

NEW STRATEGIES FOR CATALYTIC C-H AND OLEFIN HYDROSILYLATION

by

PARHAM ASGARI

Presented to the Faculty of the Graduate School of
The University of Texas at Arlington in Partial Fulfillment
of the Requirements
for the Degree of

DOCTOR OF PHILOSOPHY

THE UNIVERSITY OF TEXAS AT ARLINGTON

August, 2018

Copyright © by Parham Asgari 2018

All Rights Reserved



Acknowledgements

Foremost, I would like to express my sincere gratitude to my advisor and mentor Dr. Junha Jeon, for giving me the opportunity to learn and experience. I would like to thank him for sharing his immense knowledge, and for his continuous support and patience. His guidance helped me throughout every stage of my journey. It was truly an honor for me to be a member of Dr. Jeon's research group.

I owe a great debt of gratitude to my talented friend and post-doctoral fellow, Dr. Yuanda Hua. What I learned from Yuanda goes beyond the boundaries of chemistry and science. His exceptional modesty, his willingness to help others and his tendency to acknowledge every single contribution has been extremely inspiring for me.

I am also appreciative of all the advice and support I received from my research committee members, Dr. Carl J. Lovely, Dr. Frank W. Foss and Dr. Jongyun Heo. I am deeply thankful to all other faculty members at the University of Texas at Arlington Department of Chemistry and Biochemistry, especially my valuable professor and the department chair, Dr. Frederick MacDonnell, who has always been truly supportive, . and my graduate advisor, Dr. Peter Kroll, who has relentlessly guided me through my doctoral studies

I am equally indebted to my mentors and professors during my Master's studies, especially Dr. Mehdi Ghani and Dr. Abdoljalil Mostashari, who kept my enthusiasm for science alive during my hardest days.

A very special gratitude goes out to the Department of Chemistry kind and helpful staff, the Administrative Assistants, Mrs. Jill Howard, Mrs. Debbie Cooke, and Mrs. Natalie Croy, and the Graduate Program Coordinator, Stephanie Henry. Special thanks to the Research Engineering Scientists, Drs. Brian Edward, Roy McDougald and Chuck Savage,

and our IT support, Noor Alwachi, for making the research facilities available to me. Many thanks to Dr. William Cleaver and Heidi Conrad for their support as Lab Coordinators, as well as the stockroom supervisors, Mrs. Beth Klimek, Mr. Jason Lloyd and James Garner.

I am also grateful to all the research funding sources at UT Arlington, NIH, NSF and ACS-PRF that supported my research.

I want to express my gratitude to my lab-mates and fellow graduate students. Udaya Dakarapu, Hiep Nguyen, Apparao Bokka, Thirupataiah Avullala, Gabriela Trog, and all other fellow doctoral students for their feedback, cooperation and, of course, friendship, with a special mention to all my research collaborators, Drs. Brad S. Pierce, Kwangho Nam, Gyu Leem, Jiali Gao, Xin Chen, and Sinjinee Sardar. My gratitude also goes to our undergraduate researchers, Chanachon Thiamsiri, Watcharapon Prasitwatcharakorn, James Roh, Seongjeong Jung, and Ashif Karedath.

I am grateful to my siblings, Pouya and Parnia, my parents, who have always been there for me, and my closest friends, Ehsan, Sharmin, Hakop, Ron and Niloo.

And last but by no means least, I want to thank Bahar, my dearest wife, for her endurance and unconditional love and support. She stood by my side through thick and thin during all the hardships of immigration and enabled me to pursuit my dream. I am truly obliged to her for all the love and encouragement she gave me during my studies.

July 19, 2018

Abstract

NEW STRATEGIES FOR CATALYTIC C-H AND OLEFIN
HYDROSILYLATION

Parham Asgari PhD

The University of Texas at Arlington, 2018

Supervising Professor: Name Junha Jeon

In the works described here, new catalytic hydrosilylation strategies were explored. First, a highly selective, bond functionalization strategy, achieved via relay of two transition metal catalysts and use of traceless acetal directing groups, was introduced. Specifically, this approach involves the relay of Ir-catalyzed hydrosilylation and Rh-catalyzed ortho-C–H silylation. This acetal directing group strategy was used for catalytic ortho-C–H silylation of phenols and benzoate esters derivatives. Additionally, we developed a transition metal free, catalytic vinyl arenes hydrosilylation method. We describe our discovery on unprecedented, sustainable HAT process and report a mechanism involving Lewis base-catalyzed, complexation-induced HAT (LBCI-HAT), followed by highly selective cross-radical coupling. In this reaction, earth abundant, alkali metal Lewis base catalysts play a dual-role. They first served as a HAT initiator and subsequently a silyl radical protecting group for selective downstream processes. This efficient, and sustainable HAT permits highly controlled access to either branch-selective hydrosilylation or polymerization of vinylarenes.

Table of Contents

Chapter 1 Intramolecular Silylation of Aromatic Esters Via Silylacetal	
Directing Group	16
1.1. Silyl Chemistry and Importance of Organosilanes	17
1.2. Catalytic Approach Toward Arene C-H Silylation.....	18
1.3. Intramolecular silylation of aryl C-H bonds with a tethered silane.....	19
1.4. Establishing the catalytic system for one-pot reductive silylation	22
1.5. Ligand optimization for rhodium catalyzed C-H silylation.....	24
Chapter 2 Reductive arene ortho-silanolization of aromatic esters	26
2.1. Introduction to Organosilanols.....	27
2.2. Accessing silanols through dual Ir/Rh catalytic method	28
2.3. Substrate scope of aromatic esters using diethylsilane	28
2.4. Addressing silanol condensation issue.	30
2.5. Mechanism study and kinetic isotope effect (KIE) studies	32
2.6. Synthetic application of cyclic silyl acetals	33
2.7. Summary of chapter 2	34
Chapter 3 Catalytic Reductive ortho-C-H Silylation of Phenols	35
3.1. Introduction	36
3.2. A Single-Pot Catalytic Reductive <i>ortho</i> -C-H Silylation of Phenols	40
3.3. Synthesis of Multi-Substituted Arenes.....	42
3.4. Dioxasilines as Halosilane Equivalents	45
3.5. Synthesis of Multi-Substituted Arenes.....	47

3.6.	Synthetic Applications of Benzodioxasilines.	50
3.6.a.	Aryne Cycloaddition of ortho-Silyl triflates.....	50
3.6.b.	Pd-Catalyzed Hiyama-Denmark Cross-Coupling.....	51
3.6.c.	Au-Catalyzed Oxidative Direct Arylation of Aryl Silanes.	52
3.6.d.	Orthogonal Cross-Coupling.	53
3.6.e.	Late-Stage Functionalization of Estrone and Estradiol.	54
3.6.f.	Catalytic Synthesis of 3,3'-Bissilyl BINOL.....	55
3.7.	Summary of chapter 3	56
Chapter 4 Aryne cycloaddition reactions of benzodioxasilines phenols		57
4.1.	Introduction	58
4.2.	. Preparation of silylaryl triflates from benzodioxasilines.....	61
4.3.	Investigations on the possible desilylation pathways	62
4.4.	Preparation of sterically hindered silylaryl triflates.....	63
4.5.	Fluoride-mediated [4+2] aryne cycloaddition reaction of... ..	64
4.6.	. Synthetic approach to estrone derivative 4-20.....	65
4.7.	Summary of chapter 4	66
Chapter 5 Hydrogen Atom Transfer from Hydrosilanes by LB Catalysis		68
5.1.	Introduction	69
5.2.	Mechanistic discussion.....	72
5.3.	LBCI-HAT reactions: Discovery and development.....	74
5.4.	Mechanistic investigations of the LBCI-HAT.	76
5.5.	NMR Spectroscopic studies for the LBCI-HAT.....	78
5.6.	Cation- π interaction in the LBCI-HAT.	80
5.7.	EPR Spectroscopic studies for the LBCI-HAT.	82
5.8.	Hammett Plot Analysis	89

5.9.	Kinetic Isotope Effect (KIE) Studies.....	91
5.9.a.	Parallel KIE experiment.....	91
5.9.b.	Intermolecular competition KIE experiment	92
5.10.	Computational studies on LBCI-HAT.....	94
5.11.	Scope of the LBCI-HAT.....	97
5.12.	Synthetic applications.....	99
5.13.	Summary of chapter 5	101
Appendix A List of all abbreviations		103
Appendix B Materials and method		107
Appendix C Experimental Procedures for Chapter 1 and 2.....		110
C.1.	General Procedure for Preparation of Diethylhydridosilyl Aetals	111
C.2.	General Procedure for Preparation of (1-2 ^{iPr}):.....	111
C.3.	General Procedure for Preparation of Cyclic Silyl Acetals (1-3):	111
C.4.	General Procedure for Preparation e (2-1) and (2-2)	112
C.5.	Gram Scale Synthesis of (2-1-1)	112
C.6.	Compound Characterization for chapter 1 and 2	113
C.7.	Procedure for Preparation of (2-3):.....	133
C.8.	Procedure for Oxidation of 6a to Salicylic aldehyde (2-4):	134
C.9.	Procedure for Oxidation of 1-3-1 to Catechol (2-5):	135
C.10.	Procedure for Allylation of 1-3-1	135
C.11.	Procedure for Iodo <i>ipso</i> -Desilylation of 2a/3	136
C.12.	Procedure for Oxidative Lactonization of 3a	137
C.13.	Procedure for Horner-Wadsworth-Emmons Homologatin (2-9):	138
C.14.	Procedure for intermolecular KIE:	140
C.15.	Procedure for intramolecular KIE:	141

Appendix D Experimental Procedures for Chapter 3	144
D.1. General Procedure to Prepare Benzodioxasilines	145
D.2. General Procedure for Nucleophilic Addition	145
D.3. Compound chrecterization.....	146
D.4. Procedure for 3-9.....	170
D.5. Procedure for Preparation of Chloroacetates.....	178
D.6. Procedure for Preparation of (3-8d-Et).....	182
D.7. Procedure for Preparation of Trifluoromethanesulfonate	188
D.8. General Procedure for Benzyne Cycloaddition Reaction.....	191
D.9. Procedure for <i>ipso</i> -Desilylative Boronation)	192
D.10. Procedure for Iodo <i>ipso</i> -Desilylation of 3-12a to 3-2-Iodophenol	
D.11. General Procedure for Palladium Catalyzed Cross-Coupling	193
D.12. General Procedure for Gold Catalyzed Cross-Coupling Reaction:	194
D.13. Procedure for Palladium Catalyzed Suzuki Reaction (3-29)	201
D.14. Procedure for Palladium Catalyzed Heck Reaction (30).....	202
D.15. Procedure for Preparation of (SI-2a)	203
Appendix E Experimental Procedures for Chapter 5	237
E.1. Survey of Silanes.....	238
E.2. Survey of Lewis Base	239
E.3. Survey of KOtBu Loading	241
E.4. Survey of Solvent.....	242
E.5. Control Experiments in the Absence of KOtBu.....	243
E.6. Effects of the Order of Addition of Reagents and Catalyst.....	244
E.7. Control Reactions with KOtBu of Different Grades Vendors	246
E.8. Control experiments with various transition metals	247

E.9.	Investigation of Mechanism Involving HAT	
E.10.	Studies on Potassium Cation- π Interaction	251
E.11.	Mechanism Involving Silyl Radicals.....	253
E.12.	Radical Clock Experiments.....	254
E.13.	NMR Studies.....	258
E.14.	EPR Spectroscopy Procedure.....	260
E.15.	Addition Control Experiments	262
E.16.	Computational Details	265
E.17.	Hammett Plot Analysis	269
E.18.	Kinetic Isotope Effect (KIE) Studies.....	270
E.19.	General Procedure for Transition Metal-Free,	271
E.20.	Polymerization Procedure and Characterization:	286
E.21.	KO ^t Bu-catalyzed dual olefin hydrosilylation and ...:	288
References:	293

List of Illustrations

Figure 1-1 Examples of organosilanes with Industrial application	17
Figure 1-2. Versatility of C-Si bond in chemical transformations	18
Figure 1-3 Hartwig's group contribution in CH silylation	20
Figure 1-4 Brookhart's hydrosilylation of esters.....	21
Figure 1-5 Brookhart's proposed hydrosilylation mechanism	21
Figure 1-6 Difference in rate of electron rich and electron poor esters	22
Figure 1-7 One-pot reductive arene ortho-silylation	23
Figure 1-8 Failure of CH silylation with Ir/Phen	23
Figure 1-9 Takai's synthesis of siloles	24
Figure 2-1 Conventional methods for synthesis of silanols	27
Figure 2-2 Accessing silanols through dual catalytic method and hydrolysis.....	28
Figure 2-3 KIE studies.....	32
Figure 2-4 Synthetic application of 1-3-1	33
Figure 3-1 Examples of bioactive phenolic compounds	36
Figure 3-2 Gevorgyan's silanol directing group	38
Figure 3-3 Prior approaches for catalyzed C–H silylation of protected phenols.....	38
Figure 3-4 <i>ortho</i> -C–H silylation of phenols using a traceless acetal directing group.....	39
Figure 3-5 Proposed strategy of acetal directing group.....	40
Figure 3-6 Synthesis of multi-substituted arenes.....	44
Figure 3-7 Dioxasilines as halosilane equivalents	46
Figure 3-8 Challenges involving sterically hindered substrates.....	47
Figure 3-9 Discovery of α -chloroester directing group.....	48

Figure 3-10 Synthetic applications of benzodioxasilines	50
Figure 3-11 Au-catalyzed oxidative direct arylation	52
Figure 3-12 Orthogonal Cross-Coupling	53
Figure 3-13 C2-Silylation of estrone	54
Figure 3-14 C2-Silylation of estradiol.....	55
Figure 3-15 3,3' Silylation of BINOL.....	55
Figure 3-16 X-ray of 3,3' Silylated BINOL.....	56
Figure 4-1 Precedents of 1,2-silylaryl triflates synthesis.....	58
Figure 4-2 Single pot synthesis of silylaryl triflates	59
Figure 4-3 Possible desilylation mechanism.....	62
Figure 4-4 Synthesis of estrone derivative 4-20	66
Figure 5-1 Branch-selective hydrofunctionalizations involving HAT	69
Figure 5-2 Pentacoordinated silicate reactivity	71
Figure 5-3 Silyl radical transfer can not explain the regio-selectivity	73
Figure 5-4 Modes of substrates-hypercoordinate silicate interaction	74
Figure 5-5 Discovery of LB-catalyzed transition metal-free, hydrosilylation	75
Figure 5-6 Effect of addition of radical traps	76
Figure 5-7 Radical clock experiment.....	77
Figure 5-8 NMR studies	78
Figure 5-9 NMR studies	79
Figure 5-10 Reactivity test of silaketal 5-10	80
Figure 5-11 Inversitgation of Cation- π interaction	81
Figure 5-12. X-band EPR spectra of the reactions Carried out with spin-trap.....	84
Figure 5-13. Expanded X-band EPR Difference Spectra [6–7]	85
Figure 5-14, 50 K EPR spectra of freeze-quenched HAT reactions	89

Figure 5-15 Hammett plots using σ	90
Figure 5-16 Hammett plots using σ values.	90
Figure 5-17 Designed KIE experiments	91
Figure 5-18, $^1\text{H-NMR}$ spectra of competition KIE	92
Figure 5-19 Computed reaction energy profile for the LBCI-HAT reactions.....	94
Figure 5-20 Substrate scope of LBCI-HAT reaction	98
Figure 5-21 HAT initiated polymerization.....	99
Figure 5-22 Effect of concentration of polymerization	99
Figure 5-23 Synthetic application of benzyl silanes	100

List of Tables

Table 1-1 Ligand screening for the CH activation process	24
Table 2-1 Steric effect of bulky esters.....	29
Table 2-2 Substrate scope using H_2SiEt_2	30
Table 2-3 Expansion of substrate scope with $\text{H}_2\text{Si}^i\text{Pr}_2$	31
Table 3-1 Substrate scope of benzodioxalilenes	41
Table 3-2 Optimazation of Hiyama-Denmark coupling reaction	51
Table 4-1 Substrate scope of 1,2-silylaryl triflates	61
Table 4-2 Sterically hindered 1,2,3, substituted silylaryl triflates	63
Table 4-3 Aryne cycloaddition reaction of silylaryl triflates	64
Table 4. Survey of Silanes	238

Note

Portions of this thesis have been taken, with permission, from the following publications:

- Asgari, P.; Dakarapu, U. S.; Nguyen, H. H.; Jeon, J. Aryne cycloaddition reactions of benzodioxasilines as aryne precursors generated by catalytic reductive ortho-C H silylation of phenols with traceless acetal directing groups. *Tetrahedron* **2017**, *73*, 4052-4061.
- Hua, Y. §; Asgari, P. §; Avullala, T.; Jeon, J., Catalytic Reductive ortho-C–H Silylation of Phenols with Traceless, Versatile Acetal Directing Groups and Synthetic Applications of Dioxasilines. *J. Am. Chem. Soc.* **2016**, *138*, 7982–7991. § contributed equally to this work. **Reprinted with permission Copyright 2016 American Chemical Society.**
- Hua, Y.; Asgari, P.; Dakarapu, U. S.; Jeon, J., Reductive arene ortho-silanolization of aromatic esters with hydridosilyl acetals. *Chem. Commun.* **2015**, *51*, 3778-3781. **Reproduced with permission from The Royal Society of Chemistry.**
- Dakarapu, U. S.; Bokka, A.; Asgari, P.; Trog, G.; Hua, Y.; Nguyen, H. H.; Rahman, N.; Jeon, J., Lewis Base Activation of Silyl Acetals: Iridium-Catalyzed Reductive Horner–Wadsworth–Emmons Olefination. *Org. Lett.* **2015**, *17*, 5792-5795.

Chapter 1

Intramolecular Silylation of Aromatic Esters Via Silylacetal Directing Group

1.1. Silion Chemistry and Imporntance of Organosilanes

In recent years silicon chemistry has become one of the developing fields of research in chemistry. Silicon is the second most abundant element in the earth's crust and the eighth most abundant element in the universe. The similarity of silicon to carbon, has motivated researchers to investigate the possibility of the replacement of carbon with silicon,¹ to modify the biological and chemical behavior of molecules. Although the bond strength of carbon-silicon is considered to be relatively strong, there are few natural molecules containing silicon-carbon bonds. Silicon carbide is one of the few examples of this class of molecules.² The discovery and development of organosilane polymers³ has led to versatile usage of silicones (siloxanes) in everyday commodities. In addition organosilanes are being used in variety of fields including drug discovery,⁴ biomedical agents,⁵ electronics and photonics³.(Figure 1-1)

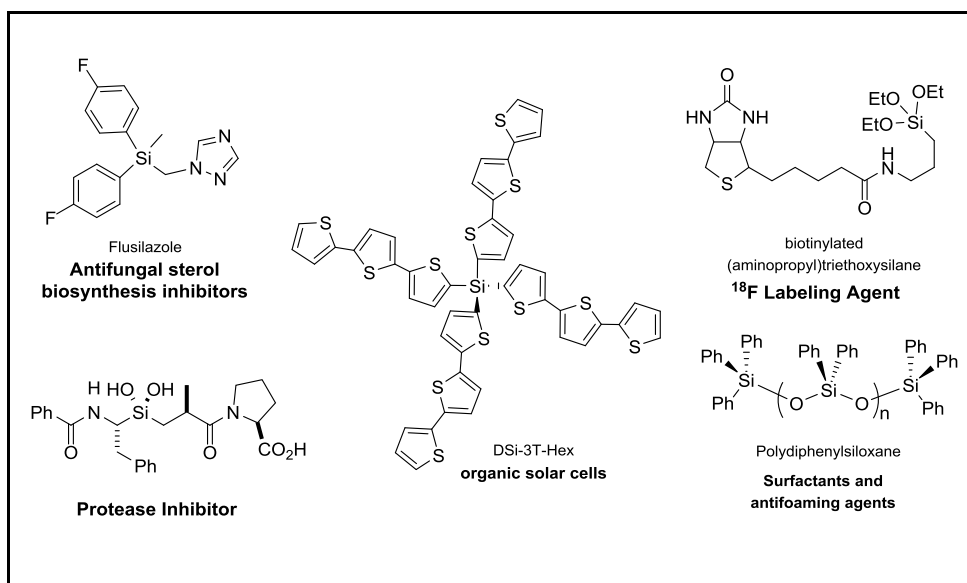


Figure 1-1 Examples of organosilanes with Industrial application

Beside abundance of silicon resources, another important feature of organosilanes is that they are mostly environmentally benign and compared to toxic heavier element of

group 4 (lead and tin) silicon compounds are considered relatively non-toxic. Organosilanes are also versatile intermediates from a synthetic point of view. For instance, Hiyama-Denmark cross-coupling^{6, 7} and Tamao oxidation⁸ are well known methods for chemical transformations of carbon-silicon bond. (Figure 1-2)

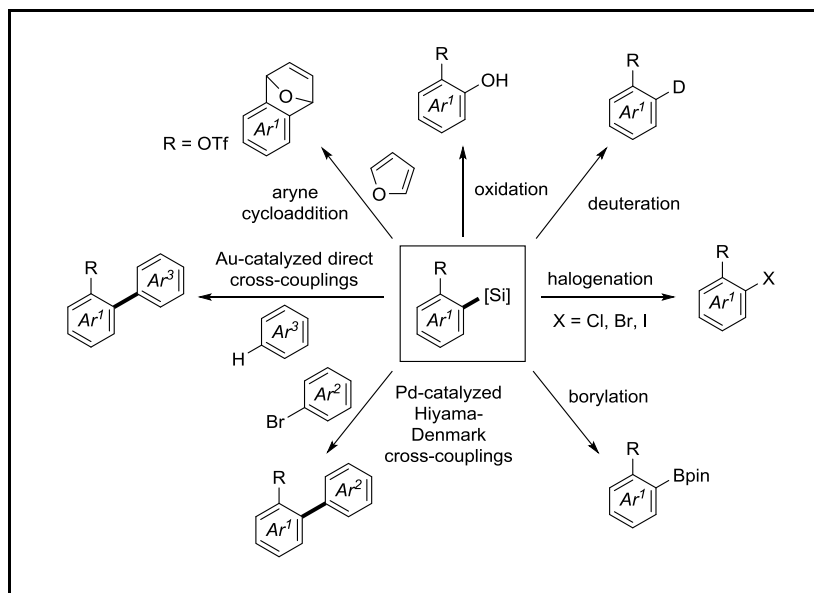


Figure 1-2. Versatility of C-Si bond in chemical transformations

1.2. Catalytic Approach Toward Arene C-H Silylation

There are various methods reported for synthesis of arylsilanes. Traditional approach is addition of Grignard or organolithium reagent to silylchloride^{9, 10} or cyclosiloxanes^{11, 12}. An alternative approach can be cross coupling of aryl halides with hydrosilanes^{13, 14}, which is more versatile and has higher functional group compatibility compared to Grignard or organolithium reagents. We can categorize these synthetic methods into the following classes, including: 1) lithium-halogen exchange/silylation, 2) metal-catalyzed silylation of haloarenes, and 3) arene directed ortho-metalation (DoM)/silylation. Although these methods exhibit excellent site-selectivity, the cryogenic conditions and stoichiometric uses of reagents can be drawbacks of such methods.

Furthermore, poor functional group tolerance and the necessity for pre-functionalized moieties such as halides and pseudo halides can be drawbacks of the mentioned methods. To overcome these difficulties, direct metal-catalyzed arene dehydrogenative silylation methods have been developed in recent years.¹⁵ These strategies can be divided in three main classes. 1) Intramolecular silylation 2) directed controlled silylation and 3) sterically directed C-H silylation. Each one of these methods has advantages and disadvantages. For example, intramolecular silylation has high yield and benefits from one to one molar ratio of silane to arene, however it requires a specific design of a tethered silane moiety. Directed control methods which are remarkably site selective, are mostly limited to *ortho* silylation and to access meta or para silylation a sterically hindered moiety or a bulky directing group is required. In recent years Hartwig group has developed various catalytic methods to achieve selective silylation of arenes.

1.3. Intramolecular silylation of aryl C–H bonds with a tethered silane.

As mentioned earlier the intramolecular strategy requires the availability of a tethered hydrosilane on the target arene molecule. The tether can comprise carbon chain or hetero atom containing moieties. In 2005 Hartwig and Tsukada developed a method involving, Pt-catalyzed intramolecular silylation of dimethylphenethylsilane and dimethyl(3-phenylpropyl)silane to access the corresponding silylarenes(Figure 1-3) ¹⁶

Hartwig and co-workers have done extensive studies on various tethering groups derived from alcohols¹⁷, amines¹⁸, or ketones¹⁷, which can generate the precursor of intramolecular silylation to form new carbon silicon bond. (Figure 1-3) Hartwig's arene intramolecular hydrosilylation strategies are generally involve a sequence of hydrosilylation (for ketones and aldehydes) or dehydrogenative silylation (in case of alcohols) followed by

Csp²-H bond activation. It was shown that addition of norbornene (nbe) as hydrogen acceptor facilitates the reaction (Figure 1-3)

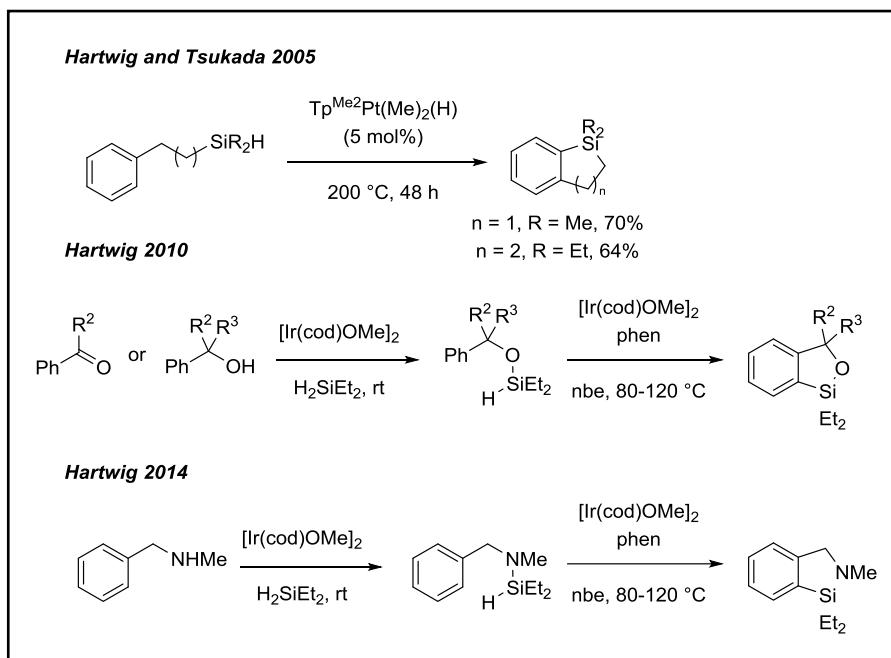


Figure 1-3 Hartwig's group contribution in CH silylation

Intramolecular silylation of aryl C–H bonds with silyl acetal tethering group.

Inspired by the synthetic method developed by Hartwig's group, we envisioned the possibility of intramolecular silylation of aromatic esters via formation of a silyl acetal intermediate. To access the silyl acetal tethering group we utilized the iridium catalyzed hydrosilylation method which was introduced by Brookhart laboratory to controllably reduce esters to aldehydes (Figure 1-4).¹⁹

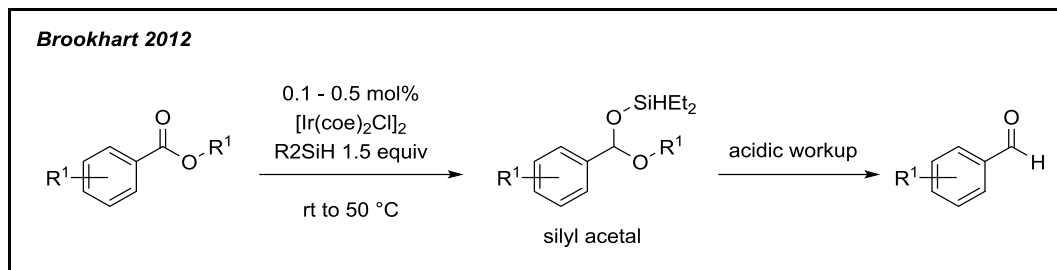


Figure 1-4 Brookhart's hydrosilylation of esters

Mechanism study of the iridium catalyzed hydrosilylation reaction suggests presence of a binuclear silylene-bridged iridium dimer as the active catalytic species. Brookhart group has previously isolated and crystallographically characterized an analogous complex from $t\text{Bu}_2\text{SiH}_2$.²⁰ Formation of such complex is possible through sequential displacement of cyclooctene (coe) and chloride ligands. (Figure 1-5)

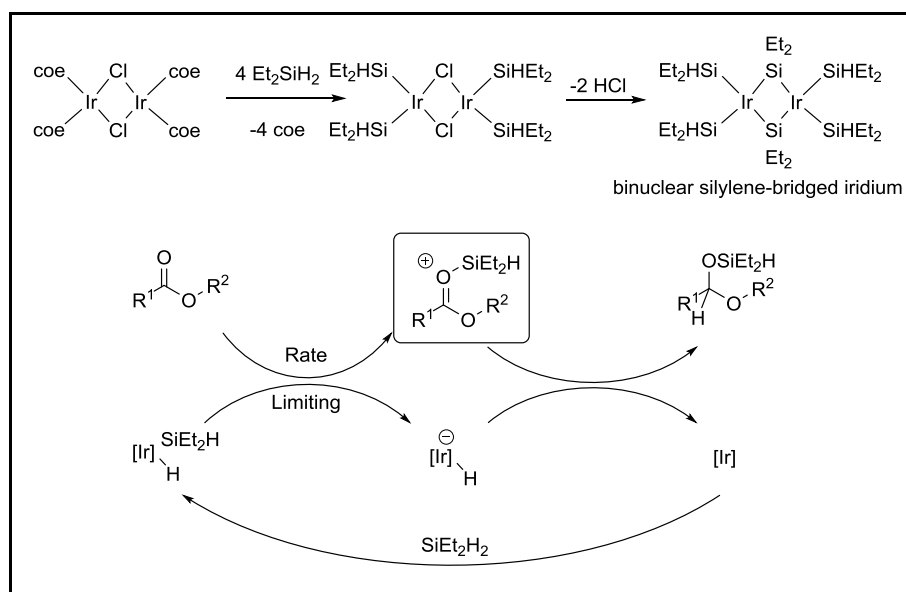


Figure 1-5 Brookhart's proposed hydrosilylation mechanism

The rate determining step of the reaction seems to be the transfer of silylium ion (SiHEt_2^+) to the lone pair of carbonyl oxygen, which can be supported by comparing the rate of hydrosilylation of electron rich carbonyls versus electron deficient ones (Figure 1-6).

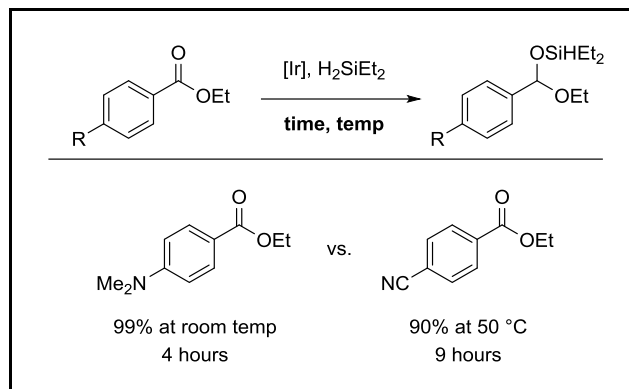


Figure 1-6 Difference in rate of electron rich and electron poor esters

The iridium catalyzed reduction process goes through a silyl acetal intermediate which has the capability of serving as a silyl directing group to obtain intramolecular C-H silylation (Figure 1-7). Notably, the versatile, yet labile silyl acetal directing groups for catalytic C-H silylation, has not been reported to date. Nonetheless, our strategy for the single-pot reductive *ortho*-silylation of arenes required the resolution of two challenges: first, the compatibility of the two catalysts toward a combined single-pot reaction sequence had to be established. Secondly, the discovery of a catalytic system suitable for C-H functionalization directed by labile hydridosilyl acetals was required.

1.4. Establishing the catalytic system for one-pot reduction silylation of aromatic esters.

From the outset, diethylhydridosilyl acetal **1-2** were prepared via a controlled hydrosilylation of aromatic esters utilizing $[\text{Ir}(\text{coe})_2\text{Cl}]_2$ (0.1 mol%) and diethylsilane (2 equiv.).¹⁹ The resultant diethylhydridosilyl acetal **1-2** did not require additional purification for the next steps. We then investigated arene *ortho*-silylation of hydridosilyl acetal.

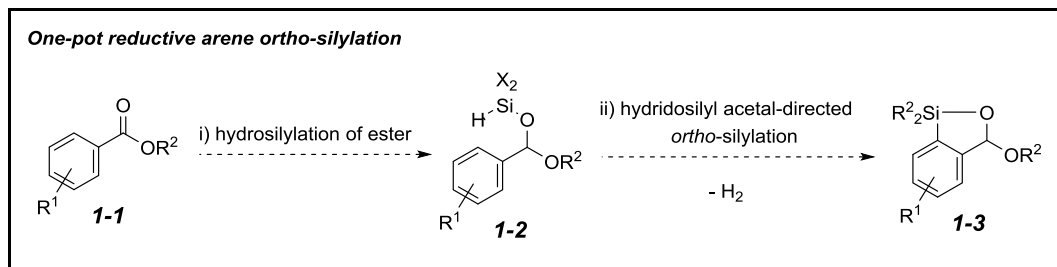


Figure 1-7 One-pot reductive arene ortho-silylation

Although we aimed to utilize a single Ir catalyst for both processes, neither the Ir/phen catalytic system which has been developed by Hartwig (or phen derivatives as ligands), nor other screened Ir/ligand complexes efficiently afforded the cyclic silyl acetal **1-3** (ca. 30% yield upon complete conversion). Instead of the expected product we observed formation of silaketal **1-4**, possibly via rearrangement of silyl acetal **1-2** (Figure 1-8)

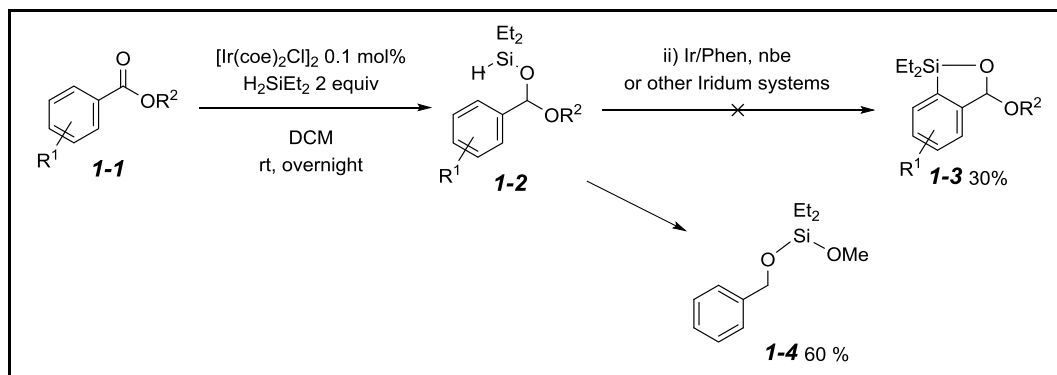


Figure 1-8 Failure of CH silylation with Ir/Phen

Steric and electronic differences of hydrosilyl ether and hydrosilyl acetal directing groups had a considerable impact on reactivity. To overcome this obstacle, we explored alternative catalytic systems. After numerous attempts, we got promising results with the use of Rhodium catalyst which was utilized by Takai in the synthesis of Spirosilabifluorene (Figure 1-9)^{21, 22} where it was shown Rh-catalyzed C–H silylation, by employing monodentate triphenylphosphine ligands.

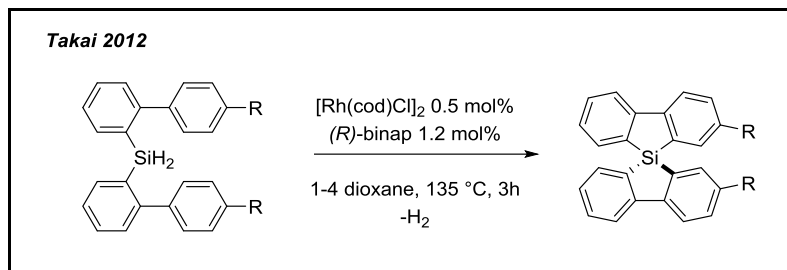


Figure 1-9 Takai's synthesis of siloles

1.5. Ligand optimization for rhodium catalyzed C-H sialylation of aromatic esters.

During our preliminary screening it was clear that monodentate phosphine ligands readily promotes the hydridosilyl acetal-directed dehydrogenative cyclization in the presence of norbornene as a hydrogen acceptor (Table 1-1)

Table 1-1 Ligand screening for the CH activation process

Entry	Ligand	Time (min)	Yield (%) ^a
1	PPh ₃	10	98
2	PPh ₂ (<i>o</i> -tol)	60	10
3	PPh ₂ Me	60	20
4	P(4-MeOPh) ₃	10	98
5	P(4-MeNPh) ₃	60	20
6	P(C ₆ F ₅) ₃	60	20
7	P(2-furyl) ₃	60	95

^a Determined by ¹H NMR spectroscopy utilizing an internal standard (CH₂Br₂).

For instance, triphenylphosphine afforded **1-3** in excellent yield (entry 1). However, sterically hindered and alkyl substituted phosphines, PPh₂(*o*-tol) and PPh₂Me, were not effective ligands (entries 2–3). To systematically study the influence of electronic

perturbation of phosphine ligands on the C–H silylation, we examined a series of electronically tuned phosphine ligands (entries 4–7). Electron donating ligand P(4-MeOPh)₃ efficiently promotes the cyclization to afford **1-3** in excellent yield (98%) within only 10 min. In comparison, well-established hydridosilyl ether-directed arene C–H silylation took 11–48 h at 80–120 °C employing 1 mol% of [Ir(cod)OMe]₂/phen.¹⁷ However, other phosphines such as P(4-Me₂NPh)₃ and P(C₆F₅)₃ drastically reduced the overall reaction efficiency (entries 5–6). Upon addition of P(2-furyl)₃ to the reaction, the yield was improved, but not comparable to P(4-MeOPh)₃. Moreover, the Rh/(4-MeOPh)₃ catalytic system achieved the reaction with sterically hindered 2- and 3-methyl benzoates to afford the corresponding cyclic silyl acetals (98% and 92% yields vis-a`-vis 63% and 54% with PPh₃, respectively) within 10 min. These results showed that the two catalytic systems (Ir and Rh) are compatible, and that a single-pot reductive arene ortho-silylation directed by hydridosilyl acetals is feasible.

In the chapter 2 and 3 we will discuss in details the utilization of Ir/Rh dual catalytic system for selective ortho silylation/salinization of aromatic esters and the synthetic application of the silicon containing cyclic compounds.

Chapter 2

Reductive arene ortho-silanolization of aromatic esters with hydridosilyl acetals

Yuanda Hua, Parham Asgari, Udaya Sree Dakarapu and Junha Jeon

This work has been published in *Chem. Commun.*, **2015**, 51, 3778

2.1. Introduction to Organosilanols

Organosilanols²³ are well known for their synthetic and industrial applications. They are widely being used in polymer industries of polydisiloxanes²⁴ and silicon coupling agents²⁵. Additionally it has been shown that silanols possess remarkable antimicrobial activity.^{26, 27} Organosilanols are, in general, environmentally benign and they readily decompose to silica, carbon dioxide, and water,²⁸ and their use has been significantly increased with wide application for silicon-based materials and biomedically relevant agents.^{29, 30} They are also useful synthetic agents for a variety of chemical transformations, including silicon-based cross-coupling reactions,³¹ oxidations,⁸ silanol hydrogen bond donor catalysis,^{32, 33, 34} and directing groups for C–H bond functionalization.³⁵ In particular, arylsilanol synthesis often involves a two-step sequence of silylation and hydrolysis. Several silanolization methods have been developed (Figure 2-1).

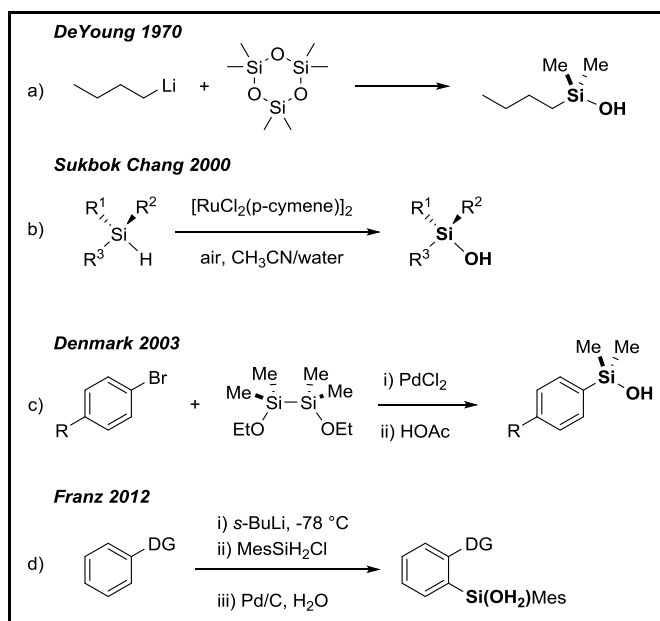


Figure 2-1 Conventional methods for synthesis of silanols

These methods include: (a) metal-halogen exchange/silylation,³⁶ (b) hydrolytic oxidation of hydrosilanes,³⁷ (c) metal-catalyzed silylation of haloarenes followed by

hydrolysis,³⁸ and (d) a sequence of directed arene *ortho*-metalation, silylation, and hydrolysis.³⁹ These methods offer excellent site-selectivity, yet often require strongly basic and cryogenic conditions or a stoichiometric amount of reagents, thereby displaying poor functional group compatibility. Alternative to direct silylation, prefunctionalized moieties [e.g., aryl (pseudo)halides] are demanded within substrates.

2.2. Accessing silanols through dual Ir/Rh catalytic method

Metal-catalyzed arene dehydrogenative silylation has emerged as a powerful method for preparation of useful organosilanes. To access diverse, functionalized organosilanols, which were previously difficult to access in an atom- and step-economical fashion, we envisioned dehydrogenative silanolization via catalytic C–H activation. Using the dual Ir/Rh catalytic strategy which has been introduced in the previous chapter.

Our approach could directly prepare arylsilanols, via the sequence of two transition metal-catalyzed reactions followed by a facile hydrolysis in a single vessel. Upon simple aqueous work-up, *ortho*-formyl arylsilanols could be produced.

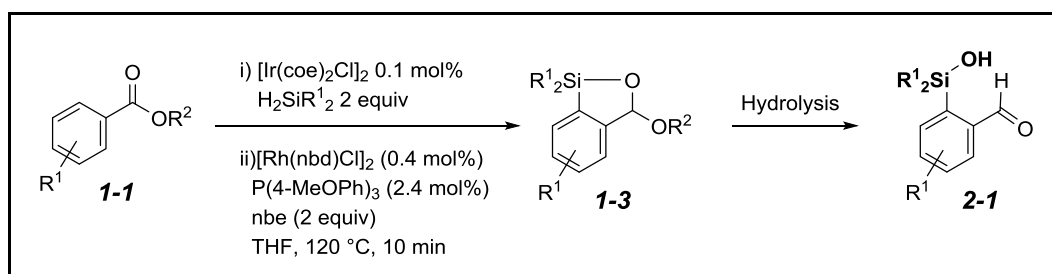


Figure 2-2 Accessing silanols through dual catalytic method and hydrolysis

2.3. Substrate scope of aromatic esters using diethylsilane

Upon determination of optimal reaction conditions for the hydrosilylation of esters and concomitant C–H silylation via Ir/Rh sequential catalysis, first we explored the compatibility of different aryl/alkyl benzoate esters with the iridium catalyzed hydrosilylation

protocol. Methyl and benzyl esters **1-1-Me** and **1-1-Bn** were most efficient while sterically hindered tert-butyl ester **1-1-^tBu** did not efficiently undergo the hydrosilylation.

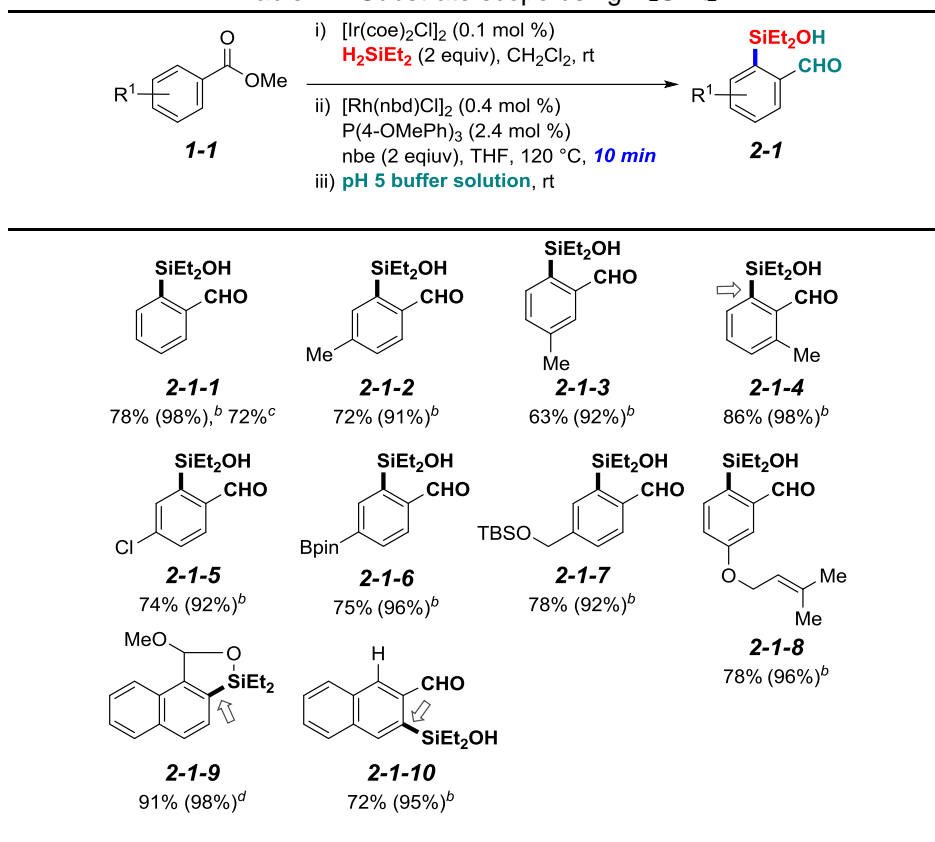
Table 2-1 Steric effect of bulky esters

	R	Yield (%)
1-1-Me	Me	98
1-1-Et	Et	85
1-1-ⁱPr	ⁱ Pr	61
1-1-^tBu	^t Bu	4
1-1-Ph	Ph	6
1-1-Bn	Bn	98

After that we investigated the substrate scope of the reductive arene *ortho*-silylation of esters **1-1**, bearing variety of electron donating or electron withdrawing substituents on the aryl ring. The sequential processes utilizing diethylsilane produce cyclic silyl acetals **1-3** in generally good yields, regardless of electronic and steric differences of arenes. However, the propensity for silanol condensation to afford disiloxanes during hydrolysis resulted in inconsistent yields of *ortho*-formyl arylsilanols **2-1**. Denmark's method resolved this issue by utilizing a buffer solution (pH 5) to reliably produce **2-1** (Table 2-2).³⁸ Under these conditions, the tandem reactions with electron-rich and deficient esters yielded the corresponding arylsilanols (**2-1-1 to 2-1-10**) in good yields. A boronic ester, a silyl blocking group, and trisubstituted alkene were tolerated in the reaction system to afford **2-1-5 to 2-1-8**. We observed chemoselective silylation of aryl C_{sp2}-H over benzylic C_{sp3}-H within **2-1-4**. Highly regioselective C-H silylation of 1-naphthoate was achieved, where the corresponding hydrosilyl acetal exclusively triggers C-H activation of hydrogen at C2 over the hydrogen at C8 to afford **2-1-9**. Hydrolysis of **2-1-9** in a wide range of pH

buffer solutions, however, provided either the recovered starting material or a significant desilylation product. In 2-naphthoate, silanolization occurred at the C3 position regioselectivity to provide **2-1-10**. Lastly, to show the compatibility of the reaction with large scale synthesis we performed a 12 mmol scale reaction which provided **2-1-1** in 72% isolation yield.

Table 2-2 Substrate scope using H₂SiEt₂



^a Conditions: **1** (1.0 mmol), CH₂Cl₂ (3.3 M); THF (1 M). ^b Yield of isolated product **2-1**. Yield of cyclic silyl acetals **1-3** determined by ¹H NMR spectroscopy utilizing an internal standard (CH₂Br₂) is shown in parentheses. ^c Reaction of **1-1-1** on 12 mmol (1.63 g) scale yielded **2-1-1** in 72% isolation yield. ^d Isolated yield of **2-1-9**.

2.4. Addressing silanol condensation issue.

As it mentioned earlier, silanols are prone to undergo condensation and forming siloxanes. Although using Denmark buffer system³⁸ reduced condensation byproduct, the

issue still persisted in most of the substrates. It has been shown that sterically hindered silanols are relatively more stable. Therefore, we turned our attention toward Silicon groups bearing larger substituents, such as isopropyl groups, which greatly suppressed the silanol condensation, thereby consistently improving yields (Table 2-3). The reaction with electron-rich and deficient esters provided the corresponding silanols (**2-2-2 to 2-2-11**) in good yields.

Table 2-3 Expansion of substrate scope with H₂SiⁱPr₂

		yield of 1-3 (%) ^b			
2-2-1	H	91 (98)		2-2-14	71% (82%) ^b
2-2-2	4-Me	90 (98)		2-2-15	41% (54%) ^b
2-2-3	5-Me	67 (86)		2-2-16	62% (73%) ^b
1-3-4	6-Me	90 ^c		2-2-17	71% (87%) ^b
2-2-4	4-F	85 (96)		2-2-18	57% (71%) ^{b,d}
2-2-5	4-Cl	75 (86)		1-3-9	91% ^e
2-2-6	5-Cl	78 (93)		2-2-19	77% (96%) ^b
2-2-7	4-CF ₃	72 (98)		2-2-20	75% (91%) ^{b,f}
2-2-8	4-OMe	56 (92)			
2-2-9	5-OMe	77 (91)			
2-2-10	6-OMe	36 (48)			
2-2-11	5-NMe ₂	91 (98)			
2-2-12	4-Bpin	77 (91)			
2-2-13	5-Bpin	72 (97)			

^a Conditions: **1** (1.0 mmol), CH₂Cl₂ (3.3 M); THF (1 M). ^b Yield of isolated product **3**. Yield of cyclic silyl acetals **1-3** determined by ¹H NMR spectroscopy utilizing an internal standard (CH₂Br₂) is shown in parentheses. ^c Isolated yield of cyclic silyl acetal **1-3-4**. ^d H₂SiⁱPr₂ (1.1 equiv), rt, 48 h. ^e Isolated yield of **1-3-9**. ^f H₂SiⁱPr₂ (4 equiv); [Rh(nbd)Cl]₂ (0.8 mol %), P(4-OMePh)₃ (4.8 mol %).

The reactions demonstrated reasonably good functional group tolerance in the presence of an amine, boronic ester, or trisubstituted alkene (**2-2-11 to 2-2-14**). Heterocyclic indolyl and furanyl esters were tolerated by the reaction conditions to provide

3-silanol indole 2-carbaldehyde **2-2-15** and silanol furanals **2-2-16** and **2-2-17**. In particular, **2-2-17** was the sole product with excellent regioselectivity. Remarkably, chemoselective arene C–H ortho-silanolization (methyl vs. isopropyl esters) within diester **1-1-18** was viable, exclusively affording **2-2-18**. As seen in Table 2-3, reactions using naphthoates and diisopropylsilane exhibited complete regioselectivity to afford **1-3-9**, which did not productively undergo hydrolysis, and **2-2-19**. Dual reductive C–H silanolization was also achieved with additional reagents to yield doubly functionalized disilanol **2-2-20**. It is worth noting that silyl hemi-acetal formation was only observed when diisopropylsilane was used. Presumably, this is due to a substantial structure and reactivity difference of silanols and alcohols as well as conformational preference by diisopropyl silane substituents (cf., diethylsilane).

2.5. Mechanism study and kinetic isotope effect (KIE) studies

To gain insight into the reaction mechanism, we performed two KIE experiments (Figure 2-3).

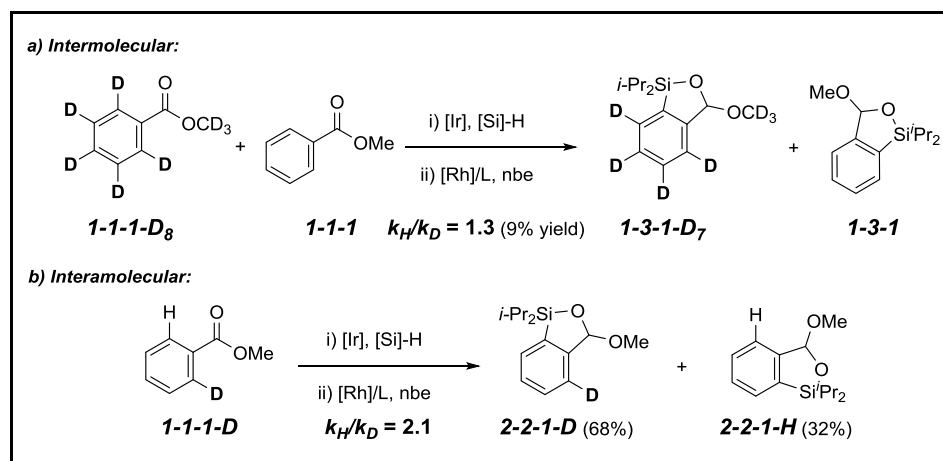


Figure 2-3 KIE studies

The observed minimal isotopic selectivity ($k_H/k_D = 1.3$) in the intermolecular KIE experiment suggests that C–H bond cleavage is not turnover-limiting and the small KIE

suggests that a preceding, irreversible step (likely substrate binding) is the product-determining step (Figure 2-3a). Assuming that C–H bond cleavage is irreversible, the significant KIE observed in the intramolecular experiment ($k_H/k_D = 2.1$) arises only from the C–H bond cleavage step being product-determining in this case, as the proceeding irreversible and turnover-limiting step cannot select the product (Figure 2-3b).⁴⁰ Together, these studies indicate that the turnover-determining step is an irreversible step involving substrate metal coordination that proceeds C–H bond cleavage.

2.6. Synthetic application of cyclic silyl acetals

Cyclic silyl acetals **1-3** and *ortho*-formyl arylsilanols **2-1** and **2-2** are versatile intermediates for a number of transformations (Scheme 3):

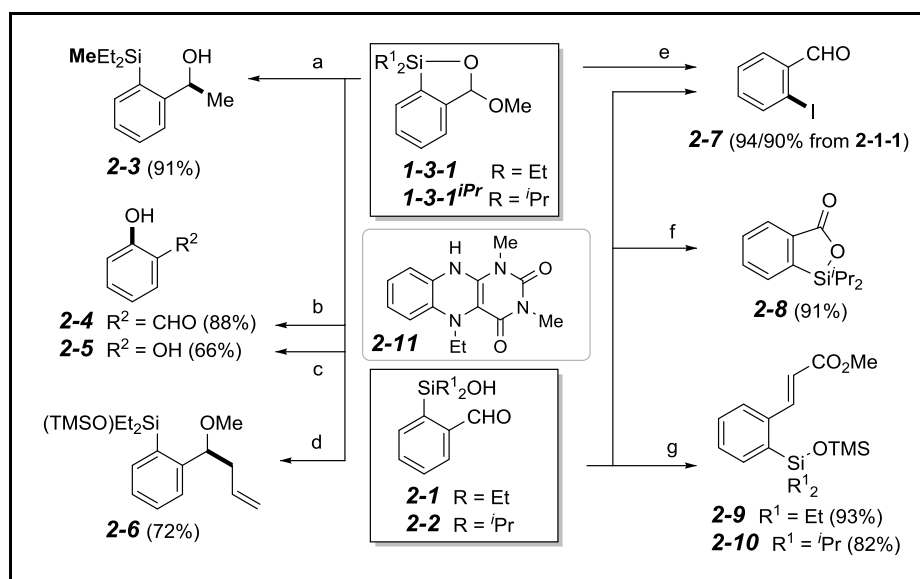


Figure 2-4 Synthetic application of **1-3-1**

First, we tried (a) nucleophilic addition to **1-3-1**, using $MeMgBr$ to furnish silane **2-3**; (b) oxidation of **1-3-1** provided salicylic aldehyde **2-4**;¹⁷ (c) Fleming-Tamao/ Dakin oxidation cascade of **1-3-1** employing the flavin-type catalyst **2-11** afforded catechol **2-5**;⁴¹ (d) Lewis acid-catalyzed allylation of **1-3-1** yielded homoallylic methyl ether **2-6**;⁴² (e) iodo

ipso-desilylation of **2-2/1-3-1** installed halogen to afford **2-7**. (f) IBX-mediated oxidation of **2-2** furnished benzosilalactone **2-8**; and (g) Horner–Wadsworth–Emmons reaction of **2-1/2-2** gave enoates **2-9/2-10**.

2.7. Summary of chapter 2

To summarize, we have developed a single-pot reductive arene ortho-silanolization of esters **1-1**. Two sequential transition metal catalytic reactions, followed by a mild hydrolysis step, allow direct access to ortho-formyl arylsilanols **2-1** and **2-2**. Our strategy interconnects Ir-catalyzed ester hydrosilylation with Rh-catalyzed C–H silylation to facilitate the reductive arene ortho-silylation in a single vessel. Hydrolysis reveals ortho-silanol and aldehyde functionalities. Notably, ester hydrosilylation was achieved with 0.1 mol % of $[\text{Ir}(\text{coe})_2\text{Cl}]_2$ and the labile hydridosilyl acetal-directed C–H silylation was accomplished within 10 min, employing 0.4 mol % of $[\text{Rh}(\text{nbd})\text{Cl}]_2/\text{P}(4\text{-MeOPh})_3$. We were able to provide Kinetic isotope effect studies to elucidate evidences for the possible C-H activation mechanism. And finally, it was shown that the ortho-formyl arylsilanols are capable of variety of synthetic transformations.

Chapter 3

Catalytic Reductive ortho-C–H Silylation of Phenols with Trace-less, Versatile Acetal
Directing Groups and Synthetic Applications of Dioxasilines

Yuanda Hua*, **Parham Asgari***, **Thirupataiah Avullala** and **Junha Jeon**

This work has been published in *J. Am. Chem. Soc.* **2016**, *138*, 7982–7991

*Equally contributed to the paper

3.1. Introduction

selective silylative functionalization of phenols is important because many bioactive natural products and unnatural congeners, including medically important molecules, contain phenolic moieties that contribute to their biological activities.⁴³ For example, well-known pharmaceuticals such as L-DOPA⁴⁴, nelfinavir,⁴⁵ and enterobactin⁴⁶ hold multi-substituted phenols(Figure 3-1).

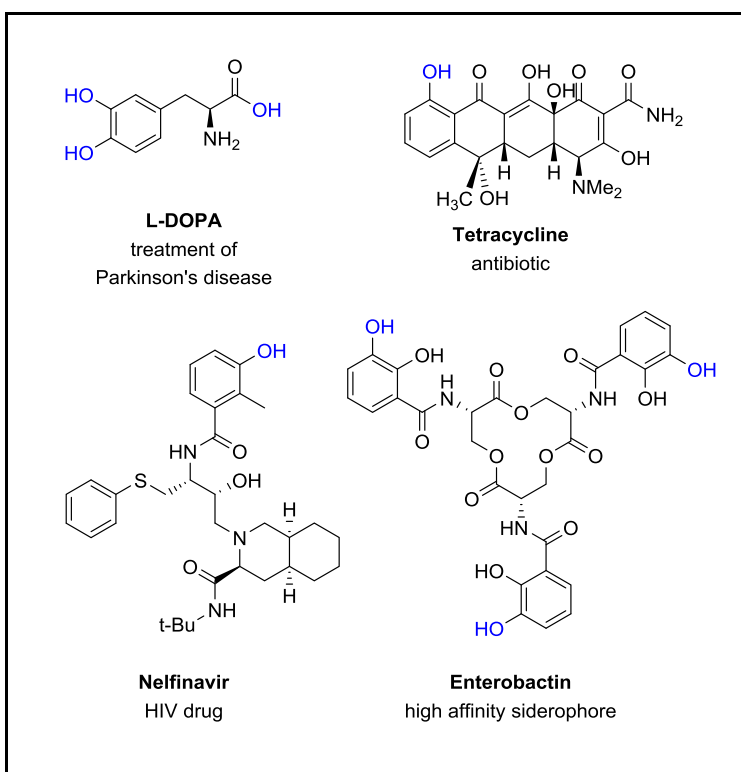


Figure 3-1 Examples of bioactive phenolic compounds

In light of this fact, there is a fundamental need for development of more efficient catalytic strategies that provide site-selective access to this motif from readily available precursors. Thus far, several very useful phenol silylation methods have been developed: 1) a sequence of (non-)selective bromination, O-silylation, and lithium-halogen exchange followed by retro-Brook reactions,^{36, 47} 2) metal-catalyzed silylation of prefunctionalized,

protected halophenols,^{38, 48} 3) directed *ortho*-metalation (DoM)/silylation of phenols,^{39, 49} and 4) KO^tBu-catalyzed silylation of aromatic heterocycles.⁵⁰ These methods offer excellent site-selectivity. However, limitations in these systems exist as they generally require a (sub-)stoichiometric amount of basic reagents, thereby displaying modest functional group compatibility, or involve a limited substrate scope and/or moderate yields.

Significant advances to transition metal-catalyzed selective C–H bond functionalizations for preparing structurally diverse, bioactive molecules.^{51, 52, 53, 54, 55, 56, 57, 58, 59, 60, 61, 62, 63, 64, 65, 66} have been made through directing group-assisted^{51, 57, 58, 60, 61, 66, 67} or direct^{54, 56} C–H bond activation strategies. Although directing group-assisted C–H bond functionalization strategies can achieve the desired transformation with high reactivity and selectivity, directing groups are often difficult to install and manipulate after processes are completed. Additional functional group interconversions, typically involving redox adjustment, are usually carried out under harsh reaction conditions, if indeed removal of the directing group is at all possible. To resolve these limitations, strategies for traceless directing group-assisted C–H functionalization have been developed.^{35, 68, 69, 70, 71, 72, 73, 74, 75, 76, 77} For instance, Gevorgyan^{35, 71, 78} and Ge⁷⁴ (Figure 3-2) reported remarkable C–H *ortho*-alkenylation, oxygenation, and carboxylation of phenols with silanol traceless directing groups. However, a traceless directing group approach for *ortho*-C–H silylation has not been reported to date.

Although diverse catalytic arene dehydrogenative silylations have been developed to prepare valuable organosilanes,^{15, 17, 22, 79, 80, 81, 82, 83, 84, 85, 86, 87, 88, 89, 90, 91, 92, 93, 94} surprisingly, only one example of catalytic *ortho*-C–H silylation of phenol derivatives has been developed (Hou group, 2011)⁸⁴ as depicted in Figure 3-3. While this scandium metallocene-catalyzed directed *ortho*-silylation of anisoles exhibited excellent site-selectivity, despite requiring a highly strained, four-membered metallacycle **3-2**, it suffers

from requiring excess anisole substrates (10-fold), limited substrate scope (inaccessible to 1,2,3-trisubstituted arenes, **3-3** to **3-4**), and use of a non-commercially available catalyst. Furthermore, the removal of alkyl masking groups in the presence of silanes is not trivial.

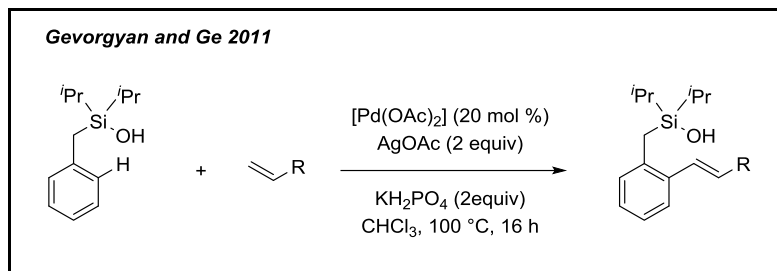


Figure 3-2 Gevorgyan's silanol directing group

Miyaura⁹⁵ and Hartwig⁹⁶ have reported Rh and Ir-catalyzed steric-controlled *meta*- or *para*-silylation of anisoles, respectively (Figure 3-3). While Miyaura's Ir-catalyzed silylation required 60-fold excess of anisole substrates **3-5**, the method developed by Hartwig showed broad substrate scope and high site-selectivity, yet the removal of a hydroxyl masking group in the presence of silanes is again questionable.

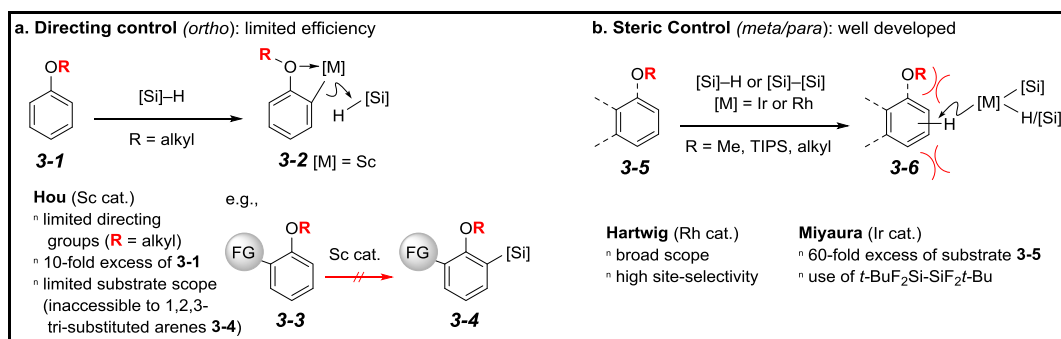


Figure 3-3 Prior approaches for catalyzed C–H silylation of protected phenols

As it was shown in previous chapters, we have developed a catalytic (exhaustive) reductive C_{sp2}–H and C_{sp3}–H silylation and silanolization of aromatic carboxylic acid derivatives.^{97, 98} In the studies, we established the mechanism for the hydridosilyl *O,O*-silyl acetal-directed catalytic C–H silylation, where the turnover-determining step is an irreversible substrate-metal coordination that proceeds to C–H bond cleavage.^{40, 99} To

develop a more general, catalytic method to improve arene *ortho*-C–H silylation of phenols, we have designed a novel approach to sequential catalytic reductive C–H silylation. This process centers on post-installation of other useful moieties on a silicon center that includes spontaneous removal of directing groups by employing versatile silyl acetal directing groups. Hence, we specifically address the aforementioned challenges and limitations in synthesis of diversely functionalized silyl phenols and significantly expand the versatility of C–H functionalization (Figure 3-4).

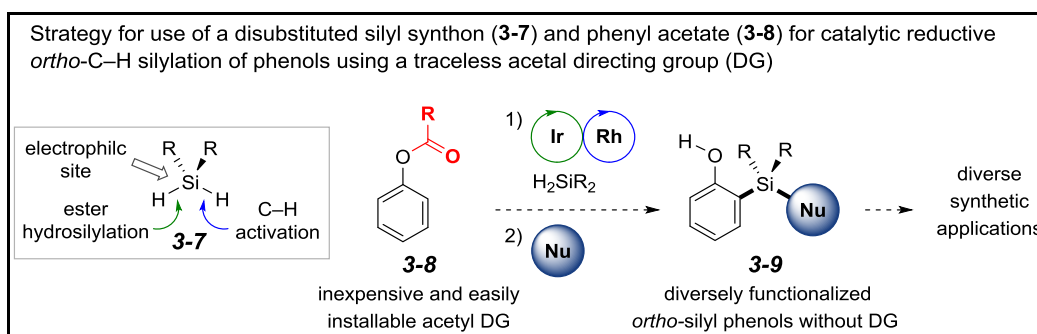


Figure 3-4 *ortho*-C–H silylation of phenols using a traceless acetal directing group

We developed a single-pot sequential metal-catalyzed reductive *ortho*-C–H silylation of phenols, with traceless mixed acetal directing groups, utilizing inexpensive and easily installable acetyl formal directing group and readily available catalyst and silane. This strategy involves the relay of Ir-catalyzed hydrosilylation of phenyl acetates **3-8**^{19, 100, 101, 102, 103, 104} exploiting disubstituted silyl synthons **3-7** to afford silyl acetals **3-10** and Rh-catalyzed C–H silylation^{22, 80, 81, 90, 93, 94} to provide dioxasilines **3-12**. A subsequent nucleophilic addition to silicon removes the acetal directing groups and provides unmasked phenol products **3-9** in a single vessel. (Figure 3-5)

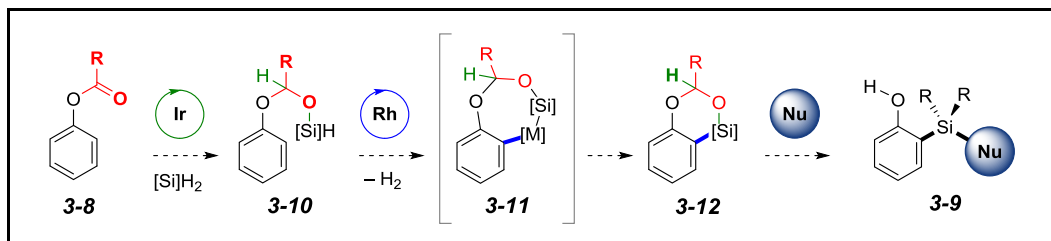


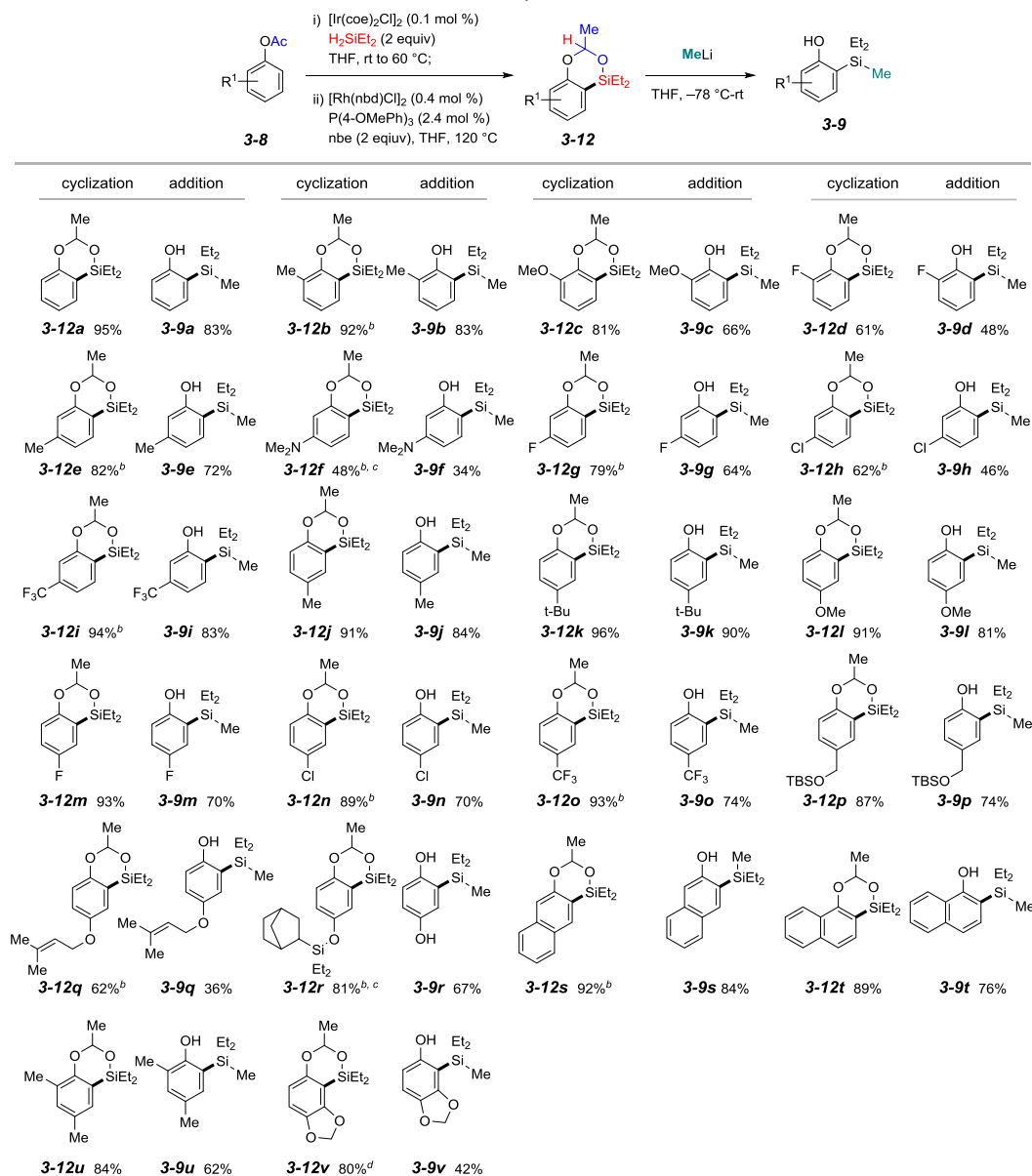
Figure 3-5 Proposed strategy of acetal directing group

Importantly, the resulting *ortho*-silyl phenols **3-9** are useful synthetic vehicles for direct applications to many other important transformations, examples of which include: harnessing aryne chemistry;^{105, 106, 107, 108, 109, 110} Au-catalyzed oxidative cross-coupling;^{111, 112} synthesis of dibenzosiloles;^{113, 114} and catalytic synthesis of a chiral BINOL^{115, 116} scaffold.

3.2. A Single-Pot Catalytic Reductive *ortho*-C–H Silylation of Phenols with Traceless Mixed *O,O*-Acetal Directing group.

Prevalent directed C–H bond functionalizations proceed through five- or six-membered cyclometallated intermediates.³¹ However, our initial concern was that our proposed process conceivably requires a rather unfavorable rhodacycloheptane intermediate **3-11** (Figure 3-5). To address this concern, we demonstrated the strategy for traceless, formal acetate directing group-assisted *ortho*-silylation of phenols (Table 1). Gratifyingly, the single-pot, two-step strategy involving Ir-catalyzed ester hydrosilylation (0.1 mol % of [Ir(coe)Cl]₂) and Rh-catalyzed C–H bond silylation using [Rh(nbd)Cl]₂ (0.4 mol %) and monodentate phosphine P(4-MeOPh)₃²² (2.4 mol %) directly produced benzodioxasilane **3-12a** in excellent yield (95%). A distinctive feature of this mixed *O,O*-acetal directed Rh-catalyzed C–H silylation was essentially complete reaction within 15 min, despite the fact that a putative cyclometallated rhodacycloheptane intermediate might be involved.

Table 3-1 Substrate scope of benzodioxalilenes



^aConditions: phenol acetates **3-8** (1 mmol), $[\text{Ir}(\text{coe})_2\text{Cl}]_2$ (0.1 mol %), THF (3.3 M); $[\text{Rh}(\text{nbd})\text{Cl}]_2$ (0.4 mol %), $\text{P}(4\text{-OMePh})_3$ (2.4 mol %), norbornene (2 equiv), THF (1M), 120 °C, 15 min; MeLi (3 equiv), THF (0.5 M), -78 °C.

^bDetermined by ^1H NMR spectroscopy utilizing an internal standard (CH_2Br_2). ^c $[\text{Ir}(\text{coe})_2\text{Cl}]_2$ (0.5 mol %), H_2SiEt_2 (4 equiv); $[\text{Rh}(\text{nbd})\text{Cl}]_2$ (1 mol %), $\text{P}(4\text{-OMePh})_3$ (6 mol %), 120 °C, 60 min; MeLi (6 equiv). ^d3:1 regioisomeric ratio of **3-12v**.

We then investigated the scope of the single-pot sequential catalytic reductive *ortho*-C–H silylation of phenyl acetates (Table 3-1). Phenyl acetates bearing a substituent at the *ortho* position (i.e., methyl, methoxy, fluoro) underwent the C–H silylation to provide benzodioxasilines (**3-12b** to **3-12d**) in good yields. The reaction of phenyl acetates possessing a *meta* substituent (**3-12e** to **3-12i**) exhibited high site selectivity favoring silylation at less congested C–H bonds (>20:1 regioselectivity). *para*-Substituted phenyl acetates holding methyl, *t*-butyl, methoxy, halogens (F and Cl), trifluoromethyl, silyl blocking group (TBS), and trisubstituted alkene groups were tolerated by the reaction conditions to afford benzodioxasilines (**3-12j** to **3-12q**). Interestingly, 4-hydroxyphenyl acetate initially afforded C–H silylation product **3-12r**, wherein unprotected hydroxy group efficiently underwent dehydrogenative silylation with excess diethylsilane, followed by hydrosilylation with norbornene (hydrogen acceptor). Reductive C–H silylation of both 1- and 2-naphthyl acetates provided single regioisomers (**3-12s** and **3-12t**, respectively) with excellent yields. Disubstituted 2,4-dimethylphenyl acetate also generated product **3-12u** via selective activation of C(sp²)–H bond over C(sp³)–H bond, with good yield (84%). C–H silylation of sesamol acetate afforded the major product **3-12v** (4-Si:6-Si = 3:1) at the more sterically hindered position. The subsequent nucleophilic ring-opening reactions of the resulting **3-12** with MeLi in the same vessel afforded *ortho*-silyl phenols, which allow concomitant removal of acetal directing group, thereby revealing hydroxy groups. These results clearly establish that the sequence of Ir and Rh-catalyzed reactions, followed by the ring-opening process, provides a viable catalytic synthesis of *ortho*-silyl phenols.

3.3. Synthesis of Multi-Substituted Arenes

. Catalytic transformation of diacetates or *N*-acetyl acetates into multi-substituted arenes, were examined with this C–H bond silylation strategy using traceless mixed *O,O*-

and *N,O*-acetal directing groups (Figure 3-6). Dual catalytic reductive C–H silylation of 1,4-phenylene diacetate **3-8x**, followed by the double-fold ring-opening with MeLi furnished tetra-substituted arene (**3-9x**) in excellent yield (88%). Furthermore, highly chemoselective reductive C–H silylation/ring-opening of 4-acetoxyphenyl pivalate **3-8y** to afford tri-substituted arene (**3-9y**) in 72% yield was observed, as achieved by selective hydrosilylation of acetate over pivalate (2 equiv of H₂SiEt₂ at rt). However, under dual hydrosilylation conditions (4 equiv of H₂SiEt₂ at 60 °C) dual C–H silylation of **3-8y** provided tetra-substituted arene (**3-12z**) (83% yield), which underwent ring-opening reaction with MeLi to give **3-9z**. *N*-Acetyl-4-indolyl acetate **3-8aa** also tolerated the reaction conditions to provide dual C–H silylation product **3-12aa**, via formation of the intermediate containing mixed *O,O*- and *N,O*-silyl acetals (not shown). Upon treatment with MeLi, **3-9aa** was generated in 38% yield over three steps. Several conditions were employed in attempts to remove the hemiaminal group; however protodesilylation (at C-5) was observed under most reaction conditions studied. Notably, when *para*-acetamide substituted phenyl acetate (i.e., *O*-acetyl acetaminophen) was subjected to the hydrosilylation conditions mixed *O,O*-silyl acetal, with concomitant reduction of amide to secondary silyl amine, initially formed which subsequently underwent C–H silylation to provide **3-12ab**, after pivalation of the amine. Subsequent treatment with MeLi afforded trisubstituted arene **3-9ab**.

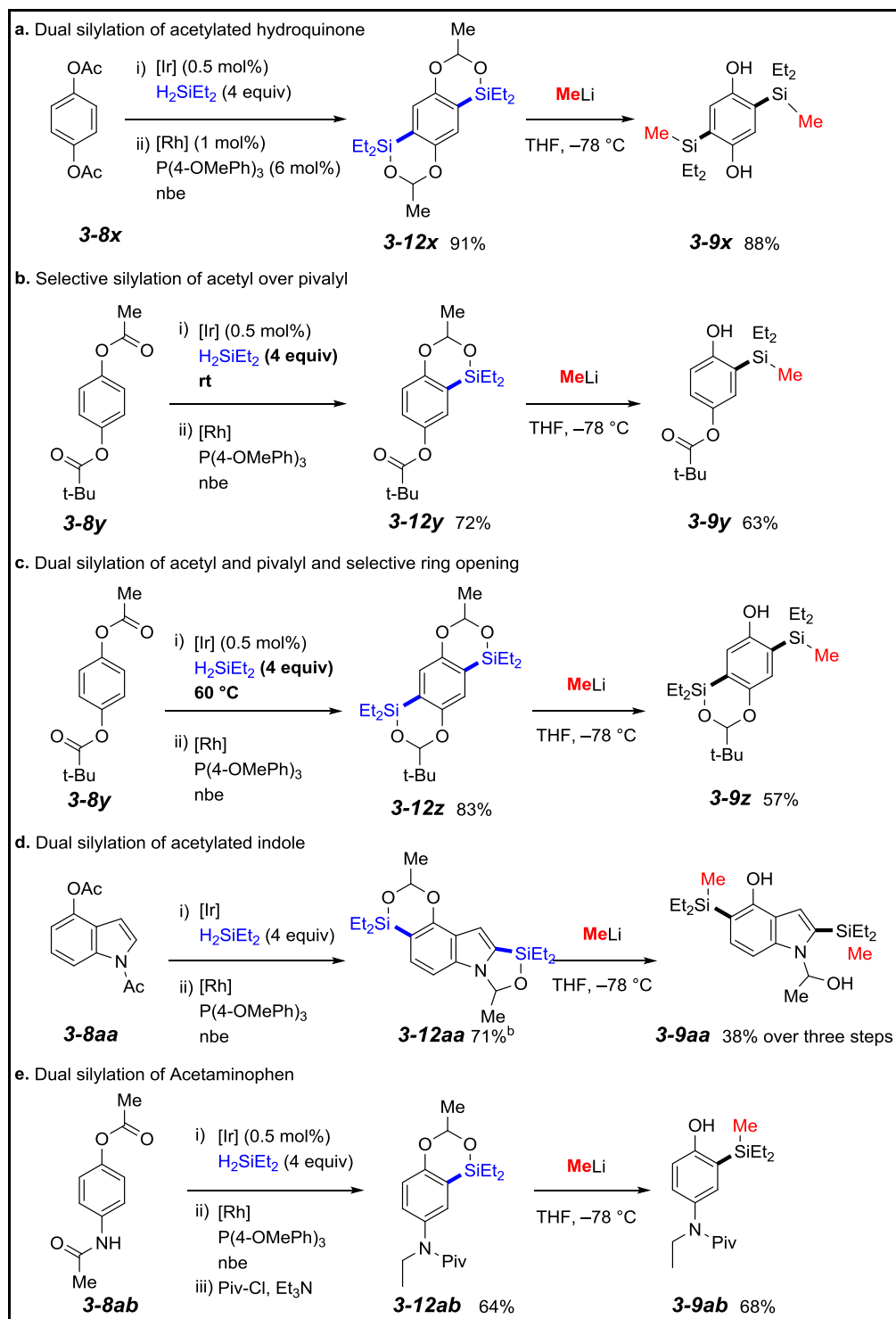


Figure 3-6 Synthesis of multi-substituted arenes

3.4. Dioxasilines as Halosilane Equivalents for Synthesis of Functionalized Silanes.

Organosilanes and organosilanols have been utilized for their unique biological functions and biomedically relevant agents.^{5, 29, 117, 118} For instance, biarylspirosilanes, synthetic mimics of (bipy)₂Cu(I) complexes, have been utilized for probing catalytic antibodies' biological functions.¹¹⁹ Although advances have been achieved, syntheses of diverse silanes by catalytic means remain significantly limited. For example, Brookhart reported only two synthetically useful silanes (Et₂SiH₂ and PhMeSiH₂) for Ir-catalyzed ester hydrosilylation.¹⁹ Furthermore, a stoichiometric method for synthesis of functionalized phenolic silanes **3-15**, involving (non-)selective bromination/retro-Brook reactions, requires substantial effort (i.e., preparation of chloroarylsilanes **3-14** bearing various aryl moieties) and the overall yield is unknown (Figure 3-7.a).⁴⁷ Alternatively, directed *ortho*-metalation (DoM)/silylation of phenols^{39, 49} also has limitations imposed by generation of chromatographically unstable chlorosilanes **3-17** and a difficult directing group removal step, associated with facile protodesilylation (Figure 3-7.b). To improve this limited silane scope, and thereby prepare diversely functionalized silanes, we investigated sequential catalytic C–H silylation, coupled with nucleophilic ring-opening reactions of “dioxasilines as stable halosilane equivalents” that readily incorporate a variety of motifs (Figure 3-7.c). Advantages of this method would be two-fold; first, it provides a post-introduction of silyl substituents containing useful functional groups, which may be not compatible with an Ir/Rh-catalytic cascade; second, it eliminates the need to prepare a variety of the not readily available dihydrosilanes for hydrosilylation. Therefore, we explored an array of nucleophiles; hydride (lithium aluminum hydride) (to **3-9ac**), carbon nucleophiles MeLi (or MeMgBr) (to **3-9a**), *n*-BuLi (to **3-9ad**), PhLi (or PhMgBr) (to **3-9ae**), vinyl magnesium

chloride (to **3-9af**), allyl magnesium chloride (to **3-9ag**), lithium trimethylsilyl acetylide (to **3-9ah**), heteroaryl

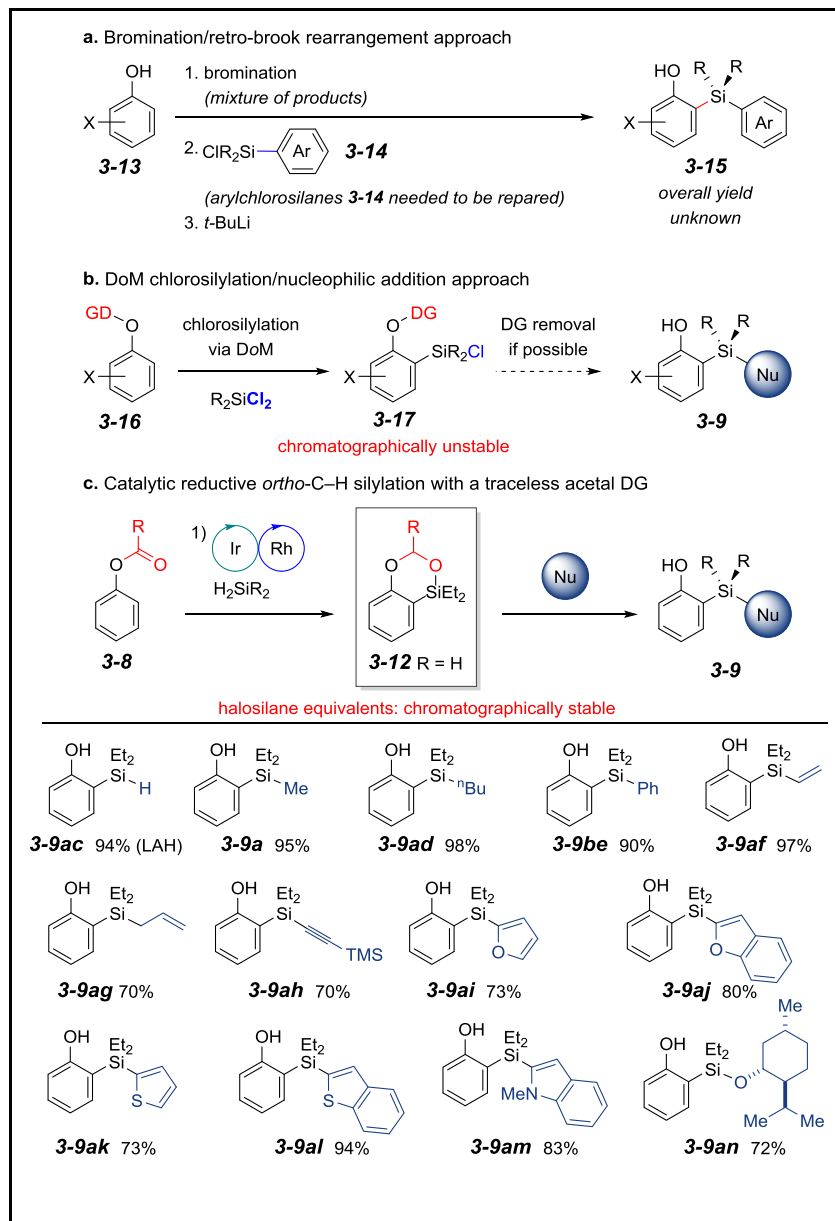


Figure 3-7 Dioxasilines as halosilane equivalents

lithium reagents (to 2-silyl furan **3-9ai**, 2-silyl benzofuran **3-9aj**, 2-thiofuran **3-9ak**, 2-silyl benzothiofuran **3-9al**, and 2-silyl indole **3-9am**, and oxygen nucleophiles (lithium

mentholate) (to **3-9an**). All these nucleophiles afforded excellent to good yields of corresponding silyl phenols.

3.5. Synthesis of Multi-Substituted Arenes.

Based on the wide substrate scope presented in Table 3-1, we investigated the potential of catalytic reductive *ortho*-C–H silylation of phenols directed by silyl acetal. However, we encountered a problem during our investigation of the substrate scope of *ortho*-C–H silylation of sterically hindered phenols.

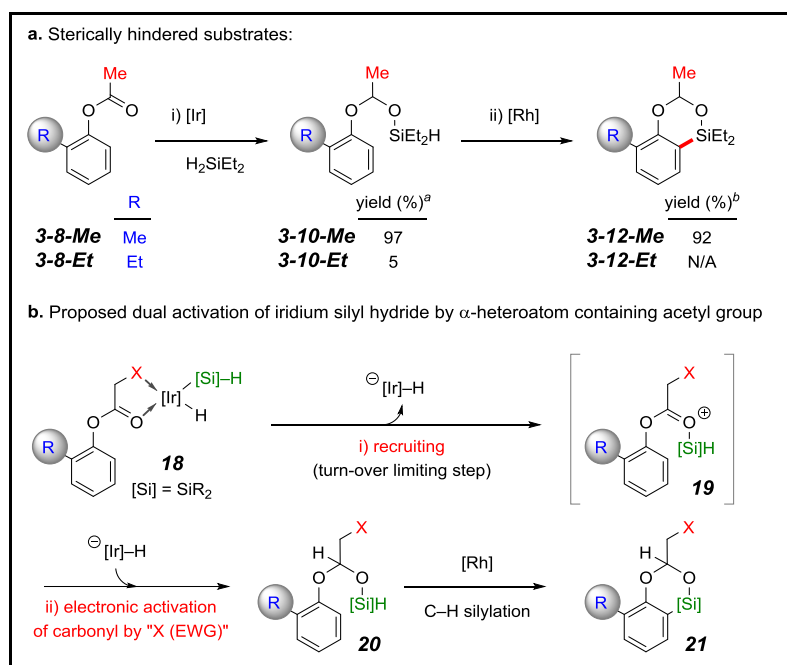


Figure 3-8 Challenges involving sterically hindered substrates

Surprisingly, minor steric variation on a substrate, such as **3-8-Et** (cf., **3-8-Me**), drastically hindered the hydrosilylation (Figure 3-8 and Figure 3-9). The Hou group also observed similar reactivity, in fact even more sensitive to the sterics, with Sc-catalyzed arene *ortho*-silylation, where even *ortho*-methyl anisole did not react (see **3-3** to **3-4** in Figure 3-3).⁸⁴ Of note, efficient catalytic synthesis of 1,2,3-trisubstituted arenes are not trivial

owing to the necessity of high reactivity over steric hindrance and high regioselectivity. Although A-values of methyl and ethyl are fairly similar (1.7 vs. 1.75 kcal/mol, respectively),^{120, 121} it is speculated that the population of reactive conformers by rotation perhaps dictates this unusual reactivity difference.

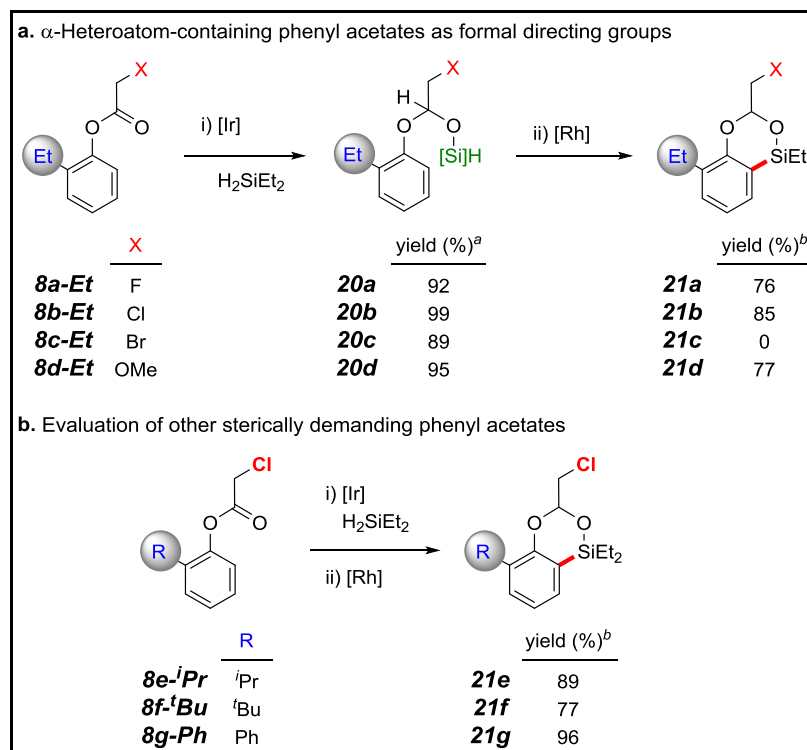


Figure 3-9 Discovery of α -chloroester directing group

To overcome this obstacle, we explored a development of other efficient traceless directing groups (Figure 3-8.b). Brookhart proposed that the turnover-limiting step of Ir-catalyzed hydrosilylation would be transfer of silylium ions (R_2HSi^+) to the carbonyl oxygen of esters.^{19, 77, 122} We speculated that effective recruiting of iridium silyl hydride species to esters could be a crucial factor for hindered esters (**3-18** to **3-19** Figure 3-8). In addition, the electron withdrawing X atom (group) could facilitate Ir-mediated hydride transfer to carbonyl (**3-19** to **3-20**). Therefore, to transfer the silylium ions to carbonyl and succeeding iridium hydride more easily, we designed and examined an α -heteroatom-containing acetyl

formal directing group as a bidentate chelating moiety (e.g., an α -fluoro, chloro, bromo, methoxy acetyl) to metal (Figure 3-9.a). We found that α -chloroacetate was among the most effective formal directing groups. This method was expanded to more sterically demanding *ortho*-substituted substrates. Remarkably, the phenyl α -chloroacetate smoothly underwent sequential hydrosilylation/C–H silylation of substrates bearing *ortho*-isopropyl, *tert*-butyl, and phenyl moieties (Figure 3-9.b). These are surprising results because only a few successful chelation-controlled nucleophilic addition to α -halo carbonyl or imino electrophiles have been reported, owing to the relatively low basicity of halogens and all these prior examples utilized α -fluoro carbonyl derivatives.^{123, 124, 125} Although the Walsh group demonstrated diastereoselective chelation-controlled addition of carbon nucleophiles to α -chloro aldimines, transition metal-catalyzed chelation-controlled hydrosilylation of α -chloroesters has not previously been described.¹²⁶

3.6. Synthetic Applications of Benzodioxasilines.

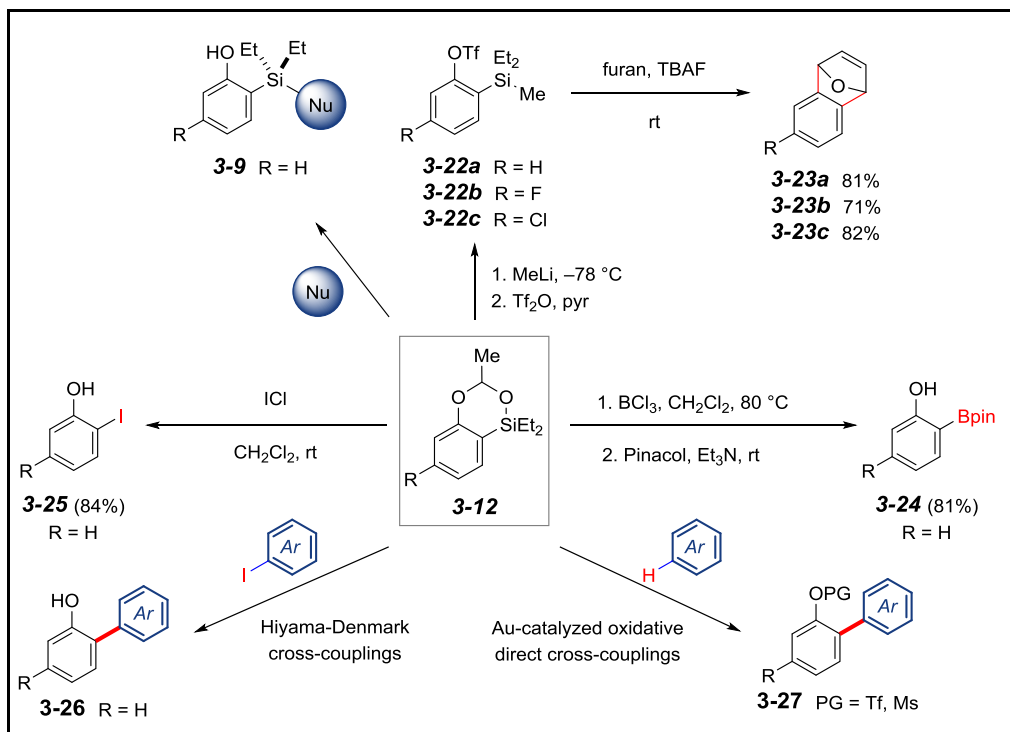


Figure 3-10 Synthetic applications of benzodioxasilines

A major aspect of this work is to introduce a novel strategy to catalytic *ortho*-C–H silylation via sequential C–H silylation post-installation of other useful moieties on a silicon center. This approach permits spontaneous removal of a directing group and simultaneously addresses the challenges of synthesis of diversely functionalized unmasked *ortho*-silyl phenols **3-9** (Figure 3-7). We further explored the powerful synthetic utilities of catalytically generated *ortho*-silyl phenols to other important transformations (Figure 3-10).

3.6.a. Aryne Cycloaddition of *ortho*-Silyl triflates and Halo and Boro ipso-desilylations.

1,2-Silyl triflates are versatile motifs for a variety of areas in organic synthesis. Our catalytic *ortho*-silylation method permits access to 1,2-diethylmethylsilyl triflates **3-22**

containing a variety of substituents in an extremely straightforward fashion. Some of such substrates were previously difficult to prepare owing to functional group incompatibility or electronic bias. We demonstrated aryne–furan cycloaddition which produced **3-23a-c** in good yields (Figure 3-10).^{105, 106, 107, 108, 109, 110} In the next chapter we will explore more details about the arylsilyl triflates. In addition, benzodioxasilane **3-12** could easily undergo iodo and boro-induced *ipso*-desilylations to generate **3-24** and **3-25** in good yields, respectively (Figure 3-10).

3.6.b. Pd-Catalyzed Hiyama-Denmark Cross-Coupling.

Table 3-2 Optimazation of Hiyama-Denmark coupling reaction

entry	PdL _n	ligand	yield of 3-26a (%) ^c
1	Pd(OAc) ₂	PCy ₃	20
2	Pd(OAc) ₂	P(<i>t</i> -Bu) ₃	50
3	Pd(OAc) ₂	RuPhos	5
4	Pd(OAc) ₂	XPhos	5
5	Pd(OAc) ₂	SPhos	11
6	Pd(OAc) ₂	P(4-MeOPh) ₃	6
7	Pd(OAc) ₂	dcpe	3
8	Pd(OAc) ₂	dppe	12
9	Pd(OAc) ₂	dppp	9
10	Pd(OAc) ₂	dppb	10
11	Pd(OAc) ₂	dppf	12
12	Pd(OAc) ₂	XantPhos	21
13	Pd ₂ (dba) ₃	P(<i>t</i> -Bu) ₃	5
14	Pd(PPh ₃) ₂ Cl ₂	P(<i>t</i> -Bu) ₃	15
15	[allylPdCl] ₂	P(<i>t</i> -Bu) ₃	11
16	PdCl ₂	P(<i>t</i> -Bu) ₃	5
17	Pd(CF ₃ CO ₂) ₂	P(<i>t</i> -Bu) ₃	23

^aConditions: silane **3-12a** (0.1 mmol), solvent (0.2 M). ^bDetermined by GC/MS analysis. ^cDetermined by ¹H NMR spectroscopy utilizing an internal standard (CH₂Br₂). RuPhos = 2-dicyclohexylphosphino-2',6'-diisopropoxybiphenyl, XPhos = 2-dicyclohexylphosphino-2',4',6'-triisopropylbiphenyl, SPhos = 2-dicyclohexylphosphino-2',6'-dimethoxybiphenyl, dcpe = 1,2-bis(dicyclohexylphosphino)ethane, dppe = 1,2-bis(diphenylphosphino)ethane, dppp = 1,3-bis(diphenylphosphino)propane, dppb = 1,4-bis(diphenylphosphino)butane, dppf = 1,1'-bis(diphenylphosphino)ferrocene, Xantphos = 4,5-bis(diphenylphosphino)-9,9-dimethylxanthene.

The biaryl scaffold is prevalent in biologically active molecules and is an ubiquitous functional motif in medicines.¹²⁷ The Hiyama-Denmark cross-coupling, using non-toxic aryl

silanes, is among the most versatile catalytic method for biaryl synthesis.^{6, 7, 31} Nonetheless, this strategy suffers from the requirements for aryl halide sources in the C–C bond-forming reaction and basic conditions for activating silanes. When attempting Pd-catalyzed Hiyama-Denmark cross-coupling of benzodisiloxane **3-12a**, we observed product **3-26a** in low to moderate yields (3-50%), along with significant desilylation byproduct **3-28a** (Table 2). Based upon our literature survey the efficiency of silicon-based cross-coupling of sterically encumbered *ortho*-substituted silanes (or siloxanes) with corresponding haloarene cross-coupling partners has been generally poor.^{128, 129, 130}

3.6.c. Au-Catalyzed Oxidative Direct Arylation of Aryl Silanes.

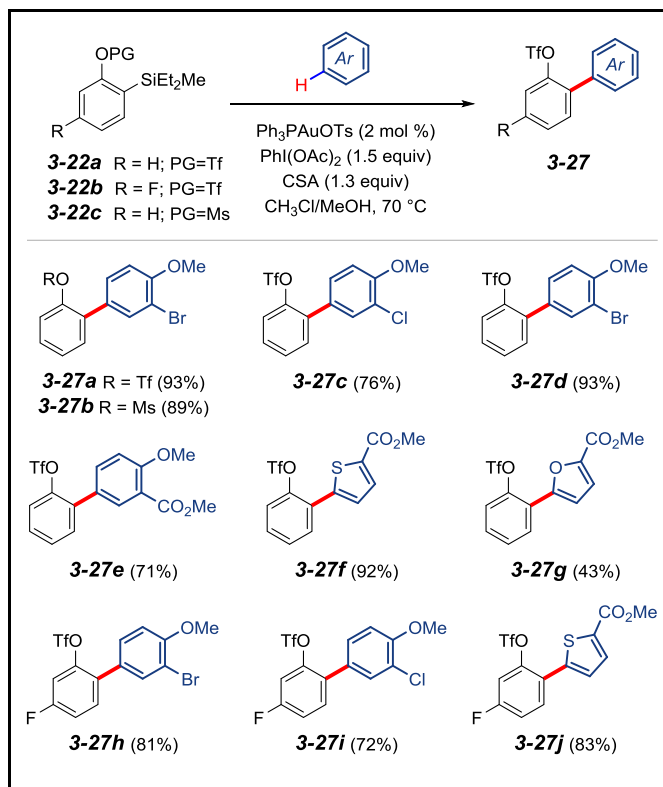


Figure 3-11 Au-catalyzed oxidative direct arylation

A direct alternative to the Hiyama-Denmark cross-coupling would be the oxidative direct cross-coupling of aryl silanes, with simple arenes as a partner,^{53, 56, 60, 131, 132, 133, 134,}

135, 136, 137, 138 as recently reported by Lloyd-Jones and Russel.^{111, 112} This strategy is, however, underexploited in 2-silyl triflates derived from dioxasilines as oxidative direct coupling partners (Figure 3-11). Our developed reductive C–H silylation strategy would enable the rapid preparation of such triflate-containing partners for the silane-based oxidative direct coupling. Gratifyingly, gold(I)-catalyzed oxidative cross-coupling of 1,2-silyl triflates **3-22** with non-prefunctionalized arenes afforded biaryls **3-27** in moderate to excellent yields (Figure 3-11). With brief optimization, the Au-catalyzed silane-based oxidative cross-coupling directly provided biaryls **3-27a** to **3-27j**, holding useful functional groups and moieties (e.g., triflate, mesylate, ester, bromide, chloride, fluoride, furan, and thiophene). These functional groups are useful for subsequent downstream reactions such as other metal-catalyzed cross-couplings.

3.6.d. Orthogonal Cross-Coupling.

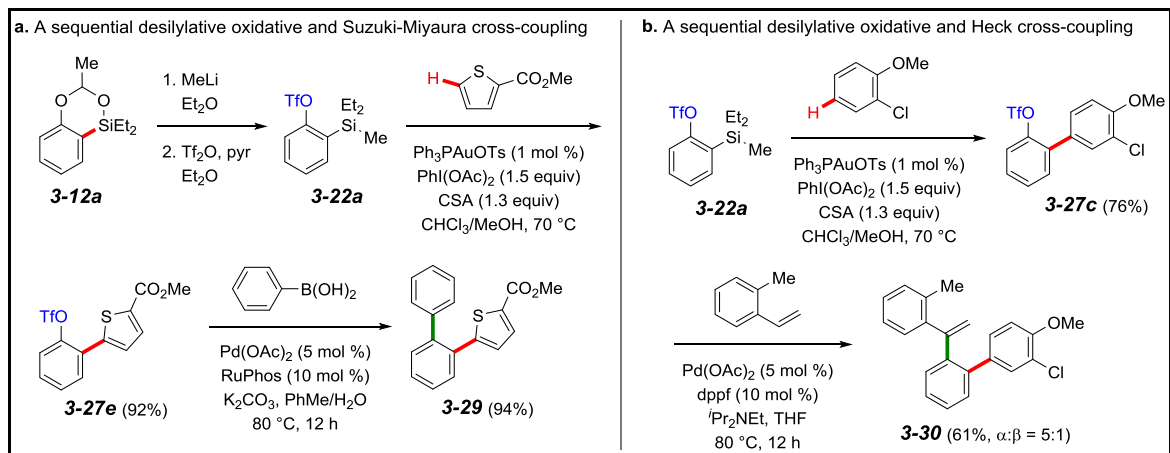


Figure 3-12 Orthogonal Cross-Coupling

The Au-catalyzed oxidative cross-coupling of biaryls **3-27a**, **3-27c** to **3-27j**, bearing triflate groups, can be used for subsequent cross-coupling reactions. Examples include Suzuki cross-coupling of **3-27e** with phenyl boronic acid to generate 1,2-diaryl benzene **3-29** (94%) (Figure 3-12a) and Heck reaction of **3-27c** with 2-methylstyrene to furnish 1,1-disubstituted alkene **3-30** (61%) (Figure 3-12b).

3.6.e. Late-Stage Functionalization of Phenol-Containing Bioactive Molecules Estrone and Estradiol.

We explored the synthetic utility of the catalytic reductive acetal directing group-assisted *ortho*-C–H silylation of phenols in known bioactive molecules (Figure 3-13 and Figure 3-14). We again exhibited that α -chloroacetyl-derived silyl acetal was crucial to afford ester hydrosilylation/C–H bond silylation (only C2 position) of estrone to provide **3-32b** (88% yield) (cf., the parent acetyl directing group only afforded **3-32a** in 30% yield), presumably due to remote steric influence (Figure 3-13).

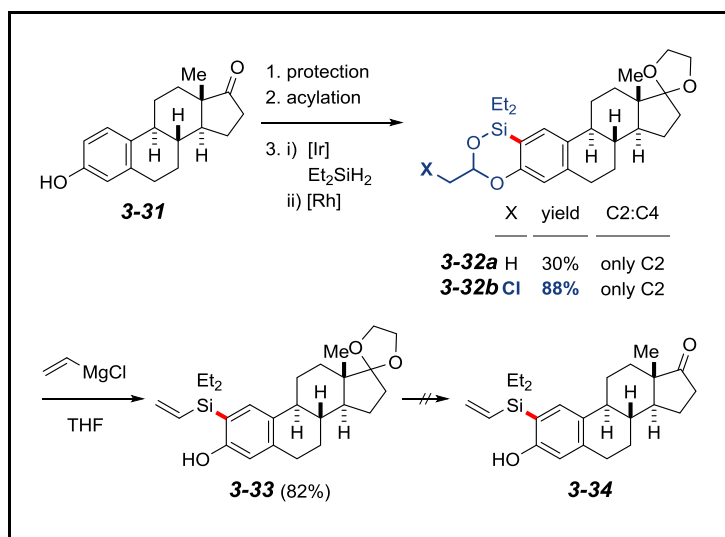


Figure 3-13 C2-Silylation of estrone

Ring-opening of **3-32b** by vinyl lithium furnished **3-33** (80% yield).^{35, 78, 139} Unfortunately, we were unable to remove the ketal protecting group within **3-33** under a variety of reaction conditions, due to concomitant protodesilylation of C2-silane.¹³⁹

We then studied a more direct method involving late-stage functionalization of estradiol **3-35** (Figure 3-14). A four-step sequence, involving bis-chloroacetylation, reductive C–H silylation, and vinyl addition, directly permits C2-silyl estradiol **3-37** (via **3-36**) without protecting group manipulation.

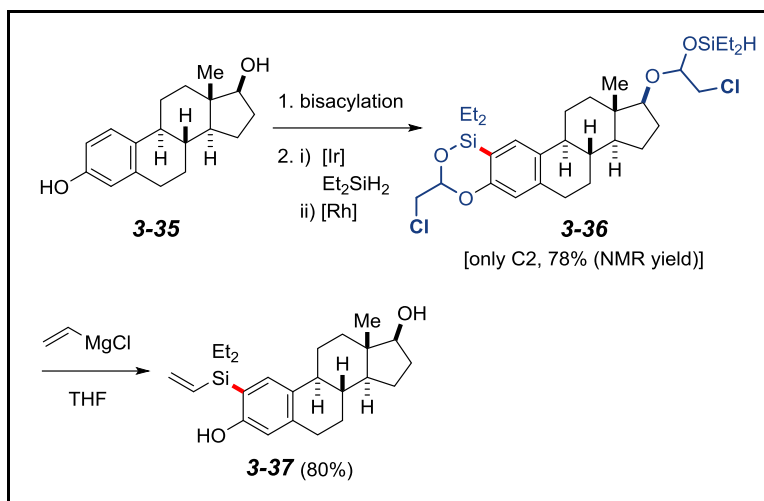


Figure 3-14 C2-Silylation of estradiol

3.6.f. Catalytic Synthesis of 3,3'-Bissilyl BINOL Using a Traceless Acetal Directing Group.

Lastly, we examined whether this catalytic silylation method is applicable to preparation of a 3,3'-bis-silylation of binaphthol (BINOL), which has been extensively utilized for asymmetric catalysis. 3,3'-Bis-silyl BINOL **3-40** was synthesized from *rac*-BINOL, in high yield, in a four steps operation—of note, only one enantiomer of the BINOL racemic mixture is presented in Figure 3-15.

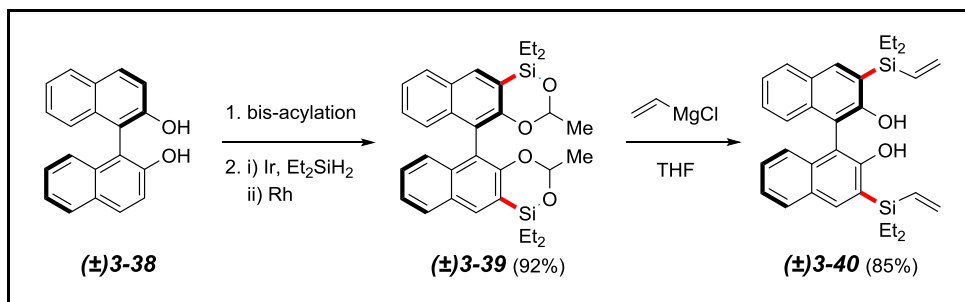


Figure 3-15 3,3' Silylation of BINOL

Overall, our development of a strategy for late-stage modification enables synthesis of structurally unique bioactive molecules and chiral scaffolds in a rapid and

highly site-selective manner and obviates a stepwise, multi-step synthesis, which would be difficult through the existing catalytic *ortho*-C–H silylation.⁸⁴

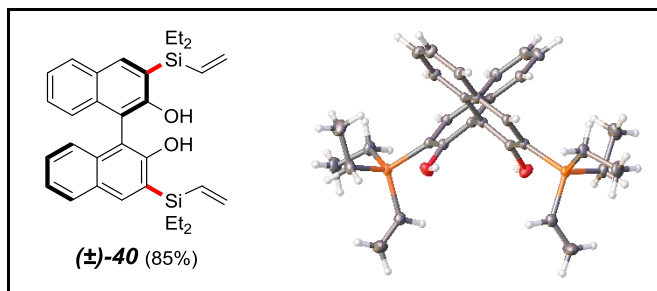


Figure 3-16 X-ray of 3,3' Silylated BINOL

3.7. Summary of chapter 3

A new strategy, employing disubstituted silyl synthons and phenyl acetates, for a single-pot sequential metal-mediated, catalytic reductive C–H silylation of phenols with traceless acetal directing groups, has been successfully achieved. The relay of Ir-catalyzed hydrosilylation of phenyl acetates and Rh-catalyzed C–H silylation provides dioxasilines. A subsequent nucleophilic addition of diverse nucleophiles to dioxasilines serving halosilane equivalents not only readily incorporates a variety of functional moieties, but also concomitantly removes the acetal directing groups in a single vessel. This approach eliminates the need to prepare a variety of not readily accessible dihydrosilanes. To resolve synthetic challenges of 1,2,3-trisubstituted, hindered arenes, we developed a new α -chloroacetyl formal directing group which allows catalytic reductive *ortho*-C–H silylation of sterically hindered phenols. We also demonstrated several important downstream reactions of the resulting 1,2-silyl phenols, including Au-catalyzed oxidative direct cross-coupling, aryne cycloaddition chemistry, and late-stage silylation of phenolic bioactive molecules and BINOL scaffold, exploiting the traceless acetal directing group strategy to afford C2-silyl estrone, C2-silyl estradiol, and 3,3'-bissilyl BINOL

Chapter 4

Aryne cycloaddition reactions of benzodioxasilines as aryne precursor generated by catalytic reductive *ortho*-C–H silylation of phenols with traceless acetal directing groups

Parham Asgari, Udaya Dakarapu, Hiep Nguyen and Junha Jeon

This work has been published in *Tetrahedron* **2017**, 73, 4052-4061.

4.1. Introduction

Ever since the discovery of benzyne in mid 50s¹⁴⁰, these highly reactive intermediates were employed in wide variety of important applications such as synthesis of bioactive molecules,^{109, 141} organic materials,^{142, 143} and catalysts.¹⁴⁴ Additionally, benzyne enable formation of diverse heterocyclic frameworks, which are difficult to obtain by conventional methods, via reactions with various arynophiles.^{145, 146, 147, 148, 149, 150, 151, 152, 153, 154, 155, 156, 157, 158, 159} Among several methods have been developed for efficient generation of arynes,^{106, 107, 108, 110, 160, 161, 162, 163, 164, 165, 166, 167, 168, 169, 170} the reaction of silylaryl triflates with fluoride is one of the most widely used approach.^{171, 172} These stable benzyne precursors, which can undergo aryne cycloadditions under mild conditions, have led to a resurgence in aryne chemistry. Generally, these highly useful 1,2-silylaryl triflates have been prepared through one of the following three methods: 1) a sequence of directed *ortho* metalation (DoM), silylation and triflation, 2) catalytic cross-coupling of *ortho*-haloarenes¹⁷³ and triflation, and 3) *ortho*-halo-phenols via retro-Brook rearrangement followed by triflation (Figure 4-1).

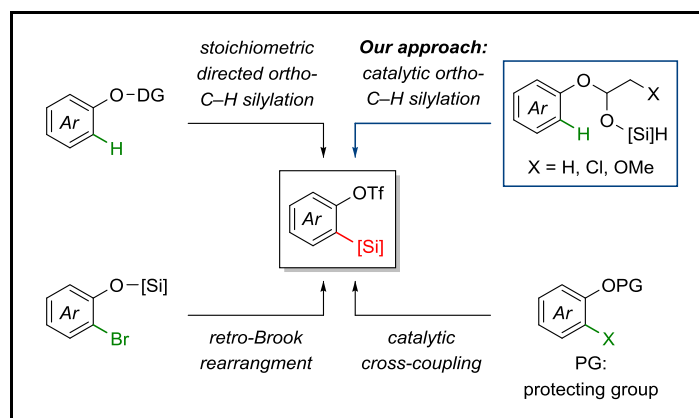


Figure 4-1 Precedents of 1,2-silylaryl triflates synthesis

However, each of these methods suffer from the challenges and/or limitations: commercial availability of starting materials, challenging post-directing group manipulation

due to potential protodesilylation, the need for either pre-functionalization of arene substrates or stoichiometric basic reagents, and limited functional group compatibility.^{174, 175, 176} Furthermore, preparation of regioselectively installed silyl and triflates moieties within multi-substituted arenes for regioselective aryne cycloaddition is often difficult to access by these methods.

As it was described in chapter 3 benzodioxasilines can be obtained from readily accessible phenyl acetates (derived from simple phenols), via catalytic reductive C–H *ortho*-silylation with traceless acetal directing groups (Figure 4-2a).^{17, 19, 98, 177}

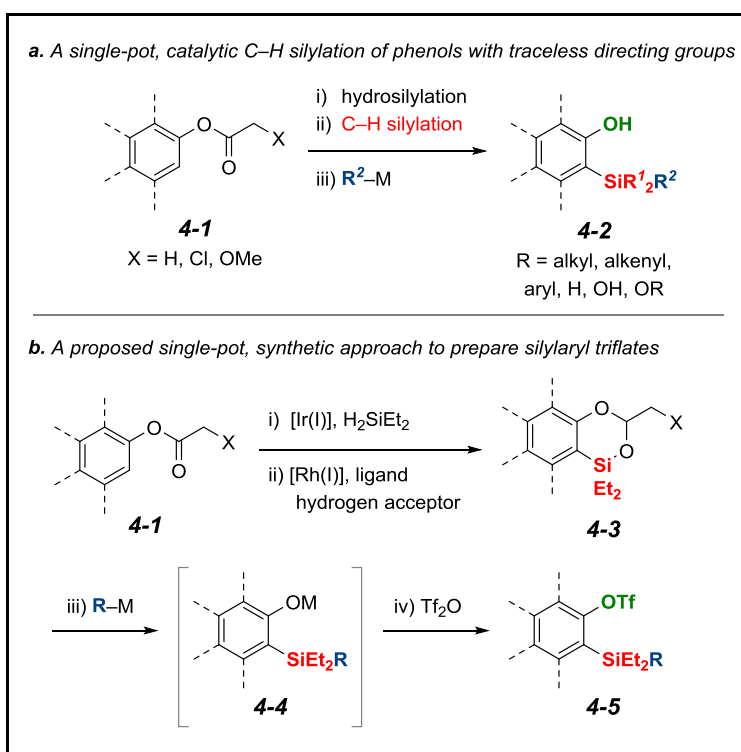


Figure 4-2 Single pot synthesis of silylaryl triflates

Specifically, a relay of iridium and rhodium catalysts involving hydrosilylation of esters with dihydrosilanes and arene *ortho*-C–H silylation, respectively, which were followed by a subsequent facile nucleophile addition to electrophilic silicon to remove the acetal directing groups, directly provides unmasked *ortho*-silyl phenol products in a single

vessel. This strategy was successfully applied to preparation of multi-substituted arenes through exploiting a new, formal α -chloroacetyl directing group. In particular, this new directing group tactic permits access to sterically hindered *ortho*-silyl phenols. Synthesis of 1,2,3-trisubstituted phenolic arenes was established, compounds which are difficult to obtain by other catalytic means. Following this study, we speculated that diversely substituted benzodioxasilines **4-3** could be excellent precursors for preparation of silylaryl triflates. For example, addition of organometallic agents to silicon and the subsequent trapping of the resulting *ortho*-silyl oxyanion intermediates **4-4** by trifluoromethanesulfonic anhydride can directly afford diversely substituted silylaryl triflates (Figure 4-2b).

Benzodioxasilines were efficiently prepared through Ir-catalyzed hydrosilylation of phenyl acetates followed by Rh-catalyzed C–H silylation in a single pot. We then examined the efficiency of nucleophilic ring-opening reaction of benzodioxasilines **4-3** with simple, readily available organometallic reagents (e.g., organolithium reagents), followed by direct triflation with trifluoromethanesulfonic anhydride. The single-pot, sequential reactions with benzodioxasiline **4-3a**, which was generated from phenyl acetate **4-1a** via catalytic reductive *ortho*-C–H silylation and used without purification, produced desired silylaryl triflates **4-5a** in excellent yield (91% from **4-1a**) (Table 4-1). We then explored the scope of the single-pot sequential reactions involving ring-opening of benzodioxasilines **4-3** by MeLi and triflation (Table 4-1). Electronically differentiated, diverse substituted benzodioxasilines provided silylaryl triflates **4-5** in moderate to excellent yields (four steps from **4-1**) under the reaction conditions. Specifically, halogens, trifluoromethyl, primary TBS protecting group, *ortho*-methyl, methoxy within benzodioxasilines **4-3** were tolerated by the four-step reaction conditions to furnish silylaryl triflates (**4-5b** to **4-5i**). 1- and 2-naphthyl silyl triflates (**4-5j** and **4-5k**) were produced from **4-1j** and **4-1k** in modest yields via the reaction sequence. Disubstituted benzodioxasilines **4-3l** and **4-3m** afforded **4-5l**

and **4-5m** in 53% and 72% yields, respectively. Finally, dual functionalization produced bis-silylaryl triflate **4-5n** in 74% yield.

4.2. . Preparation of silylaryl triflates from benzodioxasilines

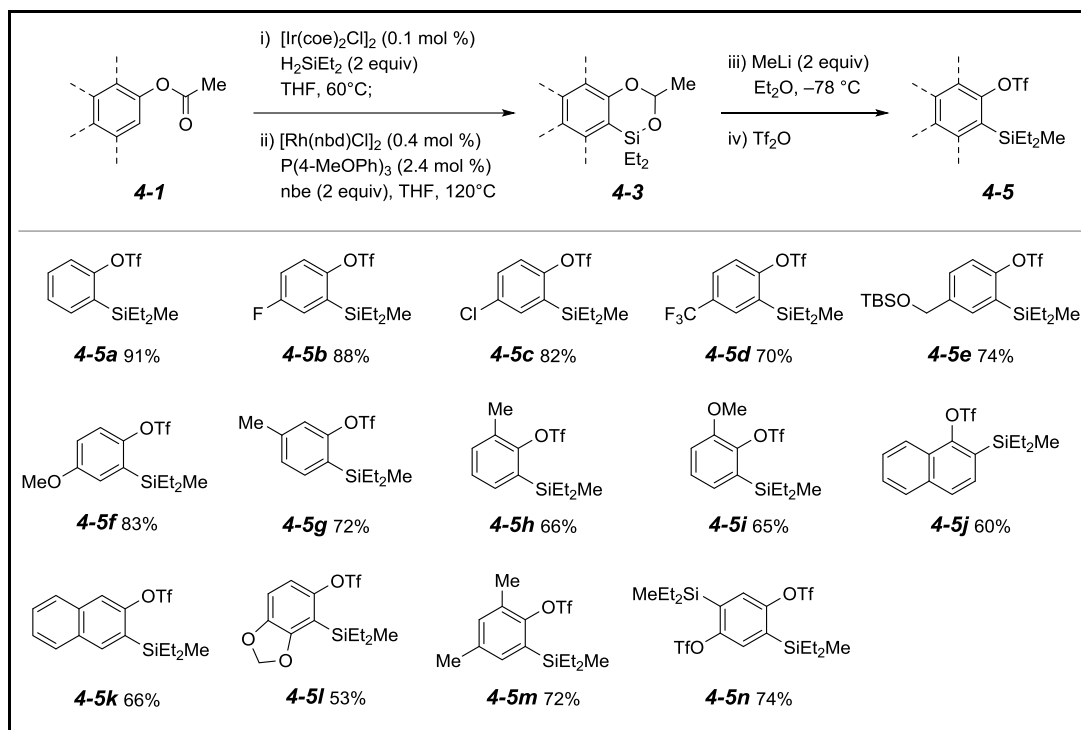


Table 4-1 Substrate scope of 1,2-silylaryl triflates

Next we investigated the single-pot, sequential strategy concerning nucleophilic attack of MeLi and triflation of sterically demanding benzodioxasilines **4-3** bearing substituents at *ortho* position to the hydroxyl group (Table 4-1). These substrates consistently produced substantial desilylation adducts **4-7** even in a short period of reaction time. We found that purity of dioxasilines **4-3** was crucial to affect the MeLi addition reaction. Specifically, when purified benzodioxasilines **4-3o-r**, obtained through a column chromatography after the reductive C–H silylation, was employed under the reaction

conditions, we were able to isolate **4-5o-r** in good yields. Of note, these 1,2,3-trisubstituted arylsilyl triflates are difficult to access by other catalytic means.

4.3. Investigations on the possible desilylation pathways

During these processes, we found that noticeable, yet minor desilylation phenol byproducts **4-7** were also produced with most substrates (Table 4-1).

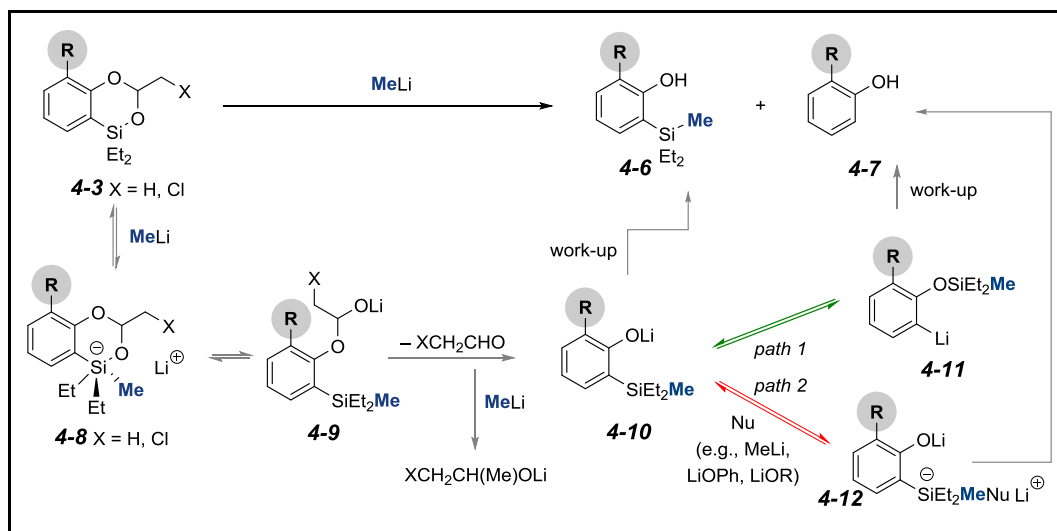


Figure 4-3 Possible desilylation mechanism

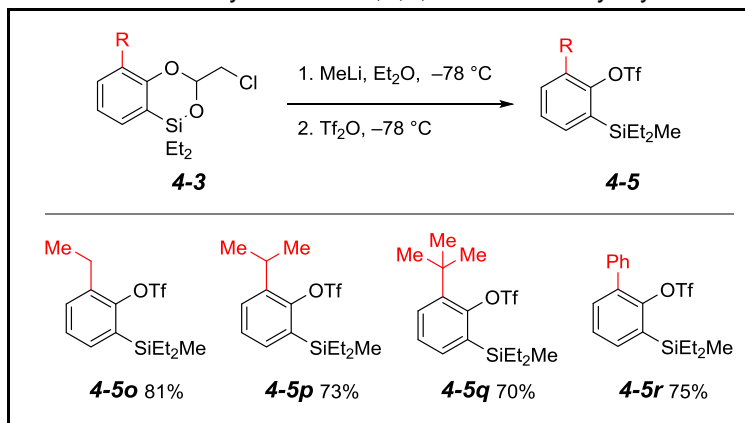
Especially, substrates such as **4-5d**, **4-5j**, and **4-5k** produced a significant amount of **7**. For the desilylation event we reasoned that a nucleophilic attack of MeLi to dioxasilines first generates putative penta-coordinate silicate species **4-8**, which undergoes a fragment process to afford lithium *ortho*-silyl phenoxide **4-10** (via lithio acetal **4-9**) and acetaldehyde. A nucleophilic addition of MeLi to acetaldehyde can furnish XCH₂CH(Me)OLi. At this moment two possible scenarios explaining the observed desilylation are feasible: 1) Intramolecular silyl transfer—a [1,3]-silyl tropic rearrangement can be attributed to this issue. For example, a [1,3]-Brook rearrangement^{178, 179} of *ortho*-silyl phenols to afford silyl ethers has been reported, however, this process was explored

mainly under acidic conditions,¹⁸⁰ elevated temperatures^{181, 182, 183} or catalytic aerobic conditions.¹⁸⁴ Additionally, under strong basic conditions a retro-[1,3]-sigmatropic process within *ortho*-silyl phenols has been well reported.^{185, 186} 2) Intermolecular silyl transfer–nucleophiles (e.g., MeLi, LiOPh, LiOR), present in the reaction, can engage with **4-10** to produce dianions **4-12**, which eventually afford phenols **4-7** upon work-up. To minimize the potential rearrangement (**4-10** to **4-11**) or reversible association of nucleophiles (**4-10** to **4-12**) to silyl moiety after the first fragmentation (**4-3** to **4-10**), we quickly quenched the reaction within <1 min with Tf₂O at –78 °C (achieving a full consumption of **4-3**). This procedure substantially reduced the formation of **4-7**, thereby enhancing yields.

4.4. Preparation of sterically hindered silylaryl triflates from benzodioxasilines

Next we investigated the single-pot, sequential strategy concerning nucleophilic attack of MeLi and triflation of sterically demanding benzodioxasilines **4-3** bearing substituents at *ortho* position to the hydroxyl group (Table 4-2).

Table 4-2 Sterically hindered 1,2,3, substituted silylaryl triflates

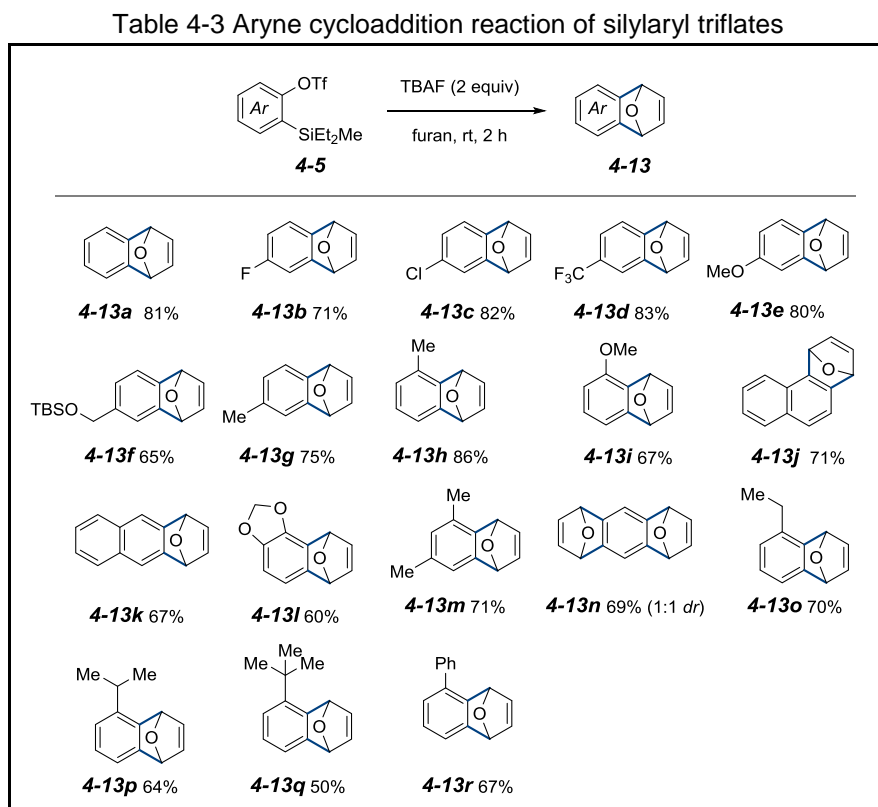


These substrates consistently produced substantial desilylation adducts **4-7** even in a short period of reaction time. We found that purity of dioxasilines **4-3** was crucial to affect the MeLi addition reaction. Specifically, when purified benzodioxasilines **4-3o** to **4-**

3r, obtained through a column chromatography after the reductive C–H silylation, was employed under the reaction conditions, we were able to isolate **4-5o** to **4-5r** in good yields. Of note, these 1,2,3-trisubstituted arylsilyl triflates are difficult to access by other catalytic means.

4.5. Fluoride-mediated [4+2] aryne cycloaddition reaction of diethylmethylsilylaryl triflates

We explored fluoride-mediated [4+2] aryne cycloaddition reactions of diethylmethylsilylaryl triflates **4-5** prepared from the corresponding phenols with furan (Table 4-3).



Cycloaddition reactions with electron-rich and -deficient arylsilyl triflates with furan (solvent) provided a variety of 1,4-dihydro-1,4-epoxynaphthalenes **4-13**, demonstrating

good functional group tolerance. Under these reaction conditions *meta* and *para*-substituted arylsilyl triflates (**4-5b** to **4-5g**) produced the corresponding 6-substituted 1,4-dihydro-1,4-epoxynaphthalenes (**4-13b** to **4-13g**) in good yields. In particular, a TBS blocking group within **4-5f** survived when the reaction was cool to 0 °C. *ortho*-substituted arylsilyl triflates (**4-5h** and **4-5i**) underwent aryne cycloaddition reaction to provide **4-13h** and **4-13i** in 86% and 67% yields, respectively. This approach is also successful with 1- and 2-silylnaphthyl triflates (**4-5j** and **4-5k**, respectively) to afford **4-13j** and **4-13k** in modest yields. Cycloaddition reactions with disubstituted arylsilyl triflates (i.e., **4-5l** and **4-5m**) and dual cycloadditions (i.e., **4-5n**) were compatible with the cycloaddition to provide **4-13l**, **4-13m**, and **4-13n** (1:1 *dr*) in good yields. Next, we studied the cycloaddition of sterically hindered, 1,2,3-trisubstituted arylsilyl triflates **4-5o** to **4-5r**. The corresponding cycloadducts **4-13o** to **4-13r** were successfully produced in moderate yields.

4.6. . Synthetic approach to estrone derivative 4-20

An important component of this project was broadening the scope of the approach towards synthesis of bioactive molecules. For this purpose, we examined [4+2] aryne cycloaddition of arylsilyl triflates derived from estrone **4-14**. C17 ketone in estrone, which was not compatible in Ir-catalyzed ester hydrosilylation, was first protected with a ketal group. α -Chloroacetyl group was then installed to the phenol for effective arene C–H silylation reaction in a hindered environment. Catalytic reductive *ortho*-C–H bond silylation of the resulting phenyl acetate with α -chloroacetyl formal directing group provided dioxasiline **4-16** (only C2). A MeLi addition to **4-16** afforded C2-silyl phenol **4-17** in 82% yield over 3 steps. The reaction of **4-17** and Tf₂O in the presence of pyridine gave arylsilyl triflate **4-18**, which in turn was utilized for the aryne cycloaddition with furan to afford cycloadduct **4-19**. During the course of the cycloaddition reaction partial deprotection of

ketal group was observed. The ketal deprotection of **4-19** afforded **4-20** (96% yield, 1.2:1 *dr*). (Figure 4-4)

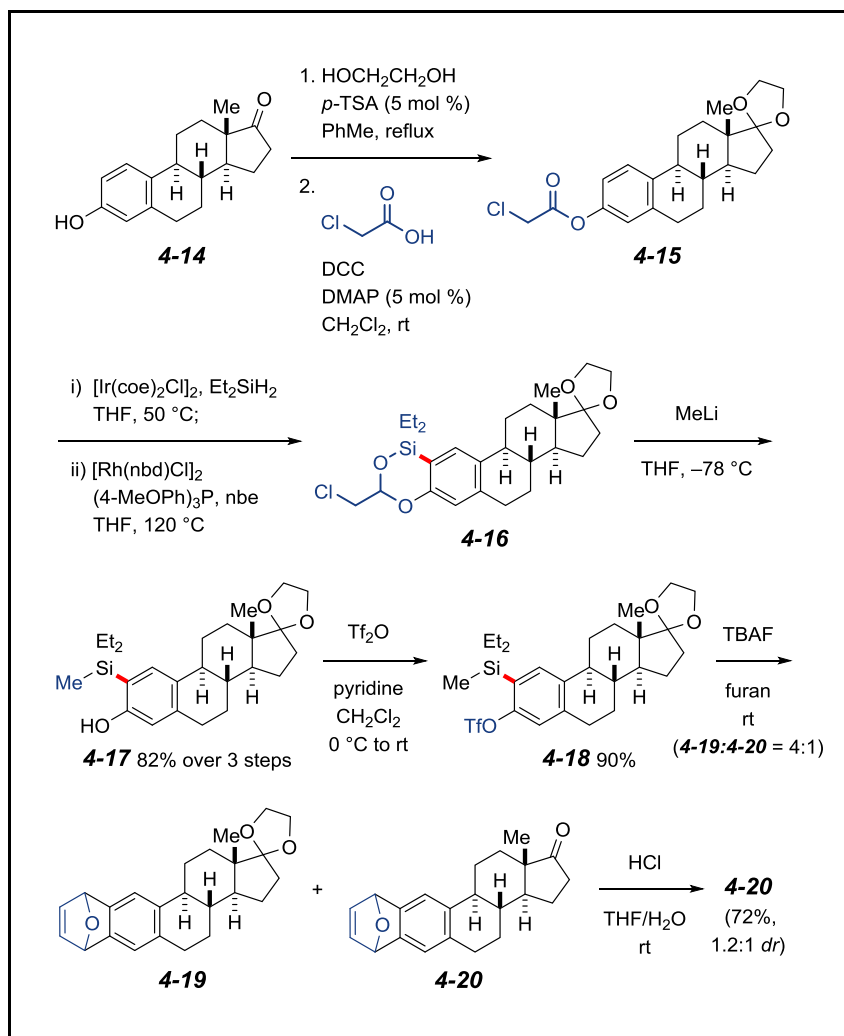


Figure 4-4 Synthesis of estrone derivative **4-20**

4.7. Summary of chapter 4

To summarize, we have developed an efficient strategy to prepare diversely substituted arylsilyl triflates. The catalytic reductive *ortho*-C–H silylation of phenols via traceless acetal directing groups to afford benzodioxasilines **4-3**, followed by a sequential addition of MeLi and trifluoromethanesulfonic anhydride, furnished arylsilyl triflates **4-5** in

a single pot. In particular, α -chloroacetyl formal directing group was required for the effective reductive *ortho*-C–H silylation to afford 1,2,3-tri-substitued arylsilyl triflates **4-5**. Furthermore, this class of arylsilyl triflates demanded purification of benzodioxasilines **3o-r** for subsequent nucleophilic ring-opening and triflation processes, in order to minimize unwanted desilylation byproduct **4-7**. We demonstrated that fluoride-mediated [4+2] aryne cycloaddition reaction of the resulting diethylmethylsilylaryl triflates **4-5** with furan, which afforded distinctly substituted, **4-13o** to **4-13r**, some of which were not accessed previously.

Chapter 5

Hydrogen Atom Transfer from Hydrosilanes by Lewis Base Catalysis

5.1. Introduction

Hydrogen atom transfer (HAT), a concerted migration of a proton and electron from a donor to an acceptor molecule in a single kinetic step, is ubiquitous and one of the most fundamental chemical processes in chemistry and biology.^{187, 188} Examples include regio and stereoselective processes catalyzed by transition metal catalysts (e.g., Co, Mn, Fe)^{187, 189, 190} (Figure 5-1a) and in the active sites of metalloenzymes (e.g., cytochrome P450s and non-heme Fe and Cu oxidases).^{191, 192}

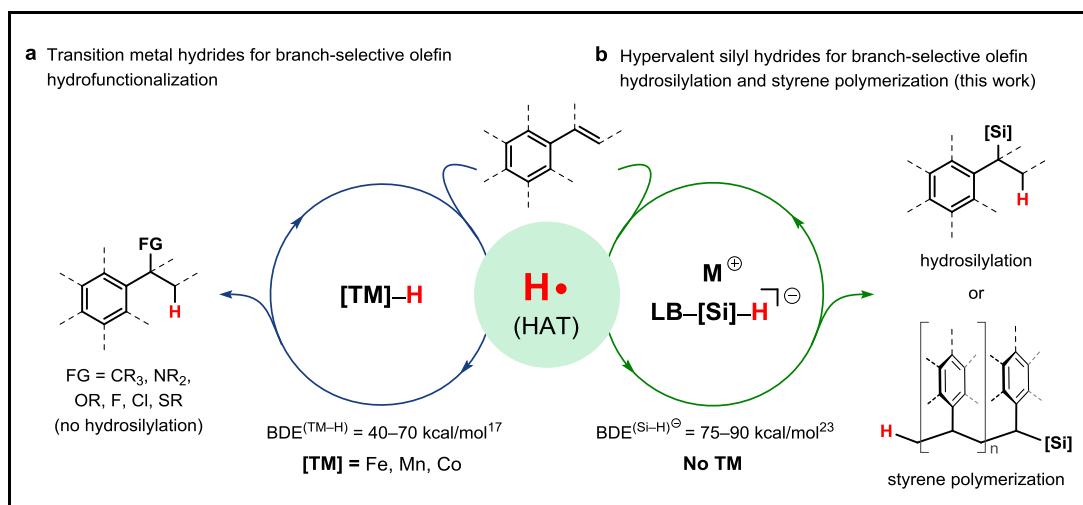


Figure 5-1 Branch-selective hydrofunctionalizations involving HAT

In chemical synthesis, HAT is closely related to free radical chemistry, often called hydrogen atom abstraction, and typically involves in the termination step of radical reactions between group 14 metal(oid) hydrides and carbon-centered radicals.¹⁹⁰ Despite substantial advances in this field, the wide and sustainable application of current thermal radical chemistry are hindered by the need for a stoichiometric amount of toxic reducing agents (e.g., organotin hydrides), excess solvent, and operational inconvenience.

Group 14 metal(loid) hydrides have been widely exploited in chemical processes which include radical and reduction chemistries to construct transformative molecules and

materials.¹⁹³ In particular, environmentally benign organosilicon hydrides have displayed an impressive range of applications, including hydrogen storage source,¹⁹⁴ silicon-based materials,¹⁹⁵ biomedically relevant agents,²⁹ and medical applications.¹⁹⁶ Since demonstration of diverse utility of organosilanes, significant advances have been made with respect to more selective Si–C forming reactions.¹⁹⁷ For example, the linear-selective olefin hydrosilylation with late transition metal catalysts (e.g., Pt, Rh, Ir, Fe, Co, Ni),¹⁹⁸ organocatalysts,¹⁹⁹ and radical initiators is well-established and applied to a wide variety of industrial processes.²⁰⁰ In contrast, relatively few catalytic systems have been identified and studied for branch-selective olefin hydrosilylation. Examples include Hayashi's chiral Pd-MOP catalyst with trichlorosilane,²⁰¹ Buchwald's chiral Cu-H/Ph-BPE catalyst with diphenylsilane,²⁰² and Lu's Co-OIP with phenylsilanes.²⁰³ Owing to the high cost of late transition metals, catalytic strategies utilizing less expensive first-row transition metals (e.g., Fe, Mn, Co) have also been explored with respect to the expansion of their synthetic utility and understanding of new catalytic olefin hydrosilylation mechanisms.^{198, 204} First-row transition metal hydrides bearing relatively weak metal-hydride (M–H) bonds (ca. 40-70 kcal/mol) allow a facile generation of carbon-centered radicals from olefins by HAT.^{205, 206} Such a process has been recently shown to be remarkably useful for branch-selective olefin hydrofunctionalization and in the preparation of cyclic small molecules (Figure 1a).^{187, 190, 207, 208, 209, 210} To date, however, no HAT-initiated hydrosilylation has been reported.

A sustainable approach toward elimination of the use of transition metals is to develop low-cost, environmentally benign, transition metal-free silylations. Because such approach could offer synthetic advantages and distinctive reaction mechanisms, there was a growing interest to develop strategies for carbonyl hydrosilylation²¹¹ and, more recently, for heteroaryl and alkynyl C–H bond silylations,^{50, 212} utilizing Lewis base catalysts (e.g., TABF, KO^tBu, KOH) with hydrosilanes. In 2017, Grubbs-Stoltz-Krenske-Houk-Zare

reported mechanistic studies of KO^tBu-catalyzed cross-dehydrogenative C–H silylation of heteroarenes.^{213, 214} Two plausible mechanisms were proposed involving either silyl radical transfer via homolytic Si–H cleavage or an anionic process via heterolytic Si–H cleavage from the common pentacoordinate silicate intermediate.²¹⁵ Although Corriu and coworkers previously showed that pentacoordinate silicates (e.g., K[HSi(OR)₄]) are capable of a single electron transfer (SET) to benzylic halides and metal complexes,²¹⁶ it has been widely accepted that Lewis base-activation of hydrosilanes for carbonyl hydrosilylation involves hydride transfer to a carbon-oxygen double bond. (Figure 5-2)

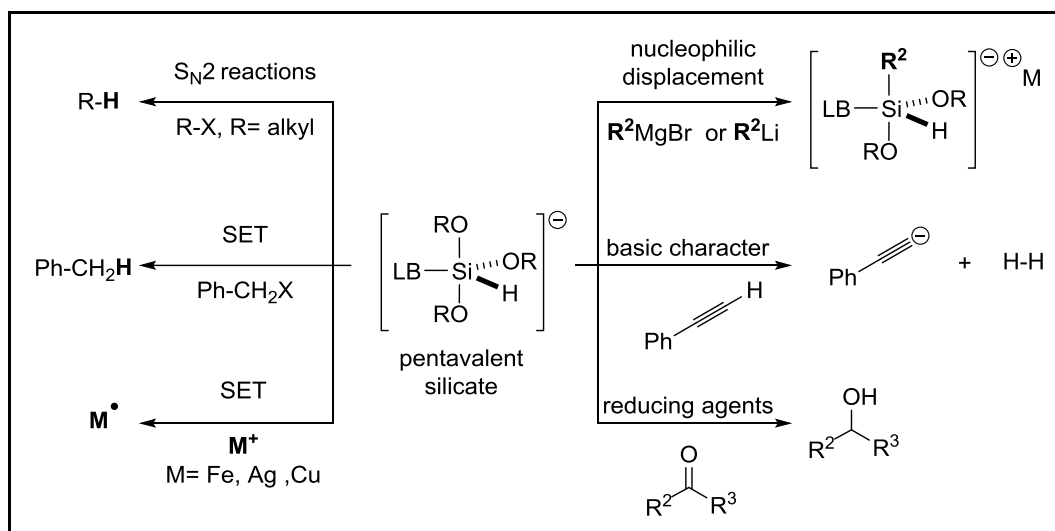


Figure 5-2 Pentacoordinated silicate reactivity

To this end, several groups have recently proposed a hydride transfer mechanism in catalytic alkene/alkyne hydrosilylation using Lewis base.^{217, 218} Nevertheless, a general strategy for transition metal-free, branch-selective olefin hydrosilylation has not been explored. In this work, we present an operationally simple, sustainable, alkali metal Lewis base-catalyzed, complexation-induced HAT (LBCI-HAT) with olefin substrates. This catalytic process exploits organosilicon hydrides and earth abundant, alkali metals base catalysts to yield either a highly branch-selective olefin hydrosilylation, or styrene

polymerization in a highly selective manner, depending on the Lewis base catalyst used (Figure 1b). The protocol offers secondary organosilanes or polymers with silane-end functional groups. In addition, we demonstrated the synthetic utility of the LCBI-HAT manifold, which ultimately provides an environmentally sustainable alternative to conventional catalytic hydrofunctionalization using transition metal catalyst and chemical wastes such as excess oxidants and solvent.

5.2. Mechanistic discussion.

The mechanism of the LBCI-HAT process, utilizing Lewis base catalyst and hydrosilanes **I** which bear reasonably strong Si–H bonds (ca. 75-90 kcal/mol),^{219, 220, 221} differs substantially from the well-established HAT-promoted olefin hydrofunctionalization with transition metal catalysts (Figure 5-1).¹⁹⁰ Specifically, the nucleophilic activation of **I**, with alkali metal Lewis base catalyst through $n-\sigma^*$ interactions, initially produces alkali metal pentacoordinate silicate **II**.²²² Si–H bond strength of **II** (81.9 kcal/mol) is reduced by 15% relative to **I** (96 kcal/mol), determined at the G3B3 level of theory.²²³ The activated hydridosilicate **II** delivers a hydrogen atom (H^\bullet) to the olefin, mediated by a cation- π interaction (**III**),²²⁴ to provide a putative intimate benzylic and silyl radical anion pair cage **IV** (Figure 5-4, left) [cf., the donor (carbonyl)/acceptor (pentacoordinate silicate) binding through $n(O, N)-\sigma^*(Si)$ complexation permits silicon to expand its valency, leading to hydride (H^-) transfer (**II** to **VIII** to **IX**),²¹¹ Figure 5-4, right]. The reaction proceeds further to produce the branch-selective hydrosilylation product **VI** via the cross-radical coupling of the benzylic and silyl radicals within the radical-radical anion pair cage **IV**, and regenerate the alkali metal Lewis base for catalytic turn-over. Although Zare and coworkers established a similar K^+ -heteroarene π interaction in the context of a C–H silylation process,²¹⁴ a mode of Lewis base activation of a Si–H bond leading to the HAT to an olefin,

without any further energetic activation (e.g., transition metal-mediated photoredox catalysis), has not been previously reported. Furthermore, the silyl radical transfer mechanism to heteroarenes, proposed by Grubbs-Stoltz-Krenske-Houk-Zare in the context of the cross-dehydrogenative arene C–H silylation,^{213, 214} is unlikely in our vinylarene system to explain the observed regioselectivity (Figure 5-3). The resulting primary radical or anion from the preferential silyl transfer, if any, is not expected to have β -silyl effect (cf., carbocation stabilization by β -silyl moiety).²²⁵

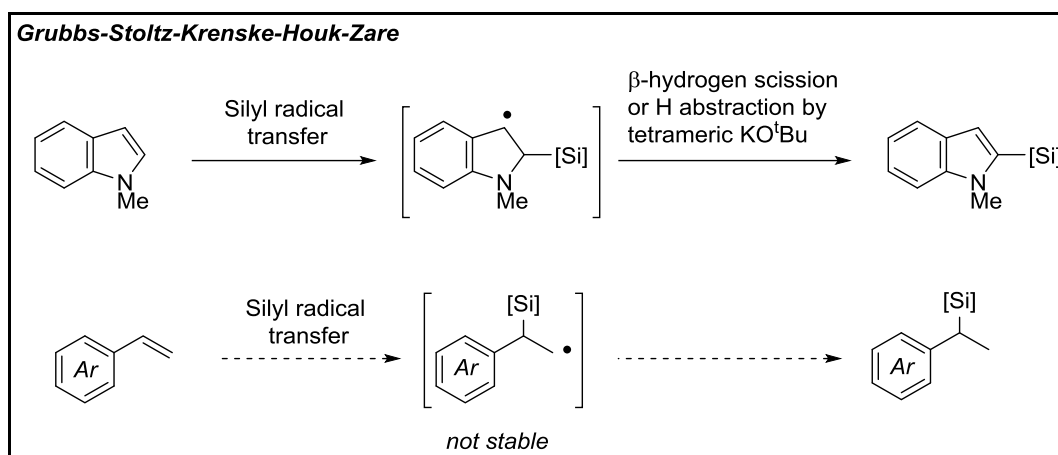


Figure 5-3 Silyl radical transfer can not explain the regio-selectivity

In general, the proposed highly selective cross-radical coupling between two reactive radical species appears challenging because of their intrinsic reactivity and minimal effective concentrations. In the present case, the success of such highly selective cross-radical coupling can be attributed to the formation of the intimate ion pair **IV**. In particular, the attenuated reactivity of the transient, unstable silyl radical with incoming Lewis base can form the relatively stable silyl radical anion (in equilibrium between **IV** and **V**), which possesses the capacity for slow-release of the unstable silyl radical for the coupling. Namely, the “protected radicals” masked with alkali metal Lewis base could dictate the reaction with stable yet transient, benzylic radicals by protecting the radical center from

potential radical-mediated reactions (e.g., hydrogen abstraction, self-termination dimerization, disproportionation, and polymerization with abundant olefins), to yield **VI**.²²⁶ Interestingly, when highly coordinating agents such as 18-crown-6 ether which can sequester alkali metal cations from **IV** are employed, free radical polymerization takes place, leading to polystyrene **VII** (Figure 5-4 left). Together, the reaction strategy depicted in Figure 5-4 can offer advantages for sustainability and operational simplicity, as well as site-selectivity and product selectivity, in comparison with the presently predominant transition metal-based linear-selective hydrosilylation.²⁰⁴

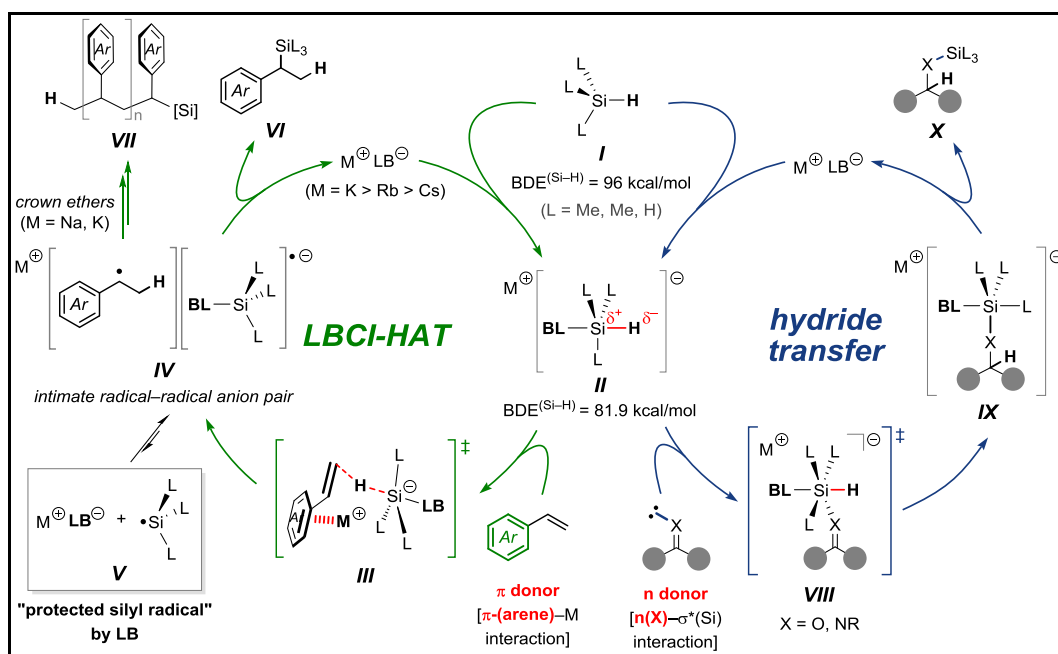


Figure 5-4 Modes of substrates-hypercoordinate silicate interaction

5.3. Lewis base-catalyzed, complexation-induced HAT (LBCI-HAT) reactions:

Discovery and development.

The benzylic radicals generated from vinylarenes via LBCI-HAT can engage in two competing reaction pathways (Figure 5-4): (1) branch-selective hydrosilylation and (2) HAT-initiated polymerization. To establish the reaction parameters of the LBCI-HAT, we

first investigated the origin of the activation mode of the Lewis base catalyst and hydrosilane for HAT, dictating high site- and product-selectivity. Unexpected, metal cations played a crucial role in promoting and controlling the reaction pathways. While large metals (i.e., K⁺, Rb⁺, Cs⁺, Ba²⁺, La³⁺, and Yb³⁺) promote the reaction, small cations (i.e., Li⁺ and Na⁺) were unable or inefficient to catalyze the reaction²¹³ (Figure 5-5).

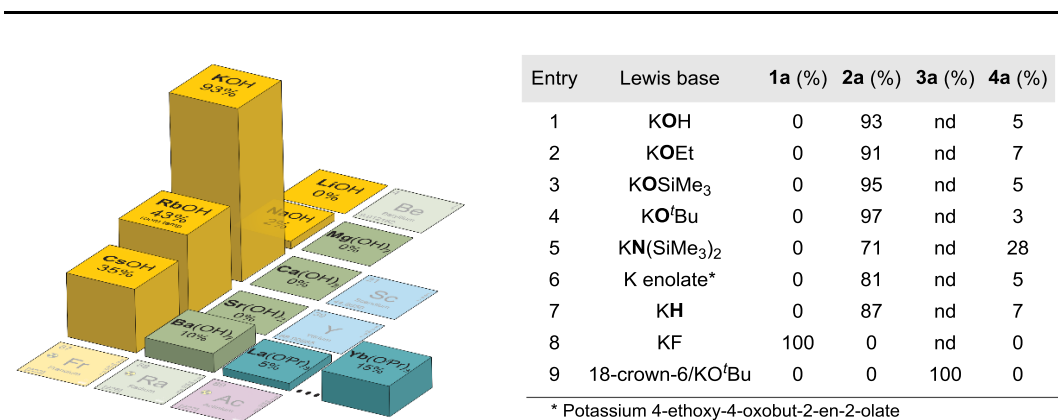
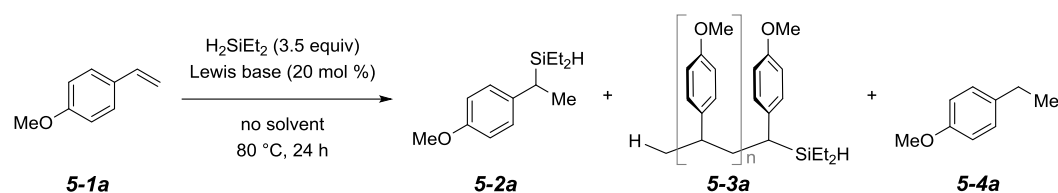


Figure 5-5 Discovery of LB-catalyzed transition metal-free, hydrosilylation of vinylarenes

Initial screening of Lewis base revealed that not only the widely-used oxyanions (entries 1-4),^{50, 212} but also various anionic bases such as amide (entry 5), enolate (entry 6), and hydride (entry 7) were effective for the hydrosilylation (Figure 5-5). Overall, the LBCl-HAT was generally efficient when the *p*K_a of the corresponding acid of Lewis base is greater than ca. 11 (e.g., β-keto ester potassium enolate, entry 6). Among them, KO^tBu was found to be most effective, which can be lowered down to 1 mol% (70%, 80 °C, 40 h; Appendix E, Table S2). In addition, when 18-crown-6 (20 mol%) was doped to the reaction mixture (entry 9), complete polymerization was observed to afford polystyrene **5-3a**. To the

best of our knowledge, this is the first example of LBCI-HAT-initiated radical polymerization of styrene. The result indicates that the departure of the cation from the ion pair cage triggers the fragments from **IV** (Figure 5-4), leading to a free radical polymerization manifold to afford **5-3a**.

5.4. Mechanistic investigations of the LBCI-HAT.

Addition of several radical initiators to our reaction conditions in the absence of KO^tBu, led to the exclusive styrene polymerization, strongly suggesting that the LBCI-HAT does not generate a transient, free benzylic radical, although it could reside in an ion pair cage (cf., Figure 5-4, left). To validate the formation of the benzylic radical by HAT, radical trapping agents, TEMPO and galvinoxyl radical were added to the reaction mixture (Figure 5-6), where TEMPO adduct **5-5b** (49% isolation yield) and reduced galvinoxyl **5-6** (40% isolation yield) were isolated.

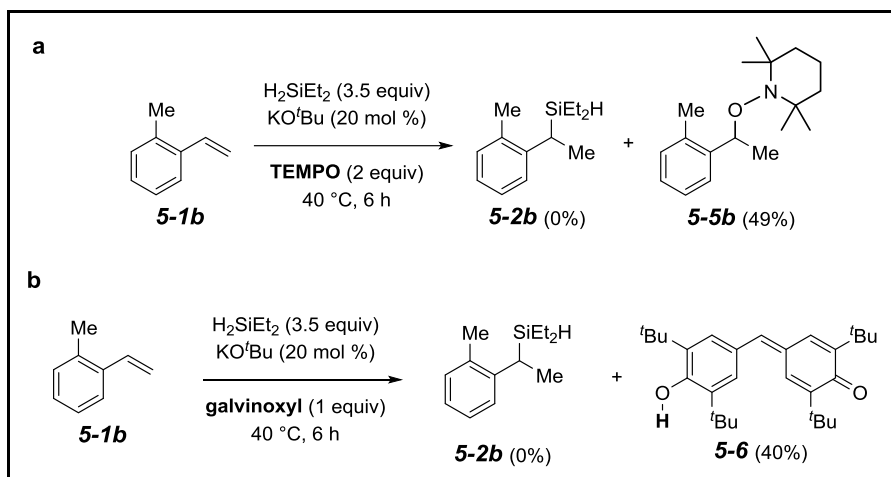


Figure 5-6 Effect of addition of radical traps

An excess of molecular oxygen also inhibited the reaction. In addition, radical clock experiments were carried out. When α -cyclopropyl-substituted styrene **5-1c- α** was subjected to the identical conditions, the ring-opened product **5-7c- α -Et** was produced in

81% yield (Figure 5-7). When $\text{HMe}_2\text{SiOSiMe}_2\text{H}$ was used, which produces smaller silane $\text{HMe}_2\text{SiO}^t\text{Bu}$ *in situ* after reacting with KO^tBu , to our surprise, the non-rearranged benzylic radical was kinetically trapped to afford **5-2c- α -Me** (15% isolation yield) along with the rearranged adduct **5-7c- α -Me** (80% isolation yield). The occurrence of the rearrangement adduct is indicative of the presence of the benzylic radical species, produced through a preceding HAT to the β -position of styrene.

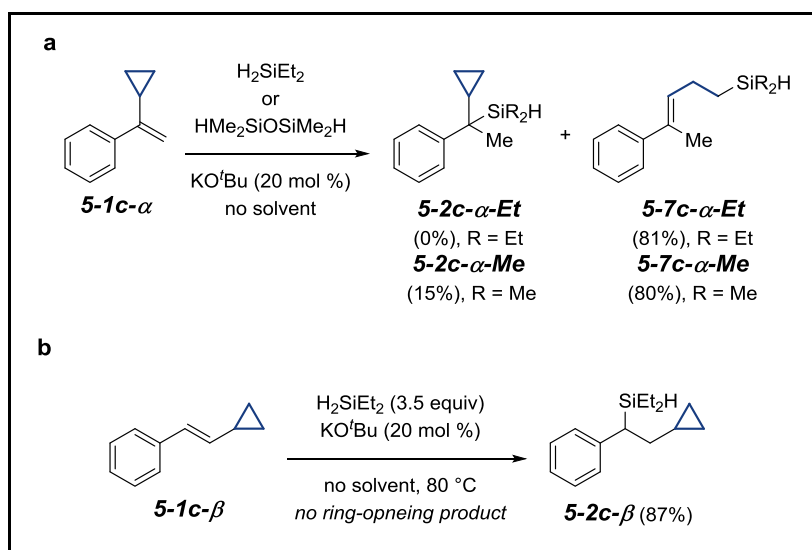


Figure 5-7 Radical clock experiment

Furthermore, the non-rearranged adduct allows one to approximate the rate of the silyl radical addition to the benzylic radical after the HAT (cf., cyclopropylbenzyl radical, $k_{\text{ring-opening}} = 3.6 \times 10^5 \text{ s}^{-1}$ at 22 °C²²⁷). A control experiment with β -cyclopropyl styrene **5-1c- β** demonstrated that the preceding HAT occurred at β -position **5-2c- β** (Figure 5-7b). On the other hand, alkyl-substituted alkenes were completely inert toward the LBCI-HAT-mediated hydrosilylation, inferring that the proposed cation- π interaction involving arene next to the olefin is key for the LBCI-HAT. Furthermore, it was not successful to trap the carbon-center benzylic radical via a 6-*exo-trig* radical cyclization (Appendix F, Scheme S14), which implies that the LBCI-HAT does not produce a free benzylic radical, but an intimate radical-radical

anion pair cage. In this scenario, the cross-radical coupling within the cage can be feasible by the slow-release of silyl radical from the Lewis base-protected radical anion, as depicted in Figure 5-4. The present study suggests that LBCI-HAT is feasible only with the larger metal Lewis base catalysts, and a cation- π interaction dictates the reaction pathways (5-1 to 5-2 vs. 5-1 to 5-3).

5.5. NMR Spectroscopic studies for the LBCI-HAT.

To directly identify reaction intermediates, experiments exploiting ^1H NMR spectroscopy were performed (Figure 5-8 and Figure 5-9).

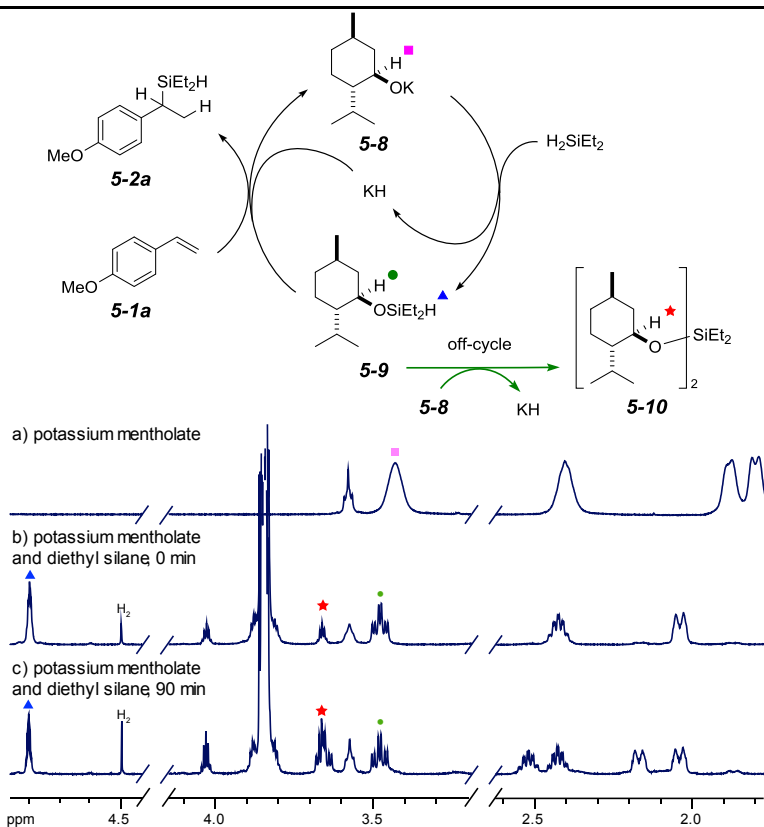


Figure 5-8 NMR studies

First, Lewis base [e.g., potassium L-mentholate **5-8** (20 mol%)] reacted with H_2SiEt_2 (1 equiv) to quickly establish the equilibrium of the (LB)SiEt₂H **5-9** and (LB)₂SiEt₂

5-10 (ca. 2:1 of **5-5-9** and **5-5-10**) (Figure 5-8). When **5-1a** was added to the reaction mixture, the reaction immediately turned red and eventually afforded **5-2a** in 4 h. Second, further insights into the Lewis base (i.e., KH)-catalyzed silane disproportionation were gathered by carrying out the reaction of **5-9** (2.5 equiv) and KH (50 mol %) (Figure 5-9). The previously observed **5-10** was formed slowly, along with a formation of H_2SiEt_2 . After 16 h, the equilibrium again was established to provide ca. 3:1 of **5-9** and **5-10**.

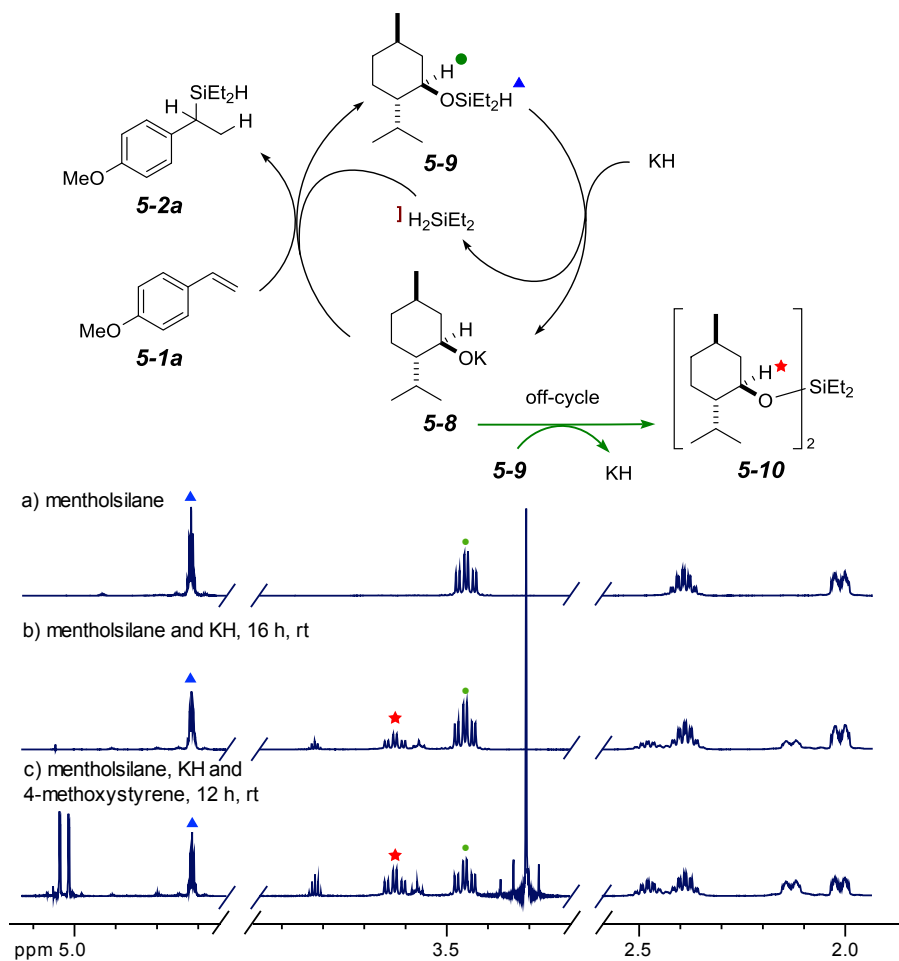


Figure 5-9 NMR studies

A subsequent addition of **5-1a** to the mixture at 80 °C furnished **5-2a**. In both experiments, homosilaketal **5-10** was formed, but it was unclear whether formation of **5-10**

was reversible or not. To establish the reversibility and examine a catalyst consuming route (i.e., **5-8** to **5-9** to **5-10**), **5-10** was independently prepared and reacted with KH (Figure 5-5).

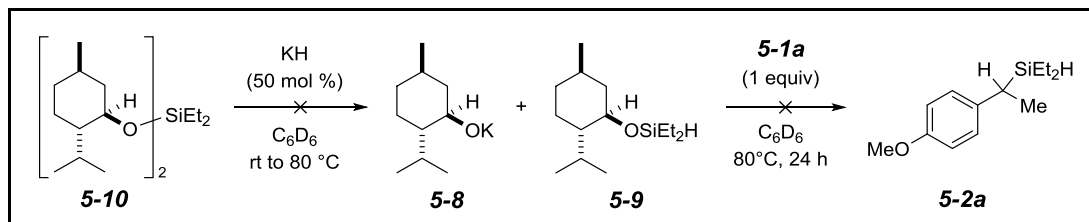


Figure 5-10 Reactivity test of silaketal **5-10**

However, **5-9** was not formed even at elevated temperatures, and an addition of **5-1a** to the reaction mixture did not affect the hydrosilylation. Together, these observations indicate that Lewis base first reacts with dihydrosilane to quickly establish the equilibrium of 1:1 LB-silane adduct (i.e., **5-9**) and 2:1 LB-silane adduct (i.e., **5-10**). Only **5-9** is responsible for the branch-selective hydrosilylation. The addition of vinylarene triggers the LBCl-HAT to furnish **5-2a**. Lewis Base is consumed by the reaction with H_2SiEt_2 to afford **5-10**, which is not a silane donor for the hydrosilylation and does not return to the catalytic cycle.

5.6. Cation- π interaction in the LBCl-HAT.

To investigate the interaction of K^+ and π system present in the vinyl arenes which is likely essential for the LBCl-HAT, the following experiments were carried out. We hypothesized that the reduction of TEMPO radical can be utilized as an indicator of HAT (Figure 5-9). First, the hydrogen atom trap with TEMPO in the absence of a π donor largely failed, suggesting that the HAT did not occur (Figure 5-4a). Secondly, upon addition of styrene as a π donor the HAT was initiated, where the reduced TEMPO was observed (Figure 5-4b). Finally, to our surprise addition of 18-crown-6 in the absence of a π donor

manifested the HAT to furnish more reduced TEMPO (Figure 5-4c) than the experiment with styrene (Figure 5-4b). We attribute more facile HAT under the reaction conditions presented in Figure 5-4c to the stronger interaction of K^+ with the crown ether (cf., vinylarene). These series of experiments suggest that the LBCI-HAT is essentially associated with the cation- π or cation- n interaction.

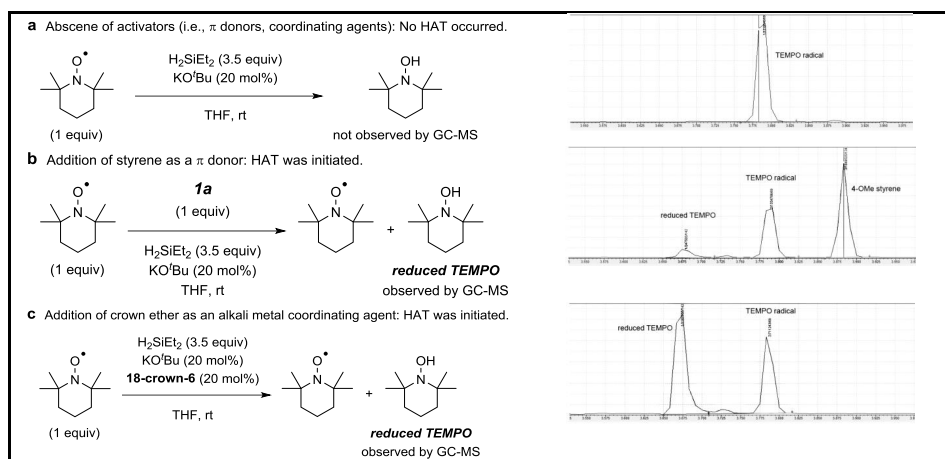


Figure 5-11 Investigation of Cation- π interaction

These results are consistent with the previous report of KO t Bu-catalyzed cross-dehydrogenative heteroarene C–H silylation, which shares virtually identical reaction parameters with the LBCI-HAT.²¹³ In the report, extensive labeling studies were carried out to understand the source of H_2 evolved during the induction period of the process. This study demonstrated that the initial H_2 formation is related to minor quantity of water.²²⁸ Therefore, with supports of the spectroscopic experiments concerning the LB-mediated silane ligand exchange in Figure 5-8 and Figure 5-9, the reaction between metal hydride and residual water in the reaction can be responsible for the production of H_2 in the beginning phase of the LBCI-HAT.

5.7. EPR Spectroscopic studies for the LBCI-HAT.

EPR spectroscopy was utilized in an attempt to directly detect radical intermediates in HAT reactions. However, due to the remarkably short lifetime of silyl and carbon-centered radicals at ambient temperature²²⁹ it is frequently not possible to accumulate sufficient concentrations of radical species for EPR detection and/or characterization. Consequently, the absence of EPR signals in HAT reactions are not sufficient strong evidence to rule out a radical mechanism. To circumvent the kinetic masking of radical intermediates in HAT reactions radical trapping agents 2,6-di-*tert*-butyl-4-[(4-hydroxy-2,5-di-*tert*-butylphenyl)-methyl]phenol (**5-6_{H2}**) and galvinoxyl [2,6-di-*tert*-butyl-4-(3,5-di-*tert*-butyl-4-hydroxybenzylidene)cyclohexa-2,5-dienone] (**5-6**) were added to reactions in the reduced form

As shown in Figure 5-12a (trace 1), data collected in the absence of **5-6_{H2}** or **5-6** exhibit no discernible features either before or after initiation of reaction. By contrast, reactions carried out in the presence of either **5-6_{H2}** and **5-6** yielded a variety of paramagnetic species which exhibit time dependent accumulation and decay. For instance, following initiation of HAT in the presence of **5-6_{H2}**, EPR data was collected at time points ranging from 2 to 20 minutes. Trace 2 (Figure 5-12a) collected 2 minutes after addition of KO^tBu exhibited broad features which cannot be attributed to any single radical species. This spectrum is likely the result of several unresolved signals overlapping and thus cannot be assigned. However, within 10 minutes a triplet centered at an isotropic *g*-value (*g_{iso}*) of 2.005 (trace 3) is observed which can be attributed to a single radical species. The differential area (1:2:1) observed for the satellite features relative to the central resonance arises from degenerate doublets produced when coupled to two equivalent nuclei [¹H] with *I* = 1/2 nuclear spin.^{230, 231} The observed spectrum can be simulated (*Sim1*, *dashed line*), assuming a single radical coupled to two equivalent protons with an isotropic

hyperfine coupling (A_{iso}) of 4.5 MHz (0.16 mT). Spin quantification of *Sim1* indicates that the concentration of this species is $1.1 \pm 0.1 \mu\text{M}$. The observed g -value, hyperfine splitting pattern, and magnitude of A_{iso} are all consistent with the **5-6**_{H2}-radical (**5-6**_{H2}[•]) shown in Figure 5-12a.^{232, 233} This experiment verifies that **5-6**_{H2} can serve as a source of hydrogen atoms in HAT reactions. Moreover, the accumulation and subsequent decay of radical-trapped species is consistent with the radical mechanism involving LBCI-HAT.

If the radical trap **5-6**_{H2} is indeed serving as a H-atom donor in HAT reactions, the observed EPR spectra should be unique to this specific spin trap. Thus, reactions using a different spin trap should yield spectroscopically distinct features. To validate this assertion a second radical trap (**6**, reduced galvinoxyl) was used in equivalent experiments. As before, no signals were observed in reactions in the absence of reduced galvinoxyl **6** or prior to imitating the reaction by addition of KO^tBu. However, following initiation of the LBCI-HAT reaction the complex spectra shown in trace 6 (Figure 5-12b) was observed at 2 minutes. The spectrum is primarily comprised of two distinct radical signals. First, an extended multiline pattern can be observed ranging from 1.997 to 2.012. This broad signal becomes the dominant species in spectra collected at 5 and 10 minutes (trace 7 and 8, respectively) before ultimately decaying. A clean spectrum of the second radical species can be obtained by subtraction of the 5 minute spectrum from trace 6, resulting in the difference spectrum (trace, [6-7]) shown in Figure 5-12b.

Before discussing the assignment of these two radical species, it is instructive to first consider the signal obtained for samples of **6**[•]. Shown in Figure 5-12b (trace 5) is the EPR signal for **6**[•] prepared under identical solvent conditions as HAT reactions to avoid the possibility of solvent dependent perturbations to g - and A -values.^{234, 235, 236} This signal is essentially a doublet of multiplets. Simulations of the **6**[•] (*Sim5*, *dashed line*) can be produced assuming coupling to inequivalent sets of protons. Strong coupling [$A_{iso} = 16.7$

MHz (0.59 mT)] to a single proton located at the α -carbon (Figure 5-12b) provides the initial separation of multiplets. The two sets of multiline (5-line) is attributed additional hyperfine coupling [$A_{iso} = 3.7$ MHz (0.13 mT)] to four equivalent protons located at carbon atoms C2', C6', C3, and C5 of **6** \cdot biphenyl ring.

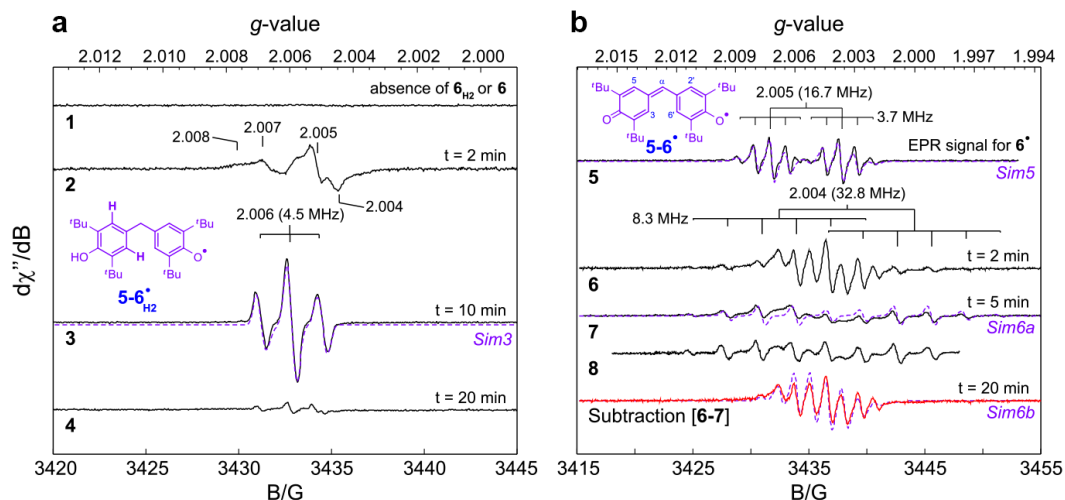


Figure 5-12. X-band EPR spectra of the reactions Carried out with spin-trap

As expected, the magnitude of this set of four protons couplings are similar in magnitude to what is observed for the equivalent set of protons [C2' and C6'] for **5-6** \cdot \cdot [$A_{iso} = 4.5$ MHz (0.16 mT)]. Additional satellite features can be observed from very weak dipolar coupling [$A_{iso} \sim 1.6$ MHz] to the *tert*-butyl groups; however, these have been neglected for simplicity. The observed g -values and hyperfine coupling constants reported here are consistent with published values for **5-6** \cdot .^{233, 237} Therefore, unlike reactions carried out in the presence of **5-6**H₂, the reduced galvinoxyl **5-6** appears to produce a unique radical signal distinct from the known spectrum of the **5-6** \cdot , suggesting a modified radical derivative of **5-6** was produced instead.

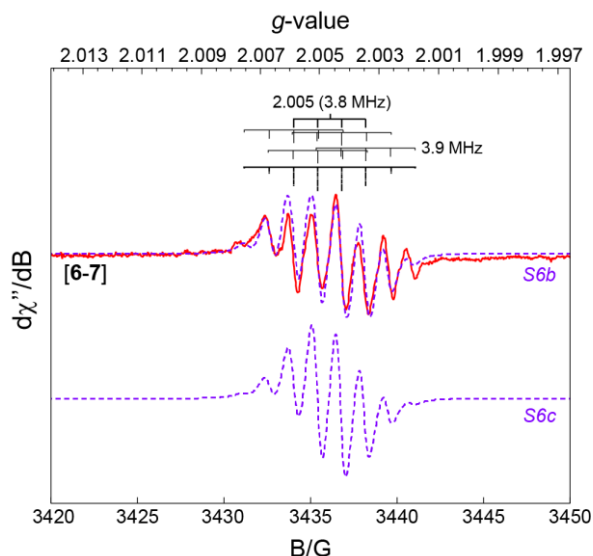


Figure 5-13. Expanded X-band EPR Difference Spectra [6–7]

The identity of this paramagnetic species produced in HAT reactions is not precisely known; however, some arguments can be made based on their spectroscopic properties and similarity to **5-6•**. For instance, the broad multiline signal shown in trace 7 and 8 has many features which are quite similar to the **5-6•**; the species observed is also a doublet of multiplets. As shown Figure 5-12b (simulation *Sim6a*), an accurate match in both hyperfine splitting and intensity of multiplets can be obtained, assuming a strong coupling to a single proton [$A_{iso} = 32.8$ MHz (1.17 mT)] with weaker coupling to a set of 5 equivalent protons [$A_{iso} = 8.3$ MHz (0.29 mT)]. Integration of this signal in trace 7 accounts for 2.2 ± 0.4 μ M. Beyond the obvious inclusion of an additional proton coupling at 8.3 MHz, both sets of hyperfine couplings increase by almost exactly 2-fold relative to couplings observed for **6•**. The fact that both sets of hyperfine features shift by a scalar quantity suggests that this observed transient species is from a modified form of **6•**.

Assignment of the remaining short-lived species represented by the difference spectra in trace [6-7] (Figure 5-12b) is slightly more complicated. To first order, an 8-line signal can be produced by assuming radical coupling to 7 equivalents [^1H , $I = 1/2$] nuclei.

However, similar to what was observed for trace 3, the resulting area for each satellite band should follow a predictable pattern due to the degeneracy of doublets produced by coupling to multiple equivalent $I = 1/2$ nuclei.^{230, 231} To illustrate, a simulation assuming coupling [$A_{iso} = 3.8$ MHz (0.13 mT)] to 7 equivalent protons is shown in Figure 5-13 (simulation *Sim6c*). Of note is the maximal intensity of the central resonance observed at $g = 2.005$ with decreasing area and intensity to either side of the central features. However, the central four doublets observed for the [6–7] difference spectrum are nearly equivalent in area. The only explanation for this behavior is that the observed hyperfine coupling involves a nucleus with a larger nuclear magnetic spin ($I > 1/2$). In this instance, the central quartet is consistent with a $I = 3/2$ nucleus. Given the proposed mechanism for radical initiated HAT shown in Figure 5-4, ^{39}K ($I = 3/2$) is a reasonable choice due to its high natural abundance (93.3%) and the absence of any other quadrupole nuclei in the reaction mixtures. As shown in Figure 5-13, simulations assuming hyperfine coupling to one ^{39}K nucleus [$A_{iso} = 3.8$ MHz (0.13 mT)] and three equivalent ^1H s [$A_{iso} = 3.9$ MHz (0.14 mT)] match both hyperfine splitting and transition intensities observed in the [6–7] difference spectrum. Least square (χ^2) analysis of spectral fits indicates a near 2-fold better agreement with the [6–7] difference spectrum for simulation *Sim6b* as compared to *Sim6c*. While satellite features from the minority ^{41}K ($I = 3/2$) isotope (6.7%) could not be resolved, the 3.8 MHz (0.13 mT) hyperfine splitting is well within the range reported for organometallic radicals exhibiting coupling to ^{39}K .^{238, 239, 240} Spin quantification of this signal represents 1.3 ± 0.3 μM .

It should be pointed out that the nearly equivalent magnitude observed for the four equivalent $I_1 = 1/2$ and single $I_2 = 3/2$ hyperfine terms [3.8 versus 3.9 MHz], suggests the possibility that rather than including four equivalent protons an additional ^{39}K nucleus might be responsible for the splitting instead. Indeed, nearly equivalent fits can be obtained

assuming radical coupling to two equivalent ^{39}K nuclei ($I = 3/2$) both with [$A_{\text{iso}} = 3.8$ MHz (0.13 mT)] rather than four ^1H nuclei. At this time, these two possibilities cannot be unambiguously differentiated but the former solution seems more likely as it is difficult to formulate a radical species not adjacent to at least one proton.

The aforementioned experiments using radical trapping reagents are consistent with the proposed radical mechanism involving LBCI-HAT. However, direct evidence of radical formation in the absence of spin-trapping reagents was not observed under ambient temperatures. Therefore, rapid freeze-quench samples were prepared for HAT reactions for analysis by cryogenic (4-50 K) EPR spectroscopy. These experiments have the benefit of interrogating reaction speciation at shorter time intervals (1-30 seconds) while simultaneously increasing instrumental sensitivity. Freeze-quench EPR samples were prepared by from parallel reactions. Reagents were dissolved in a binary mixture of diisopropyl ether and isopentane [3:1 (v/v)]. This solvent mixture was selected based on its ability to form a frozen glass and its compatibility with reaction components.²⁴¹ Reactions were initiated by addition of KO^tBu. Samples were freeze-quenched at selected time points (5 seconds, 10 seconds, and 30 seconds) by immersion in a liquid N₂ cooled acetone bath. Cryogenic X-band EPR spectra were collected

As an additional control, baseline samples of individual reaction components **5-1a** (**Error! Reference source not found.**, trace 9), H₂SiEt₂, and KO^tBu were prepared within the binary solvent mixture and analyzed by EPR under identical conditions to ensure that any paramagnetic species observed in rapid-quench samples were not introduced by base components of the HAT reaction. As shown in (**Error! Reference source not found.**, trace 10), two radical species can be observed with average g -values (g_{ave}) of 2.006 and 1.993 in samples quenched within 5 seconds. At first glance this spectrum appears much like a doublet split by 2.2 mT (62 MHz). However, the higher field resonance at $g_{\text{ave}} = 1.993$

is absent in samples quenched at 10 and 30 seconds (data not shown), indicating this species decays more rapidly than the low-field (g_{ave} , 2.006) species. Moreover, the intrinsic line width (σ_B) of the $g_{ave} = 1.993$ (σ_B , 0.9 mT) resonance is 3-fold higher than observed for the $g_{ave} = 2.002$ (σ_B , 0.3 mT) signal, indicating that these resonances are attributed to chemically distinct entities. At longer time points, the $g_{ave} = 2.006$ species accumulates, reaching maximum intensity near 10-minutes (**Error! Reference source not found.**, trace 11). This signal exhibits a triplet hyperfine splitting with a 1:2:1 intensity pattern indicating that the radical is strongly coupled [$A_{iso} = 38$ MHz (1.4 mT)] to 2-equivalent ($I = 1/2$) ^1H -nuclei. The concentration of this species observed at 10-min (8.4 μM) was determined by quantitative simulation (**Error! Reference source not found.**, *Sim 11*). However by 30-minutes (**Error! Reference source not found.**, trace 12) this species decreases to 1.6 μM . Collectively, these experiments demonstrate the formation of at least two distinct radical species in HAT reactions in the absence of spin-trapping reagents. Further, the $g_{ave} = 2.006$ species persists at a steady-state concentrations throughout the time course of the reaction (~45 minutes).

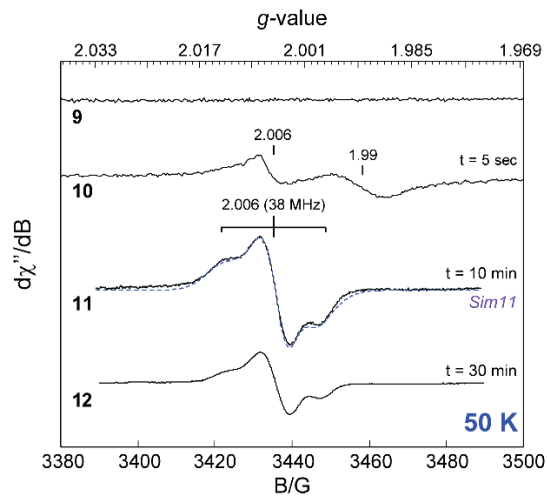


Figure 5-14, 50 K EPR spectra of freeze-quenched HAT reactions

One caveat of with cryogenic measurements of frozen solutions is that the spectral line width is much broader due to unresolved g - and A -anisotropy. In solution, these quantities are time-averaged by molecular motion and therefore the observed spectra appear isotropic in both g - and A -values. By contrast, frozen spectra yield a 'powder pattern' as all possible molecular orientations are trapped. The resulting spectrum is then comprised of a weighted sum of resonances along each principal molecular axis.²⁴² The resulting anisotropy makes it difficult to resolve weaker hyperfine interactions contributing to the increased line width. Therefore, additional experiments are needed to verify if the observed species represents a Si- or C-centered radical, only that it is strongly coupled to 2-equivalent ^1H -protons, suggesting direct bonding to the atom with unpaired electron density

5.8. Hammett Plot Analysis

The effect of *para*-Substituents on the rate of the reaction was investigated. To overcome the issue of polymerization which usually happens with the electron withdrawing substrates, we selected 5 mostly electron rich arenes for this study (Figure 5-15).

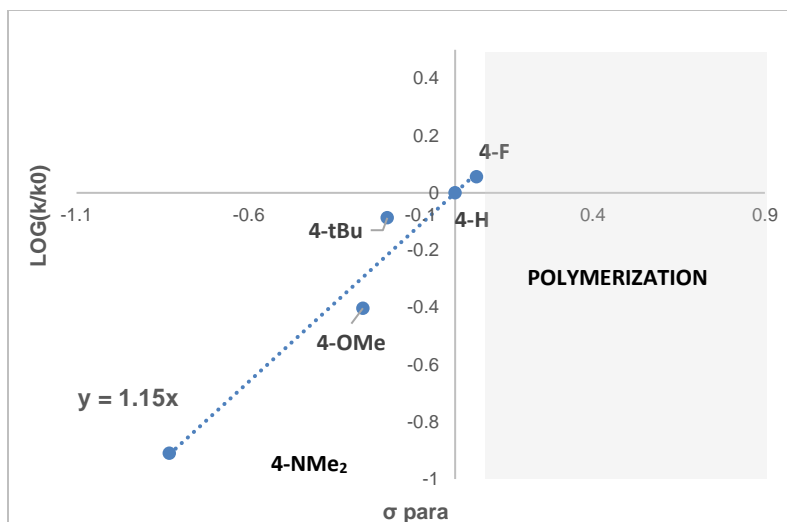


Figure 5-15 Hammett plots using σ

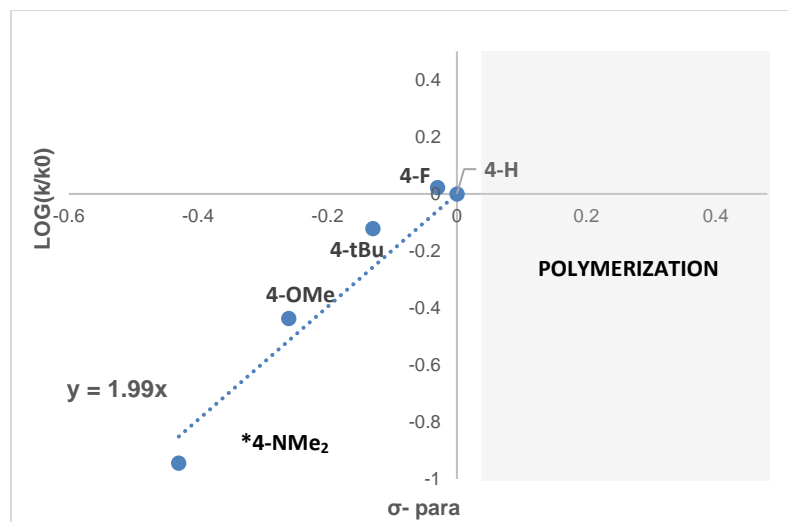


Figure 5-16 Hammett plots using σ^- values. * sigma value of NEt_2 was used.

The observed rho value ($\rho = 1.15$ and $\rho = 1.99$) suggests decline of reactivity with more electron rich systems, which implies possibility of presence of partial negative charge in the RDS. This may be an indication of the proposed radical anion or partially negative intermediates in the catalytic cycle of LBCl-HAT. It should be mentioned that in the

previously reported radical polymerization of styrene, the trend of reactivity is in agreement with our finding.²⁴³

5.9. Kinetic Isotope Effect (KIE) Studies

To have a better understanding of the reaction mechanism and the corresponding intermediates, we designed the following KIE studies: a) parallel reactions, b) intramolecular competition (Figure 5-15). The parallel reaction can be challenging in terms of reproducibility and accuracy of rate measurement, which can be addressed by averaging multiple data points. We chose diphenylsilane because of its higher boiling point and ease of handling and purification. Moreover, in the competition reaction, we added equimolar portion of deuterated silane and its proto form to the reaction mixture

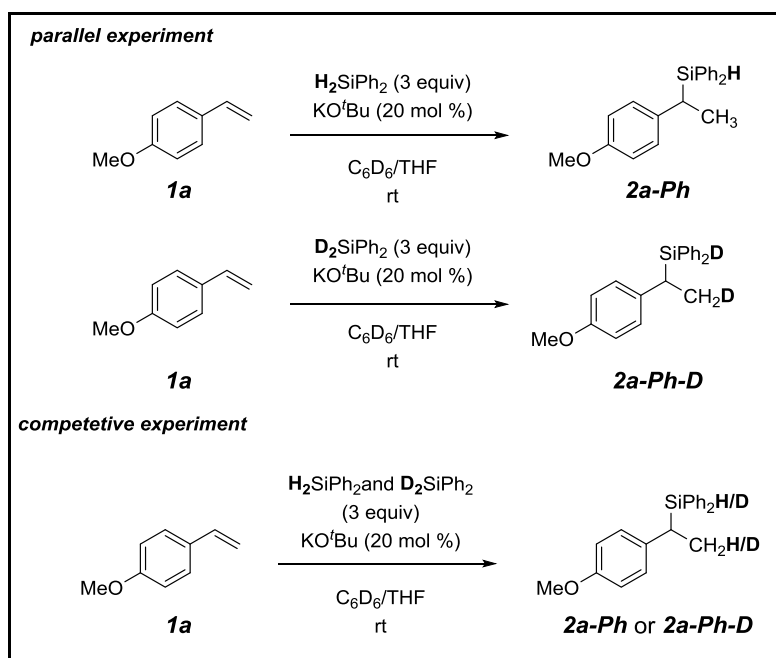


Figure 5-17 Designed KIE experiments

5.9.a.Parallel KIE experiment

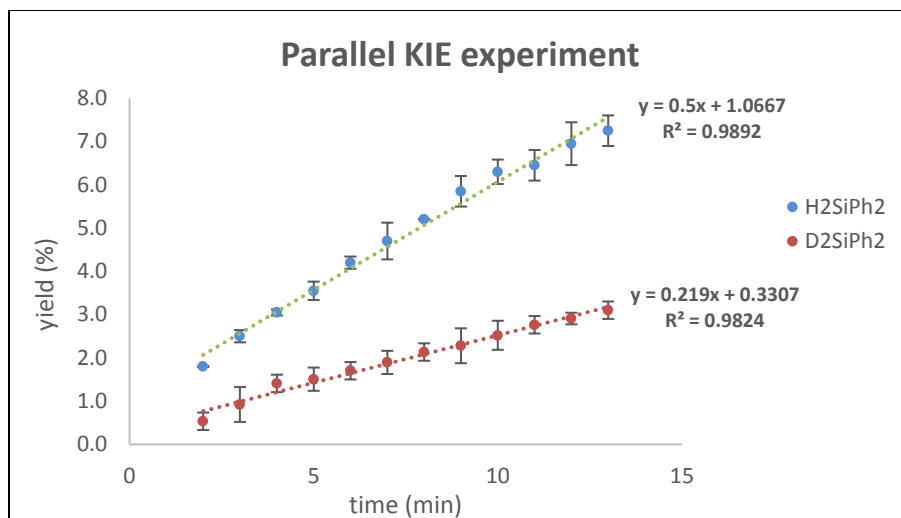


Figure S1. Parallel KIE experiment

$$KIE = \frac{k_H}{k_D} = \frac{0.5}{0.219} = 2.28$$

5.9.b. Intermolecular competition KIE experiment

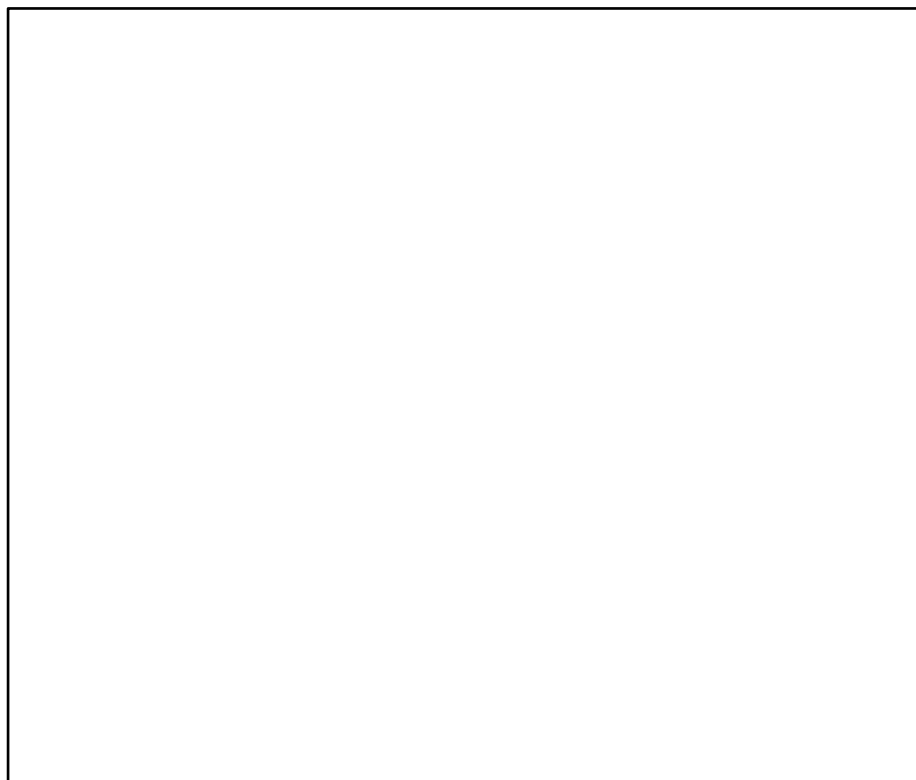
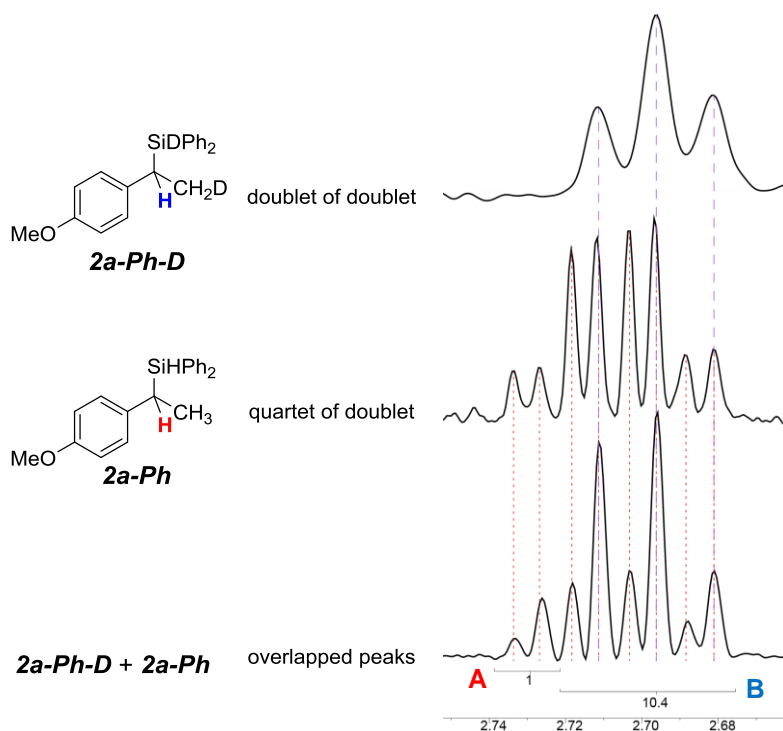


Figure 5-18, ¹H-NMR spectra of competition KIE



Due to overlapping of the corresponding peaks, we did the following calculations to obtain the ratio of k_H/k_D . We presumed that the integration value **A** is 1/8 of area of the methine peak in the **2a-Ph**. And integration value **B** is equal to the 7/8 of methine in **2a-Ph** and all of methane area in **2a-Ph-D**.

Area of **A**=1

Area of **2a-Ph** = 8**A** = 8

The total area of **2a-Ph-D + 2a-Ph** = **A**+**B** = 11.4

Area of **2a-Ph-D** = 11.4 – 8 = 3.4

$$KIE = \frac{k_H}{k_D} = \frac{\text{area of } \mathbf{A} \times \mathbf{8}}{\mathbf{A} + \mathbf{B} - (\text{area of } \mathbf{A} \times \mathbf{8})} = \frac{8}{3.4} = 2.35$$

$$KIE = \frac{k_H}{k_D} = \frac{8}{3.4} = 2.35$$

The observed primary KIE value in both experiments, implies that the rate determining step probably involves homolytic cleavage of Si-H bond.

5.10. Computational studies on LBCI-HAT

Since the LBCI-HAT mechanism involves the formation of an open-shell free radical pair as the key intermediate, which also competes with a hydride transfer process, we employed multistate density function theory (MSDFT) to characterize the intrinsically multiconfigurational features of reaction pathways.^{244, 245, 246} Although a weighted broken-symmetry approach may be employed with standard Kohn-Sham DFT, it only works well for simple situations.²⁴⁷

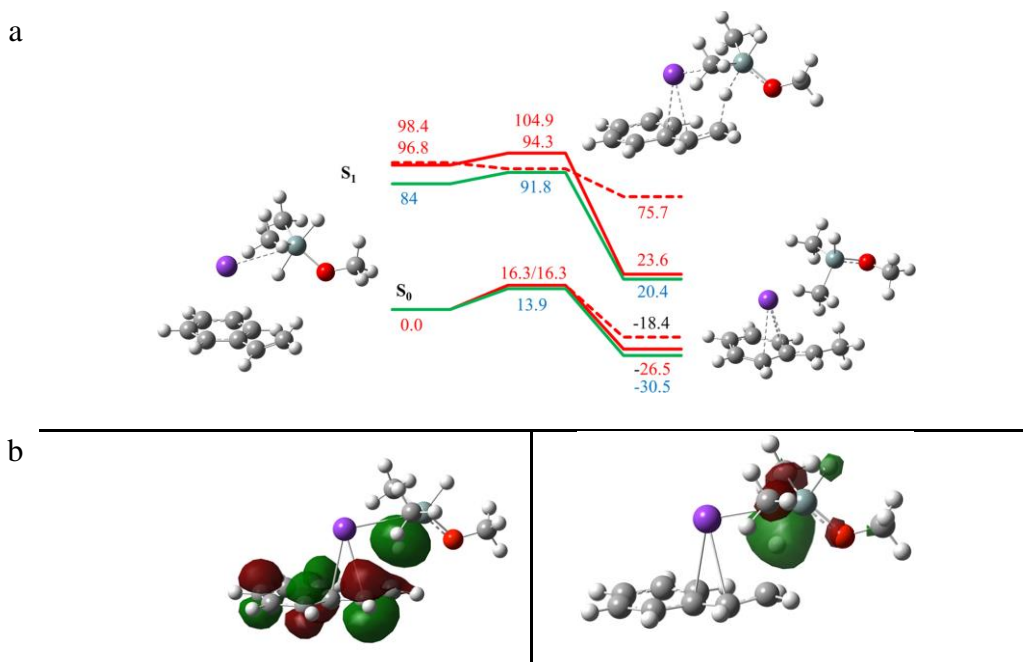


Figure 5-19 Computed reaction energy profile for the LBCI-HAT reactions.

The performance of MSDFT on photochemical processes,²⁴⁴ proton-coupled electron transfer reactions,²⁴⁶ and singlet-triplet energy splitting of diradicals²⁴⁵ is comparable to CASPT2 calculations with less computational costs since dynamic correlation is included

first in the configurational states via DFT. To this end, MSDFT calculations were carried out on the model reactions between $\text{Me}_2\text{H}_2\text{SiR}$ ($\text{R} = \text{OMe}$ or H) and styrene, CH_2CHPh , with and without K^+ as the mediating alkali metal ion. In MSDFT, spin-adapted singlet and triplet biradical states were constructed with the two free radicals localized, respectively, on the $[\text{CH}_3\text{CHPh}\dots\text{K}]^{+\bullet}$ complex and on the reagent $[\text{Me}_2\text{HSiR}]^{-\bullet}$ anion fragment (Figure 5-19). In addition, states corresponding to the HAT mechanism, electron transfer and hydride transfer processes were defined. In all, a total of seven to eleven determinant configurations for the reactions with or without the metal cation, respectively, were included in the multiconfigurational active space. These spin-adapted configurations correspond to valence bond-like states, whose configuration interaction promotes an avoided crossing to yield the adiabatic ground and excited states, and the energies of the latter are shown in Figure 5-19. Consequently, all reaction pathways were treated on the same footing (Appendix F, Table S6). In essence, Figure 5-19 depicts a Shaik-like diagram^{248, 249, 250} that correlates the transition from a closed-shell reactant state of single determinant character to the product with diradical and multiconfigurational character; note that it does not imply that the reaction takes place in the excited state.

The calculations showed that K^+ binds the reactant CH_2CHPh via a cation- π complex that forms a salt-bridge with the pentacoordinate silicon species (Figure 5-19). The computed reaction barriers are 16.3 kcal/mol for R (i.e., LB) = OMe and 13.9 kcal/mol for $\text{R} = \text{H}$ (Figure 5-19a and Appendix F, Table S6) using the PBE0 density functional²⁵¹ and 6-311++G(d,p) basis set. Interestingly, there was essentially no effect on the barrier height with the inclusion of the K^+ ion, suggesting that there is little charge variation from the reactant to the transition state on the styrene substrate to alter cation- π interactions. However, there was a remarkable stabilizing effect on the diradical intermediate/product state by more than 50 kcal/mol (Figure 5-19a), highlighting the importance of cationic

counterion in the reaction. We have computed the Coulson structural weights of the electronic states to gain an insight on their relative contributions to the adiabatic potential energy surface (Appendix F, Table S6). Figure 5-19b shows the two fragment-localized singly occupied molecular orbitals (SOMO) at the transition state where the fragments are defined as $[\text{Me}_2\text{HSiOMe}]^{\bullet-}$ and $[\text{H-styrene-K}]^{\bullet+}$, corresponding to a free radical transfer from the silyl anion to styrene- K^+ complex. This is the predominant configuration at the TS with a Coulson structural weight of about 75% for all reactions.

In all cases, the reactant state complexes were dominated by the closed-shell pentacoordinate silicon anion, and the hydrogen-transfer intermediates comprised about 75% of the hydride transfer configuration and about 25% of biradical character. The transition state structures were of highly multiconfigurational character, consisting of 60-70% of biradical character mixed with about equal contributions from the closed-shell reactant and product configurations. The diradical species correspond to an excited state with less than 1 kcal/mol splitting between the singlet and triplet configurations; however, the energy difference was reduced from about 100 kcal/mol in the reactant state to about 40-50 kcal/mol in the hydrogen transfer intermediate, corresponding to emission of red light, further highlighting the importance of multiconfiguration interaction.

Taken together, all experimental and computational studies presented suggest that the LBCl-HAT produces an intimate radical-radical anion pair cage via the cation- π interaction with weakly coordinating counter cations. This is followed by the cross-radical coupling to provide the branch-selective hydrosilylation product. The reaction can be shifted toward the HAT-initiated polymerization by trapping the cations with 18-crown-6. This observation suggests that the alkali metal ion-mediated complexation is the key for the hydrosilylation product formation. Otherwise, the benzylic radical undergoes rapid polymerization.

5.11. Scope of the LBCI-HAT, branch-selective hydrosilylation and polymerization of vinylarenes.

Upon the establishment of the LBCI-HAT mechanism, the scope of the hydrosilylation and LBCI-HAT-initiated polymerization was investigated. The results are summarized in Figure 8. First, the reaction of vinylarenes with mono- and dihydrosilanes afforded exclusively branched products (**5-2a-Me** to **5-2a-MePh**) (Figure 5-20). Smaller, electron-donating hydrosilanes were generally better reactant for the hydrosilylation. Although LBCI-HAT-initiated polymerization was observed with electron-deficient vinylarenes, most of the hydrosilylations with electron-neutral and -rich vinylarenes worked well with regioselectivity. For example, various mono and di-substituted styrenes only furnished the branched product (**5-2b**, **5-2e** to **5-2o**). In cases of sterically hindered substrates (**5-2b** and **5-2e** to **5-2i**), tetramethyldisiloxane was superior to diethylsilane with substantially improved yields. 1,2-Disubstituted alkenes also underwent the hydrosilylation to give **5-2p** to **5-2s** in excellent yields (92-94%) with regioselectivity. More sterically hindered trisubstituted alkene required elevated temperature to produce **5-2t**. Notably, the exceptional chemoselectivity was observed within **5-1u**, where the catalytic conditions nicely differentiated aryl- versus alkyl-substituted alkenes. Specifically, silane selectively reacted with aryl-substituted alkene and the allyl group remained intact. Finally, to validate the viability of the LBCI-HAT-mediated, late-stage modification of a complex, bioactive natural products leading to their biologically relevant analogues, C2-vinylestradiol was subjected to the identical reaction conditions, which afforded **5-2v** (74% yield, 1:1 *dr*) and potentially sensitive TBS functional group survived.

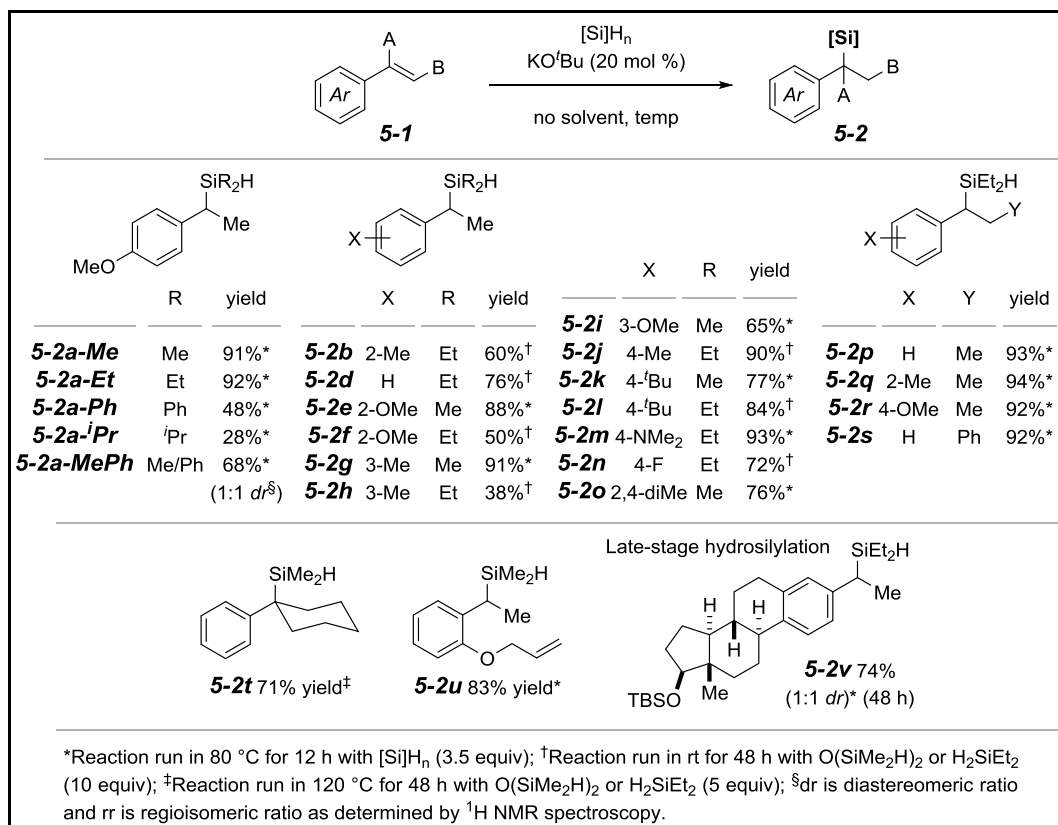


Figure 5-20 Substrate scope of LBCI-HAT reaction

Next, we turned our attention to the LBCI-HAT-initiated polymerization of styrene. 4-Chlorostyrene provided the polystyrenes **5-3w** (M_n 27,600; PDI 2.64) in complete conversion (Figure 5-21a). The more exciting result was that an addition of 18-crown-6 (10 mol%) permitted the polymerization of electron-rich vinylarenes (e.g., 4-methoxystyrene) to afford **5-3a** (M_n 10,400; PDI 1.46) in complete conversion (Figure 5-21b).

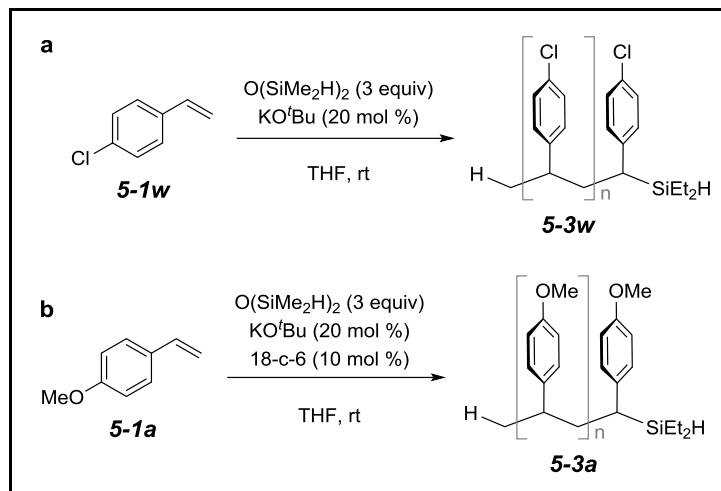


Figure 5-21 HAT initiated polymerization

Furthermore, effect of concentration of silane and KOtBu on Mn, Mw and PDI was examined and our preliminary results suggest that the by lowering the Lewis base concentration, narrower PDIs can be obtained. Effect of silane concentration changes was minimal. (Figure 5-22)

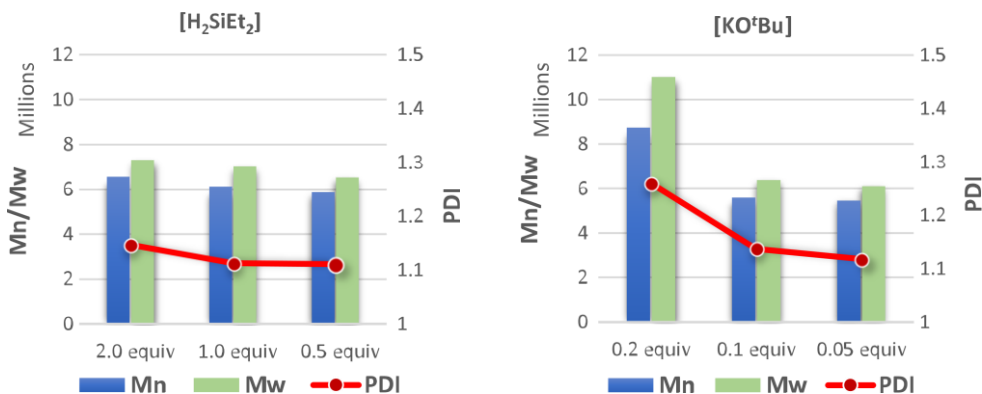


Figure 5-22 Effect of concentration of polymerization

5.12. Synthetic applications.

Having explored the reaction scope presented in Figure 5-20, the synthetic applicability of the catalytically generated, branched benzylic silanes **5-2** was highlighted. First, a single catalytic protocol harnessing the Lewis base permitted dual olefin

hydrosilylation and cross-dehydrogenative arene C–H silylation of 5-vinylindole and 5-vinylbenzofuran.

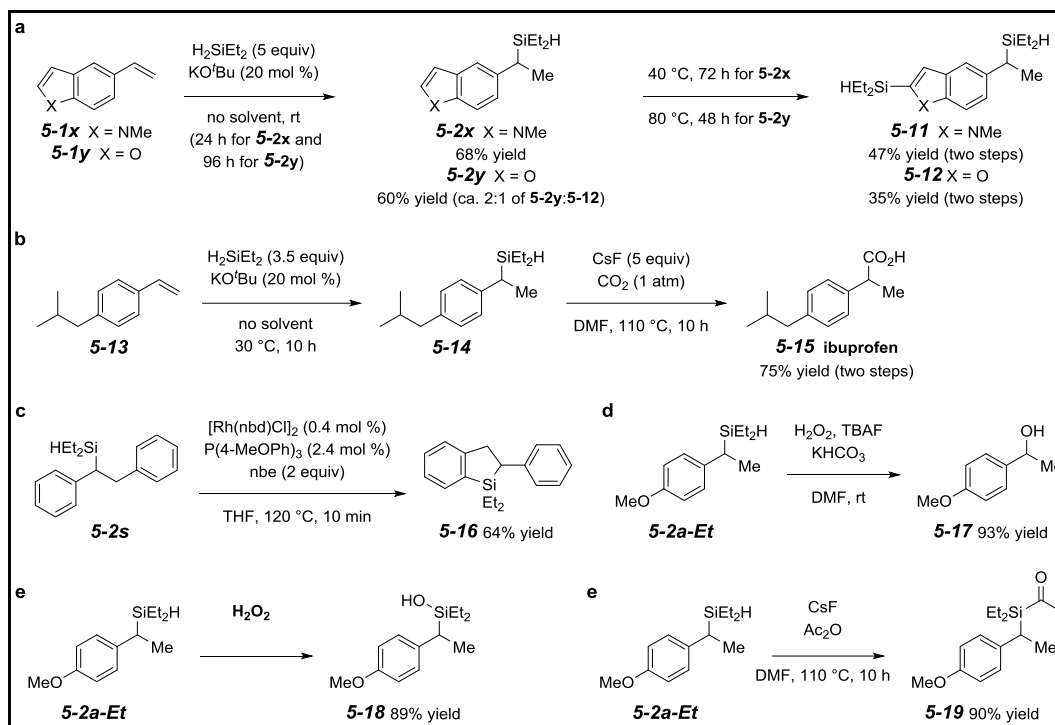


Figure 5-23 Synthetic application of benzyl silanes

Given an interesting reactivity profile of the LBCI-HAT olefin hydrosilylation, the olefin hydrosilylation of vinyl-substituted heterocycles occurred first at room temperature to afford **5-2x** (68% yield) and **5-2y** (60% yield, ca. 2:1 of **2y:12**) (Figure 5-23a). Upon mild heating cross-dehydrogenative silylation of **5-2x** provided **5-11** (47% yield; single-pot, single catalytic system). Although KO^tBu-catalyzed cross-dehydrogenative C2-silylation of benzofuran was not reported by Stoltz and Grubbs,⁵⁰ the reaction of **5-2y** at 80 °C permitted dual olefin and C–H silylation to provide **5-12** (35% from **5-1y**). Second, utilization of carbon dioxide, a renewable C1 source, has emerged as a sustainable chemical technology for the production of value-added products.²⁵² Although the strategy involving stable, yet low polarizable C–Si bond activation as a carbanion synthon has been challenging, transition

metal-free, desilylative carboxylation permitted direct conversion of **5-14** to the 2-arylpropionate derivative. For example, ibuprofen **5-15**, non-steroidal anti-inflammatory drug was synthesized in only two steps without any transition metal catalysts (Figure 5-23b). Third, in recent years siloles have been identified as attractive targets for organic materials, particularly in electronic and optoelectronic devices.²⁵³ The LBCI-HAT hydrosilylation is an appealing tool to rapidly access such molecules, because a Si–H bond present in the hydrosilylation product of stilbene (e.g., **5-2s**) was rapidly relayed to Rh-catalyzed C–H silylation to furnish dihydrobenzosilole **5-16** toward applications to an organic light-emitting diode (OLED) (Figure 5-23c).¹⁷⁷ Oxidation of **5-2a-Et** afforded benzylic alcohol **5-17** in 93% yield (Figure 5-23d). The presented examples illustrate the synthetic utility of the olefin hydrosilylation involving the LBCI-HAT. Furthermore to convert the silanes to silanols we followed procedure reported by Buchwald group²⁰² to access silanol **5-18** in high yield. And finally, we demonstrated the possibility of direct acylation by using a silaphile (CsF) and an acylation source, to obtain **5-19**. These reactions are currently under optimization and development in our group to access them in enantioselective fashion.

5.13. Summary of chapter 5

In this work we demonstrated the Lewis base-catalyzed, complexation-induced HAT (LBCI-HAT) reaction with olefins as a new paradigm for convenient production of synthetically useful, non-toxic small organosilanes, as well as a new class of HAT-initiated styrene polymers for pharmaceutical and materials science applications. The experimental and computational studies were conducted to understand how hydrogen atom and silyl moiety were transferred to unsaturated C–C bonds upon Lewis base catalysis, and provided important insights for the finding of the new, high-performance earth abundant alkali metal Lewis base catalysts to expand the scope of the reaction. Most importantly,

the presented results suggested that the LBCI-HAT manifold developed can function as a more sustainable alternative to the conventional transition metal hydride-catalyzed hydrofunctionalization. It can also serve as a new toolbox for diverse chemical processes, offering advantages for production of new materials and pharmaceutical precursors, which can ultimately address important issues in chemistry, biology, and medicine.

Appendix A

List of all abbreviations

δ : chemical shift (ppm)
 μL : microliter
FG: functional groups
[M⁺]: molecular ion
18.C.6: 1,4,7,10,13,16-hexaoxacyclooctadecane
Ac: acetate
Ad: adamantyl
Aiso: isotropic hyperfine coupling constants
APCI: Atmospheric-pressure chemical ionization
Ar: aryl group or substituent, general
B: anisotropic hyperfine coupling constant
BDE, bond dissociation energy;
Bis(diphenylphosphino)ferrocene
Bn: benzyl
Bu: butyl
C: Celsius
calcd: calculated
cat.: catalyst, catalytic amount
cf: compare to
COD: 1,5-cyclooctadiene
DCM: dichloromethane
Dcpe: 1,2-Bis(dicyclohexylphosphino)ethane
dpp: 1,n-bis(diphenylphosphino)
dppf: 1,1'-Bis(diphenylphosphino)ferrocene
EPR: electron paramagnetic resonance
Eq.: equation
equiv.: equivalent
Et: ethyl

g: gram
G: magnetic field strength
GCMS: gas chromatography mass spectrometry
GHz: gigahertz
GPC: gel permeation chromatography
h: hours
HAT: hydrogen atom transfer
HOMO: Highest occupied molecular orbital
HPLC: high pressure chromatography
HRMS: high resolution mass spectrometry
Hz: hertz
IR: infrared spectroscopy
J: coupling constant, NMR spectroscopy
LB: Lewis Base
LBCI: Lewis base catalyzed complexation induced
LUMO: lowest unoccupied molecular orbital
M: metal, general
M: molar
Me: methyl
mg: milligram
MHz: megahertz
min.: minutes
mL: milliliter
mmol: millimole
 M_n : number average molar mass
 M_w : Mass average molar mass
MPLC: medium pressure chromatography
MSDFT: multistate density function theory

mT: militesla
MW: molecular weight
n/a: not applicable
nbd: norbornadiene
nbe : norbornene
nfom: (non-first-order multiplet)
NHC: N-heterocyclic carbene ligand
NMR: nuclear magnetic resonance spectroscopy
PDI: polydispersity index
RuPhos: 2-Dicyclohexylphosphino-2',6'-diisopropoxybiphenyl
SET: single electron transfer
SOMO: singly occupied molecular orbital
SPhos: 2-Dicyclohexylphosphino-2',6'-dimethoxybiphenyl
tBu: tert-butyl
TEMPO: 2,2,6,6-Tetramethyl-1-piperidinyloxy
TM: transition metals;
TLC: thin layer chromatography
TOF: time of flight
TS: transition state
Xantphos: 4,5-Bis(diphenylphosphino)-9,9-dimethylxanthene
Xantphos: 4,5-Bis(diphenylphosphino)-9,9-dimethylxanthene
XPhos: 2-Dicyclohexylphosphino-2',4',6'-triisopropylbiphenyl

Apendix B

Materials and method

Reactions requiring anhydrous conditions were performed under an atmosphere of nitrogen or argon in flame or oven-dried glassware. Anhydrous toluene and dichloromethane (DCM) were distilled from CaH₂. Anhydrous tetrahydrofuran (THF) and diethyl ether (Et₂O) were distilled from sodium and benzophenone. Triethylamine and pyridine were distilled from KOH. DMF and DMSO were stored over 4 Å molecular sieves. All other solvents and reagents from commercial sources were used as received. NMR spectra were recorded on a 500 or 300 MHz NMR spectrometer. ¹H NMR chemical shifts are referenced to chloroform (7.26 ppm) and DMSO-*d*₆ (2.50 ppm). ¹³C NMR chemical shifts are referenced to ¹³CDCl₃ (77.23 ppm) and DMSO-*d*₆ (39.52 ppm). The following abbreviations are used to describe multiplets: s (singlet), d (doublet), t (triplet), q (quartet), pent (pentet), m (multiplet), nfom (nonfirst-order multiplet), and br (broad). The following format was used to report peaks: chemical shift in ppm [multiplicity, coupling constant(s) in Hz, integral, and assignment]. ¹H NMR assignments are indicated by structure environment (e.g., CH_aH_b). ¹H NMR and ¹³C NMR were processed with the iNMR software program. Infrared (IR) spectra were recorded using neat (for liquid compound) or a thin film from a concentrated DCM solution. Absorptions are reported in cm⁻¹. Only the most intense and/or diagnostic peaks are reported. MPLC refers to medium pressure liquid chromatography (25–200 psi) using hand-packed columns of silica gel (20–45 μm, spherical, 70 Å pore size), an HPLC pump, and a differential refractive index detector. High-resolution mass spectra (HRMS) were recorded in atmospheric-pressure chemical ionization and time-of-flight (APCI/TOF) mode. Samples were introduced as solutions in a mixed solution of methanol and DCM. GC/MS data were recorded on a Varian 450-GC/Varian 240-MS System and Shimadzu GCMS-QP2010 SE. GC-MS experiments using electron impact ionization (EI) were performed at 70 eV using a mass-selective detector. Analytical TLC experiments were performed on an F254 plate with 250 μm thickness. Detection was

performed by UV light or potassium phosphomolybdic acid, potassium permanganate, and *p*-anisaldehyde staining. Gel permeation chromatography (GPC) analyses were conducted on a TOSOH HLC-8320 system with THF as eluent at 1 mL min⁻¹ flow rate. The system was calibrated against linear polystyrene standards in THF. X-band (9 GHz) electron paramagnetic resonance (EPR) spectra were recorded on a Bruker (Billerica, MA) EMX Plus spectrometer equipped with a bimodal resonator (Bruker model 4116DM). A modulation frequency and amplitude of 100 kHz and 0.1 mT was used for all EPR measurements. All experimental data used for spin-quantification were collected under non-saturating conditions. EPR spectra were calculated by diagonalization of the general spin Hamiltonian^{230, 231, 254} for a single electron wavefunction using the software SpinCount (ver. 6.0.6325.21642), written by Professor M. P. Hendrich at Carnegie Mellon University.²⁵⁵ Nuclear hyperfine interactions (**A**) are treated with second order perturbation theory. The simulations were generated with consideration of all intensity factors, both theoretical and experimental, to allow for determination of species concentration. The only unknown factor relating the spin concentration to signal intensity was an instrumental factor that is specific to the microwave detection system. However, this was determined by a spin standard, Cu(EDTA), prepared from a copper atomic absorption standard solution purchased from Sigma-Aldrich.

Appendix C

Experimental Procedures for Chapter 1 and 2

C.1. General Procedure for Preparation of Diethylhydridosilyl Aetals (1-2):

$[\text{Ir}(\text{coe})_2\text{Cl}]_2$ (0.9 mg, 0.1 mol %) and ester **1-1** (1 mmol) were dissolved with CH_2Cl_2 (0.3 mL, 3.3 M). Diethylsilane (0.28 mL, 2 mmol) was added to the mixture. The septum on the vial was replaced by a screw cap with a Teflon liner. The reaction mixture was kept at rt and stirred for 3-12 h. The volatiles were removed *in vacuo* to afford the silyl acetals **1-2**, which were directly used for subsequent reactions without further purification.

C.2. General Procedure for Preparation of Hydridodiisopropylsilyl Aetals (1-2^{iPr}):

$[\text{Ir}(\text{coe})_2\text{Cl}]_2$ (0.9 mg, 0.1 mol %) and ester **1-1** (1 mmol) were dissolved with CH_2Cl_2 (0.3 mL, 3.3 M). Diisopropylsilane (0.38 mL, 2 mmol) was added to the mixture in one portion. The septum on the vial was replaced by a screw cap with a Teflon liner. The reaction mixture was kept at 45 °C and stirred for 24-36 h. The volatiles were removed *in vacuo* to afford the silyl acetals **1-2^{iPr}**, which were directly used for subsequent reactions without further purification.

C.3. General Procedure for Preparation of Cyclic Silyl Acetals (1-3):

$[\text{Rh}(\text{nbd})\text{Cl}]_2$ (1.84 mg, 0.4 mol %), *tris*(4-methoxyphenyl)phosphine (8.45 mg, 2.4 mol %) and norbornene (188 mg, 2 mmol) were dissolved with THF (1 mL, 1 M), silyl acetal **1-2** (1 mmol) was added to the mixture in one portion. The septum on the vial was replaced by a screw cap with a Teflon liner, and the mixture was stirred at 120 °C for 10 min. The reaction progress was monitored by GC/MS spectrometry. The yield of the cyclic silyl acetals **1-3** was determined by ¹H NMR spectroscopy by an addition of CH_2Br_2 (1 mmol) as an internal standard after the volatiles were removed *in vacuo*. Crude material was directly subjected to hydrolysis.

C.4. General Procedure for Preparation of 2-[Diethyl(hydroxy)silyl]benzaldehyde (2-1) and 2-(Hydroxydiisopropylsilyl)benzaldehyde (2-2)

The crude cyclic silyl acetal **1-3** (1 mmol) was dissolved by a 1:1 mixture (v/v) of acetonitrile and pH 5 buffer (1 mL:1 mL, total concentration = 0.5 M) and stirred at rt for 10 h. The mixture was extracted with diethyl ether (5 mL×4). The combined organic layer was washed with water (10 mL) and brine (10 mL), and dried over anhydrous sodium sulfate. The volatiles were removed *in vacuo*, and the crude mixture was purified by MPLC to afford silanol aldehyde **2-2**

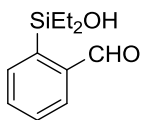
C.5. Gram Scale Synthesis of 2-[Diethyl(hydroxy)silyl]benzaldehyde (2-1-1)

[Ir(coe)₂Cl]₂ (10 mg, 0.1 mol %) and methyl benzoate **1a-Me** (1.5 mL, 12 mmol) were dissolved with CH₂Cl₂ (6 mL, 2 M). Diethylsilane (2.0 mL, 14.4 mmol, 1.2 equiv) was added to the mixture slowly (the reaction was exothermic). The septum on the vial was replaced by a screw cap with a Teflon liner. The reaction mixture was stirred at rt for 10 h. The volatiles were removed *in vacuo* to afford the silyl acetal **4a-Me**, which was directly used for subsequent C–H silylation without further purification. [Rh(nbd)Cl]₂ (22.1 mg, 0.4 mol %), *tris*(4-methoxyphenyl)phosphine (101 mg, 2.4 mol %), and norbornene (2.26 g, 24 mmol) were dissolved with THF (6 mL, 2 M), the crude silyl acetal **4a-Me** was added to the mixture. The septum on the vial was replaced by a screw cap with a Teflon liner, and the mixture was stirred at 120 °C for 10 min. The yield of cyclic silyl acetal **6a-Me** was determined by ¹H NMR spectroscopy by an addition of CH₂Br₂ as an internal standard after the volatiles were removed *in vacuo*. The crude material **6a-Me** was dissolved by a 1:1 mixture (v/v) of acetonitrile and pH 5 buffer (6 mL: 6 mL, total concentration = 1 M) and stirred at rt for 10 h. The mixture was extracted with diethyl ether (20 mL×4). The combined organic layer was washed with water (20 mL) and brine (20 mL), and dried over anhydrous

sodium sulfate. The volatiles were removed *in vacuo*, and the crude mixture was purified by MPLC (hexanes/EtOAc = 5:1, 7 mL/min, retention time 8 min) to afford *ortho*-formyl arylsilanol **2a** (1.8 g, 72% yield) as a pale yellow liquid.

C.6. Compound Characterization for chapter 1 and 2

2-[Diethyl(hydroxy)silyl]benzaldehyde (2-1-1)



Yield: 1 mmol scale, 162 mg, 78%; 12 mmol scale, 1.80 g, 72%.

¹H NMR (CDCl₃, 500 MHz): δ 10.0 (s, 1H, CHO), 7.89 (dd, *J* = 7.0, 1.6 Hz, 1H, CHOCC*H*), 7.79 (dd, *J* = 7.0, 1.6 Hz, 1H, SiCCH), 7.64 (ddd, *J* = 7.4, 7.4, 1.6 Hz, 1H, CHOCC*HCH* or SiCCH*CH*), 7.61 (ddd, *J* = 7.4, 7.4, 1.6 Hz, 1H, CHOCC*HCH* or SiCCH*CH*), 3.15 (br, 1H, SiOH), 0.99-0.95 [m, 6H, Si(CH₂CH₃)₂], and 0.92-0.89 [m, 4H, Si(CH₂CH₃)₂].

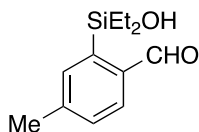
¹³C NMR (CDCl₃, 75 MHz): δ 196.0, 141.2, 139.6, 136.1, 135.5, 133.8, 129.9, 7.1, and 6.5.

IR (neat): 3409 (br, m), 2955 (w), 1685 (s), 1200 (m), 1039 (s), 1003 (s), and 707 (s) cm⁻¹.

TLC: R_f = 0.5 in 5:1 hexanes: EtOAc.

HRMS (ESI/TOF): Calcd for (M+K)⁺ (C₁₁H₁₆KO₂Si)⁺: 247.0551. Found: 247.0568.

2-[Diethyl(hydroxy)silyl]-4-methylbenzaldehyde (2-1-2)



Yield: 1 mmol scale, 160 mg, 72%.

¹H NMR (CDCl₃, 500 MHz): δ 9.94 (s, 1H, CHO), 7.77 (d, *J* = 7.7 Hz, 1H, CHOCC*H*), 7.57 (d, *J* = 1.6 Hz, 1H, SiCCH), 7.39 (dd, *J* = 7.7, 1.6 Hz, 1H, CHOCC*HCH*), 3.14 (br s, 1H, SiOH), 0.98-0.95 [m, 6H, Si(CH₂CH₃)₂], and 0.91-0.88 [m, 4H, Si(CH₂CH₃)₂].

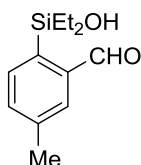
^{13}C NMR (CDCl_3 , 75 MHz): δ 195.5, 144.8, 139.5, 139.0, 137.1, 136.2, 130.4, 22.2, 7.2, and 6.5.

IR (neat): 3372 (br, w), 2955 (m), 2874 (m), 1692 (m), 1592 (m), 1200 (m), 1039 (s), 1003 (s), 792 (s), and 704 (s) cm^{-1} .

TLC: R_f = 0.5 in 5:1 hexanes: EtOAc.

HRMS (ESI/TOF): Calcd for $(\text{M}+\text{Na})^+$ ($\text{C}_{12}\text{H}_{18}\text{NaO}_2\text{Si}$): 245.0968. Found: 245.0987.

2-[Diethyl(hydroxy)silyl]-5-methylbenzaldehyde (2-1-3)



Yield: 1 mmol scale, 140 mg, 63%.

^1H NMR (CDCl_3 , 500 MHz): δ 9.98 (s, 1H, CHO), 7.68 (d, J = 1.6 Hz, 1H, CHOCC H), 7.66 (d, J = 7.4 Hz, 1H, SiCCH), 7.57 (dd, J = 7.4, 1.6 Hz, 1H, CHOCC H CH), 3.00 (br s, 1H, SiOH), 0.98-0.94 [m, 6H, Si(CH $_2$ CH $_3$) $_2$], and 0.92-0.89 [m, 4H, Si(CH $_2$ CH $_3$) $_2$].

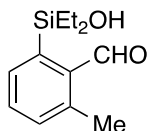
^{13}C NMR (CDCl_3 , 125 MHz): δ 196.3, 141.5, 140.1, 136.7, 136.2, 136.0, 134.6, 21.2, 7.2, and 6.5.

IR (neat): 3407 (br, m), 2955 (m), 1684 (m), 1461 (m), 1189 (m), 1045 (s), 1015 (s), 977 (s), and 712 (s) cm^{-1} .

TLC: R_f = 0.45 in 5:1 hexanes: EtOAc.

HRMS (ESI/TOF): Calcd for $(\text{M}+\text{Na})^+$ ($\text{C}_{12}\text{H}_{18}\text{NaO}_2\text{Si}$): 245.0968. Found: 245.0983.

2-[Diethyl(hydroxy)silyl]-6-methylbenzaldehyde (2-1-4)



Yield: 1 mmol scale, 191 mg, 86%.

^1H NMR (CDCl_3 , 500 MHz): δ 10.5 (s, 1H, CHO), 7.77 (d, J = 7.5 Hz, 1H, SiCCH or MeCCH), 7.41 (dd, J = 7.5, 7.5 Hz, 1H, SiCCHCH), 7.26 (d, J = 7.5 Hz, 1H, SiCCH or MeCCH), 2.68 (s, 3H, ArCH $_3$), 2.08 (br s, 1H, SiOH), 1.01-0.97 [m, 2H, Si(CH $_2$ CH $_3$) $_2$], and

0.93-0.90 [m, 8H, Si(CH₂CH₃)₂ and Si(CH₂CH₃)₂].

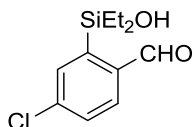
¹³C NMR (CDCl₃, 125 MHz): δ 193.4, 141.7, 141.4, 139.3, 134.8, 133.1, 132.7, 20.4, 8.5, and 7.7.

IR (neat): 3407 (br, m), 2956 (m), 1683 (m), 1459 (m), 1179 (m), 1046 (s), 1004 (s), 978 (s), and 711 (s) cm⁻¹.

TLC: R_f = 0.45 in 5:1 hexanes: EtOAc.

HRMS (ESI/TOF): Calcd for (M+Na)⁺ (C₁₂H₁₈NaO₂Si)⁺: 245.0968. Found: 245.0992.

4-Chloro-2-[diethyl(hydroxy)silyl]benzaldehyde (2-1-5)



Yield: 1 mmol scale, 179 mg, 74%.

¹H NMR (CDCl₃, 500 MHz): δ 9.97 (s, 1H, CHO), 7.82 (d, *J* = 8.1 Hz, 1H, CHOCC*H*), 7.76 (d, *J* = 2.1 Hz, 1H, SiC*C**H*), 7.57 (dd, *J* = 8.1, 2.1 Hz, 1H, CHOCC*H**C**H*), 3.00 (br s, 1H, SiOH), 0.98-0.94 [m, 6H, Si(CH₂CH₃)₂], and 0.92-0.89 [m, 4H, Si(CH₂CH₃)₂].

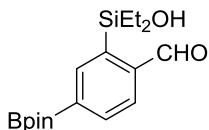
¹³C NMR (CDCl₃, 125 MHz): δ 194.3, 142.2, 141.0, 139.3, 136.39, 136.30, 129.9, 7.0, and 6.3.

IR (neat): 3440 (br, w), 2957 (m), 2876 (m), 1694 (s), 1547 (m), 1039 (s), 1003 (s), 728 (s), 698 (s), and 442 (s) cm⁻¹.

TLC: R_f = 0.45 in 5:1 hexanes: EtOAc.

HRMS (ESI/TOF): Calcd for (M+Na)⁺ (C₁₁H₁₅NaO₂Si)⁺: 265.0422. Found: 265.0437.

2-[Diethyl(hydroxy)silyl]-4-(4,4,5,5-tetramethyl-1,3,2-dioxaborolan-2-yl)benzaldehyde (2-1-6)



Yield: 1 mmol scale, 250 mg, 75%.

¹H NMR (CDCl₃, 500 MHz): δ 10.0 (s, 1H, CHO), 8.19 (d, *J* = 1.2 Hz, 1H, SiC*C**H*), 8.02 (dd, *J* = 7.4, 1.2 Hz, 1H, CHOCC*H**C**H*), 7.86 (d, *J* = 7.4 Hz, 1H, CHOCC*H*), 3.03 (br s,

1H, SiOH), 1.36 {s, 12H, B[OC(CH₃)₂]₂}, 0.99-0.96 [m, 6H, Si(CH₂CH₃)₂], and 0.94-0.91 [m, 4H, Si(CH₂CH₃)₂].

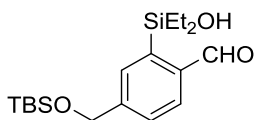
¹³C NMR (CDCl₃, 125 MHz): δ 196.2, 143.0, 142.1, 138.3, 136.3 (2), 134.4, 84.5, 25.1, 7.2, and 6.6.

IR (neat): 3441 (br, m), 2977 (m), 2875 (m), 1695 (s), 1473 (m), 1354 (s), 1141 (s), 1095 (s), 962 (s), 821 (s), 666 (s), and 430 (s) cm⁻¹.

TLC: R_f = 0.4 in 5:1 hexanes: EtOAc.

HRMS (ESI/TOF): Calcd for (M+H)⁺ (C₁₇H₂₈BO₄Si)⁺: 335.1844. Found: 335.1828.

4-[[*tert*-Butyldimethylsilyloxy]methyl]-2-[diethyl(hydroxy)silyl]benzaldehyde (2-1-7)



Yield: 1 mmol scale, 274 mg, 78%.

¹H NMR (CDCl₃, 500 MHz): δ 9.98 (s, 1H, CHO), 7.85 (d, *J* = 7.8 Hz, 1H, CHOCH), 7.72 (s, 1H, SiCCH), 7.56 (d, *J* = 7.8 Hz, 1H, CHOCHCH), 4.83 (s, 2H, CH₂OTBS), 3.29 (br s, 1H, SiOH), 0.98-0.95 [m, 6H, Si(CH₂CH₃)₂], 0.96 [s, 9H, Si(CH₃)₂(CH₃)₃], 0.92-0.89 [m, 4H, Si(CH₂CH₃)₂], and 0.12 [s, 6H, Si(CH₃)₂(CH₃)₃].

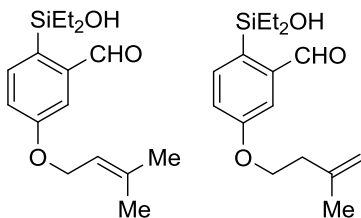
¹³C NMR (CDCl₃, 125 MHz): δ 195.7, 147.7, 140.2, 139.6, 136.1, 133.4, 127.0, 64.7, 26.1, 18.5, 7.2, 6.5, and 5.1.

IR (neat): 3449 (br, m), 2954 (m), 2877 (m), 1692 (s), 1462 (m), 1253 (m), 1098 (s), 834 (s), 776 (s), 731 (s), and 708 (s) cm⁻¹.

TLC: R_f = 0.4 in 10:1 hexanes: EtOAc.

HRMS (ESI/TOF): Calcd for (M+Na)⁺ (C₁₈H₃₂NaO₃Si₂)⁺: 375.1782. Found: 375.1794.

2-[Diethyl(hydroxy)silyl]-5-[(3-methylbut-2-en-1-yl)oxy]benzaldehyde (2-1-8)



1,1-Disubstituted alkene via alkene migration were isolated along with the desired

product as an inseparable mixture. The ratio of isomers' is 1: 0.09.

Total Yield: 1 mmol scale, 223 mg, 78%.

¹H NMR (CDCl₃, 500 MHz) for internal alkene: δ 9.98 (s, 1H, CHO), 7.67 (d, *J* = 8.1 Hz, 1H, SiCCH), 7.42 (d, *J* = 2.6 Hz, 1H, CHOCCH), 7.14 (dd, *J* = 8.1, 2.6 Hz, 1H, SiCCHCH), 5.50 (app t, *J* = 6.8 Hz, 1H, ArOCH₂CH=CMe₂), 4.59 (d, *J* = 6.8 Hz, 2H, ArOCH₂CH=CMe₂), 3.06 (br s, 1H, SiOH), 1.81 [s, 3H, ArOCH₂CH=C(CH₃)₂], 1.76 [s, 3H, ArOCH₂CH=C(CH₃)₂], 0.97-0.94 [m, 6H, Si(CH₂CH₃)₂], and 0.89-0.86 [m, 4H, Si(CH₂CH₃)₂].

¹H NMR (CDCl₃, 500 MHz) for terminal alkene: 9.98 (s, 0.09H, CHO), 7.67 (d, *J* = 8.1 Hz, 0.09H, SiCCH), 7.42 (d, *J* = 2.6 Hz, 0.09H, CHOCCH), 7.14 (dd, *J* = 8.1, 2.6 Hz, 0.09H, SiCCHCH), 4.86 (app s, 0.09H, CH_aH_b=CMe₂), 4.81 (app s, 0.09H, CH_aH_b=CMe₂), 4.16 (t, *J* = 6.8 Hz, 0.18H, ArOCH₂CH₂), 2.53 (t, *J* = 6.8 Hz, 0.18H, ArOCH₂CH₂), 1.81 [s, 0.27H, CH_aH_b=CCH₃], 0.97-0.94 [m, 0.54H, Si(CH₂CH₃)₂], and 0.89-0.86 [m, 0.36H, Si(CH₂CH₃)₂].

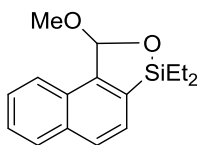
¹³C NMR (CDCl₃, 125 MHz) only for internal alkene: δ 195.6, 160.4, 142.9, 139.2, 137.6, 130.2, 121.6, 119.6, 119.1, 65.1, 26.0, 18.4, 7.2, and 6.7.

IR (neat): 3408 (br, m), 2955 (m), 2875 (m), 1688 (s), 1591 (s), 1267 (s), 1231 (m), 1071 (s), 1002 (s), 825 (s), and 707 (s) cm⁻¹.

TLC: R_f = 0.45 in 5:1 hexanes: EtOAc.

HRMS (ESI/TOF): Calcd for (M+H)⁺ (C₁₆H₂₅O₃Si)⁺: 293.1567. Found: 293.1578.

3,3-Diethyl-1-methoxy-1,3-dihydronaphtho[2,1-c][1,2]oxasilole (2-1-9)



Yield: 1 mmol scale, 247 mg, 91%.

¹H NMR (CDCl₃, 500 MHz): δ 8.14 (dddd, *J* = 8.1, 1.5, 0.6, 0.6 Hz, 1H, naphthalene-H5), 7.92 (ddd, *J* = 8.1, 1.5, 0.6 Hz, 1H, naphthalene-H8), 7.89 (dd, *J* = 8.0, 0.6 Hz, 1H, naphthalene-H4), 7.62 (d, *J* = 8.0 Hz, 1H, naphthalene-H3), 7.60 (ddd, *J* = 8.1, 6.9, 1.5 Hz, 1H, naphthalene-H6 or naphthalene-H7), 7.56 (ddd, *J* = 8.1, 6.9, 1.5 Hz, 1H, naphthalene-H6 or naphthalene-H7), 6.60 (s, 1H, SiOCHOMe), 3.64 (s, 3H, OMe), 1.11-1.07 [m, 3H, Si(CH₂CH₃)₂], 1.03-0.94 [m, 7H, Si(CH₂CH₃)₂ and Si(CH₂CH₃)₂].

¹³C NMR (CDCl₃, 125 MHz): δ 146.3, 134.8, 132.7, 129.5, 129.2, 128.6, 126.79, 126.75(2), 124.3, 104.2, 54.4, 7.1, 6.7, 6.64 and 6.61.

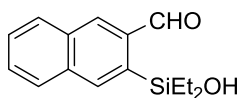
IR (neat): 3047 (w), 2955 (m), 2875 (m), 1507 (m), 1234 (m), 1097 (s), 1045 (s), 862 (s), 728 (s), 705 (s), and 435 (s) cm⁻¹.

TLC: R_f = 0.4 in 10:1 hexanes: EtOAc.

GCMS (5029017): t_R = 12.08 min, m/z 272 (M⁺, 20), 271 [(M-H)⁺, 25], and 241 [(M-OMe)⁺, 100].

HRMS (ESI/TOF): Calcd for (M+Na)⁺ (C₁₆H₂₀NaO₂Si)⁺: 295.1125. Found: 295.15138.

3-[Diethyl(hydroxy)silyl]-2-naphthaldehyde (2-1-10)



Yield: 1 mmol scale, 186 mg, 72%.

¹H NMR (CDCl₃, 500 MHz): δ 10.1 (s, 1H, CHO), 8.37 (s, 1H, naphthalene-H1 or naphthalene-H4), 8.22 (s, 1H, naphthalene-H1 or naphthalene-H4), 8.00 (dd, J = 8.1, 1.3 Hz, 1H, naphthalene-H8 or naphthalene-H5), 7.93 (dd, J = 8.1, 1.3 Hz, 1H, naphthalene-H8 or naphthalene-H5), 7.69 (ddd, J = 8.1, 7.0, 1.3 Hz, 1H, naphthalene-H6 or naphthalene-H7), 7.62 (ddd, J = 8.1, 7.0, 1.3 Hz, 1H, naphthalene-H6 or naphthalene-H7), 3.25 (br s, 1H, SiOH), 1.03-0.96 [m, 10H, Si(CH₂CH₃)₂ and Si(CH₂CH₃)₂].

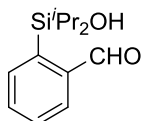
¹³C NMR (CDCl₃, 125 MHz): δ 195.7, 139.4, 138.6, 137.7, 135.7, 133.3, 132.9, 129.9, 129.3, 128.7, 128.0, 7.3, and 6.6.

IR (neat): 3441 (br, m), 2954 (m), 2873 (m), 1688 (s), 1450 (m), 1212 (m), 1141 (m), 1031 (s), 746 (s), 702 (s), and 477 (s) cm⁻¹.

TLC: R_f = 0.4 in 5:1 hexanes: EtOAc.

HRMS (ESI/TOF): Calcd for (M+H)⁺ (C₁₅H₁₉O₂Si)⁺: 259.1149. Found: 259.1157.

2-(Hydroxydiisopropylsilyl)benzaldehyde (2-2-1)



The ratio of aldehyde and silyl hemiacetal is 1:0.07.

Yield: 1 mmol scale, 215 mg, 91%; 6 mmol scale, 1.19 g, 84%.

¹H NMR (CDCl₃, 500 MHz): δ 10.0 (s, 1H, CHO), 7.90 (dd, *J* = 7.3, 1.6 Hz, 1H, CHOCCH), 7.81 (dd, *J* = 7.3, 1.6 Hz, 1H, SiCCH), 7.62 (ddd, *J* = 7.3, 7.3, 1.6 Hz, 1H, CHOCCHCH or SiCCHCH), 7.59 (ddd, *J* = 7.3, 7.3, 1.6 Hz, 1H, CHOCCHCH or SiCCHCH), 3.51 (br s, 1H, SiOH), 1.34 [septet, *J* = 7.4 Hz, 2H, CH(CH₃)₂], 1.08 [d, *J* = 7.4 Hz, 6H, CH(CH₃)₂], and 0.90 [d, *J* = 7.4 Hz, 6H, CH(CH₃)₂].

¹H NMR (CDCl₃, 500 MHz) for silyl hemiacetal: 7.55 [dd, *J* = 7.0, 1.2 Hz, 0.07H, C(OSi)CCH or SiCCH], 7.50 (dd, *J* = 7.6, 1.2 Hz, 0.07H, C(OSi)CCH or SiCCH], 7.47 [ddd, *J* = 7.6, 7.0, 1.2 Hz, 0.07H, C(OSi)CCH or SiCCHCH], 7.39 (ddd, *J* = 7.0, 7.0, 1.2 Hz, 0.07H, C(OSi)CCH or SiCCHCH], 6.36 (br s, 0.07H, SiOCH₂OH), 1.37 [septet, *J* = 7.4 Hz, 0.07H, CH(CH₃)₂], 1.30 [septet, *J* = 7.4 Hz, 0.07H, CH(CH₃)₂], 1.06 [d, *J* = 7.4 Hz, 0.21H, CH(CH₃)₂], 1.04 [d, *J* = 7.4 Hz, 0.21H, CH(CH₃)₂], 1.00 [d, *J* = 7.4 Hz, 0.21H, CH(CH₃)₂], and 0.98 [d, *J* = 7.4 Hz, 0.21H, CH(CH₃)₂].

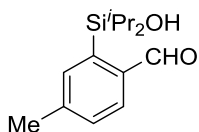
¹³C NMR (CDCl₃, 125 MHz): δ 196.2, 141.8, 139.0, 136.4, 135.6, 133.5, 129.7, 17.9, 17.7, and 13.3.

IR (neat): 3441 (br, m), 2944 (m), 2864 (m), 1686 (s), 1462 (s), 1202 (s), 1076 (m), 879 (s), 755 (s), 661 (s), and 505 (s) cm⁻¹.

TLC: R_f = 0.5 in 5:1 hexanes: EtOAc.

HRMS (ESI/TOF): Calcd for (M+K)⁺ (C₁₃H₂₀KO₂Si)⁺: 275.0864. Found: 275.0844.

2-(Hydroxydiisopropylsilyl)-4-methylbenzaldehyde (2-2-2)



The ratio of aldehyde and silyl hemiacetal is 1:0.02.

Yield: 1 mmol scale, 225 mg, 90%.

¹H NMR (CDCl₃, 500 MHz) only for aldehyde: δ 9.94 (s, 1H, CHO), 7.78 (d, *J* = 7.7 Hz, 1H, CHOCCH), 7.59 (s, 1H, SiCCH), 7.37 (d, *J* = 7.7 Hz, 1H, CHOCCHCH), 3.61 (br s, 1H, SiOH), 2.44 (s, 3H, ArCH₃), 1.33 [septet, *J* = 7.4 Hz, 2H, CH(CH₃)₂], 1.07 [d, *J* = 7.4 Hz, 6H, CH(CH₃)₂], and 0.89 [d, *J* = 7.4 Hz, 6H, CH(CH₃)₂].

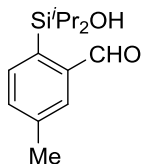
¹³C NMR (CDCl₃, 125 MHz) only for aldehyde: δ 195.5, 144.4, 139.4, 138.9, 137.3, 136.0, 120.2, 22.2, 18.0, 17.7, and 13.3.

IR (neat): 3443 (br, m), 2944 (m), 2864 (m), 1685 (s), 1462 (s), 880 (s), 817 (s), 790 (s), and 485 (s) cm⁻¹.

TLC: $R_f = 0.5$ in 5:1 hexanes: EtOAc.

HRMS (ESI/TOF): Calcd for $(M+K)^+$ ($C_{14}H_{22}KO_2Si$): 289.1021. Found: 289.1011.

2-(Hydroxydiisopropylsilyl)-5-methylbenzaldehyde (2-2-3)



The ratio of aldehyde and silyl hemiacetal is 1:0.04.

Yield: 1 mmol scale, 167 mg, 67%.

1H NMR ($CDCl_3$, 500 MHz) only for aldehyde: δ 9.99 (s, 1H, CHO), 7.71 (d, $J = 1.6$ Hz, 1H, CHOCC H), 7.67 (d, $J = 7.5$ Hz, 1H, SiCCH), 7.44 (dd, $J = 7.5, 1.6$ Hz, 1H, SiCCHCH), 3.47 (br s, 1H, SiOH), 2.45 (s, 3H, ArCH $_3$), 1.34 [septet, $J = 7.4$ Hz, 2H, CH(CH $_3$) $_2$], 1.07 [d, $J = 7.4$ Hz, 6H, CH(CH $_3$) $_2$], and 0.90 [d, $J = 7.4$ Hz, 6H, CH(CH $_3$) $_2$].

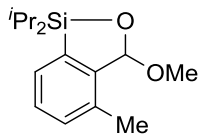
^{13}C NMR ($CDCl_3$, 125 MHz) only for aldehyde: δ 196.4, 142.0, 139.8, 136.5 (2), 135.3, 134.3, 21.2, 17.9, 17.6, and 13.3.

IR (neat): 3450 (br, m), 2944 (m), 2864 (m), 1681 (s), 1462 (s), 880 (s), 823 (s), 660 (s), and 479 (s) cm^{-1} .

TLC: $R_f = 0.5$ in 5:1 hexanes: EtOAc.

HRMS (ESI/TOF): Calcd for $(M+Na)^+$ ($C_{14}H_{22}NaO_2Si$): 273.1281. Found: 273.1269.

1,1-Diisopropyl-3-methoxy-4-methyl-1,3-dihydrobenzo[*c*][1,2]oxasilole (1-3-4)



Yield: 1 mmol scale, 238 mg, 90%.

1H NMR ($CDCl_3$, 500 MHz): δ 7.36 (d, $J = 7.4$ Hz, 1H, MeCCH or SiCCH), 7.27 (dd, $J = 7.4, 7.4$ Hz, 1H, MeCCHCH), 7.21 (d, $J = 7.4$ Hz, 1H, MeCCH or SiCCH), 6.00 (s, 1H, SiOCHOMe), 3.56 (s, 3H, OCH $_3$), 2.36 (s, 3H, ArCH $_3$), 1.25 [septet, $J = 7.4$ Hz, 1H, CH(CH $_3$) $_2$], 1.21 [septet, $J = 7.4$ Hz, 1H, CH(CH $_3$) $_2$], 1.08 [d, $J = 7.4$ Hz, 3H, CH(CH $_3$) $_2$], 1.06 [d, $J = 7.4$ Hz, 3H, CH(CH $_3$) $_2$], 1.01 [d, $J = 7.4$ Hz, 3H, CH(CH $_3$) $_2$] and 0.95 [d, $J = 7.4$ Hz, 3H, CH(CH $_3$) $_2$].

¹³C NMR (CDCl₃, 125 MHz): δ 147.8, 134.4, 132.9, 132.0, 129.3, 128.8, 104.5, 55.1, 18.6, 17.41, 17.37, 17.19, 17.13, 12.76 and 12.67.

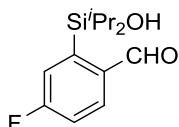
IR (neat): 2943 (m), 2864 (m), 1461 (s), 1071 (s), 1019 (m), 880 (s), 708 (s), and 471 (s) cm⁻¹.

TLC: R_f = 0.6 in 10:1 hexanes: EtOAc.

GCMS (5029017): t_R = 10.01 min, m/z 264 (M⁺, 5), 263 [(M-H)⁺, 20], 233 [(M-OMe)⁺, 100], and 221[(M-Pr)⁺, 10].

HRMS (ESI/TOF): Calcd for (M+Na)⁺ (C₁₅H₂₄NaO₂Si)⁺: 287.1438. Found: 287.1449.

4-Fluoro-2-(hydroxydiisopropylsilyl)benzaldehyde (2-2-4)



The ratio of aldehyde and silyl hemiacetal is 1:0.04.

Yield: 1 mmol scale, 216 mg, 85%.

¹H NMR (CDCl₃, 500 MHz) only for aldehyde: δ 9.96 (s, 1H, CHO), 7.92 [dd, J = 8.3, 5.3 (J^{F-H}) Hz, 1H, CHOCC_H], 7.54 [dd, 1H, J = 9.3 (J^{β-F-H}), 2.5 Hz, SiCC_H], 7.24 [ddd, J = 8.3, 8.3 (J^{β-F-H}), 2.5 Hz, 1H, CHOCC_HCH], 3.12 (br s, 1H, SiOH), 1.35 [septet, J = 7.4 Hz, 2H, CH(CH₃)₂], 1.09 [d, J = 7.4 Hz, 6H, CH(CH₃)₂], and 0.88 [d, J = 7.4 Hz, 6H, CH(CH₃)₂].

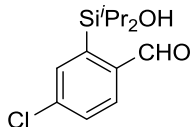
¹³C NMR (CDCl₃, 125 MHz) only for aldehyde: δ 193.9, 166.0 (d, J^{F-C} = 260.3 Hz), 143.8 (d, J^{β-F-C} = 5.8 Hz), 138.1 (d, J^{α-F-C} = 2.1 Hz), 137.9 (d, J^{β-F-C} = 9.3 Hz), 123.9 (d, J^{F-C} = 20.4 Hz), 116.5 (d, J^{F-C} = 21.7 Hz), 18.0, 17.7, and 13.2.

IR (neat): 3453 (br, m), 2945 (m), 2866 (m), 1689 (s), 1566 (s), 1464 (m), 1257(m), 1210 (s), 880 (s), 798 (s), 680 (s), and 456 (s) cm⁻¹.

TLC: R_f = 0.55 in 5:1 hexanes: EtOAc.

HRMS (ESI/TOF): Calcd for (M+Na)⁺ (C₁₃H₁₉FN₂O₂Si)⁺: 277.1031. Found: 277.1047.

4-Chloro-2-(hydroxydiisopropylsilyl)benzaldehyde (2-2-5)



The ratio of aldehyde and silyl hemiacetal is 1:0.08.

Total Yield: 1 mmol scale, 203 mg, 75%.

¹H NMR (CDCl₃, 500 MHz) for aldehyde: δ 9.99 (s, 1H, CHO), 7.83 (d, *J* = 8.2 Hz, 1H, CHOCC_H), 7.82 (d, *J* = 2.2 Hz, 1H, SiCCHC_HCl), 7.55 (dd, *J* = 8.2, 2.2 Hz, 1H, ClCCHCHCCHO), 3.08 (br s, 1H, SiOH), 1.35 [septet, *J* = 7.4 Hz, 2H, CH(CH₃)₂], 1.08 [d, *J* = 7.4 Hz, 6H, CH(CH₃)₂], and 0.87 [d, *J* = 7.4 Hz, 6H, CH(CH₃)₂].

¹H NMR (CDCl₃, 500 MHz) for silyl hemiacetal: 7.48 (s, 0.08H, SiCCH), 7.419-7.417 (m, 0.16H, ClCCHCHCHO and ClCCHCHCHO), 6.33 (s, 0.08H, SiOCHOH), 1.25 [septet, *J* = 7.4 Hz, 0.08H, CH(CH₃)₂], 1.23 [septet, *J* = 7.4 Hz, 0.08H, CH(CH₃)₂], 1.05 [d, *J* = 7.4 Hz, 0.24H, CH(CH₃)₂], 1.03 [d, *J* = 7.4 Hz, 0.24H, CH(CH₃)₂], 0.99 [d, *J* = 7.4 Hz, 0.24H, CH(CH₃)₂], and 0.97 [d, *J* = 7.4 Hz, 0.24H, CH(CH₃)₂].

¹³C NMR (CDCl₃, 125 MHz) for aldehyde: δ 194.3, 141.9, 140.9, 139.8, 136.6, 136.0, 129.8, 18.0, 17.7, and 13.2.

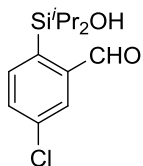
¹³C NMR (CDCl₃, 125 MHz) for silyl hemiacetal: 139.1, 137.9, 135.3, 131.4, 130.6, 125.8, 98.3, 17.23, 17.12, 16.99, 16.98, 12.5, and 12.4.

IR (neat): 3456 (br, m), 2945 (m), 2865 (m), 1692 (s), 1546 (m), 1462 (m), 1138 (s), 821 (s), 665 (s), and 483 (s) cm⁻¹.

TLC: R_f = 0.5 in 5:1 hexanes: EtOAc.

HRMS (ESI/TOF): Calcd for (M+H)⁺ (C₁₃H₂₀ClO₂Si)⁺: 271.0916. Found: 271.0947.

5-Chloro-2-(hydroxydiisopropylsilyl)benzaldehyde (2-2-6)



The ratio of aldehyde and silyl hemiacetal is 1:0.22.

Total Yield: 1 mmol scale, 211 mg, 78%.

¹H NMR (CDCl₃, 500 MHz) for aldehyde: δ 10.0 (s, 1H, CHO), 7.87 (d, *J* = 2.1 Hz, 1H, CHOCC_H), 7.77 (d, *J* = 7.9 Hz, 1H, SiCCH), 7.59 (dd, *J* = 7.9, 2.1 Hz, 1H, SiCCHCHC_HCl), 2.96 (br s, 1H, SiOH), 1.33 [septet, *J* = 7.4 Hz, 2H, CH(CH₃)₂], 1.08 [d, *J* = 7.4 Hz, 6H, CH(CH₃)₂], and 0.87 [d, *J* = 7.4 Hz, 6H, CH(CH₃)₂].

¹H NMR (CDCl₃, 500 MHz) for silyl hemiacetal: 7.48 (d, *J* = 1.8 Hz, 0.22H, CHOCC_H), 7.46 (d, *J* = 7.7 Hz, 0.22H, SiCCH), 7.36 (dd, *J* = 7.7, 1.8 Hz, 0.22H, SiCCHCHC_HCl), 6.31 (s, 0.22H, SiOCHOH), 1.25 [septet, *J* = 7.4 Hz, 0.22H, CH(CH₃)₂], 1.22 [septet, *J* = 7.4

Hz, 0.22H, $CH(CH_3)_2$], 1.04 [d, $J = 7.4$ Hz, 0.66H, $CH(CH_3)_2$], 1.03 [d, $J = 7.4$ Hz, 0.66H, $CH(CH_3)_2$], 0.98 [d, $J = 7.4$ Hz, 0.66H, $CH(CH_3)_2$], and 0.97 [d, $J = 7.4$ Hz, 0.66H, $CH(CH_3)_2$].

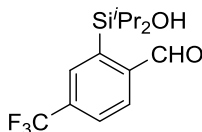
^{13}C NMR ($CDCl_3$, 125 MHz) for aldehyde: δ 194.4, 143.3, 137.9, 136.4, 134.2, 133.4, 124.8, 17.9, 17.7, and 13.3. For partial assignment of silyl hemiacetal: 137.3, 136.9, 133.0, 129.3, 98.2, 17.27, 17.15, 17.09, 17.03, 12.55, and 12.40.

IR (neat): 3450 (br, m), 2945 (m), 2865 (m), 1698 (m), 1587 (m), 1462 (m), 1191 (s), 1058 (s), 978 (s), 801 (s), 774 (s), and 497 (s) cm^{-1} .

TLC: $R_f = 0.5$ in 5:1 hexanes: EtOAc.

HRMS (ESI/TOF): Calcd for $(M+H)^+$ ($C_{13}H_{20}ClO_2Si$) $^+$: 271.0916. Found: 271.0958.

2-(Hydroxydiisopropylsilyl)-4-(trifluoromethyl)benzaldehyde (2-2-7)



The ratio of aldehyde and silyl hemiacetal is 1:0.55.

Total Yield: 1 mmol scale, 219 mg, 72%.

1H NMR ($CDCl_3$, 500 MHz) for aldehyde: δ 10.1 (s, 1H, CHO), 8.13 (d, $J = 1.9$ Hz, 1H, $SiCCHCCF_3$), 8.01 (d, $J = 7.9$ Hz, 1H, $CHOCC$), 7.84 (dd, $J = 7.9, 1.9$ Hz, 1H, $CF_3CCHCHCCHO$), 2.72 (br s, 1H, $SiOH$), 1.38 [septet, $J = 7.4$ Hz, 2H, $CH(CH_3)_2$], 1.11 [d, $J = 7.4$ Hz, 6H, $CH(CH_3)_2$], and 0.86 [d, $J = 7.5$ Hz, 6H, $CH(CH_3)_2$].

1H NMR ($CDCl_3$, 500 MHz) for silyl hemiacetal: 7.78 (d, $J = 1.6$ Hz, 0.55H, $SiCCH$), 7.72 (dd, $J = 8.1, 1.6$ Hz, 0.55H, $CHOCC$), 7.61 (d, $J = 8.1$ Hz, 0.55H, $CF_3CCHCHCCHO$), 6.39 (d, $J = 6.7$ Hz, 0.55H, $SiOCHOH$), 2.98 (d, $J = 6.7$ Hz, 0.55H, $SiOCHOH$), 1.29 [septet, $J = 7.4$ Hz, 0.55H, $CH(CH_3)_2$], 1.23 [septet, $J = 7.4$ Hz, 0.55H, $CH(CH_3)_2$], 1.06 [d, $J = 7.4$ Hz, 1.65 H, $CH(CH_3)_2$], 1.05 [d, $J = 7.4$ Hz, 1.65H, $CH(CH_3)_2$], 1.00 [d, $J = 7.4$ Hz, 1.65H, $CH(CH_3)_2$], and 0.99 [d, $J = 7.4$ Hz, 1.65H, $CH(CH_3)_2$].

^{13}C NMR ($CDCl_3$, 125 MHz) for aldehyde: δ 194.5, 140.9, 134.0, 133.1 (q, $J^{F-C} = 3.6$ Hz), 131.1 (q, $J^{F-C} = 32.1$ Hz), 126.7 (q, $J^{F-C} = 3.7$ Hz), 126.0 (q, $J^{F-C} = 273.1$ Hz), 124.9, 18.0, 17.7, 13.2.

^{13}C NMR ($CDCl_3$, 125 MHz) for silyl hemiacetal: 154.5, 134.4, 131.1 (q, $J^{F-C} = 31.3$ Hz), 128.5 (q, $J^{F-C} = 3.6$ Hz), 127.6 (q, $J^{F-C} = 3.0$ Hz), 125.0, 124.5 (q, $J^{F-C} = 262.1$ Hz), 98.4,

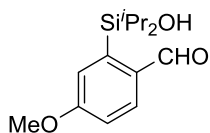
17.22, 17.13, 17.00 (2), 12.5, and 12.4.

IR (neat): 3460 (br, w), 2947 (m), 2868 (m), 1754 (w), 1706 (w), 1463 (m), 1321 (s), 1124 (s), 1075 (s), 977 (s), 802 (s), 639 (s), and 486 (s) cm^{-1} .

TLC: $R_f = 0.5$ in 5:1 hexanes: EtOAc.

HRMS (ESI/TOF): Calcd for $(M+H)^+$ ($\text{C}_{14}\text{H}_{20}\text{F}_3\text{O}_2\text{Si}$) $^+$: 305.1179. Found: 305.1199.

2-(Hydroxydiisopropylsilyl)-4-methoxybenzaldehyde (2-2-8)



The ratio of aldehyde and silyl hemiacetal is 1:0.01.

Yield: 1 mmol scale, 149 mg, 56%.

$^1\text{H NMR}$ (CDCl_3 , 500 MHz) only for aldehyde: δ 9.83 (s, 1H, CHO), 7.85 (d, $J = 8.5$ Hz, 1H, CHOCC H), 7.30 (d, 1H, $J = 2.6$ Hz, SiC CH), 7.01 (dd, $J = 8.5, 2.6$ Hz, 1H, CHOCC HCH), 3.90 (s, 3H, OCH $_3$), 3.82 (br s, 1H, SiOH), 1.32 [septet, $J = 7.4$ Hz, 2H, CH(CH $_3$) $_2$], 1.07 [d, $J = 7.4$ Hz, 6H, CH(CH $_3$) $_2$], and 0.91 [d, $J = 7.4$ Hz, 6H, CH(CH $_3$) $_2$].

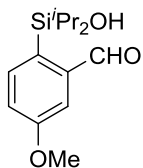
$^{13}\text{C NMR}$ (CDCl_3 , 125 MHz) only for **3i**: δ 194.3, 163.7, 141.7, 139.1, 134.9, 123.4, 113.2, 55.7, 17.9, 17.6, and 13.2.

IR (neat): 3453 (br, m), 2943 (m), 2864 (m), 1680 (s), 1582 (m), 1555 (m), 1462 (s), 1230 (s), 1212 (s), 881 (s), 665 (s), and 486 (s) cm^{-1} .

TLC: $R_f = 0.4$ in 5:1 hexanes: EtOAc.

HRMS (ESI/TOF): Calcd for $(M+\text{Na})^+$ ($\text{C}_{14}\text{H}_{22}\text{NaO}_3\text{Si}$) $^+$: 289.1230. Found: 289.1252.

2-(Hydroxydiisopropylsilyl)-5-methoxybenzaldehyde (2-2-9)



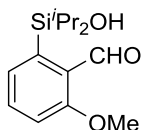
The ratio of aldehyde and silyl hemiacetal is 1:0.05.

Yield: 1 mmol scale, 205 mg, 77%.

$^1\text{H NMR}$ (CDCl_3 , 500 MHz) only for aldehyde: δ 10.0 (s, 1H, CHO), 7.70 (d, $J = 8.2$ Hz, 1H, SiC CH), 7.44 (d, 1H, $J = 2.6$ Hz, CHOCC H), 7.15 (dd, $J = 8.2, 2.6$ Hz, 1H,

SiCCHCH), 3.89 (s, 3H, ArOCH₃), 3.15 (br s, 1H, SiOH), 1.30 [septet, *J* = 7.4 Hz, 2H, CH(CH₃)₂], 1.07 [d, *J* = 7.4 Hz, 6H, CH(CH₃)₂], and 0.90 [d, *J* = 7.4 Hz, 6H, CH(CH₃)₂].
¹³C NMR (CDCl₃, 125 MHz) only for aldehyde: δ 195.7, 160.9, 143.6, 137.9, 129.6, 120.1, 119.0, 55.6, 17.9, 17.6, and 13.4.
IR (neat): 3400 (br, m), 2943 (m), 2865 (m), 1738 (m), 1686 (m), 1593 (m), 1462 (s), 1238 (s), 1048 (s), 1025 (s), 880 (s), 662 (s), and 464 (s) cm⁻¹.
TLC: R_f = 0.4 in 5:1 hexanes: EtOAc.
HRMS (ESI/TOF): Calcd for (M+Na)⁺ (C₁₄H₂₂NaO₃Si)⁺: 289.1230. Found: 289.1260.

2-(Hydroxydiisopropylsilyl)-6-methoxybenzaldehyde (2-2-10)



The ratio of aldehyde and corresponding silyl hemiacetal is 1:0.45.

Total Yield: 1 mmol scale, 96 mg, 36%.

¹H NMR (CDCl₃, 500 MHz) for aldehyde: δ 10.5 (s, 1H, CHO), 7.56 (dd, *J* = 8.3, 7.4 Hz, 1H, SiCCHCH), 7.42 (d, *J* = 7.4 Hz, 1H, SiCCH), 7.03 (d, *J* = 8.3 Hz, 1H, MeOCCH), 3.92 (s, 3H, ArOCH₃), 3.16 (br s, 1H, SiOH), 1.34 [septet, *J* = 7.4 Hz, 2H, CH(CH₃)₂], 1.08 [d, *J* = 7.4 Hz, 6H, CH(CH₃)₂], and 0.85 [d, *J* = 7.4 Hz, 6H, CH(CH₃)₂].

¹H NMR (CDCl₃, 500 MHz) for silyl hemiacetal: 7.36 (dd, *J* = 8.0, 7.2 Hz, 0.45H, SiCCHCH), 7.10 (d, *J* = 7.4 Hz, 0.45H, SiCCH), 6.92 (d, *J* = 8.0 Hz, 0.45H, MeOCCH), 6.49 (s, 0.45H, SiOCHOH), 3.88 (s, 1.35H, ArOCH₃), 1.26 [septet, *J* = 7.4 Hz, 0.45H, CH(CH₃)₂], 1.20 [septet, *J* = 7.4 Hz, 0.45H, CH(CH₃)₂], 1.07 [d, *J* = 7.4 Hz, 1.35H, CH(CH₃)₂], 1.06 [d, *J* = 7.4 Hz, 1.35H, CH(CH₃)₂], 0.97 [d, *J* = 7.4 Hz, 1.35H, CH(CH₃)₂], and 0.96 [d, *J* = 7.4 Hz, 1.35H, CH(CH₃)₂].

¹³C NMR (CDCl₃, 125 MHz) for aldehyde: δ 193.0, 163.6, 141.1, 135.4, 128.5, 123.7, 112.8, 55.8, 18.3, 18.1, and 13.3.

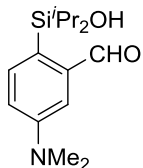
¹³C NMR (CDCl₃, 125 MHz) for silyl hemiacetal: 155.8, 138.8, 134.7, 130.7, 129.5, 112.0, 97.0, 55.3, 17.37, 17.24, 17.05 (2), 12.52, and 12.48.

IR (neat): 3435 (br, m), 2943 (m), 2864 (m), 1738 (m), 1676 (m), 1570 (m), 1466 (s), 1258 (s), 1024 (s), 963 (s), 786 (s), 668 (s), and 502 (s) cm⁻¹.

TLC: R_f = 0.4 in 3:1 hexanes: EtOAc.

HRMS (ESI/TOF): Calcd for (M+Na)⁺ (C₁₄H₂₂NaO₃Si)⁺: 289.1230. Found: 289.1257.

5-(Dimethylamino)-2-(hydroxydiisopropylsilyl)benzaldehyde (2-2-11)



The ratio of aldehyde and silyl hemiacetal is 1:0.04.

Yield: 1 mmol scale, 254 mg, 91%.

¹H NMR (CDCl₃, 500 MHz) only for aldehyde: δ 9.99 (s, 1H, CHO), 7.59 (d, *J* = 8.3 Hz, 1H, SiCCH), 7.22 (d, 1H, *J* = 2.7 Hz, CHOCCH), 6.91 (dd, *J* = 8.3, 2.7 Hz, 1H, SiCCHCH), 3.34 (br s, 1H, SiOH), 3.05 [s, 6H, N(CH₃)₂], 1.28 [septet, *J* = 7.4 Hz, 2H, CH(CH₃)₂], 1.06 [d, *J* = 7.4 Hz, 6H, CH(CH₃)₂], and 0.91 [d, *J* = 7.4 Hz, 6H, CH(CH₃)₂].

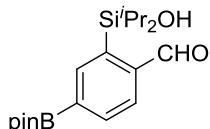
¹³C NMR (CDCl₃, 125 MHz) only for aldehyde: δ 197.0, 151.1, 143.0, 137.5 (2), 119.2, 116.3, 40.2, 17.9, 17.7, and 13.5.

IR (neat): 3436 (br, m), 2942 (m), 2863 (m), 1682 (s), 1595 (s), 1359 (m), 1208 (m), 1061 (s), 816 (s), 662 (s), and 485 (s) cm⁻¹.

TLC: R_f = 0.35 in 5:1 hexanes: EtOAc.

HRMS (ESI/TOF): Calcd for (M+H)⁺ (C₁₅H₂₆NO₂Si)⁺: 280.1727. Found: 280.1746.

2-(Hydroxydiisopropylsilyl)-4-(4,4,5,5-tetramethyl-1,3,2-dioxaborolan-2-yl)benzaldehyde (2-2-12)



The ratio of aldehyde and silyl hemiacetal is 1:0.22.

Total Yield: 1 mmol scale, 279 mg, 77%.

¹H NMR (CDCl₃, 500 MHz) for aldehyde: δ 10.0 (s, 1H, CHO), 8.21 (app s, 1H, SiCCHCBpin), 8.01 (dd, *J* = 7.5, 1.1 Hz, 1H, pinBCCCHCHCCHO), 7.87 (d, *J* = 7.5 Hz, 1H, CHOCCH), 3.17 (br s, 1H, SiOH), 1.38 [septet, *J* = 7.4 Hz, 2H, CH(CH₃)₂], 1.36 {s, 12H, B[OC(CH₃)₂]₂}, 1.09 [d, *J* = 7.4 Hz, 6H, CH(CH₃)₂], and 0.88 [d, *J* = 7.5 Hz, 6H, CH(CH₃)₂].

¹H NMR (CDCl₃, 500 MHz) for silyl hemiacetal: 7.98 (app s, 0.22H, SiCCHCBpin), 7.91

(dd, $J = 7.7, 1.1$ Hz, 0.22H, pinBCC $CHCCHO$), 7.49 (d, $J = 7.7$ Hz, 0.22H, CHOCC H), 6.35 (s, 0.22H, SiOCHOH), 1.36 {s, 2.6H, B[OC(CH $_3$) $_2$] $_2$ }, 1.27 [septet, $J = 7.4$ Hz, 0.22H, CH(CH $_3$) $_2$], 1.24 [septet, $J = 7.4$ Hz, 0.22H, CH(CH $_3$) $_2$], 1.053 [d, $J = 7.4$ Hz, 0.66 H, CH(CH $_3$) $_2$], 1.046 [d, $J = 7.4$ Hz, 0.66H, CH(CH $_3$) $_2$], 0.987 [d, $J = 7.4$ Hz, 0.66H, CH(CH $_3$) $_2$], and 0.984 [d, $J = 7.4$ Hz, 0.66H, CH(CH $_3$) $_2$].

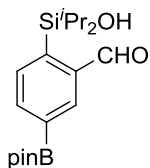
^{13}C NMR (CDCl $_3$, 125 MHz) for aldehyde: δ 196.2, 143.5, 142.4, 137.7, 137.0, 136.1, 134.1, 84.5, 25.1, 18.1, 17.8, and 13.3. For partial assignment of silyl hemiacetal: 138.5, 123.6, 98.8, 84.1, 24.9, 17.35, 17.27, 17.10 (2), 12.6, and 12.4.

IR (neat): 3442 (br, w), 2945 (m), 2866 (m), 1696 (w), 1464 (m), 1356 (s), 1260 (s), 1094 (s), 1011 (s), 795 (s), 736 (s), and 482 (s) cm $^{-1}$.

TLC: $R_f = 0.5$ in 5:1 hexanes: EtOAc.

HRMS (ESI/TOF): Calcd for (M+H) $^+$ (C $_{19}$ H $_{32}$ BO $_4$ Si) $^+$: 363.2157. Found: 363.2189.

2-(Hydroxydiisopropylsilyl)-5-(4,4,5,5-tetramethyl-1,3,2-dioxaborolan-2-yl)benzaldehyde (2-2-13)



The ratio of aldehyde and silyl hemiacetal is 1:0.05.

Yield: 1 mmol scale, 261 mg, 72%.

1H NMR (CDCl $_3$, 500 MHz) only for aldehyde: δ 10.0 (s, 1H, CHO), 8.31 (app s, 1H, CHOCC H), 8.03 (dd, $J = 7.2, 1.2$ Hz, 1H, SiCCH CH), 7.81 (d, $J = 7.2$ Hz, 1H, SiCCH), 3.53 (br s, 1H, SiOH), 1.37 {s, 12H, B[OC(CH $_3$) $_2$] $_2$ }, 1.34 [septet, $J = 7.4$ Hz, 2H, CH(CH $_3$) $_2$], 1.07 [d, $J = 7.4$ Hz, 6H, CH(CH $_3$) $_2$], and 0.87 [d, $J = 7.4$ Hz, 6H, CH(CH $_3$) $_2$].

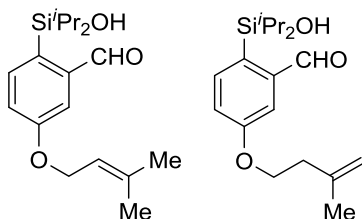
^{13}C NMR (CDCl $_3$, 125 MHz) only for aldehyde: δ 196.6, 142.5, 142.2, 141.1, 139.6 (2), 135.9, 84.6, 25.1, 17.9, 17.7, and 13.2.

IR (neat): 3443 (br, w), 2943 (m), 2865 (m), 1690 (w), 1463 (m), 1356 (s), 1141 (s), 881 (s), 673 (s), and 497 (m) cm $^{-1}$.

TLC: $R_f = 0.4$ in 10:1 hexanes: EtOAc.

HRMS (ESI/TOF): Calcd for (M+Na) $^+$ (C $_{19}$ H $_{31}$ BNaO $_4$ Si) $^+$: 385.1977. Found: 385.1997.

2-(Hydroxydiisopropylsilyl)-5-[(3-methylbut-2-en-1-yl)oxy]benzaldehyde (2-2-14)



1,1-Disubstituted alkene via alkene migration were isolated along with the desired product as an inseparable mixture. The ratio of three compounds (internal alkene: terminal alkene: silyl hemiacetal of internal alkene) is 1:0.18:0.08.

Total Yield: 1 mmol scale, 227 mg, 71%.

¹H NMR (CDCl₃, 500 MHz) for internal alkene aldehyde: δ 10.04 (s, 1H, CHO), 7.683 (d, *J* = 8.2 Hz, 1H, SiCCH), 7.448 (d, *J* = 2.6 Hz, 1H, CHOCC), 7.150 (dd, *J* = 8.2, 2.6 Hz, 1H, SiCCHCH), 5.51 (app t, *J* = 6.8 Hz, 1H, ArOCH₂CH=CMe₂), 4.59 (d, *J* = 6.8 Hz, 2H, ArOCH₂CH=CMe₂), 3.16 (br s, 1H, SiOH), 1.81 [s, 3H, ArOCH₂CH=C(CH₃)₂], 1.77 [s, 3H, ArOCH₂CH=C(CH₃)₂], 1.30 [septet, *J* = 7.4 Hz, 2H, CH(CH₃)₂], 1.06 [d, *J* = 7.4 Hz, 6H, CH(CH₃)₂], and 0.901 [d, *J* = 7.4 Hz, 6H, CH(CH₃)₂].

¹H NMR (CDCl₃, 500 MHz) for terminal alkene aldehyde: 10.05 (s, 0.18H, CHO), 7.685 (d, *J* = 8.2 Hz, 0.18H, SiCCH), 7.439 (d, *J* = 2.6 Hz, 0.18H, CHOCC), 7.142 (dd, *J* = 8.2, 2.6 Hz, 0.18H, SiCCHCH), 4.87 (app s, 0.18H, CH_aH_b=CMe), 4.82 (app s, 0.18H, CH_aH_b=CMe), 4.16 (t, *J* = 6.8 Hz, 0.36H, ArOCH₂CH₂), 2.54 (t, *J* = 6.8 Hz, 0.36H, ArOCH₂CH₂), 2.25 (br s, 0.18H, SiCHOH), 1.81 [s, 0.54H, ArOCH₂CH=C(CH₃)₂], 1.32-1.17 [m, 0.36H, CH(CH₃)₂], 1.038 [d, *J* = 7.4 Hz, 1.08H, CH(CH₃)₂], and 0.898 [d, *J* = 7.4 Hz, 1.08H, CH(CH₃)₂].

¹H NMR (CDCl₃, 500 MHz) for silyl hemiacetal of internal alkene: 7.427 (d, *J* = 8.0 Hz, 0.08H, SiCCH), 7.02 (d, *J* = 2.2 Hz, 0.08H, CH₂OCC_HCCHO), 6.96 (dd, *J* = 8.0, 2.2 Hz, 0.08H, SiCCHCH), 6.29 (d, *J* = 7.4 Hz, 0.08H, SiCHOH), 5.51 (app t, *J* = 6.8 Hz, 0.08H, ArOCH₂CH=CMe₂), 4.57-4.50 (m, 0.16H, ArOCH₂CH=CMe₂), 2.88 (d, *J* = 7.4 Hz, 0.08H, SiCHOH), 1.80 [s, 0.24H, ArOCH₂CH=C(CH₃)₂], 1.32-1.17 [m, 0.16H, CH(CH₃)₂], 1.75 [s, 0.24H, ArOCH₂CH=C(CH₃)₂], 1.046 [d, *J* = 7.4 Hz, 0.24H, CH(CH₃)₂], 1.028 [d, *J* = 7.4 Hz, 0.24H, CH(CH₃)₂], 0.989 [d, *J* = 7.4 Hz, 0.24H, CH(CH₃)₂], and 0.969 [d, *J* = 7.4 Hz, 0.24H, CH(CH₃)₂].

¹³C NMR (CDCl₃, 125 MHz) only for aldehyde: δ 195.7, 160.2, 143.5, 139.3, 137.9, 129.4, 120.9, 119.7, 119.2, 65.1, 26.1, 18.5, 17.9, 17.6, and 13.4.

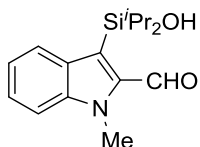
IR (neat): 3457 (br, w), 2942 (m), 2864 (m), 1686 (s), 1591 (s), 1462 (m), 1297 (s), 1267

(s), 1232 (s), 1069 (s), 995 (s), 826 (s), 662 (s), and 487 (m) cm^{-1} .

TLC: $R_f = 0.4$ in 5:1 hexanes: EtOAc.

HRMS (ESI/TOF): Calcd for $(M+Na)^+$ ($\text{C}_{18}\text{H}_{28}\text{NaO}_3\text{Si}$): 343.1700. Found: 343.1735.

3-(Hyoxydiisopropylsilyl)-1-methyl-1*H*-indole-2-carbaldehyde (2-2-15)



Yield: 1 mmol scale, 118 mg, 41%.

$^1\text{H NMR}$ (CDCl_3 , 500 MHz): δ 10.3 (s, 1H, CHO), 7.94 (ddd, $J = 8.1, 0.9, 0.9$ Hz, 1H, ArH), 7.44-7.40 (nfom, 2H, ArH), 7.17 (ddd, $J = 8.1, 4.9, 3.0$ Hz, 1H, ArH), 4.12 (s, 3H, NCH_3), 3.25 (br s, 1H, SiOH), 1.39 [septet, $J = 7.4$ Hz, 2H, $\text{CH}(\text{CH}_3)_2$], 1.12 [d, $J = 7.4$ Hz, 6H, $\text{CH}(\text{CH}_3)_2$], and 0.99 [d, $J = 7.4$ Hz, 6H, $\text{CH}(\text{CH}_3)_2$].

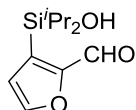
$^{13}\text{C NMR}$ (CDCl_3 , 125 MHz): δ 186.6, 141.4, 141.0, 132.2, 126.7, 125.2, 121.5, 121.2, 110.6, 32.2, 17.4, 17.1, and 14.4.

IR (neat): 3382 (br, w), 3052 (w), 2943 (m), 2864 (m), 1642 (s), 1465 (m), 1385 (m), 1346 (m), 878 (s), and 488 (m) cm^{-1} .

TLC: $R_f = 0.6$ in 5:1 hexanes: EtOAc.

HRMS (ESI/TOF): Calcd for $(M+Na)^+$ ($\text{C}_{16}\text{H}_{23}\text{NNaO}_2\text{Si}$): 312.1390. Found: 312.1412.

3-(Hyoxydiisopropylsilyl)furan-2-carbaldehyde (2-2-16)



The ratio of aldehyde and silyl hemiacetal is 1:0.04.

Yield: 1 mmol scale, 140 mg, 62%.

$^1\text{H NMR}$ (CDCl_3 , 500 MHz) only for aldehyde: δ 9.78 (d, $J = 0.7$ Hz, 1H, CHO), 7.76 (d, $J = 1.5$ Hz, 1H, ArH), 6.62 (dd, $J = 1.5, 0.7$ Hz, 1H, ArH), 4.82 (br s, 1H, SiOH), 1.15 [septet, $J = 7.2$ Hz, 2H, $\text{CH}(\text{CH}_3)_2$], 1.04 [d, $J = 7.2$ Hz, 6H, $\text{CH}(\text{CH}_3)_2$], and 0.96 [d, $J = 7.3$ Hz, 6H, $\text{CH}(\text{CH}_3)_2$].

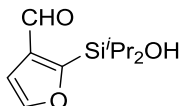
$^{13}\text{C NMR}$ (CDCl_3 , 125 MHz) only for aldehyde: δ 182.6, 157.8, 148.1, 128.9, 118.0, 17.1, 16.8, and 13.2.

IR (neat): 3397 (br, w), 2945 (m), 2866 (m), 1734 (m), 1664 (s), 1460 (s), 1353 (m), 821 (s), 762 (s), and 493 (m) cm^{-1} .

TLC: $R_f = 0.5$ in 5:1 hexanes: EtOAc.

HRMS (ESI/TOF): Calcd for $(M+Na)^+$ ($\text{C}_{11}\text{H}_{18}\text{NaO}_3\text{Si}$): 249.0917. Found: 249.0937.

2-(Hydroxydiisopropylsilyl)furan-3-carbaldehyde (2-2-17)



The ratio of aldehyde and silyl hemiacetal is 1:0.05.

Yield: 1 mmol scale, 160 mg, 71%.

$^1\text{H NMR}$ (CDCl_3 , 500 MHz) only for aldehyde: δ 9.88 (d, $J = 0.7$ Hz, 1H, CHO), 8.23 (d, $J = 1.3$ Hz, 1H, ArH), 7.42 (dd, $J = 1.3, 0.7$ Hz, 1H, ArH), 4.74 (br s, 1H, SiOH), 1.09 [septet, $J = 7.2$ Hz, 2H, $\text{CH}(\text{CH}_3)_2$], 1.02 [d, $J = 7.2$ Hz, 6H, $\text{CH}(\text{CH}_3)_2$], and 0.96 [d, $J = 7.2$ Hz, 6H, $\text{CH}(\text{CH}_3)_2$].

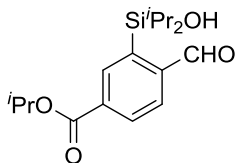
$^{13}\text{C NMR}$ (CDCl_3 , 125 MHz) only for aldehyde: δ 187.1, 155.9, 149.9, 133.1, 113.3, 17.2, 17.0, and 13.5.

IR (neat): 3382 (br, w), 2945 (m), 2867 (m), 1734 (m), 1670 (s), 1463 (s), 996 (s), 882 (s), 674 (s), and 479 (m) cm^{-1} .

TLC: $R_f = 0.5$ in 5:1 hexanes: EtOAc.

HRMS (ESI/TOF): Calcd for $(M+Na)^+$ ($\text{C}_{11}\text{H}_{18}\text{NaO}_3\text{Si}$): 249.0917. Found: 249.0940.

Isopropyl 4-formyl-3-(hydroxydiisopropylsilyl)benzoate (2-2-18)



The ratio of aldehyde and silyl hemiacetal is 1:0.40.

Total Yield: 1 mmol scale, 184 mg, 57%.

$^1\text{H NMR}$ (CDCl_3 , 500 MHz) for aldehyde: δ 10.1 (s, 1H, CHO), 8.46 (d, $J = 1.7$ Hz, 1H, SiCCH), 8.20 (dd, $J = 7.9, 1.7$ Hz, 1H, CHOCCCHCCO₂iPr), 7.96 (d, $J = 7.9$ Hz, 1H, CHOCCCH), 5.27 [septet, $J = 6.3$ Hz, 1H, ArCO₂CH(CH₃)₂], 3.35 (br s, 1H, SiOH), 1.39 [d, $J = 6.3$ Hz, 6H, ArCO₂CH(CH₃)₂], 1.35 [septet, $J = 7.4$ Hz, 2H, Si[CH(CH₃)₂]₂], 1.09 [d, $J = 7.4$ Hz, 6H, SiCH(CH₃)₂], and 0.89 [d, $J = 7.4$ Hz, 6H, SiCH(CH₃)₂].

¹H NMR (CDCl₃, 500 MHz) for silyl hemiacetal: 8.19 (d, *J* = 1.6 Hz, 0.4H, SiCCH), 8.11 (dd, *J* = 8.0, 1.6 Hz, 0.4H, CHOCCHCHCCO₂Pr), 7.54 (d, *J* = 8.0 Hz, 1H, CHOCCH), 6.38 (s, 0.4H, SiOCHOH), 5.26 [septet, *J* = 6.3 Hz, 0.4H, ArCO₂CH(CH₃)₂], 1.38 [d, *J* = 6.3 Hz, 2.4H, ArCO₂CH(CH₃)₂], 1.27 {septet, *J* = 7.4 Hz, 0.4H, Si[CH(CH₃)₂]₂}, 1.25 {septet, *J* = 7.4 Hz, 0.4H, Si[CH(CH₃)₂]₂}, 1.05 [d, *J* = 7.4 Hz, 1.2H, SiCH(CH₃)₂], 1.04 [d, *J* = 7.4 Hz, 1.2H, SiCH(CH₃)₂], 0.99 [d, *J* = 7.4 Hz, 1.2H, SiCH(CH₃)₂], and 0.98 [d, *J* = 7.4 Hz, 1.2H, SiCH(CH₃)₂].

¹³C NMR (CDCl₃, 125 MHz) for aldehyde: δ 195.3, 165.6, 139.6, 137.2, 134.6, 134.1, 131.7, 130.7, 69.5, 22.09, 18.0, 17.7, and 13.3.

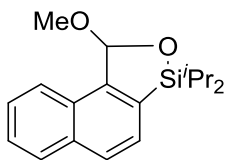
¹³C NMR (CDCl₃, 125 MHz) for silyl hemiacetal: 166.3, 155.4, 144.5, 133.2, 131.4, 126.6, 124.3, 98.5, 68.8, 22.14 (2), 17.24, 17.15, 17.02 (2), 12.5, and 12.4.

IR (neat): 3492 (br, w), 2944 (m), 2866 (m), 1716 (s), 1463 (m), 1276 (m), 1244 (m), 1099 (s), 806 (s), and 483 (m) cm⁻¹.

TLC: R_f = 0.3 in 10:1 hexanes: EtOAc.

HRMS (ESI/TOF): Calcd for (M+Na)⁺ (C₁₇H₂₆NaO₄Si)⁺: 345.1493. Found: 345.1515.

3,3-Diisopropyl-1-methoxy-1,3-dihydronaphtho[2,1-c][1,2]oxasilole (1-3-9)



Yield: 1 mmol scale, 273 mg, 91%.

¹H NMR (CDCl₃, 500 MHz): δ 8.11 (dddd, *J* = 8.1, 1.5, 0.6, 0.6 Hz, 1H, naphthalene-*H*5), 7.91 (ddd, *J* = 8.1, 1.5, 0.6 Hz, 1H, naphthalene-*H*8), 7.87 (dd, *J* = 8.0, 0.6 Hz, 1H, naphthalene-*H*4), 7.60 (d, *J* = 8.0 Hz, 1H, naphthalene-*H*3), 7.58 (ddd, *J* = 8.1, 6.9, 1.5 Hz, 1H, naphthalene-*H*6 or naphthalene-*H*7), 7.54 (ddd, *J* = 8.1, 6.9, 1.5 Hz, 1H, naphthalene-*H*6 or naphthalene-*H*7), 6.54 (s, 1H, SiOCHOMe), 3.68 (s, 3H, OCH₃), 1.35 [septet, *J* = 7.4 Hz, 1H, CH(CH₃)₂], 1.31 [septet, *J* = 7.4 Hz, 1H, CH(CH₃)₂], 1.15 [d, *J* = 7.2 Hz, 3H, CH(CH₃)₂], 1.13 [d, *J* = 7.2 Hz, 3H, CH(CH₃)₂], 1.06 [d, *J* = 7.2 Hz, 3H, CH(CH₃)₂], and 1.01 [d, *J* = 7.2 Hz, 3H, CH(CH₃)₂].

¹³C NMR (CDCl₃, 125 MHz): δ 146.7, 134.9, 131.4, 129.32, 129.22, 128.6, 127.4, 126.74, 126.72, 124.4, 104.4, 54.9, 17.51, 17.41, 17.21, 17.19, and 12.8 (2).

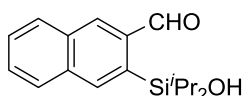
IR (neat): 3047 (w), 2943 (m), 2864 (m), 1461 (m), 1244 (m), 1065 (s), 801 (s), 671 (s), and 435 (m) cm^{-1} .

TLC: $R_f = 0.4$ in 10:1 hexanes: EtOAc.

GCMS (5029017): $t_R = 12.48$ min, m/z 300 (M^+ , 18), 299 [($M-H$) $^+$, 10], 269 [($M-OMe$) $^+$, 100], and 257 [($M-Pr$) $^+$, 15].

HRMS (ESI/TOF): Calcd for ($M+Na$) $^+$ ($C_{18}H_{24}NaO_2Si$) $^+$: 323.1438. Found: 323.1456.

3-(Hydroxydiisopropylsilyl)-2-naphthaldehyde (2-2-19)



The ratio of aldehyde and silyl hemiacetal is 1:0.01.

Yield: 1 mmol scale, 220 mg, 77%.

1H NMR ($CDCl_3$, 500 MHz) only for aldehyde: δ 10.1 (s, 1H, CHO), 8.38 (s, 1H, naphthalene-*H1* or naphthalene-*H4*), 8.26 (s, 1H, naphthalene-*H1* or naphthalene-*H4*), 8.00 (dd, $J = 8.1, 1.3$ Hz, 1H, naphthalene-*H8* or naphthalene-*H5*), 7.93 (dd, $J = 8.1, 1.3$ Hz, 1H, naphthalene-*H8* or naphthalene-*H5*), 7.68 (ddd, $J = 8.1, 6.9, 1.3$ Hz, 1H, naphthalene-*H6* or naphthalene-*H7*), 7.62 (ddd, $J = 8.1, 6.9, 1.3$ Hz, 1H, naphthalene-*H6* or naphthalene-*H7*), 3.39 (br s, 1H, SiOH), 1.44 [septet, $J = 7.2$ Hz, 2H, $CH(CH_3)_2$], 1.12 [d, $J = 7.2$ Hz, 6H, $CH(CH_3)_2$], and 0.92 [d, $J = 7.2$ Hz, 6H, $CH(CH_3)_2$].

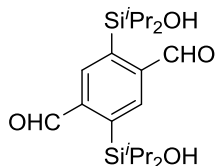
^{13}C NMR ($CDCl_3$, 125 MHz) only for aldehyde: δ 195.8, 139.6, 138.9, 138.0, 135.6, 132.8, 132.5, 129.9, 129.3, 128.7, 128.0, 18.2, 17.9, and 13.4.

IR (neat): 3455 (br, w), 2943 (m), 2863 (m), 1686 (s), 1461 (m), 1211 (s), 881 (s), 744 (s), and 477 (m) cm^{-1} .

TLC: $R_f = 0.4$ in 10:1 hexanes: EtOAc.

HRMS (ESI/TOF): Calcd for ($M+H$) $^+$ ($C_{17}H_{23}O_2Si$) $^+$: 287.1462. Found: 287.1488.

2,5-Bis(hydroxydiisopropylsilyl)terephthalaldehyde (2-2-20)



Yield: 1 mmol scale, 295 mg, 75%.

¹H NMR (DMSO-d₆, 500 MHz): δ 10.4 (s, 2H, CHO), 8.39 (s, 2H, SiCCH), 6.15 (s, 2H, SiOH), 3.33 (H₂O), 1.30 [septet, *J* = 7.4 Hz, 4H, CH(CH₃)₂], 1.03 [d, *J* = 7.4 Hz, 12H, CH(CH₃)₂], and 0.76 [d, *J* = 7.4 Hz, 12H, CH(CH₃)₂].

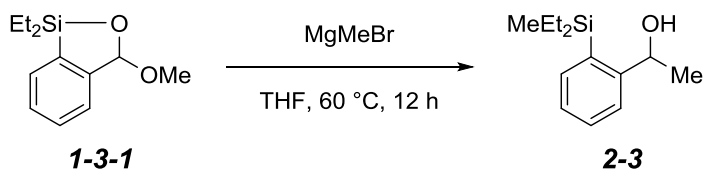
¹³C NMR (DMSO-d₆, 125 MHz): δ 195.3, 143.5, 141.2, 137.9, 17.9, 17.5, and 12.7.

IR (neat): 3489 (br, w), 2944 (s), 2865 (s), 1694 (s), 1463 (s), 1086 (s), 1018 (s), 880 (s), and 672 (m) cm⁻¹.

TLC: R_f = 0.2 in 5:1 hexanes: EtOAc.

HRMS (ESI/TOF): Calcd for (M+H)⁺ (C₂₀H₃₅O₄Si₂)⁺: 395.2068. Found: 395.2089.

C.7. Procedure for Preparation of 1-{2-[Diethyl(methyl)silyl]phenyl}ethanol (2-3):



Crude cyclic silyl acetal **1-3-1** (1 mmol) was dissolved with THF (1 mL, 1 M). Methylmagnesium bromide (3 M in diethyl ether, 1 mL, 3 mmol) was added to the mixture in one portion. The septum on the vial was replaced by a screw cap with a Teflon liner. The reaction mixture was kept at 60 °C and stirred for 12 h. The reaction was quenched by adding saturated aqueous ammonium chloride (5 mL) and extracted with diethyl ether (8 mL×4). The combined organic layer was washed with water (10 mL) and brine (10 mL), and dried over anhydrous sodium sulfate. The volatiles were removed *in vacuo*, and the crude mixture was purified by MPLC (hexanes/EtOAc = 20:1, 7 mL/min, retention time 9 min) to afford **2-3** (202 mg, 91%) as a colorless liquid.

¹H NMR (CDCl₃, 500 MHz): δ 7.62 [dd, *J* = 7.5, 1.5 Hz, 1H, CH(OH)CCH or SiCCH], 7.47 [dd, *J* = 7.5, 1.5 Hz, 1H, CH(OH)CCH or SiCCH], 7.43 (ddd, *J* = 7.5, 7.5, 1.5 Hz, 1H, SiCCHCH or SiCCHCHCH), 7.27 (ddd, *J* = 7.5, 7.5, 1.5 Hz, 1H, SiCCHCH or SiCCHCHCH), 5.12 [q, *J* = 6.3 Hz, 1H, CH(OH)CH₃], 2.12 (br s, 1H, OH), 1.49 (d, *J* = 6.3

Hz, 3H, CH(OH)CH₃], 1.00-0.96 [m, 6H, Si(CH₂CH₃)₂], 0.88-0.83 [m, 4H, Si(CH₂CH₃)₂], and 0.34 (s, 3H, SiCH₃).

¹³C NMR (CDCl₃, 125 MHz): δ 152.0, 135.06, 135.00, 129.9, 127.1, 125.4, 69.8, 25.4, 7.84, 7.81, 6.94, 6.85, and 3.9.

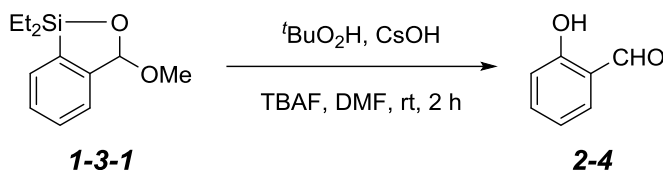
IR (neat): 3466 (br, w), 2954 (w), 2875 (w), 1077 (s), 1006 (s), and 732 (m) cm⁻¹.

TLC: R_f = 0.6 in 20:1 hexanes: EtOAc.

GCMS (5029017): t_R = 9.68 min, m/z 207 [(M-Me)⁺, 10], 193 [(M-Et)⁺, 12], and 177 [(M-CH(OH)Me)⁺, 100].

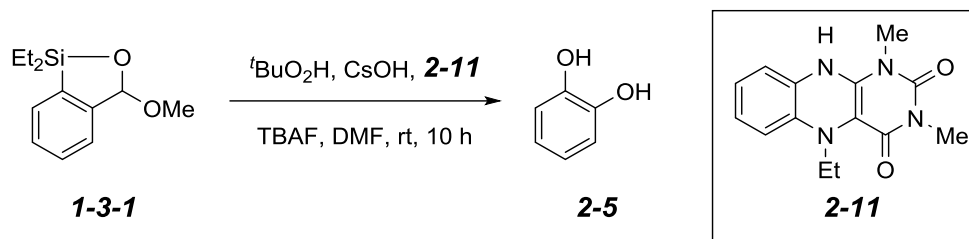
HRMS (ESI/TOF): Calcd for (M+H)⁺ (C₁₃H₂₃OSi)⁺: 223.1513. Found: 223.1530.

C.8. Procedure for Oxidation of 6a to Salicylic aldehyde (2-4):



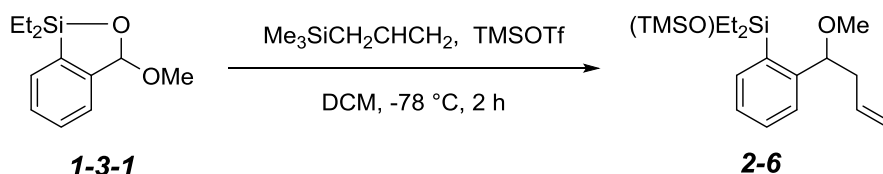
Crude cyclic silyl acetal **1-3-1** (0.2 mmol), cesium hydroxide (45 mg, 0.3 mmol), and TBAF·3H₂O (126 mg, 0.4 mmol) were dissolved with DMF (0.2 mL, 1 M). *tert*-Butyl hydrogen peroxide (70% in water, 1 mL, 7 mmol) was added to the mixture. The reaction mixture was kept at rt and stirred for 2 h. The reaction was quenched by adding saturated aqueous sodium thiosulfate (5 mL) and acidified by HCl (1 N) and extracted with diethyl ether (8 mL×4). The combined organic layer was washed with water (10 mL) and brine (10 mL), and dried over anhydrous sodium sulfate. The volatiles were removed *in vacuo*, and the crude mixture was purified by MPLC (hexanes/EtOAc = 5:1, 7 mL/min, retention time 8 min) to provide salicylic aldehyde **2-4** (21.5 mg, 88%) as a colorless liquid.

C.9. Procedure for Oxidation of 1-3-1 to Catechol (2-5):



Crude cyclic silyl acetal **1-3-1** (0.2 mmol), cesium hydroxide (45 mg, 0.3 mmol), flavin **2-11** (5.4 mg, 10 mol %) and TBAF \cdot 3H₂O (126 mg, 0.4 mmol) were dissolved with DMF (0.2 mL, 1 M). *tert*-Butyl hydrogen peroxide (70% in water, 1 mL, 7 mmol) was added to the mixture. The reaction mixture was kept at rt and stirred for 10 h. The reaction was quenched by adding saturated aqueous sodium thiosulfate (5 mL) and acidified by HCl (1 N) and extracted with diethyl ether (8 mL \times 4). The combined organic layer was washed with water (10 mL), brine (10 mL), and dried over anhydrous sodium sulfate. The volatiles were removed *in vacuo*, and the crude mixture was purified by MPLC (hexanes/EtOAc = 3:1, 7 mL/min, retention time 6 min) to provide catechol **2-5** (14.5 mg, 66%).

C.10. Procedure for Allylation of 1-3-1 to 1,1-Diethyl-1-[2-(1-methoxybut-3-en-1-yl)phenyl]-3,3,3-trimethyldisiloxane (2-6):



Crude cyclic silyl acetal **1-3-1** (12 mmol) and allyltrimethylsilane (2.4 mL, 15 mmol) were dissolved with CH₂Cl₂ (6 mL, 2 M), and the solution was cooled to -78°C . Trimethylsilyl trifluoromethanesulfonate (TMSOTf, 0.18 mL, 1 mmol) was added into the reaction mixture. The reaction was kept at -78°C for 2 h. The reaction was warmed to rt

and quenched by adding saturated aqueous ammonium chloride (20 mL) extracted with diethyl ether (20 mL×4). The combined organic layer was washed with water (20 mL) and brine (20 mL), and dried over anhydrous sodium sulfate. The volatiles were removed *in vacuo*, and the crude mixture was purified by MPLC (hexanes/EtOAc = 20:1, 7 mL/min, retention time 7 min) to provide **2-6** (2.90 g, 72% yield) as a colorless liquid.

¹H NMR (CDCl₃, 500 MHz): δ 7.55 [dd, *J* = 7.4, 1.3 Hz, 1H, SiCCH or C(OMe)CCH], 7.52 [dd, *J* = 7.4, 1.3 Hz, 1H, SiCCH or C(OMe)CCH], 7.42 [ddd, *J* = 7.4, 7.4, 1.3 Hz, 1H, SiCCHCH or C(OMe)CCHCH], 7.28 [ddd, *J* = 7.4, 7.4, 1.3 Hz, 1H, SiCCHCH or C(OMe)CCHCH], 5.94 (dddd, *J* = 17.0, 10.3, 6.7, 6.7 Hz, 1H, CH₂CH=CH₂), 5.11 (dddd, *J* = 17.0, 2.0, 1.3, 1.3 Hz, 1H, CH₂CH=CH_{cis}H_{trans}), 5.08 (dddd, *J* = 10.3, 2.0, 1.3, 1.3 Hz, 1H, CH₂CH=CH_{cis}H_{trans}), 4.66 (dd, *J* = 8.9, 3.6 Hz, 1H, MeOCH), 3.22 (s, 3H, OCH₃), 2.46 (dddd, *J* = 14.7, 8.9, 6.7, 1.3, 1.3, 1H, MeOCHCH_aH_b), 2.37 (dddd, *J* = 14.7, 6.7, 3.6, 1.3, 1.3, 1H, MeOCHCH_aH_b), 0.99-0.94 [m, 6H, Si(CH₂CH₃)₂], 0.88-0.81 [m, 4H, Si(CH₂CH₃)₂], and 0.21 [s, 9H, Si(CH₃)₃].

¹³C NMR (CDCl₃, 125 MHz): δ 148.6, 135.7, 135.5, 134.8, 129.9, 126.7, 125.8, 116.6, 81.4, 56.5, 43.5, 9.14, 9.03, 7.1 (2) and 2.3.

IR (neat): 3059 (w), 2954 (w), 2876 (w), 1252 (s), 1047 (s), 837 (s), and 719 (m) cm⁻¹.

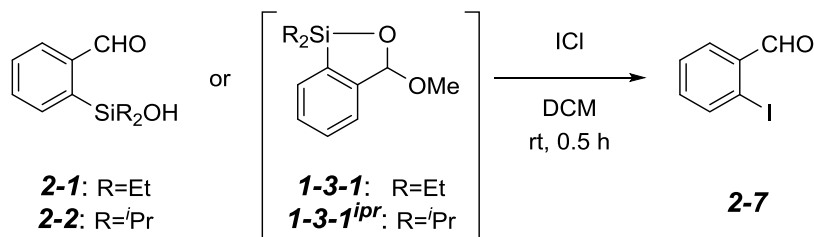
TLC: R_f = 0.6 in 20:1 hexanes: EtOAc.

GCMS (5029017): t_R = 10.79 min, m/z 335 [(M-H)⁺, 5], 295 [(M-allyl)⁺, 100], 234, and 192.

HRMS (ESI/TOF): Calcd for (M+Na)⁺ (C₁₈H₃₂NaO₂Si₂)⁺: 359.1833. Found: 359.1854.

C.11. Procedure for Iodo *ipso*-Desilylation of **2a/3a** or **6a/7a** to **2-**

Iodobenzaldehyde (**13**):



ortho-Formyl arylsilanols **2-1** or **2-2**, or cyclic silyl acetals **1-3-1** or **1-3-1^{ipr}** (0.2 mmol) and iodine chloride (65 mg, 0.4 mmol) were dissolved with DCM (1 mL, 0.2 M). The reaction mixture was stirred at rt for 2 h. The reaction was quenched by adding saturated aqueous sodium chloride (2 mL) and extracted with diethyl ether (4 mLx4). The combined organic layer was washed with water (4 mL) and brine (4 mL), and dried over anhydrous sodium sulfate. The volatiles were removed *in vacuo*, and the crude mixture was purified by flash column (hexanes as eluent) to afford 2-iodobenzaldehyde **2-7** (43.6 mg, 94% from **2-1**; 41.8 mg, 90% from **2-2**; 41.3 mg, 89% from **1-3-1**; 39.4 mg, 85% from **1-3-1^{ipr}**).

¹H NMR (CDCl₃, 500 MHz): δ 10.1 [d, *J* = 1.0 Hz (coupled with CHOCCCH), 1H, CHO], 7.95 (dd, *J* = 7.9, 1.0 Hz, 1H, ICCH), 7.88 (dd, *J* = 7.7, 1.8 Hz, 1H, CHOCCCH), 7.46 [dddd, *J* = 7.7, 7.4, 1.0 (coupled with CHO), 1.0 Hz, 1H, CHOCCCH], and 7.29 (ddd, *J* = 7.9, 7.4, 1.8 Hz, 1H, ICCHCH).

¹³C NMR (CDCl₃, 125 MHz): δ 196.0, 140.9, 135.7, 135.3, 130.5, 128.9, and 100.9.

TLC: R_f = 0.7 in 20:1 hexanes: EtOAc.

GCMS (5029017): t_R = 8.52 min, m/z 232 (M⁺, 100), 231 [(M-H)⁺, 35], and 104 [(M-I)⁺, 40].

C.12. Procedure for Oxidative Lactonization of 3a to 1,1-

Diisopropylbenzo[*c*][1,2]oxasilol-3-one (**2-2**):



ortho-Formyl phenylsilanol **2-2** (1 mmol) and 2-iodoxybenzoic acid (IBX, 560 mg, 2 mmol) were mixed with DMSO (2 mL, 0.5 M). The suspension was warmed to 40 °C and stirred for 10 h. The reaction was quenched by adding saturated aqueous sodium chloride (5 mL) and extracted with diethyl ether (8 mLx4). The combined organic layer was washed

with water (10 mL) and brine (10 mL), and dried over anhydrous sodium sulfate. The volatiles were removed *in vacuo*, and the crude mixture was purified by MPLC (hexanes/EtOAc = 5:1, 7 mL/min, retention time 6 min) to afford silalactone **2-8** (212 mg, 91%) as a colorless liquid.

¹H NMR (CDCl₃, 500 MHz): δ 8.08 [dd, *J* = 7.2, 1.3 Hz, 1H, SiCCH or C(O)CCH], 7.68 [dd, *J* = 7.2, 1.3 Hz, 1H, SiCCH or C(O)CCH], 7.64 [ddd, *J* = 7.2, 7.2, 1.3 Hz, 1H, C(O)CCHCH or SiCCHCH], 7.60 [ddd, *J* = 7.2, 7.2, 1.3 Hz, 1H, C(O)CCHCH or SiCCHCH], 1.41 [septet, *J* = 7.5 Hz, 2H, CH(CH₃)₂], 1.08 [d, *J* = 7.5 Hz, 6H, CH(CH₃)₂], and 1.04 [d, *J* = 7.5 Hz, 6H, CH(CH₃)₂].

¹³C NMR (CDCl₃, 125 MHz): δ 169.1, 138.4, 138.0, 133.2, 132.1, 131.3, 127.8, 16.8 (2), and 11.7.

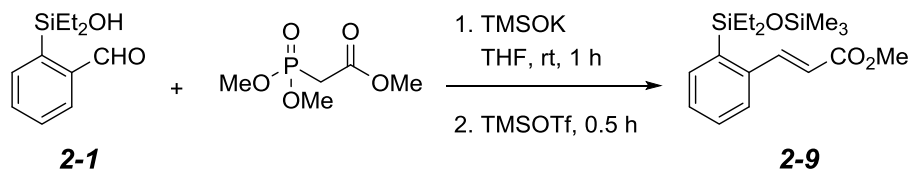
TLC: R_f = 0.5 in 5:1 hexanes: EtOAc.

GCMS (5029017): t_R = 10.58 min, m/z 235 [(M+H)⁺, 5], 234 (M⁺, 5), and 191 [(M-Pr)⁺, 100].

HRMS (ESI/TOF): Calcd for (M+H)⁺ (C₁₃H₁₉O₂Si)⁺: 235.1149. Found: 235.1170.

C.13. Procedure for Horner-Wadsworth-Emmons Homologation of **2a** into (*E*)-

Methyl 3-[2-(1,1-diethyl-3,3,3-trimethyldisiloxanyl)phenyl]acrylate (**2-9**):



ortho-Formyl phenylsilanol **2-1** (1 mmol) and trimethyl phosphonoacetate (0.19 mL, 1.2 mmol) were dissolved with THF (2 mL, 0.5 M). Potassium trimethylsilanolate (141 mg, 1 mmol) was added into the reaction mixture. After being stirred for 1 h at rt, the reaction was quenched by adding saturated aqueous ammonium chloride (5 mL), and extracted with diethyl ether (8 mLx4). The combined organic layer was washed with water (10 mL) and brine (10 mL) and dried over anhydrous sodium sulfate. The volatiles were removed

in vacuo. The crude mixture was dissolved with CH₂Cl₂ (2 mL, 0.5 M). TMSOTf (0.09 mL, 0.5 mmol) was added into the reaction mixture. After being stirred for 0.5 h at rt, the reaction was quenched by adding saturated aqueous sodium bicarbonate (5 mL) and extracted with diethyl ether (8 mL×4). The combined organic layer was washed with water (10 mL) and brine (10 mL) and dried over anhydrous sodium sulfate. The volatiles were removed *in vacuo*, and the crude mixture was purified by MPLC (hexanes/EtOAc = 10:1, 7 mL/min, retention time 6 min) to afford enoate **2-9** (312 mg, 93%, *E/Z* >20:1).

¹H NMR (CDCl₃, 500 MHz): δ 8.17 (d, *J* = 15.7 Hz, 1H, ArCH=CHCO₂Me), 7.66 [dd, *J* = 7.4, 1.3 Hz, 1H, SiCCH or (MeO₂CCH=CH)CCH], 7.60 [dd, *J* = 7.4, 1.3 Hz, 1H, SiCCH or (MeO₂CCH=CH)CCH], 7.39 [ddd, *J* = 7.4, 7.4, 1.3 Hz, 1H, SiCCHCH or (MeO₂CCH=CH)CCHCH], 7.36 [ddd, *J* = 7.4, 7.4, 1.3 Hz, 1H, SiCCHCH or (MeO₂CCH=CH)CCHCH], 6.36 (d, *J* = 15.7 Hz, 1H, ArCH=CHCO₂Me), 3.81 (s, 3H, OCH₃), 0.98-0.91 [m, 6H, Si(CH₂CH₃)₂], 0.88-0.82 [m, 4H, Si(CH₂CH₃)₂] and 0.15 [s, 9H, Si(CH₃)₃].

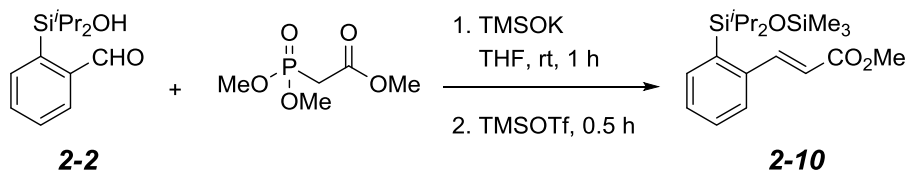
¹³C NMR (CDCl₃, 125 MHz): δ 167.5, 146.2, 140.2, 139.5, 135.3, 129.8, 129.1, 126.2, 118.6, 51.8, 8.4, 7.0 and 2.1.

IR (neat): 3055 (w), 2954 (w), 2877 (w), 1720 (m), 1052 (s), 836 (s), and 719 (m) cm⁻¹.

TLC: R_f = 0.4 in 10:1 hexanes: EtOAc.

HRMS (ESI/TOF): Calcd for (M+Na)⁺ (C₁₇H₂₈NaO₃Si₂)⁺: 359.1469. Found: 359.1482.

(*E*)-Methyl 3-(2-(1,1-diisopropyl-3,3,3-trimethyldisiloxanyl)phenyl)acrylate (2-10**)**



The procedure for the preparation of **2-10** is the same as one of **2-9**. The crude reaction mixture was purified by MPLC (hexanes/EtOAc = 20:1, 7 mL/min, retention time 5 min) to afford product **16** (298 mg, 82%, *E/Z* >20:1).

¹H NMR (CDCl₃, 500 MHz): δ 8.07 (d, *J* = 15.7 Hz, 1H, ArCH=CHCO₂Me), 7.66 [dd, *J* = 7.4, 1.3 Hz, 1H, SiCCH or (MeO₂CCH=CH)CCH], 7.62 [dd, *J* = 7.4, 1.3 Hz, 1H, SiCCH or (MeO₂CCH=CH)CCH], 7.38 [ddd, *J* = 7.4, 7.4, 1.3 Hz, 1H, SiCCHCH or (MeO₂CCH=CH)CCHCH], 7.36 [ddd, *J* = 7.4, 7.4, 1.3 Hz, 1H, SiCCHCH or (MeO₂CCH=CH)CCHCH], 6.36 (d, *J* = 15.7 Hz, 1H, ArCH=CHCO₂Me), 3.80 (s, 3H, OCH₃), 1.25 [septet, 2H, *J* = 7.4 Hz, CH(CH₃)₂], 1.05 [d, *J* = 7.4 Hz, 6H, CH(CH₃)₂], and 0.92 [d, *J* = 7.4 Hz, 6H, CH(CH₃)₂].

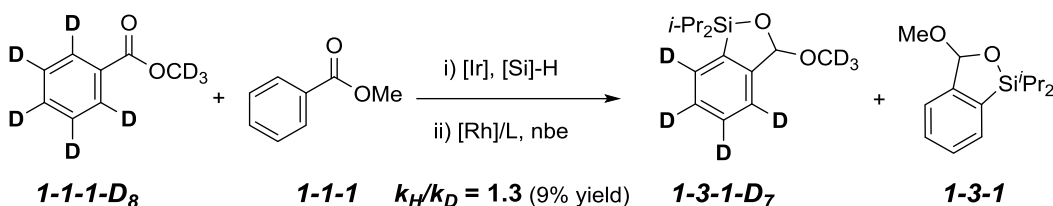
¹³C NMR (CDCl₃, 125 MHz): δ 167.5, 146.9, 140.3, 138.8, 136.0, 129.5, 128.9, 126.2, 118.4, 51.8, 17.709, 17.689, 14.5 and 2.4.

IR (neat): 3057 (w), 2944 (w), 2877 (w), 1721 (m), 1048 (s), 838 (s), and 714 (m) cm⁻¹.

TLC: R_f = 0.4 in 20:1 hexanes: EtOAc.

HRMS (ESI/TOF): Calcd for (M+Na)⁺ (C₁₉H₃₂NaO₃Si₂)⁺: 387.1782. Found: 387.1798.

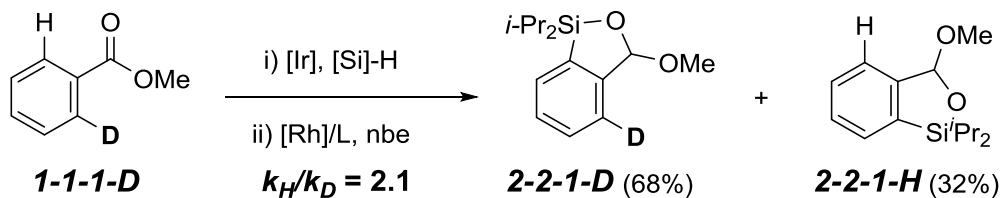
C.14. Procedure for intermolecular KIE:



[Ir(coe)₂Cl]₂ (0.45 mg, 0.1 mol %), ester **1-1-1** (0.25 mmol, 31.5 μ L) and ester **1-1-1-D₈** (0.25 mmol, 30.5 μ L) were dissolved with CH₂Cl₂ (0.2 mL, 2.5 M). Diisopropylsilane (0.2 mL, 1 mmol) was added to the mixture in one portion. The septum on the vial was replaced by a screw cap with a Teflon liner. The reaction mixture was kept at 45 °C and stirred for 24 h. The volatiles were removed *in vacuo* to afford the silyl acetals, which were directly used for subsequent reaction without further purification. [Rh(nbd)Cl]₂ (1 mg, 0.4 mol %), *tris*(4-methoxyphenyl)phosphine (4.2 mg, 2.4 mol %) and norbornene (94 mg, 1 mmol) were dissolved with THF (0.5 mL, 1 M), the previous prepared silyl acetals mixture (0.5 mmol) was added to the mixture in one portion. The septum on the vial was replaced

by a screw cap with a Teflon liner, and the mixture was stirred at 120 °C for 50 s. The yield of the cyclic silyl acetals (9%) was determined by ^1H NMR spectroscopy by an addition of CH_2Br_2 (0.5 mmol) as an internal standard after the volatiles were removed *in vacuo*. The crude mixture was purified by MPLC (hexanes/EtOAc = 40:1, 7 mL/min, retention time 7 min) to provide **1-3-1-D₇** and **1-3-1** as a colorless liquid. The isolated cyclic silyl acetal products were analyzed by ^1H NMR using CDCl_3 as solvent and 20s relaxation delay on a 500 MHz NMR spectrometer. The reactions were run 6 times, the average KIE was 1.3 ± 0.1 .

C.15. Procedure for intramolecular KIE:



$[\text{Ir}(\text{coe})_2\text{Cl}]_2$ (0.23 mg, 0.1 mol %) and ester **1-1-1-D** (0.25 mmol, 34.2 mg) were dissolved with CH_2Cl_2 (0.1 mL, 2.5 M). Diisopropylsilane (0.1 mL, 0.5 mmol) was added to the mixture in one portion. The septum on the vial was replaced by a screw cap with a Teflon liner. The reaction mixture was kept at 45 °C and stirred for 24 h. The volatiles were removed *in vacuo* to afford the silyl acetals, which were directly used for subsequent reaction without further purification. $[\text{Rh}(\text{nbd})\text{Cl}]_2$ (0.5 mg, 0.4 mol %), *tris*(4-methoxyphenyl)phosphine (2.1 mg, 2.4 mol %) and norbornene (47 mg, 0.5 mmol) were dissolved with THF (0.5 mL, 1 M), the silyl acetals mixture (0.25 mmol) was added to the mixture in one portion. The septum on the vial was replaced by a screw cap with a Teflon liner, and the mixture was stirred at 120 °C for 1h. The yield of the cyclic silyl acetals was determined by ^1H NMR spectroscopy by an addition of CH_2Br_2 (0.25 mmol) as an internal

standard after the volatiles were removed *in vacuo*. The crude mixture was purified by MPLC (hexanes/EtOAc = 40:1, 7 mL/min, retention time 7 min) to provide **2-2-1-D** and **2-1-H** as a colorless liquid. The conditions for ¹H NMR are: 500 MHz NMR; CDCl₃ as solvent; 20s relaxation delay. The reactions were run 3 times, the average KIE was **2.1 ± 0.1**.

Apendix D

Experimental Procedures for Chapter 3

D.1. General Procedure for C-H Silylation to Prepare Benzodioxasilines (3-12):

(i) $[\text{Ir}(\text{coe})_2\text{Cl}]_2$ (0.9 mg, 0.1 mol %) and aryl acetates **3-8** (1 mmol) were added to a flame-dried, nitrogen-purged septum-capped vial. The mixture was dissolved with THF (0.3 mL, 3.3 M), and diethylsilane (0.26 mL, 2 mmol) was added to the mixture. The septum on the vial was replaced by a screw cap with a Teflon liner under a N_2 atmosphere [note: diethylsilane (bp 56 °C and density 0.686 g/mL) is volatile]. The reaction mixture was stirred for 3-12 h at 60 °C. Volatiles were removed *in vacuo* to afford silyl acetals **3-10**, which were directly used for subsequent reactions without further purification. (ii) $[\text{Rh}(\text{nbd})\text{Cl}]_2$ (1.84 mg, 0.4 mol %), *tris*(4-methoxyphenyl)phosphine (8.45 mg, 2.4 mol %), norbornene (188 mg, 2 mmol), and THF (1 mL, 1 M) were added to the crude silyl acetals **3-10** (1 mmol). The septum on the vial was replaced by a screw cap with a Teflon liner, and the mixture was stirred at 120 °C for 15 min (unless otherwise mentioned in Table 3-1). The reaction progress was monitored by GC/MS spectrometry. Volatiles were removed *in vacuo*, and the resulting mixture was dissolved with pentane, filtered through a pad of Celite®, and concentrated *in vacuo* to afford the crude benzodioxasilines **3-12**, which were directly used for a subsequent reaction without further purification. For an analytical purpose, the product was purified by MPLC (hexanes/EtOAc =80:1, 5 mL/min, retention time 5-15 min).

D.2. General Procedure for Nucleophilic Addition to Benzodioxasilines to Prepare of 2-Silyl Phenols (3-9)

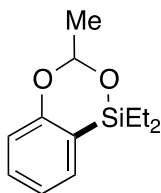
The crude benzodioxasilines **3-12** (1 mmol) were dissolved with THF (2 mL, 0.5 M) and cooled to -78 °C, then nucleophiles (3 equiv) were added into the reaction mixture and stirred at -78 °C for 30 min. The reaction was quenched at -78 °C by adding saturated

aqueous ammonium chloride solution, then the mixture was acidified to ca. pH 4-5 with aqueous HCl (1 M). The mixture was extracted with diethyl ether. The combined organic layer was washed with water and brine, and dried over anhydrous sodium sulfate. Volatiles were removed *in vacuo*, and the crude mixture was purified by MPLC to afford 2-silyl phenols **3-9** (hexanes/EtOAc = 20:1, 5 mL/min, retention time 6-20 min).

Note: When MeLi addition reactions were carried out over 30 min, significant desilylation occurred in cases of compounds **3-9f**, **3-9r**, **3-9x**, **3-9y**, and **3-9aa**.

D.3. Compound characterization

1,1-Diethyl-3-methyl-benzo[*c*][1,5,2]dioxasiline (**3-12a**)



Yield: 1 mmol scale, 210 mg, 95%; 12 mmol scale, 1.92 g, 72%.

¹H NMR (CDCl₃, 500 MHz): δ 7.56 (ddd, *J* = 8.1, 7.2, 1.7 Hz, 1H, SiCCHCH or OCCHCH), 7.55-7.53 (mfom, 1H, SiCCH or OCCH), 7.26 (ddd, *J* = 7.2, 7.2, 0.9 Hz, 1H, OCCHCH or SiCCHCH), 7.15 (app d, *J* = 8.1 Hz, 1H, OCCH or SiCCH), 5.67 (q, *J* = 5.0 Hz, 1H, OCHMe), 1.80 (d, *J* = 5.0 Hz, 3H, OCHCH₃), 1.31 (t, *J* = 7.8 Hz, 3H, SiCH₂CH₃), 1.15 (t, *J* = 7.8 Hz, 3H, SiCH₂CH₃), and 1.15-0.93 [m, 4H, Si(CH₂CH₃)₂].

¹³C NMR (CDCl₃, 125 MHz): δ 164.3, 133.5, 131.5, 122.1, 119.4, 117.7, 95.9, 23.8, 7.0, 6.9, 6.4, and 6.37.

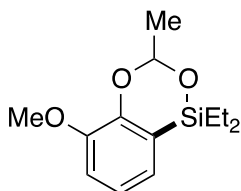
IR (neat): 2957 (w), 1596 (m), 1491 (m), 1265 (s), 1224 (s), 1091 (s), and 934 (s) cm⁻¹.

TLC: R_f = 0.5 in 20:1 hexanes: EtOAc.

GCMS (5029017): t_R = 8.65 min, m/z 223 [(M+H)⁺, 57], 222 (M⁺, 100), 223 [(M-H)⁺, 60], 193 [(M-Et)⁺, 51], and 178 [(M-MeCHO)⁺, 16].

HRMS (APCI/TOF): Calcd for (M+H)⁺ (C₁₂H₁₉O₂Si)⁺: 223.1149. Found: 223.1134.

1,1-Diethyl-5-methoxy-3-methyl-benzo[*c*][1,5,2]dioxasiline (**3-12c**)



Total Yield: 1 mmol scale, 204 mg, 81%.

¹H NMR (CDCl₃, 500 MHz): δ 7.00 (dd, *J* = 7.9, 7.2 Hz, 1H, SiCCHCH), 6.92 [dd, *J* = 7.9, 1.5 Hz, 1H, SiCCH or C(OMe)CH], 6.87 [dd, *J* = 7.2, 1.5 Hz, 1H, SiCCH or C(OMe)CH], 5.45 (q, *J* = 5.0 Hz, 1H, OCHMe), 3.85 (s, 3H, OCH₃), 1.64 (d, *J* = 5.0 Hz, 3H, OCHCH₃), 1.07 (t, *J* = 7.9 Hz, 3H, SiCH₂CH₃), 0.89 (t, *J* = 7.9 Hz, 3H, SiCH₂CH₃), and 0.89-0.68 [m, 4H, Si(CH₂CH₃)₂].

¹³C NMR (CDCl₃, 125 MHz): δ 153.3, 148.4, 124.4, 122.3, 120.2, 113.4, 96.2, 55.8, 23.7, 6.9, 6.7, and 6.3 (2).

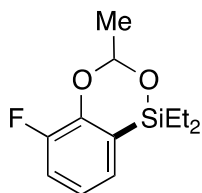
IR (neat): 2956 (w), 2937 (w), 1466 (s), 1403 (s), 1229 (s), 1091 (s), 933 (s), and 801 (s) cm⁻¹.

TLC: R_f = 0.4 in 20:1 hexanes: EtOAc.

GCMS (5029017): t_R = 9.94 min, m/z 253 [(M+H)⁺, 1], 252 (M⁺, 1), 224 [(M+H-Et)⁺, 100], and 209 [(M-MeCHO)⁺, 10].

HRMS (APCI/TOF): Calcd for (M+H)⁺ (C₁₃H₂₁O₃Si)⁺: 253.1254. Found: 253.1267.

1,1-Diethyl-5-fluoro-3-methyl-benzo[*c*][1,5,2]dioxasiline (3-12d)



Yield: 1 mmol scale, 146 mg, 61%.

¹H NMR (CDCl₃, 500 MHz): δ 7.10 [ddd, *J* = 11.1 (³J_{F-H}), 7.9, 1.6 Hz, 1H, FCCH], 7.03 [ddd, *J* = 7.3, 1.6, 0.7 (⁵J_{F-H}) Hz, 1H, SiCCH], 6.99 [ddd, *J* = 7.9, 7.3, 4.1 (⁴J_{F-H}) Hz, 1H, SiCCHCH], 5.47 (q, *J* = 5.0 Hz, 1H, OCHMe), 1.62 (d, *J* = 5.0 Hz, 3H, OCHCH₃), 1.07 (t, *J* = 7.7 Hz, 3H, SiCH₂CH₃), 0.92 (t, *J* = 7.7 Hz, 3H, SiCH₂CH₃), and 0.90-0.67 [m, 4H, Si(CH₂CH₃)₂].

¹³C NMR (CDCl₃, 125 MHz): δ 151.60 (d, ¹J_{F-C} = 250.4 Hz), 151.59 (d, ²J_{F-C} = 8.8 Hz),

128.2 (d, $^3J_{F-C} = 4.6$ Hz), 122.50, 122.48 (d, $^3J_{F-C} = 5.7$ Hz), 118.0 (d, $^2J_{F-C} = 18.4$ Hz), 96.5, 23.6, 7.0, 6.8, 6.30, and 6.28.

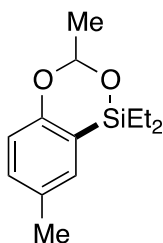
IR (neat): 2956 (w), 1690 (w), 1505 (s), 1259 (s), 1066 (s), 1007 (s), and 747 (m) cm^{-1} .

TLC: $R_f = 0.6$ in 20:1 hexanes: EtOAc.

GCMS (5029017): $t_R = 8.77$ min, m/z 241 [(M+H)⁺, 45], 240 (M⁺, 100), 221 [(M-F)⁺, 2], 211 [(M-Et)⁺, 12], and 196 [(M-MeCHO)⁺, 27].

HRMS (APCI/TOF): Calcd for (M+H)⁺ (C₁₂H₁₈FO₂Si)⁺: 241.1055. Found: 241.1046.

1,1-Diethyl-3,7-dimethyl-benzo[c][1,5,2]dioxasiline (3-12j)



Yield: 1 mmol scale, 215 mg, 91%.

¹H NMR (CDCl₃, 500 MHz): δ 7.13 (dd, $J = 8.3, 2.2$ Hz, 1H, OCCHCH), 7.10 (d, $J = 2.2$ Hz, 1H, SiCCH), 6.82 (d, $J = 8.3$ Hz, 1H, OCCH), 5.39 (q, $J = 5.0$ Hz, 1H, OCHMe), 2.32 (s, 3H, SiCCHCCH₃), 1.56 (d, $J = 5.0$ Hz, 3H, OCHCH₃), 1.09 (t, $J = 7.8$ Hz, 3H, SiCH₂CH₃), 0.93 (t, $J = 7.8$ Hz, 3H, SiCH₂CH₃), and 0.91-0.70 [m, 4H, Si(CH₂CH₃)₂].

¹³C NMR (CDCl₃, 125 MHz): δ 162.2, 133.4, 132.2, 131.1, 119.1, 117.3, 95.8, 23.7, 20.8, 6.9, 6.8, 6.4, and 6.3.

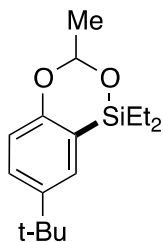
IR (neat): 2993 (m), 1470 (m), 1388 (s), 1223 (s), 1092 (s), and 714 (s) cm^{-1} .

TLC: $R_f = 0.4$ in 20:1 hexanes: EtOAc.

GCMS (5029017): $t_R = 9.23$ min, m/z 236 (M⁺, 70), 235 [(M-H)⁺, 100], 230 [(M-Me)⁺, 31], 207 [(M-Et)⁺, 62], and 192 [(M-MeCHO)⁺, 16].

HRMS (APCI/TOF): Calcd for (M+H)⁺ (C₁₃H₂₁O₂Si)⁺: 237.1305. Found: 237.1296.

7-(tert-Butyl)-1,1-diethyl-3-methyl-benzo[c][1,5,2]dioxasiline (3-12k)



Yield: 1 mmol scale, 267 mg, 96%.

¹H NMR (CDCl₃, 500 MHz): δ 7.37 (dd, *J* = 8.6, 2.5 Hz, 1H, OCCHCH), 7.29 (d, *J* = 2.5 Hz, 1H, SiCCH), 6.86 (d, *J* = 8.6 Hz, 1H, OCCH), 5.43 (q, *J* = 5.0 Hz, 1H, OCHMe), 1.57 (d, *J* = 5.0 Hz, 3H, OCHCH₃), 1.32 [s, 9H, C(CH₃)₃], 1.10 (t, *J* = 7.8 Hz, 3H, SiCH₂CH₃), 0.94 (t, *J* = 7.8 Hz, 3H, SiCH₂CH₃), and 0.87-0.73 [m, 4H, Si(CH₂CH₃)₂].

¹³C NMR (CDCl₃, 125 MHz): δ 162.1, 144.5, 129.7, 128.7, 118.7, 117.1, 95.8, 34.4, 31.7, 23.8, 7.0, 6.9, 6.47, and 6.45.

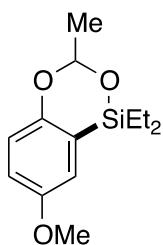
IR (neat): 2956 (m), 2874 (m), 1475 (m), 1362 (m), 1231 (s), 1092 (s), 935 (s), and 788 (s) cm⁻¹.

TLC: R_f = 0.5 in 20:1 hexanes: EtOAc.

GCMS (5029017): t_R = 10.44 min, m/z 279 [(M+H)⁺, 2], 263 [(M-Me)⁺, 6], 251 (100), and 234 [(M-MeCHO)⁺, 7].

HRMS (APCI/TOF): Calcd for (M+H)⁺ (C₁₆H₂₇O₂Si)⁺: 279.1775. Found: 279.1762.

1,1-Diethyl-7-methoxy-3-methyl-benzo[c][1,5,2]dioxasiline (3-12I)



Yield: 1 mmol scale, 229 mg, 91%.

¹H NMR (CDCl₃, 500 MHz): δ 6.88 [dd, *J* = 8.9, 2.7 Hz, 1H, SiCCHC(OMe)CH], 6.86 [d, *J* = 8.9 Hz, 1H, SiCCHC(OMe)CHCH], 6.80 (d, *J* = 2.7 Hz, 1H, SiCCH), 5.37 (q, *J* = 5.0 Hz, 1H, OCHMe), 3.78 (s, 3H, OCH₃), 1.55 (d, *J* = 5.0 Hz, 3H, OCHCH₃), 1.07 (t, *J* = 7.9 Hz, 3H, SiCH₂CH₃), 0.92 (t, *J* = 7.9 Hz, 3H, SiCH₂CH₃), and 0.90-0.70 [m, 4H, Si(CH₂CH₃)₂].

¹³C NMR (CDCl₃, 125 MHz): δ 158.3, 154.6, 120.5, 118.7, 117.5, 117.2, 96.2, 55.8, 23.8, 6.94, 6.88, 6.48 and 6.40.

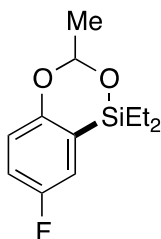
IR (neat): 2934 (w), 1469 (s), 1407 (s), 1233 (s), 1092 (s), 934 (s), and 798 (s) cm^{-1} .

TLC: $R_f = 0.4$ in 20:1 hexanes: EtOAc.

GCMS (5029017): $t_R = 9.93$ min, m/z 253 [(M+H)⁺, 27], 252 (M⁺, 100), 237 [(M-Me)⁺, 1], 223 [(M-Et)⁺, 6], and 208 [(M-MeCHO)⁺, 85].

HRMS (APCI/TOF): Calcd for (M+H)⁺ (C₁₃H₂₁O₃Si)⁺: 253.1254. Found: 253.1246.

1,1-Diethyl-7-fluoro-3-methyl-benzo[c][1,5,2]dioxasiline (3-12m)



Yield: 1 mmol scale, 223 mg, 91%.

¹H NMR (CDCl₃, 500 MHz): δ 7.00 [ddd, $J = 8.9, 8.9$ (³ J_{F-H}), 3.1 Hz, 1H, OCCHCH], 6.95 [dd, $J = 7.6$ (³ J_{F-H}), 3.1 Hz, 1H, SiCCH], 6.87 [dd, $J = 8.9, 4.2$ (⁴ J_{F-H}) Hz, 1H, OCCH], 5.38 (q, $J = 5.0$ Hz, 1H, OCHMe), 1.55 (d, $J = 5.0$ Hz, 3H, OCHCH₃), 1.06 (t, $J = 7.7$ Hz, 3H, SiCH₂CH₃), 0.91 (t, $J = 7.7$ Hz, 3H, SiCH₂CH₃), and 0.91-0.69 [m, 4H, Si(CH₂CH₃)₂].

¹³C NMR (CDCl₃, 125 MHz): δ 160.2 (d, ⁴ $J_{F-C} = 2.3$ Hz), 158.1 (d, ¹ $J_{F-C} = 242.3$ Hz), 121.1 (d, ³ $J_{F-C} = 4.6$ Hz), 119.3 (d, ³ $J_{F-C} = 7.0$ Hz), 118.6 (d, ² $J_{F-C} = 20.4$ Hz), 118.4 (d, ² $J_{F-C} = 24.0$ Hz), 96.3, 23.7, 6.9, 6.8, 6.31, and 6.26.

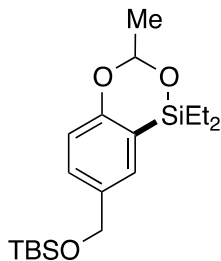
IR (neat): 2954 (m), 2853 (w), 1460 (w), 1108 (s), and 962 (s) cm^{-1} .

TLC: $R_f = 0.5$ in 20:1 hexanes: EtOAc.

GCMS (5029017): $t_R = 8.52$ min, m/z 241 [(M+H)⁺, 27], 240 (M⁺, 61), 239 [(M-H)⁺, 22], 221 [(M-F)⁺, 2], 211 [(M-Et)⁺, 15], and 196 [(M-MeCHO)⁺, 100].

HRMS (APCI/TOF): Calcd for (M+H)⁺ (C₁₂H₁₈FO₂Si)⁺: 241.1055. Found: 241.1071.

7-[(*tert*-Butyldimethylsilyloxy)ariamethyl]-1,1-diethyl-3-methyl-benzo[c][1,5,2]dioxasiline (3-12p)



Yield: 1 mmol scale, 318 mg, 87%.

¹H NMR (CDCl₃, 500 MHz): δ 7.26 (dd, *J* = 8.0, 2.2 Hz, 1H, OCCHCH), 7.25 (d, *J* = 2.2 Hz, 1H, SiCCH), 6.87 (d, *J* = 8.0 Hz, 1H, OCCH), 5.41 (q, *J* = 5.0 Hz, 1H, OCHMe), 4.70 (d, *J* = 17.6 Hz, 1H, ArCH_aH_bO), 4.67 (d, *J* = 17.6 Hz, 1H, ArCH_aH_bO), 1.56 (d, *J* = 5.0 Hz, 3H, OCHCH₃), 1.06 (t, *J* = 7.8 Hz, 3H, SiCH₂CH₃), 0.92 [s, 9H, OSi(CH₃)₃], 0.90 (t, *J* = 7.8 Hz, 3H, SiCH₂CH₃), 0.90-0.69 [m, 4H, Si(CH₂CH₃)₂], and 0.08 [s, 6H, OSi(CH₃)₂].

¹³C NMR (CDCl₃, 125 MHz): δ 163.3, 134.7, 131.1, 129.6, 118.9, 117.4, 95.9, 64.8, 26.0, 23.6, 18.4, 6.8, 6.7, 6.2 (2), and 5.1 (2).

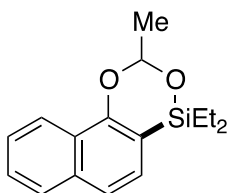
IR (neat): 2955 (m), 2876 (m), 1597 (m), 1479 (m), 1230 (s), 1098 (s), and 825 (s) cm⁻¹.

TLC: R_f = 0.5 in 20:1 hexanes: EtOAc.

GCMS (5029017): t_R = 11.97 min, m/z 366 (M⁺, 28), 365 [(M-H)⁺, 85], 265 [(M-OSiEt₂)⁺, 100], and 235 [(M-OTBS)⁺, 30].

HRMS (APCI/TOF): Calcd for (M+H)⁺ (C₁₉H₃₅O₃Si₂)⁺: 367.2119. Found: 367.2103.

4,4-Diethyl-2-methyl-naphtho[2,1-c][1,5,2]dioxasiline (3-12t)



Yield: 1 mmol scale, 242 mg, 89%.

¹H NMR (CDCl₃, 500 MHz): δ 8.25 (app d, *J* = 8.0 Hz, 1H, Ar-*H*), 7.82 (app d, *J* = 7.3 Hz, 1H, Ar-*H*), 7.55-7.48 (m, 3H, Ar-*H*), 7.34 (d, *J* = 8.1 Hz, 1H, Ar-*H*), 5.61 (q, *J* = 5.0 Hz, 1H, OCHMe), 1.74 (d, *J* = 5.0 Hz, 3H, OCHCH₃), 1.12 (t, *J* = 7.8 Hz, 3H, SiCH₂CH₃), 1.01 (t, *J* = 7.8 Hz, 3H, SiCH₂CH₃), and 0.95-0.76 [m, 4H, Si(CH₂CH₃)₂].

¹³C NMR (CDCl₃, 125 MHz): δ 161.0, 135.5, 128.5, 127.6, 127.3, 125.7, 125.2, 122.2, 121.4, 112.4, 96.2, 23.7, 7.1, 7.0, 6.5, and 6.3.

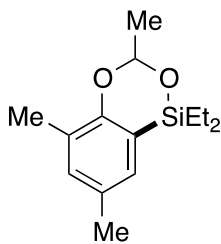
IR (neat): 3046 (w), 2956 (m), 1500 (m), 1396 (m), 1325 (s), 1088 (s), 958 (s), and 742 (s) cm⁻¹.

TLC: R_f = 0.5 in 20:1 hexanes: EtOAc.

GCMS (5029017): t_R = 11.73 min, m/z 273 [(M+H)⁺, 7], 272 (M⁺, 61), 243 [(M-Et)⁺, 6], and 228 [(M-MeCHO)⁺, 100].

HRMS (APCI/TOF): Calcd for (M+H)⁺ (C₁₆H₂₁O₂Si)⁺: 273.1305. Found: 273.1320.

1,1-Diethyl-3,5,7-trimethyl-benzo[c][1,5,2]dioxasiline (3-12u)



Yield: 1 mmol scale, 210 mg, 84%.

¹H NMR (CDCl₃, 500 MHz): δ 7.01 (app s, 1H, Ar-H), 6.93 (app s, 1H, Ar-H), 5.37 (q, J = 5.0 Hz, 1H, OCHMe), 2.27 (s, 3H, ArCH₃), 2.18 (s, 3H, ArCH₃), 1.58 (d, J = 5.0 Hz, 3H, OCHCH₃), 1.07 (t, J = 7.8 Hz, 3H, SiCH₂CH₃), 0.92 (t, J = 7.8 Hz, 3H, SiCH₂CH₃), and 0.91-0.69 [m, 4H, Si(CH₂CH₃)₂].

¹³C NMR (CDCl₃, 125 MHz): δ, 160.3, 133.5, 130.79, 130.73, 126.3, 118.6, 95.8, 23.7, 20.7, 16.0, 6.85, 6.81, 6.4, and 6.3.

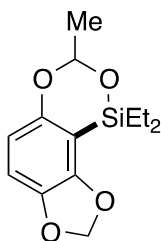
IR (neat): 2957 (m), 2877 (m), 1460 (m), 1392 (m), 1217 (s), 1091 (s), and 740 (m) cm⁻¹.

TLC: R_f = 0.5 in 20:1 hexanes: EtOAc.

GCMS (5029017): t_R = 9.46 min, m/z 251 [(M+H)⁺, 15], 250 (M⁺, 27), 221 [(M-Et)⁺, 7], and 206 [(M-MeCHO)⁺, 100].

HRMS (APCI/TOF): Calcd for (M+H)⁺ (C₁₄H₂₃O₂Si)⁺: 251.1462. Found: 251.1443.

1,1-Diethyl-3-methyl-[1,3]dioxolo[4',5':5,6]benzo[1,2-c][1,5,2]dioxasiline (3-12v)



Total Yield: 1 mmol scale, 213 mg, 80%. (regioisomer ratio 3:1)

¹H NMR (CDCl₃, 500 MHz): δ 6.75 (d, *J* = 8.3 Hz, 1H, Ar-*H*), 6.38 (d, *J* = 8.3 Hz, 1H, Ar-*H*), 5.92 (d, *J* = 17.6 Hz, 1H, ArOCH_aH_bO), 5.89 (d, *J* = 17.6 Hz, 1H, ArOCH_aH_bO), 5.35 (q, *J* = 5.0 Hz, 1H, OCHMe), 1.53 (d, *J* = 5.0 Hz, 3H, OCHCH₃), 1.06 (t, *J* = 7.8 Hz, 3H, SiCH₂CH₃), 0.95 (t, *J* = 7.8 Hz, 3H, SiCH₂CH₃), and 0.90-0.74 [m, 4H, Si(CH₂CH₃)₂].

¹³C NMR (CDCl₃, 125 MHz): δ 158.4, 151.4, 141.1, 110.6, 109.4, 101.9, 101.2, 96.3, 23.6, 7.2, 6.6, 6.2, and 5.9.

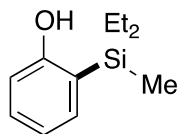
IR (neat): 2958 (m), 2877 (m), 1636 (m), 1429 (s), 1395 (s), 1219 (s), 1091 (s), 1044 (s), 934 (s), and 731 (m) cm⁻¹.

TLC: R_f = 0.4 in 20:1 hexanes: EtOAc.

GCMS (5029017): t_R = 10.48 min, m/z 267 [(M+H)⁺, 16], 266 (M⁺, 100), 238 [(M+H-Et)⁺, 2], and 223 [(M+H-MeCHO)⁺, 22].

HRMS (APCI/TOF): Calcd for (M+H)⁺ (C₁₃H₁₉O₄Si)⁺: 267.1047. Found: 267.1026.

2-[Diethyl(methyl)silyl]phenol (3-9a)



Yield: 1 mmol scale, 161 mg, 83%.

¹H NMR (CDCl₃, 500 MHz): δ 7.35 [dd, *J* = 7.3, 1.5 Hz, 1H, C(O)CH or SiCCH], 7.23 [ddd, *J* = 8.0, 7.3, 1.5 Hz, 1H, C(O)CHCH or SiCCHCH], 6.92 [dd, *J* = 7.3, 7.3 Hz, 1H, C(O)CHCH or SiCCHCH], 6.67 [d, *J* = 8.0 Hz, 1H, C(O)CH or SiCCH], 4.73 (s, 1H, ArOH), 0.95 [t, *J* = 8.5 Hz, 6H, Si(CH₂CH₃)₂], 0.86-0.78 [m, 4H, Si(CH₂CH₃)₂], and 0.27 (s, 3H, SiCH₃).

¹³C NMR (CDCl₃, 125 MHz): δ 160.7, 136.2, 130.7, 123.6, 120.5, 114.7, 7.7, 5.6, and 5.5.

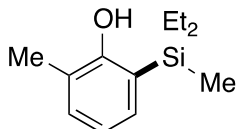
IR (neat): 3536 (br, w), 2953 (m), 2874 (m), 1435 (s), 1322 (s), 1122 (m), 1006 (m), and 752 (s) cm⁻¹.

TLC: $R_f = 0.4$ in 10:1 hexanes: EtOAc.

GCMS (5029017): $t_R = 9.25$ min, m/z 195 [(M+H)⁺, 1], 179 [(M-Me)⁺, 2], 165 [(M-Et)⁺, 29], and 137 (100).

HRMS (APCI/TOF): Calcd for (M+H)⁺ (C₁₁H₁₉OSi)⁺: 195.1200. Found: 195.1213.

2-[Diethyl(methyl)silyl]-6-methylphenol (3-9b)



Yield: 1 mmol scale, 173 mg, 83%.

¹H NMR (CDCl₃, 500 MHz): δ 7.23 [dd, $J = 7.3, 1.7$ Hz, 1H, C(OH)C(Me)CH or SiCCH], 7.15 [dd, $J = 7.3, 1.7$ Hz, 1H, C(OH)C(Me)CH or SiCCH], 6.87 (dd, $J = 7.3, 7.3$ Hz, 1H, SiCCHCH), 4.75 (s, 1H, ArOH), 2.25 (s, 3H, Ar-CH₃), 0.98 [t, $J = 7.7$ Hz, 6H, Si(CH₂CH₃)₂], 0.88-0.82 [m, 4H, Si(CH₂CH₃)₂], and 0.30 (s, 3H, SiCH₃).

¹³C NMR (CDCl₃, 125 MHz): δ 159.0, 134.0, 132.2, 123.0, 121.8, 120.6, 16.0, 7.8, 5.8, and -5.3.

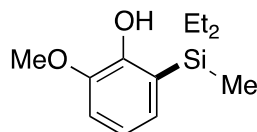
IR (neat): 3541 (br, w), 2952 (m), 2873 (m), 1577 (w), 1455 (m), 1432 (s), 1275 (s), 1215 (s), 1073 (m), and 735 (m) cm⁻¹.

TLC: $R_f = 0.5$ in 10:1 hexanes: EtOAc.

GCMS (5029017): $t_R = 9.37$ min, m/z 209 [(M+H)⁺, 100], 208 (M⁺, 20), 192 [(M-H-Me)⁺, 1], and 178 [(M-H-Et)⁺, 60].

HRMS (APCI/TOF): Calcd for (M+H)⁺ (C₁₂H₂₁OSi)⁺: 209.1356. Found: 209.1366.

2-[Diethyl(methyl)silyl]-6-methoxyphenol (3-9c)



Yield: 1 mmol scale, 148 mg, 66%.

¹H NMR (CDCl₃, 500 MHz): δ 6.95 [dd, $J = 6.9, 2.0$ Hz, 1H, C(OH)C(OMe)CH or SiCCH], 6.88 [dd, $J = 7.9, 2.0$ Hz, 1H, C(OH)C(OMe)CH or SiCCH], 6.85 (dd, $J = 7.9, 6.9$ Hz, 1H, SiCCHCH), 5.84 (s, 1H, ArOH), 3.88 (s, 3H, Ar-OCH₃), 0.97 [t, $J = 7.3$ Hz, 6H, Si(CH₂CH₃)₂], 0.88-0.81 [m, 4H, Si(CH₂CH₃)₂], and 0.28 (s, 3H, SiCH₃).

¹³C NMR (CDCl₃, 125 MHz): δ 150.6, 145.9, 127.4, 122.8, 119.8, 111.7, 56.0, 7.8, 5.5, and -5.6.

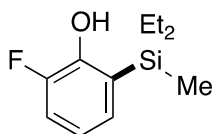
IR (neat): 3611 (br, w), 2952 (m), 2873 (m), 1577 (w), 1416 (m), 1201 (s), 1006 (m), and 741 (s) cm⁻¹.

TLC: R_f = 0.6 in 10:1 hexanes: EtOAc.

GCMS (5029017): t_R = 9.94 min, m/z 225 [(M+H)⁺, 26], 224 (M⁺, 100), 209 [(M-Me)⁺, 10], and 195 [(M-Et)⁺, 16].

HRMS (APCI/TOF): Calcd for (M+H)⁺ (C₁₂H₂₁O₂Si)⁺: 225.1305. Found: 225.1310.

2-[Diethyl(methyl)silyl]-6-fluorophenol (3-9d)



Yield: 1 mmol scale, 102 mg, 48%.

¹H NMR (CDCl₃, 300 MHz): δ 7.08 (dd, *J* = 7.1, 1.5 Hz, 1H, SiCCH), 7.06 [ddd, *J* = 9.6 (³*J*_{F-H}), 8.2, 1.5 Hz, 1H, C(OH)C(F)CH], 6.83 [ddd, *J* = 8.2, 7.1, 4.6 (⁴*J*_{F-H}) Hz, 1H, SiCCHCH], 5.21 [d, *J* = 5.7 (⁴*J*_{F-H}) Hz, 1H, ArOH], 0.98-0.76 [m, 10H, Si(CH₂CH₃)₂], and 0.27 (s, 3H, SiCH₃).

¹³C NMR (CDCl₃, 75 MHz): δ 150.8 (d, ¹*J*_{F-C} = 238.1 Hz), 148.0 (d, ²*J*_{F-C} = 12.5 Hz), 130.9 (d, ³*J*_{F-C} = 4.2 Hz), 126.7, 120.6 (d, ³*J*_{F-C} = 5.6 Hz), 116.4 (d, ²*J*_{F-C} = 28.5 Hz), 7.7, 5.5, and -5.6.

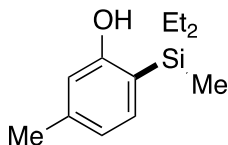
IR (neat): 3588 (br, w), 2953 (m), 283 (m), 1606 (m), 1443 (s), 1256 (s), 1168 (s), and 741 (s) cm⁻¹.

TLC: R_f = 0.6 in 10:1 hexanes: EtOAc.

GCMS (5029017): t_R = 8.69 min, m/z 212 (M⁺, 8), 197 [(M-Me)⁺, 3], 183 [(M-Et)⁺, 74], 169 (10), 155 (100), and 141 (15).

HRMS (APCI/TOF): Calcd for (M+H)⁺ (C₁₁H₁₈FOSi)⁺: 213.1105. Found: 213.1105.

2-[Diethyl(methyl)silyl]-5-methylphenol (3-9e)



Yield: 1 mmol scale, 150 mg, 72%.

¹H NMR (CDCl₃, 500 MHz): δ 7.24 (d, *J* = 7.4, 1H, SiCCH), 6.76 (app d, *J* = 7.4, 1H, SiCCHCH), 6.51 [app s, 1H, C(OH)CH], 4.70 (s, 1H, ArOH), 2.30 (s, 3H, ArCH₃), 0.96 [t, *J* = 7.6 Hz, 6H, Si(CH₂CH₃)₂], 0.86-0.77 [m, 4H, Si(CH₂CH₃)₂], and 0.27 (s, 3H, SiCH₃).

¹³C NMR (CDCl₃, 125 MHz): δ 160.8, 141.2, 136.1, 121.6, 119.9, 115.6, 21.4, 7.8, 5.7, and -5.4.

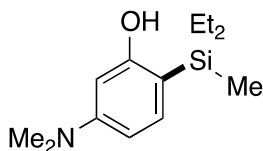
IR (neat): 3532 (br, w), 2952 (m), 2874 (m), 1605 (m), 1397 (s), 1283 (s), 1070 (s), 758 (s), and 742 (s) (m) cm⁻¹.

TLC: R_f = 0.5 in 10:1 hexanes: EtOAc.

GCMS (5029017): t_R = 9.37 min, m/z 208 (M⁺, 17), 207 [(M-H)⁺, 100], 192 [(M-H-Me)⁺, 88], and 178 [(M-Et)⁺, 31].

HRMS (APCI/TOF): Calcd for (M+H)⁺ (C₁₁H₂₁OSi)⁺: 209.1356. Found: 209.1339.

2-[Diethyl(methyl)silyl]-5-(dimethylamino)phenol (3-9f)



Yield: 1 mmol scale, 81 mg, 34%.

¹H NMR (CDCl₃, 300 MHz): δ 7.20 (d, *J* = 8.2 Hz, 1H, SiCCH), 6.33 (dd, *J* = 8.2, 2.2 Hz, 1H, SiCCHCH), 6.05 [d, *J* = 2.2 Hz, 1H, C(OH)CH], 4.76 (s, 1H, ArOH), 2.92 [s, 6H, ArN(CH₃)₂], 0.95 [t, *J* = 7.2 Hz, 6H, Si(CH₂CH₃)₂], 0.88-0.74 [m, 4H, Si(CH₂CH₃)₂], and 0.24 (s, 3H, SiCH₃).

¹³C NMR (CDCl₃, 75 MHz): δ 162.1, 153.1, 136.8, 109.4, 105.4, 99.3, 40.5, 7.8, 6.0, and -5.2.

IR (neat): 3331 (br, w), 2954 (m), 2875 (m), 1612 (s), 1577 (s), 1502 (s), 1443 (s), 1233 (s), 1150 (s), 974 (s), and 685 (m) cm⁻¹.

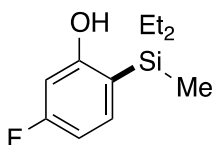
TLC: R_f = 0.1 in 10:1 hexanes: EtOAc.

GCMS (5029017): t_R = 10.18 min, m/z 238 [(M+H)⁺, 62], 237 (M)⁺, 100), 123 [(M-Me)⁺, 1],

and 209 [(M-Et)⁺, 4].

HRMS (APCI/TOF): Calcd for (M+H)⁺ (C₁₃H₂₄NOSi)⁺: 238.1622. Found: 238.1613.

2-[Diethyl(methyl)silyl]-5-fluorophenol (3-9g)



Yield: 1 mmol scale, 136 mg, 64%.

¹H NMR (CDCl₃, 500 MHz): δ 7.28 [dd, *J* = 8.4, 7.6 (⁴*J*_{F-H}) Hz, 1H, SiCCH], 6.64 [ddd, *J* = 8.4 (³*J*_{F-H}), 8.4, 2.2 Hz, 1H, SiCCHCH], 6.43 [dd, *J* = 10.4 (³*J*_{F-H}), 2.2 Hz, 1H, OCC_H], 5.09 (s, 1H, ArOH), 0.94 [t, *J* = 7.6 Hz, 6H, Si(CH₂CH₃)₂], 0.86-0.76 [m, 4H, Si(CH₂CH₃)₂], and 0.26 (s, 3H, SiCH₃).

¹³C NMR (CDCl₃, 125 MHz): δ 164.8 (d, ¹*J*_{F-C} = 247.0 Hz), 162.0 (d, ³*J*_{F-C} = 9.6 Hz), 137.3 (d, ³*J*_{F-C} = 9.6 Hz), 119.1 (d, ⁴*J*_{F-C} = 3.1 Hz), 107.6 (d, ²*J*_{F-C} = 19.7 Hz), 102.6 (d, ²*J*_{F-C} = 23.5 Hz), 7.7, 5.6, and -5.4.

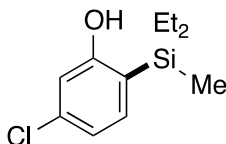
IR (neat): 3598 (br, w), 2954 (m), 2875 (m), 1590 (s), 1398 (s), 1283 (m), 1067 (m), 972 (s), and 785 (m) cm⁻¹.

TLC: R_f = 0.5 in 10:1 hexanes: EtOAc.

GCMS (5029017): t_R = 9.40 min, m/z 213 [(M+H)⁺, 15], 197 [(M-Me)⁺, 11], 193 [(M-F)⁺, 3], 183 [(M-Et)⁺, 80], and 155 (100).

HRMS (APCI/TOF): Calcd for (M+H)⁺ (C₁₁H₁₈FOSi)⁺: 213.1105. Found: 213.1114.

5-Chloro-2-[diethyl(methyl)silyl]phenol (3-9h)



Yield: 1 mmol scale, 106 mg, 46%.

¹H NMR (CDCl₃, 500 MHz): δ 7.25 (d, *J* = 7.8 Hz, 1H, SiCCH), 6.91 (dd, *J* = 7.8, 1.8 Hz, 1H, SiCCHCH), 6.70 [d, *J* = 1.8 Hz, 1H, C(OH)CH], 4.93 (s, 1H, ArOH), 0.93 [t, *J* = 7.4 Hz, 6H, Si(CH₂CH₃)₂], 0.83-0.77 [m, 4H, Si(CH₂CH₃)₂], and 0.26 (s, 3H, SiCH₃).

¹³C NMR (CDCl₃, 125 MHz): δ 161.3, 137.1, 136.0, 122.2, 120.9, 115.0, 7.6, 5.5, and -

5.5.

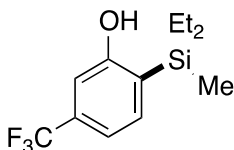
IR (neat): 3557 (br, w), 2953 (m), 2874 (m), 1584 (m), 1385 (s), 1229 (m), 1006 (m), 894 (s), 785 (s), and 742 (m) cm^{-1} .

TLC: $R_f = 0.5$ in 10:1 hexanes: EtOAc.

GCMS (5029017): $t_R = 10.55$ min, m/z 231 [(M+H+2)⁺, 18], 229 [(M+H)⁺, 57], 213 [(M-Me)⁺, 11], and 199 [(M-Et)⁺, 100].

HRMS (APCI/TOF): Calcd for (M+H)⁺ ($\text{C}_{11}\text{H}_{18}\text{ClOSi}$)⁺: 229.0810. Found: 229.0817.

2-[Diethyl(methyl)silyl]-5-(trifluoromethyl)phenol (3-9i)



Yield: 1 mmol scale, 217 mg, 83%.

¹H NMR (CDCl_3 , 500 MHz): δ 7.45 (d, $J = 7.6$ Hz, 1H, SiCCH), 7.16 (app d, $J = 7.6$ Hz, 1H, SiCCHCH), 6.90 [app s, 1H, C(OH)CH], 5.12 (s, 1H, ArOH), 0.99-0.90 [m, 6H, $\text{Si}(\text{CH}_2\text{CH}_3)_2$], 0.99-0.89-0.78 [m, 4H, $\text{Si}(\text{CH}_2\text{CH}_3)_2$], and 0.29 (s, 3H, SiCH₃).

¹³C NMR (CDCl_3 , 125 MHz): δ 160.7, 136.8, 132.8 (q, $^2J_{\text{F-C}} = 32.3$ Hz), 128.7, 124.1 (q, $^1J_{\text{F-C}} = 272.1$ Hz), 117.2 (q, $^3J_{\text{F-C}} = 3.6$ Hz), 111.1 (q, $^3J_{\text{F-C}} = 3.6$ Hz), 7.6, 5.4, and -5.6.

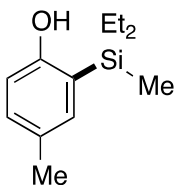
IR (neat): 3612 (br, w), 2956 (m), 2877 (m), 1402 (s), 1328 (s), 1123 (s), 909 (s), and 745 (m) cm^{-1} .

TLC: $R_f = 0.5$ in 10:1 hexanes: EtOAc.

GCMS (5029017): $t_R = 9.30$ min, m/z 261 [(M-H)⁺, 1], 243 [(M-F)⁺, 100], 247 [(M-Me)⁺, 1], and 233 [(M-Et)⁺, 2].

HRMS (APCI/TOF): Calcd for (M+H)⁺ ($\text{C}_{12}\text{H}_{18}\text{F}_3\text{OSi}$)⁺: 263.1074. Found: 263.1068.

2-[Diethyl(methyl)silyl]-4-methylphenol (3-9j)



Yield: 1 mmol scale, 175 mg, 84%.

$^1\text{H NMR}$ (CDCl_3 , 500 MHz): δ 7.13 (app s, 1H, SiCCH), 7.03 [app d, $J = 8.1$, 1H, C(OH)CHCH], 6.59 [d, $J = 8.1$ Hz, 1H, C(OH)CH], 4.65 (s, 1H, ArOH), 2.28 (s, 3H, ArCH₃), 0.97 [t, $J = 8.1$ Hz, 6H, Si(CH₂CH₃)₂], 0.88-0.78 [m, 4H, Si(CH₂CH₃)₂], and 0.28 (s, 3H, SiCH₃).

$^{13}\text{C NMR}$ (CDCl_3 , 125 MHz): δ 158.5, 136.6, 131.2, 129.5, 123.3, 114.5, 20.8, 7.8, 5.7, and -5.4.

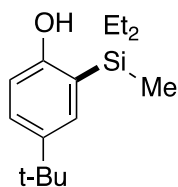
IR (neat): 3538 (br, w), 2952 (m), 2873 (m), 1598 (m), 1388 (m), 1243 (m), 1071 (m), 738 (s), and 679 (m) cm^{-1} .

TLC: $R_f = 0.4$ in 10:1 hexanes: EtOAc.

GCMS (5029017): $t_R = 9.78$ min, m/z 208 (M^+ , 17), 193 [(M-Me)⁺, 3], 179 [(M-Et)⁺, 78], 161 (50), 151 (100), and 91 (34).

HRMS (APCI/TOF): Calcd for (M+H)⁺ (C₁₁H₂₁OSi)⁺: 209.1356. Found: 209.1344.

4-(*tert*-Butyl)-2-[Diethyl(methyl)silyl]phenol (**3-9k**)



Yield: 1 mmol scale, 225 mg, 90%.

$^1\text{H NMR}$ (CDCl_3 , 500 MHz): δ 7.36 (d, $J = 2.5$ Hz, 1H, SiCCH), 7.24 [dd, $J = 8.3$, 2.5 Hz, 1H, C(OH)CHCH], 6.62 [d, $J = 8.3$ Hz, 1H, C(OH)CH], 4.64 (s, 1H, ArOH), 1.30 [s, 9H, C(CH₃)₃], 0.93 [t, $J = 7.4$ Hz, 6H, Si(CH₂CH₃)₂], 0.87-0.81 [m, 4H, Si(CH₂CH₃)₂], and 0.28 (s, 3H, SiCH₃).

$^{13}\text{C NMR}$ (CDCl_3 , 125 MHz): δ 158.4, 142.8, 132.8, 127.6, 122.8, 114.2, 34.3, 31.8, 7.8, 5.7, and -5.3.

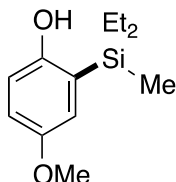
IR (neat): 3531 (br, w), 2954 (m), 2874 (m), 1595 (w), 1484 (m), 1387 (m), 1287 (s), 1071 (m), 788 (s), and 739 (m) cm^{-1} .

TLC: $R_f = 0.5$ in 10:1 hexanes: EtOAc.

GCMS (5029017): $t_R = 10.67$ min, m/z 250 (M^+ , 18), 235 [(M-Me)⁺, 4], 221 [(M-Et)⁺, 42], 205 (36), 193 (100), and 177 (16).

HRMS (APCI/TOF): Calcd for (M+H)⁺ (C₁₅H₂₇OSi)⁺: 251.1826. Found: 251.1815.

2-[Diethyl(methyl)silyl]-4-methoxyphenol (3-9I)



Yield: 1 mmol scale, 181 mg, 81%.

¹H NMR (CDCl₃, 500 MHz): δ 6.90 (d, *J* = 3.1 Hz, 1H, SiCCH), 6.76 [dd, *J* = 8.6, 3.1 Hz, 1H, SiCCHC(OMe)CH], 6.62 [d, *J* = 8.6 Hz, 1H, SiCC(OH)CH], 4.64 (s, 1H, ArOH), 3.77 (s, 3H, Ar-OCH₃), 0.95 [t, *J* = 7.5 Hz, 6H, Si(CH₂CH₃)₂], 0.86-0.78 [m, 4H, Si(CH₂CH₃)₂], and 0.27 (s, 3H, SiCH₃).

¹³C NMR (CDCl₃, 125 MHz): δ 154.7, 153.5, 125.1, 121.6, 115.4, 115.2, 55.9, 7.7, 5.6, and -5.5.

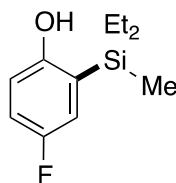
IR (neat): 3405 (br, w), 2953 (m), 2874 (m), 1585 (w), 1461 (m), 1400 (m), 1322 (m), 1165 (m), 1006 (m), 790 (s), and 720 (m) cm⁻¹.

TLC: R_f = 0.3 in 10:1 hexanes: EtOAc.

GCMS (5029017): t_R = 10.55 min, m/z 224 (M⁺, 18), 209 [(M-Me)⁺, 3], 195 [(M-Et)⁺, 18], 167 (100), and 151 (13).

HRMS (APCI/TOF): Calcd for (M+H)⁺ (C₁₂H₂₁O₂Si)⁺: 225.1305. Found: 225.1321.

2-[Diethyl(methyl)silyl]-4-fluorophenol (3-9m)



Yield: 1 mmol scale, 148 mg, 70%.

¹H NMR (CDCl₃, 300 MHz): δ 7.01 [dd, *J* = 8.5 (³J_{F-H}), 3.1 Hz, 1H, SiCCH], 6.89 [ddd, *J* = 8.4 (³J_{F-H}), 8.4, 3.1 Hz, 1H, C(OH)CHCH], 6.61 [dd, *J* = 8.4, 3.9 (⁴J_{F-H}) Hz, 1H, C(OH)CH], 4.73 (s, 1H, ArOH), 0.94 [t, *J* = 7.0 Hz, 6H, Si(CH₂CH₃)₂], 0.86-0.75 [m, 4H, Si(CH₂CH₃)₂], and 0.27 (s, 3H, SiCH₃).

¹³C NMR (CDCl₃, 75 MHz): δ 157.3 (d, ¹J_{F-C} = 239.6 Hz), 156.4 (d, ⁴J_{F-C} = 1.6 Hz), 125.9 (d, ³J_{F-C} = 3.6 Hz), 121.8 (d, ²J_{F-C} = 20.7 Hz), 116.8 (d, ²J_{F-C} = 23.2 Hz), 115.5 (d, ³J_{F-C} =

7.2 Hz), 7.6, 5.4 and -5.7.

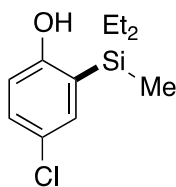
IR (neat): 3440 (br, w), 2954 (m), 2875 (m), 1487 (m), 1397 (s), 1257 (m), 1162 (m), 808 (s), and 749 (s) cm^{-1} .

TLC: $R_f = 0.4$ in 10:1 hexanes: EtOAc.

GCMS (5029017): $t_R = 9.44$ min, m/z 212 (M^+ , 11), 197 [(M -Me) $^+$, 4], 183 [(M -Et) $^+$, 98], 155 (100), and 141 (24).

HRMS (APCI/TOF): Calcd for ($M+H$) $^+$ ($C_{11}H_{18}FOSi$) $^+$: 213.1105. Found: 213.1109.

4-Chloro-2-[diethyl(methyl)silyl]phenol (3-9n)



Yield: 1 mmol scale, 161 mg, 70%.

$^1\text{H NMR}$ (CDCl_3 , 500 MHz): δ 7.24 (d, $J = 2.6$ Hz, 1H, SiCCH), 7.16 [dd, $J = 8.5, 2.6$ Hz, 1H, C(OH)CHCH], 6.60 [d, $J = 8.5$ Hz, 1H, C(OH)CH], 4.89 (s, 1H, ArOH), 0.94 [t, $J = 7.6$ Hz, 6H, Si(CH_2CH_3) $_2$], 0.86-0.77 [m, 4H, Si(CH_2CH_3) $_2$], and 0.26 (s, 3H, SiCH $_3$).

$^{13}\text{C NMR}$ (CDCl_3 , 125 MHz): δ 159.1, 135.6, 130.3, 126.3, 125.8, 116.0, 7.6, 5.4, and -5.6.

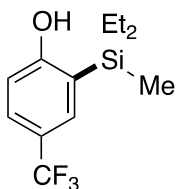
IR (neat): 3560 (br, w), 2953 (m), 2874 (w), 1588 (w), 1464 (m), 1377 (s), 1263 (m), 1105 (m), 1006 (m), 786 (s), and 645 (s) cm^{-1} .

TLC: $R_f = 0.4$ in 10:1 hexanes: EtOAc.

GCMS (5029017): $t_R = 10.58$ min, m/z 230 [($M+2$) $^+$, 4], 228 (M^+ , 12), 213 [(M -Me) $^+$, 2], 199 [(M -Et) $^+$, 74], 171 (100), and 137 (18).

HRMS (APCI/TOF): Calcd for ($M+H$) $^+$ ($C_{11}H_{18}ClOSi$) $^+$: 229.0810. Found: 229.0816.

2-[Diethyl(methyl)silyl]-4-(trifluoromethyl)phenol (3-9o)



Yield: 1 mmol scale, 193 mg, 74%.

¹H NMR (CDCl₃, 500 MHz): δ 7.57 [app s, 1H, C(OH)C(Si)CH], 7.47 [app d, *J* = 8.3 Hz, 1H, C(OH)CHCH], 6.73 [d, *J* = 8.3 Hz, 1H, C(OH)CH], 5.32 (s, 1H, ArOH), 1.00-0.79 [m, 10H, Si(CH₂CH₃)₂], and 0.30 (s, 3H, SiCH₃).

¹³C NMR (CDCl₃, 125 MHz): δ 163.2, 133.3 (q, ³*J*_{F-C} = 3.6 Hz), 128.1 (q, ³*J*_{F-C} = 3.6 Hz), 124.9 (q, ¹*J*_{F-C} = 272.1 Hz), 124.7, 122.9 (q, ²*J*_{F-C} = 32.5 Hz), 114.5, 7.6, 5.4, and -5.7.

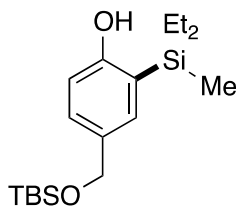
IR (neat): 3352 (br, w), 2955 (m), 2876 (m), 1610 (s), 1405 (w), 1318 (s), 1115 (s), 1075 (s), 788 (m), and 746 (m) cm⁻¹.

TLC: R_f = 0.4 in 10:1 hexanes: EtOAc.

GCMS (5029017): t_R = 9.43 min, m/z 262 (M⁺, 1), 247 [(M-Me)⁺, 2], 233 [(M-Et)⁺, 96], 205 (100), 191 (14), and 153 (22).

HRMS (APCI/TOF): Calcd for (M+H)⁺ (C₁₂H₁₈F₃OSi)⁺: 263.1074. Found: 263.1078.

4-[[*tert*-Butyldimethylsilyloxy]methyl]-2-[diethyl(methyl)silyl]phenol (3-9p)



Yield: 1 mmol scale, 250 mg, 74%.

¹H NMR (CDCl₃, 500 MHz): δ 7.29 (d, *J* = 2.2 Hz, 1H, SiCCH), 7.17 [dd, *J* = 8.1, 2.2 Hz, 1H, SiCCHC(CH₂OTBS)CH], 6.63 [d, *J* = 8.1 Hz, 1H, SiCC(OH)CH], 4.76 (s, 1H, ArOH), 4.67 (s, 2H, ArCH₂OTBS), 0.94 [t, *J* = 7.6 Hz, 6H, Si(CH₂CH₃)₂], 0.93 [s, 9H, Si(CH₃)₂C(CH₃)₃], 0.86-0.77 [m, 4H, Si(CH₂CH₃)₂], 0.27 (s, 3H, SiCH₃), and 0.09 [s, 6H, Si(CH₃)₂C(CH₃)₃].

¹³C NMR (CDCl₃, 125 MHz): δ 159.8, 134.3, 133.1, 129.0, 123.2, 114.5, 65.1, 26.2, 18.6, 7.7, 5.7, -4.9, and -5.4.

IR (neat): 3317 (br, w), 2953 (m), 2874 (w), 1597 (w), 1407 (m), 1254 (m), 1220 (m),

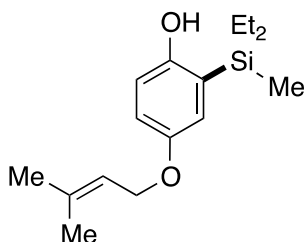
1069 (m), 833 (s), and 720 (s) cm^{-1} .

TLC: $R_f = 0.5$ in 10:1 hexanes: EtOAc.

GCMS (5029017): $t_R = 12.67$ min, m/z 338 (M^+ , 1), 323 [($M\text{-Me}$) $^+$, 5], 309 [($M\text{-Et}$) $^+$, 6], 281 (100), 191 (42), and 177 (54).

HRMS (APCI/TOF): Calcd for ($M+H$) $^+$ ($C_{18}H_{35}O_2Si_2$) $^+$: 339.2170. Found: 339.2157.

2-[Diethyl(methyl)silyl]-4-[(3-methylbut-2-en-1-yl)oxy]phenol (3-9q)



Yield: 1 mmol scale, 98 mg, 36%.

$^1\text{H NMR}$ (CDCl_3 , 500 MHz): δ 6.92 (d, $J = 2.9$ Hz, 1H, SiCCH), 6.78 [dd, $J = 8.6, 2.9$ Hz, 1H, C(OH)CHCH], 6.61 [d, $J = 8.6$ Hz, 1H, C(OH)CH], 5.49 (tq, $J = 6.8, 1.2$ Hz, 1H, CH=CCH₃CH₃), 4.58 (s, 1H, ArOH), 4.46 (d, $J = 6.8$ Hz, 2H, ArOCH₂), 1.79 (s, 3H, CH=CCH₃CH₃), 1.74 (s, 3H, CH=CCH₃CH₃), 0.95 [t, $J = 8.0$ Hz, 6H, Si(CH₂CH₃)₂], 0.87-0.77 [m, 4H, Si(CH₂CH₃)₂], and 0.26 (s, 3H, SiCH₃).

$^{13}\text{C NMR}$ (CDCl_3 , 125 MHz): δ 154.6, 152.8, 138.2, 125.0, 122.6, 120.2, 116.1, 115.3, 65.5, 26.0, 18.4, 7.7, 5.6, and -5.4.

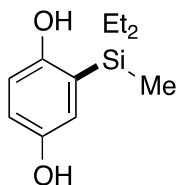
IR (neat): 3403 (br, w), 2952 (m), 2873 (m), 1675 (w), 1581 (w), 1489 (m), 1397 (m), 1197 (m), 1004 (m), 788 (s), and 737 (s) cm^{-1} .

TLC: $R_f = 0.5$ in 10:1 hexanes: EtOAc.

GCMS (5029017): $t_R = 11.34$ min, m/z 279 [($M+H$) $^+$, 100], 278 (M^+ , 54), 263 [($M\text{-Me}$) $^+$, 4], and 249 [($M\text{-Et}$) $^+$, 3].

HRMS (APCI/TOF): Calcd for ($M+H$) $^+$ ($C_{16}H_{27}O_2Si$) $^+$: 279.1775. Found: 279.1763.

2-[Diethyl(methyl)silyl]benzene-1,4-diol (3-9r)



Yield: 1 mmol scale, 141 mg, 67%.

¹H NMR (CDCl₃, 500 MHz): δ 6.81 (d, *J* = 3.0 Hz, 1H, SiCCH), 6.70 [dd, *J* = 8.5, 3.0 Hz, 1H, SiCC(OH)CHCH], 6.57 [d, *J* = 8.5 Hz, 1H, SiCC(OH)CH], 4.68 (br s, 2H, ArOH), 0.95 [t, *J* = 7.6 Hz, 6H, Si(CH₂CH₃)₂], 0.86-0.77 [m, 4H, Si(CH₂CH₃)₂], and 0.25 (s, 3H, SiCH₃).

¹³C NMR (CDCl₃, 125 MHz): δ 154.6, 149.1, 125.3, 122.3, 117.2, 115.7, 7.7, 5.5, and –5.6.

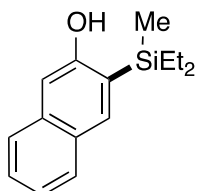
IR (neat): 3262 (br, w), 2954 (m), 2875 (m), 1481 (w), 1264 (m), 1189 (m), 1064 (w), and 734 (s) cm⁻¹.

TLC: R_f = 0.3 in 10:1 hexanes: EtOAc.

GCMS (5029017): t_R = 11.00 min, m/z 211 [(M+H)⁺, 26], 210 (M⁺, 100), and 194 [(M-H-Me)⁺, 2].

HRMS (APCI/TOF): Calcd for (M+H)⁺ (C₁₁H₁₉O₂Si)⁺: 211.1149. Found: 211.1143.

3-[Diethyl(methyl)silyl]naphthalen-2-ol (3-9s)



Yield: 1 mmol scale, 205 mg, 84%.

¹H NMR (CDCl₃, 500 MHz): δ 7.88 [s, 1H, C(OH)CH (naphthalene-H1) or SiCCH (naphthalene-H4)], 7.78 (d, *J* = 8.1 Hz, 1H, naphthalene-H5 or naphthalene-H8), 7.64 (d, *J* = 8.0 Hz, 1H, naphthalene-H5 or naphthalene-H8), 7.43 (ddd, *J* = 8.1, 6.8, 1.2 Hz, 1H, naphthalene-H6 or naphthalene-H7), 7.33 (ddd, *J* = 8.0, 6.8, 1.2 Hz, 1H, naphthalene-H6 or naphthalene-H7), 6.98 [s, 1H, C(OH)CH (naphthalene-H1) or SiCCH (naphthalene-H4)], 5.08 (s, 1H, ArOH), 1.04-0.88 [m, 10H, Si(CH₂CH₃)₂], and 0.38 (s, 3H, SiCH₃).

¹³C NMR (CDCl₃, 125 MHz): δ 158.1, 137.5, 135.5, 129.0, 128.1, 127.1, 126.9, 125.9, 123.6, 108.2, 7.8, 5.7, and –5.4.

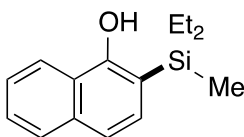
IR (neat): 3265 (br, w), 2952 (w), 2873 (w), 1623 (m), 1459 (m), 1320 (m), 1070 (m), 740 (s), and 539 (m) cm^{-1} .

TLC: $R_f = 0.5$ in 10:1 hexanes: EtOAc.

GCMS (5029017): $t_R = 12.57$ min, m/z 245 [(M+H)⁺, 2], 229 [(M-Me)⁺, 23], and 215 [(M-Et)⁺, 100].

HRMS (APCI/TOF): Calcd for (M+H)⁺ (C₁₅H₂₁OSi)⁺: 245.1356. Found: 245.1341.

2-[Diethyl(methyl)silyl]naphthalen-1-ol (3-9t)



Yield: 1 mmol scale, 185 mg, 76%.

¹H NMR (CDCl₃, 300 MHz): δ 8.09-8.02 (m, 1H, Ar-H), 7.88-7.80 (m, 1H, Ar-H), 7.56-7.42 (m, 4H, Ar-H), 5.56 (s, 1H, ArOH), 1.10-0.90 [m, 10 H, Si(CH₂CH₃)₂], and 0.45 (s, 3H, SiCH₃).

¹³C NMR (CDCl₃, 75 MHz): δ 156.9, 135.6, 131.5, 128.1, 126.8, 125.6, 123.9, 120.6, 120.4, 116.0, 7.7, 6.1, and -4.9.

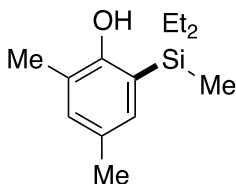
IR (neat): 3406 (br, w), 2955 (m), 2875 (m), 1654 (m), 1460 (m), 1091 (m), 1014 (m), 881 (s), and 750 (s) cm^{-1} .

TLC: $R_f = 0.4$ in 10:1 hexanes: EtOAc.

GCMS (5029017): $t_R = 12.50$ min, m/z 245 [(M+H)⁺, 32], 244 (M⁺, 100), 229 [(M-Me)⁺, 6], and 215 [(M-Et)⁺, 27].

HRMS (APCI/TOF): Calcd for (M+H)⁺ (C₁₅H₂₁OSi)⁺: 245.1356. Found: 245.1347.

2-[Diethyl(methyl)silyl]-4,6-dimethylphenol (3-9u)



Yield: 1 mmol scale, 138 mg, 62%.

¹H NMR (CDCl₃, 300 MHz): δ 6.98 [d, *J* = 2.2 Hz, 1H, SiCCH or C(OH)C(Me)CH], 6.94 [d, *J* = 2.2 Hz, 1H, C(OH)C(Me)CH or SiCCH], 4.56 (s, 1H, ArOH), 2.25 (s, 3H, ArCH₃), 2.20 (s, 3H, ArCH₃), 0.96 [t, *J* = 7.0 Hz, 6H, Si(CH₂CH₃)₂], 0.86-0.77 [m, 4H, Si(CH₂CH₃)₂], and 0.27 (s, 3H, SiCH₃).

¹³C NMR (CDCl₃, 75 MHz): δ 156.8, 134.2, 132.9, 129.5, 122.9, 121.7, 20.7, 16.0, 7.8, 5.8, and -5.2.

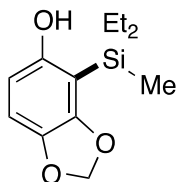
IR (neat): 3570 (br, w), 2952 (m), 2873 (m), 1465 (m), 1234 (m), 1172 (s), 850 (s), and 738 (s) cm⁻¹.

TLC: R_f = 0.7 in 10:1 hexanes: EtOAc.

GCMS (5029017): t_R = 9.75 min, m/z 223 [(M+H)⁺, 5], 207 [(M-Me)⁺, 6], 193 [(M-Et)⁺, 11], and 165 (100).

HRMS (APCI/TOF): Calcd for (M+H)⁺ (C₁₃H₂₃OSi)⁺: 223.1513. Found: 223.1524.

5-[Diethyl(methyl)silyl]benzo[d][1,3]dioxol-4-ol (3-9v)



Yield: 1 mmol scale, 100 mg, 42%.

¹H NMR (CDCl₃, 300 MHz): δ 6.62 [d, *J* = 8.1 Hz, 1H, C(OH)CH or C(OH)CHCH], 6.12 [d, *J* = 8.1 Hz, 1H, C(OH)CH or C(OH)CHCH], 5.85 (s, 2H, OCH₂O), 4.59 (s, 1H, ArOH), 1.02-0.76 [m, 10H, Si(CH₂CH₃)₂], and 0.32 (s, 3H, SiCH₃).

¹³C NMR (CDCl₃, 75 MHz): δ 155.5, 153.6, 140.5, 109.1, 106.2, 106.0, 100.5, 7.7, 6.3, and -4.4.

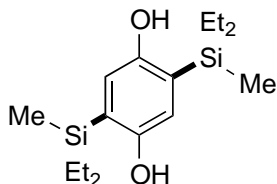
IR (neat): 3491 (br, w), 2953 (m), 2874 (m), 1628 (m), 1497 (s), 1243 (s), 1048 (s), 788 (s), and 737 (s) cm⁻¹.

TLC: R_f = 0.4 in 10:1 hexanes: EtOAc.

GCMS (5029017): t_R = 11.08 min, m/z 238 (M⁺, 30), 223 [(M-Me)⁺, 8], 208 [(M+H-Et)⁺, 100], 181 (53), and 151 (94).

HRMS (APCI/TOF): Calcd for (M+H)⁺ (C₁₂H₁₉O₃Si)⁺: 239.1098. Found: 239.1088.

2,5-Bis[diethyl(methyl)silyl]benzene-1,4-diol (3-9x)



Yield: 1 mmol scale, 273 mg, 88%.

¹H NMR (CDCl₃, 300 MHz): δ 6.64 (s, 2H, SiCCH), 4.47 (s, 2H, ArOH), 0.96 [t, *J* = 7.2 Hz, 12H, Si(CH₂CH₃)₂], 0.86-0.77 [m, 8H, Si(CH₂CH₃)₂], and 0.26 (s, 6H, SiCH₃).

¹³C NMR (CDCl₃, 75 MHz): δ 154.2, 126.2, 121.5, 7.8, 5.5, and -5.5.

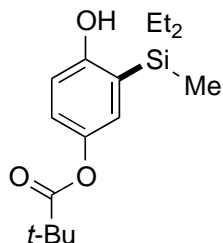
IR (neat): 3432 (br, w), 2953 (m), 2874 (m), 1459 (w), 1369 (m), 1160 (w), 789 (m), and 733 (s) cm⁻¹.

TLC: R_f = 0.5 in 10:1 hexanes: EtOAc.

GCMS (5029017): t_R = 12.95 min, m/z 311 [(M+H)⁺, 29], 310 (M⁺, 54), 243 [(M-F)⁺, 100], 295 [(M-Me)⁺, 3], 281 [(M-Et)⁺, 4], 264 (48), and 250 (100).

HRMS (APCI/TOF): Calcd for (M+H)⁺ (C₁₆H₃₁O₂Si₂)⁺: 311.1857. Found: 311.1862.

3-[Diethyl(methyl)silyl]-4-hydroxyphenyl pivalate (3-9y)



Yield: 1 mmol scale, 185 mg, 63%.

¹H NMR (CDCl₃, 300 MHz): δ 6.93 (d, *J* = 2.7, 1H, SiCCH), 6.83 [dd, *J* = 8.6, 2.7 Hz, 1H, C(OH)CHCH], 6.53 [d, *J* = 8.6 Hz, 1H, C(OH)CH], 5.32 (s, 1H, ArOH), 1.35 [s, 9H, C(CH₃)₃], 0.94 [t, *J* = 7.0 Hz, 6H, Si(CH₂CH₃)₂], 0.87-0.75 [m, 4H, Si(CH₂CH₃)₂], and 0.25 (s, 3H, SiCH₃).

¹³C NMR (CDCl₃, 75 MHz): δ 178.3, 158.3, 144.4, 128.0, 125.1, 123.3, 115.3, 39.2, 27.4, 7.7, 5.4, and -5.7.

IR (neat): 3458 (br, w), 2957 (m), 2875 (m), 1727 (m), 1398 (m), 1266 (m), 1131 (s), 738

(s), and 596 (m) cm^{-1} .

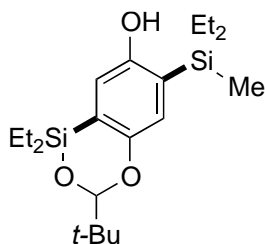
m.p. 88-90 $^{\circ}\text{C}$.

TLC: $R_f = 0.3$ in 10:1 hexanes: EtOAc.

GCMS (5029017): $t_R = 11.84$ min, m/z 295 $[(M+H)^+, 8]$, 294 (M^+ , 9), 279 $[(M-\text{Me})^+, 20]$, and 265 $[(M-\text{Et})^+, 100]$.

HRMS (APCI/TOF): Calcd for $(M+H)^+$ ($\text{C}_{16}\text{H}_{27}\text{O}_3\text{Si}$): 295.1724. Found: 295.1735.

1,1-Diethyl-3-methyl-benzo[*c*][1,5,2]dioxasilin-7-yl pivalate (3-9z)



Yield: 1 mmol scale, 217 mg, 57%.

$^1\text{H NMR}$ (CDCl_3 , 300 MHz): δ 6.90 (s, 1H, Ar-*H*), 6.58 (s, 1H, Ar-*H*), 4.76 (s, 1H, *t*-BuCH), 4.62 (s, 1H, ArOH), 1.06-0.81 [m, 20H, $\text{Si}(\text{CH}_2\text{CH}_3)_2$], and 1.03 (s, 9H, *t*-Bu).

$^{13}\text{C NMR}$ (CDCl_3 , 75 MHz): δ 158.5, 155.0, 128.1, 124.6, 122.1, 117.8, 104.3, 36.4, 24.6, 7.79, 7.76, 6.93, 6.87, 6.55, 6.45, 5.60, 5.50, and -5.6.

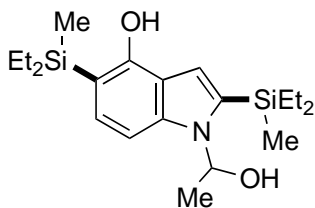
IR (neat): 3417 (br, w), 2956 (m), 2876 (m), 1461 (w), 1377 (m), 1264 (m), 1041 (m), and 736 (s) cm^{-1} .

TLC: $R_f = 0.5$ in 10:1 hexanes: EtOAc.

GCMS (5029017): $t_R = 12.89$ min, m/z 380 (M^+ , 1), 379 $[(M+H)^+, 6]$, 278 $[(M-\text{OSiEt}_2)^+, 19]$, 265 (24), and 264 (100).

HRMS (APCI/TOF): Calcd for $(M+H)^+$ ($\text{C}_{20}\text{H}_{37}\text{O}_3\text{Si}_2$): 381.2276. Found: 381.2260.

2,5-Bis[diethyl(methyl)silyl]-1-(1-hydroxyethyl)-1H-indol-4-ol (3-9aa)



Yield: 1 mmol scale, 147 mg, 38% (over 3 steps).

¹H NMR (CDCl₃, 300 MHz): δ 7.40 [d, *J* = 8.3 Hz, 1H, C(OH)C(Si)CH or C(OH)C(Si)CHCH], 7.15 [d, *J* = 8.3 Hz, 1H, C(OH)C(Si)CHCH or C(OH)C(Si)CH], 6.63 [s, 1H, C(N)(Si)CH], 6.06 [qd, *J* = 6.0, 1.9 Hz, 1H, CH₃C(OH)H], 5.17 (s, 1H, ArOH), 2.66 (d, *J* = 1.9 Hz, 1H, MeCHOH), 1.80 [d, *J* = 6.0 Hz, 3H, CH₃C(OH)H], 1.05-0.82 [m, 20 H, Si(CH₂CH₃)₂], 0.35 (s, 3H, SiCH₃), and 0.33 (s, 3H, SiCH₃).

¹³C NMR (CDCl₃, 75 MHz): δ 154.2, 140.3, 136.4, 129.5, 119.7, 110.1, 108.6, 106.3, 80.6, 21.8, 7.86, 7.75, 7.73, 6.25, 6.21, -4.82, and -4.85.

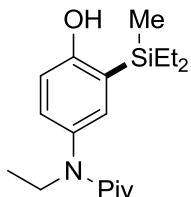
IR (neat): 3383 (br, w), 2954 (m), 2875 (m), 1458 (w), 1241 (m), 1003 (m), 788 (m), and 733 (s) cm⁻¹.

TLC: R_f = 0.3 in 10:1 hexanes: EtOAc.

GCMS (5029017): t_R = 12.87 min, m/z 378 [(M+H)⁺, 77], 377 (M⁺, 100), 362 [(M-Me)⁺, 9], 348 [(M-Et)⁺, 12], 261 (10), and 204 (31).

HRMS (APCI/TOF): Calcd for (M+H)⁺ (C₂₀H₃₆NO₂Si₂)⁺: 378.2279. Found: 378.2268.

***N*-[3-(diethyl(methyl)silyl)-4-hydroxyphenyl]-*N*-ethylpivalamide (3-9ab)**



Yield: 1 mmol scale, 218 mg, 68%.

¹H NMR (CDCl₃, 500 MHz): δ 7.19 (s, 1H, ArOH), 7.07 (d, *J* = 2.6 Hz, 1H, SiCCH), 7.00 [dd, *J* = 8.4, 2.6 Hz, 1H, C(OH)CHCH], 6.82 [d, *J* = 8.4 Hz, 1H, C(OH)CH], 3.64 (q, *J* = 7.1 Hz, 2H, NCH₂CH₃), 1.11 (t, *J* = 7.1 Hz, 3H, NCH₂CH₃), 1.02 [s, 9H, C(CH₃)₃], 0.93 [t, *J* = 7.2 Hz, 6H, Si(CH₂CH₃)₂], 0.88-0.74 [m, 4H, Si(CH₂CH₃)₂], and 0.26 (s, 3H, SiCH₃).

¹³C NMR (CDCl₃, 125 MHz): δ 178.4, 161.3, 137.1, 134.9, 131.5, 124.5, 114.9, 48.2, 41.0, 12.8, 7.7, 5.39, 5.37, and -5.6.

IR (neat): 3147 (br, m), 2954 (m), 2875 (m), 1594 (m), 1571 (s), 1483 (m), 1272 (s), 1208 (s), 1069 (m), 790 (s), and 735 (m) cm⁻¹.

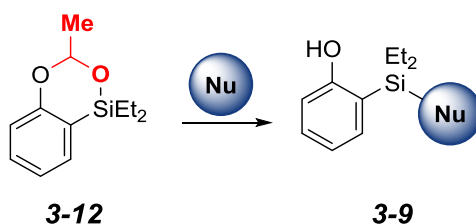
m.p. 192-194 °C.

TLC: R_f = 0.25 in 10:1 hexanes: EtOAc.

GCMS (5029017): t_R = 12.98 min, m/z 322 [(M+H)⁺, 1], 220 [(M-SiEt₂Me)⁺, 0.5], 190 (0.5), and 112 (100).

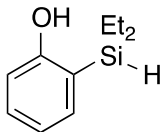
HRMS (APCI/TOF): Calcd for (M+H)⁺ (C₁₈H₃₂NO₂Si)⁺: 322.2197. Found: 322.2178.

D.4. Procedure for Nucleophilic Opening of Dioxasilines to 2-Silyl Phenols (3-9)
with Non-Commercially Available Nucleophiles ⁵



Nucleophiles were generated by treatment of pronucleophiles (3 mmol) with ⁿBuLi (1.4 mL, 2 M in THF, 2.8 mmol) in THF (3 mL) at -78 °C for 30 min (when furan and *N*-methyl indole were used for pronucleophiles, Et₂O was used as solvent and the deprotonation reactions were carried out at 45 °C for 8 h). The crude dioxasiline **3-12a** (1 mmol) was added into the reaction mixture, which was stirred at -78 °C for 30 min and rt for 30 min. The reaction was quenched by adding saturated aqueous ammonium chloride solution, then the mixture was acidified to ca. pH 4-5 with aqueous HCl (1 M). The mixture was extracted with diethyl ether. The combined organic layer was washed with water and brine, and dried over anhydrous sodium sulfate. The volatiles were removed *in vacuo*, and the crude mixture was purified by MPLC to afford 2-silyl phenols **3-9** (hexanes/EtOAc = 20:1, 5 mL/min, retention time 5-20 min).

2-(Diethylsilyl)phenol (3-9ac)



Yield: 1 mmol scale, 169 mg, 94%. LiAlH₄ was used to prepare **3-9ac**.

¹H NMR (CDCl₃, 500 MHz): δ 7.34 [dd, *J* = 7.3, 1.7 Hz, 1H, C(O)CH or SiCCH], 7.27 [ddd, *J* = 8.0, 7.3, 1.7 Hz, 1H, C(O)CHCH or SiCCHCH], 6.93 [ddd, *J* = 7.3, 7.3, 0.7 Hz,

1H, C(O)CHCH or SiCCHCH], 6.74 [d, $J = 8.0$ Hz, 1H, C(O)CH or SiCCH], 5.10 (s, 1H, ArOH), 4.28 (p, $J = 3.5$ Hz, 1H, SiH), 1.37-1.24 (m, 5H SiCH₂CH₂CH₂CH₃), 1.02 [t, $J = 8.1$ Hz, 6H, Si(CH₂CH₃)₂], and 0.93-0.86 [m, 8H, Si(CH₂CH₃)₂].

¹³C NMR (CDCl₃, 125 MHz): δ 160.6, 136.7, 131.3, 120.8 (2), 114.7, 8.5, and 3.5.

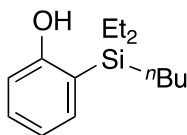
IR (neat): 3538 (br, w), 2954 (m), 2873 (m), 2100 (m), 1594 (w), 1463 (s), 1276 (m), 1008 (w), 805 (s), and 754 (s) cm⁻¹.

TLC: R_f = 0.5 in 10:1 hexanes: EtOAc.

GCMS (5029017): t_R = 8.77 min, m/z 181 [(M+H)⁺, 65], 180 (M⁺, 63), 179 [(M-H)⁺, 100], 151 [(M-Et)⁺, 47], and 123 (84).

HRMS (APCI/TOF): Calcd for (M+H)⁺ (C₁₀H₁₇OSi)⁺: 181.1043. Found: 181.1036.

2-(Butyldiethylsilyl)phenol (3-9ad)



Yield: 1 mmol scale, 231 mg, 98%. ⁿBuLi was used to prepare **3-9ad**.

¹H NMR (CDCl₃, 500 MHz): δ 7.34 [dd, $J = 7.3, 1.6$ Hz, 1H, C(O)CH or SiCCH], 7.23 [ddd, $J = 8.0, 7.3, 1.6$ Hz, 1H, C(O)CHCH or SiCCHCH], 6.92 [ddd, $J = 7.3, 7.3, 1.0$ Hz, 1H, C(O)CHCH or SiCCHCH], 6.67 [dd, $J = 8.0, 1.0$ Hz, 1H, C(O)CH or SiCCH], 4.72 (s, 1H, ArOH), 1.37-1.24 (m, 4H SiCH₂CH₂CH₂CH₃), 0.95 [t, $J = 8.0$ Hz, 6H, Si(CH₂CH₃)₂], and 0.95-0.89 [m, 9H, Si(CH₂CH₃)₂ and SiCH₂CH₂CH₂CH₃].

¹³C NMR (CDCl₃, 125 MHz): δ 160.7, 136.4, 130.7, 122.8, 120.6, 114.6, 27.0, 26.3, 14.0, 11.7, 7.8, and 4.1.

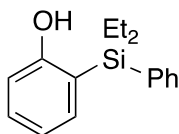
IR (neat): 3351 (br, w), 2954 (m), 2883 (m), 1594 (m), 1435 (m), 1296 (w), 1072 (m), 752 (s), and 700 (s) cm⁻¹.

TLC: R_f = 0.5 in 10:1 hexanes: EtOAc.

GCMS (5029017): t_R = 10.71 min, m/z 237 [(M+H)⁺, 79], 236 (M⁺, 27), 207 [(M-Et)⁺, 100], 179 [(M-ⁿBu)⁺, 43], and 151 (48).

HRMS (APCI/TOF): Calcd for (M+H)⁺ (C₁₄H₂₅OSi)⁺: 237.1669. Found: 237.1686.

2-[Diethyl(phenyl)silyl]phenol (3-9ae)



Yield: 1 mmol scale, 230 mg, 90%. PhLi was used to prepare **3-9ae**.

¹H NMR (CDCl₃, 500 MHz): δ 7.60-7.57 (m, 2H, Ar-*H*), 7.43-7.36 (m, 3H, Ar-*H*), 7.36 [dd, *J* = 7.3, 1.7 Hz, 1H, C(O)CH or SiCCH], 7.28 [ddd, *J* = 8.0, 7.3, 1.7 Hz, 1H, C(O)CHCH or SiCCHCH], 6.95 [ddd, *J* = 7.3, 7.3, 1.0 Hz, 1H, C(O)CHCH or SiCCHCH], 6.72 [dd, *J* = 8.0, 1.0 Hz, 1H, C(O)CH or SiCCH], 4.75 (s, 1H, ArOH), 1.21-1.08 [m, 4H Si(CH₂CH₃)₂], and 1.00 [t, *J* = 7.8 Hz, 6H, Si(CH₂CH₃)₂].

¹³C NMR (CDCl₃, 125 MHz): δ 160.9, 136.7, 136.9, 135.0 (2), 131.4, 129.8, 128.4 (2), 121.1, 120.7, 115.4, 7.6, and 4.0.

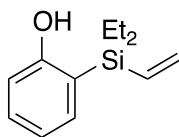
IR (neat): 3530 (br, w), 3067 (w), 2954 (m), 2873 (m), 1593 (m), 1427 (s), 1276 (m), 1070 (m), 756 (s), and 698 (s) cm⁻¹.

TLC: R_f = 0.4 in 10:1 hexanes: EtOAc.

GCMS (5029017): t_R = 12.14 min, m/z 257 [(M+H)⁺, 2], 256 (M⁺, 1), 227 [(M-Et)⁺, 14], 199 (23), 179 [(M-Ph)⁺, 56], and 178 (100).

HRMS (APCI/TOF): Calcd for (M+H)⁺ (C₁₆H₂₁OSi)⁺: 257.1356. Found: 257.1342.

2-[Diethyl(vinyl)silyl]phenol (**3-9af**)



Yield: 1 mmol scale, 200 mg, 97%. Vinylmagnesium chloride was used to prepare **3-9af**.

¹H NMR (CDCl₃, 500 MHz): δ 7.34 [dd, *J* = 7.3, 1.7 Hz, 1H, C(O)CH or SiCCH], 7.27 [ddd, *J* = 8.0, 7.3, 1.7 Hz, 1H, C(O)CHCH or SiCCHCH], 6.93 (ddd, *J* = 7.3, 7.3, 1.0 Hz, 1H, C(O)CHCH or SiCCHCH], 6.75 (d, *J* = 8.0, 1.0 Hz, 1H, C(O)CH or SiCCH], 6.42 (dd, *J* = 20.5, 14.8 Hz, 1H, SiCH=CH₂), 6.24 (dd, *J* = 14.8, 3.7 Hz, 1H, SiCH=CH_{cis}H_{trans}), 5.95 (dd, *J* = 20.5, 3.7 Hz, 1H, SiCH=CH_{cis}H_{trans}), 5.24 (s, 1H, ArOH), 1.00-0.96 [m, 6H, Si(CH₂CH₃)₂], and 0.95-0.89 [m, 4H, Si(CH₂CH₃)₂].

¹³C NMR (CDCl₃, 125 MHz): δ 161.0, 136.2 (2), 135.7, 131.4, 120.9, 120.7, 115.4, 7.5, and 3.9.

IR (neat): 3492 (br, m), 3049 (w), 2954 (m), 2874 (m), 1593 (m), 1436 (m), 1276 (w),

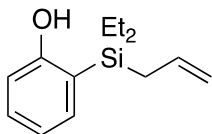
1071 (m), 1020 (s), and 714 (s) cm^{-1} .

TLC: $R_f = 0.5$ in 10:1 hexanes: EtOAc.

GCMS (5029017): $t_R = 9.59$ min, m/z 207 [(M+H)⁺, 9], 206 (M⁺, 7), 179 [(M-CH=CH₂)⁺, 40], 177 [(M-Et)⁺, 40], and 149 (100).

HRMS (APCI/TOF): Calcd for (M+H)⁺ (C₁₂H₁₉OSi)⁺: 207.1200. Found: 207.1189.

2-(Allyldiethylsilyl)phenol (3-9ag)



Yield: 1 mmol scale, 154 mg, 70%. Allylmagnesium chloride was used to prepare **9ag**.

¹H NMR (CDCl₃, 500 MHz): δ 7.34 [dd, $J = 7.3, 1.7$ Hz, 1H, C(O)CH or SiCCH], 7.25 [ddd, $J = 8.0, 7.3, 1.7$ Hz, 1H, C(O)CHCH or SiCCHCH], 6.93 (dd, $J = 7.3, 7.3$ Hz, 1H, C(O)CHCH or SiCCHCH], 6.68 (d, $J = 8.0$ Hz, 1H, C(O)CH or SiCCH], 5.84 (dddd, $J = 17.0, 10.1, 8.0, 8.0$ Hz, 1H, SiCH₂CHCH₂), 4.91 (app d, $J = 17$ Hz, 1H, SiCH₂CH=CH_{cis}H_{trans}), 4.83 (app d, $J = 10.1$ Hz, 1H, SiCH₂CH=CH_{cis}H_{trans}), 4.81 (s, 1H, ArOH), 1.91 (d, $J = 8.0$, 2H, SiCH₂CH=CH₂), 0.97 [t, $J = 8.0$ Hz, 6H, Si(CH₂CH₃)₂], and 0.95-0.89 [m, 4H, Si(CH₂CH₃)₂].

¹³C NMR (CDCl₃, 125 MHz): δ 160.6, 136.4, 135.7, 131.0, 122.0, 120.7, 114.8, 113.4, 20.0, 7.6, and 3.7.

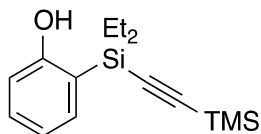
IR (neat): 3351 (br, w), 3073 (w), 2953 (m), 2874 (m), 1593 (m), 1435 (s), 1275 (m), 1072 (m), 752 (s), and 690 (s) cm^{-1} .

TLC: $R_f = 0.5$ in 10:1 hexanes: EtOAc.

GCMS (5029017): $t_R = 10.36$ min, m/z 220 (M⁺, 0.5), 179 [(M-allyl)⁺, 69], 151 (52), and 123 (100).

HRMS (APCI/TOF): Calcd for (M+H)⁺ (C₁₃H₂₁OSi)⁺: 221.1356. Found: 221.1346.

2-[Diethyl{(trimethylsilyl)ethynyl}silyl]phenol (3-9ah)



Yield: 1 mmol scale, 193 mg, 70%. Trimethylsilylacetylene was used as pronucleophile

to prepare **3-9ah**.

¹H NMR (CDCl₃, 500 MHz): δ 7.29 [ddd, *J* = 8.0, 7.3, 1.7 Hz, 1H, C(OH)CHCH or SiCCHCH], 7.25 [dd, *J* = 7.3, 1.7 Hz, 1H, C(OH)CH or SiCCH], 6.924 (s, 1H, ArOH), 6.917 [ddd, *J* = 7.3, 7.3, 1.0 Hz, 1H, C(OH)CHCH or SiCCHCH], 6.72 (app d, *J* = 8.0 Hz, 1H, C(OH)CH or SiCCH], 1.03 [t, *J* = 7.8 Hz 6H, Si(CH₂CH₃)₂], 0.90-0.83 [m, 4H, Si(CH₂CH₃)₂], and 0.24 [s, 9H, Si(CH₃)₃].

¹³C NMR (CDCl₃, 125 MHz): δ 161.8, 135.1, 131.8, 121.7, 120.4, 118.4, 116.1, 109.7, 7.5, 5.8, and -0.1.

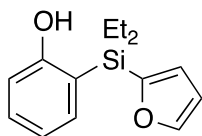
IR (neat): 3459 (br, m), 2957 (m), 2875 (w), 2359 (w), 1595 (m), 1473 (m), 1279 (m), 840 (s), and 752 (s) cm⁻¹.

TLC: R_f = 0.6 in 10:1 hexanes: EtOAc.

GCMS (5029017): t_R = 10.31 min, m/z 277 [(M+H)⁺, 45], 276 (M⁺, 27), 247 [(M-Et)⁺, 66], 179 [(M-CCTMS)⁺, 84], and 178 (100).

HRMS (APCI/TOF): Calcd for (M+H)⁺ (C₁₅H₂₅OSi₂)⁺: 277.1438. Found: 277.1448.

2-[Diethyl(furan-2-yl)silyl]phenol (**3-9ai**)



Yield: 1 mmol scale, 180 mg, 73%. Furan was used as pronucleophile to prepare **3-9ai**.

¹H NMR (CDCl₃, 500 MHz): δ 7.75 (d, *J* = 1.6 Hz, 1H, Furan-H3 or Furan-H5), 7.31 [dd, *J* = 7.3, 1.7 Hz, 1H, C(OH)CH or SiCCH], 7.28 [ddd, *J* = 8.1, 7.3, 1.7 Hz, 1H, C(OH)CHCH or SiCCHCH], 6.93 (ddd, *J* = 7.3, 7.3, 1.0 Hz, 1H, C(OH)CHCH or SiCCHCH], 6.84 (d, *J* = 3.0 Hz, 1H, , Furan-H3 or Furan-H5), 6.76 [app d, *J* = 8.1 Hz, 1H, C(OH)CH or SiCCH], 6.46 (dd, *J* = 3.0, 1.7 Hz, 1H, Furan-H4), 5.29 (s, 1H, ArOH), 1.11-1.07 [m, 4H, Si(CH₂CH₃)₂], and 1.04-1.00 [m, 6H, Si(CH₂CH₃)₂].

¹³C NMR (CDCl₃, 125 MHz): δ 161.0, 156.7, 147.8, 136.3, 131.7, 122.7, 120.7, 120.0, 115.7, 109.9, 7.6, and 4.2.

IR (neat): 3423 (br, w), 2955 (m), 2874 (m), 1593 (m), 1435 (m), 1277 (m), 1004 (s), 830 (w), and 690 (s) cm⁻¹.

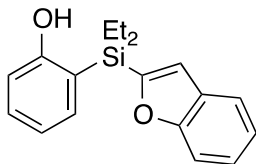
TLC: R_f = 0.4 in 10:1 hexanes: EtOAc.

GCMS (5029017): t_R = 11.13 min, m/z 247 [(M+H)⁺, 1], 217 [(M-Et)⁺, 5], 179 [(M-furyl)⁺,

40], and 178 (100).

HRMS (APCI/TOF): Calcd for (M+H)⁺ (C₁₄H₁₉O₂Si)⁺: 247.1149. Found: 247.1156.

2-(Benzofuran-2-yl-diethylsilyl)phenol (**3-9aj**)



Yield: 1 mmol scale, 237 mg, 80%. 2,3-Benzofuran was used as pronucleophile to prepare **3-9aj**.

¹H NMR (CDCl₃, 500 MHz): δ 7.60 (ddd, *J* = 7.8, 1.3, 0.6 Hz, 1H, benzofuran *H7*), 7.53 (dddd, *J* = 8.2, 1.7, 0.9, 0.6 Hz, 1H, benzofuran *H4*), 7.36 [dd, *J* = 7.3, 1.0 Hz, 1H, C(OH)CH or SiCCH], 7.300 (ddd, *J* = 8.2, 7.2, 1.3 Hz, 1H, benzofuran *H5*), 7.297 (ddd, *J* = 7.8, 7.2, 1.7 Hz, 1H, benzofuran *H6*), 7.22 [ddd, *J* = 7.8, 7.3, 1.0 Hz, 1H, C(OH)CHCH or SiCCHCH], 7.15 (d, *J* = 0.9 Hz, 1H, benzofuran *H3*), 6.94 [ddd, *J* = 7.3, 7.3, 1.0 Hz, 1H, C(OH)CHCH or SiCCHCH], 6.76 [dd, *J* = 7.8, 1.0 Hz, 1H, C(OH)CH or SiCCH], 5.45 (s, 1H, ArOH), 1.29-1.19 [m, 4H, Si(CH₂CH₃)₂], and 1.05 [t, *J* = 7.5, 6H, Si(CH₂CH₃)₂].

¹³C NMR (CDCl₃, 125 MHz): δ 160.9, 160.3, 158.4, 136.6, 131.8, 128.0, 124.8, 122.7, 121.3, 120.9, 119.8, 118.9, 115.6, 111.7, 7.7, and 4.1.

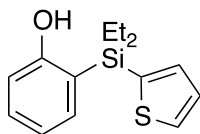
IR (neat): 3531 (br, w), 3065 (w), 2995 (m), 2875 (m), 1594 (m), 1436 (s), 1295 (m), 1007 (m), 741 (s), and 717 (s) cm⁻¹.

TLC: R_f = 0.4 in 10:1 hexanes: EtOAc.

GCMS (5029017): t_R = 13.83 min, m/z 296 (M⁺, 2), 267 [(M-Et)⁺, 6], 239 (10), 221 (10), 179 [(M-benzofuryl)⁺, 34], and 178 (100).

HRMS (APCI/TOF): Calcd for (M+H)⁺ (C₁₈H₂₁O₂Si)⁺: 297.1305. Found: 297.1323.

2-[Diethyl(thiophen-2-yl)silyl]phenol (**3-9ak**)



Yield: 1 mmol scale, 191 mg, 73%. Thiophene was used as pronucleophile to prepare **3-9ak**.

¹H NMR (CDCl₃, 500 MHz): δ 7.72 (dd, *J* = 4.6, 0.8 Hz, 1H, thiophene-*H3* or thiophene-*H5*), 7.45 (dd, *J* = 3.2, 0.8 Hz, 1H, thiophene-*H3* or thiophene-*H5*), 7.38 [dd, *J* = 7.3, 1.7 Hz, 1H, C(OH)CH or SiCCH], 7.31 [ddd, *J* = 8.0, 7.3, 1.7 Hz, 1H, C(OH)CHCH or SiCCHCH], 7.28 (dd, *J* = 4.6, 3.2 Hz, 1H, thiophene-*H4*), 6.97 [ddd, *J* = 7.3, 7.3, 0.9 Hz, 1H, C(OH)CHCH or SiCCHCH], 6.74 [dd, *J* = 8.0, 0.9 Hz, 1H, C(OH)CH or SiCCH], 5.13 (s, 1H, ArOH), 1.22-1.17 [m, 4H, Si(CH₂CH₃)₂], and 1.05 [t, *J* = 7.8 Hz, 6H, Si(CH₂CH₃)₂].

¹³C NMR (CDCl₃, 125 MHz): δ 161.0, 136.6, 136.4, 135.0, 132.2, 131.7, 128.7, 120.71, 120.68, 115.5, 7.6, and 5.3.

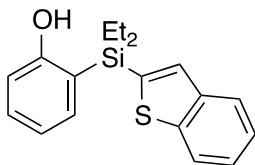
IR (neat): 3474 (br, m), 2955 (m), 2874 (m), 1594 (m), 1435 (m), 1276 (m), 1071 (m), and 730 (s) cm⁻¹.

TLC: R_f = 0.4 in 10:1 hexanes: EtOAc.

GCMS (5029017): t_R = 12.16 min, m/z 263 [(M+H)⁺, 11], 233 [(M-Et)⁺, 11], 205 (13), 179 [(M-thiophene)⁺, 83], and 178 (100).

HRMS (APCI/TOF): Calcd for (M+H)⁺ (C₁₄H₁₉OSSi)⁺: 263.0920. Found: 263.0932.

2-(Benzo [b]thiophen-2-yl)diethylsilylphenol (3-9al)



Yield: 1 mmol scale, 293 mg, 94%. 2,3-Benzothiophene was used as pronucleophile to prepare **3-9al**.

¹H NMR (CDCl₃, 500 MHz): δ 7.92-7.90 (nfom, 1H, benzothiophene), 7.86-7.84 (nfom, 1H, benzothiophene), 7.62 (s, 1H, benzothiophene *H3*), 7.41 [dd, *J* = 7.3, 1.7 Hz, 1H, C(OH)CH or SiCCH], 7.37 (dd, *J* = 7.0, 7.0, 1.5 Hz, 1H, benzothiophene), 7.35 (dd, *J* = 7.0, 7.0, 1.7 Hz, 1H, benzothiophene), 7.31 [ddd, *J* = 8.0, 7.3, 1.7 Hz, 1H, C(OH)CHCH or SiCCHCH], 6.97 [ddd, *J* = 7.3, 7.3, 0.9 Hz, 1H, C(OH)CHCH or SiCCHCH], 6.74 [dd, *J* = 8.0, 0.9 Hz, 1H, C(OH)CH or SiCCH], 4.98 (s, 1H, ArOH), 1.24-1.19 [m, 4H, Si(CH₂CH₃)₂], and 1.05 [t, *J* = 7.6, 6H, Si(CH₂CH₃)₂].

¹³C NMR (CDCl₃, 125 MHz): δ 160.9, 144.2, 141.2, 137.9, 136.7, 133.3, 131.8, 124.6, 124.2, 123.8, 122.4, 120.9, 120.4, 115.4, 7.7, and 5.1.

IR (neat): 3537 (br, m), 2954 (m), 2873 (m), 1593 (m), 1486 (s), 1277 (m), 1070 (m), 848

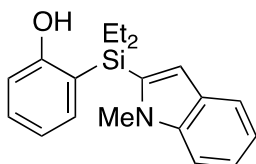
(m), and 710 (s) cm^{-1} .

TLC: $R_f = 0.4$ in 10:1 hexanes: EtOAc.

GCMS (5029017): $t_R = 13.83$ min, m/z 313 [(M+H)⁺, 0.1], 283 [(M-Et)⁺, 0.3], 239 (20), 221 (21), 179 [(M-benzothiophene)⁺, 18], and 178 (100).

HRMS (APCI/TOF): Calcd for (M+H)⁺ ($\text{C}_{18}\text{H}_{21}\text{OSSi}$)⁺: 313.1077. Found: 313.1092.

2-[Diethyl(1-methyl-indol-2-yl)silyl]phenol (**3-9am**)



Yield: 1 mmol scale, 256 mg, 83%. N-methylindole was used as pronucleophile to prepare **3-9am**.

¹H NMR (CDCl_3 , 500 MHz): δ 7.66 (ddd, $J = 7.9, 1.1, 0.9$ Hz, 1H, Indole *H7*), 7.34 [dd, $J = 7.3, 1.7$ Hz, 1H, C(OH)CH or SiCCH], 7.31 (dddd, $J = 8.2, 0.9, 0.9, 0.9$ Hz, 1H, Indole *H4*), 7.30 [ddd, $J = 8.1, 7.3, 1.7$ Hz, 1H, C(OH)CHCH or SiCCHCH], 7.25 (ddd, $J = 8.2, 6.9, 1.1$ Hz, 1H, Indole *H5*), 7.11 (ddd, $J = 7.9, 6.9, 0.9$ Hz, 1H, indole *H6*), 6.95 (d, $J = 0.9$ Hz, 1H, Indole *H3*), 6.94 [ddd, $J = 7.3, 7.3, 1.0$ Hz, 1H, C(OH)CHCH or SiCCHCH], 6.73 [dd, $J = 8.1, 1.0$ Hz, 1H, C(OH)CH or SiCCH], 5.13 (s, 1H, ArOH), 3.66 (s, 3H, NCH_3), 1.33-1.15 [m, 4H, $\text{Si}(\text{CH}_2\text{CH}_3)_2$], and 1.02 [t, $J = 7.8$, 6H, $\text{Si}(\text{CH}_2\text{CH}_3)_2$].

¹³C NMR (CDCl_3 , 125 MHz): δ 161.1, 141.9, 136.3, 135.9, 131.8, 128.7, 122.7, 121.1, 120.7, 120.2, 119.5, 115.7, 114.2, 109.5, 33.1, 7.5, and 4.2.

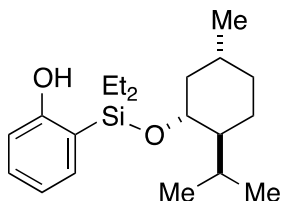
IR (neat): 3440 (br, w), 2954 (m), 2874 (m), 1593 (m), 1463 (s), 1276 (m), 1069 (s), 751 (s), and 634 (m) cm^{-1} .

TLC: $R_f = 0.3$ in 10:1 hexanes: EtOAc.

GCMS (5029017): $t_R = 14.82$ min, m/z 310 [(M+H)⁺, 40], 309 (M^+ , 86), 280 [(M-Et)⁺, 14], 204 (8), 179 {[M-(N-Methyl indole)]⁺, 2}, and 131 (N-Methyl indole, 100).

HRMS (APCI/TOF): Calcd for (M+H)⁺ ($\text{C}_{19}\text{H}_{24}\text{NOSi}$)⁺: 310.1622. Found: 310.1636.

2-[Diethyl{[(1R,2R,5R)-2-isopropyl-5-methylcyclohexyl]oxy}silyl]phenol (**3-9an**)



Yield: 1 mmol scale, 240 mg, 72%. *L*-Menthol was used as pronucleophile to prepare **3-9an**.

¹H NMR (CDCl₃, 500 MHz): δ 8.89 (s, 1H, ArOH), 7.28 [ddd, *J* = 8.2, 7.3, 1.7 Hz, 1H, C(OH)CHCH or SiCCHCH], 7.14 [dd, *J* = 7.3, 1.7 Hz, 1H, C(OH)CH or SiCCH], 6.86 [app dd, *J* = 7.3, 7.3 Hz, 1H, C(OH)CHCH or SiCCHCH], 6.83 [d, *J* = 8.2 Hz, 1H, C(OH)CH or SiCCH], 3.69 (ddd, *J* = 10.4, 10.4, 4.4 Hz, 1H, SiOCH), 2.24 [septet of doublet, *J* = 7.0, 2.4 Hz, 1H, CH(CH₃)₂], 2.06-2.01 (m, 1H, Alk-*H*), 1.70-1.65 (m, 2H, Alk-*H*), 1.46-1.37 (m, 1H, Alk-*H*), 1.27 (dddd, *J* = 12.3, 10.1, 3.1, 3.1 Hz, 1H, Alk-*H*), 1.18 (ddd, *J* = 12.2, 12.2, 10.8 Hz, 1H, Alk-*H*), 1.05-0.86 [m, 19H, Si(CH₂CH₃)₂ and Alk-*H*], and 0.77 [d, *J* = 7.0 Hz, 3H, CH₃CHCH₃].

¹³C NMR (CDCl₃, 125 MHz): δ 163.4, 134.0, 131.7, 119.4, 118.0, 116.1, 74.8, 50.5, 45.1, 34.4, 32.0, 25.4, 22.9, 22.4, 21.6, 16.0, 7.6, 7.2, 7.1, and 6.6.

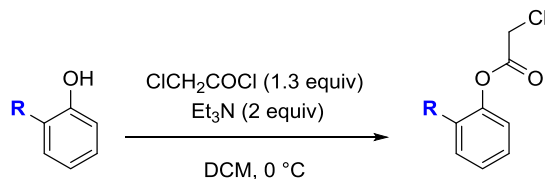
IR (neat): 3327 (br, w), 2955 (m), 2874 (m), 1609 (w), 1479 (m), 1250 (m), 1043 (s), 756 (s), and 702 (s) cm⁻¹.

TLC: R_f = 0.7 in 10:1 hexanes: EtOAc.

GCMS (5029017): t_R = 12.73 min, m/z 334 (M⁺, 59), 305 [(M-Et)⁺, 3], 281 (4), 231 (12), and 197 (100).

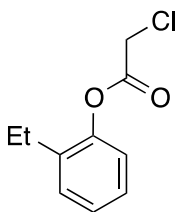
HRMS (APCI/TOF): Calcd for (M+H)⁺ (C₂₀H₃₅O₂Si)⁺: 335.2401. Found: 335.2412.

D.5. Procedure for Preparation of Chloroacetates



2-Alkylphenol **8** (10 mmol) and Et₃N (2.8 mL, 20 mmol) were dissolved with CH₂Cl₂ (20 mL), the reaction mixture was cooled to 0 °C by an ice bath. Chloroacetyl chloride (1.0 mL, 13 mmol) was added into the reaction mixture slowly. Then the reaction mixture was stirred at rt for 0.5 h. The reaction was quenched by adding saturated aqueous ammonium chloride (40 mL) and was extracted with diethyl ether (30 mL×4). The combined organic extracts were washed with water (30 mL) and brine (30 mL), and dried over anhydrous sodium sulfate. The volatiles were removed *in vacuo*, and the crude mixture was purified by flash column (hexanes: EtOAc 10:1) to afford the corresponding ester (**3-8b-Et**, **3-8e-ⁱPr**, **3-8f-^tBu**, **3-8g-Ph**).

2-Ethylphenyl 2-chloroacetate (**3-8b-Et**)



Yield: 10 mmol scale, 1.68 g, 85%.

¹H NMR (CDCl₃, 500 MHz): δ 7.30-7.28 (m, 1H, Ar-*H*), 7.25-7.22 (m, 2H, Ar-*H*), 7.07-7.05 (m, 1H, Ar-*H*), 4.32 (s, 2H, CH₂Cl), 2.58 (q, *J* = 7.6 Hz, 2H, ArCH₂CH₃), and 1.23 (t, *J* = 7.6 Hz, 3H, ArCH₂CH₃).

¹³C NMR (CDCl₃, 125 MHz): δ 166.1, 148.6, 135.8, 129.8, 127.2, 127.0, 121.9, 40.9, 23.2, and 14.3.

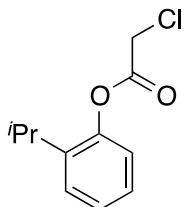
IR (neat): 2970 (w), 1774 (s), 1489 (m), 1212 (m), 1170 (s), 928 (m), and 787 (s) cm⁻¹.

TLC: R_f = 0.5 in 10:1 hexanes: EtOAc.

GCMS (5029017): t_R = 8.88 min, m/z 200 [(M+2)⁺, 1], 198 (M⁺, 3), 178 (29), 176 (100), and 91 (5).

HRMS (APCI/TOF): Calcd for (M+H)⁺ (C₁₀H₁₂ClO₂)⁺: 199.0520. Found: 199.0503.

2-Isopropylphenyl 2-chloroacetate (**3-8e-ⁱPr**)



Yield: 10 mmol scale, 1.87 g, 90%.

¹H NMR (CDCl₃, 500 MHz): δ 7.35 [dd, *J* = 7.5, 1.9 Hz, 1H, OCCH or OCC(*i*Pr)CH], 7.26 [ddd, *J* = 7.5, 7.3, 1.6 Hz, 1H, OCCHCH or OCC(*i*Pr)CHCH], 7.23 [ddd, *J* = 7.7, 7.3, 1.9 Hz, 1H, OCCHCH or OCC(*i*Pr)CHCH], 7.04 [dd, *J* = 7.7, 1.6 Hz, 1H, OCCH or OCC(*i*Pr)CH], 4.33 (s, 2H, CH₂Cl), 3.05 [septet, *J* = 6.9 Hz, 1H, ArCH(CH₃)₂], and 1.23 [d, *J* = 6.9 Hz, 6H, ArCH(CH₃)₂].

¹³C NMR (CDCl₃, 125 MHz): δ 166.2, 147.8, 140.1, 127.05, 127.01, 126.94, 122.0, 40.9, 27.4, and 23.1.

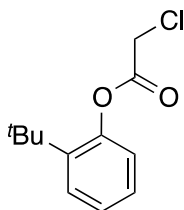
IR (neat): 2965 (w), 1774 (s), 1488 (m), 1449 (m), 1243 (m), 1144 (s), 924 (m), and 760 (s) cm⁻¹.

TLC: R_f = 0.5 in 10:1 hexanes: EtOAc.

GCMS (5029017): t_R = 9.18 min, m/z 214 [(M+2)⁺, 4], 212 (M⁺, 12), 197 [(M-Me)⁺, 3], 136 (96), and 121 (100).

HRMS (APCI/TOF): Calcd for (M+H)⁺ (C₁₁H₁₄ClO₂)⁺: 213.0677. Found: 213.0650.

2-(*tert*-Butyl)phenyl 2-chloroacetate (3-8f-^tBu)



Yield: 10 mmol scale, 2.02 g, 91%.

¹H NMR (CDCl₃, 500 MHz): δ 7.42 [dd, *J* = 7.7, 1.9 Hz, 1H, OCCH or OCC(^tBu)CH], 7.24 [ddd, *J* = 7.7, 7.3, 1.9 Hz, 1H, OCCHCH or OCC(^tBu)CHCH], 7.20 [ddd, *J* = 7.7, 7.3, 1.9 Hz, 1H, OCCHCH or OCC(^tBu)CHCH], 7.03 [dd, *J* = 7.7, 1.9 Hz, 1H, OCCH or OCC(^tBu)CH], 4.33 (s, 2H, CH₂Cl), and 1.36 [s, 9H, ArC(CH₃)₃].

¹³C NMR (CDCl₃, 125 MHz): δ 166.1, 149.1, 141.1, 127.6, 127.2, 126.5, 123.6, 41.3, 34.7, and 30.4.

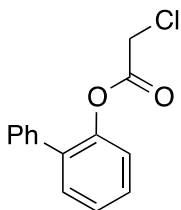
IR (neat): 2958 (w), 1775 (s), 1486 (m), 1442 (m), 1241 (m), 1181 (s), 1125 (s), 923 (m), and 756 (s) cm⁻¹.

TLC: R_f = 0.5 in 10:1 hexanes: EtOAc.

GCMS (5029017): t_R = 9.77 min, m/z 228 [(M+2)⁺, 9], 226 (M⁺, 28), 211 [(M-Me)⁺, 17], 193 (18), 150 (88), and 135 (100).

HRMS (APCI/TOF): Calcd for (M+H)⁺ (C₁₂H₁₆ClO₂)⁺: 227.0833. Found: 227.0821.

[1,1'-Biphenyl]-2-yl 2-chloroacetate (3-8g-Ph)



Yield: 10 mmol scale, 2.10 g, 87%.

¹H NMR (CDCl₃, 500 MHz): δ 7.45-7.34 (m, 8H, Ar-*H*), 7.18 (dd, *J* = 7.8, 1.4 Hz, 1H, Ar-*H*), and 4.06 (s, 2H, CH₂Cl).

¹³C NMR (CDCl₃, 125 MHz): δ 165.9, 147.5, 137.2, 134.9, 131.3, 129.1, 128.9, 128.6, 127.9, 127.1, 122.6, and 40.8.

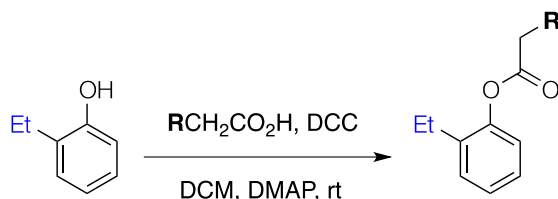
IR (neat): 3061 (w), 2951 (w), 1775 (s), 1477 (m), 1434 (m), 1276 (m), 1183 (s), 925 (m), and 737 (s) cm⁻¹.

TLC: R_f = 0.4 in 10:1 hexanes: EtOAc.

GCMS (5029017): t_R = 11.41 min, m/z 248 [(M+2)⁺, 13], 246 (M⁺, 41), 170 (100), 141 (38), and 115 (54).

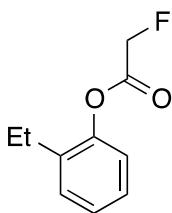
HRMS (APCI/TOF): Calcd for (M+H)⁺ (C₁₄H₁₂ClO₂)⁺: 247.0520. Found: 247.0512.

D.6. Procedure for Preparation of 2-Ethylphenyl 2-fluoroacetate (3-8a-Et), 2-Ethylphenyl 2-bromoacetate (3-8c-Et) and 2-Ethylphenyl 2-methoxyacetate (3-8d-Et).



2-Ethylphenol 8-Et (1.2 mL, 10 mmol), substituted acetic acid (13 mmol) and 4-dimethyl aminopyridine (122 mg, 1 mmol) were dissolved with CH₂Cl₂ (20 mL). 1,3-Dicyclohexyl carbodiimide (2.7 g, 13 mmol) was added into the reaction mixture slowly at 0 °C. After 10 min the reaction mixture was warmed to rt and stirred for 1 h before it was filtered through a pad of Celite®, and the volatiles were removed *in vacuo*, and the crude mixture was purified by flash column (hexanes: EtOAc 10:1) to afford the desired product.

2-Ethylphenyl 2-fluoroacetate (3-8a-Et)



Yield: 10 mmol scale, 1.47 g, 81%.

¹H NMR (CDCl₃, 500 MHz): δ 7.31-7.29 (m, 1H, Ar-*H*), 7.25-7.23 (m, 2H, Ar-*H*), 7.09-7.06 (m, 1H, Ar-*H*), 5.13 [d, *J* = 46.9 (²*J*_{F-H}), 2H, CH₂F], 2.56 (q, *J* = 7.6, 2H, ArCH₂CH₃), and 1.20 (t, *J* = 7.6, 3H, ArCH₂CH₃).

¹³C NMR (CDCl₃, 125 MHz): δ 166.6 (d, ²*J*_{F-C} = 21.7 Hz), 148.0, 135.8, 129.9, 127.3, 127.0, 122.0, 77.6 (d, ¹*J*_{F-C} = 183.7 Hz), 23.3, and 14.3.

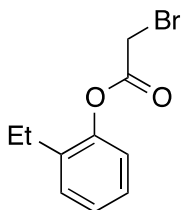
IR (neat): 3037 (w), 2972 (w), 1779 (s), 1489 (m), 1240 (s), 1169 (s), 1074 (s), 916 (w), and 771 (s) cm⁻¹.

TLC: $R_f = 0.7$ in 5:1 hexanes: EtOAc.

GCMS (5029017): $t_R = 7.73$ min, m/z 181 [(M-H)⁺, 25], 120 (100), and 106 (85).

HRMS (APCI/TOF): Calcd for (M+H)⁺ (C₁₀H₁₂FO₂)⁺: 183.0816. Found: 183.0806.

2-Ethylphenyl 2-bromoacetate (3-8c-Et)



Yield: 10 mmol scale, 2.02 g, 83%.

¹H NMR (CDCl₃, 500 MHz): δ 7.30-7.27 (m, 1H, Ar-H), 7.27-7.22 (m, 2H, Ar-H), 7.06-7.03 (m, 1H, Ar-H), 4.07 (s, 2H, CH₂Br), 2.59 (q, $J = 7.7$ Hz, 2H, ArCH₂CH₃), and 1.21 (t, $J = 7.7$ Hz, 3H, ArCH₂CH₃).

¹³C NMR (CDCl₃, 125 MHz): δ 166.1, 148.6, 136.0, 129.9, 127.2, 127.0, 121.8, 25.4, 23.2, and 14.5.

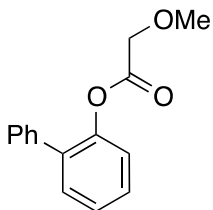
IR (neat): 2969 (w), 1752 (s), 1488 (m), 1258 (s), 1209 (s), 1113(s), 927 (m), and 748 (s) cm⁻¹.

TLC: $R_f = 0.5$ in 10:1 hexanes: EtOAc.

GCMS (5029017): $t_R = 9.41$ min, m/z 240 (M⁺, 16), 238 [(M-2)⁺, 16], 178 (29), 120 (45), and 106 (100).

HRMS (APCI/TOF): Calcd for (M+H)⁺ (C₁₀H₁₂BrO₂)⁺: 243.0015. Found: 243.0012.

2-Ethylphenyl 2-methoxyacetate (3-8d-Et)



Yield: 10 mmol scale, 1.67 g, 86%.

¹H NMR (CDCl₃, 500 MHz): δ 7.27 [dd, *J* = 7.4, 2.2 Hz, 1H, OCCH or OCC(Et)CH], 7.23 [ddd, *J* = 7.4, 7.2, 2.2 Hz, 2H, OCCHCH or OCC(Et)CHCH], 7.20 [ddd, *J* = 7.4, 7.4, 1.8 Hz, 1H, OCCHCH or OCC(Et)CHCH], 7.04 [dd, *J* = 7.2, 1.8 Hz, 1H, OCCH or OCC(Et)CH], 4.32 (s, 2H, CH₂OMe), 3.55 (s, 3H, OCH₃), 2.55 (q, *J* = 7.6 Hz, 2H, ArCH₂CH₃), and 1.20 (t, *J* = 7.6 Hz, 3H, ArCH₂CH₃).

¹³C NMR (CDCl₃, 125 MHz): δ 169.0, 148.4, 135.8, 129.7, 127.1, 126.6, 122.1, 69.9, 59.7, 23.3, and 14.3.

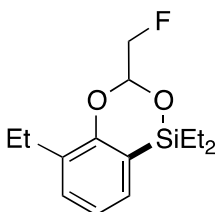
IR (neat): 2969 (w), 1771 (s), 1489 (m), 1451 (m), 1214 (m), 1164 (s), 1114 (s), 938 (m), and 771 (m) cm⁻¹.

TLC: R_f = 0.4 in 10:1 hexanes: EtOAc.

GCMS (5029017): t_R = 8.83 min, m/z 195 [(M+H)⁺, 89], 176 (28), 166 (100), 134 (63), and 121 {[M-C(O)CH₂OMe]⁺, 57}.

HRMS (APCI/TOF): Calcd for (M+H)⁺ (C₁₁H₁₅O₃)⁺: 195.1016. Found: 195.1002.

1,1,5-Triethyl-3-(fluoromethyl)-benzo[*c*][1,5,2]dioxasiline (3-18a)



Yield: 1 mmol scale, 201 mg, 75%.

¹H NMR (CDCl₃, 500 MHz): δ 7.25 [dd, *J* = 7.3, 1.7 Hz, 1H, SiCCH or OCC(Et)CH], 7.18 [dd, *J* = 7.3, 1.7 Hz, 1H, OCC(Et)CH or SiCCH], 7.04 (dd, *J* = 7.3, 7.3 Hz, 1H, SiCCHCH), 5.46 (ddd, *J* = 7.3 (³J_{F-H}), 5.6, 3.8 Hz, 1H, OCHCH₂F), 4.57 (ddd, *J* = 47.0 (²J_{F-H}), 9.5, 5.6 Hz, 1H, FCH_aH_b), 4.53 (ddd, *J* = 46.3 (²J_{F-H}), 9.5, 3.8 Hz, 1H, FCH_aH_b), 2.71 (dq, *J* = 14.8, 7.6 Hz, 1H, PhCH_aH_b), 2.63 (dq, *J* = 14.8, 7.6 Hz, 1H, PhCH_aH_b), 1.22 (t, *J* = 7.6 Hz, 3H, PhCH₂CH₃), 1.10 (t, *J* = 7.5 Hz, 3H, SiCH₂CH₃), 0.97-0.74 [m, 7H, Si(CH₂CH₃)₂ and SiCH₂CH₃].

¹³C NMR (CDCl₃, 125 MHz): δ 161.3, 133.2, 131.4, 130.9, 122.8, 119.6, 95.4 (d, ²J_{F-C} = 25.9 Hz), 84.0 (d, ¹J_{F-C} = 173.7 Hz), 23.4, 14.4, 6.81, 6.79, 6.6, 6.3

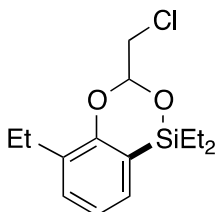
IR (neat): 2960 (m), 2877 (m), 1588 (w), 1420 (m), 1214 (m), 1191 (m), 1142 (s), and 729 (m) cm⁻¹.

TLC: R_f = 0.4 in 20:1 hexanes: EtOAc.

GCMS (5029017): $t_R = 9.60$ min, m/z 267 [(M-F)⁺, 64], 205 (100), and 191 (22).

HRMS (APCI/TOF): Calcd for (M+H)⁺ (C₁₄H₂₂FO₂Si)⁺: 269.1368. Found: 269.1354.

3-(Chloromethyl)-1,1,5-triethyl-benzo[c][1,5,2]dioxasiline (3-18b)



Yield: 1 mmol scale, 211 mg, 85%.

¹H NMR (CDCl₃, 500 MHz): δ 7.25 [app d, $J = 7.4$ Hz, 1H, SiCCH or OCC(Et)CH], 7.17 [dd, $J = 7.4, 1.6$ Hz, 1H, OCC(Et)CH or SiCCH], 7.03 (dd, $J = 7.4, 7.4$ Hz, 1H, SiCCHCH), 5.34 (dd, $J = 6.0, 3.8$ Hz, 1H, OCHCH₂Cl), 3.76 (dd, $J = 11.4, 6.0$ Hz, 1H, ClCH_aH_b), 3.70 (dd, $J = 11.4, 3.8$ Hz, 1H, ClCH_aH_b), 2.72 (dq, $J = 14.7, 7.5$ Hz, 1H, PhCH_aH_b), 2.64 (dq, $J = 14.7, 7.5$ Hz, 1H, PhCH_aH_b), 1.26 (dd, $J = 7.5, 7.5$ Hz, 1H, PhCH₂CH₃), 1.09 (t, $J = 7.8$ Hz, 3H, SiCH₂CH₃), 0.93 (t, $J = 7.8$ Hz, 3H, SiCH₂CH₃), and 0.91-0.72 [m, 4H, Si(CH₂CH₃)₂].

¹³C NMR (CDCl₃, 125 MHz): δ 161.3, 133.3, 131.4, 131.0, 122.8, 119.4, 97.2, 46.3, 23.3, 14.5, 6.81, 6.78, 6.62, and 6.33.

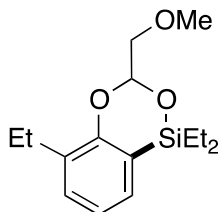
IR (neat): 2961 (m), 2877 (m), 1588 (w), 1420 (s), 1215 (s), 1018 (s), and 754 (s) cm⁻¹.

TLC: $R_f = 0.8$ in 10:1 hexanes: EtOAc.

GCMS (5029017): $t_R = 10.61$ min, m/z 286 [(M+2)⁺, 2], 284 (M⁺, 7), 255 [(M-Et)⁺, 2], 249 [(M-Cl)⁺, 3], 206 [(M-CH₂ClCHO)⁺, 100], and 191 (15).

HRMS (APCI/TOF): Calcd for (M+H)⁺ (C₁₄H₂₂ClO₂Si)⁺: 285.1072. Found: 285.1061.

1,1,5-Triethyl-3-(methoxymethyl)-benzo[c][1,5,2]dioxasiline (3-18d)



Yield: 1 mmol scale, 215 mg, 77%.

¹H NMR (CDCl₃, 500 MHz): δ 7.23 [dd, *J* = 7.3, 1.4 Hz, 1H, SiCCH or OCC(Et)CH], 7.17 [dd, *J* = 7.3, 1.4 Hz, 1H, SiCCH or OCC(Et)CH], 7.00 (dd, *J* = 7.3, 7.3 Hz, 1H, SiCCHCH), 5.37 (dd, *J* = 4.7, 4.7 Hz, 1H, OCHO), 3.70 (dd, *J* = 12.3, 4.7 Hz, 1H, CH_aH_bOMe), 3.67 (dd, *J* = 12.3, 4.7 Hz, 1H, CH_aH_bOMe), 3.52 (s, 3H, OCH₃), 2.69 (dq, *J* = 14.7, 7.5 Hz 1H, ArCH_aH_b), 2.61 (dq, *J* = 14.7, 7.5 Hz 1H, ArCH_aH_b), 1.21 (dd, *J* = 7.5, 7.5 Hz 3H, ArCH₂CH₃), 1.09 [t, *J* = 7.9 Hz, 3H, SiCH₂CH₃], and 0.96-0.71 [m, 7H, SiCH₂CH₃ and Si(CH₂CH₃)₂].

¹³C NMR (CDCl₃, 125 MHz): δ 161.8, 132.9, 131.1, 130.9, 122.4, 119.5, 96.7, 75.5, 59.8, 23.4, 14.4, 6.8 (2), 6.6, and 6.4.

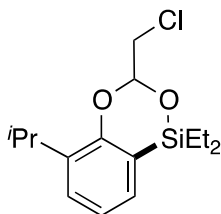
IR (neat): 2959 (m), 2877 (m), 1694 (s), 1587 (w), 1420 (s), 1086 (s), 1035 (s), 830 (m), and 728 (s) cm⁻¹.

TLC: R_f = 0.6 in 10:1 hexanes: EtOAc.

GCMS (5029017): t_R = 10.44 min, m/z 281 [(M+H)⁺, 42], 235 [(M-CH₂OCH₃)⁺, 100], 251 [(M-OMe)⁺, 11], 206 {[M-CH₂(OMe)CHO]⁺, 14}, and 163 (15).

HRMS (APCI/TOF): Calcd for (M+H)⁺ (C₁₅H₂₅O₃Si)⁺: 281.1567. Found: 281.1552.

3-(Chloromethyl)-1,1-diethyl-5-isopropyl-benzo[c][1,5,2]dioxasiline (3-18e)



Yield: 1 mmol scale, 265 mg, 89%.

¹H NMR (CDCl₃, 500 MHz): δ 7.31 [dd, *J* = 7.4, 1.7 Hz, 1H, OCC(ⁱPr)CH or SiCCH], 7.16 [dd, *J* = 7.4, 1.7 Hz, 1H, OCC(ⁱPr)CH or SiCCH], 7.06 (dd, *J* = 7.4, 7.4 Hz, 1H, SiCCHCH), 5.34 (dd, *J* = 6.0, 3.7 Hz, 1H, OCHCH₂Cl), 3.76 (dd, *J* = 11.4, 6.0 Hz 1H, ClCH_aH_b), 3.70 (dd, *J* = 11.4, 3.7 Hz 1H, ClCH_aH_b), 3.38 [septet, *J* = 7.0 Hz 1H, PhCH(CH₃)₂], 1.25 [d, *J* = 7.0 Hz, 3H, PhCH(CH_{3a})(CH_{3b})], 1.23 [d, *J* = 7.0 Hz 3H, PhCH(CH_{3a})(CH_{3b})], 1.09 (t, *J* = 7.8 Hz, 3H, SiCH₂CH₃), 0.92 (t, *J* = 7.8 Hz, 3H, SiCH₂CH₃), and 0.97-0.72 [m, 4H, Si(CH₂CH₃)₂].

¹³C NMR (CDCl₃, 125 MHz): δ 160.7, 137.7, 130.7, 128.5, 122.9, 119.6, 97.2, 46.3, 27.0, 23.2, 22.5, 6.78, 6.77, 6.67, and 6.35.

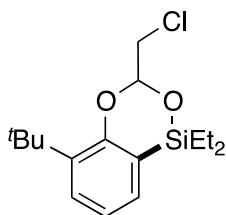
IR (neat): 2959 (m), 2877 (m), 1587 (w), 1420 (m), 1214 (m), 1018 (s), 882 (s), and 754 (s) cm^{-1} .

TLC: $R_f = 0.8$ in 10:1 hexanes: EtOAc.

GCMS (5029017): $t_R = 10.80$ min, m/z 300 $[(M+2)^+, 2]$, 298 (M^+ , 3), 263 $[(M-Cl)^+, 5]$, 220 $[(M-CH_2ClCHO)^+, 100]$, and 205 (83).

HRMS (APCI/TOF): Calcd for $(M+H)^+$ ($C_{15}H_{24}ClO_2Si$) $^+$: 299.1229. Found: 299.1120.

5-(*tert*-Butyl)-3-(chloromethyl)-1,1-diethyl-benzo[*c*][1,5,2]dioxasiline (3-18f)



Total Yield: 1 mmol scale, 241 mg, 77%.

$^1\text{H NMR}$ (CDCl_3 , 500 MHz): δ 7.37 [dd, $J = 7.8, 1.7$ Hz, 1H, OCC(*t*Bu)CH or SiCCH], 7.16 [dd, $J = 7.1, 1.7$ Hz, 1H, OCC(*t*Bu)CH or SiCCH], 7.02 (dd, $J = 7.8, 7.1$ Hz, 1H, SiCCHCH), 5.37 (dd, $J = 4.9, 4.0$ Hz, 1H, OCHCH₂Cl), 3.80 (dd, $J = 11.5, 4.9$ Hz 1H, ClCH_aH_b), 3.74 (dd, $J = 11.5, 4.0$ Hz 1H, ClCH_aH_b), 1.40 [s, 9H, ArC(CH₃)₃], 1.09 (t, $J = 7.5$ Hz, 3H, SiCH₂CH₃), 0.96-0.91 (m, 2H, SiCH₂CH₃), 0.89 (t, $J = 7.5$ Hz, 3H, SiCH₂CH₃), and 0.86-0.68 (m, 2H, SiCH₂CH₃).

$^{13}\text{C NMR}$ (CDCl_3 , 125 MHz): δ 162.5, 138.9, 131.2, 129.1, 122.6, 120.4, 96.9, 46.6, 35.0, 30.2, 6.82, 6.79, 6.66, and 6.30.

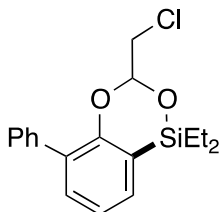
IR (neat): 2957 (m), 2877 (m), 1580 (w), 1408 (m), 1213 (m), 1017 (s), 848 (m), and 725 (s) cm^{-1} .

TLC: $R_f = 0.8$ in 10:1 hexanes: EtOAc.

GCMS (5029017): $t_R = 11.20$ min, m/z 315 $[(M+2)^+, 4]$, 313 (M^+ , 12), 277 $[(M-Cl)^+, 8]$, 234 $[(M-CH_2ClCHO)^+, 62]$, and 219 (100).

HRMS (APCI/TOF): Calcd for $(M+H)^+$ ($C_{16}H_{26}ClO_2Si$) $^+$: 313.1385. Found: 313.1375.

3-(Chloromethyl)-1,1-diethyl-5-phenyl-benzo[*c*][1,5,2]dioxasiline (3-18g)



Yield: 1 mmol scale, 318 mg, 96%.

¹H NMR (CDCl₃, 500 MHz): δ 7.60 – 7.57 (m, 2H, Ar-H), 7.45 [dd, *J* = 7.4, 1.7 Hz, 1H, OCC(Ph)CH or SiCCH], 7.44 – 7.40 (m, 2H, Ar-H), 7.35 (app d, *J* = 7.4 Hz, 1H, Ar-H), 7.32 [dd, *J* = 7.4, 1.7 Hz, 1H, OCC(Ph)CH or SiCCH], 7.17 (dd, *J* = 7.4, 7.4 Hz, 1H, SiCCHCH), 5.45 (dd, *J* = 5.2, 4.3 Hz, 1H, OCHCH₂Cl), 3.68 (dd, *J* = 11.5, 5.2 Hz 1H, ClCH_aH_b), 3.65 (dd, *J* = 11.5, 4.3 Hz 1H, ClCH_aH_b), 1.14 (t, *J* = 7.5 Hz, 3H, SiCH₂CH₃), and 1.01-0.75 [m, 7H, SiCH₂CH₃ and Si(CH₂CH₃)₂].

¹³C NMR (CDCl₃, 125 MHz): δ 160.1, 137.7, 133.1, 132.7, 131.2, 130.0, 128.1, 127.3, 123.1, 120.5, 97.4, 46.3, 6.83, 6.81, 6.62, and 6.35.

IR (neat): 2960 (m), 2877 (m), 1585 (w), 1407 (m), 1213 (s), 1015 (s), 847 (m), and 731 (s) cm⁻¹.

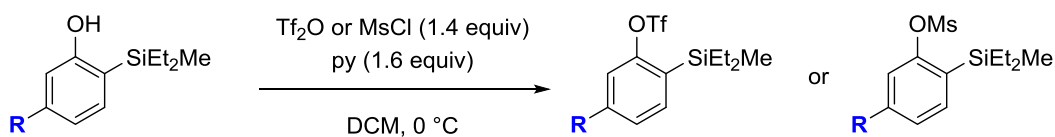
TLC: R_f = 0.7 in 10:1 hexanes: EtOAc.

GCMS (5029017): t_R = 13.23 min, m/z 334 [(M+2)⁺, 14], 332 (M⁺, 31), 297 [(M-Cl)⁺, 4], 254 [(M-CH₂ClCHO)⁺, 100], and 153 (24).

HRMS (APCI/TOF): Calcd for (M+H)⁺ (C₁₈H₂₂ClO₂Si)⁺: 333.1072. Found: 333.1068.

D.7. Procedure for Preparation of Trifluoromethanesulfonate and

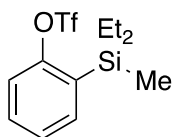
Methanesulfonate



2-Silylphenol (5 mmol) and pyridine (0.64 mL, 8 mmol) in CH₂Cl₂ (10 mL) were cooled to 0 °C with an ice bath. Trifluoromethanesulfonyl anhydride (1.2 mL, 7 mmol) or methanesulfonyl chloride (0.54 mL, 7 mmol) was added into the reaction mixture slowly.

The reaction mixture was stirred at 0 °C for 0.5 h before it was quenched by saturated aqueous sodium bicarbonate (10 mL) and was extracted with diethyl ether (15 mLx4). The combined organic extracts were washed with water (10 mL) and brine (10 mL), and dried over anhydrous sodium sulfate. The volatiles were removed *in vacuo*, and the crude mixture was purified by MPLC (hexanes/EtOAc =80:1, 5 mL/min, retention time 5-10 min) to afford the desired product **3-22**.

2-[Diethyl(methyl)silyl]phenyl trifluoromethanesulfonate (**3-22a**)



Yield: 5 mmol scale, 1.56 g, 96%.

¹H NMR (CDCl₃, 500 MHz): δ 7.54-7.52 (nfom, 1H, OCCH or SiCCH), 7.44 (ddd, *J* = 8.4, 7.2, 1.8 Hz, 1H, SiCCHCH or OCCHCH), 7.37-7.34 (nfom, 1H, OCCH or SiCCH), 7.34 (ddd, *J* = 7.4, 1.0 Hz, 1H, OCCHCH or SiCCHCH), 0.97-0.93 [m, 6H, Si(CH₂CH₃)₂], 0.90-0.84 [m, 4H, Si(CH₂CH₃)₂], and 0.35 (s, 3H, SiCH₃).

¹³C NMR (CDCl₃, 125 MHz): δ 155.5, 137.1, 131.4, 130.8, 127.6, 119.7, 118.5 (q, ¹*J*_{F-C} = 322 Hz), 7.4, 5.5, and -5.4.

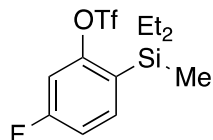
IR (neat): 2957 (m), 2877 (w), 1596 (w), 1417 (s), 1206 (s), 1136 (s), 1055 (m), 885 (s), and 766 (s) cm⁻¹.

TLC: R_f = 0.6 in 20:1 hexanes: EtOAc.

GCMS (5029017): t_R = 8.85 min, m/z 326 (M⁺, 0.1), 311 [(M-Me)⁺, 11], 297 [(M-Et)⁺, 65], and 177 [(M-OTf)⁺, 100].

HRMS (APCI/TOF): Calcd for (M+H)⁺ (C₁₂H₁₈F₃O₃SSi)⁺: 327.0693. Found: 327.0698.

2-[Diethyl(methyl)silyl]-5-fluorophenyl trifluoromethanesulfonate (**3-22b**)



Yield: 5 mmol scale, 1.62 g, 94%.

¹H NMR (CDCl₃, 500 MHz): δ 7.49 [dd, *J* = 8.2, 6.9 (⁴*J*_{F-H}) Hz, 1H, SiCCH], 7.13 [dd, *J* = 9.4 (³*J*_{F-H}), 2.2 Hz, 1H, C(OTf)CH], 7.08 [ddd, *J* = 8.2, 8.2 (³*J*_{F-H}), 2.2 Hz, 1H, SiCCHCH], 0.95-0.91 [m, 6H, Si(CH₂CH₃)₂], 0.88-0.82 [m, 4H, Si(CH₂CH₃)₂], and 0.32 (s, 3H, SiCH₃).

¹³C NMR (CDCl₃, 125 MHz): δ 163.9 (¹*J*_{F-C} = 253 Hz), 155.3 (d, ³*J*_{F-C} = 9.7 Hz), 138.0 (d, ³*J*_{F-C} = 8.4 Hz), 126.2 (d, ⁴*J*_{F-C} = 3.4 Hz), 118.7 (d, ¹*J*_{CF₃} = 321 Hz), 115.0 (d, ²*J*_{F-C} = 19.2 Hz), 108.2 (d, ²*J*_{F-C} = 24.9 Hz), 7.4, 5.5, and -5.4.

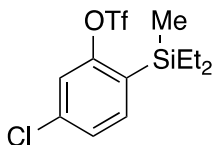
IR (neat): 2955 (m), 2877 (m), 1607 (m), 1422 (m), 1213 (s), 1134 (s), 1005 (s), 880 (s), and 599 (m) cm⁻¹.

TLC: R_f = 0.6 in 20:1 hexanes: EtOAc.

GCMS (5029017): t_R = 8.49 min, m/z 344 (M⁺, 0.2), 329 [(M-Me)⁺, 25], 315 [(M-Et)⁺, 100], and 195 [(M-OTf)⁺, 50].

HRMS (APCI/TOF): Calcd for (M+H)⁺ (C₁₂H₁₇F₄O₃SSi)⁺: 345.0598. Found: 345.0593.

5-Chloro-2-(diethyl(methyl)silyl)phenyl trifluoromethanesulfonate (3-22c)



Yield: 1 mmol scale, 338 mg, 94%.

¹H NMR (CDCl₃, 500 MHz): δ 7.43 [d, *J* = 2.6 Hz 1H, C(OTf)CH], 7.39 (dd, *J* = 8.7, 2.6 Hz, 1H, SiCCHCH), 7.28 (d, *J* = 8.7 Hz, 1H, SiCCH), 0.97-0.93 [m, 6H, Si(CH₂CH₃)₂], 0.90-0.84 [m, 4H, Si(CH₂CH₃)₂], and 0.34 (s, 3H, SiCH₃).

¹³C NMR (CDCl₃, 125 MHz): δ 153.5, 136.6, 133.7, 133.6, 131.2, 121.1, 118.5 (q, ¹*J*_{F-C} = 320 Hz), 7.4, 5.4, and -5.5.

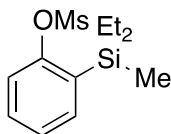
IR (neat): 2957 (m), 2877 (w), 1590 (w), 1489 (s), 1208 (s), 1136 (s), 1005 (m), 884 (m), and 612 (s) cm⁻¹.

TLC: R_f = 0.6 in 20:1 hexanes: EtOAc.

GCMS (5029017): t_R = 9.60 min, m/z 345 [(M-Me)⁺, 10], 325 [(M-Cl)⁺, 0.2], 315 [(M-Et)⁺, 66], 211 [(M-OTf)⁺, 46], and 198 (100).

HRMS (APCI/TOF): Calcd for (M+H)⁺ (C₁₂H₁₇ClF₃O₃SSi)⁺: 361.0303. Found: 361.0316.

2-[Diethyl(methyl)silyl]phenyl methanesulfonate (3-22d)



Yield: 5 mmol scale, 1.25 g, 92%.

¹H NMR (CDCl₃, 500 MHz): δ 7.50 [dd, *J* = 8.3, 1.0 Hz, 1H, C(OMs)CH or SiCCH], 7.48 [dd, *J* = 7.3, 1.8 Hz, 1H, C(OMs)CH or SiCCH], 7.40 [ddd, *J* = 8.3, 7.8, 1.8 Hz, 1H, C(OMs)CHCH or SiCCHCH], 7.26 [ddd, *J* = 7.8, 7.3, 1.0 Hz, 1H, C(OMs)CHCH or SiCCHCH], 3.19 (s, 3H, SO₂CH₃), 0.97-0.93 [m, 6H, Si(CH₂CH₃)₂], 0.87-0.82 [m, 4H, Si(CH₂CH₃)₂], and 0.32 (s, 3H, SiCH₃).

¹³C NMR (CDCl₃, 125 MHz): δ 155.1, 136.9, 131.1, 130.0, 126.4, 119.4, 38.8, 7.6, 5.8, and -5.1.

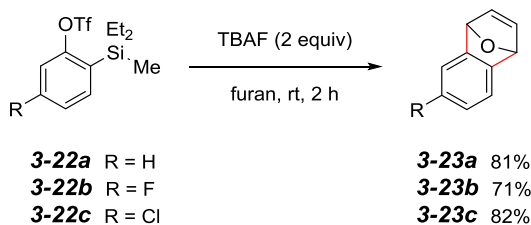
IR (neat): 2953 (m), 2874 (w), 1592 (w), 1425 (m), 1190 (m), 1145 (s), 1005 (m), 865 (s), 784 (s), and 529 (s) cm⁻¹.

TLC: R_f = 0.2 in 20:1 hexanes: EtOAc.

GCMS (5029017): t_R = 11.31 min, m/z 257 [(M-Me)⁺, 9], 243 [(M-Et)⁺, 100], and 180 (11).

HRMS (APCI/TOF): Calcd for (M+H)⁺ (C₁₂H₂₁O₃SSi)⁺: 273.0975. Found: 273.0969.

D.8. General Procedure for Benzyne Cycloaddition Reaction



Silane (0.2 mmol) and furan (0.4 mL) were placed in a 4 mL vial. TBAF (0.2 mL, 1 M in THF) was added into the reaction mixture at rt. The septum on the vial was replaced by a screw cap with a Teflon liner, and the mixture was stirred at rt for 2 h. The reaction was quenched by adding saturated aqueous ammonium chloride (2 mL). The reaction mixture was extracted with diethyl ether (3×1 mL) and concentrated *in vacuo* to afford the

crude mixture, which was purified by MPLC (hexanes/EtOAc =10:1, 5 mL/min, retention time 7-15 min). The compounds **3-23a**, **3-23b** and **3-23c** have been reported.

D.9. Procedure for *ipso*-Desilylative Boronation to Synthesize 2-(4,4,5,5-Tetramethyl-1,3,2-dioxaborolan-2-yl)phenol (3-24**)**



Dioxasiline **3-12a** (0.2 mmol) was dissolved with CH₂Cl₂ (0.2 mL). BCl₃ (1 M in heptane, 1 mL, 1 mmol) was added to the mixture in one portion. The septum on the vial was replaced by a screw cap with a Teflon liner. The reaction mixture was kept at 80 °C and stirred for 2 d. A solution of pinacol (177 mg, 1.5 mmol) and triethylamine (0.4 ml, 3 mmol) in dry DCM (0.50 ml) was injected to the above mixture and stirred at rt for 12 h. After completion, saturated aqueous NaHCO₃ (2 ml) was added. The mixture was extracted with diethyl ether (3 mLx4). The combined organic layer was washed with water (3 mL) and brine (3 mL), and dried over anhydrous sodium sulfate. The volatiles were removed *in vacuo*, and the crude mixture was purified by MPLC (hexanes/EtOAc = 3:1, 5 mL/min, retention time 9 min) to afford **3-24** (36 mg, 81%) as a colorless liquid.

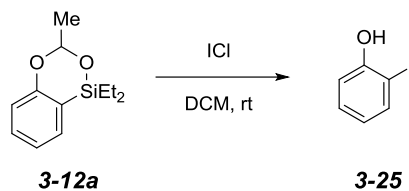
¹H NMR (CDCl₃, 500 MHz): δ 7.81 (s, 1H, ArOH), 7.61 [dd, *J* = 7.6, 1.8 Hz, 1H, BCCH or C(OH)CH], 7.37 [ddd, *J* = 7.6, 7.6, 1.8 Hz, 1H, BCCHCH or C(OH)CHCH], 6.88 [ddd, *J* = 7.6, 7.6, 1.3 Hz, 1H, BCCHCH or C(OH)CHCH], 7.88 [dd, *J* = 7.6, 1.3 Hz, 1H, BCCH or C(OH)CH], and 1.37 {s, 12H, B[OC(CH₃)₂]₂}.

¹³C NMR (CDCl₃, 125 MHz): δ 163.8, 135.9, 134.1, 119.7, 115.7, 84.7, and 25.0.

TLC: R_f = 0.6 in 2:1 hexanes: EtOAc.

GCMS (5029017): t_R=9.63 min, m/z 221 [(M+H)⁺, 2], 220 (M⁺, 3), 135 (1), 89 (13), and 63 (100).

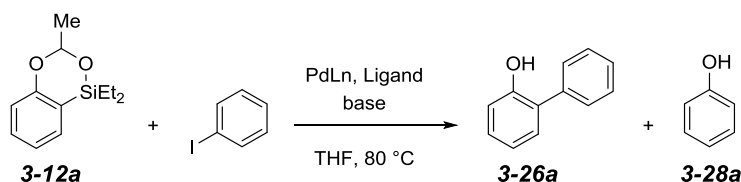
D.10. Procedure for Iodo *ipso*-Desilylation of **3-12a** to **3-2-Iodophenol (3-25)**:-



Dioxasiline **3-12a** (0.2 mmol) and iodine chloride (65 mg, 0.4 mmol) were dissolved with DCM (1 mL, 0.2 M). The reaction mixture was stirred at rt for 2 h. The reaction was quenched by adding saturated aqueous sodium chloride (2 mL) and extracted with diethyl ether (4 mL×4). The combined organic layer was washed with water (4 mL) and brine (4 mL), and dried over anhydrous sodium sulfate. The volatiles were removed *in vacuo*, and the crude mixture was purified by flash column (hexanes: EtOAc 10:1) to afford 2-iodophenol **3-25** (36.9 mg, 84%).

D.11. General Procedure for Palladium Catalyzed Hiyama Cross-Coupling

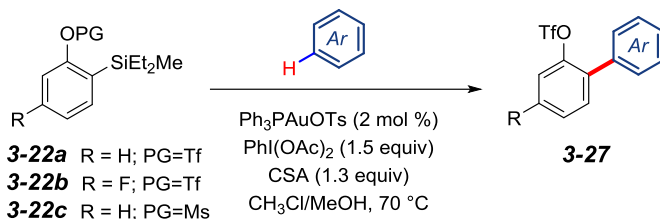
Reaction



PdLn (5 mol %), ligand (5 mol % for bidentate, 10 mol% for monodentate) and iodobenzene (22 μ L, 0.2 mmol) were dissolved with THF (0.4 mL) and base (2 equiv) in a 4 mL vial. Dioxasiline **3-12a** (22 mg, 0.1 mmol) was added into the reaction mixture. The septum on the vial was replaced by a screw cap with a Teflon liner. The reaction mixture was kept at 80 °C and stirred for 12 h. The reaction mixture was extracted with diethyl ether (3×1 mL) and concentrated *in vacuo* to afford the crude mixture. The yield of **3-26a**

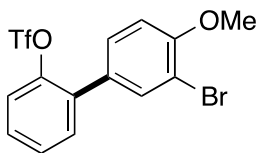
was determined by ^1H NMR spectroscopy by adding CH_2Br_2 (7 μL , 0.1 mmol) as an internal standard. (Table 3-2)

D.12. General Procedure for Gold Catalyzed Cross-Coupling Reaction:⁹



Silane **3-22** (0.2 mmol) and arene (0.4 mmol, as specified for individual compounds) were added to a 4 mL vial containing Ph₃PAuOTs (2.8 mg, 2 mol %) in CHCl₃ (1 mL) and MeOH (40 μL). Iodobenzene diacetate (84 mg, 0.26 mmol) and camphorsulfonic acid (70 mg, 0.3 mmol) were added into the reaction mixture. The septum on the vial was replaced by a screw cap with a Teflon liner. The reaction mixture was stirred at 70 °C and stirred for 24 h. The volatiles were removed *in vacuo*, and the resulting mixture was dissolved with diethyl ether, filtered through a pad of Celite[®], and concentrated *in vacuo* to afford the crude mixture, which was purified by MPLC (hexanes/EtOAc = 5:1, 7 mL/min, retention time 10-20 min) to give desired product **3-27** as a colorless liquid.

3'-Bromo-4'-methoxy-[1,1'-biphenyl]-2-yl trifluoromethanesulfonate (**3-27a**)



Yield: 0.2 mmol scale, 76 mg, 93%.

^1H NMR (CDCl₃, 500 MHz): δ 7.67 (d, J = 2.3 Hz, 1H, BrCCH), 7.45-7.36 (m, 5H, Ar-H), 6.98 [d, J = 8.5 Hz, 1H, CHC(OMe)], and 3.95 (s, 3H, OCH₃).

^{13}C NMR (CDCl₃, 125 MHz): δ 156.2, 146.9, 134.3, 134.0, 132.0, 129.8, 129.4, 129.3,

128.8, 122.4, 119.8, 121.1 (q, $^1J_{CF_3} = 321.6$ Hz), 111.8, and 56.5.

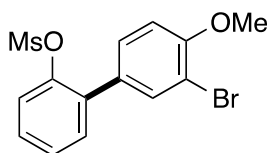
IR (neat): 2952 (w), 2875 (w), 1730 (s), 1464 (s), 1287 (s), 1208 (s), 1135 (s), 1016 (m), 885 (s), and 740 (s) cm^{-1} .

TLC: $R_f = 0.5$ in 5:1 hexanes: EtOAc.

GCMS (5029017): $t_R = 12.47$ min, m/z 412 [(M+2)⁺, 5], 410 (M⁺, 5), 261 [(M-OTf)⁺, 1], 198 (100), and 183 [(M-ArOTf)⁺, 41].

HRMS (APCI/TOF): Calcd for (M+H)⁺ (C₁₄H₁₁BrF₃O₄S)⁺: 410.9508. Found: 410.9501.

3'-Bromo-4'-methoxy-[1,1'-biphenyl]-2-yl methanesulfonate
3'-bromo-4'-methoxy-[1,1'-biphenyl]-2-yl methanesulfonate (3-27b)



Yield: 0.2 mmol scale, 63 mg, 89%.

¹H NMR (CDCl₃, 500 MHz): δ 7.73 (d, $J = 2.0$ Hz, 1H, BrCCH), 7.48-7.44 (m, 2H, Ar-H), 7.42-7.37 (m, 3H, Ar-H), 7.00 [d, $J = 8.5$ Hz, 1H, CHC(OMe)], 3.95 (s, 3H, OCH₃), and 2.68 (s, 3H, SO₂CH₃).

¹³C NMR (CDCl₃, 125 MHz): δ 155.9, 146.4, 134.2, 133.5, 131.3, 130.6, 129.8, 129.3, 128.0, 124.0, 112.0, 111.9, 56.5, and 38.2.

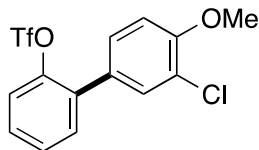
IR (neat): 3061 (w), 3010 (w), 1476 (m), 1365 (s), 1155 (s), 967 (m), 1056 (m), 865 (s), 720 (s), and 577 (s) cm^{-1} .

TLC: $R_f = 0.4$ in 5:1 hexanes: EtOAc.

GCMS (5029017): $t_R = 14.58$ min, m/z 358 [(M+2)⁺, 12], 356 (M⁺, 12), 261 [(M-OTf)⁺, 1], 198 (100), and 183 [(M-ArOTf)⁺, 41].

HRMS (APCI/TOF): Calcd for (M+H)⁺ (C₁₄H₁₄BrO₄S)⁺: 356.9791. Found: 356.9775.

3'-Chloro-4'-methoxy-[1,1'-biphenyl]-2-yl trifluoromethanesulfonate (3-27c)



Yield: 0.2 mmol scale, 56 mg, 76%.

¹H NMR (CDCl₃, 500 MHz): δ 7.50 [d, *J* = 2.2 Hz, 1H, C(Cl)CH], 7.45-7.36 (m, 4H, Ar-*H*), 7.35 [dd, *J* = 8.5, 2.2 Hz, 1H, C(OMe)CHCH], 7.01 [d, *J* = 8.5 Hz, 1H, C(OMe)CH], and 3.95 (s, 3H, OCH₃).

¹³C NMR (CDCl₃, 125 MHz): δ 155.3, 146.9, 134.1, 132.0, 131.2, 129.3, 129.0, 128.9, 128.8, 122.8, 122.4, 118.51 (q, ¹*J*_{CF₃} = 320.8 Hz), 112.0, and 56.4.

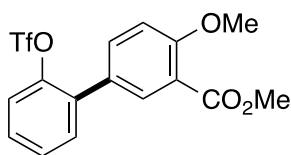
12IR (neat): 3056 (w), 2962 (w), 1747 (w), 1478 (m), 1295 (m), 1167 (m), 881 (m), 1056 (m), 865 (s), 750 (s), and 539 (s) cm⁻¹.

TLC: R_f = 0.5 in 5:1 hexanes: EtOAc.

GCMS (5029017): t_R = 12.03 min, m/z 368 [(M+2)⁺, 17], 366 (M⁺, 46), 233 (31), 217 [(M-OTf)⁺, 5], 198 (100), and 183 (34).

HRMS (APCI/TOF): Calcd for (M+H)⁺ (C₁₄H₁₁ClF₃O₄S)⁺: 367.0013. Found: 367.0004.

Methyl 4-methoxy-2'-[[(trifluoromethyl)sulfonyl]oxy]-[1,1'-biphenyl]-3-carboxylate (3-27d)



Yield: 0.2 mmol scale, 55 mg, 71%.

¹H NMR (CDCl₃, 500 MHz): δ 7.92 [d, *J* = 2.4 Hz, 1H, C(CO₂Me)CH], 7.59 [dd, *J* = 8.6, 2.4 Hz, 1H, C(OMe)CHCH], 7.48-7.36 (m, 4H, Ar-*H*), 7.07 [d, *J* = 8.7 Hz, 1H, C(OMe)CH], 3.96 (s, 3H, CO₂CH₃), and 3.90 (s, 3H, ArOCH₃).

¹³C NMR (CDCl₃, 125 MHz): δ 166.4, 159.4, 146.9, 134.6, 134.3, 132.9, 132.0, 129.2, 128.8, 127.7, 122.4, 120.3, 118.53 (q, ¹*J*_{CF₃} = 320.4 Hz), 112.3, 56.3, and 52.5.

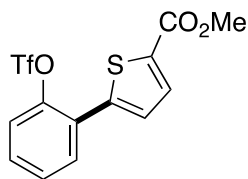
IR (neat): 3065 (w), 2953 (m), 1730 (s), 1419 (m), 1206 (s), 1136 (s), 889 (s), 737 (s), and 570 (m) cm⁻¹.

TLC: R_f = 0.3 in 5:1 hexanes: EtOAc.

GCMS (5029017): t_R = 12.86 min, m/z 390 (M⁺, 37), 359 [(M-OMe)⁺, 13], 241 [(M-OTf)⁺, 2], 225 [(ArOTf)⁺, 48], and 198 (100).

HRMS (APCI/TOF): Calcd for (M+H)⁺ (C₁₆H₁₄F₃O₆S)⁺: 391.0458. Found: 391.0453.

Methyl 5-[2-[[[(trifluoromethyl)sulfonyl]oxy]phenyl]thiophene-2-carboxylate (3-27e)



Yield: 0.2 mmol scale, 67 mg, 92%.

¹H NMR (CDCl₃, 500 MHz): δ 7.80 [d, *J* = 3.8 Hz, 1H, SCCH or C(CO₂Me)CH], 7.64-7.61 (nfm, 1H, Ar-*H*), 7.48-7.42 (m, 3H, Ar-*H*), 7.34 [d, *J* = 3.9 Hz, 1H, SCCH or C(CO₂Me)CH], and 3.91 (s, 3H, CO₂CH₃).

¹³C NMR (CDCl₃, 125 MHz): δ 162.6, 146.6, 143.3, 134.7, 134.1, 131.8, 130.4, 129.0, 128.8, 127.6, 122.7, 118.6 (¹*J*_{CF₃} = 320.4 Hz), and 52.6.

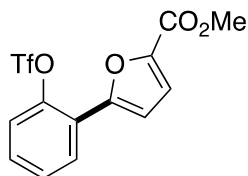
IR (neat): 3095 (w), 2955 (w), 1712 (s), 1421 (s), 1195 (s), 872 (s), 747 (s), and 640 (m) cm⁻¹.

TLC: R_f = 0.5 in 5:1 hexanes: EtOAc.

GCMS (5029017): t_R = 12.18 min, m/z 367 [(M+H)⁺, 32], 366 (M⁺, 72), 335 [(M-OMe)⁺, 6], 217 [(M-OTf)⁺, 6], 233 (71), and 174 (100).

HRMS (APCI/TOF): Calcd for (M+H)⁺ (C₁₃H₁₀F₃O₅S₂)⁺: 366.9916. Found: 366.9923.

Methyl 5-[2-((trifluoromethyl)sulfonyl)oxy]phenyl]furan-2-carboxylate (3-27f)



Yield: 1 mmol scale, 30 mg, 43%.

¹H NMR (CDCl₃, 500 MHz): δ 8.02 [dd, *J* = 7.1, 1.9 Hz, 1H, C(OTf)C(furyl)CH or C(OTf)CH], 7.47 [ddd, *J* = 7.1, 7.1, 1.6 Hz, 1H, C(OTf)CHCH or C(OTf)CHCHCH], 7.43 [ddd, *J* = 8.1, 7.1, 1.9 Hz, 1H, C(OTf)CHCH or C(OTf)CHCHCH], 7.40 [dd *J* = 8.1, 1.6 Hz, 1H, C(OTf)C(furyl)CH or C(OTf)CH], 7.28 [d, *J* = 3.7 Hz, 1H, OCCH or C(CO₂Me)CH], 7.01 [d, *J* = 3.7 Hz, 1H, OCCH or C(CO₂Me)CH], and 3.93 (s, 3H, CO₂CH₃).

¹³C NMR (CDCl₃, 125 MHz): δ 159.2, 151.0, 146.0, 144.5, 130.3, 129.1, 128.8, 123.4, 122.1, 120.0, 118.6 (¹*J*_{CF₃} = 325.7 Hz), 112.8, and 52.3.

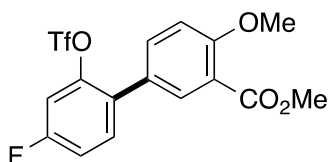
IR (neat): 2955 (w), 1720 (s), 1421 (s), 1301 (s), 1206 (s), 1132 (s), 874 (s), 746 (s), and 597 (m) cm⁻¹.

TLC: $R_f = 0.5$ in 5:1 hexanes: EtOAc.

GCMS (5029017): $t_R = 11.49$ min, m/z 351 [(M+H)⁺, 10], 350 (M⁺, 27), 319 [(M-OMe)⁺, 3], 217 [(M-OTf)⁺, 21], 189 (100), and 161 (86).

HRMS (APCI/TOF): Calcd for (M+H)⁺ (C₁₃H₁₀F₃O₆S)⁺: 351.0145. Found: 351.0134.

Methyl 4'-fluoro-4-methoxy-2'-[[(trifluoromethyl)sulfonyl]oxy]-[1,1'-biphenyl]-3-carboxylate (3-27g)



Yield: 0.2 mmol scale, 64 mg, 77%.

¹H NMR (CDCl₃, 500 MHz): δ 7.87 [d, $J = 2.4$ Hz, 1H, C(CO₂Me)CH], 7.54 [dd, $J = 8.7$, 2.4 Hz, 1H, C(OMe)CHCH], 7.45 [dd, $J = 8.6$, 6.1 (⁴J_{F-H}) Hz, 1H, C(F)CHCH], 7.18 [ddd, $J = 8.6$, 7.7 (³J_{F-H}), 2.5 Hz, 1H, C(F)CHCH], 7.15 (dd, $J = 8.4$ (³J_{F-H}), 2.5 Hz, 1H, C(F)CHC(OTf)], 7.10 [d, $J = 8.7$ Hz, 1H, C(OMe)CH], and 3.96 (s, 3H, CO₂CH₃), and 3.90 (s, 3H, ArOCH₃).

¹³C NMR (CDCl₃, 125 MHz): δ 166.3, 161.9 (d, ¹J_{F-C} = 251.8 Hz), 159.5, 146.7 (d, ³J_{F-C} = 10.7 Hz), 134.5, 132.9, 132.8 (d, ³J_{F-C} = 8.6 Hz), 130.6 (d, ⁴J_{F-C} = 3.8 Hz), 126.8, 120.4, 118.4 (q, ¹J_{CF3} = 320.5 Hz), 116.1 (d, ²J_{F-C} = 20.6 Hz), 112.4, 110.5 (d, ²J_{F-C} = 25.7 Hz), 56.4, and 52.4.

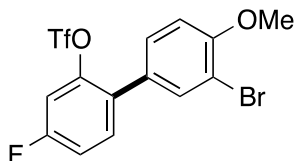
IR (neat): 2952 (w), 1730 (s), 1609 (m), 1489 (s), 1422 (s), 1190 (s), 1135 (s), and 832 (s) cm⁻¹.

TLC: $R_f = 0.2$ in 5:1 hexanes: EtOAc.

GCMS (5029017): $t_R = 12.49$ min, m/z 409 [(M+H)⁺, 93], 408 (M⁺, 100), 377 [(M-OMe)⁺, 40], 243 (36), 216 (75), and 201 (36).

HRMS (APCI/TOF): Calcd for (M+H)⁺ (C₁₆H₁₃F₄O₆S)⁺: 409.0363. Found: 409.0346.

3'-Bromo-4'-fluoro-4'-methoxy-[1,1'-biphenyl]-2-yl trifluoromethanesulfonate (3-27h)



Yield: 0.2 mmol scale, 69 mg, 81%.

¹H NMR (CDCl₃, 500 MHz): δ 7.62 [d, *J* = 2.3 Hz, 1H, C(Br)CH], 7.42 [dd, *J* = 8.6, 6.2 (⁴*J*_{F-H}) Hz, 1H, C(F)CHCH], 7.35 [dd, *J* = 8.5, 2.3 Hz, 1H, C(OMe)CHCH], 7.18 [ddd, *J* = 8.6, 7.6 (³*J*_{F-H}), 2.5 Hz, 1H, C(F)CHCH], 7.15 [dd, *J* = 8.3 (³*J*_{F-H}), 2.5 Hz, 1H, C(F)CH], 6.97 [d, *J* = 8.5 Hz, 1H, C(OMe)CH], and 3.95 (s, 3H, OCH₃).

¹³C NMR (CDCl₃, 125 MHz): δ 162.0 (d, ¹*J*_{F-C} = 254.3 Hz), 156.2, 146.6 (d, ³*J*_{F-C} = 10.3 Hz), 134.2, 132.8 (d, ³*J*_{F-C} = 8.5 Hz), 130.3 (d, ⁴*J*_{F-C} = 3.6 Hz), 129.8, 128.5, 118.6 (q, ¹*J*_{CF₃} = 320.6 Hz), 116.1 (d, ²*J*_{F-C} = 21.3 Hz), 112.0, 111.9, 110.6 (d, ²*J*_{F-C} = 25.7 Hz), and 56.5.

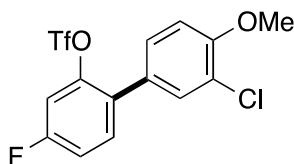
IR (neat): 2843 (w), 1602 (m), 2863 (m), 1466 (s), 1422 (s), 1206 (s), 1134 (s), 861 (m), and 597 (s) cm⁻¹.

TLC: R_f = 0.5 in 5:1 hexanes: EtOAc.

GCMS (5029017): t_R = 12.11 min, m/z 430 [(M+2)⁺, 23], 428 (M⁺, 23), 216 (100), and 201 (40).

HRMS (APCI/TOF): Calcd for (M+H)⁺ (C₁₄H₁₀BrF₄O₄S)⁺: 428.9414. Found: 428.9426.

3'-Chloro-4'-fluoro-4'-methoxy-[1,1'-biphenyl]-2-yl trifluoromethanesulfonate (3-27i)



Yield: 0.2 mmol scale, 55 mg, 72%.

¹H NMR (CDCl₃, 500 MHz): δ 7.45 [d, *J* = 2.3 Hz, 1H, C(Cl)CH], 7.42 [dd, *J* = 8.6, 6.2 (⁴*J*_{F-H}) Hz, 1H, C(F)CHCH], 7.30 [dd, *J* = 8.5, 2.3 Hz, 1H, C(OMe)CHCH], 7.18 [ddd, *J* = 8.6, 7.6 (³*J*_{F-H}), 2.5 Hz, 1H, C(F)CHCH], 7.14 [dd, *J* = 8.3 (³*J*_{F-H}), 2.5 Hz, 1H, C(F)CHC(OTf)], 7.00 [d, *J* = 8.5 Hz, 1H, C(OMe)CH], and 3.96 (s, 3H, OCH₃).

¹³C NMR (CDCl₃, 125 MHz): δ 162.0 (d, ¹*J*_{F-C} = 252.0 Hz), 155.4, 146.7 (d, ³*J*_{F-C} = 10.8

Hz), 132.7 (d, $^3J_{F-C} = 9.4$ Hz), 131.2, 130.5 (d, $^4J_{F-C} = 3.6$ Hz), 129.0, 128.0, 122.9, 118.5 (q, $^1J_{CF_3} = 320.7$ Hz), 116.1 (d, $^2J_{F-C} = 20.6$ Hz), 112.1, 110.5 (d, $^2J_{F-C} = 25.9$ Hz), and 56.4.

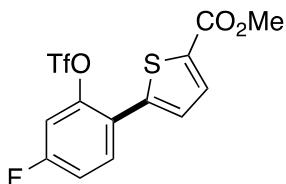
IR (neat): 2843 (w), 1604 (m), 1487 (m), 1221 (s), 861 (m), 738 (s), and 598 (s) cm^{-1} .

TLC: $R_f = 0.5$ in 5:1 hexanes: EtOAc.

GCMS (5029017): $t_R = 11.66$ min, m/z 386 [(M+2)⁺, 17], 384 (M⁺, 52), 251 (23), 235 [(M-OTf)⁺, 5], 216 (100), and 201 (35).

HRMS (APCI/TOF): Calcd for (M+H)⁺ (C₁₄H₁₀ClF₄O₄S)⁺: 384.9919. Found: 384.9927.

Methyl 5-[4-fluoro-2-[(trifluoromethyl)sulfonyl]oxy]phenyl]thiophene-2-carboxylate (3-27j)



Yield: 0.2 mmol scale, 64 mg, 83%.

¹H NMR (CDCl₃, 500 MHz): δ 7.79 [d, $J = 3.9$ Hz, 1H, SCCH or C(CO₂Me)CH], 7.60 (dd, $J = 8.2, 6.0$ ($^4J_{F-H}$) Hz, 1H, C(F)CHCH], 7.28 [d, $J = 3.9$ Hz, 1H, SCCH or C(CO₂Me)CH], 7.22-7.17 (m, 2H, Ar-H), and 3.91 (s, 3H, CO₂CH₃).

¹³C NMR (CDCl₃, 125 MHz): δ 162.5 (d, $^1J_{F-C} = 254.3$ Hz), 162.4, 146.6 (d, $^3J_{F-C} = 10.8$ Hz), 142.3, 134.8, 134.0, 132.8 (d, $^3J_{F-C} = 9.5$ Hz), 128.7, 124.0 (d, $^4J_{F-C} = 4.7$ Hz), 118.6 (q, $^1J_{CF_3} = 320.7$ Hz), 116.4 (d, $^2J_{F-C} = 20.7$ Hz), 111.0 (d, $^2J_{F-C} = 26.2$ Hz), and 52.6.

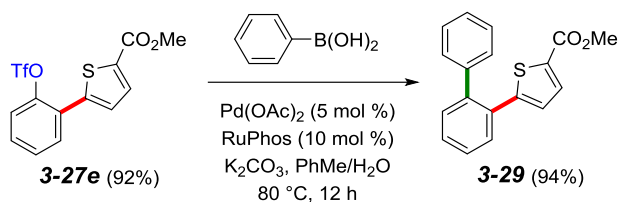
IR (neat): 3081 (w), 2955 (w), 1713 (s), 1425 (s), 1207 (s), 816 (s), 748 (s), and 596 (m) cm^{-1} .

TLC: $R_f = 0.5$ in 5:1 hexanes: EtOAc.

GCMS (5029017): $t_R = 11.74$ min, m/z 385 [(M+H)⁺, 39], 384 (M⁺, 100), 353 [(M-OMe)⁺, 8], 251 (42), and 192 (59).

HRMS (APCI/TOF): Calcd for (M+H)⁺ (C₁₃H₉F₄O₅S₂)⁺: 384.9822. Found: 384.9813.

D.13. Procedure for Palladium Catalyzed Suzuki Reaction to Synthesize Methyl 5-([1,1'-biphenyl]-2-yl)thiophene-2-carboxylate (3-29)



Pd(OAc)₂ (2.2 mg, 5 mol %), RuPhos (4.7 mg, 10 mol %), phenylboronic acid (37 mg, 0.3 mmol), and K₂CO₃ (55 mg, 0.4 mmol) were dissolved with toluene and water (3:1 V:V, 0.4 mL in total) in a 4 mL vial. Compound **27e** (0.2 mmol) was added into the reaction mixture. The septum on the vial was replaced by a screw cap with a Teflon liner. The reaction was stirred at 80 °C for 12 h. The volatiles were removed *in vacuo*, and the resulting mixture was dissolved with diethyl ether, filtered through a pad of silica gel, and concentrated *in vacuo* to afford the crude mixture, which was purified by MPLC (hexanes/EtOAc = 5:1, 7 mL/min, retention time 10 min) to give desired product **29** as a yellow solid (55 mg, 94%).

¹H NMR (CDCl₃, 500 MHz): δ 7.57-7.54 (m, 1H, Ar-*H*), 7.54 [d, *J* = 3.9 Hz, 1H, SC(CO-Me)CH], 7.46-7.39 (m, 3H, Ar-*H*), 7.33-7.29 (m, 3H, Ar-*H*), 7.25-7.22 (m, 2H, Ar-*H*), 6.61 (d, *J* = 3.9 Hz, 1H, SCCH), and 3.85 (s, 3H, CO₂CH₃).

¹³C NMR (CDCl₃, 125 MHz): δ 162.9, 150.7, 141.4, 141.0, 133.6, 132.8, 132.4, 131.1, 130.7, 129.7, 128.9, 128.4, 128.0, 127.9, 127.4, and 52.2.

IR (neat): 2950 (m), 1708 (s), 1686 (s), 1430 (m), 1257 (s), 1093 (s), 881 (s), and 699 (m) cm⁻¹.

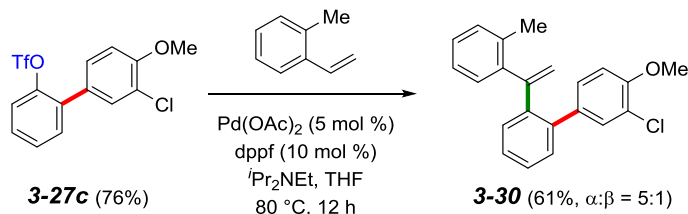
m.p. 71-73 °C.

TLC: R_f = 0.5 in 5:1 hexanes: EtOAc.

GCMS (5029017): t_R = 14.08 min, m/z 295 [(M+H)⁺, 27], 294 (M⁺, 100), 263 [(M-OMe)⁺, 7], 234 (42), and 202 (14).

HRMS (APCI/TOF): Calcd for (M+H)⁺ (C₁₈H₁₅O₂S)⁺: 295.0787. Found: 295.0791.

D.14. Procedure for Palladium Catalyzed Heck Reaction to Synthesize 3'-Chloro-4'-methoxy-2-(1-(*o*-tolyl)vinyl)-1,1'-biphenyl (30)



Pd(OAc)₂ (2.2 mg, 5 mol %), dppf (5.5 mg, 10 mol %), 2-methylstyrene (64 μ L, 0.5 mmol), and *i*Pr₂NEt (70 μ L, 0.4 mmol) were dissolved with THF (0.4 mL) with a 4 mL vial. Compound **27c** (0.2 mmol) was added into the reaction mixture. The septum on the vial was replaced by a screw cap with a Teflon liner. The reaction was stirred at 80 °C for 12 h. The volatiles were removed *in vacuo*, and the resulting mixture was dissolved with diethyl ether, filtered through a pad of silica gel, and concentrated *in vacuo* to afford the crude mixture ($\alpha:\beta = 5:1$), which was purified by MPLC (hexanes/EtOAc = 10:1, 5 mL/min, retention time 7 min) to give desired product **30** as a colorless liquid (41 mg, 61%).

¹H NMR (CDCl₃, 500 MHz): δ 7.45 (dd, $J = 7.2, 1.8$ Hz, 1H, Ar-*H*), 7.36 (ddd, $J = 7.4, 7.4, 1.6$ Hz, 1H, Ar-*H*), 7.33 (ddd, $J = 7.4, 7.4, 1.6$ Hz, 1H, Ar-*H*), 7.14 (dd, $J = 7.2, 1.7$ Hz, 1H, Ar-*H*), 7.05 [d, $J = 2.2$ Hz, 1H, C(Cl)CH], 6.97 (ddd, $J = 7.4, 7.4, 1.5$ Hz, 1H, Ar-*H*), 6.89 (app d, $J = 7.5$ Hz, 1H, Ar-*H*), 6.87 [dd, $J = 8.4, 2.2$ Hz, 1H, C(OMe)CHCH], 6.86 (app d, $J = 7.2$ Hz, 1H, Ar-*H*), 6.76 (dd, $J = 7.6, 1.4$ Hz, 1H, Ar-*H*), 6.66 [d, $J = 8.4$ Hz, 1H, C(OMe)CH], 5.52 (d, $J = 1.7$ Hz, 1H, C=CH_aH_b), 5.53 (d, $J = 1.7$ Hz, 1H, C=CH_aH_b), 3.84 (s, 3H, ArOCH₃), and 1.95 (s, 3H, ArCH₃).

¹³C NMR (CDCl₃, 125 MHz): δ 153.8, 150.1, 142.0, 141.3, 139.5, 135.6, 135.3, 130.9, 130.8, 130.4, 130.3, 130.1, 128.3, 127.7 (2), 127.0, 125.2, 121.6, 120.0, 111.5, 56.4, and 21.2.

IR (neat): 2953 (w), 1604 (m), 1506 (m), 1438 (m), 1249 (s), 1064 (s), and 729 (s) cm⁻¹.

TLC: R_f = 0.6 in 5:1 hexanes: EtOAc.

GCMS (5029017): t_R = 14.39 min, m/z 336 [(M+2)⁺, 37], 334 (M⁺, 100), 299 [(M-Cl)⁺, 69],

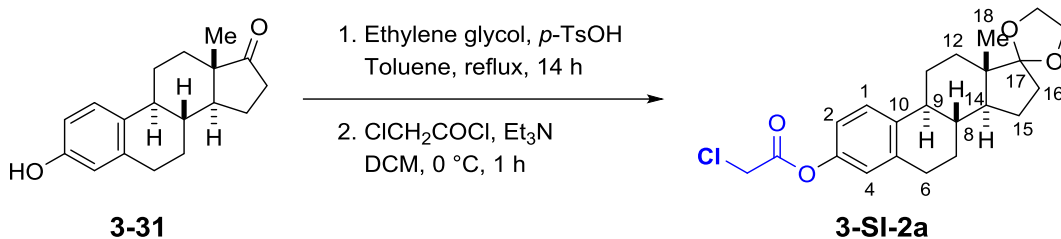
and 284 (24).

HRMS (APCI/TOF): Calcd for (M+H)⁺ (C₂₂H₂₀ClO)⁺: 335.1197. Found: 335.1082.

D.15. Procedure for Preparation of (8*R*,9*S*,13*S*,14*S*)-13-Methyl-

6,7,8,9,11,12,13,14,15,16-decahydrospiro[cyclopenta[*a*]phenanthrene-17,2'-

[1,3]dioxolan]-3-yl 2-chloroacetate (SI-2a)¹⁰



A round-bottom flask (100 mL) with a magnetic stir bar and a Dean-Stark apparatus was charged with estrone **3-31** (3.0 g, 11.0 mmol) and *p*-TsOH (96 mg, 0.55 mmol). Toluene (60 mL) and ethylene glycol (55 mmol) were added and the reaction mixture was heated at reflux for 14 h. The reaction was cooled to rt, and the solvent was removed *in vacuo*, ethyl acetate (30 mL) and brine (50 mL) were added. The mixture was extracted with ethyl acetate (3×50 mL), and the combined organic extract was washed with water (40 mL) and brine (40 mL), and dried over anhydrous sodium sulfate. The volatiles were removed *in vacuo* to afford the crude product, which was directly used for a subsequent reaction without further purification. The crude product (11 mmol) and Et₃N (2.8 mL, 20 mmol) were dissolved with CH₂Cl₂ (20 mL), the reaction mixture was cooled to 0 °C with an ice bath. Chloroacetyl chloride (1.0 mL, 13 mmol) was added into the reaction mixture slowly. The reaction mixture was stirred at 0 °C for 1 h before it was quenched with saturated aqueous ammonium chloride (50 mL). The mixture was separated and the aqueous phase was extracted with ethyl acetate (3×50 mL). The combined organic extracts were washed with water (50 mL) and brine (50 mL), and dried over anhydrous sodium

sulfate. The volatiles were removed *in vacuo*, and the crude mixture was purified by flash column (hexanes: EtOAc 3:1) to afford the ester **3-SI-2a** (3.27 g, 76% over two steps).

¹H NMR (CDCl₃, 500 MHz): δ 7.30 [d, *J* = 8.1 Hz, 1H, *H*(1)], 6.88 [dd, *J* = 8.1, 2.6 Hz, 1H, *H*(2)], 6.83 [d, *J* = 2.6 Hz, 1H, *H*(4)], 4.28 (s, 2H, CH₂Cl), 3.98-3.88 (m, 4H, OCH₂CH₂O), 2.88-2.84 (m, 2H, alkyl-*H*), 2.32 (dddd, *J* = 13.2, 4.2, 4.2, 2.7 Hz, 1H, alkyl-*H*), 2.26 (ddd, *J* = 10.6, 10.6, 4.1 Hz, 1H, alkyl-*H*), 2.03 (ddd, *J* = 14.0, 11.2, 3.1 Hz, 1H, alkyl-*H*), 1.93-1.74 (m, 4H, alkyl-*H*), 1.63 (ddd, *J* = 12.1, 10.8, 7.0 Hz, 1H, alkyl-*H*), 1.55-1.31 (m, 5H, alkyl-*H*), and 0.88 [s, 3H, CH(18)].

¹³C NMR (CDCl₃, 125 MHz): δ 166.4, 148.2, 138.9, 138.8, 126.8, 121.2, 119.6, 118.2, 65.5, 64.8, 49.6, 46.3, 44.0, 41.1, 38.8, 34.4, 30.9, 29.7, 26.9, 26.2, 22.6, and 14.5.

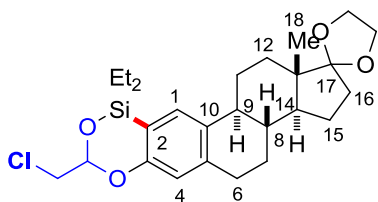
IR (neat): 2935 (m), 2864 (m), 1775 (s), 1724 (m), 1493 (m), 1304 (m), 1190 (s), 1042 (m), and 804 (m) cm⁻¹.

m.p. 76-78 °C.

TLC: R_f = 0.5 in 3:1 hexanes: EtOAc.

HRMS (APCI/TOF): Calcd for (M+H)⁺ (C₂₂H₂₈ClO₄)⁺: 391.1671. Found: 391.1659.

(3a*S*,3b*R*,11b*S*,13a*S*)-8-(Chloromethyl)-10,10-diethyl-13a-methyl-3,3a,3b,4,5,10,11b,12,13,13a-decahydro-2*H*-spiro[cyclopenta[7,8]phenanthro[3,2-*c*][1,5,2]dioxasiline-1,2'-[1,3]dioxolane] (3-32b)



Yield: 0.2 mmol scale, 84 mg, 88% (dr: 1:1).

¹H NMR (CDCl₃, 500 MHz): δ 7.19 [s, 1H, *H*(1) or *H*(4)], 7.18 [s, 1H, *H*(1) or *H*(4)], 6.72, [s, 1H, *H*(1) or *H*(4)], 6.71 [s, 1H, *H*(1) or *H*(4)], 5.33 (dd, *J* = 5.3, 4.0 Hz, 1H, OCHCH₂Cl), 5.32 (dd, *J* = 5.3, 4.0 Hz, 1H, OCHCH₂Cl), 3.97-3.88 (m, 8H, OCH₂CH₂O), 3.69 (dd, *J* = 11.4, 5.3 Hz, 2H, ClCH_aH_b), 3.64 (dd, *J* = 11.4, 4.0 Hz, 2H, ClCH_aH_b), 2.86-2.82 (m, 4H, alkyl-*H*), 2.35-2.28 (m, 2H, alkyl-*H*), 2.25-2.19 (m, 2H, alkyl-*H*), 2.06-1.99 (m, 2H, alkyl-*H*), 1.91-1.73 (m, 8H, alkyl-*H*), 1.67-1.60 (m, 2H, alkyl-*H*), 1.55-1.32 (m, 10H, alkyl-*H*), 1.08 [t, *J* = 7.8, 3H, SiCH₂CH₃], 1.06 [t, *J* = 7.8, 3H, SiCH₂CH₃], and 0.94-0.70 [m, 20H,

Si(CH₂CH₃)₂, SiCH₂CH₃ and CH(18)₃].

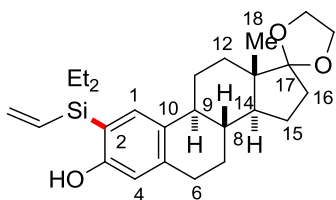
¹³C NMR (CDCl₃, 125 MHz): δ 161.3 (2), 141.2 (2), 135.1, 135.0, 130.1, 130.0, 119.6 (2), 117.7, 117.6, 116.42, 116.37, 96.9, 96.8, 65.4 (2), 64.7 (2), 49.6 (2), 46.32, 46.26, 43.9, 43.7, 39.10, 39.07, 34.4 (2), 30.9 (2), 30.8 (2), 30.0, 29.9, 27.0, 26.9, 26.4, 26.2, 22.6 (2), 14.6, 14.5, 7.04, 6.92, 6.8, 6.62, 6.56, 6.50, 6.43, and 6.39.

IR (neat): 2957 (w), 1606 (w), 1474 (m), 1238 (m), 1116 (w), 1077 (w), 1041 (w), 732 (s), and 703 (s) cm⁻¹.

TLC: R_f = 0.5 in 5:1 hexanes: EtOAc.

HRMS (APCI/TOF): Calcd for (M+H)⁺ (C₂₆H₃₈ClO₄Si)⁺: 477.2222. Found: 477.2201.

(8R,9S,13S,14S)-2-(Diethyl(vinyl)silyl)-13-methyl-6,7,8,9,11,12,13,14,15,16-decahydrospiro[cyclopenta[a]phenanthrene-17,2'-[1,3]dioxolan]-3-ol (3-33)



Yield: 0.2 mmol scale, 74 mg, 87%.

¹H NMR (CDCl₃, 500 MHz): δ 7.25 [s, 1H, H(1) or H(4)], 6.49 [s, 1H, H(4) or H(1)], 6.40 (dd, J = 20.5, 14.7 Hz, 1H, SiCH=CH₂), 6.22 (dd, J = 14.7, 3.8 Hz, 1H, SiCH=CH_{cis}H_{trans}), 5.94 (dd, J = 20.5, 3.8 Hz, 1H, SiCH=CH_{cis}H_{trans}), 5.13 (s, 1H, ArOH), 3.98-3.89 (m, 4H, OCH₂CH₂O), 2.83-2.78 (m, 2H, alkyl-H), 2.33 (dddd, J = 13.2, 4.2, 4.2, 2.7 Hz, 1H, alkyl-H), 2.23 (ddd, J = 11.3, 11.3, 4.3 Hz, 1H, alkyl-H), 2.03 (ddd, J = 14.4, 11.9, 3.1 Hz, 1H, alkyl-H), 1.90-1.74 (m, 4H, alkyl-H), 1.63 (ddd, J = 12.3, 10.7, 7.2 Hz, 1H, alkyl-H), 1.54 (ddd, J = 12.5, 3.9, 2.7 Hz, 1H, alkyl-H), 1.48-1.31 (m, 4H, alkyl-H-H), 1.01-0.97 [(m, 6H, Si(CH₂CH₃)₂], 0.94-0.88 [(m, 4H, Si(CH₂CH₃)₂], and 0.88 [s, 3H, CH(18)₃].

¹³C NMR (CDCl₃, 125 MHz): δ 158.8, 140.4, 136.5, 135.2, 133.0, 132.4, 119.6, 117.6, 115.2, 65.3, 64.7, 49.4, 46.3, 43.7, 39.2, 34.3, 30.8, 29.7, 27.0, 26.2, 22.4, 14.4, 7.5 (2), 4.01, and 3.96.

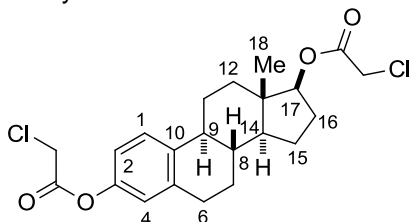
IR (neat): 3853 (br, w), 2938 (m), 1601 (m), 1393 (m), 1264 (m), 1180 (m), 1041 (m), 952 (m), 733 (s), and 703 (s) cm⁻¹.

TLC: R_f = 0.5 in 5:1 hexanes: EtOAc.

HRMS (APCI/TOF): Calcd for (M+H)⁺ (C₂₆H₃₉O₃Si)⁺: 477.2222. Found: 477.2201.

(8R,9S,13S,14S)-13-methyl-7,8,9,11,12,13,14,15,16,17-decahydro-6H-cyclopenta[a]phenanthrene-3,17-diyl bis(2-chloroacetate) (3-SI-2b)

For the procedure, see page SI-67, double the amount of chloroacetyl chloride and triethylamine.



Yield: 5 mmol scale, 1.4 g, 84%.

¹H NMR (CDCl₃, 500 MHz): δ 7.29 [d, *J* = 8.3 Hz, 1H, *H*(1)], 6.88 [dd, *J* = 8.1, 2.6 Hz, 1H, *H*(2)], 6.83 [d, *J* = 2.6 Hz, 1H, *H*(4)], 4.78 [dd, *J* = 9.2, 7.8 Hz, 1H, C(17)*H*], 4.28 (s, 2H, CH₂Cl), 4.07 (s, 2H, CH₂Cl), 2.89-2.85 (m, 2H, alkyl-*H*), 2.33-2.21 (m, 3H, alkyl-*H*), 1.93-1.87 (m, 2H, alkyl-*H*), 1.77 (dddd, *J* = 12.4, 9.6, 7.0, 3.2 Hz, 1H, alkyl-*H*), 1.61 (dddd, *J* = 13.7, 11.8, 7.8, 3.2 Hz, 1H, alkyl-*H*), 1.54-1.25 (m, 6H, alkyl-*H*), and 0.85 [s, 3H, CH(18)₃].

¹³C NMR (CDCl₃, 125 MHz): δ 167.5, 166.2, 148.2, 138.5, 138.4, 126.7, 121.1, 118.2, 84.6, 49.8, 44.0, 43.2, 41.2, 41.0, 38.2, 36.8, 29.6, 27.5, 27.0, 26.0, 23.3, and 12.1.

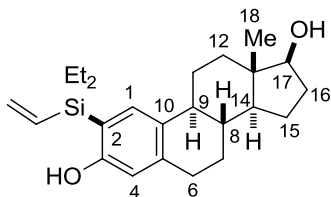
IR (neat): 2955 (m), 2858 (w), 1773 (m), 1756 (s), 1494 (m), 1308 (s), 1192 (s), 1032 (m), and 798 (m) cm⁻¹.

m.p. 113-115 °C.

TLC: R_f = 0.6 in 3:1 hexanes: EtOAc.

HRMS (APCI/TOF): Calcd for (M+H)⁺ (C₂₂H₂₇Cl₂O₄)⁺: 425.1281. Found: 425.1268.

(8R,9S,13S,14S,17S)-2-(diethyl(vinyl)silyl)-13-methyl-7,8,9,11,12,13,14,15,16,17-decahydro-6H-cyclopenta[a]phenanthrene-3,17-diol (3-37)



Yield: 0.2 mmol scale, 61 mg, 80%.

¹H NMR (CDCl₃, 500 MHz): δ 7.24 [s, 1H, *H*(1) or *H*(4)], 6.59 [s, 1H, *H*(4) or *H*(1)], 6.40 (dd, *J* = 14.8, 20.5 Hz, 1H, SiCH=CH₂), 6.22 (dd, *J* = 14.8, 3.8 Hz, 1H, SiCH=CH_{cis}H_{trans}), 5.94 (dd, *J* = 20.5, 3.8 Hz, 1H, SiCH=CH_{cis}H_{trans}), 5.15 [br s, 1H, C(17)(OH)], 4.1 (s, 1H, ArOH), 3.74 [dd, *J* = 8.3, 8.3, 1H, *H*(17)], 2.87-2.76 (m, 2H, alkyl-*H*), 2.33 (dddd, *J* = 13.4, 4.0, 4.0, 2.6 Hz, 1H, alkyl-*H*), 2.18 (ddd, *J* = 11.3, 11.3, 4.0 Hz, 1H, alkyl-*H*), 2.12 (dddd, *J* = 13.3, 9.2, 9.2, 5.7 Hz, 1H, alkyl-*H*), 1.95 (ddd, *J* = 12.5, 3.8, 2.7 Hz, 1H, alkyl-*H*), 1.85 (dddd, *J* = 12.7, 6.0, 2.6, 2.6 Hz, 1H, alkyl-*H*), 1.70 (dddd, *J* = 12.2, 9.4, 7.1, 3.2 Hz, 1H, alkyl-*H*), 1.53-1.25 (m, 6H, alkyl-*H*), 1.19 (ddd, *J* = 12.4, 10.9, 7.2 Hz, 1H, alkyl-*H*), 1.02-0.97 [m, 6H, Si(CH₂CH₃)₂], 0.93-0.88 [m, 4H, Si(CH₂CH₃)₂], and 0.78 [s, 3H, C(18)H₃].

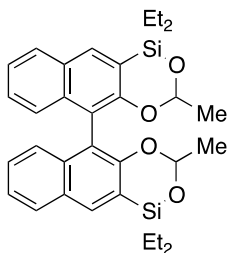
¹³C NMR (CDCl₃, 125 MHz): δ 158.9, 140.4, 136.5, 135.4, 133.1, 132.4, 117.8, 115.4, 82.2, 50.2, 44.2, 43.5, 39.1, 36.9, 30.8, 39.8, 27.3, 26.5, 23.3, 11.3, 7.6 (2), 4.12, and 4.05.

IR (neat): 3320 (br, w), 2953 (w), 1601 (w), 1393 (w), 1264 (m), 1011 (m), 732 (s), and 704 (s) cm⁻¹.

TLC: R_f = 0.2 in 5:1 hexanes: EtOAc.

HRMS (APCI/TOF): Calcd for (M+H)⁺ (C₂₄H₃₇O₂Si)⁺: 385.2557. Found: 385.2536.

1,1,1',1'-Tetraethyl-3,3'-dimethyl-1*H*,1'*H*-5,5'-binaphtho[2,3-*c*][1,5,2]dioxasiline (3-39)



Yield: 1 mmol scale, 500 mg, 92%. 4 sets of diastereomers = 1.56:1.56:1.0:1.56.

¹H NMR (CDCl₃, 500 MHz): δ 8.01-7.98 (m, 2H, Ar-*H*), 7.89 (d, *J* = 8.2 Hz, 1H, Ar-*H*), 7.88 (d, *J* = 8.2 Hz, 1H, Ar-*H*), 7.36 (dd, *J* = 8.0, 8.0 Hz, 1H, Ar-*H*), 7.35 (dd, *J* = 8.0, 8.0 Hz, 1H, Ar-*H*), 7.30-7.21 (m, 3H, Ar-*H*), 7.13 (dd, *J* = 8.3, 8.3 Hz, 1H, Ar-*H*), 5.53 (q, *J* = 5.0 Hz, 0.55 H, OCHMe), 5.47 (q, *J* = 5.0 Hz, 0.55 H, OCHMe), 5.40 (q, *J* = 5.0 Hz, 0.35 H, OCHMe), 5.32 (q, *J* = 5.0 Hz, 0.55 H, OCHMe), 1.37 (d, *J* = 5.0 Hz, 1.65H, OCHCH₃), 1.33 (d, *J* = 5.0 Hz, 1.65H, OCHCH₃), 1.19 (d, *J* = 5.0 Hz, 1.65H, OCHCH₃), 1.19-1.14

(m, 6H, SiCH₂CH₃), 1.12 (d, *J* = 5.0 Hz, 1.05H, OCHCH₃), and 1.09-0.84 [m, 14H, SiCH₂CH₃ and Si(CH₂CH₃)₂].

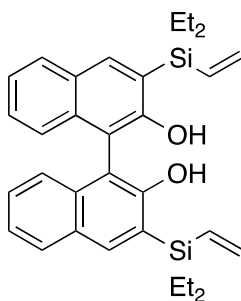
¹³C NMR (CDCl₃, 125 MHz): δ 159.3, 158.19, 158.09, 157.92, 135.39, 135.33, 135.01, 134.86, 134.76, 134.73, 129.84, 129.80, 129.76, 129.72, 128.35, 128.27, 127.13, 127.05, 126.81, 126.78, 126.4, 126.05, 126.01, 125.5, 124.13, 124.05, 123.99, 123.95, 122.7, 122.4, 121.9, 121.6, 119.21, 119.15, 119.04, 118.97, 97.6, 96.84, 96.68, 96.3, 23.84, 23.75, 23.59, 23.48, 7.3, 7.14, 7.12, 7.10, 7.08, 6.99, 6.97, 6.91, 6.60, 6.55, 6.52, and 6.51.

IR (neat): 2958 (m), 1619 (w), 1586 (w), 1391 (m), 1232 (m), 1088 (s), 1043 (m), 931 (s), 734 (s), and 702 (s) cm⁻¹.

TLC: R_f = 0.4 in 20:1 hexanes: EtOAc.

HRMS (APCI/TOF): Calcd for (M+H)⁺ (C₃₂H₃₉O₄Si₂)⁺: 543.2381. Found: 543.2360.

3,3'-Bis[diethyl(vinyl)silyl]-[1,1'-binaphthalene]-2,2'-diol (3-40) (Racemic)



Yield: 0.2 mmol scale, 87 mg, 85%.

¹H NMR (CDCl₃, 500 MHz): δ 8.10 (s, 2H, Binol *H*₄ and *H*_{4'}), 7.88 (d, *J* = 8.0 Hz, 2H, Binol *H*₅, *H*_{5'} or *H*₈, *H*_{8'}), 7.35 (ddd, *J* = 8.0, 6.7, 1.2 Hz, 2H, Binol *H*₆, *H*_{6'} or *H*₇, *H*_{7'}), 7.29 (ddd, *J* = 8.0, 6.7, 1.2 Hz, 2H, Binol *H*₆, *H*_{6'} or *H*₇, *H*_{7'}), 7.09 (d, *J* = 8.0 Hz, 2H, Binol *H*₅, *H*_{5'} or *H*₈, *H*_{8'}), 6.46 (dd, *J* = 14.8, 20.5 Hz, 2H, SiCH=CH₂), 6.19 (dd, *J* = 14.8, 3.7 Hz, 2H, SiCH=CH_{cis}H_{trans}), 5.90 (dd, *J* = 20.5, 3.7 Hz, 2H, SiCH=CH_{cis}H_{trans}), 5.24 (s, 2H, ArOH), and 1.02 [app s, 20H, Si_a(CH₂CH₃)₂ and Si_b(CH₂CH₃)₂].

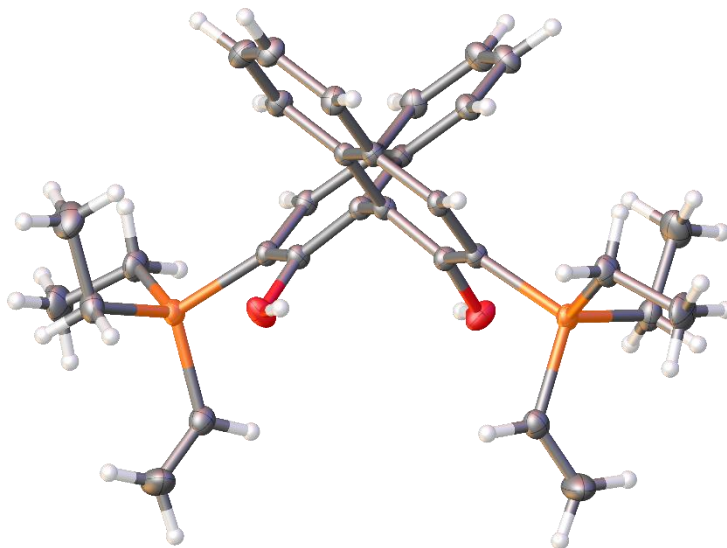
¹³C NMR (CDCl₃, 125 MHz): δ 157.1, 139.7, 135.8, 134.5, 133.8, 129.5, 128.8, 127.9, 125.7, 124.1, 123.9, 109.8, 7.9, 7.8, 4.2, and 4.1.

IR (neat): 3485 (br, w), 3422 (br, w), 2955 (m), 1573 (m), 1444 (m), 1207 (s), 1129 (s), 1007 (s), and 736 (s) cm⁻¹.

TLC: R_f = 0.3 in 20:1 hexanes: EtOAc.

HRMS (APCI /TOF): Calcd for (M+H)⁺ (C₃₂H₃₉O₂Si₂)⁺: 511.2483. Found: 511.2467.

Table SI-2 Crystal data and structure refinement for 3,3'-bis(diethyl(vinyl)silyl)-[1,1'-binaphthalene]-2,2'-diol (3-40).



Empirical formula	C ₃₂ H ₃₈ O ₂ Si ₂
Formula weight	510.80
Temperature/K	102(2)
Crystal system	monoclinic
Space group	C2/c
a/Å	26.3946(14)
b/Å	11.3169(6)
c/Å	21.4863(12)
α/°	90
β/°	115.3270(10)
γ/°	90
Volume/Å ³	5801.2(5)
Z	8
ρ _{calc} /cm ³	1.170
μ/mm ⁻¹	0.148
F(000)	2192.0
Crystal size/mm ³	0.598 × 0.354 × 0.219
Radiation	MoKα (λ = 0.71073)

2 θ range for data collection/ $^{\circ}$ 5.866 to 66.284
 Index ranges $-40 \leq h \leq 40, -17 \leq k \leq 17, -33 \leq l \leq 32$
 Reflections collected 51174
 Independent reflections 11030 [$R_{\text{int}} = 0.0244, R_{\text{sigma}} = 0.0192$]
 Data/restraints/parameters 11030/0/331
 Goodness-of-fit on F^2 1.037
 Final R indexes [$|I| \geq 2\sigma(I)$] $R_1 = 0.0433, wR_2 = 0.1609$
 Final R indexes [all data] $R_1 = 0.0517, wR_2 = 0.1751$
 Largest diff. peak/hole / $e \text{ \AA}^{-3}$ 1.06/-0.53

Fractional Atomic Coordinates ($\times 10^4$) and Equivalent Isotropic Displacement Parameters ($\text{\AA}^2 \times 10^3$) for 3,3'-bis(diethyl(vinyl)silyl)-[1,1'-binaphthalene]-2,2'-diol (39). U_{eq} is defined as 1/3 of the trace of the orthogonalised U_{ij} tensor.

Atom	x	y	z	U(eq)
Si1	6303.1(2)	2288.6(2)	6755.1(2)	16.38(8)
O1	5161.8(3)	2174.6(7)	6762.9(4)	23.13(16)
C1	6067.9(4)	1350.2(8)	7309.2(5)	14.93(16)
C2	6432.2(4)	600.8(8)	7804.1(5)	15.16(16)
C3	6262.6(3)	-145.2(8)	8212.8(4)	14.45(15)
C4	6648.3(4)	-891.9(9)	8726.0(5)	18.70(17)
C5	6473.8(4)	-1641.5(9)	9099.0(5)	21.76(19)
C6	5902.9(4)	-1671.6(9)	8970.6(5)	20.62(18)
C7	5516.9(4)	-955.2(9)	8475.3(5)	17.13(17)
C8	5687.3(3)	-164.4(8)	8086.9(4)	13.53(15)
C9	5304.0(3)	607.0(8)	7576.5(4)	13.60(15)
C10	5501.3(4)	1359.2(8)	7225.0(5)	15.32(16)
C11	7018.6(5)	1762.3(10)	6899.5(6)	26.3(2)
C12	7252.9(6)	2372.2(14)	6444.9(9)	42.3(4)
C13	6337.4(6)	3885.3(10)	7000.3(7)	29.2(2)
C14	6773.8(8)	4399.4(15)	7501.4(10)	48.7(4)
C15	5803.7(5)	2154.0(13)	5830.0(6)	31.5(3)
C16	5641.6(10)	895.3(17)	5574.8(8)	56.7(5)
Si2	3715.4(2)	3760.1(2)	5336.9(2)	17.99(8)
O2	4252.6(4)	3775.5(7)	6893.8(4)	23.03(16)
C17	4337.5(4)	4637.3(8)	5943.5(4)	16.20(16)
C18	4623.8(4)	5386.3(9)	5700.2(4)	16.38(16)
C19	5077.6(4)	6099.4(8)	6143.8(4)	15.44(16)
C20	5369.0(4)	6854.5(9)	5880.4(5)	20.19(18)
C21	5802.7(5)	7549(1)	6312.5(6)	23.8(2)
C22	5961.5(5)	7518.2(10)	7030.3(6)	23.3(2)
C23	5679.7(4)	6810.7(9)	7300.5(5)	19.12(17)
C24	5230.7(4)	6082.3(8)	6864.8(4)	14.75(16)

C25	4935.3(4)	5314.3(8)	7126.1(4)	15.17(16)
C26	4520.0(4)	4592.0(8)	6670.9(5)	16.28(16)
C27	3482.9(5)	4439.0(11)	4459.5(5)	25.3(2)
C28	2973.1(5)	3859.7(13)	3909.2(6)	34.4(3)
C29	3927.0(5)	2195.2(10)	5310.6(5)	23.2(2)
C30	3619.9(7)	1289.9(11)	5313.8(9)	41.2(3)
C31	3119.5(5)	3816.5(11)	5591.8(6)	26.3(2)
C32	2939.7(6)	5073.7(14)	5671.8(8)	38.8(3)

Anisotropic Displacement Parameters ($\text{\AA}^2 \times 10^3$) for 3,3'-bis(diethyl(vinyl)silyl)-[1,1'-binaphthalene]-2,2'-diol (39).. The Anisotropic displacement factor exponent takes the form: $-2\pi^2[h^2a^{*2}U_{11}+2hka^*b^*U_{12}+\dots]$.

Atom	U_{11}	U_{22}	U_{33}	U_{23}	U_{13}	U_{12}
Si1	13.53(13)	19.43(14)	18.08(14)	4.44(8)	8.57(10)	1.37(8)
O1	13.6(3)	27.5(4)	29.3(4)	14.0(3)	10.2(3)	6.4(3)
C1	12.2(3)	18.0(4)	15.4(4)	1.8(3)	6.6(3)	0.6(3)
C2	10.6(3)	19.2(4)	15.6(4)	1.0(3)	5.5(3)	0.5(3)
C3	11.7(3)	17.3(4)	13.2(3)	0.9(3)	4.3(3)	1.0(3)
C4	15.0(4)	20.8(4)	17.6(4)	3.3(3)	4.4(3)	2.7(3)
C5	20.5(4)	21.9(4)	19.3(4)	5.8(3)	5.1(3)	2.3(3)
C6	22.0(4)	20.3(4)	18.1(4)	3.0(3)	7.2(3)	-3.6(3)
C7	16.4(4)	18.9(4)	16.5(4)	0.2(3)	7.4(3)	-2.9(3)
C8	12.0(3)	15.3(4)	12.7(3)	-1.0(3)	4.7(3)	-0.8(3)
C9	10.1(3)	16.4(4)	14.7(3)	0.0(3)	5.7(3)	0.0(3)
C10	12.1(3)	17.4(4)	16.9(4)	2.9(3)	6.5(3)	2.3(3)
C11	21.8(5)	28.3(5)	36.5(6)	12.0(4)	19.7(4)	6.6(4)
C12	39.9(7)	43.4(7)	64(1)	22.1(7)	41.9(7)	14.0(6)
C13	36.7(6)	21.3(5)	39.2(6)	5.2(4)	25.5(5)	3.5(4)
C14	59.8(10)	32.4(7)	62.9(10)	-16.4(7)	34.7(9)	-11.9(7)
C15	27.0(5)	45.6(7)	18.9(5)	7.0(4)	6.8(4)	-7.8(5)
C16	81.1(13)	56.2(10)	26.0(6)	-8.9(6)	16.4(7)	-35.8(10)
Si2	15.11(13)	21.31(15)	13.71(13)	-1.51(8)	2.48(10)	-0.22(9)
O2	26.6(4)	27.0(4)	14.5(3)	0.2(2)	7.9(3)	-9.2(3)
C17	15.9(4)	18.8(4)	11.6(3)	0.0(3)	3.6(3)	0.7(3)
C18	16.2(4)	20.4(4)	11.3(3)	0.3(3)	4.6(3)	1.8(3)
C19	15.9(4)	17.3(4)	13.2(3)	0.7(3)	6.4(3)	2.3(3)
C20	20.5(4)	25.6(5)	16.3(4)	1.6(3)	9.7(3)	-1.3(3)
C21	24.7(5)	26.3(5)	23.5(5)	-0.9(4)	13.2(4)	-5.5(4)
C22	23.7(5)	24.4(5)	23.0(5)	-5.3(3)	11.2(4)	-5.8(4)
C23	20.6(4)	20.9(4)	15.5(4)	-4.1(3)	7.5(3)	-2.6(3)
C24	15.9(4)	15.9(4)	12.3(3)	-0.7(3)	5.9(3)	1.4(3)
C25	17.2(4)	16.8(4)	10.6(3)	0.1(3)	5.0(3)	0.7(3)
C26	17.2(4)	17.8(4)	12.7(3)	0.9(3)	5.2(3)	-0.7(3)
C27	21.4(4)	31.2(5)	16.1(4)	1.0(4)	1.3(3)	1.5(4)

C28	24.5(5)	43.9(7)	21.0(5)	2.3(4)	-3.5(4)	-2.4(5)
C29	21.6(4)	25.9(5)	19.2(4)	-1.6(3)	6.1(3)	1.6(4)
C30	35.7(7)	22.8(6)	64.2(10)	7.3(6)	20.6(7)	1.0(5)
C31	18.5(4)	32.0(6)	27.3(5)	-5.9(4)	9.0(4)	-2.1(4)
C32	30.0(6)	42.4(7)	43.6(7)	-10.8(6)	15.5(5)	6.5(5)

Bond Lengths for 3,3'-bis(diethyl(vinyl)silyl)-[1,1'-binaphthalene]-2,2'-diol (39).

Atom	Atom	Length/Å	Atom	Atom	Length/Å
Si1	C15	1.8629(12)	Si2	C29	1.8650(11)
Si1	C13	1.8735(12)	Si2	C31	1.8747(12)
Si1	C11	1.8754(11)	Si2	C27	1.8791(11)
Si1	C1	1.8874(9)	Si2	C17	1.8840(9)
O1	C10	1.3708(11)	O2	C26	1.3677(12)
C1	C2	1.3783(12)	C17	C18	1.3787(13)
C1	C10	1.4277(12)	C17	C26	1.4259(12)
C2	C3	1.4213(12)	C18	C19	1.4205(13)
C3	C4	1.4163(12)	C19	C20	1.4192(13)
C3	C8	1.4242(12)	C19	C24	1.4241(12)
C4	C5	1.3748(14)	C20	C21	1.3715(15)
C5	C6	1.4113(14)	C21	C22	1.4152(15)
C6	C7	1.3786(14)	C22	C23	1.3787(14)
C7	C8	1.4215(12)	C23	C24	1.4182(13)
C8	C9	1.4279(12)	C24	C25	1.4328(13)
C9	C10	1.3796(12)	C25	C26	1.3816(13)
C9	C9 ¹	1.4938(16)	C25	C25 ¹	1.4929(17)
C11	C12	1.5265(16)	C27	C28	1.5090(16)
C13	C14	1.328(2)	C29	C30	1.3081(18)
C15	C16	1.521(2)	C31	C32	1.5325(18)

¹1-X,+Y,3/2-Z

Bond Angles for 3,3'-bis(diethyl(vinyl)silyl)-[1,1'-binaphthalene]-2,2'-diol (39).

Atom	Atom	Atom	Angle/°	Atom	Atom	Atom	Angle/°
C15	Si1	C13	107.82(6)	C29	Si2	C31	109.92(5)
C15	Si1	C11	110.69(6)	C29	Si2	C27	109.35(5)
C13	Si1	C11	109.62(6)	C31	Si2	C27	108.93(5)
C15	Si1	C1	110.71(5)	C29	Si2	C17	109.73(5)
C13	Si1	C1	110.78(5)	C31	Si2	C17	111.82(5)
C11	Si1	C1	107.25(4)	C27	Si2	C17	107.01(5)
C2	C1	C10	116.70(8)	C18	C17	C26	117.05(8)
C2	C1	Si1	121.59(7)	C18	C17	Si2	121.24(7)
C10	C1	Si1	121.69(7)	C26	C17	Si2	121.68(7)
C1	C2	C3	122.83(8)	C17	C18	C19	122.45(8)

C4	C3	C2	121.60(8)	C20	C19	C18	121.31(8)
C4	C3	C8	119.45(8)	C20	C19	C24	119.48(9)
C2	C3	C8	118.92(8)	C18	C19	C24	119.18(8)
C5	C4	C3	120.90(9)	C21	C20	C19	120.86(9)
C4	C5	C6	119.80(9)	C20	C21	C22	119.73(9)
C7	C6	C5	120.76(9)	C23	C22	C21	120.77(10)
C6	C7	C8	120.56(9)	C22	C23	C24	120.58(9)
C7	C8	C3	118.52(8)	C23	C24	C19	118.56(8)
C7	C8	C9	122.52(8)	C23	C24	C25	122.36(8)
C3	C8	C9	118.96(8)	C19	C24	C25	119.07(8)
C10	C9	C8	119.23(8)	C26	C25	C24	118.78(8)
C10	C9	C9 ¹	120.07(8)	C26	C25	C25 ¹	120.60(8)
C8	C9	C9 ¹	120.70(7)	C24	C25	C25 ¹	120.61(8)
O1	C10	C9	121.95(8)	O2	C26	C25	121.58(8)
O1	C10	C1	114.92(8)	O2	C26	C17	115.16(8)
C9	C10	C1	123.13(8)	C25	C26	C17	123.26(8)
C12	C11	Si1	113.93(8)	C28	C27	Si2	114.05(9)
C14	C13	Si1	124.84(12)	C30	C29	Si2	123.32(10)
C16	C15	Si1	115.02(10)	C32	C31	Si2	113.78(9)

¹1-X,+Y,3/2-Z

Hydrogen Atom Coordinates ($\text{\AA}\times 10^4$) and Isotropic Displacement Parameters ($\text{\AA}^2\times 10^3$) for 3,3'-bis(diethyl(vinyl)silyl)-[1,1'-binaphthalene]-2,2'-diol (39).

Atom	x	y	z	U(eq)
H1	4830	2078	6708	35
H2A	6813	582	7875	18
H4	7033	-874	8814	22
H5	6737	-2138	9442	26
H6	5783	-2192	9229	25
H7	5134	-990	8393	21
H11A	7279	1895	7388	32
H11B	7002	901	6813	32
H12A	7028	2153	5963	63
H12B	7642	2125	6585	63
H12C	7239	3231	6495	63
H13	6019	4362	6747	35
H14A	7100	3951	7766	58
H14B	6760	5216	7596	58
H15A	5459	2597	5753	38
H15B	5973	2534	5549	38
H16A	5979	447	5643	85
H16B	5385	907	5084	85

H16C 5456	520	5833	85
H2 4366	3836	7322	35
H18 4514	5427	5218	20
H20 5262	6879	5399	24
H21 5996	8049	6131	29
H22 6266	7990	7330	28
H23 5787	6811	7783	23
H27A 3400	5285	4487	30
H27B 3796	4393	4322	30
H28A 3057	3031	3860	52
H28B 2871	4272	3471	52
H28C 2660	3900	4040	52
H29 4275	2048	5294	28
H30A 3270	1413	5330	49
H30B 3747	509	5300	49
H31A 2794	3397	5240	32
H31B 3231	3391	6033	32
H32A 3250	5476	6045	58
H32B 2615	5039	5780	58
H32C 2839	5510	5241	58

Apendix E

Experimental Procedures for Chapter 4

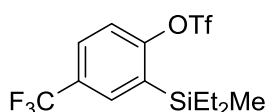
E.1. 4.2. General procedure for preparation of arylsilyl triflates from phenyl acetates (4-5)

(i) $[\text{Ir}(\text{coe})_2\text{Cl}]_2$ (0.9 mg, 0.1 mol %) and aryl acetates **4-1** (1 mmol) were added to a flame-dried, nitrogen-purged septum-capped vial. The mixture was dissolved with THF (0.3 mL, 3.3 M), and diethylsilane (0.26 mL, 2 mmol) was added to the mixture. The septum on the vial was replaced by a screw cap with a Teflon liner under a N_2 atmosphere [note: diethylsilane (bp 56 °C and density 0.686 g/mL) is volatile]. The reaction mixture was stirred for 3–12 h at 60 °C. Volatiles were removed *in vacuo* to afford silyl acetals, which were directly used for subsequent reactions without further purification. (ii) $[\text{Rh}(\text{nbd})\text{Cl}]_2$ (1.8 mg, 0.4 mol %), *tris*(4-methoxyphenyl)phosphine (8.4 mg, 2.4 mol %), norbornene (188 mg, 2 mmol), and THF (1 mL, 1 M) were added to the crude silyl acetals (1 mmol). The septum on the vial was replaced by a screw cap with a Teflon liner, and the mixture was stirred at 120 °C for 15 min. The reaction progress was monitored by GC/MS spectrometry. The resulting benzodioxasilines **4-3** were directly used for a subsequent reaction without further purification. For hindered substrates **4-3o-r**, the resulting benzodioxasilines **3** were purified for the subsequent reactions; volatiles were removed *in vacuo*, and the resulting mixture was dissolved with pentane, filtered through a pad of Celite[®], and concentrated *in vacuo*. The crude product was purified by MPLC (hexanes/EtOAc = 80:1, 5 mL/min, retention time 5–15 min). (iii) The crude benzodioxasilines **4-3** (1 mmol, THF, 1 M) were diluted with diethyl ether (3 mL, 0.33 M) and cooled to –78 °C. MeLi (3 mmol, 1.6 M in Et₂O) were added into the reaction mixture at –78 °C and stirred for 1 min. (iv) Trifluoromethanesulfonyl anhydride (1.2 mmol, 0.2 mL) was added into the reaction mixture. The reaction mixture was warmed to rt and stirred for 30 min. The reaction mixture was cooled to 0 °C and saturated aqueous ammonium

chloride solution was added. The mixture was extracted with diethyl ether three times. The combined organic layer was washed with water and brine, and dried over anhydrous sodium sulfate. Volatiles were removed *in vacuo*, and the crude mixture was purified by MPLC to afford arylsilyl triflates **5** (hexanes/EtOAc = 40:1, 5 mL/min, retention time 6–20 min).

E.2. Compounds characterization

2-[Diethyl(methyl)silyl]-4-(trifluoromethyl)phenyl trifluoromethanesulfonate (4-5d)



Yield: 1 mmol scale, 296 mg, 75%.

¹H NMR (CDCl₃, 500 MHz): δ 7.76 (d, *J* = 2.4 Hz, 1H, Ar-*H*), 7.71 (dd, *J* = 8.7, 2.4 Hz, 1H, Ar-*H*), 7.49 (d, *J* = 8.7 Hz, 1H, Ar-*H*), 0.98-0.90 [m, 10H, Si(CH₂CH₃)₂], and 0.38 (s, 3H, SiCH₃).

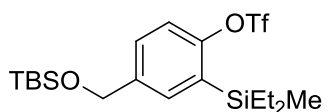
¹³C NMR (CDCl₃, 125 MHz): δ 157.3, 134.0 (q, ³*J*_{F-C} = 3.6 Hz), 132.6, 129.9 (q, ²*J*_{F-C} = 32.5 Hz), 128.7 (q, ³*J*_{F-C} = 3.6 Hz), 123.8 (q, ¹*J*_{F-C} = 273.2 Hz), 119.9, 118.8 (q, ¹*J*_{F-C} = 320.3 Hz), 7.3, 5.3, and -5.6.

IR (neat): 2962 (m), 2857 (w), 1566 (w), 1421 (s), 1201 (s), 1131 (s), 1045 (m), 889 (s), and 773 (s) cm⁻¹.

TLC: R_f = 0.5 in 40:1 hexanes: EtOAc.

HRMS (APCI/TOF): Calcd for (M+H)⁺ (C₁₃H₁₆F₆O₃SSi)⁺: 394.0494. Found: 394.0463.

4-[[*Tert*-butyldimethylsilyl]oxy]methyl]-2-(diethyl[methyl]silyl)phenyl trifluoromethanesulfonate (4-5e)



Yield: 1 mmol scale, 174 mg, 37%.

¹H NMR (CDCl₃, 500 MHz): δ 7.48 (d, *J* = 2.2 Hz, 1H, Ar-*H*), 7.37 (dd, *J* = 8.6, 2.2 Hz, 1H, Ar-*H*), 7.30 (d, *J* = 8.6 Hz, 1H, Ar-*H*), 4.76 (s, 2H, Ar-CH₂OTBS), 0.95 [s, 9H,

OSi(CH₃)₃], 0.97-0.85 [m, 10H, Si(CH₂CH₃)₂], 0.34 (s, 3H, SiCH₃), and 0.11 [s, 6H, OSi(CH₃)₂].

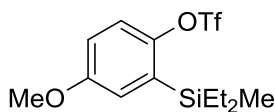
¹³C NMR (CDCl₃, 125 MHz): δ 154.3, 140.7, 134.3, 130.4, 128.8, 119.4, 118.7 (q, ¹J_{F-C} = 320.3 Hz), 64.3, 26.1, 18.5, 7.5, 5.6, -5.1, and -5.3.

IR (neat): 2954 (m), 2873 (w), 1571 (w), 1454 (s), 1244 (s), 1133 (s), 1061 (m), 888 (s), and 621 (s) cm⁻¹.

TLC: R_f = 0.5 in 40:1 hexanes: EtOAc.

HRMS (APCI/TOF): Calcd for (M+H)⁺ (C₁₉H₃₄F₃O₄SSi₂)⁺: 471.1663. Found: 471.1689.

2-[Diethyl(methyl)silyl]-4-methoxyphenyl trifluoromethanesulfonate (4-5f)



Yield: 1 mmol scale, 325 mg, 91%.

¹H-NMR (CDCl₃, 500 MHz): δ 7.26 (d, *J* = 9.0 Hz, 1H, Ar-*H*), 7.00 (d, *J* = 3.2 Hz, 1H, Ar-*H*), 6.90 (dd, *J* = 9.0, 3.2 Hz, 1H, Ar-*H*), 3.82 (s, 3H, Ar-OCH₃), 0.98-0.84 [m, 10H, Si(CH₂CH₃)₂], and 0.34 (s, 3H, SiCH₃).

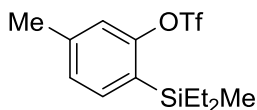
¹³C NMR (CDCl₃, 125 MHz): δ 158.1, 148.6, 132.4, 122.2, 120.8, 118.7 (q, ¹J_{F-C} = 320.3 Hz), 115.0, 55.6, 7.3, 5.4, and -5.5.

IR (neat): 2957 (m), 2878 (w), 1576 (w), 1467 (s), 1211 (s), 1121 (s), 1034 (m), 889 (s), and 618 (s) cm⁻¹.

TLC: R_f = 0.5 in 40:1 hexanes: EtOAc.

HRMS (APCI/TOF): Calcd for (M+H)⁺ (C₁₃H₂₀F₃O₄SSi)⁺: 357.0798. Found: 357.0815.

2-[Diethyl(methyl)silyl]-5-methylphenyl trifluoromethanesulfonate (4-5g)



Yield: 1 mmol scale, 278 mg, 82%.

¹H NMR (CDCl₃, 500 MHz): δ 7.39 (d, *J* = 7.9 Hz, 1H, Ar-*H*), 7.17-7.14 (m, 2H, Ar-*H*), 2.39 (s, 3H, Ar-CH₃), 0.95-0.83 [m, 10H, Si(CH₂CH₃)₂], and 0.32 (s, 3H, SiCH₃).

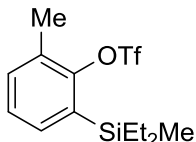
¹³C NMR (CDCl₃, 125 MHz): δ 155.6, 142.2, 136.9, 128.5, 127.0, 120.3, 118.7 (q, ¹*J*_{F-C} = 320.3 Hz), 21.5, 7.5, 5.6, and -5.3.

IR (neat): 2957 (m), 2877 (w), 1610 (w), 1417 (s), 1204 (s), 1139 (s), 1046 (m), 839 (s), and 597 (s) cm⁻¹.

TLC: R_f = 0.5 in 40:1 hexanes: EtOAc.

HRMS (APCI/TOF): Calcd for (M+H)⁺ (C₁₃H₂₀F₃O₃SSi)⁺: 341.0849. Found: 341.0873.

2-[Diethyl(methyl)silyl]-6-methylphenyl trifluoromethanesulfonate (4-5h)



Yield: 1 mmol scale, 312 mg, 92%.

¹H NMR (CDCl₃, 500 MHz): δ 7.39 (dd, *J* = 6.9, 2.2 Hz, 1H, Ar-*H*), 7.31 (dd, *J* = 7.5, 2.2 Hz, 1H, Ar-*H*), 7.28 (dd, *J* = 7.5, 6.9 Hz, 1H, Ar-*H*), 2.40 (s, 3H, Ar-CH₃), 0.99-0.87 [m, 10H, Si(CH₂CH₃)₂], and 0.37 (s, 3H, SiCH₃).

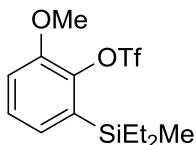
¹³C NMR (CDCl₃, 125 MHz): δ 151.6, 135.3, 134.0, 132.8, 131.7, 128.1, 118.9 (q, ¹*J*_{F-C} = 319.8 Hz), 17.6, 7.5, 6.1, and -4.5.

IR (neat): 2957 (m), 2875 (w), 1587 (w), 1455 (s), 1232 (s), 1115 (s), 1026 (m), 881 (s), and 610 (s) cm⁻¹.

TLC: R_f = 0.5 in 40:1 hexanes: EtOAc.

HRMS (APCI/TOF): Calcd for (M+H)⁺ (C₁₃H₂₀F₃O₃SSi)⁺: 341.0849. Found: 341.0818.

2-[Diethyl(methyl)silyl]-6-methoxyphenyl trifluoromethanesulfonate (4-5i)



Yield: 1 mmol scale, 288 mg, 81%.

¹H NMR (CDCl₃, 500 MHz): δ 7.30 (dd, *J* = 7.8, 7.8 Hz, 1H, Ar-*H*), 7.04 (dd, *J* = 7.8, 1.5 Hz, 1H, Ar-*H*), 7.03 (dd, *J* = 7.8, 1.5 Hz, 1H, Ar-*H*), 3.86 (s, 3H, Ar-OCH₃), 0.96-0.86 [m, 10H, Si(CH₂CH₃)₂], and 0.35 (s, 3H, SiCH₃).

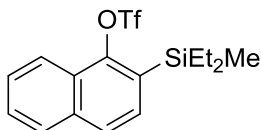
¹³C NMR (CDCl₃, 125 MHz): δ 150.3, 143.6, 133.4, 128.7, 127.6, 119.2 (q, ¹*J*_{F-C} = 321.6 Hz), 114.1, 55.7, 7.5, 5.6, and -5.1.

IR (neat): 2957 (m), 2879 (w), 1575 (w), 1461 (s), 1203 (s), 1137 (s), 1030 (m), 870 (s), and 631 (s) cm⁻¹.

TLC: R_f = 0.5 in 40:1 hexanes: EtOAc.

HRMS (APCI/TOF): Calcd for (M+H)⁺ (C₁₃H₂₀F₃O₄SSi)⁺: 357.0798. Found: 357.0776.

2-[Diethyl(methyl)silyl]naphthalen-1-yl trifluoromethanesulfonate (4-5j)



Yield: 226 mg, 60%, colorless oil;

¹H NMR (CDCl₃, 500 MHz) δ 7.90 (dd, *J* = 7.0, 1.3 Hz, 1H, Ar-*H*), 7.87 (ddd, *J* = 8.1, 1.1, 0.4 Hz, 1H, Ar-*H*), 7.82 (dd, *J* = 8.2, 1.4 Hz, 1H, Ar-*H*), 7.77 (dd, *J* = 8.1, 1.1 Hz, 1H, Ar-*H*), 7.53 (dd, *J* = 8.1, 7.0 Hz, 1H, Ar-*H*), 7.45 (dd, *J* = 8.1, 8.1 Hz, 1H, Ar-*H*), 0.99–0.90 [m, 10H, Si(CH₂CH₃)₂], and 0.40 (s, 3H, SiCH₃).

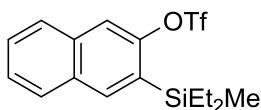
¹³C NMR (CDCl₃, 76 MHz) δ 148.6, 137.9, 136.0, 132.2, 129.9, 129.3, 129.0, 126.2, 124.6, 118.9 (q, ¹*J*_{F-C} = 320.2 Hz), 114.9, 7.9, 7.3, -2.7.

IR (neat): 2956 (m), 2877 (w), 1485 (s), 1192 (s), 1111 (s), 1051 (w), 890 (s), and 650 (s) cm⁻¹.

TLC R_f = 0.5 in 80:1 hexanes: EtOAc.

HRMS (APCI/TOF) calcd for (M+H)⁺ (C₁₆H₂₀F₃O₃SSi)⁺: 376.0776. Found: 376.0759.

3-[Diethyl(methyl)silyl]naphthalen-2-yl trifluoromethanesulfonate (4-5k)



Yield: 1 mmol scale, 334 mg, 89%.

¹H NMR (CDCl₃, 500 MHz): δ 8.00 (s, 1H, Ar-*H*), 7.88 (dd, *J* = 6.8, 2.2 Hz, 1H, Ar-*H*), 7.85 (dd, *J* = 6.8, 2.2 Hz, 1H, Ar-*H*), 7.82 (s, 1H, Ar-*H*), 7.59-7.53 (m, 2H, Ar-*H*), 1.01-0.92 [m, 10H, Si(CH₂CH₃)₂], and 0.42 (s, 3H, SiCH₃).

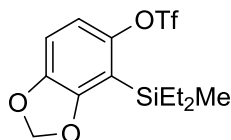
¹³C NMR (CDCl₃, 125 MHz): δ 152.9, 138.5, 134.3, 131.9, 129.2, 128.15, 127.99, 127.95, 127.1, 118.8 (q, ¹*J*_{F-C} = 320.3 Hz), 116.6, 7.5, 5.6, and -5.2.

IR (neat): 2957 (m), 2874 (w), 1532 (w), 1474 (s), 1202 (s), 1109 (s), 1046 (m), 874 (s), and 637 (s) cm⁻¹.

TLC: R_f = 0.5 in 40:1 hexanes: EtOAc.

HRMS (APCI/TOF): Calcd for (M+H)⁺ (C₁₆H₂₀F₃O₃SSi)⁺: 377.0849. Found: 377.0817.

4-[Diethyl(methyl)silyl]benzo[d][1,3]dioxol-5-yl trifluoromethanesulfonate (4-5l)



Yield: 1 mmol scale, 296 mg, 80%.

¹H NMR (CDCl₃, 500 MHz): δ 6.79 (app s, 2H, Ar-*H*), 5.98 (s, 2H, OCH₂O), 0.98-0.84 (m, 10H, Si(CH₂CH₃)₂), and 0.38 (s, 3H, SiCH₃).

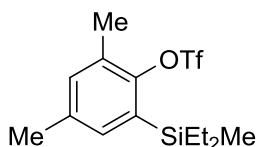
¹³C NMR (CDCl₃, 125 MHz): δ 153.8, 148.7, 145.8, 118.7 (q, ¹*J*_{F-C} = 320.3 Hz), 113.5, 112.7, 109.1, 101.6, 7.4, 6.0, and -4.6.

IR (neat): 2955 (m), 2865 (w), 1581 (w), 1465 (s), 1208 (s), 1124 (s), 1030 (m), 869 (s), and 661 (s) cm⁻¹.

TLC: R_f = 0.5 in 40:1 hexanes: EtOAc.

HRMS (APCI/TOF): Calcd for (M+H)⁺ (¹³H₁₈F₃O₅SSi)⁺: 371.0591. Found: 371.0585.

2-[Diethyl(methyl)silyl]-4,6-dimethylphenyl trifluoromethanesulfonate (4-5m)



Yield: 1 mmol scale, 310 mg, 84%.

¹H NMR (CDCl₃, 500 MHz): δ 7.18 (d, *J* = 2.3 Hz, 1H, Ar-*H*), 7.13 (d, *J* = 2.3 Hz, 1H, Ar-*H*), 2.38 (s, 3H, Ar-CH₃), 2.36 (s, 3H, Ar-CH₃), 1.01-0.92 [m, 10H Si(CH₂CH₃)₂], and 0.39 (s, 3H, SiCH₃).

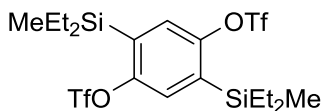
¹³C NMR (CDCl₃, 125 MHz): δ 149.6, 137.7, 135.7, 134.6, 132.4, 131.2, 119.0 (q, ¹*J*_{F-C} = 320.1 Hz), 20.9, 17.5, 7.6, 6.1, and -4.5.

IR (neat): 2956 (m), 2877 (w), 1460 (s), 1221 (s), 900 (s), 1039 (m), 865 (s), and 633 (s) cm⁻¹.

TLC: R_f = 0.5 in 40:1 hexanes: EtOAc.

HRMS (APCI/TOF): Calcd for (M+H)⁺ (C₁₄H₂₂F₃O₃SSi)⁺: 355.1006. Found: 355.1013.

2,5-bis[diethyl(methyl)silyl]-1,4-phenylene bis(trifluoromethanesulfonate) (4-5n)



Yield: 1 mmol scale, 522 mg, 91%.

¹H NMR (CDCl₃, 500 MHz): δ 7.47 (s, 2H, Ar-*H*), 0.99-0.88 [m, 20H, Si(CH₂CH₃)₂], and 0.37 (s, 6H, SiCH₃).

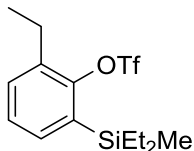
¹³C NMR (CDCl₃, 125 MHz): δ 153.5, 135.8, 127.7, 118.8 (q, ¹*J*_{F-C} = 320.6 Hz), 7.2, 5.2, and -5.7.

IR (neat): 2958 (m), 2879 (w), 1461 (w), 1422 (s), 1223 (s), 1137 (s), 1078 (m), 884 (s), and 615 (s) cm⁻¹.

TLC: R_f = 0.5 in 20:1 hexanes: EtOAc.

HRMS (APCI/TOF): Calcd for (M+H)⁺ (C₈H₂₉F₆O₆S₂Si₂)⁺: 575.0843. Found: 575.0817.

2-[Diethyl(methyl)silyl]-6-ethylphenyl trifluoromethanesulfonate (4-5o)



Yield: 1 mmol scale, 287 mg, 81%.

¹H NMR (CDCl₃, 500 MHz): δ 7.40 (dd, *J* = 7.3, 2.1 Hz, 1H, Ar-*H*), 7.37 (dd, *J* = 7.3, 2.1 Hz, 1H, Ar-*H*), 7.33 (dd, *J* = 7.3, 7.3 Hz, 1H, Ar-*H*), 2.79 (q, *J* = 7.6 Hz, 2H, Ar-CH₂CH₃),

1.25 (t, $J = 7.6$ Hz, 3H, Ar-CH₂CH₃), 0.99-0.87 [m, 10H, Si(CH₂CH₃)₂], and 0.37 (s, 3H, SiCH₃).

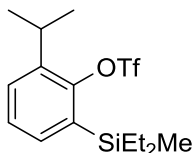
¹³C NMR (CDCl₃, 125 MHz): δ 150.7, 137.5, 135.3, 132.9, 131.9, 128.3, 118.9 (q, $^1J_{F-C} = 319.35$ Hz), 23.5, 14.2, 7.5, 6.2, and -4.4.

IR (neat): 2957 (m), 2878 (w), 1576 (w), 1467 (s), 1211 (s), 1121 (s), 1034 (m), 889 (s), and 618 (s) cm⁻¹;

TLC: R_f = 0.5 in 80:1 hexanes: EtOAc.

HRMS (APCI/TOF): Calcd for (M+H)⁺ (C₁₄H₂₂F₃O₃SSi)⁺: 355.1006. Found: 355.1018.

2-[Diethyl(methyl)silyl]-6-isopropylphenyl trifluoromethanesulfonate (4-5p)



Yield: 1 mmol scale, 269 mg, 73%.

¹H NMR (CDCl₃, 500 MHz): δ 7.42 (dd, $J = 7.0, 2.5$ Hz, 1H, Ar-*H*), 7.38-7.33 (m, 2H, Ar-*H*), 3.31 [hept, $J = 6.8$ Hz, 1H, Ar-CH(CH₃)₂], 1.24 [d, $J = 6.8$ Hz, 6H, Ar-CH(CH₃)₂], 0.96-0.87 [m, 10H, Si(CH₂CH₃)₂], and 0.35 (s, 3H, SiCH₃).

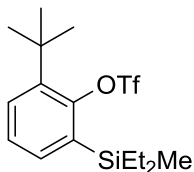
¹³C NMR (CDCl₃, 125 MHz): δ 149.5, 142.2, 135.2, 133.0, 129.3, 128.4, 118.8 (q, $^1J_{F-C} = 317.3$ Hz), 27.3, 23.7, 7.6, 6.2, and -4.3.

IR (neat): 2958 (m), 2877 (w), 1571 (w), 1447 (s), 1201 (s), 1154 (s), 1027 (m), 892 (s), and 636 (s) cm⁻¹.

TLC: R_f = 0.5 in 80:1 hexanes: EtOAc.

HRMS (APCI/TOF): Calcd for (M+H)⁺ (C₁₅H₂₄F₃O₃SSi)⁺: 369.1162. Found: 369.1145.

2-(*Tert*-butyl)-6-[diethyl(methyl)silyl]phenyl trifluoromethanesulfonate (4-5q)



Yield: 1 mmol scale, 267 mg, 70%.

¹H NMR (CDCl₃, 500 MHz): δ 7.55 (dd, *J* = 7.8, 1.9 Hz, 1H, Ar-*H*), 7.37 (dd, *J* = 7.2, 1.9 Hz, 1H, Ar-*H*), 7.30 (dd, *J* = 7.8, 7.2 Hz, 1H, Ar-*H*), 1.43 [s, 9H, C(CH₃)₃], 0.95-0.84 [m, 10H Si(CH₂CH₃)₂], and 0.32 (s, 3H, SiCH₃).

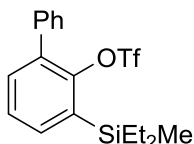
¹³C NMR (CDCl₃, 125 MHz): δ 148.2, 143.8, 135.6, 134.6, 131.8, 127.6, 118.6 (q, ¹*J*_{F-C} = 320.3 Hz), 36.5, 32.1, 7.6, 6.9, and -3.6.

IR (neat): 2957 (m), 2878 (w), 1564 (w), 1443 (s), 1236 (s), 1163 (s), 1041 (m), 874 (s), and 608 (s) cm⁻¹.

TLC: R_f = 0.5 in hexanes.

HRMS (APCI/TOF): Calcd for (M+H)⁺ (C₁₆H₂₆F₃O₃SSi)⁺: 383.1319. Found: 383.1304.

3-[Diethyl(methyl)silyl]-(1,1'-biphenyl)-2-yl trifluoromethanesulfonate (4-5r)



Yield: 1 mmol scale, 301 mg, 75%.

¹H NMR (CDCl₃, 500 MHz): δ 7.54-7.52 (m, 1H, Ar-*H*), 7.45-7.37 (m, 7H, Ar-*H*), 1.02-0.93 [m, 10H, Si(CH₂CH₃)₂], and 0.42 (s, 3H, SiCH₃).

¹³C NMR (CDCl₃, 125 MHz): δ 150.1, 137.1, 136.5, 133.96, 133.85, 129.8, 128.6, 128.2, 118.2 (q, ¹*J*_{F-C} = 320.7 Hz), 7.6, 6.2, and -4.3.

IR (neat): 2957 (m), 2878 (w), 1556 (w), 1435 (s), 1221 (s), 1133 (s), 1024 (m), 869 (s), and 798 (s) cm⁻¹.

TLC: R_f = 0.5 in 80:1 hexanes: EtOAc.

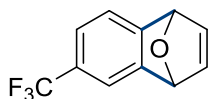
HRMS (APCI/TOF): Calcd for (M+H)⁺ (C₁₈H₂₂F₃O₃SSi)⁺: 403.1006. Found: 403.9985.

E.3. General procedure for fluoride-mediated benzyne cycloaddition reactions (4-13)

Arylsilyl triflate (0.5 mmol) **5** was dissolved in furan (0.2 mL) and placed in a 4 mL vial. TBAF (1.2 equiv, 1 M in THF) was added into the reaction mixture at rt. The septum on the vial was replaced by a screw cap with a Teflon liner, and the mixture was stirred at rt for 2 h. The reaction was quenched by adding saturated aqueous ammonium chloride. The reaction mixture was extracted with diethyl ether and concentrated *in vacuo* to afford

the crude mixture, which was purified by MPLC (hexanes/EtOAc = 10:1, 5 mL/min, retention time 7–15 min) to afford 1,4-dihydro-1,4-epoxynaphthalenes **4-13**.

6-(Trifluoromethyl)-1,4-dihydro-1,4-epoxynaphthalene (4-13d)



Yield: 1 mmol scale, 182 mg, 86%.

¹H NMR (CDCl₃, 300 MHz): δ 7.46 (s, 1H, Ar-*H*), 7.33 (d, *J* = 7.4 Hz, 1H, Ar-*H*), 7.29 (d, *J* = 7.4 Hz, 1H, Ar-*H*), 7.06 (dd, *J* = 5.5, 1.7 Hz, 1H, CH(O)CH=CH), 7.04 (dd, *J* = 5.5, 1.8 Hz, 1H, CH(O)CH=CH), and 5.77 (app s, 2H, CHOCH).

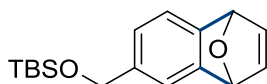
¹³C NMR (CDCl₃, 76 MHz) δ 153.4, 150.5, 143.3, 142.9, 127.7 (q, ²*J*_{F-C} = 32.3 Hz), 124.3 (q, ¹*J*_{F-C} = 271.6 Hz), 123.2 (q, ³*J*_{F-C} = 4.3 Hz), 120.2, 117.2 (q, ³*J*_{F-C} = 3.6 Hz), and 82.3 (2).

IR (neat): 3035 (w), 2956 (m), 2924 (m), 2853 (m), 1703 (w), 1631 (m), 1527 (m), 1222 (s), 1087 (s), 1031 (s), and 826 (m) cm⁻¹;

TLC *R*_f = 0.5 in 5:1 hexanes:EtOAc;

HRMS (APCI/TOF) calcd for (M+H)⁺ (C₁₁H₈F₃O)⁺: 213.0522. Found: 213.0514.

***Tert*-butyl[(1,4-dihydro-1,4-epoxynaphthalen-6-yl)methoxy]dimethylsilane (4-13e)**



Yield: 0.5 mmol scale, 94 mg, 80%.

¹H NMR (CDCl₃, 500 MHz): δ 7.24 (s, 1H, Ar-*H*), 7.18 (d, *J* = 7.2 Hz, 1H, Ar-*H*), 7.01 [m, 2H, CH(O)CH=CH], 6.91 (d, *J* = 7.2 Hz, 1H, Ar-*H*), 5.70 (s, 2H, CHOCH), 4.67 (s, 2H, Ar-CH₂OTBS), 0.93 [s, 9H, OSi(CH₃)₃], and 0.09 [s, 6H, OSi(CH₃)₂].

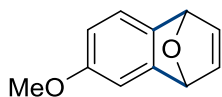
¹³C NMR (CDCl₃, 125 MHz): δ 149.5, 147.9, 143.27, 143.12, 138.8, 122.7, 120.0, 118.8, 82.58, 82.41, 65.2, 26.2, 18.6, and -5.0.

IR (neat): 3053 (m), 2874 (w), 1600 (w), 1460 (m), 1415 (s), 1278 (m), 1209 (s), 1139 (s), 1045 (s), 845 (w), 695 (s), 571 (m) cm⁻¹.

TLC: *R*_f = 0.5 in 5:1 hexanes: EtOAc.

HRMS (APCI/TOF): Calcd for (M+H)⁺ (C₁₇H₂₅O₂Si)⁺: 289.1618. Found: 289.1602.

6-Methoxy-1,4-dihydro-1,4-epoxynaphthalene (4-13f)



Yield: 1 mmol scale, 139 mg, 80%.

¹H NMR (CDCl₃, 500 MHz): δ 7.13 (d, *J* = 7.8 Hz, 1H, Ar-*H*), 7.03 [dd, *J* = 5.6, 1.8 Hz, 1H CH(O)CH=CH], 6.99 [dd, *J* = 5.6, 1.8 Hz, 1H CH(O)CH=CH], 6.91 (d, *J* = 2.2 Hz, 1H, Ar-*H*), 6.42 (dd, *J* = 7.8, 2.2 Hz, 1H, Ar-*H*), 5.68 (app s, 1H, CHOCH), 5.66 (app s, 1H, CHOCH), and 3.77 (s, 3H, Ar-OCH₃).

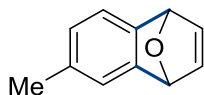
¹³C NMR (CDCl₃, 125 MHz): δ 157.6, 151.2, 143.7, 142.4, 140.6, 120.6, 109.9, 107.4, 82.6, 82.2, and 55.8.

IR (neat): 3036 (w), 2961 (w), 2909 (w), 1632 (m), 1516 (m), 1481 (m), 1264 (s), 1217 (s), 1030 (m), 812 (s), 560 (m) cm⁻¹.

TLC: R_f = 0.5 in 5:1 hexanes: EtOAc.

HRMS (APCI/TOF): Calcd for (M+H)⁺ (C₁₁H₁₁O₂)⁺: 175.0754. Found: 175.0737.

6-Methyl-1,4-dihydro-1,4-epoxynaphthalene (4-13g)



Yield: 0.5 mmol scale, 69 mg, 75%.

¹H NMR (CDCl₃, 500 MHz): δ 7.13 (d, *J* = 7.2 Hz, 1H, Ar-*H*), 7.10 (s, 1H, Ar-*H*), 7.02 [dd, *J* = 5.5, 1.7 Hz, 1H CH(O)CH=CH], 7.01 [dd, *J* = 5.5, 1.7 Hz, 1H CH(O)CH=CH], 6.77 (d, *J* = 7.2 Hz, 1H, Ar-*H*), 5.69 (app s, 1H, CHOCH), 5.67 (app s, 1H, CHOCH), and 2.30 (s, 3H, Ar-CH₃).

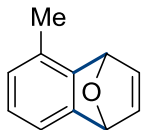
¹³C NMR (CDCl₃, 125 MHz): δ 149.5, 146.2, 143.4, 143.0, 135.0, 125.2, 121.8, 120.1, 82.50, 82.38, and 21.5.

IR (neat): 3038(m), 2954(w), 1620(w), 1599(w), 1459(m), 1279(s), 1165(m), 1020(s), 845(s), 641(s), 573(s) cm⁻¹.

TLC: R_f = 0.5 in 5:1 hexanes: EtOAc.

HRMS (APCI/TOF): Calcd for (M+H)⁺ (C₁₁H₁₁O)⁺: 159.0804. Found: 159.0821.

4.3.5. 5-Methyl-1,4-dihydro-1,4-epoxynaphthalene (13h)



Yield: 0.5 mmol scale, 66 mg, 83%.

¹H NMR (CDCl₃, 300 MHz): δ 7.09 (d, *J* = 6.9 Hz, 1H, Ar-*H*), 7.07-6.99 [m, 2H, CH(O)CH=CH], 6.88 (dd, *J* = 7.6, 6.9 Hz, 1H, Ar-*H*), 6.78 (d, *J* = 7.6 Hz, 1H, Ar-*H*), 5.81 (app s, 1H, CHOCH), 5.71 (app s, 1H, CHOCH), and 2.32 (s, 3H, ArCH₃).

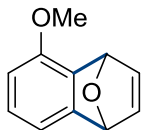
¹³C NMR (CDCl₃, 76 MHz) δ 148.7, 147.4, 143.2, 142.7, 130.1, 126.8, 125.1, 117.9, 82.6, 80.9, and 18.2

IR (neat): 3036 (m), 2841(w), 1632(w), 1465(m), 1522(s), 1216(s), 1347(s), 1014(s), 835(m), 662(s), 573(m) cm⁻¹.

TLC: R_f = 0.5 in 5:1 hexanes: EtOAc.

HRMS (APCI/TOF): Calcd for (M+H)⁺ (C₁₁H₁₁O)⁺: 159.0804. Found: 159.0791.

5-Methoxy-1,4-dihydro-1,4-epoxynaphthalene (4-13i)



Yield: 0.5 mmol scale, 58 mg, 67%.

¹H NMR (CDCl₃, 500 MHz): δ 7.07 [dd, *J* = 5.5, 1.8 Hz, 1H, CH(O)CH=CH], 7.03 [dd, *J* = 5.5, 1.8 Hz, 1H, CH(O)CH=CH], 6.97 (dd, *J* = 8.0, 7.0 Hz, 1H, Ar-*H*), 6.93 (dd, *J* = 7.0, 0.8 Hz, 1H, Ar-*H*), 6.59 (dd, *J* = 8.0, 0.8 Hz, 1H, Ar-*H*), 5.95 (app s, 1H, CHOCH), 5.70 (app s, 1H, CHOCH), and 3.83 (s, 3H, Ar-CH₃).

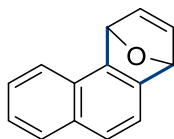
¹³C NMR (CDCl₃, 76 MHz) δ 153.1, 151.7, 143.23, 143.08, 135.2, 127.2, 113.9, 110.5, 82.7, 80.3, and 55.9

IR (neat): 3042(m), 2874(w), 1642(w), 1453(m), 1538(s), 1312(m), 1167(s), 1041(m), 844(m), 521(m) cm⁻¹.

TLC: R_f = 0.5 in 5:1 hexanes: EtOAc.

HRMS (APCI/TOF): Calcd for (M+H)⁺ (C₁₁H₁₁O₂)⁺: 175.0754. Found: 175.0731.

1,4-Dihydro-1,4-epoxyphenanthrene (4-13j)



Yield (71%, 69 mg); pale yellow solid, mp 85–87 °C;

¹H NMR (CDCl₃, 300 MHz) δ 7.83 (dd, *J* = 8.3, 8.3 Hz, 2H, Ar-*H*), 7.56 (ddd, *J* = 7.9, 7.9, 7.9 Hz, 2H, Ar-*H*), 7.47 (dd, *J* = 8.1, 7.4 Hz, 1H, Ar-*H*), 7.39 (dd, *J* = 8.1, 7.6 Hz, 1H, Ar-*H*), 7.31–7.12 [m, 2H, CH(O)CH=CH], 6.28 (app s, 1H, CHOCH), and 5.94 (app s, 1H, CHOCH).

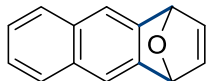
¹³C NMR (CDCl₃, 76 MHz) δ 148.5, 148.0, 145.1, 143.6, 132.0, 129.0, 127.8, 126.4, 125.6, 125.3, 122.9, 119.5, 83.6, and 81.4

IR (neat) 3050 (m), 2855 (w), 1655 (w), 1517 (m), 1451 (m), 1345 (s), 1147 (s), 1039 (s), 683 (s), and 482 (s).

TLC *R_f* = 0.5 in 5:1 hexanes:EtOAc.

HRMS (APCI/TOF) calcd for (M+H)⁺ (C₁₄H₁₁O)⁺: 194.0732. Found: 194.0741.

1,4-Dihydro-1,4-epoxyanthracene (4-13k)



Yield (67%, 65 mg) pale yellow solid, mp 160–162 °C;

¹H NMR (CDCl₃, 500 MHz): δ 7.76–7.67 (m, 2H, Ar-*H*), 7.59 (s, 2H, Ar-*H*), 7.45–7.42 (m, 2H, Ar-*H*), 7.01–6.94 [m, 2H CH(O)CH=CH], and 5.81 (app s, 2H, CHOCH).

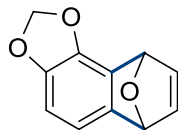
¹³C NMR (CDCl₃, 125 MHz): δ 144.3, 141.9, 132.1, 128.3, 126.3, 118.8, and 82.0.

IR (neat): 3042(m), 2857(w), 1637(w), 1435(m), 1518(m), 1311(s), 1132(s), 1021(s), 631(s), 456(m) cm⁻¹.

TLC: *R_f* = 0.5 in 5:1 hexanes: EtOAc.

HRMS (APCI/TOF): Calcd for (M+H)⁺ (C₁₄H₁₁O)⁺: 195.0804. Found: 195.0788.

6,9-Dihydro-6,9-epoxynaphtho[1,2-d][1,3]dioxole (4-13l)



Yield: 0.5 mmol scale, 56 mg, 60%.

¹H NMR (CDCl₃, 500 MHz): δ 7.00 [dd, *J* = 5.6, 1.7 Hz, 1H, CH(O)CH=CH], 6.97 [dd, *J* = 5.6, 1.7 Hz, 1H, CH(O)CH=CH], 6.72 (d, *J* = 7.2 Hz, 1H, Ar-*H*), 6.38 (d, *J* = 7.2 Hz, 1H, Ar-*H*), 5.90 (d, *J* = 10.7 Hz, 1H, OCH_aH_bO), 5.90 (d, *J* = 10.7 Hz, 1H, OCH_aH_bO), 5.85 (app s, 1H, CHOCH), and 5.65 (app s, 1H, CHOCH).

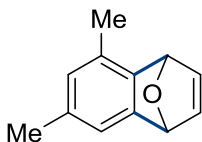
¹³C NMR (CDCl₃, 125 MHz): δ 146.5, 143.2 (2), 141.5, 140.6, 127.3, 113.3, 103.5, 101.1, 82.5, and 79.7.

IR (neat): 3053(m), 2960(w), 2777(w), 1650(w), 1572(m), 1458(s), 1232(s), 1042(s), 954(s), 829(m), 638(s), 522(m) cm⁻¹.

TLC: R_f = 0.5 in 5:1 hexanes: EtOAc.

HRMS (APCI/TOF): Calcd for (M+H)⁺ (C₁₁H₉O₃)⁺: 189.0546. Found: 189.0565.

5,7-Dimethyl-1,4-dihydro-1,4-epoxynaphthalene (4-13m)



Yield: 1 mmol scale, 61 mg, 71%.

¹H NMR (CDCl₃, 500 MHz): δ 7.03 [dd, *J* = 5.5, 1.7 Hz, 1H, CH(O)CH=CH], 7.02 [dd, *J* = 5.5, 1.7 Hz, 1H, CH(O)CH=CH], 6.94 (s, 1H, Ar-*H*), 6.60 (s, 1H, Ar-*H*), 5.78 (app s, 1H, CHOCH), 5.66 (app s, 1H, CHOCH), 2.28 (s, 3H, Ar-CH₃), and 2.27 (s, 3H, Ar-CH₃).

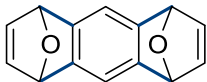
¹³C NMR (CDCl₃, 125 MHz): δ 149.2, 144.5, 143.08, 143.03, 134.9, 129.8, 127.0, 119.4, 82.7, 80.9, 21.3, and 18.2.

IR (neat): 3047(m), 2964(m), 2872(w), 1612(w), 1481(m), 1532(s), 1214(s), 1121(s), 644(s), 521(m) cm⁻¹.

TLC: R_f = 0.5 in 5:1 hexanes: EtOAc.

HRMS (APCI/TOF): Calcd for (M+H)⁺ (C₁₂H₁₃O)⁺: 173.0961. Found: 173.0942.

1,4,5,8-Tetrahydro-1,4:5,8-diepoxyanthracene (4-13n)



Yield: (69%, 72 mg) (1:1 *dr*); white solid, mp 189–191 °C;

¹H NMR (CDCl₃, 500 MHz): δ 7.20 (s, 2H, Ar-*H*), 7.06-6.99 (m, 4H, CH(O)CH=CH], and 5.63 (app s, 4H, CHOCH).

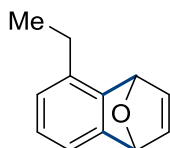
¹³C NMR (CDCl₃, 125 MHz): δ 148.0, 143.6, 114.3, and 82.6.

IR (neat): 3047(w), 2963(m), 2877(w), 1640(w), 1603(w), 1485(m), 1528(s), 1222(s), 1147(s), 1029(s), 845(m), 635(s), 516(m) cm⁻¹.

TLC: R_f = 0.5 in 3:1 hexanes: EtOAc.

HRMS (APCI/TOF): Calcd for (M+H)⁺ (C₁₄H₁₁O₂)⁺: 211.0754. Found: 211.0767.

5-Ethyl-1,4-dihydro-1,4-epoxynaphthalene (4-13o)



Yield: 0.2 mmol scale, 24 mg, 70%.

¹H NMR (CDCl₃, 500 MHz): δ 7.12 (d, *J* = 7.0 Hz, 1H, Ar-*H*), 7.05-7.02 [nform, 2H, CH(O)CH=CH], 6.92 (dd, *J* = 7.9, 7.0 Hz, 1H, Ar-*H*), 6.81 (d, *J* = 7.9 Hz, 1H, Ar-*H*), 5.84 (app s, 1H, CHOCH), 5.72 (app s, 1H, CHOCH), 2.70 (dq, *J* = 14.1, 7.6 Hz, 1H, Ar-CH_aH_bCH₃), 2.63 (dq, *J* = 14.1, 7.6 Hz, 2H, Ar-CH_aH_bCH₃), and 1.21 (dd, *J* = 7.7, 7.7 Hz, 3H, Ar-CH_aH_bCH₃).

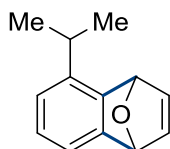
¹³C NMR (CDCl₃, 125 MHz): δ 148.7, 146.9, 143.4, 142.9, 136.7, 125.40, 125.34, 118.2, 82.6, 81.0, 26.2, and 16.0.

IR (neat): 3050(m), 2963(m), 2871(w), 1643(w), 1609(w), 1470(m), 1278(m), 1141(m), 1087(m), 1003(s), 870(s), 675(s), 603(m) cm⁻¹.

TLC: R_f = 0.5 in 10:1 hexanes: EtOAc.

HRMS (APCI/TOF): Calcd for (M+H)⁺ (C₁₂H₁₃O)⁺: 173.0961. Found: 173.0942.

5-Isopropyl-1,4-dihydro-1,4-epoxynaphthalene (4-13p)



Yield: 0.2 mmol scale, 24 mg, 64%.

¹H NMR (CDCl₃, 500 MHz): δ 7.11 (d, *J* = 6.9 Hz, 1H, Ar-*H*), 7.05-7.01 [nfom, 2H, CH(O)CH=CH], 6.94 (dd, *J* = 7.9, 6.9 Hz, 1H, Ar-*H*), 6.86 (d, *J* = 7.9, 0.5 Hz, 1H, Ar-*H*), 5.91 (app s, 1H, CHOCH), 5.70 (app s, 1H, CHOCH), 3.05 (hept, *J* = 6.9 Hz, 1H), 1.29 (d, *J* = 6.9 Hz, 3H), and 1.21 (d, *J* = 6.9 Hz, 3H).

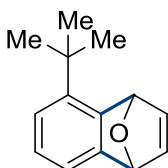
¹³C NMR (CDCl₃, 125 MHz): δ 148.7, 146.4, 143.5, 142.9, 141.2, 125.5, 122.8, 118.3, 82.6, 81.2, 31.8, 24.3, and 23.2.

IR (neat): 3052(m), 2956(m), 2872(w), 1641(w), 1611(w), 1475(m), 1274(m), 1121(m), 1065(m), 671(s), 653(m) cm⁻¹.

TLC: R_f = 0.5 in 10:1 hexanes: EtOAc.

HRMS (APCI/TOF): Calcd for (M+H)⁺ (C₁₃H₁₅O)⁺: 187.1117. Found: 187.1103.

5-(*Tert*-butyl)-1,4-dihydro-1,4-epoxynaphthalene (4-13q)



Yield: 0.2 mmol scale, 20 mg, 50%. white solid, mp 53–54 °C;

¹H NMR (CDCl₃, 500 MHz): δ 7.12 (d, *J* = 6.8, 1.1 Hz, 1H, Ar-*H*), 7.06-7.02 [nfom, 2H, CH(O)CH=CH], 6.97 (dd, *J* = 8.1, 1.1 Hz, 1H, Ar-*H*), 6.93 (dd, *J* = 8.1, 6.8 Hz, 1H, Ar-*H*), 6.15 (app s, 1H, CHOCH), 5.68 (app s, 1H, CHOCH), and 1.36 (s, 9H).

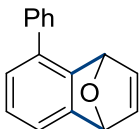
¹³C NMR (CDCl₃, 125 MHz): δ 149.2, 146.7, 144.1, 143.8, 142.8, 125.2, 122.6, 118.4, 83.2, 82.1, 35.5, and 31.5.

IR (neat): 3066(m), 2963(m), 2869(w), 1686(w), 1588(w), 1470(m), 1279(m), 1187(m), 1120(m), 1008(m), 878(s), 710(s), 658(m) cm⁻¹.

TLC: R_f = 0.5 in 10:1 hexanes: EtOAc.

HRMS (APCI/TOF): Calcd for (M+H)⁺ (C₁₄H₁₇O)⁺: 201.1274. Found: 201.1294.

4.3.15. 5-Phenyl-1,4-dihydro-1,4-epoxynaphthalene (4-13r)



Yield: 0.2 mmol scale, 29 mg, 67%. pale yellow solid, mp 63–65 °C

¹H NMR (CDCl₃, 500 MHz): δ 7.51-7.45 (m, 2H, Ar-H), 7.42-7.35 (m, 3H, Ar-H), 7.29-7.25 (m, 1H, Ar-H), 7.20-7.10 [m, 2H, CH(O)CH=CH], 7.09-7.04 (m, 2H, Ar-H), 5.84 (app s, 1H, CHOCH), and 5.78 (app s, 1H, CHOCH).

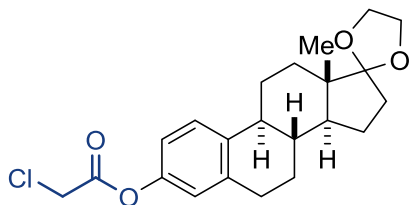
¹³C NMR (CDCl₃, 125 MHz): δ 149.3, 147.1, 143.5, 143.0, 139.8, 135.1, 128.9, 128.3, 127.6, 125.6, 125.4, 119.5, 82.7, and 82.0.

IR (neat): 3063(m), 2962(m), 2872(w), 1662(w), 1581(w), 1473(m), 1282(m), 1193(m), 1117(m), 1003(m), 871(s), 710(s), cm⁻¹.

TLC: R_f = 0.5 in 10:1 hexanes: EtOAc.

HRMS (APCI/TOF): Calcd for (M+H)⁺ (C₁₆H₁₃O)⁺: 221.0961. Found: 221.0945.

Procedure for preparation of (8R,9S,13S,14S)-13-methyl-6,7,8,9,11,12,13,14,15,16-deca-hydrospiro[cyclopenta[a]phenanthrene-17,2'-[1,3]dioxolan]-3-yl 2-chloroacetate (4-15)



A round-bottom flask (100 mL) with a magnetic stir bar and a Dean-Stark apparatus was charged with estrone **4-14** (3.0 g, 11.0 mmol) and *p*-TsOH (105 mg, 5 mol %). Toluene (60 mL) and ethylene glycol (3.1 mL, 55 mmol) were added and the reaction mixture was heated at reflux for 14 h. The reaction was cooled to rt, and the solvent was removed *in vacuo*, ethyl acetate (30 mL) and brine (50 mL) were added. The mixture was extracted with ethyl acetate three times, and the combined organic extract was washed with water and brine, and dried over anhydrous sodium sulfate. The volatiles were removed *in vacuo* to afford the crude product, which was directly used for a subsequent reaction without further purification. The crude product (11 mmol) and chloroacetic acid (1.9 g, 20 mmol) and DMAP (67 mg, 5 mol %) were dissolved with CH₂Cl₂ (20 mL), the reaction mixture was cooled to 0 °C with an ice bath. DCC (2.7 g, 13 mmol) was added

into the reaction mixture slowly. The reaction mixture was warmed to rt and stirred for 10 h. Diethyl ether (30 mL) was added to precipitate the urea byproduct. The mixture was filtered and the filtrate was treated with saturated aqueous sodium bicarbonate. Aqueous phase was extracted with ethyl acetate three times. The combined organic extracts were washed with water and brine, and dried over anhydrous sodium sulfate. The volatiles were removed *in vacuo*, and the crude mixture was purified by flash column (hexanes: EtOAc 3:1) to afford the ester **4-15** (3.27 g, 76% over two steps).

White solid, mp 113–115 °C;

¹H NMR (CDCl₃, 500 MHz) δ 7.30 [d, *J* = 8.1 Hz, 1H, *H*(1)], 6.88 [dd, *J* = 8.1, 2.6 Hz, 1H, *H*(2)], 6.83 [d, *J* = 2.6 Hz, 1H, *H*(4)], 4.28 (s, 2H, CH₂Cl), 3.98–3.88 (m, 4H, OCH₂CH₂O), 2.88–2.84 (m, 2H, alkyl-*H*), 2.32 (dddd, *J* = 13.2, 4.2, 4.2, 2.7 Hz, 1H, alkyl-*H*), 2.26 (ddd, *J* = 10.6, 10.6, 4.1 Hz, 1H, alkyl-*H*), 2.03 (ddd, *J* = 14.0, 11.2, 3.1 Hz, 1H, alkyl-*H*), 1.93–1.74 (m, 4H, alkyl-*H*), 1.63 (ddd, *J* = 12.1, 10.8, 7.0 Hz, 1H, alkyl-*H*), 1.55–1.31 (m, 5H, alkyl-*H*), and 0.88 [s, 3H, CH(18)].

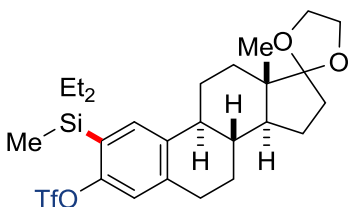
¹³C NMR (CDCl₃, 125 MHz) δ 166.4, 148.2, 138.9, 138.8, 126.8, 121.2, 119.6, 118.2, 65.5, 64.8, 49.6, 46.3, 44.0, 41.1, 38.8, 34.4, 30.9, 29.7, 26.9, 26.2, 22.6, and 14.5.

IR (neat) 2935 (m), 2864 (m), 1775 (s), 1724 (m), 1493 (m), 1304 (m), 1190 (s), 1042 (m), and 804 (m) cm⁻¹. m.p. 76–78 °C.

TLC *R*_f = 0.5 in 3:1 hexanes:EtOAc.

HRMS (APCI/TOF) calcd for (M+H)⁺ (C₂₂H₂₈ClO₄)⁺: 391.1671. Found: 391.1659.

E.4. Procedure for preparation of (8*R*,9*S*,13*S*,14*S*)-3-[diethyl(methyl)silyl]-13-methyl-6,7,8,9,11,12,13,14,15,16-decahydrospiro(cyclopenta[*a*]phenanthrene-17,2'-[1,3]dioxolan)-2-yl trifluoromethanesulfonate (4-18)



C2-silyl phenol **4-17** (414 mg, 1 mmol) and pyridine (0.12 mL, 1.5 mmol) in CH₂Cl₂ (2 mL, 1 M) were cooled to 0 °C with an ice bath. Trifluoromethanesulfonyl anhydride (0.25 mL, 1.5 mmol) was added into the reaction mixture dropwise. The reaction mixture was stirred at 0 °C for 1 h and an additional 30 min at rt. The reaction was quenched by saturated aqueous sodium bicarbonate and was extracted with diethyl ether three times. The combined organic extracts were washed with water two times and brine, and dried over anhydrous sodium sulfate. The volatiles were removed *in vacuo*, and the crude mixture was purified by MPLC (hexanes/EtOAc = 5:1, 5 mL/min) to afford arylsilyl triflate **4-18**.

White solid; Yield (90%, 491 mg)

¹H NMR (CDCl₃, 500 MHz) δ 7.39 (s, 1H, Ar-*H*), 7.01 (s, 1H, Ar-*H*), 3.99–3.88 (m, 4H, OCH₂CH₂O), 2.87 (dd, *J* = 8.4, 4.0 Hz, 2H, alkyl-*H*), 2.37–2.31 (m, 1H, alkyl-*H*), 2.30–2.25 (m, 1H, alkyl-*H*), 2.04 (ddd, *J* = 14.1, 11.6, 2.7 Hz, 1H, alkyl-*H*), 1.94–1.76 (m, 4H alkyl-*H*), 1.64 (ddd, *J* = 11.9, 10.9, 7.0 Hz, 1H alkyl-*H*), 1.56 (ddd, *J* = 12.6, 3.3, 2.6 Hz, 1H alkyl-*H*), 1.55–1.33 (m, 4H), 0.89 [s, 3H CH(18)₃], 0.97–0.80 [m, 10H, Si(CH₂CH₃)₂], and 0.30 (s, 3H, SiCH₃).

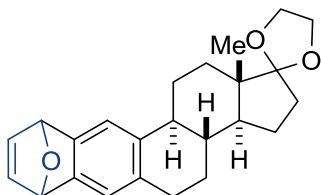
¹³C NMR (CDCl₃, 125 MHz) δ 153.5, 141.0, 139.8, 134.1, 126.8, 119.58, 119.51, 118.7 (q, ¹*J*_{F-C} = 319.6 Hz), 65.5, 64.8, 49.5, 46.3, 44.0, 38.8, 34.4, 30.8, 29.9, 26.8, 26.1, 22.6, 14.5, 7.6, 5.68, 5.59, and -5.2.

IR (neat) 2957 (m), 2874 (w), 1493 (m), 1304 (m), 1190 (s), 1042 (m), and 804 (m) (s) cm⁻¹.

TLC *R_f* = 0.5 in 5:1 hexanes:EtOAc.

HRMS (APCI/TOF) calcd for (M+H)⁺ (C₂₆H₃₈F₃O₅SSi)⁺: 547.2156. Found: 547.2139.

(3aS,3bR,11bS,13aS)-13a-Methyl-2,3,3a,3b,4,5,7,10,11b,12,13,13a-dodecahydrospiro[7,10-epoxycyclopenta[*c*]tetraphene-1,2'-[1,3]dioxolane] (4-19)



C2-Silyl triflate **4-18** (109 mg, 0.2 mmol) was dissolved in furan (0.2 mL). TBAF (0.6 mL, 0.24 mmol, 1 M in THF) was added to the reaction mixture at rt. The septum on the vial was replaced by a screw cap with a Teflon liner, and the mixture was stirred at rt for 2 h. Reaction progress was monitored by TLC until full conversion of **4-18**. TLC showed two spots, indicating formation of compound **4-19** and **4-20**. The reaction was quenched by adding saturated aqueous ammonium chloride. The reaction mixture was extracted with diethyl ether and concentrated *in vacuo* to afford a mixture of **4-19** and **4-20** (4:1), which was used for next step without further purification.

White solid; Yield (60%, 44 mg) (1.2:1 *dr*).

¹H NMR (CDCl₃, 500 MHz) δ 7.25 (s, 0.45H, Ar—H), 7.24 (s, 0.55H, Ar—H), 7.02–6.98 [m, 3H, Ar—H and CH(O)CH=CH], 5.66–5.65 (m, 2H, CHOCH), 3.98–3.87 (m, 4H, OCH₂CH₂O), 2.85–2.72 (m, *J* = 2.9 Hz, 2H, Alkyl-H), 2.32–2.28 (m, 1H, Alkyl-H), 2.27–2.19 (m, 1H, Alkyl-H), 2.05–1.99 (m, 1H, Alkyl-H), 1.89–1.73 (m, 4H, Alkyl-H), 1.65–1.59 (m, 1H, Alkyl-H), 1.56–1.51 (m, 1H, Alkyl-H), 1.49–1.31 (m, 4H, Alkyl-H), 0.88 [s, 1.35H, CH(18)₃], and 0.86 [s, 1.65H CH(18)₃]

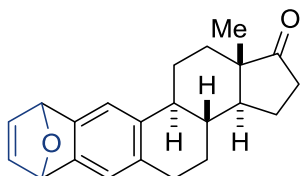
³C NMR (CDCl₃, 125 MHz) δ 146.34, 146.32, 146.21, 146.09, 143.24, 143.20, 143.01 (2), 136.84, 136.73, 133.31, 133.27, 121.57, 121.52, 119.62, 119.60, 118.0 (2), 82.58, 82.55, 82.36, 82.28, 65.5 (2), 64.8 (2), 49.61, 49.57, 46.34, 46.32, 44.47, 44.39, 39.18, 39.13, 34.4 (2), 31.0 (2), 30.1 (2), 27.11, 27.09, 26.44, 26.30, 22.6 (2), and 14.5 (2).

IR (neat) 3061 (m), 2957 (m), 2873 (w), 1491 (m), 1205 (m), 1192 (s), 1041 (m), and 814 (m) (s) cm⁻¹

TLC *R_f* = 0.4 in 5:1 hexanes:EtOAc.

HRMS (APCI/TOF) calcd for (M+H)⁺ (C₂₄H₂₉O₃)⁺: 365.2111. Found: 365.2085.

E.5. Procedure for preparation of (3a*S*,3b*R*,11b*S*,13a*S*)-13a-Methyl-2,3,3a,3b,4,5,7,10,11b,12,13,13a-dodecahydro-1*H*-7,10-epoxycyclopenta[*c*]tetraphen-1-one (4-20)



The crude mixture of **4-19** was dissolved in a mixture of THF/H₂O (0.5 mL, 1:1, 0.1 M). Hydrochloric acid (0.5 mL, 1 M) was added and the mixture was stirred at rt for 5 h. The reaction was quenched by adding saturated aqueous sodium bicarbonate. The reaction mixture was extracted with diethyl ether three times and concentrated *in vacuo* to afford the crude mixture, which was purified by MPLC (hexanes/EtOAc = 5:1, 5 mL/min, retention time 15 min) to provide **4-20**.

Yield (72%, 46 mg) (1.2:1 *dr*); White solid.

¹H NMR (CDCl₃, 500 MHz) δ 7.24 (s, 0.45H, Ar—*H*), 7.24 (s, 0.55H, Ar—*H*), 7.02–6.98 [m, 3H, Ar—*H* and CH(O)CH=CH], 5.66 (app s, 2H, CHOCH), 2.86–2.82 (m, 2H, Alkyl-*H*), 2.50 (ddd, *J* = 19.0, 8.7, 2.3 Hz, 1H, Alkyl-*H*), 2.41–2.35 (m, 1H, Alkyl-*H*), 2.27–2.24 (m, 1H, Alkyl-*H*), 2.18–2.10 (m, 1H, Alkyl-*H*), 2.07–1.94 (m, 3H, Alkyl-*H*), 1.63–1.42 (m, 6H, Alkyl-*H*), 0.91 [s, 1.35H, CH(18)₃], and 0.89 [s, 1.65H, CH(18)₃].

¹³C NMR (CDCl₃, 125 MHz) δ 221.1 (2), 146.60, 146.58, 146.44 (2), 143.25, 143.23, 142.99, 142.96, 136.17, 136.07, 133.08, 133.05, 121.58, 121.54, 117.9 (2), 82.57, 82.54, 82.35, 82.27, 50.6 (2), 48.21, 48.19, 44.81, 44.73, 38.51, 38.47, 36.1 (2), 31.8 (2), 30.0 (2), 26.7 (2), 26.23, 26.10, 21.8 (2), and 14.1 (2).

IR (neat) 3053 (m), 2961 (m), 2874 (w), 1631 (w), 1442 (m), 1222 (m), 1191 (m), 1115 (m), 1001 (m), 851 (s), 706 (s), cm⁻¹.

TLC *R*_f = 0.5 in 3:1 hexanes:EtOAc; HRMS (APCI/TOF) calcd for (M+H)⁺(₂₂H₂₅O₂)⁺: 321.1849. Found: 321.1855.

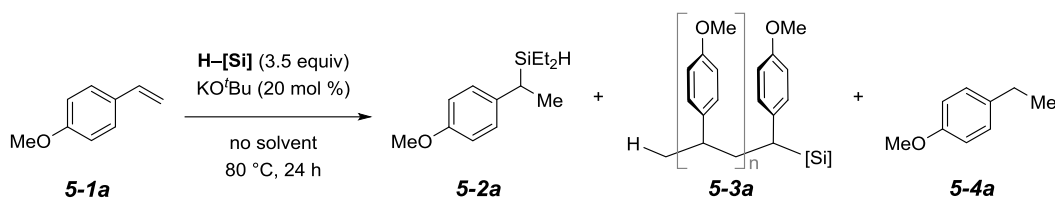
Apendix F

Experimental Procedures for Chapter 5

F.1. Survey of Silanes

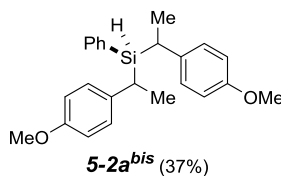
Styrene **5-1a** (0.2 mmol, 28 μ L), silane (3.5 equiv) were added to a 4 mL flame-dried vial. KO^tBu (40 μ L, 1 M in THF, 20 mol %) was added to the mixture. The septum on the vial was replaced by a screw cap with a Teflon liner. The reaction mixture was stirred for 24 h at 23 °C or 80 °C.

Table 4. Survey of Silanes



entry	H-[Si]	5-1a (%) ^a	5-2a (%) ^a	5-3a ^a	5-4a (%) ^a
1	O(SiMe ₂ H) ₂	0	91	nd	5
2	NH(SiMe ₂ H) ₂	100	0	nd	0
3	HSiMe(OTMS) ₂	50	28	yes	1
4	HSiEt ₃	75	1	yes	12
5	HSiPh ₃	60	12	yes	0
6	HSi(OEt) ₃	60	20	yes	0
7	H ₂ SiEt ₂	0	96 (97) ^c	nd	4(3) ^c
8	H ₂ Si ⁱ Pr ₂	0	28	yes	2
9	H ₂ SiPh ₂	0	48	yes	2
10	H ₂ SiMePh	25	68 ^b	yes	3
11 ^d	H ₃ SiPh	0	34	yes	2
12	Me ₃ Si-SiMe ₃	100	0	0	0

^aDetermined by ¹H NMR spectroscopy using mesitylene as internal standard. ^bA diastereomeric mixture of **5-2a** (1:1 *dr*) was formed. ^cReaction at 23 °C for 24 h. ^dBesides monosilylation product **5-2a** a diastereomeric mixture of the disilylation product **5-2a^{bis}** were produced.

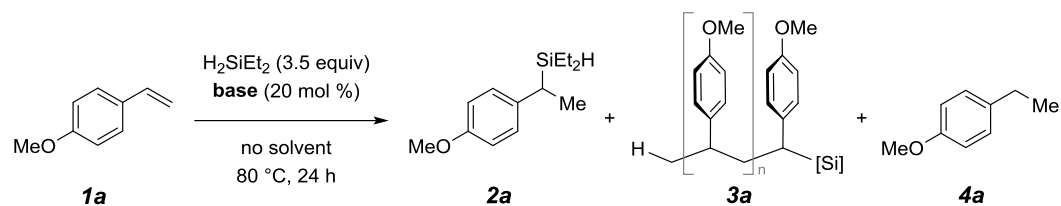


The silane screening showed that smaller and electron-donating hydrosilanes are generally better for the hydrosilylation and required >2 equiv for higher conversion.

F.2. Survey of Lewis Base

Styrene **5-1a** (0.2 mmol, 28 μ L) and diethylsilane (90 μ L, 3.5 equiv) were added to a 4 mL flame-dried vial. Lewis base (20 mol %) was added to the mixture. The septum on the vial was replaced by a screw cap with a Teflon liner. The reaction mixture was stirred for 24 h at 23 $^{\circ}$ C or 80 $^{\circ}$ C.

Table S1. Survey of Metal Lewis Base



entry	base	5-1a (%) ^a	5-2a (%) ^a	5-3a ^a	5-4a (%) ^a
1	LiOH	100	0	-	0
2	NaOH	95	2	-	3
3	KOH	0	93	-	5
4	RbOH	0	0 (43) ^b	-	100 (12) ^b
5	CsOH	0	35	-	64
6	Mg(OH) ₂	100	0	-	0
7	Ca(OH) ₂	0	0	-	0
8	Sr(OH) ₂	100	0	-	0
9	Ba(OH) ₂	0	10	Yes	19
10 ^b	La(O ⁱ Pr) ₃	87	5	-	4
11 ^b	Yb(O ⁱ Pr) ₃	15	27	-	53
12	KOEt	0	91	-	7
13	KO ^t Bu	0	97	-	3
14	KOSiMe ₃	0	95	-	5
15	KN(SiMe ₃) ₂	0	71	-	28
16	K enolate ^c	0	81	-	5
17	KH	0	87	-	7
18	KF	100	0	-	0
19	KCN	100	0	-	0
20	K	0	10	-	18
21	LiOSiMe ₃	96	2	-	2
22	NaOSiMe ₃	100	0	-	0
23	NaO ^t Bu	79	7	-	2
24	NaOEt	95	0	-	1
25	NaH	78	7	-	1

26	Na	5	5	-	6
27 ^d	TBAF	6.5	6.2	Yes	6.7
28	18.crown.6/KO ^t Bu	0	0	Yes	0

^aDetermined by ¹H NMR spectroscopy using mesitylene as internal standard. ^bReaction at 23 °C for 24 h. ^cPotassium 4-ethoxy-4-oxobut-2-en-2-olate. ^dAfter 168 h at 100 °C.

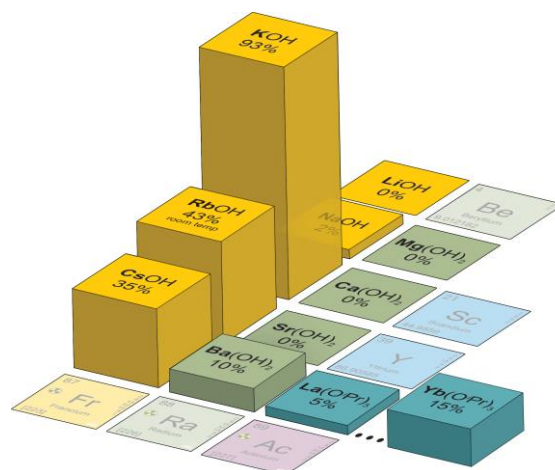
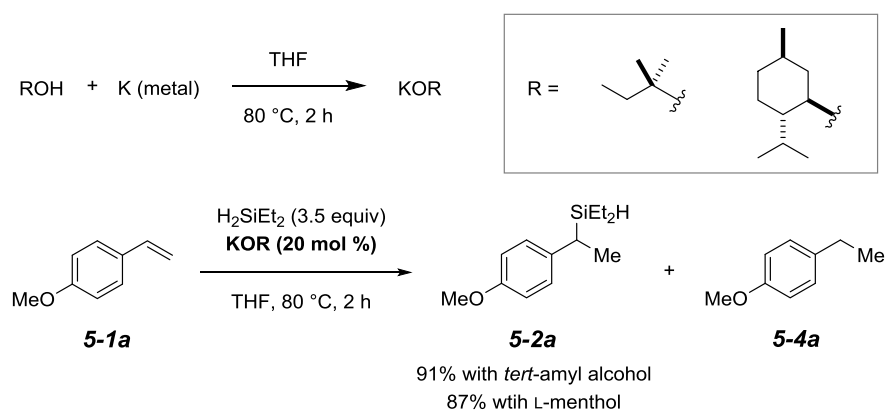


Figure S2. Survey of Lewis base catalysts and impact of cations using metal hydroxide (MOH) for branch-selective Markovnikov olefin silylation. Yields of hydrosilylation product **2a** with MOH (20 mol%) are indicated.

Scheme S1. Preparation of Bulky Potassium Alkoxy Lewis Bases and Use for Branch-Selective, Markovnikov Olefin Hydrosilylation



tert-Amyl alcohol (0.2 mmol) or L-menthol (0.2 mmol), excess potassium and THF (0.1 mL, 2 M) were added to a vial. The reaction mixture was heated at 80 °C for 2 h. The solution was transferred to another vial via syringe. 4-Methoxystyrene **5-1a** (28 μL, 0.2

mmol), H₂SiEt₂ (90 μL, 3.5 equiv), and THF (0.1 mL, 2M) were added to the vial. The reaction mixture was heated at 80 °C for 2 h. The yield of **5-2a**, based on ¹H NMR spectroscopy using an internal standard was 91% and 87% for *tert*-amyl alcohol and L-menthol, respectively, based on ¹H NMR spectroscopy using an internal standard. These results imply that other potassium tertiary alkoxide and bulky secondary alkoxide can serve as an effective Lewis base for the branch-selective, Markovnikov olefin hydrosilylation.

Screening of Lewis base shows the effectiveness of widely-used oxyanions, amide, enolate, and hydride on hydrosilylation of vinylarenes, but not carbanion and fluoride. The LBCI-HAT was generally efficient when the *p*K_a of the corresponding acid of Lewis base was >ca. 11 (e.g., β-keto ester potassium anion entry 16). Among them, KO^tBu was found to be the most effective Lewis base catalyst. Counter cations played a crucial role in promoting and controlling the reaction pathways; while larger alkali metals (i.e., K⁺, Rb⁺, Cs⁺) promote the reaction, small cations (i.e., Li⁺ and Na⁺) were unable to or inefficiently catalyze the reaction (Figure S2).

F.3. Survey of KO^tBu Loading

Styrene **5-1a** (0.2 mmol, 28 μL), diethylsilane (90 μL, 3.5 equiv), and KO^tBu (X mol %) were dissolved in C₆D₆ (0.1 mL), THF (0.3 mL) and internal standard mesitylene (28 μL, 0.2 mmol) were placed in a Norell[®] pressure NMR tube and heated at 80 °C for 24 h.

Table S2. Survey of KO^tBu Loading

Reaction scheme: **5-1a** (4-methoxystyrene) + H₂SiEt₂ (3.5 equiv) + KO^tBu (X mol %) → **5-2a** (4-methoxy-1-methyl-1-(diethylhydro)silylbenzene) in C₆D₆/THF at 80 °C, 24 h.

entry	KO ^t Bu (mol %)	Time (h)	Conv. (%) ^a	5-2a (%) ^a
1	1	40	100	70
2	2	24	100	78
3	5	10	100	81

4	10	6	100	91
5	20	0.5	100	96

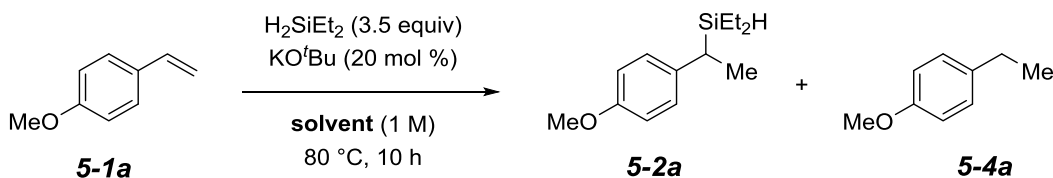
^aDetermined by ¹H NMR spectroscopy using mesitylene as internal standard.

KO^tBu was shown to be most effective Lewis base catalyst, and the catalyst loading can be lowered down to 1 mol%. However, the highest efficiency was achieved with 20 mol% KO^tBu.

F.4. Survey of Solvent

Styrene **5-1a** (0.2 mmol, 28 μ L) and diethylsilane (90 μ L, 3.5 equiv) were dissolved with solvent (0.2 mL, 1M) in a 4 mL flame-dried vial. KO^tBu (40 μ L, 1 M in THF, 20 mol %) was added to the mixture. The septum on the vial was replaced by a screw cap with a Teflon liner. The reaction mixture was stirred for 10 h at 80 °C.

Table S3. Survey of Solvent



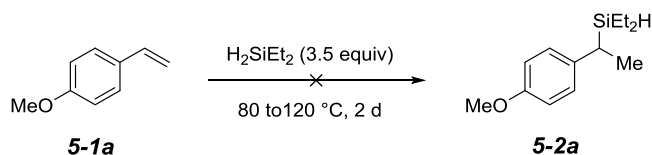
entry	Solvent Snyder polarity index ^a	5-1a (%) ^b	5-2a (%) ^b	5-4a (%) ^b
1	neat	0	97	3
2	hexanes (0.1)	0	94	6
3	toluene (2.4)	0	94	6
4	Et ₂ O (2.8)	0	97	3
5	benzene (3.0)	0	96	4
6	THF (4.0)	0	94	7
7	1,4-dioxane (4.8)	0	90	7
8	DME(NA) ^c	100	0	0
9	DMF (6.4)	100	0	0
10	DMSO (7.2)	82	0	0

^a See reference ²⁵⁶. ^bDetermined by ¹H NMR spectroscopy using mesitylene as internal standard. ^cDME: 1,2-dimethoxyethylene.

We found that solvent is indeed not necessary which fits well with perspective of development of a sustainable chemical process. If needed, non-polar solvents that have Snyder polarity index < ca. 5 were generally better with higher concentration >1 M. as shown in Table S3. Choice of temperature (23 °C to 120 °C) was dependent on substrates (steric and electronics).

F.5. Control Experiments in the Absence of KO^tBu

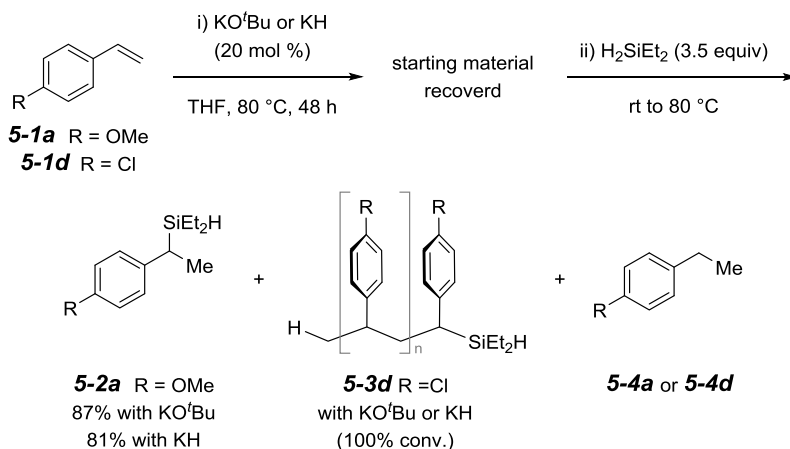
Scheme S2. Control Experiments in the Absence of KO^tBu



4-Methoxystyrene (**5-1a**, 28 μL , 0.2 mmol) and diethylsilane (90 μL , 3.5 equiv) were placed in a flame-dried vial. The septum on the vial was replaced by a screw cap with a Teflon liner. The mixture was stirred at 80 °C for 1 d. No desired product was observed. The reaction mixture was warmed to 120 °C and stirred for 2 d. No desired product **2a** was observed and **5-1a** was cleanly recovered.

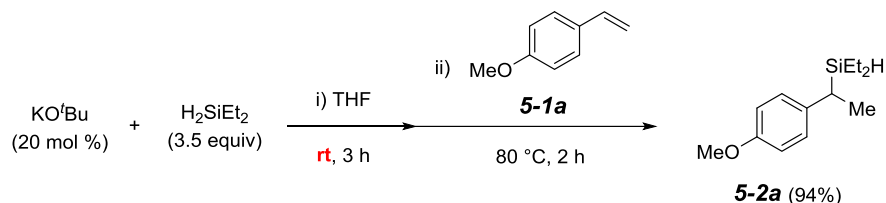
F.6. Effects of the Order of Addition of Reagents and Catalyst

Scheme S3. Effects of the Order of Addition of Reagents and Catalyst: Olefin–Lewis Base–Silane



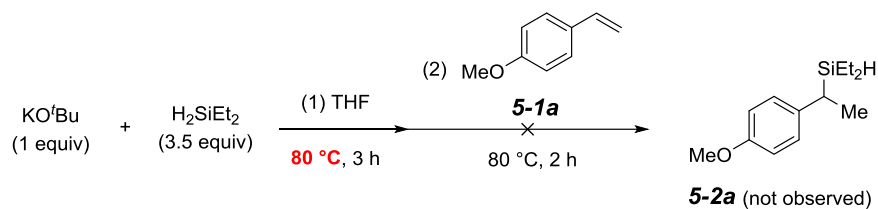
KO^tBu (40 μ L, 1 M in THF, 20 mol %) or KH (2 mg, 20 mol %) and styrene (**5-1a** or **5-1w**, 0.2 mmol) were placed in a flame-dried vial. The septum on the vial was replaced by a screw cap with a Teflon liner and the mixture was heated at 80 °C. [Note: THF (0.2 mL, 1M) was used when KH was used as Lewis base.] After being stirred for 2 d, styrenes were cleanly recovered and no obvious polymerization was observed. Then diethylsilane (90 μ L, 3.5 equiv) was added to the reaction mixture which was stirred for 16 h at rt (with KO^tBu) or for 3 h at 80 °C (with KH), to produce the corresponding hydrosilylation products **5-2a** (87% yield, 100% conversion with KO^tBu; 81%, 100% conversion with KH) based on ¹H NMR spectroscopy using an internal standard or styrene polymer **5-3w** with 100% conversion with KO^tBu or KH.

Scheme S4. Effects of the Order of Addition of Reagents and Catalyst: Lewis Base–Silane–Olefin



KO^tBu (40 μ L, 1 M in THF, 20 mol %) and diethylsilane (90 μ L, 0.7 mmol) were placed in a flame-dried vial. The septum on the vial was replaced by a screw cap with a Teflon liner. The mixture was stirred at rt for 3 h. 4-methoxystyrene **5-1a** (28 μ L, 0.2 mmol) was added into the solution. The reaction mixture was heated at 80 °C for 2 h to afford **5-2a** (94% yield) based on ¹H NMR spectroscopy using an internal standard.

Scheme S5. Effects of the Order of Addition of Reagents and Catalyst: Lewis Base–Silane–heating–Olefin



KO^tBu (0.2 mL, 1 M in THF, 100 mol %) and diethylsilane (90 μ L, 0.7 mmol) were placed in a flame-dried vial. The septum on the vial was replaced by a screw cap with a Teflon liner. The mixture was stirred at 80 °C for 3 h, and **5-1a** (28 μ L, 0.2 mmol) was added into the solution. The reaction mixture was heated at 80 °C for 2 h. The reaction resulted in a complex mixture and no desired product **5-2a** was observed.

During a series of experiments in Scheme S3 to Scheme S5, no obvious color change of the reaction mixture from a combination of KO^tBu/diethylsilane, KO^tBu/vinylarene (i.e., **5-1a**), or vinylarene/diethylsilane was observed in a wide range of

temperatures (23 °C to 120 °C). However, as soon as the three components (i.e., vinylarene, KO^tBu and diethylsilane) were all present in the solution, yellow, brown, or intense red color appeared, depending upon the nature of vinylarenes and the reaction concentrations. It suggests that the reaction might involve anion or radical-mediated processes.

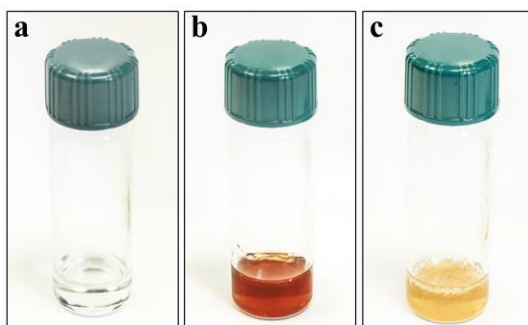
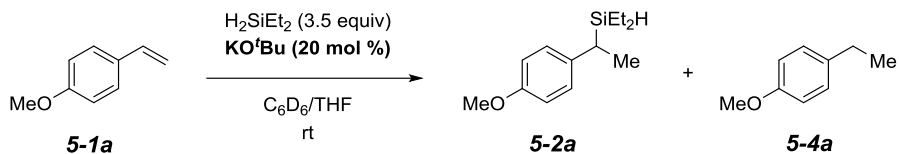


Figure S3. Reaction Color Change at Various Stages of Olefin Hydrosilylation. **a**, Mixture of diethylsilane and vinylarene (e.g., 4-methoxystyrene). **b**, Color changes to red after addition of KO^tBu. **c**, Discharge of color after exposure to air.

To summarize, the reaction is insensitive to the order of addition of reagent and catalyst. However, the premature heating of the reaction mixture of Lewis base and hydrosilane, prior to the addition of olefin, did not produce the hydrosilylation product, likely due to the consumption of the Lewis base and some of the hydrosilane by a formation of disiloxane (See Figure 5-8, Figure 5-9).

F.7. Control Reactions with KO^tBu of Different Grades from Various Vendors

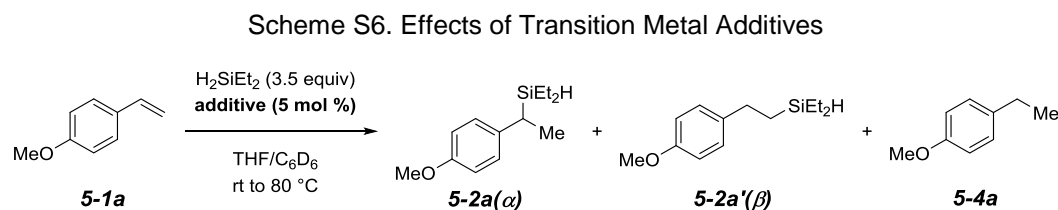
Table S4. The conversion with various vendors of KO^tBu monitored by NMR spectroscopy



entry	KO ^t Bu	Vendor	0.5h	1h	1.2h	4h	8h	18h	28h	84h	120h
1	98% in THF 99.99%	Acros	67	100							
2	solid (sublimated)	Aldrich	32	63	69	88	100				
3	98% in solid	Aldrich	1	3	6	12	25	47	64	94	100
4	95% in solid	Aldrich	0	0	0	0	2	9	16	50	60

4-Methoxystyrene **5-1a** (28 μ L, 0.2 mmol), H₂SiEt₂ (90 μ L, 3.5 equiv), C₆D₆ (0.1 mL), THF (0.2 mL, 1 M) and internal standard mesitylene (28 μ L, 0.2 mmol) were placed in a Norell[®] pressure NMR tube. Then, KO^tBu (20 mol %) from various sources was added to the NMR tubes. The NMR tubes were kept at rt and the conversion was monitored by ¹H NMR spectroscopy over time. Different purities of KO^tBu gave different kinetic profiles. For example, KO^tBu (98%, 1 M in THF), sublimated (99.99%), 98% in solid and 95% in solid completed the olefin hydrosilylation in 1 h, 8 h, 120 h and 200 h, respectively (Table S4). However, the overall yield and selectivity were virtually identical.

F.8. Control experiments with various transition metals



To address the question as to whether this reaction is simply mediated by trace metals, many transition-metals were examined in the absence of KO^tBu.

No reaction occurred with transition metals such as Sc(OTf)₃, Ti(OⁱPr)₄, V₂O₅, Cr(acac)₃, MnO₂, FeSO₄•7H₂O, FeCl₃•6H₂O, Co(acac)₂, CuBr, CuI, ZnCl₂•4H₂O, RuCl₃•6H₂O at rt or elevated temperatures for 24 h.

Other metal salts such as Pd, Rh, Ir, and Pt exhibited slow conversion with poor site selectivity. For instance, i) Pd(OAc)₂ [at 80 °C for 24 h, 28% conversion, **5-2a**(α): **5-4a**: **5-2a'**(β)=19:1:9], ii) [Rh(nbd)Cl]₂ [at 80 °C for 24 h, 18% conversion, **5-2a**(α): **5-4a**: **5-2a'**(β)=4:7:7], iii) [Ir(coe)₂Cl]₂ (at 80 °C for 24 h, 19% conversion, only **5-4a**), and iv) Pt(dvds)₂ [at 80 °C for 24 h, 33% conversion, **5-2a**(α) **5-4a**: **5-2a'**(β)=13:5:15].

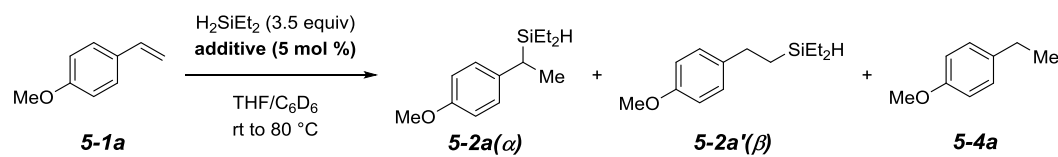
While NiCl₂•6H₂O provided the full conversion (rt, 17 h) favoring the Markovnikov product [**5-2a**(α) **5-2a'**(β) = 3.3:1], Ni(OAc)₂•4H₂O [the full conversion (rt, 36 h)] produced the *anti*-Markovnikov product as major [**5-2a**(α): **5-2a'**(β) = 1:1.5].

In summary, a trace amount of transition metals unlikely catalyzes the proposed highly branch-selective, Markovnikov hydrosilylation.

F.9. Investigation of Mechanism Involving Hydrogen Atom Transfer (HAT) Effect of Additives

Styrene **5-1a** (0.2 mmol, 28 μL), diethylsilane (90 μL, 3.5 equiv), and an additive were added to a 4 mL flame-dried vial. KO^tBu (40 μL, 1 M in THF, 20 mol %) was added to the mixture. The septum on the vial was replaced by a screw cap with a Teflon liner. The reaction mixture was stirred for 18 h at 80 °C.

Table S5. Effect of Additives



Entry	additive (equiv)	5-1a (%) ^a	5-2a (%) ^a	5-4a (%) ^a
1	H ₂ O (0.1)	0	91	9
2	H ₂ O (2.0)	0	74	10
3	H ₂ O (4.0)	35	18	13
4	BHT (0.1)	97	0	3
5	BHT (0.2)	100	0	0
6	O ₂ (2.2 mL, 0.5)	84	0	0

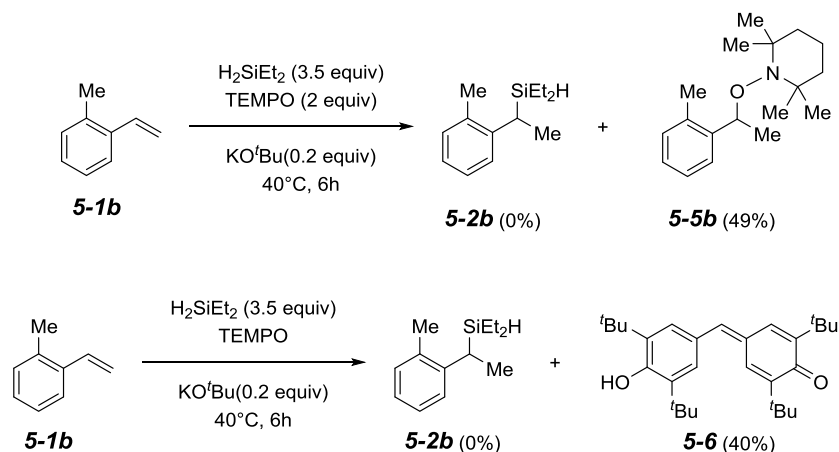
7	TEMPO (0.1)	0	90	4
8	TEMPO (0.2)	0	84	5
9	TEMPO (0.5)	0	65	6
10	TEMPO (1)	0	34	6
11 ^b	TEMPO (2)	0	0	6
12	Galvinoxyl (0.2)	70	20	6
13	Galvinoxyl (1)	80	0	0
14	in dark	0	95	3

^aDetermined by ¹H NMR spectroscopy using mesitylene as internal standard. ^bThe

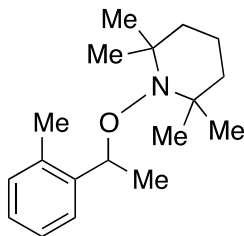
adduct produced from the reaction of TEMPO and 4-methoxystyrene was observed (47% isolation yield). For details, see Scheme S6.

Additives were examined in this reaction. A proton donor such as H₂O did not shut down the reaction, but it lowered the yield. But a radical scavenger such as 2,6-di-*tert*-butyl-4-methylphenol (0.1 and 0.2 equiv) completely shut down the reaction. O₂ (0.5 equiv) also prevented the reaction. The reaction was shut down completely when TEMPO (2 equiv) or Galvinoxyl radical (1 equiv) was used. In case of TEMPO, **5-5b** (47%; for details, see Scheme S7) was obtained, which indicates a formation of benzylic radical intermediate. The addition of galvinoxyl radical resulted in formation of **5-6** (40%) which presumably signifies formation of hydrogen atom radical (Scheme S7).

Scheme S7. Additions of TEMPO and Galvinoxyl Radicals.



2,2,6,6-Tetramethyl-1-[1-(*o*-tolyl)ethoxy]piperidine (5-5b)



Yield: 0.4 mmol scale, 135 mg, 49%. (White solid, Melting point: 56-59 °C).

¹H NMR (CDCl₃, 500 MHz): δ 7.44 (d, *J* = 7.7 Hz, 1H, Ar-*H*), 7.21 (dd, *J* = 7.7, 7.3 Hz, 1H, Ar-*H*), 7.13 (dd, *J* = 7.5, 7.3 Hz, 1H, Ar-*H*), 7.09 (d, *J* = 7.5 Hz, 1H, Ar-*H*), 5.00 [q, *J* = 6.6 Hz, 1H, Ar-CH(OR)Me], 2.33 (s, 3H, Ar-CH₃), 1.45 [d, *J* = 6.6 Hz, 3H, CH(OR)CH₃], 1.33 [br s, 3H, ONC(CH₃)₂], 1.19 [br s, 3H, ONC(CH₃)₂], 1.03 [br s, 3H, ONC(CH₃)₂], and 0.71 [br s, 3H, ONC(CH₃)₂].

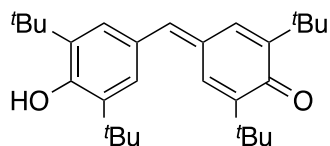
¹³C NMR (CDCl₃, 125 MHz): δ 144.9, 133.8, 130.1, 126.51, 126.48, 126.1, 80.6, 59.9, 59.6, 40.5 (2), 34.8, 33.6, 23.1, 20.61, 20.46, 19.5, and 17.4.

IR (neat): 2953 (s), 2870 (s), 1707 (s), 1462 (m), 1361 (m), 1062 (s), and 758 (s) cm⁻¹.

TLC: R_f = 0.5 in 20:1 hexanes:EtOAc.

HRMS (APCI/TOF): Calcd for (M+H)⁺ (C₁₈H₃₀NO)⁺: 276.2322. Found: 276.2315.

2,6-Di-*tert*-butyl-4-(3,5-di-*tert*-butyl-4-hydroxybenzylidene)cyclohexa-2,5-dienone (5-6)



Yield: 0.4 mmol scale, 67 mg, 40%. (Yellow solid, Melting point: 156-158 °C).

Yellow solids

¹H NMR (CDCl₃, 500 MHz): δ 7.61 (d, *J* = 2.3 Hz, 1H, Ar-*H*), 7.36 [s, 2H, C(*t*Bu)CH], 7.17 (s, 1H, Ar-CH=C), 7.01 (d, *J* = 2.3 Hz, 1H, Ar-*H*), 5.56 (s, 1H, OH), 1.48 [s, 18H, (CH₃)₃], 1.334 [s, 9H, (CH₃)₃], and 1.327 [s, 9H, (CH₃)₃].

¹³C NMR (CDCl₃, 125 MHz): δ 186.7, 155.7, 149.0, 147.1, 144.7, 136.6, 135.9, 130.1, 128.39, 128.36, 127.8, 35.7, 35.2, 34.6, 30.5, 29.88, and 29.74.

IR (neat): 3629 (m), 2954 (m), 2868 (m), 1632 (m), 1610 (s), 1551(s), 1435 (s), 1359 (s), 1213 (s), 887 (s), and 502 (m) cm⁻¹.

TLC: R_f = 0.5 in 20:1 hexanes:EtOAc.

HRMS (APCI/TOF): Calcd for (M+H)⁺ (C₂₉H₄₃O₂)⁺: 423.3258. Found: 423.3246.

F.10. Studies on Potassium Cation- π Interaction

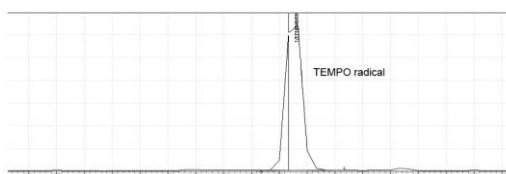
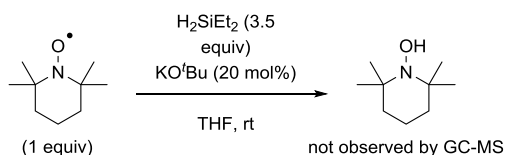
To investigate the interaction of K⁺ and π system which is likely essential for the homolytic cleavage of Si-H bond within pentavalent silicate for the LBCI-HAT, the following experiments were carried out. We hypothesized that the reduction of TEMPO radical can be utilized as an indicator of HAT. 1) The first experiment performed was whether the HAT occurs in the absence of π system. A solution of TEMPO radical (0.2 mmol, 31 mg, 1 equiv) in THF (0.2 mL, 1 M) was added to a flame-dried vial under nitrogen atmosphere. Then, H₂SiEt₂ (3.5 equiv) and KO^tBu (20 mol %) were added to the mixture (Fig. S3a). 2) The second experiment was carried out in presence of vinylarene **5-1a** (0.2 mmol, 27 μ L) (Fig. S3b). 3) In the third experiment, 18-crown-6 (20 mol%) was added to a mixture of KO^tBu, H₂SiEt₂, and TEMPO (Fig. S3c).

The TEMPO free radical (retention time = 3.78 min) and its reduced form (H-TEMPO, retention time = 3.67 min) are easily distinguishable on GC-MS spectrometry. In the studies, the formation of the reduced TEMPO in the absence of styrene was generally negligible (Fig. S3a). However, the presence of vinylarene **5-1a** in the reaction triggered the formation of the reduced TEMPO (Fig. S3b). The most noticeable result (Fig. S3c) was that more reduced TEMPO was observed vis-à-vis Fig. S3b, when 18-crown-6 was added in the absence of **5-1a**. We presume that the stronger interaction of K⁺ with the crown ether

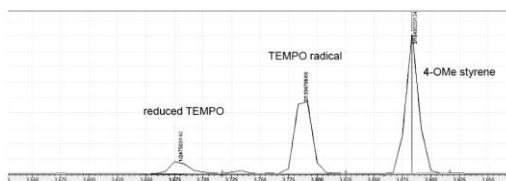
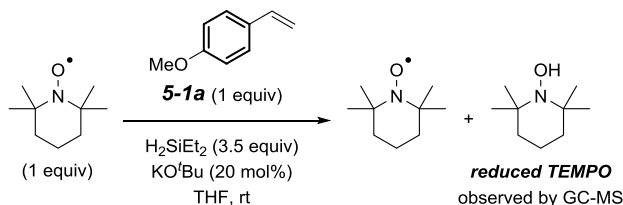
(cf., vinylarene) allows more facile HAT under the reaction conditions. These series of experiments suggest that the LBCI-HAT is essentially associated with the cation- π or cation- n interaction.

During the experiments, H_2 evolution was observed in the beginning phase of the reaction.²¹³ These results are consistent with the previous report of KO^tBu -catalyzed cross-dehydrogenative heteroarene C–H silylation, which shares virtually identical reaction parameters with the LBCI-HAT.²¹³ In the report, the initial H_2 formation is related to minor quantity of water.²²⁸ Therefore, with supports of the NMR spectroscopic experiments concerning the LB-mediated silane ligand exchange

a Absence of activators (i.e., π donors, coordinating agents): No HAT occurred.



b Addition of styrene as a π donor: HAT was initiated via the $K^+ - \pi$ interaction.



c Addition of crown ether: HAT was initiated via $K^+ - n$ interaction.

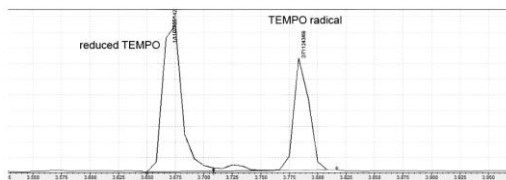
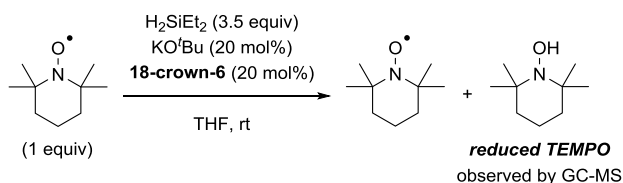


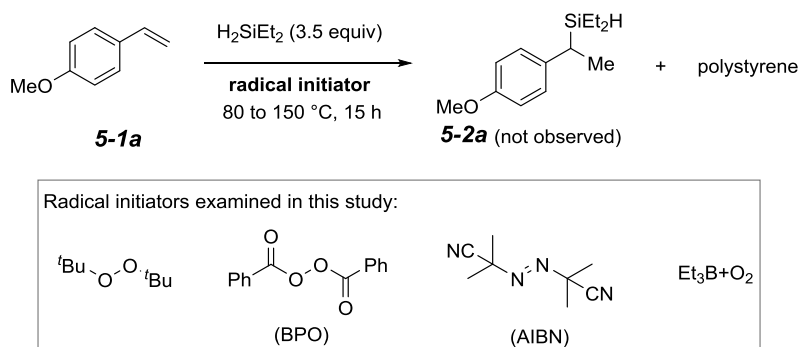
Figure S4. Hydrogen Atom Trapping Experiments for Elucidating Potassium Cation- π Interaction in the LBCI-HAT, Monitored by GC-MS Spectrometry. **a**, The reaction of H_2SiEt_2 with KO^tBu in the presence of TEMPO radical. **b**, The reaction of H_2SiEt_2 and KO^tBu with 4-methoxystyrene in the presence of TEMPO radical. **c**, The reaction of H_2SiEt_2 and KO^tBu with 18-crown-6 in the presence of TEMPO radical.

in Figure 5-8 and Figure 5-9, the reaction between metal hydride and residual water in the reaction can be responsible for the production of H₂ in the beginning phase of the LBCI-HAT. Alternatively, the generation of H₂ and silylpotassium species can also be possible within the coordination sphere of hypercoordinate silicon species.²²² Further efforts toward elucidating the dehydroeogenation mechanism are currently underway.

F.11. Mechanism Involving Silyl Radicals

While the radical polymerization of styrenes have been well established, we added several radical initiators to our reaction conditions in the absence of KO^tBu. Radical Initiators such as di-*tert*-butyl peroxide, benzoyl peroxide (BPO), AIBN, triethylborane with O₂, and potassium were examined, which led to the polymerization of styrene as the major product and a trace amount of the desired compound **5-2a**.

Scheme S8. Survey of Different Radical Initiators for Generation of Silyl Radicals



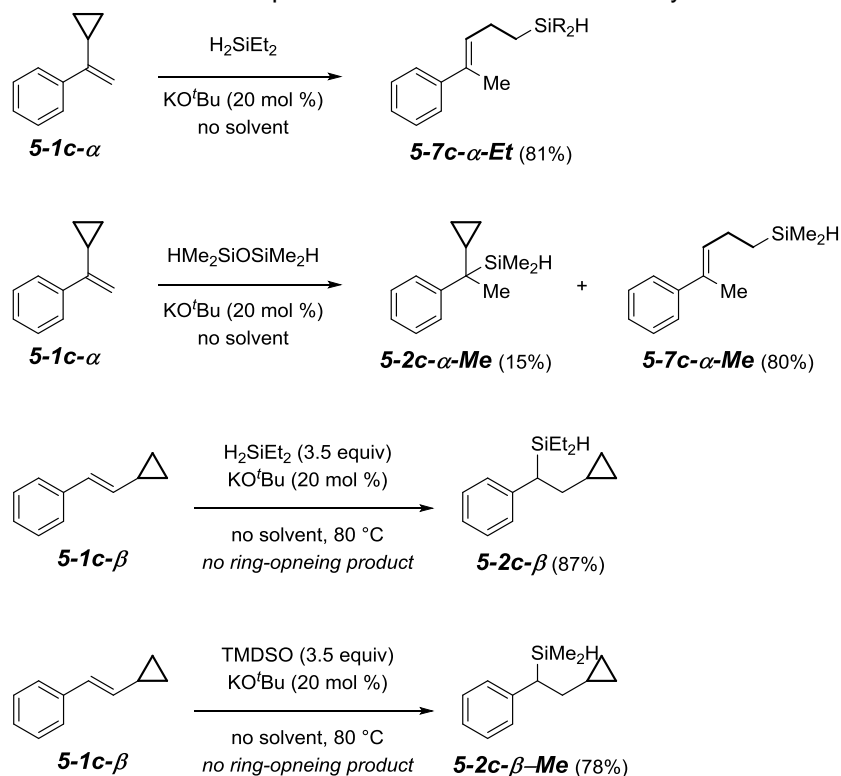
These series of the reactions (Schemes S5 to S7) indicate that our catalytic hydrosilylation with KO^tBu and hydrosilane involves a radical process, either HAT or silyl radical transfer to alkene. We speculate that HAT (Galvinoxyl trapped hydrogen atom, see Scheme S7) first and likely produces benzylic radical with vinylarene (see the TEMPO experiment, see Scheme S7), and a subsequent silyl group transfers. Because the silyl radical transfer mechanism should exclusively lead to the formation of *anti*-Markovnikov

hydrosilylation product. In addition, when the free radical polymerization experiment was designed to produce silyl radical which can react with vinylarene, we did not observe either Markovnikov or *anti*-Markovnikov hydrosilylation products. The result suggested that the silyl radical transfer is unlikely responsible for the initial stage of our transition metal-free hydrosilylation involving the Lewis base-catalyzed, complexation-induced hydrogen atom transfer (LBCI-HAT) to olefins, which leads to the formation of the Markovnikov hydrosilylation product.

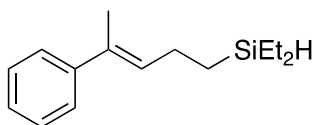
F.12. Radical Clock Experiments

When **5-1c- α** was treated with diethylsilane and KOtBu at 80 °C, the cyclopropyl ring was opened to form the rearranged product **5-7c- α -Et** in 81% isolation yield, indicating a benzylic radical was, indeed, involved in the reaction. When HMe₂SiOSiMe₂H (TMDSO) was used, the non-rearranged benzylic radical was kinetically trapped to afford **5-2c- α -Me** (15% isolation yield) along with the rearranged adduct **5-7c- α -Me** (80% isolation yield). The occurrence of the rearrangement adduct is indicative of the presence of the benzylic radical species, produced through a preceding HAT to the β -position of styrene. A control experiment with β -cyclopropyl styrene **5-1c- β** clearly demonstrated the preceding HAT occurs at β -position **5-2c- β** . (Scheme S9)

Scheme S9. Radical Clock Experiments and LBCI-HAT with Alkyl-Substituted Alkenes



(E)-Diethyl(4-phenylpent-3-en-1-yl)silane (5-7c-α-Et)



Yield: 0.2 mmol scale, 38 mg, 81%.

$^1\text{H NMR}$ (CDCl_3 , 500 MHz): δ 7.41-7.38 (d, $J = 8.0$ Hz, 2H, Ar- H), 7.34-7.31 (dd, $J = 8.0$, 7.4 Hz, 2H, Ar- H), 7.23 (dd, $J = 7.4$, 7.4 Hz, 1H, Ar- H), 5.83 [tq, $J = 7.1$, 1.3 Hz, 1H, C(Me)=CHCH $_2$], 3.74 (triplet of pent, $J = 3.2$, 3.2 Hz, 1H, Si- H), 2.29 [td, $J = 7.1$, 7.1 Hz, 2H, C(Me)=CHCH $_2$ CH $_2$], 2.05 [app s, 3H, Ar-C(CH $_3$)], 1.03 [t, $J = 7.9$ Hz, 6H, Si(CH $_2$ CH $_3$) $_2$], 0.83-0.78 [nfom, 2H, CH $_2$ (SiEt $_2$ H)], and 0.65 [qd, $J = 7.9$, 3.2 Hz, 4H, Si(CH $_2$ CH $_3$) $_2$].

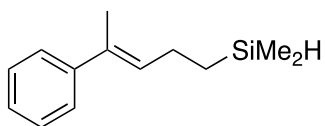
¹³C NMR (CDCl₃, 125 MHz): δ 144.2, 133.7, 131.2, 128.3, 126.6, 125.8, 24.0, 15.9, 11.0, 8.4, and 3.1.

IR (neat): 2955 (m), 2173(w), 1720 (m), 1447 (w), 1253 (s), 1027 (s), and 699 (s) cm⁻¹.

TLC: R_f = 0.6 in hexanes.

HRMS (APCI/TOF): Calcd for (M+H)⁺ (C₁₅H₂₅Si)⁺: 223.1720. Found: 223.1732.

(E)-Dimethyl(4-phenylpent-3-en-1-yl)silane (5-7c-α-Me)



Yield: 0.2 mmol scale, 33 mg, 80%.

¹H NMR (500 MHz): δ 7.38 (ddd, *J* = 7.0, 1.4, 1.4 Hz, 2H, Ar-*H*), 7.31 (app t, *J* = 7.3 Hz, 2H, Ar-*H*), 7.21 (dddd, *J* = 7.2, 7.2, 1.4, 1.4 Hz, 1H, Ar-*H*), 5.81 [tq, *J* = 7.1, 1.3 Hz, 1H, Ar-C(Me)CH], 3.92 (triplet of septet, *J* = 3.6, 3.6 Hz, 1H, Si-*H*), 2.27 (dt, *J* = 7.1, 7.1 Hz, 2H, C=CHCH₂), 2.03 (app s, 3H, Ar-CCH₃), 0.80-0.75 [nfom, 2H, CH₂(SiMe₂H)], and 0.12 [d, *J* = 3.6 Hz, 6H, Si(CH₃)₂].

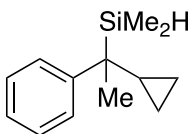
¹³C NMR (CDCl₃, 125 MHz): δ 144.2, 133.7, 131.1, 128.4, 126.6, 125.8, 23.7, 15.9, 14.5, and -4.1.

IR (neat): 2953 (m), 2176(w), 1722 (m), 1447 (w), 1255 (s), 1027 (s), and 701 (s) cm⁻¹.

TLC: R_f = 0.6 in hexanes.

HRMS (APCI/TOF): Calcd for (M+H)⁺ (C₁₃H₂₁Si)⁺: 205.1407. Found: 205.1410.

(1-Cyclopropyl-1-phenylethyl)dimethylsilane (5-2c-α-Me)



Yield: 0.2 mmol scale, 6 mg, 15%.

¹H NMR (500 MHz): δ 7.37-7.25 (m, 5H, Ar-*H*), 3.96 (septet, $J = 3.5$ Hz, 1H, Si-*H*), 1.89 (app t, $J = 7.2$ Hz, 1H, cyclopropyl-*H*), 1.78 (dddd, $J = 14.3, 11.8, 7.2, 5.1$ Hz, 1H, cyclopropyl-*H*), 1.62 (dddd, $J = 14.3, 11.9, 7.2, 5.1$ Hz, 1H, cyclopropyl-*H*), 1.46 [s, 3H, C(Si)CH₃], 0.93 (dddd, $J = 14.5, 11.9, 5.1, 3.0$ Hz, 1H, cyclopropyl-*H*), 0.80 (dddd, $J = 14.5, 11.8, 5.1, 3.0$ Hz, 1H), and 0.15 [d, $J = 3.5$ Hz, 6H, Si(CH₃)₂].

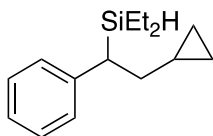
¹³C NMR (CDCl₃, 125 MHz): δ 143.5, 128.9, 128.6, 127.2, 40.2, 38.4, 20.8, 19.7, 13.6, and -4.3.

IR (neat): 2872 (m), 2109 (m), 1598 (m), 1247 (s), 1165 (w), 1031 (m), 871 (s), 836 (s), and 516 (m) cm⁻¹.

TLC: R_f = 0.6 in hexanes.

HRMS (APCI/TOF): Calcd for (M+H)⁺ (C₁₃H₂₁Si)⁺: 205.1417 Found: 205.1426.

(2-Cyclopropyl-1-phenylethyl)diethylsilane (5-2c- β)



Yield: 195 mg, 87%. (colorless liquid).

¹H NMR (CDCl₃, 500 MHz): δ 7.26-7.22 (m, 2H, Ar-*H*), 7.14-7.08 (m, 3H, Ar-*H*), 3.67 (dddd, $J = 3.5, 3.5, 3.5, 3.5, 3.5$ Hz, 1H, Si-*H*), 2.37 [ddd, $J = 10.8, 4.5, 3.5$ Hz, 1H, C(Si)HCH₂], 2.05 [ddd, $J = 14.1, 10.8, 5.2$ Hz, 1H, C(Si)HCH_aH_b], 1.33 [ddd, $J = 14.1, 8.4, 4.5$ Hz, 1H, C(Si)HCH_aH_b], 0.96 (dd, $J = 8.0, 8.0$, 3H, SiCH₂CH₃), 0.87 (dd, $J = 8.0, 8.0$, 3H, SiCH₂CH₃), 0.67 (dddd, $J = 13.2, 10, 8.4, 5.2, 5.0$ Hz, 1H, cyclopropyl-*H*), 0.64-0.53 [m, 2H, Si(CH_aH_bCH₃)], 0.50 [dq, $J = 14.9, 8.0, 3.5$ Hz, 1H, Si(CH_aH_bCH₃)], 0.44 [dq, $J = 14.9, 8.0, 3.5$ Hz, 1H, Si(CH_aH_bCH₃)], 0.38-0.31 (nfom, 2H, cyclopropyl-*H*), and 0.06-0.04 (m, 2H, cyclopropyl-*H*).

¹³C NMR (CDCl₃, 125 MHz): δ 144.4, 128.4, 128.1, 124.7, 36.8, 33.6, 11.2, 8.4, 5.3, 4.7, 2.1, and 1.7.

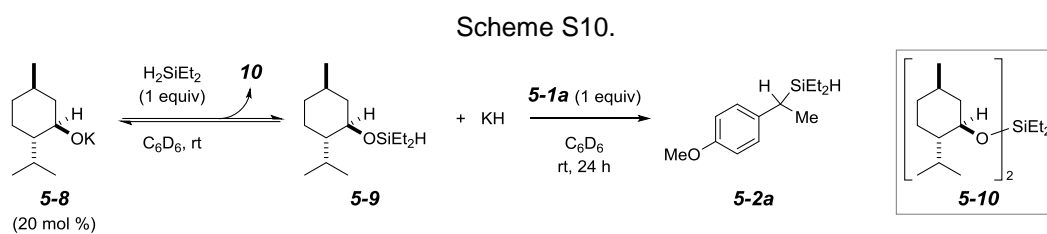
IR (neat): 2953 (m), 2874 (m), 2098 (m), 1599 (w), 1490 (w), 1234 (s), 1011 (s), 808 (s), 697 (s) and 522 (m) cm⁻¹.

TLC: $R_f = 0.9$ in 80:1 hexanes:EtOAc.

HRMS (APCI/TOF): Calcd for $(M+H)^+$ ($C_{15}H_{25}Si$): 233.1720. Found: 233.1715.

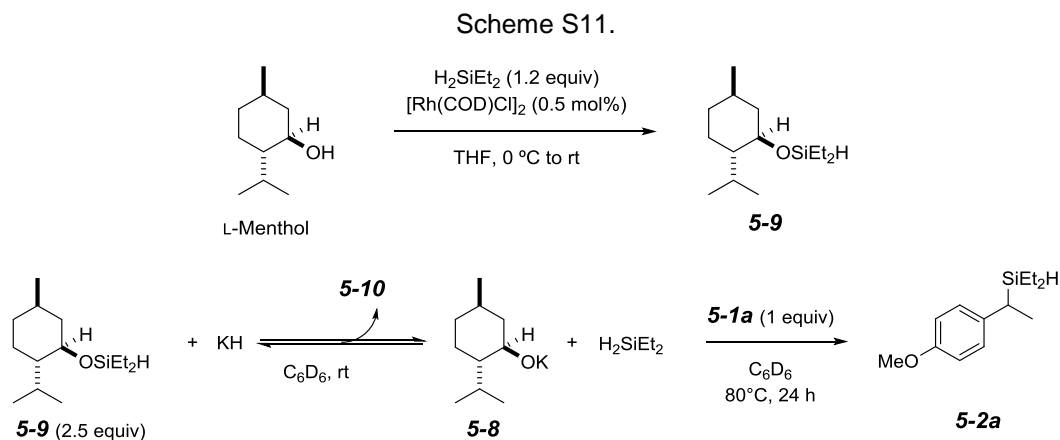
F.13. NMR Studies

Procedure for preparation of potassium L-mentholate and the corresponding 1H NMR study



In a flame dried vial, L-menthol (39.1 mg, 0.25 mmol) was dissolved in C_6D_6 (0.6 ml). Potassium metal (ca. 40 mg, ca. 1 mmol) was added at 0 °C. The septum on the vial was replaced by a screw cap with a Teflon liner, and the mixture was heated to 80 °C for 3 h. The solution was transferred to a Norell® pressure NMR tube. Reaction progress was monitored by 1H NMR spectroscopy.

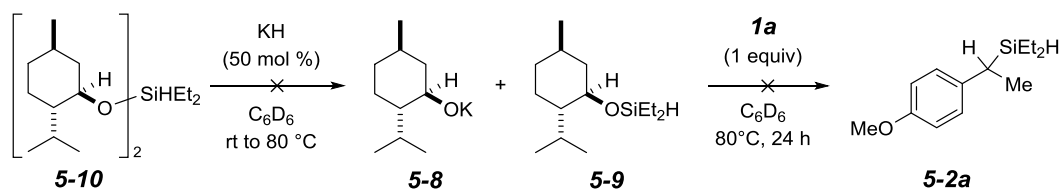
(a) Procedure for preparation of L-menthylsilane and the corresponding 1H NMR study



L-Menthol (781 mg, 5 mmol) and $[\text{Rh}(\text{COD})\text{Cl}]_2$ (5.0 mg, 0.5 mol%) were dissolved in THF (0.5 M). H_2SiEt_2 was slowly added at 0 °C, the mixture was warmed to rt. After completion of the alcoholysis, the volatiles were removed *in vacuo* and compound **5-9** was kept at -20 °C. A Norell® pressure NMR tube was purged with N_2 , and menthylsilane **5-9** (150 μL , 0.5 mmol) and C_6D_6 (0.6 ml) were added. The NMR tube was cooled to 0 °C and KH (4 mg, 0.1 mmol) was added. The mixture was warmed to rt, and the reaction progress was monitored by ^1H NMR spectroscopy.

Procedure for examining the reversibility of silaketal **5-10** to identify a Lewis base catalyst consuming route by ^1H NMR spectroscopy

Scheme S12.



A Norell® pressure NMR tube was purged with N_2 and silaketal **5-10** (80 mg, 0.2 mmol) and C_6D_6 (0.6 mL) were added. The NMR tube was cooled to 0 °C and KH (4 mg, 0.1 mmol) was added. The mixture was warmed to rt, then 80 °C. The reaction progress was monitored by ^1H NMR spectroscopy.

(b) Detection of intermediates reaction with TMDSO

Potassium mentholate was prepared same as part (a) and was transferred to a Norell® pressure NMR tube. Tetramethyldisiloxane (1 equiv) was added to the tube. After heating the mixture to 80 °C, formation of H_2SiMe_2 was observed by ^1H NMR spectroscopy.

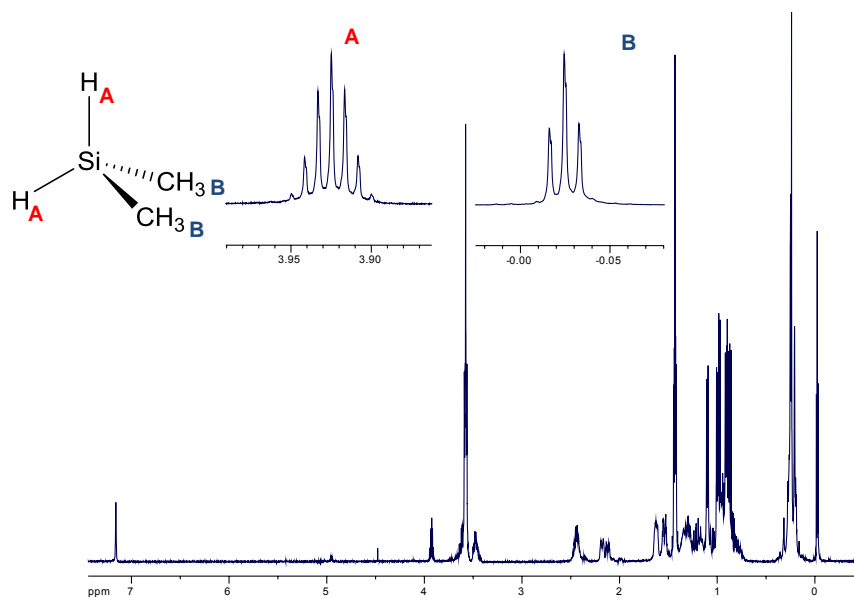


Figure S5.

F.14. EPR Spectroscopy Procedure

In these experiments, solutions containing 4-methoxystyrene **5-1a** (14 μL , 0.1 mmol), H_2SiEt_2 (45 μL , 3.5 equiv), and galvinoxyl-H (**6**) (10 mol %) in THF (0.4 mL) were added to a N_2 -purged, 4 mm quartz EPR tube (Wilmad-Labglass p/n 707-SQ-250M). Baseline measurements were made to ensure that no radical species were present in the starting reagents prior to initiating the reaction by addition of KO^tBu (20 μL , 1 M in THF, 20 mol %) via a 50 mL Hamilton gastight syringe. Following initiation of HAT reactions, the EPR spectrometer was quickly re-tuned and spectra were collected at selected time points to monitor the progress of the reaction.

Instrumental conditions: temperature, 293 K; microwave frequency, 9.641 GHz; microwave power, 200 μW ; modulation amplitude, 0.1 mT. Simulation parameters: *Sim1*, $g_{\text{iso}} = 2.0054$; I_1 , 1/2; # I_1 , (2); $A_{\text{iso}} = 4.5$ MHz (0.16 mT); $s_{\text{B}} = 0.01$ mT. *Sim5*, $g_{\text{iso}} = 2.0054$; I_1 , 1/2; # I_1 , (1); $A_{\text{iso}} = 16.7$ MHz (0.59 mT); I_2 , 1/2; # I_1 , (4); $A_{\text{iso}} = 3.7$ MHz (0.13 mT); s_{B} , 0.01 mT. *Sim6a*, $g_{\text{iso}} = 2.0035$; I_1 , 1/2; # I_1 , (1); $A_{\text{iso}} = 32.8$ MHz (1.17 mT); I_2 , 1/2; # I_1 , (5);

$A_{iso} = 8.3$ MHz (0.29 mT); s_B , 0.01 mT. *Sim6b*, $g_{iso} = 2.0047$; I_1 , 1/2; # I_1 , (4); $A_{iso} = 3.8$ MHz (0.13 mT); I_2 , 1/2; # I_1 , (1); $A_{iso} = 3.9$ MHz (0.14 mT); s_B , 0.01 mT.

. Instrumental conditions: temperature, 293 K; microwave frequency, 9.641 GHz; microwave power, 200 μ W; modulation amplitude, 0.1 mT. Simulation parameters: *Sim6b*, $g_{iso} = 2.0047$; I_1 , 1/2; # I_1 , (4); $A_{iso} = 3.8$ MHz (0.13 mT); I_2 , 3/2; # I_1 , (1); $A_{iso} = 3.9$ MHz (0.14 mT); s_B , 0.01 mT. *Sim6c*, $g_{iso} = 2.0047$; I_1 , 1/2; # I_1 , (7); s_B , 0.01 mT.

rapid freeze-quench samples were prepared for HAT reactions for analysis by cryogenic (4-50 K) EPR spectroscopy. These experiments have the benefit of interrogating reaction speciation at shorter time intervals (1-30 seconds) while simultaneously increasing instrumental sensitivity. Freeze-quench EPR samples were prepared by from parallel reactions. For each sample, an oven dried 4 mm quartz EPR tube (Wilmad-Labglass p/n 707-SQ-250M) was equipped with septum and purged with N_2 gas. Subsequently, 4-methoxystyrene **5-1a** (7 μ L, 0.05 mmol), and H_2SiEt_2 (23 μ L, 3 equiv, 0.45 mmol) were dissolved in a binary mixture of diisopropyl ether and isopentane [3:1 (v/v)] to obtain a final **5-1a** concentration of 0.25 M. This solvent mixture was selected based on its ability to form a frozen glass and its compatibility with reaction components.²⁴¹ Reactions were initiated by addition of KOtBu (40 μ L, 40 mol %, 1 M in THF) to the tubes using a Hamilton gas-tight syringe equipped with a 6-inch needle. Samples were freeze-quenched at selected time points (5 seconds, 10 seconds, and 30 seconds) by immersion in a liquid N_2 cooled acetone bath. Cryogenic X-band EPR spectra were collected using a Bruker (Billerica, MA) EMX Plus spectrometer equipped with a bimodal resonator (Bruker model 4116DM). Low-temperature measurements (4 - 50 K) were made using an Oxford ESR900 cryostat and an Oxford ITC 503 temperature controller.

Instrumental conditions: temperature, 50 K; microwave frequency, 9.645 GHz; microwave power, 6 μ W; modulation amplitude, 0.3 mT. Quantitation of $g_{ave} = 1.993$ and

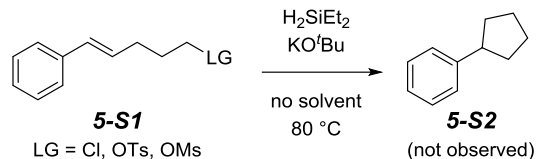
2.006 species at 5-seconds was determined to be 17 μM and 3 μM , respectively. While the $g_{\text{ave}} = 1.993$ signal is not present in samples collected at 10 and 30-seconds, the intensity of the $g_{\text{ave}} = 2.006$ signal remains largely invariant. The concentration of the $g_{\text{ave}} = 2.006$ signal at later time points (10-, 20-, and 30-minutes) was measured at 8.4, 5.5, and 1.6 μM , respectively. Simulation parameters: *Sim11*, $g_{x,y,z} = 2.0042, 2.0072, 2.0057$; $I_1, 1/2$; $\#I_1, (2)$; $A_{x,y,z} = 10, 18, 38$ MHz; $\sigma_B, 0.03$ mT.

F.15. Addition Control Experiments

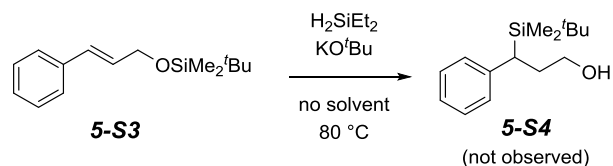
A series of experiment were carried out to detect or capture the anionic intermediates such as benzylic anions or silyl anions (Scheme S13). To detect formation of benzylic radical, we first tried a reaction with substrate **5-S1** bearing leaving groups (Cl, OTs, OMs), which is capable of 5-*exo-tet* type ring closure. Subsequently, we examined [1,4] O to C retro-Brook rearrangement with substrate **5-S3**. Finally, to investigate a possibility for the generation of silyl anions, a mixture of styrene **5-1d** and the epoxide **5-S6** was subjected to H_2SiEt_2 and KO^tBu . However, none of the expected products (i.e., benzylic anions or silyl anions) were observed, suggesting that a formation of nucleophilic benzyl or silyl anions is unlikely.

Scheme S13. Investigation on Mechanisms Involving Anionic Species

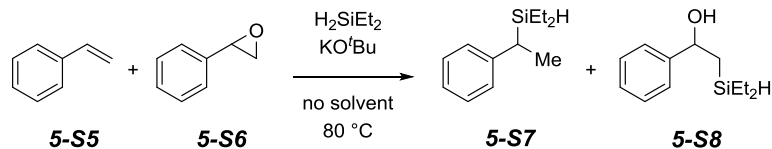
a. Benzylic anion formation: 5-*exo-tet* cyclization



b. Benzylic anion formation: [1,4] O to C retro-Brook

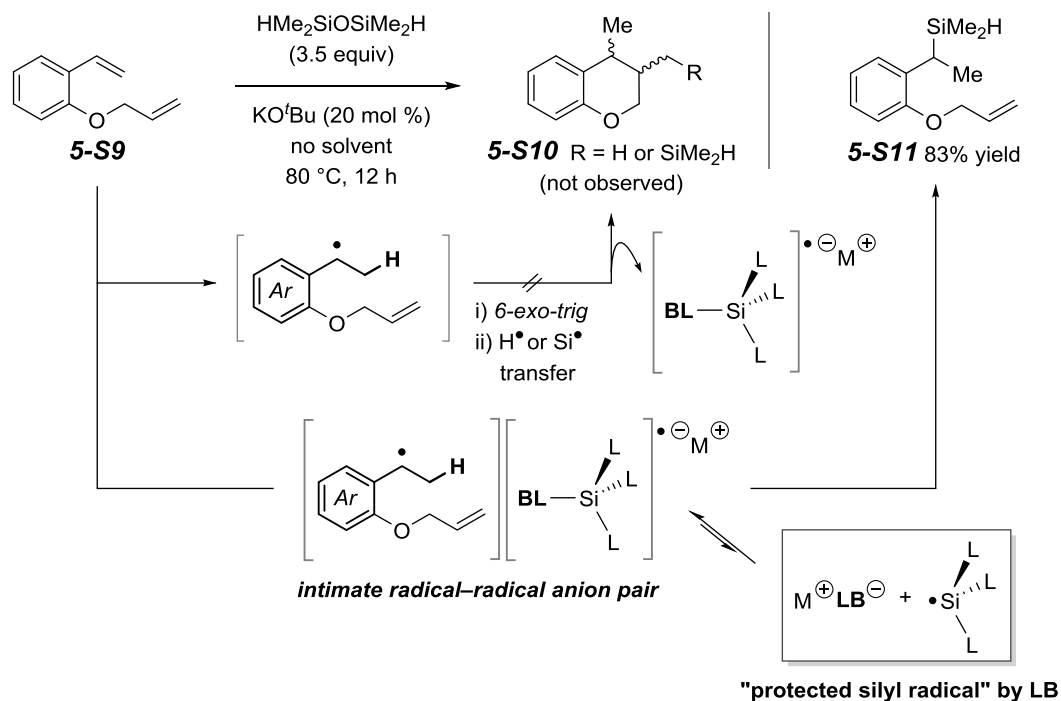


c. Silyl anion formation

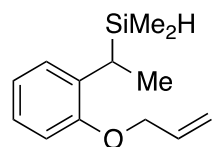


The 6-*exo-trig* Radical cyclization reaction to form carbocycle **5-S10** was investigated (Scheme S14). However, hydrosilane selectively reacted with aryl-substituted alkene and the allyl group within **5-S9** remained intact, where the cyclized adduct **5-S10** was not observed. This result suggests that the LBCl-HAT likely does not produce a benzylic free radical. Rather, we propose that the unusual radical-radical cross-coupling arose from the transient, yet effective stabilization of the silyl radical anions within an intimate radical-radical anion pair cage, can be achievable by incoming alkali metal Lewis base. Namely, the “protected radicals” masked with alkali metal Lewis base would perhaps dictate the reaction with stable yet transient, benzylic radicals, by protecting the radical center from potential radical-mediated downstream reactions (e.g., hydrogen abstraction, self-termination dimerization, disproportionation, and polymerization with abundant olefins), which ultimately leads to the hydrosilylation product.

Scheme S14. Radical-mediated cyclization reactions: An intimate radical-radical anion pair cage



{1[2-(Allyloxy)phenyl]ethyl}dimethylsilane (S11)



Yield: 183 mg, 83%. (colorless liquid).

$^1\text{H NMR}$ (CDCl_3 , 500 MHz): δ 7.09 (dd, $J = 7.5, 1.7$ Hz, 1H, Ar- H), 7.06 (ddd, $J = 8.0, 7.5, 1.7$ Hz, 1H, Ar- H), 6.92 (ddd, $J = 7.5, 7.5, 1.2$ Hz, 1H, Ar- H), 6.80 (dd, $J = 8.0, 1.2$ Hz, 1H, Ar- H), 6.08 (dddd, $J = 17.2, 10.6, 5.1, 5.1$ Hz, 1H, $\text{CH}=\text{CH}_2$), 5.43 (dddd, $J = 17.2, 1.6, 1.6, 1.6$ Hz, 1H, $\text{CH}=\text{CH}_{\text{cis}}\text{H}_{\text{trans}}$), 5.27 (dddd, $J = 10.6, 1.6, 1.6, 1.6$ Hz, 1H, $\text{CH}=\text{CH}_{\text{cis}}\text{H}_{\text{trans}}$), 4.53 (dddd, $J = 13.0, 5.1, 1.6, 1.6$ Hz, 1H, $\text{OCH}_a\text{H}_b\text{CH}=\text{CH}_2$), 4.49 (dddd, $J = 13.0, 5.1, 1.6, 1.6$ Hz, 1H, $\text{OCH}_a\text{H}_b\text{CH}=\text{CH}_2$), 3.80 (qqd, $J = 3.6, 3.6, 2.7$ Hz, 1H, Si- H), 2.82 [qd, $J = 7.6, 2.7$ Hz, 1H, $\text{C}(\text{Si})\text{HCH}_3$], 1.36 [d, $J = 7.6$ Hz, 3H, $\text{C}(\text{Si})\text{HCH}_3$], 0.03 (d, $J = 3.6$ Hz, 3H, SiCH_3), and -0.03 (d, $J = 3.6$ Hz, 3H, SiCH_3).

¹³C NMR (CDCl₃, 125 MHz): δ 155.3, 134.8, 133.9, 126.9, 125.2, 120.9, 117.1, 111.2, 68.8, 19.5, 15.2, -5.3, and -5.5.

IR (neat): 2960 (m), 2925 (m), 2853 (m), 2099 (m), 1735 (w), 1489 (w), 1259 (s), 1088 (s), 1019 (s), 799 (s), 700 (w) and 396 (m) cm⁻¹.

TLC: R_f = 0.8 in 80:1 hexanes:EtOAc.

HRMS (APCI/TOF): Calcd for (M+H)⁺ (C₁₃H₂₁OSi)⁺: 221.1356. Found: 221.1364.

F.16. Computational Details

Geometry optimizations were performed with the M06-2X functional²⁵⁷ along with the 6-311++G(2d,2p) basis set, calculated using the Gaussian suite of programs (version G09)²⁵⁸. To elucidate the origin of the hydrogen atom transfer (HAT) and hydride transfer pathways, single-point energy calculations were performed using multistate density functional theory (MSDFT)^{244, 245, 246} with a modified version of the GAMESS-US program^{259, 260}. In MSDFT, we constructed a set of valence bond (VB) states, corresponding to elementary electron, proton, hydrogen atom, and hydride transfer processes (Scheme S15). The adiabatic ground and excited state potential energy surfaces (PES) for the styrene silylation and polymerization reactions were obtained from configuration interaction among these VB states.

In particular, the formal transfer of a net hydrogen atom to produce a free radical intermediate (Ψ_{2b}) may be characterized by the admixture of proton-coupled electron transfer (PCET) and hydrogen atom transfer (HAT) mechanisms (yellow area in Scheme S15). In case of PCET, the reaction can take place via a concerted pathway, or via stepwise sequences either with an initial ET followed by PT ($\Psi_{1b} \rightarrow \Psi_{2b}$) or with a PT first followed by ET ($\Psi_{2a} \rightarrow \Psi_{2b}$). HAT and concerted PCET are distinguished by strong and weak

electronic coupling, respectively, and they are often associated with adiabatic and non-adiabatic processes. The spectrum of HAT and PCET mechanisms to yield the free radical species can be represented by the three valence bond states in Scheme S15, which along with the reactant state (Ψ_{1a}) and hydride transfer state (Ψ_{3b}) form the basis configurational states to fully characterize the mechanisms for the styrene silylation and polymerization reactions.

We studied the following three reactions:



We focused on the key reaction step to yield the reaction intermediate, and the potential energy profiles for the hydrogen transfer with and without the presence of K^+ are shown in Figure S6. We have also computed the reaction profile for a smaller model, in which the methoxy substituent is replaced by a hydride ion (Reaction 3). Since the relative energies are within 3 kcal/mol of reaction 2, it is not illustrated for clarity. The energy barrier from the pentavalent silyl anion and styrene complex is 16.3 kcal/mol for the parent system (reaction 1), which is nearly identical for Reaction 2 at 16.3 kcal/mol when K^+ is included. The reaction-product intermediate is predicted to be exothermic by -18.4 and -26.5 kcal/mol, respectively. The nature of this intermediate were then characterized by analysis of structural weights of the VB states that contribute to the total wave function, which are given in

Table S6.

	$W(S_0)$				$W(S_1)$			
	$\square E$	RS	BR	HT	$\square E$	RS	BR	HT
Reaction 1								
RC1	0.0	0.59	0.61	-0.20	98.5	0.00	1.00	0.00

TS1	16.3	0.26	0.57	0.17	131.5	0.27	0.66	0.07
PI1	-18.4	-0.02	0.28	0.74	76.1	0.00	1.00	0.00
Reaction 2								
RC3	0.0	0.67	0.23	0.13	99.4	0.01	0.99	0.00
TS3	16.3	0.27	0.46	0.27	104.9	0.27	0.66	0.07
PI3	-26.5	-0.03	0.28	0.75	24.2	0.00	1.00	0.00
Reaction 3								
RC2	0.0	0.68	0.34	0.00	91.3	0.04	0.96	0.00
TS2	13.9	0.36	0.44	0.20	112.9	0.24	0.72	0.04
PI2	-30.5	0.05	0.30	0.75	21.2	0.00	1.00	0.00

Table S6. Computed relative energies (kcal/mol) and structural weights (W) for the reactant complex (RC), transition state (TS), and product intermediate (PI) in the singlet ground state (S_0) and excited state (S_1). Structural weights are given in terms of the silyl anionic reactant state (RS), the biradical state due to a net hydrogen atom transfer (BR), and the hydride transfer product (HT). In all cases, the singlet excited state corresponds to an open shell biradical residing on the silyl reagent $[(LB)HMe_2Si]^- \cdot$ and on the hydrogen atom transfer adduct $[CH_3CHPh]^\cdot$, respectively. There is negligible (< 1 kcal/mol) energy difference with the triplet biradical state, except at the transition state geometry where strong correlation of all state functions is found with an S-T splitting as large as 37 kcal/mol.

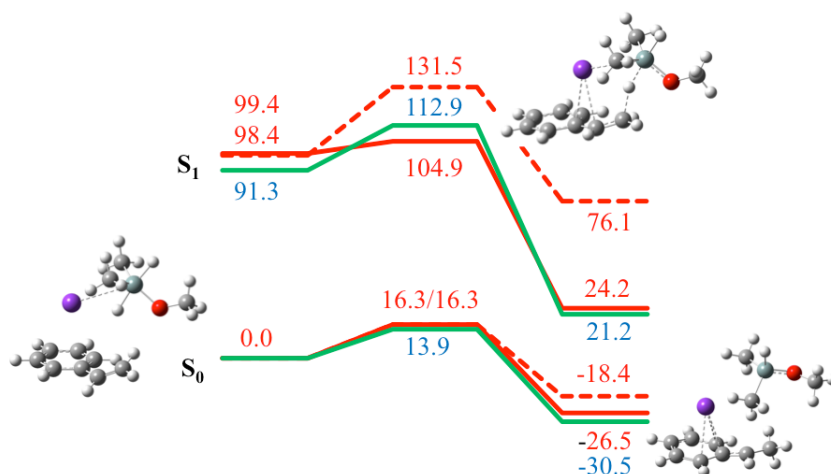
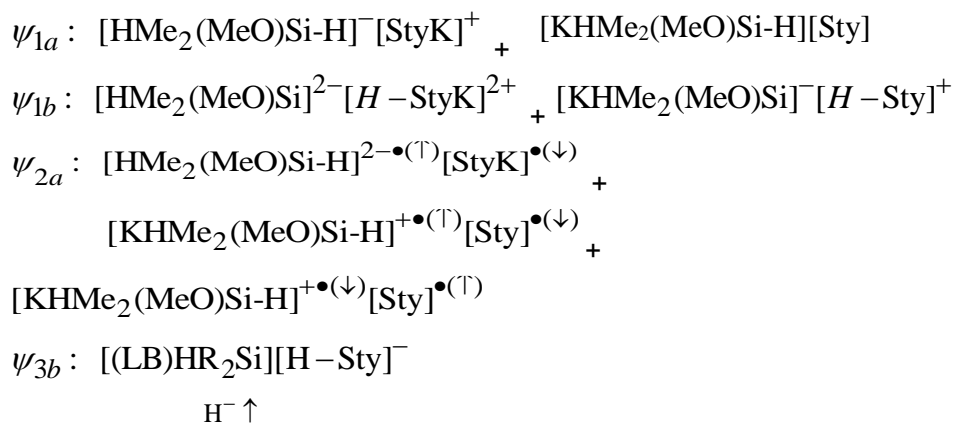
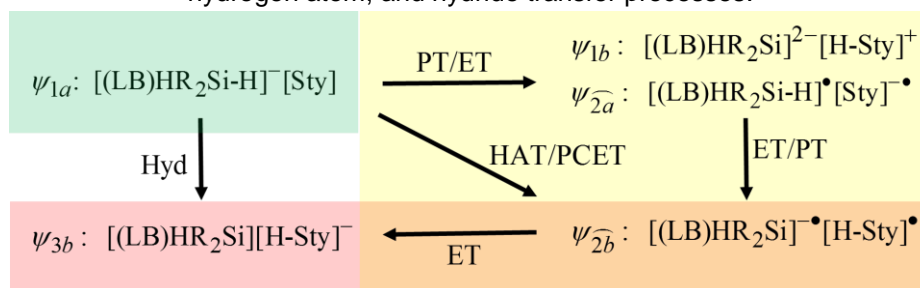
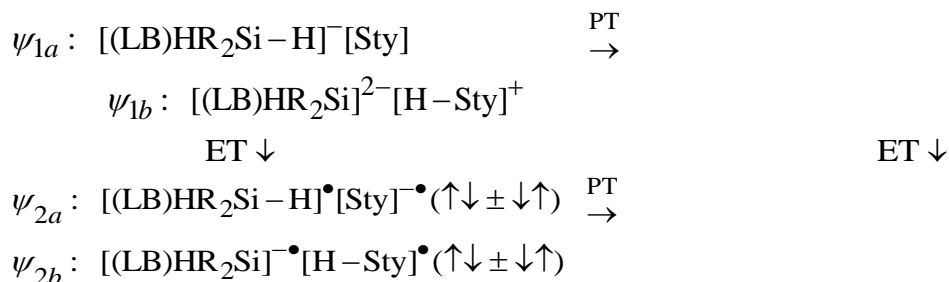


Figure S6. The key reaction step to yield the reaction intermediate, and the potential energy profiles for the hydrogen transfer with and without the presence of K⁺

Scheme S15. Valence bond (VB) states, corresponding to elementary electron, proton, hydrogen atom, and hydride transfer processes.





Computed total energies (hartree) for the ground and excited states from multistate density functional calculations.

<u>Reaction 1</u>	MeO- without K+		
S0	-794.6338651	-794.6078672	-794.6631733
T1	-794.4770261	-794.4836606	-794.5132154
S1	-794.476972	-794.4242607	-794.5126446

<u>Reaction 2</u>	MeO- with K+		
S0	-1394.328956	-1394.302931	-1394.371194
T1	-1394.174641	-1394.102527	-1394.291305
S1	-1394.170512	-1394.161845	-1394.290333

<u>Reaction 3</u>	H- with K+		
S0	-1279.878142	-1279.855977	-1279.926674
T1	-1279.743976	-1279.731787	-1279.845634
S1	-1279.732678	-1279.698231	-1279.844338

F.17. Hammett Plot Analysis

The effect of *para*-Substituents on the rate of the reaction was investigated. To overcome the issue of polymerization which usually happens with the electron withdrawing substrates, we selected 5 mostly electro reach arenes for this study.

An oven dried Norell® pressure NMR tube was purged with nitrogen and charged with vinyl arene (0.1 mmol), H₂SiEt₂ (50 μL, 0.4 mmol) and C₆D₆ (0.45 mL), along with TMS as internal standard. A Solution of KOtBu in THF (0.02 mmol, 20 μL) was added to the tube

and it was immediately capped and $^1\text{H-NMR}$ spectra was obtained over period of 30 minutes with 2-minute time intervals.

After obtaining rate constants of early yields (<15%), $\text{Log}(k/K_0)$ was plotted against the corresponding σ or σ^- values. The σ and σ^- values were taken from J.E. Leffler and E. Grunwald, *Rates and Equilibria of Organic Reactions*, Wiley, 1963 (Dover reprint) and C. Hansch, A. Leo, and R. W. Taft, *Chem. Rev.* 1991, 91, 165-195.

F.18. Kinetic Isotope Effect (KIE) Studies

(a) Parallel KIE experiment

An oven dried Norell[®] pressure NMR tube was purged with nitrogen and charged with **5-1a** (0.1 mmol), H_2SiPh_2 or D_2SiPh_2 (55 μL , 0.3 mmol) and C_6D_6 (0.45 mL), along with TMS as internal standard. A Solution of KOtBu in THF (0.02 mmol, 20 μL) was added to the tube and it was immediately capped and $^1\text{H-NMR}$ spectra was obtained over period of 15 minutes with 1-minute time intervals. The observed yields were plotted against time where the rate constants for both, normal substrate and the deuterium labeled substrate were determined from the slope of the lines.

(b) Intermolecular competition KIE experiment

An oven dried Norell[®] pressure NMR tube was purged with nitrogen and charged with **5-1a** (0.1 mmol), H_2SiPh_2 (27 μL , 0.15 mmol), D_2SiPh_2 (27 μL , 0.15 mmol) and C_6D_6 (0.45 mL), along with TMS as internal standard. A Solution of KOtBu in THF (0.02 mmol, 20 μL) was added to the tube and it was immediately capped and $^1\text{H-NMR}$ spectra was obtained (yield < 5%).

The observed primary KIE value in both experiments, implies that the rate determining step probably involves homolytic cleavage of Si-H bond.

F.19. General Procedure for Transition Metal-Free, Branch-Selective

Markovnikov Hydrosilylation and Polymerization.

Condition A:

Alkene **5-1** (1 mmol) and diethylsilane (1.3 mL, 10 mmol) were added to a flame-dried vial. KO^tBu (20 mol %; either 22 mg of solid KO^tBu or 0.2 mL, 1 M in THF) was added to the mixture. The septum on the vial was replaced by a screw cap with a Teflon liner. The reaction mixture was stirred for 48 h at rt. The volatiles were removed *in vacuo* to afford the silanes **2**, which were purified by MPLC (hexanes, 3 mL/min, retention time 3-8 min).

Condition B:

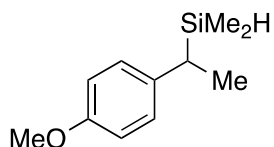
Alkene **5-1** (1 mmol) and diethylsilane (0.45 mL, 3.5 mmol) were added to a flame-dried vial. KO^tBu (20 mol %; either 22 mg of solid KO^tBu or 0.2 mL, 1 M in THF) was added to the mixture. The septum on the vial was replaced by a screw cap with a Teflon liner. The reaction mixture was stirred for 3-12 h at 80 °C. The volatiles were removed *in vacuo* to afford the silanes **2**, which were purified by MPLC (hexanes, 3 mL/min, retention time 3-8 min).

Condition C:

Alkene **5-1** (1 mmol) and diethylsilane (0.65 mL, 5 mmol) or tetramethyldisiloxane (0.88 mL, 5 mmol) were added to a flame-dried vial. KO^tBu (22 mg of solid KO^tBu or 0.2 mL, 1 M in THF, 20 mol %) was added to the mixture. The septum on the vial was replaced by a screw cap with a Teflon liner. The reaction mixture was stirred for 24 h at 120 °C.

The volatiles were removed *in vacuo* to afford the silanes **2**, which were purified by MPLC (hexanes, 3 mL/min, retention time 3-8 min).

[1-(4-Methoxyphenyl)ethyl]dimethylsilane (5-2a^{Me})



Yield: 176 mg, 91% (colorless liquid).

¹H NMR (CDCl₃, 500 MHz): δ 7.00 (d, *J* = 8.7 Hz, 2H, Ar-*H*), 6.82 (d, *J* = 8.7 Hz, 2H, Ar-*H*), 3.81 (qqd, *J* = 3.6, 3.6, 2.8 Hz, 1H, Si-*H*), 3.78 (s, 3H, OCH₃), 2.20 [qd, *J* = 7.5, 2.8 Hz, 1H, C(Si)HCH₃], 1.36 [d, *J* = 7.5 Hz, 3H, C(Si)HCH₃], 0.02 (d, *J* = 3.6 Hz, 3H, SiHCH₃), and -0.02 (d, *J* = 3.6 Hz, 3H, SiHCH₃).

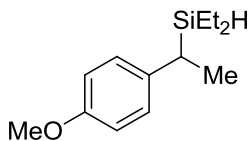
¹³C NMR (CDCl₃, 125 MHz): δ 157.0, 137.7, 127.9, 113.9, 55.4, 26.8, 15.9, -5.67, and -5.78.

IR (neat): 2954 (m), 2869 (w), 2108 (m), 1609 (m), 1508 (s), 1241 (s), 1177 (m), 1036 (s), 829 (s) and 528 (m) cm⁻¹.

TLC: R_f = 0.3 in 80:1 hexanes:EtOAc.

HRMS (APCI/TOF): Calcd for (M+H)⁺ (C₁₁H₁₉OSi)⁺: 195.1200. Found: 195.1221.

Diethyl[1-(4-methoxyphenyl)ethyl]silane (5-2a^{Et})



Yield: 204 mg, 92% (colorless liquid).

¹H NMR (CDCl₃, 500 MHz): δ 7.04 (d, *J* = 8.7 Hz, 2H, Ar-*H*), 6.83 (d, *J* = 8.7 Hz, 2H, Ar-*H*), 3.79 (s, 3H, OCH₃), 3.65 (dddd, *J* = 3.1, 3.1, 3.1, 3.1, 3.1 Hz, 1H, Si-*H*), 2.31 [qd, *J* = 7.6, 3.2 Hz, 1H, C(Si)HCH₃], 1.40 [d, *J* = 7.6 Hz, 3H, C(Si)HCH₃], 0.98 (dd, *J* = 7.9, 7.9 Hz, 3H, SiCH₂CH₃), 0.91 (dd, *J* = 7.9, 7.9 Hz, 3H, SiCH₂CH₃), 0.64-0.58 (m, 2H, SiCH₂CH₃), and 0.56-0.47 (m, 2H, SiCH₂CH₃).

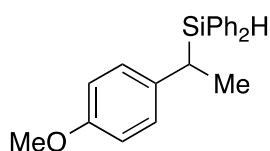
¹³C NMR (CDCl₃, 125 MHz): δ 157.0, 138.0, 128.0, 113.9, 55.4, 24.8, 16.6, 8.44, 8.41, 1.75, and 1.73.

IR (neat): 2951 (m), 2872 (w), 2094 (m), 1610 (m), 1508 (s), 1457 (m), 1242 (s), 1177 (m), 1039 (s), 1012 (s), 795 (s), 694 (m) and 528 (m) cm⁻¹.

TLC: R_f = 0.5 in 80:1 hexanes:EtOAc.

HRMS (APCI/TOF): Calcd for (M+H)⁺ (C₁₃H₂₃OSi)⁺: 223.1513. Found: 223.1520.

[1-(4-Methoxyphenyl)ethyl]diphenylsilane (5-2a^{Ph})



Yield: 153 mg, 48%. (White solid, Melting point: 57-50 °C).

¹H NMR (CDCl₃, 500 MHz): δ 7.57-7.54 (m, 2H, Ar-*H*), 7.46-7.35 (m, 6H, Ar-*H*), 7.32-7.29 (m, 2H, Ar-*H*), 6.96 (d, *J* = 8.7 Hz, 2H, Ar-*H*), 6.78 (d, *J* = 8.7 Hz, 2H, Ar-*H*), 4.86 (d, *J* = 3.4 Hz, 1H, Si-*H*), 3.79 (s, 3H, OCH₃), 2.80 [qd, *J* = 7.5, 3.4 Hz, 1H, C(Si)HCH₃], and 1.47 [d, *J* = 7.7 Hz, 3H, C(Si)HCH₃].

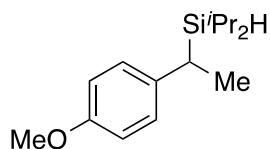
¹³C NMR (CDCl₃, 125 MHz): δ 157.30, 136.48, 135.90, 135.78, 133.40, 133.36, 129.85, 129.73, 128.74, 128.10, 127.92, 113.83, 55.41, 25.99, and 17.05.

IR (neat): 3067 (m), 2998 (w), 2116 (m), 1608 (m), 1507 (s), 1427 (m), 1242 (s), 1177 (m), 1036 (m), 830 (s), 795 (s), 695 (m) and 484 (m) cm⁻¹.

TLC: R_f = 0.2 in 80:1 hexanes:EtOAc.

HRMS (APCI/TOF): Calcd for (M+H)⁺ (C₂₁H₂₃OSi)⁺: 319.1513. Found: 319.1515.

Diisopropyl[1-(4-methoxyphenyl)ethyl]silane (5-2a^{Pr})



Yield: 58 mg, 28%. (colorless liquid).

¹H NMR (CDCl₃, 500 MHz): δ 7.09-7.06 (m, 2H, Ar-*H*), 6.83-6.80 (m, 2H, Ar-*H*), 3.79 (s, 3H, OCH₃), 3.52-3.51 (m, 1H, Si-*H*), 2.40 [qd, *J* = 7.6, 3.8 Hz, 1H, C(Si)HCH₃], 1.42 [d, *J* =

7.6 Hz, 3H, C(Si)HCH₃], 1.09-1.04 [m, 8H, SiCH(CH₃)₂], 0.97-0.94 [m, *J* = 3.5 Hz, 3H, SiCH(CH₃)₂], and 0.90-0.86 [m, 3H, SiCH(CH₃)₂].

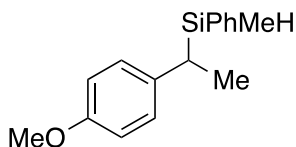
¹³C NMR (CDCl₃, 125 MHz): δ 157.0, 138.4, 128.3, 113.9, 55.4, 23.9, 19.58, 19.44 (2), 19.1, 17.7, 10.61, and 10.56.

IR (neat): 2941 (m), 2863 (m), 2089 (m), 1610 (w), 1508 (s), 1460 (m), 1242 (s), 1177 (m), 1039 (s), 1004 (s), 829 (s), 795 (s) and 539 (m) cm⁻¹.

TLC: R_f = 0.5 in 80:1 hexanes:EtOAc.

HRMS (APCI/TOF): Calcd for (M+H)⁺ (C₁₅H₂₇OSi)⁺: 251.1826. Found: 251.1835.

[1-(4-Methoxyphenyl)ethyl](methyl)(phenyl)silane (5-2a^{MePh})



Yield: 174 mg, 68%. (colorless liquid). 1:1 *dr*

¹H NMR (CDCl₃, 500 MHz): δ 7.43-7.41 (m, 1H, Ar-*H*), 7.39-7.35 (m, 2H, Ar-*H*), 7.34-7.29 (m, 2H, Ar-*H*), 6.95-6.91 (m, 2H, Ar-*H*), 6.80-6.76 (m, 2H, Ar-*H*), 4.32 (qd, *J* = 3.7, 2.4 Hz, 0.5H, Si-*H*), 4.29 (qd, *J* = 3.7, 3.3 Hz, 0.5H, Si-*H*), 3.78 (s, 1.5H, OCH₃), 3.78 (s, 1.5H, OCH₃), 2.45 [qd, *J* = 7.5, 2.4 Hz, 0.5H, C(Si)HCH₃], 2.38 [qd, *J* = 7.5, 3.3 Hz, 0.5H, C(Si)HCH₃], 1.36 [d, *J* = 2.5 Hz, 1.5H, C(Si)HCH₃], 1.34 (d, *J* = 2.5 Hz, 1.5H, C(Si)HCH₃], 0.28 (d, *J* = 3.7 Hz, 1.5H, SiCH₃), and 0.21 (d, *J* = 3.7 Hz, 3H, SiCH₃).

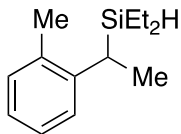
¹³C NMR (CDCl₃, 125 MHz): δ 157.06, 157.03, 136.89, 136.75, 135.3, 134.94, 134.89, 129.46, 129.45, 128.8, 128.13, 128.11, 127.80, 127.75, 113.75, 113.70, 55.3, 26.7, 26.4, 16.3, 15.6, -7.0, and -7.9.

IR (neat): 3067 (w), 2998 (w), 2953 (m), 2112 (m), 1609 (m), 1507 (s), 1460 (m), 1242 (s), 1195 (m), 1037 (m), 871 (s), 826 (s), 718 (m) and 698 (s) cm⁻¹.

TLC: R_f = 0.2 in 80:1 hexanes:EtOAc.

HRMS (APCI/TOF): Calcd for (M+H)⁺ (C₁₆H₂₁OSi)⁺: 257.1356. Found: 257.1360.

Diethyl[1-(*o*-tolyl)ethyl]silane (5-2b)



Yield: 124 mg, 60%. (colorless liquid).

¹H NMR (CDCl₃, 500 MHz): δ 7.17-7.11 (ddd, *J* = 7.8, 7.8, 1.5 Hz, 1H, Ar-*H*), 7.15-7.10 (m, 2H, Ar-*H*), 7.03-7.00 (m, 1H, Ar-*H*), 3.65 (dddd, *J* = 3.1, 3.1, 3.1, 3.1, 3.1 Hz, 1H, Si-*H*), 2.55 (qd, *J* = 7.4, 3.1 Hz, 1H, C(Si)HCH₃), 2.29 (s, 3H, Ar-CH₃), 1.40 [d, *J* = 7.4 Hz, 3H, C(Si)HCH₃], 0.96 (dd, *J* = 8.0, 8.0 Hz, 3H, SiCH₂CH₃), 0.92 (dd, *J* = 8.0, 8.0 Hz, 3H, SiCH₂CH₃), 0.66-0.61 (m, 2H, SiCH₂CH₃), and 0.58-0.50 (m, 2H, SiCH₂CH₃).

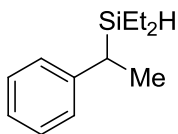
¹³C NMR (CDCl₃, 125 MHz): δ 144.62, 134.75, 130.25, 126.44, 126.26, 124.45, 21.11, 20.40, 16.56, 8.54, 8.47, 2.21, and 1.58

IR (neat): 2952 (m), 2873 (m), 2101 (m), 1486 (m), 1458 (m), 1184 (w), 1010 (m), 970 (m), 801 (s), 763 (s), 725 (s), and 445 (w) cm⁻¹.

TLC: R_f = 0.8 in 80:1 hexanes:EtOAc.

HRMS (APCI/TOF): Calcd for (M+H)⁺ (C₁₃H₂₃Si)⁺: 207.1564. Found: 207.1759.

Diethyl(1-phenylethyl)silane (5-2d)



Yield: 146 mg, 76%. (colorless liquid).

¹H NMR (CDCl₃, 500 MHz): δ 7.27-7.24 (m, 2H, Ar-*H*), 7.11-7.08 (m, 3H, Ar-*H*), 3.64 (dddd, *J* = 3.1, 3.1, 3.1, 3.1, 3.1 Hz, 1H, Si-*H*), 2.36 [qd, *J* = 7.5, 3.1 Hz, 1H, C(Si)HCH₃], 1.41 [d, *J* = 7.5 Hz, 3H, C(Si)HCH₃], 0.96 (dd, *J* = 7.9, 7.9 Hz, 3H, SiCH₂CH₃), 0.89 (dd, *J* = 7.9, 7.9 Hz, 3H, SiCH₂CH₃), 0.62-0.57 (m, 2H, SiCH₂CH₃), and 0.54-0.48 (m, 2H, SiCH₂CH₃).

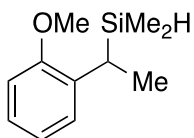
¹³C-NMR (125 MHz): δ 146.1, 128.4, 127.2, 124.7, 26.0, 16.2, 8.14, 8.13, and 1.7 (2).

IR (neat): 2951 (m), 2872 (w), 2094 (m), 1610 (m), 1508 (s), 1458 (m), 1243 (s), 1177 (m), 1039 (s), 1012 (s), 697 (m), 830 (s), 795 (s) and 533 (m) cm⁻¹.

TLC: R_f = 0.6 in 80:1 hexanes:EtOAc.

HRMS (APCI/TOF): Calcd for (M+H)⁺ (C₁₂H₂₁Si)⁺: 193.1407. Found: 193.1398.

[1-(2-Methoxyphenyl)ethyl]dimethylsilane (5-2e)



Yield: 171 mg, 88%. (colorless liquid).

¹H NMR (CDCl₃, 500 MHz): δ 7.09 (ddd, *J* = 8.1, 7.5, 1.1 Hz, 1H, Ar-*H*), 7.08 (dd, *J* = 7.5, 1.0 Hz, 1H, Ar-*H*), 6.91 (ddd, *J* = 7.5, 7.5, 1.1 Hz, 1H, Ar-*H*), 6.82 (dd, *J* = 8.1, 1.0 Hz, 1H, Ar-*H*), 3.79 (s, 3H, Ar-OCH₃), 3.78 (qqd, *J* = 3.7, 3.7, 2.7 Hz, 1H, Si-*H*), 2.74 [qd, *J* = 7.6, 2.7 Hz, 1H, C(Si)HCH₃], 1.34 [d, *J* = 7.6 Hz, 3H, C(Si)HCH₃], 0.02 (d, *J* = 3.7 Hz, 3H, SiCH₃), and -0.04 (d, *J* = 3.7 Hz, 3H, SiCH₃).

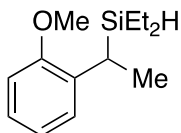
¹³C NMR (CDCl₃, 125 MHz): δ 156.4, 134.5, 126.9, 125.3, 120.7, 110.0, 55.3, 19.5, 15.2, -5.3, and -5.6.

IR (neat): 2997 (m), 2872 (m), 2092 (m), 1597 (w), 1497 (s), 1234 (s), 1114 (m), 1011 (m), 971 (m), 762 (s), 743 (s), and 462 (w) cm⁻¹.

TLC: R_f = 0.6 in 80:1 hexanes:EtOAc.

HRMS (APCI/TOF): Calcd for (M+H)⁺ (C₁₁H₁₉OSi)⁺: 195.1200. Found: 195.1194

Diethyl[1-(2-methoxyphenyl)ethyl]silane (5-2f)



Yield: 111 mg, 50%. (colorless liquid).

¹H NMR (CDCl₃, 500 MHz): δ 7.11 (dd, *J* = 7.7, 1.7 Hz, 1H, Ar-*H*), 7.09 (ddd, *J* = 8.1, 7.4, 1.7 Hz, 1H, Ar-*H*), 6.91 (ddd, *J* = 7.7, 7.4, 1.1 Hz, 1H, Ar-*H*), 6.81 (dd, *J* = 8.1, 1.1 Hz, 1H, Ar-*H*), 3.80 (s, 3H, OCH₃), 3.59 (dddd, *J* = 3.0, 3.0, 3.0, 3.0 Hz, 1H, Si-*H*), 2.81 [qd, *J* = 7.6, 2.9 Hz, 1H, C(Si)HCH₃], 1.38 [d, *J* = 7.6 Hz, 3H, C(Si)HCH₃], 0.98 (dd, *J* = 7.9, 7.9 Hz, 3H, SiCH₂CH₃), 0.88 (dd, *J* = 7.9, 7.9 Hz, 3H, SiCH₂CH₃), 0.64-0.59 (m, 2H, SiCH₂CH₃), and 0.50-0.44 (m, 2H, SiCH₂CH₃).

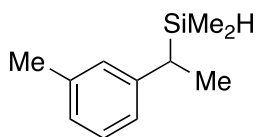
¹³C NMR (CDCl₃, 125 MHz): δ 156.3, 134.9, 127.1, 125.3, 120.8, 109.9, 55.2, 17.8, 15.9, 8.48, 8.44, 2.2, and 2.0.

IR (neat): 2996 (m), 2872 (m), 2091 (m), 1596 (w), 1488 (s), 1236 (s), 1114 (m), 1010 (m), 971 (m), 799 (s), 762 (s), 745 (s), and 460 (w) cm^{-1} .

TLC: $R_f = 0.6$ in 20:1 hexanes:EtOAc.

HRMS (APCI/TOF): Calcd for $(\text{M}+\text{H})^+$ ($\text{C}_{13}\text{H}_{23}\text{OS}$) $^+$: 223.1513. Found: 223.1519.

Dimethyl[1-(*m*-tolyl)ethyl]silane (5-2g)



Yield: 162 mg, 91%. (colorless liquid).

^1H NMR (CDCl_3 , 500 MHz): δ 7.17 (dd, $J = 7.5, 7.5$ Hz, 1H, Ar-*H*), 6.95 (d, $J = 7.5$ Hz, 1H, Ar-*H*), 6.92 (s, 1H, Ar-*H*), 6.91 (d, $J = 7.5$ Hz, 1H, Ar-*H*), 3.86 (qqd, $J = 3.6, 3.6, 2.8$ Hz, 1H, Si-*H*), 2.35 (s, 3H, Ar- CH_3), 2.25 [qd, $J = 7.5, 2.8$ Hz, 1H, C(Si)*HCH* $_3$], 1.41 [d, $J = 7.5$ Hz, 3H, C(Si)*HCH* $_3$], 0.06 (d, $J = 3.6$ Hz, 3H, Si CH_3), and 0.02 (d, $J = 3.6$ Hz, 3H, Si CH_3).

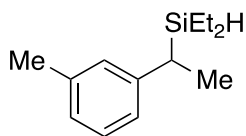
^{13}C NMR (CDCl_3 , 125 MHz): δ 145.7, 137.8, 128.3, 127.9, 125.5, 124.2, 27.8, 21.7, 15.6, -5.68, and -5.73.

IR (neat): 2956 (w), 2869 (w), 2108 (m), 1604 (w), 1487 (w), 1248 (m), 1023 (w), 871 (s), 834 (s), 699 (s) and 432 (w) cm^{-1} .

TLC: $R_f = 0.7$ in 80:1 hexanes:EtOAc.

HRMS (APCI/TOF): Calcd for $(\text{M}+\text{H})^+$ ($\text{C}_{11}\text{H}_{19}\text{Si}$) $^+$: 179.1251. Found: 179.1244

Diethyl[1-(*m*-tolyl)ethyl]silane (5-2h)



Yield: 39 mg, 19%. (colorless liquid).

^1H NMR (CDCl_3 , 500 MHz): δ 7.14 (dd, $J = 7.6, 7.6$ Hz, 1H, Ar-*H*), 6.92-6.88 (m, 3H, Ar-*H*), 3.63 (dddd, $J = 3.1, 3.1, 3.1, 3.1, 3.1$ Hz, 1H, Si-*H*), 2.32 (s, 3H, Ar- CH_3), 2.31 (qd, $J = 7.5, 3.1$ Hz, 1H, C(Si)*HCH* $_3$), 1.39 (d, $J = 7.5$ Hz, 3H C(Si)*HCH* $_3$), 0.96 (dd, $J = 8.0, 8.0$ Hz, 3H, Si CH_2CH_3), 0.89 (dd, $J = 8.0, 8.0$ Hz, 3H, Si CH_2CH_3), 0.61-0.57 (m, 2H, Si CH_2CH_3), and 0.53-0.46 (m, 2H, Si CH_2CH_3).

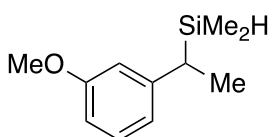
¹³C NMR (CDCl₃, 125 MHz): δ 146.0, 137.9, 128.3, 128.0, 125.5, 124.3, 25.8, 21.7, 16.3, 8.43, 8.40, 1.78, and 1.75.

IR (neat): 2956 (w), 2869 (w), 2108 (m), 1603 (w), 1486 (w), 1246 (m), 872 (s), 834 (s), 700 (s) and 431 (w) cm⁻¹.

TLC: R_f = 0.7 in 80:1 hexanes:EtOAc.

HRMS (APCI/TOF): Calcd for (M+H)⁺ (C₁₃H₂₃Si)⁺: 207.1564. Found: 207.1550.

[1-(3-Methoxyphenyl)ethyl]dimethylsilane (5-2i)



Yield: 126 mg, 65%. (colorless liquid).

¹H NMR (CDCl₃, 500 MHz): δ 7.17 (dd, *J* = 7.5, 7.5 Hz, 1H, Ar-*H*), 6.62-6.70 (m, 3H, Ar-*H*), 3.86 (qqd, *J* = 3.6, 3.6, 2.8 Hz, 1H, Si-*H*), 3.79 (s, 3H, Ar-OCH₃), 2.25 [qd, *J* = 7.5, 2.8 Hz, 1H, C(Si)HCH₃], 1.39 [d, *J* = 7.5 Hz, 3H, C(Si)HCH₃], 0.06 (d, *J* = 3.6 Hz, 3H, SiCH₃), and 0.01 (d, *J* = 3.6 Hz, 3H, SiCH₃).

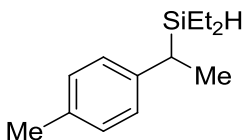
¹³C NMR (CDCl₃, 125 MHz): δ 158.7, 147.3, 128.9, 119.5, 112.9, 109.3, 55.1, 27.9, 15.5, -5.71, and -5.75.

IR (neat): 2956 (m), 2870 (w), 2110 (m), 1599 (m), 1486 (m), 1249 (m), 1013 (m), 875 (s), 834 (m), 697 (s) and 457 (w) cm⁻¹.

TLC: R_f = 0.4 in 80:1 hexanes:EtOAc.

HRMS (APCI/TOF): Calcd for (M+H)⁺ (C₁₁H₁₉OSi)⁺: 195.1200. Found: 195.1210

Diethyl[1-(*p*-tolyl)ethyl]silane (5-2j)



Yield: 185 mg, 90%. (colorless liquid).

¹H NMR (CDCl₃, 500 MHz): δ 7.09 (d, *J* = 8.1 Hz, 2H, Ar-*H*), 7.02 (d, *J* = 8.1 Hz, 2H, Ar-*H*), 3.66 (dddd, *J* = 3.1, 3.1, 3.1, 3.1, 3.1 Hz, 1H, Si-*H*), 2.34 [qd, *J* = 7.5, 3.1 Hz, 1H, C(Si)HCH₃], 2.33 (s, 3H, Ar-CH₃), 1.42 (d, *J* = 7.5 Hz, 3H, C(Si)HCH₃), 0.99 (dd, *J* = 7.9,

7.9 Hz, 3H, SiCH₂CH₃), 0.92 (dd, *J* = 7.9, 7.9 Hz, 3H, SiCH₂CH₃), 0.68-0.59 (m, 2H, SiCH₂CH₃), and 0.58-0.46 (m, 2H, SiCH₂CH₃).

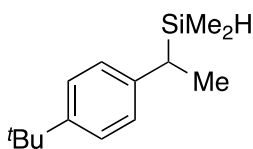
¹³C NMR (CDCl₃, 125 MHz): δ 142.9, 134.0, 129.1, 127.1, 25.4, 21.1, 16.4, 8.4 (2), and 1.7 (2).

IR (neat): 2953 (m), 2873 (m), 2098 (m), 1510 (m), 1457 (m), 1236 (w), 1196 (w), 1047 (m), 1004 (s), 795 (s), 707 (m) and 523 (m) cm⁻¹.

TLC: R_f = 0.7 in 80:1 hexanes:EtOAc.

HRMS (APCI/TOF): Calcd for (M+H)⁺ (C₁₃H₂₃Si)⁺: 207.1564. Found: 207.1559.

{1-[4-(*tert*-Butyl)phenyl]ethyl}dimethylsilane (5-2k)



Yield: 176 mg, 91% (colorless liquid).

¹H NMR (CDCl₃, 500 MHz): δ 7.32 (d, *J* = 8.4 Hz, 2H, Ar-*H*), 7.06 (d, *J* = 8.4 Hz, 2H, Ar-*H*), 3.89 (qqd, *J* = 3.6, 3.6, 2.8 Hz, 1H, Si-*H*), 2.29 [qd, *J* = 7.5, 2.7 Hz, 1H, C(Si)HCH₃], 1.43 [d, *J* = 7.5 Hz, 3H, C(Si)HCH₃], 1.36 [s, 9H, C(CH₃)₃], 0.08 (d, *J* = 3.6 Hz, 3H, SiHCH₃), and 0.05 (d, *J* = 3.6 Hz, 3H, SiHCH₃).

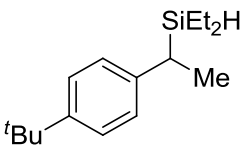
¹³C NMR (CDCl₃, 125 MHz): δ 147.3, 142.4, 126.7, 125.2, 34.4, 31.7, 27.2, 15.5, and -5.7 (2).

IR (neat): 2953 (m), 2862 (w), 2107 (m), 1505 (s), 1240 (s), 1175 (m), 1036 (m), 831 (s) and 527 (m) cm⁻¹.

TLC: R_f = 0.6 in 80:1 hexanes:EtOAc.

HRMS (APCI/TOF): Calcd for (M+H)⁺ (C₁₄H₂₅Si)⁺: 221.1720. Found: 221.1708.

{1-[4-(*tert*-Butyl)phenyl]ethyl}diethylsilane (5-2l)



Yield: 208 mg, 84%. (colorless liquid).

¹H NMR (CDCl₃, 500 MHz): δ 7.27 (d, *J* = 8.1 Hz, 2H, Ar-*H*), 7.03 (d, *J* = 8.1 Hz, 2H, Ar-*H*), 3.63 (dddd, *J* = 3.1, 3.1, 3.1, 3.1, 3.1 Hz, 1H, Si-*H*), 2.33 [qd, *J* = 7.5, 3.1 Hz, 1H, C(Si)HCH₃], 1.40 [d, *J* = 7.5 Hz, 3H, C(Si)HCH₃], 1.31 [s, 9H, CCH₃]₃, 0.96 (dd, *J* = 7.9, 7.9 Hz, 3H, SiCH₂CH₃), 0.90 (dd, *J* = 7.9, 7.9 Hz, 3H, SiCH₂CH₃), 0.66-0.57 (m, 2H, SiCH₂CH₃), and 0.56-0.47 (m, 2H, SiCH₂CH₃).

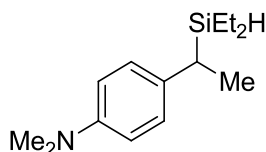
¹³C NMR (CDCl₃, 125 MHz): δ 147.3, 142.8, 126.8, 125.3, 34.4, 31.7, 25.2, 16.2, 8.44, 8.40, 1.77, and 1.74.

IR (neat): 2956 (m), 2869 (w), 2109 (m), 1513 (w), 1459 (w), 1362 (w), 1268 (m), 1008 (w), 873 (s), 832 (s) and 558 (m) cm⁻¹.

TLC: R_f = 0.7 in 80:1 hexanes:EtOAc.

HRMS (APCI/TOF): Calcd for (M+H)⁺ (C₁₆H₂₉Si)⁺: 249.2033. Found: 249.2025.

4-[1-(Diethylsilyl)ethyl]-N,N-dimethylaniline (5-2m)



Yield: 219 mg, 93%. (colorless liquid).

¹H NMR (CDCl₃, 500 MHz): δ 7.01 (d, *J* = 8.6 Hz, 2H, Ar-*H*), 6.71 (d, *J* = 8.6 Hz, 2H, Ar-*H*), 3.64 (dddd, *J* = 3.1, 3.1, 3.1, 3.1, 3.1 Hz, 1H, Si-*H*), 2.91 [s, 6H, ArN(CH₃)₂], 2.26 [qd, *J* = 7.6, 3.1 Hz, 1H, C(Si)HCH₃], 1.38 [d, *J* = 7.6 Hz, 3H, C(Si)HCH₃], 0.98 (dd, *J* = 7.9, 7.9 Hz, 3H, SiCH₂CH₃), 0.92 (dd, *J* = 7.9, 7.9 Hz, 3H, SiCH₂CH₃), 0.64-0.57 (m, 2H, SiCH_aH_bCH₃), 0.53 (dq, *J* = 11.5, 7.9, 3.5 Hz, 1H, SiCH_aH_bCH₃), and 0.49 (dq, *J* = 11.5, 7.9, 3.5 Hz, 1H, SiCH_aH_bCH₃).

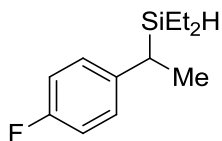
¹³C NMR (CDCl₃, 125 MHz): δ 148.4, 134.2, 127.8, 113.4, 41.2, 24.5, 16.6, 8.5 (2), 1.84, and 1.79.

IR (neat): 2951 (m), 2871 (m), 2092 (m), 1614 (m), 1515 (s), 1455 (m), 1340 (m), 1224 (m), 1131 (w), 1012 (m), 805 (s), 717 (m) and 538 (m) cm⁻¹.

TLC: R_f = 0.3 in 20:1 hexanes:EtOAc.

HRMS (APCI/TOF): Calcd for (M+H)⁺ (C₁₄H₂₆NSi)⁺: 236.1829. Found: 236.1835.

Diethyl[1-(4-fluorophenyl)ethyl]silane (5-2n)



Yield: 151 mg, 72%. (colorless liquid).

¹H NMR (CDCl₃, 500 MHz): δ 7.04 [dd, *J* = 8.7, 5.3(⁴*J*_{F-H}) Hz, 2H, Ar-*H*], 6.94 [dd, *J* = 8.7, 8.7(³*J*_{F-H}) Hz, 2H, Ar-*H*], 3.62 (dddd, *J* = 3.1, 3.1, 3.1, 3.1 Hz, 1H, Si-*H*), 2.33 [qd, *J* = 7.5, 3.1 Hz, 1H, C(Si)HCH₃], 1.38 [d, *J* = 7.5 Hz, 3H, C(Si)HCH₃], 0.95 (dd, *J* = 7.9, 7.9 Hz, 3H, SiCH₂CH₃), 0.88 (dd, *J* = 7.9, 7.9 Hz, 3H SiCH₂CH₃), 0.59 (td, *J* = 7.9, 3.1 Hz, 2H, SiCH₂CH₃), and 0.49 (td, *J* = 7.9, 3.1 Hz, 2H, SiCH₂CH₃).

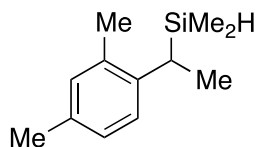
¹³C NMR (CDCl₃, 125 MHz): δ 160.63 (d, ¹*J*_{F-C} = 242.2 Hz), 141.65 (d, ⁴*J*_{F-C} = 3.7 Hz), 128.29 (d, ³*J*_{F-C} = 7.2 Hz), 115.14 (d, ²*J*_{F-C} = 21.3 Hz), 25.2, 16.5, 8.39, 8.36, 1.70, and 1.67.

IR (neat): 2959 (m), 2871 (w), 2164 (m), 1603 (w), 1506 (s), 1456 (w), 1258 (m), 1224 (m), 1158 (w), 1015 (s), 875 (s), 832 (s) 797 (s) and 523 (m) cm⁻¹.

TLC: R_f = 0.7 in 80:1 hexanes:EtOAc.

HRMS (APCI/TOF): Calcd for (M+H)⁺ (C₁₂H₂₀FSi)⁺: 211.1313. Found: 211.1321.

[1-(2,4-Dimethylphenyl)ethyl]dimethylsilane (5-2o)



Yield: 146 mg, 76%. (colorless liquid).

¹H NMR (CDCl₃, 500 MHz): δ 7.03-7.00 (m, 2H, Ar-*H*), 6.98 (s, 1H, Ar-*H*), 3.88 (qqd, *J* = 3.6, 3.6, 2.7 Hz, 1H, Si-*H*), 2.47 [qd, *J* = 7.4, 2.7 Hz, 1H, C(Si)HCH₃], 2.31 (s, 3H, Ar-CH₃), 2.28 (s, 3H, Ar-CH₃), 1.39 (d, *J* = 7.4 Hz, 3H, C(Si)HCH₃), 0.07 (d, *J* = 3.6 Hz, 3H, SiCH₃), and 0.06 (d, *J* = 3.6 Hz, 3H, SiCH₃).

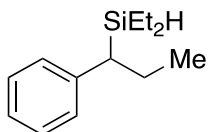
¹³C NMR (CDCl₃, 125 MHz): δ 141.1, 134.7, 133.7, 131.1, 126.9, 126.1, 22.3, 21.0, 20.4, 16.0, -5.2, and -5.9.

IR (neat): 2960 (m), 2872 (w), 2090 (w), 1513 (w), 1411 (w), 1257 (s), 1015 (s), 910 (m), 789 (s), 701 (m), 701 (m), and 562 (w) cm⁻¹.

TLC: R_f = 0.8 in 80:1 hexanes:EtOAc.

HRMS (APCI/TOF): Calcd for (M+H)⁺ (C₁₂H₂₁Si)⁺: 193.1407. Found: 193.1420.

Diethyl(1-phenylpropyl)silane (5-2p)



Yield: 192 mg, 93%. (colorless liquid).

¹H NMR (CDCl₃, 500 MHz): δ 7.25 (app t, *J* = 7.3 Hz, 2H, Ar-*H*), 7.11 (t, *J* = 7.3 Hz, 1H, Ar-*H*), 7.08 (d, *J* = 7.3 Hz, 2H, Ar-*H*), 3.68 (dddd, *J* = 3.1, 3.1, 3.1, 3.1, 3.1 Hz, 1H, Si-*H*), 2.11 [ddd, *J* = 9.4, 5.8, 3.1 Hz, 1H, C(Si)HCH₂], 1.91-1.79 [nfom, 2H, C(Si)HCH₂CH₃], 0.97 [dd, *J* = 7.9, 7.9 Hz, 3H, SiCH₂CH₃], 0.90 [t, *J* = 7.1 Hz, 3H, C(Si)HCH₂CH₃], 0.88 (dd, *J* = 7.9, 7.9 Hz, 3H, SiCH₂CH₃), 0.63-0.57 (m, 2H, SiCH₂CH₃), and 0.54-0.42 (m, 2H, SiCH₂CH₃).

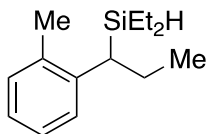
¹³C NMR (CDCl₃, 125 MHz): δ 144.0, 128.4, 128.0, 124.7, 35.3, 24.3, 14.4, 8.46, 8.45, 2.1, and 1.7.

IR (neat): 2947 (m), 2866 (w), 2092 (m), 1610 (m), 1504 (m), 1177 (m), 1043 (s), 1013 (s), 696 (m), 830 (s), 799 (s) and 523 (m) cm⁻¹.

TLC: R_f = 0.8 in 80:1 hexanes:EtOAc.

HRMS (APCI/TOF): Calcd for (M+H)⁺ (C₁₃H₂₃Si)⁺: 207.1564. Found: 207.1576.

Diethyl[1-(*o*-tolyl)propyl]silane (5-2q)



Yield: 207 mg, 94%. (colorless liquid).

¹H NMR (CDCl₃, 500 MHz): δ 7.14-7.09 (m, 3H, Ar-*H*), 7.01 (ddd, *J* = 7.3, 7.3, 1.6 Hz, 1H, Ar-*H*), 3.65 (dddd, *J* = 3.3, 3.3, 3.3, 3.3, 3.3 Hz, 1H, Si-*H*), 2.36 [ddd, *J* = 10.8, 5.3, 3.3 Hz, 1H, C(Si)HCH₂], 2.28 (s, 3H, Ar-CH₃), 1.88 [qdd, *J* = 12.0, 7.2, 5.3 Hz, 1H, C(Si)HCH_aH_bCH₃], 1.82 [ddq, *J* = 12.0, 10.8, 7.2 Hz, 1H, C(Si)HCH_aH_bCH₃], 0.96 [dd, *J* = 7.9, 7.9 Hz, 3H, C(Si)HCH₂CH₃], 0.89 (dd, *J* = 7.9, 7.9 Hz, 3H, SiCH₂CH₃), 0.85 (dd, *J* =

7.2, 7.2 Hz, 3H, SiCH₂CH₃), 0.65-0.62 (m, 2H, SiCH₂CH₃), and 0.53-0.49 (m, 2H, SiCH₂CH₃).

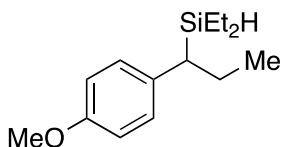
¹³C NMR (CDCl₃, 125 MHz): δ 142.5, 135.8, 130.3, 126.7, 126.2, 124.4, 29.9, 24.8, 20.7, 14.3, 8.61, 8.53, 2.13, and 2.07.

IR (neat): 2953 (m), 2872 (m), 2099 (m), 1601 (m), 1507 (s), 1486 (m), 1459 (m), 1233 (w), 1008 (s), 969 (m), 807 (s) and 446 (m) cm⁻¹.

TLC: R_f = 0.8 in 80:1 hexanes:EtOAc.

HRMS (APCI/TOF): Calcd for (M+H)⁺ (C₁₄H₂₅Si)⁺: 221.1720. Found: 221.1709.

Diethyl[1-(4-methoxyphenyl)propyl]silane (5-2r)



Yield: 217 mg, 92%. (colorless liquid).

¹H NMR (CDCl₃, 500 MHz): δ 6.98 (d, *J* = 8.7 Hz, 2H, Ar-*H*), 6.81 (d, *J* = 8.7 Hz, 2H, Ar-*H*), 3.78 (s, 3H, ArOCH₃), 3.65 (dddd, *J* = 3.3, 3.3, 3.3, 3.3 Hz, 1H, Si-*H*), 2.02 [ddd, *J* = 11.0, 4.4, 3.3 Hz, 1H, C(Si)HCH₂], 1.82 [dq, *J* = 14.1, 7.2, 4.4 Hz, 1H, C(Si)HCH_aH_bCH₃], 1.76 [ddq, *J* = 14.1, 11.0, 7.2 Hz, 1H, C(Si)HCH_aH_bCH₃], 0.96 (dd, *J* = 7.9, 7.9 Hz, 3H, SiCH₂CH₃), 0.873 (dd, *J* = 7.9, 7.9 Hz, 3H, SiCH₂CH₃), 0.865 (dd, *J* = 7.2, 7.2 Hz, 3H, CHCH₂CH₃), 0.62-0.55 (m, 2H, SiHCH_aH_bCH₃), 0.50 (dq, *J* = 14.9, 7.9, 3.3 Hz, 1H, SiHCH_aH_bCH₃), and 0.43 (dq, *J* = 14.9, 7.9, 3.3 Hz, 1H, SiHCH_aH_bCH₃).

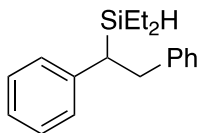
¹³C NMR (CDCl₃, 125 MHz): δ 157.0, 135.8, 128.8, 113.9, 55.4, 34.1, 24.5, 14.3, 8.5, 2.1, and 1.7.

IR (neat): 2953 (m), 2872 (m), 2094 (m), 1609 (m), 1507 (s), 1246 (s), 1177 (m), 1038 (m), 1009 (m), 832 (s), 802 (s) and 532 (m) cm⁻¹.

TLC: R_f = 0.5 in 80:1 hexanes:EtOAc.

HRMS (APCI/TOF): Calcd for (M+H)⁺ (C₁₄H₂₅OSi)⁺: 237.1669. Found: 237.1677.

(1,2-Diphenylethyl)diethylsilane (5-2s)



Yield: 247 mg, 92%. (colorless liquid).

¹H NMR (CDCl₃, 500 MHz): δ 7.28-7.22 (m, 4H, Ar-*H*), 7.18-7.12 (m, 6H, Ar-*H*), 3.84 (dddd, *J* = 3.2, 3.2, 3.2, 3.2, 3.2 Hz, 1H), 3.21 [nfom, 2H, C(Si)HCH₂Ph], 2.64 [ddd, *J* = 7.8, 7.8, 3.2 Hz, 1H, C(Si)HCH₂], 1.05 (dd, *J* = 7.9, 7.9 Hz, 3H, SiCH₂CH₃), 0.95 (dd, *J* = 7.9, 7.9 Hz, 3H, SiCH₂CH₃), 0.76-65 (m, 2H, SiCH₂CH₃), 0.60 (dq, *J* = 15.1, 7.9, 3.2 Hz, 1H, SiCH_aH_bCH₃), and 0.54 (dq, *J* = 15.1, 7.9, 3.2 Hz, 1H, SiCH_aH_bCH₃).

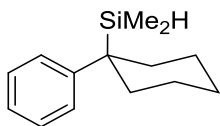
¹³C NMR (CDCl₃, 125 MHz): δ 143.3, 142.1, 128.7, 128.42, 128.23, 128.16, 125.9, 124.9, 37.5, 34.9, 8.4 (2), 2.1, and 1.8.

IR (neat): 3025 (w), 2953 (m), 2873 (m), 2099 (m), 1560 (m), 1493 (m), 1451 (m), 1007 (m), 810 (s), 788 (s), 694 (s) and 521 (m) cm⁻¹.

TLC: R_f = 0.6 in 80:1 hexanes:EtOAc.

HRMS (APCI/TOF): Calcd for (M+H)⁺ (C₁₈H₂₅Si)⁺: 269.1720. Found: 269.1724.

Dimethyl(1-phenylcyclohexyl)silane (5-2t)



Yield: 148 mg, 71%. (colorless liquid).

¹H NMR (CDCl₃, 500 MHz): δ 7.32-7.28 (m, 2H, Ar-*H*), 7.23-7.21 (m, 2H, Ar-*H*), 7.11-7.08 (dddd, *J* = 7.2, 7.2, 1.3, 1.3 Hz, 1H, Ar-*H*), 3.66 (qq, *J* = 3.6, 3.6 Hz, 1H, Si-*H*), 2.37-2.22 (nfom, 2H, alkyl-*H*), 1.73-1.67 (m, 2H, alkyl-*H*), 1.58-1.54 (m, 1H, alkyl-*H*), 1.51-1.34 (m, 5H, alkyl-*H*), and -0.11 [d, *J* = 3.6 Hz, 6H, Si(CH₃)₂].

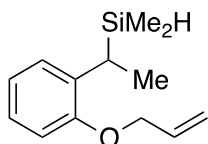
¹³C NMR (CDCl₃, 125 MHz): δ 144.4, 128.4, 127.2, 124.0, 32.6, 31.4, 27.3, 21.7, and -7.0.

IR (neat): 2928 (s), 2872 (m), 2107 (m), 1598 (m), 1491 (m), 1247 (s), 1170 (w), 1029 (m), 1009 (m), 870 (s), 837 (s), 659 (s), and 516 (m) cm⁻¹.

TLC: R_f = 0.9 in 80:1 hexanes:EtOAc.

HRMS (APCI/TOF): Calcd for (M+H)⁺ (C₁₄H₂₃Si)⁺: 219.1564. Found: 219.1566

{1[2-(Allyloxy)phenyl]ethyl}dimethylsilane (5-2u)



Yield: 183 mg, 83%. (colorless liquid).

¹H NMR (CDCl₃, 500 MHz): δ 7.09 (dd, *J* = 7.5, 1.7 Hz, 1H, Ar-*H*), 7.06 (ddd, *J* = 8.0, 7.5, 1.7 Hz, 1H, Ar-*H*), 6.92 (ddd, *J* = 7.5, 7.5, 1.2 Hz, 1H, Ar-*H*), 6.80 (dd, *J* = 8.0, 1.2 Hz, 1H, Ar-*H*), 6.08 (dddd, *J* = 17.2, 10.6, 5.1, 5.1 Hz, 1H, CH=CH₂), 5.43 (dddd, *J* = 17.2, 1.6, 1.6, 1.6 Hz, 1H, CH=CH_{cis}H_{trans}), 5.27 (dddd, *J* = 10.6, 1.6, 1.6, 1.6 Hz, 1H, CH=CH_{cis}H_{trans}), 4.53 (dddd, *J* = 13.0, 5.1, 1.6, 1.6 Hz, 1H, OCH_aH_bCH=CH₂), 4.49 (dddd, *J* = 13.0, 5.1, 1.6, 1.6 Hz, 1H, OCH_aH_bCH=CH₂), 3.80 (qqd, *J* = 3.6, 3.6, 2.7 Hz, 1H, Si-*H*), 2.82 [qd, *J* = 7.6, 2.7 Hz, 1H, C(Si)HCH₃], 1.36 [d, *J* = 7.6 Hz, 3H, C(Si)HCH₃], 0.03 (d, *J* = 3.6 Hz, 3H, SiCH₃), and -0.03 (d, *J* = 3.6 Hz, 3H, SiCH₃).

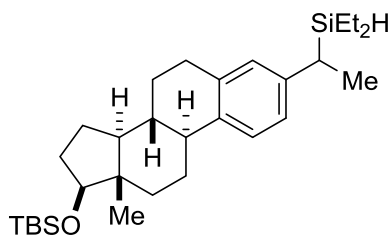
¹³C NMR (CDCl₃, 125 MHz): δ 155.3, 134.8, 133.9, 126.9, 125.2, 120.9, 117.1, 111.2, 68.8, 19.5, 15.2, -5.3, and -5.5.

IR (neat): 2960 (m), 2925 (m), 2853 (m), 2099 (m), 1735 (w), 1489 (w), 1259 (s), 1088 (s), 1019 (s), 799 (s), 700 (w) and 396 (m) cm⁻¹.

TLC: R_f = 0.8 in 80:1 hexanes:EtOAc.

HRMS (APCI/TOF): Calcd for (M+H)⁺ (C₁₃H₂₁OSi)⁺: 221.1356. Found: 221.1364.

***tert*-Butyl{[(13S)-3-[1-(diethylsilyl)ethyl]-13-methyl-7,8,9,11,12,13,14,15,16,17-decahydro-6H-cyclopenta[a]phenanthren-17-yl]oxy}dimethylsilane (5-2v)**



Yield: 0.1 mmol scale, 36 mg, 74%. 1:1 *dr*

¹H NMR (CDCl₃, 500 MHz): δ 7.18 [d, *J* = 8.0 Hz, 0.5H, C(1)*H*], 7.17 [d, *J* = 8.0 Hz, 0.5H, C(1)*H*], 6.89 [dd, *J* = 8.0, 1.8 Hz, 1H, C(2)*H*], 6.88 [dd, *J* = 8.0, 1.8 Hz, 1H, C(2)*H*], 6.81 [d,

$J = 1.8$ Hz, 1H, C(4) H], 6.80 [d, $J = 1.8$ Hz, 1H, C(4) H], 3.68-3.62 [m, 1H, C(17) H], 3.65-3.61 (m, 1H, Si- H), 2.89-2.77 (m, 2H, alkyl- H), 2.34-2.29 (m, 1H, alkyl- H), 2.28 [qd, $J = 7.5$, 3.3 Hz, 1H, C(Si) HCH_3], 2.20 (ddd, $J = 11.3$, 11.3, 4.1 Hz, 1H, alkyl- H), 1.98-1.83 (m, 3H, alkyl- H), 1.70-1.62 (m, 1H, alkyl- H), 1.53-1.44 (m, 3H, alkyl- H), 1.39 [d, $J = 7.5$ Hz, 3H, C(Si) HCH_3], 1.38-1.30 (m, 2H, alkyl- H), 1.23-1.11 (m, 2H, alkyl- H), 1.00-0.95 [m, 6H, Si(CH₂CH₃)₂], 0.91 [s, 9H, OSi(CH₃)₃], 0.75 [s, 3H, C(18) H_3], 0.66-0.59 (m, 2H, SiCH₂CH₃), 0.57-0.50 (m, 2H, SiCH₂CH₃), 0.05 (s, 3H, OSiCH₃), and 0.04 (s, 3H, OSiCH₃).

¹³C NMR (CDCl₃, 125 MHz): δ 143.0, 136.82, 136.67, 136.59, 127.9, 127.5, 125.39, 125.33, 124.8, 124.4, 82.0, 50.0, 44.6, 43.8, 39.0, 37.4, 31.2, 29.94, 29.88, 27.6, 26.4, 26.1, 25.26, 25.19, 23.5, 18.3, 16.3, 11.6, 8.5, 1.78, 1.70, -4.2, and -4.6.

IR (neat): 2953 (m), 2856 (m), 2101 (m), 1497 (w), 1460 (m), 1249 (m), 1092 (w), 1006 (m), 833 (s), 811 (s) and 721 (s) cm⁻¹.

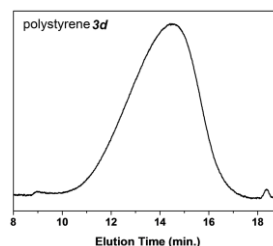
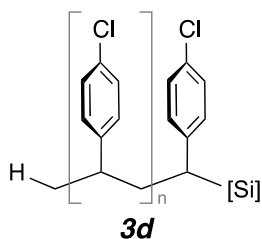
TLC: R_f = 0.7 in 80:1 hexanes:EtOAc.

HRMS (APCI/TOF): Calcd for (M+H)⁺ (C₃₀H₅₃OSi₂)⁺: 485.3629. Found: 485.3640.

F.20. Polymerization Procedure and Characterization:

Condition A: (Electron-poor arenes)

Styrene **5-1** (1 mmol) and 1,1,3,3-tetramethyldisiloxane (3 equiv) were dissolved in THF (0.2 M). KO^tBu (20 mol %) was added to the mixture. Once the polymerization was completed, the polymer was precipitated by addition of methanol to the reaction mixture. After filtration, white solids were washed with cold methanol to provide polystyrenes.



M_n

M_w

M_z

PDI

3d 27600 73000 190000 2.64
Figure S7. GPC Chromatogram of Polystyrene **5-3d**

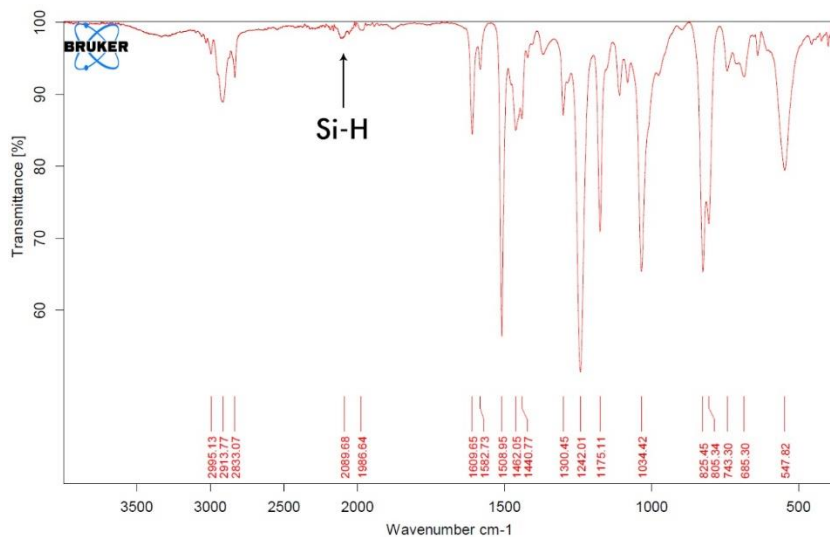
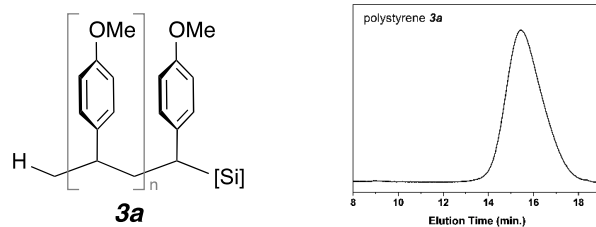


Figure S8. IR Spectrum of polystyrene **5-3d**

Condition B: (Electron-neutral and -rich arenes)

Styrene **5-1** (1 mmol), 18-crown-6 (10 mol %), and 1,1,3,3-tetramethyldisiloxane (3 equiv) were dissolved in THF (0.2 M). KO^tBu (20 mol %) was added to the mixture which immediately turned dark brown. Once the polymerization was completed, the polymer was precipitated by addition of methanol to the reaction mixture. After filtration, white solids were washed with cold methanol to obtain polystyrene **5-3a**.



	Mn	Mw	Mz	PDI
5-3a	10400	15200	21000	1.46

Figure S9. GPC Chromatogram of Polystyrene **3a**

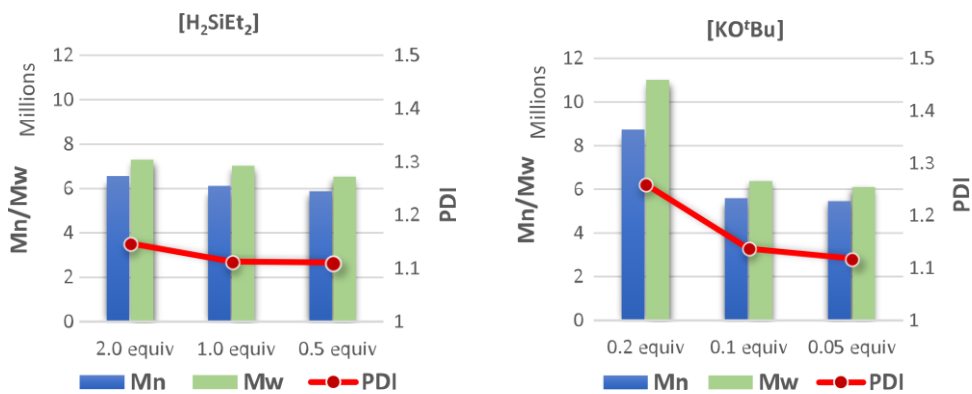
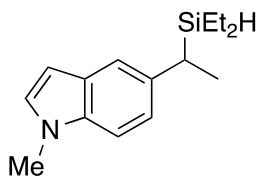


Figure S 10. Effect of concentration of silane and base on Mn/Mw and PDI

F.21. KO^tBu-catalyzed dual olefin hydrosilylation and cross-dehydrogenative arene C–H silylation of vinyl-substituted heterocycles:

5-[1-(Diethylsilyl)ethyl]-1-methyl-1H-indole (5-2x)



Yield: 0.2 mmol scale, 33 mg, 68%.

¹H NMR (500 MHz): δ 7.36 [d, J = 1.7 Hz, 1H, C(4)*H*], 7.23 [d, J = 8.4 Hz, 1H, C(7)*H*], 7.02 [dd, J = 8.4, 1.7 Hz, 1H, C(6)*H*], 7.01 [d, J = 2.9 Hz, 1H, C(2)*H*], 6.41 [d, J = 2.9 Hz, 1H, C(3)*H*], 3.77 (s, 3H, NCH₃), 3.70 (dddd, J = 3.1, 3.1, 3.1, 3.1, 3.1 Hz, 1H, Si-*H*), 2.44 [qd, J = 7.6, 3.2 Hz, 1H, C(Si)*HCH*₃], 1.48 [d, J = 7.6 Hz, 3H, C(Si)*HCH*₃], 0.99 (dd, J = 7.8, 7.8 Hz, 3H, SiCH₂CH₃), 0.91 (dd, J = 7.8, 7.8 Hz, 3H, SiCH₂CH₃), 0.65-0.60 (m, 2H, SiCH₂CH₃), and 0.59-0.45 (m, 2H, SiCH₂CH₃).

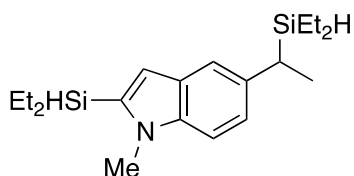
¹³C NMR (CDCl₃, 125 MHz): δ 136.8, 135.0, 128.96, 128.88, 122.0, 118.5, 109.0, 100.5, 33.0, 25.5, 17.2, 8.53, 8.50, 1.89, and 1.85.

IR (neat): 2950 (m), 2871 (m), 2091 (m), 1512 (m), 1486 (s), 1245 (m), 1179 (w), 1008 (m), 874 (s), 803 (s) and 711 (m) cm⁻¹.

TLC: R_f = 0.2 in 80:1 hexanes:EtOAc.

HRMS (APCI/TOF): Calcd for (M+H)⁺ (C₁₅H₂₄NSi)⁺: 246.1673. Found: 246.1669

2-(Diethylsilyl)-5-[1-(diethylsilyl)ethyl]-1-methyl-1H-indole (5-11)



Yield: 0.2 mmol scale, 31 mg, 47%. (with 5% mono-hydrosilylation product **5-2x**).

¹H NMR (CDCl₃, 500 MHz): δ 7.33 (d, J = 1.8 Hz, 1H), 7.22 [d, J = 8.5 Hz, 1H, C(7)*H*], 7.01 [dd, J = 8.5, 1.8 Hz, 1H, C(6)*H*], 6.67 [app s, 1H, C(3)*H*], 4.41 [dddd, J = 3.3, 3.3, 3.3, 3.3 Hz, 1H, C(2)Si-*H*], 3.82 (s, 3H, NCH₃), 3.69 [dddd, J = 3.1, 3.1, 3.1, 3.1, 3.1 Hz, 1H, C(5)CHC(Si-*H*)], 2.42 [qd, J = 7.6, 3.1 Hz, 1H, C(Si)*HCH*₃], 1.46 (d, J = 7.8 Hz, 3H, C(Si)*HCH*₃), 1.07 [app t, J = 7.9 Hz, 6H, Si(CH₂CH₃)₂], 0.99 (dd, J = 7.9, 7.9 Hz, 3H, SiCH₂CH₃), 0.95-0.87 [m, 4H, Si(CH₂CH₃)₂], 0.91 (dd, J = 7.9, 7.9 Hz, 3H, SiCH₂CH₃), 0.65-0.57 (m, 2H, SiCH₂CH₃), and 0.57-0.44 (m, 2H, SiCH₂CH₃).

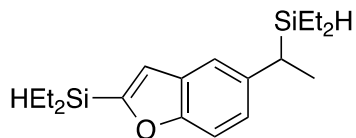
¹³C NMR (CDCl₃, 125 MHz): δ 138.5, 136.8, 136.5, 129.0, 122.7, 118.1, 112.2, 109.0, 32.9, 25.5, 17.2, 8.54, 8.51, 8.49 (2), 3.7 (2), 1.86, and 1.84.

IR (neat): 2950 (m), 2871 (m), 2092 (m), 1512 (m), 1486 (m), 1234 (m), 1008 (m), 803 (s) and 711 (s) cm⁻¹.

TLC: R_f = 0.8 in 80:1 hexanes:EtOAc.

HRMS (APCI/TOF): Calcd for (M+H)⁺ (C₁₉H₃₄NSi₂)⁺: 332.2224. Found: 332.2211

{1-[2-(Diethylsilyl)benzofuran-5-yl]ethyl}diethylsilane (5-12)



Yield: 0.2 mmol scale, 22 mg, 35%.

¹H NMR (CDCl₃, 500 MHz): δ 7.38 [d, *J* = 8.5 Hz, 1H, C(7)*H*], 7.28 [dd, *J* = 1.9, 0.9 Hz, 1H, C(4)*H*], 7.03 [dd, *J* = 8.5, 1.9 Hz, 1H, C(6)*H*], 6.99 [d, *J* = 0.9 Hz, 1H, C(3)*H*], 4.29 [dddd, *J* = 3.3, 3.3, 3.3, 3.3 Hz, 1H, C(2)Si-*H*], 3.66 [dddddd, *J* = 3.1, 3.1, 3.1, 3.1, 3.1 Hz, 1H, C(5)CHC(Si-*H*)], 2.43 [qd, *J* = 7.6, 3.1 Hz, 1H, C(Si)*H*CH₃], 1.44 [d, *J* = 7.6 Hz, 3H, C(Si)HCH₃], 1.08 [dd, *J* = 7.9, 7.9 Hz, 6H, Si(CH₂CH₃)₂], 0.97 (dd, *J* = 7.9, 7.9 Hz, 3H, SiCH₂CH₃), 0.95-0.88 [m, 4H, Si(CH₂CH₃)₂], 0.90-0.87 (dd, *J* = 7.9, 7.9 Hz, 3H, SiCH₂CH₃), 0.63-0.58 (m, 2H, SiCH₂CH₃), and 0.54-0.46 (m, 2H, SiCH₂CH₃).

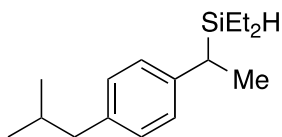
¹³C NMR (CDCl₃, 125 MHz): δ 159.2, 156.5, 140.3, 128.2, 124.5, 118.6, 118.4, 111.0, 25.6, 17.1, 8.47, 8.44, 8.2 (2), 2.9 (2), and 1.8 (2).

IR (neat): 2953 (m), 2873 (m), 2117 (m), 1528 (w), 1455 (m), 1225 (m), 1007 (m), 791 (s), 713 (s), and 451 (m) cm⁻¹.

TLC: R_f = 0.8 in 80:1 hexanes:EtOAc.

HRMS (APCI/TOF): Calcd for (M+H)⁺ (C₁₈H₃₁OSi₂)⁺: 319.1908. Found: 319.1900.

Diethyl[1-(4-isobutylphenyl)ethyl]silane (14)



Yield: 149 mg, 60%. (colorless liquid).

¹H NMR (CDCl₃, 500 MHz): δ 7.04 (d, *J* = 8.4 Hz, 2H, Ar-*H*), 7.02 (d, *J* = 8.4 Hz, 2H, Ar-*H*), 3.65 (dddd, *J* = 3.1, 3.1, 3.1, 3.1, 3.1 Hz, 1H, Si-*H*), 2.44 (app d, *J* = 7.2 Hz, 2H, CH₂CHMe₂), 2.34 [qd, *J* = 7.5, 3.1 Hz, 1H, C(Si)HCH₃], 1.85 (ddqq, *J* = 7.2, 7.2, 6.6, 6.6 Hz, 1H, CH₂CHMe₂), 1.41 [d, *J* = 7.5 Hz, 3H, C(Si)HCH₃], 0.96 (dd, *J* = 8.0, 8.0 Hz, 3H, SiCH₂CH₃).

SiCH₂CH₃), 0.91 [d, *J* = 6.6 Hz, 6H, CH(CH₃)₂], 0.89 (dd, *J* = 8.0, 8.0 Hz, 3H, SiCH₂CH₃), 0.63-0.58 (m, 2H, SiCH₂CH₃), and 0.55-0.47 (m, 2H, SiCH₂CH₃).

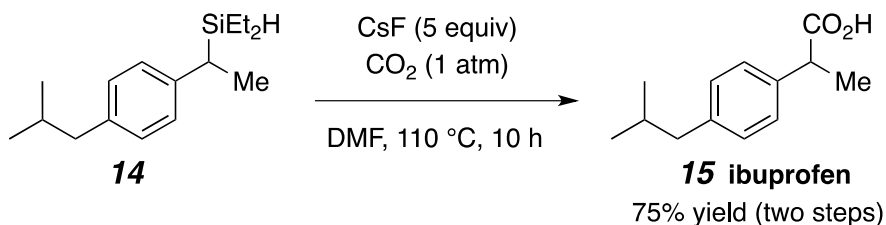
¹³C NMR (CDCl₃, 125 MHz): δ 142.8, 137.9, 129.1, 126.8, 45.2, 30.5, 27.4, 22.6 (2), 15.6, 1.18, 1.09, -5.65, and -5.74.

IR (neat): 2955 (m), 2867 (w), 2109 (m), 1513 (w), 1458 (w), 1268 (m), 1005 (w), 866 (s), 830 (s) and 554 (s) cm⁻¹.

TLC: R_f = 0.7 in 80:1 hexanes:EtOAc.

HRMS (APCI/TOF): Calcd for (M+H)⁺ (C₁₆H₂₉Si)⁺: 249.2033. Found: 249.2025.

Procedure for Desilylative Carboxylation to Ibuprofen⁸⁷

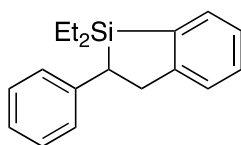


In a glove box, the hydrosilylation product **5-14** was added to freshly distilled DMF (0.1 M) and flame-dried CsF (5.0 equiv) in a flame-dried flask. The vial was taken out from the glove box, and the mixture was heated at 110 °C under 1 atm of CO₂ (balloon) for 10 h. The reaction mixture was then cooled down to room temperature and treated with aqueous NH₄Cl and extracted with ethyl acetate (x3) and the combined organic layer was washed with water (x1) and brine (x1), and then dried over with Na₂SO₄. After removal of solvent under reduced pressure, the residue was purified by flash silica-gel column chromatography to give Ibuprofen **5-15**.

F.22. E. Rh-catalyzed C–H silylation of diarylsilane to afford dihydrobenzosilole

5-16:

1,1-Diethyl-2-phenyl-2,3-dihydro-1*H*-benzo[*b*]silole (5-16)



To a flame-dried vial, **2s** (268 mg, 1 mmol) was added. [Rh(nbd)Cl]₂ (1.84 mg, 0.4 mol %), *tris*(4-methoxyphenyl)phosphine (8.45 mg, 2.4 mol %) and norbornene (188 mg, 2 mmol) were dissolved with THF, and the mixture was added to the mixture. The septum on the vial was replaced by a screw cap with a Teflon liner, and the mixture was stirred at 120 °C for 30 min. The volatiles were removed *in vacuo*, and was purified by MPLC (hexanes 5 mL/min, retention time 12 min).^{177, 261}

Yield: 1 mmol scale, 170 mg, 64%.

¹H NMR (CDCl₃, 500 MHz): δ 7.53 (d, *J* = 7.1 Hz, 1H, Ar-*H*), 7.37 (ddd, *J* = 6.9, 6.9, 1.3 Hz, 1H, Ar-*H*), 7.34 (d, *J* = 6.9 Hz, 1H, Ar-*H*), 7.25-7.21 (m, 3H, Ar-*H*), 7.10-7.07 (m, 3H, Ar-*H*), 3.51 [dd, *J* = 16.6, 8.4 Hz, 1H, C(Si)HCH_aH_b], 3.39 [dd, *J* = 16.6, 7.1 Hz, 1H, C(Si)HCH_aH_b], 2.92 [dd, *J* = 8.4, 7.1 Hz, 1H, C(Si)HCH₂], 1.06 (dd, *J* = 7.7, 7.7 Hz, 3H, SiCH₂CH₃), 0.98-0.86 (m, 2H, SiCH₂CH₃), 0.74 (dd, *J* = 7.9, 7.9 Hz, 3H, SiCH₂CH₃), and 0.56-0.42 (m, 2H, SiCH₂CH₃).

¹³C NMR (CDCl₃, 125 MHz): δ 152.5, 144.9, 137.0, 133.3, 129.8, 128.5, 126.7, 126.1, 125.7, 124.4, 39.9, 33.2, 7.8, 7.2, 4.9, and 3.6.

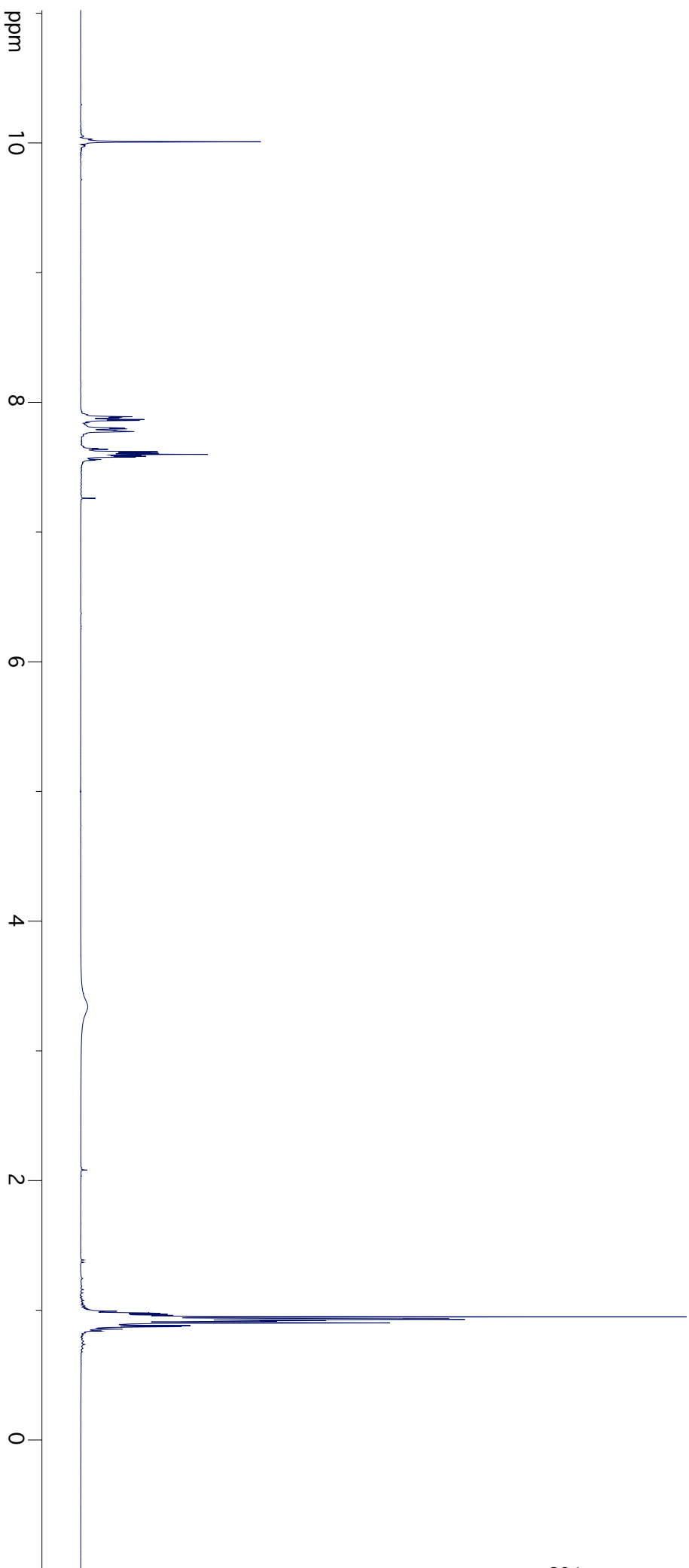
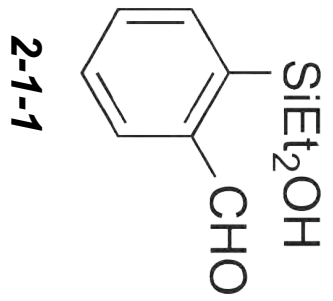
IR (neat): 3057 (w), 2954 (m), 2874 (m), 1689 (s), 1451 (w), 1412 (w), 1270 (m), 1236 (m), 1055 (s), 1004 (s), 697 (s), 490 (w), and 428 (w) cm⁻¹.

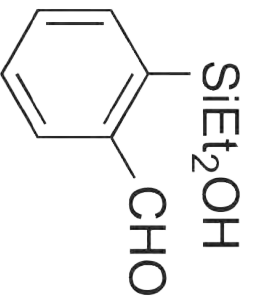
TLC: R_f = 0.5 in hexanes.

HRMS (APCI/TOF): Calcd for (M+H)⁺ (C₁₈H₂₃Si)⁺: 267.1564. Found: 267.1550.

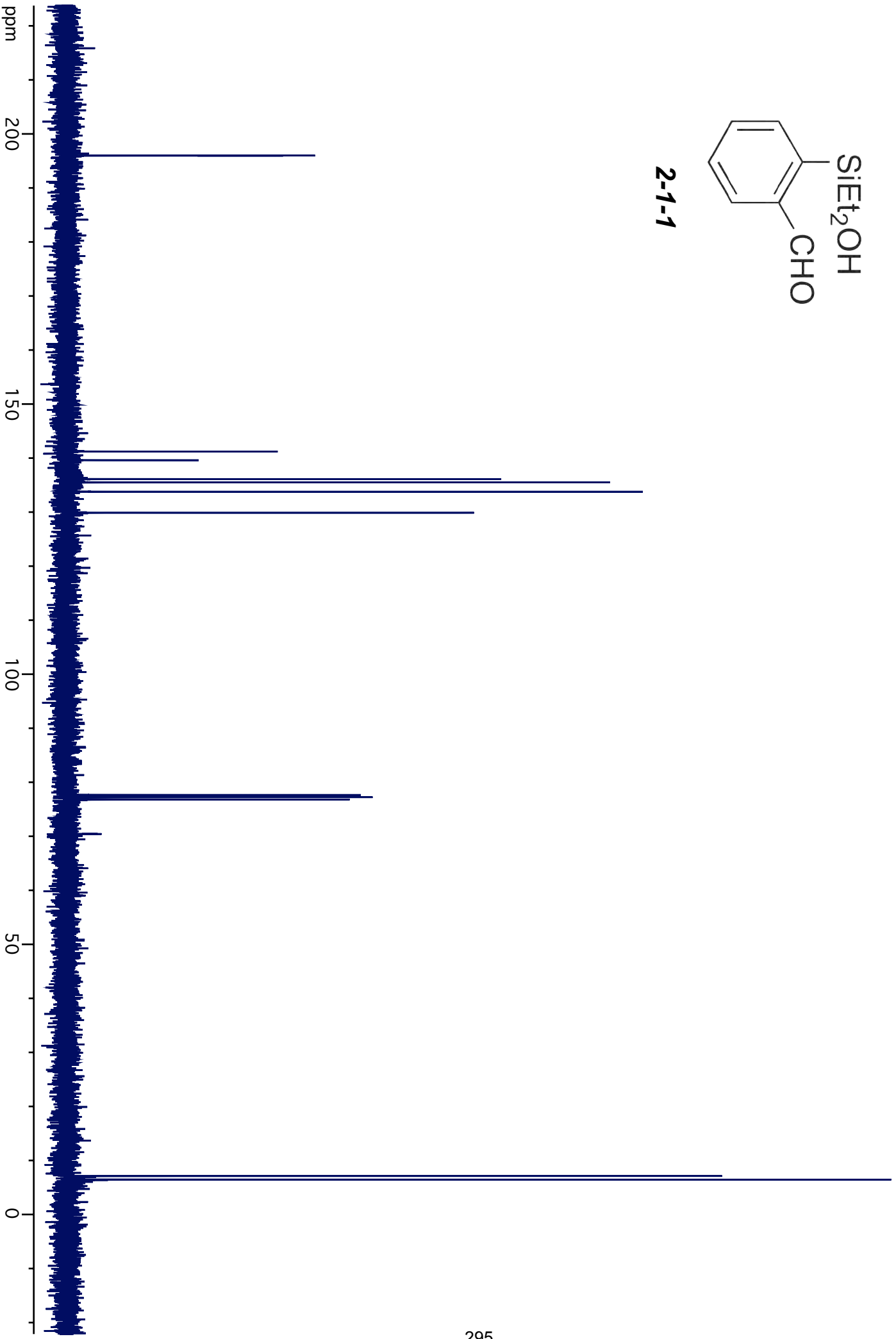
Apendix G

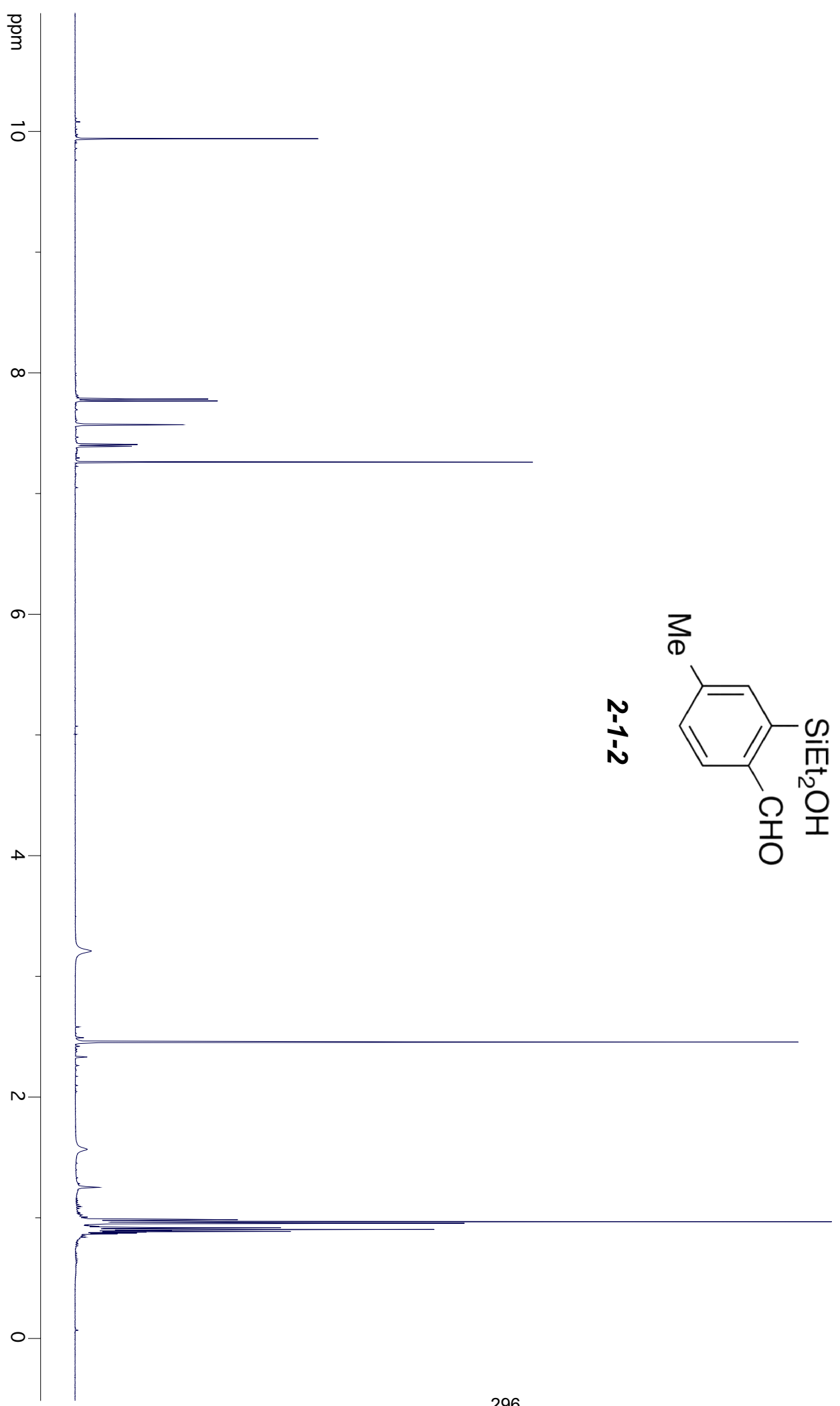
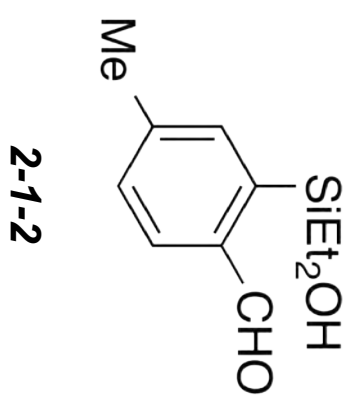
^1H - ^{13}C NMR Spectra

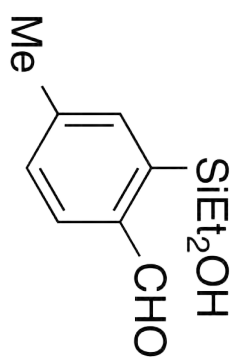




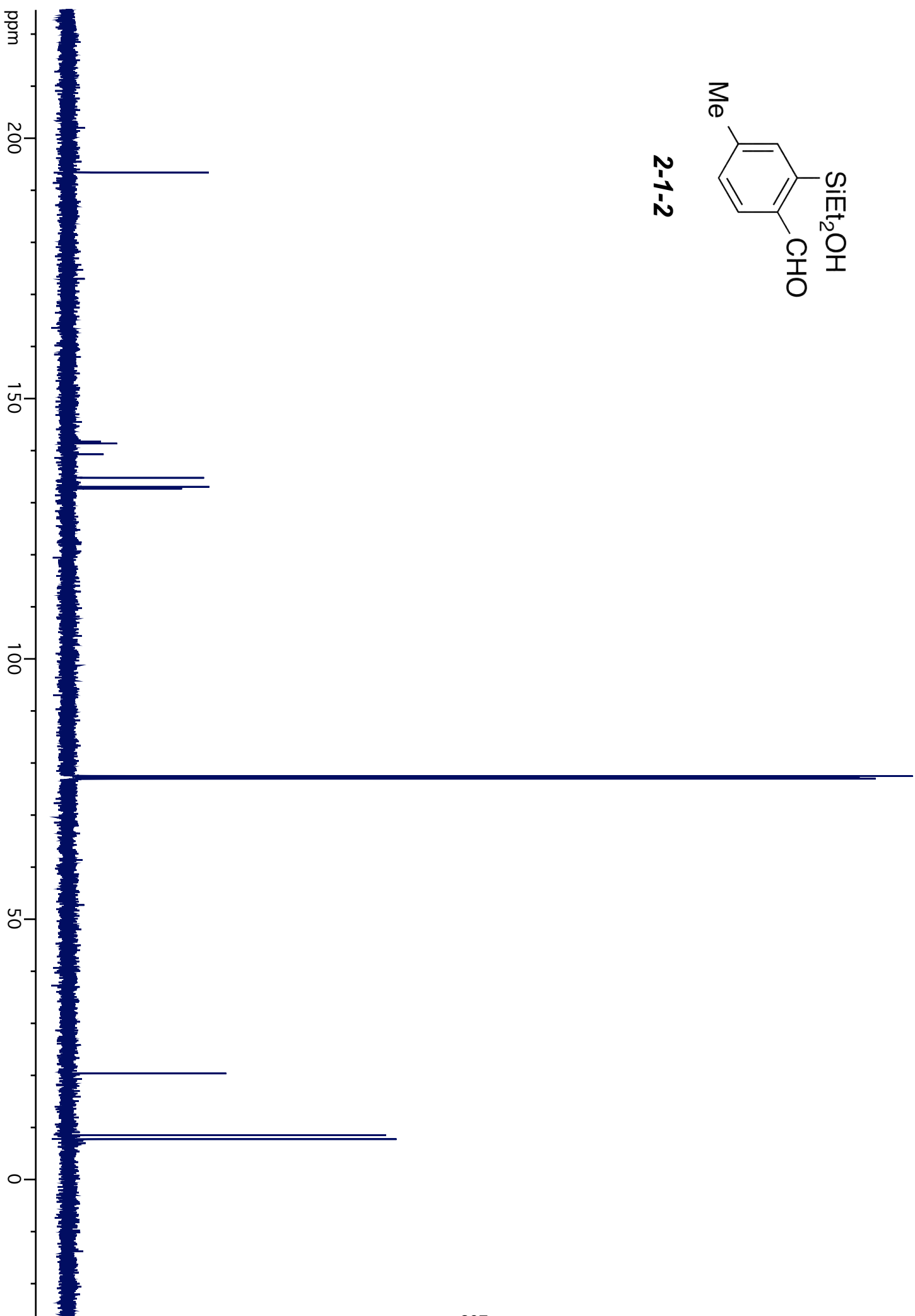
2-1-1

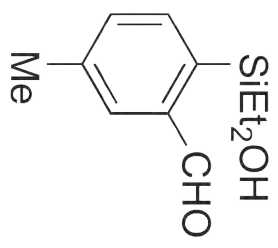




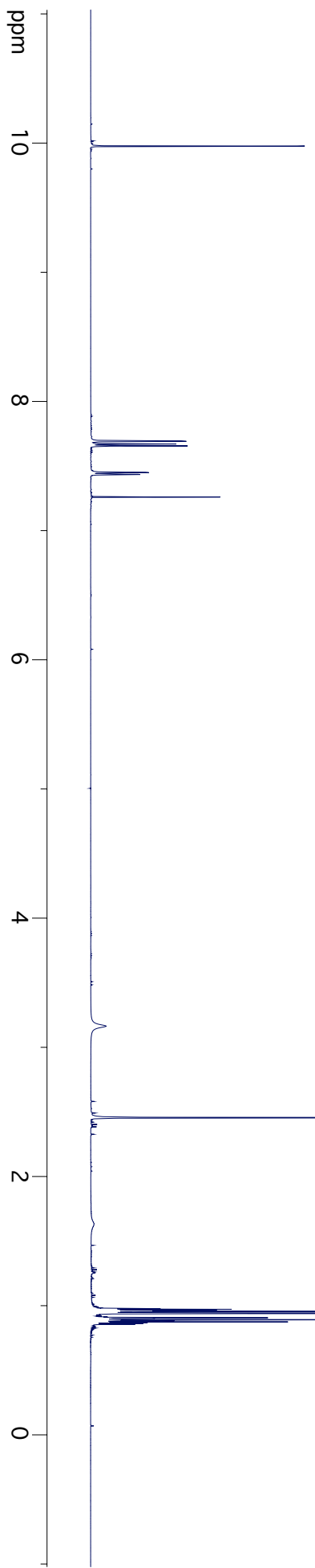


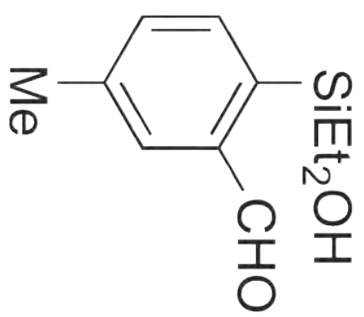
2-1-2



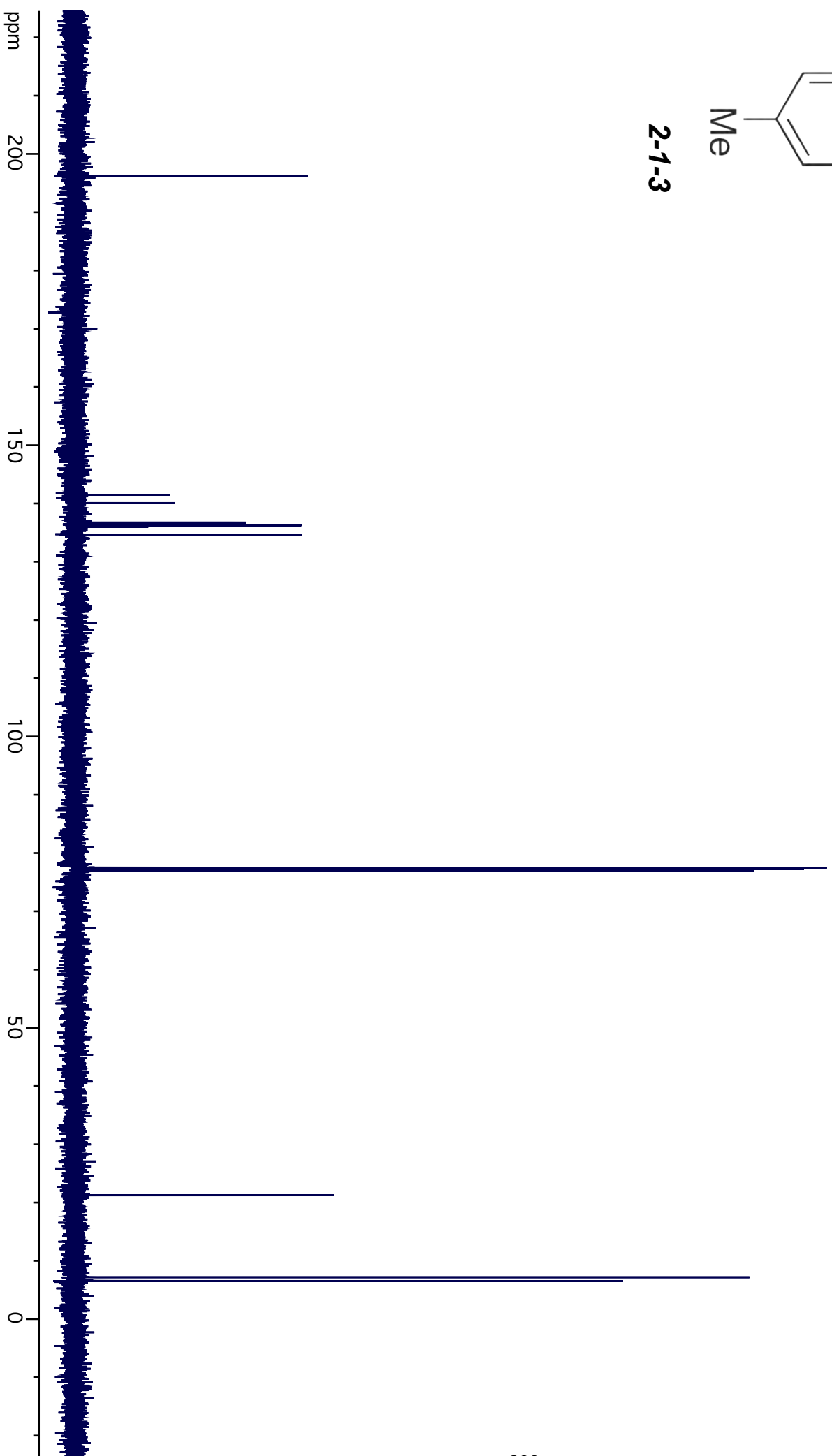


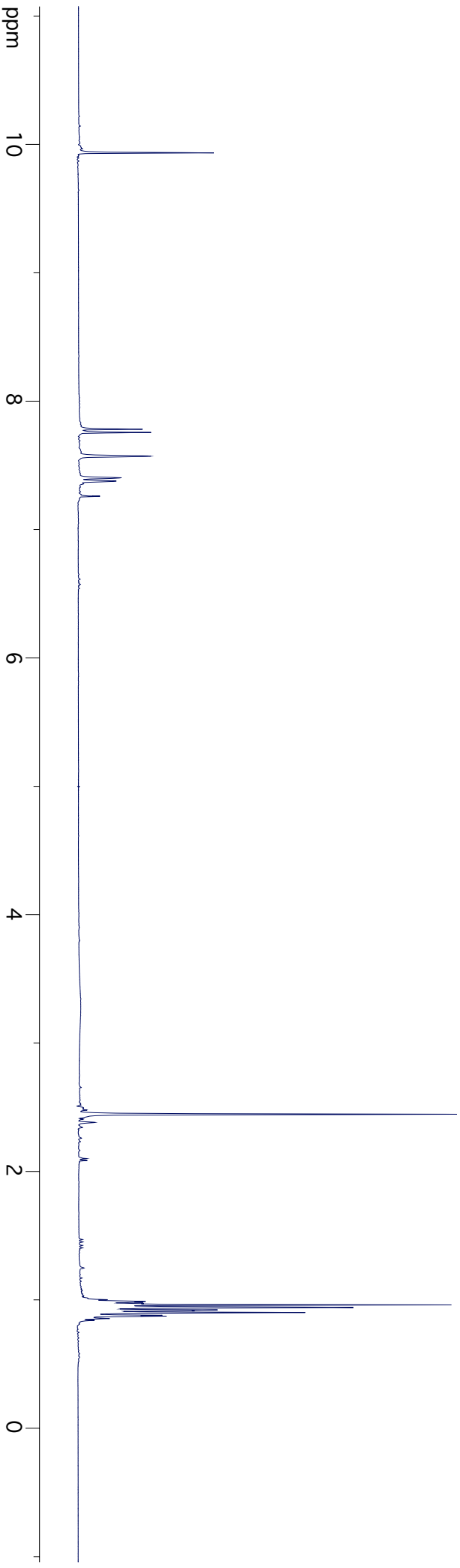
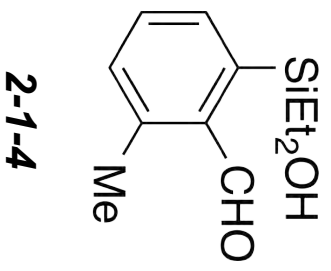
2-1-3

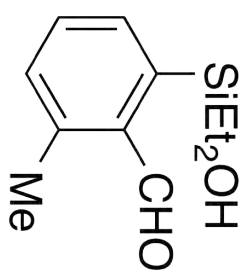




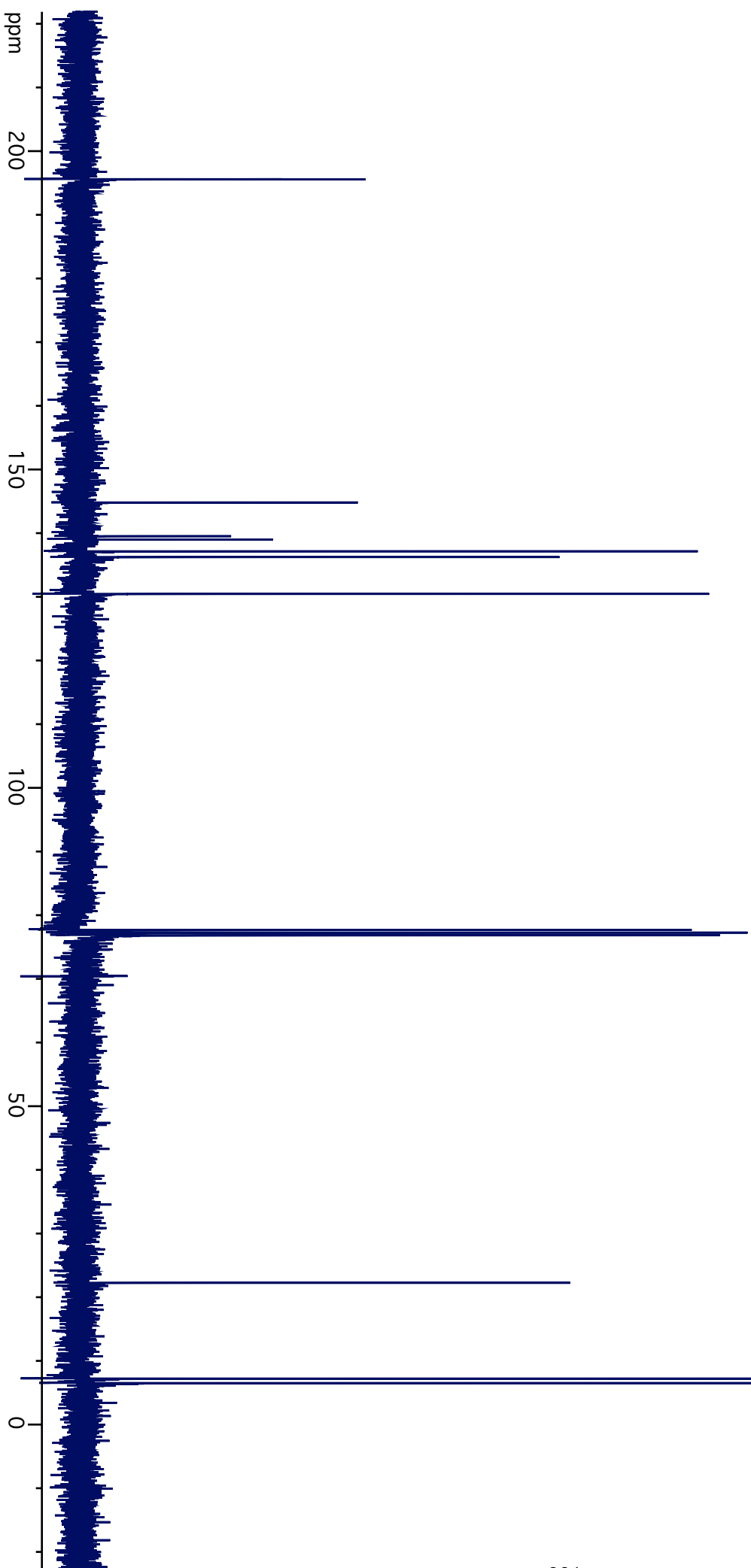
2-1-3

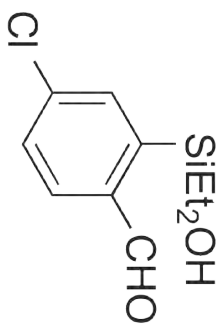




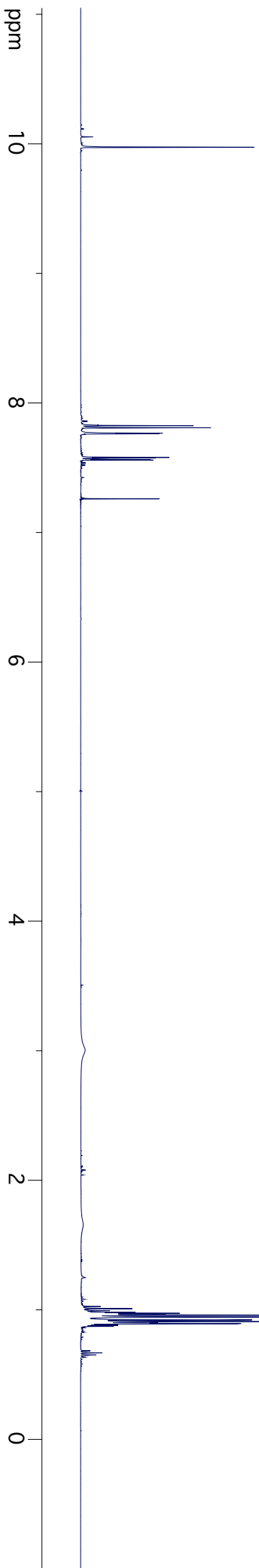


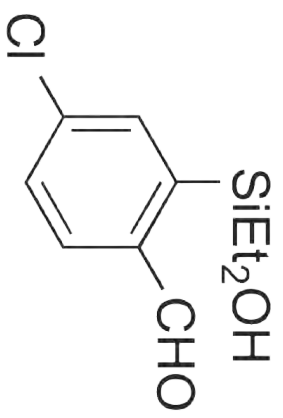
2-1-4



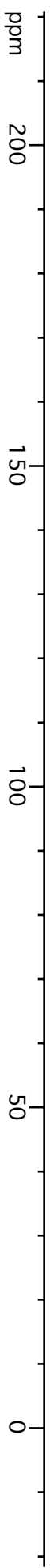


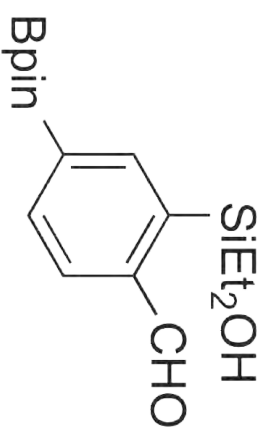
2-1-5



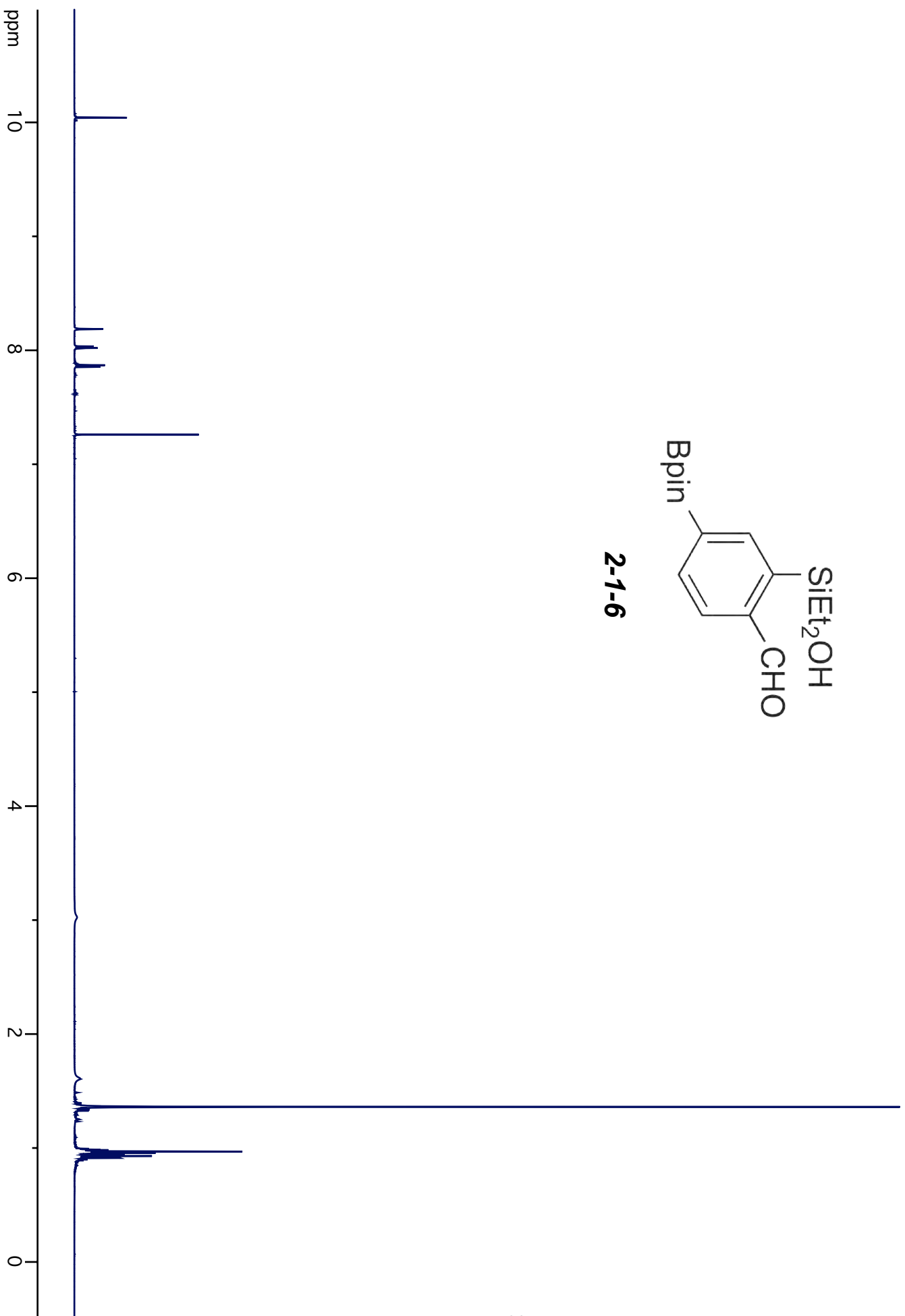


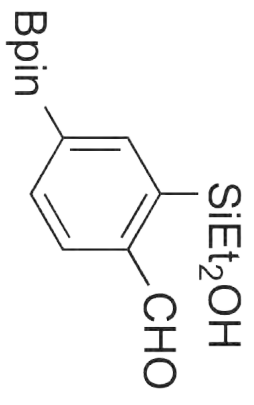
2-1-5





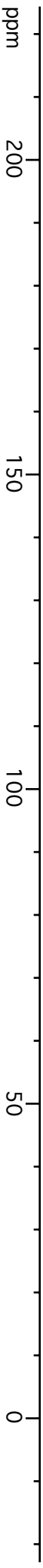
2-1-6

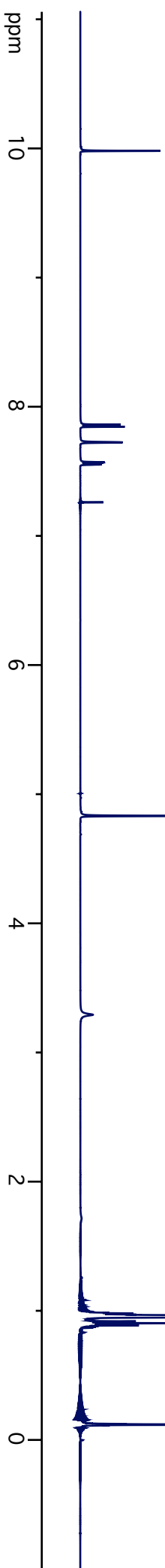
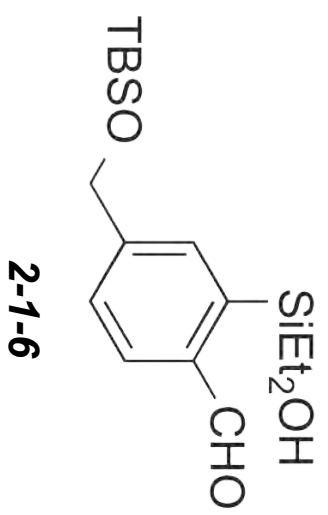


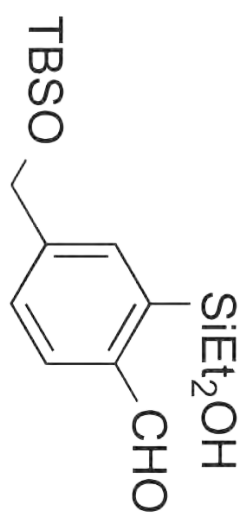


2-1-6

ppm

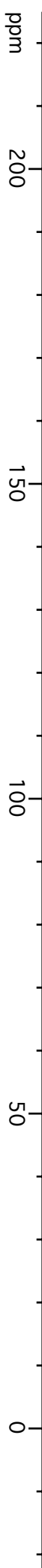


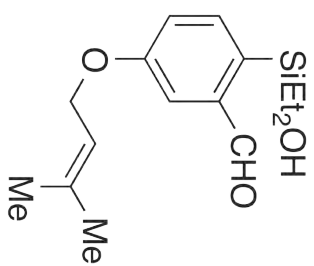




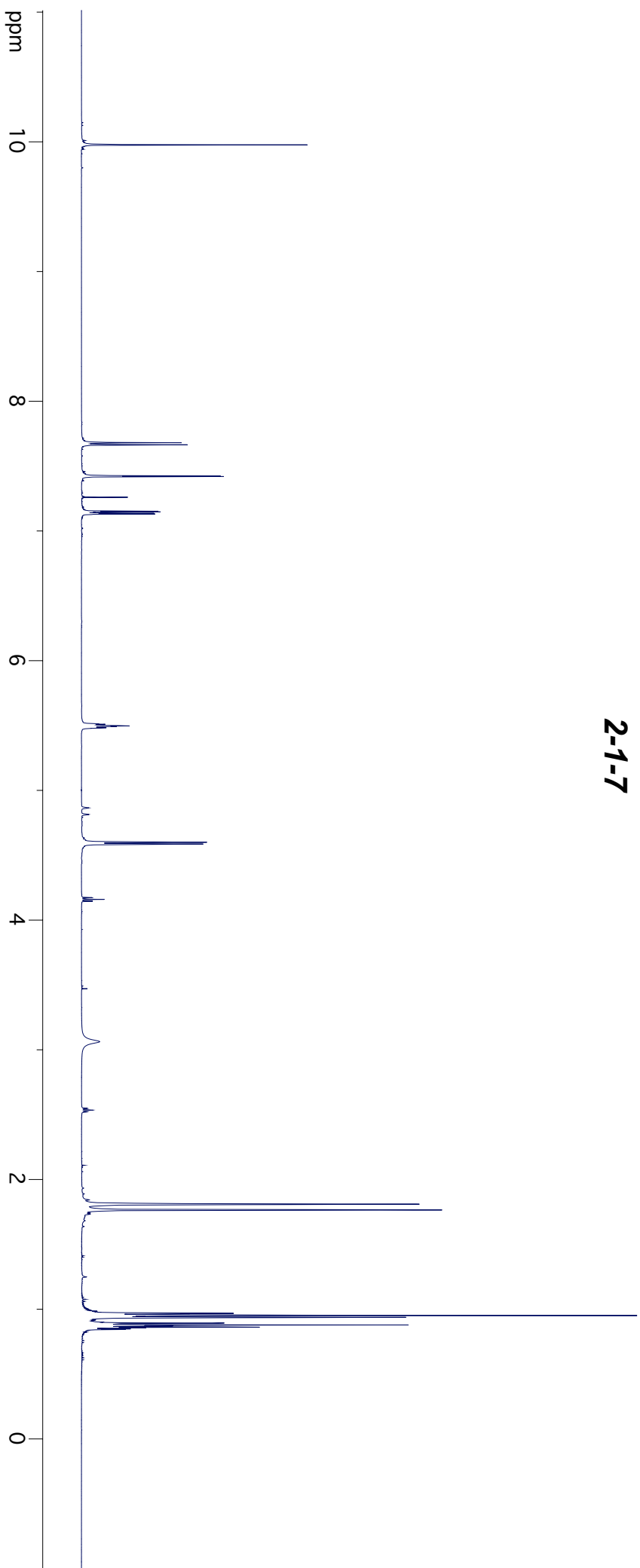
2-1-6

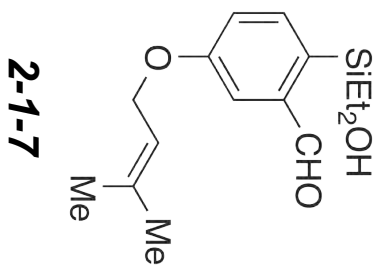
ppm



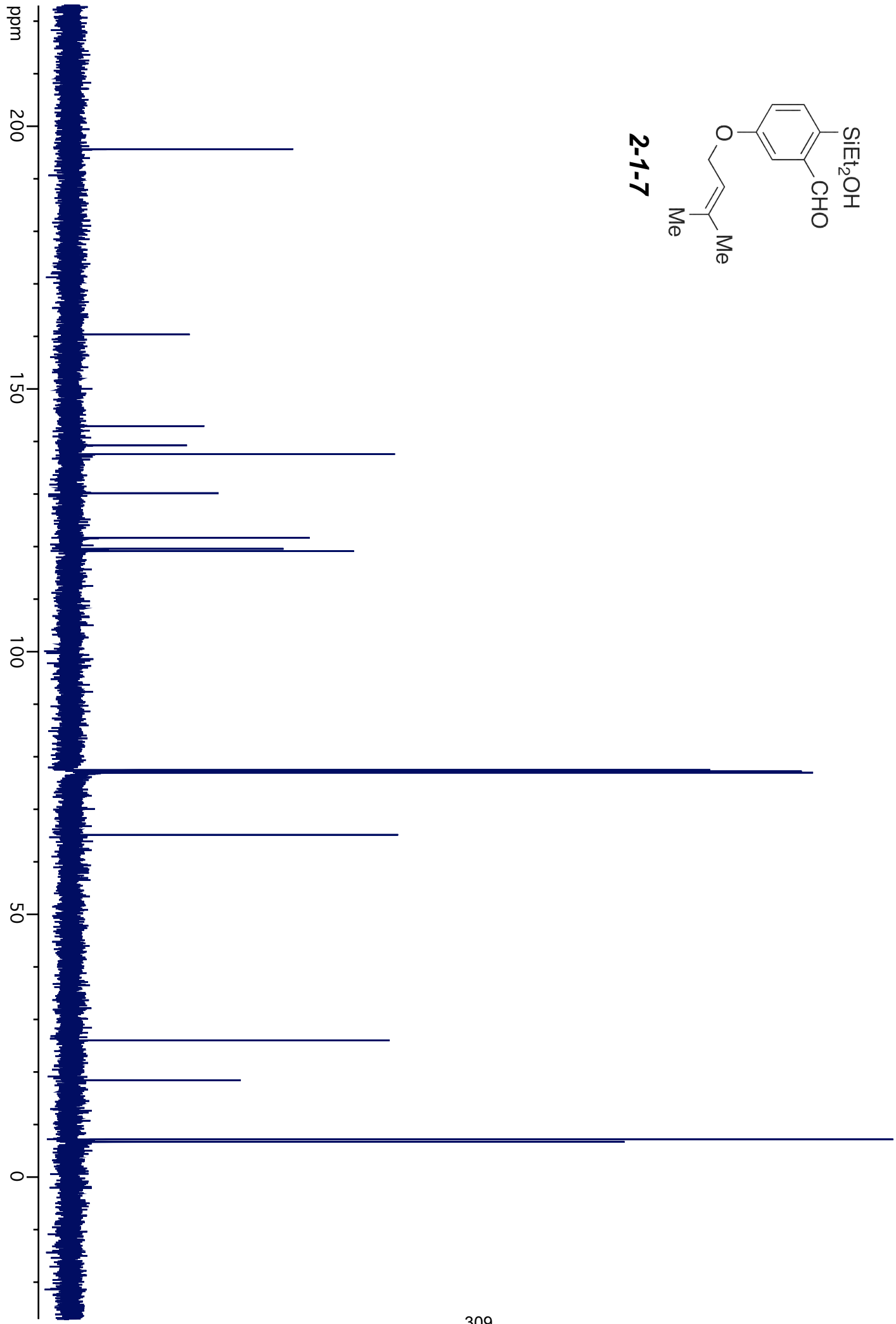


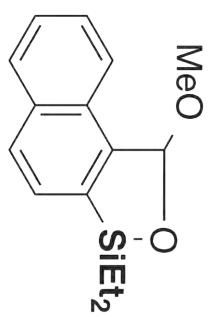
2-1-7



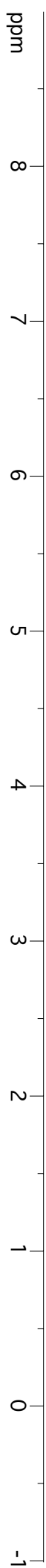


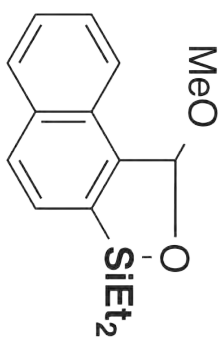
2-1-7





2-1-9





2-1-7

ppm

200

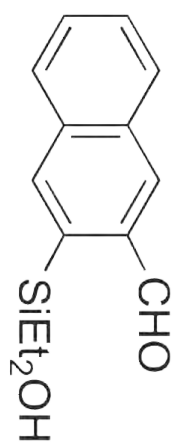
150

100

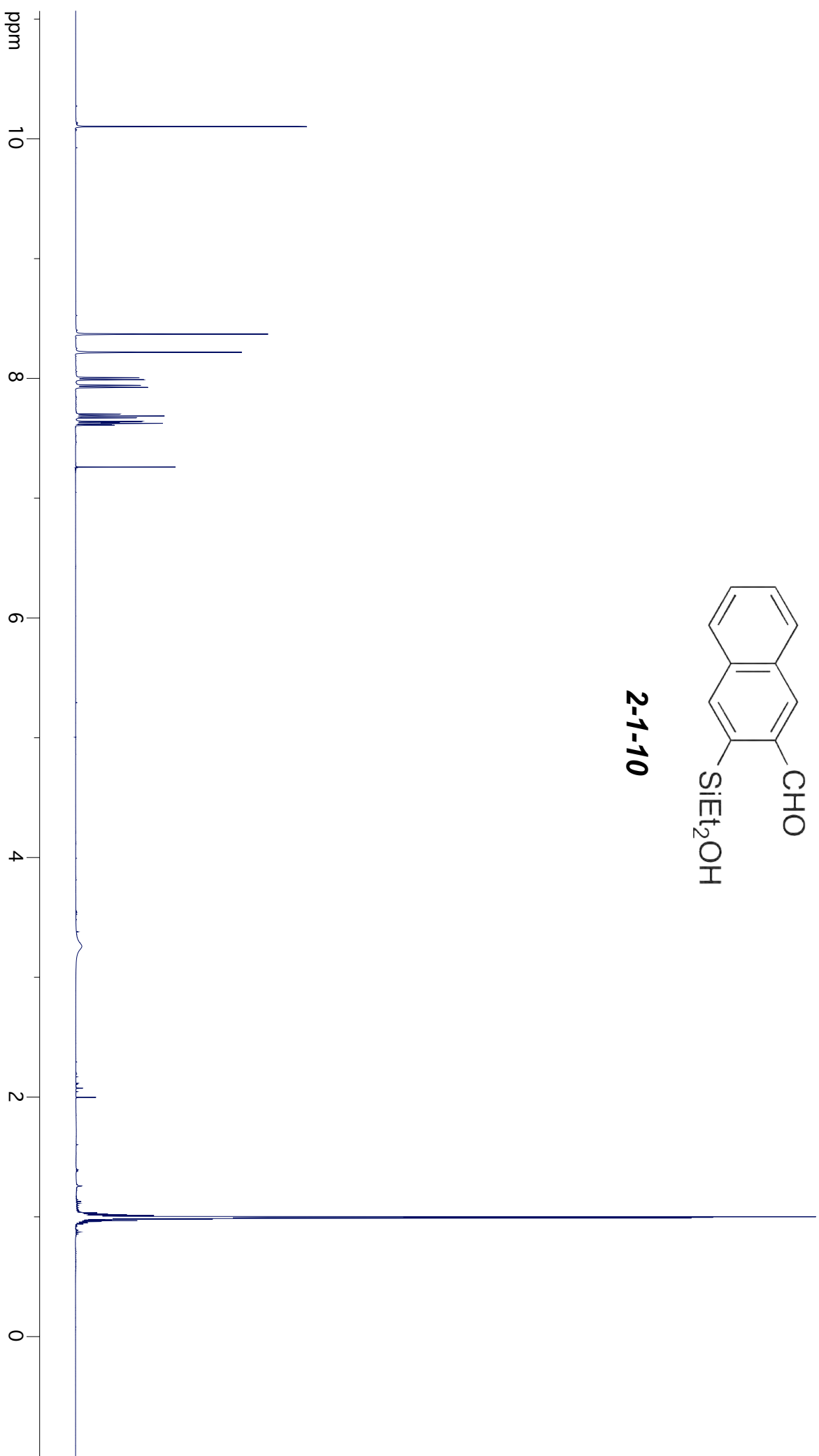
50

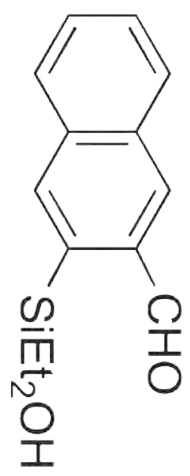
0



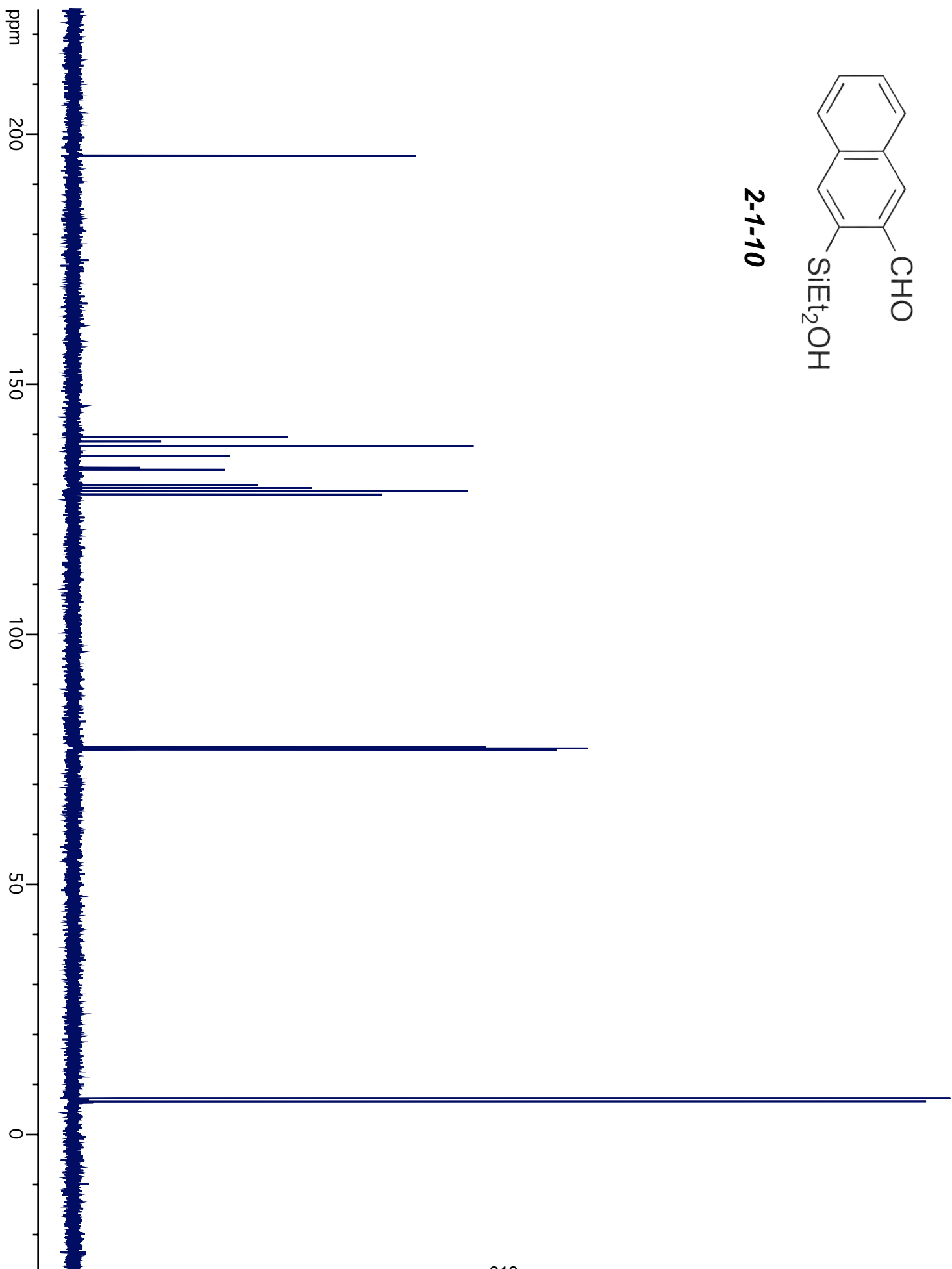


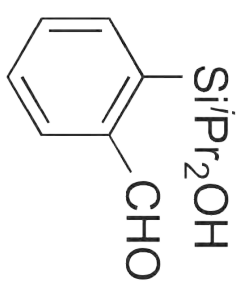
2-1-10





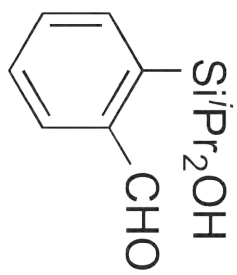
2-1-10





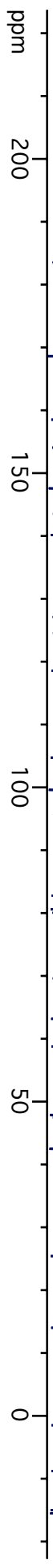
2-2-1

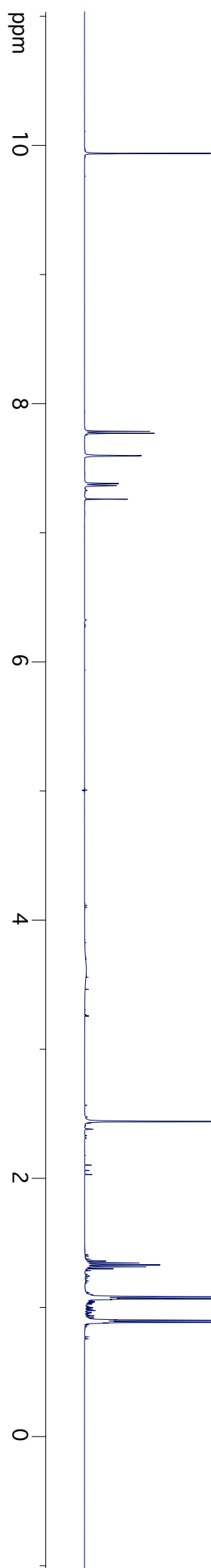
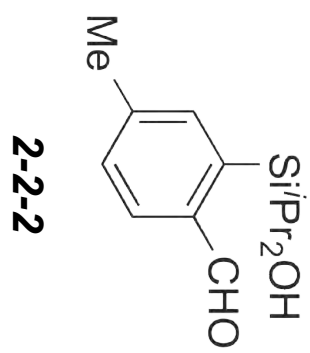


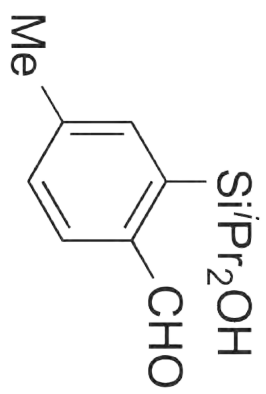


2-2-1

ppm

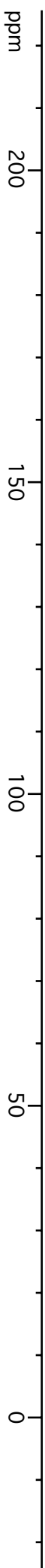


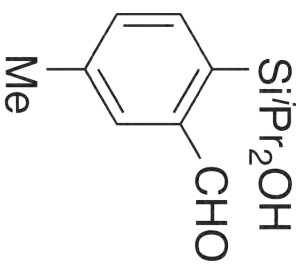




2-2-2

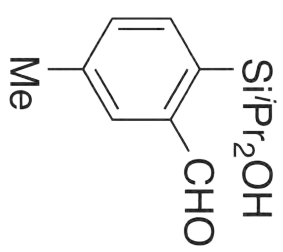
ppm



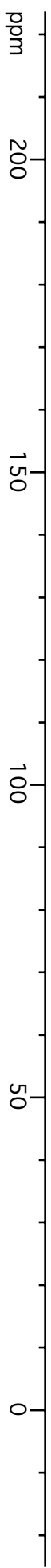


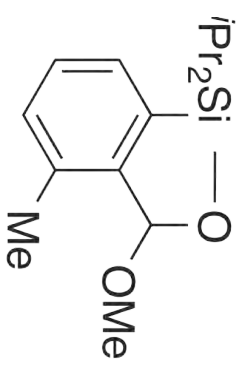
2-2-3



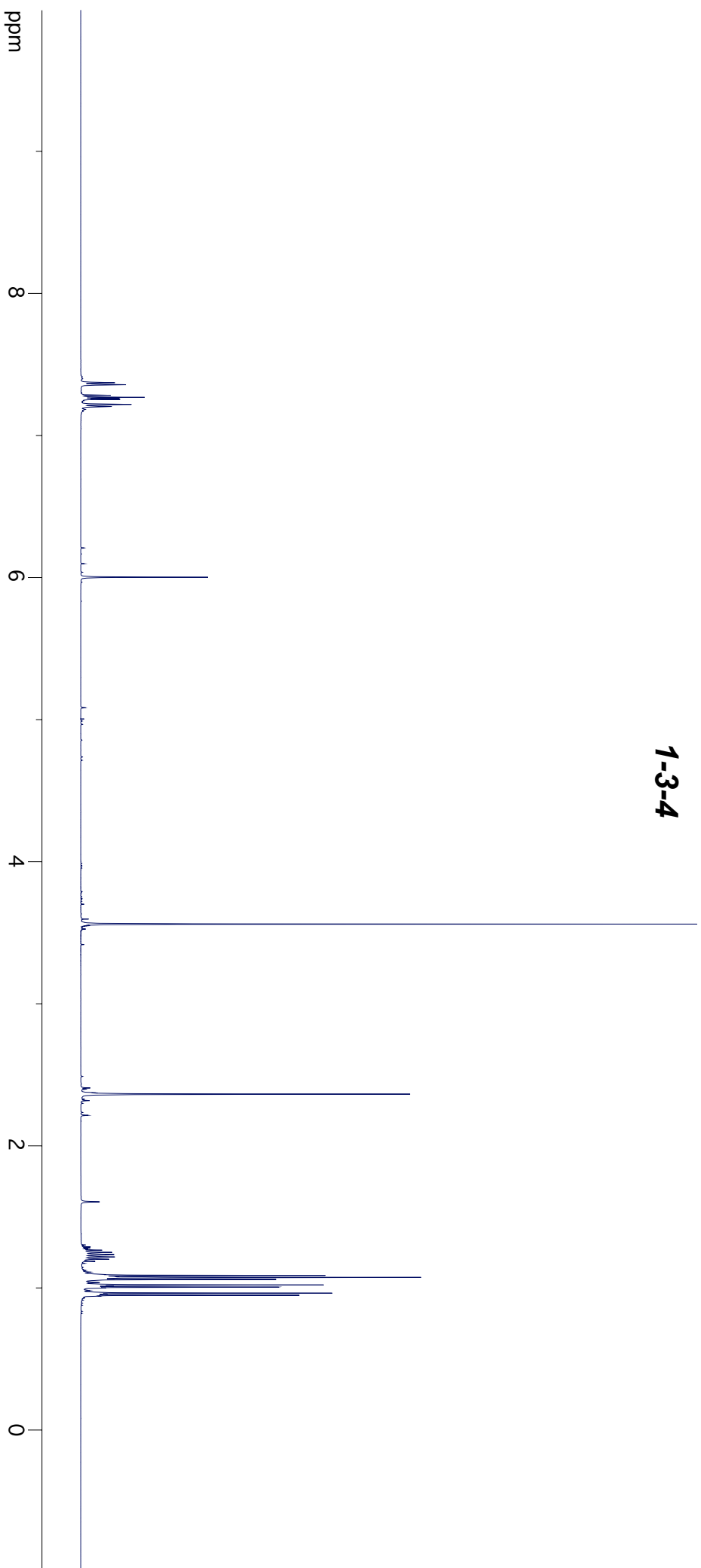


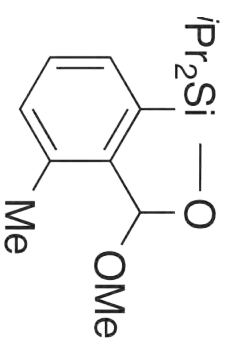
2-2-3



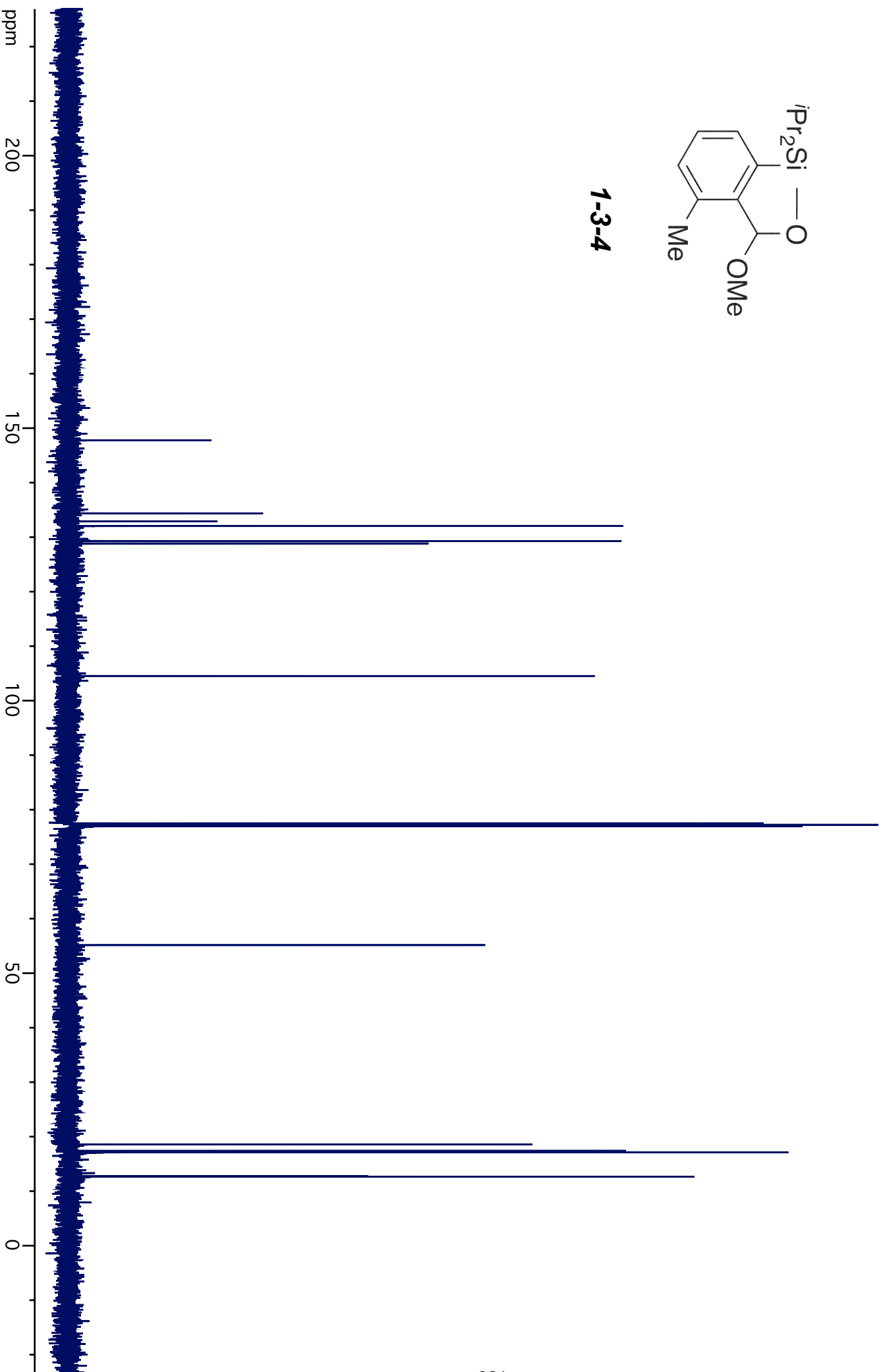


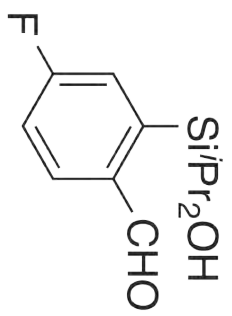
1-3-4



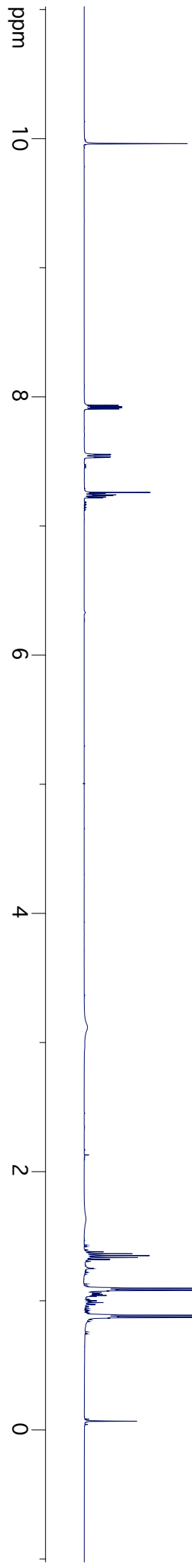


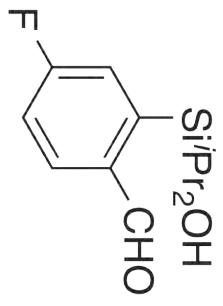
1-3-4



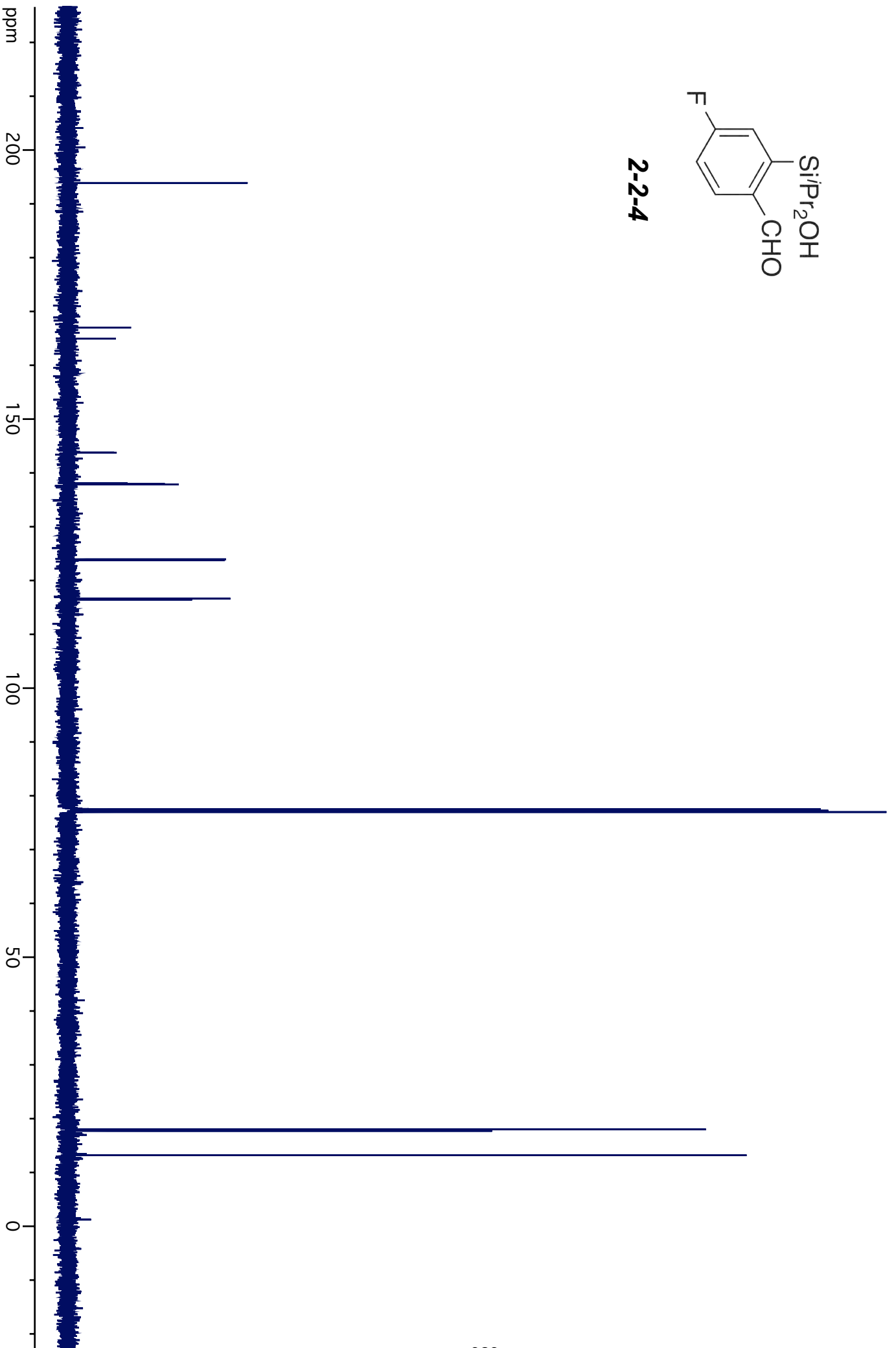


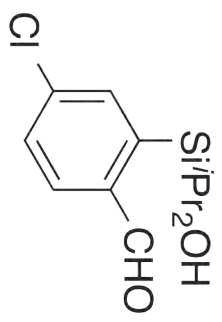
2-2-4





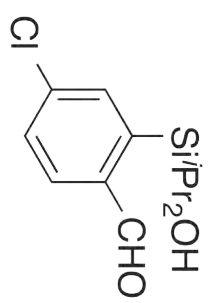
2-2-4



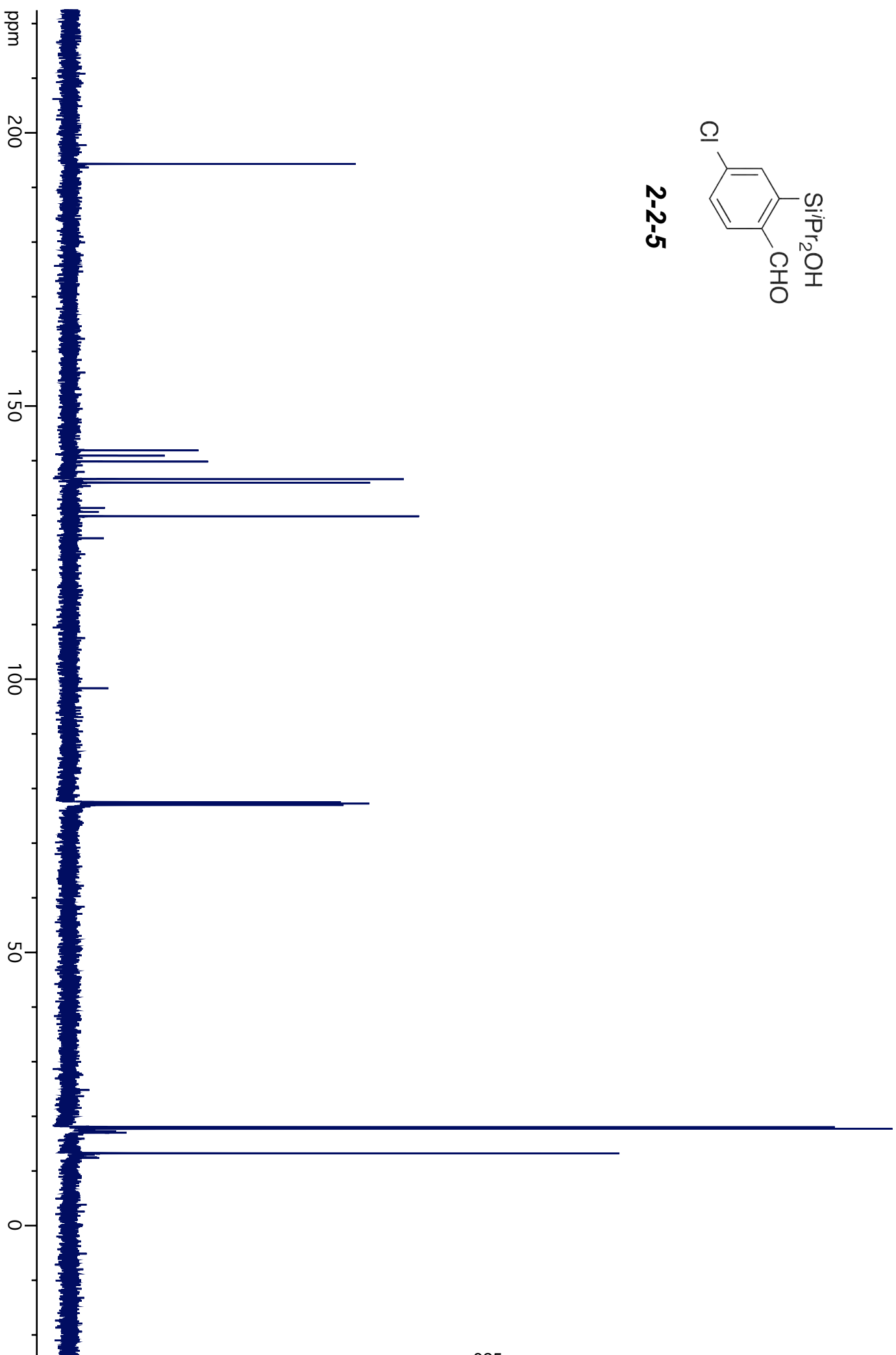


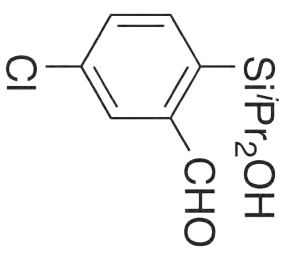
2-2-5



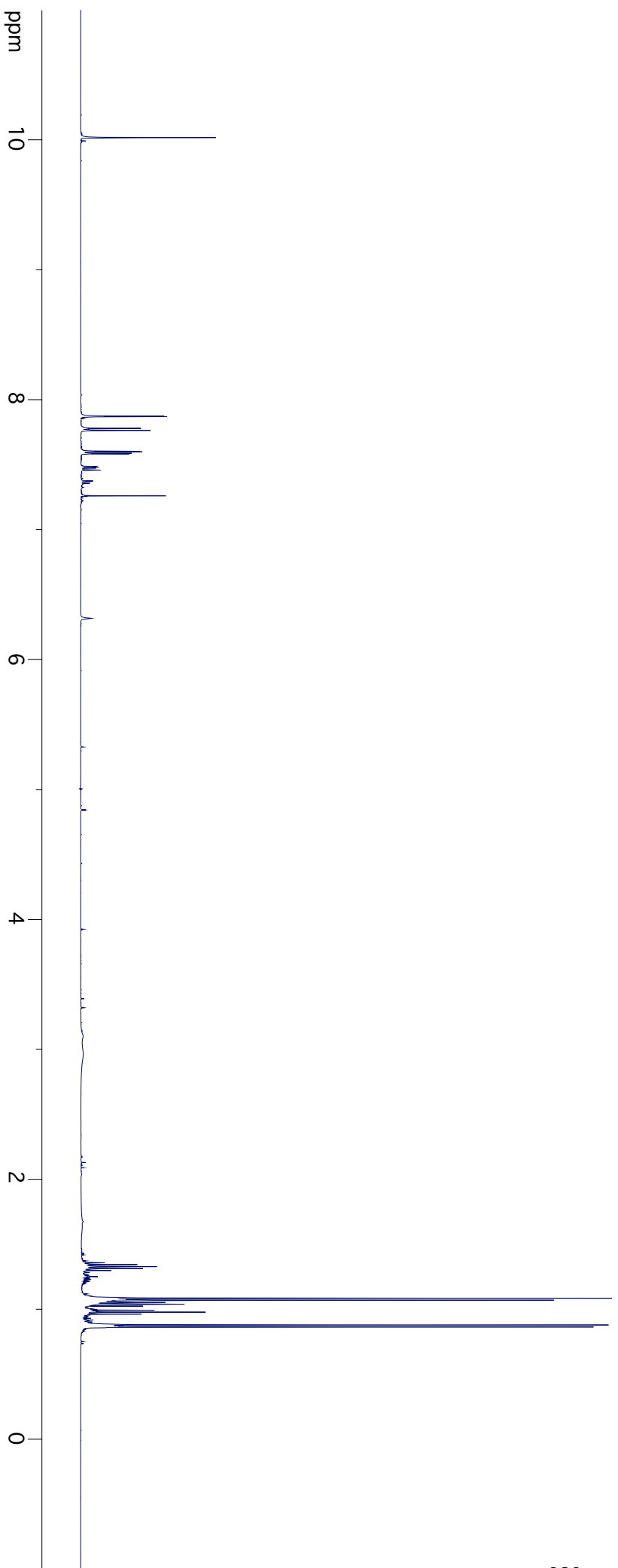


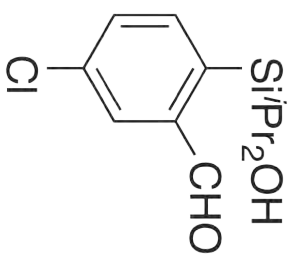
2-2-5



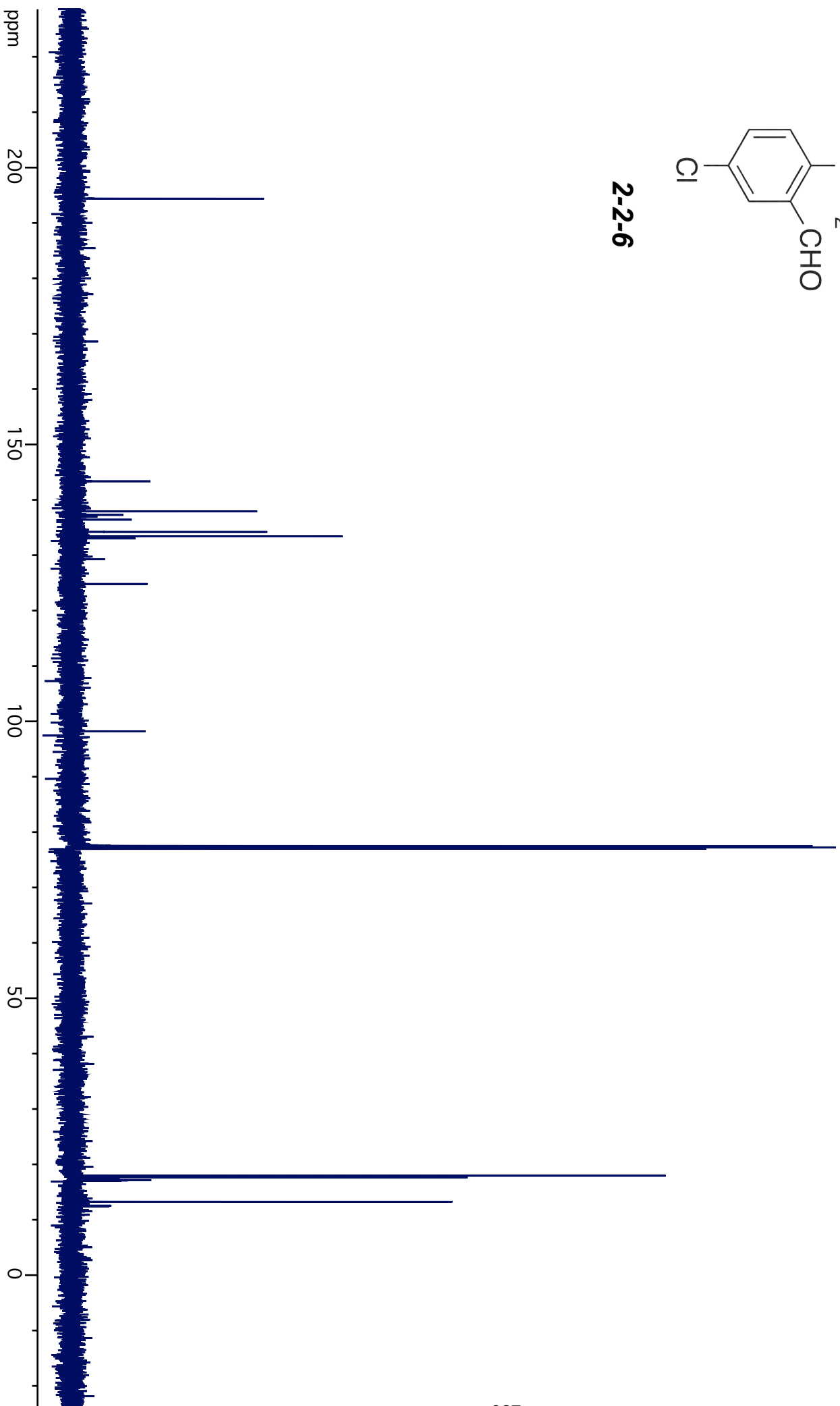


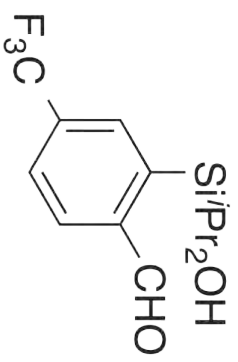
2-2-6



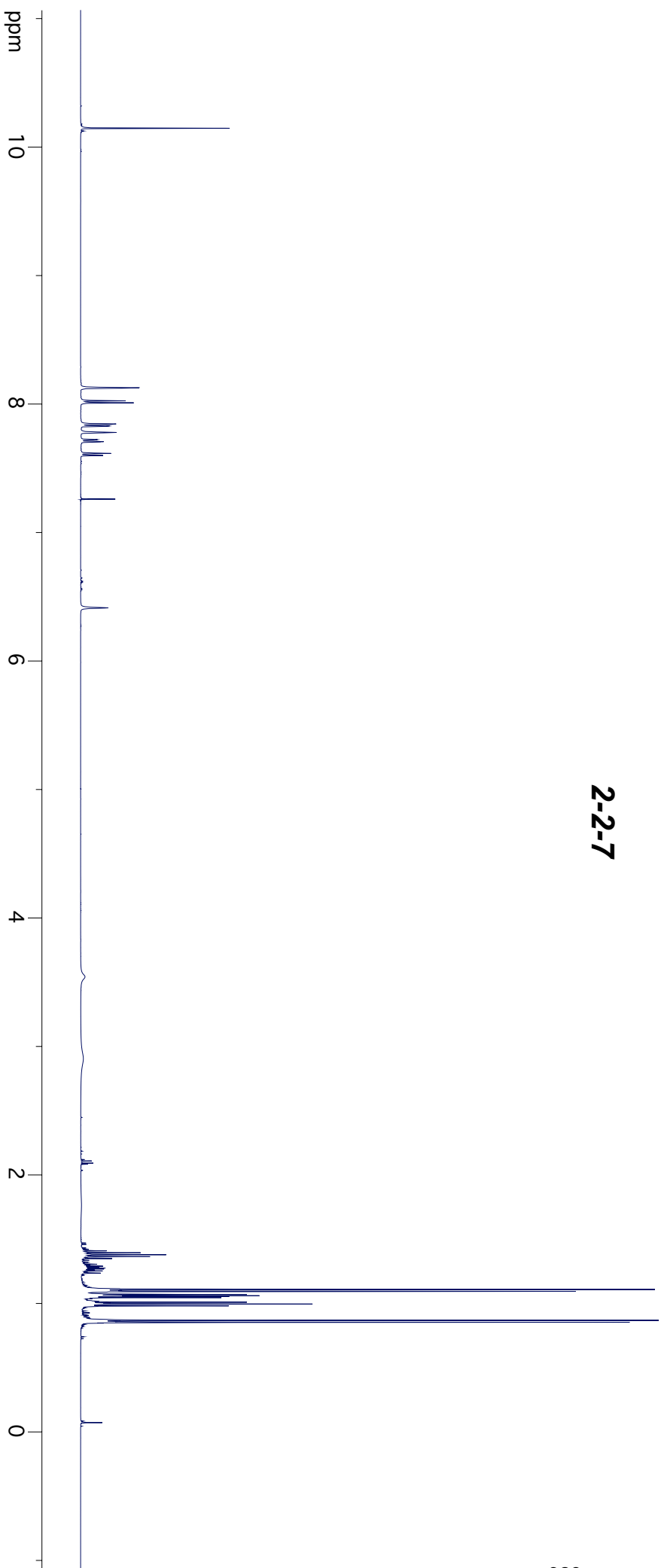


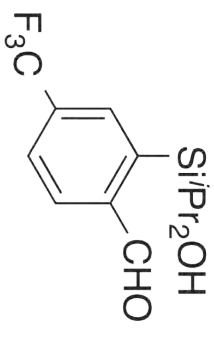
2-2-6



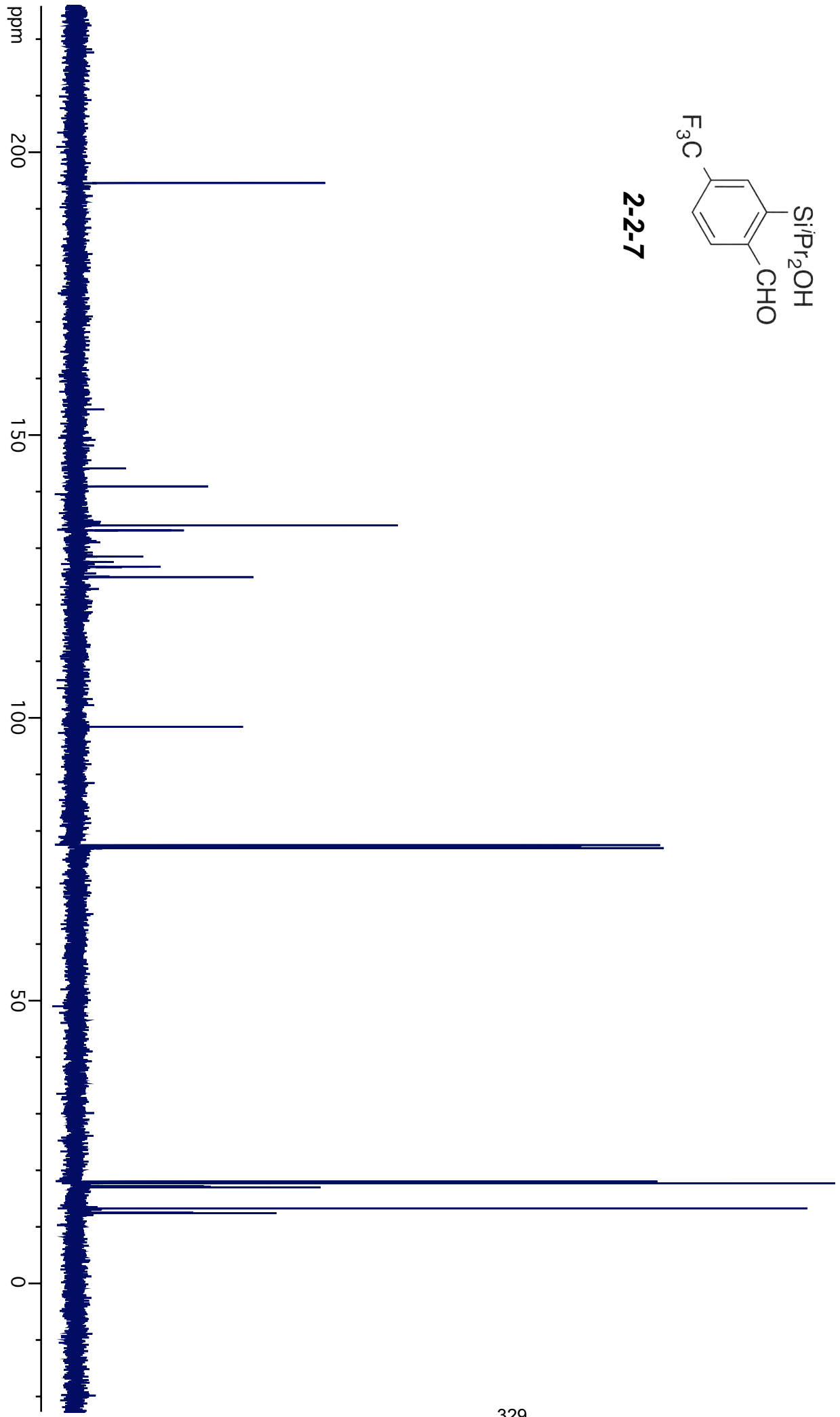


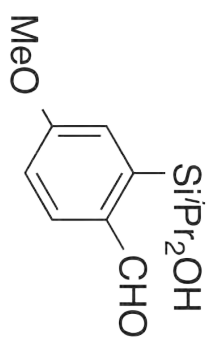
2-2-7





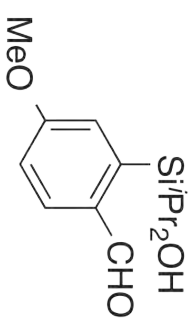
2-2-7



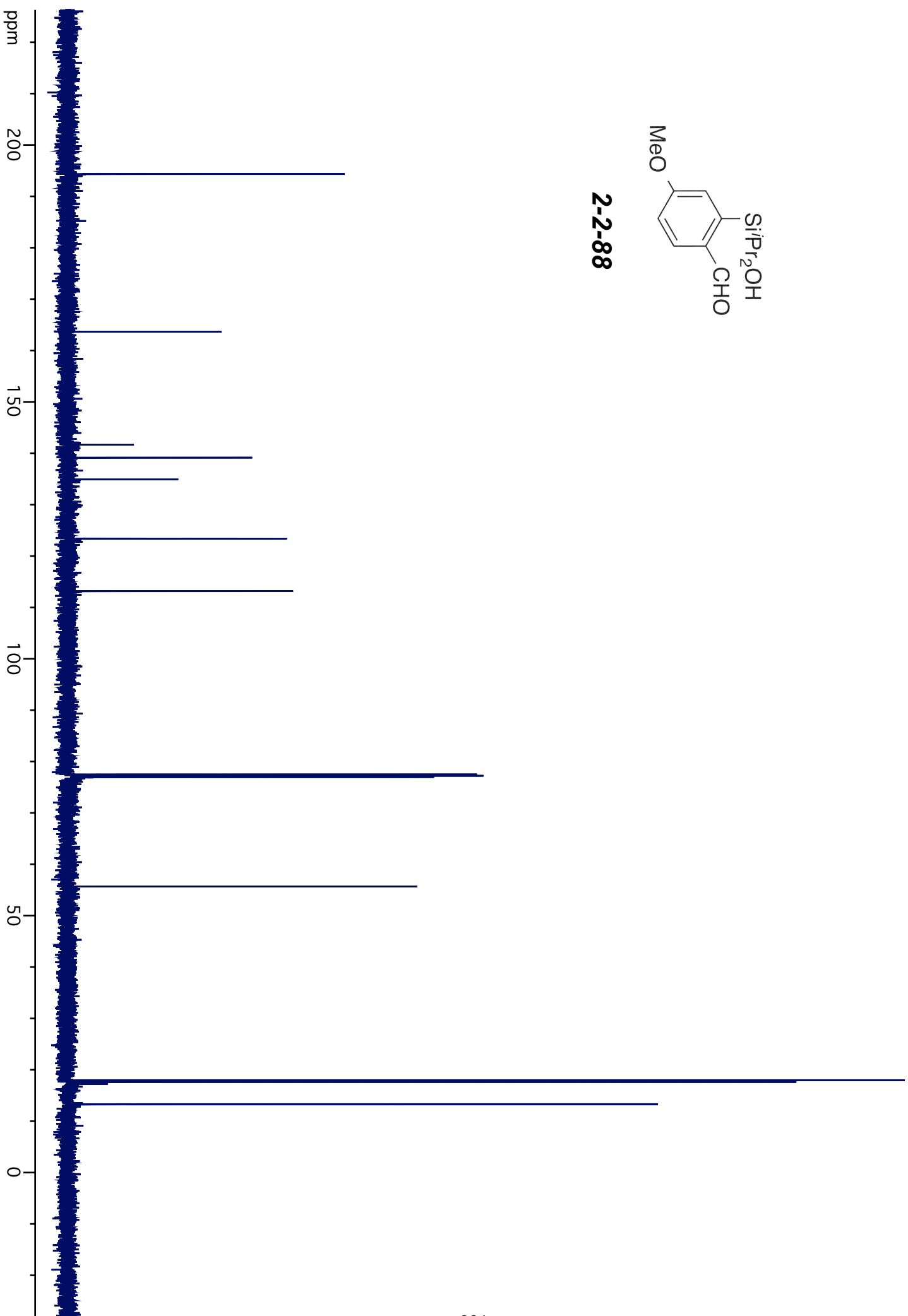


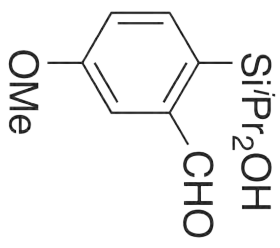
2-2-8





2-2-88





2-2-99

ppm

10

8

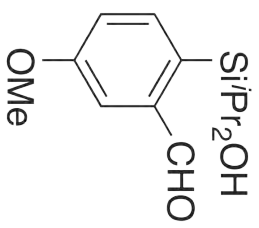
6

4

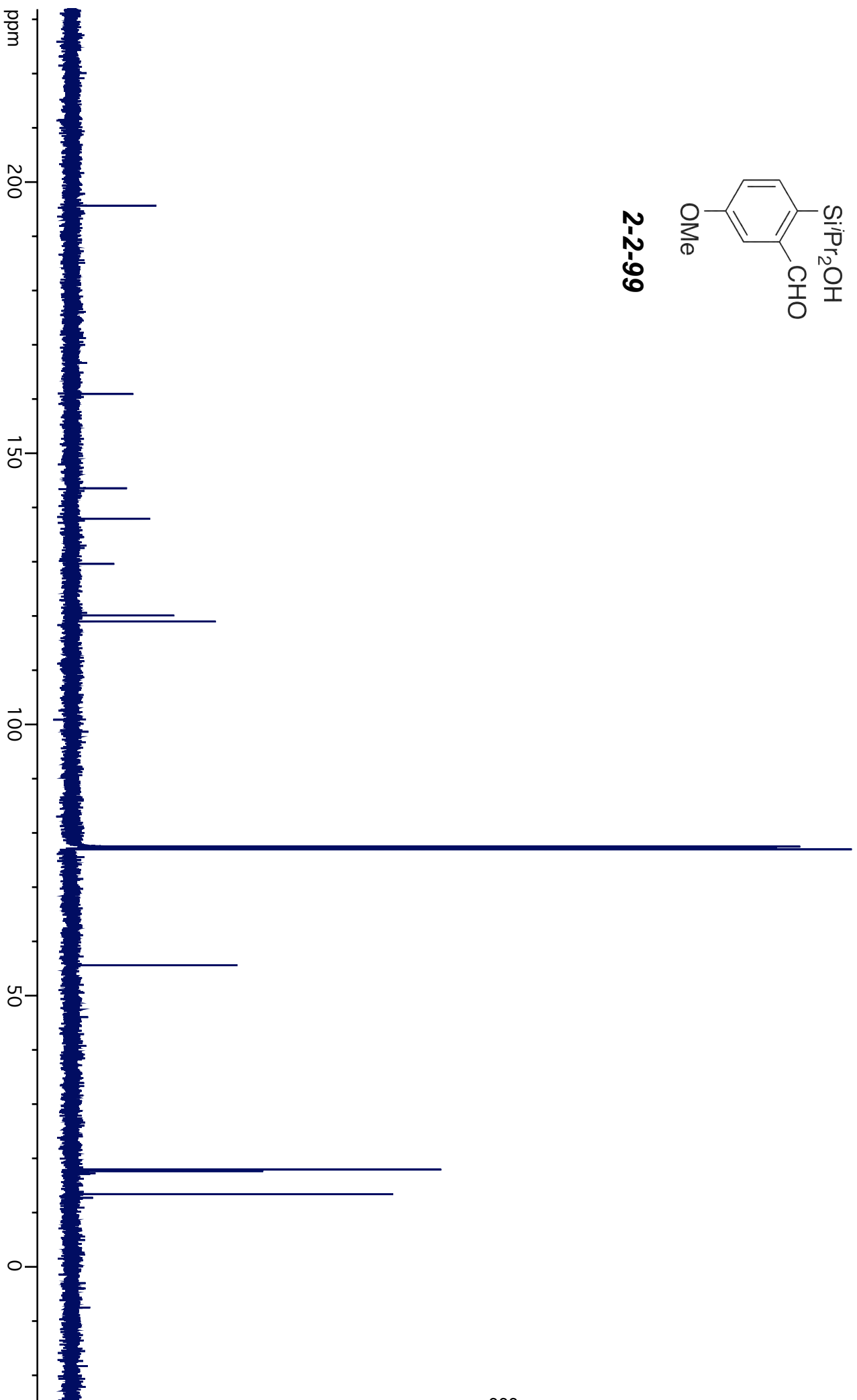
2

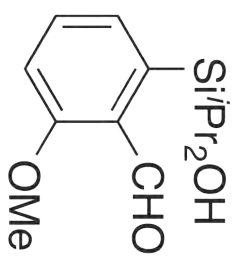
0



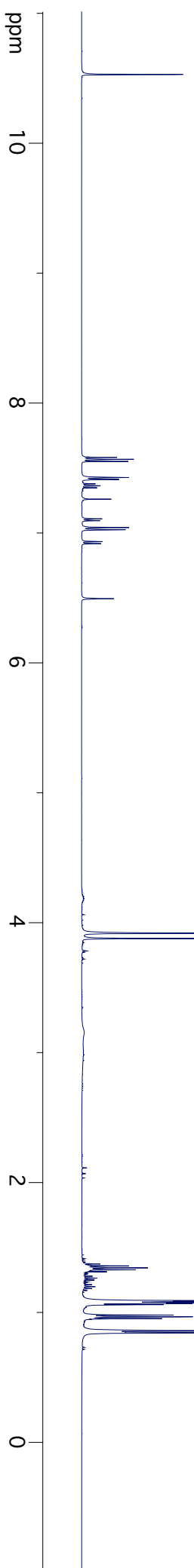


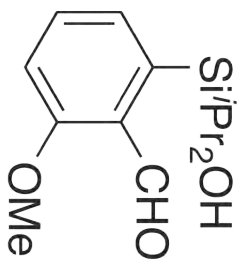
2-2-99



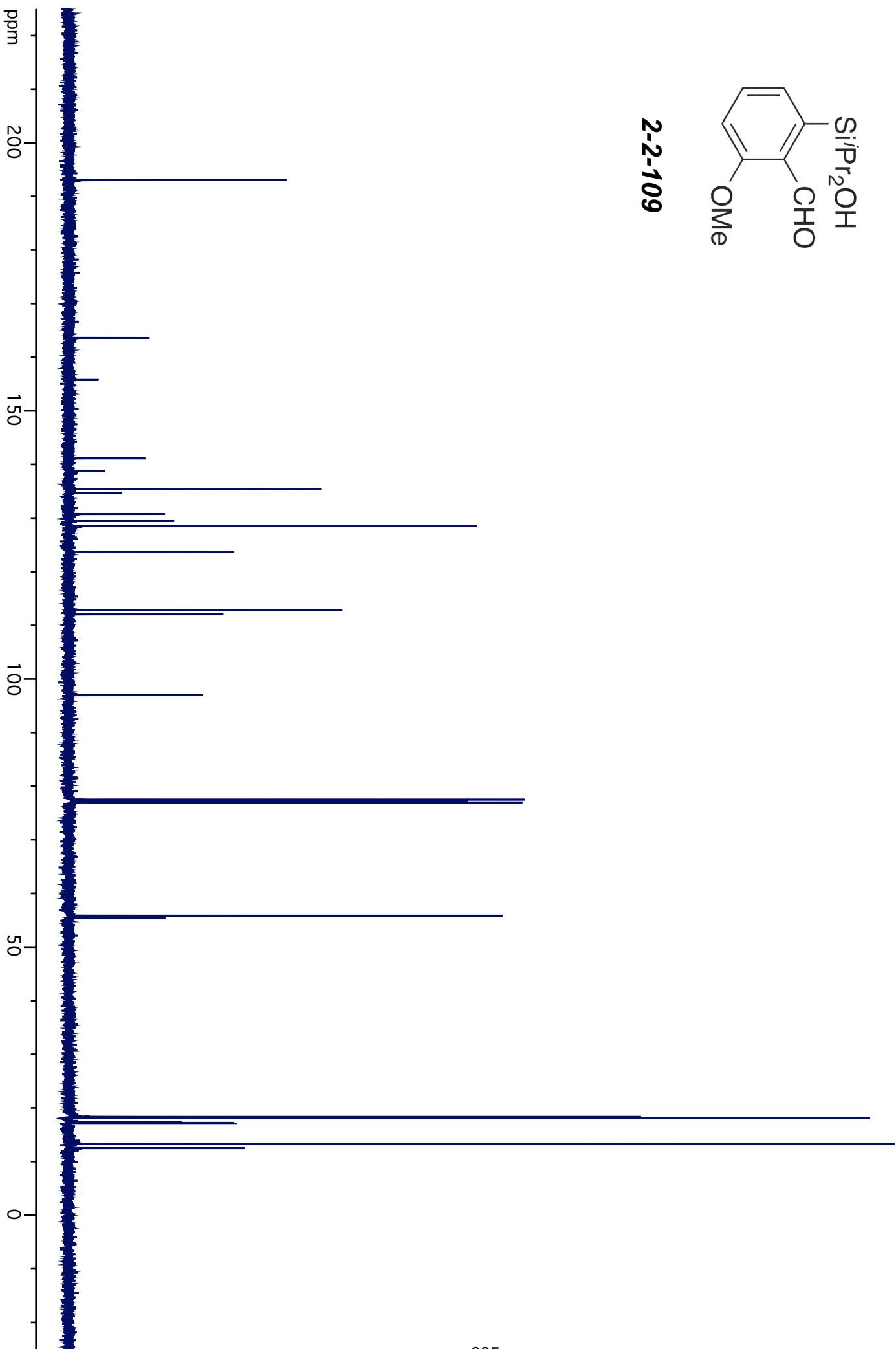


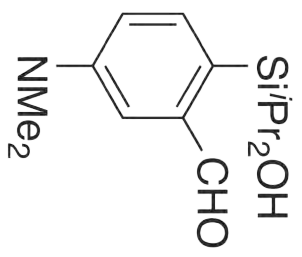
2-2-109



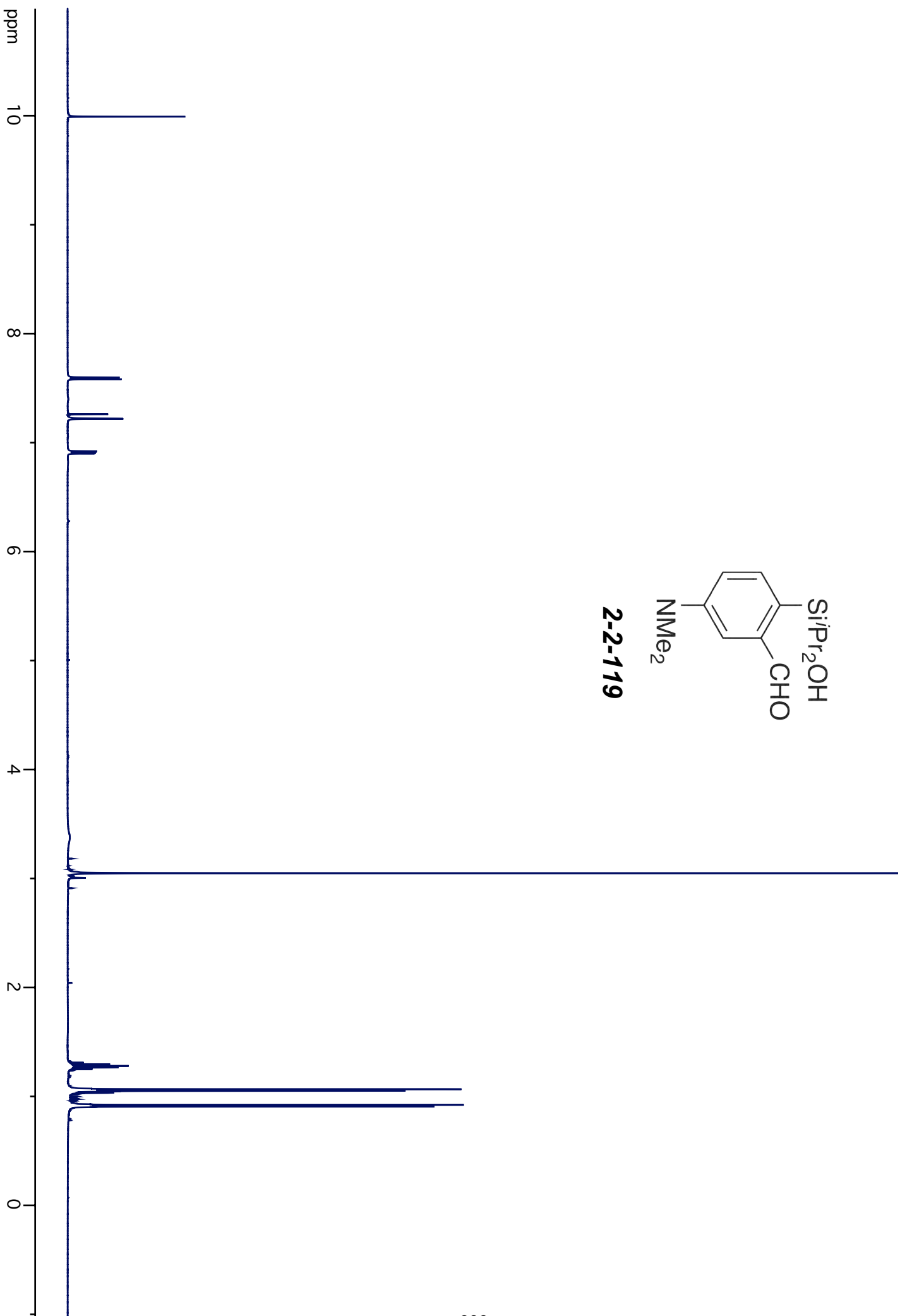


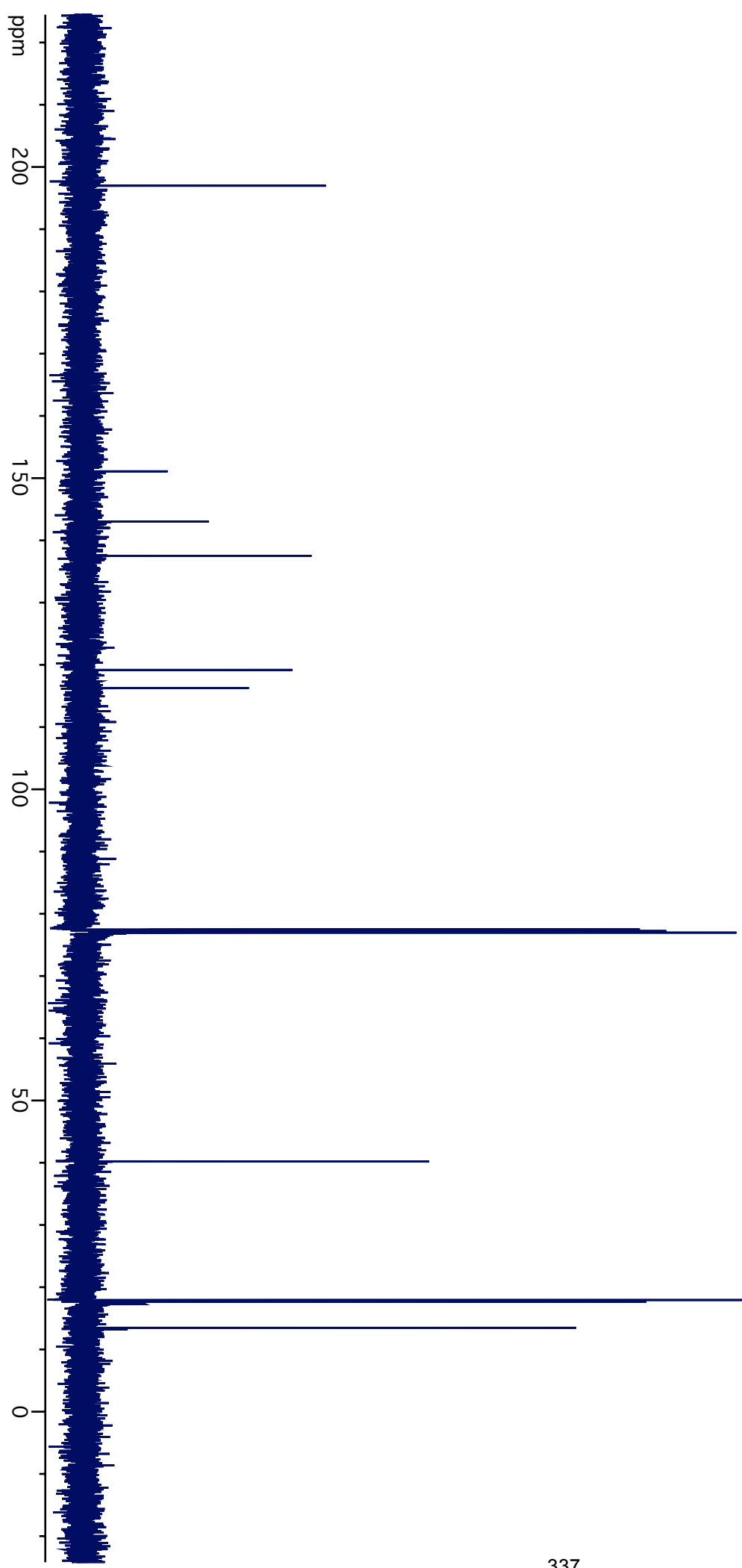
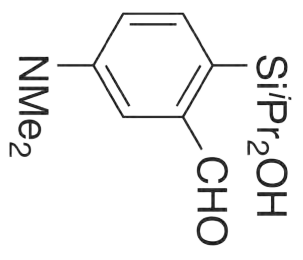
2-2-109

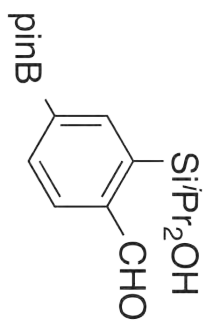




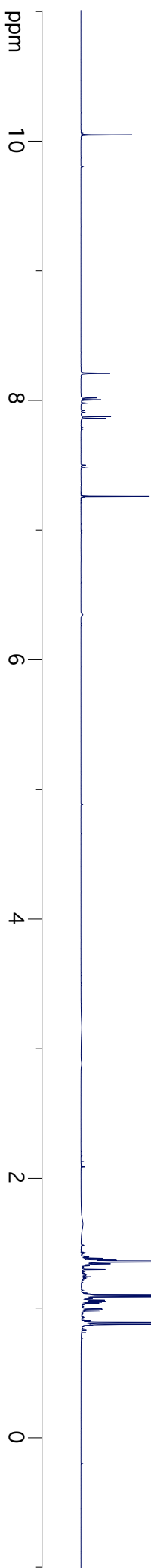
2-2-119

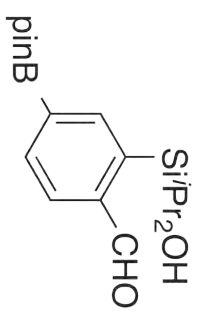




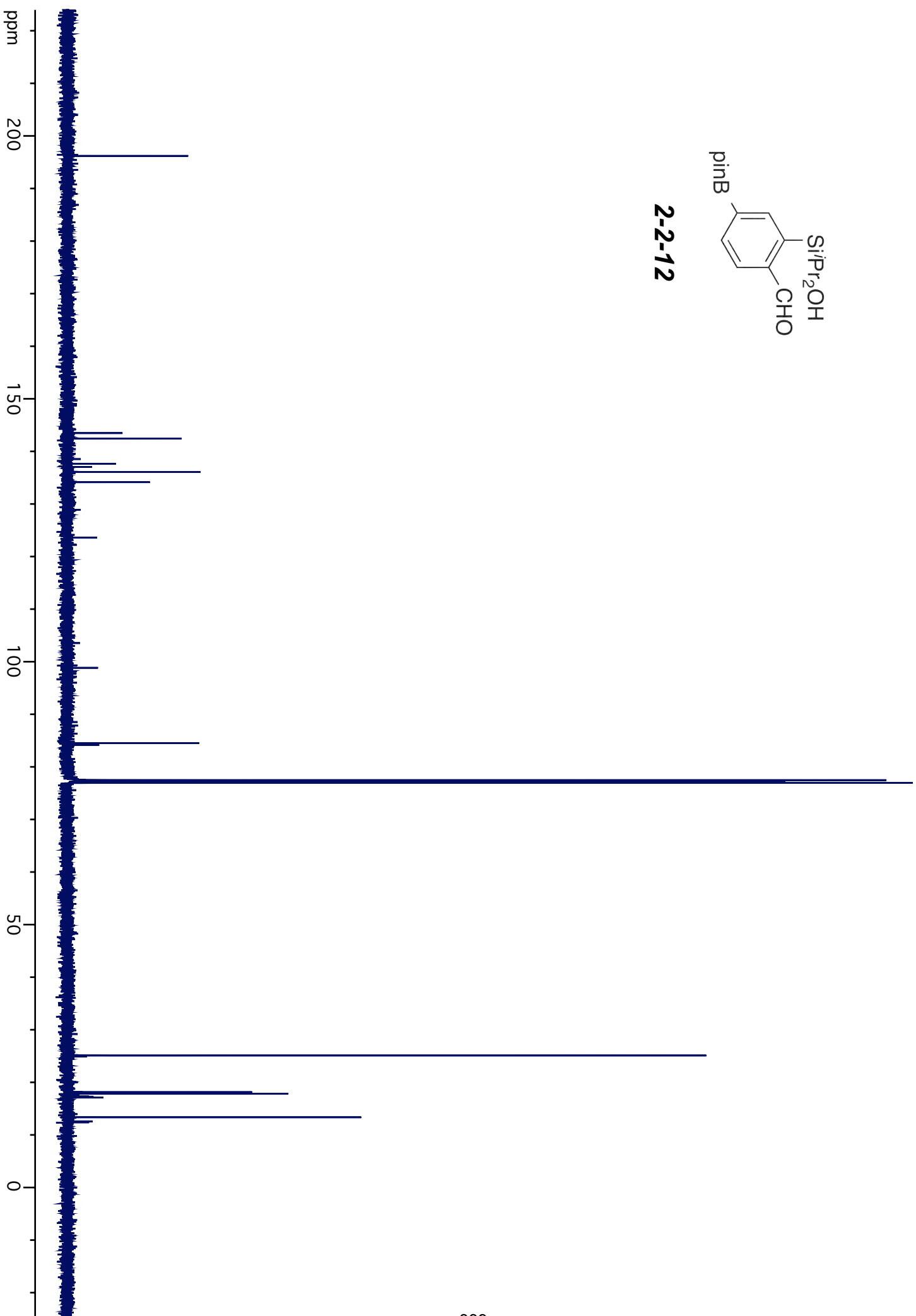


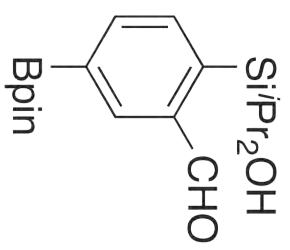
2-2-119



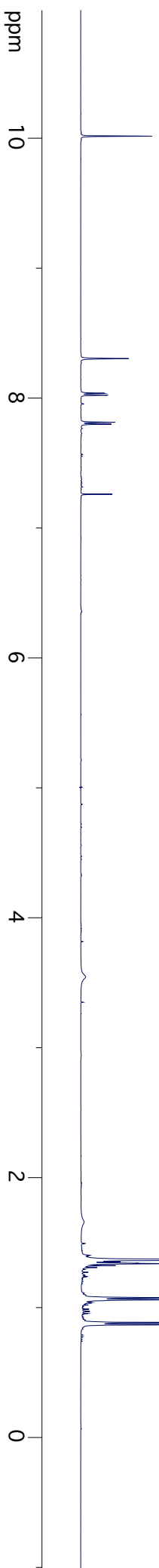


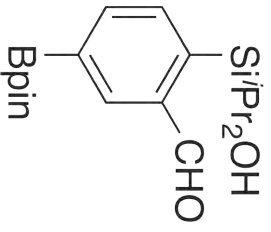
2-2-12



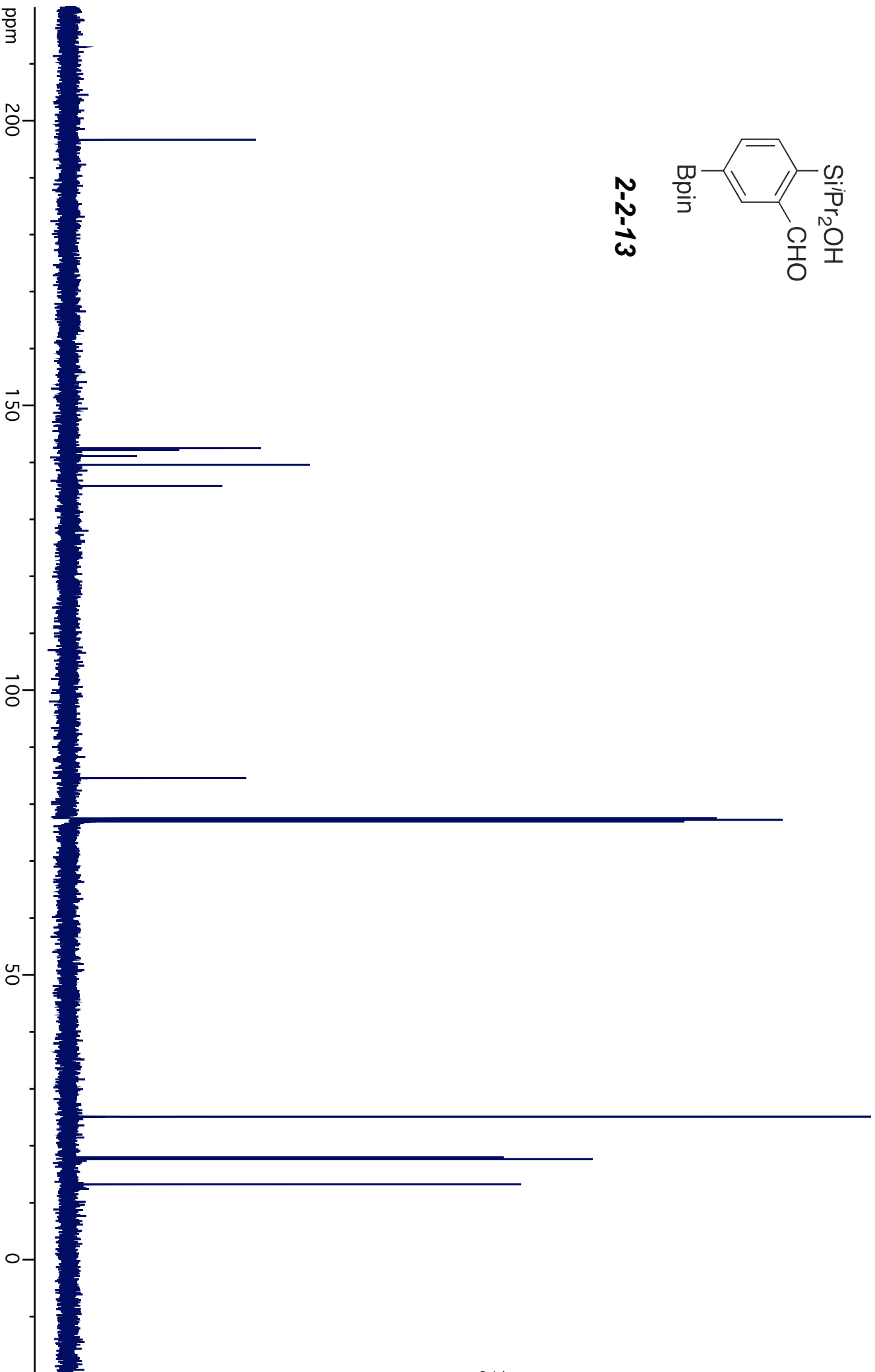


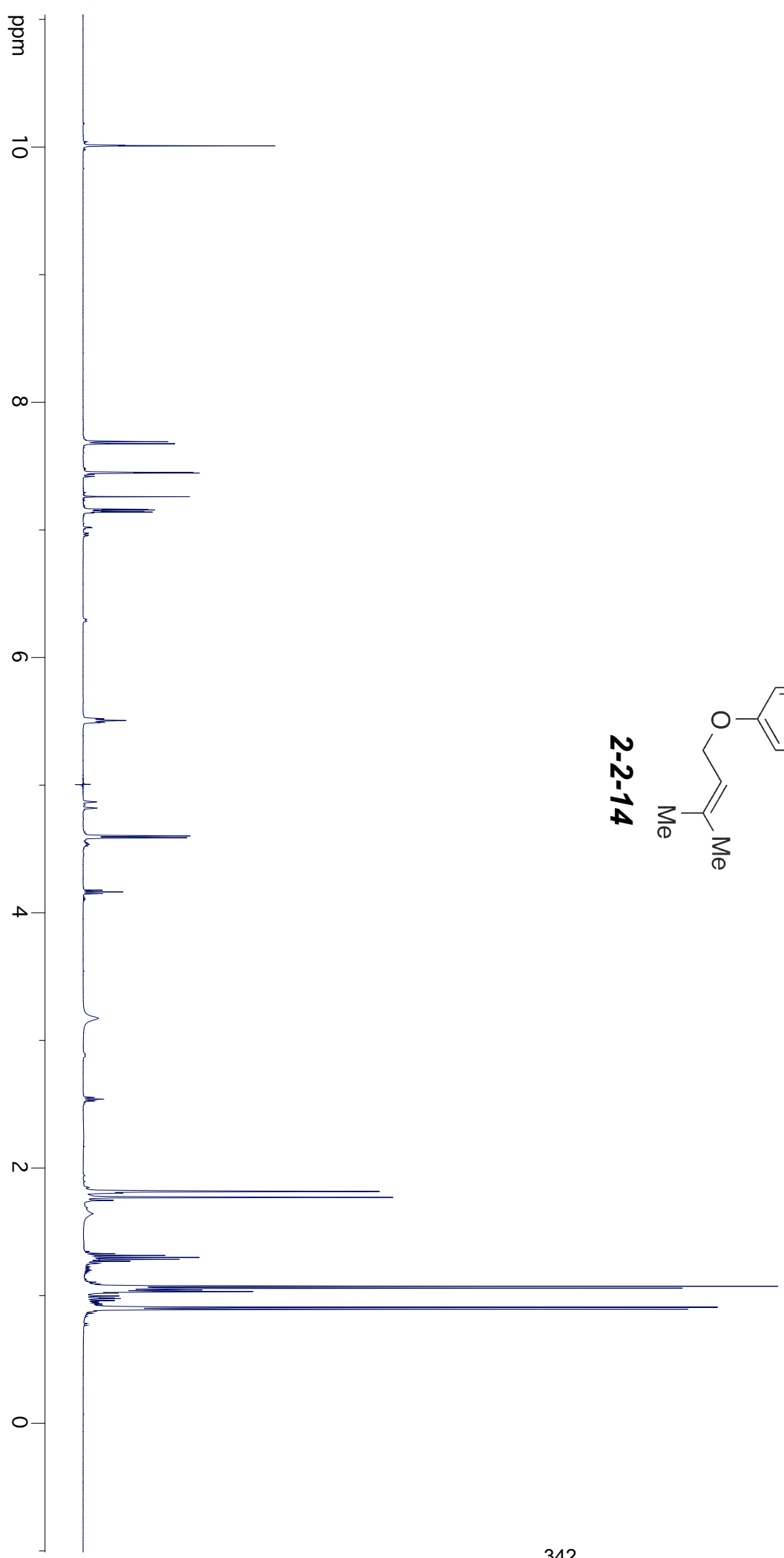
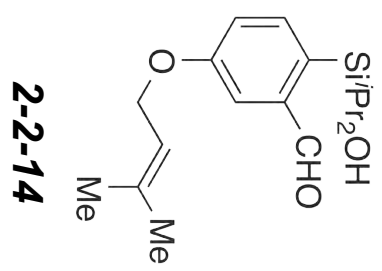
2-2-13

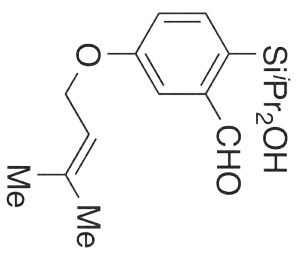




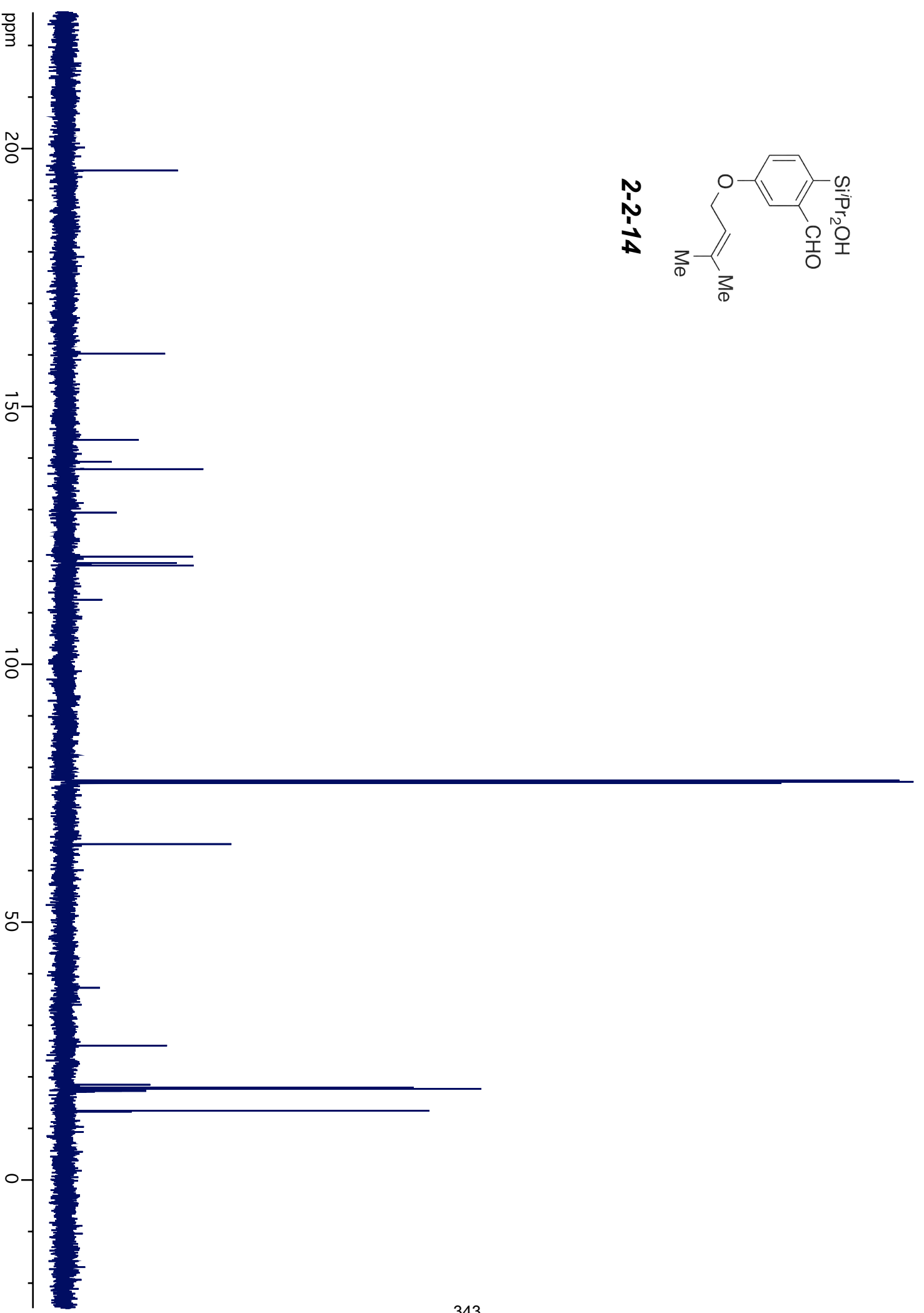
2-2-13

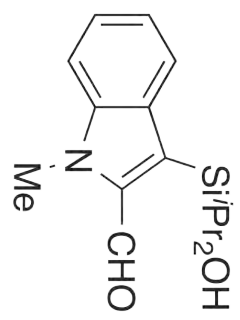






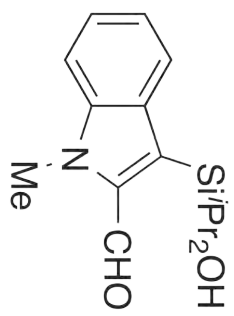
2-2-14





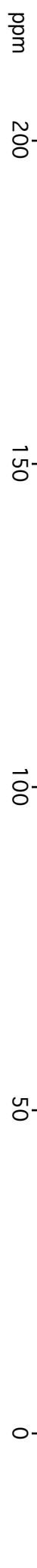
2-2-15

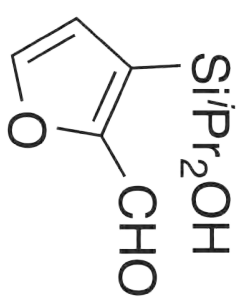




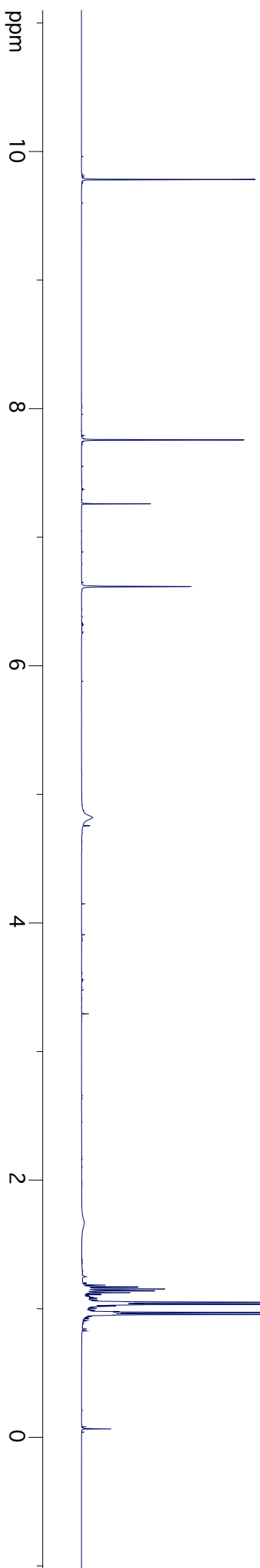
2-2-15

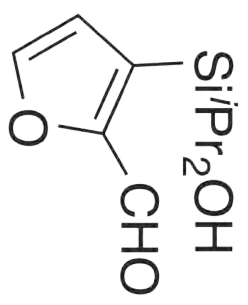
ppm



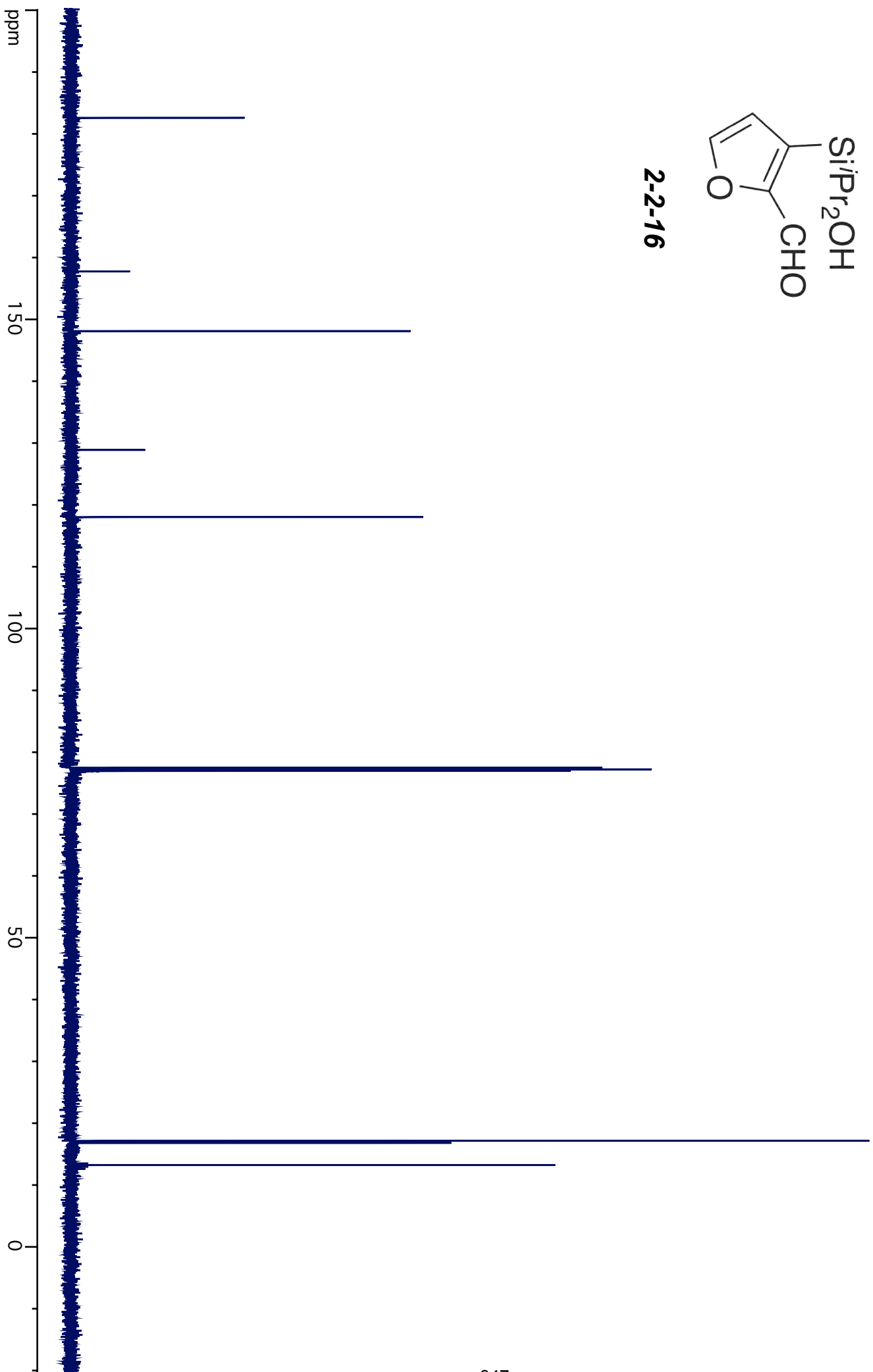


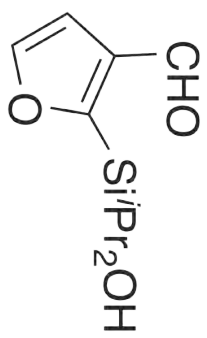
2-2-16



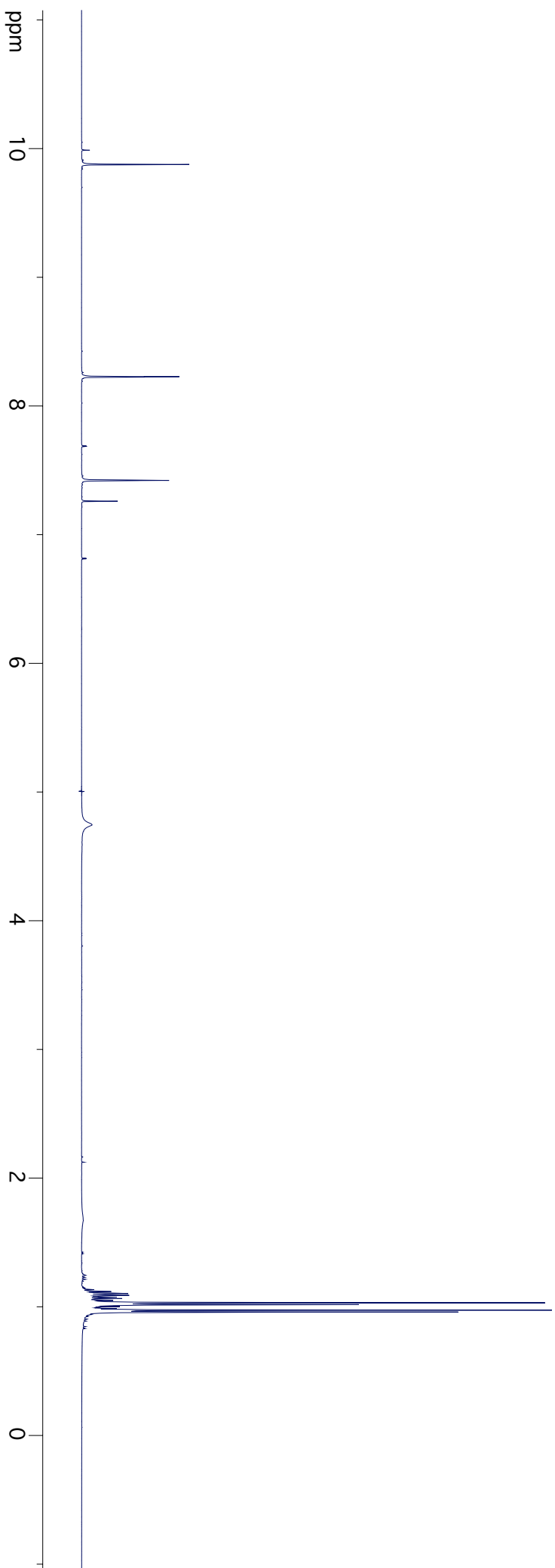


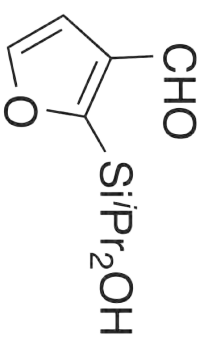
2-2-16



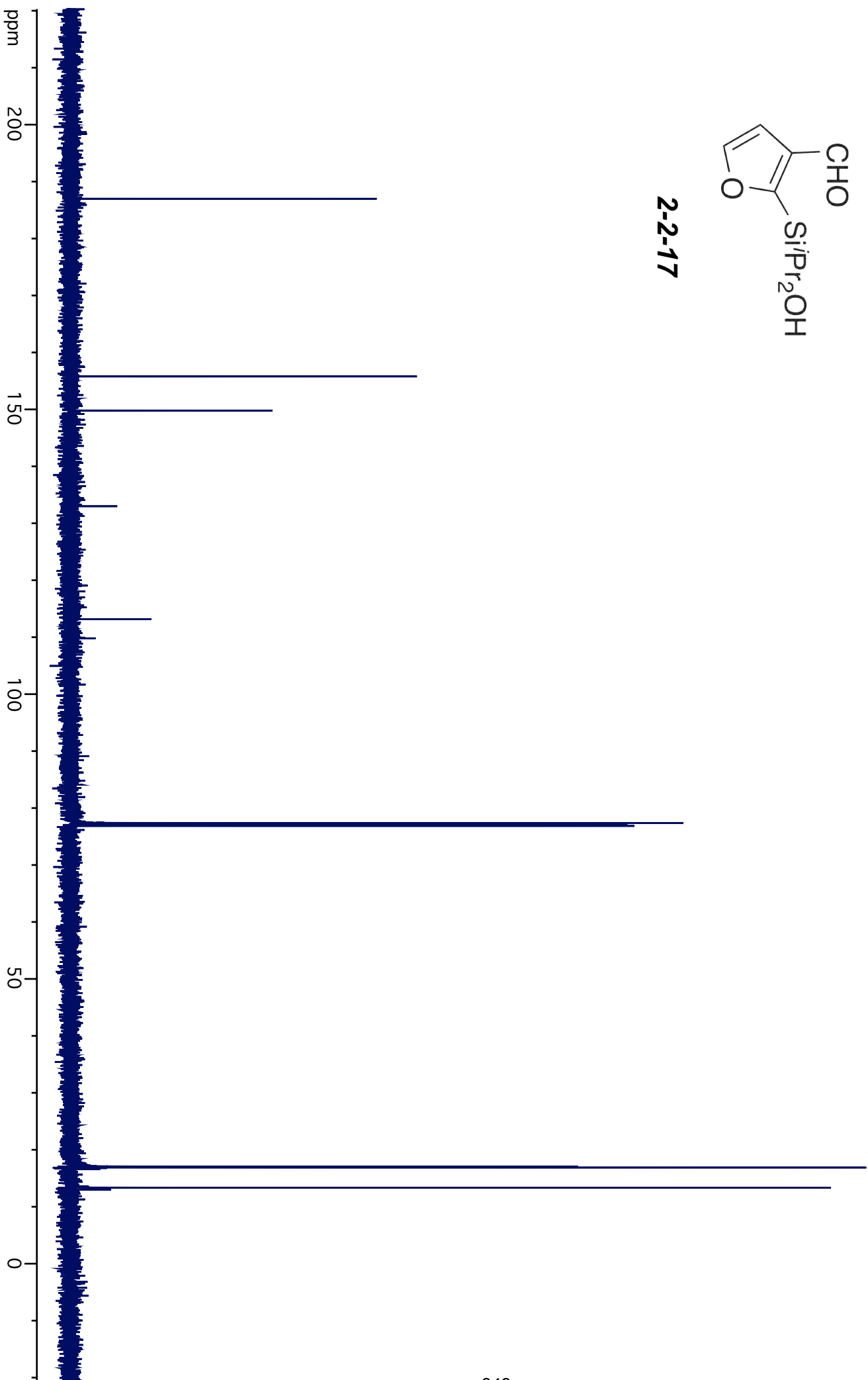


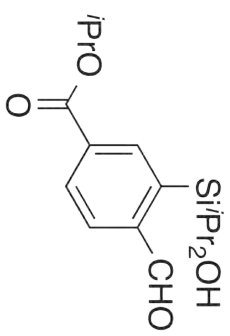
2-2-17



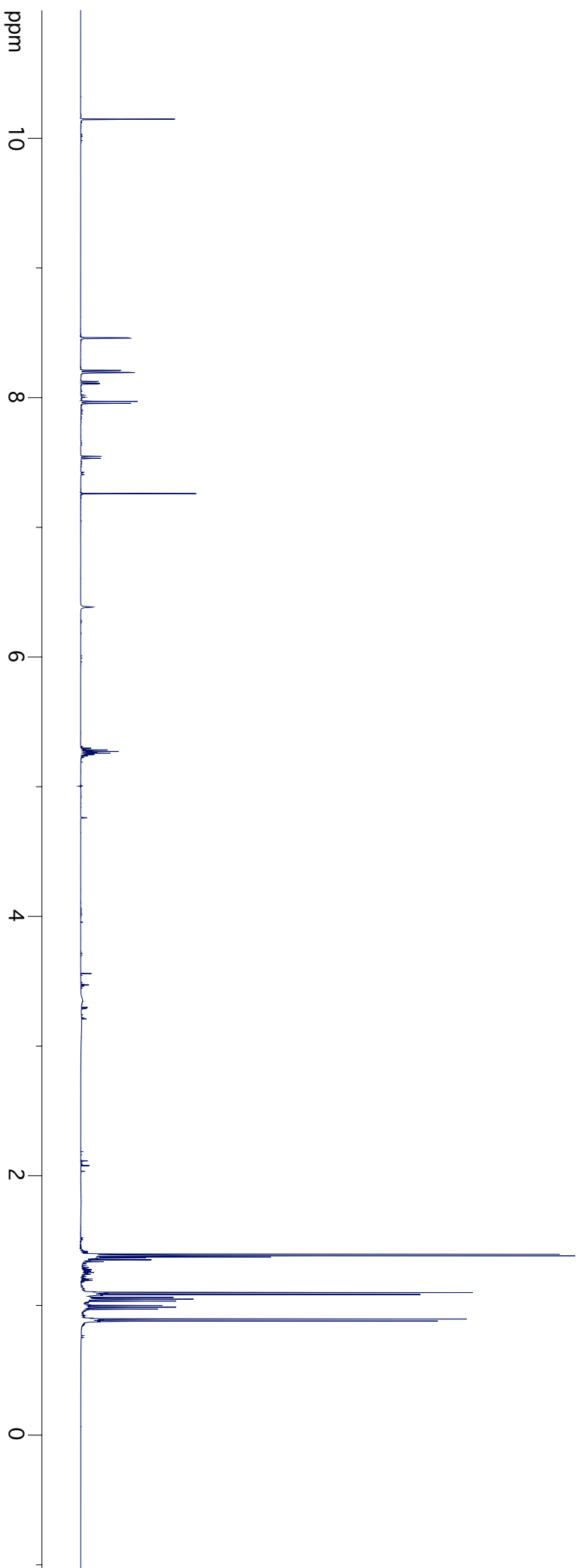


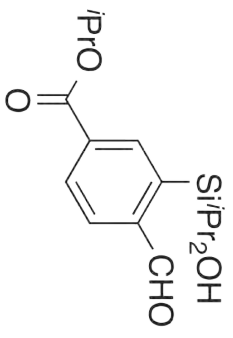
2-2-17





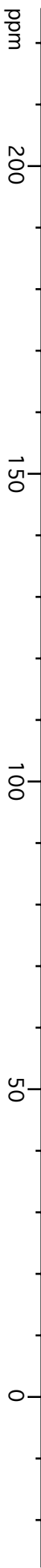
2-2-18

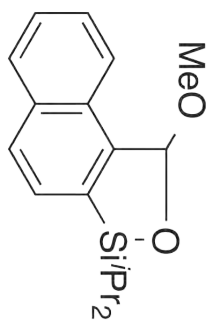




2-2-18

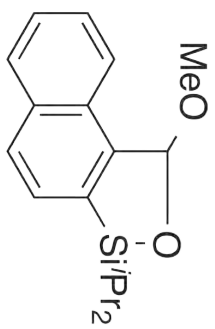
ppm



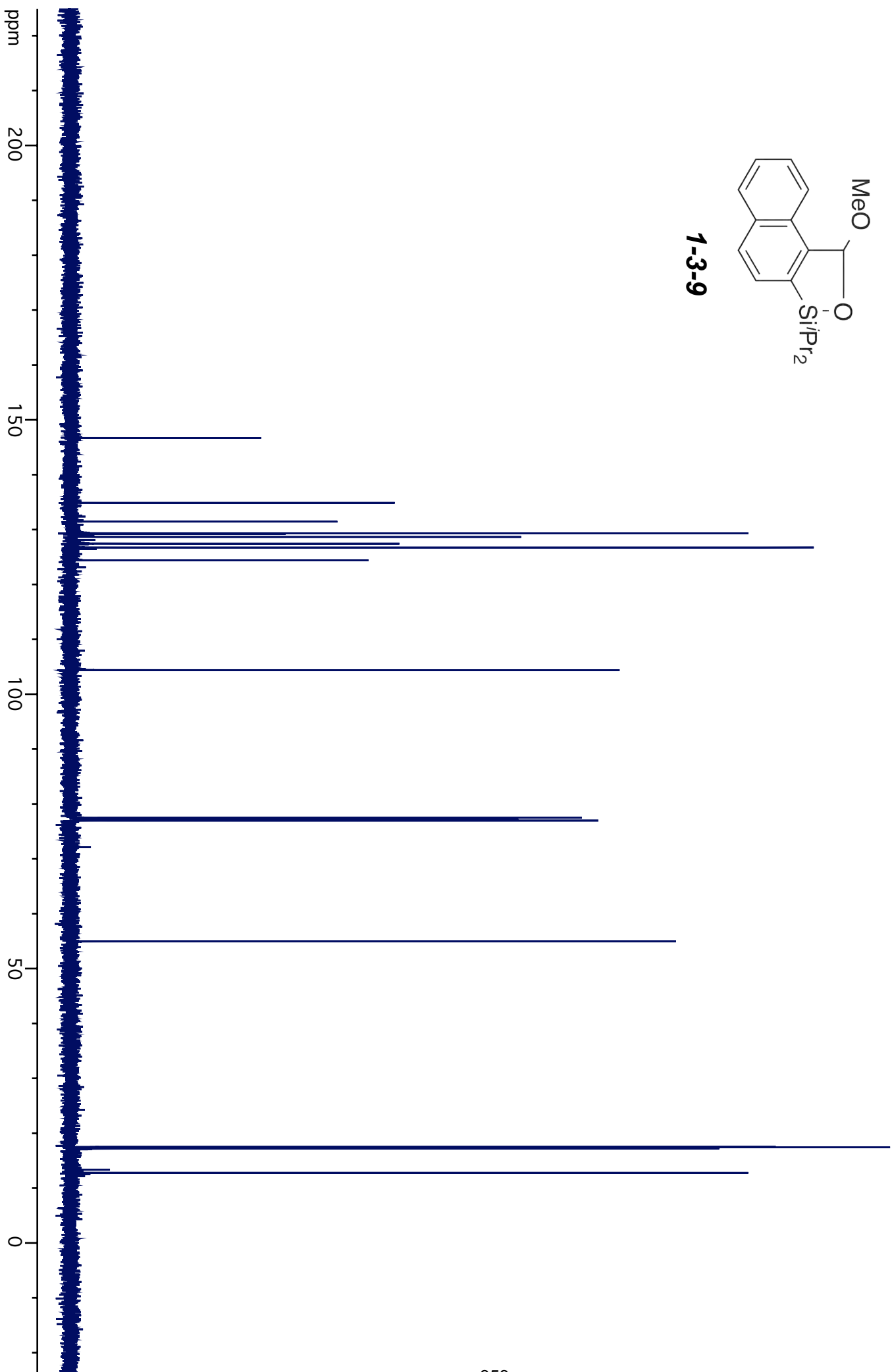


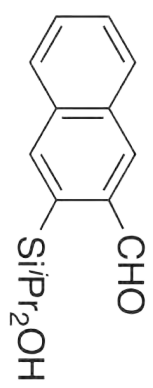
1-3-9



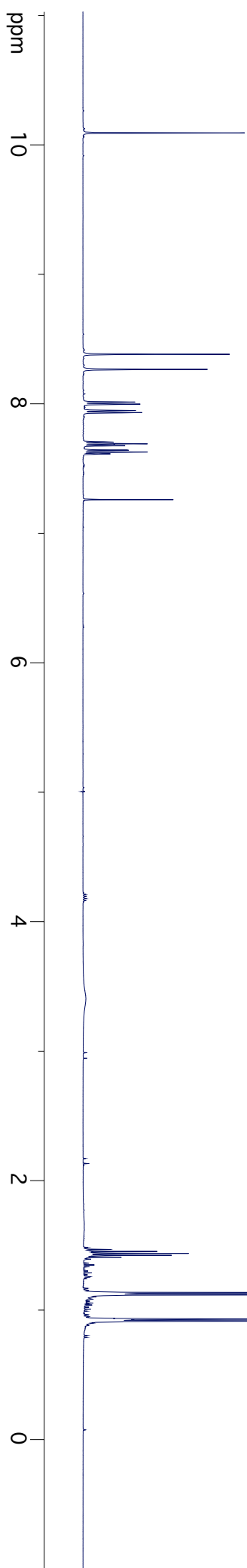


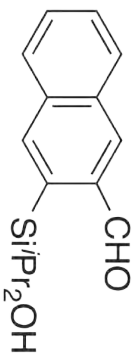
1-3-9



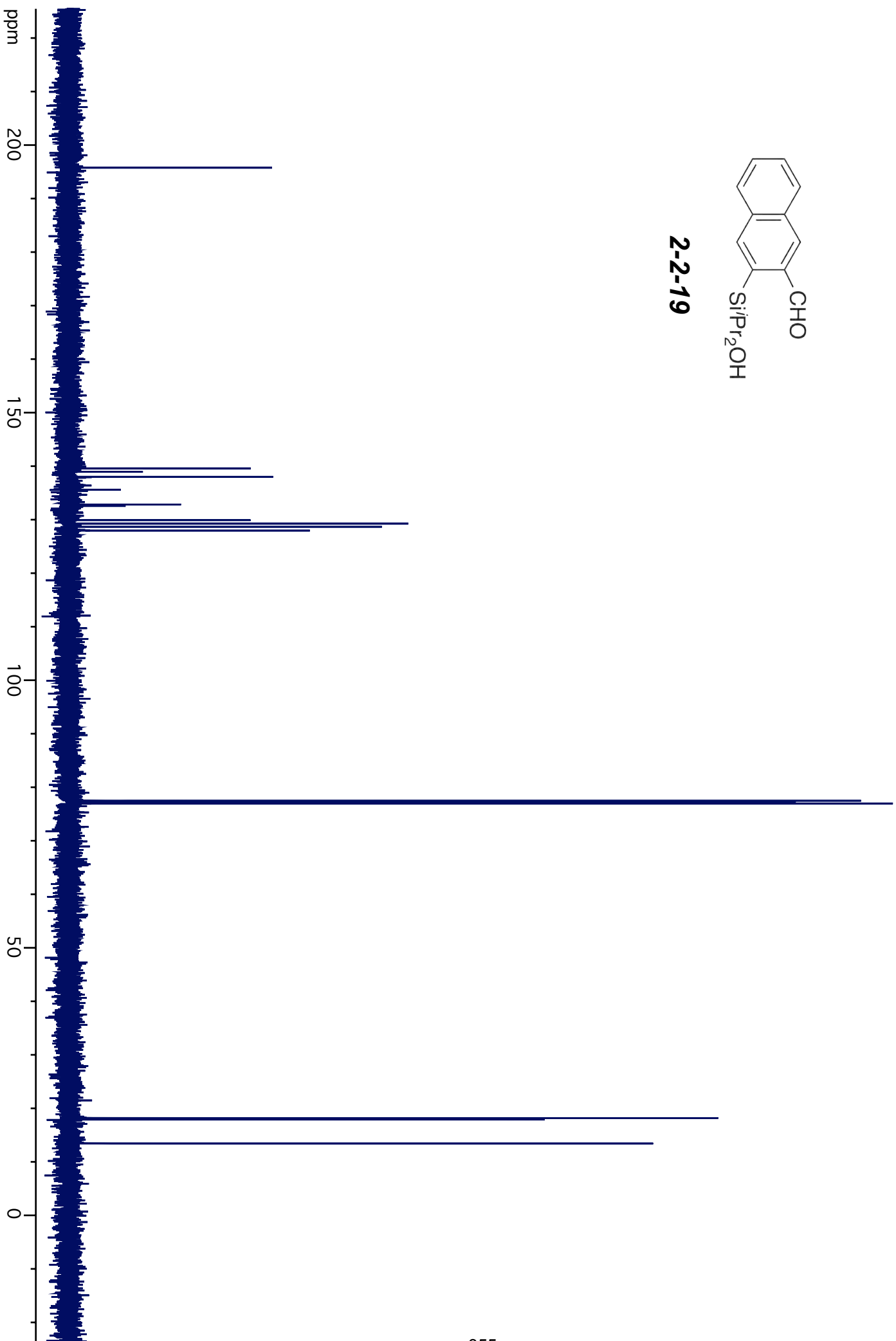


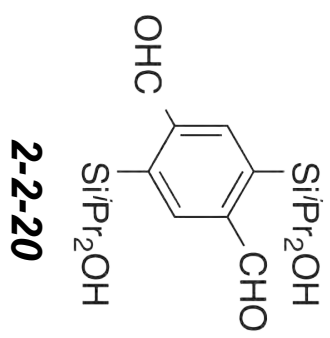
2-2-19

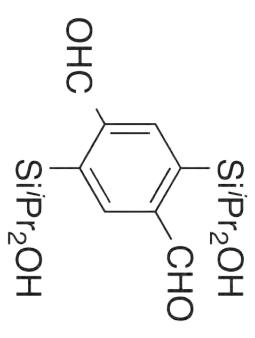




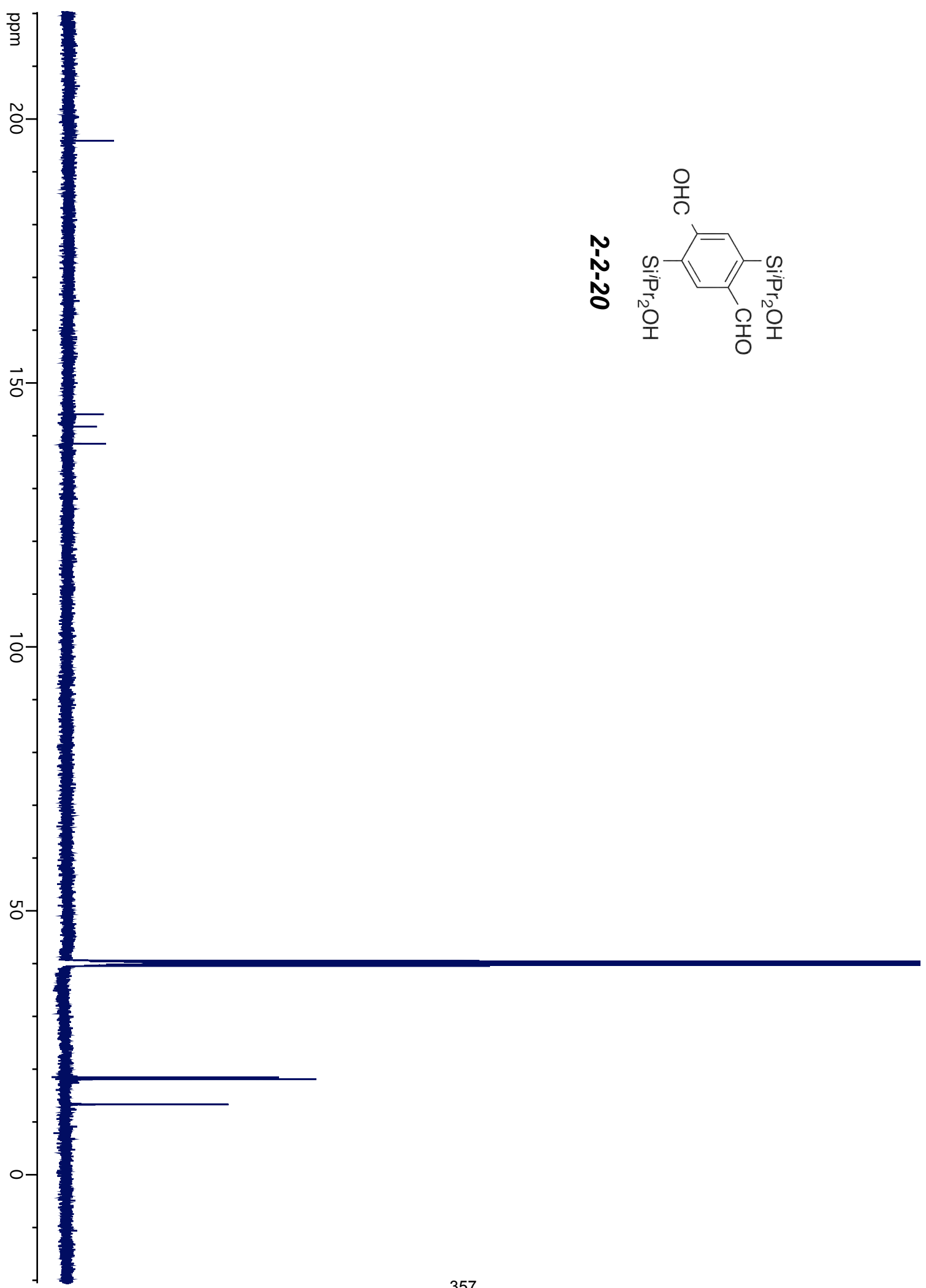
2-2-19

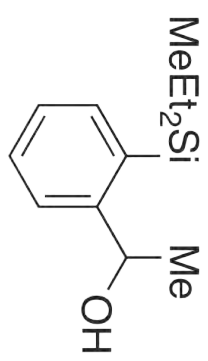






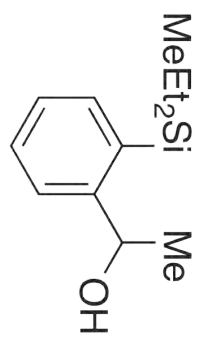
2-2-20





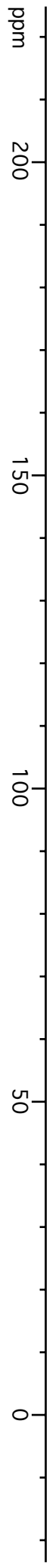
2-3

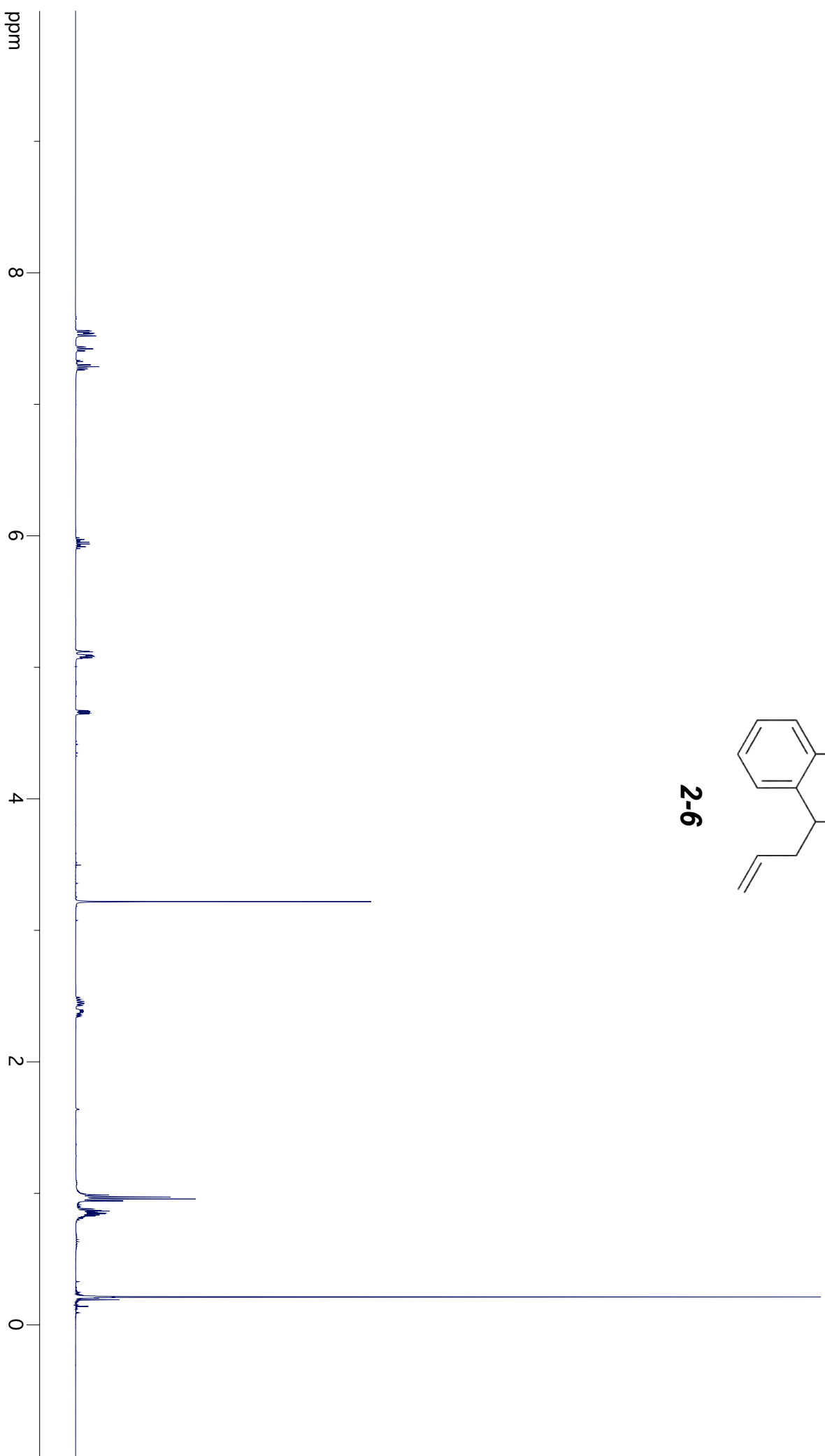
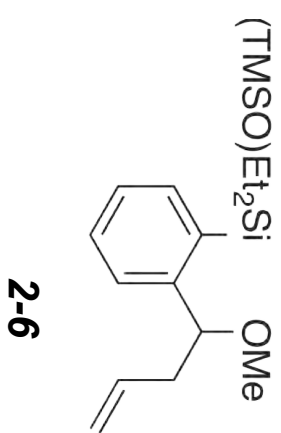


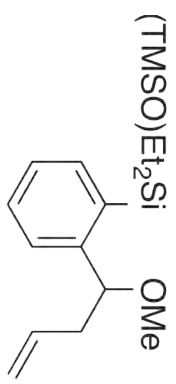


2-3

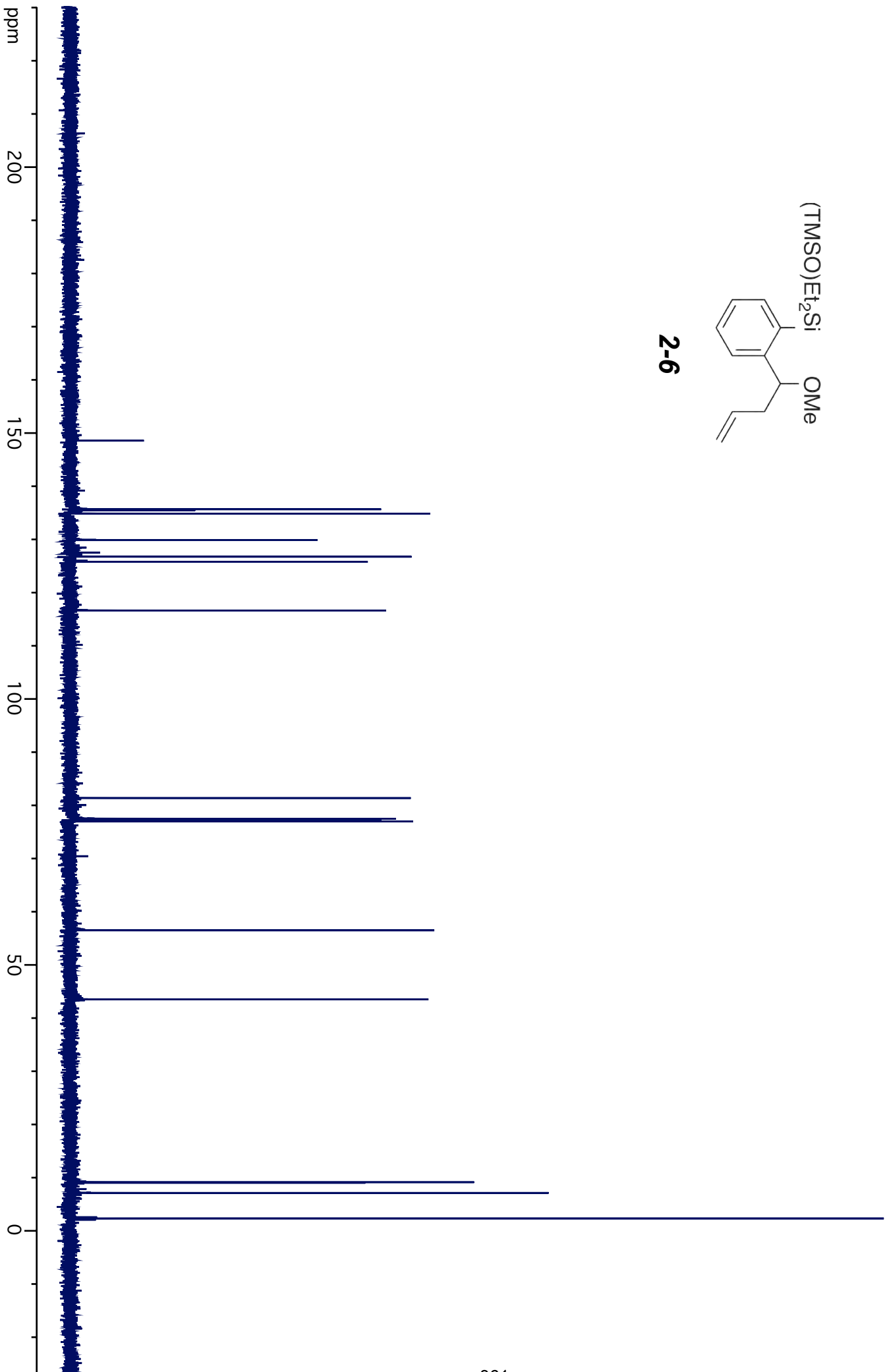
ppm

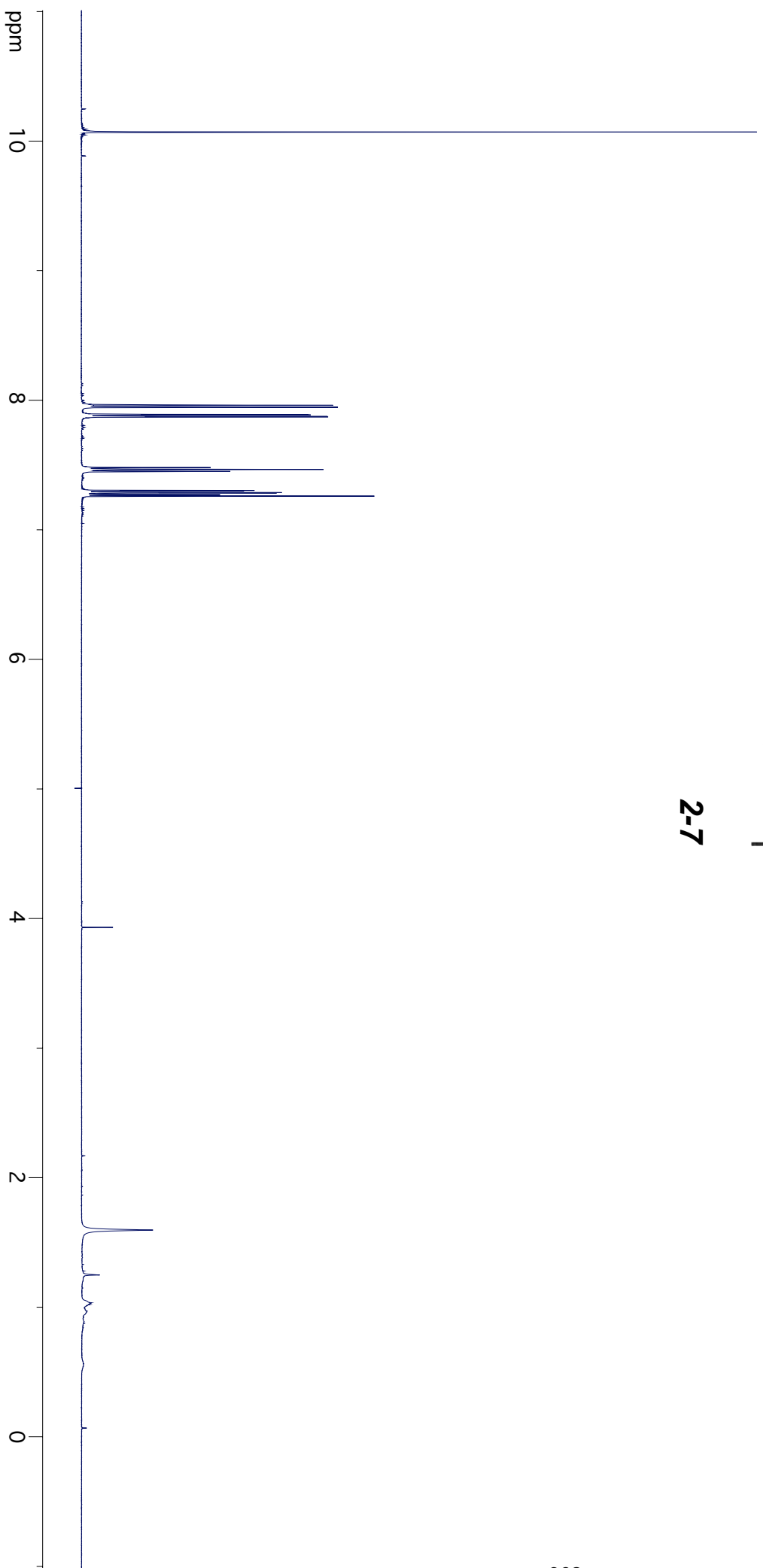
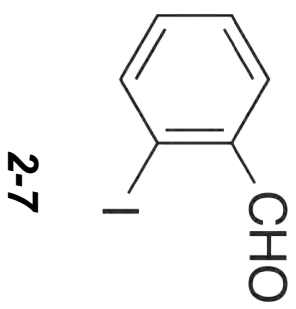


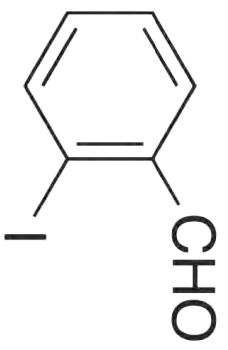




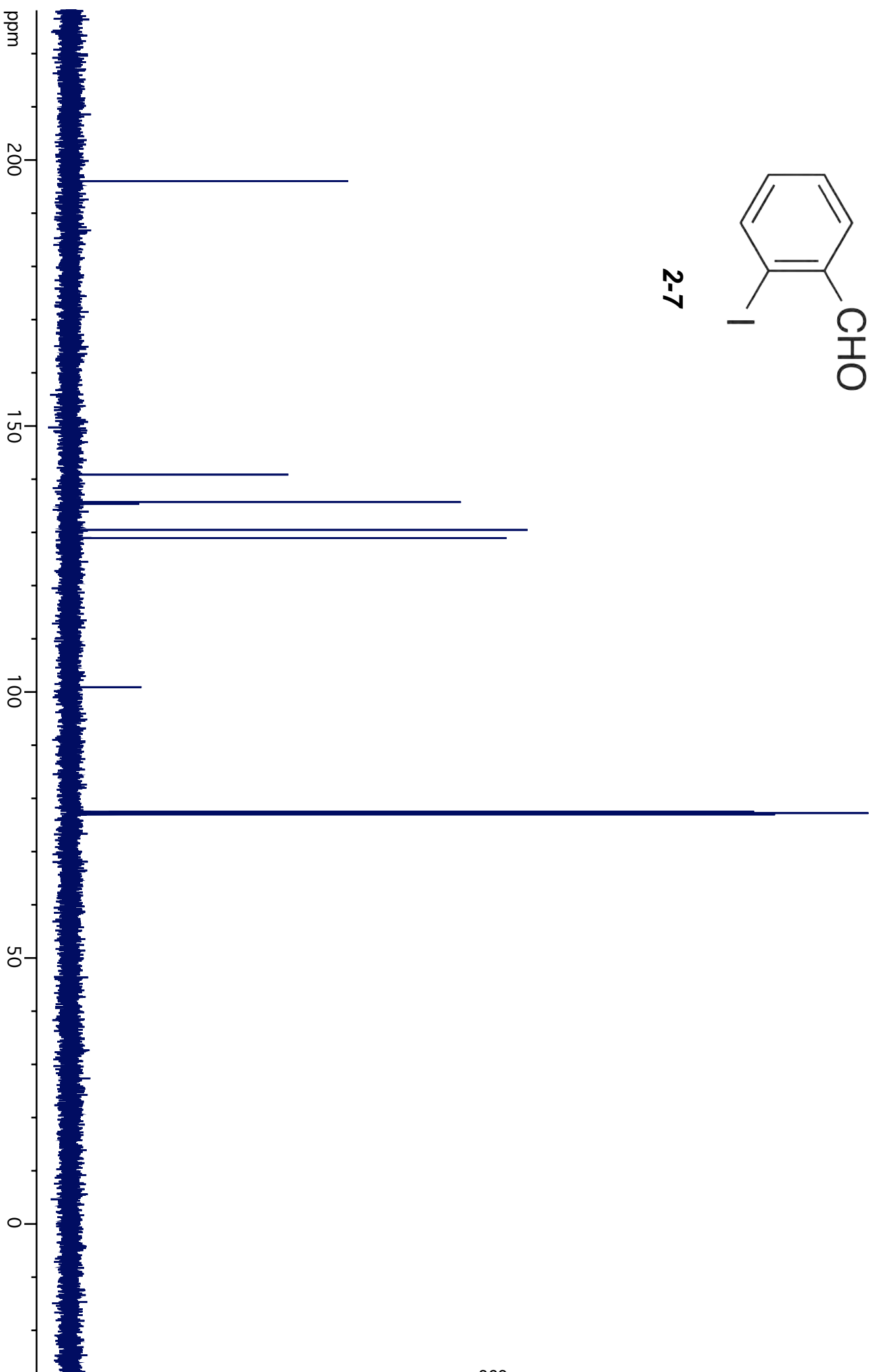
2-6

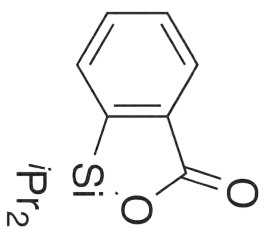




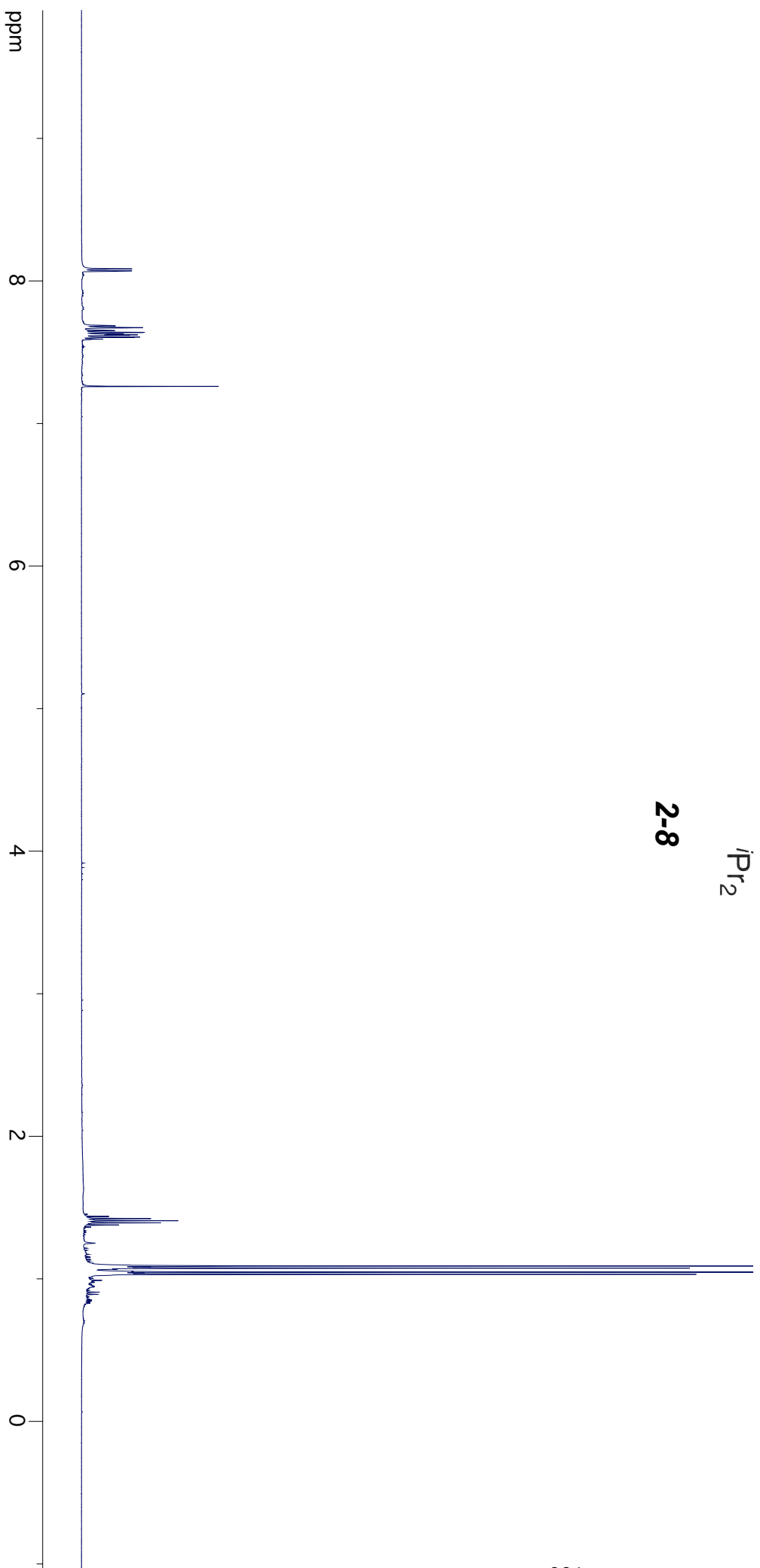


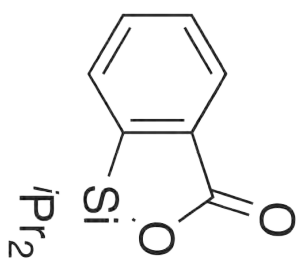
2-7



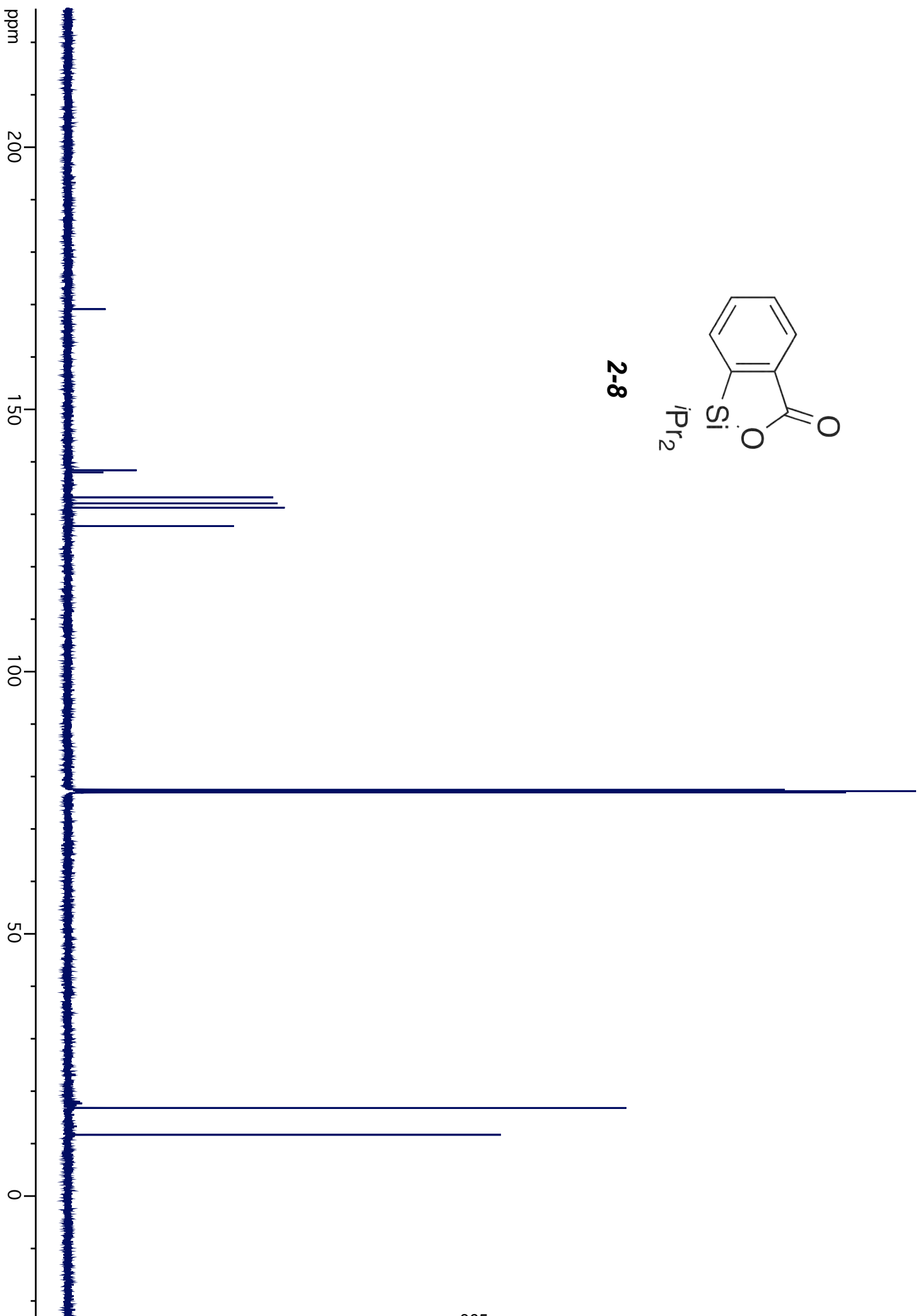


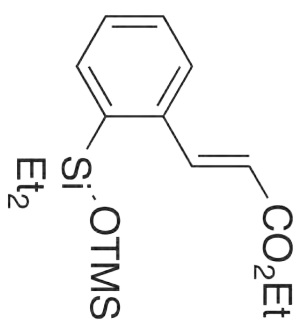
2-8





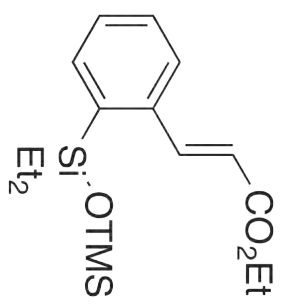
2-8





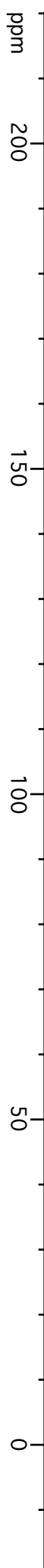
2-9

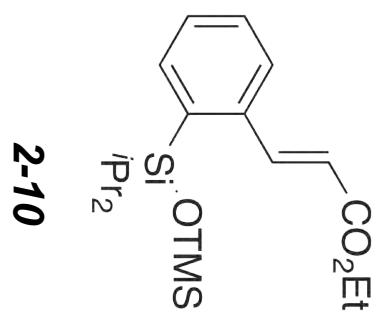




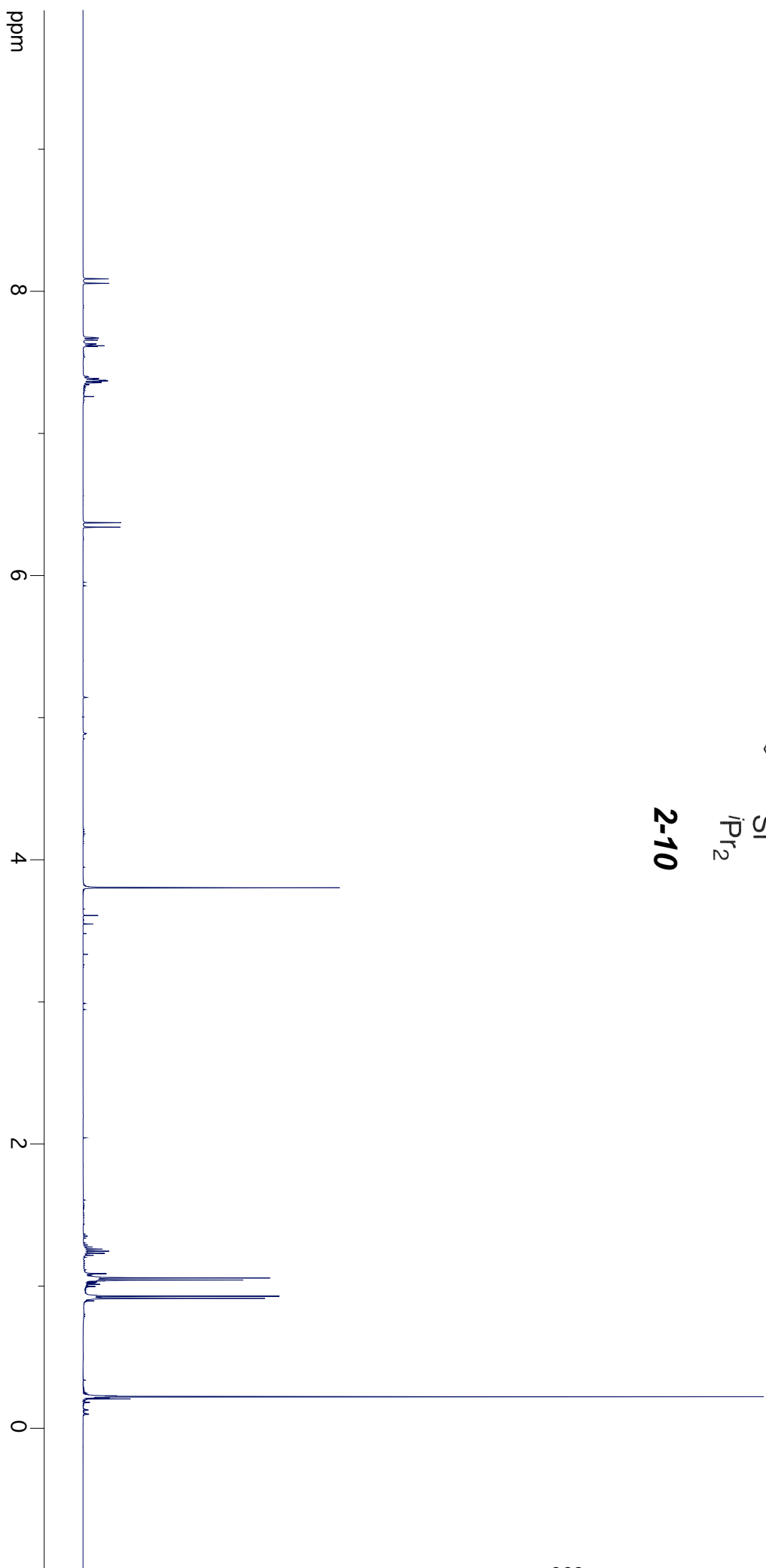
2-9

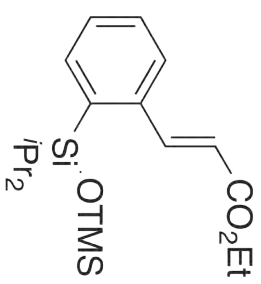
ppm



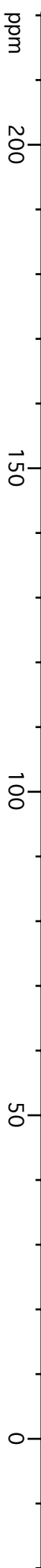


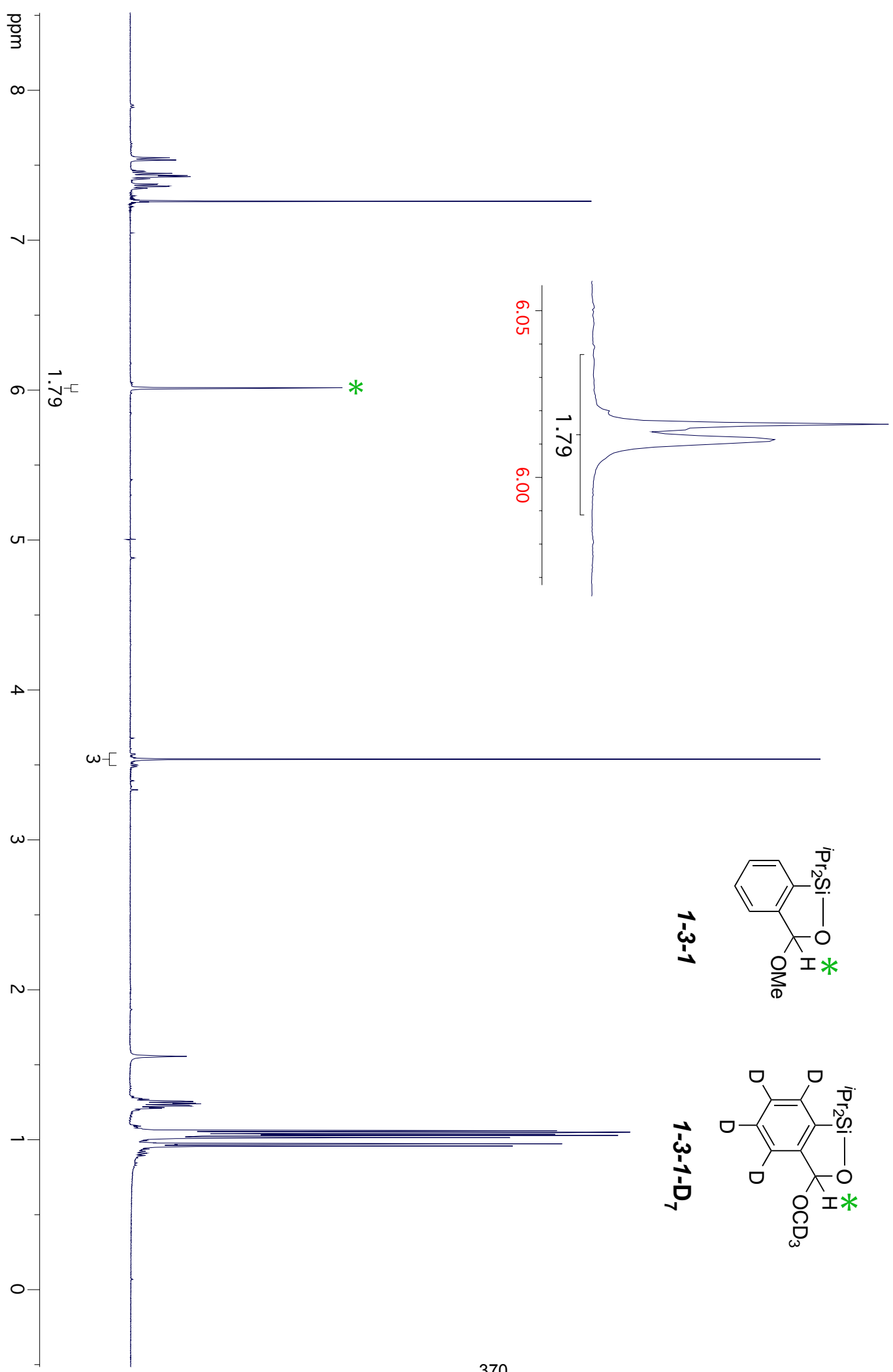
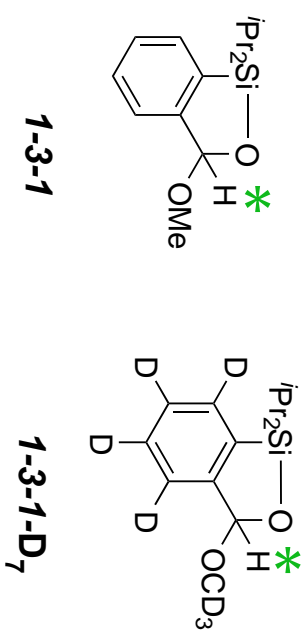
2-10

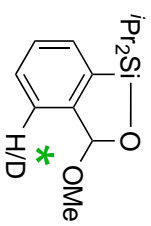




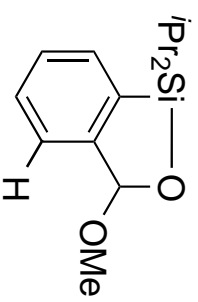
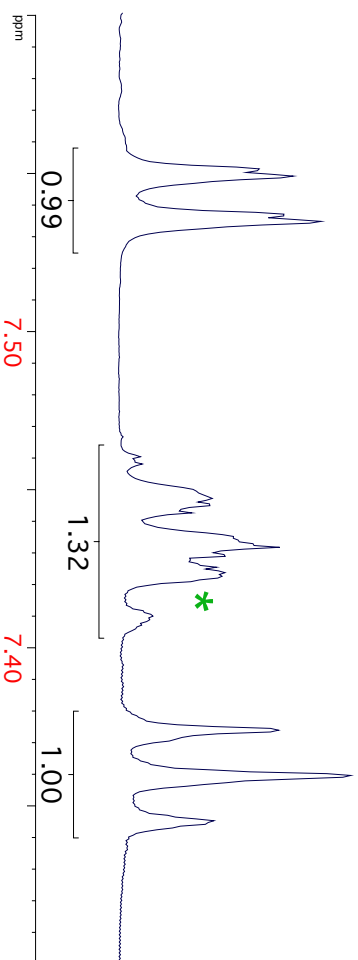
2-10



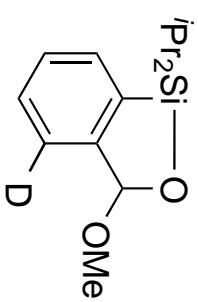




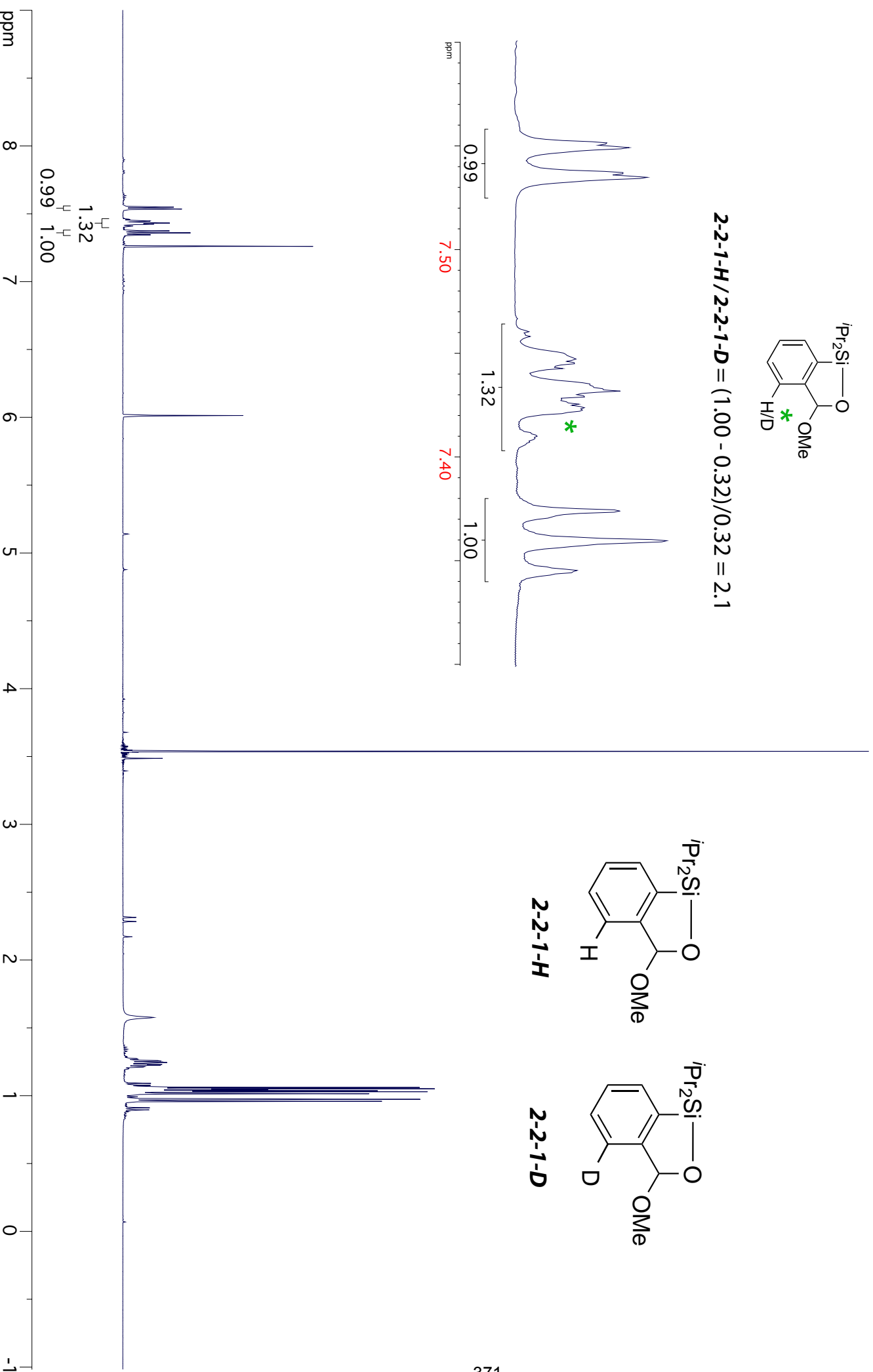
$$2\text{-}2\text{-}1\text{-}H/2\text{-}2\text{-}1\text{-}D = (1.00 - 0.32)/0.32 = 2.1$$

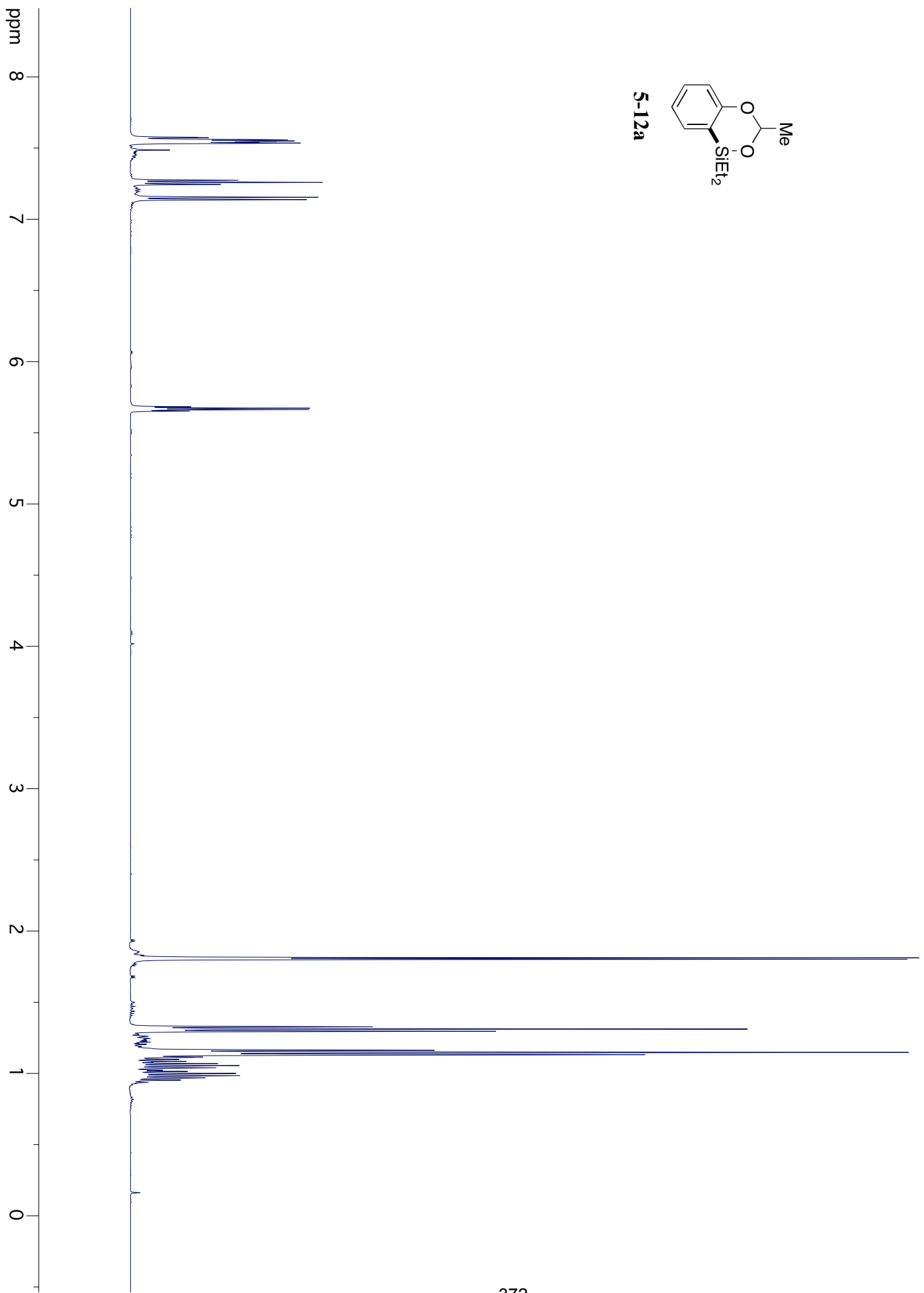
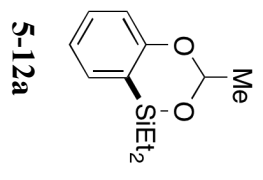


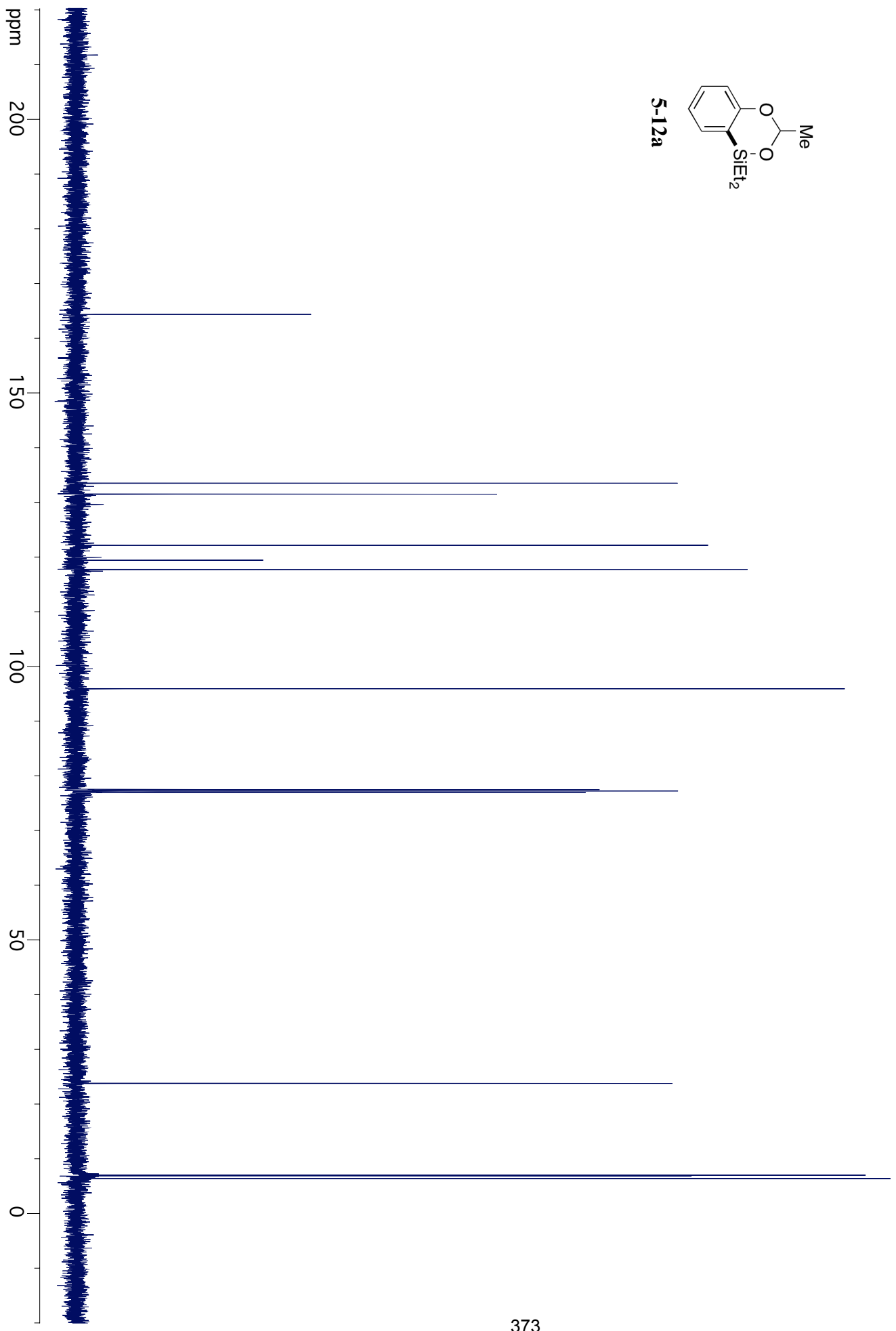
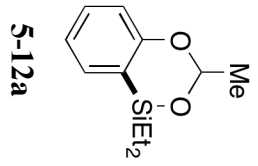
2-2-1-H

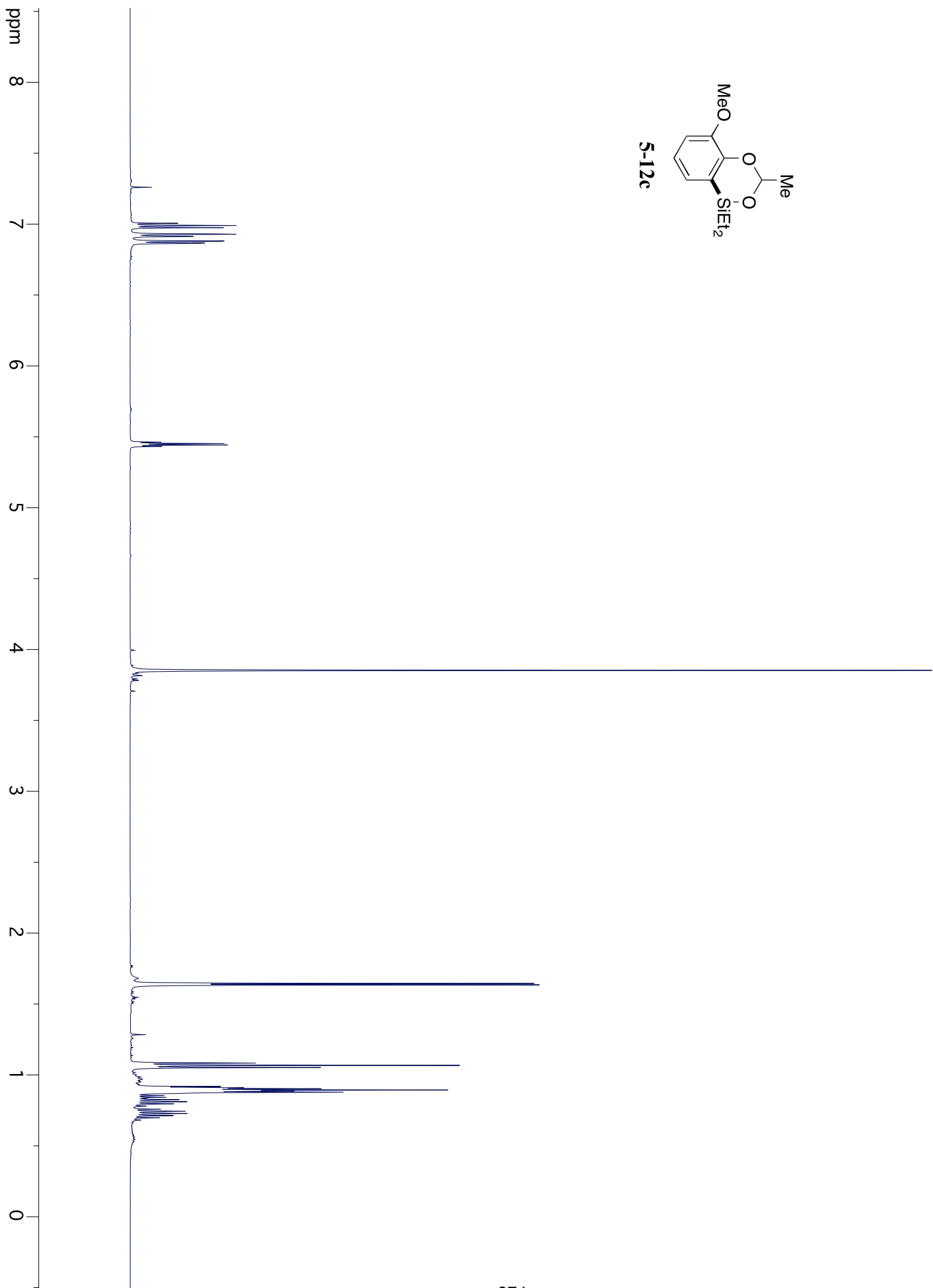
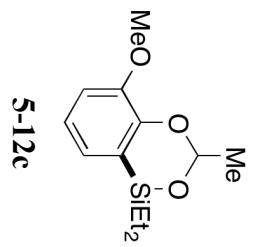


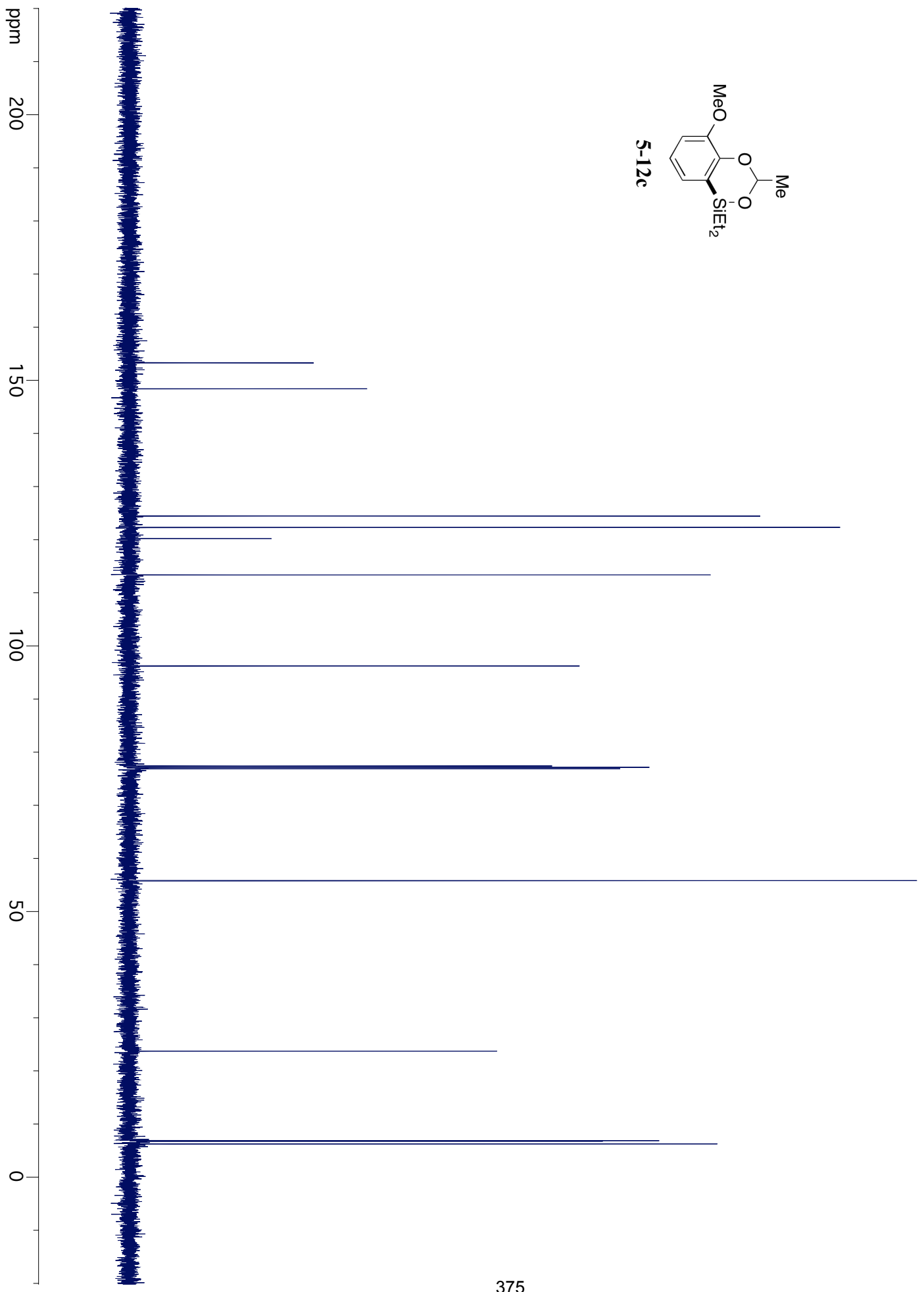
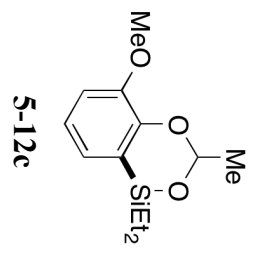
2-2-1-D

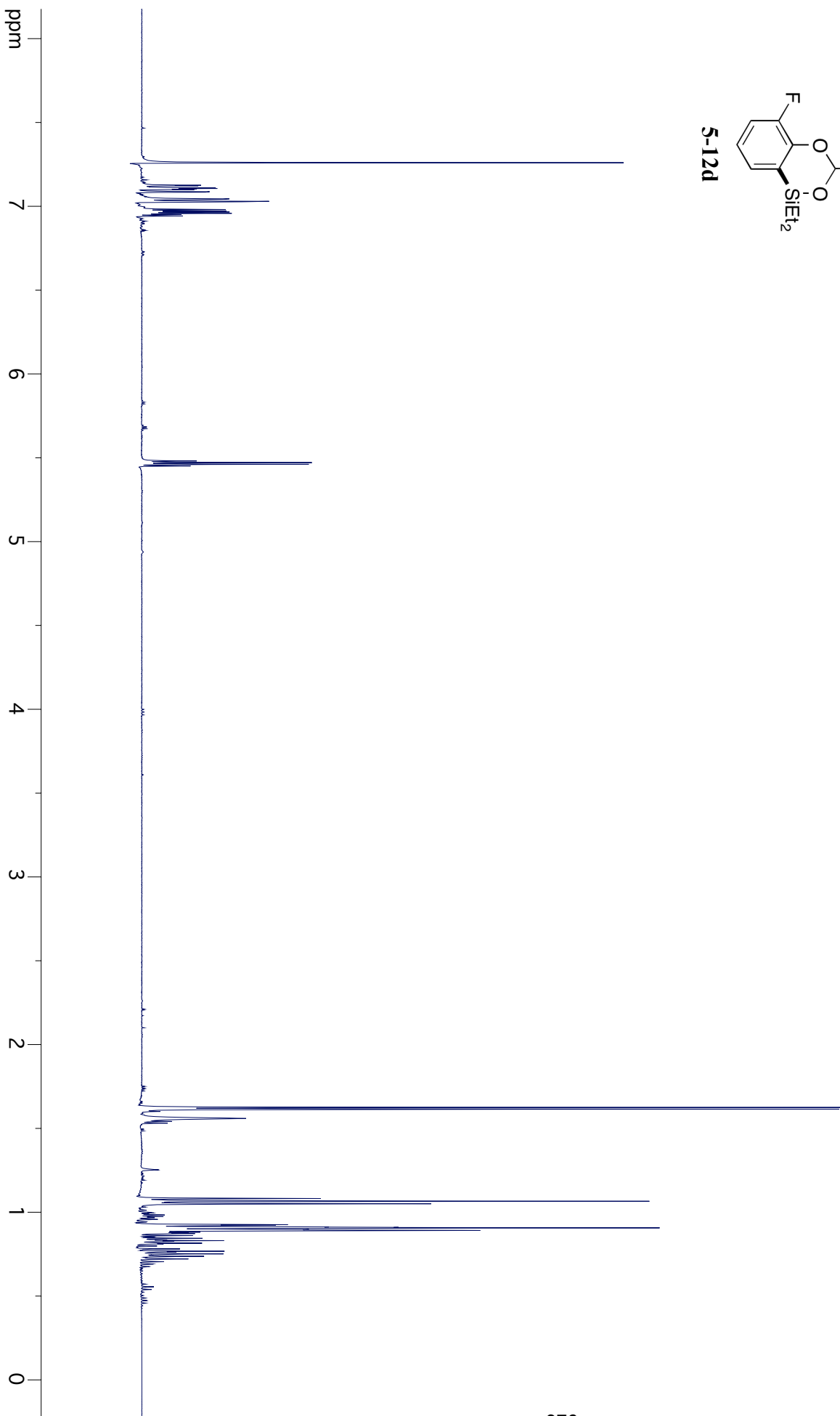
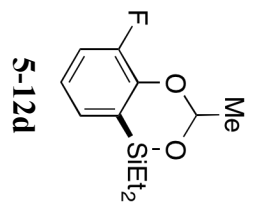


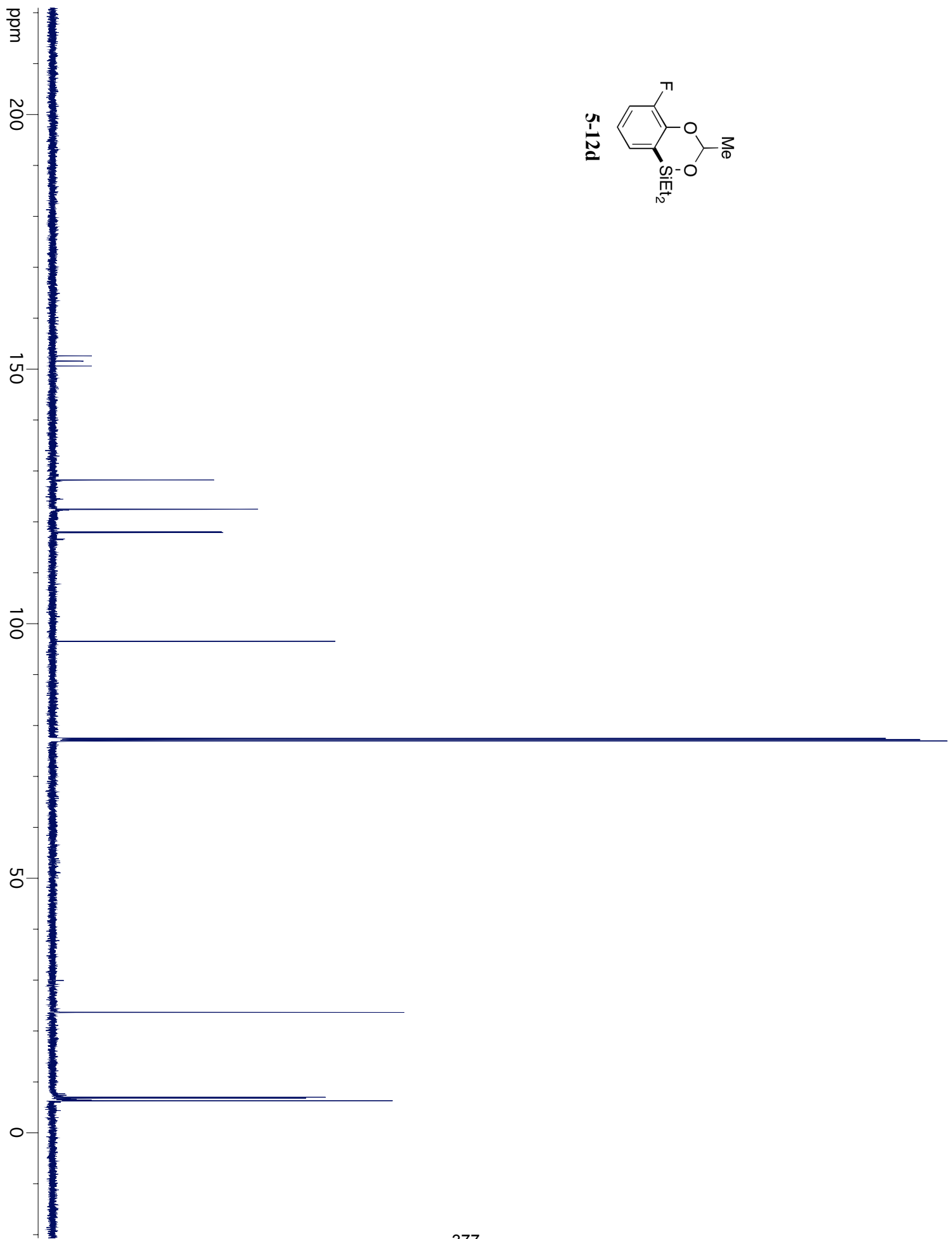
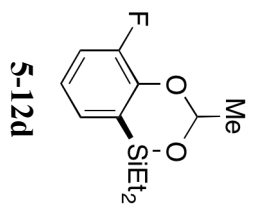


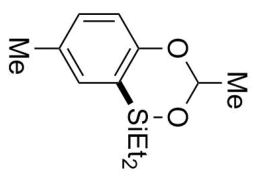




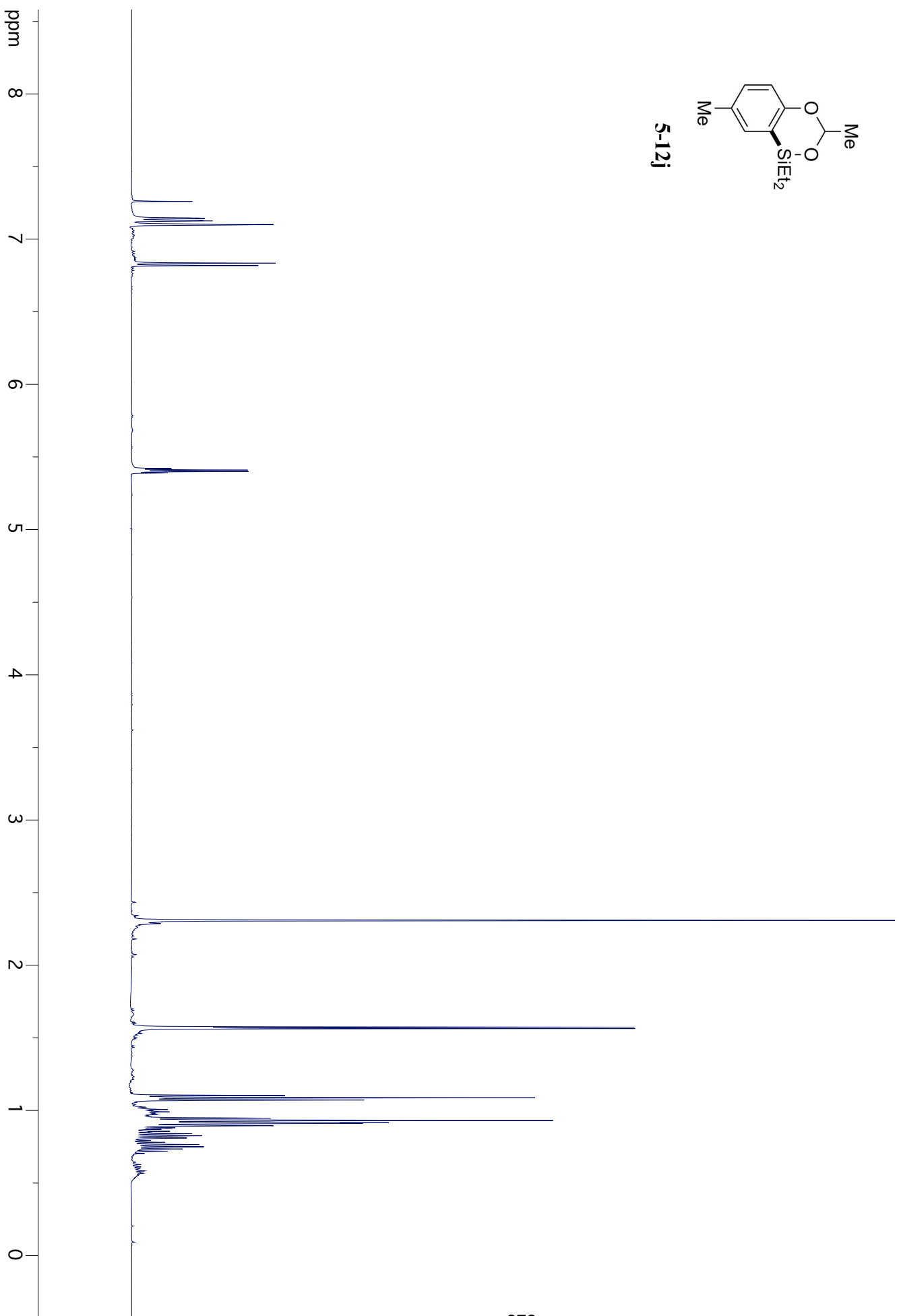


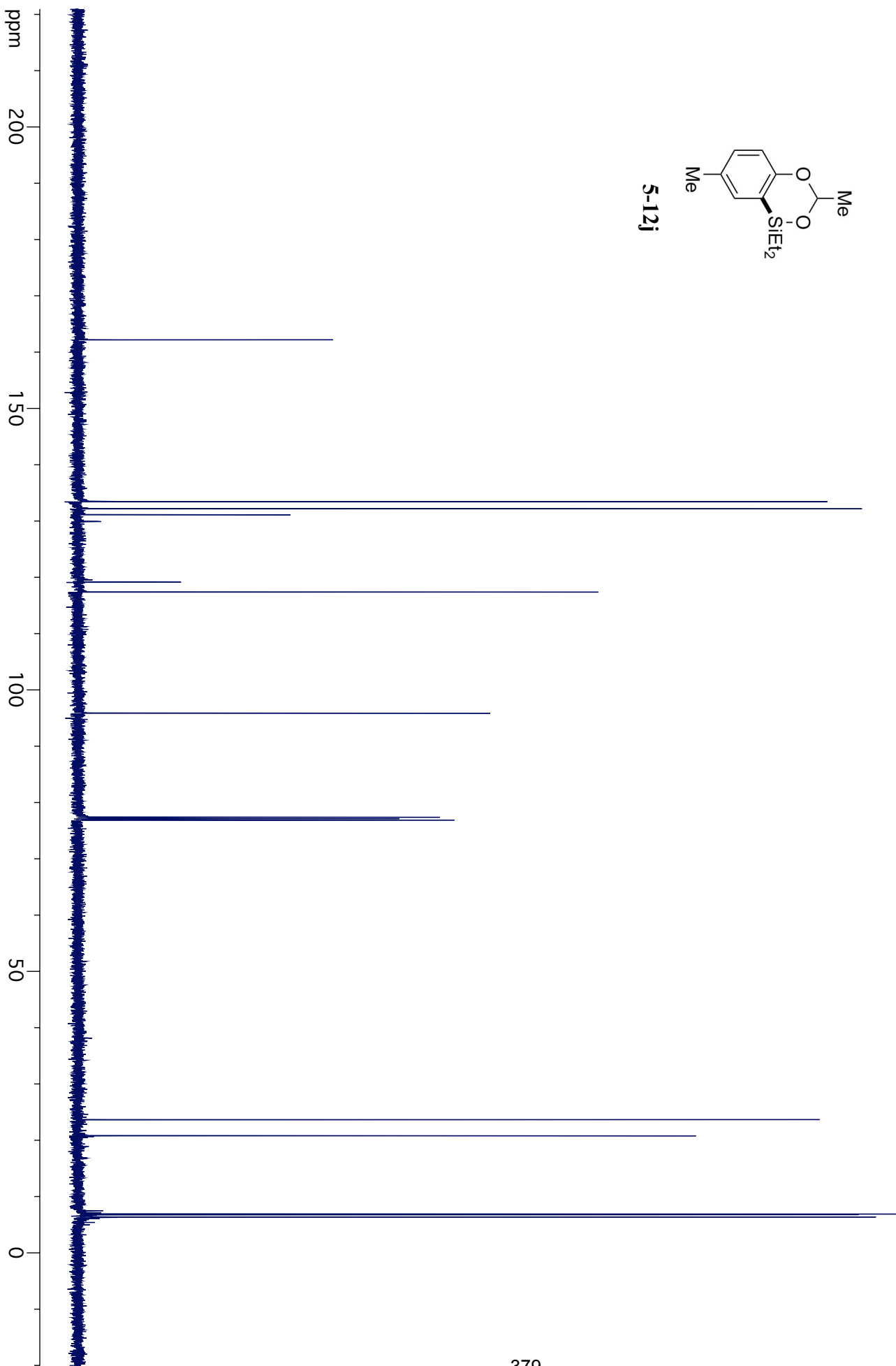
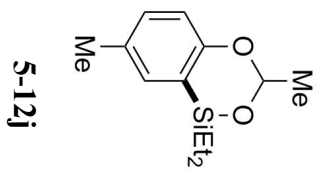


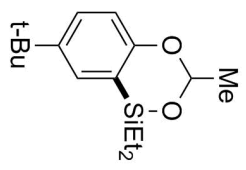




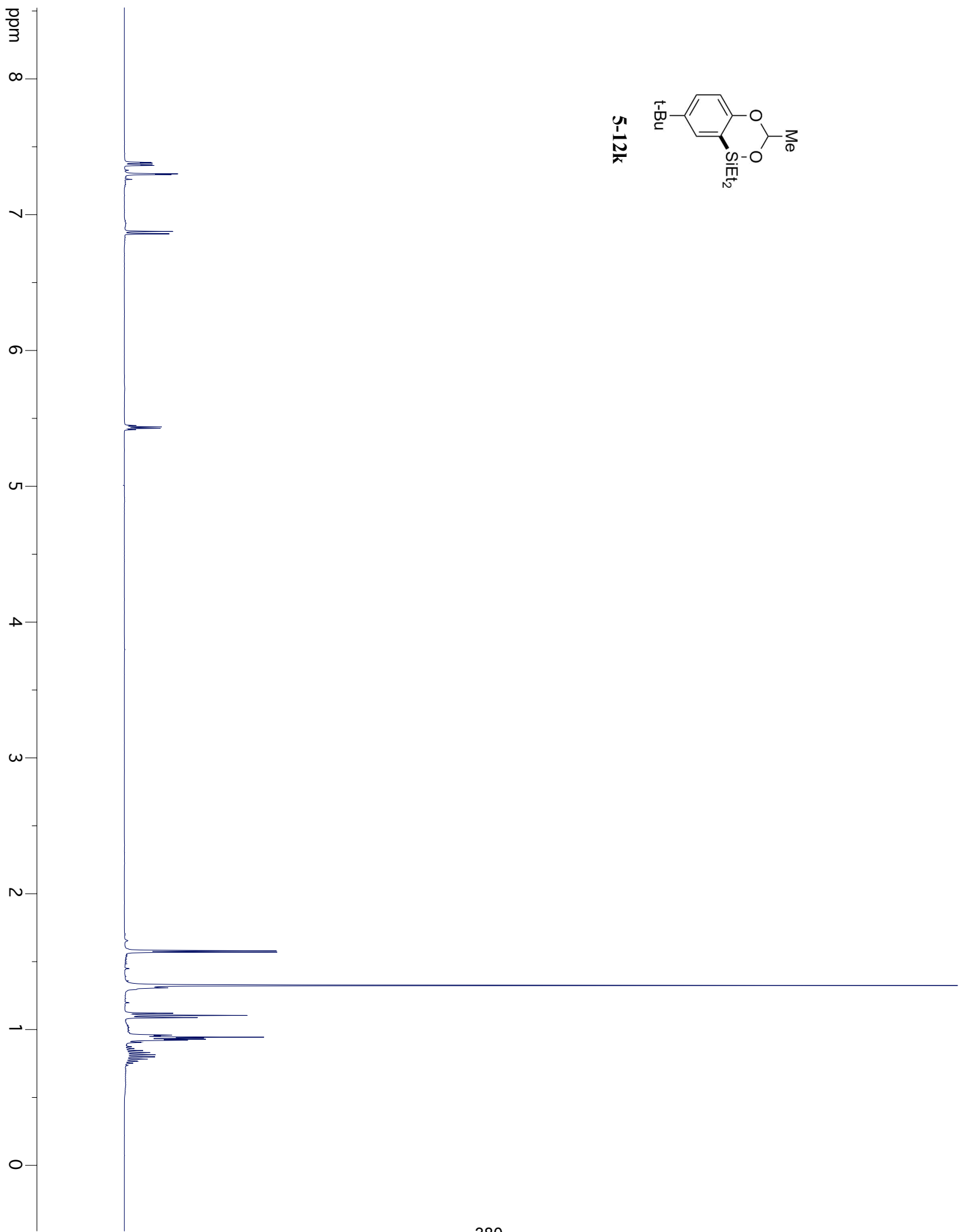
5-12j

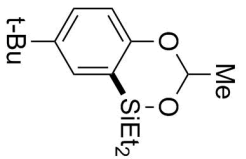




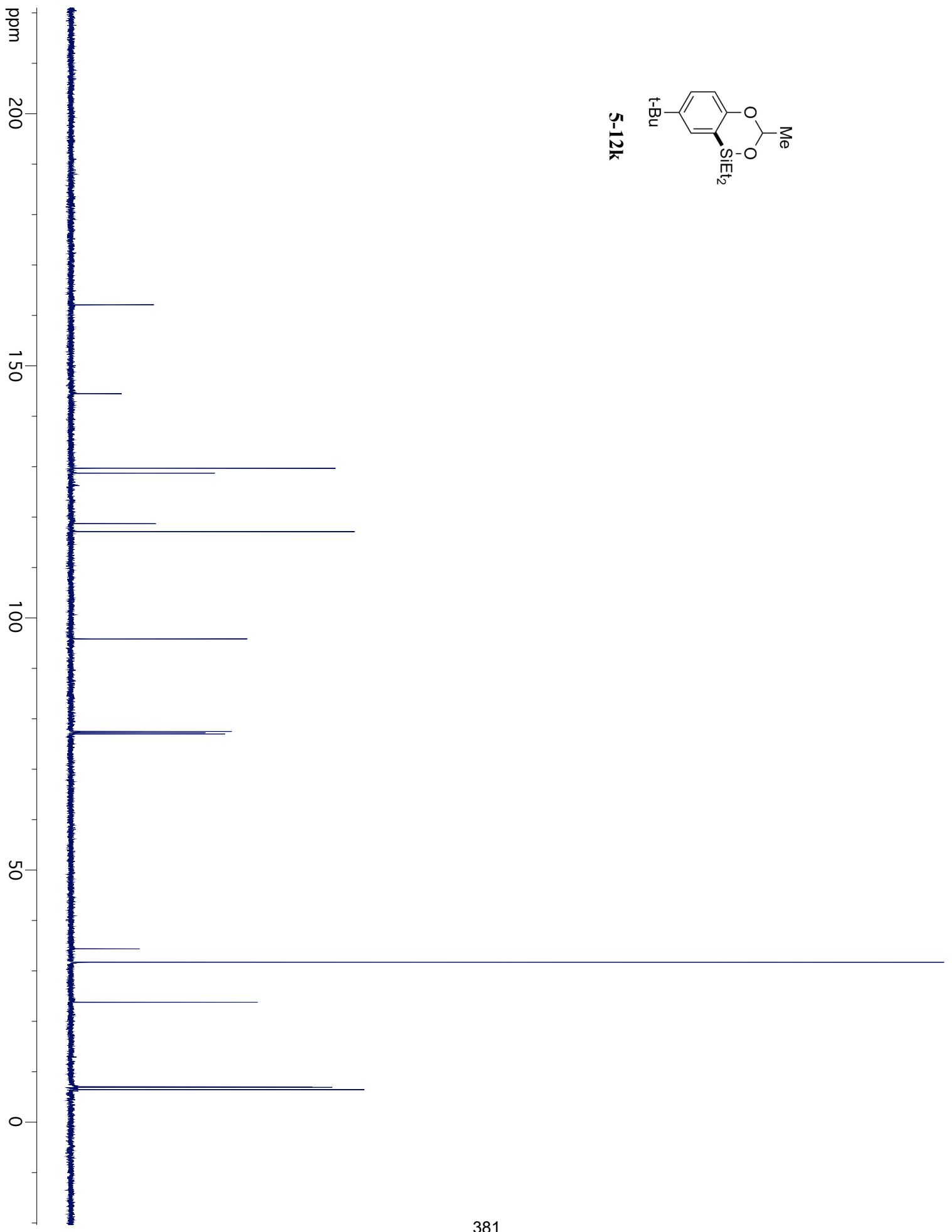


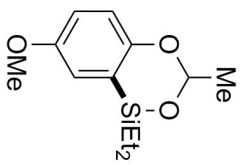
5-12k



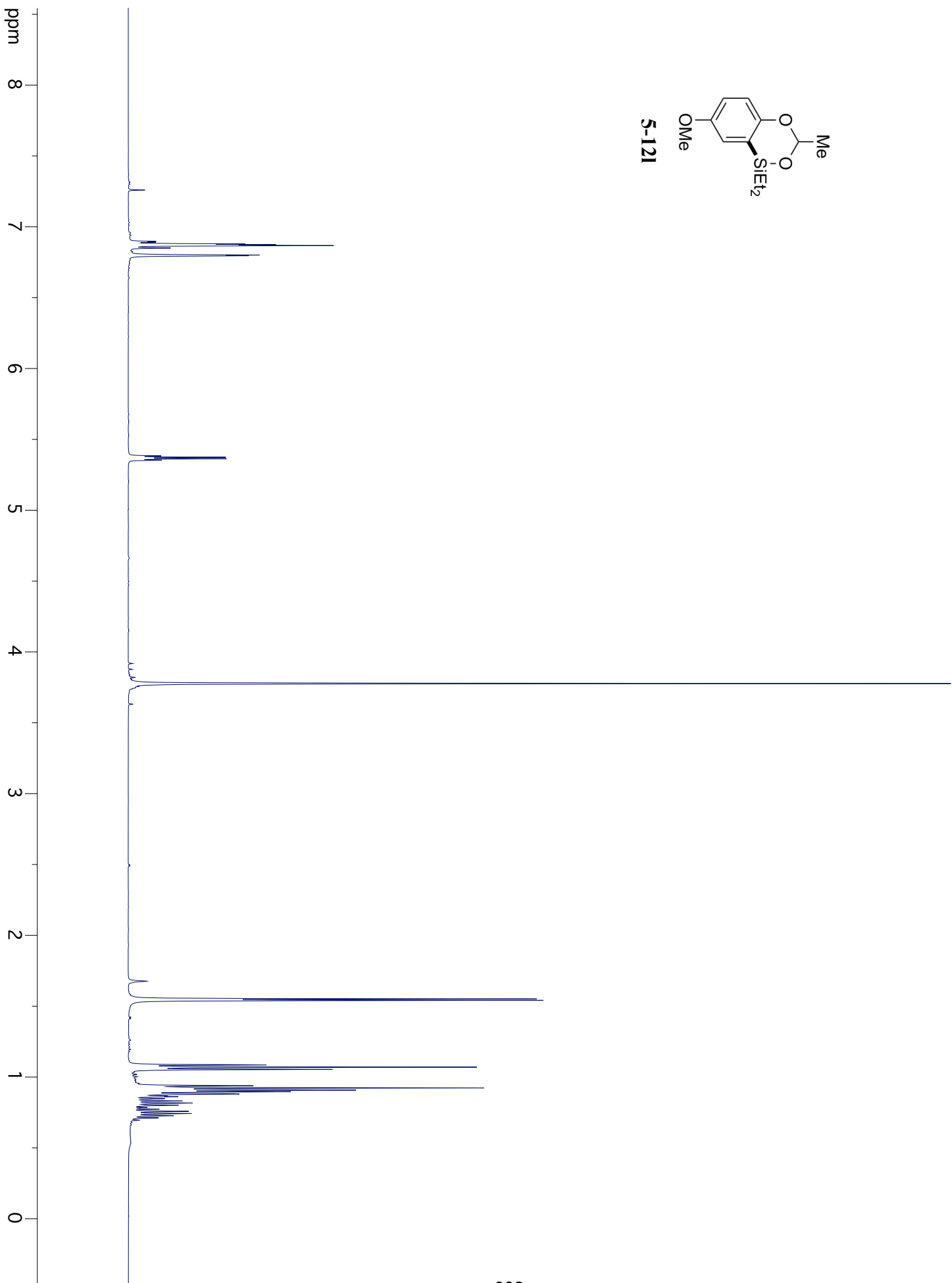


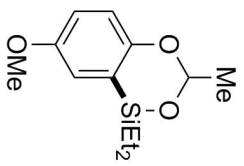
5-12K



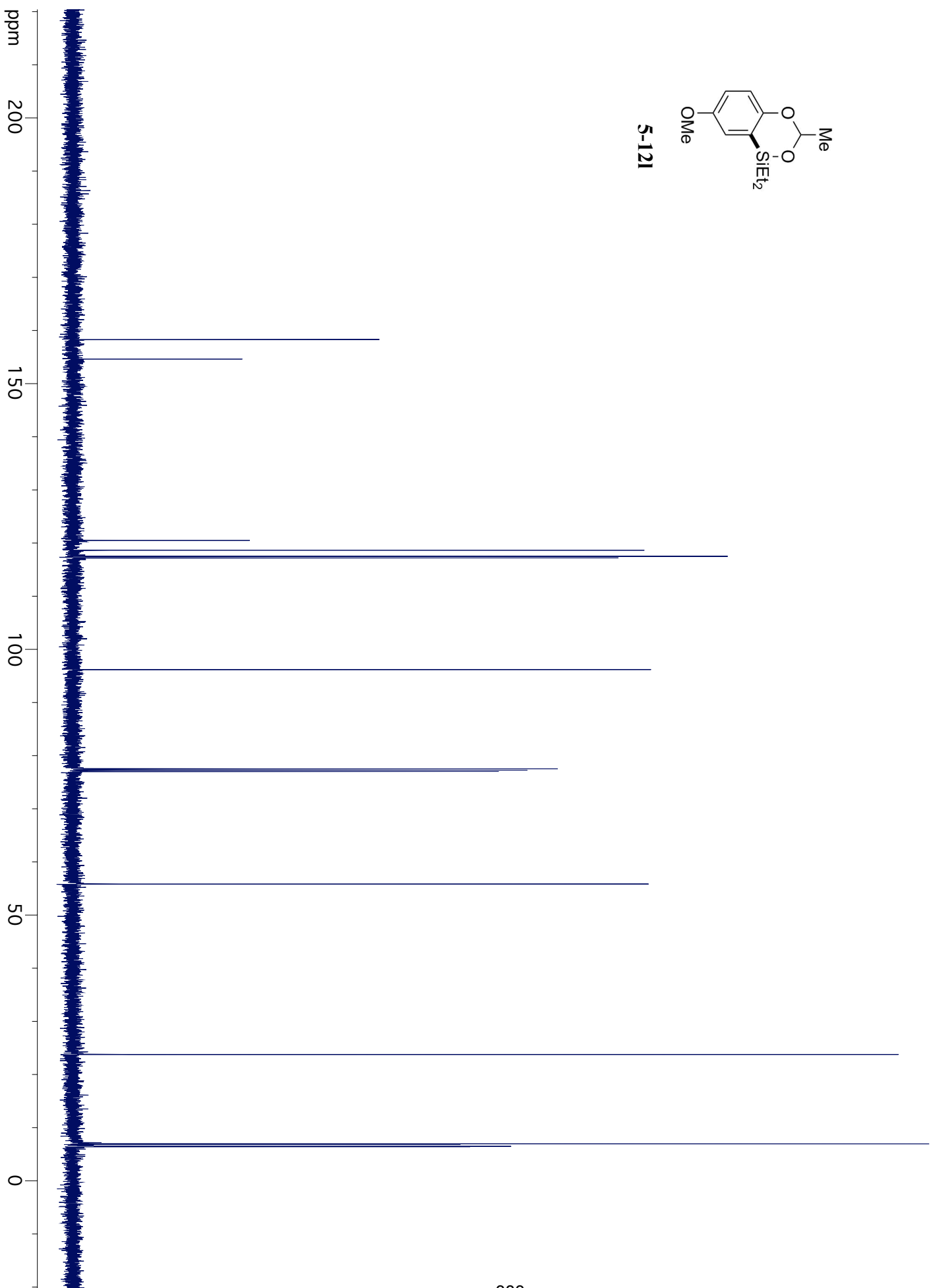


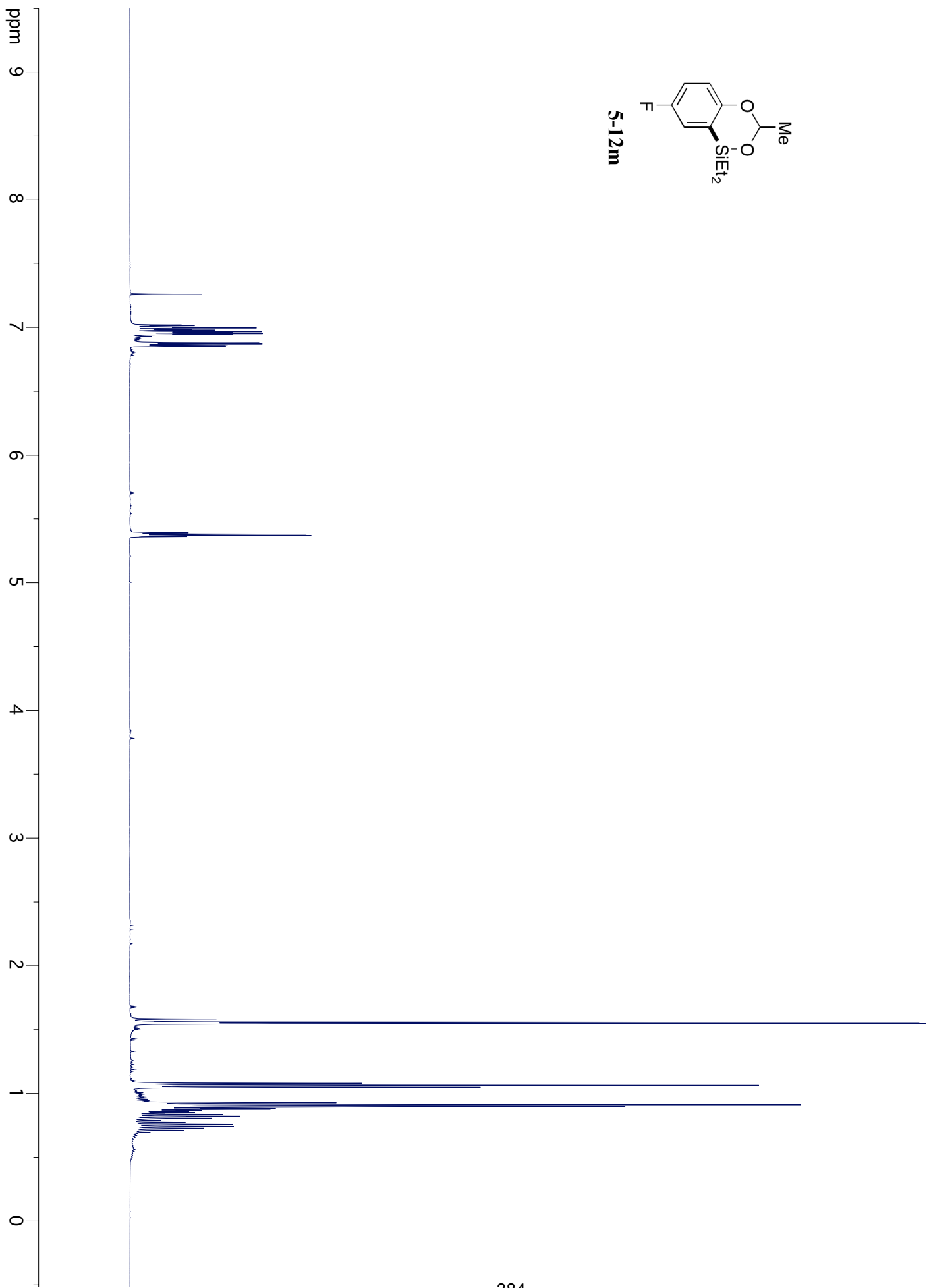
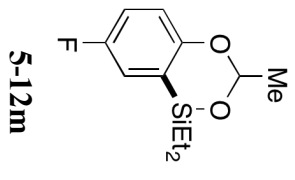
S-121

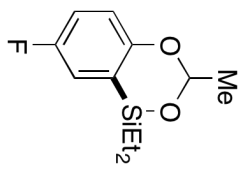




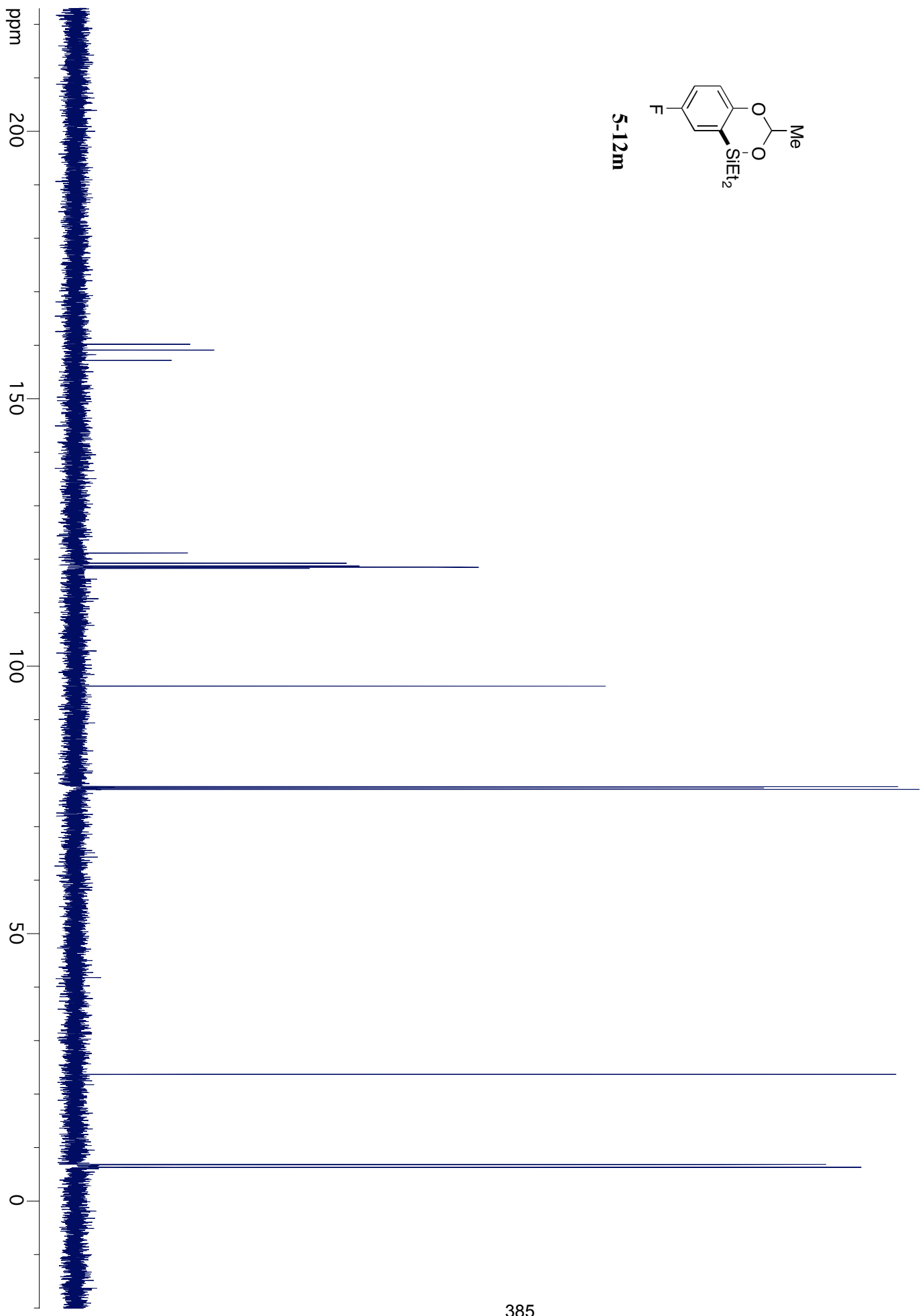
5-121

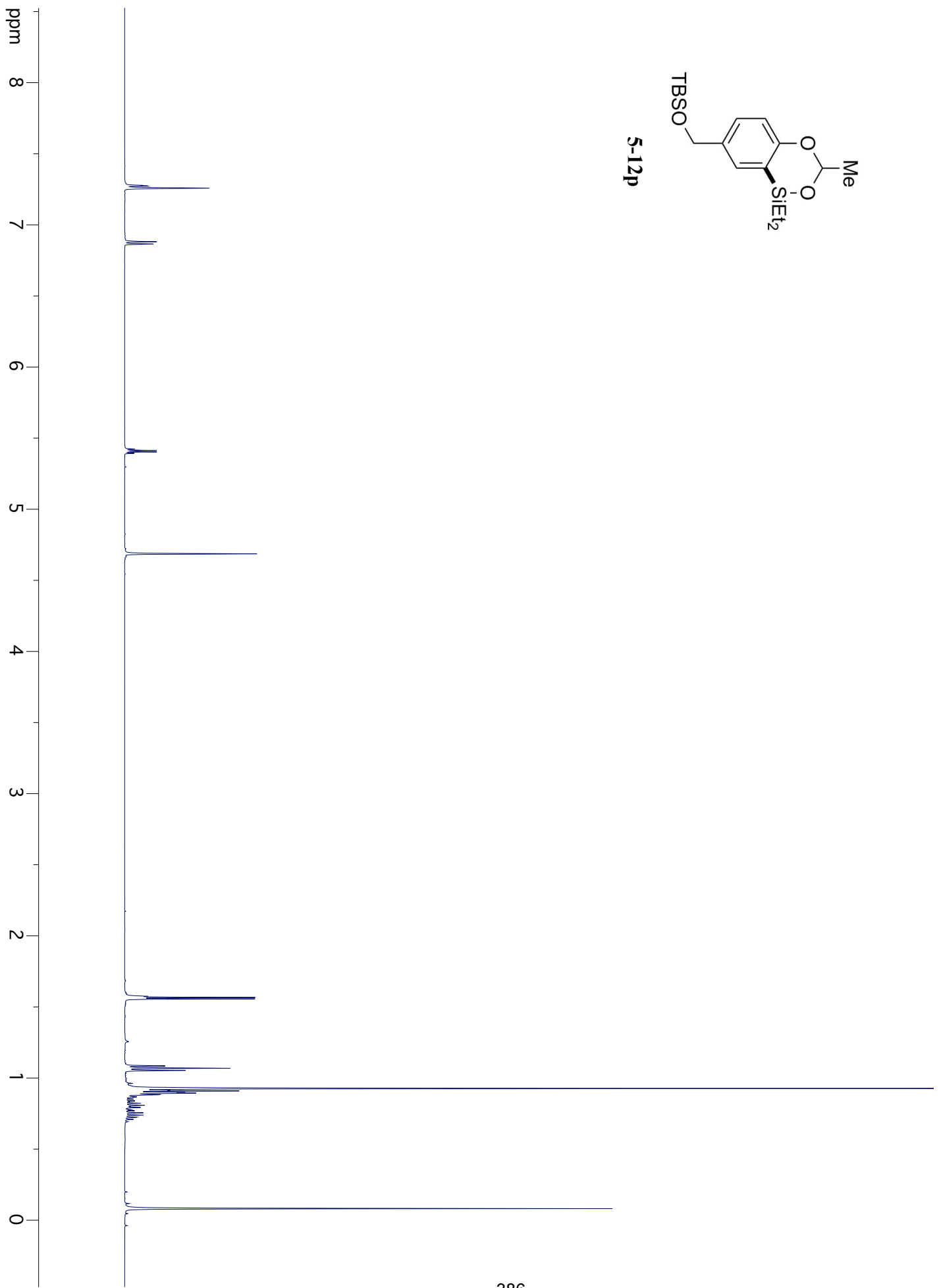
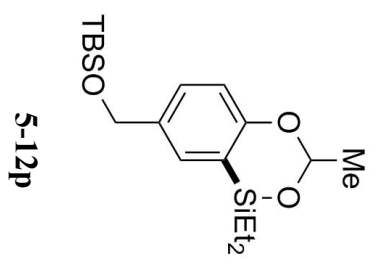


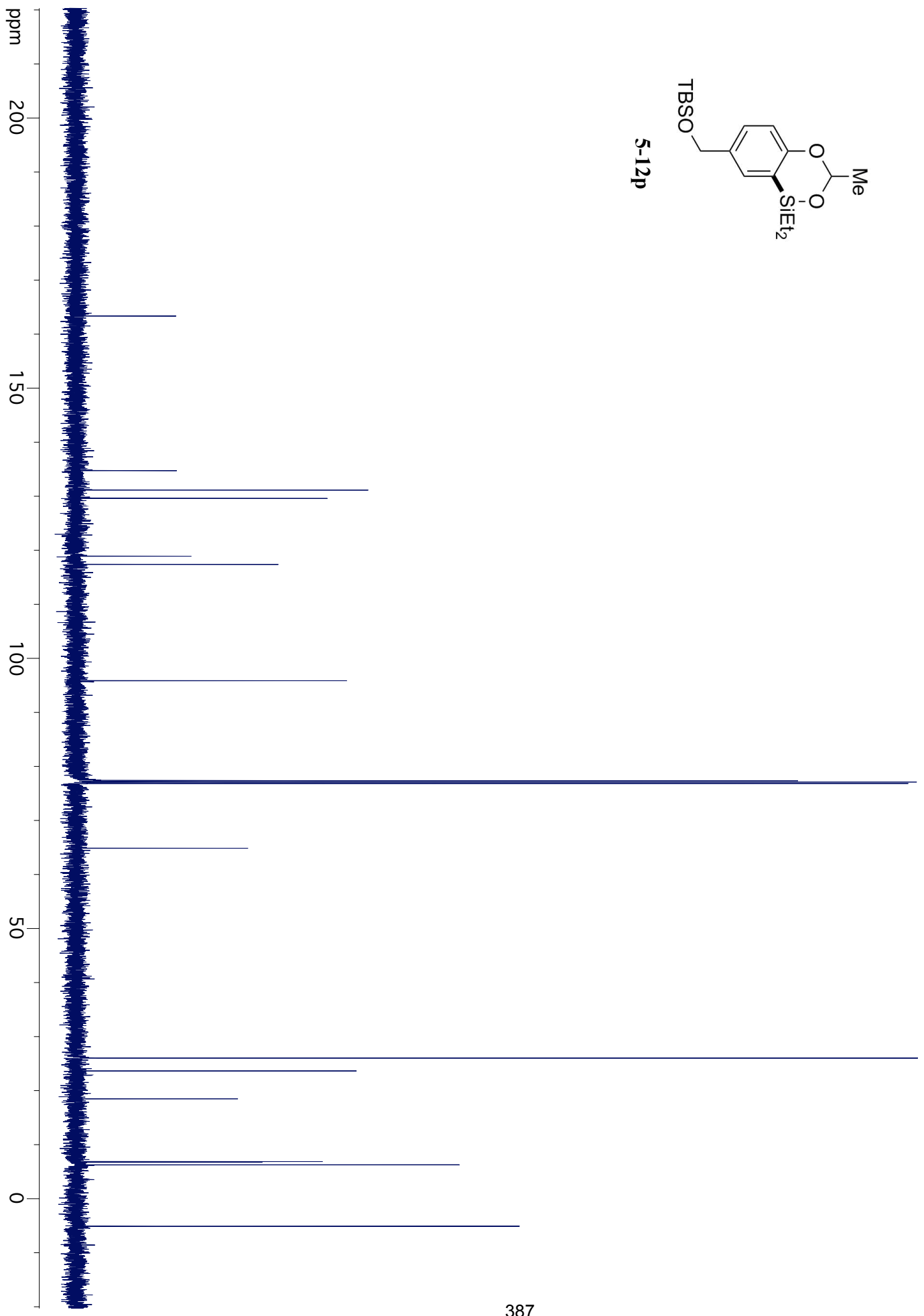
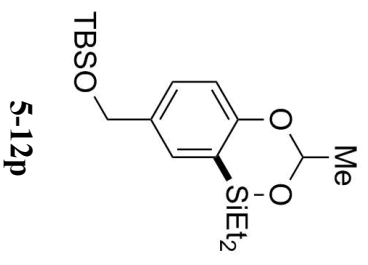


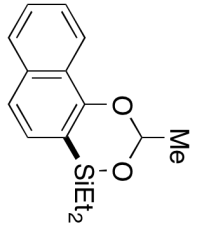


5-12m

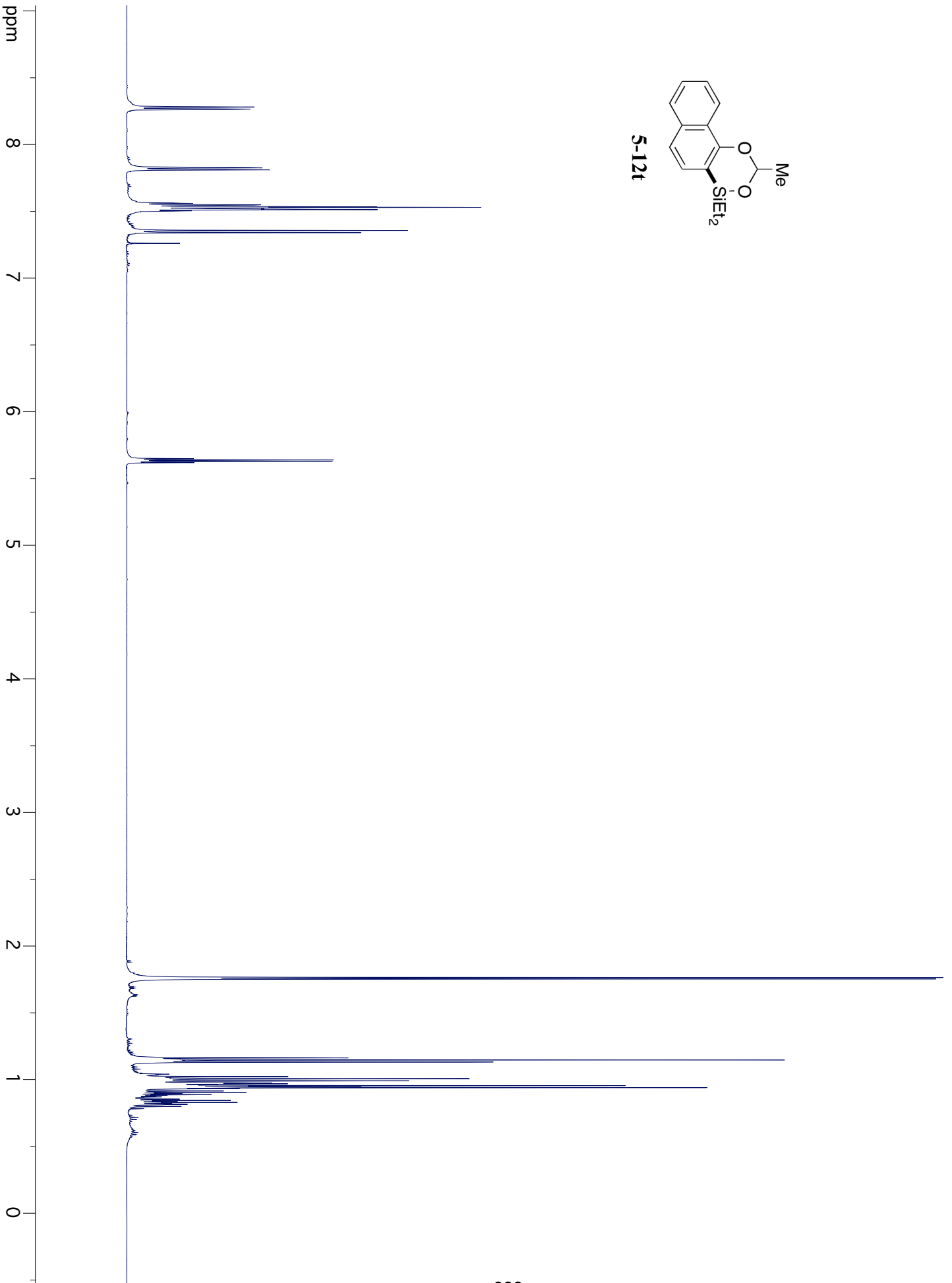


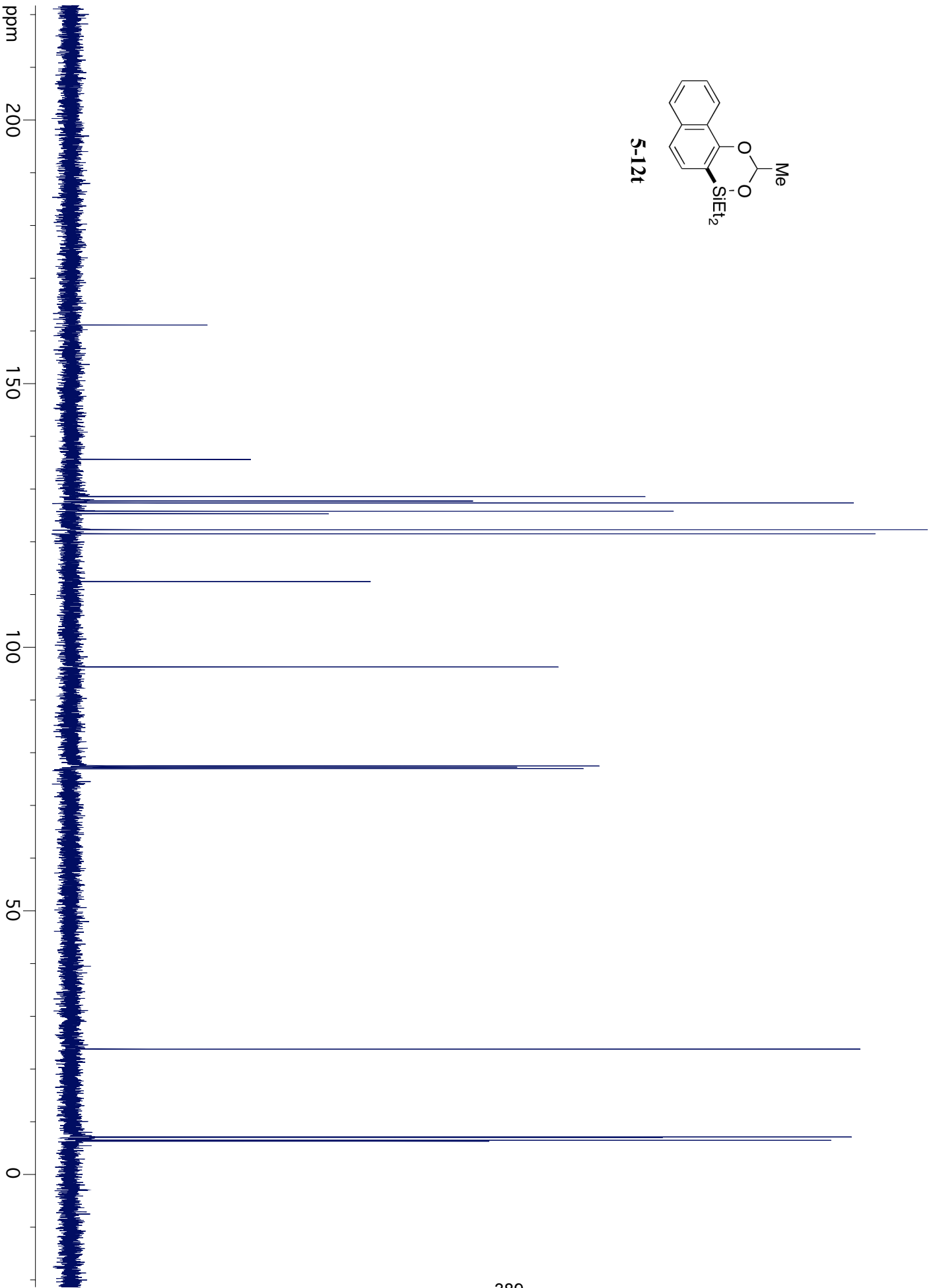
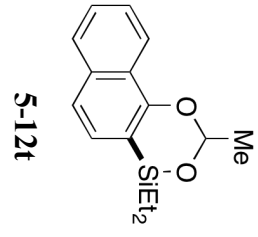


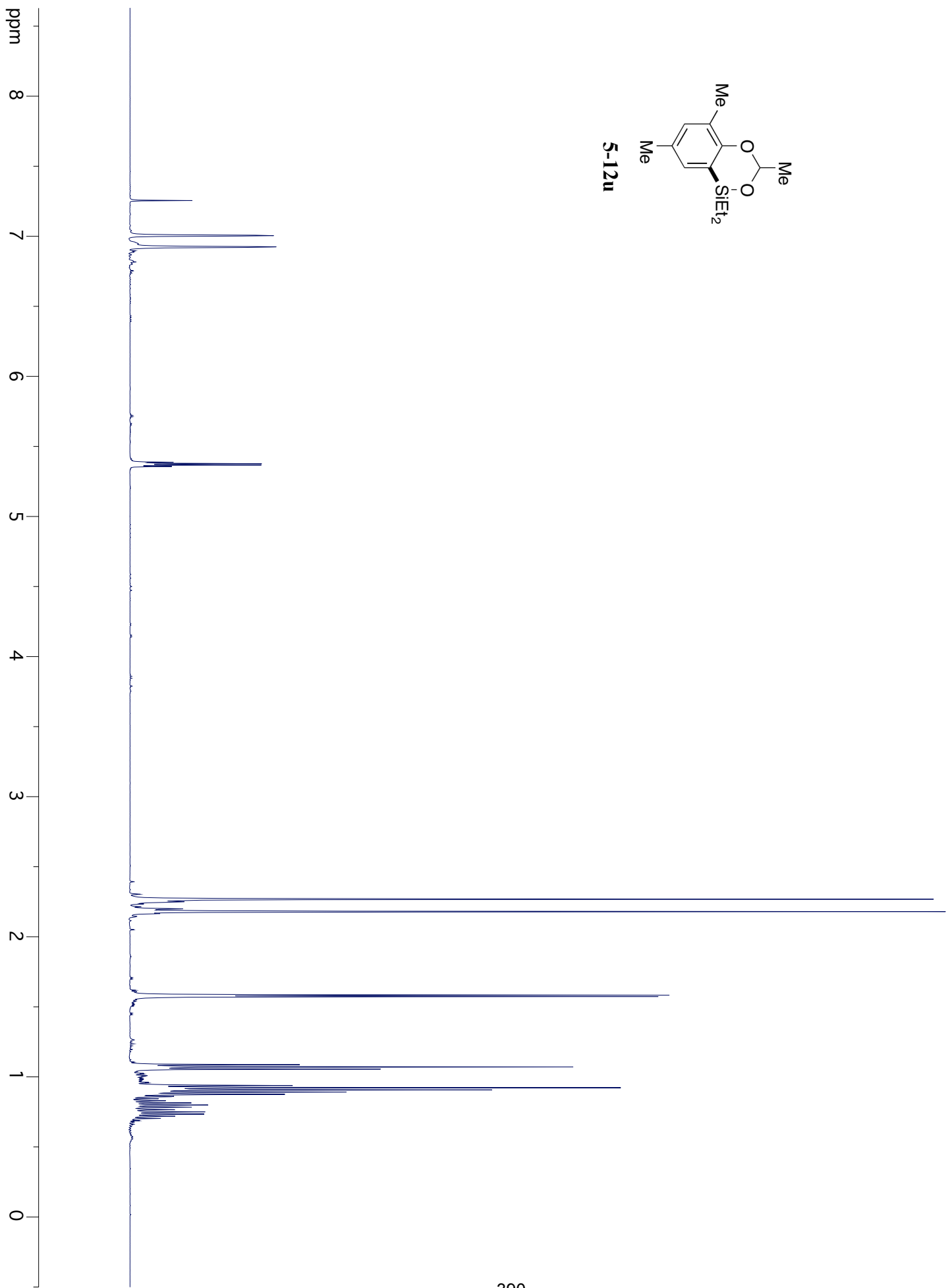
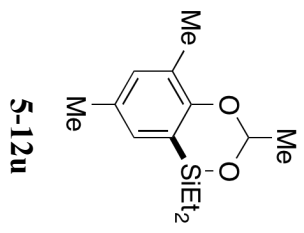


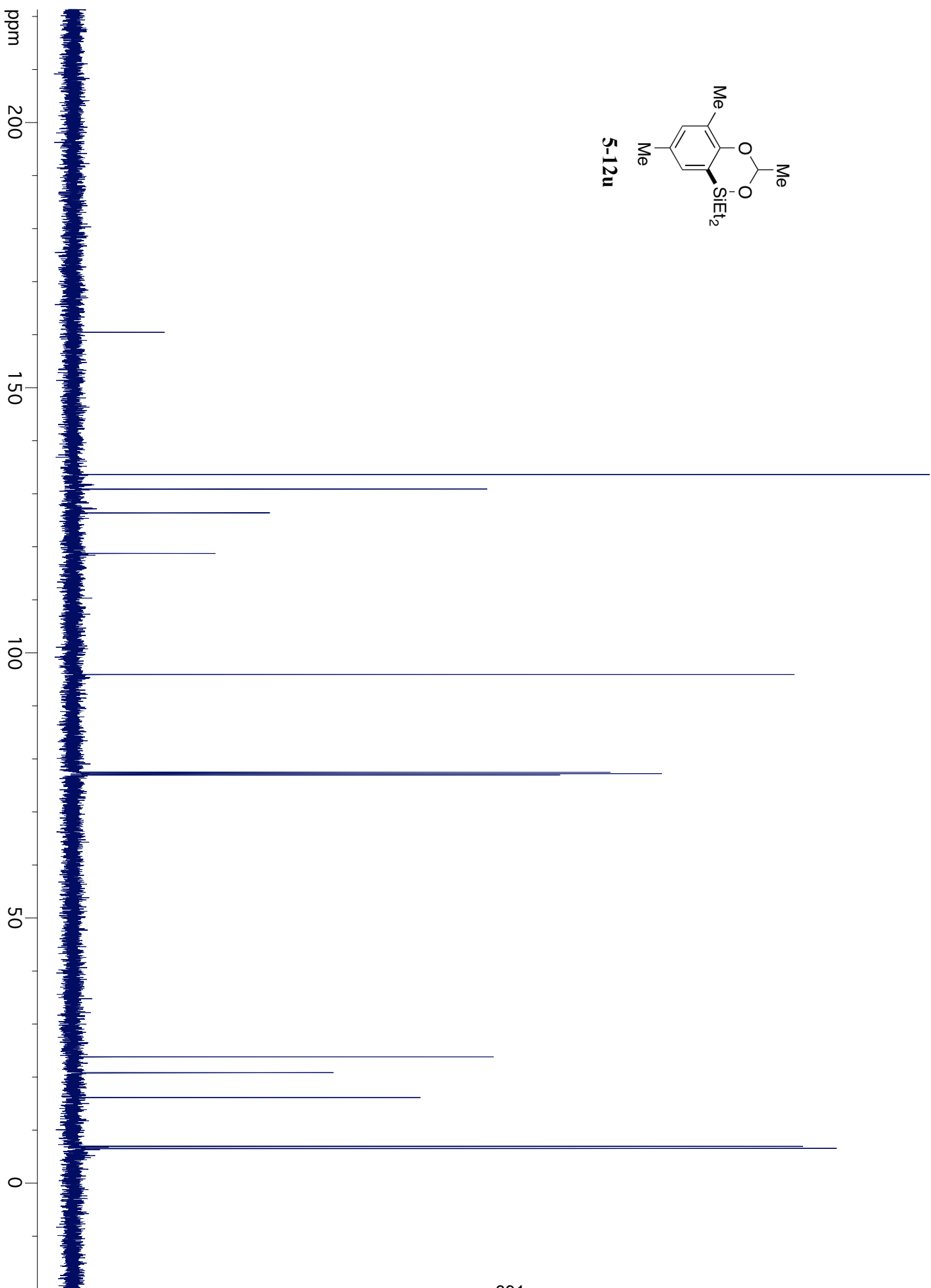
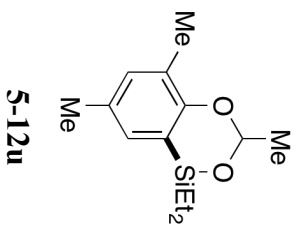


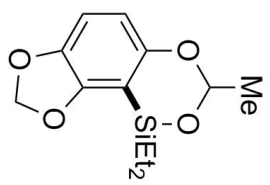
5-12t





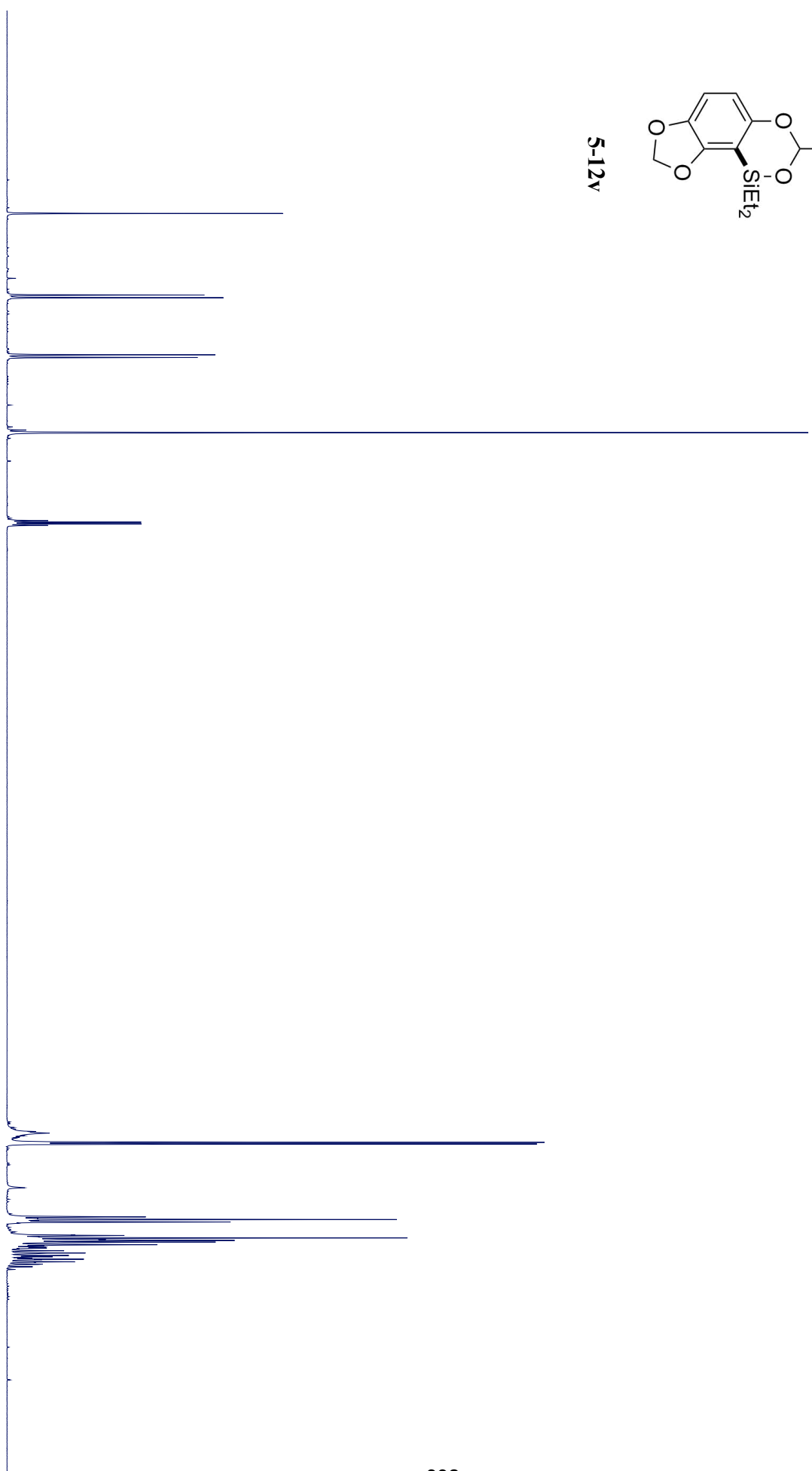


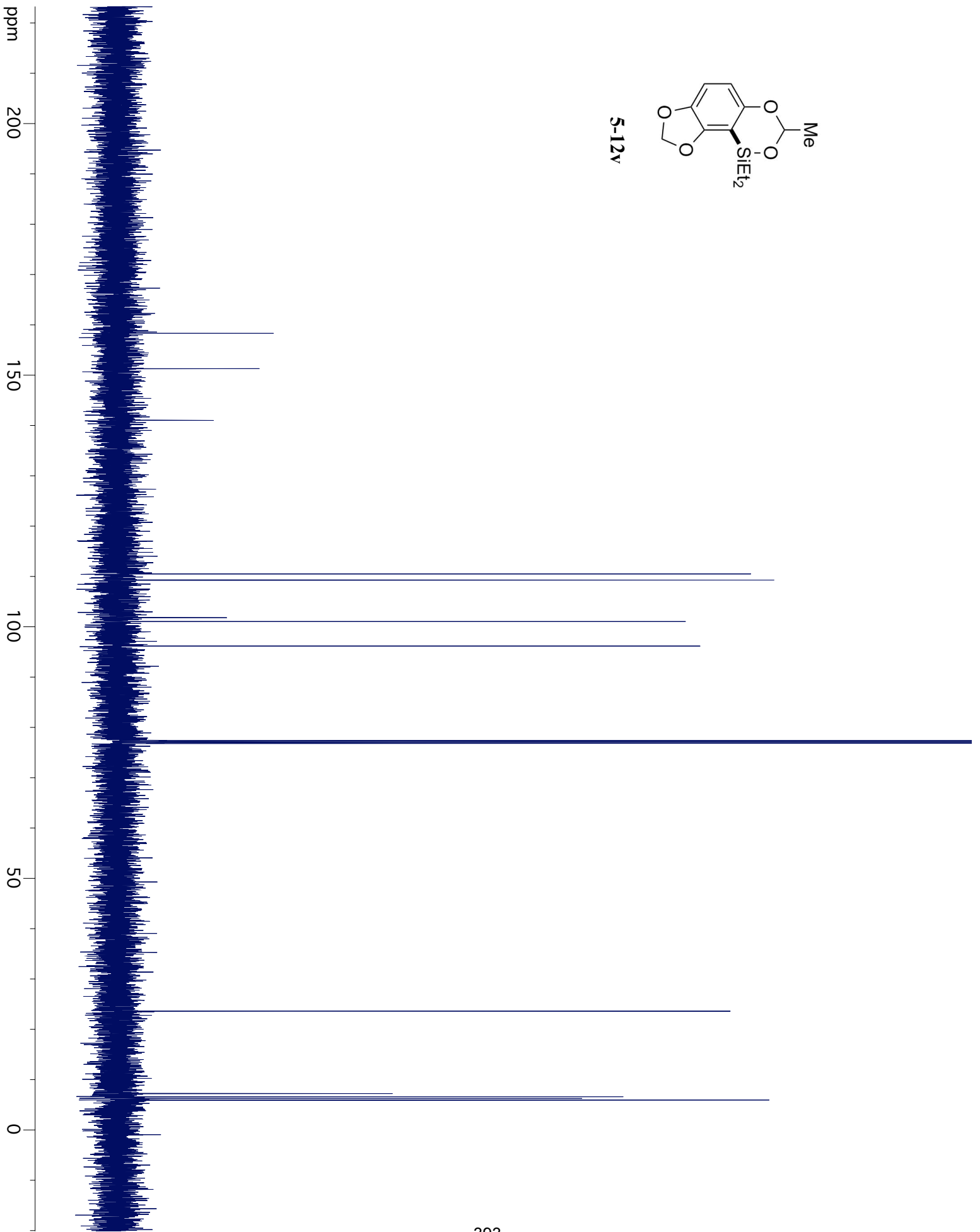
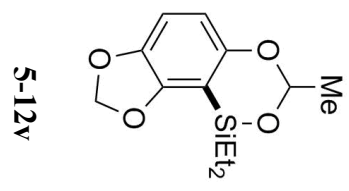


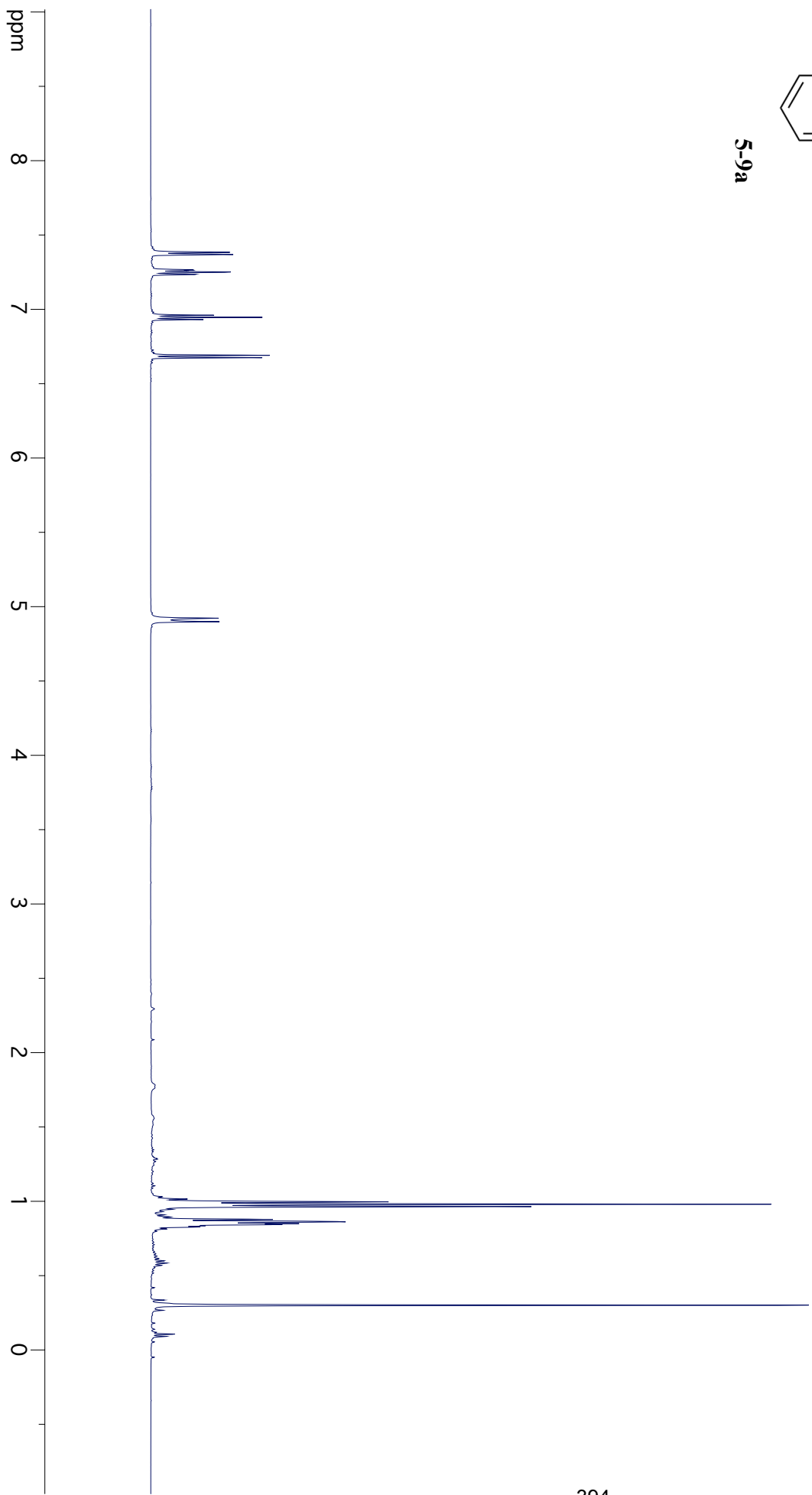
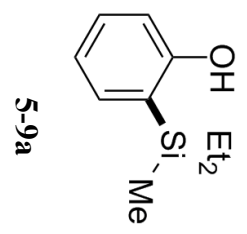


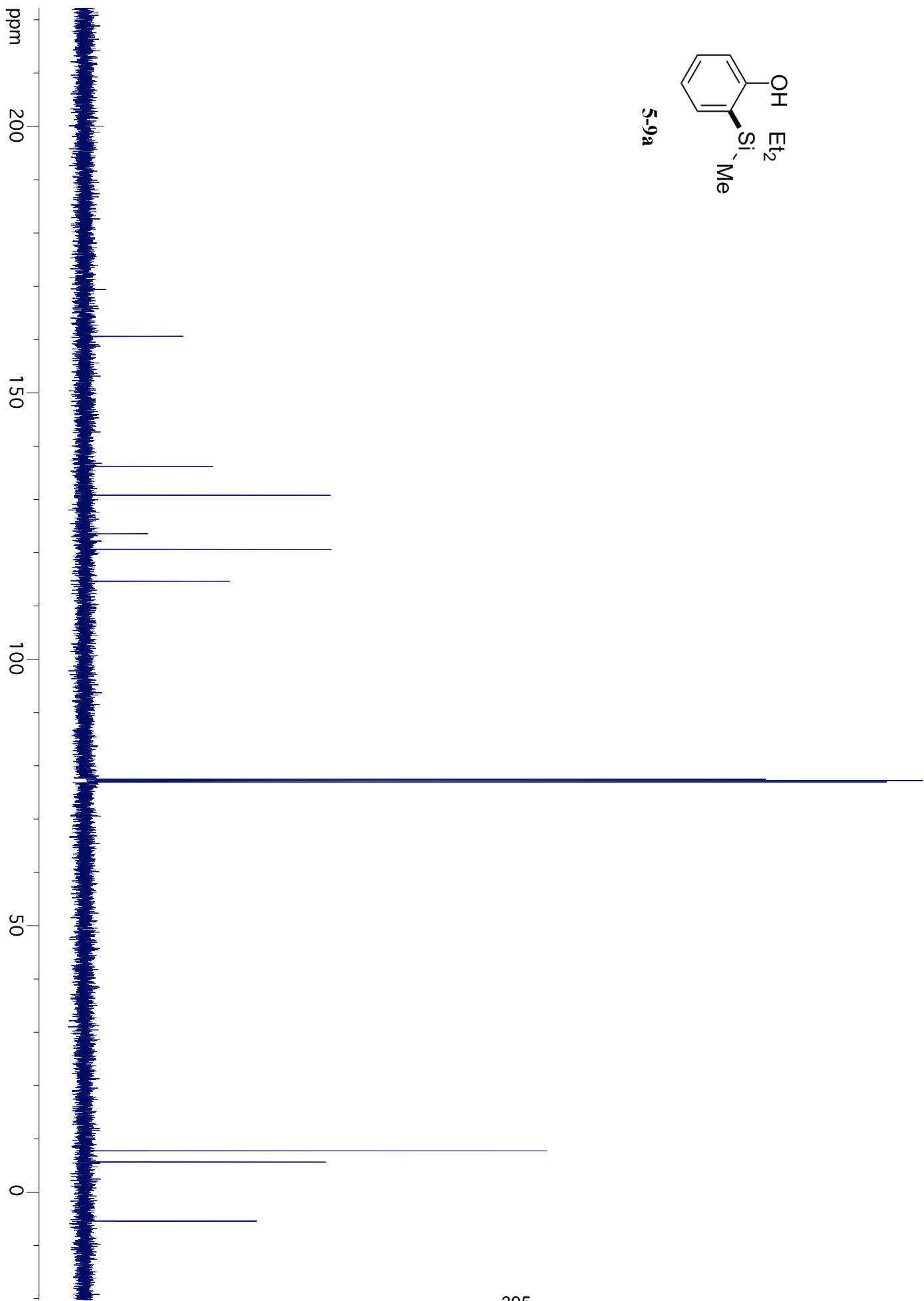
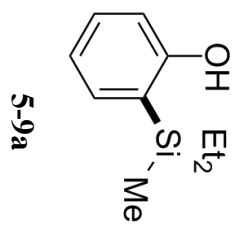
5-12v

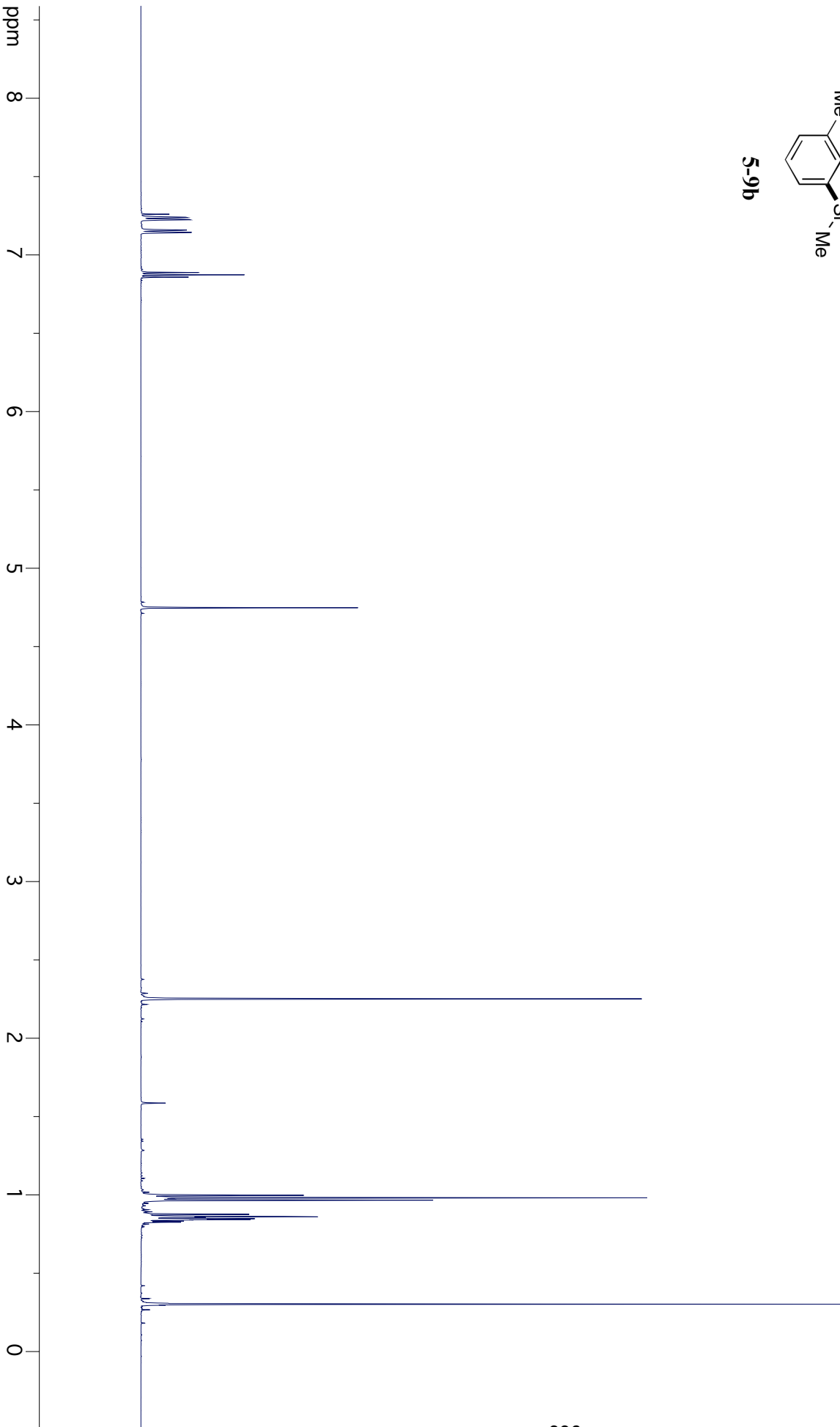
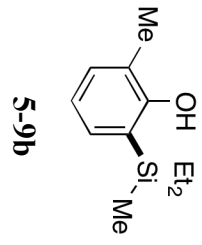
ppm 8 7 6 5 4 3 2 1 0

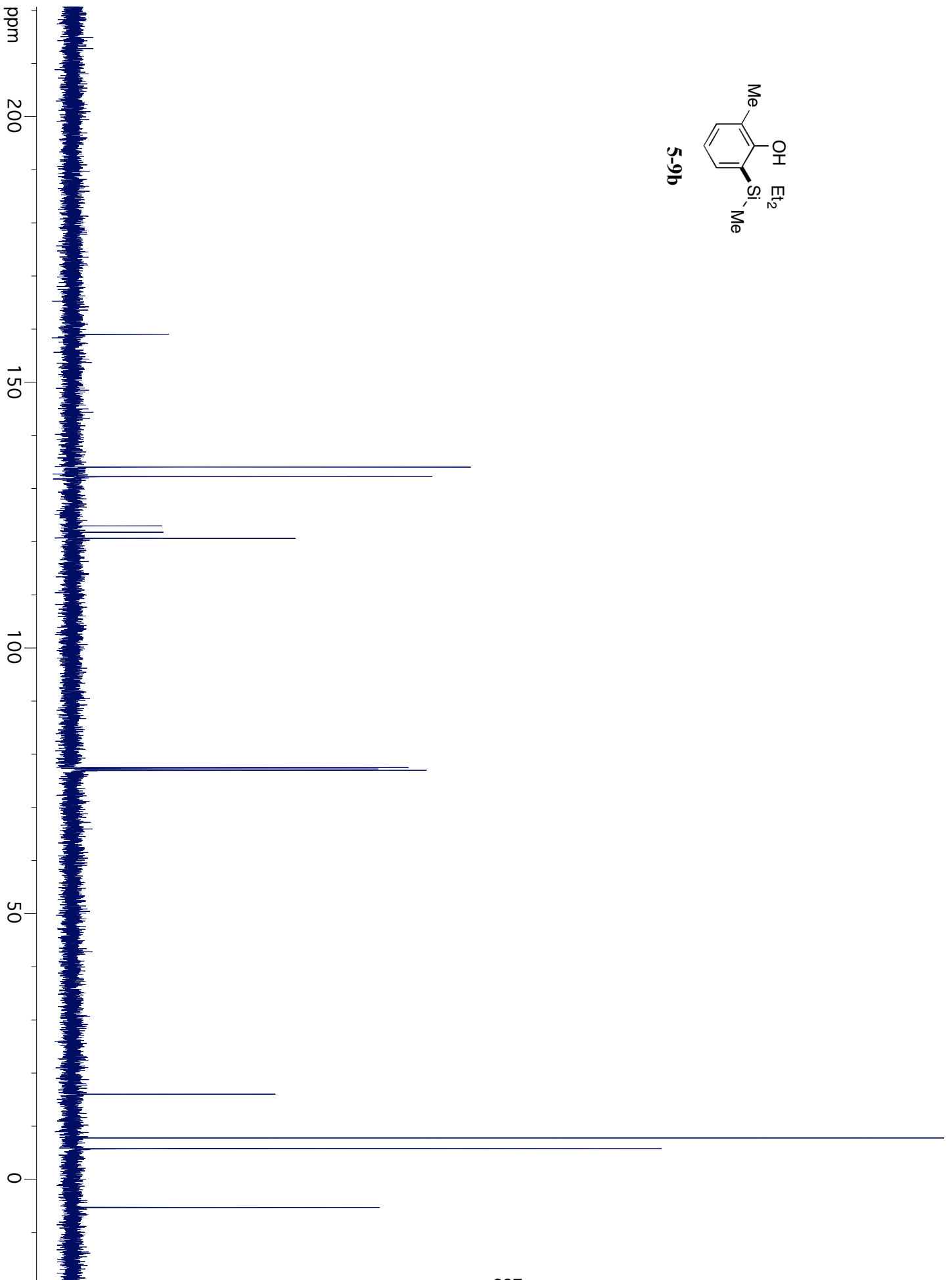
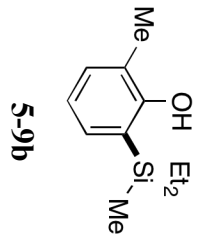


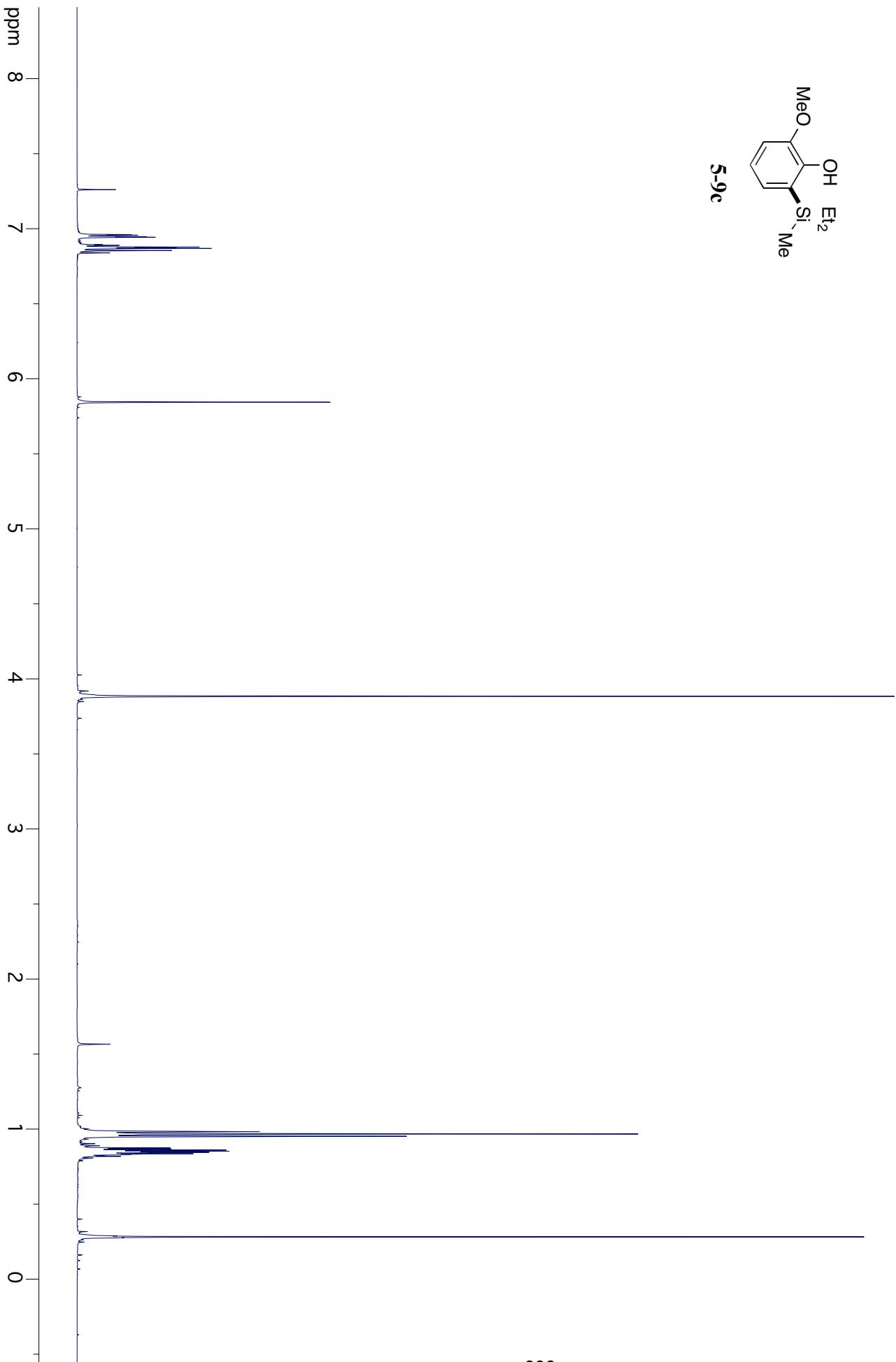
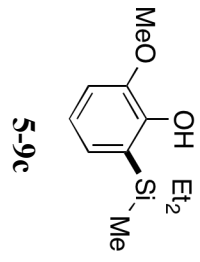


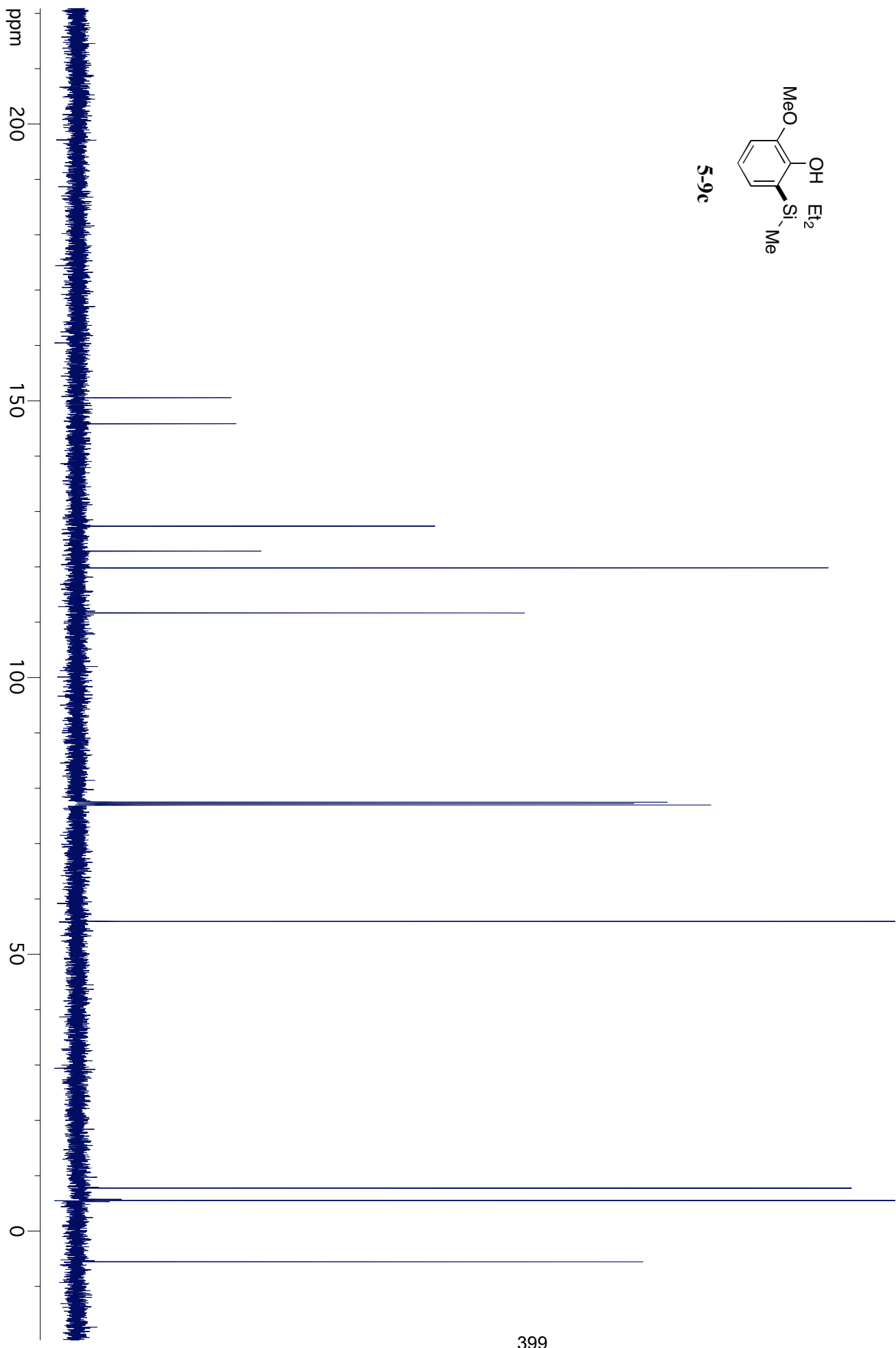
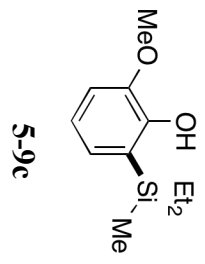


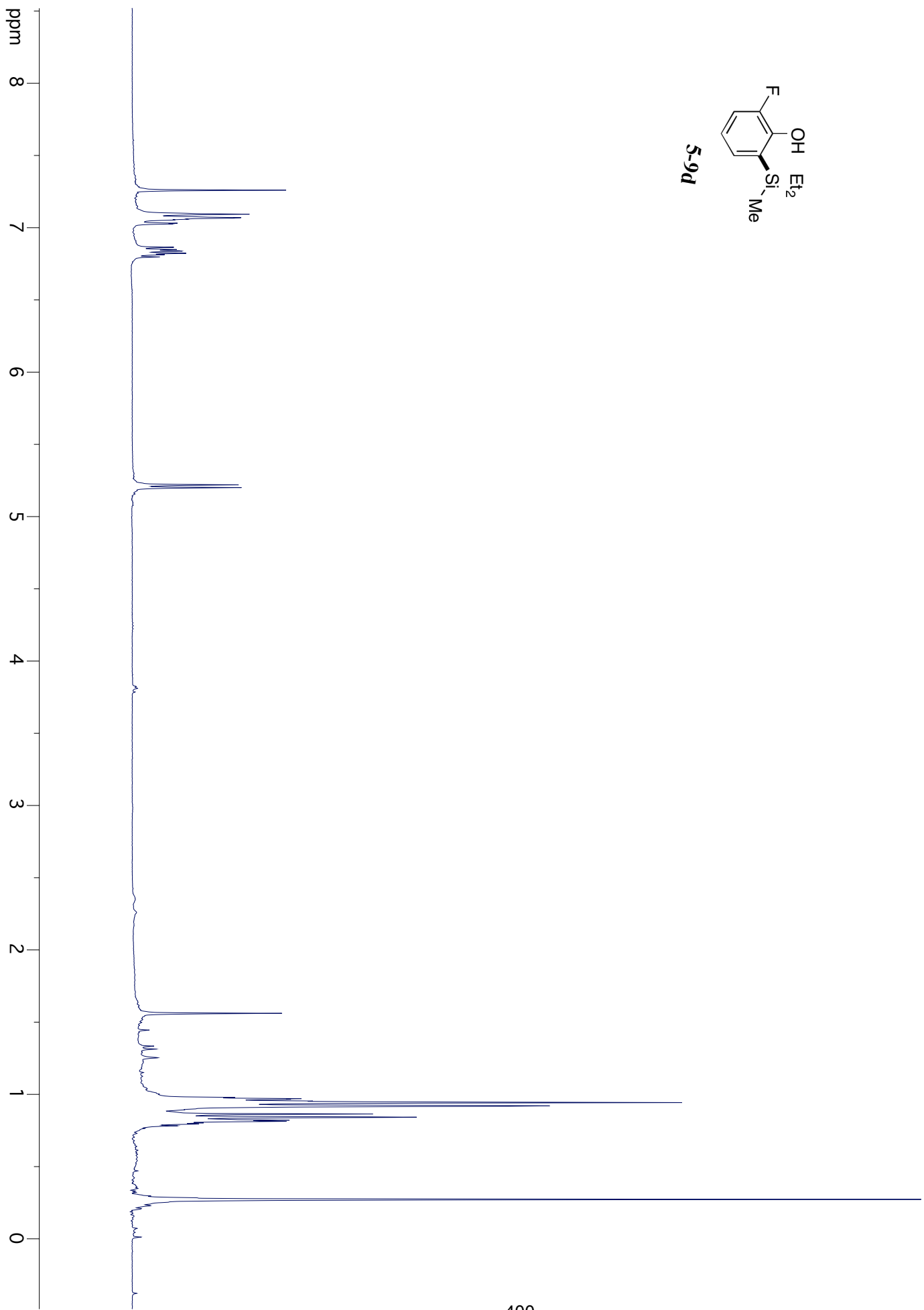
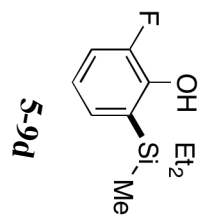


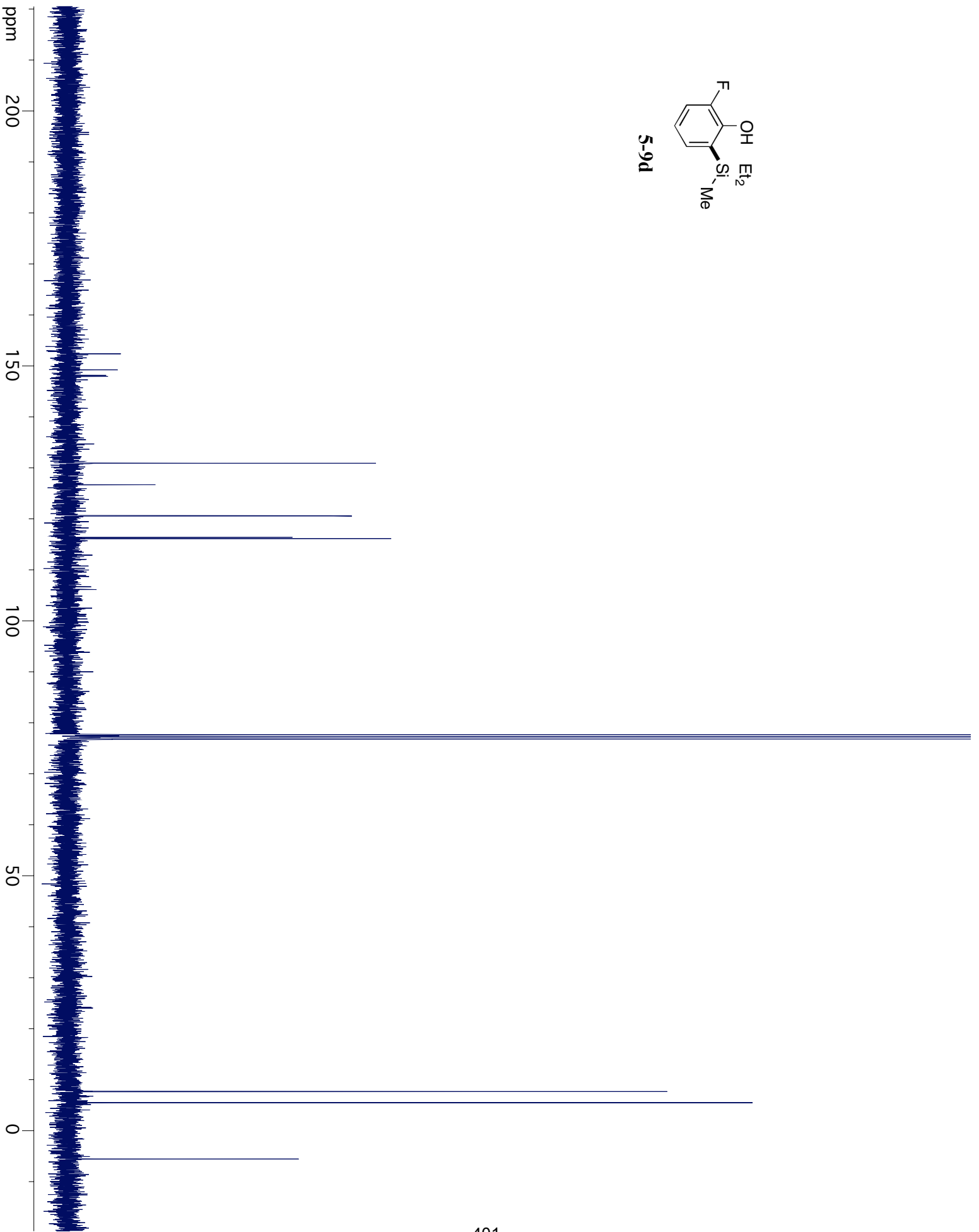
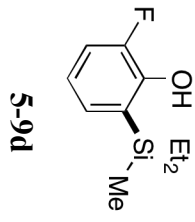


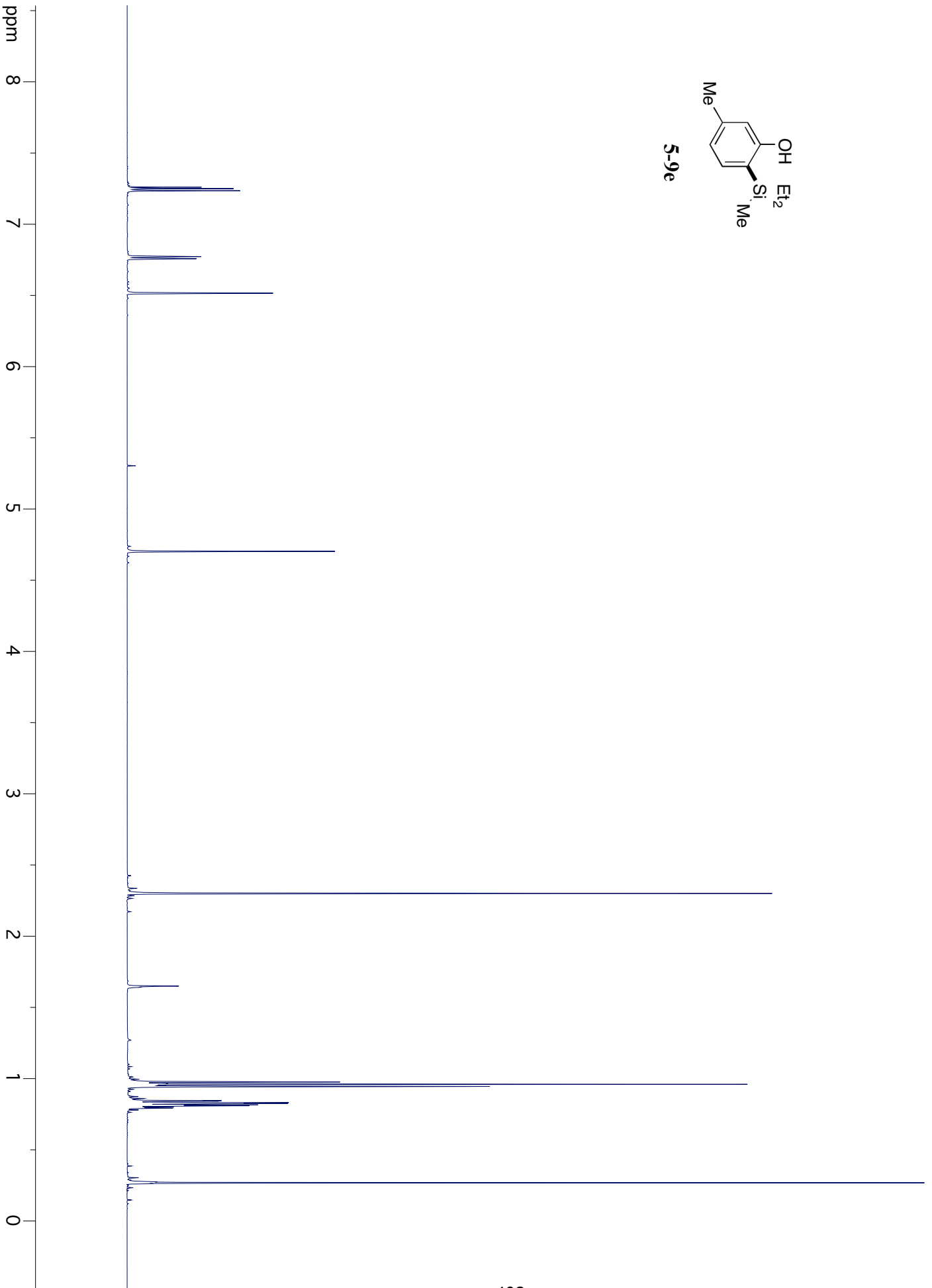
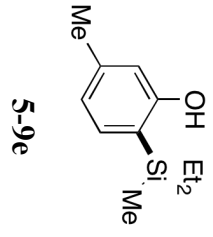


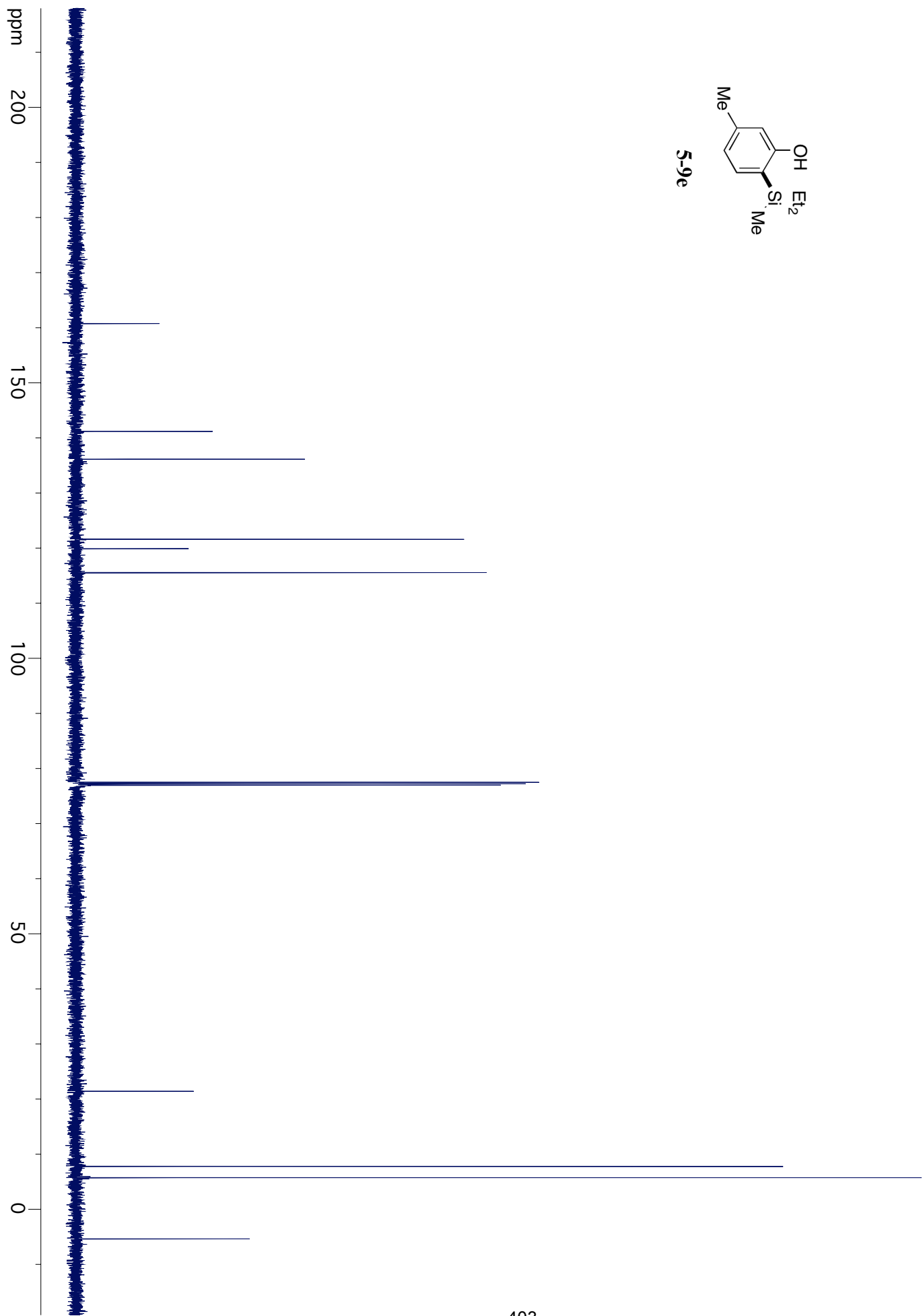
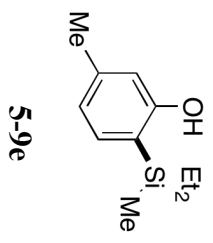


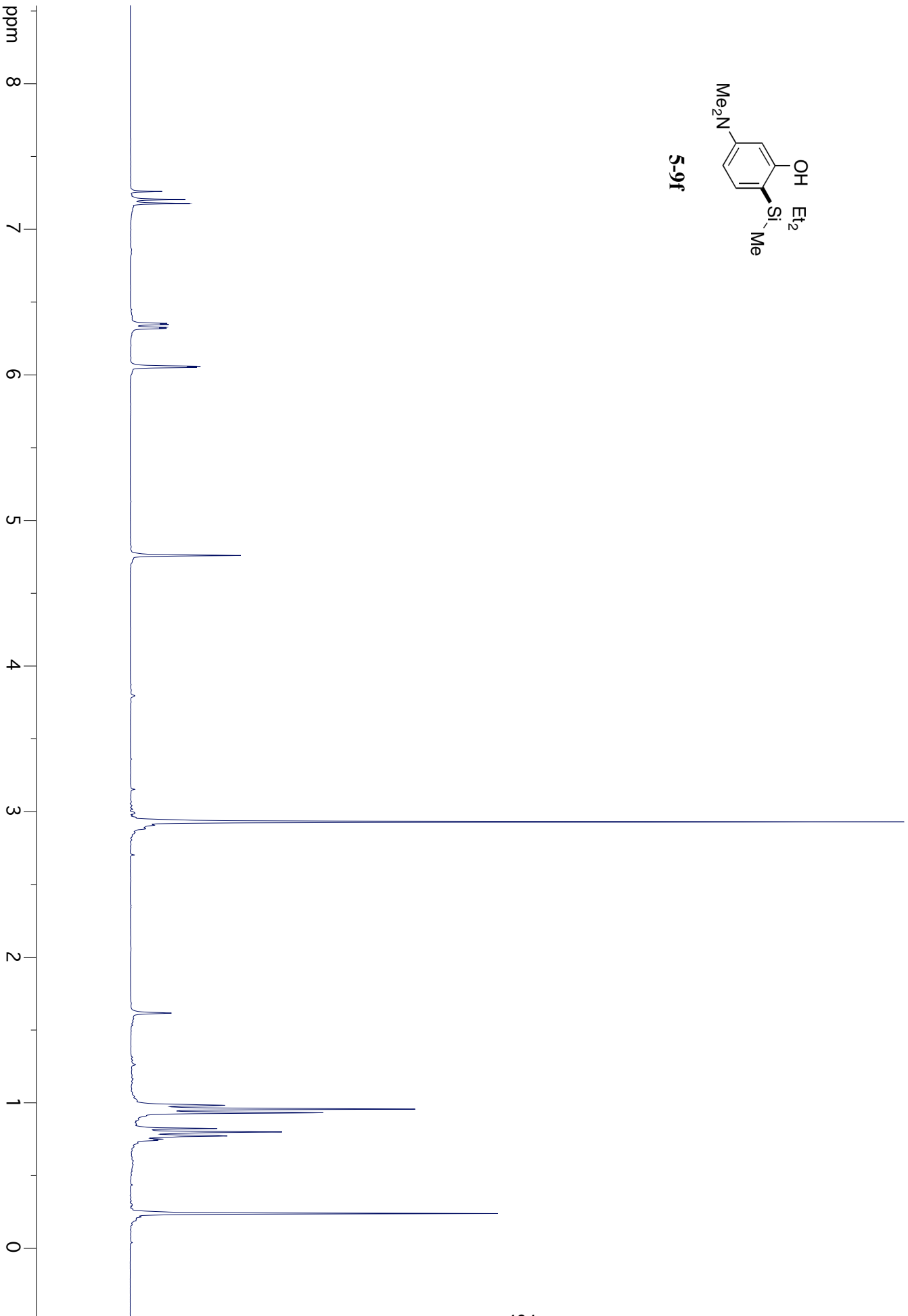
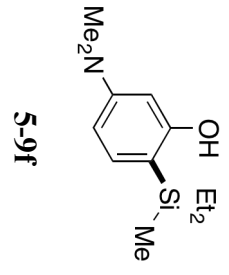


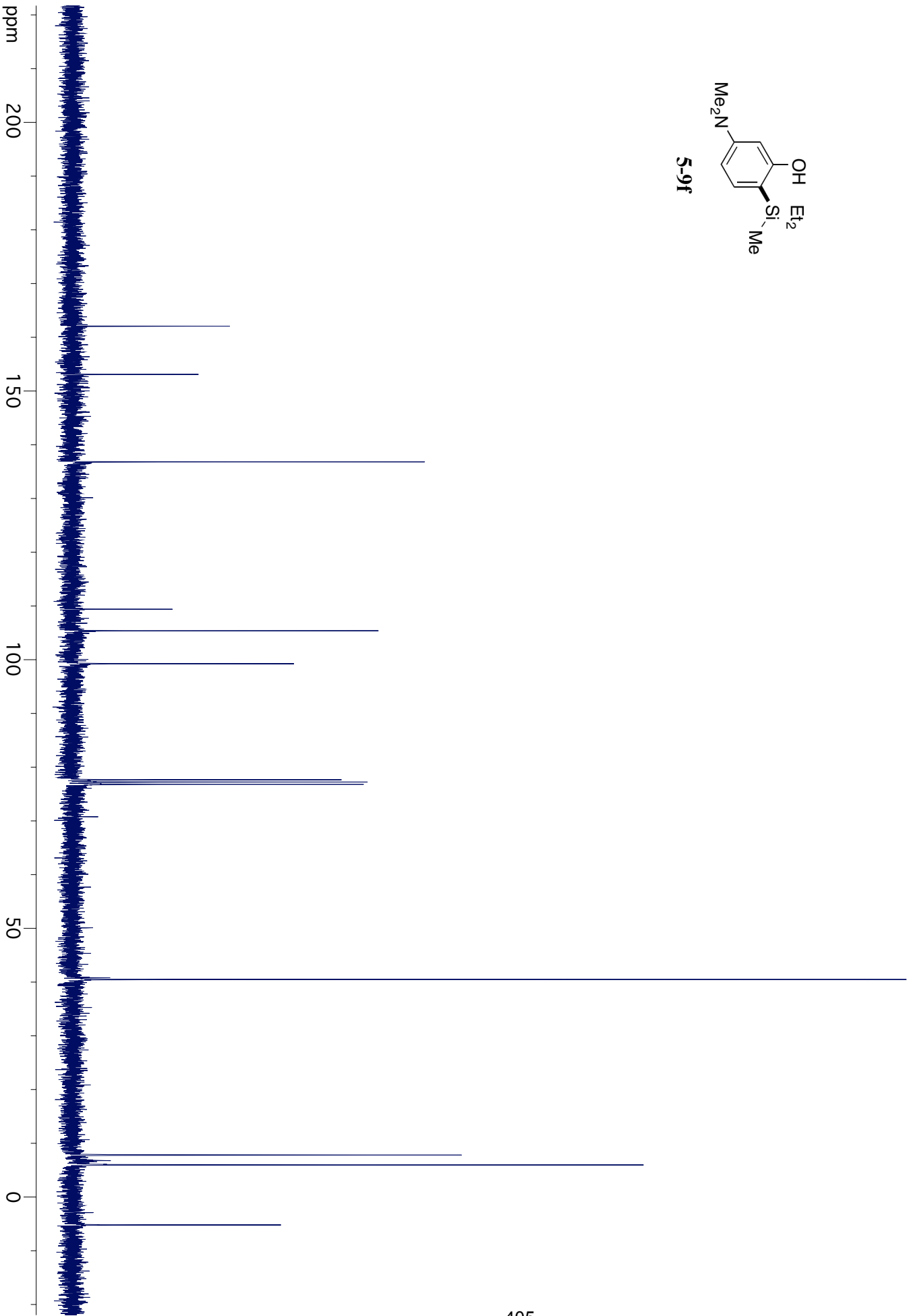
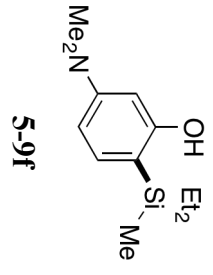


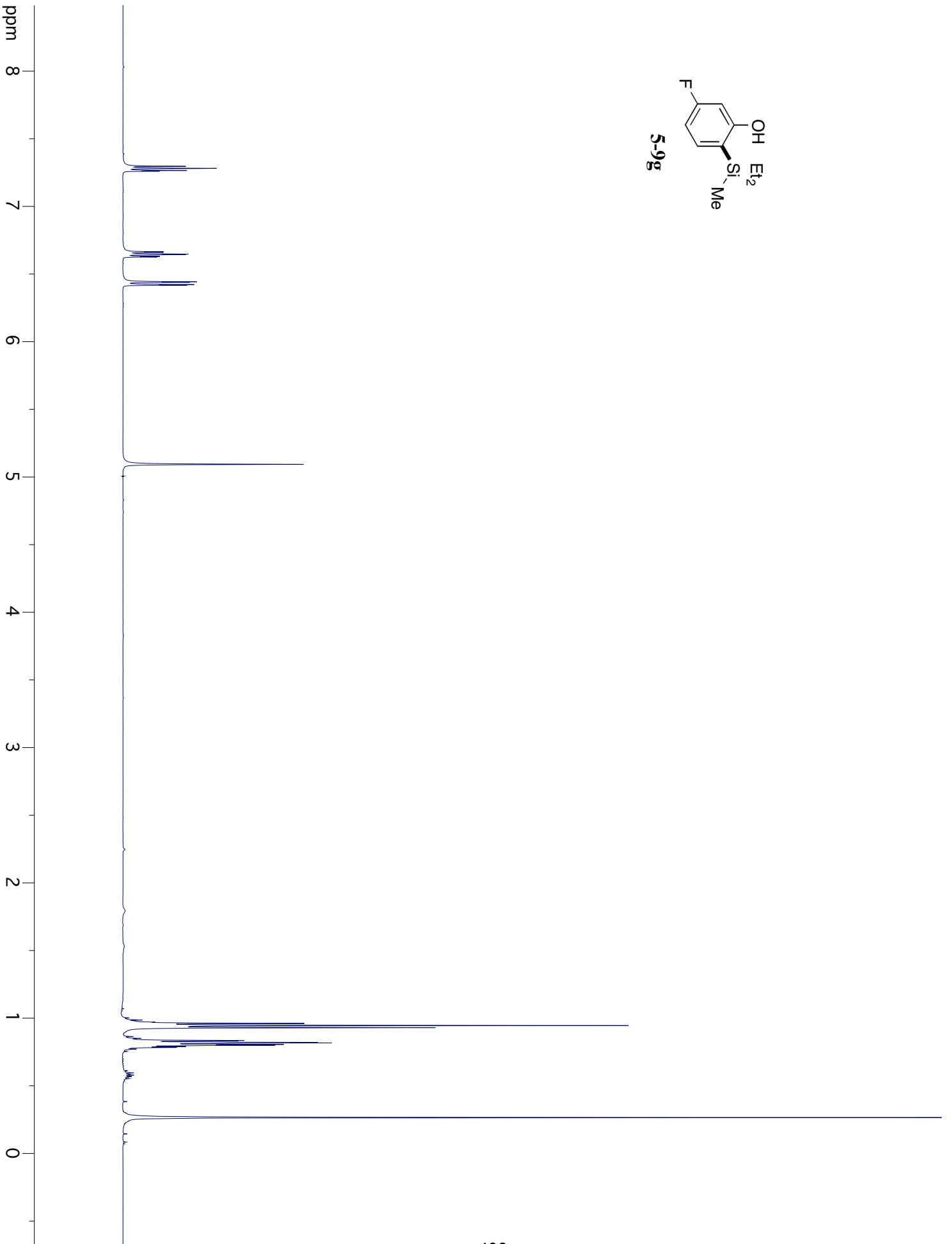
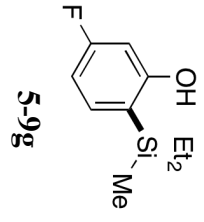


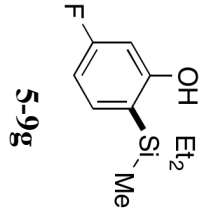




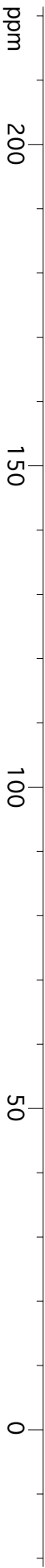


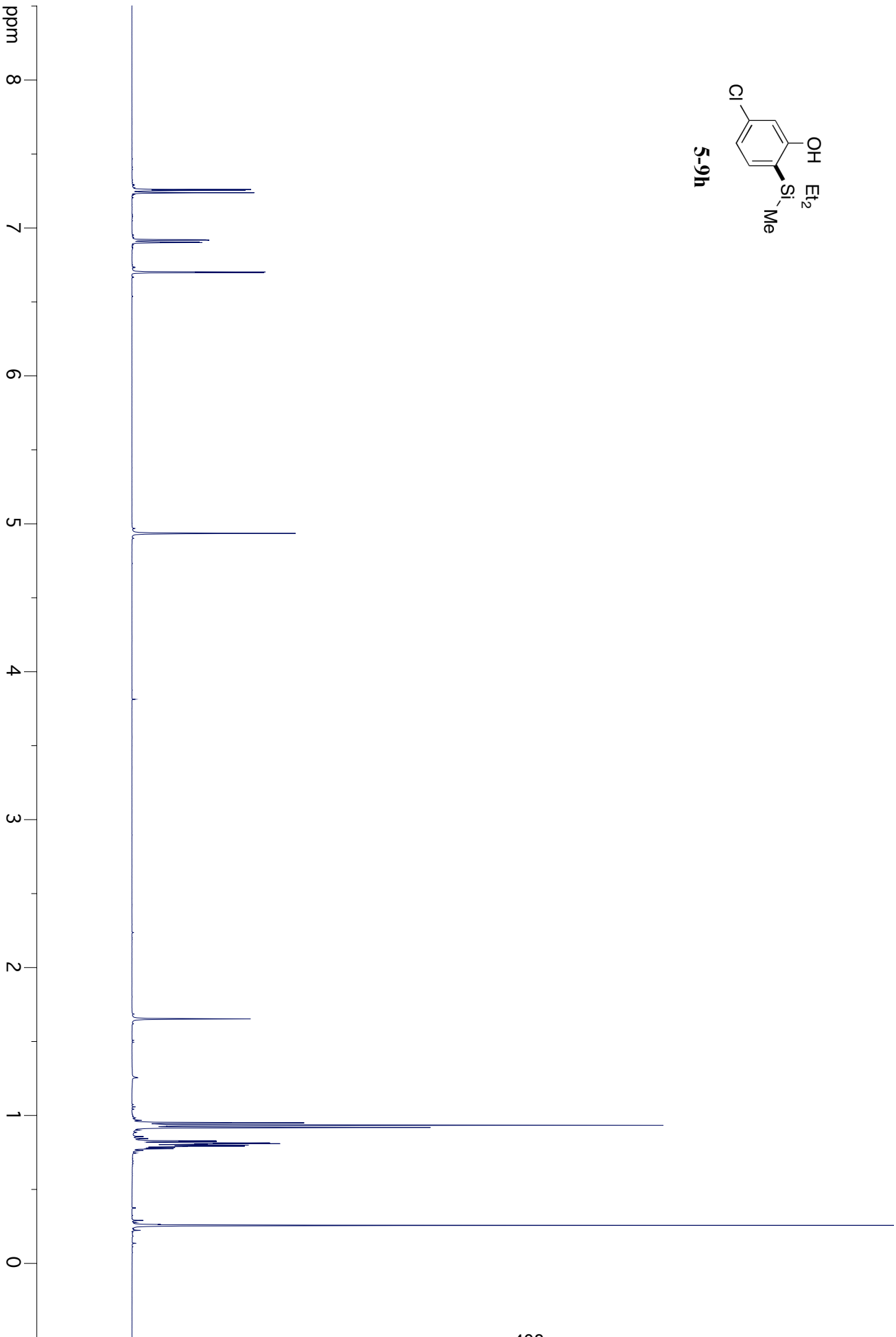
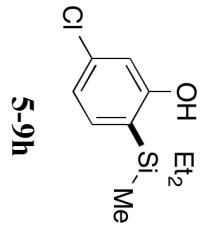


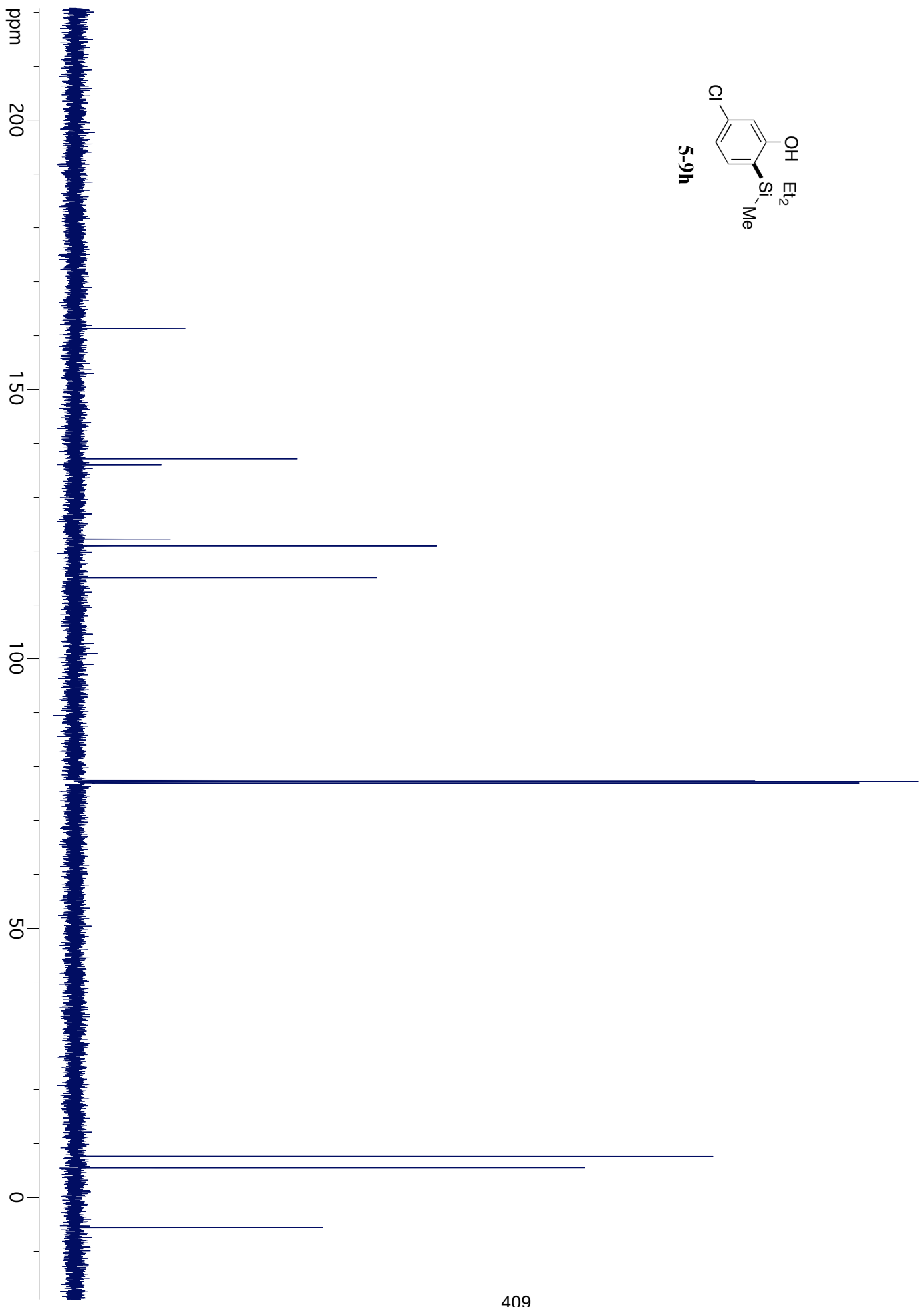
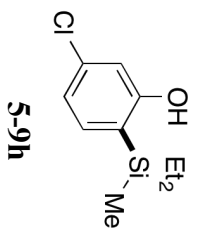


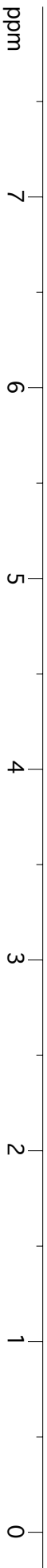
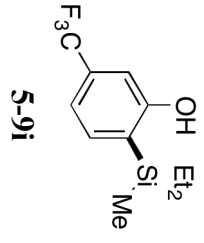


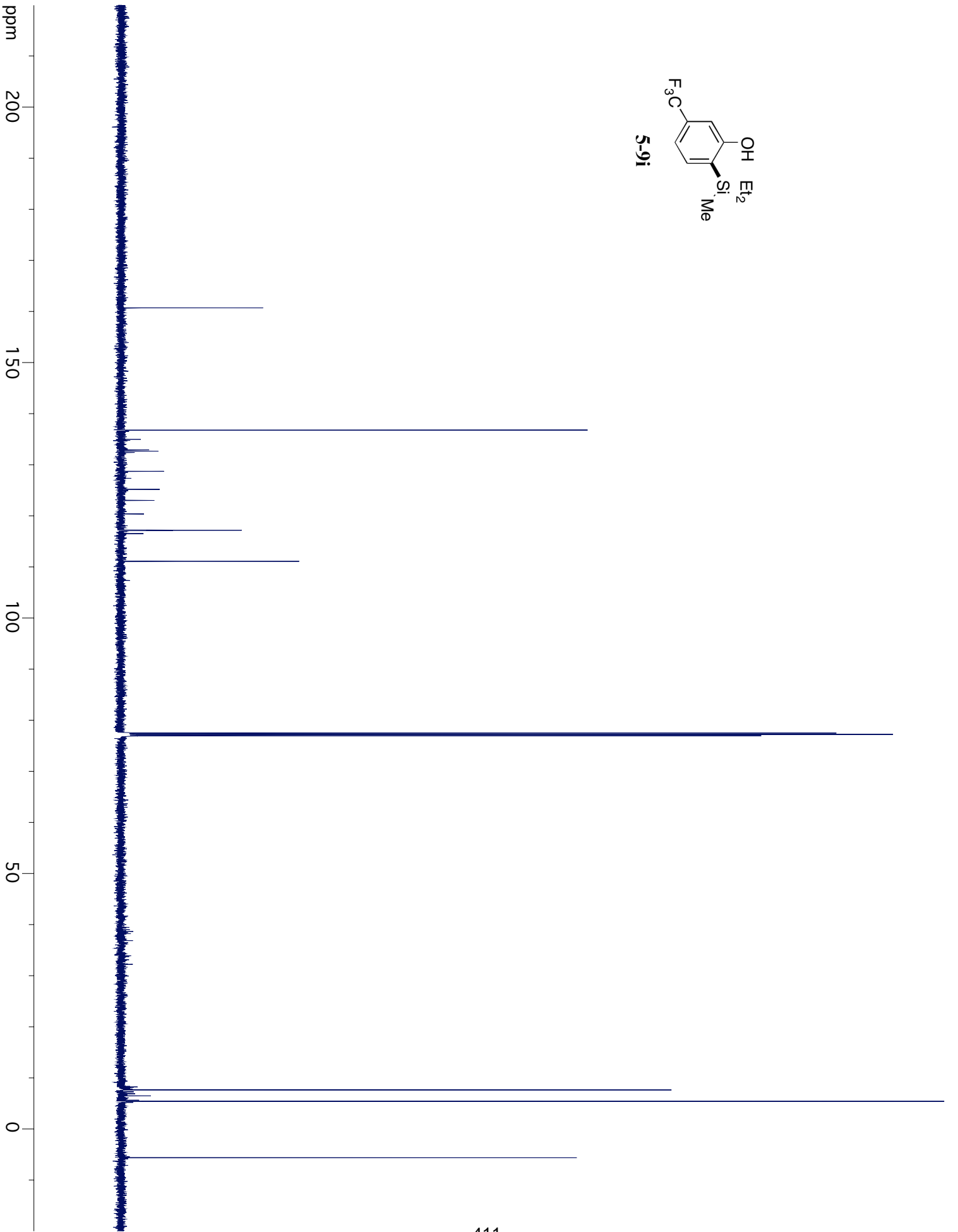
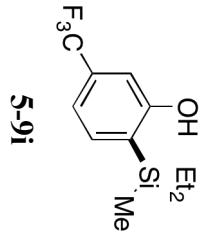
ppm

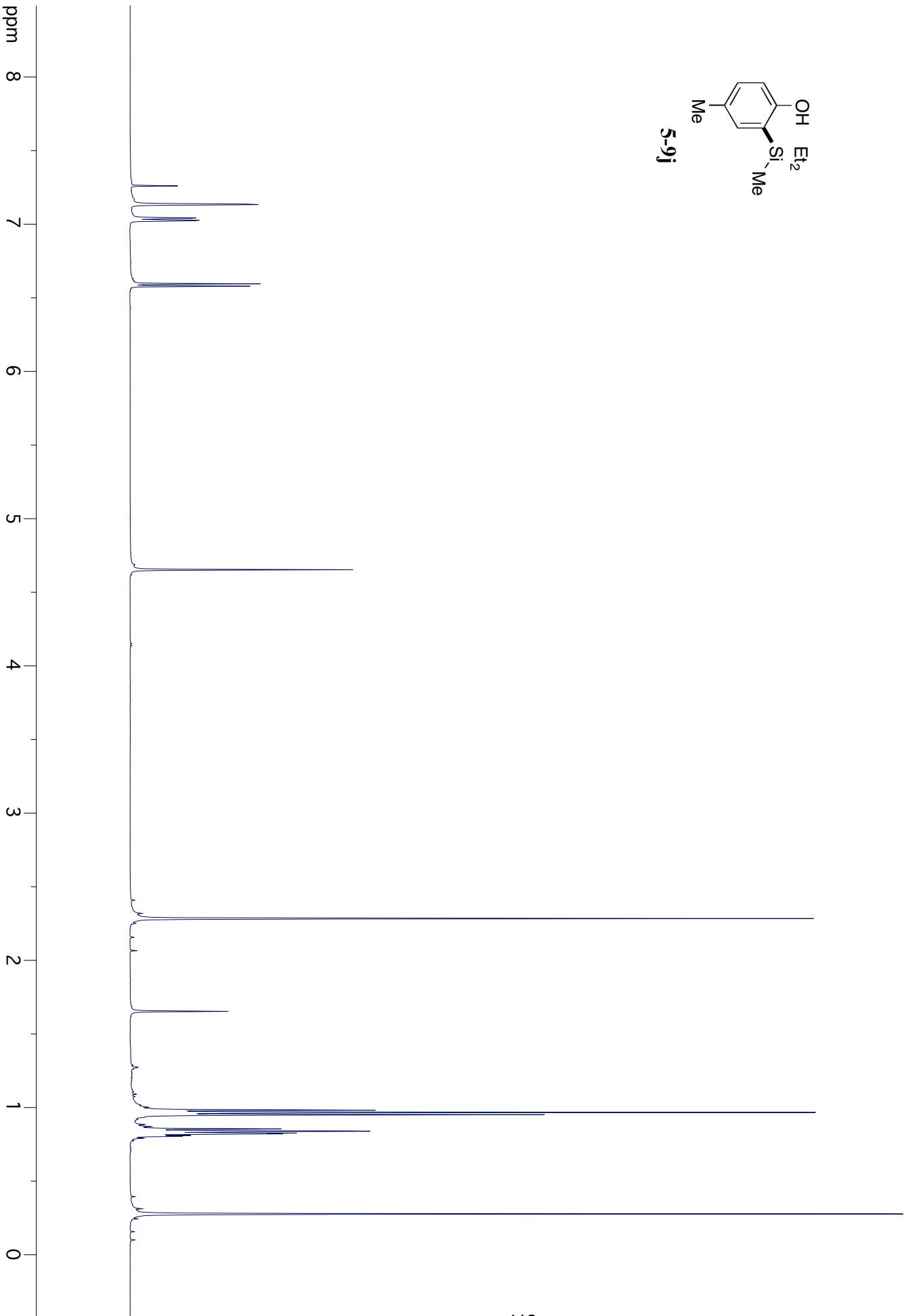
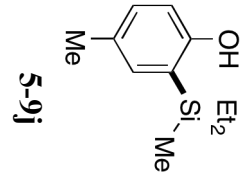


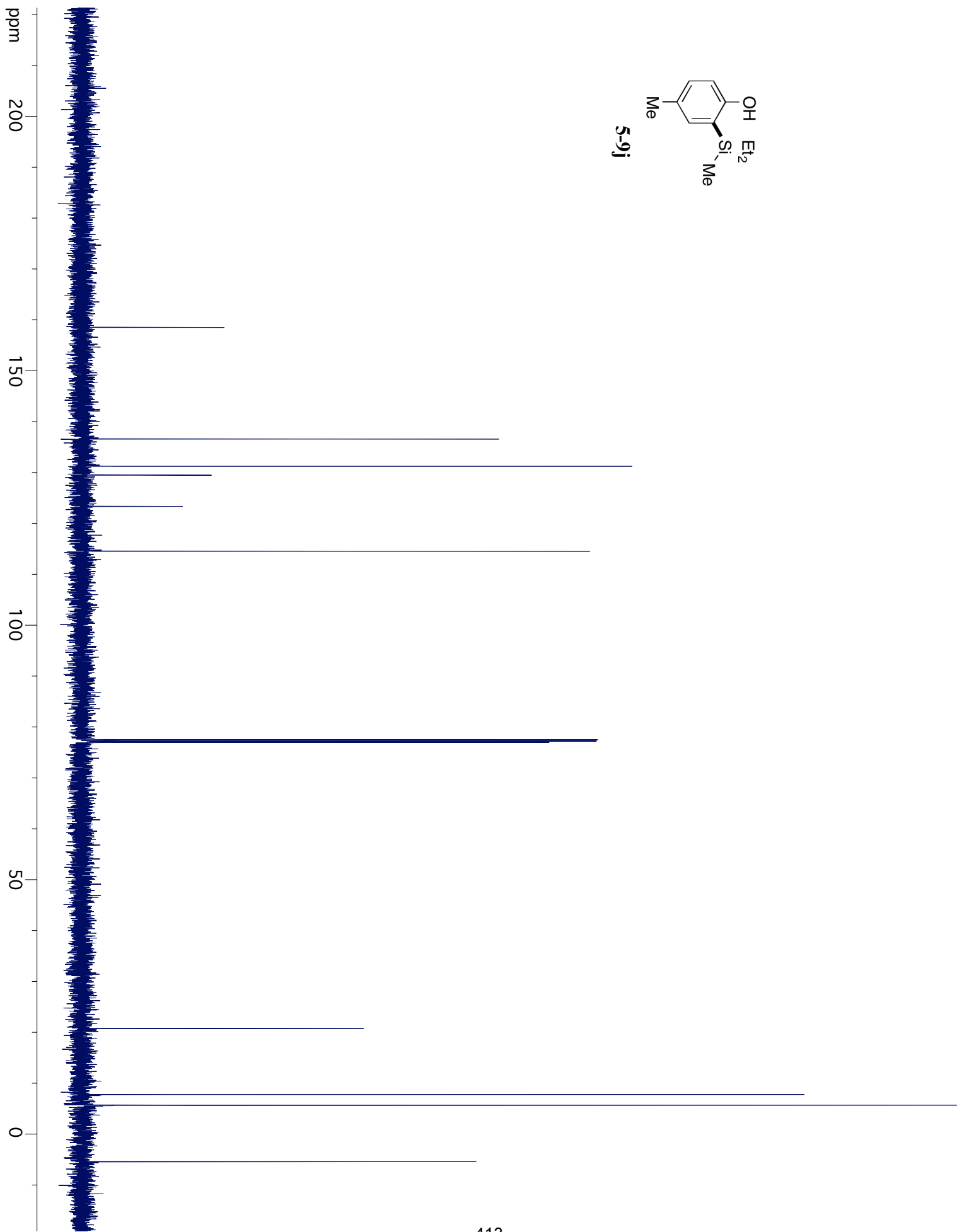
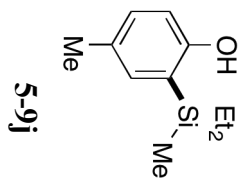


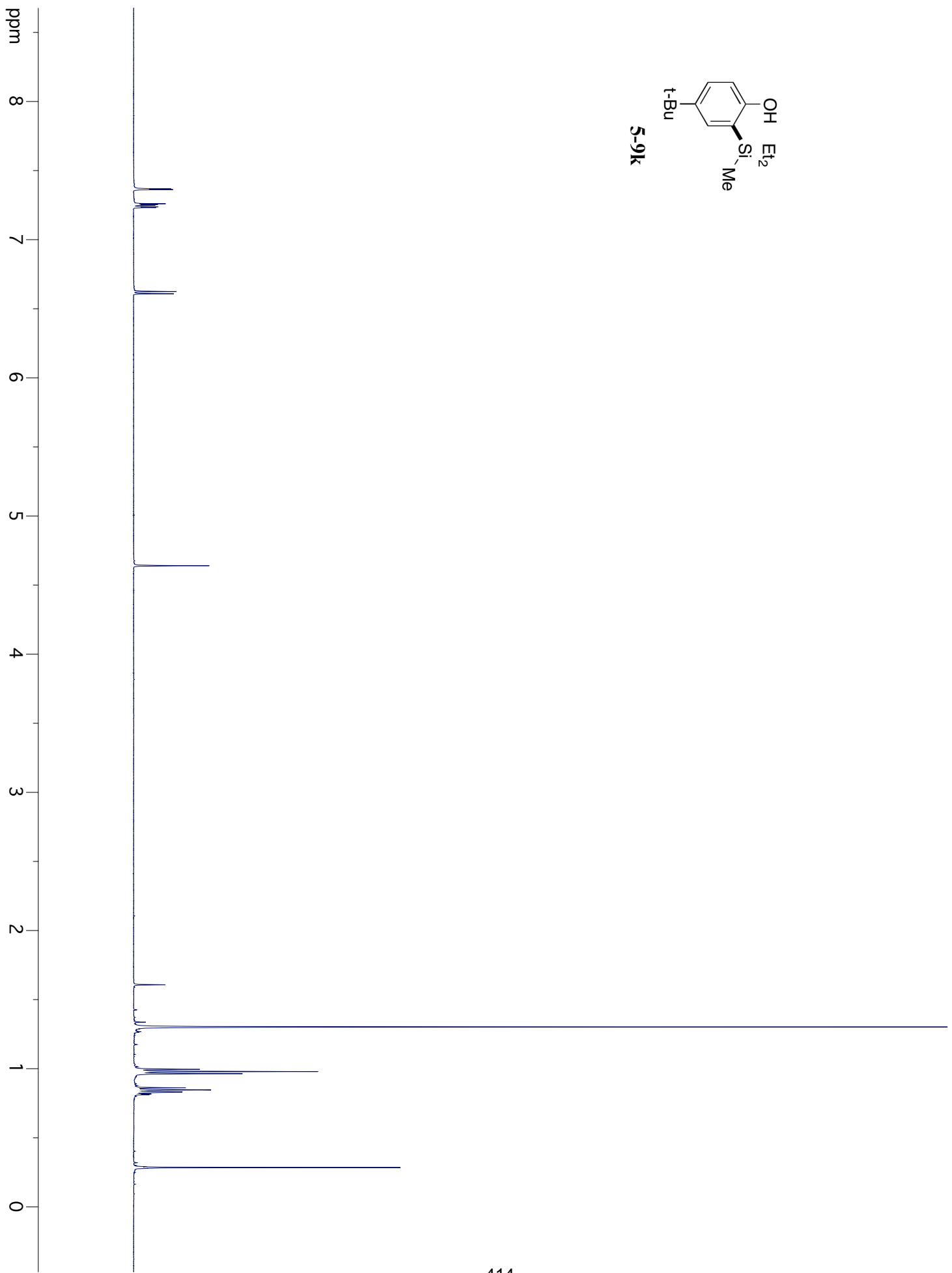
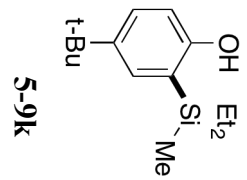


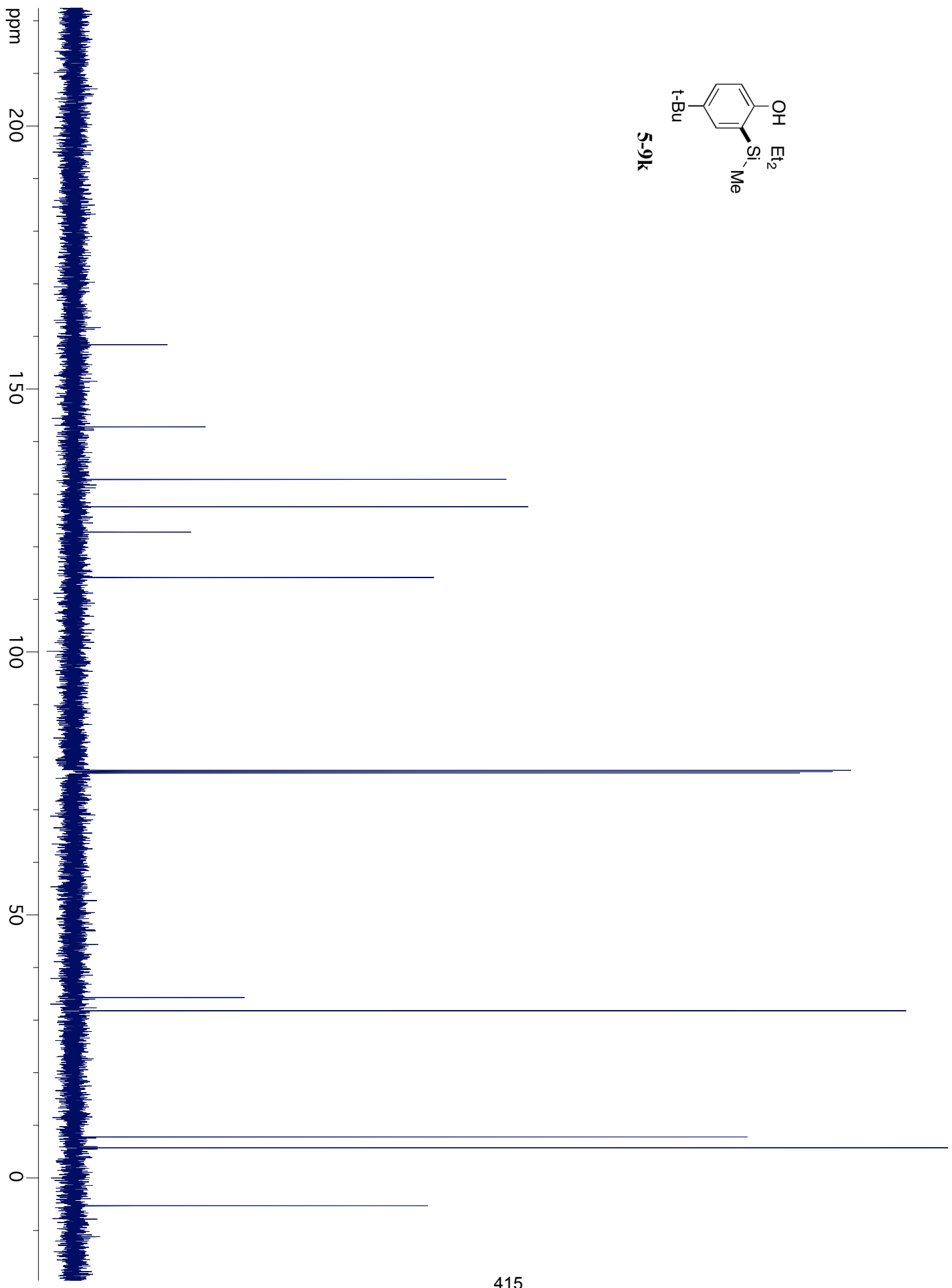
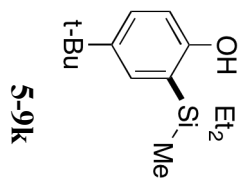


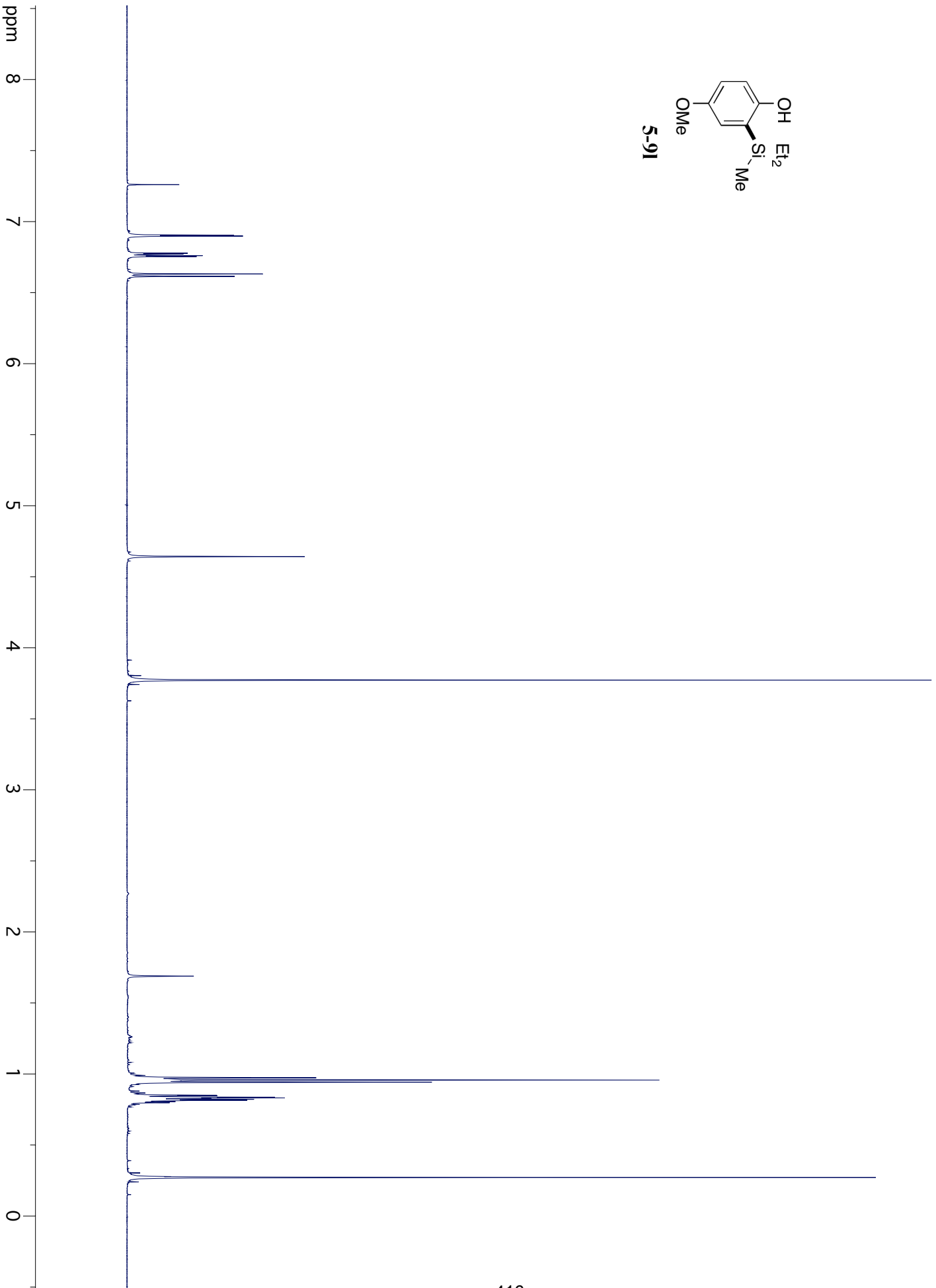
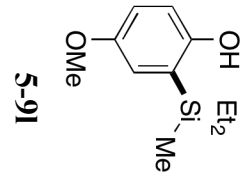


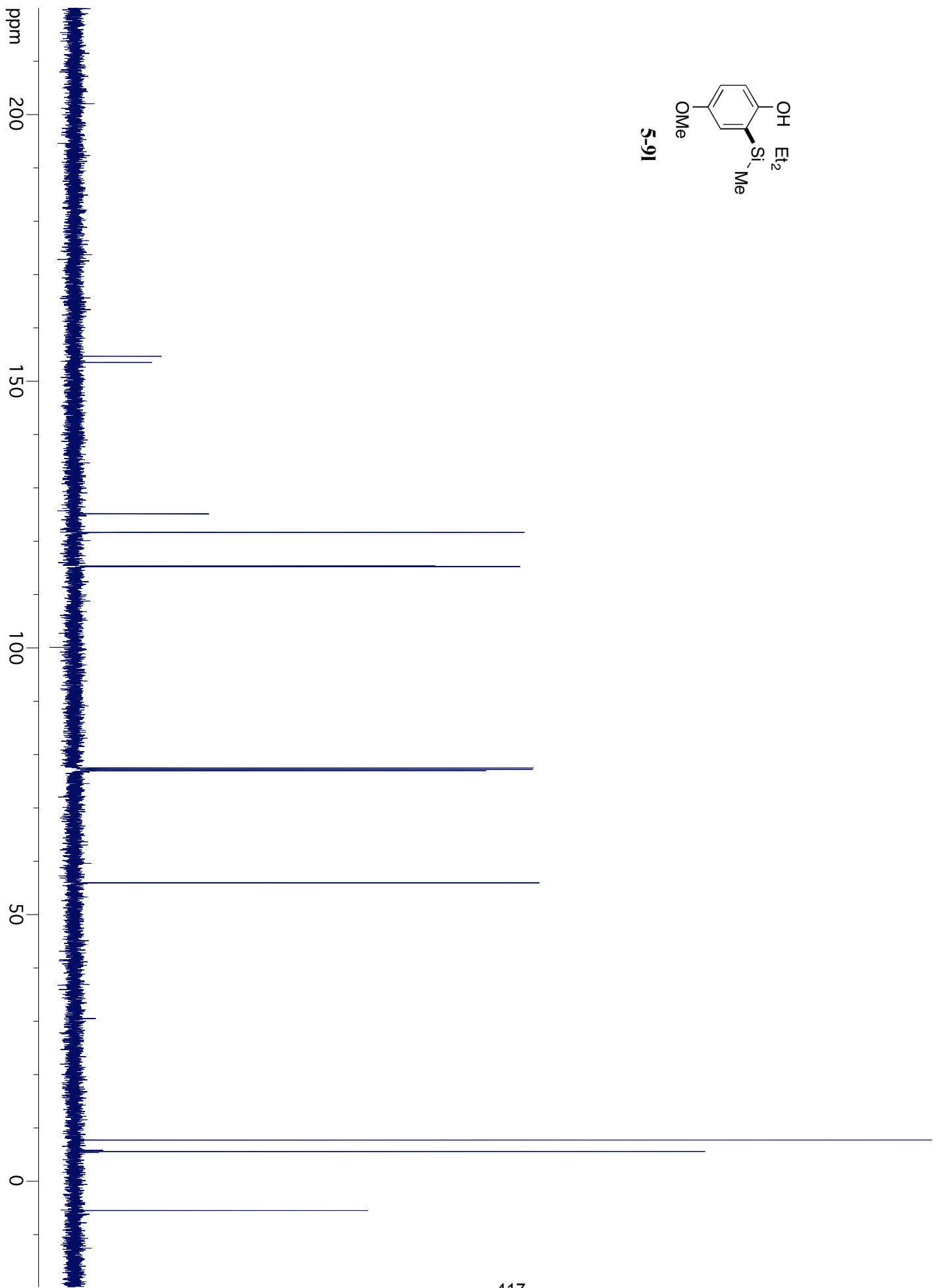
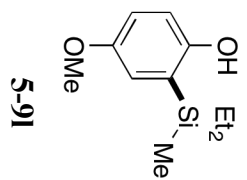


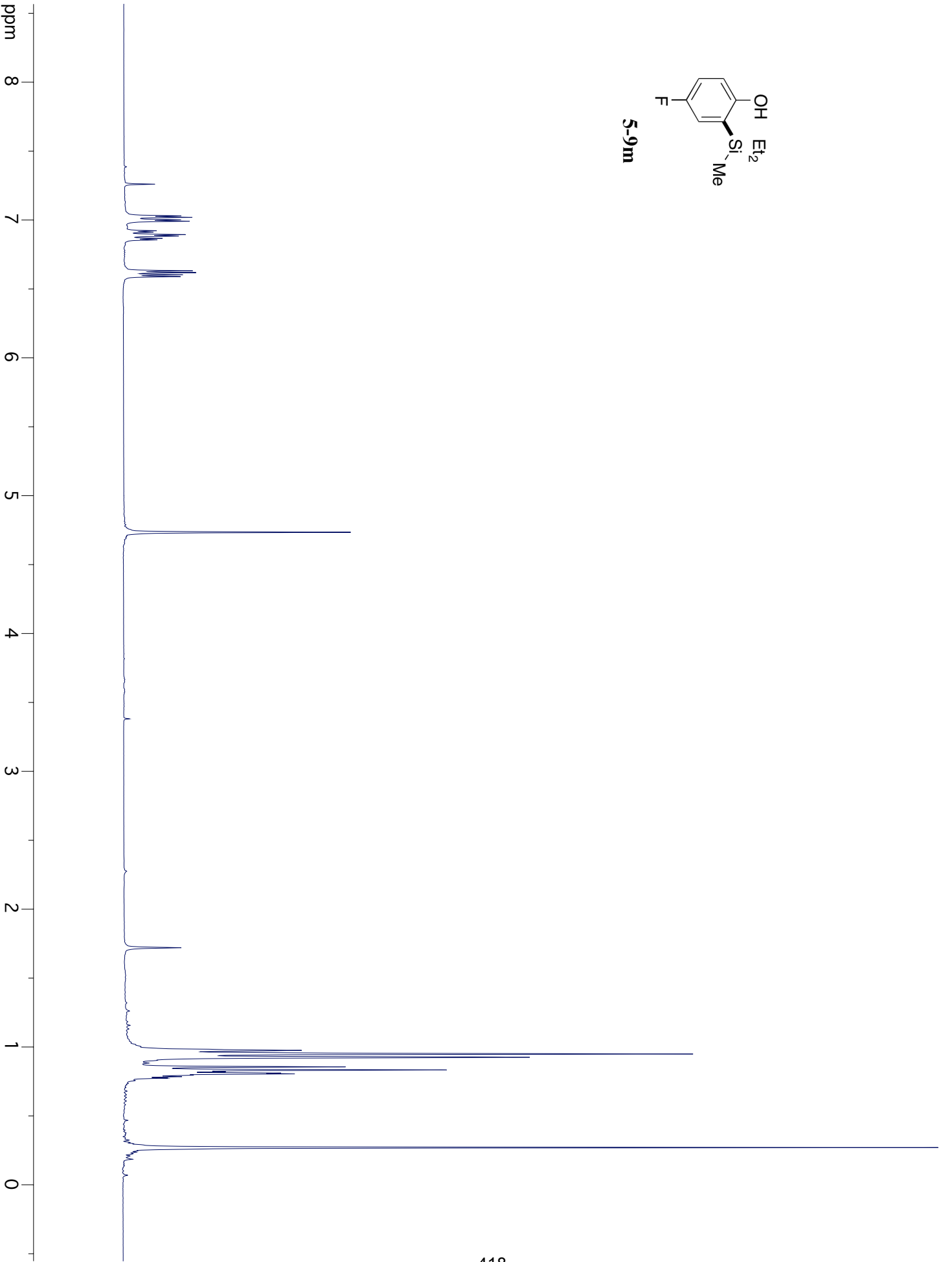
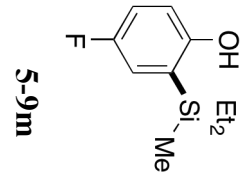


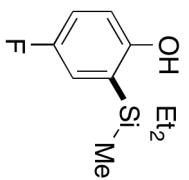




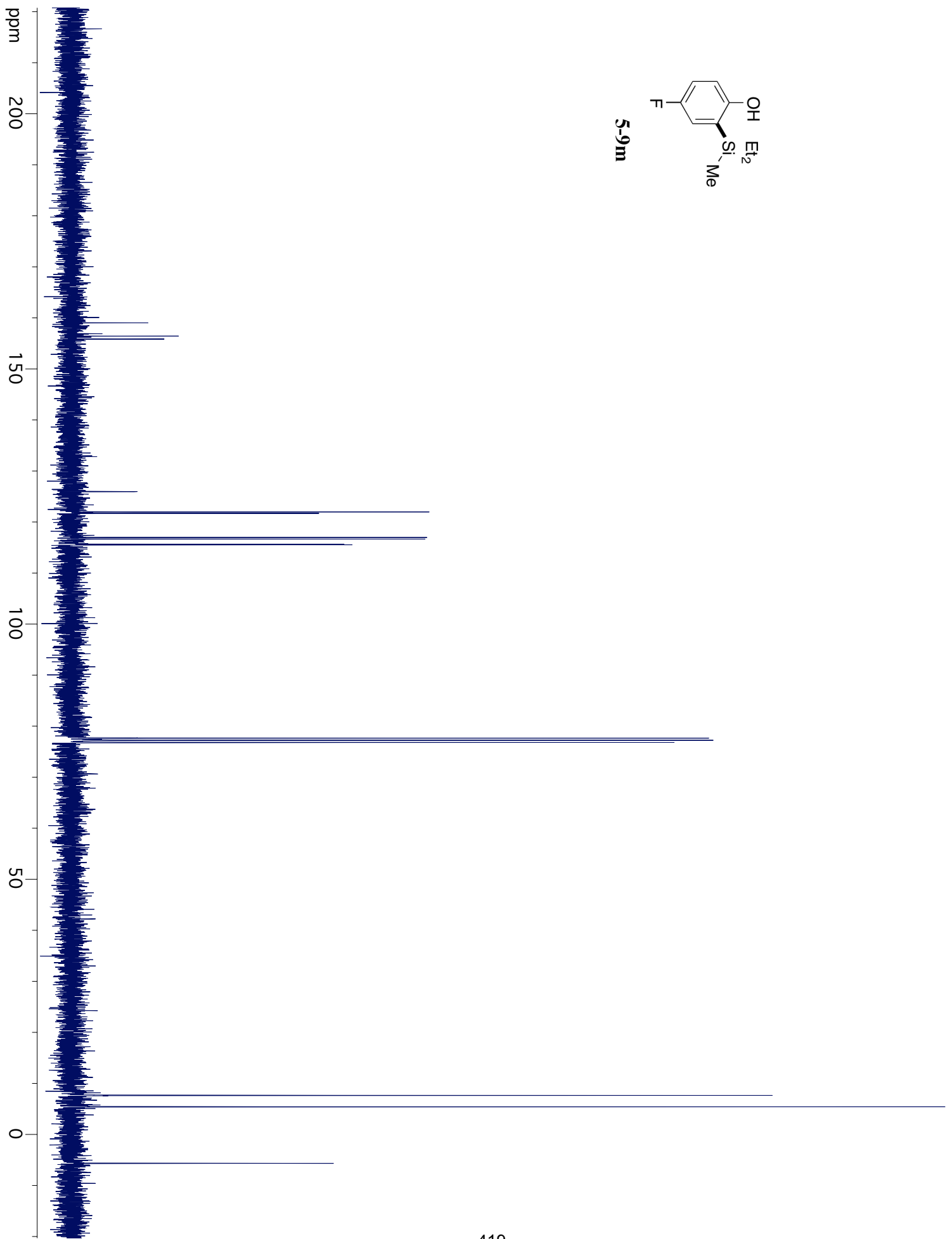


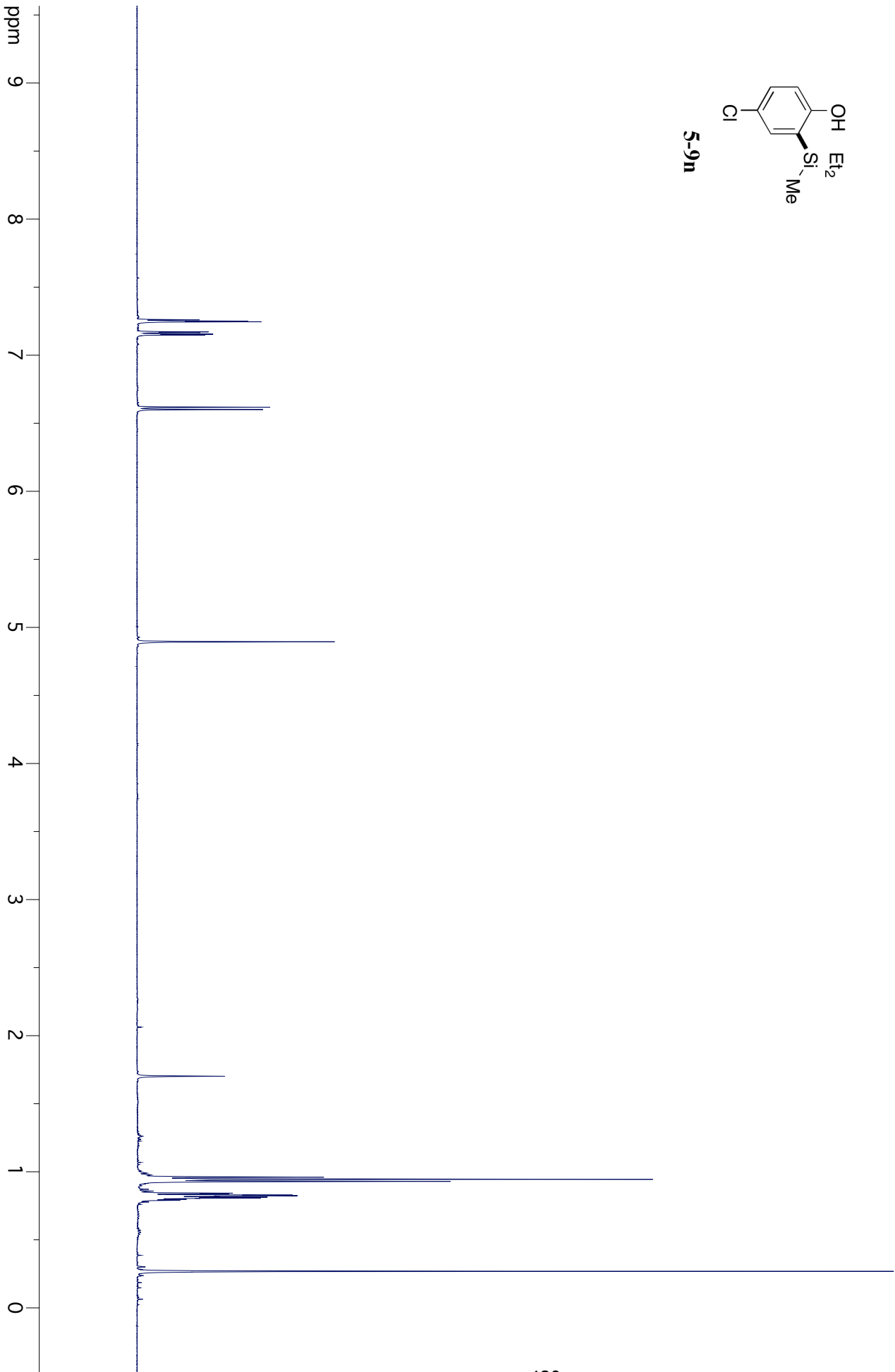
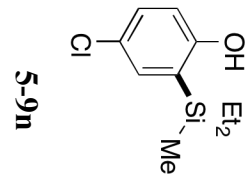


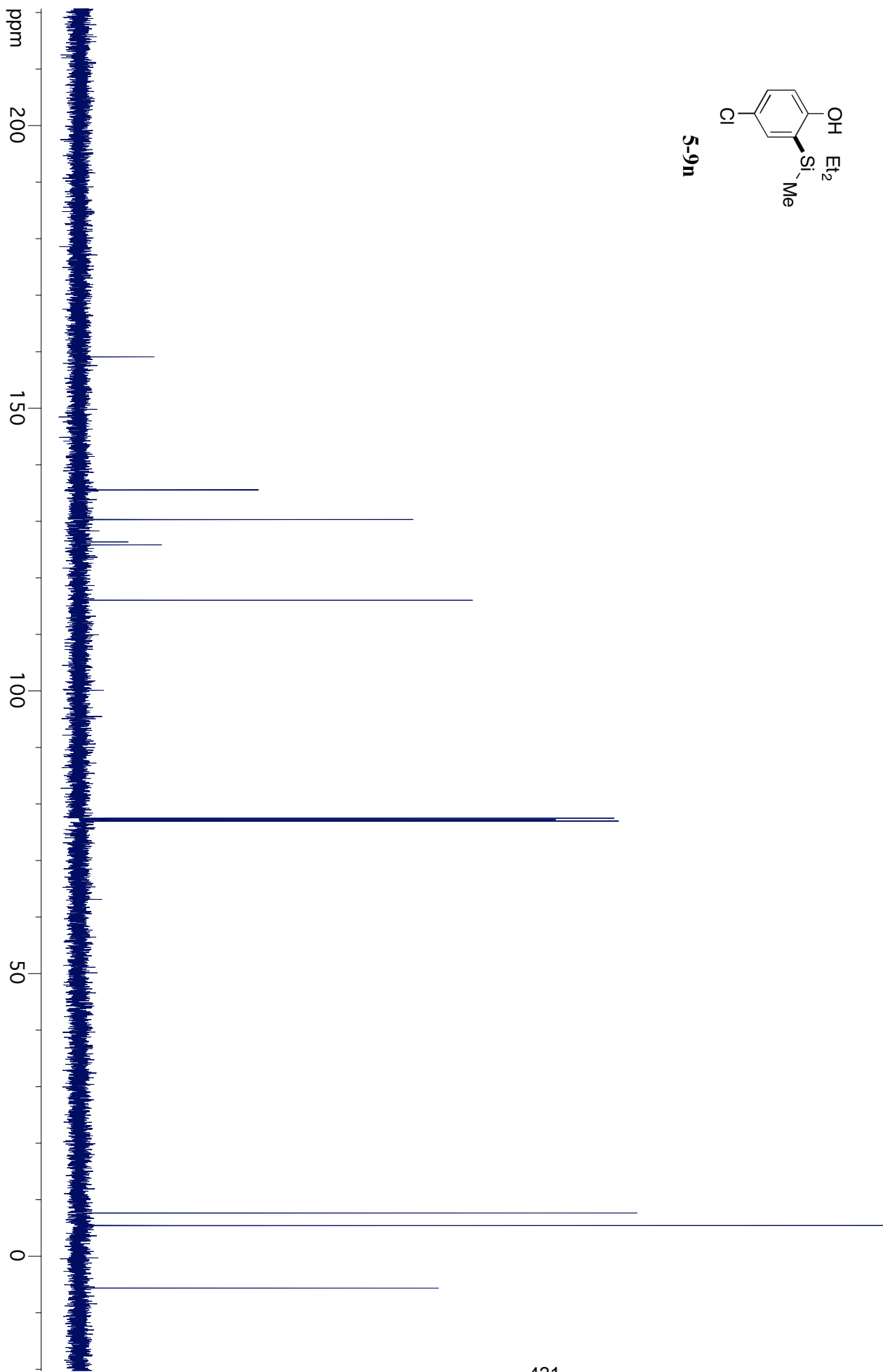
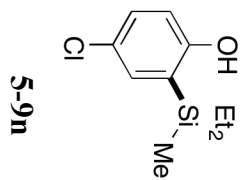


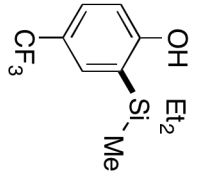


5-9m

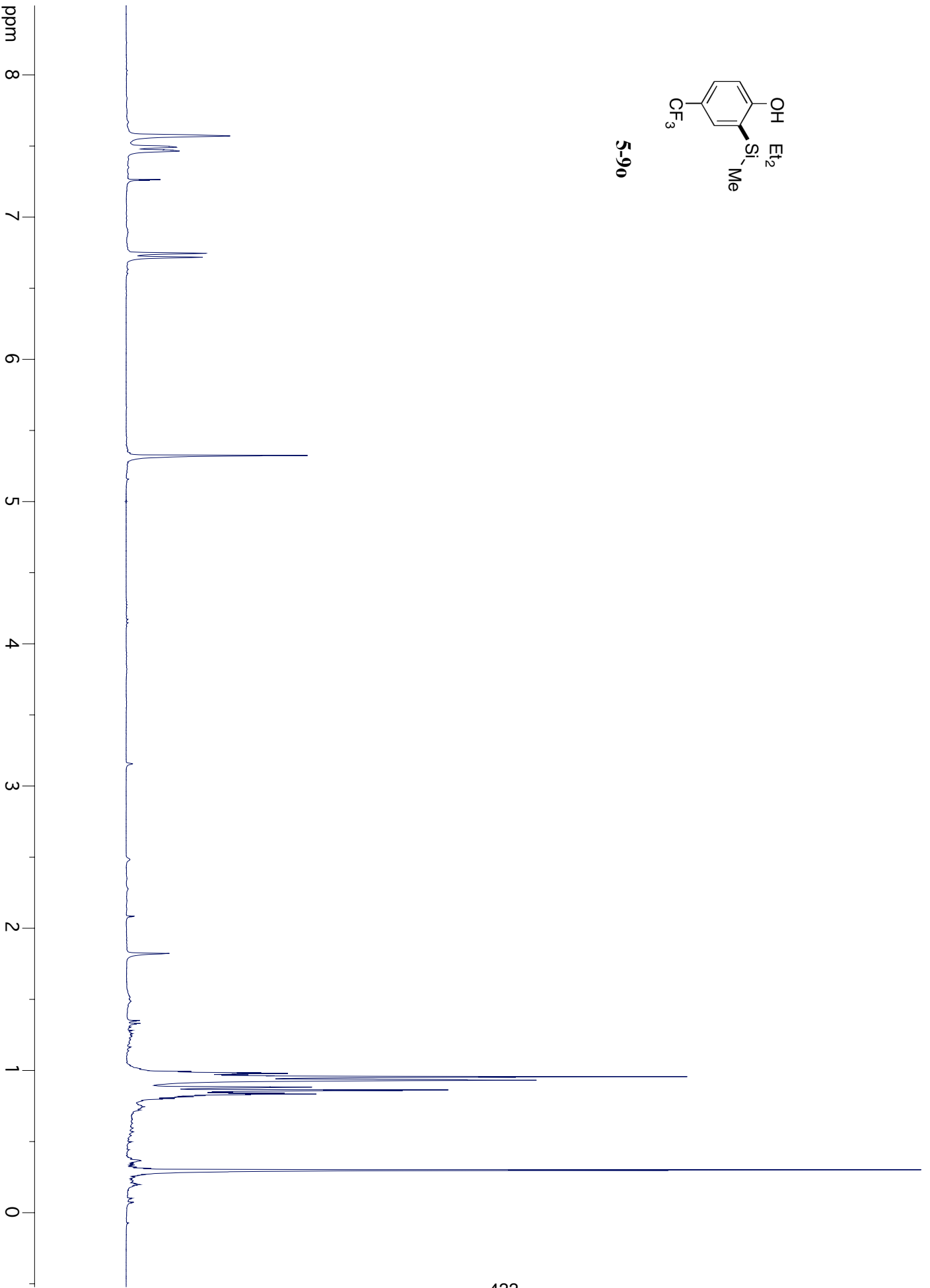


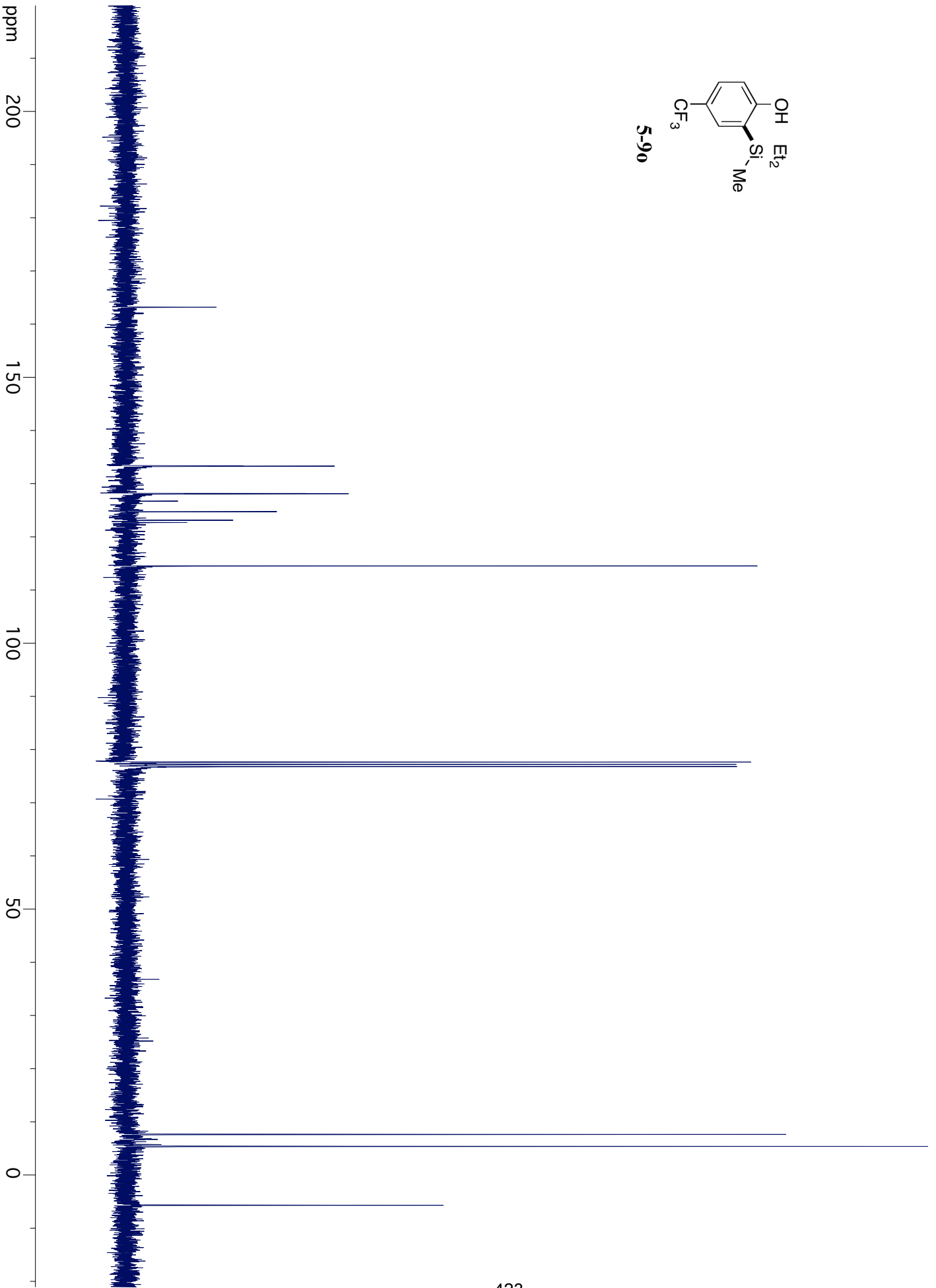
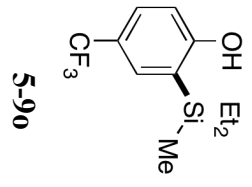


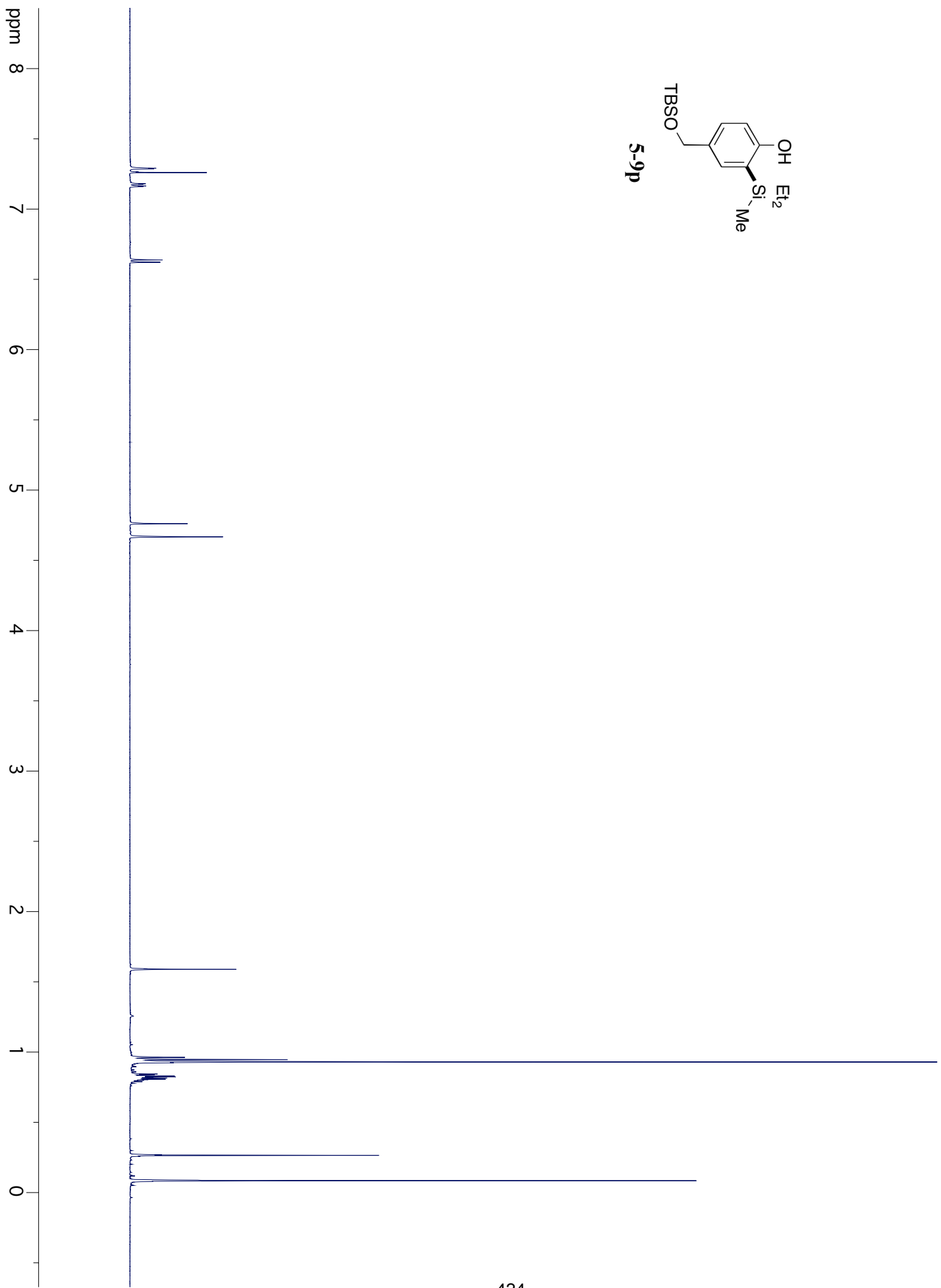
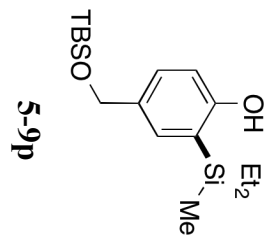


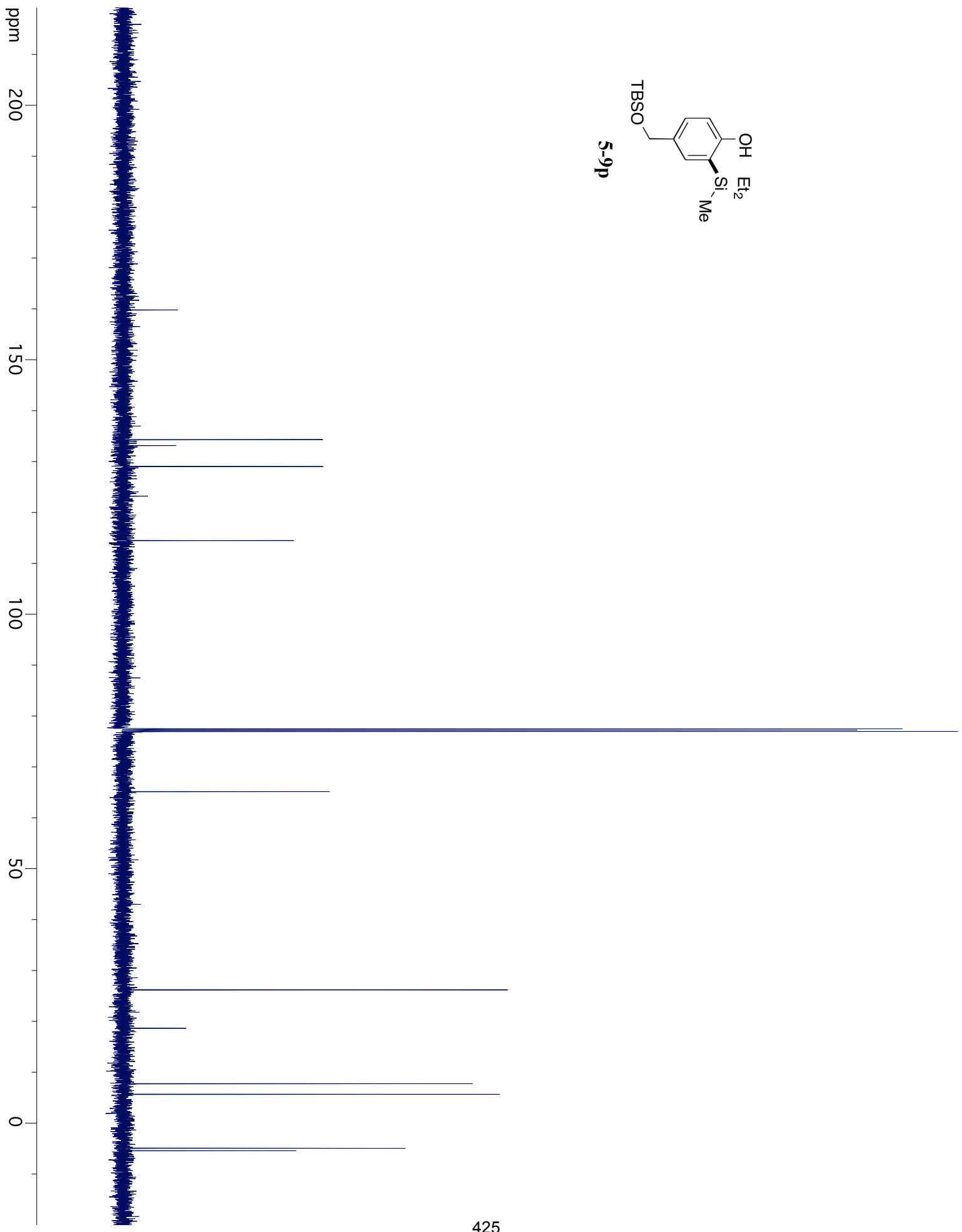
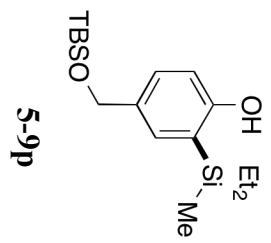


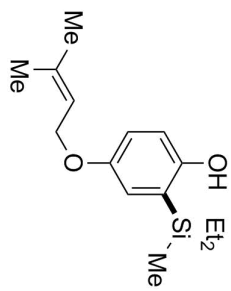
5-90



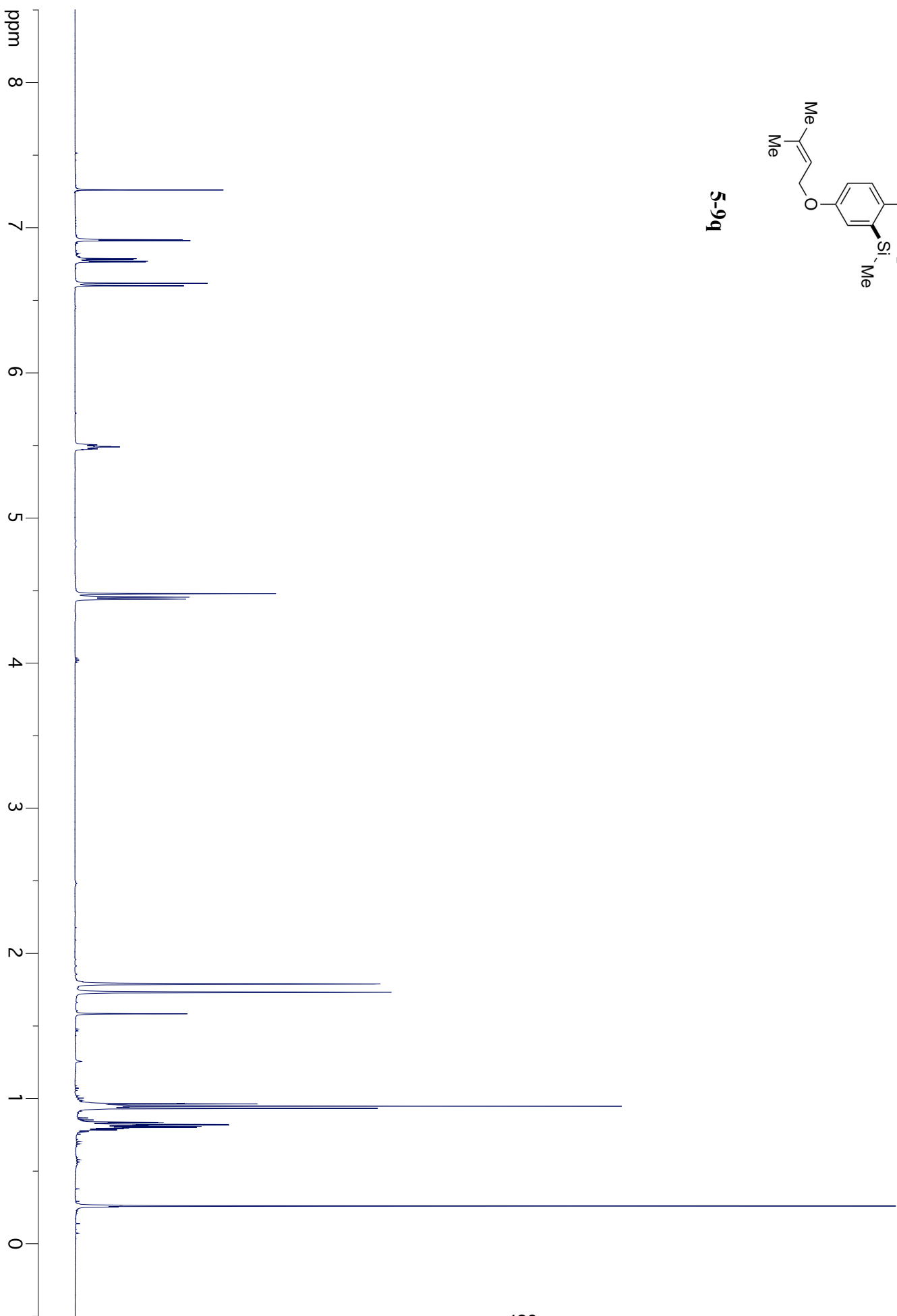


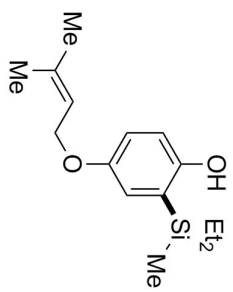




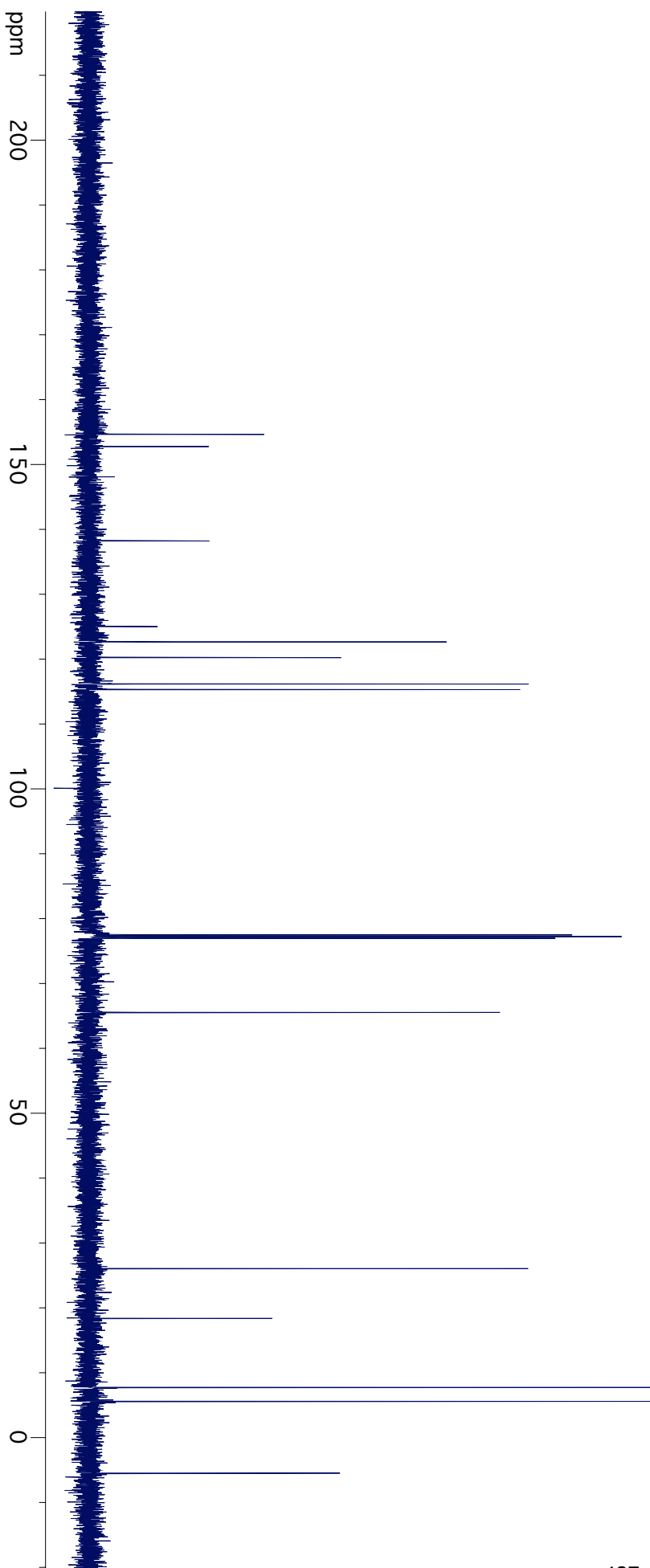


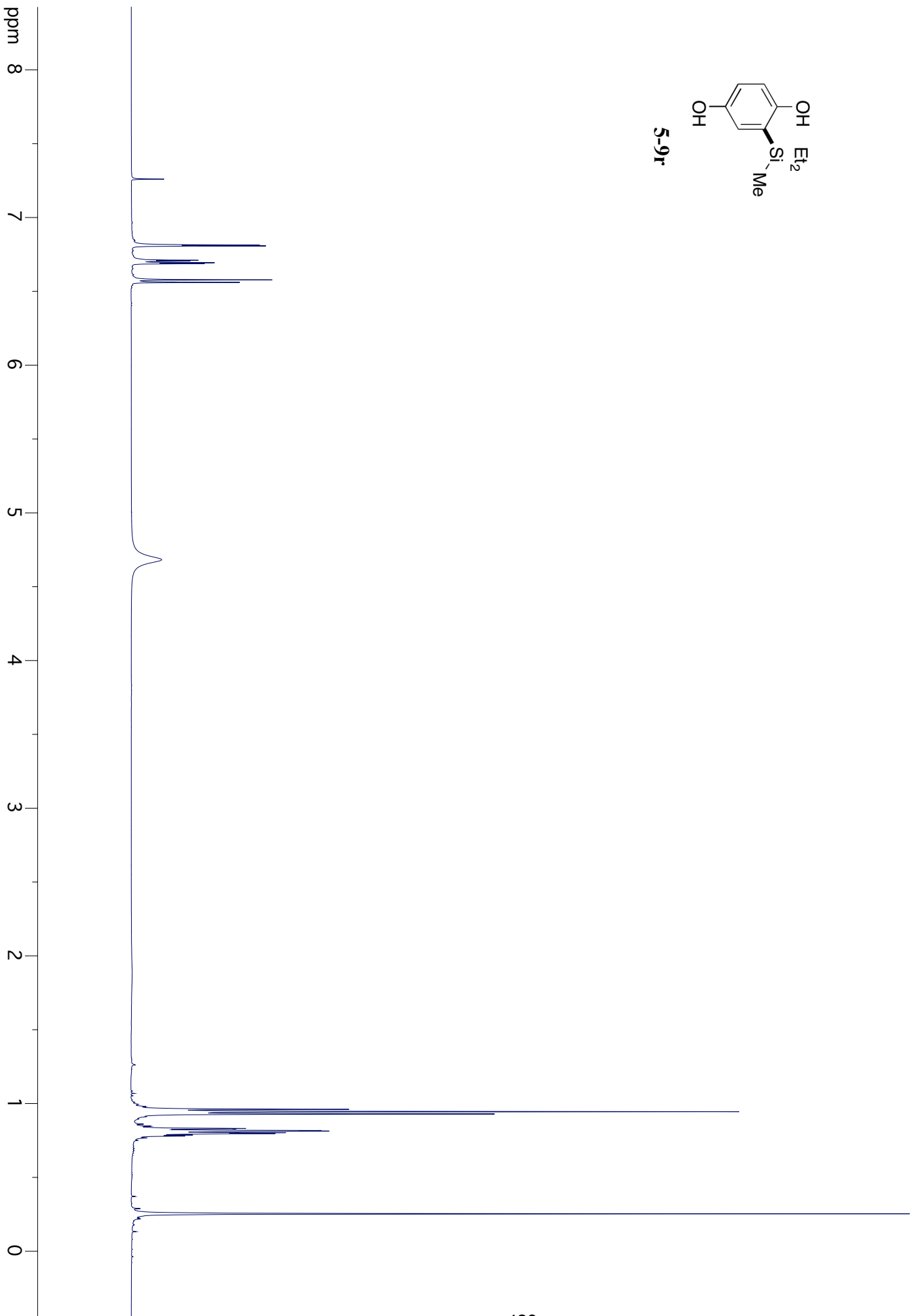
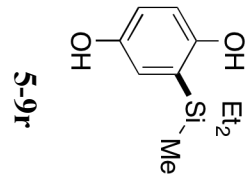
5-9q

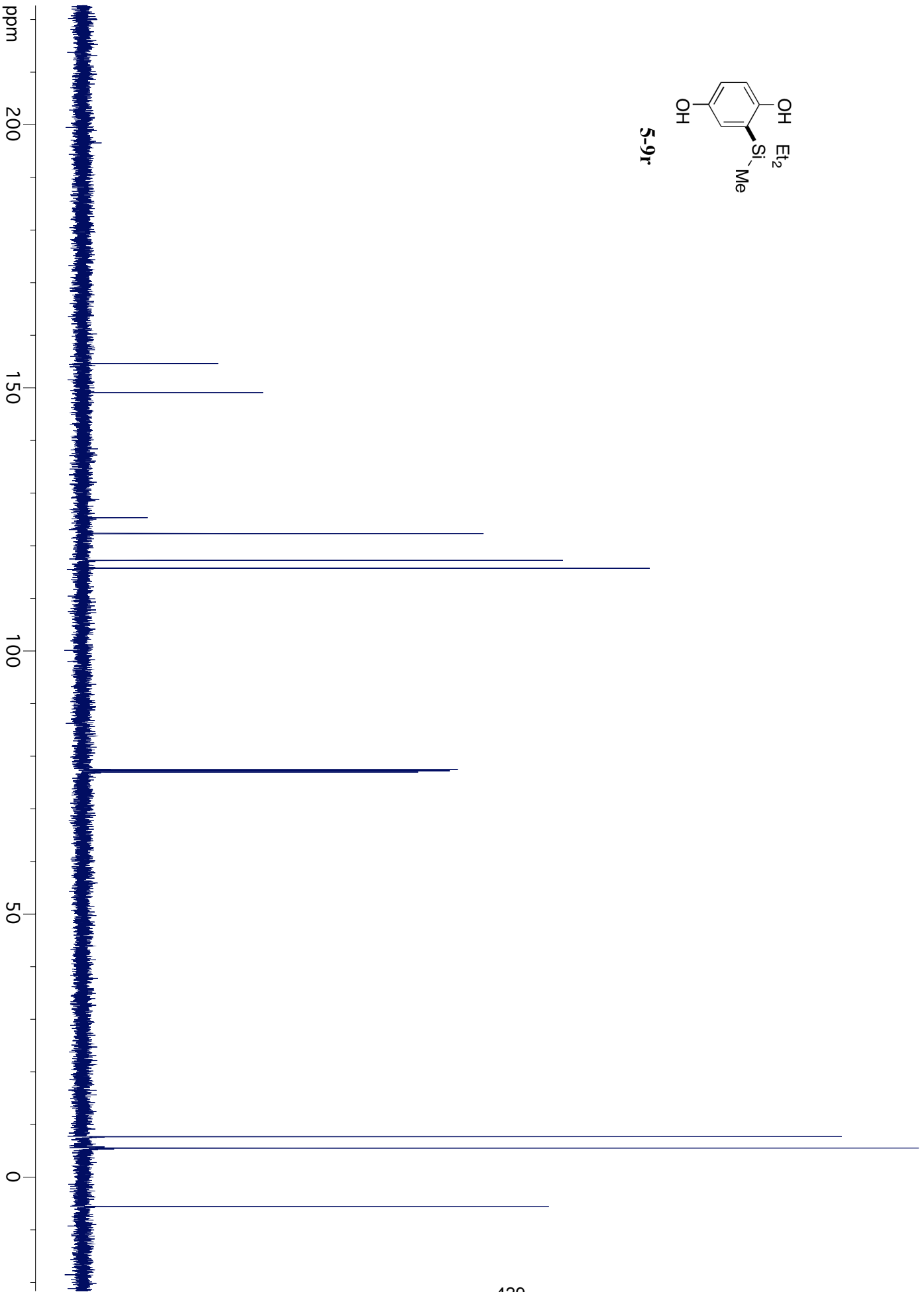
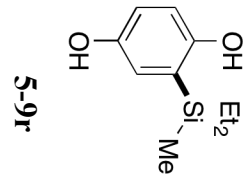


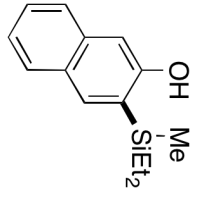


5-9q

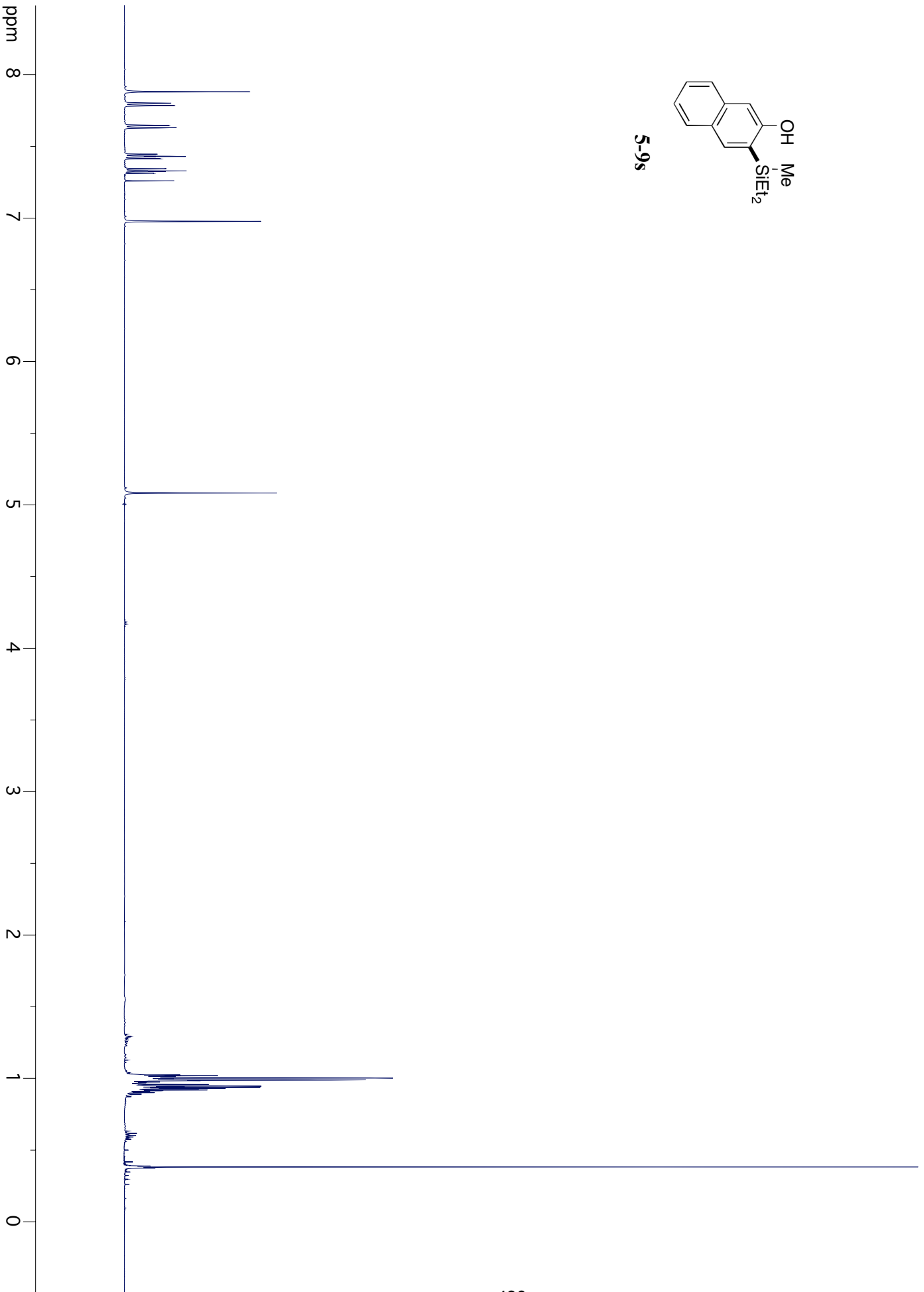


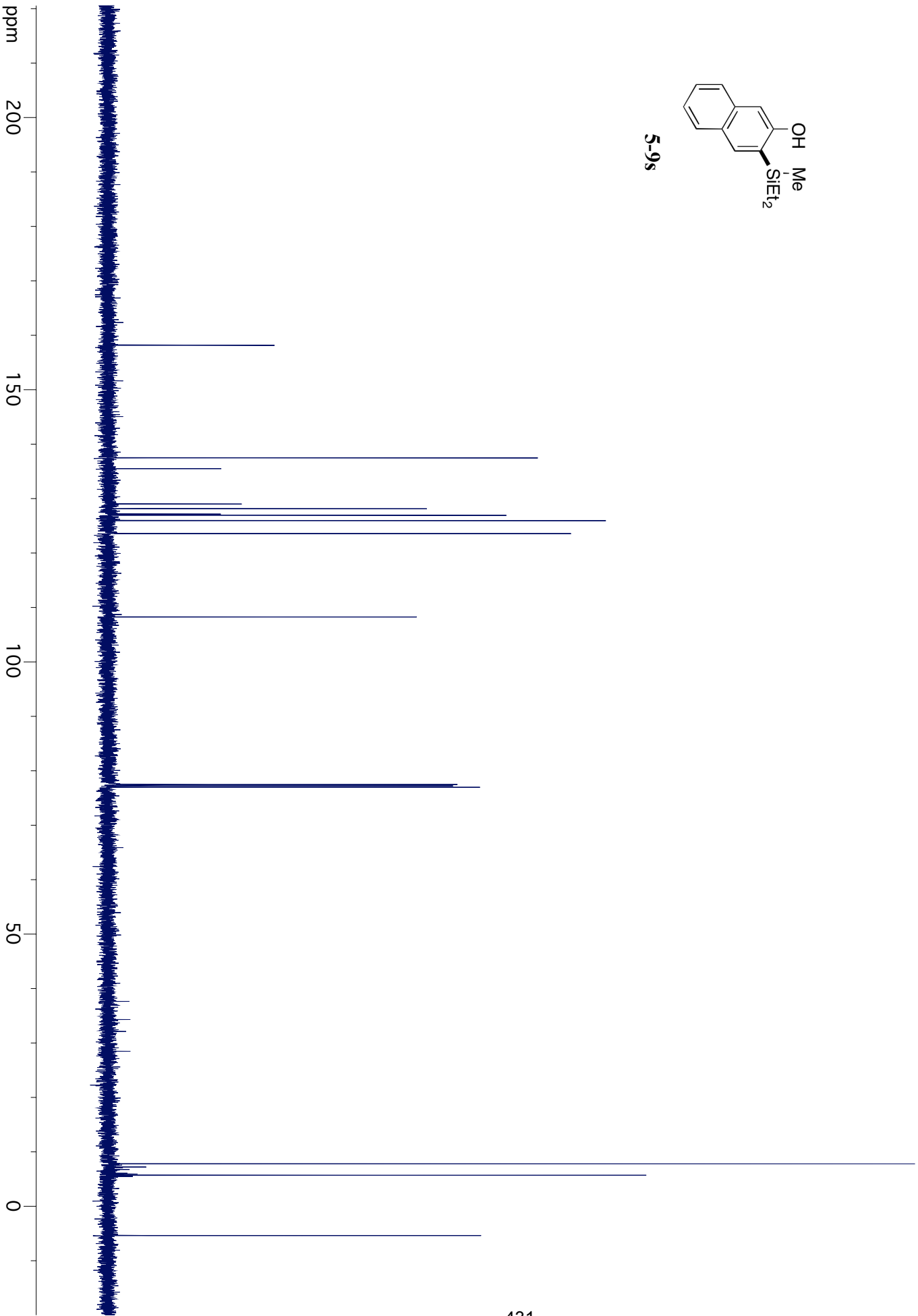
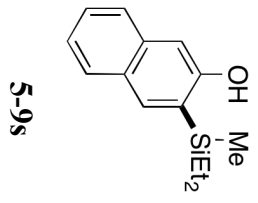


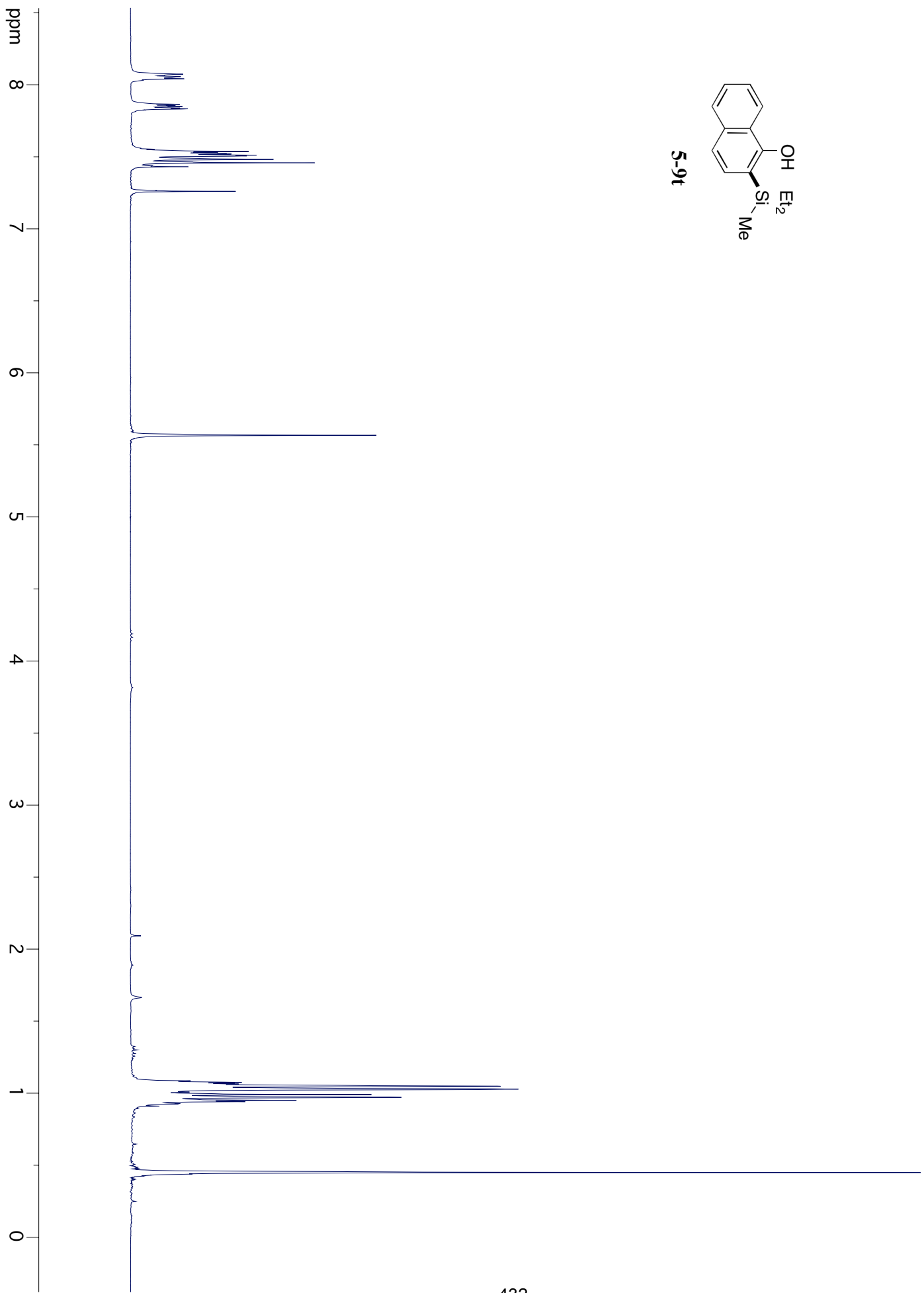
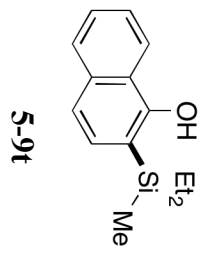


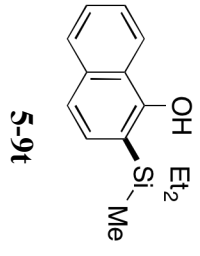


5-9s

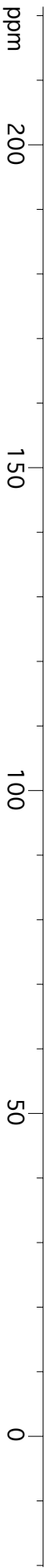


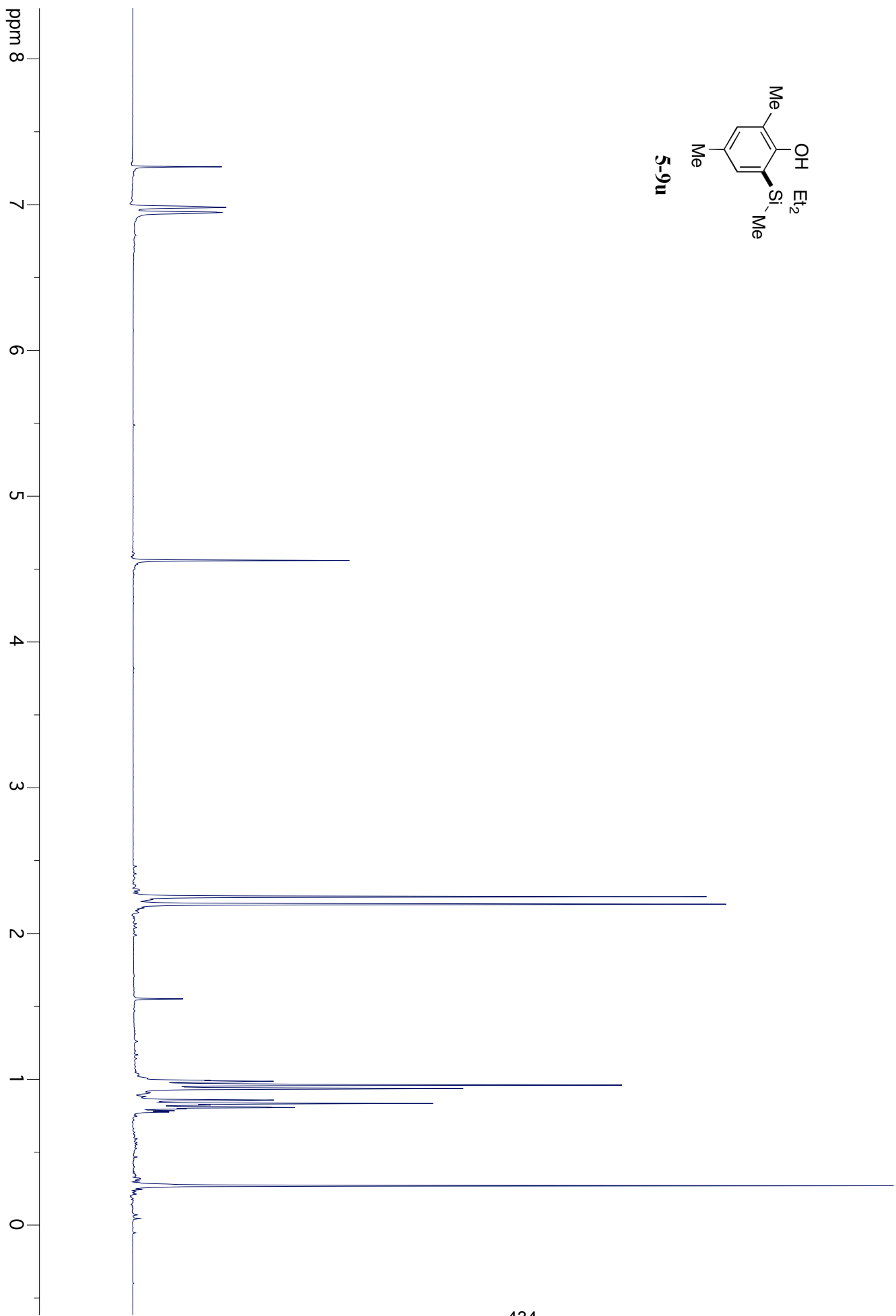
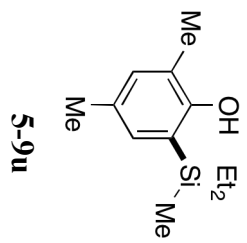


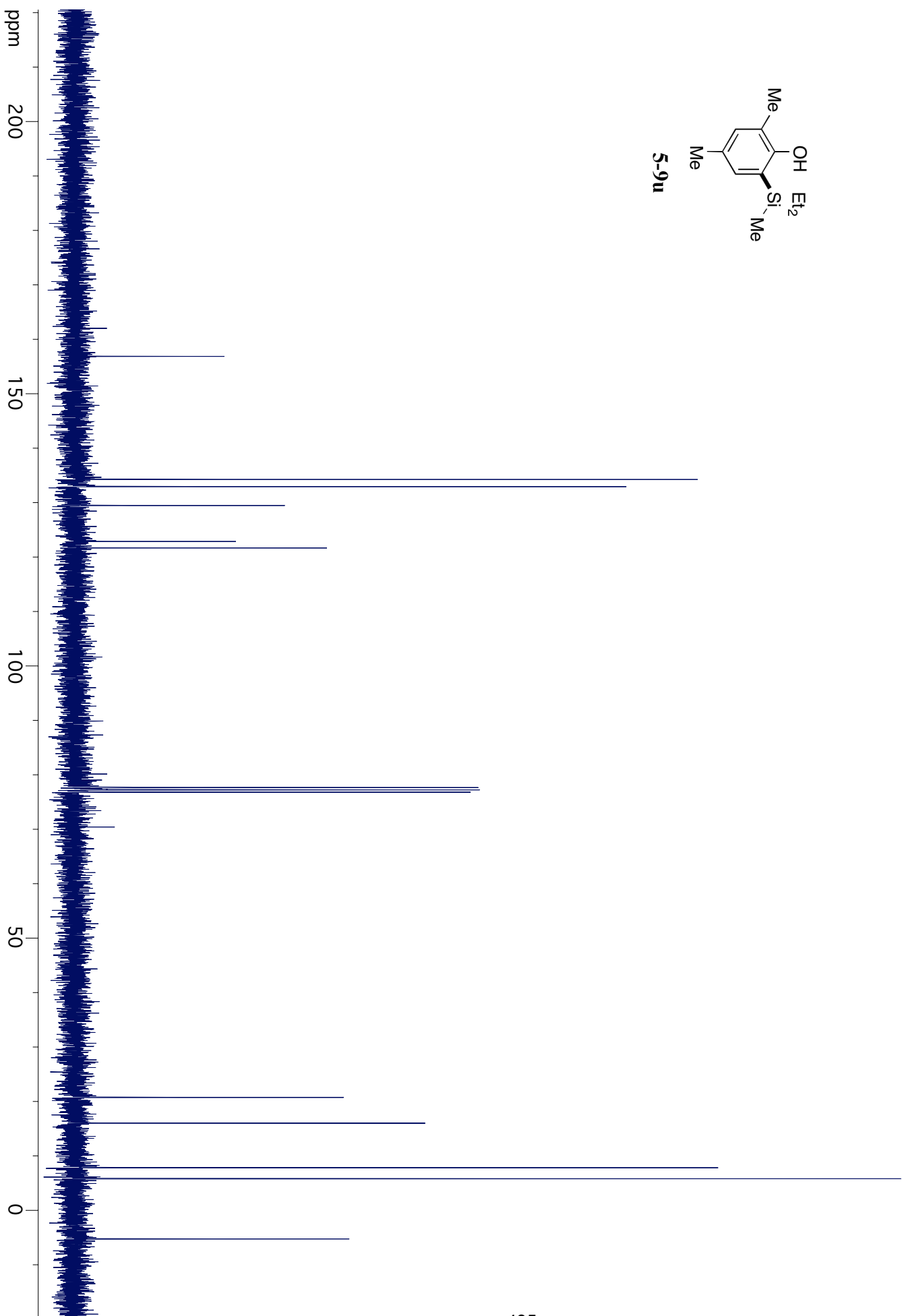
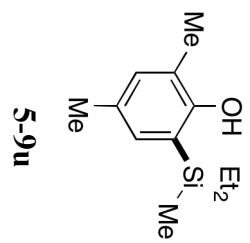


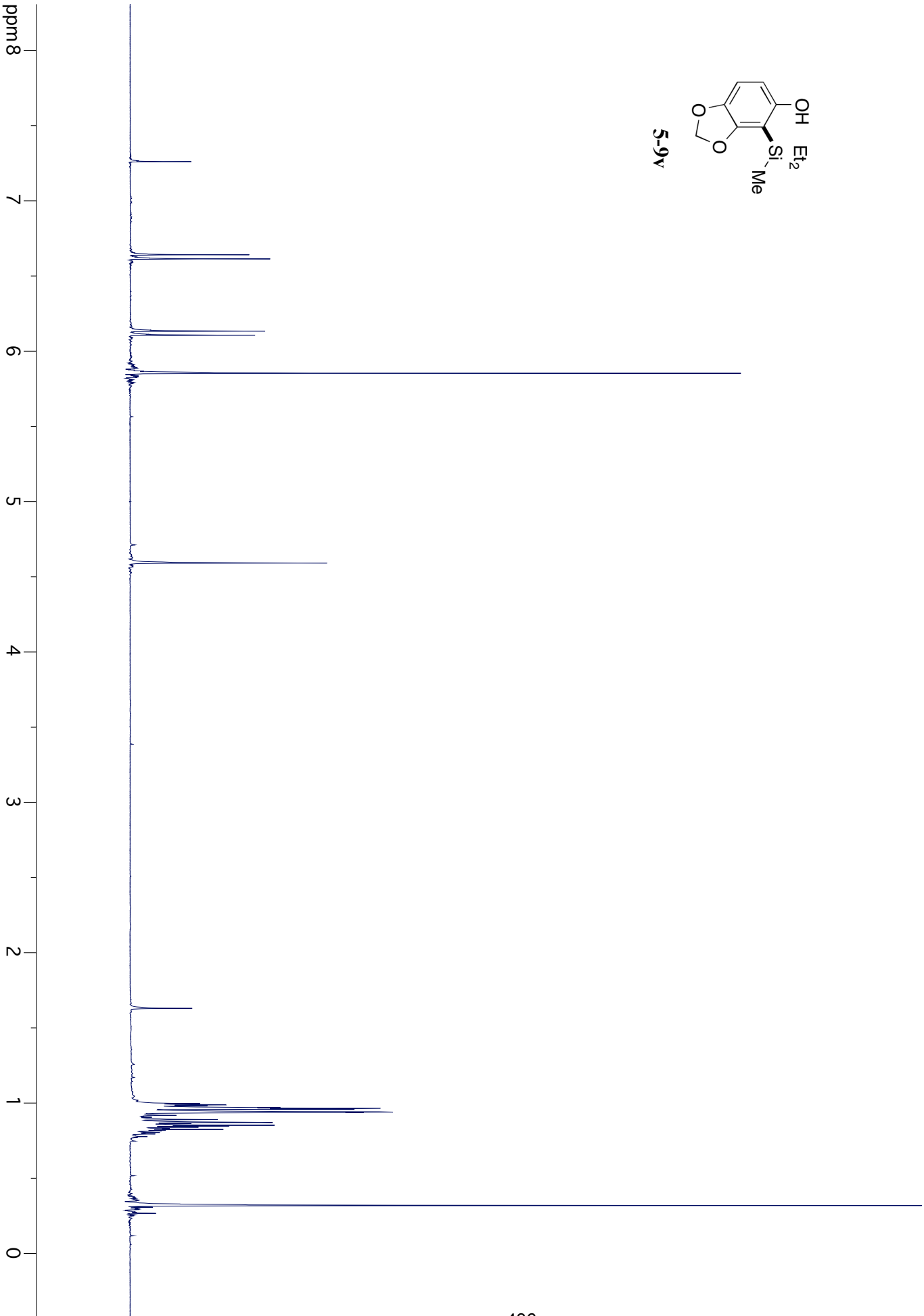
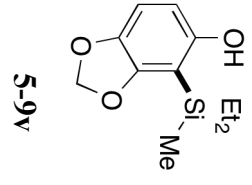


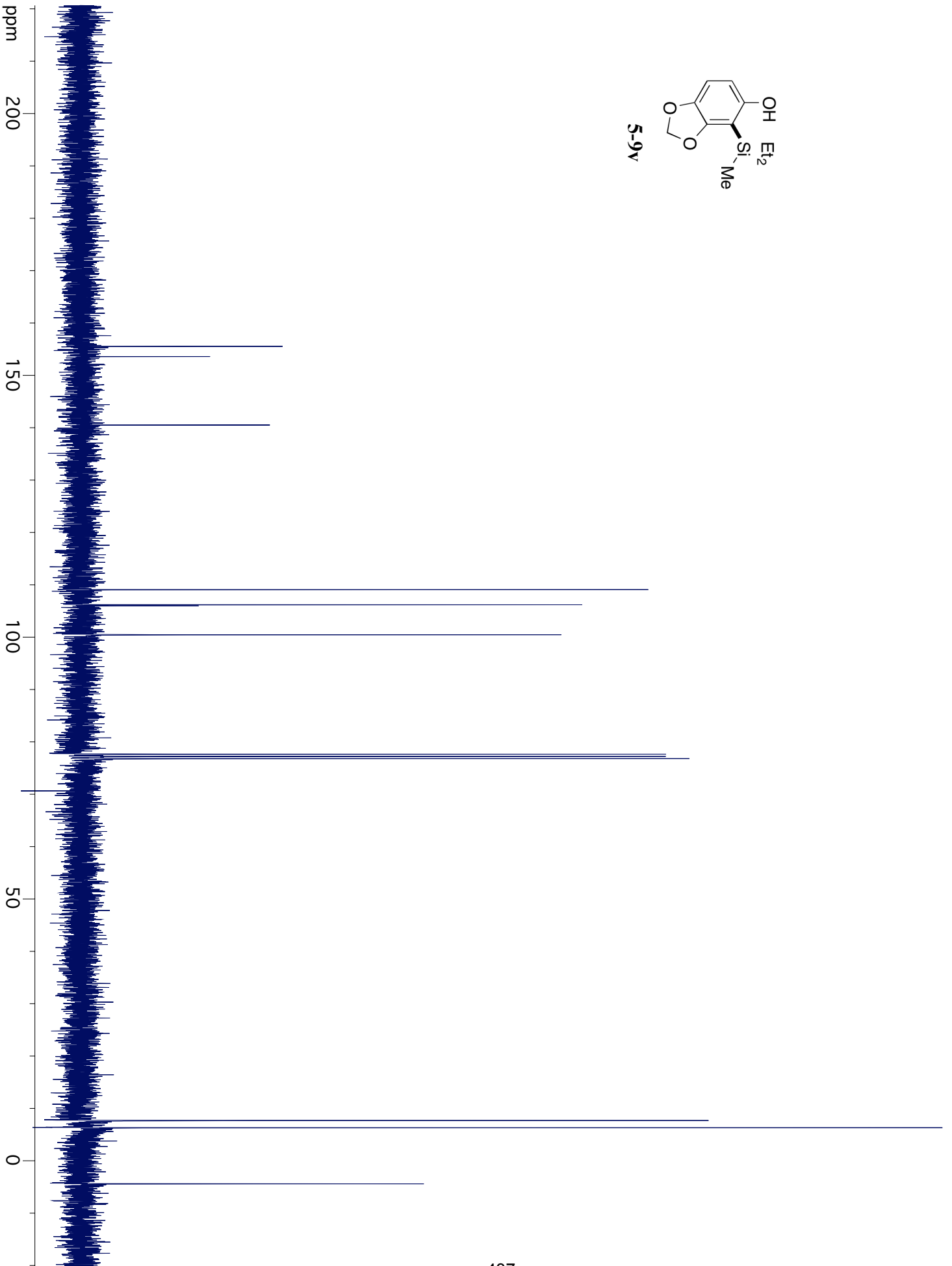
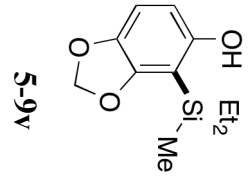
ppm

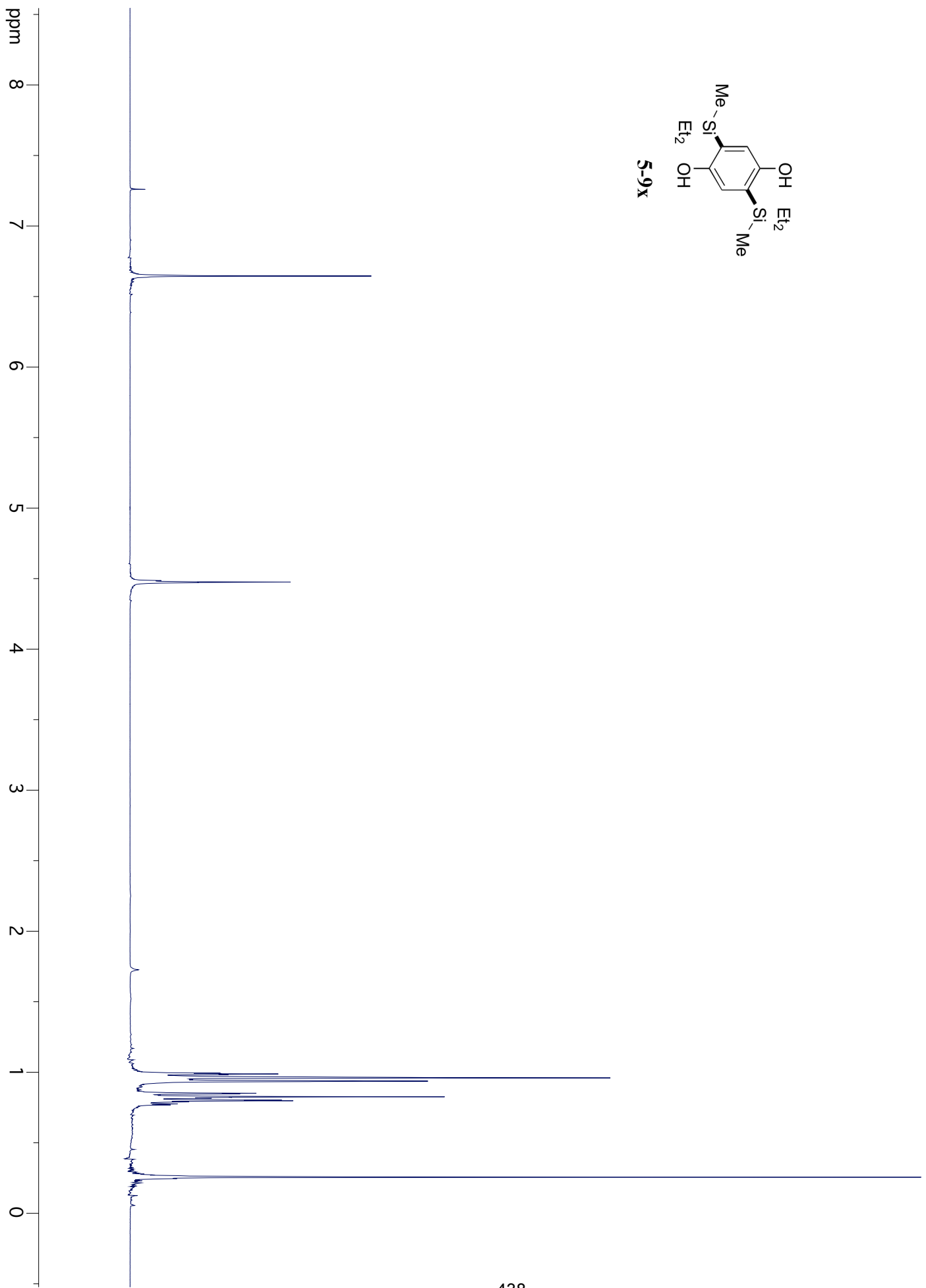
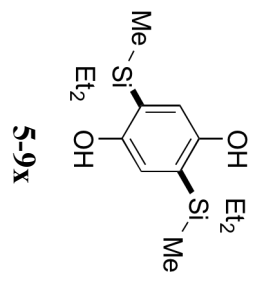


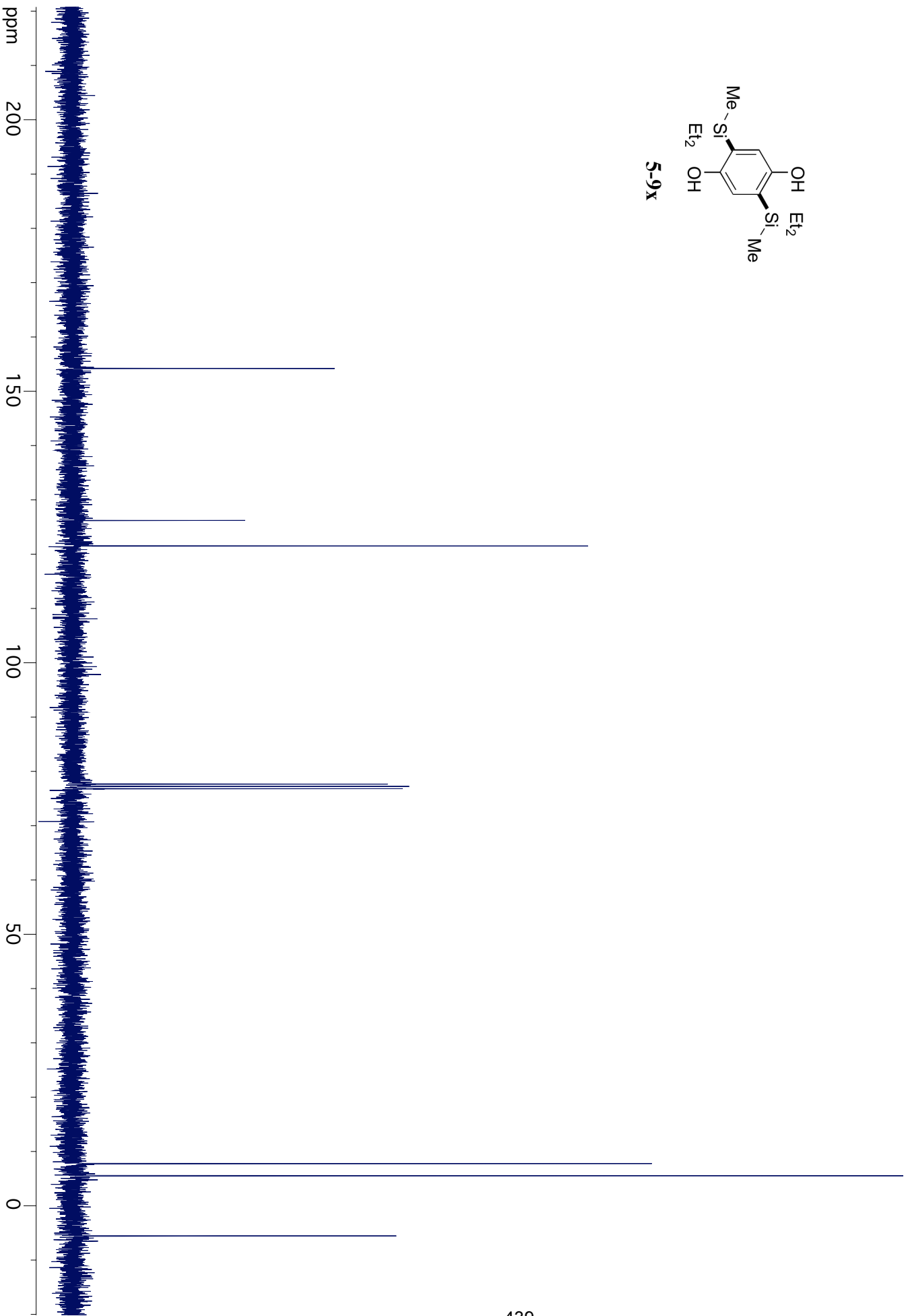
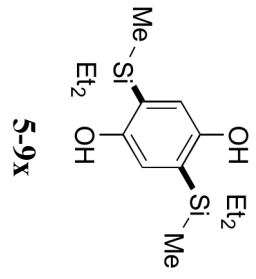


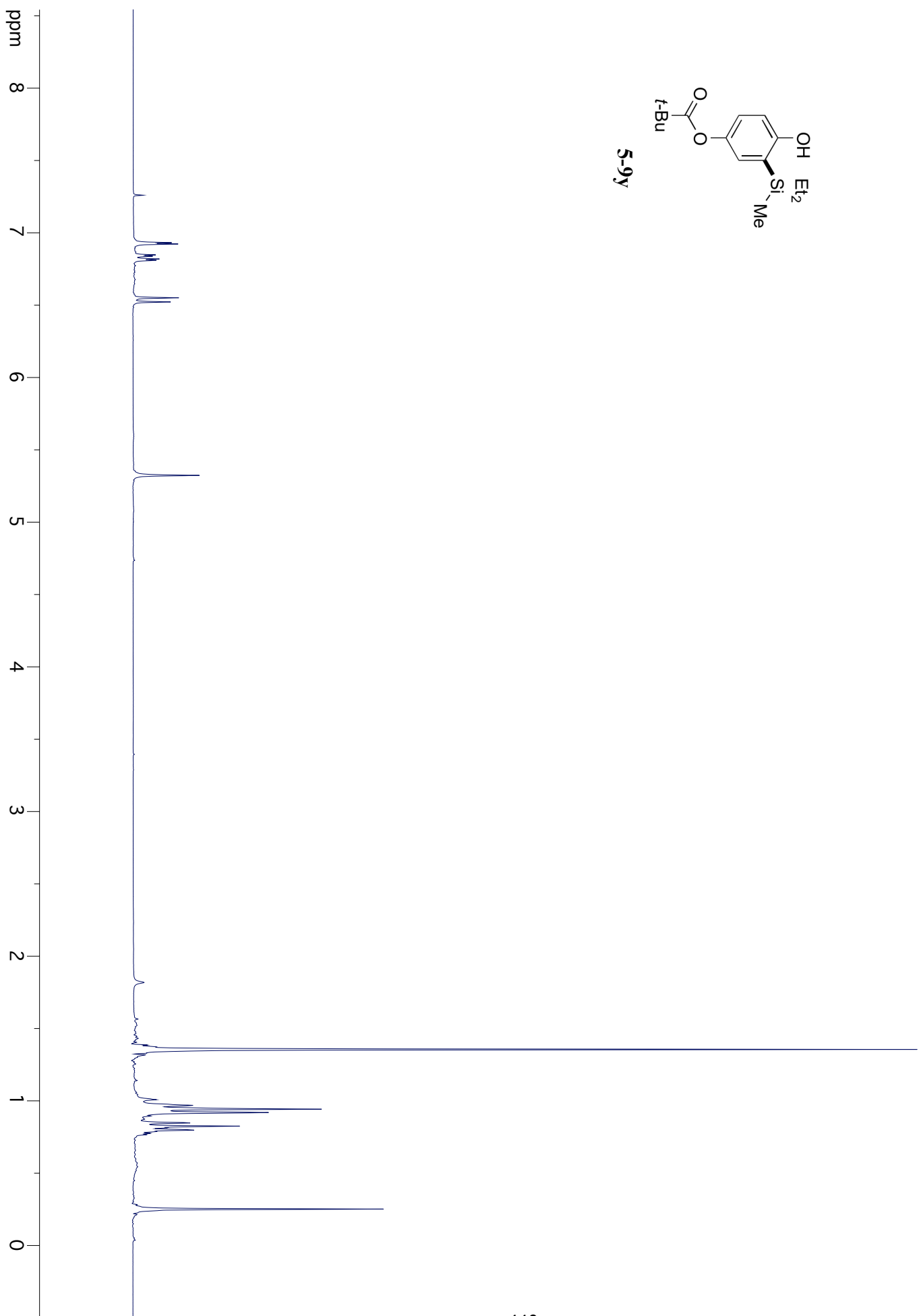
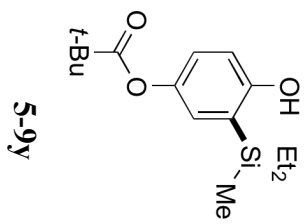


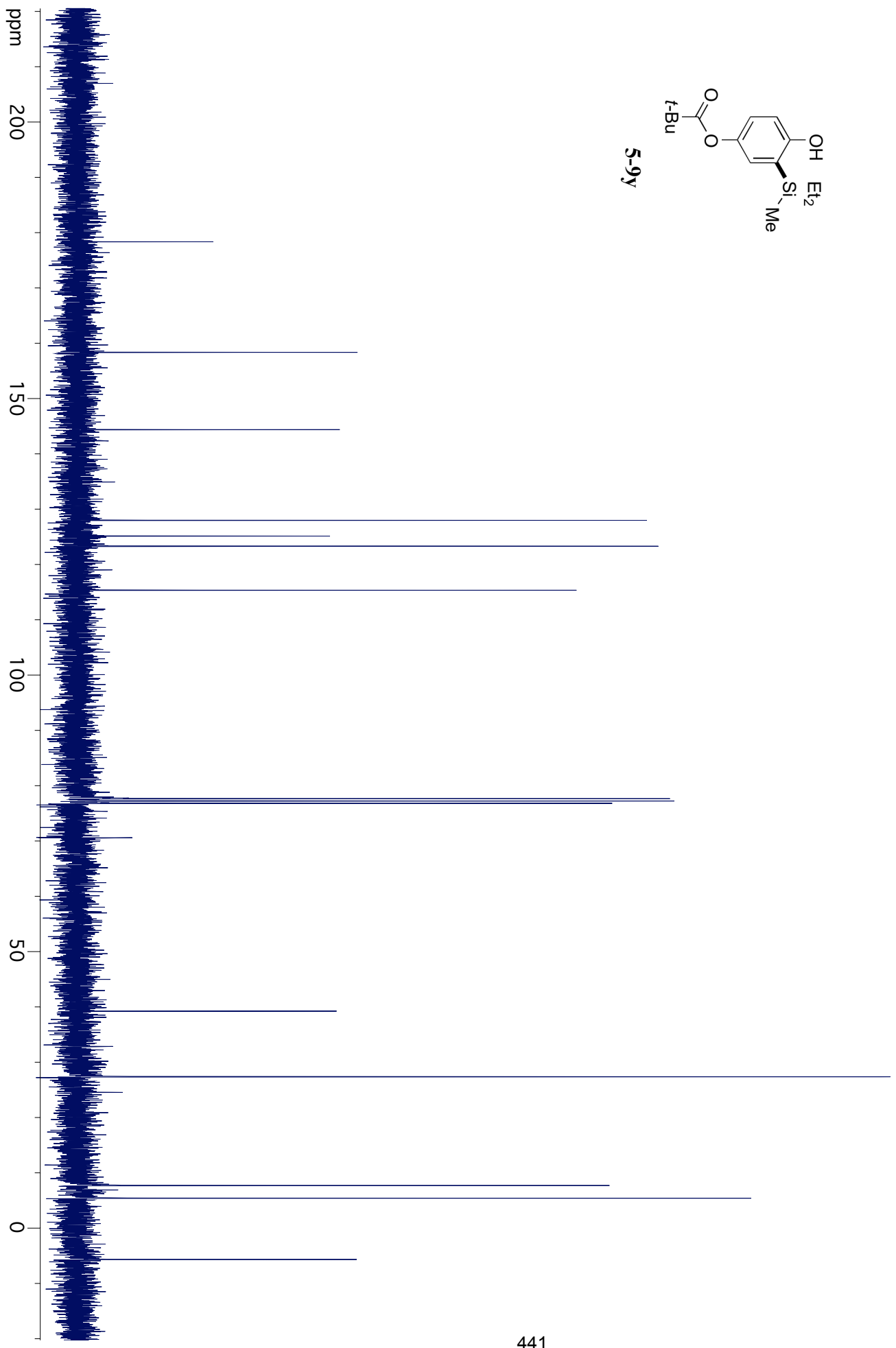
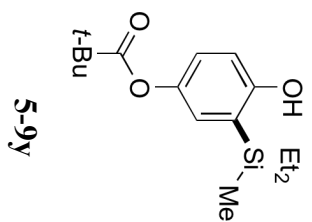


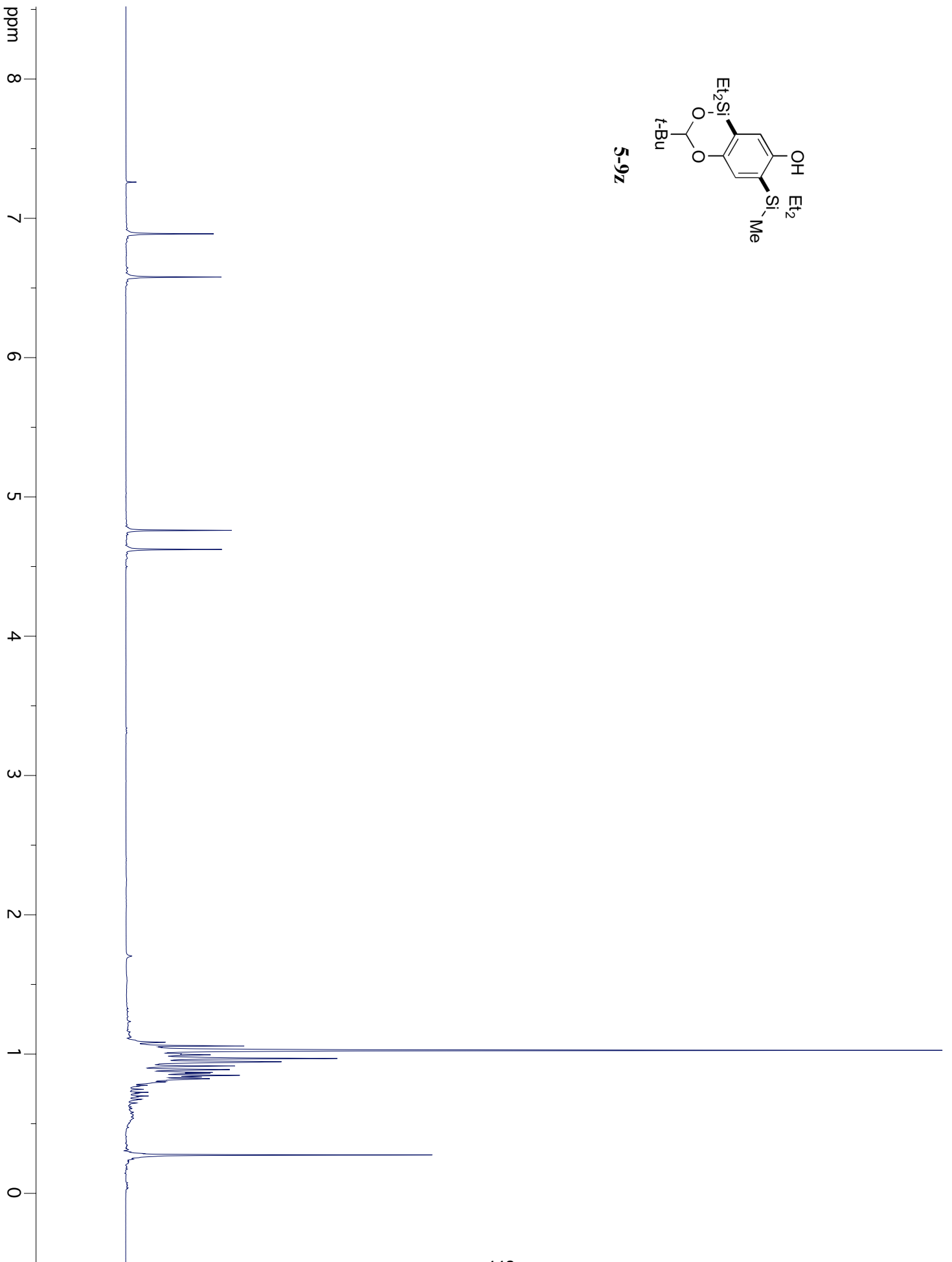
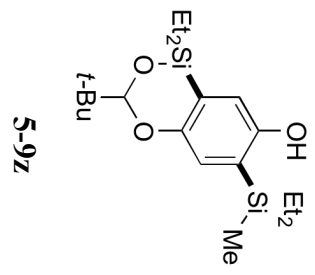


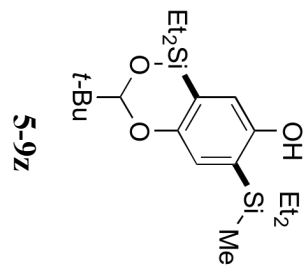






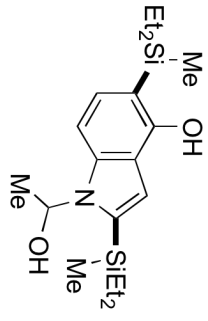




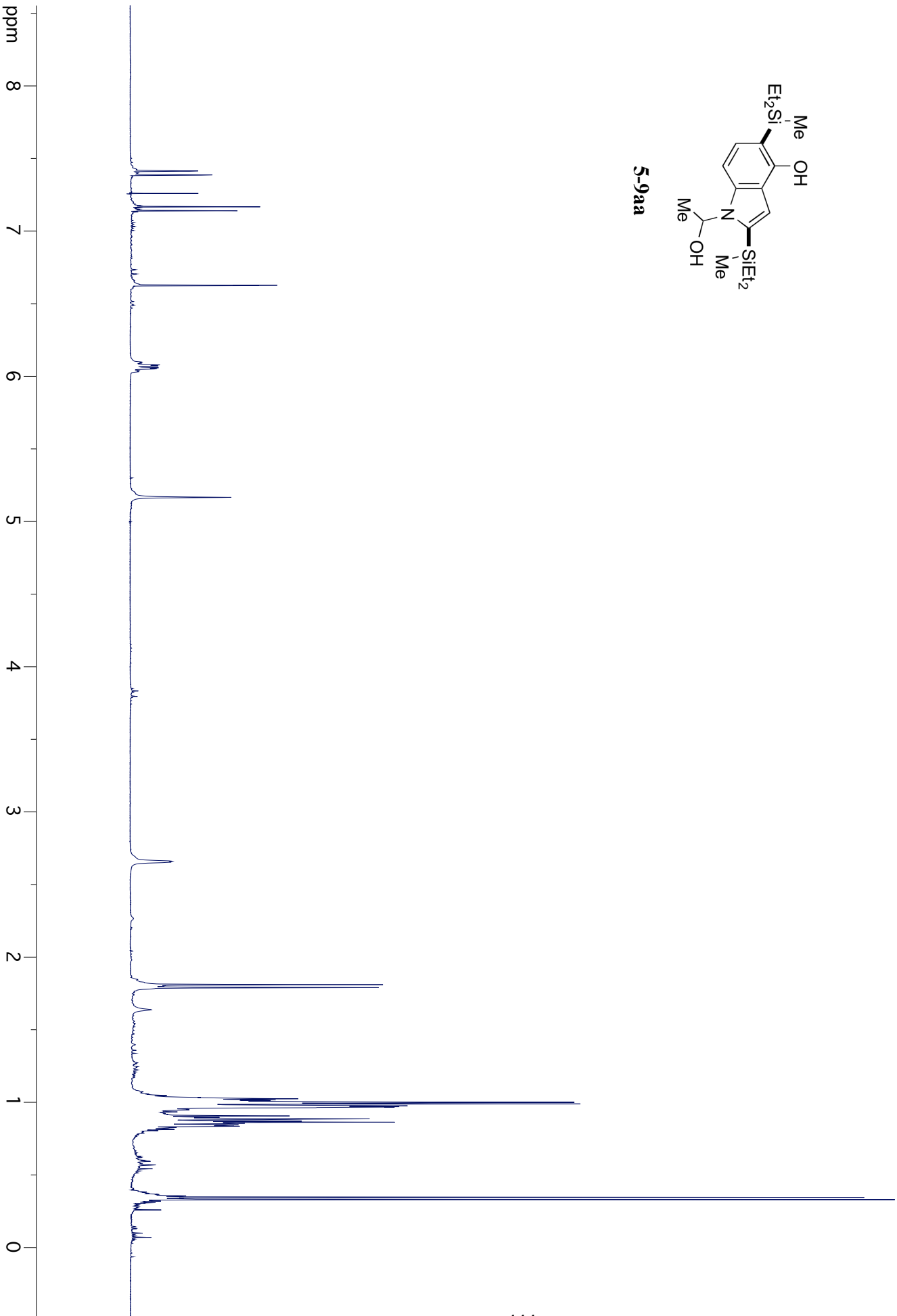


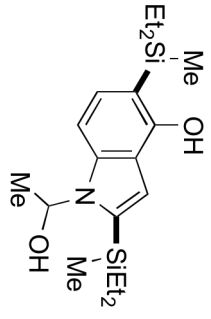
ppm 200 150 100 50 0



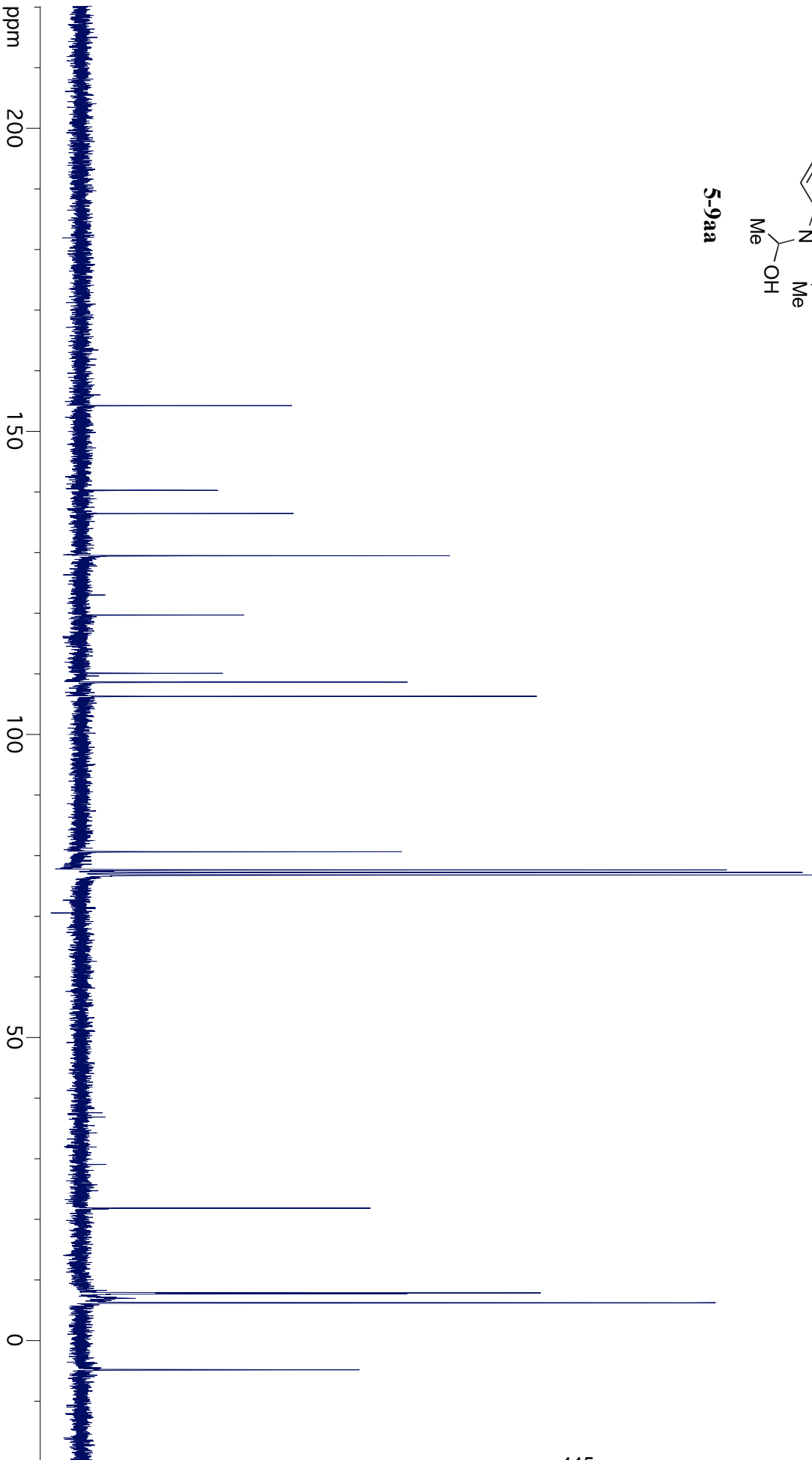


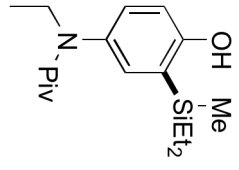
5-9aa



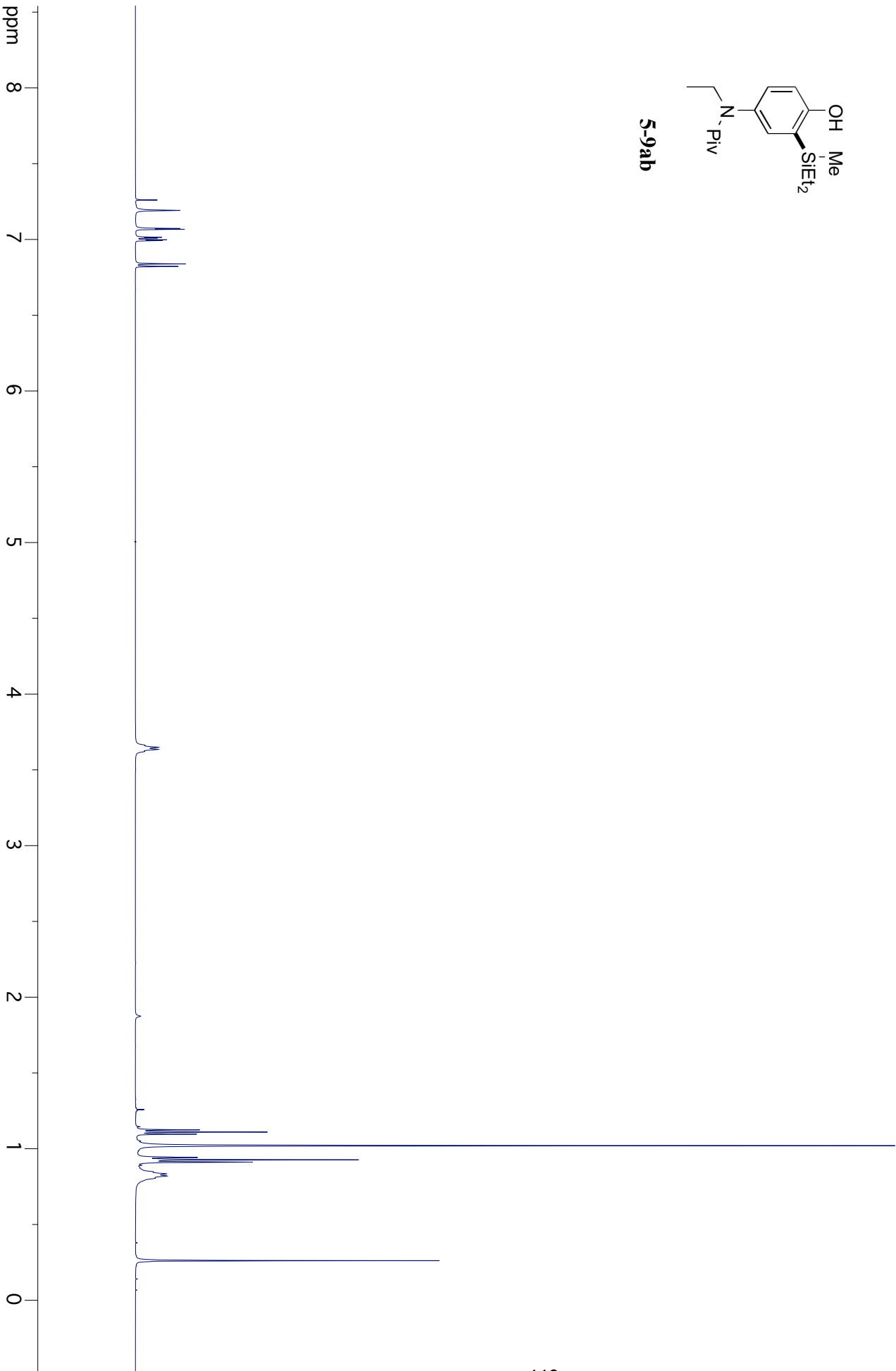


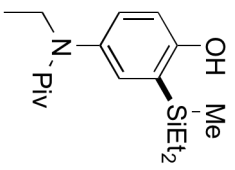
5-9aa



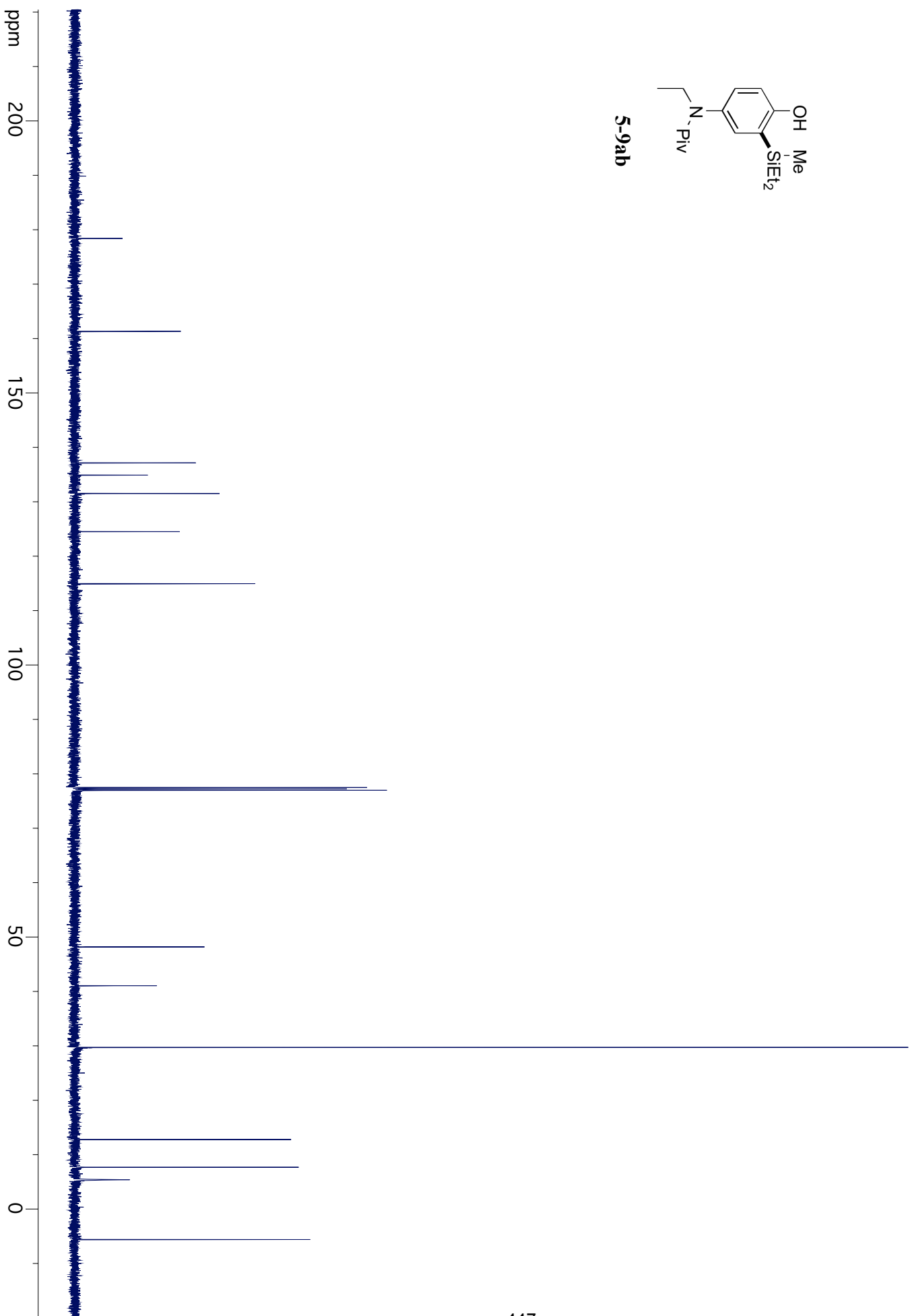


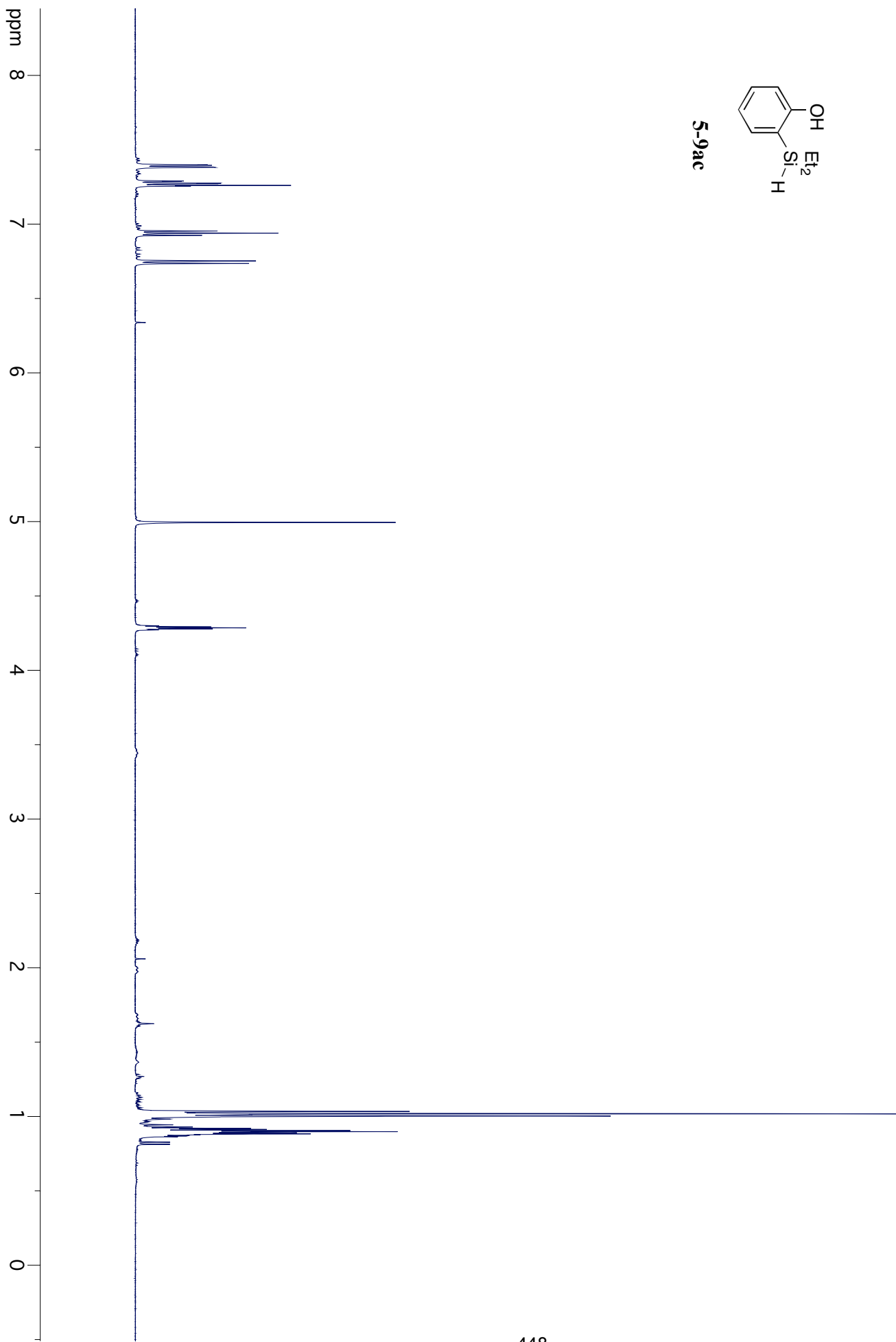
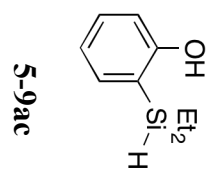
5-9ab

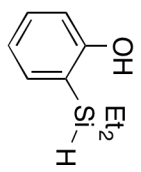




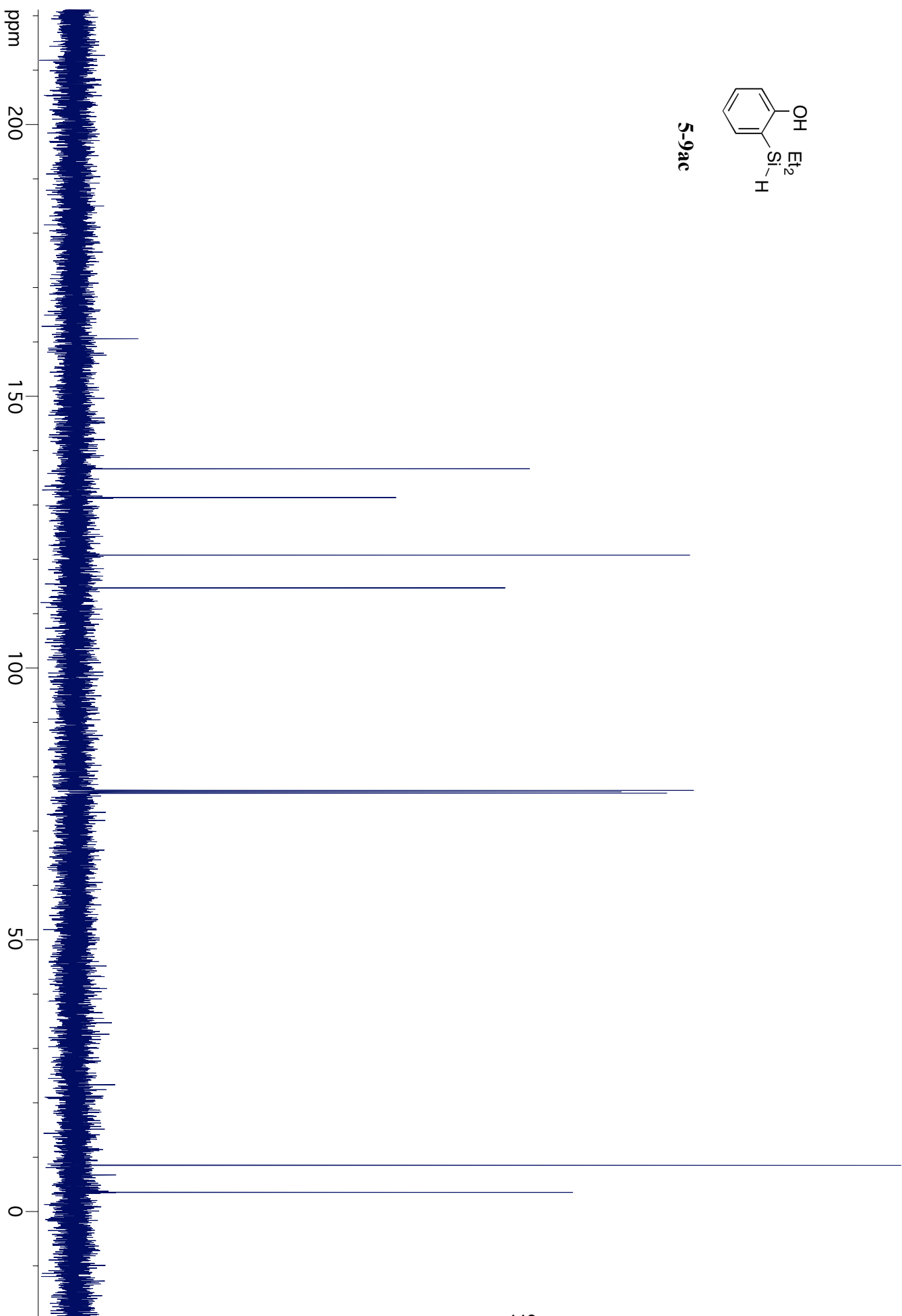
5-9ab

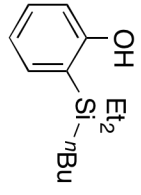




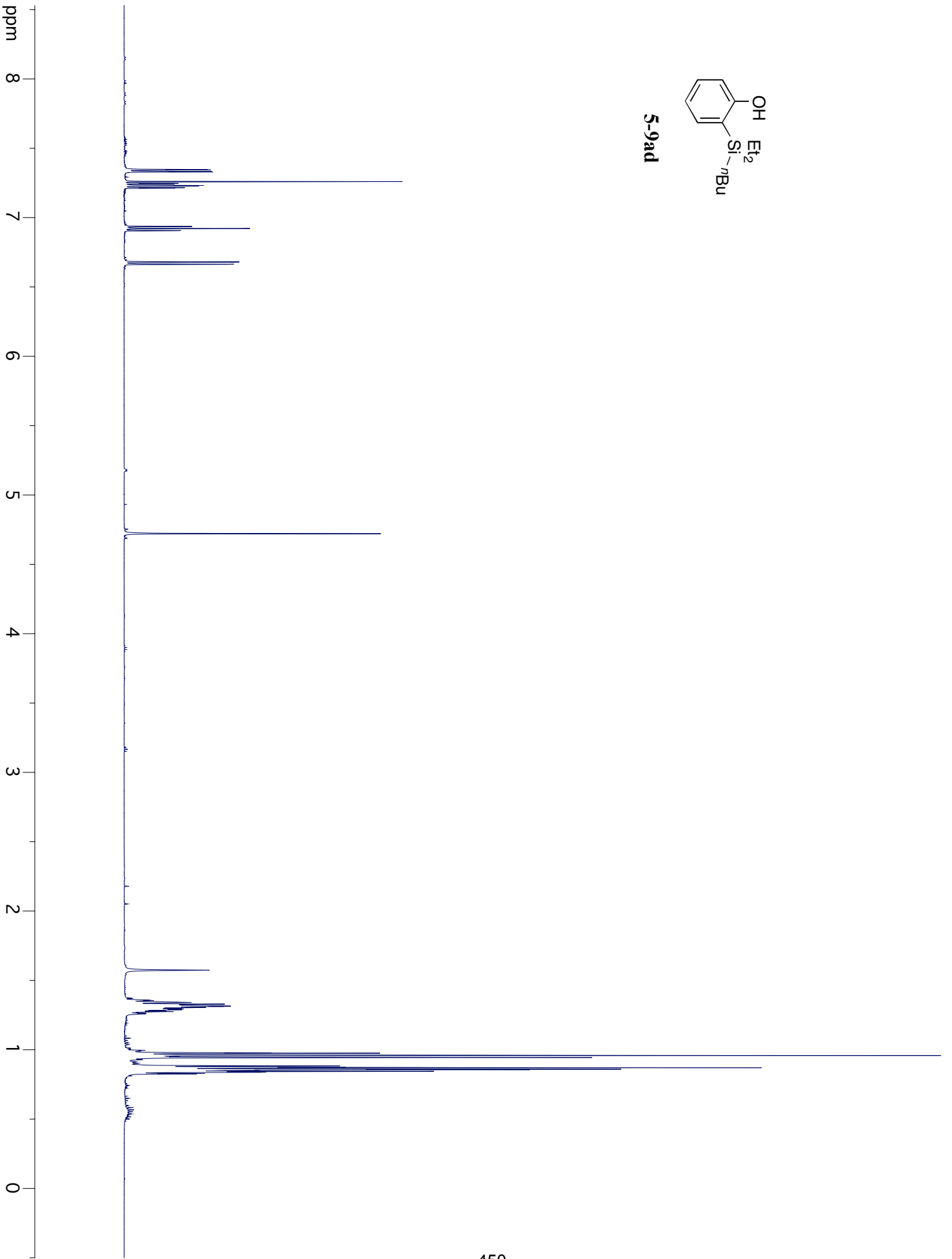


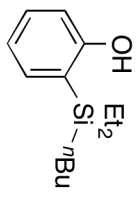
5-9ac



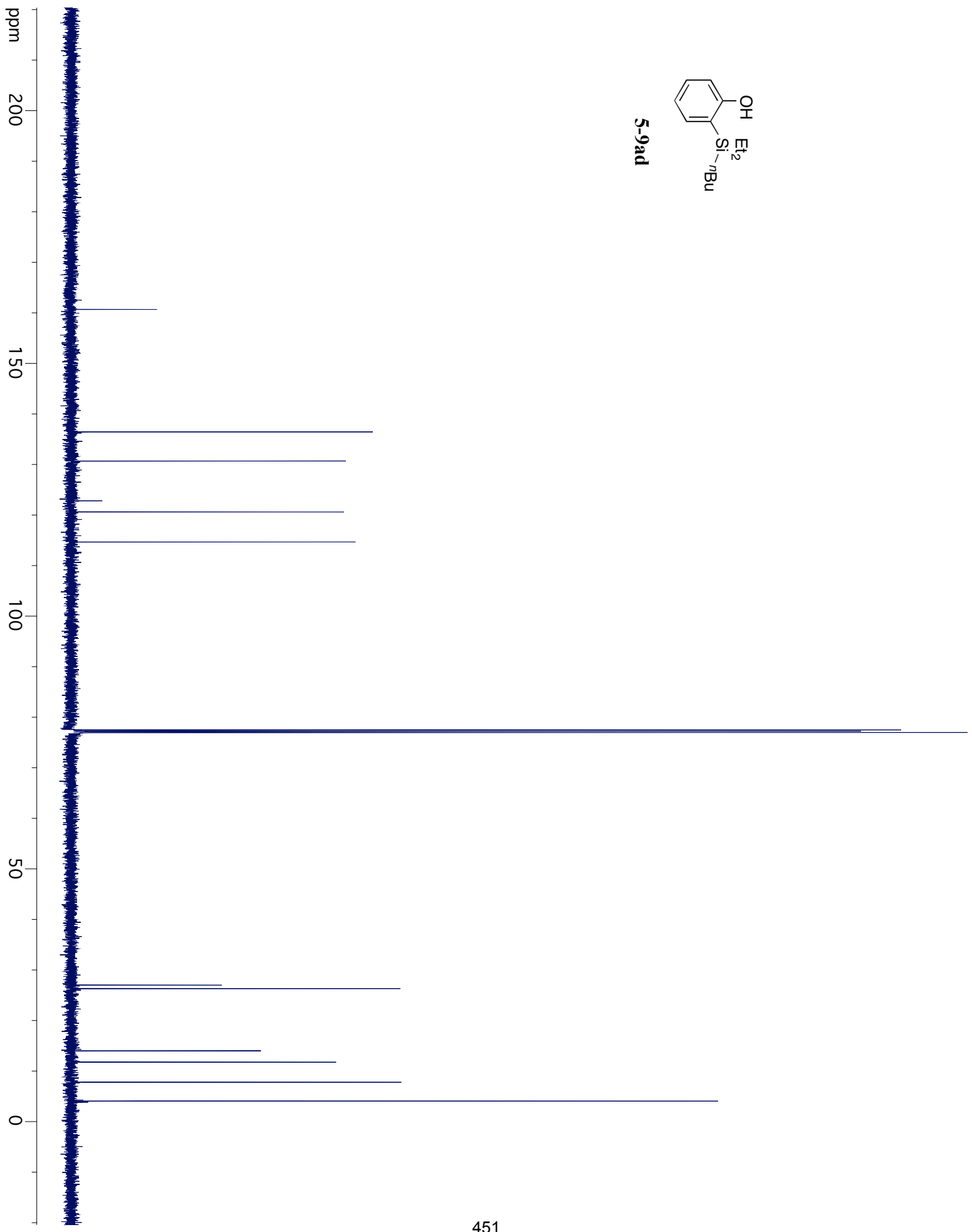


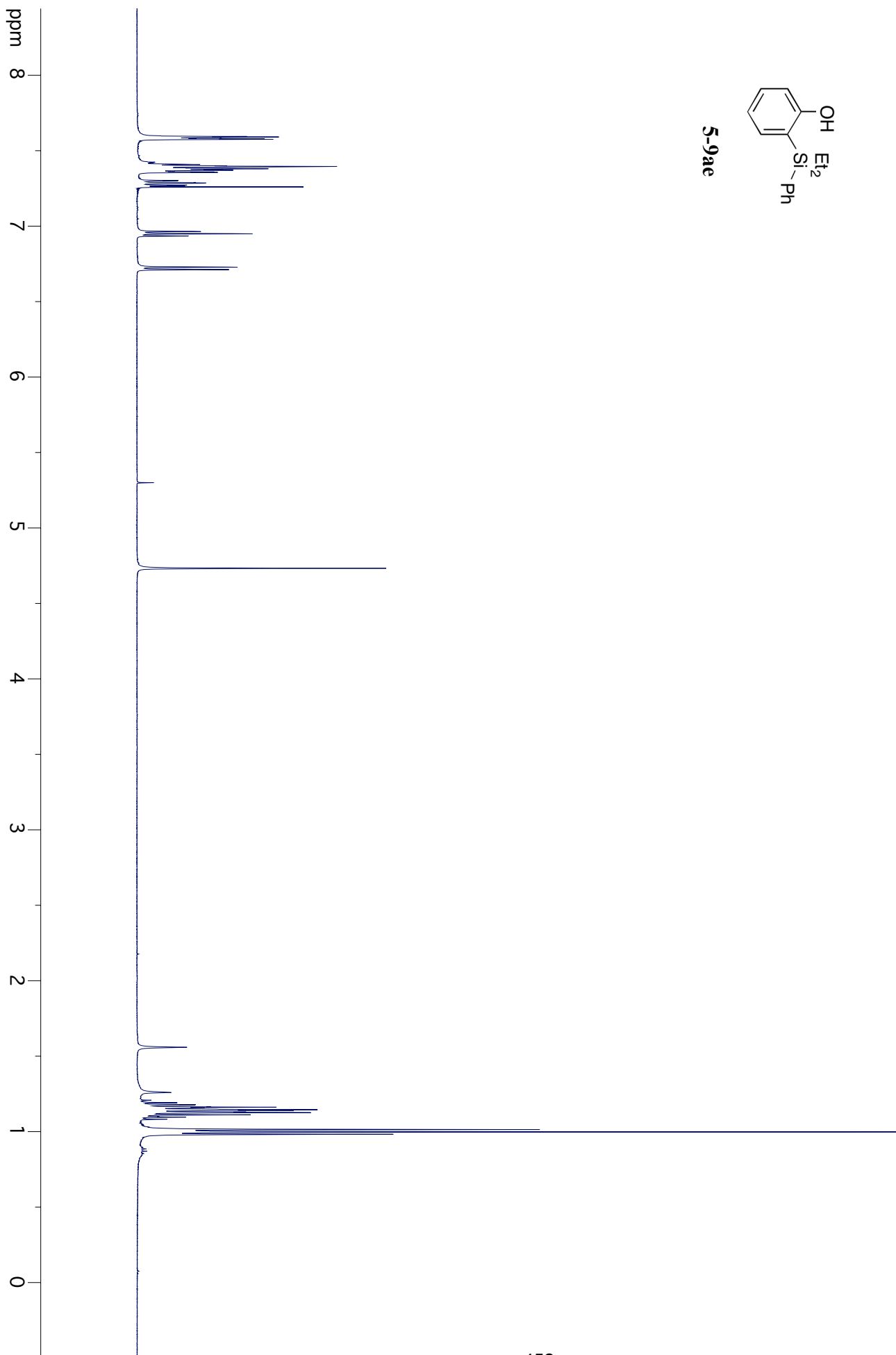
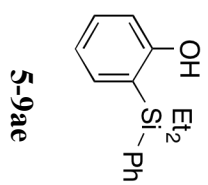
5-9ad

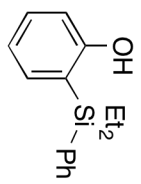




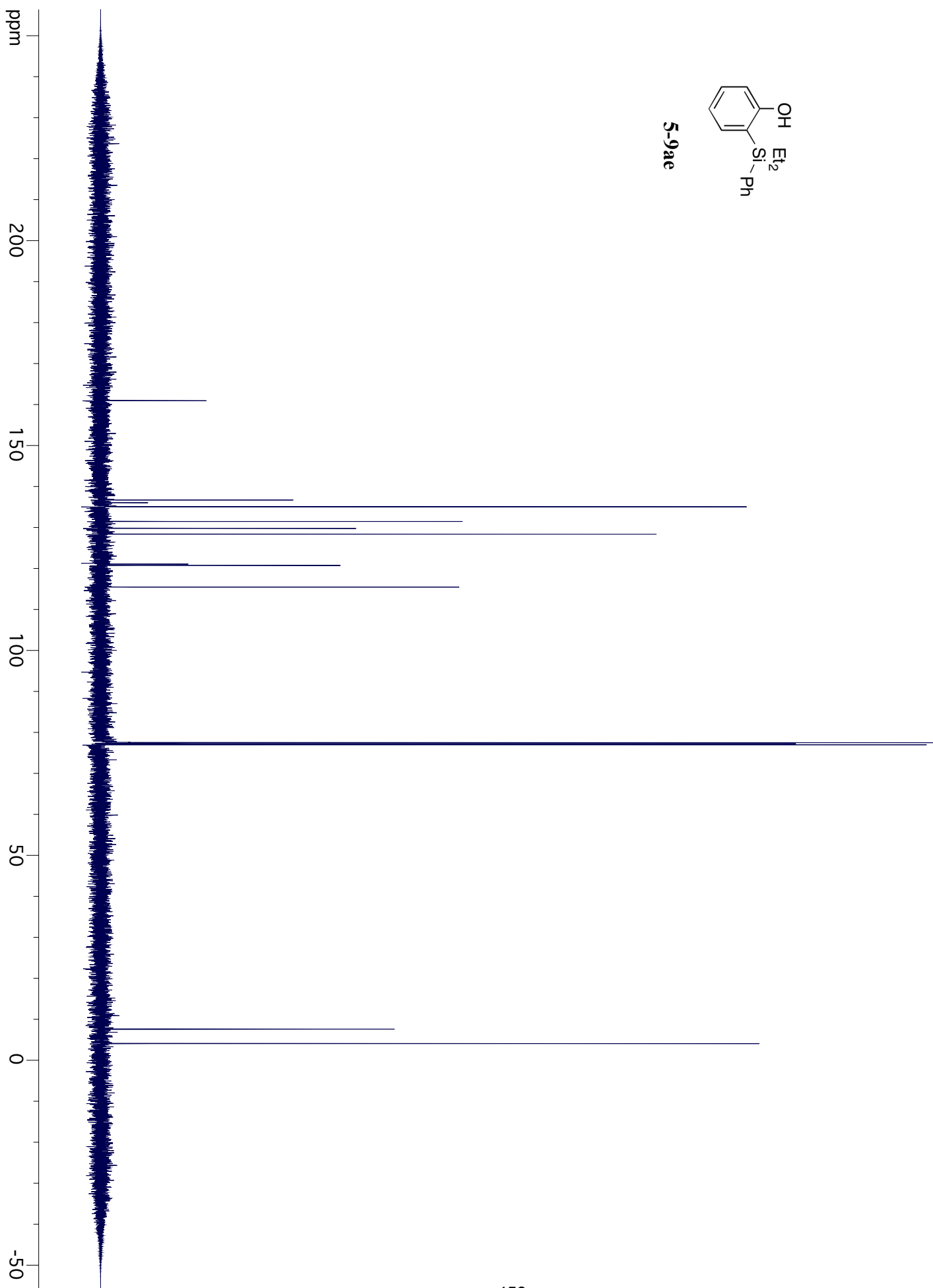
5-9ad

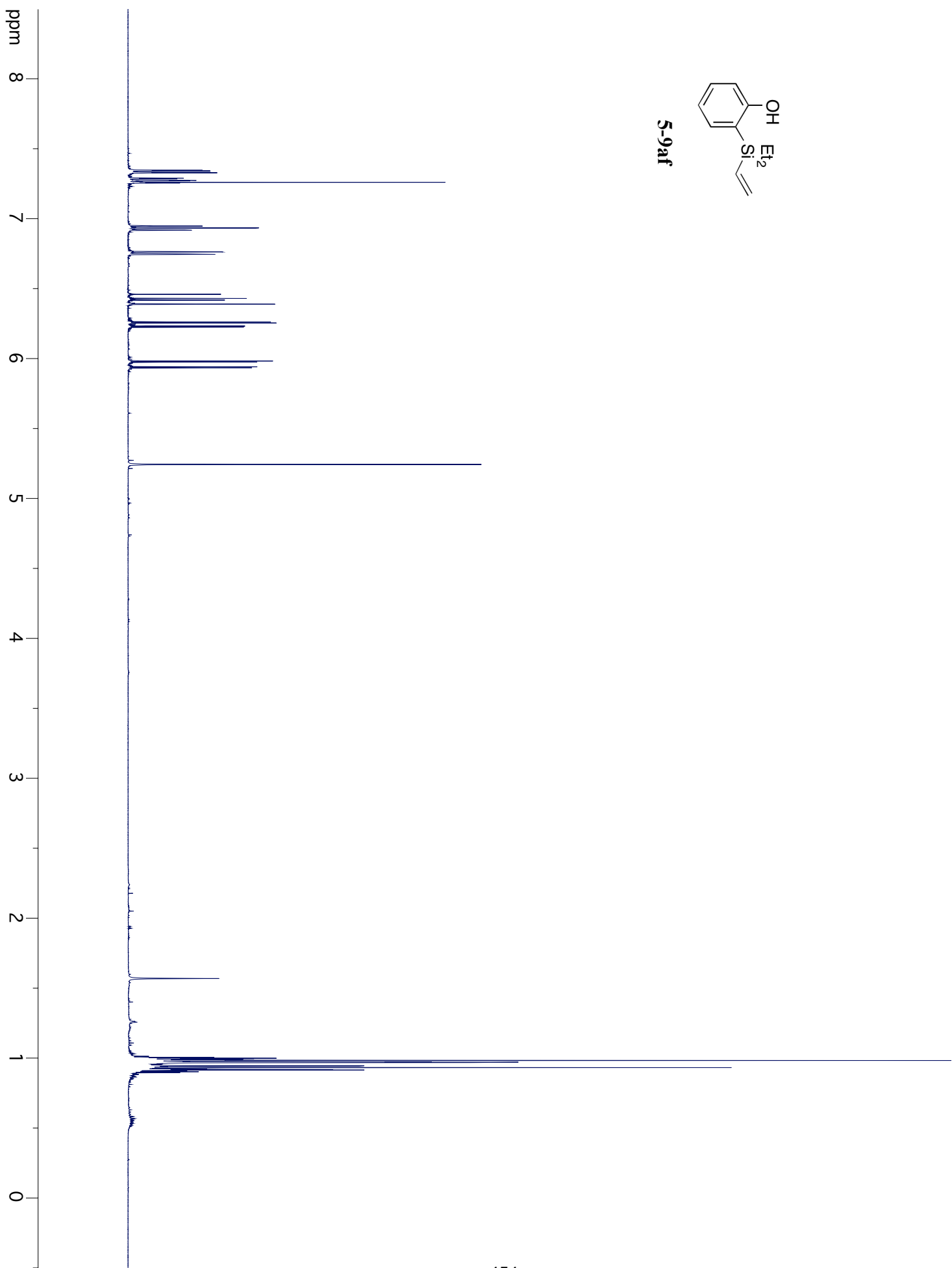
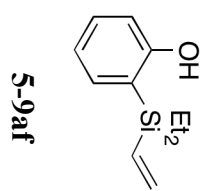


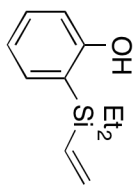




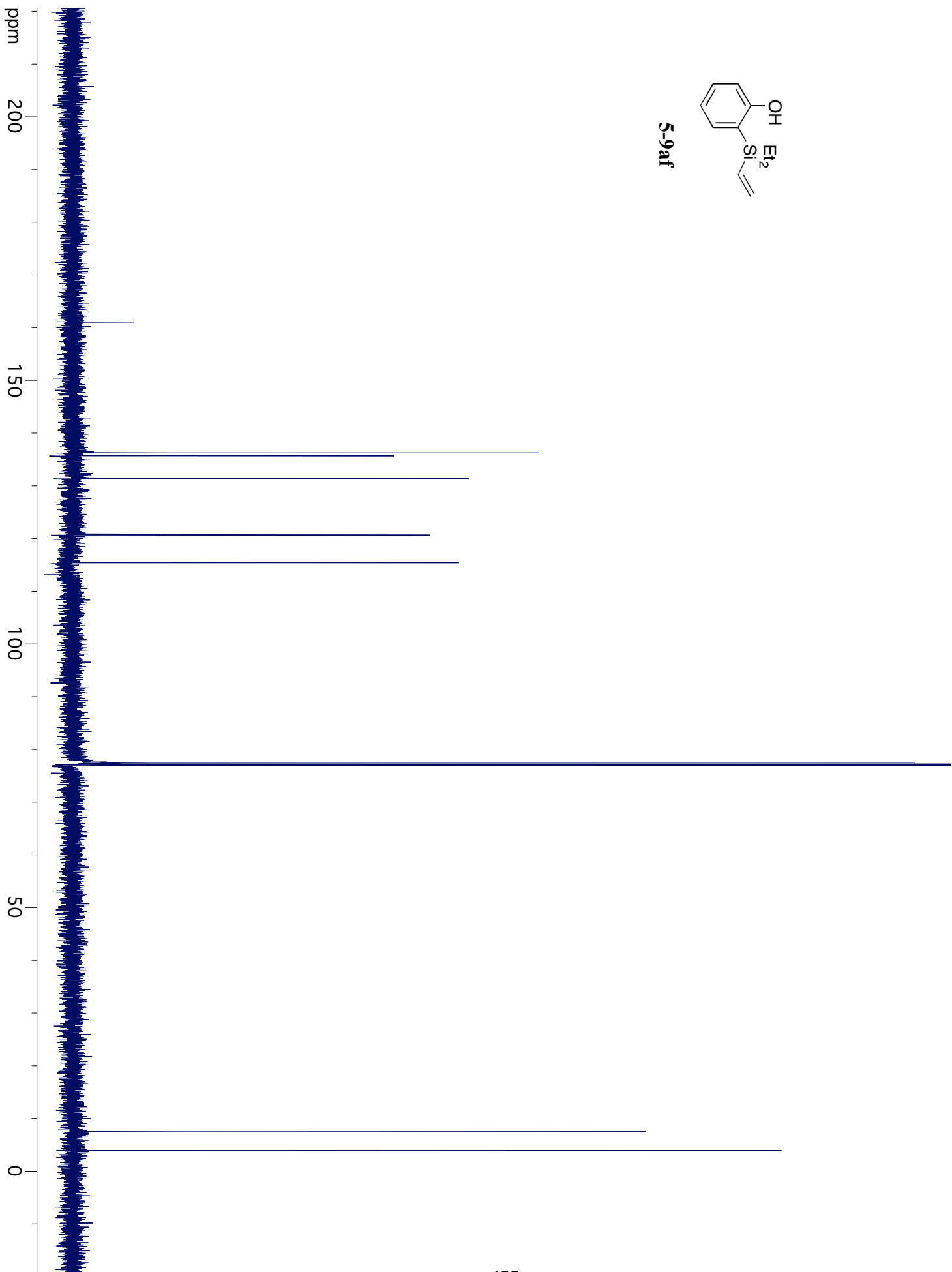
5-9ae

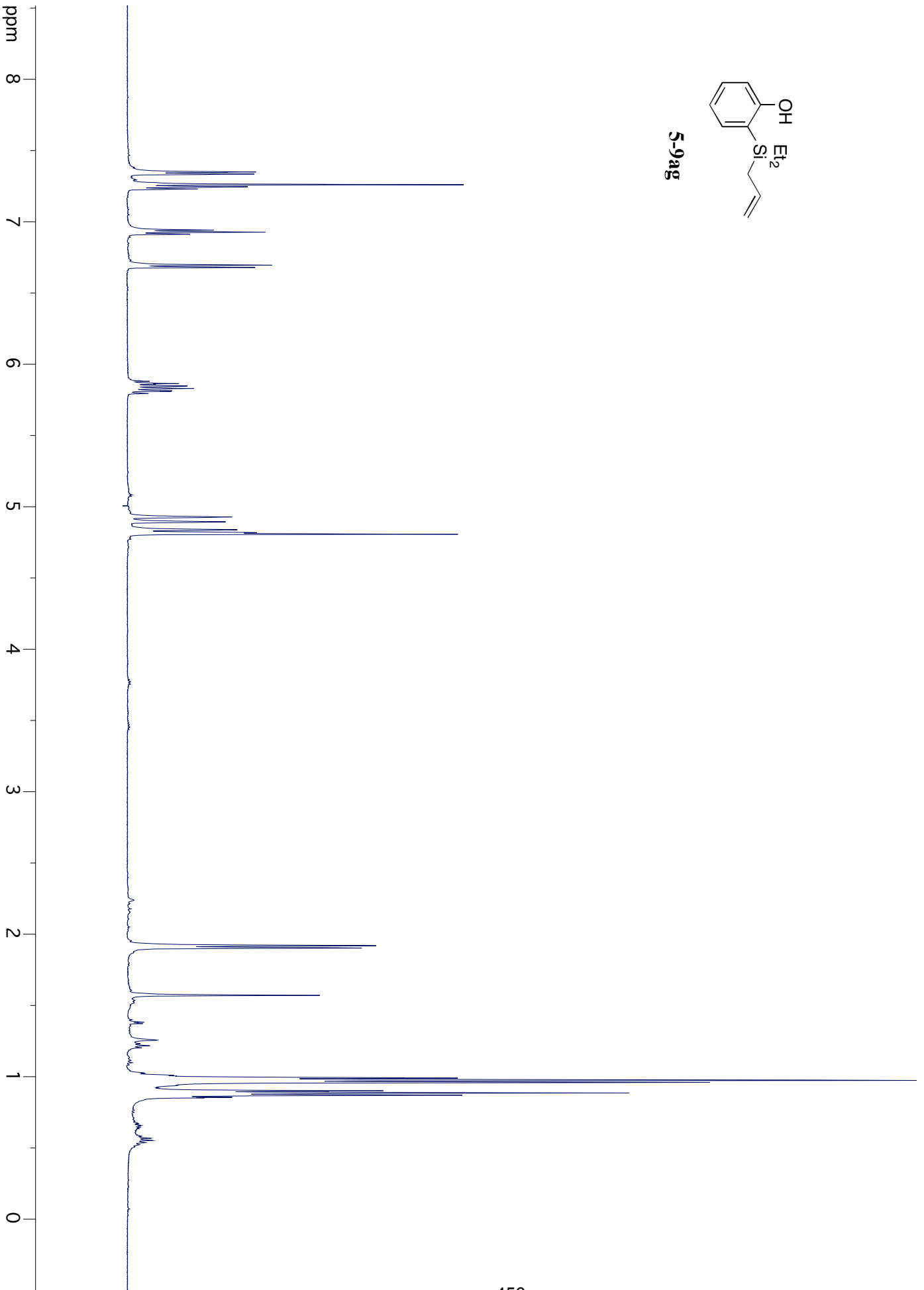
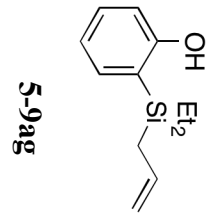


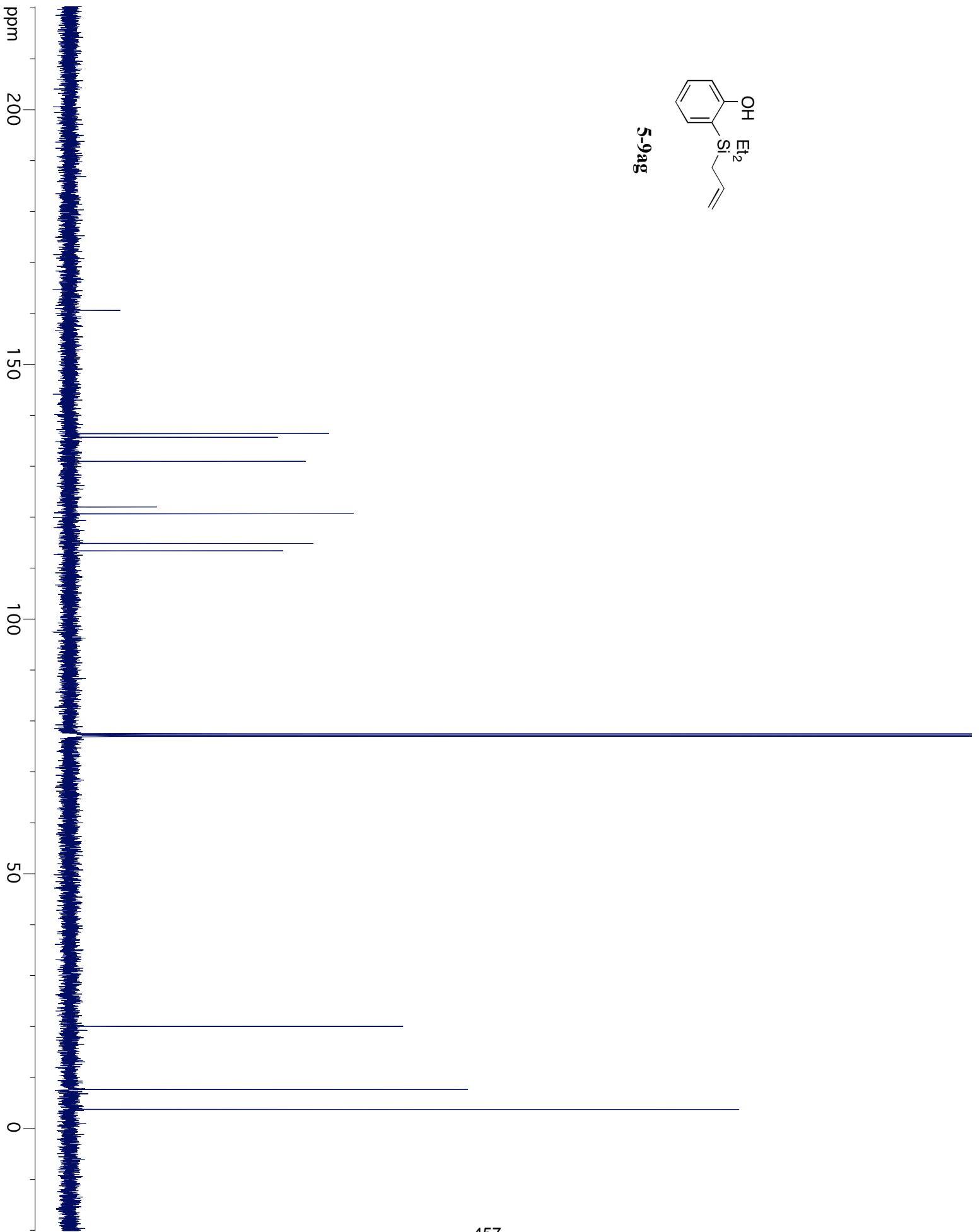
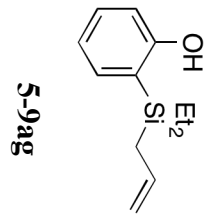


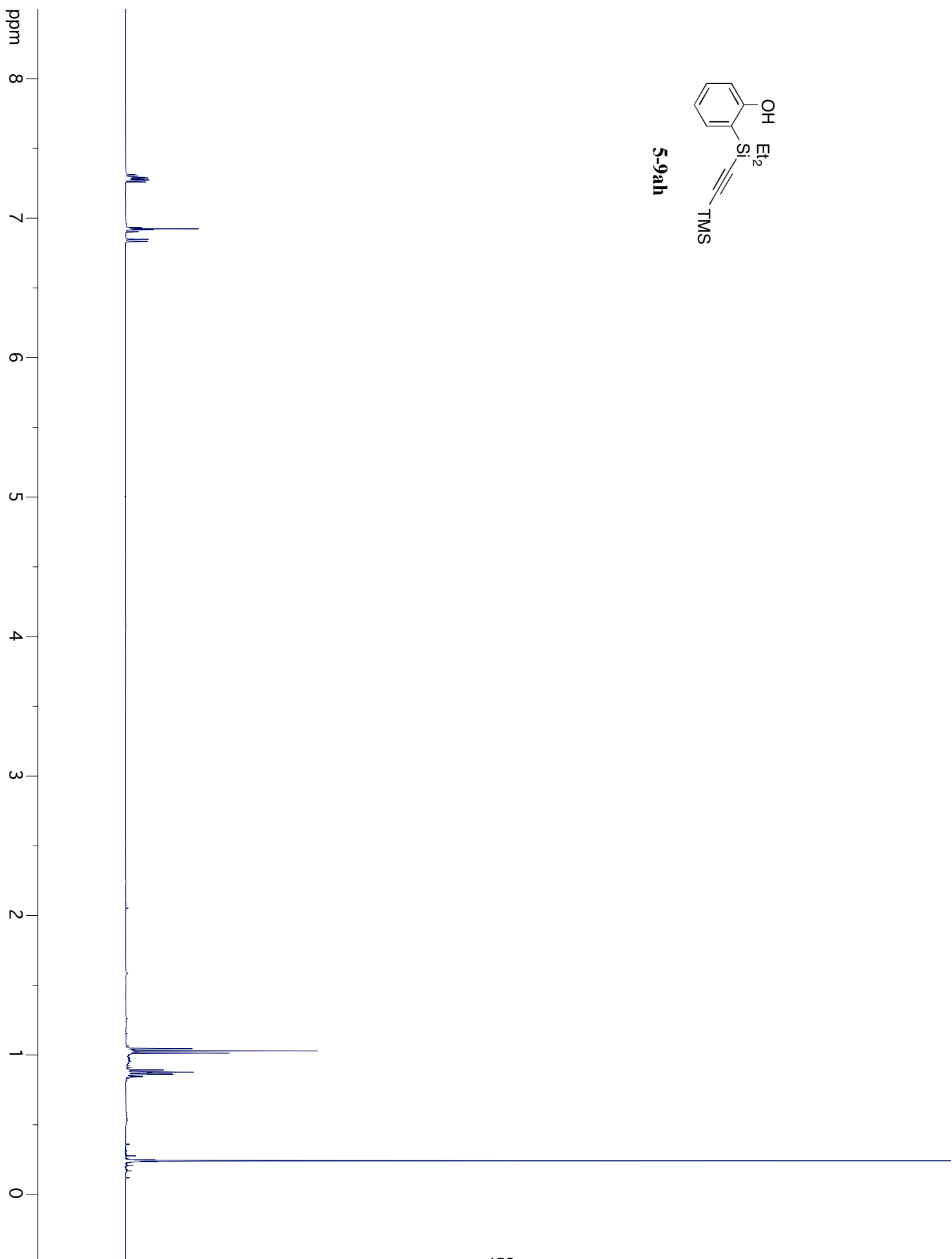
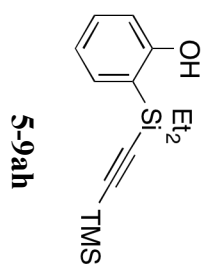


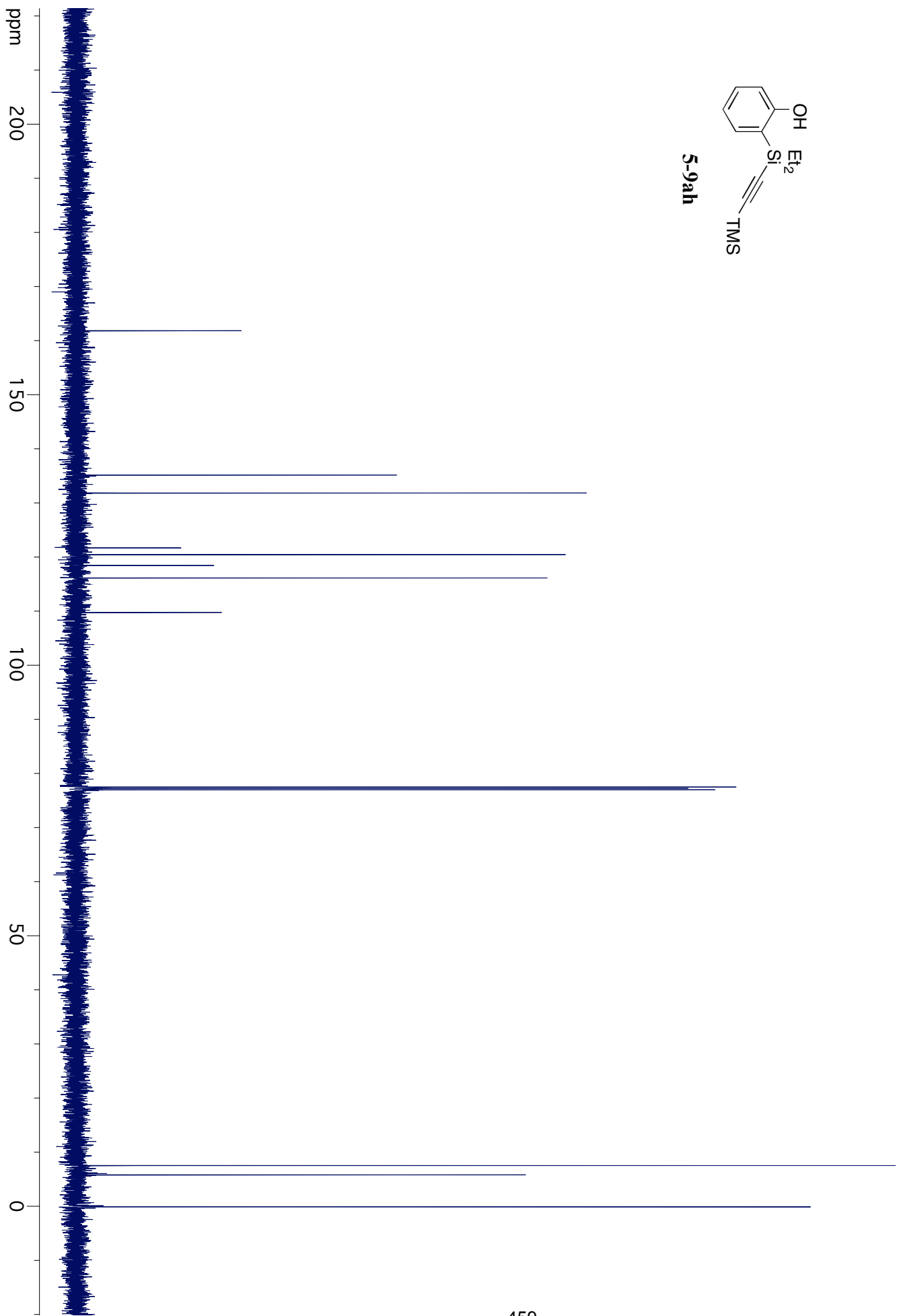
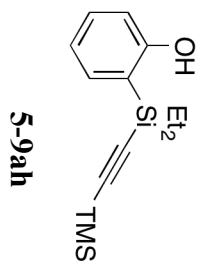
5-9af

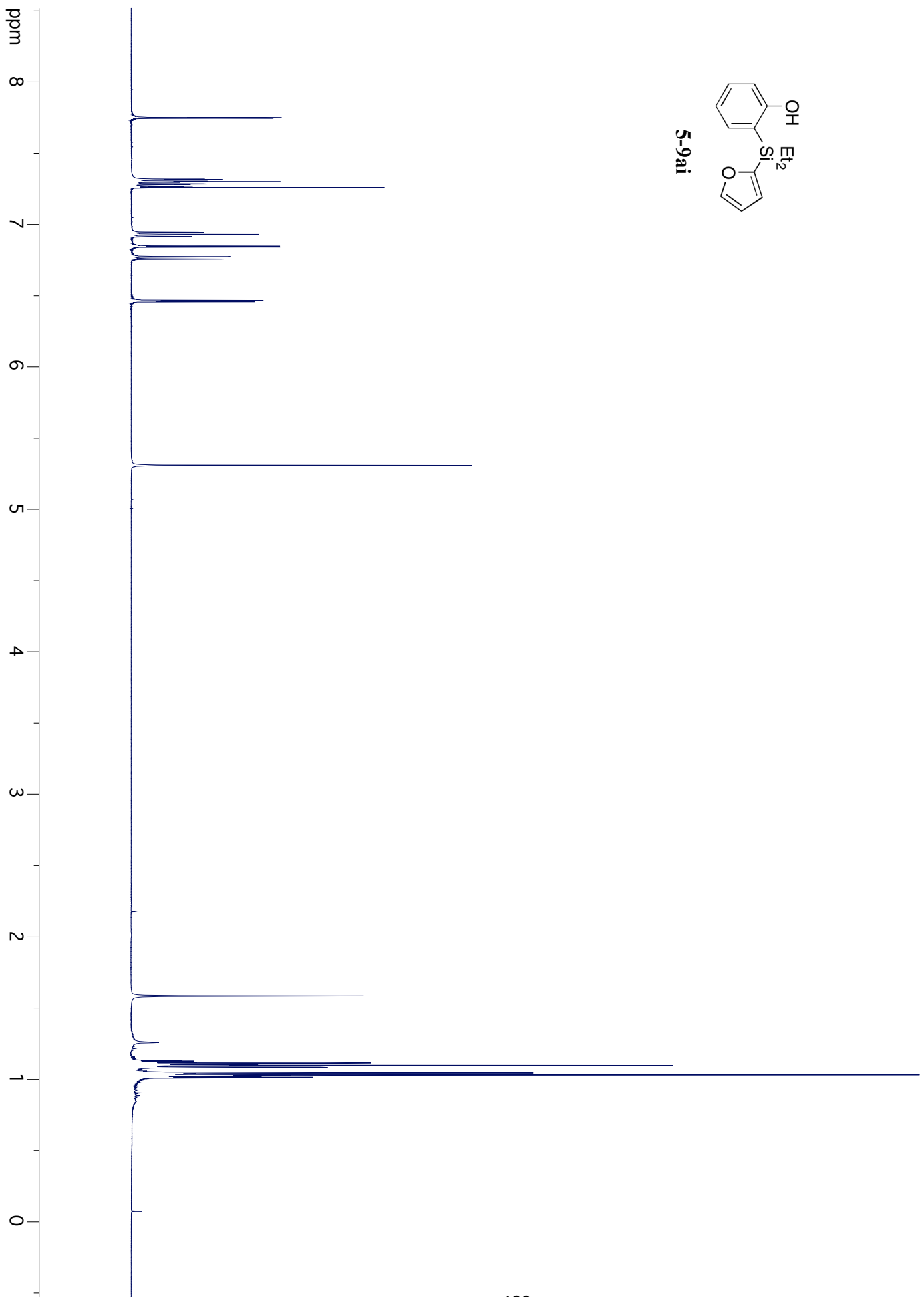
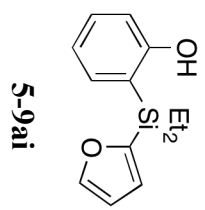


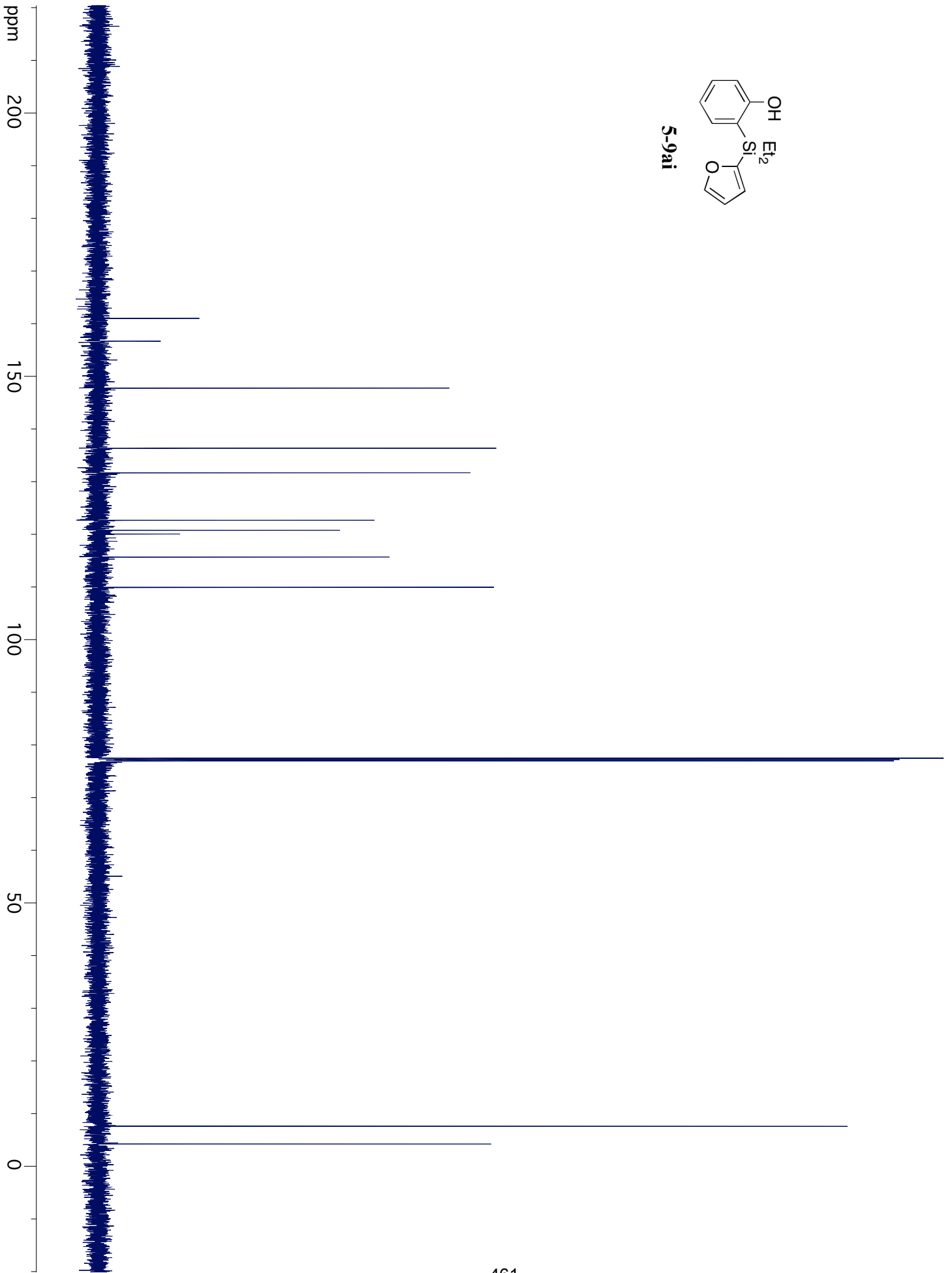
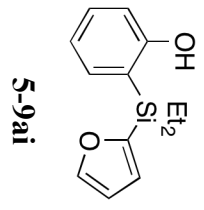


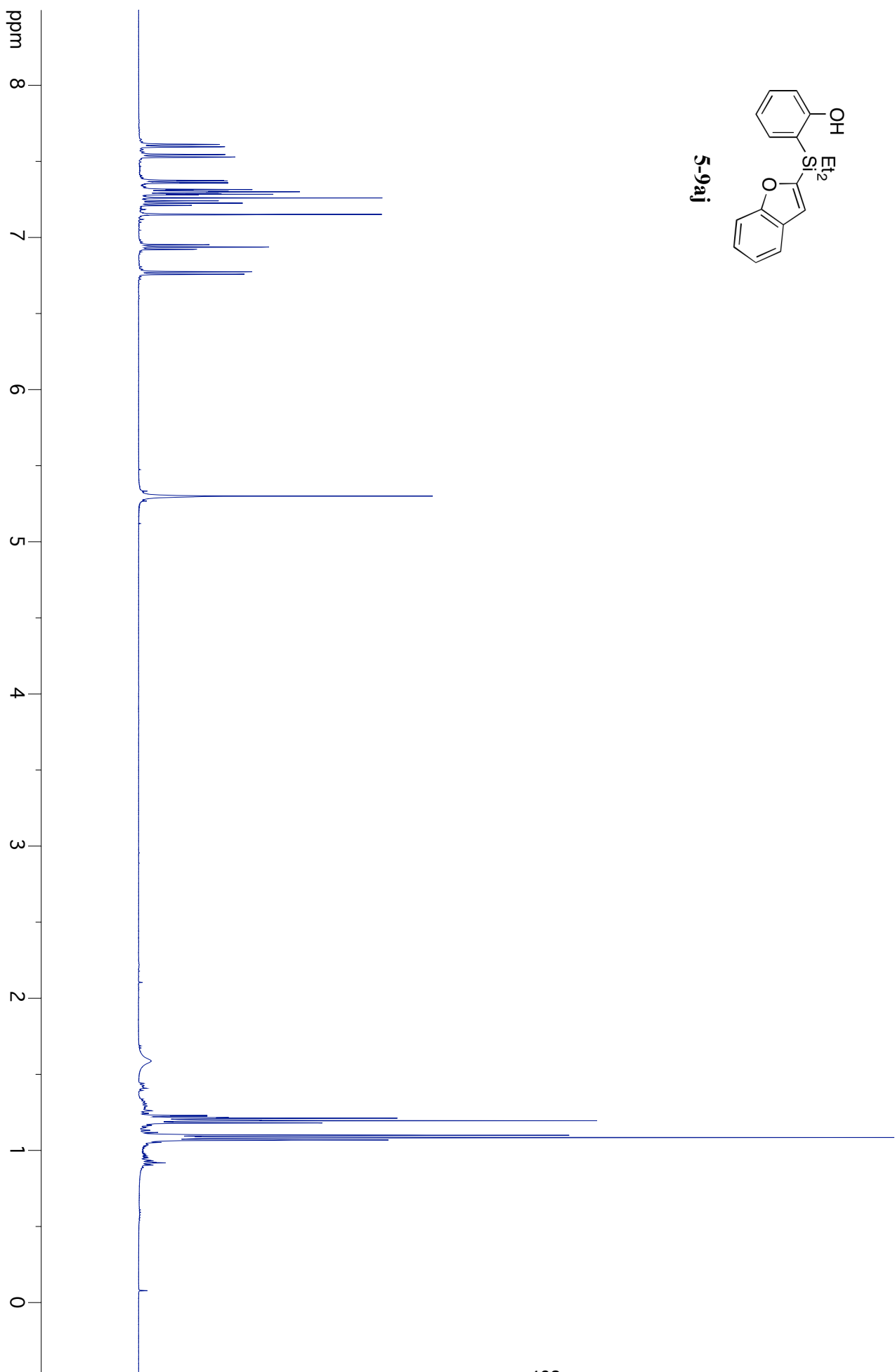
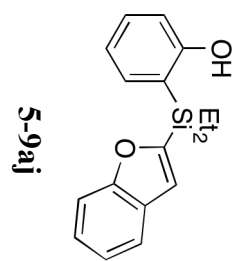


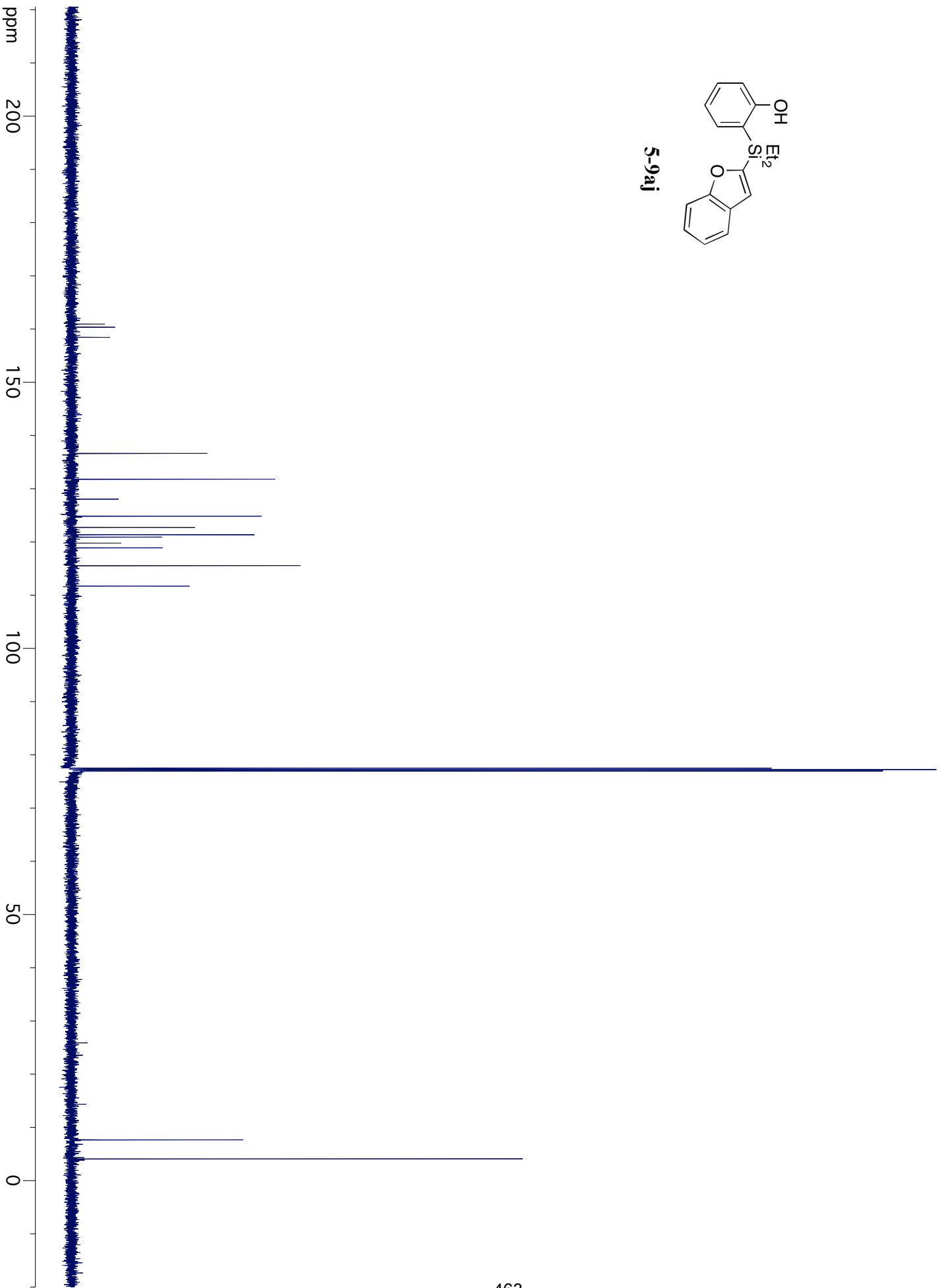
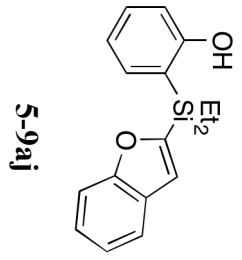


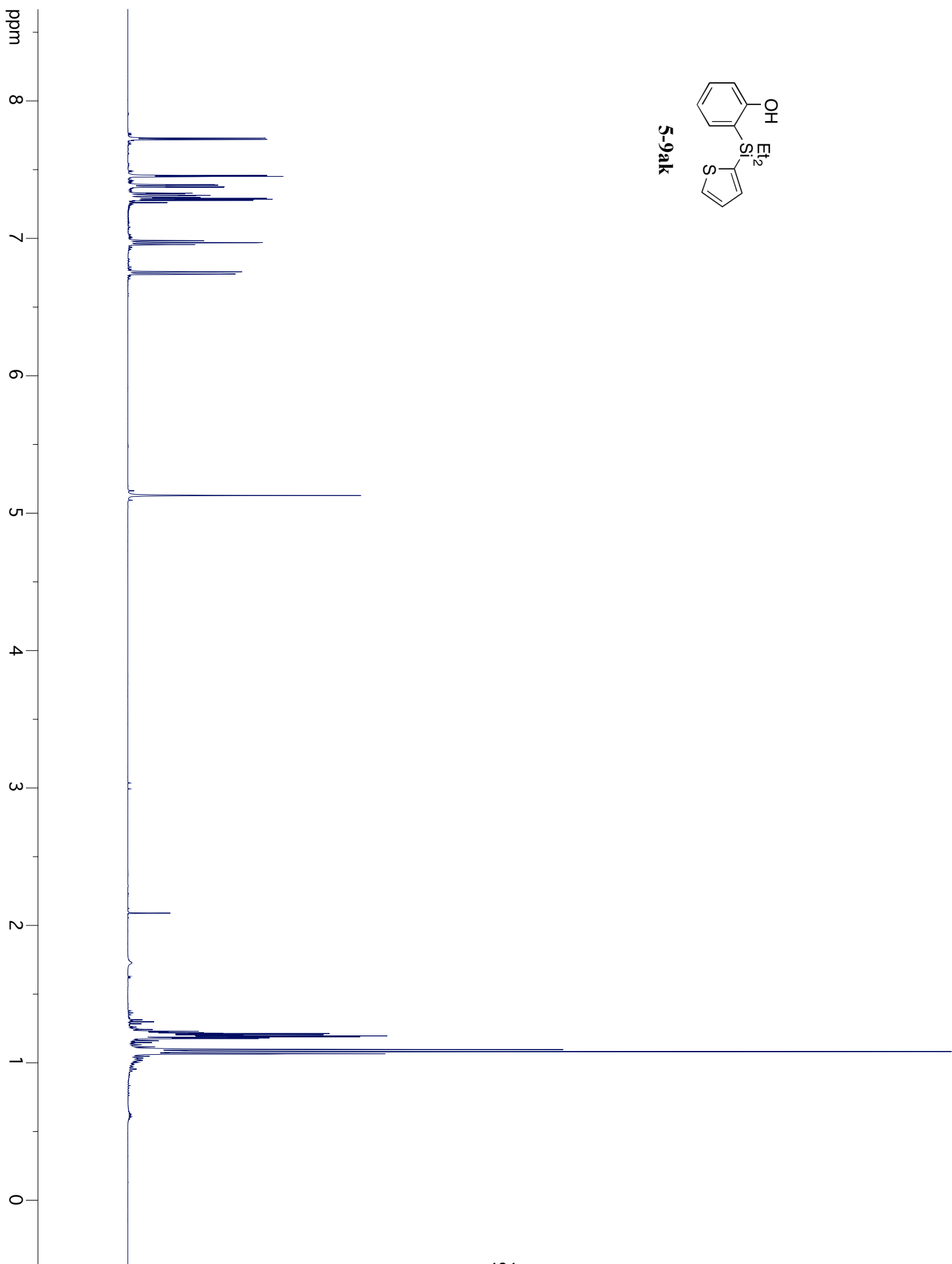
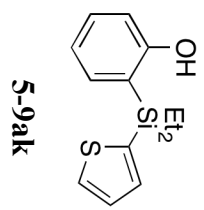


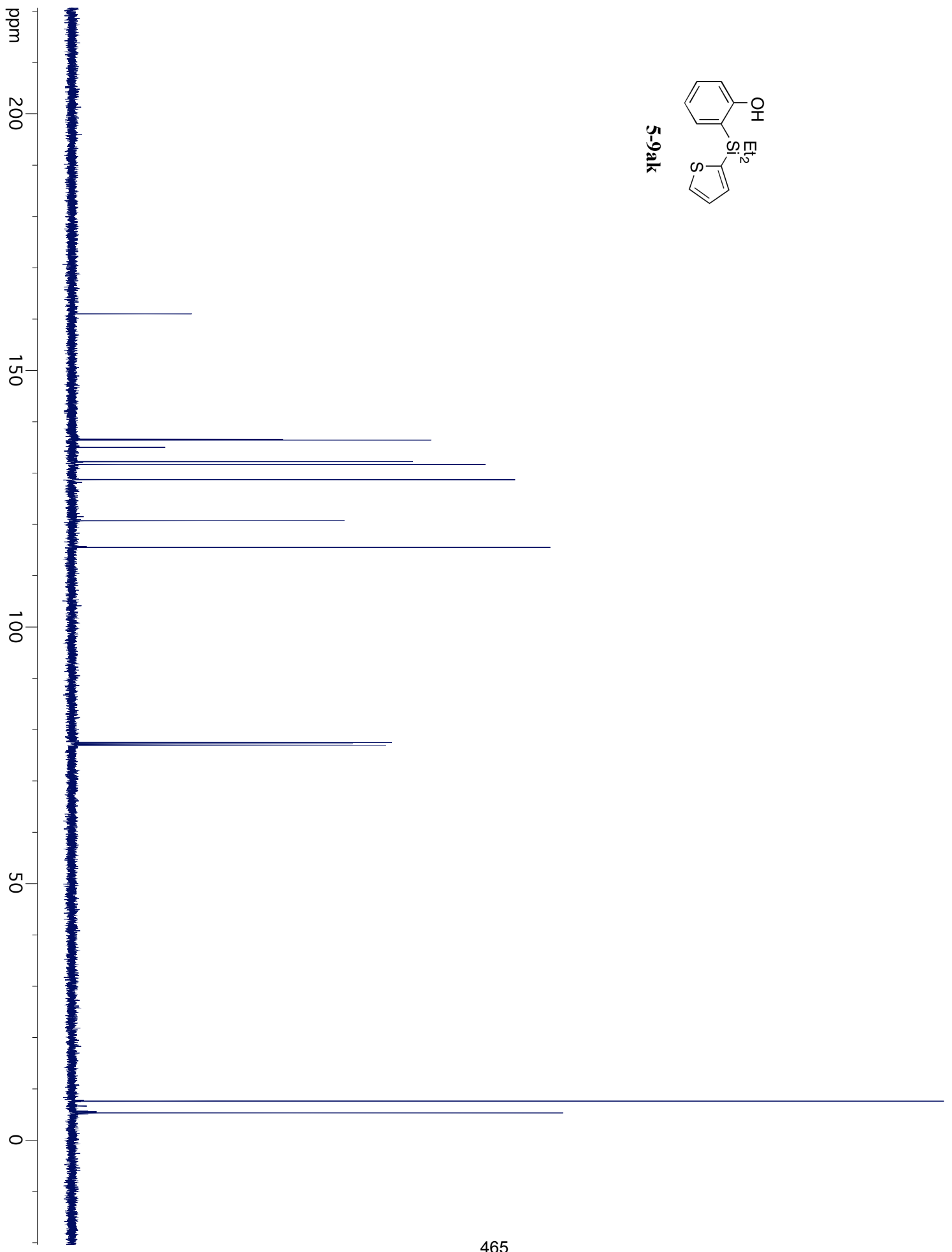
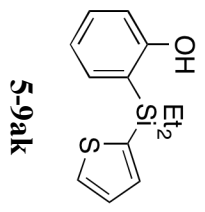


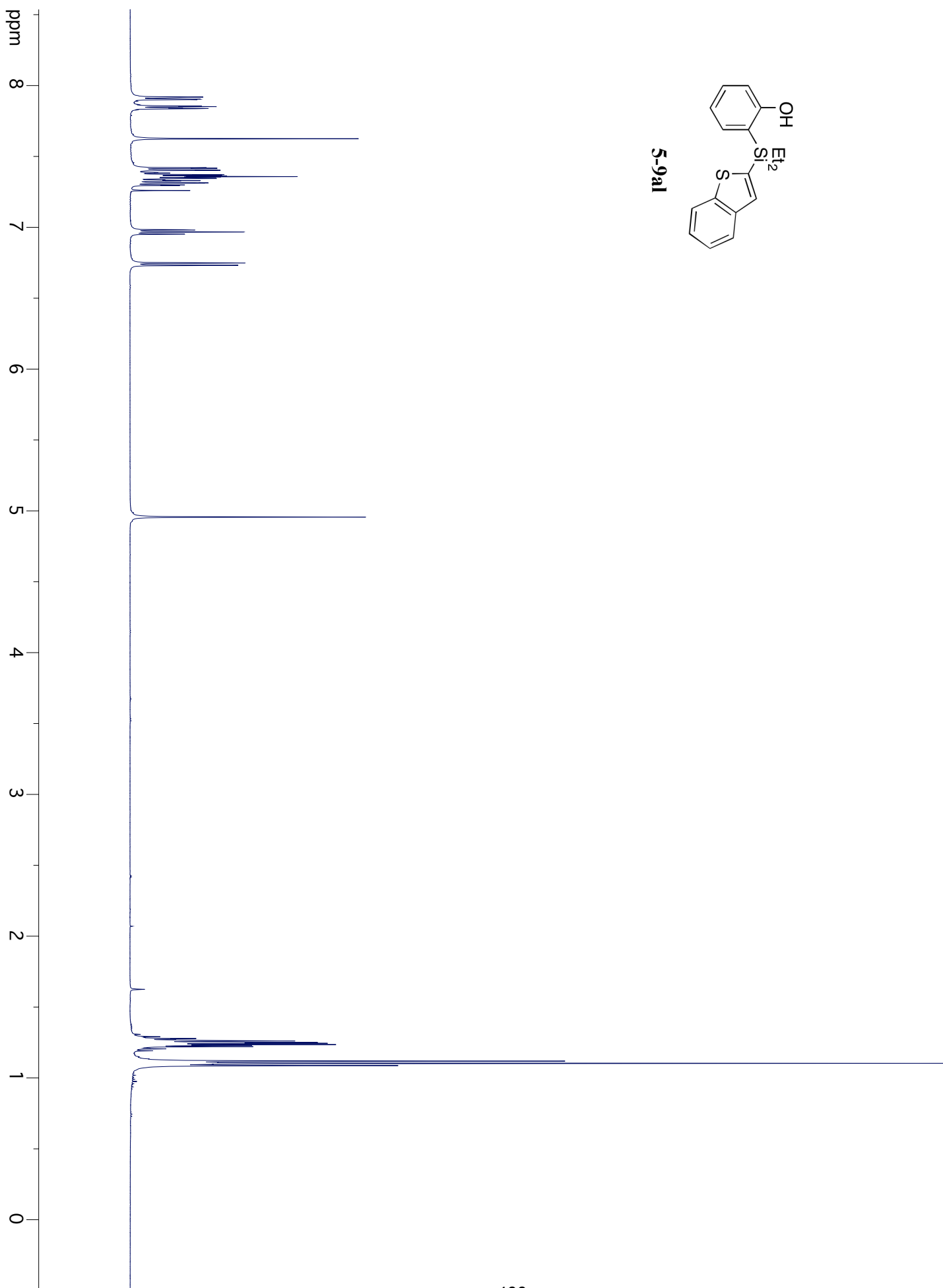
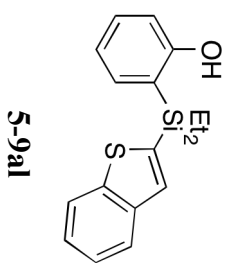


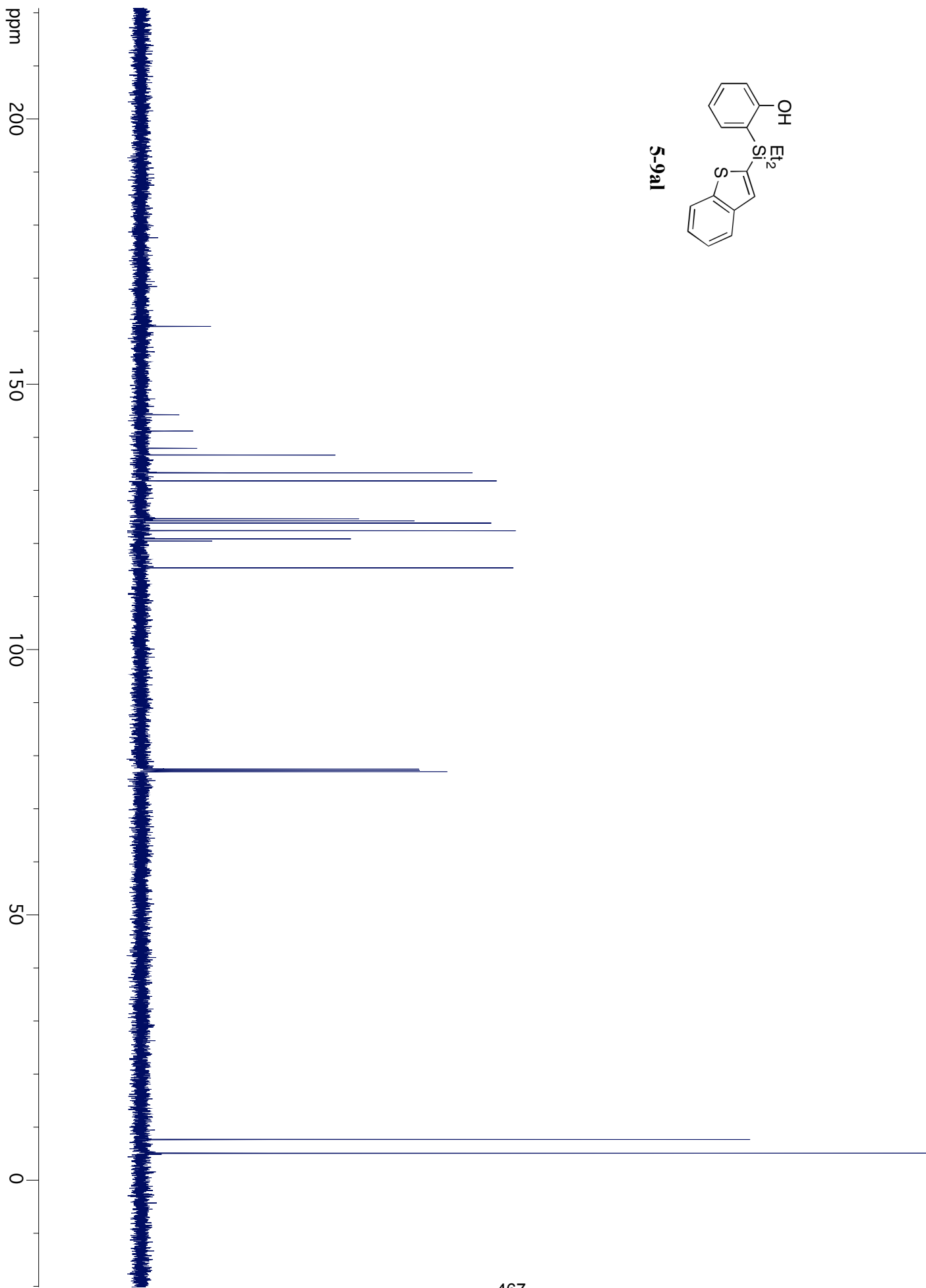
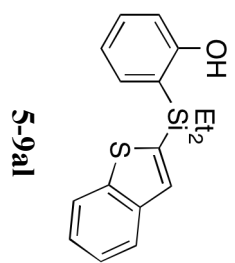


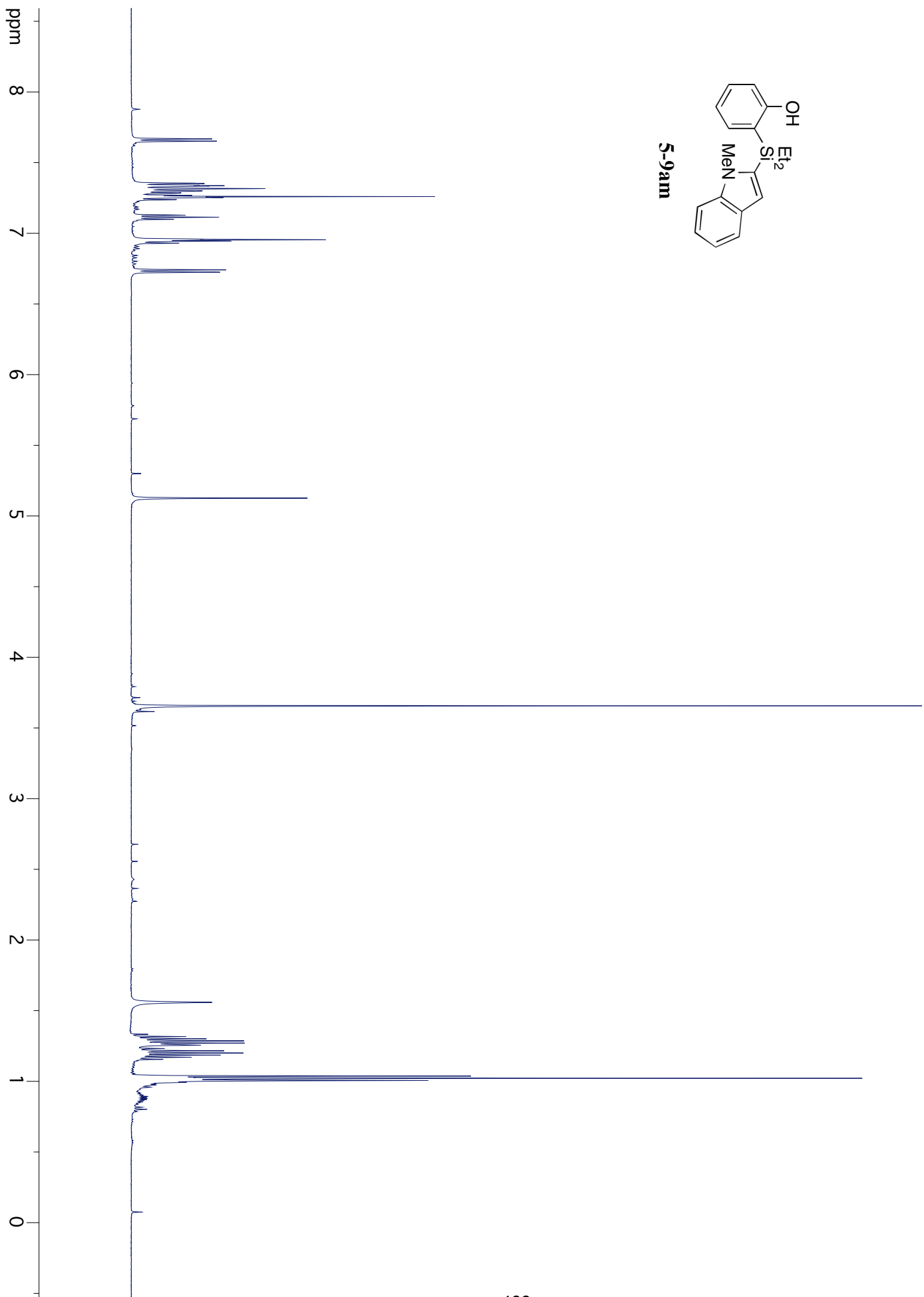
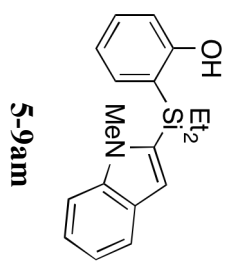


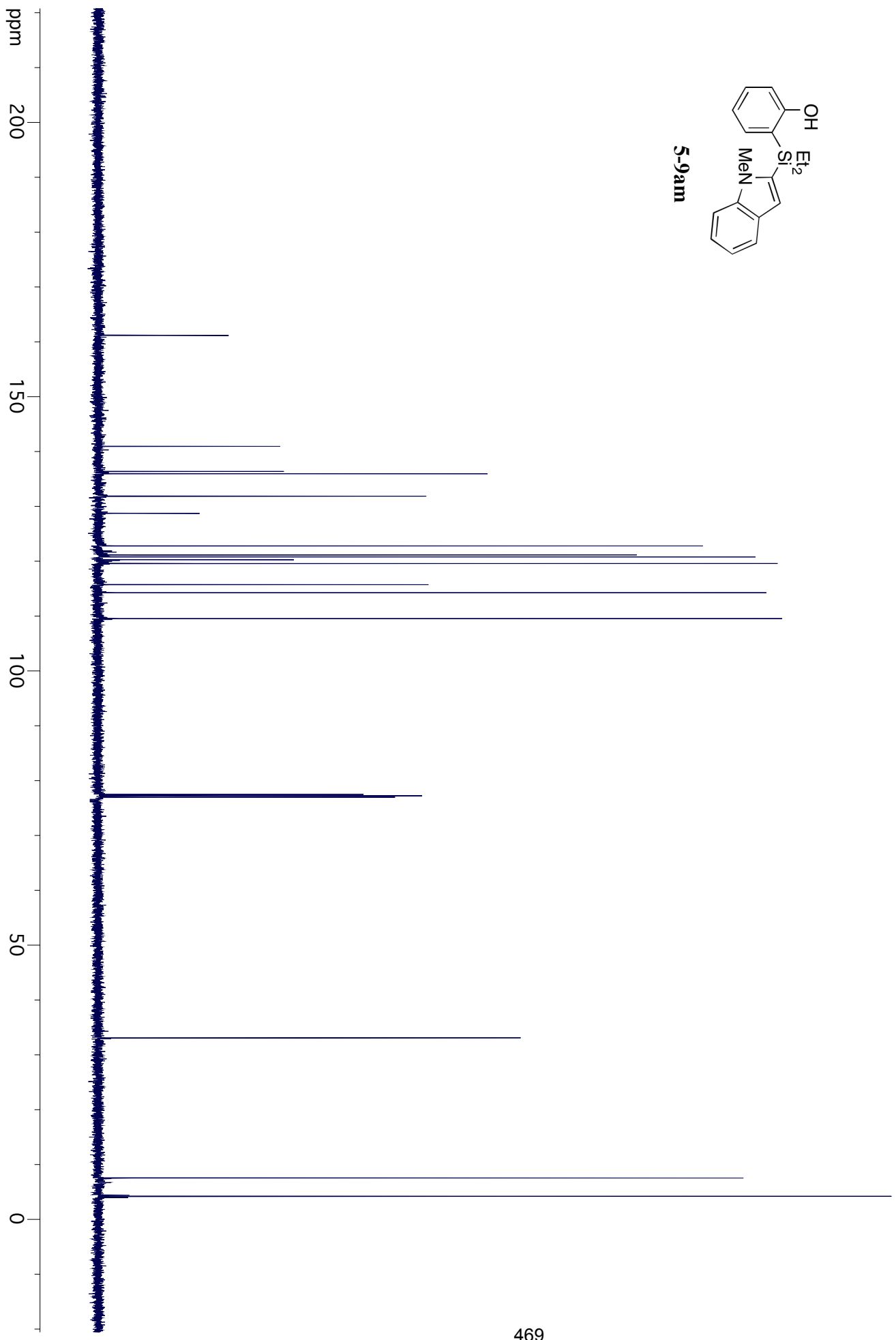
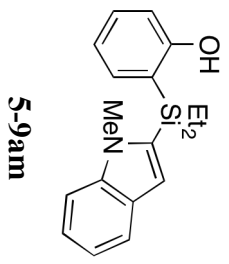


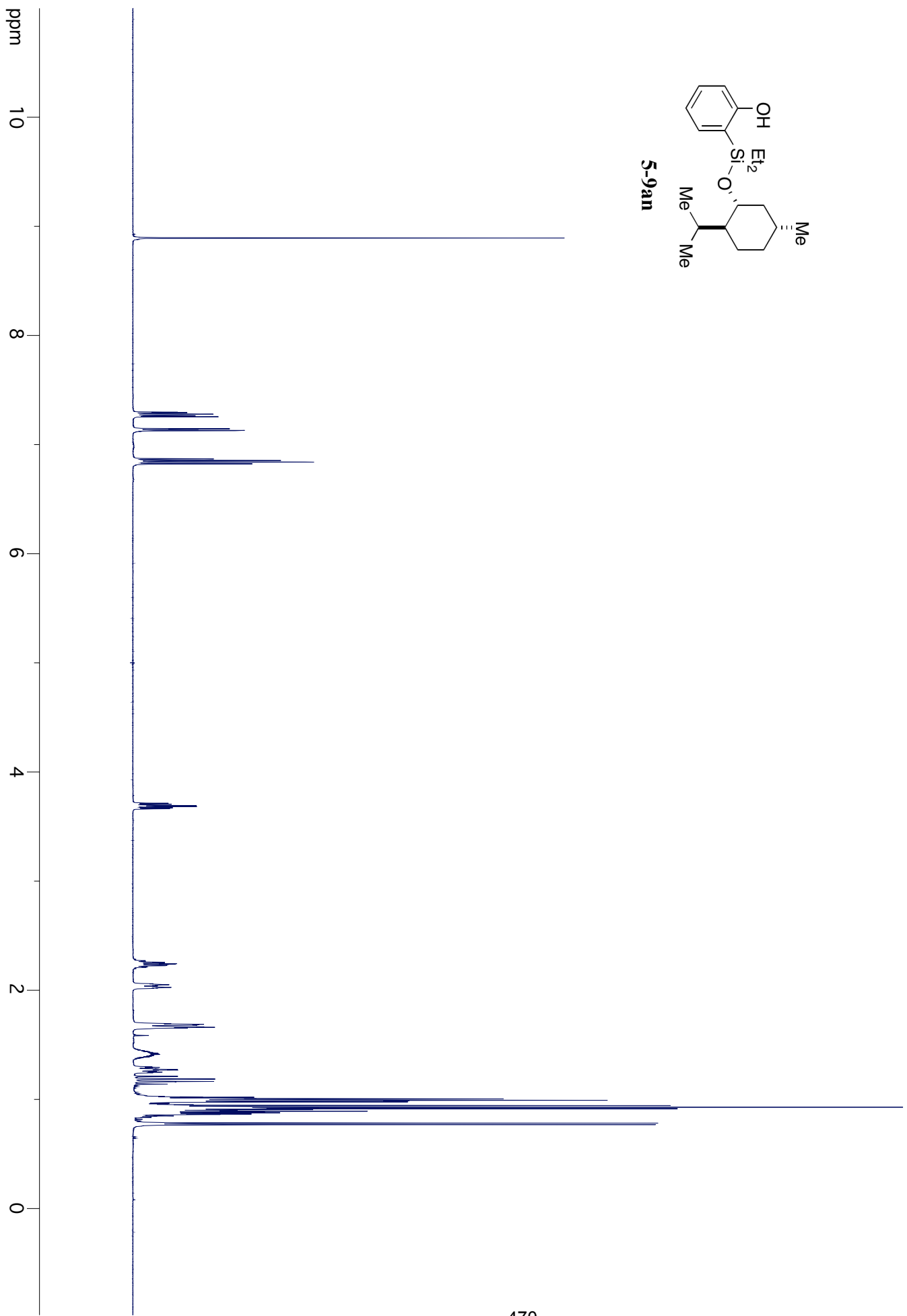
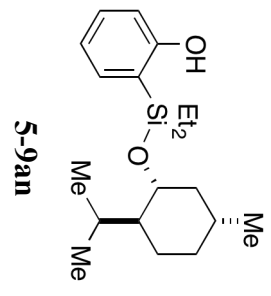


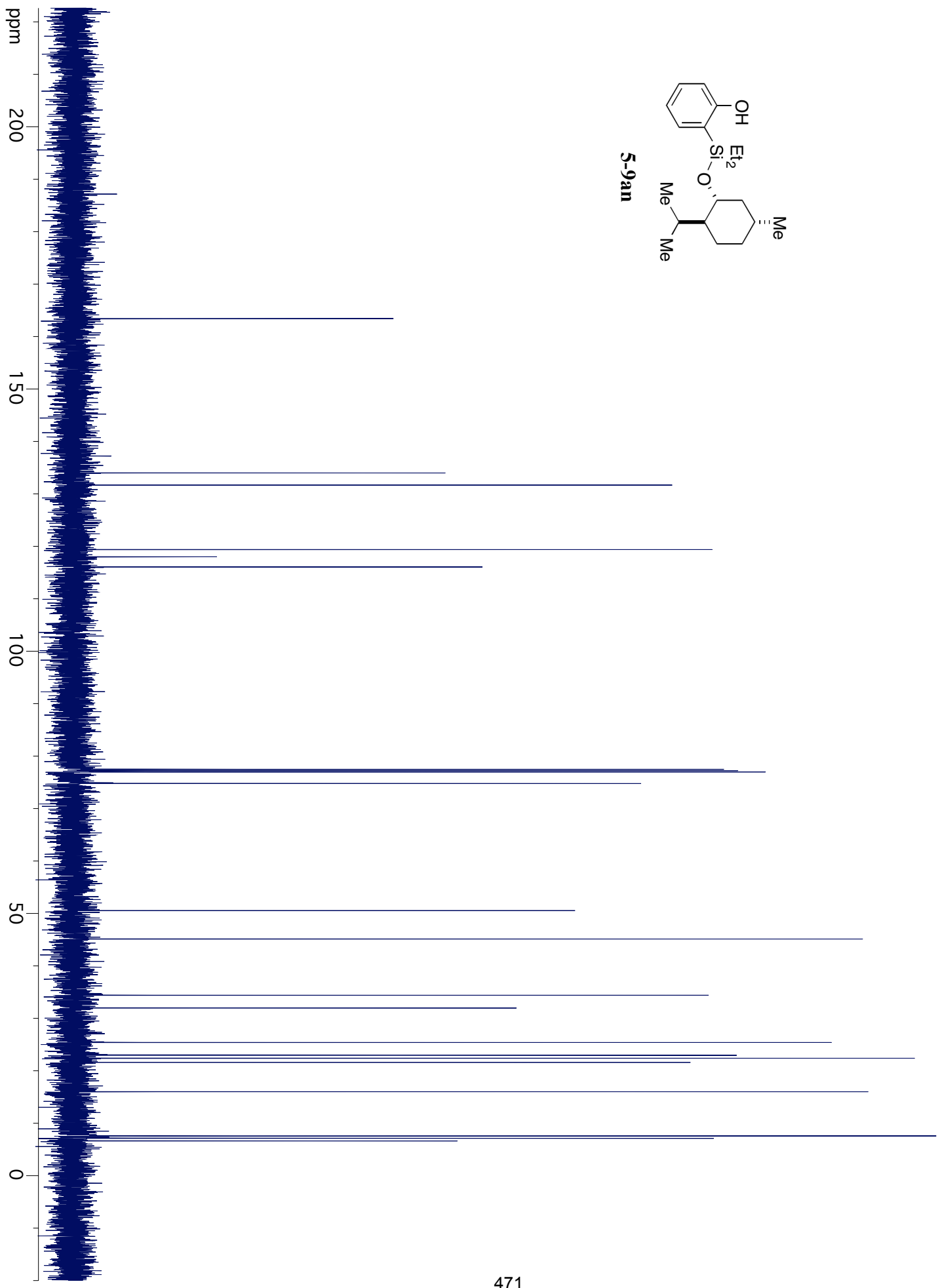
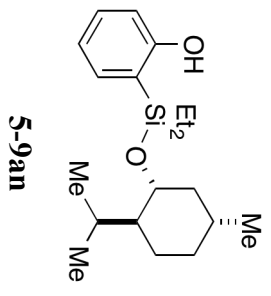


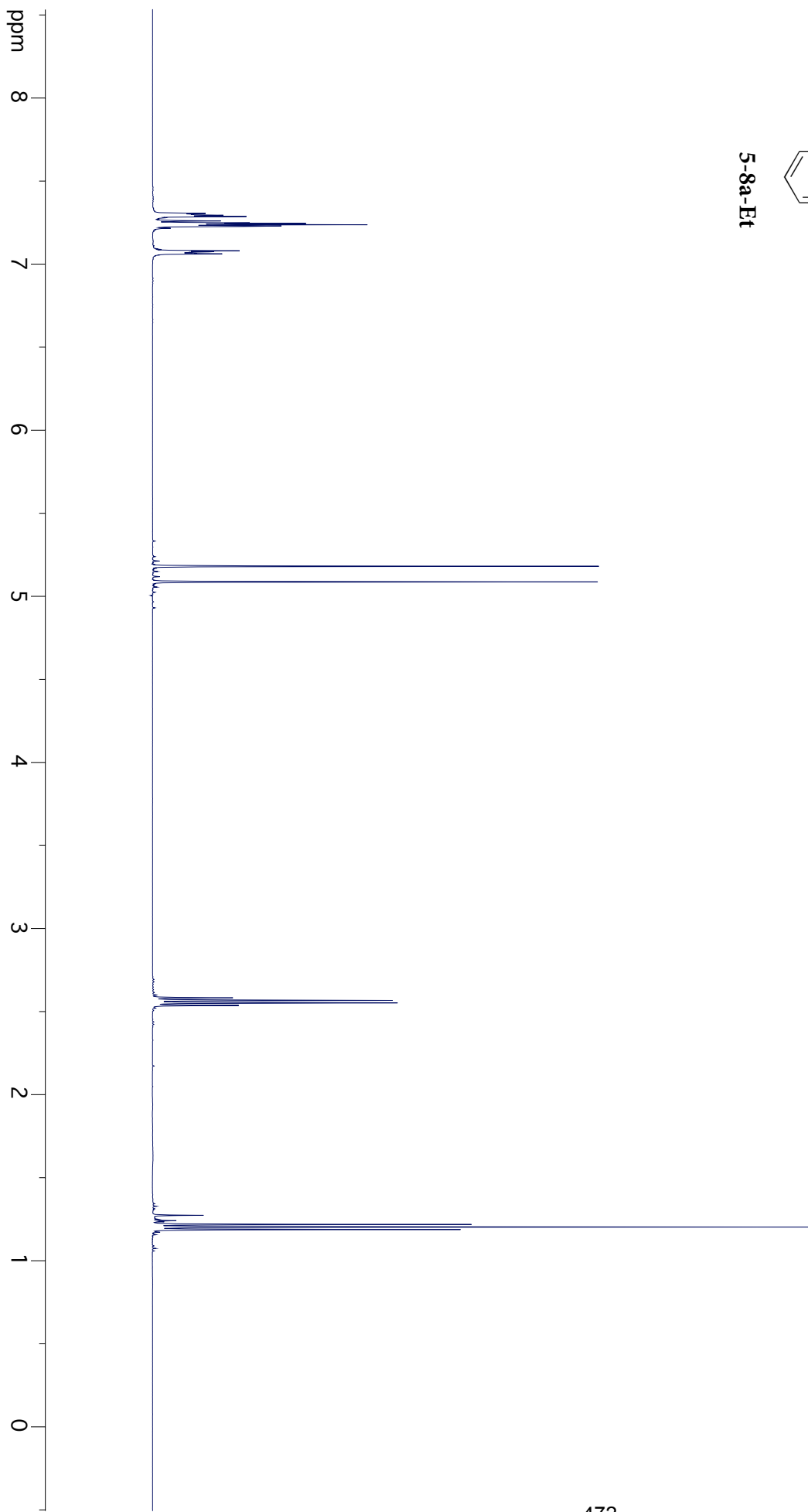
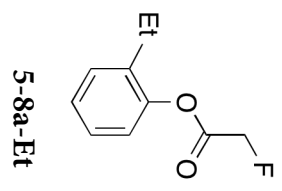


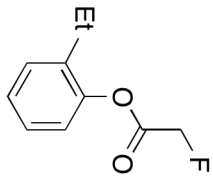




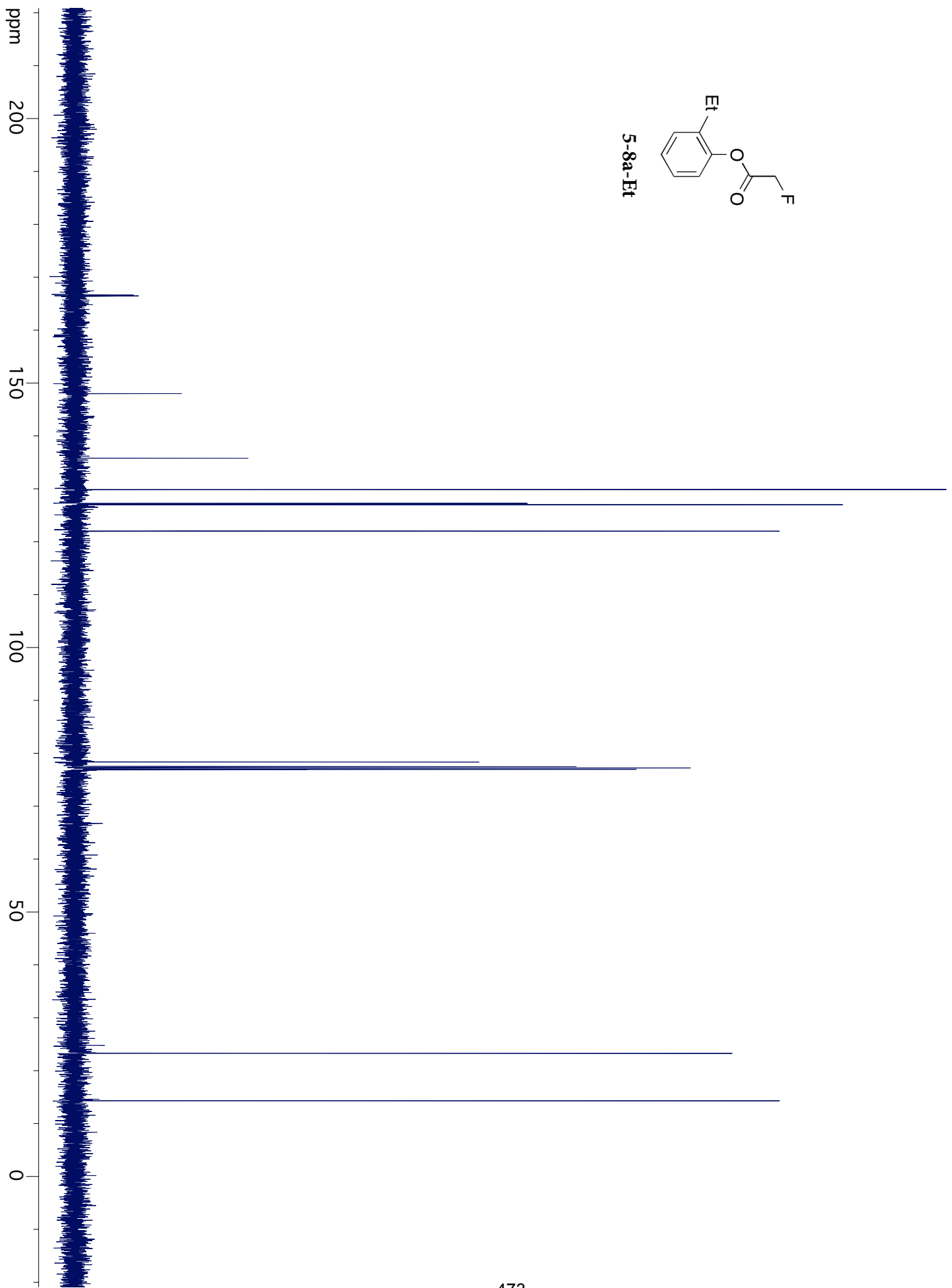


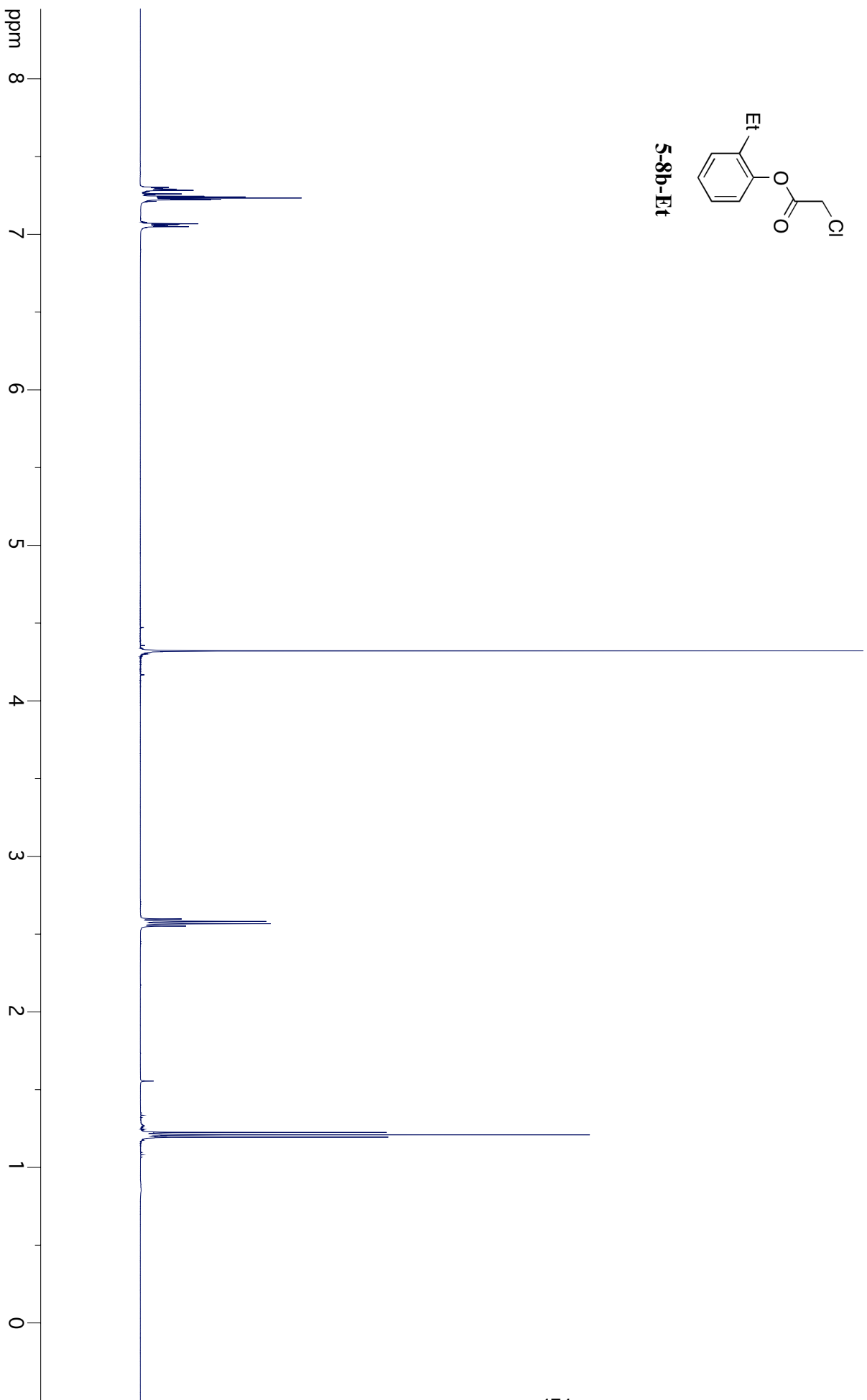
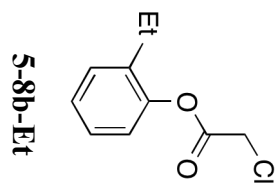


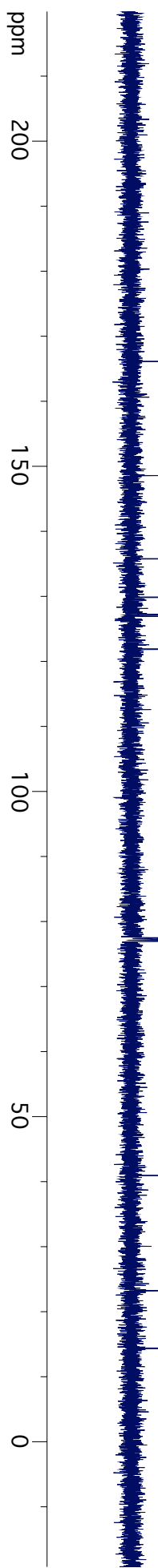
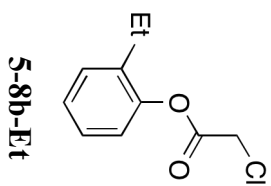


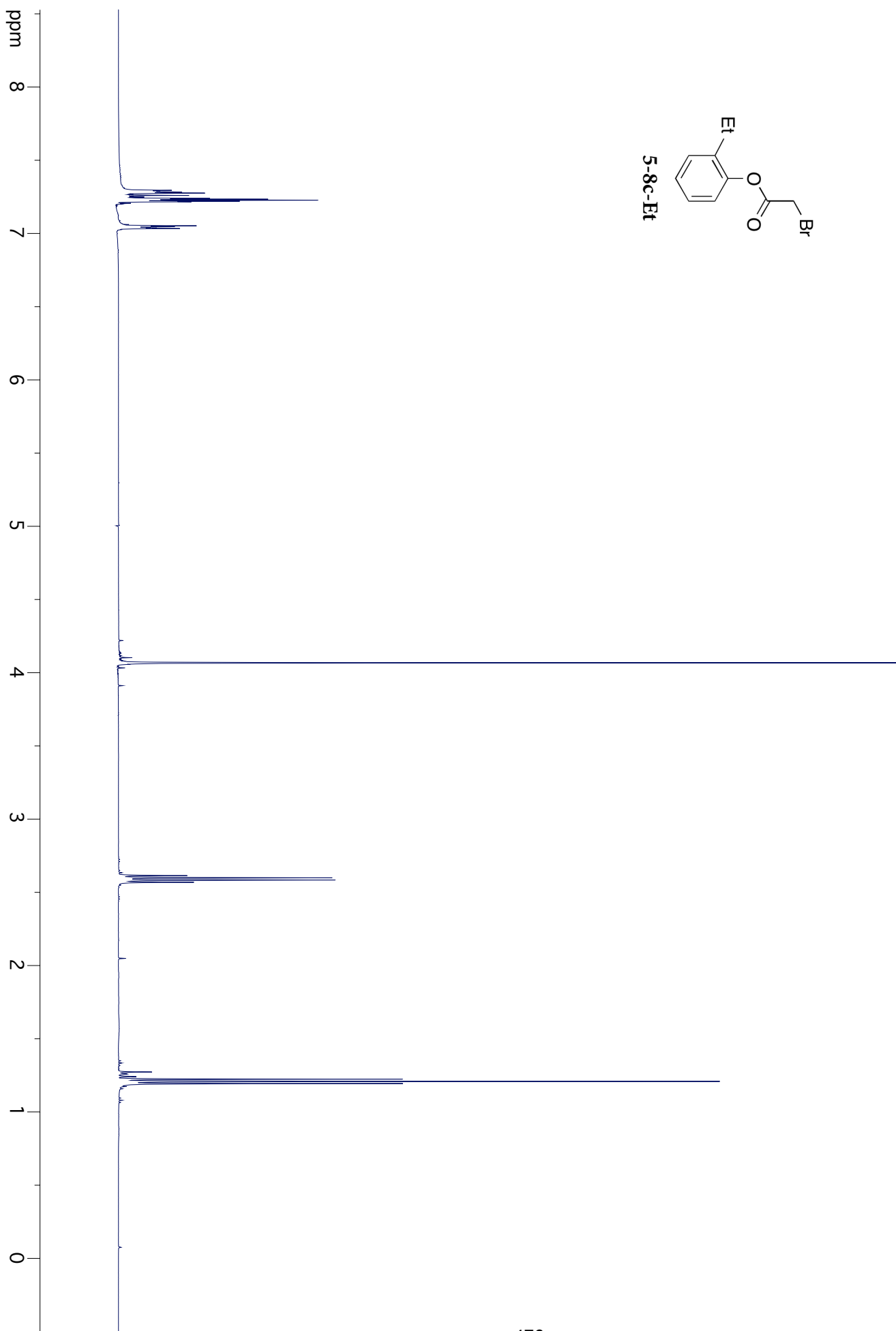
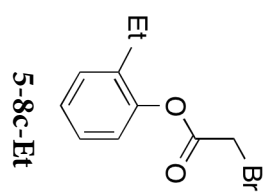


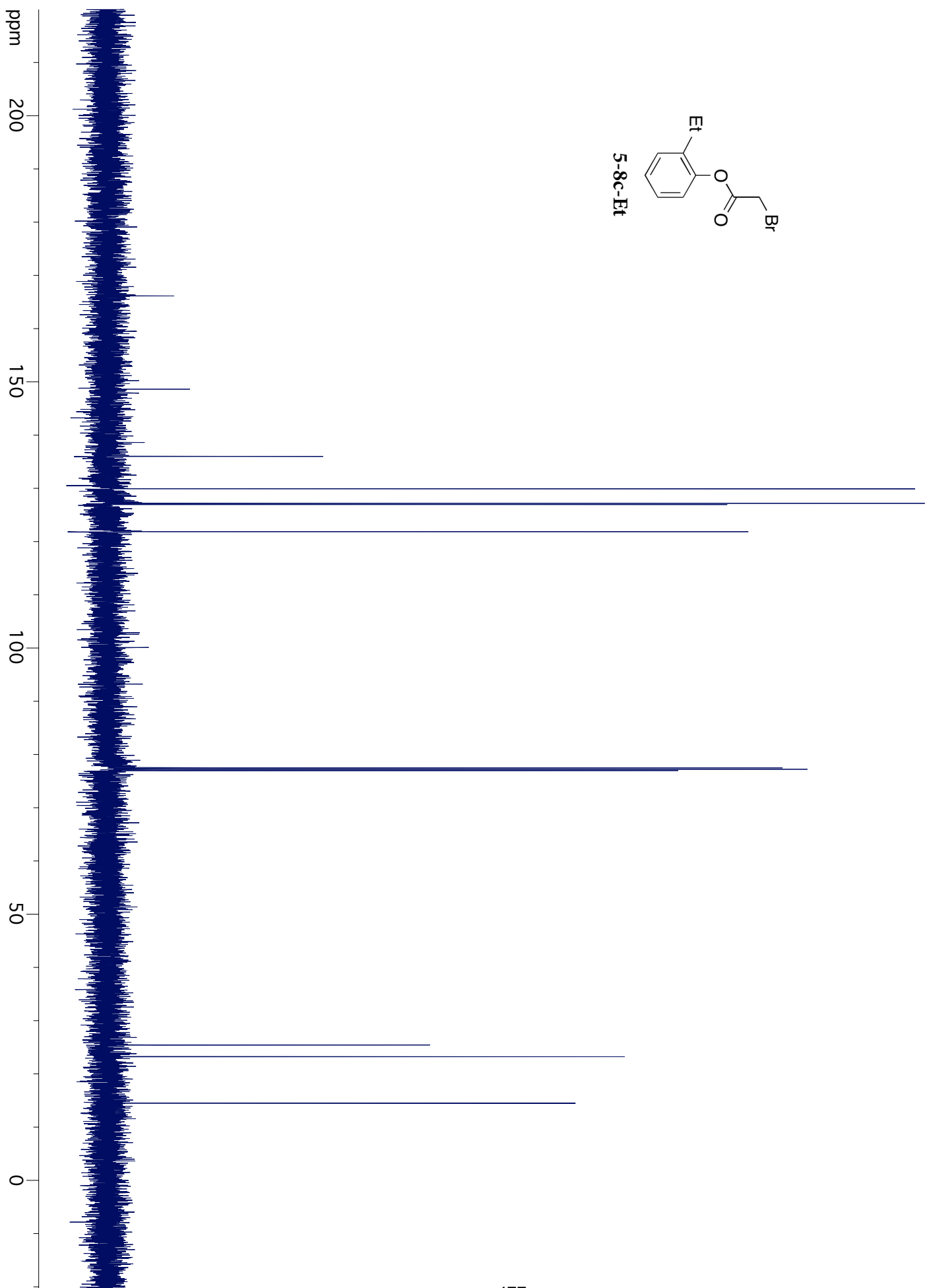
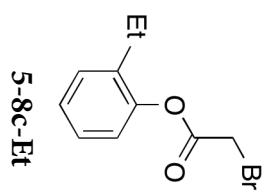
5-8a-Et

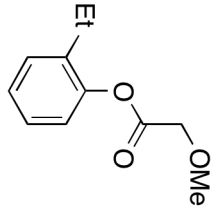




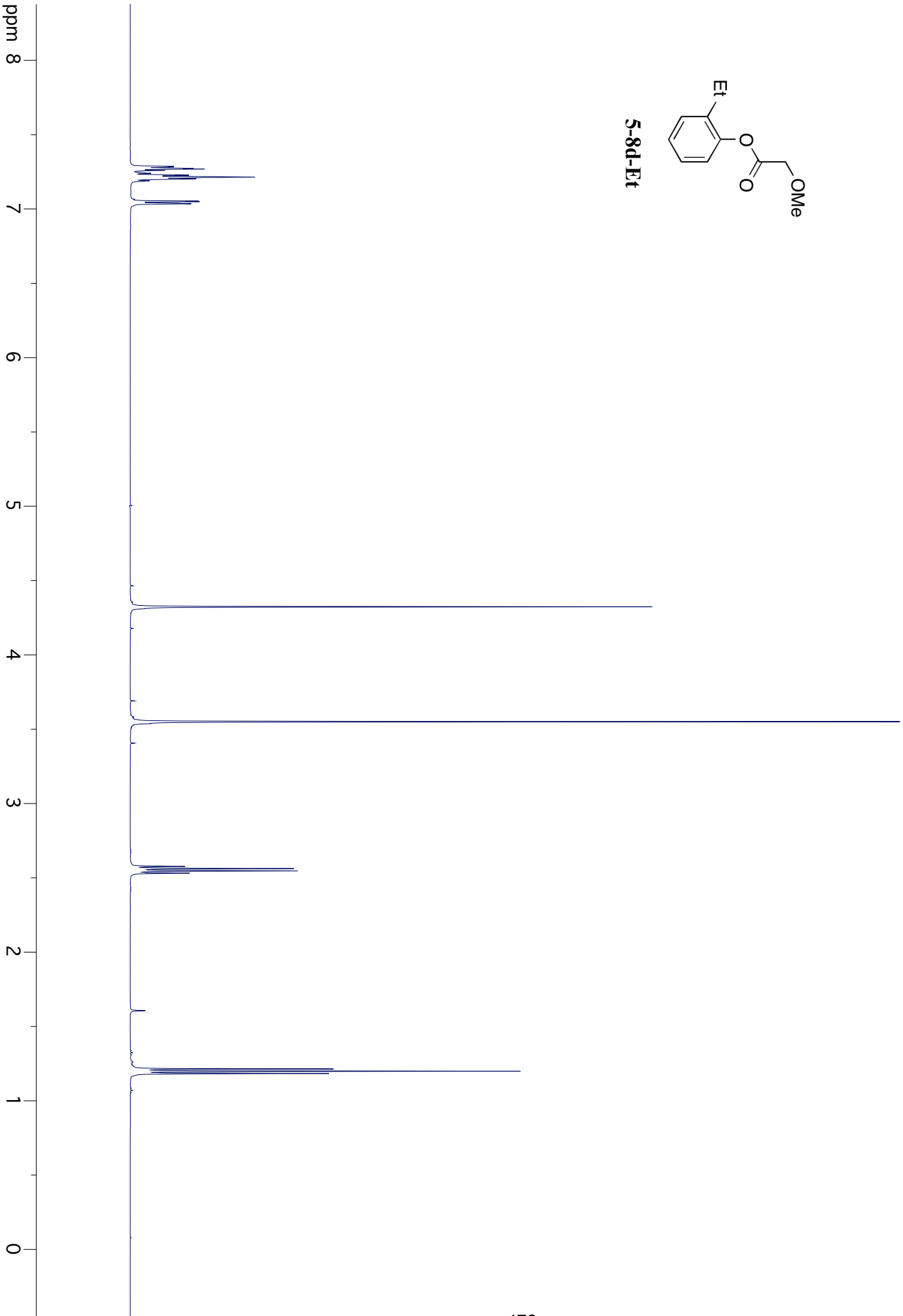


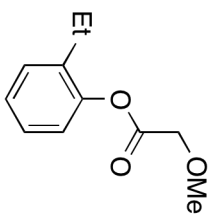




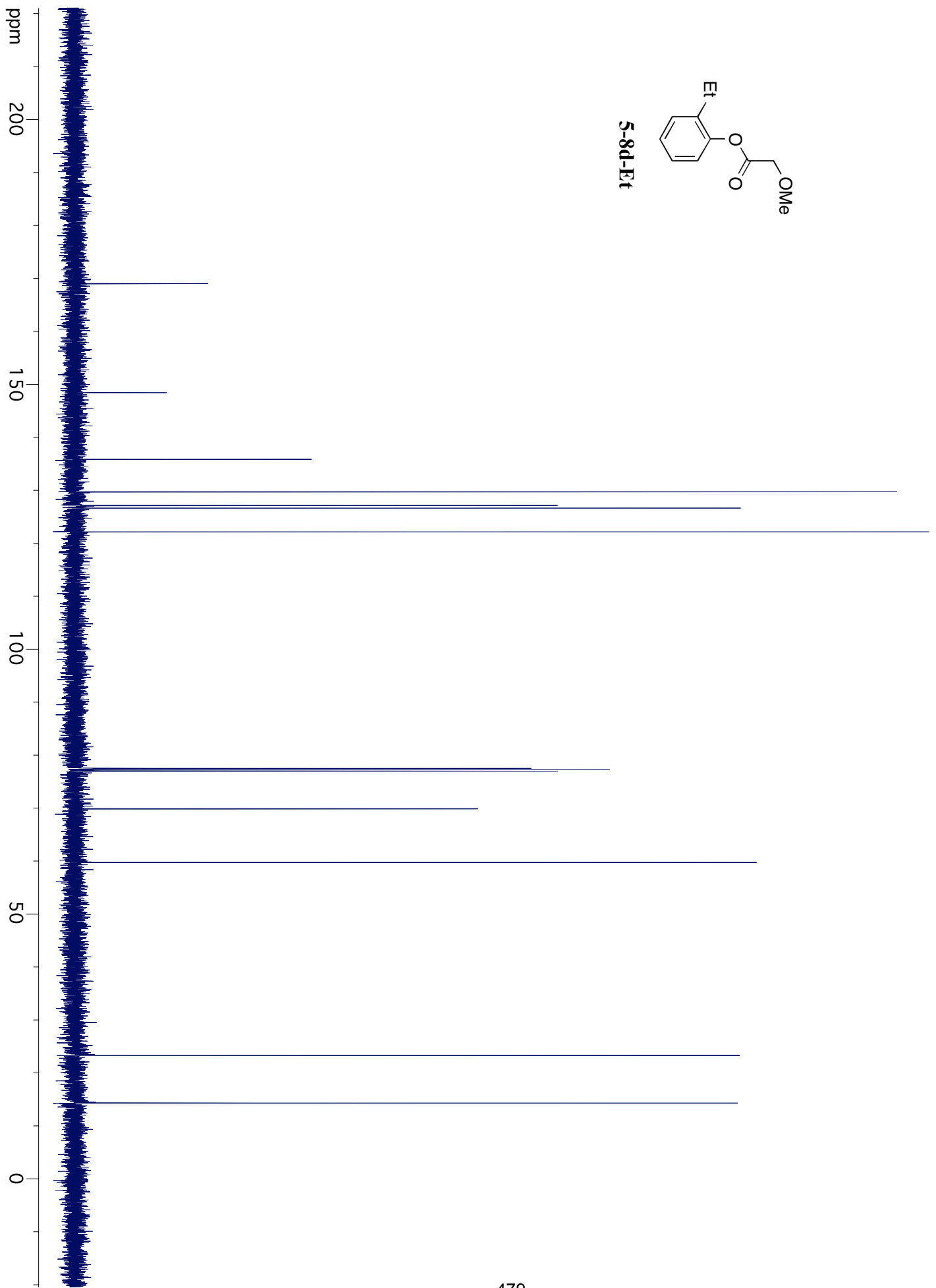


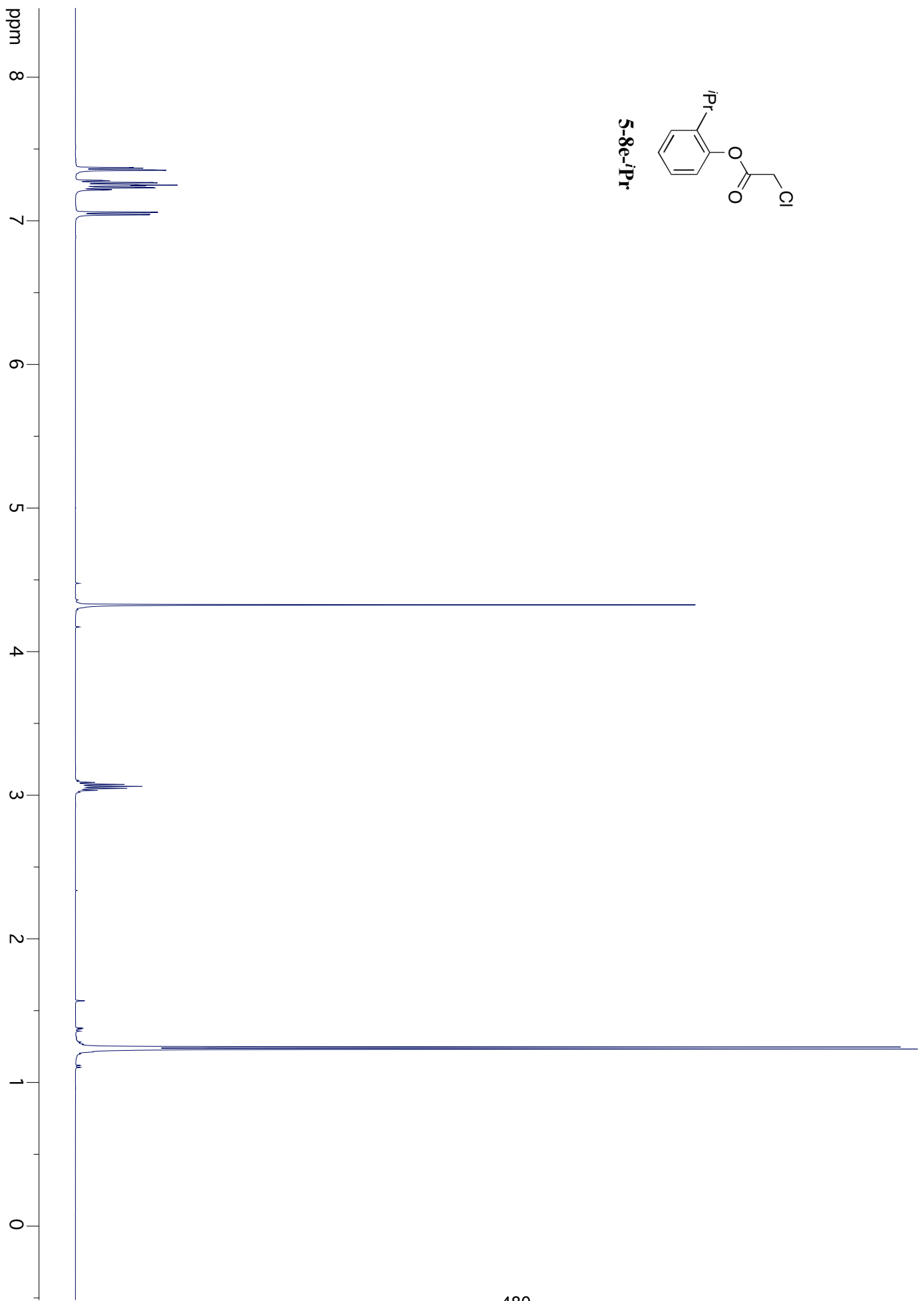
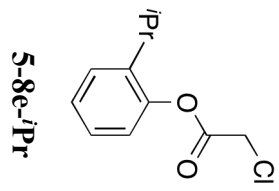
5-8d-Et

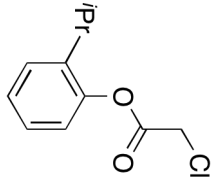




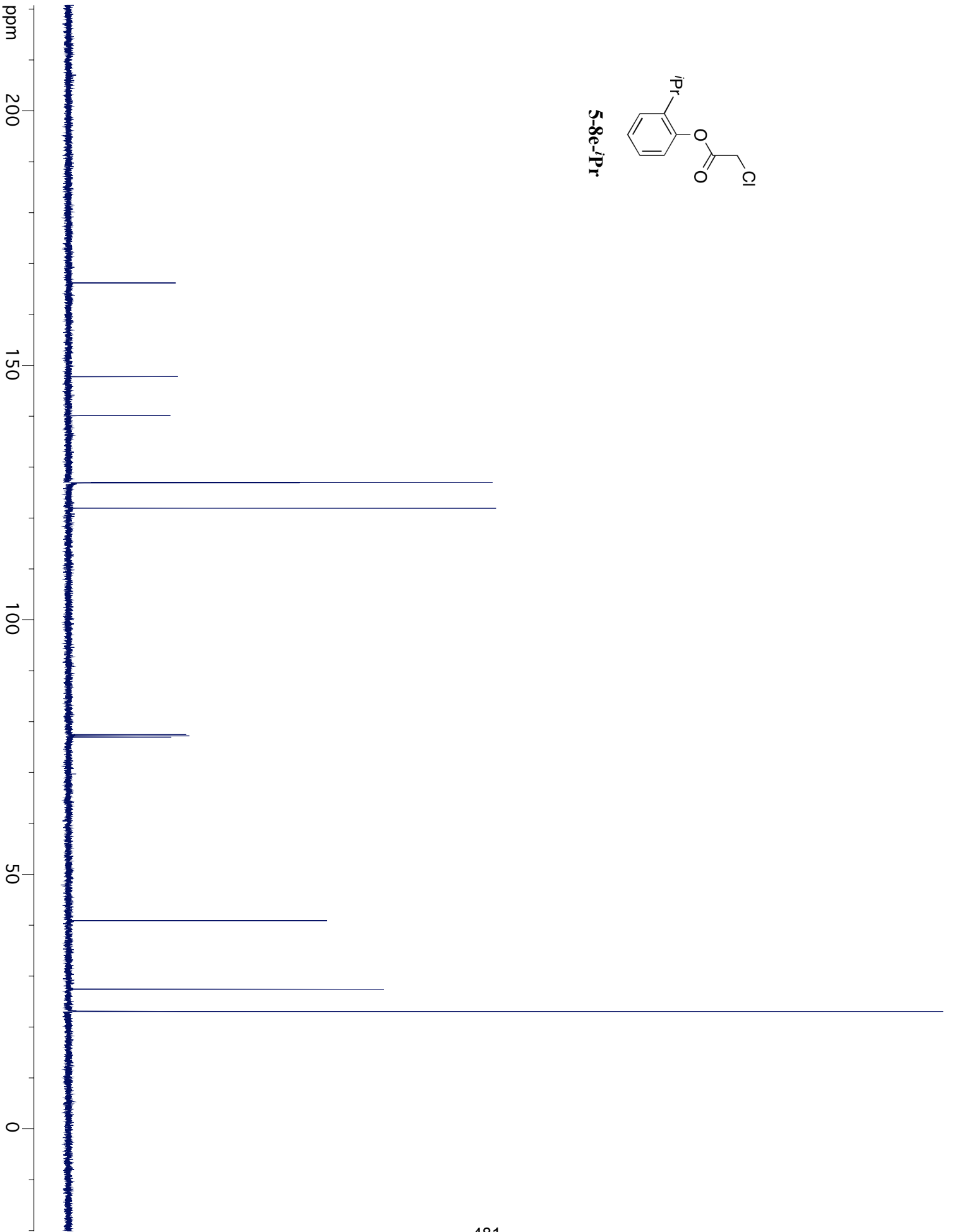
5-8d-Et

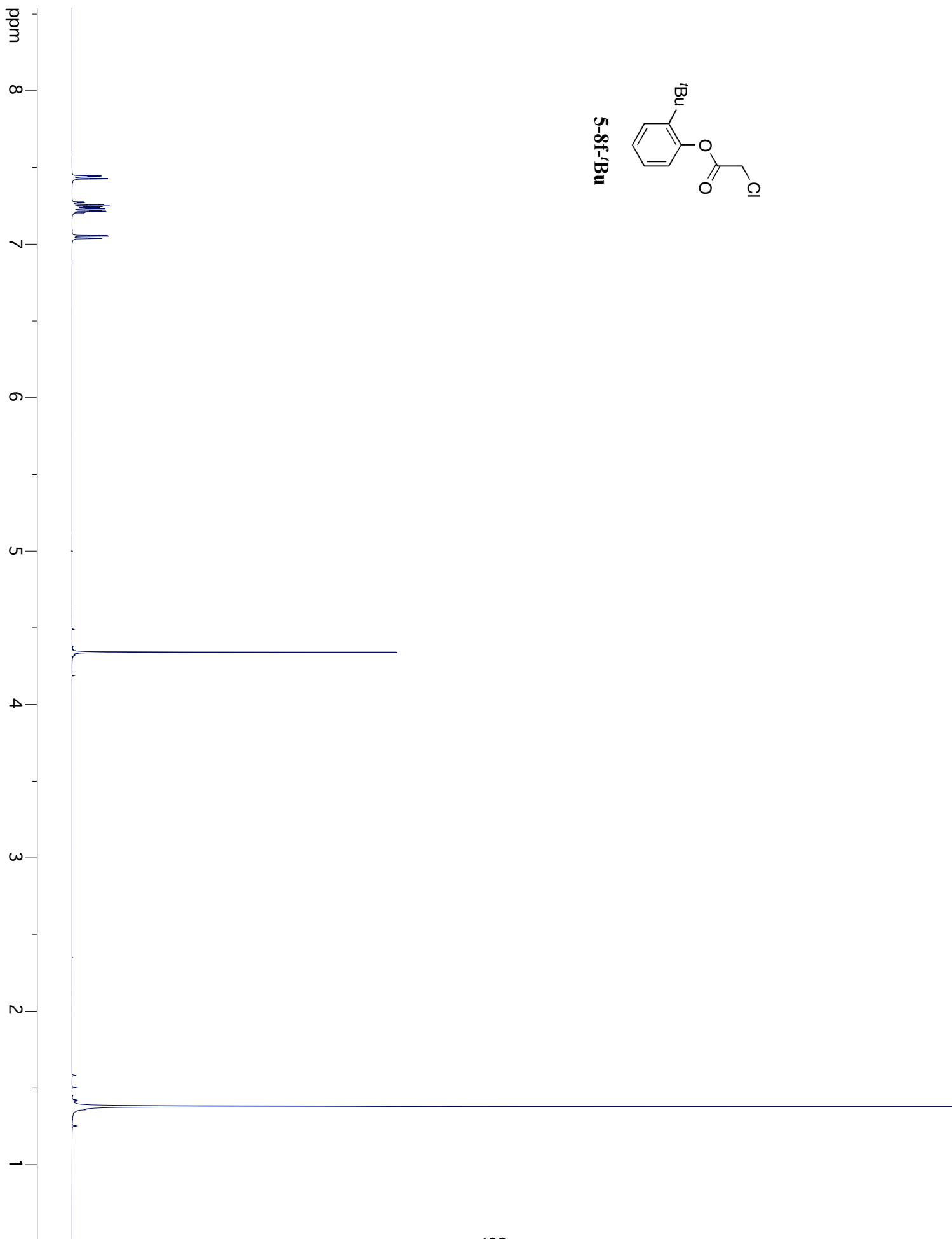
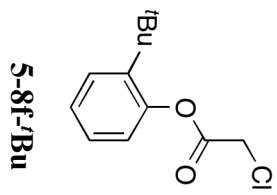


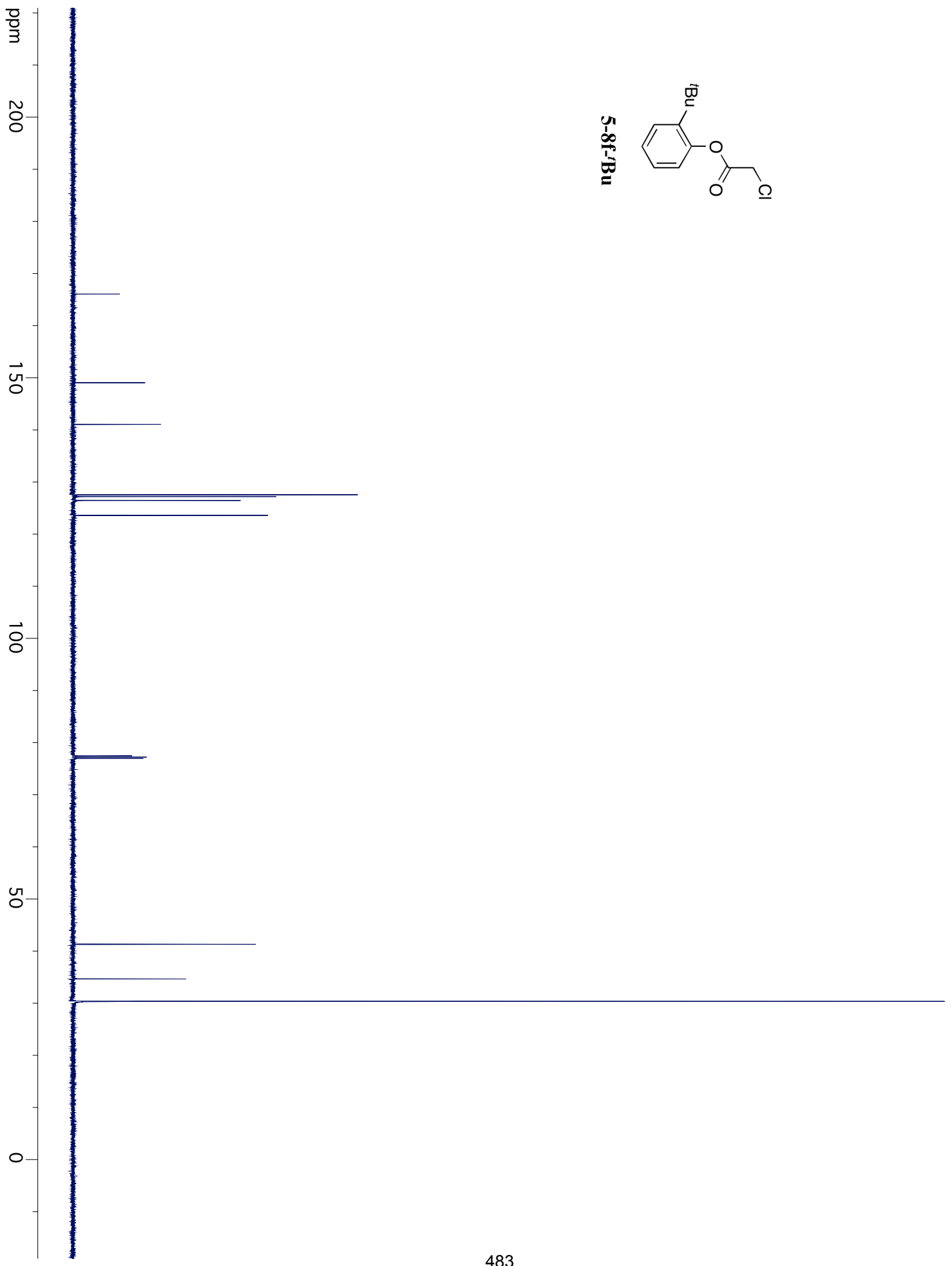
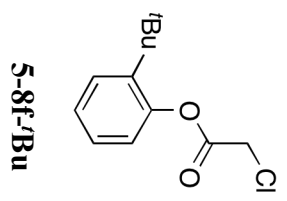


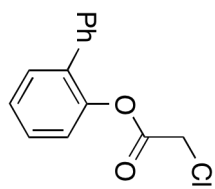


5-8-e-iPr

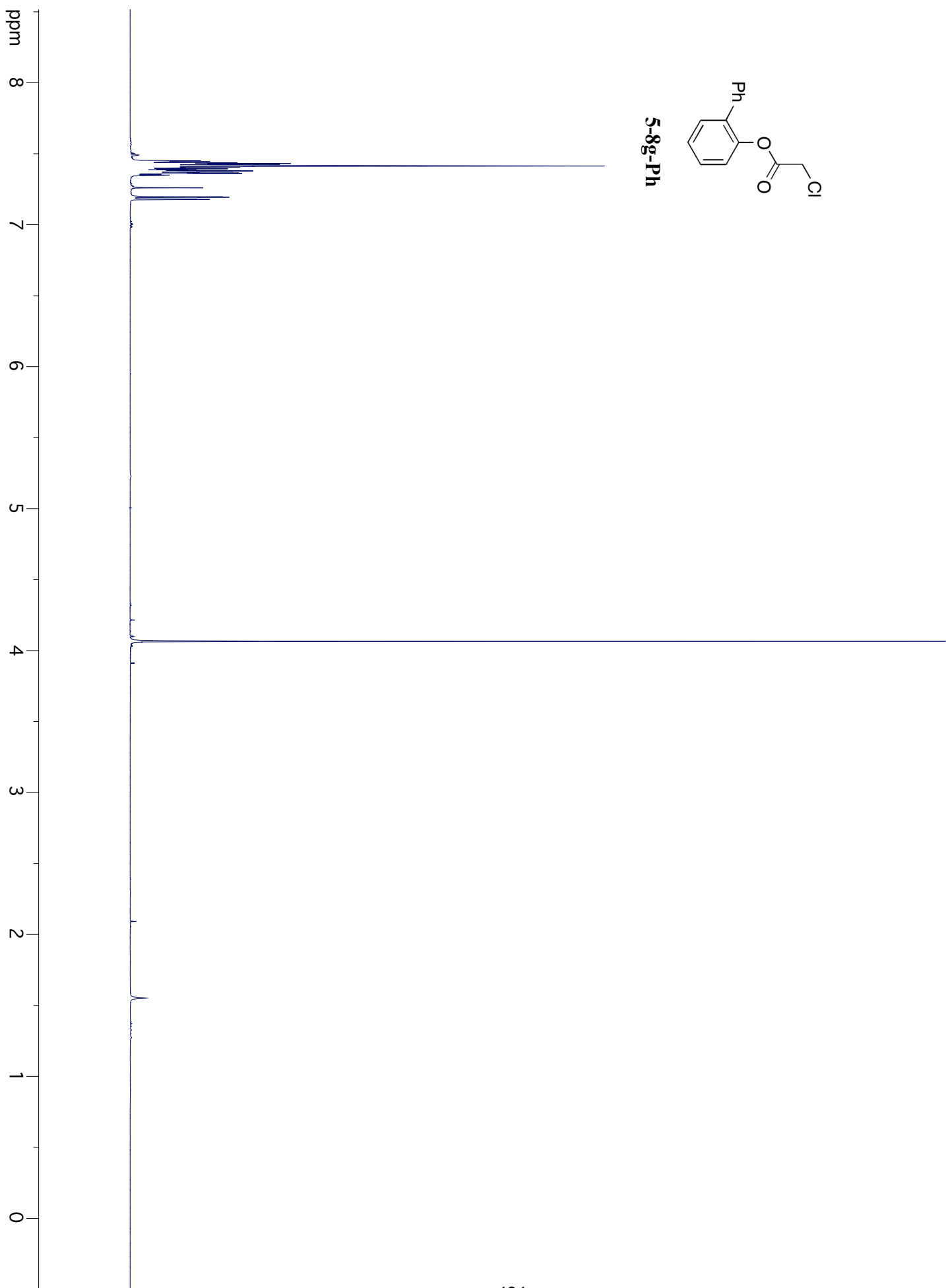


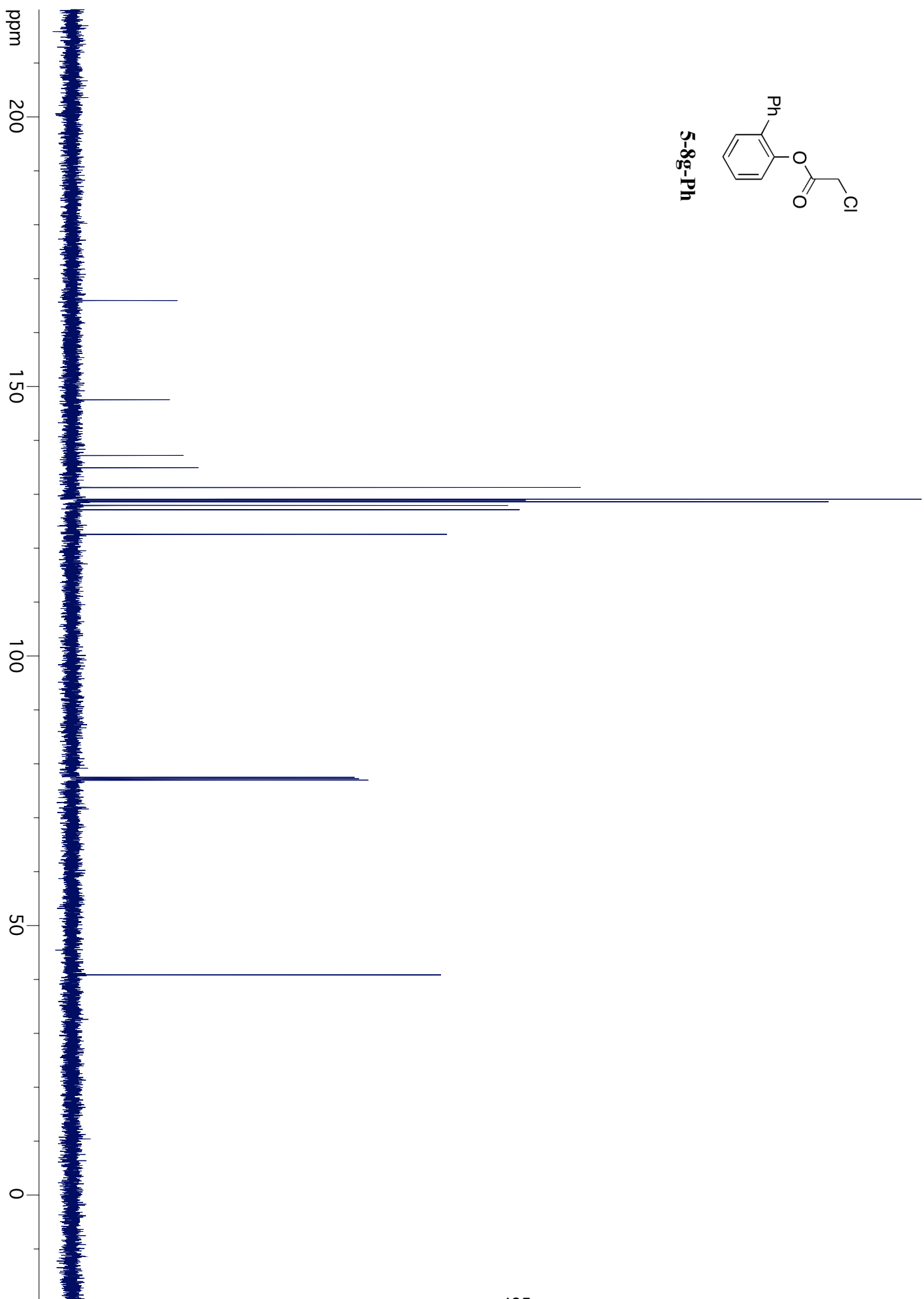
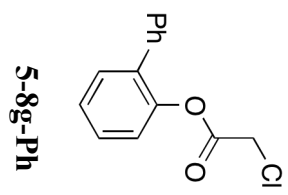


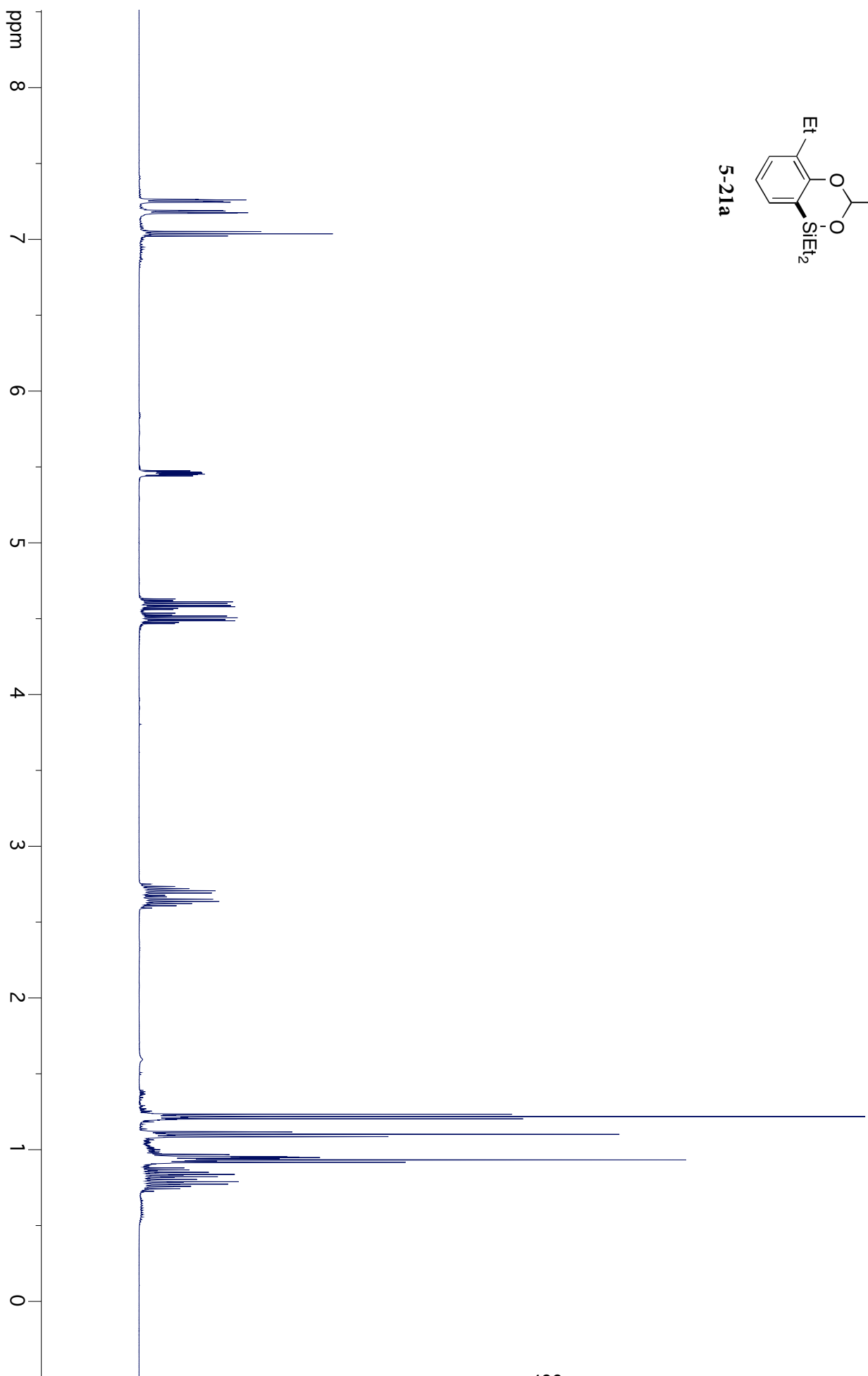
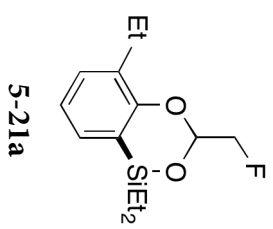


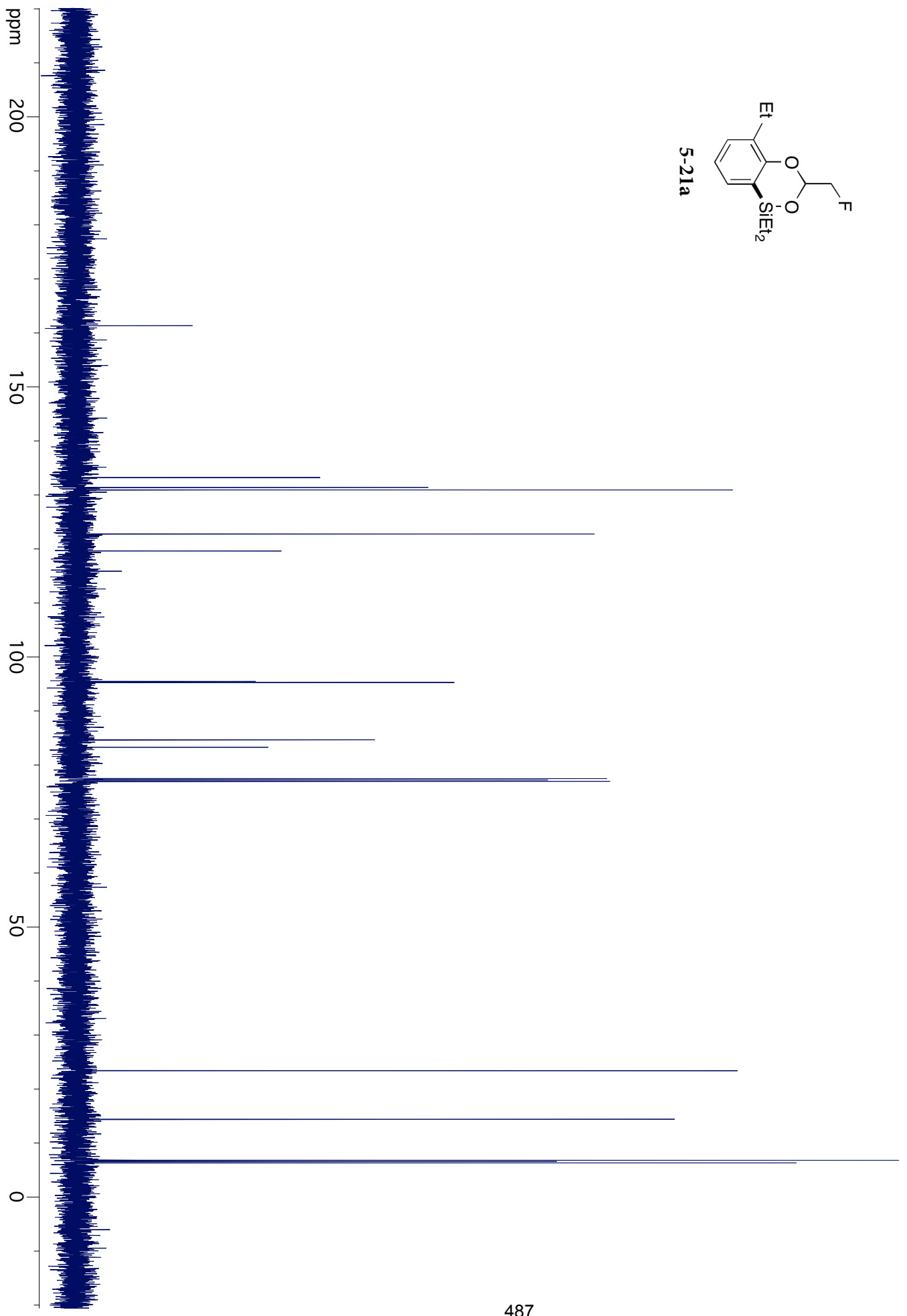
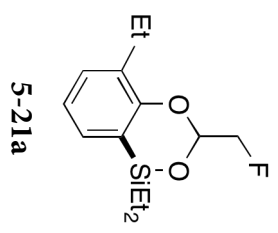


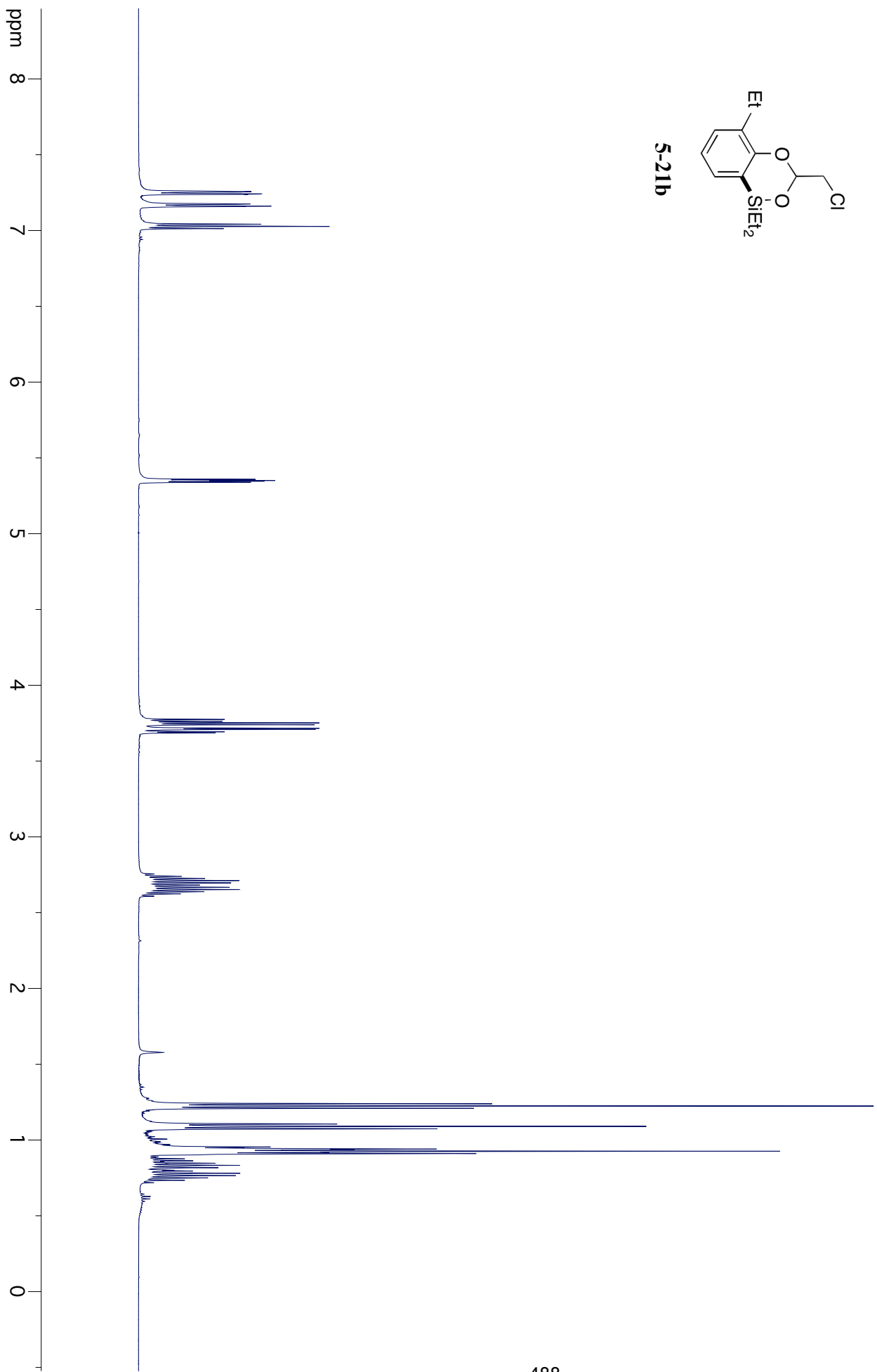
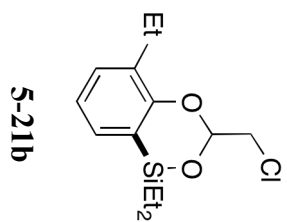
5-8g-Ph

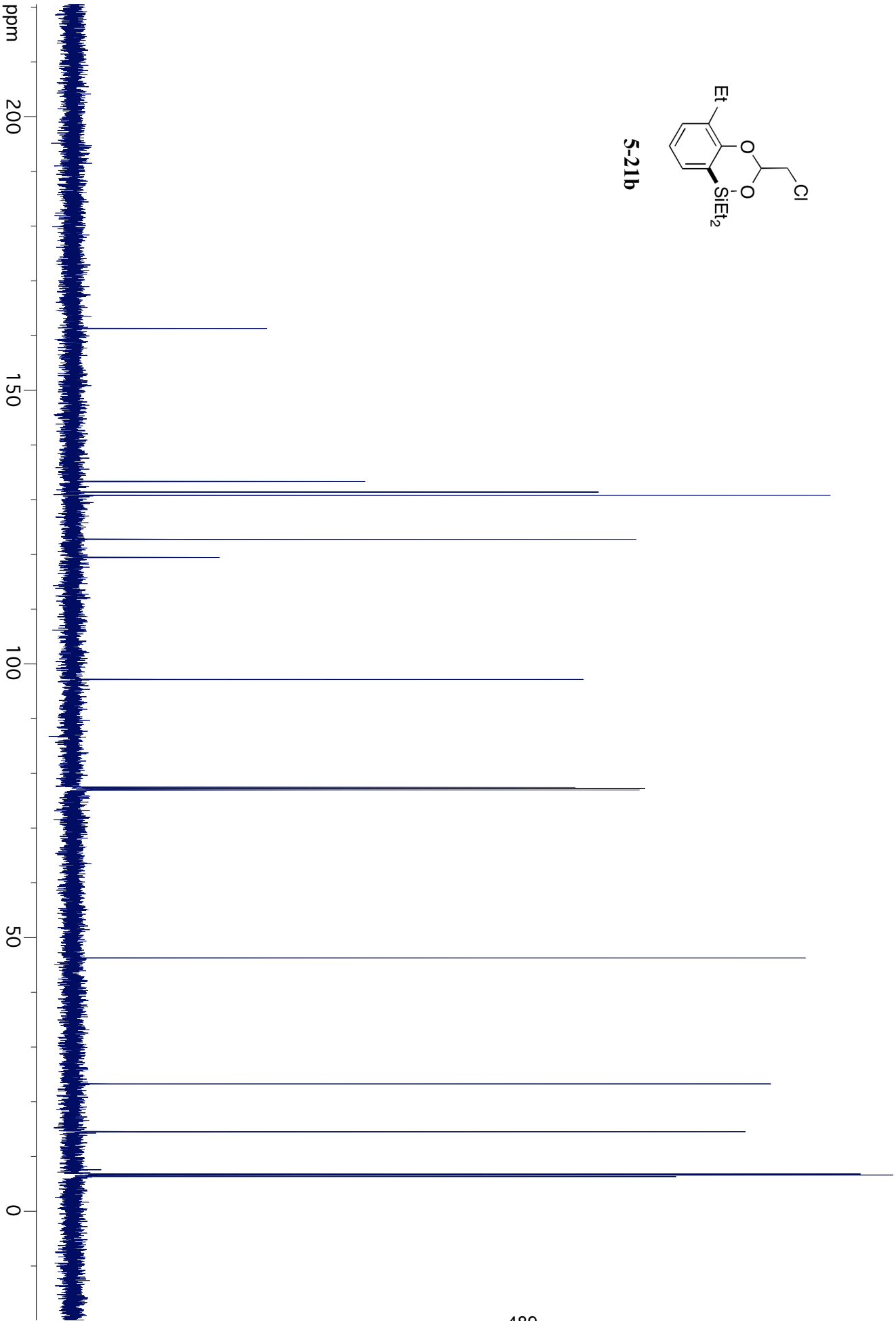
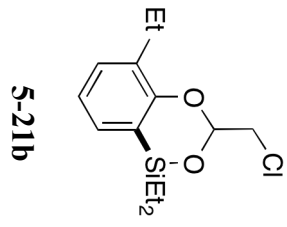


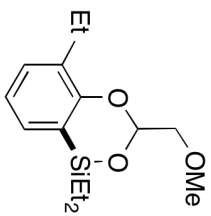




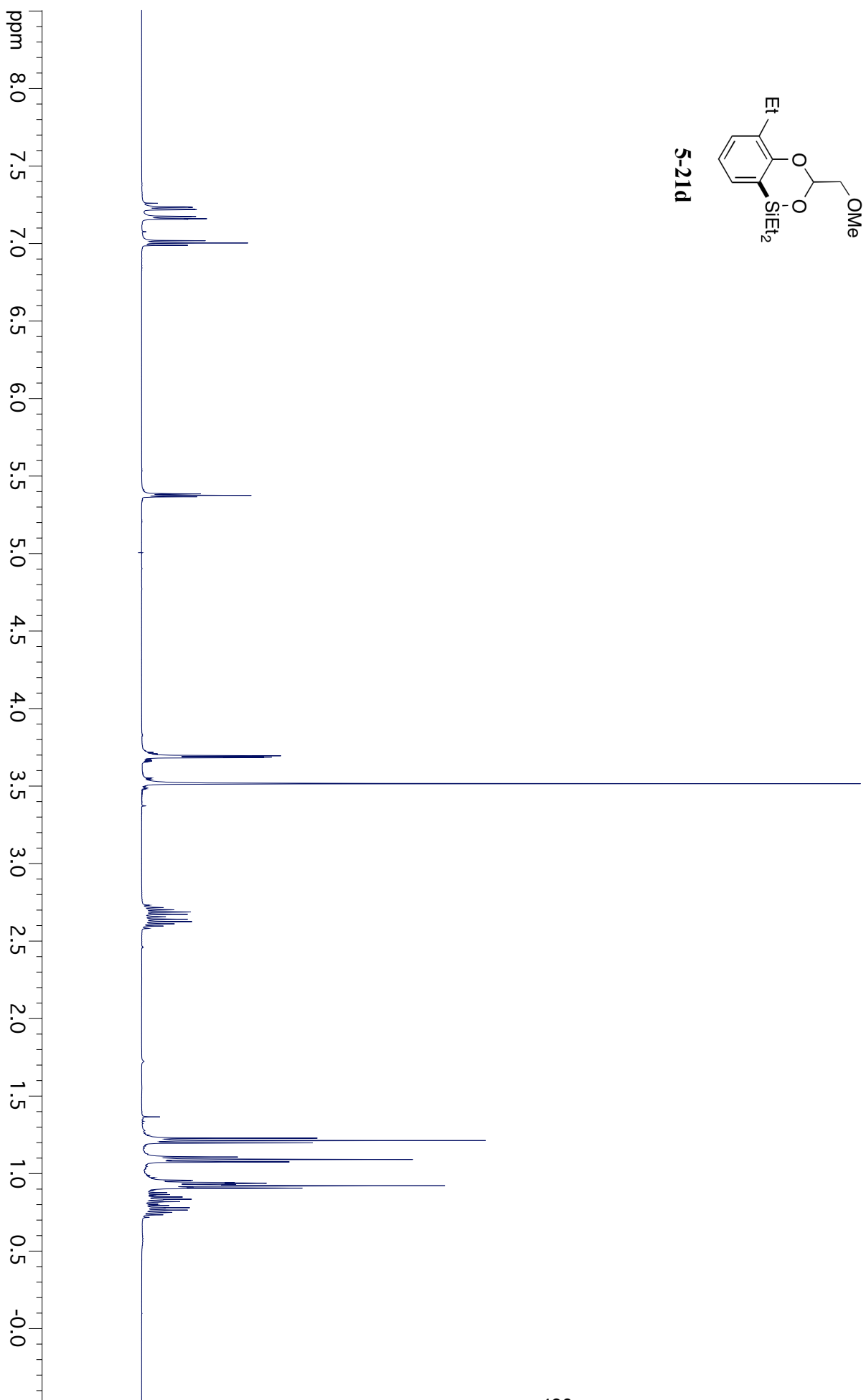


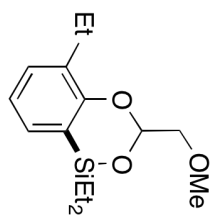




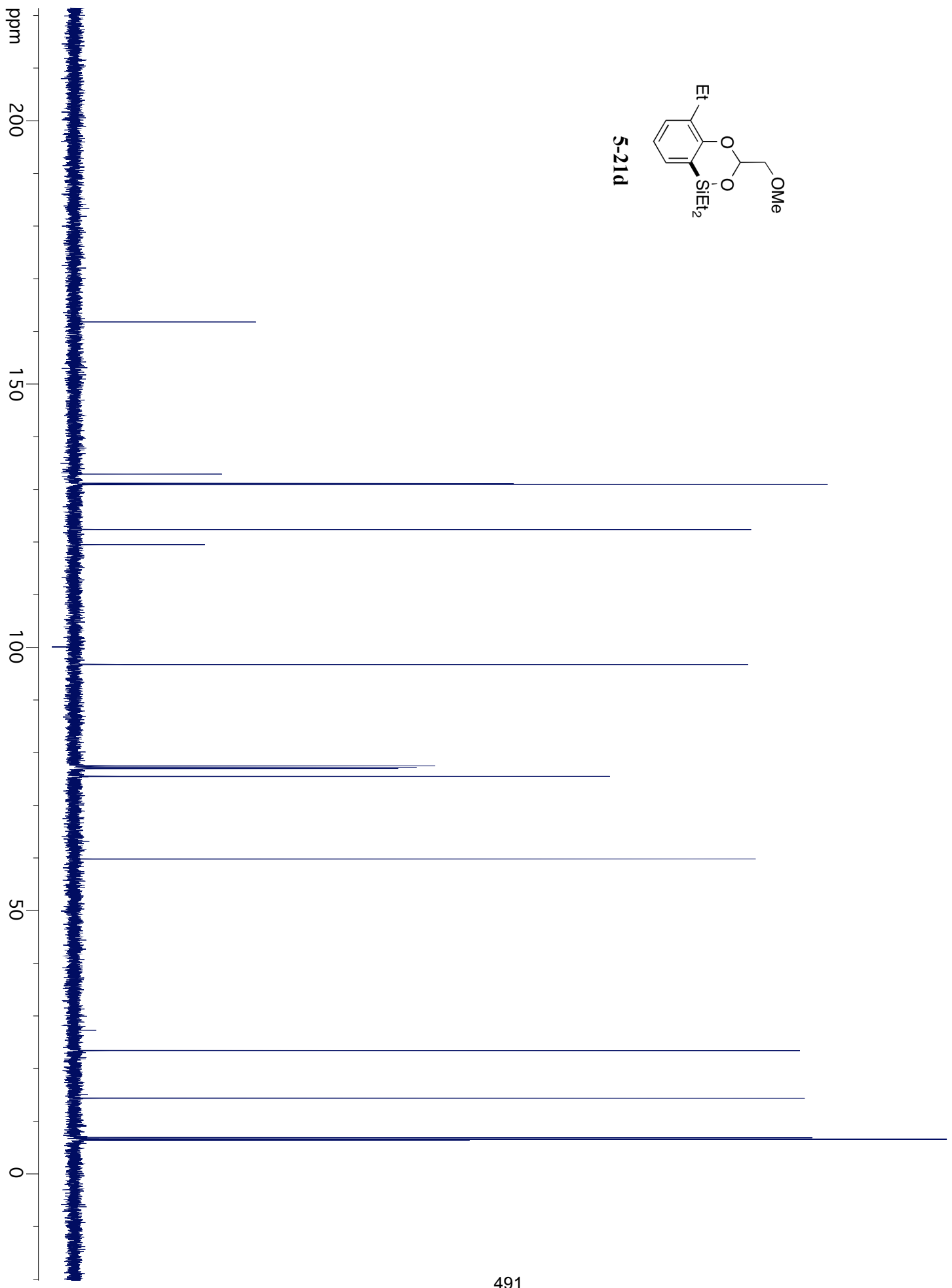


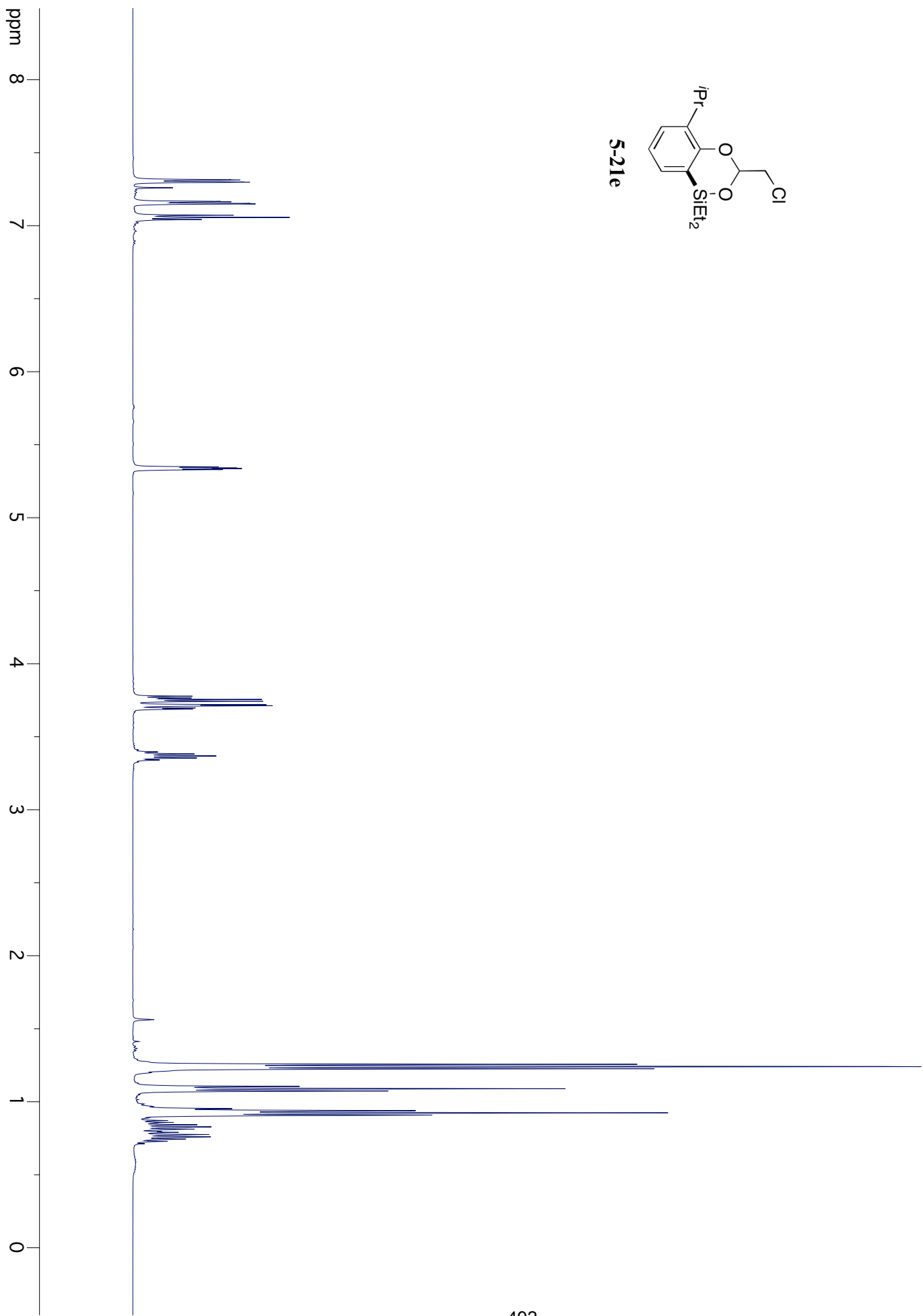
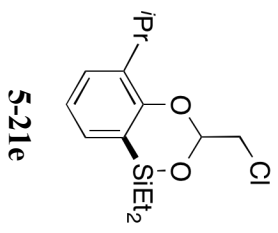
5-21d

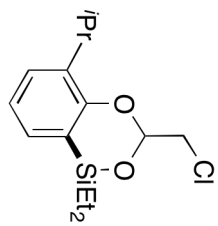




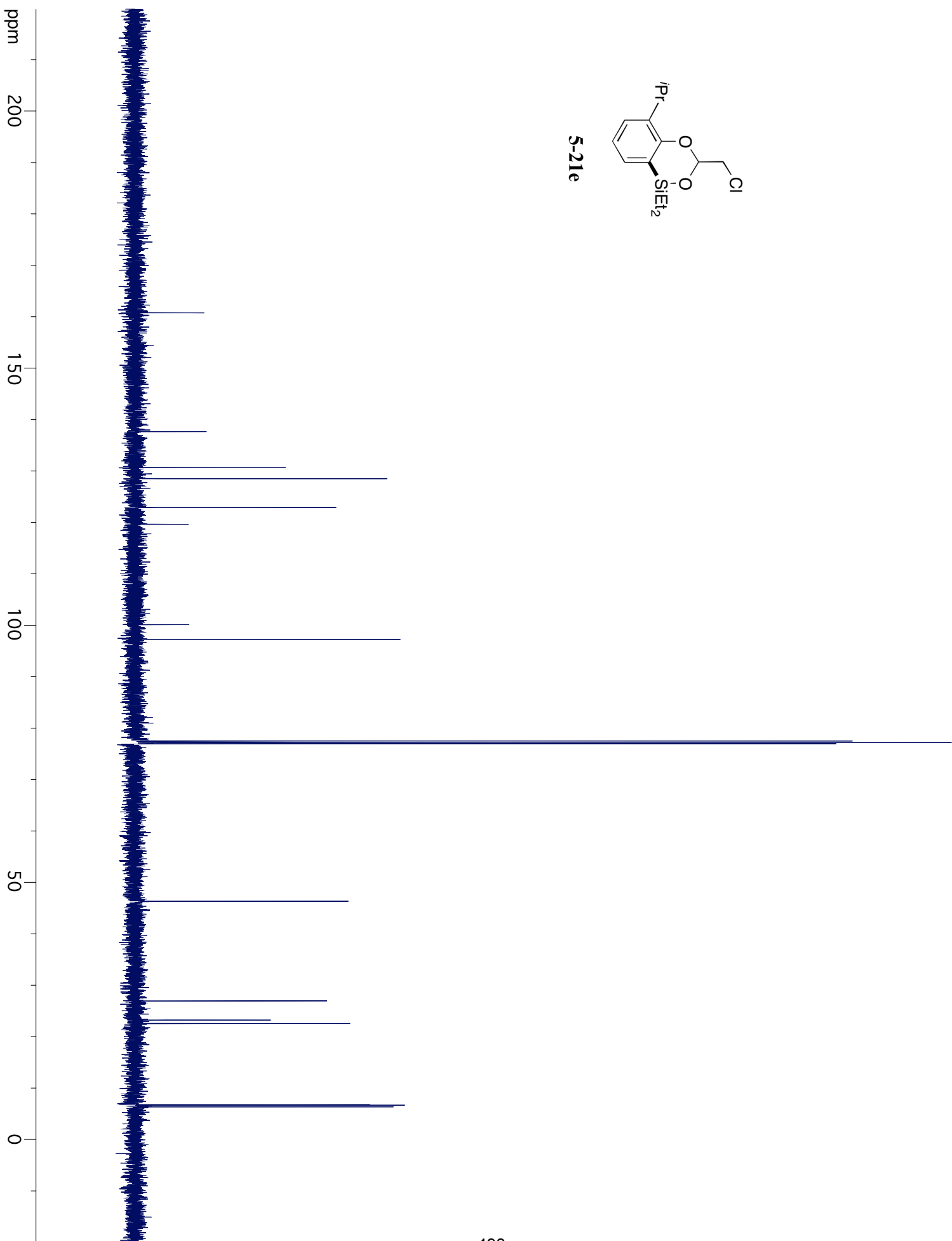
5-21d

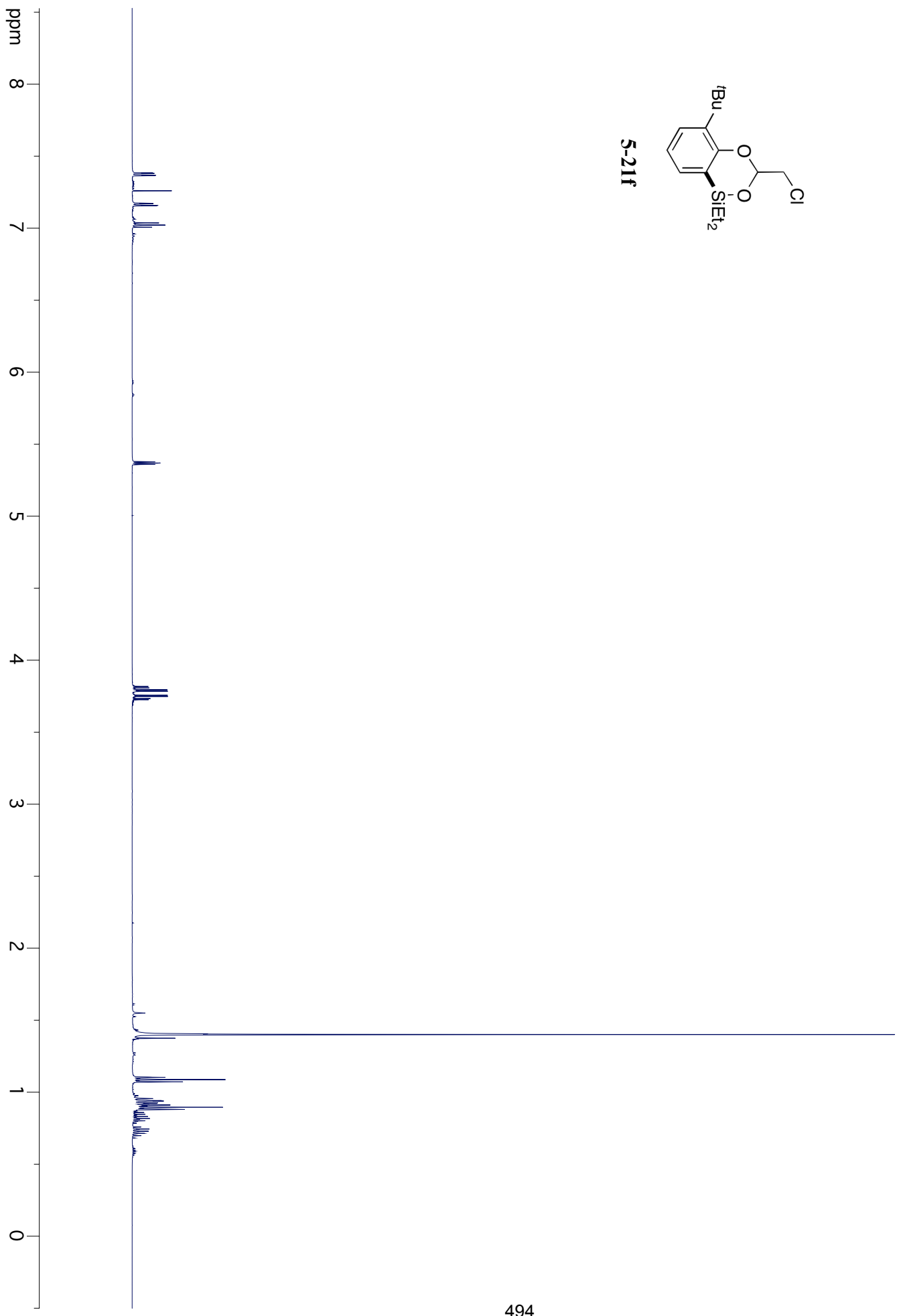
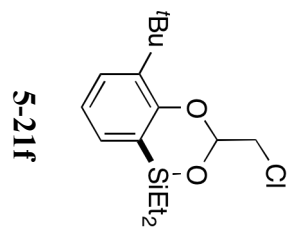


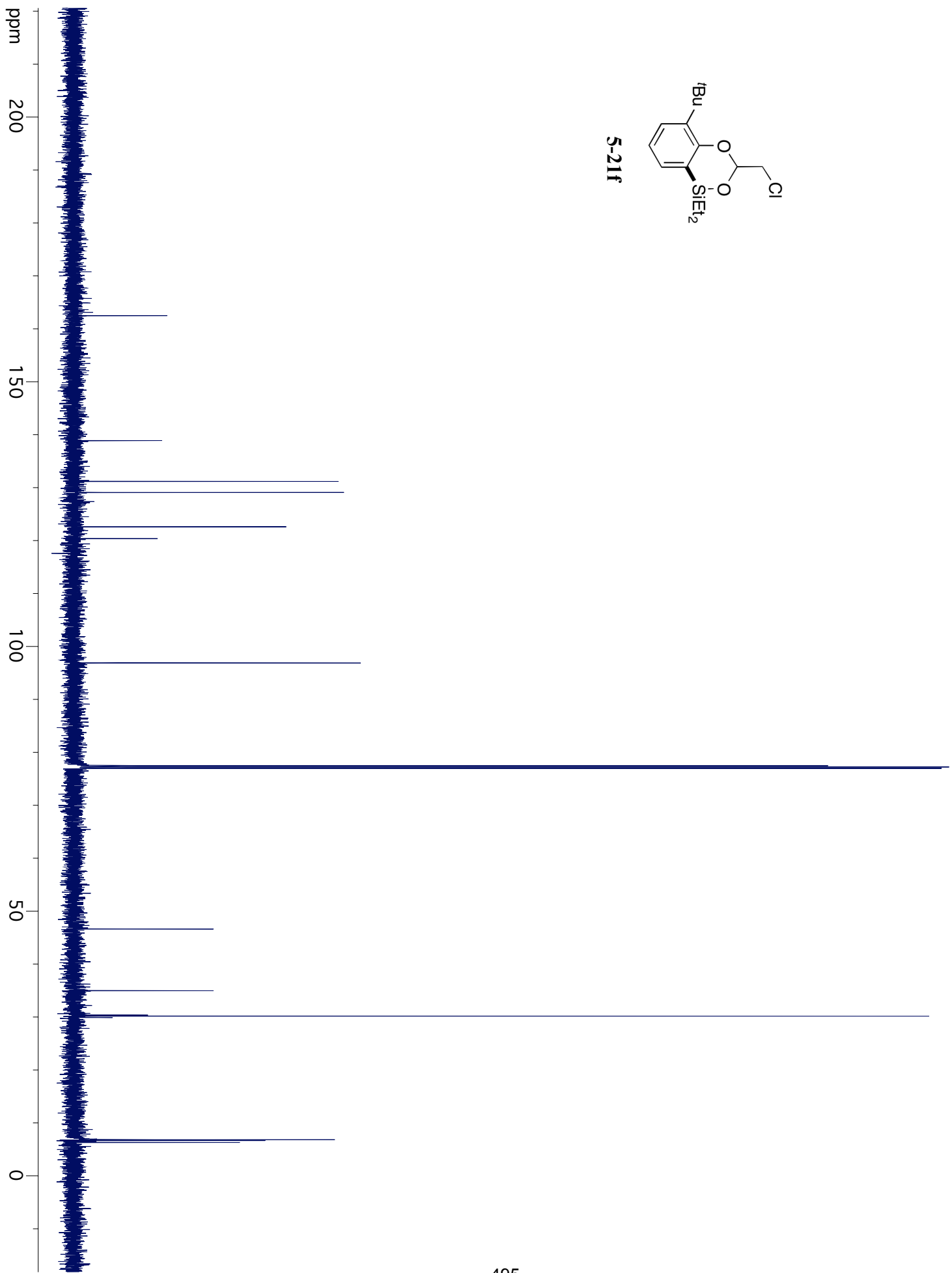
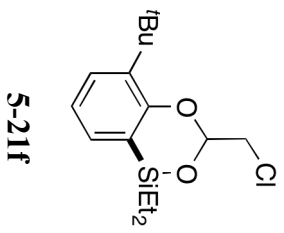


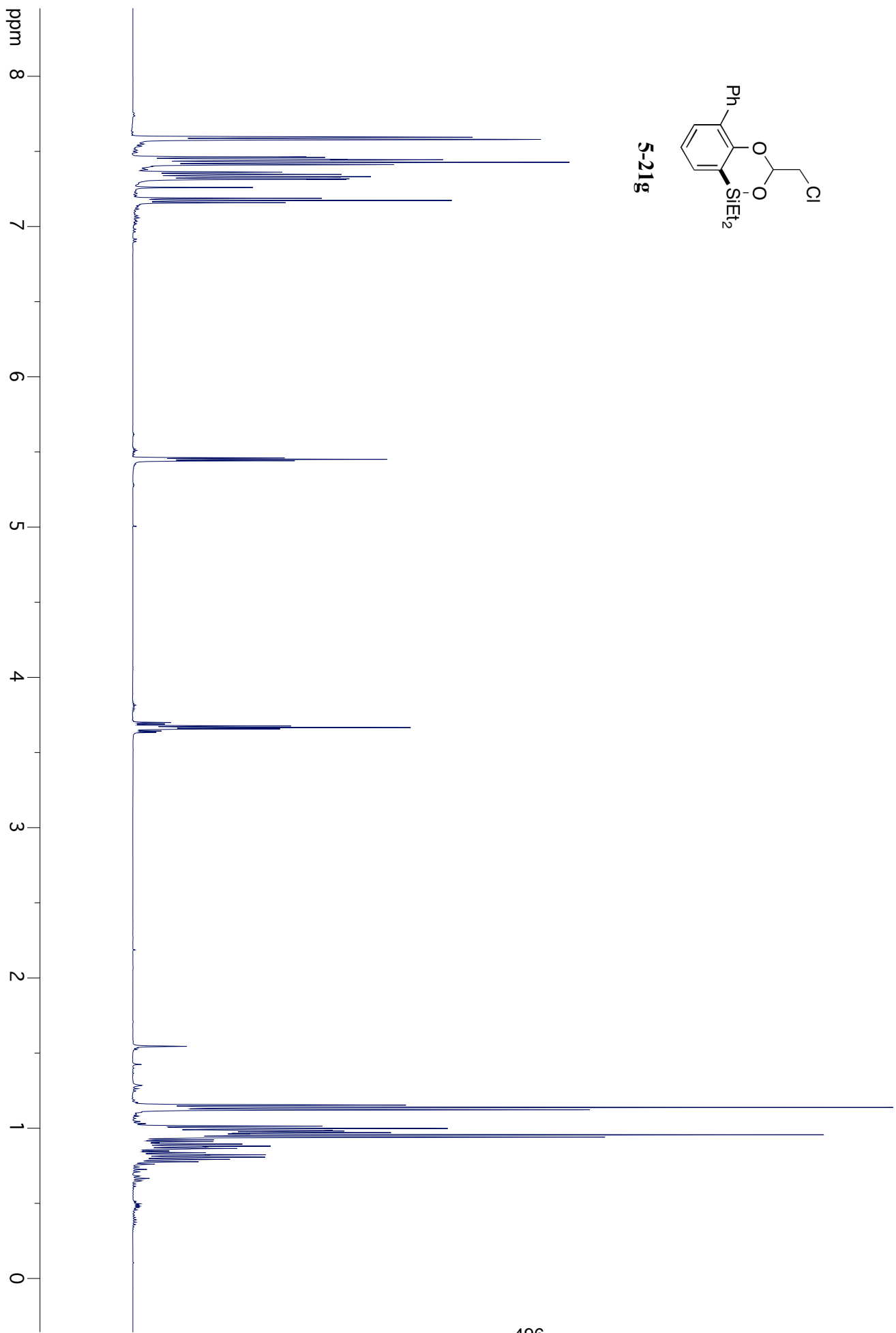
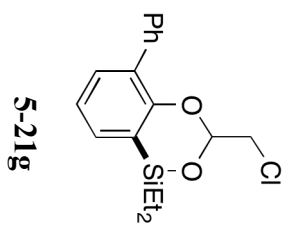


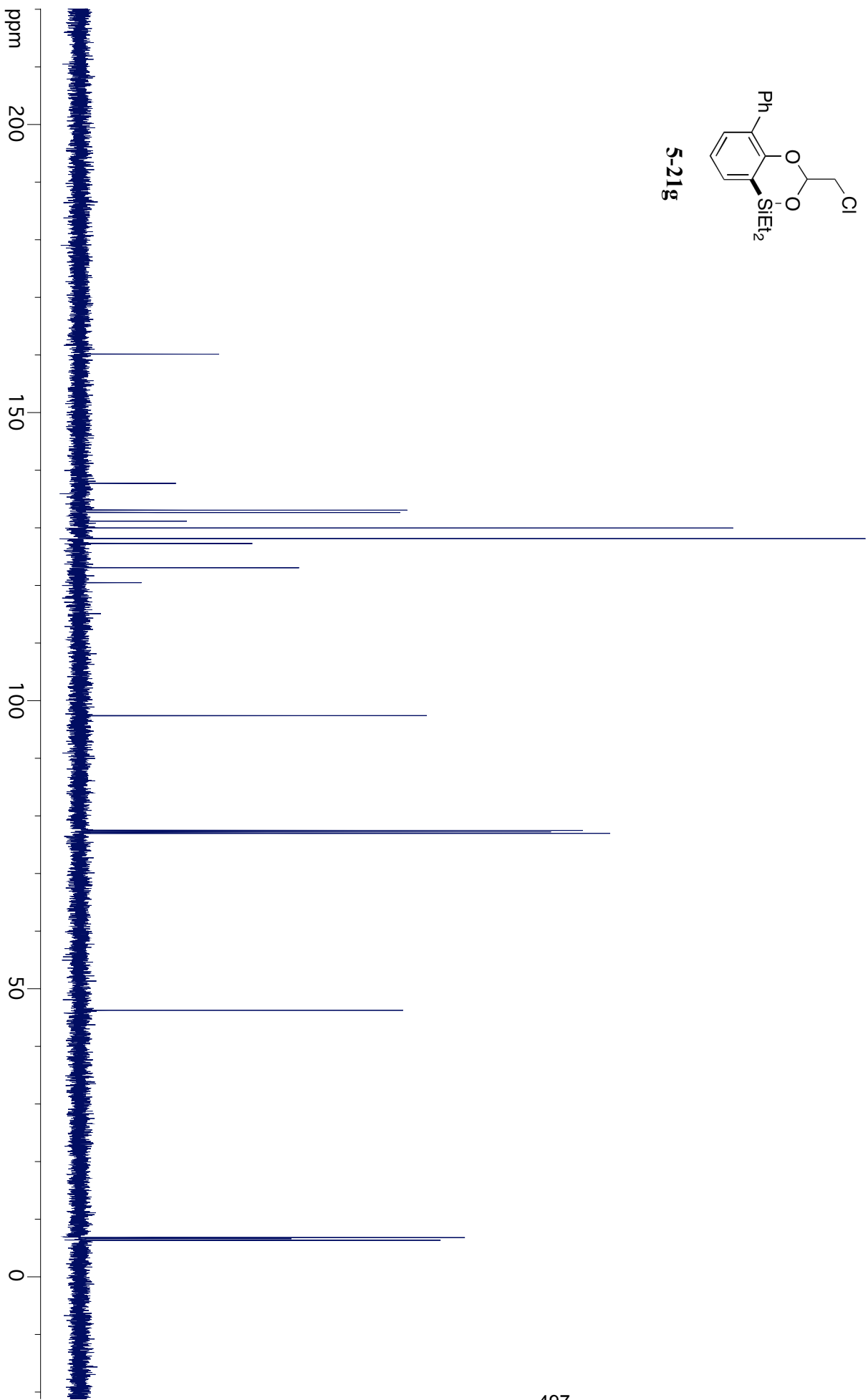
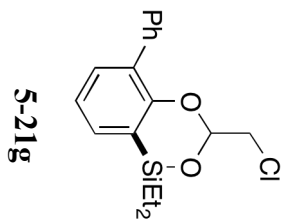
5-21e

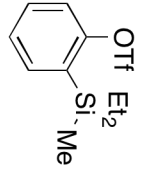






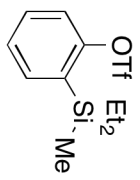




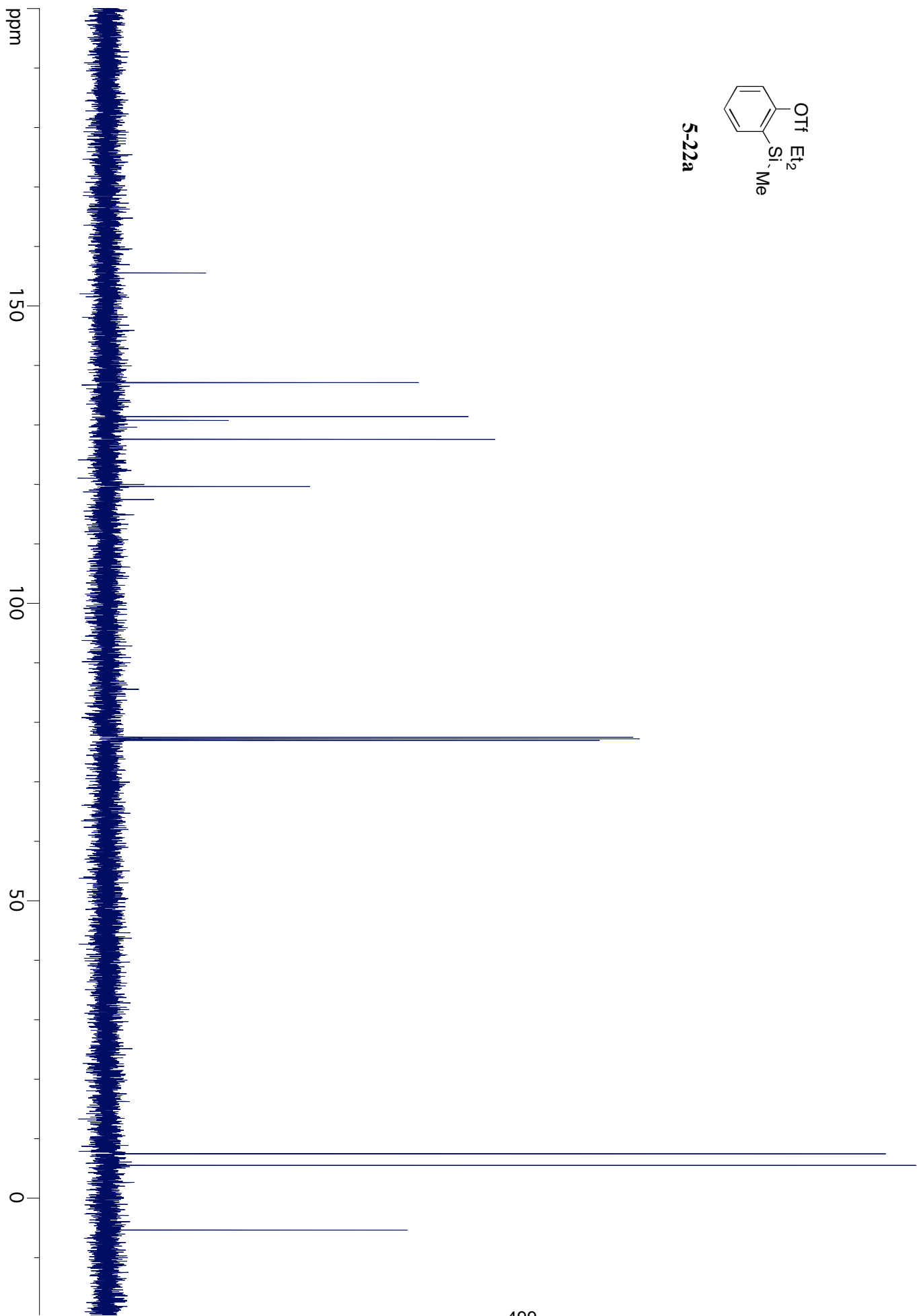


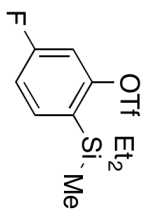
5-22a



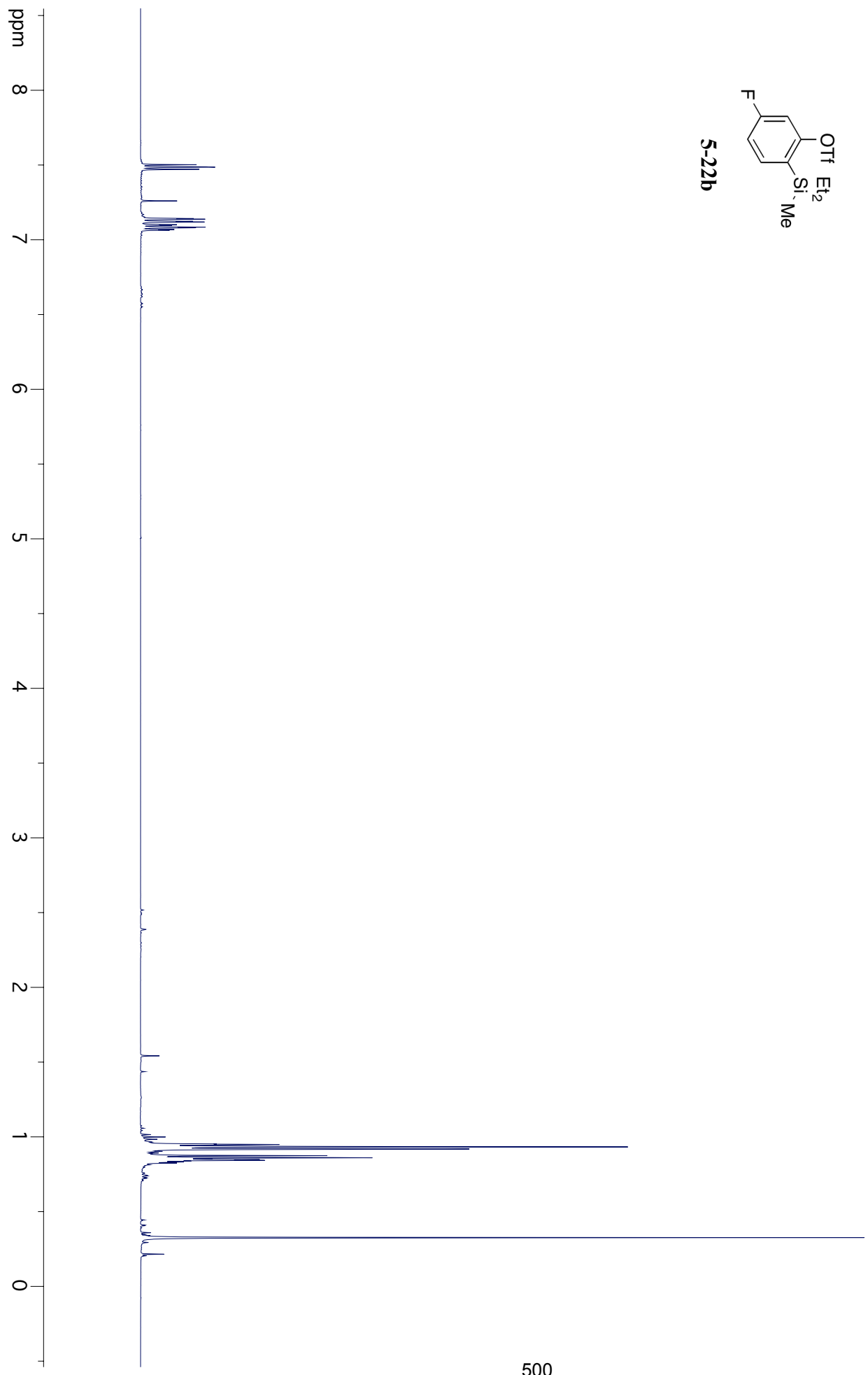


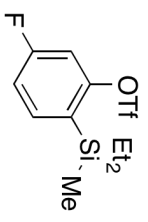
5-22a



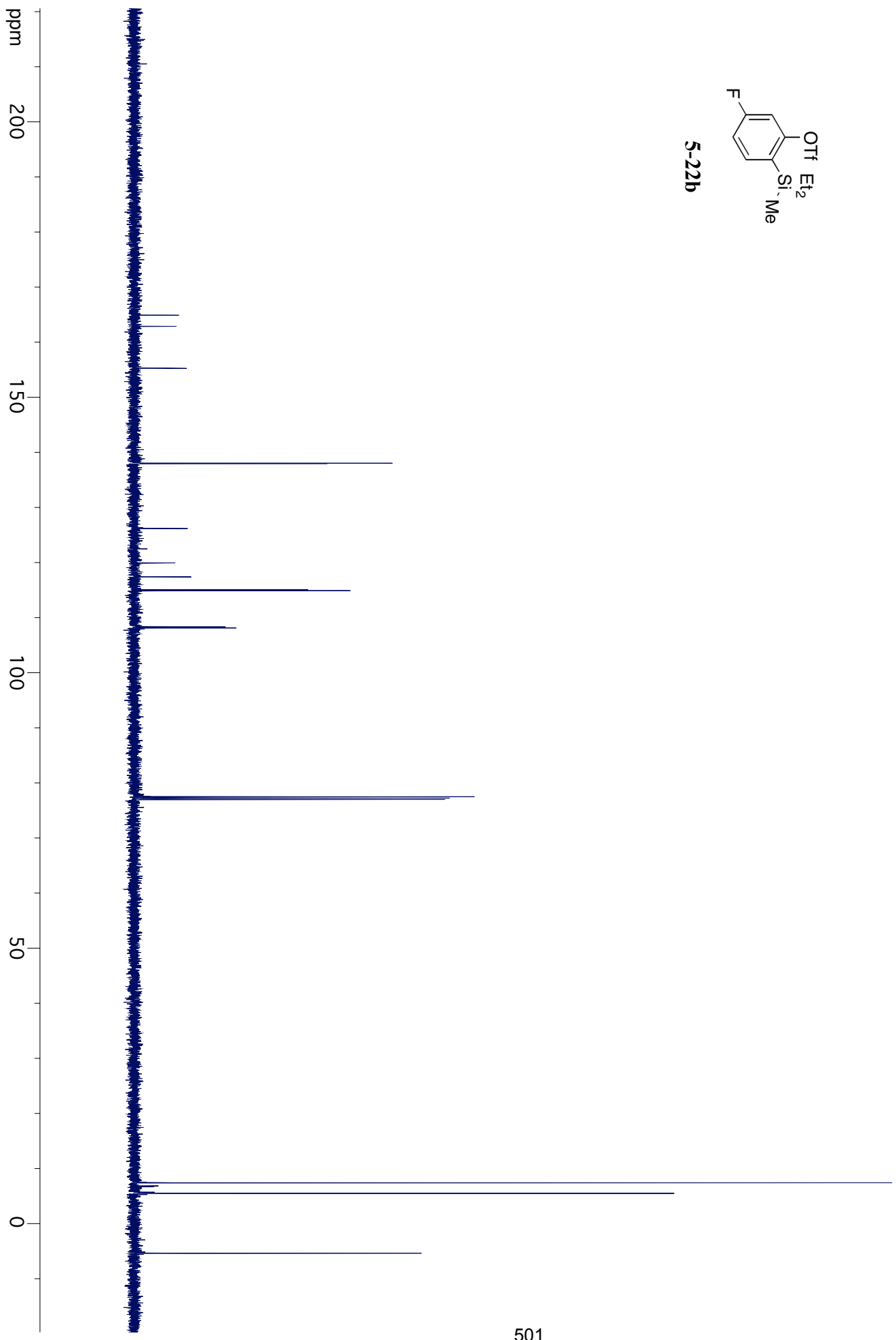


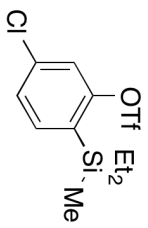
5-22b



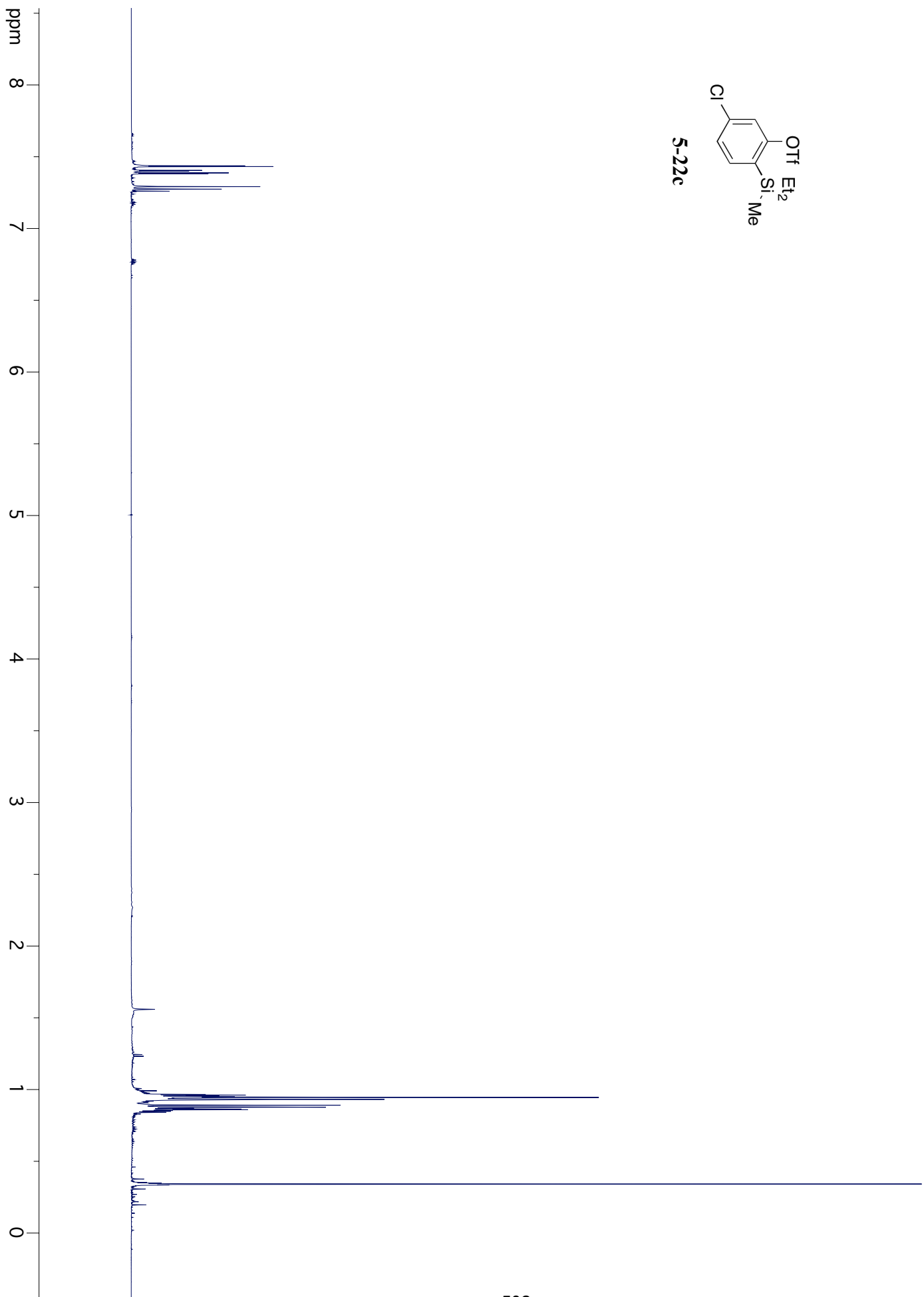


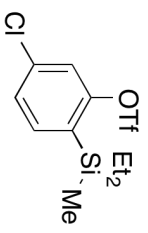
5-22b



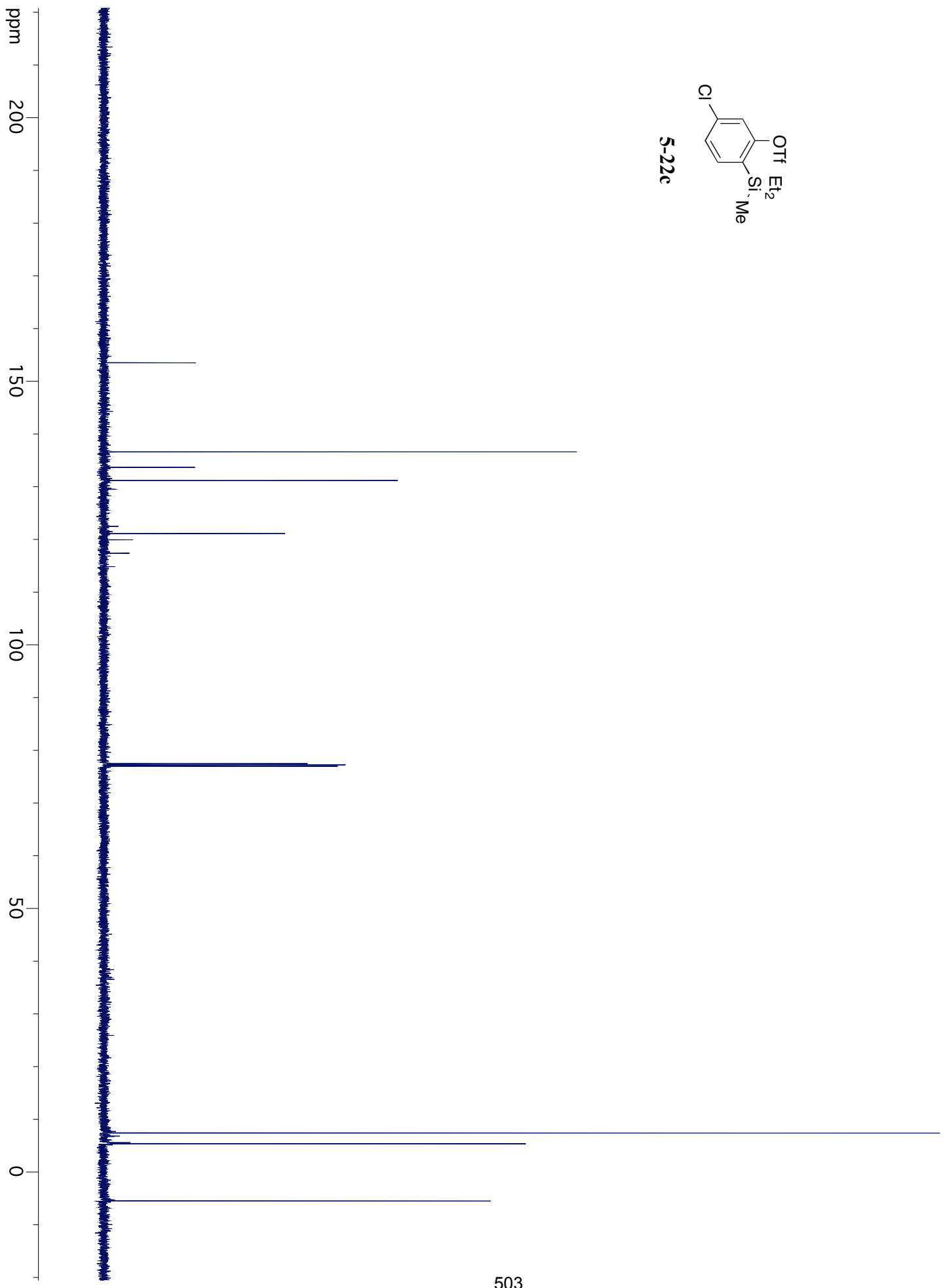


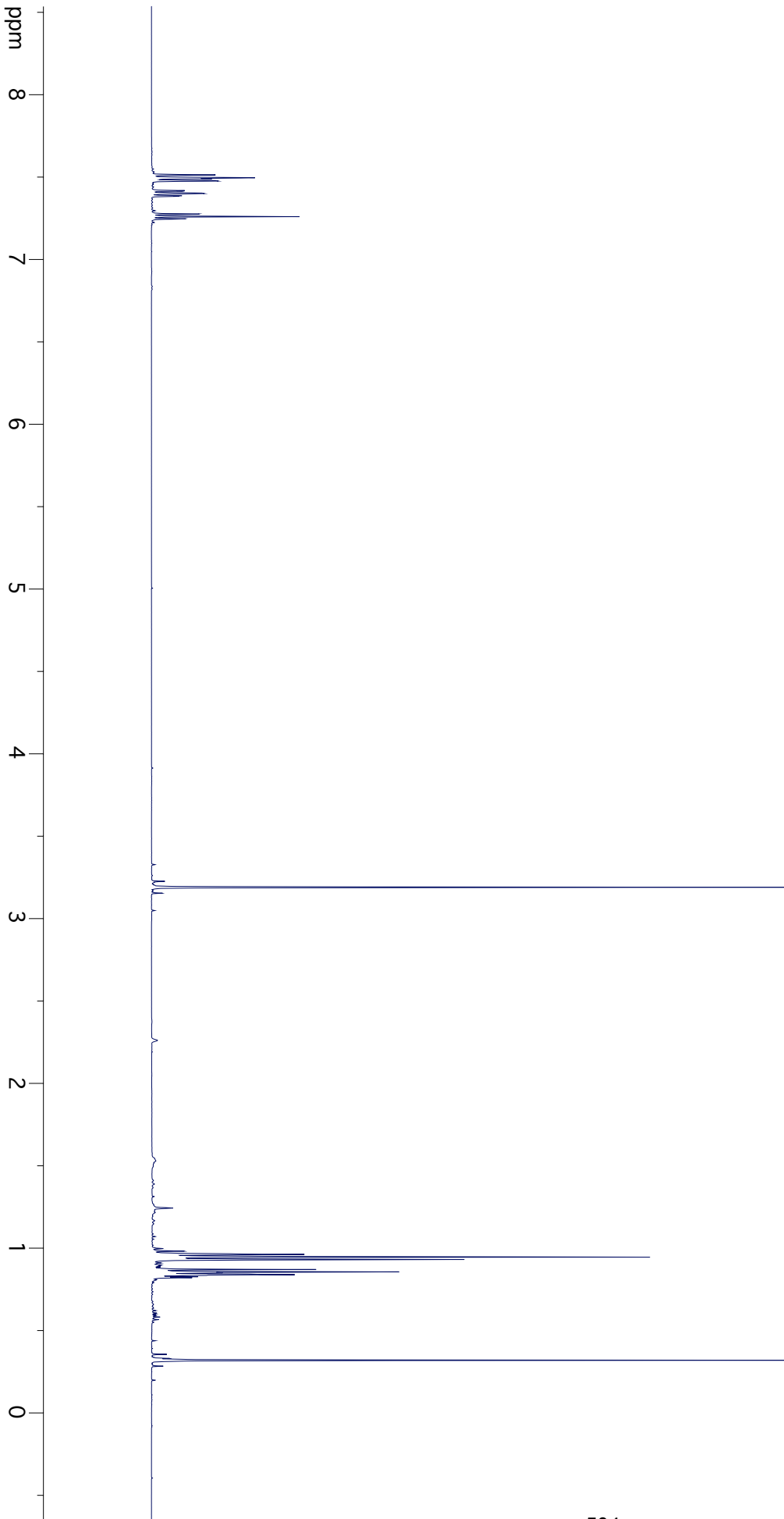
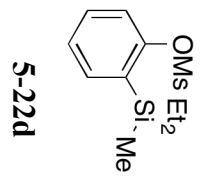
5-22c

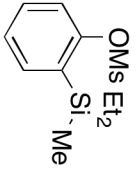




5-22c







5-22d

ppm

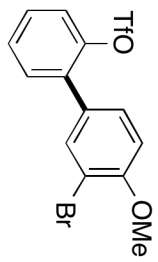
200

150

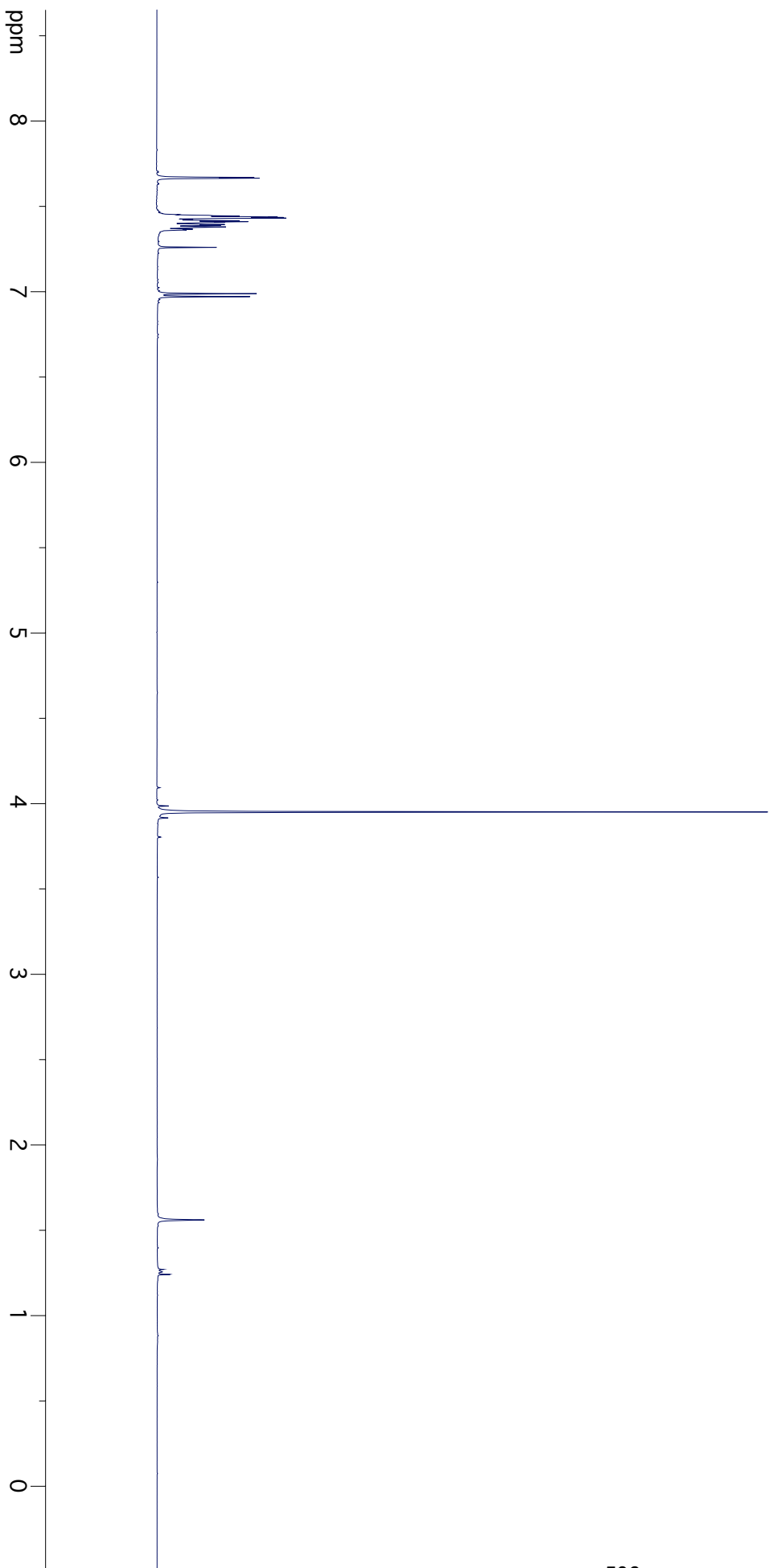
100

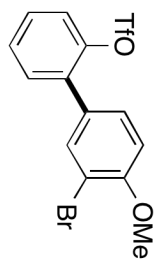
50

0

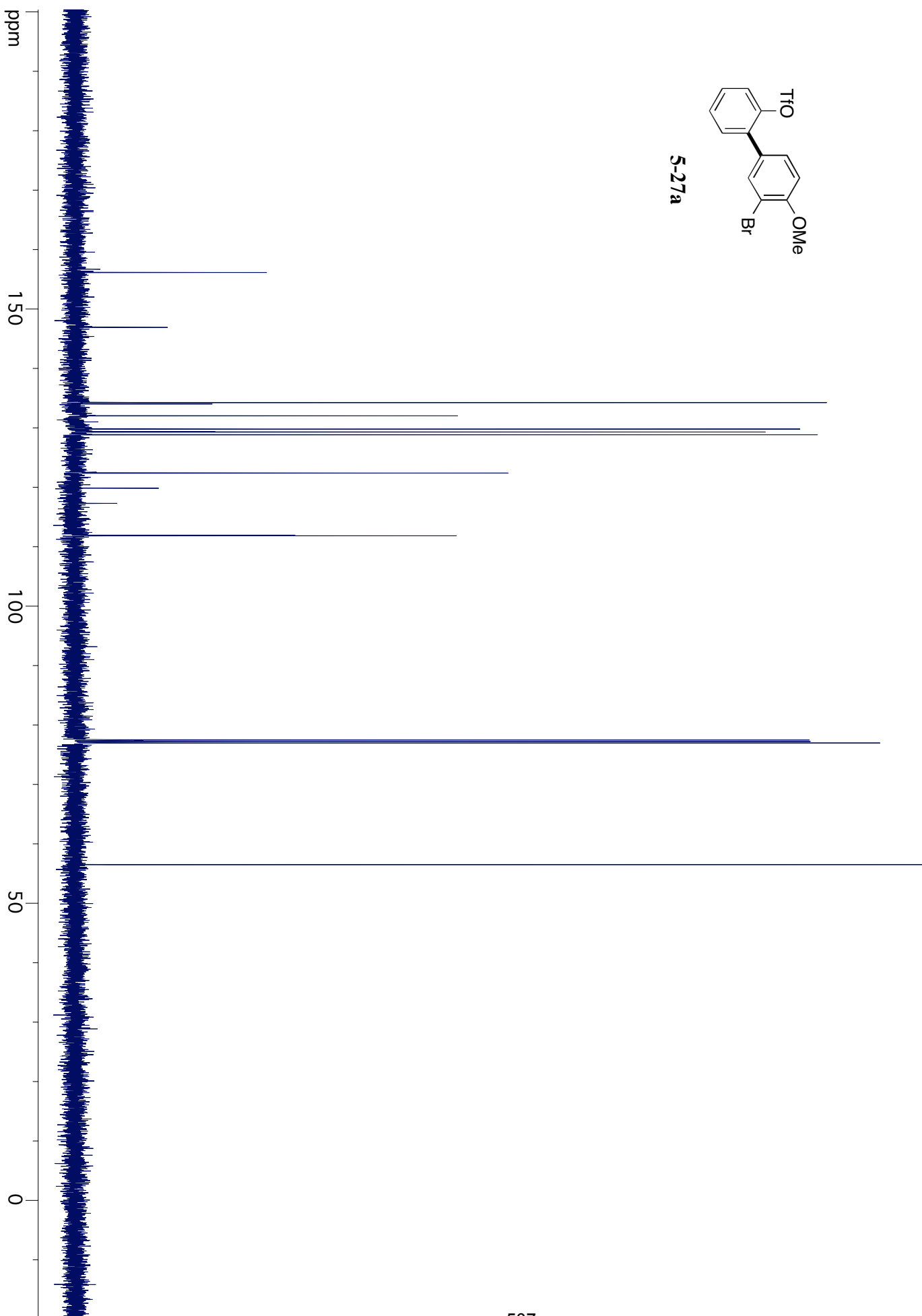


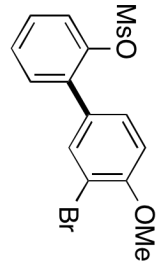
5-27a





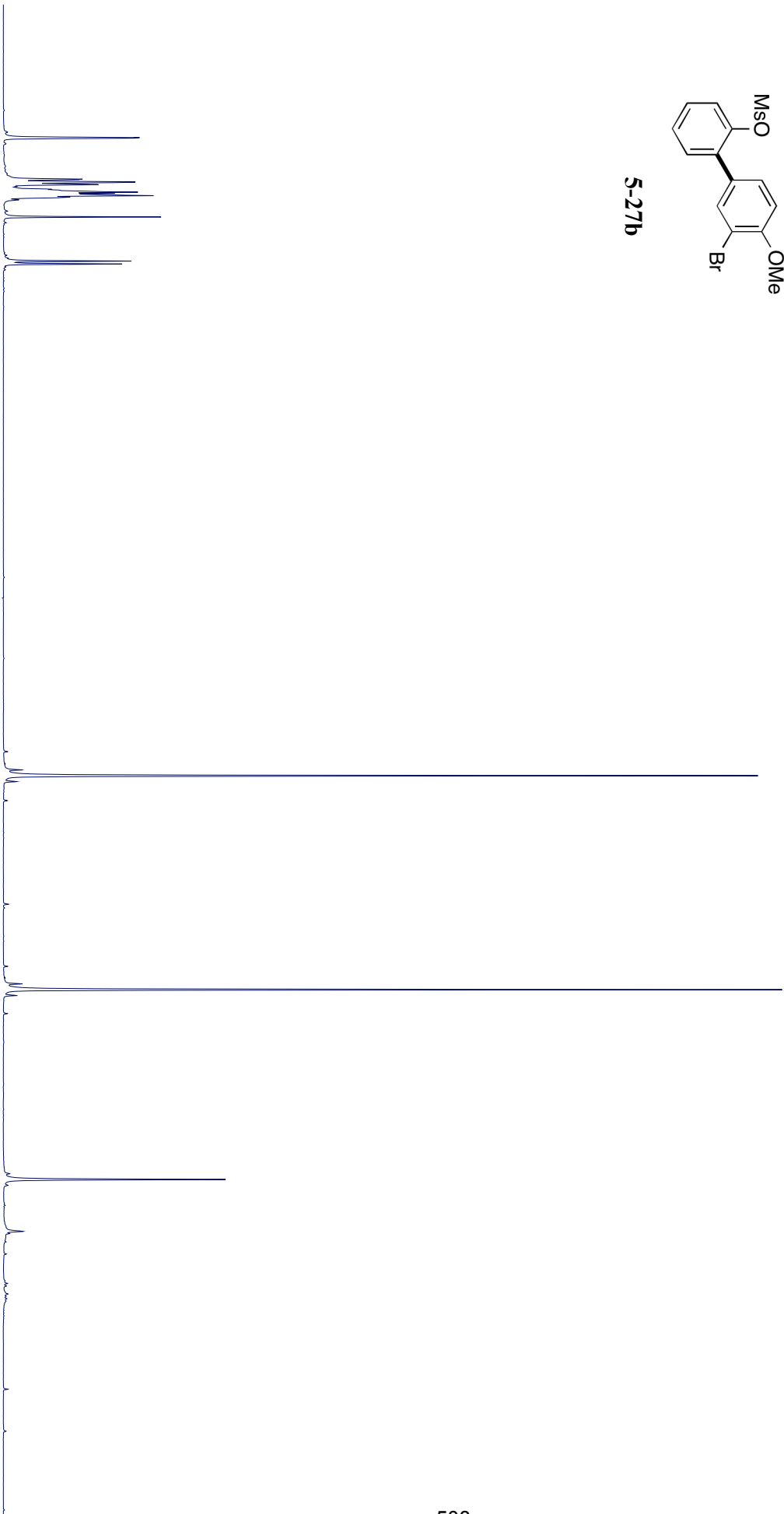
5-27a

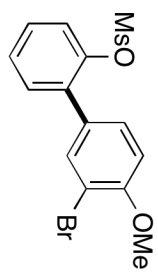




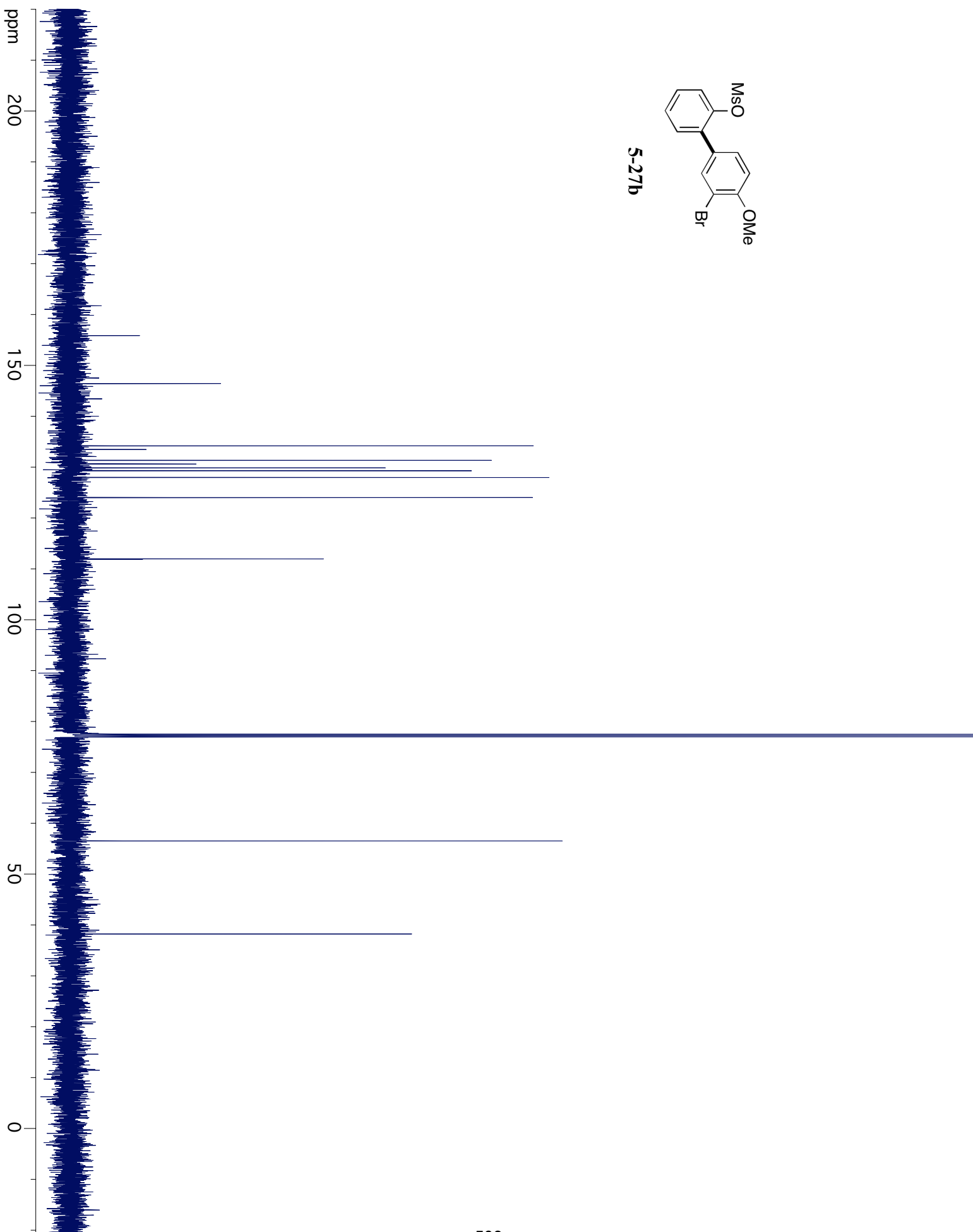
5-27b

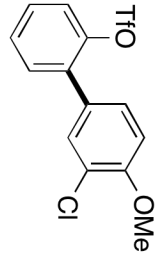
ppm 8 7 6 5 4 3 2 1 0



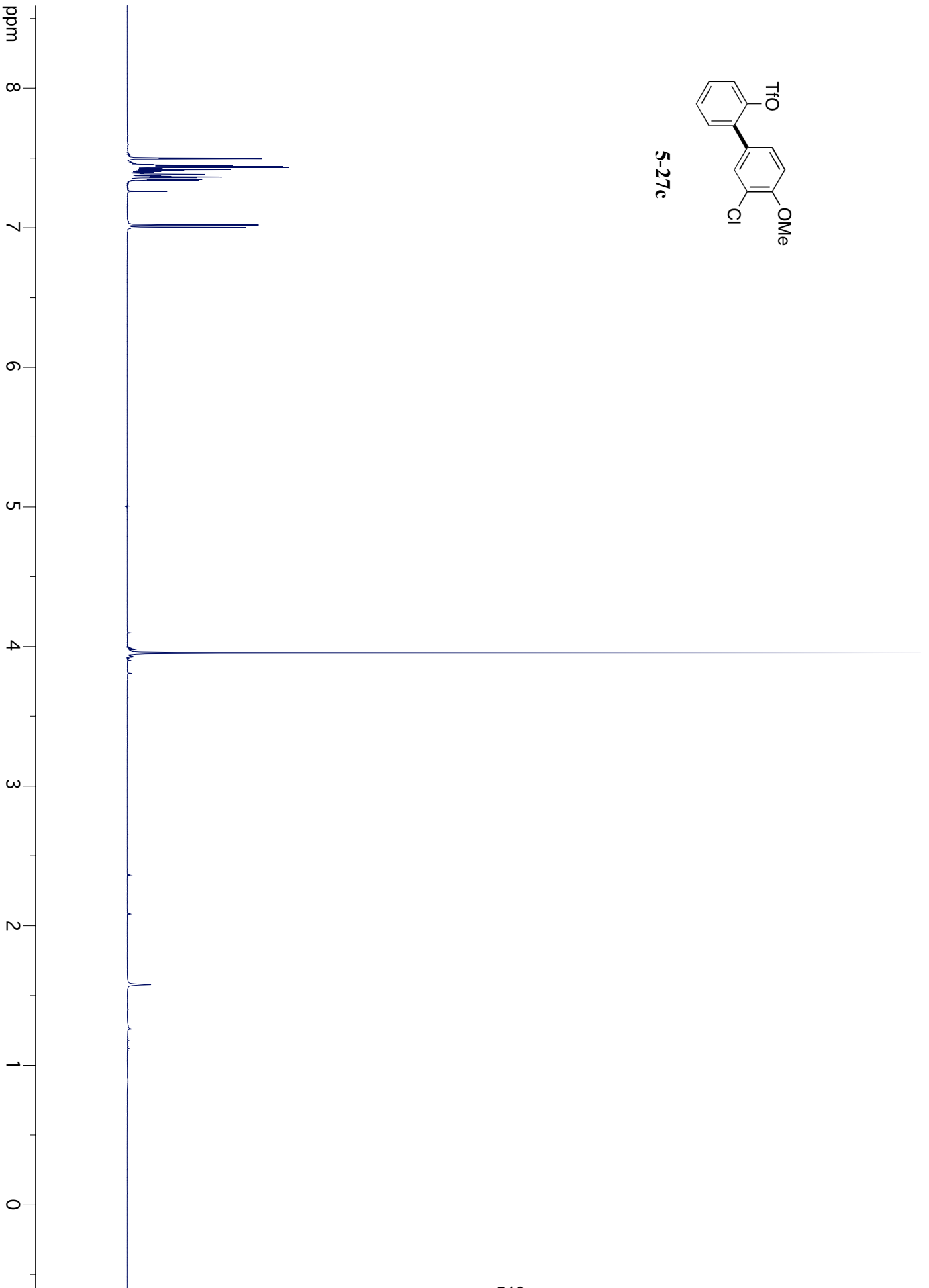


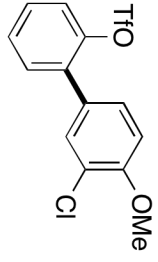
5-27b



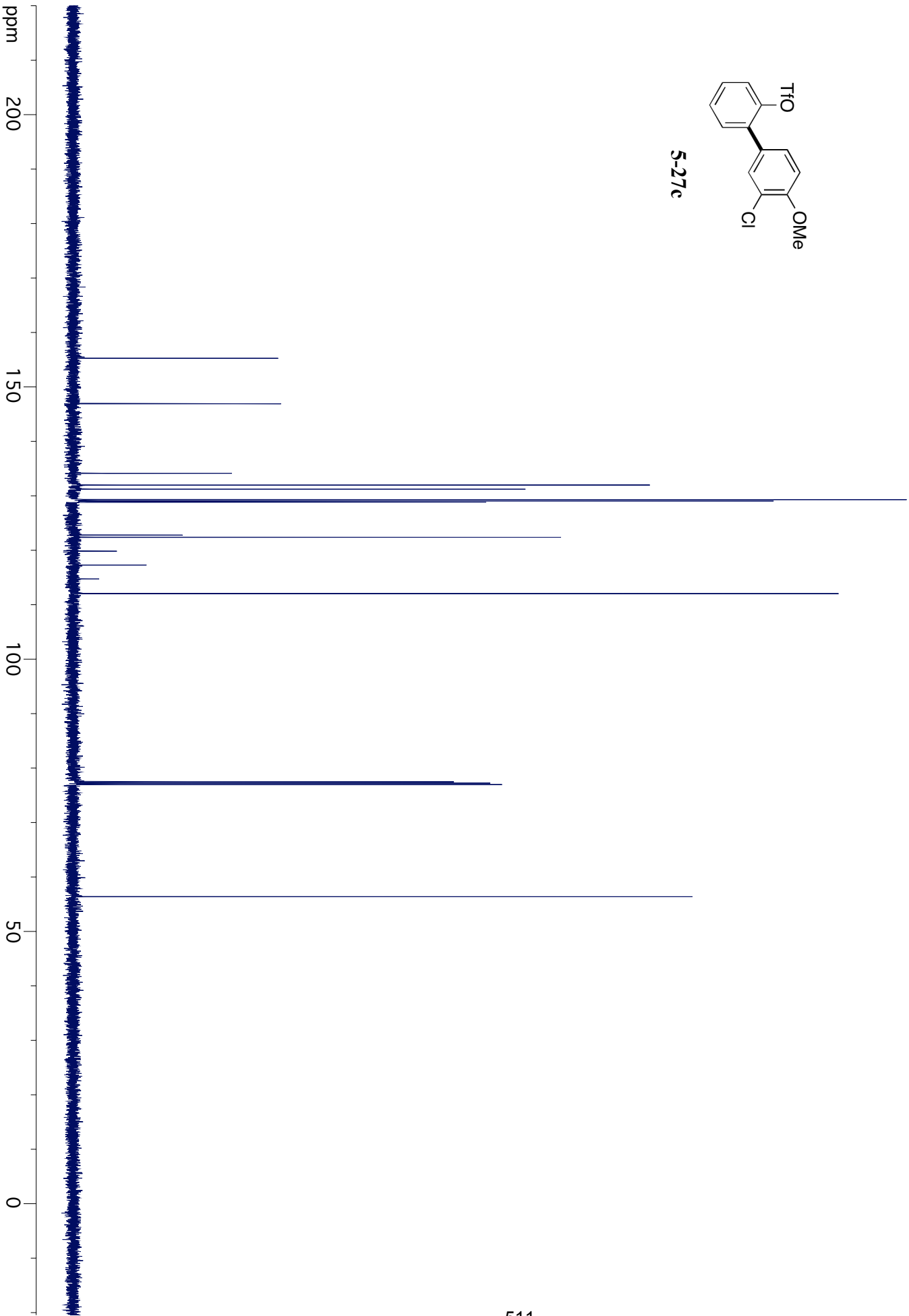


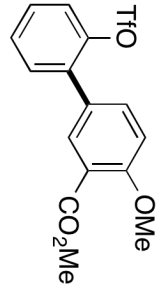
5-27c



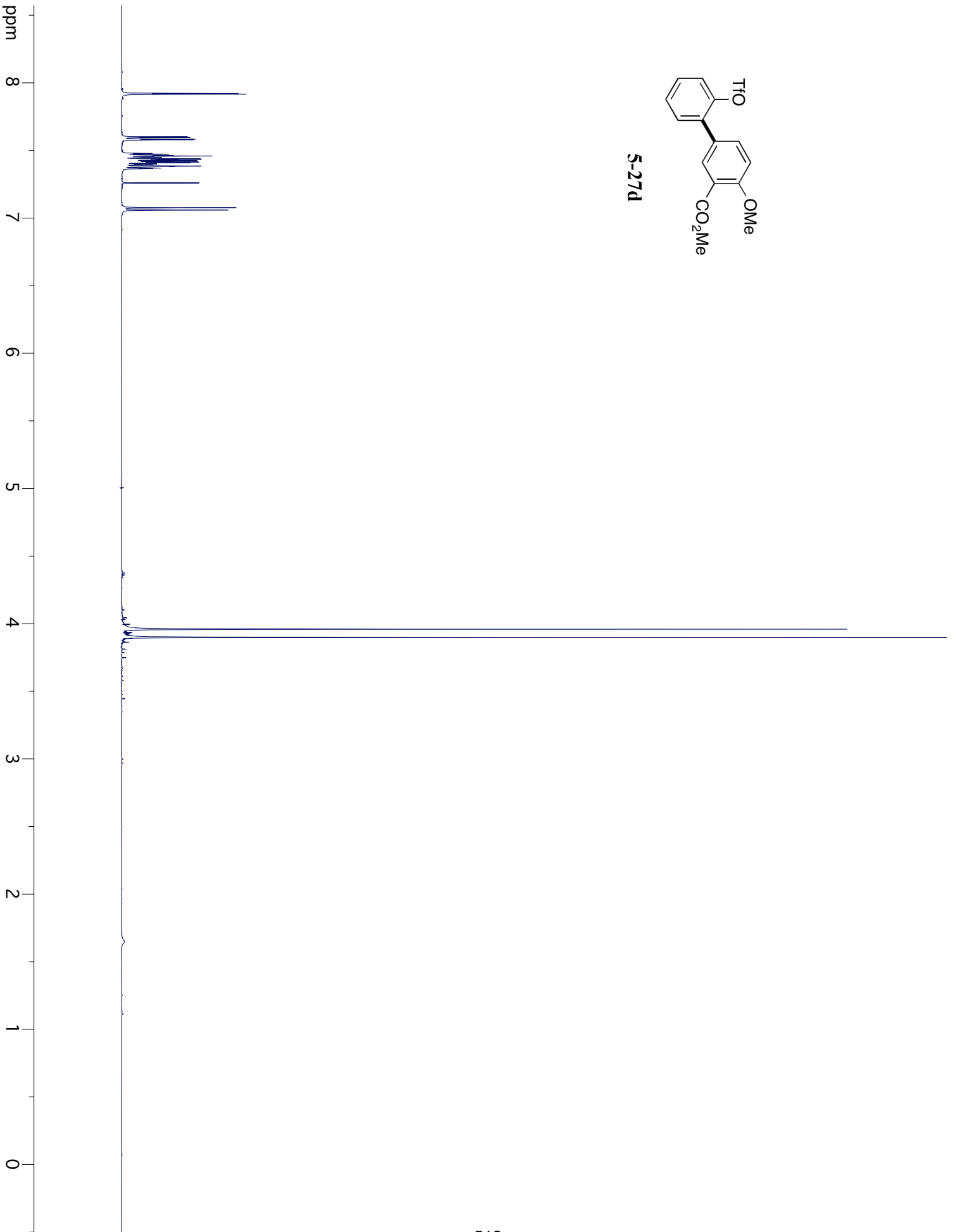


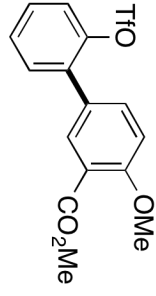
5-27c



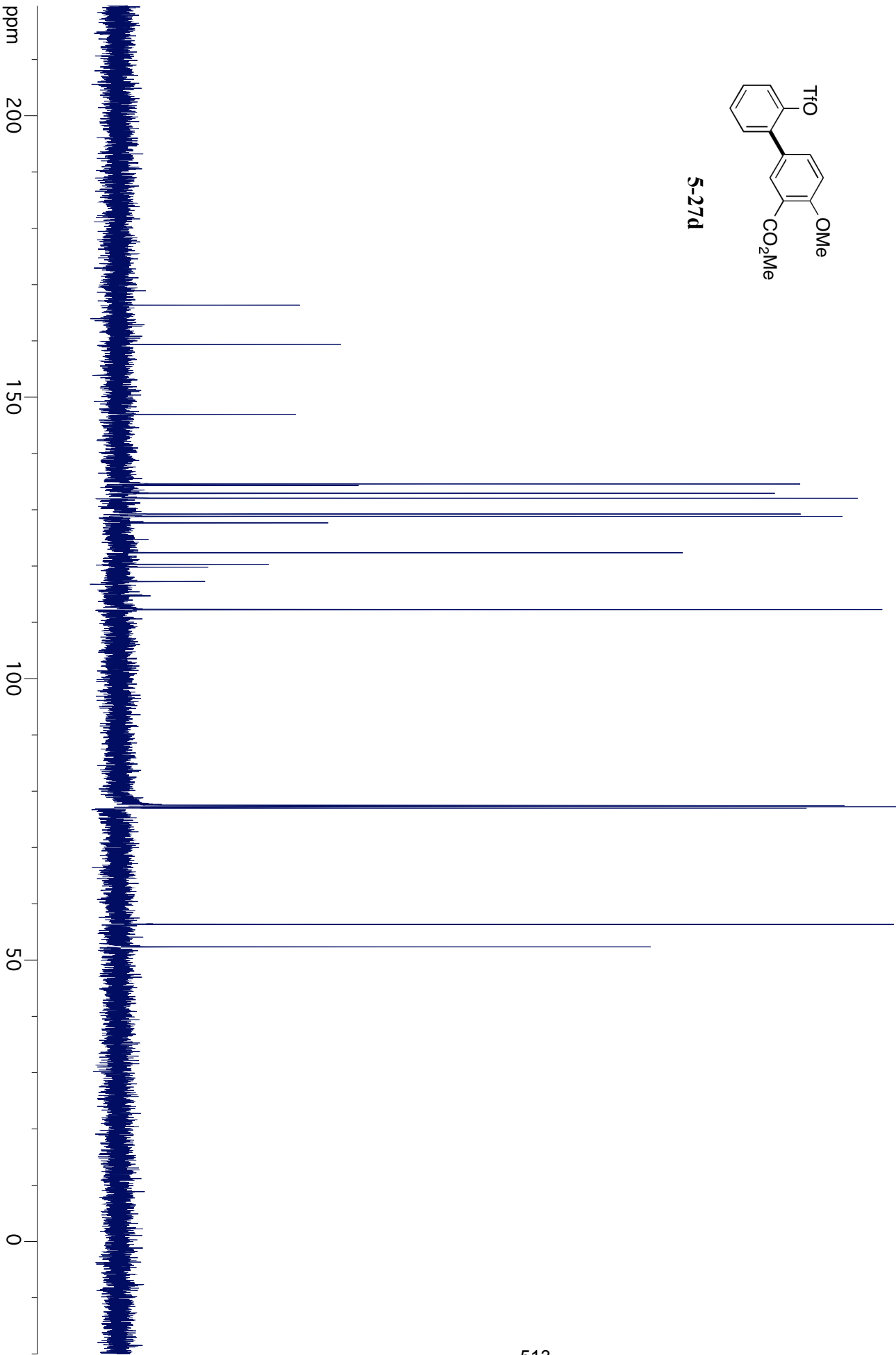


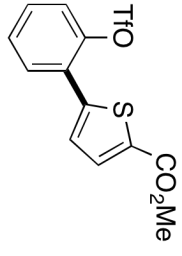
5-27d



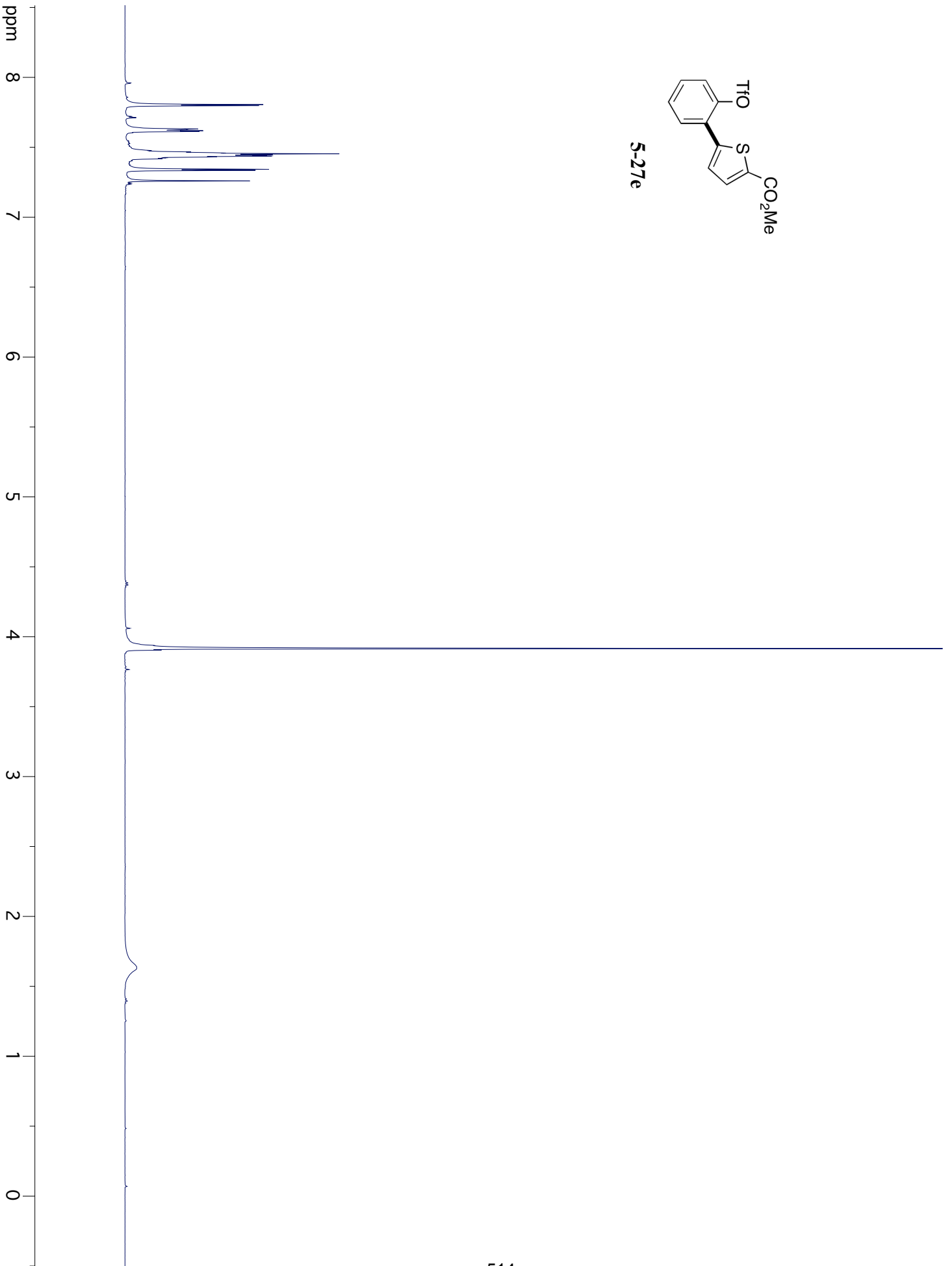


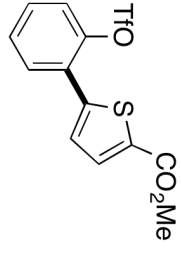
S-27d



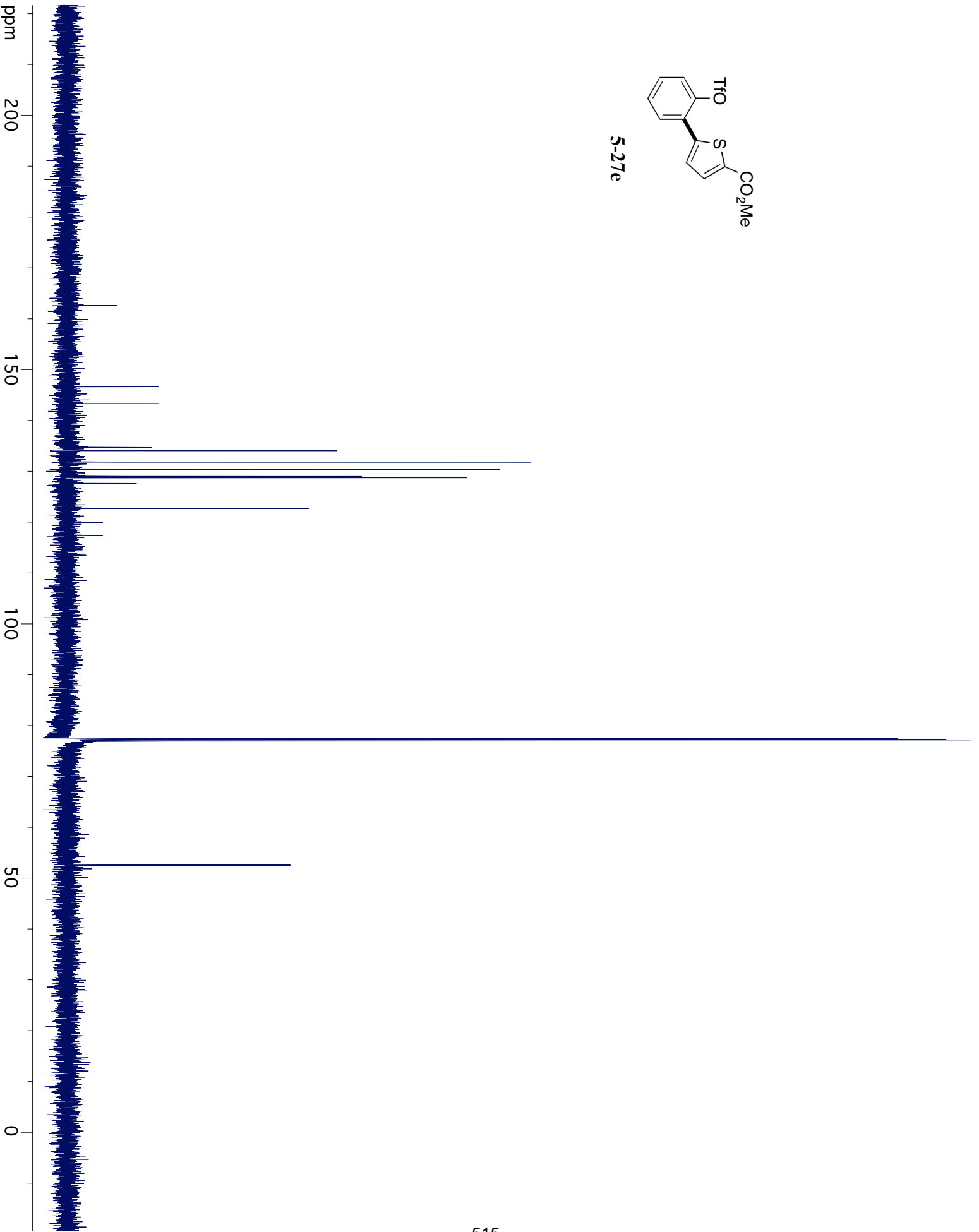


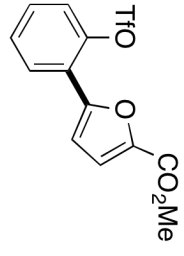
5-27e



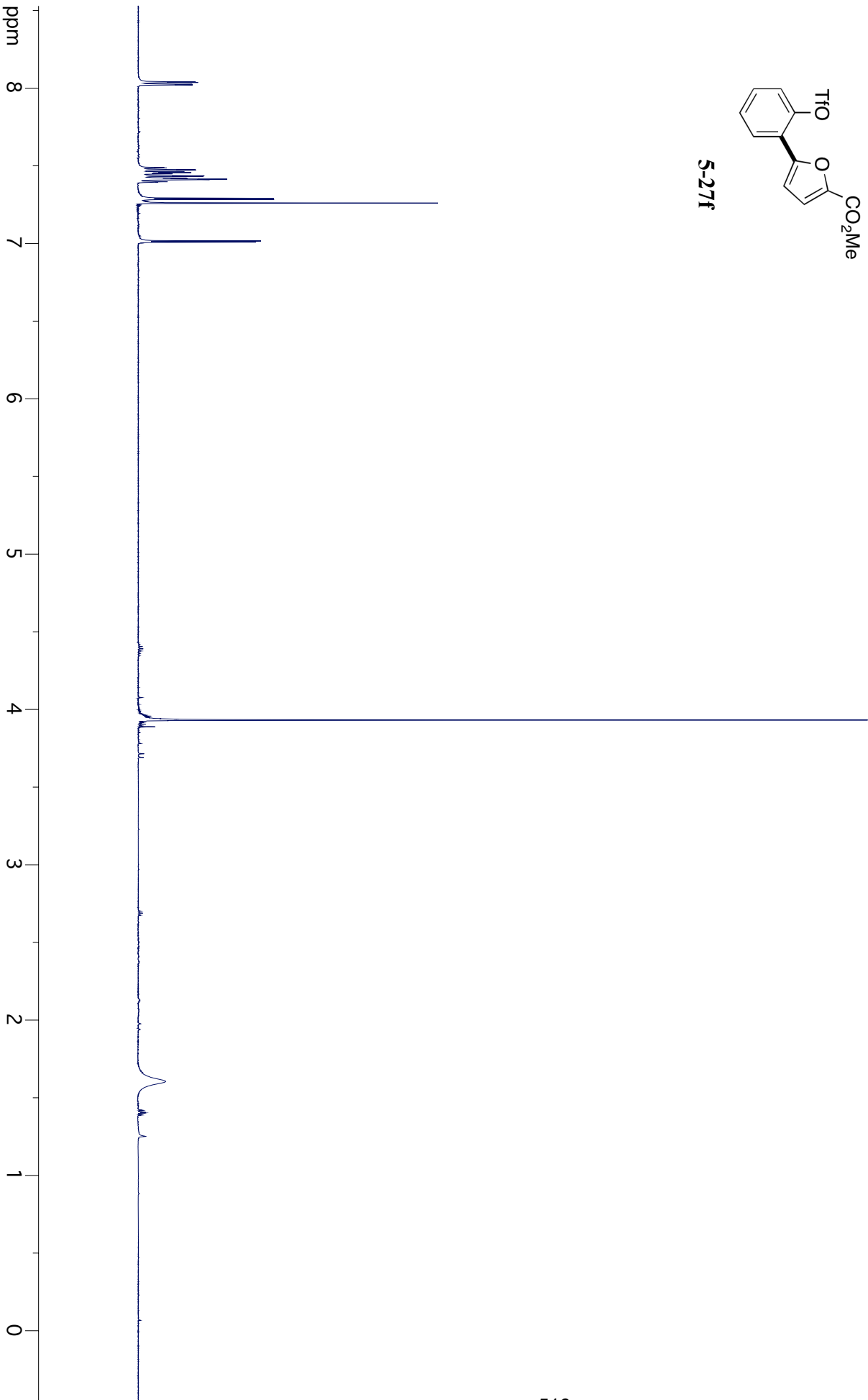


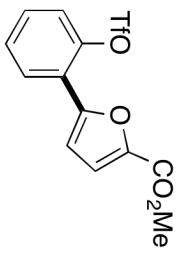
5-27e



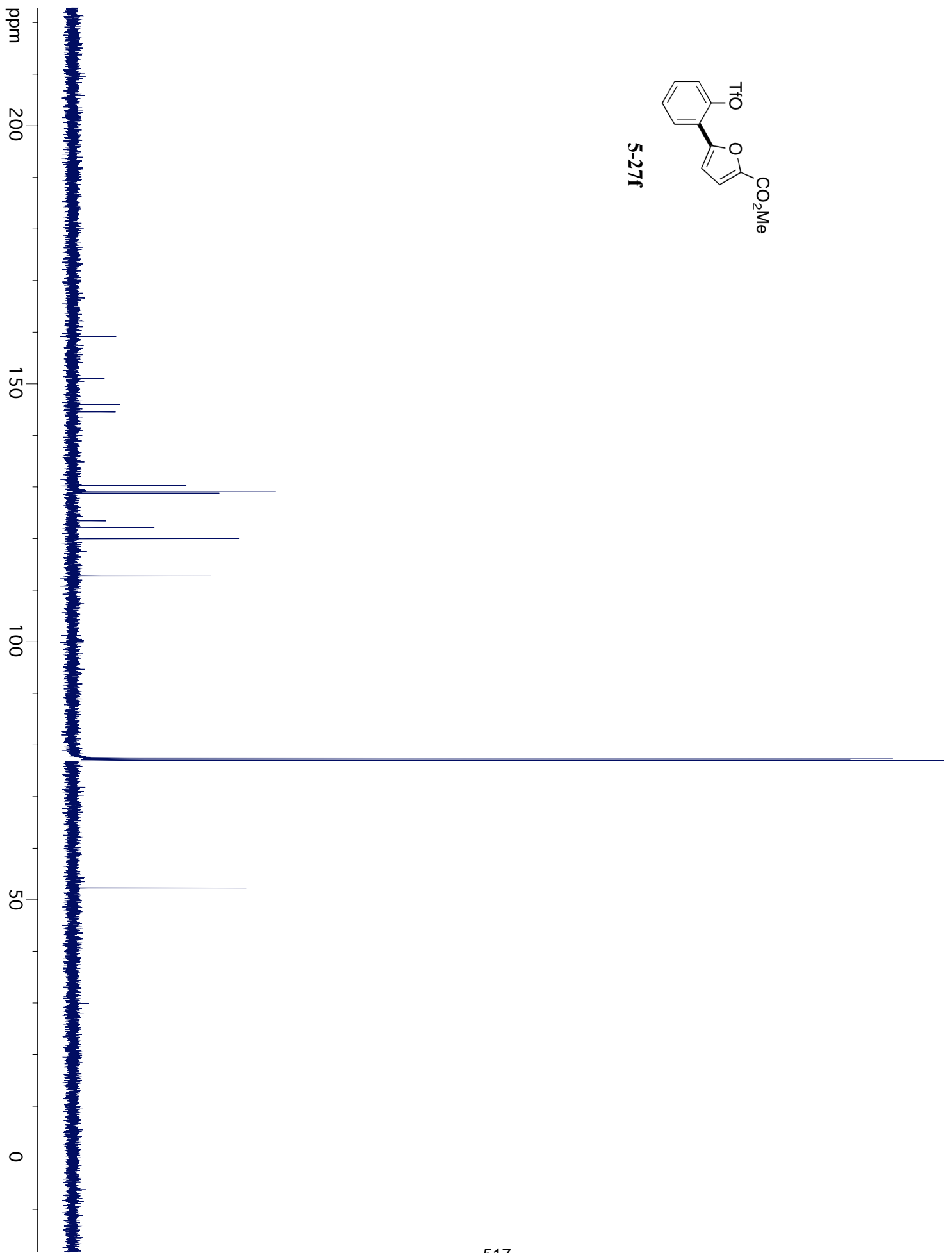


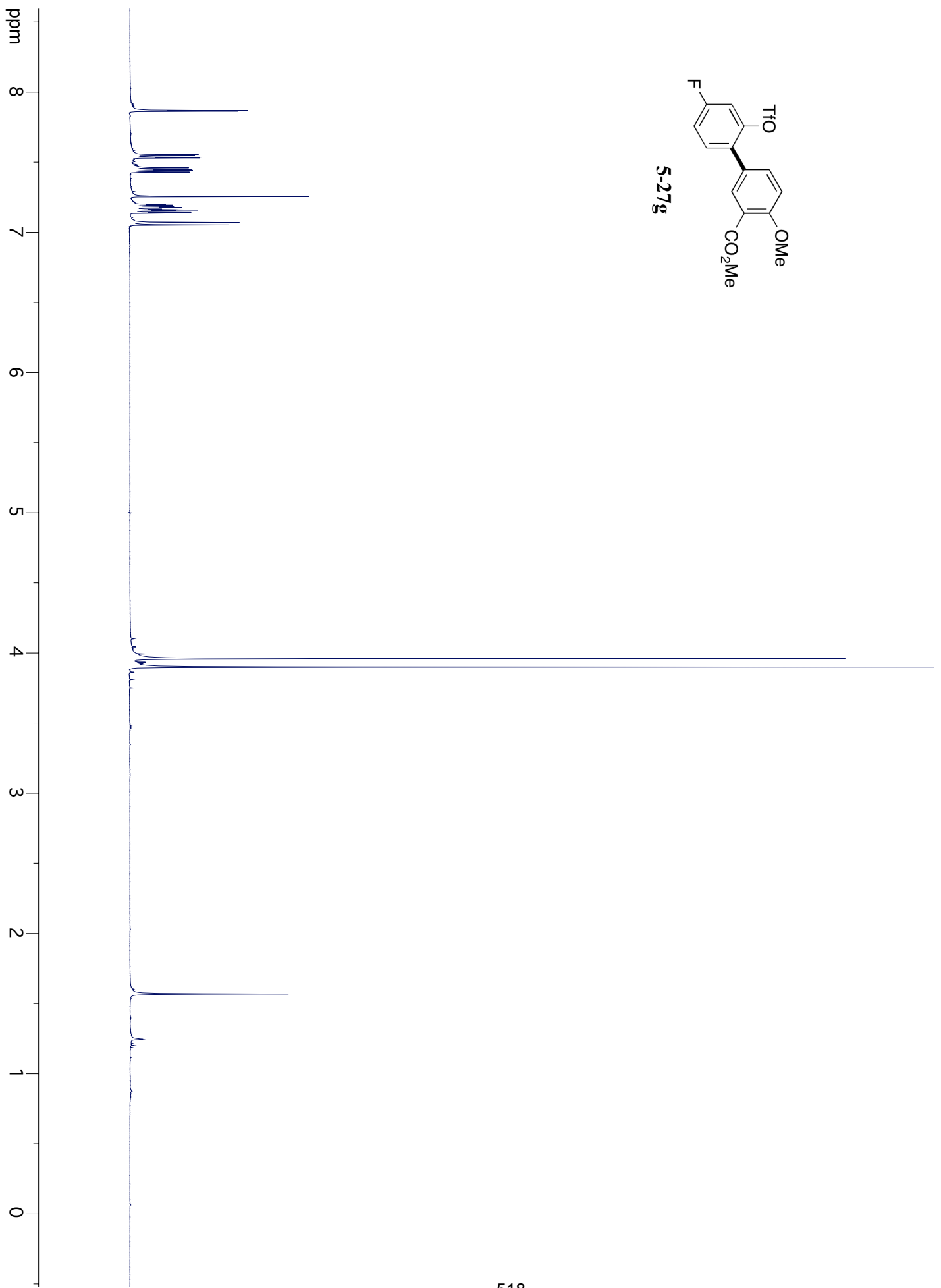
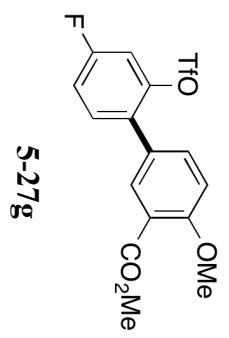
5-27f

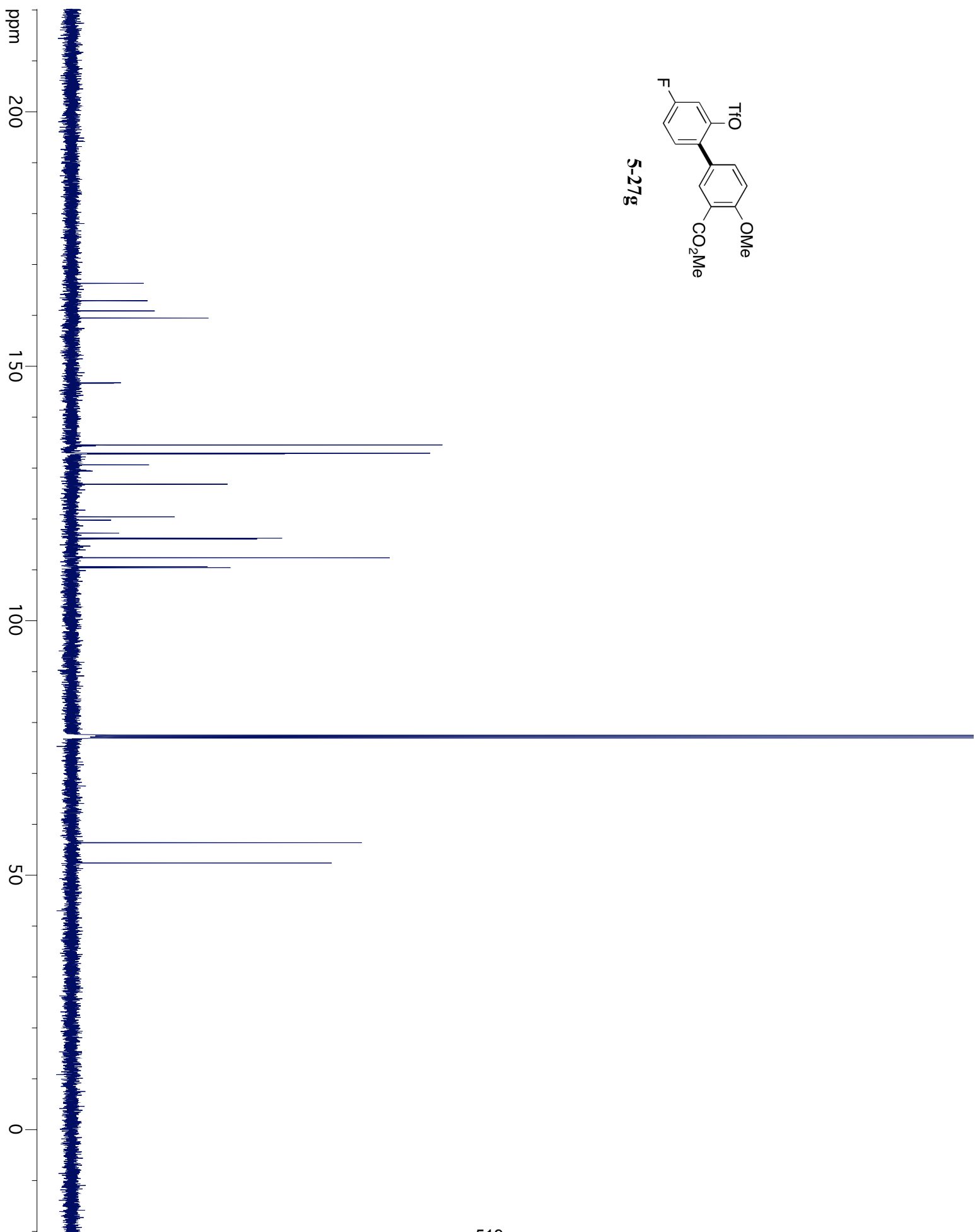
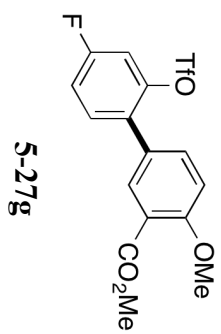


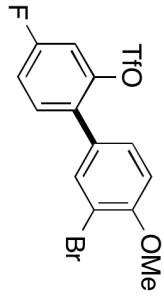


5-27f

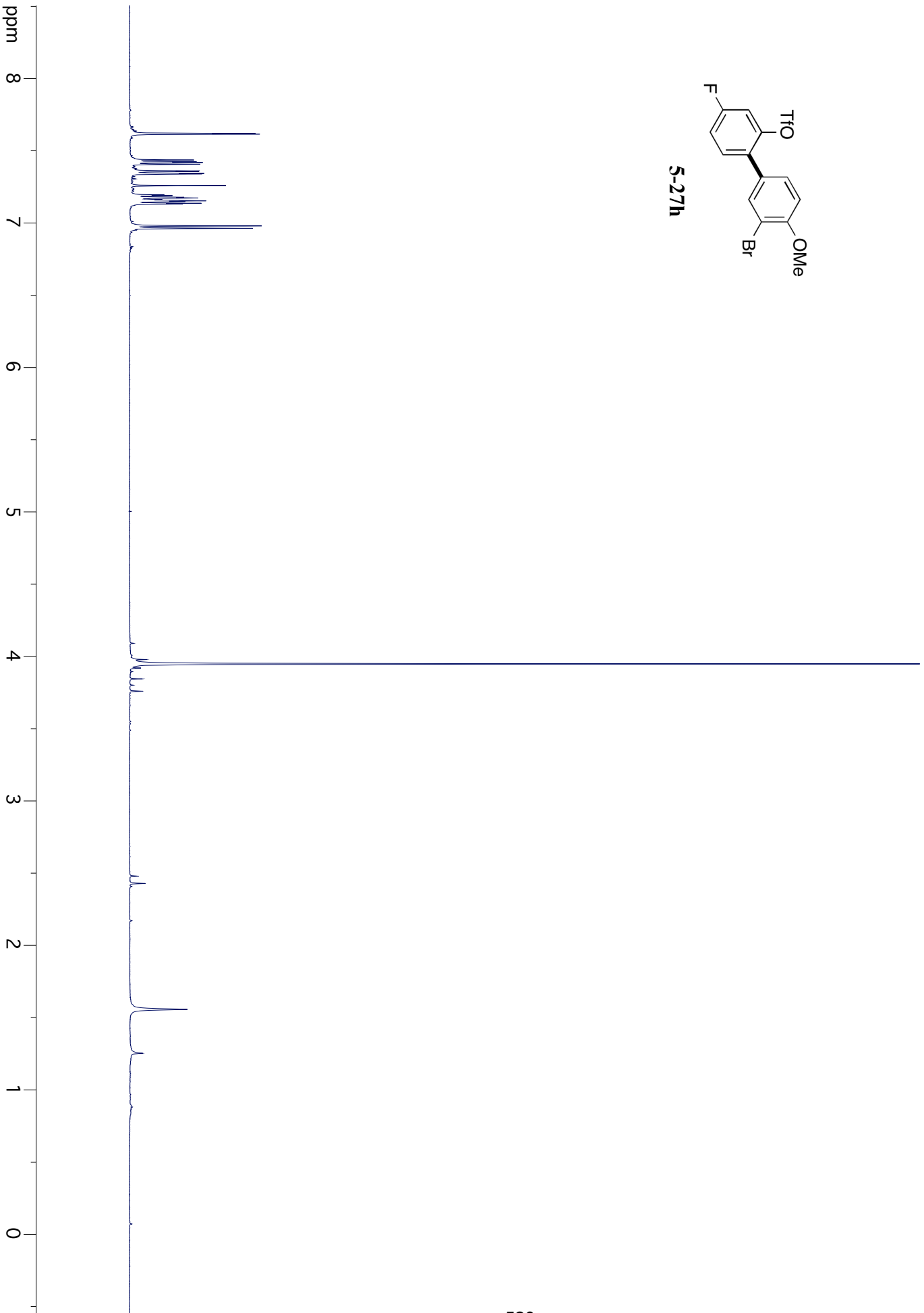


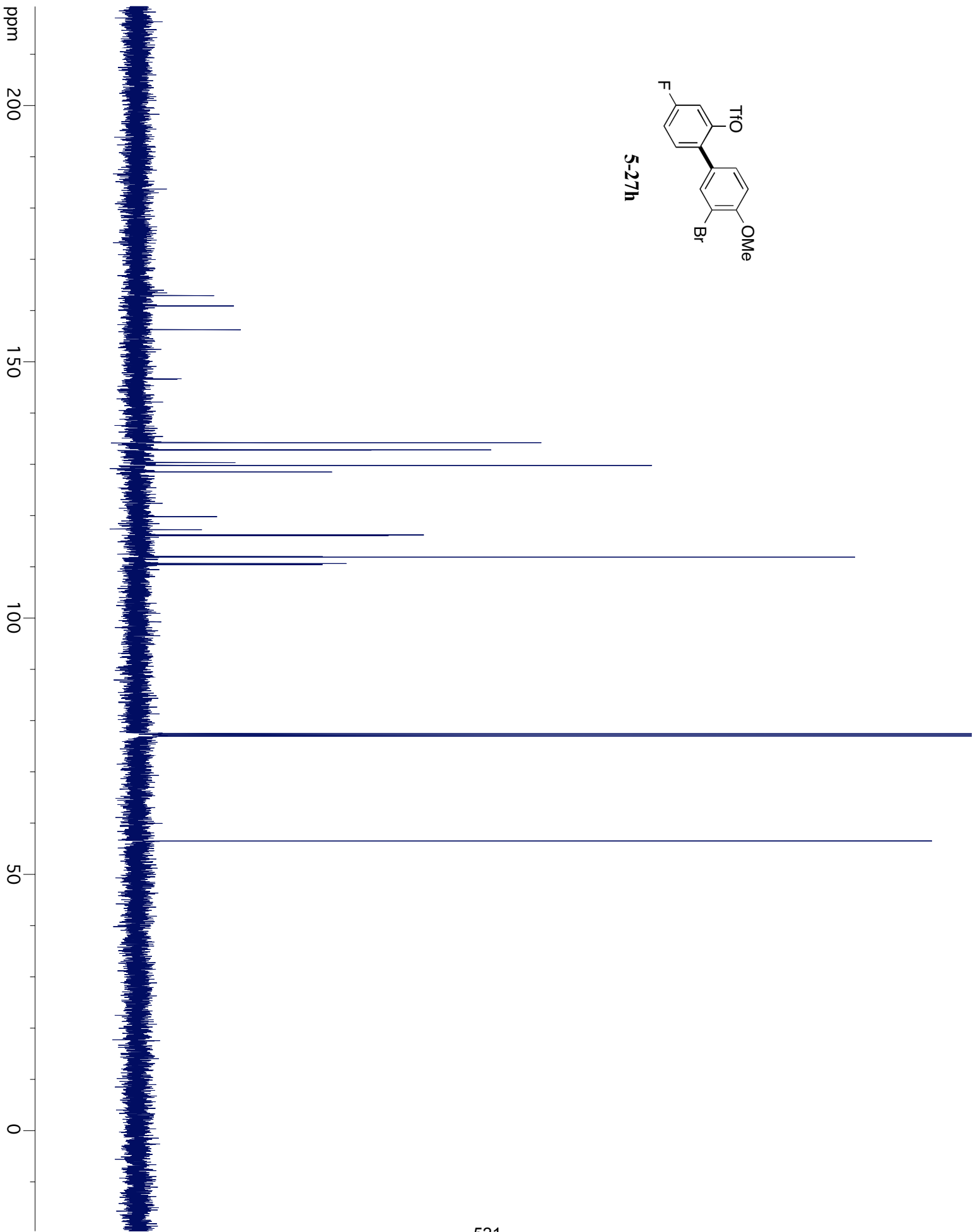
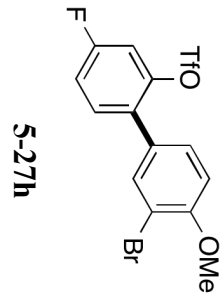


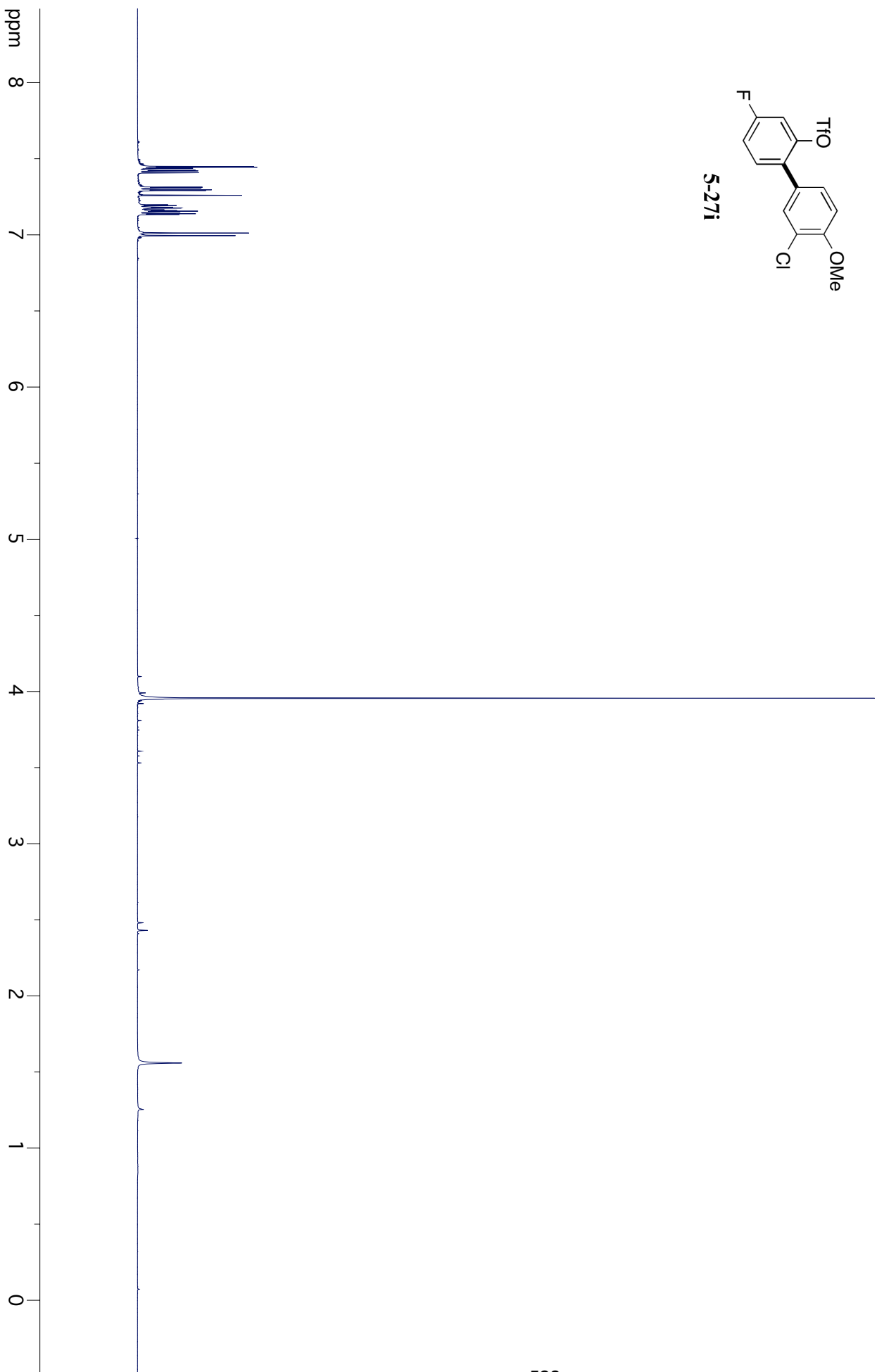
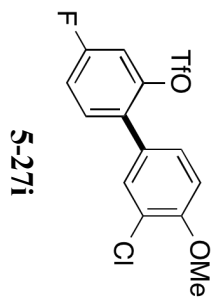


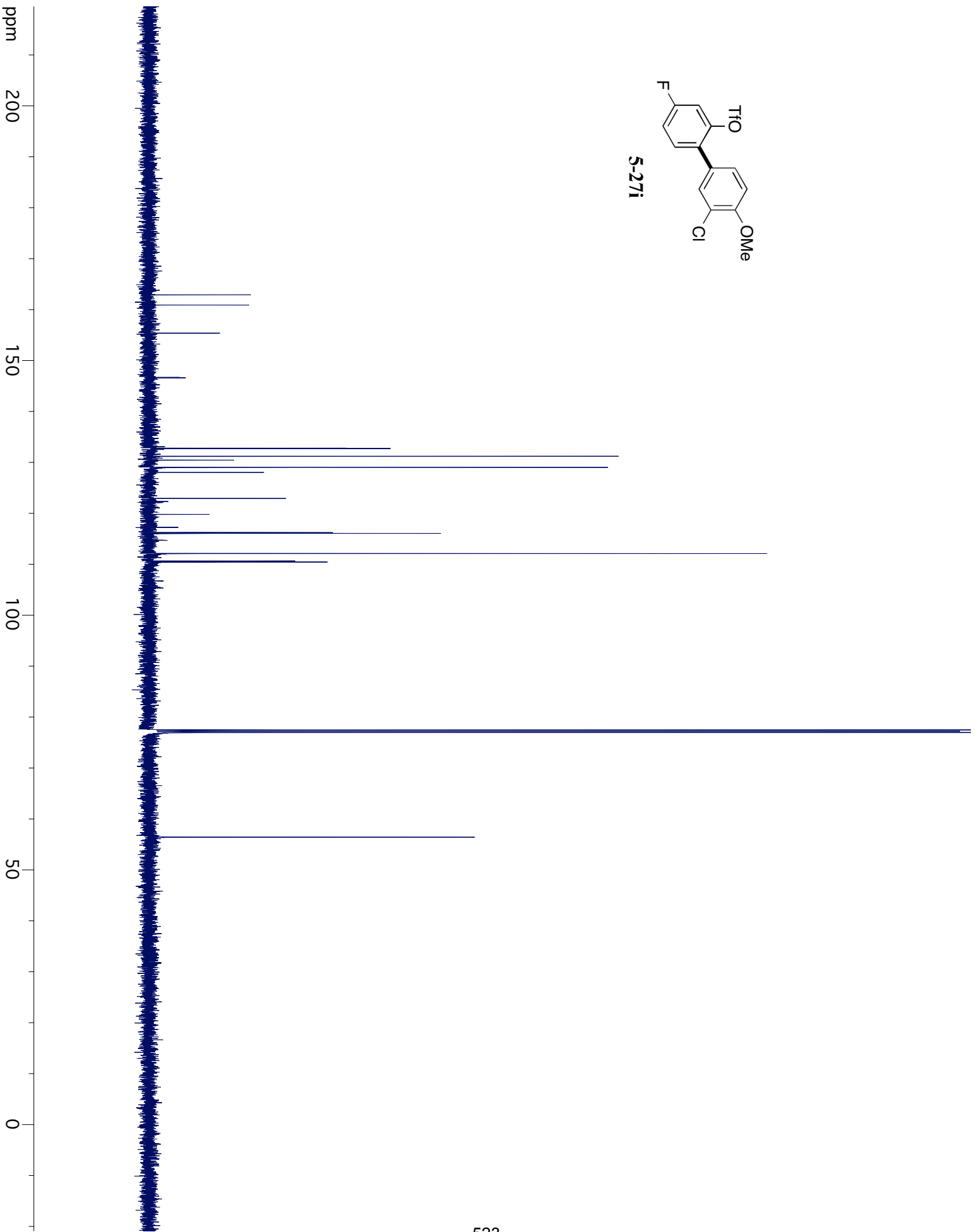
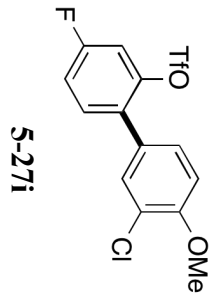


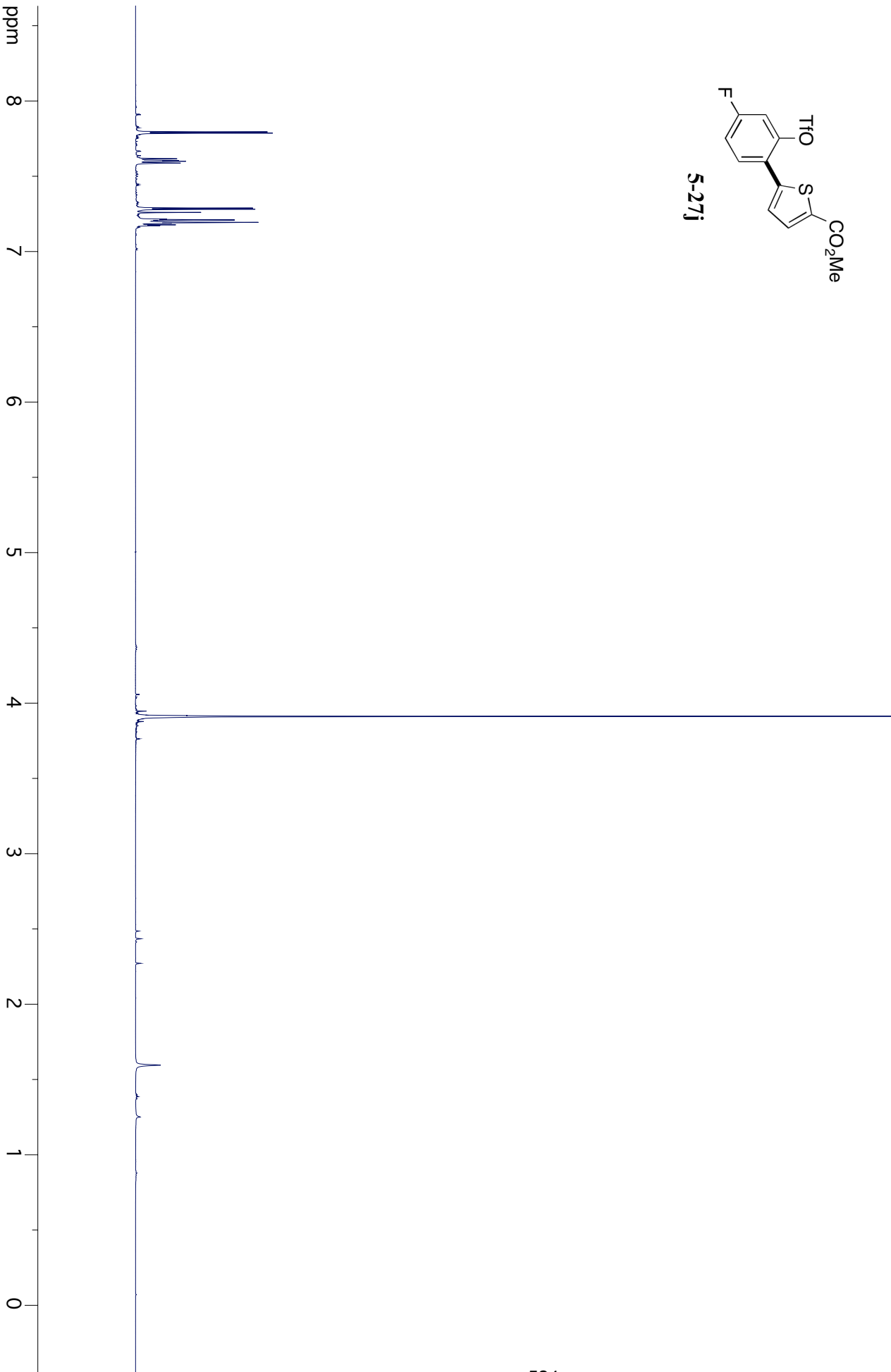
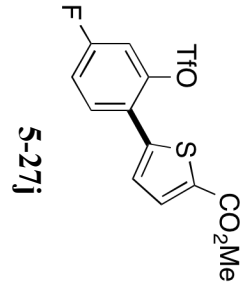
5-27h

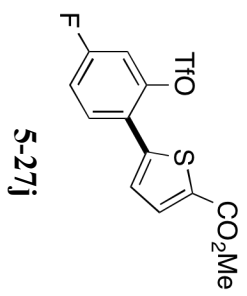






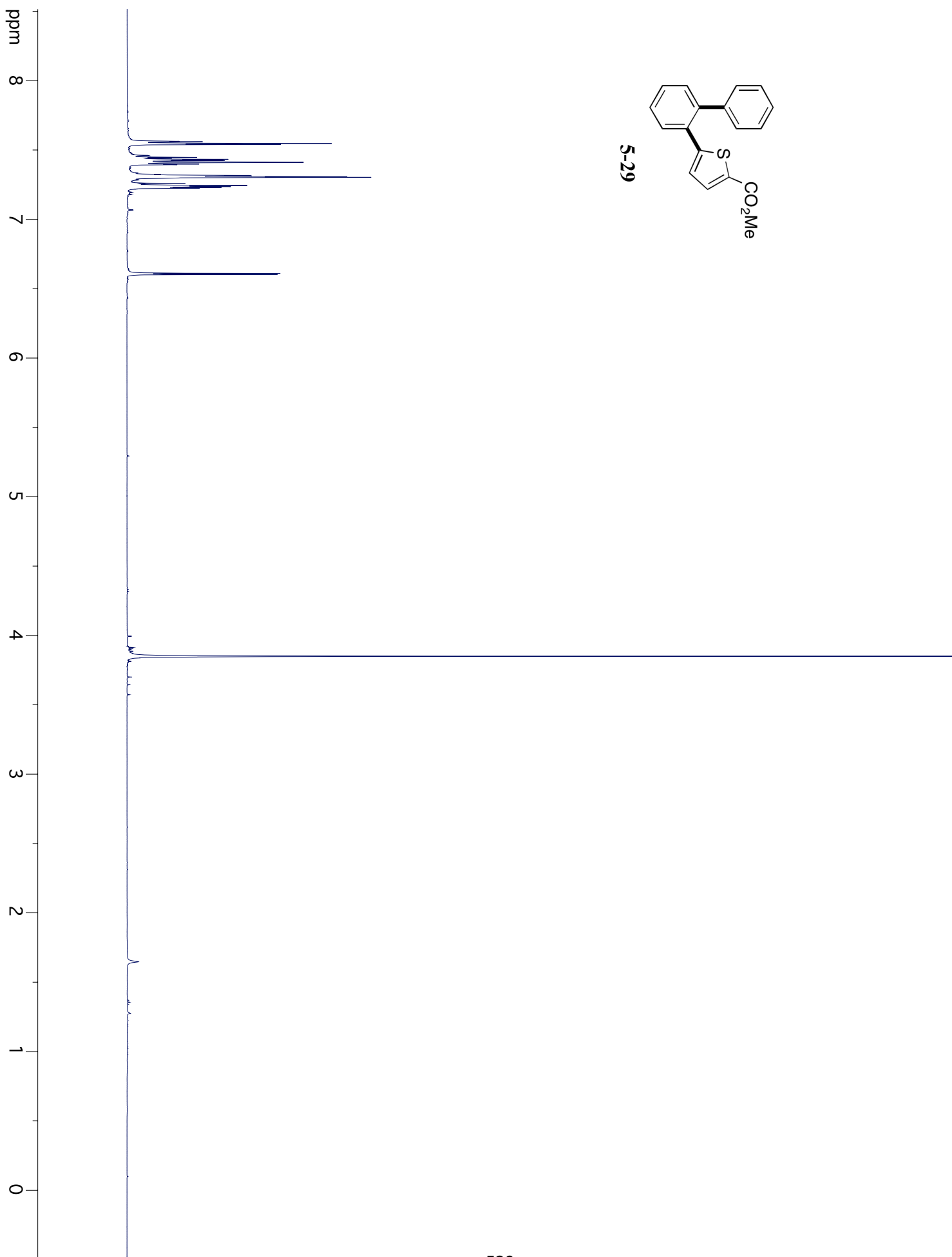
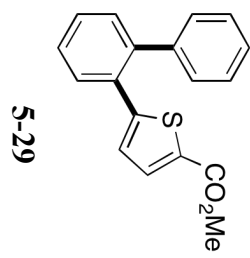


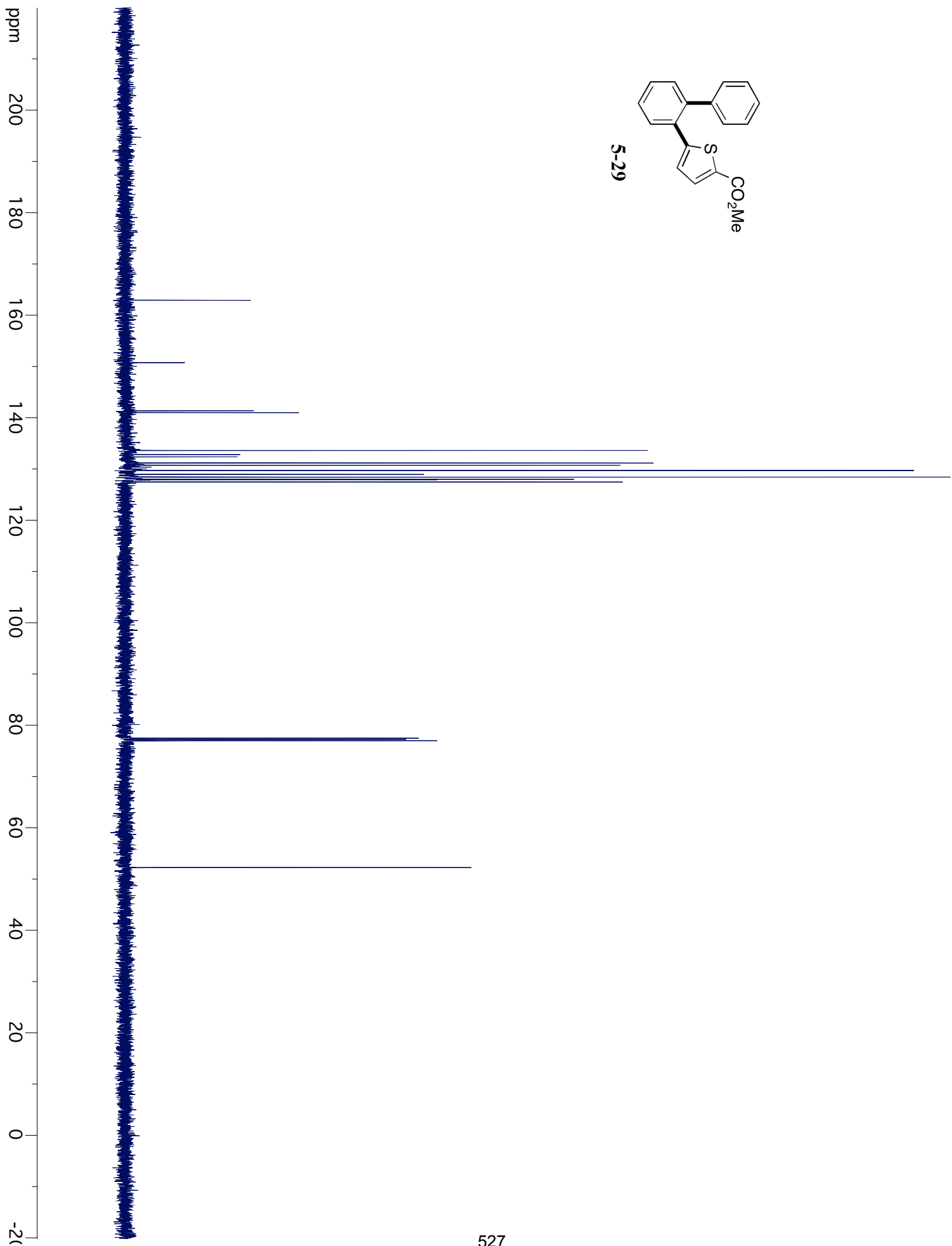
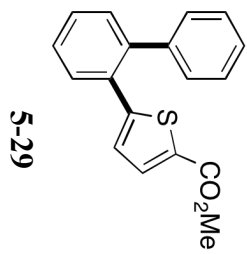


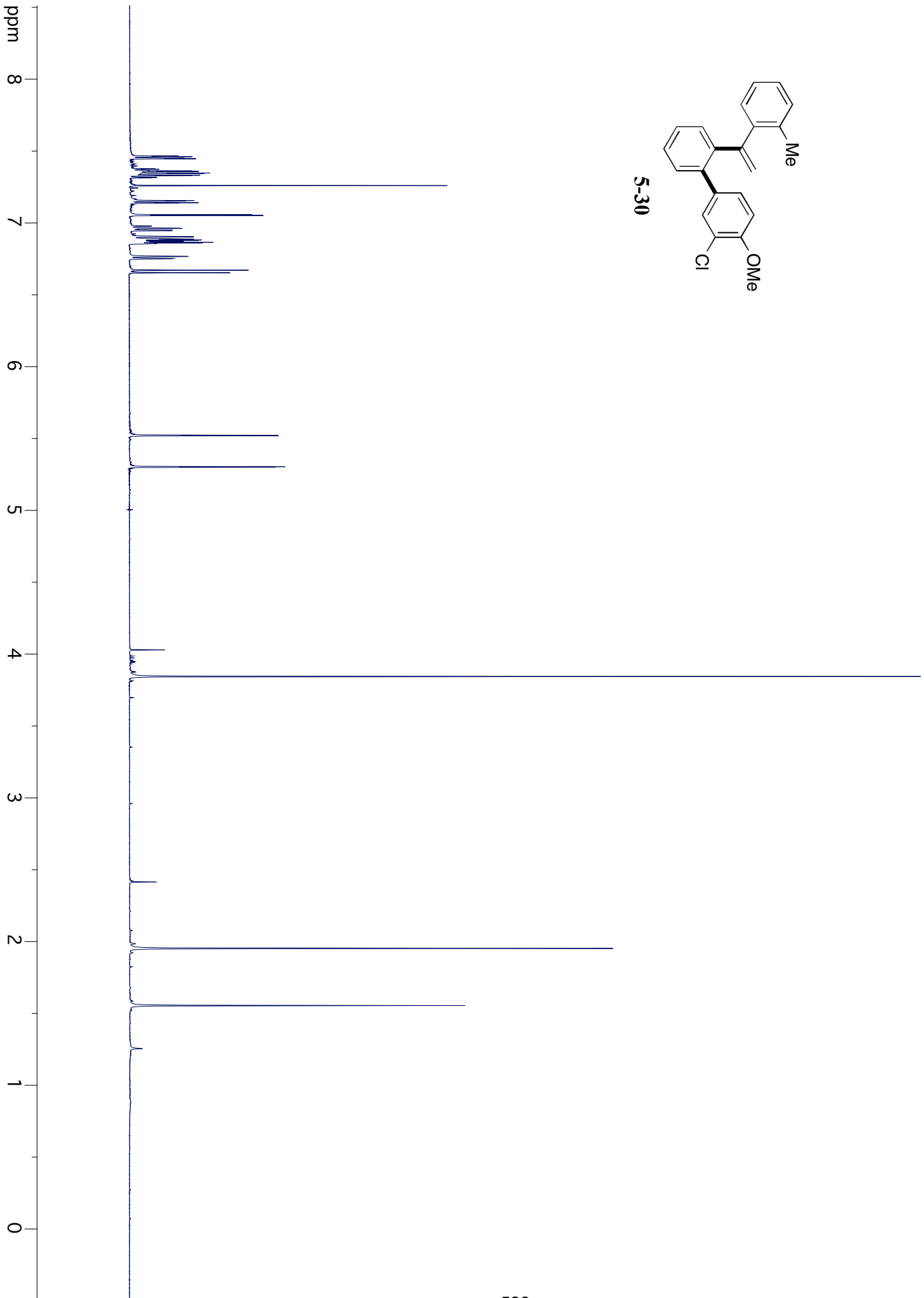
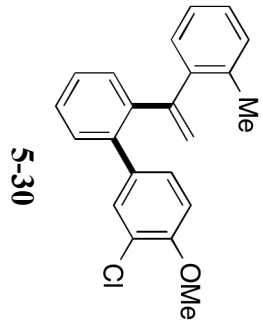


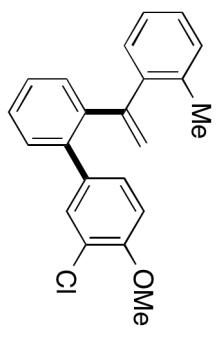
ppm



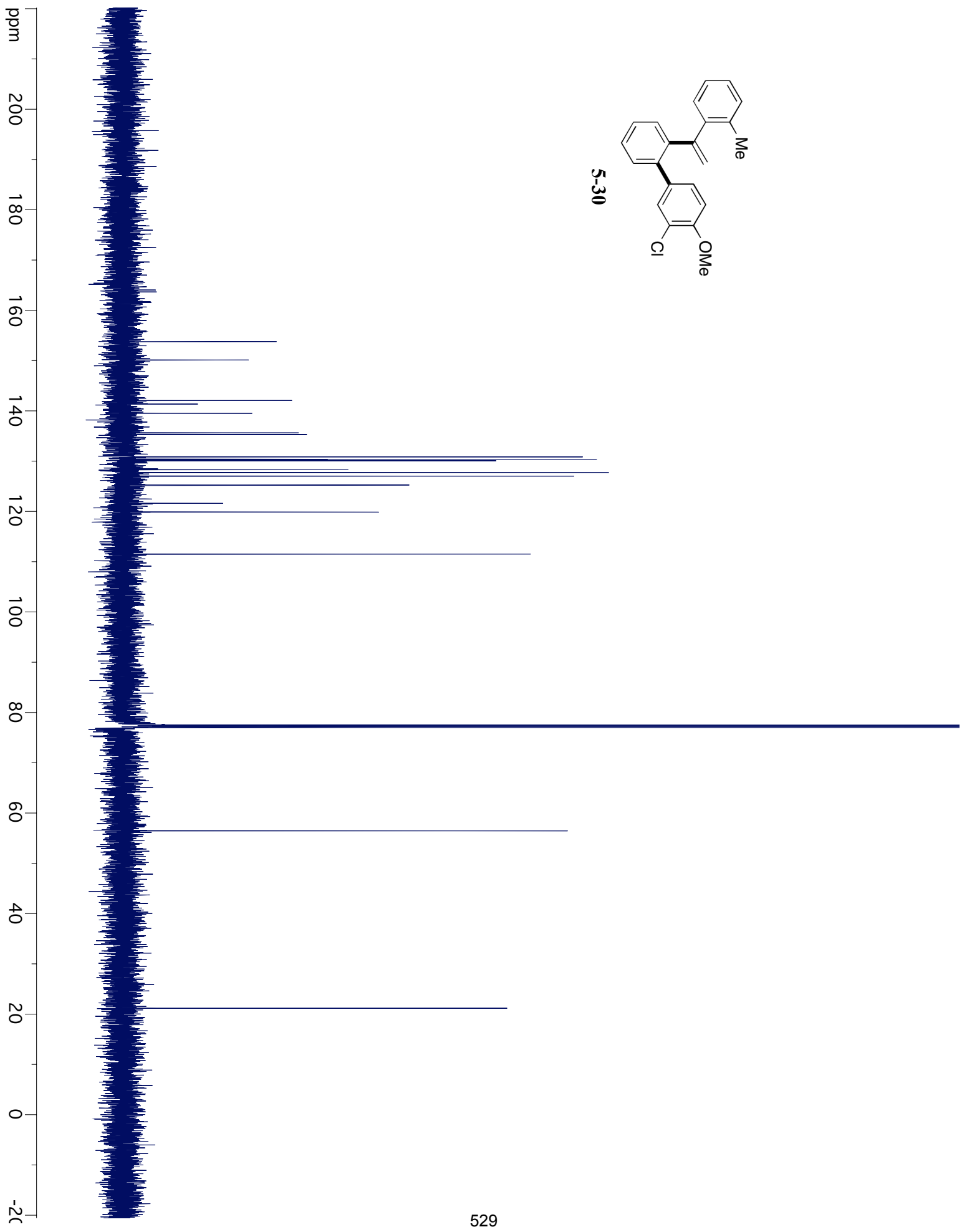


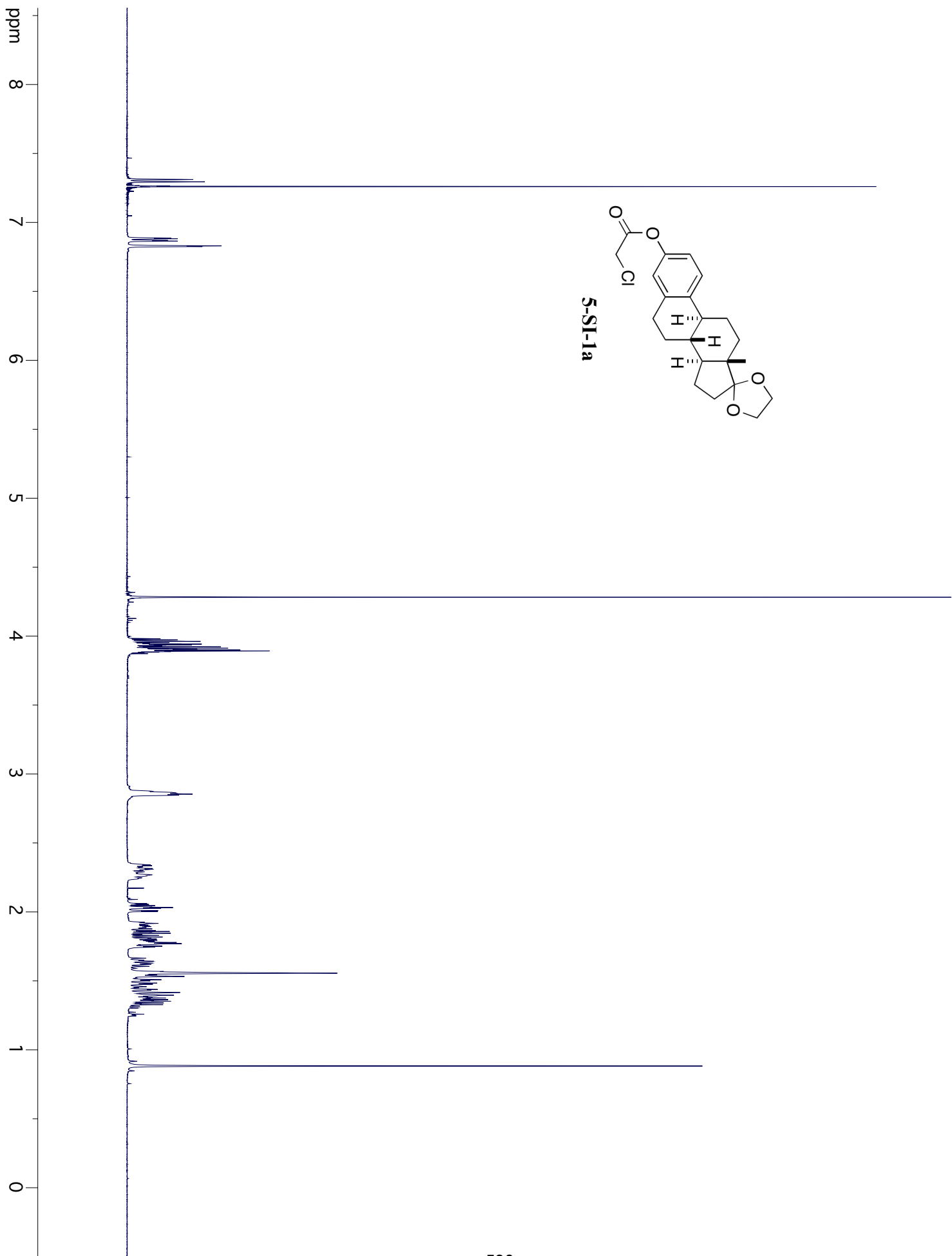
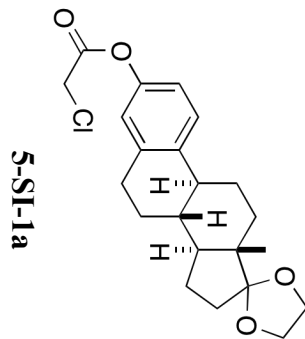


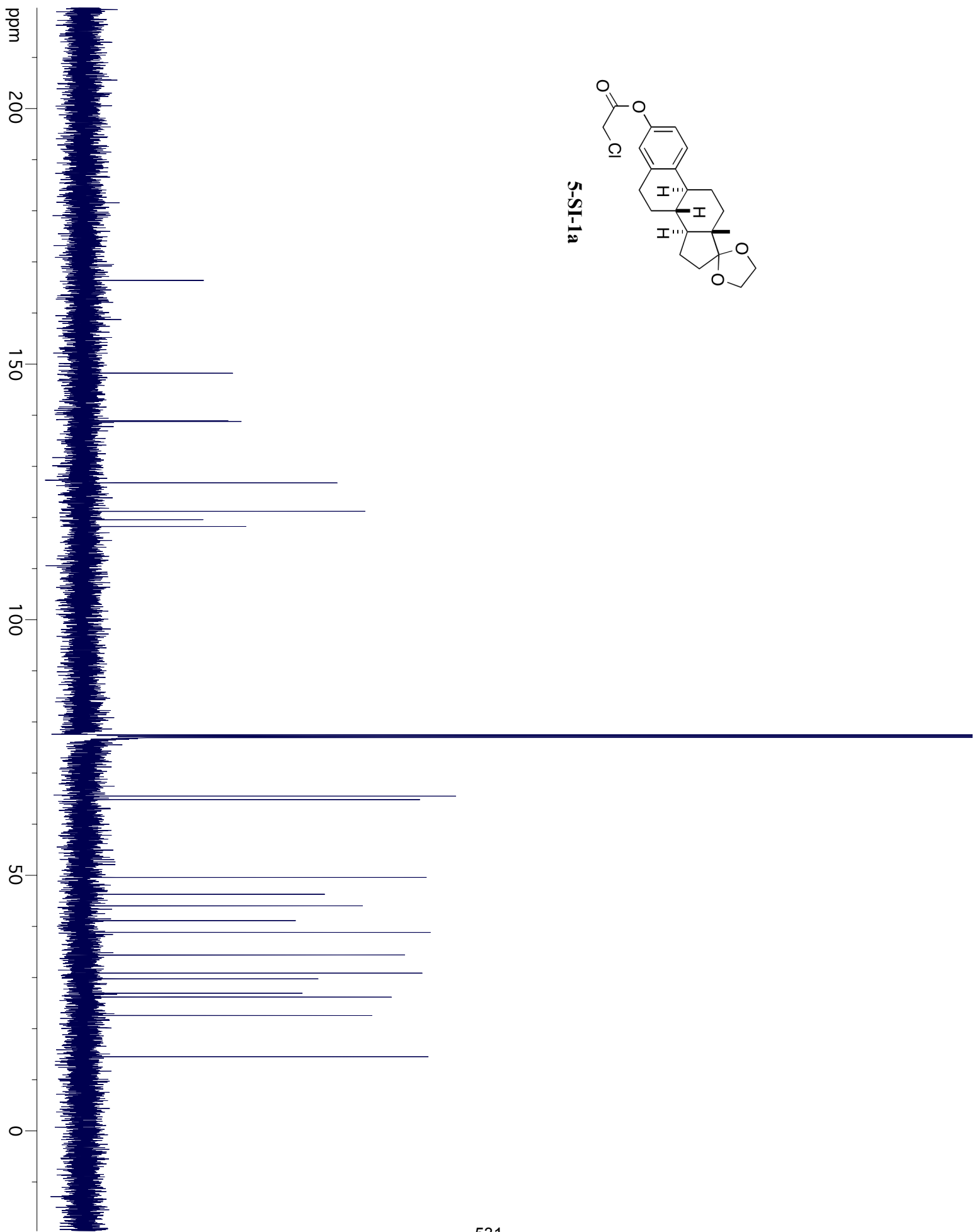
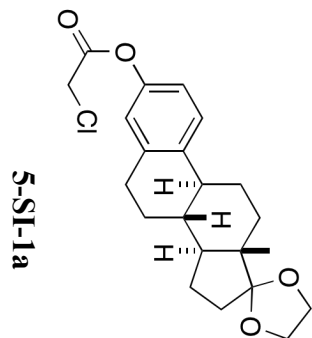


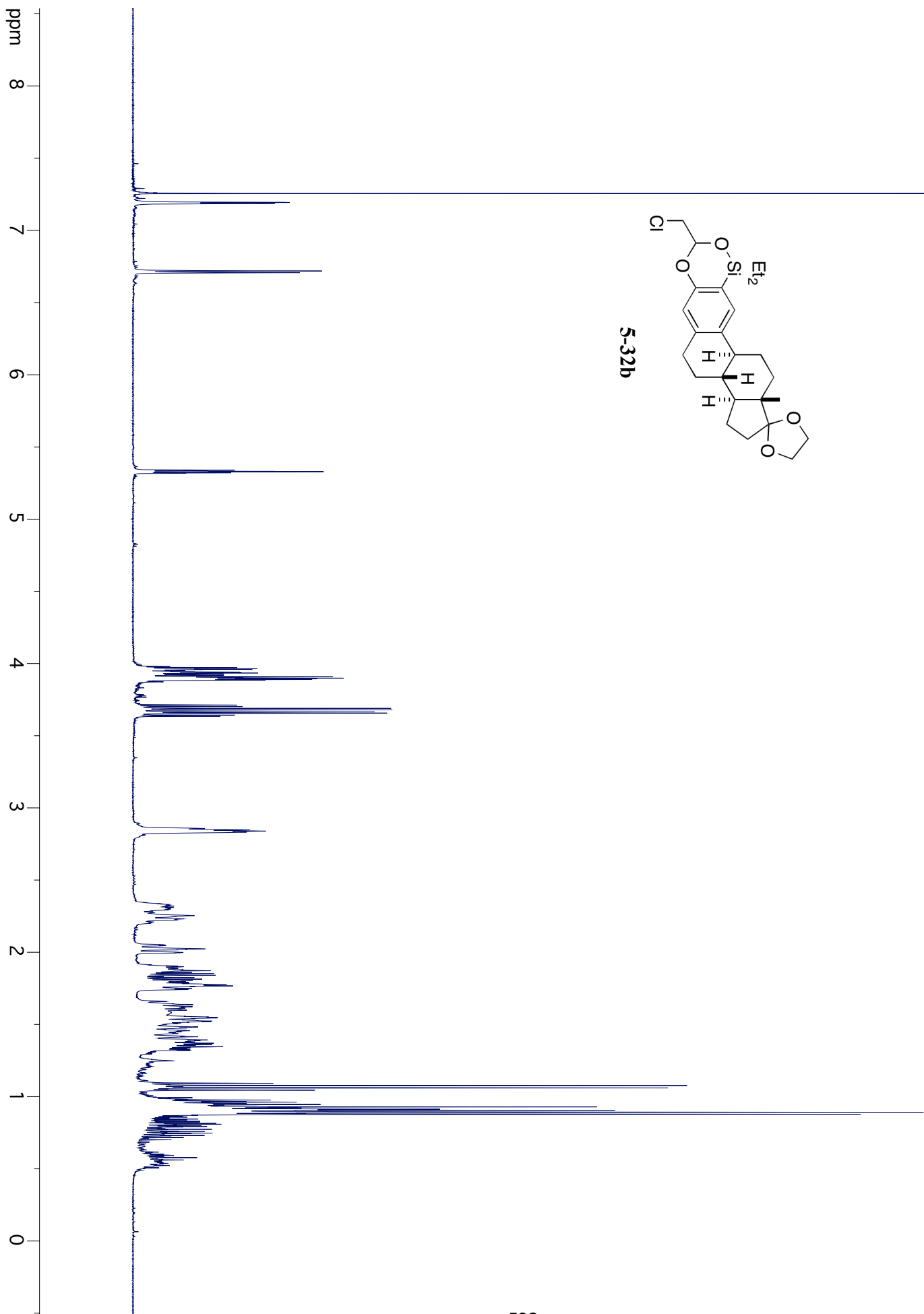
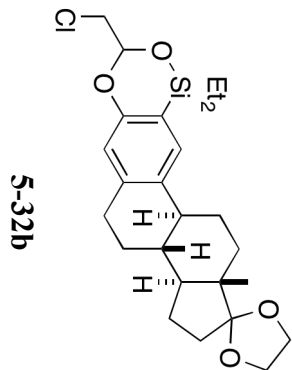


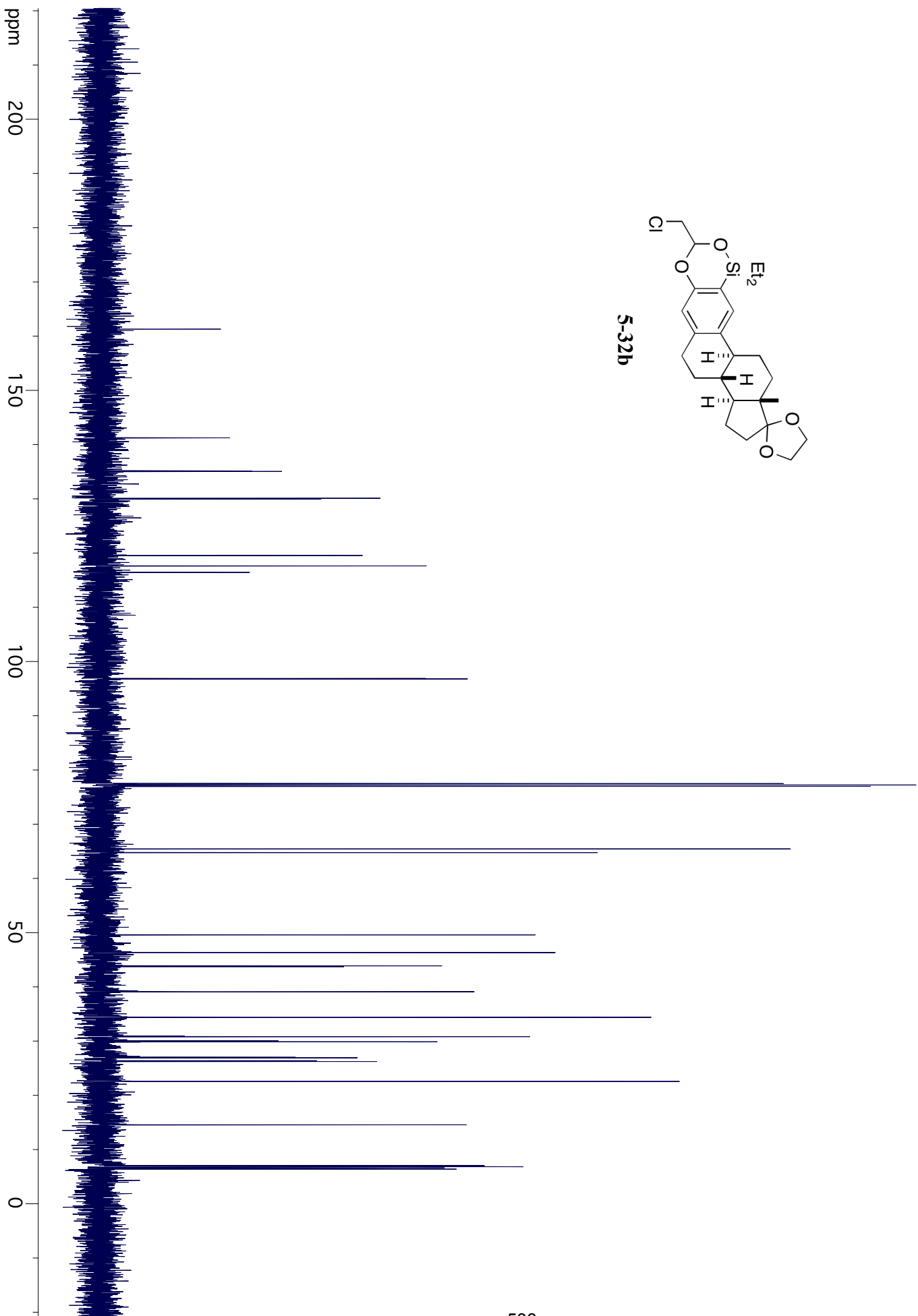
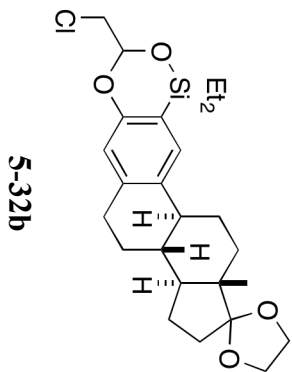
5-30

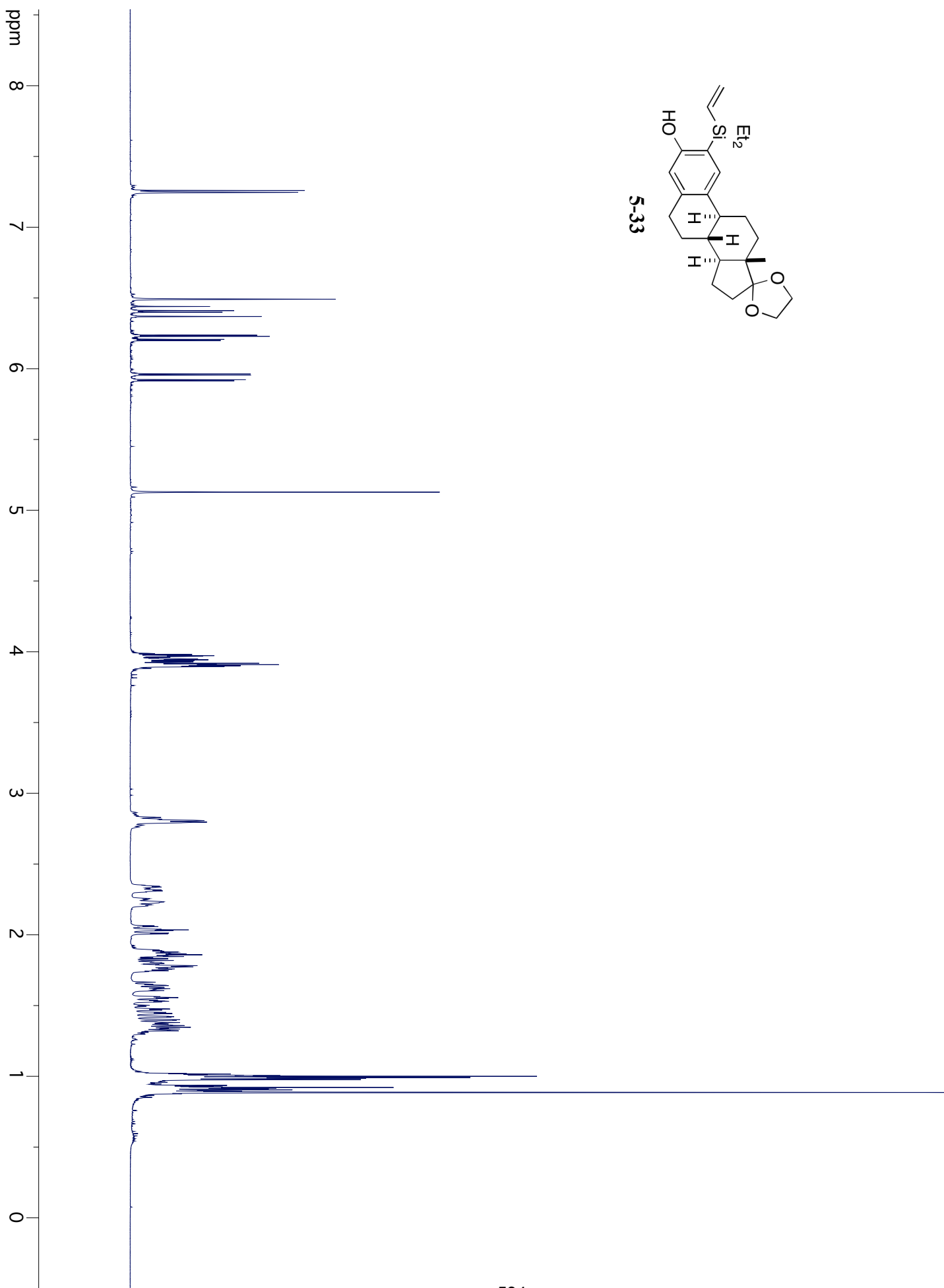
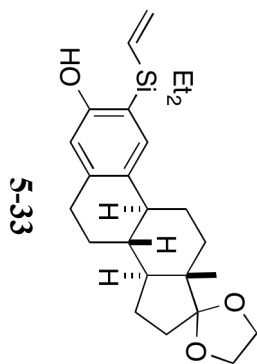


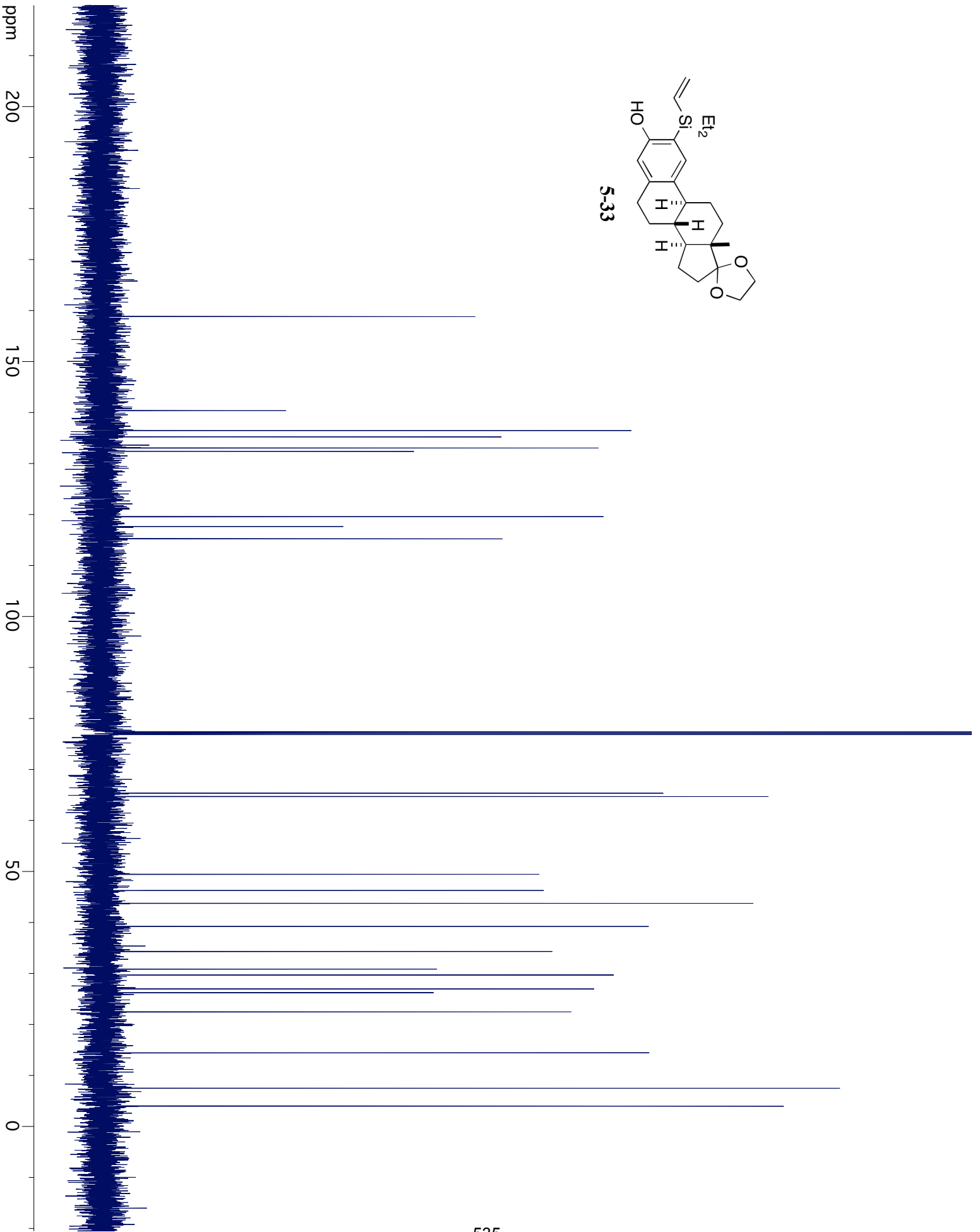
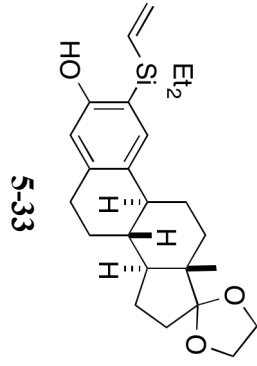


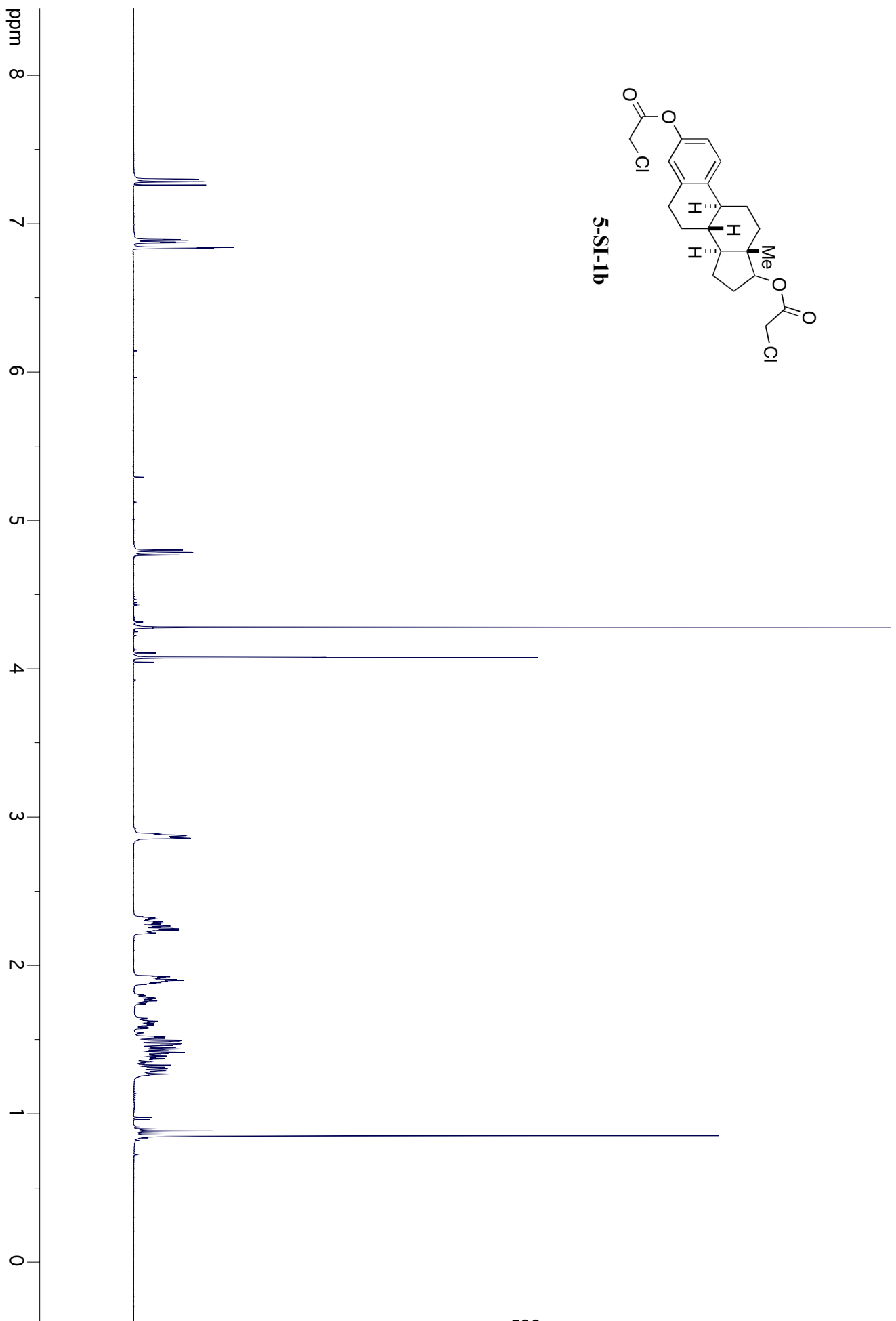
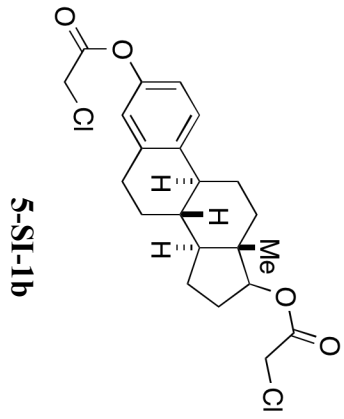


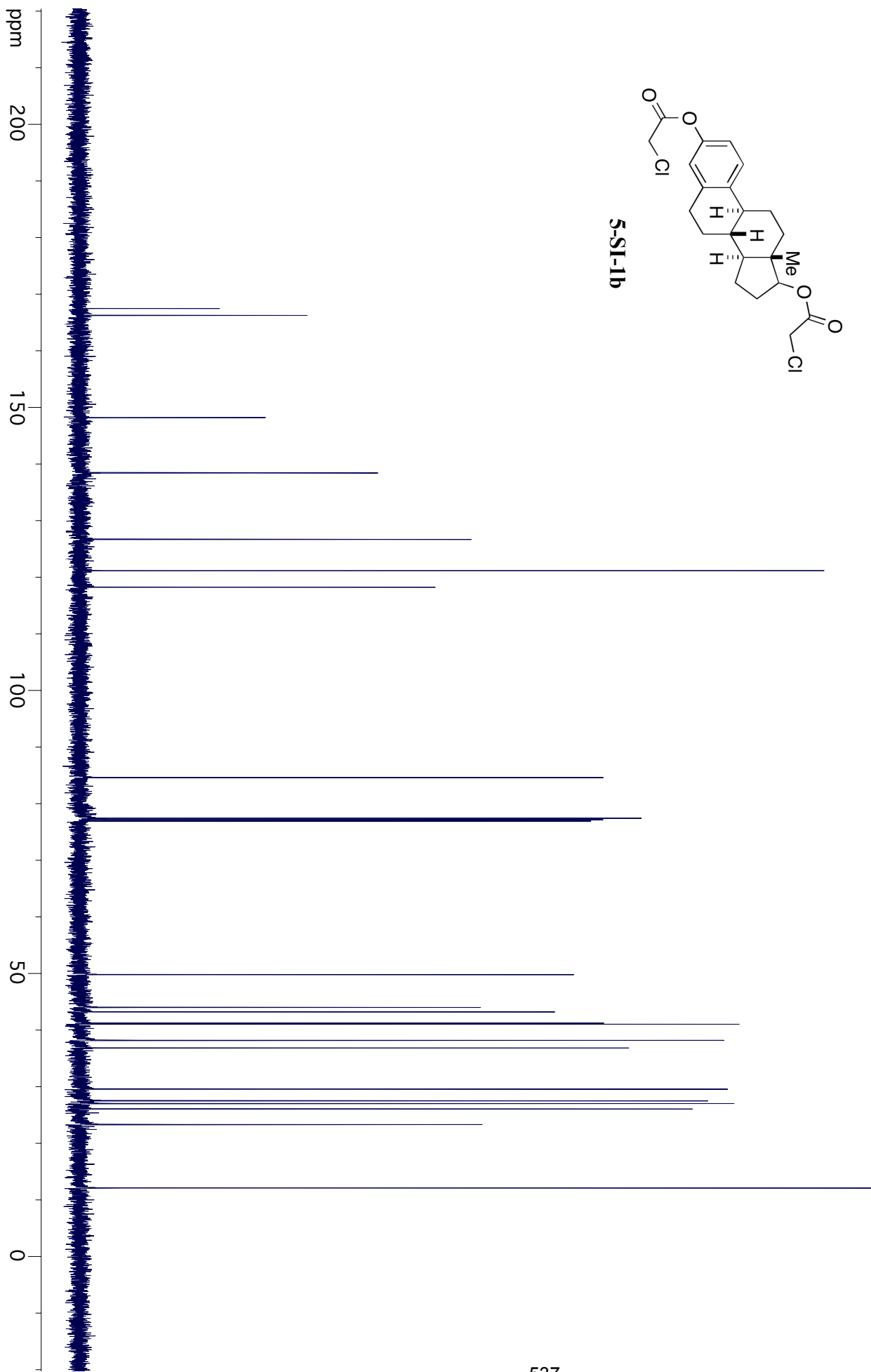
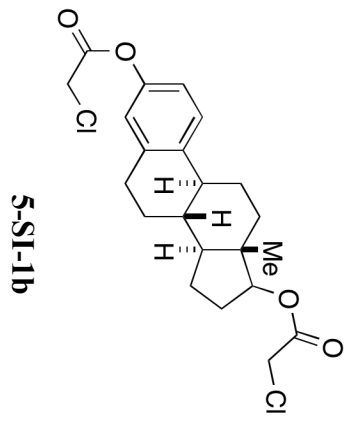


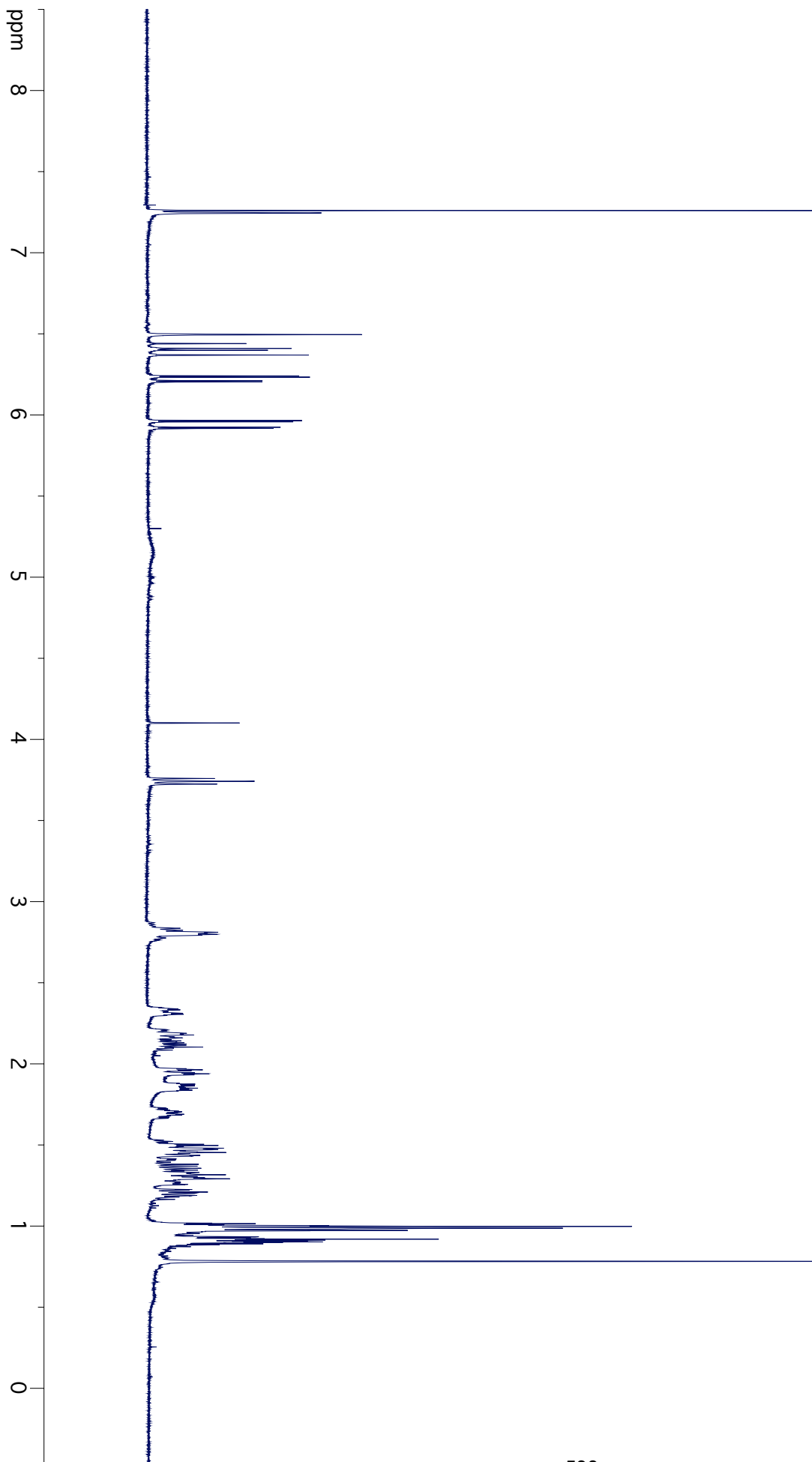
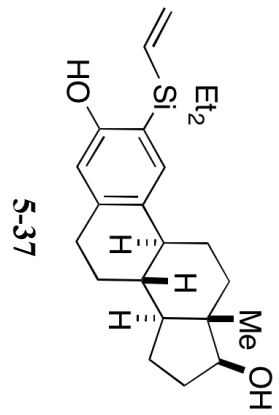


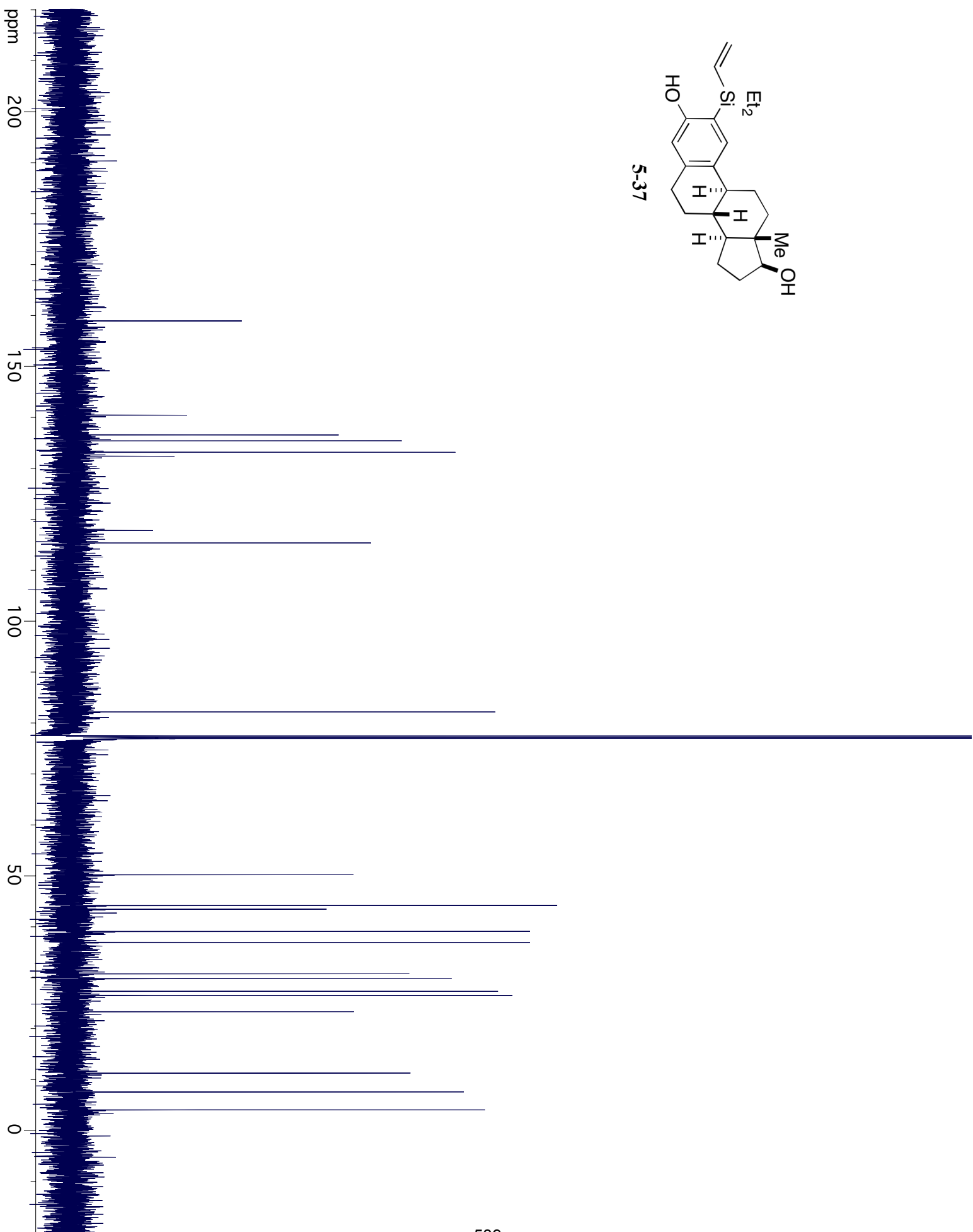
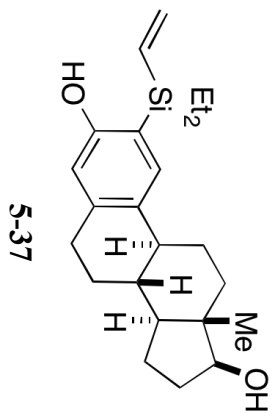


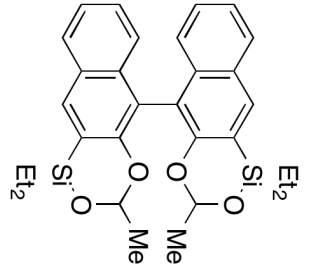




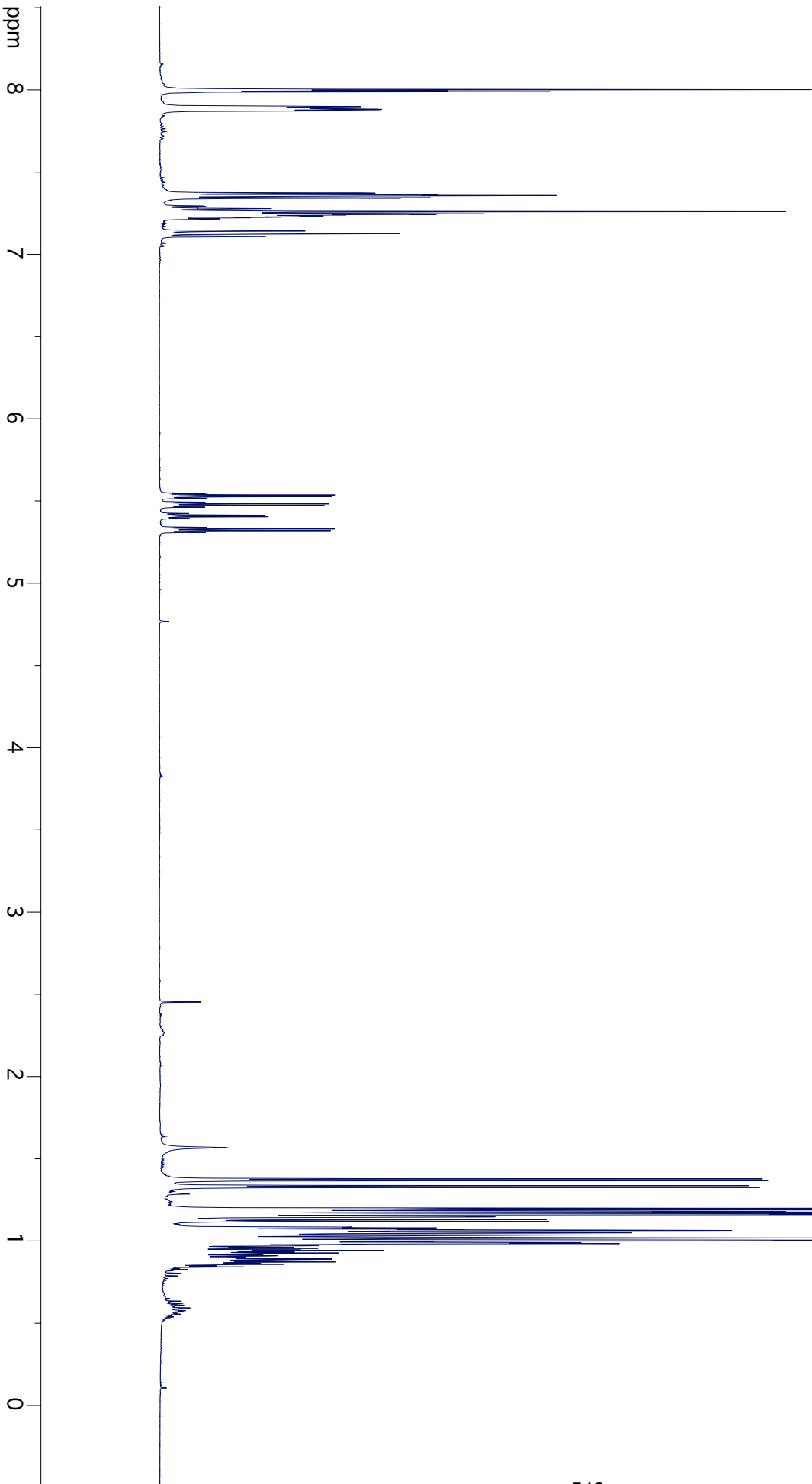


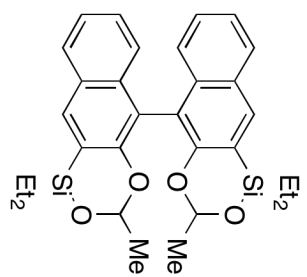




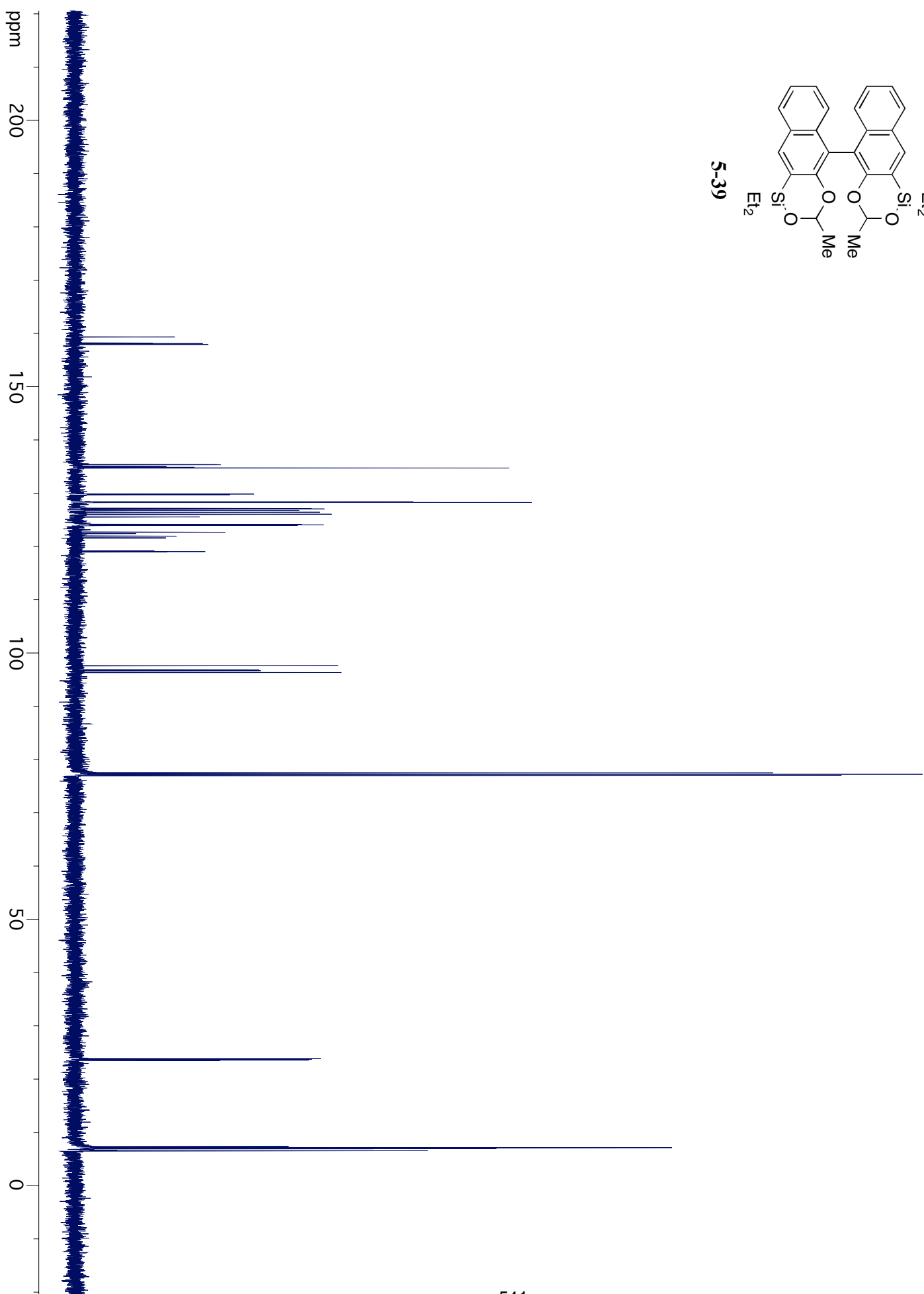


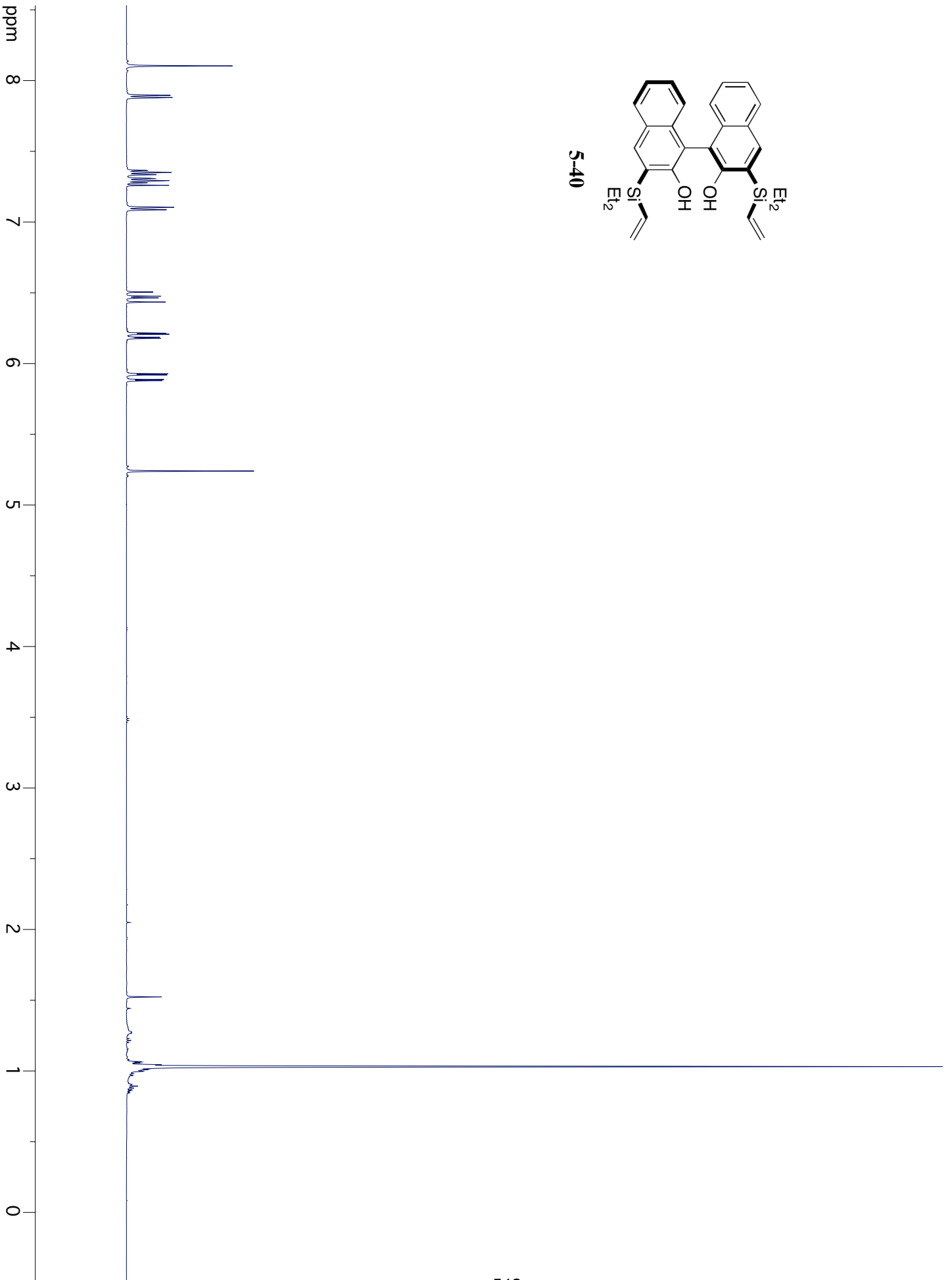
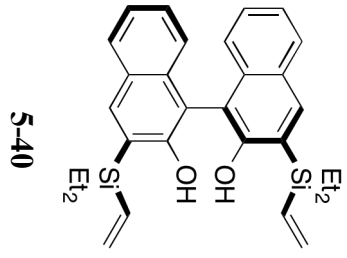
5-39

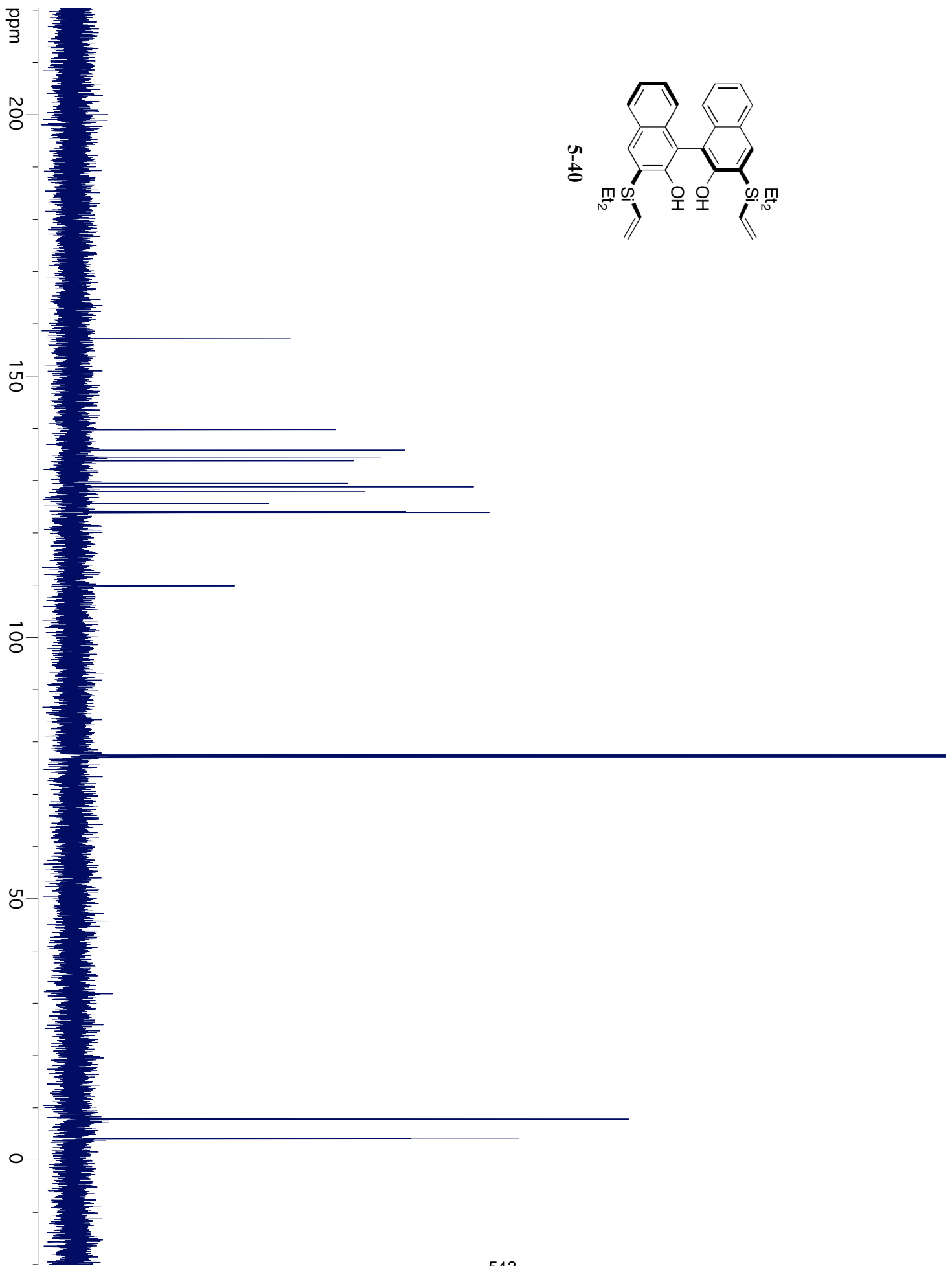
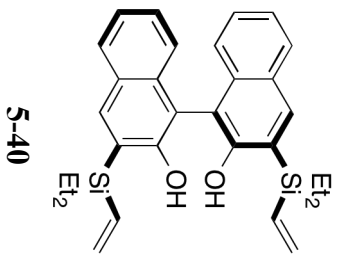


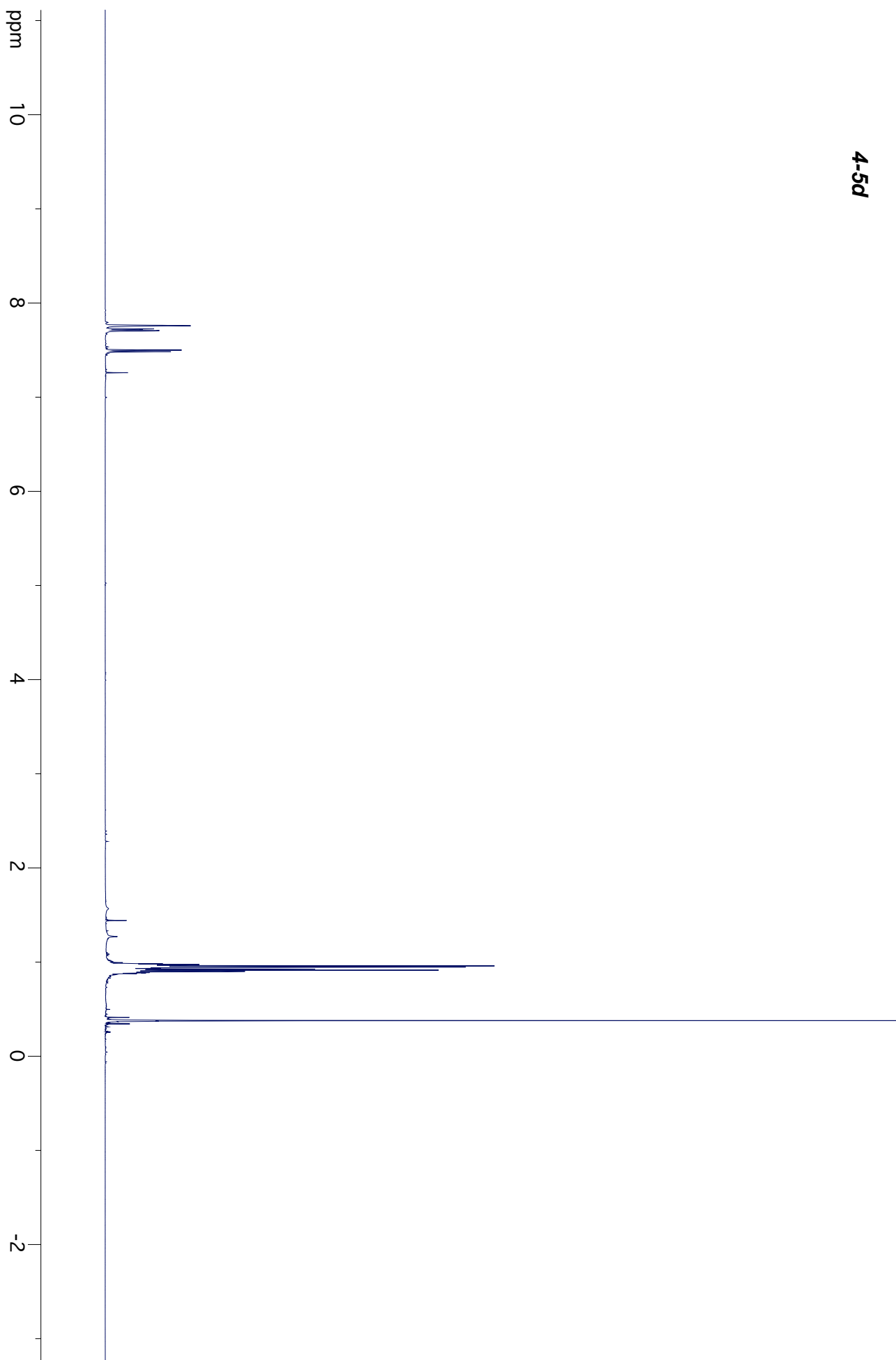
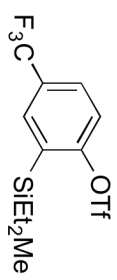


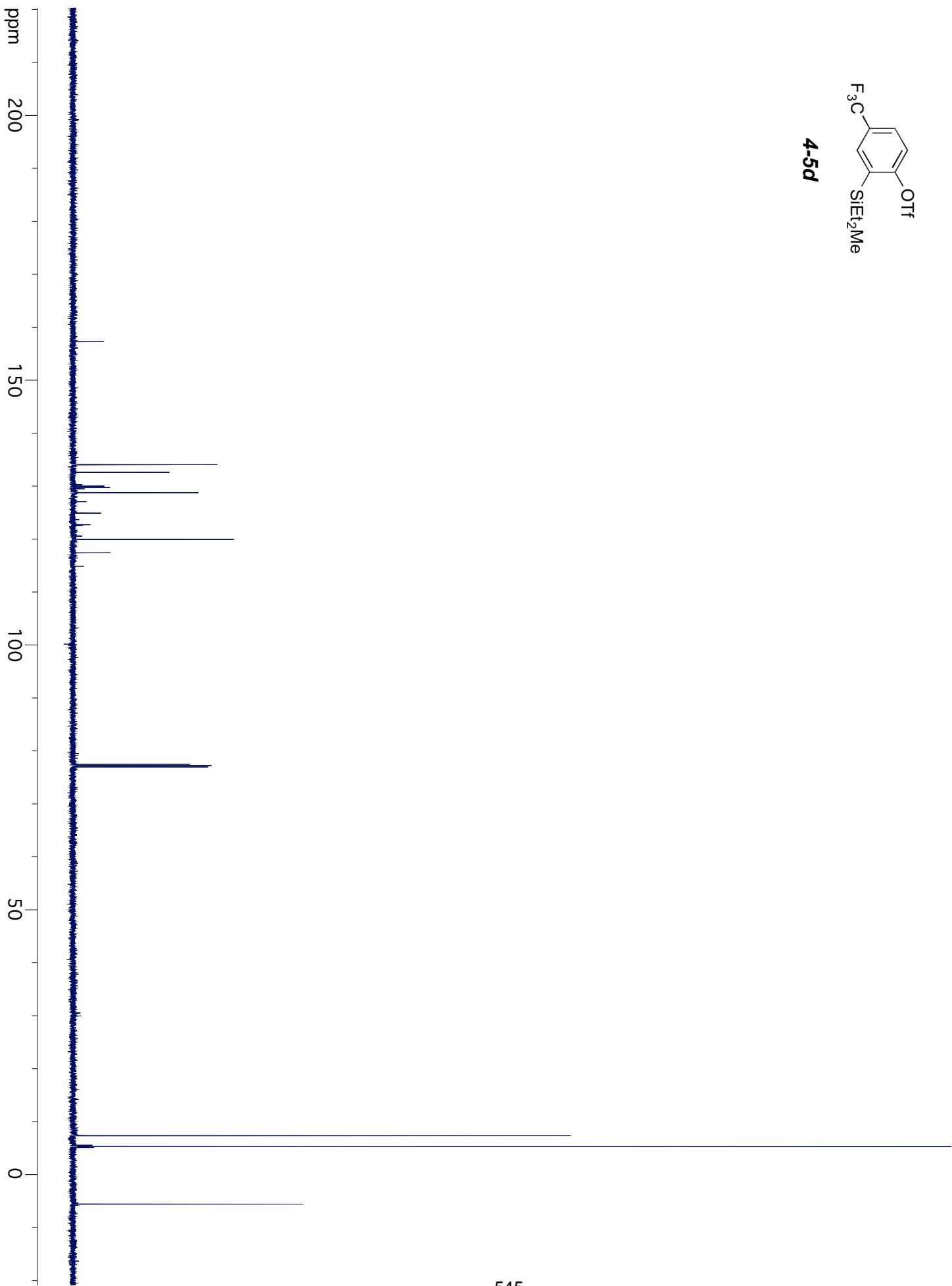
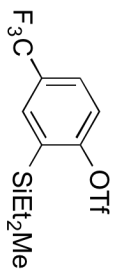
5-39

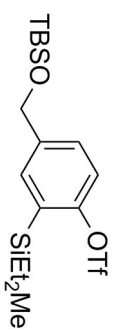




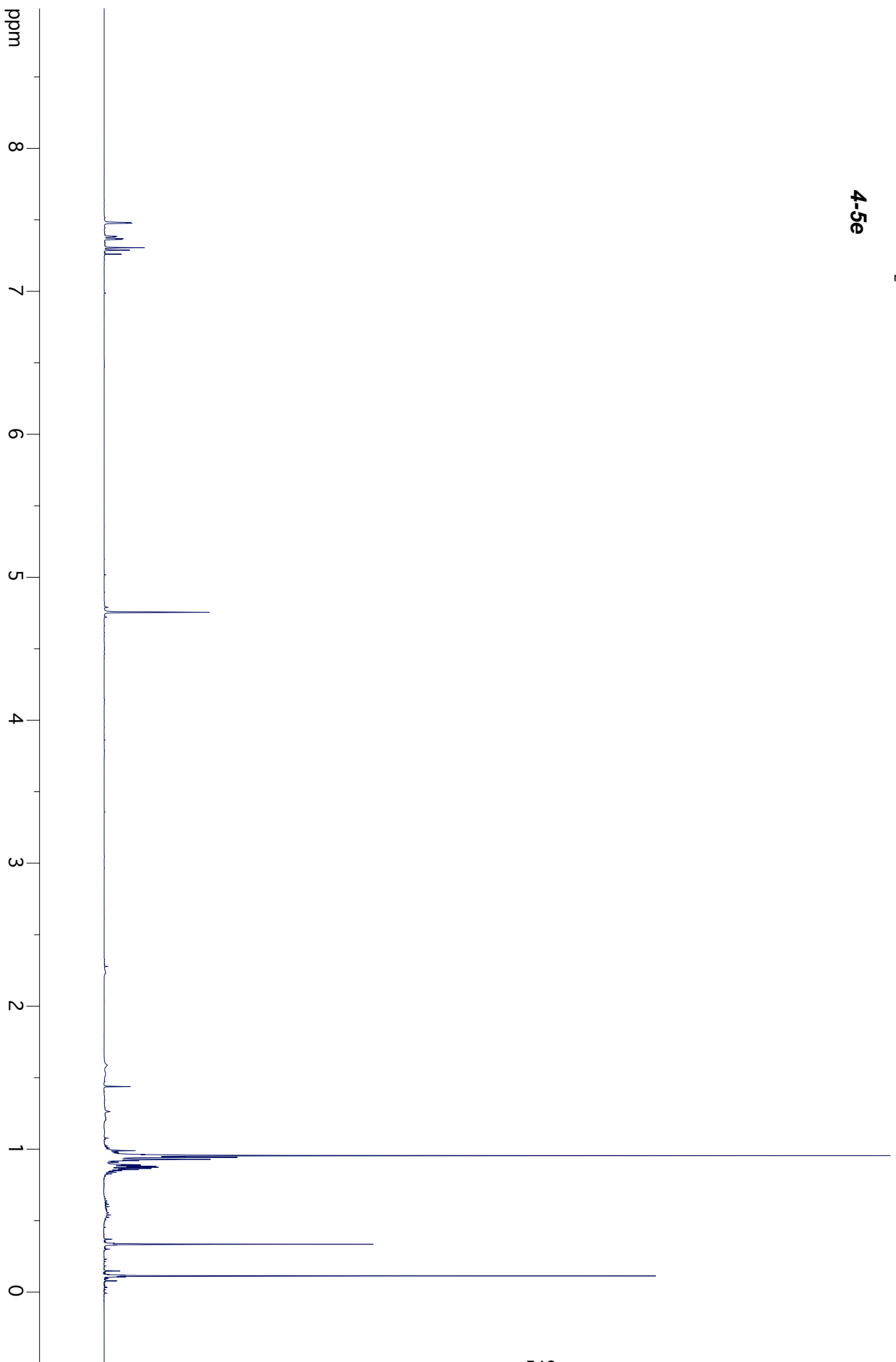


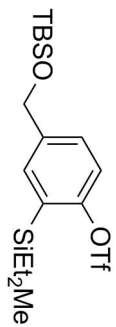




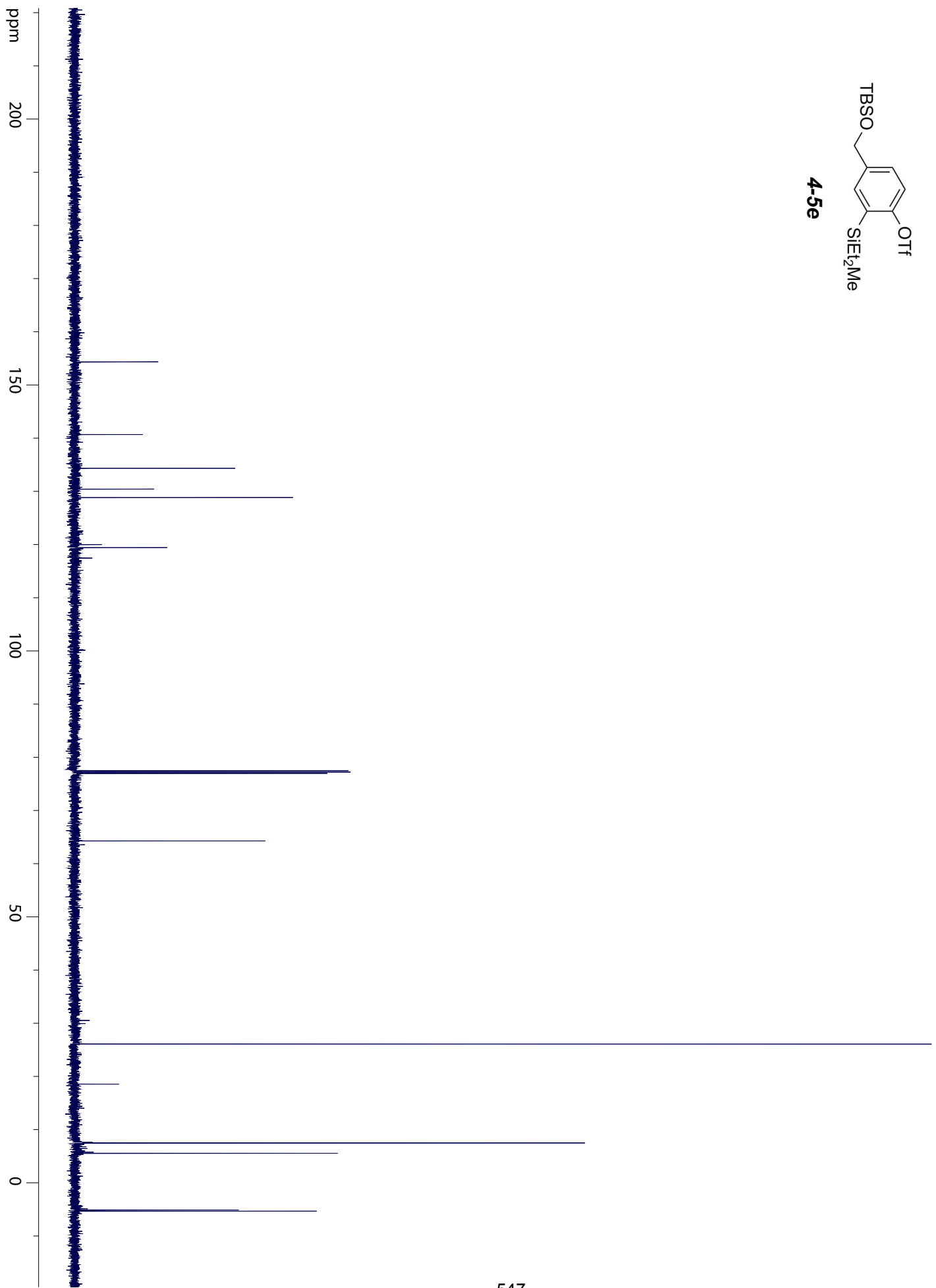


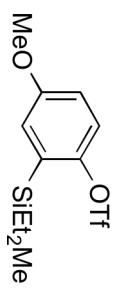
4-5e



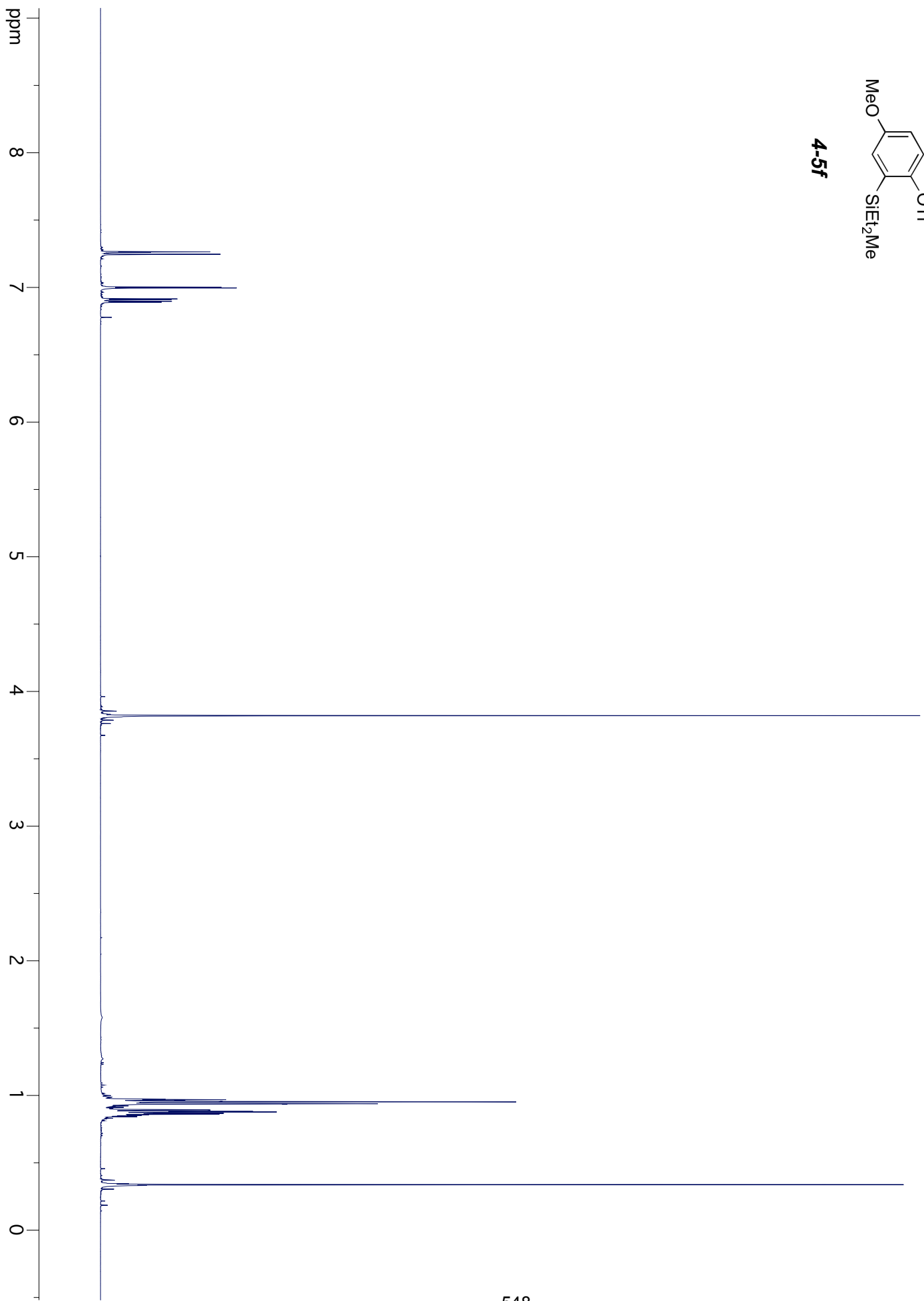


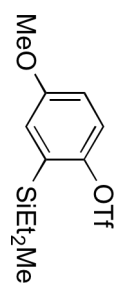
4-5e



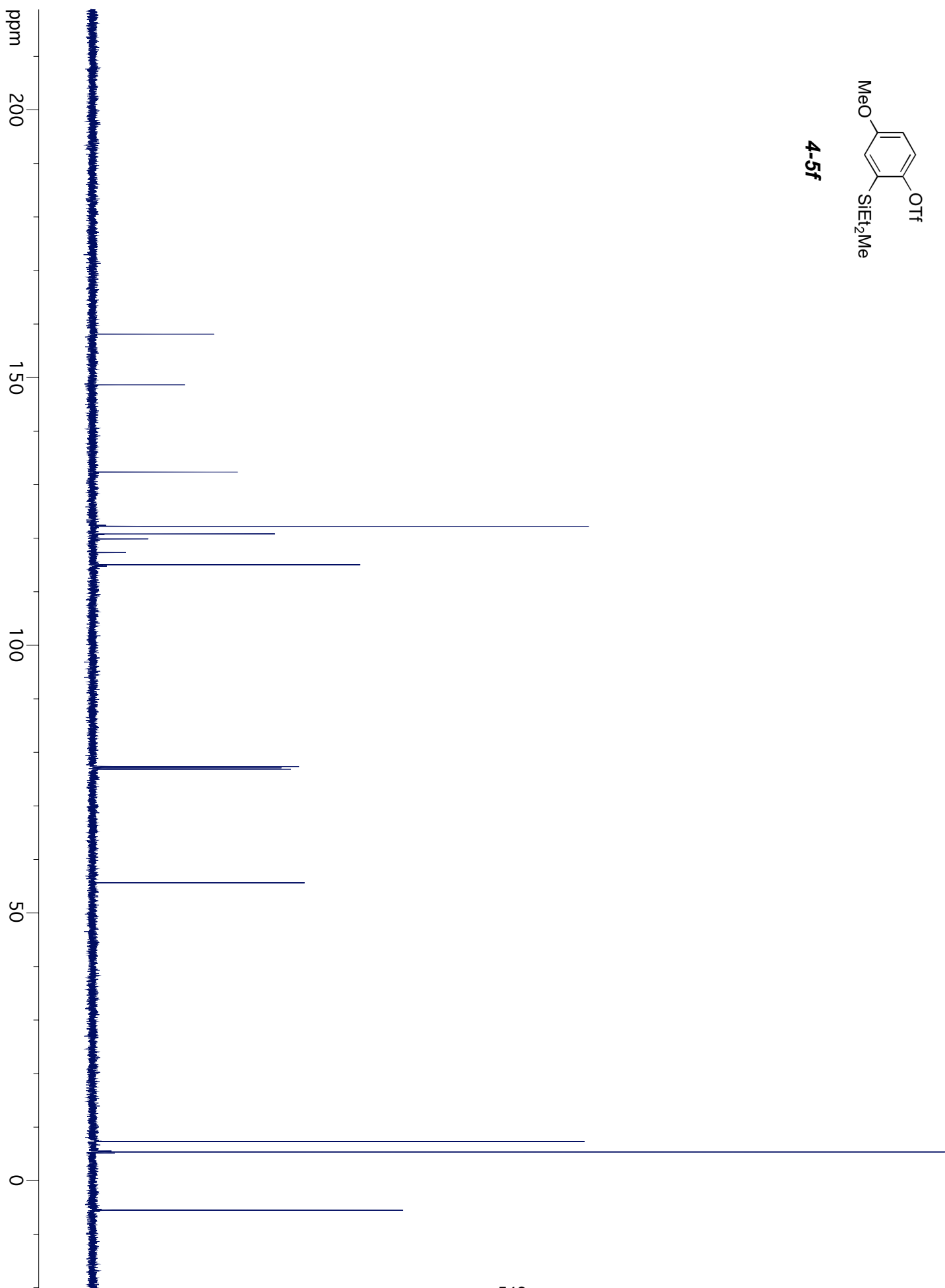


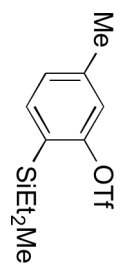
4-5f



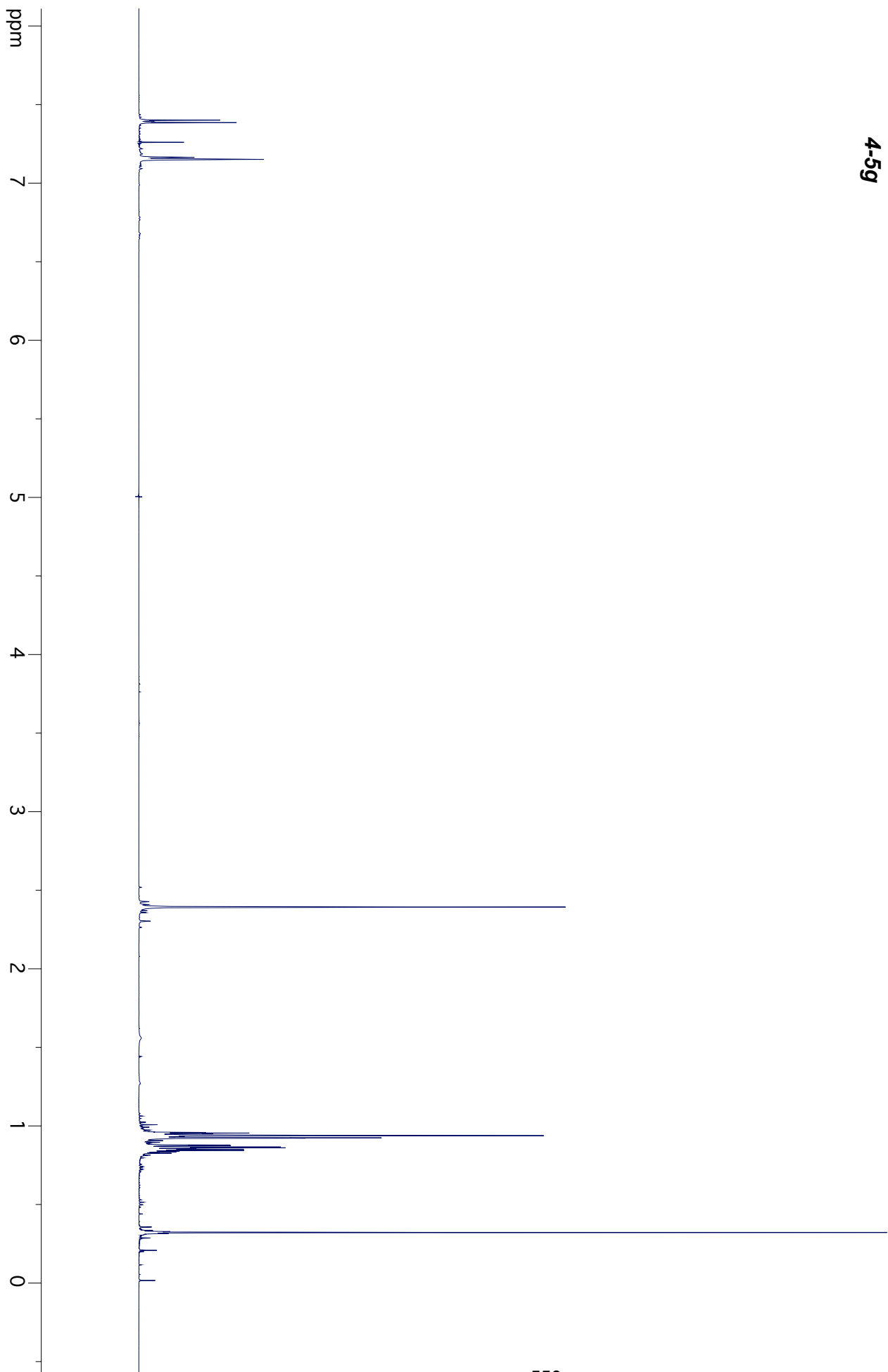


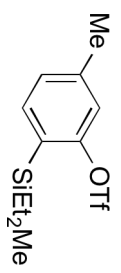
4-5f





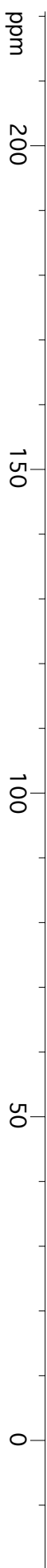
4-5g

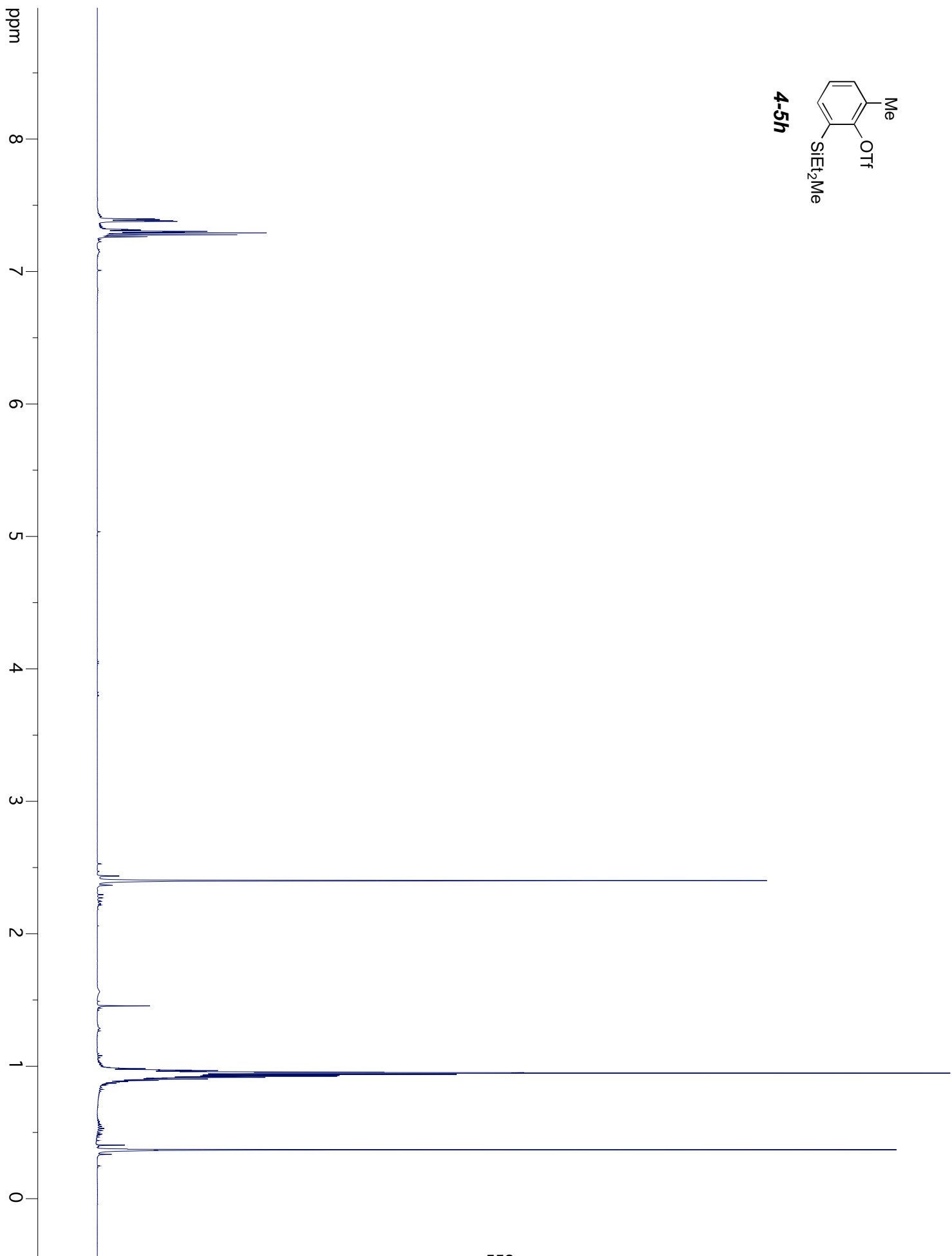
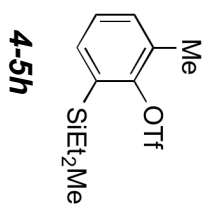


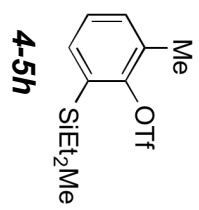


4-5g

ppm







ppm

200

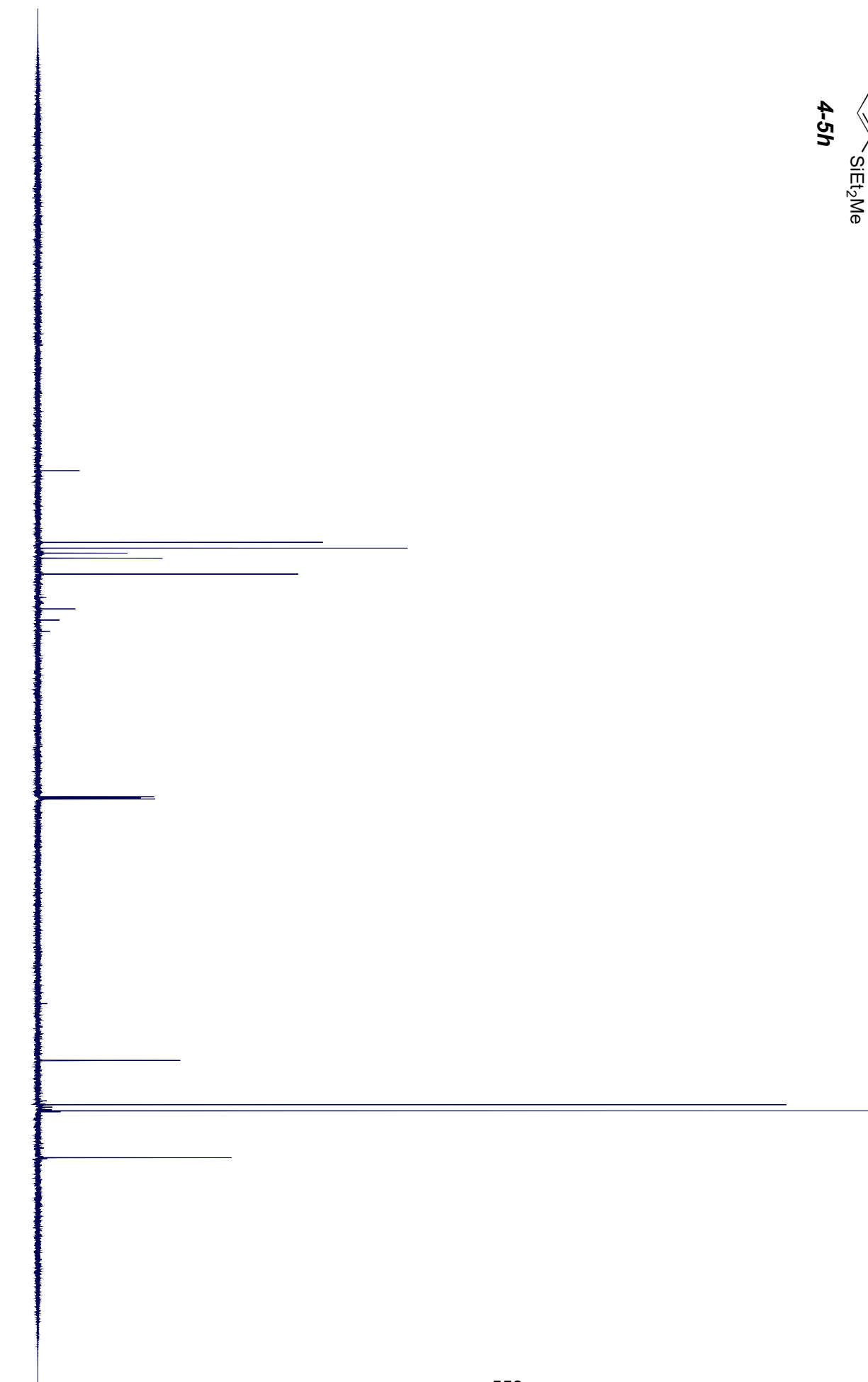
150

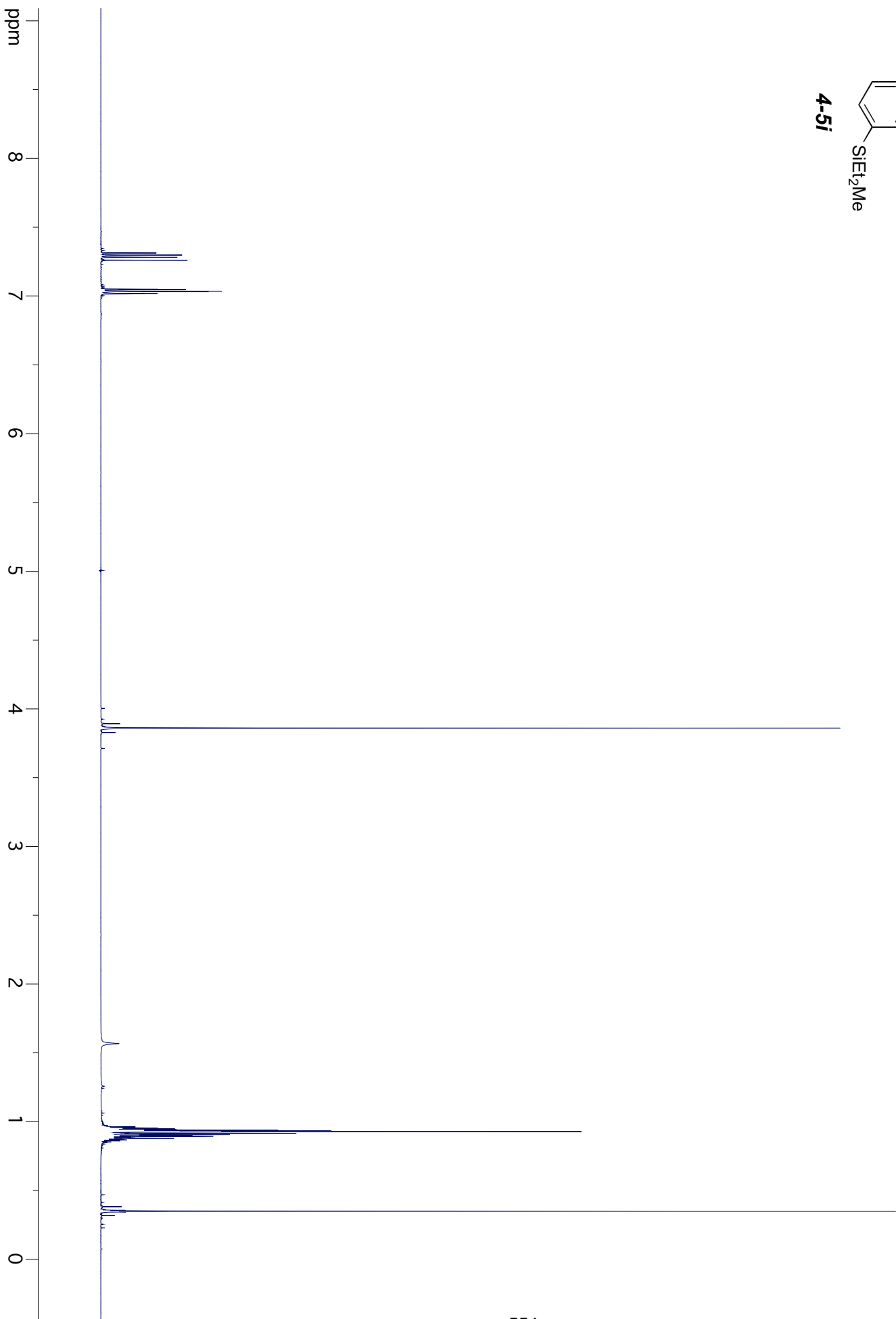
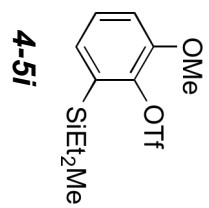
100

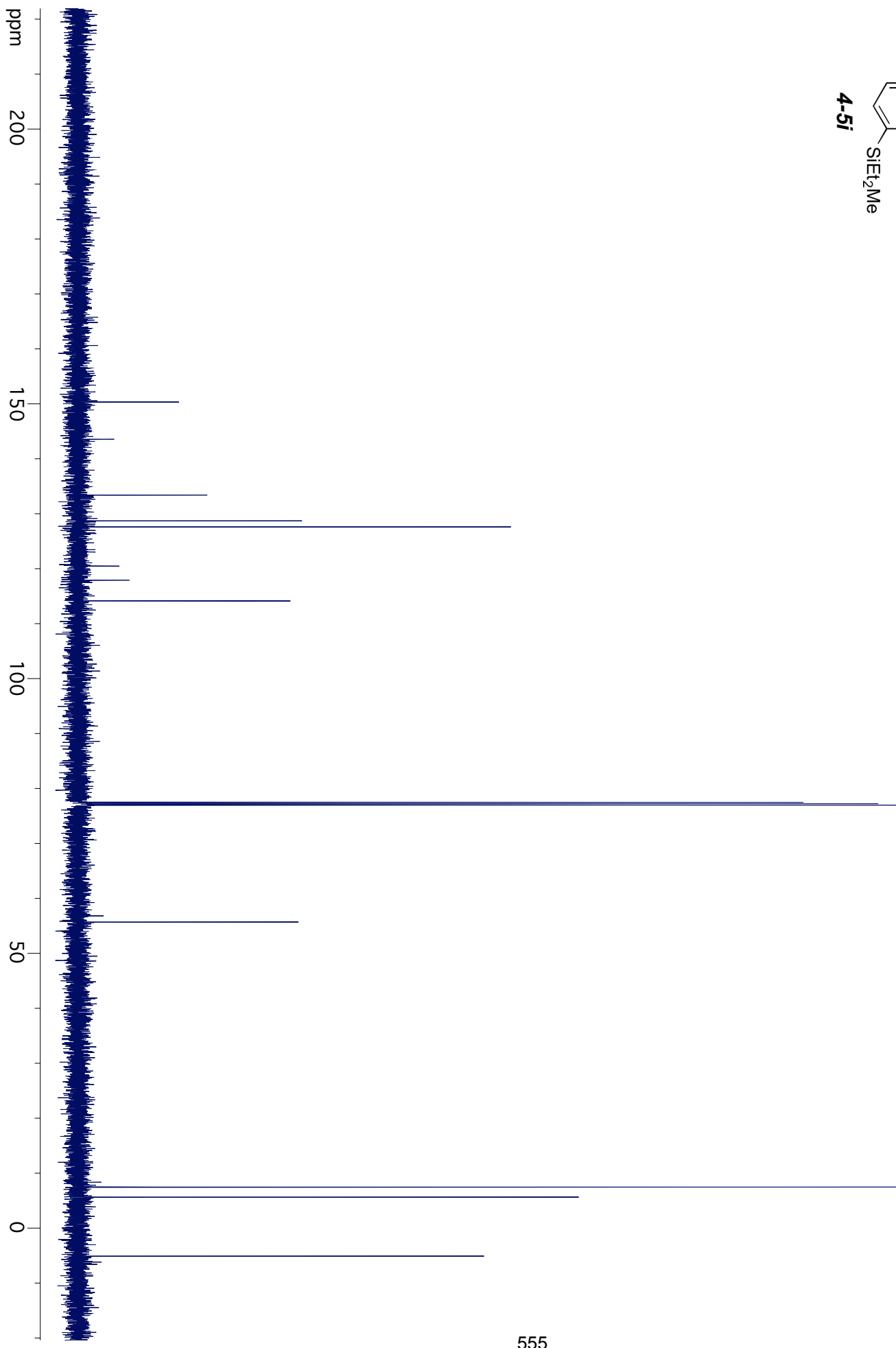
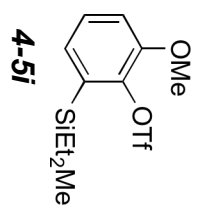
50

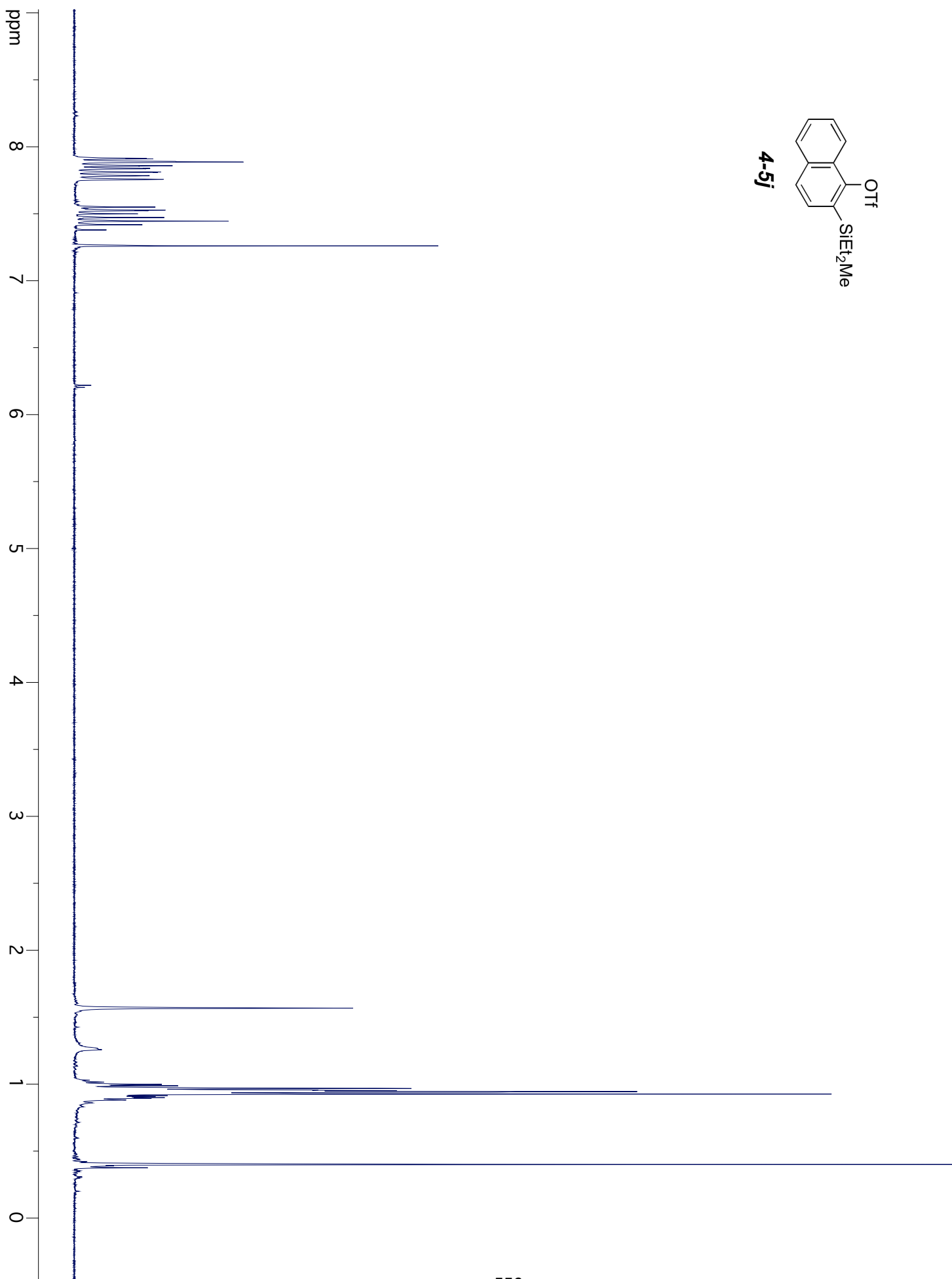
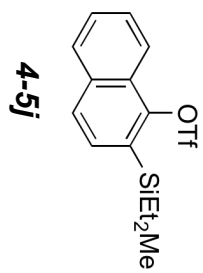
0

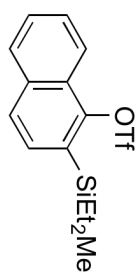
-50



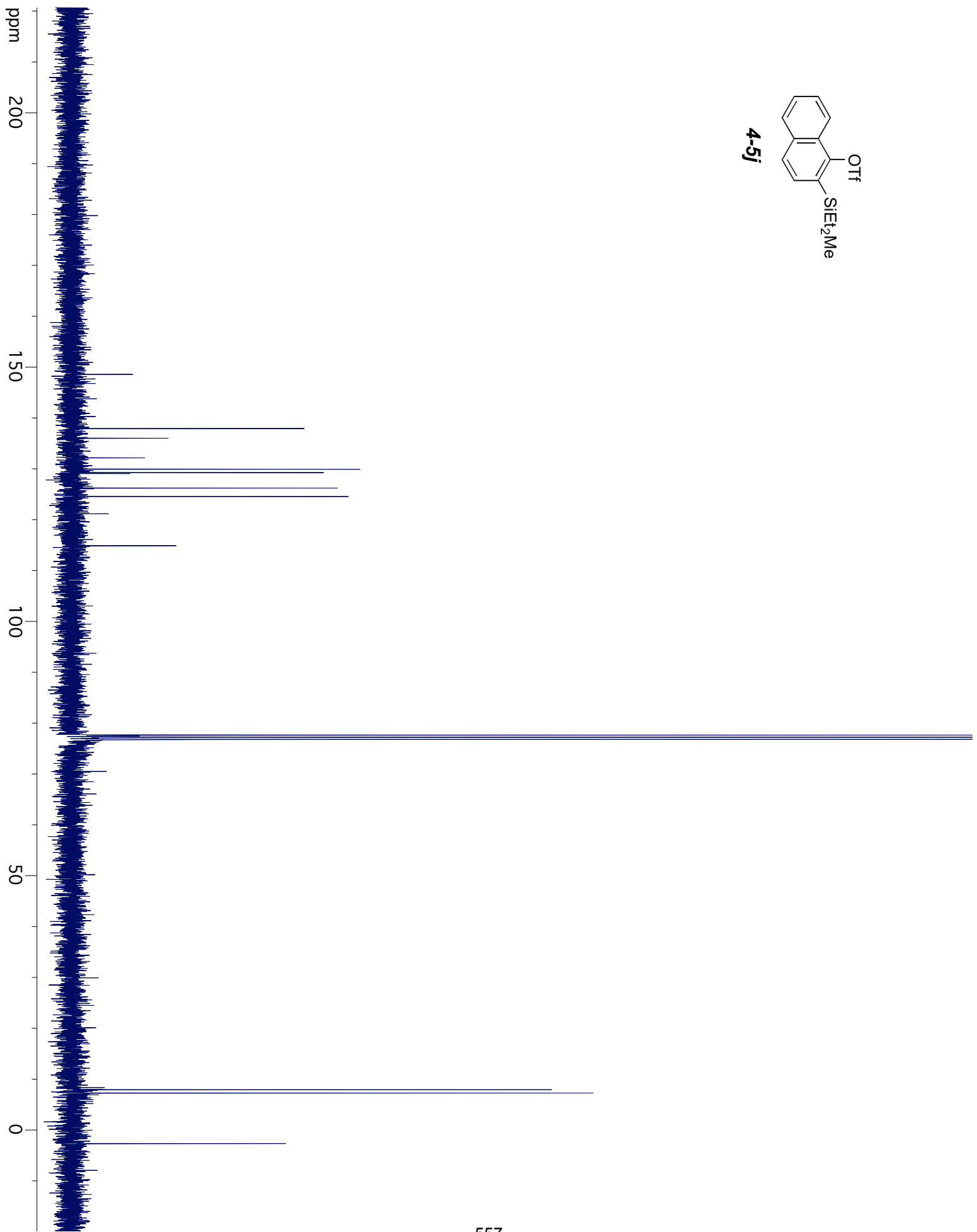


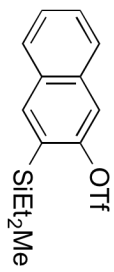




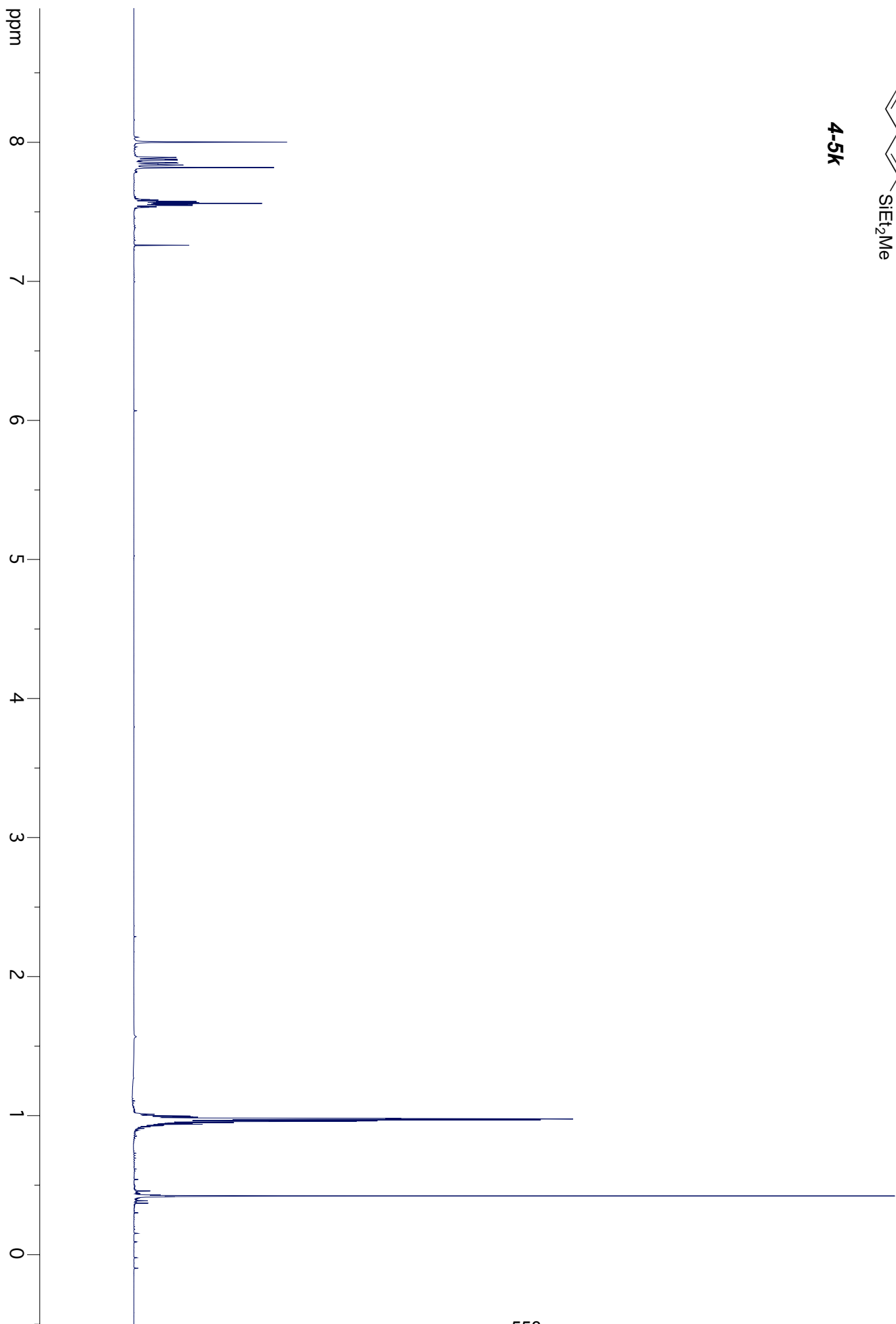


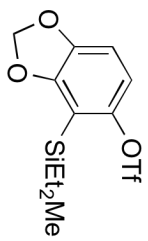
4-5j



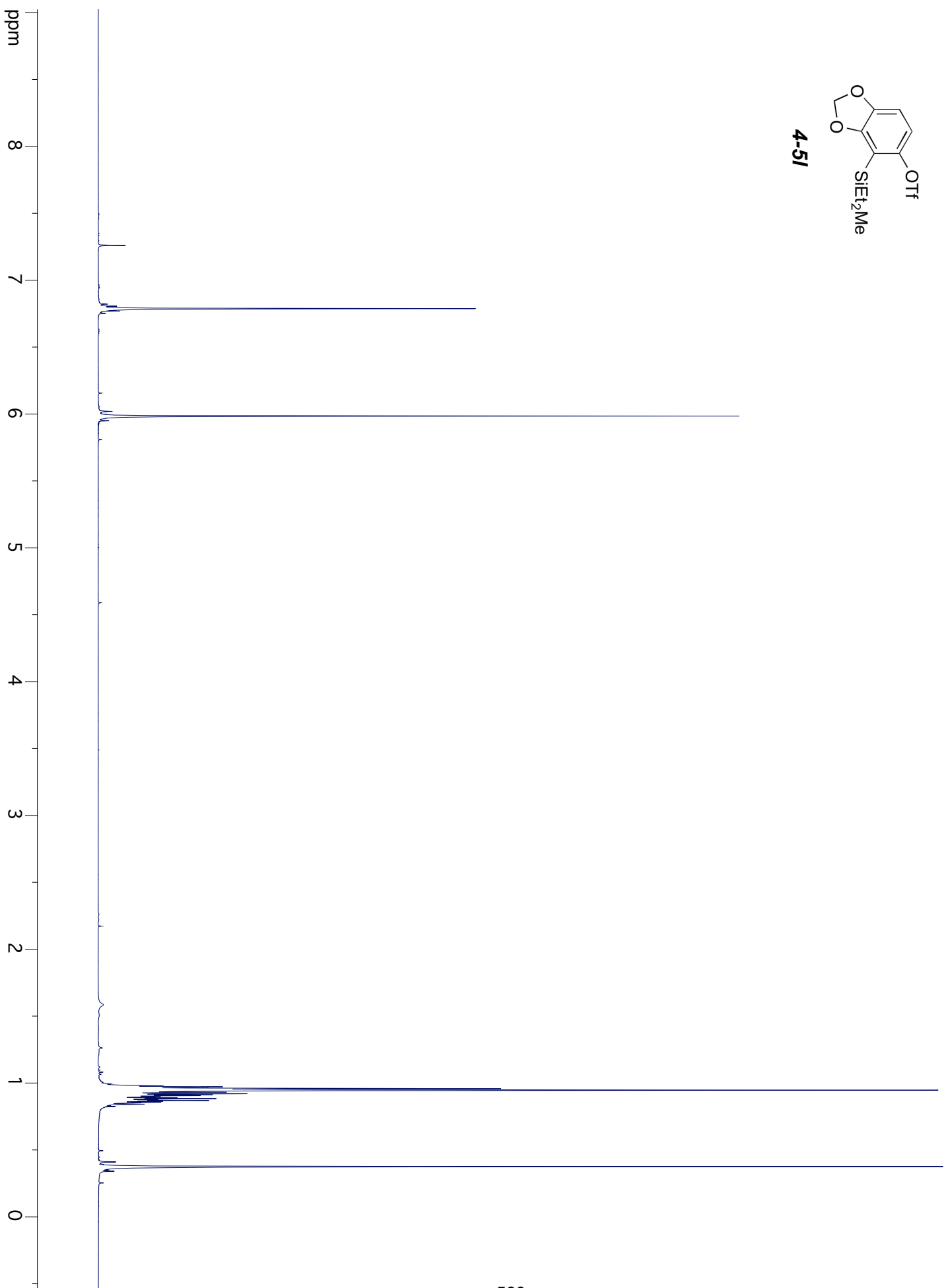


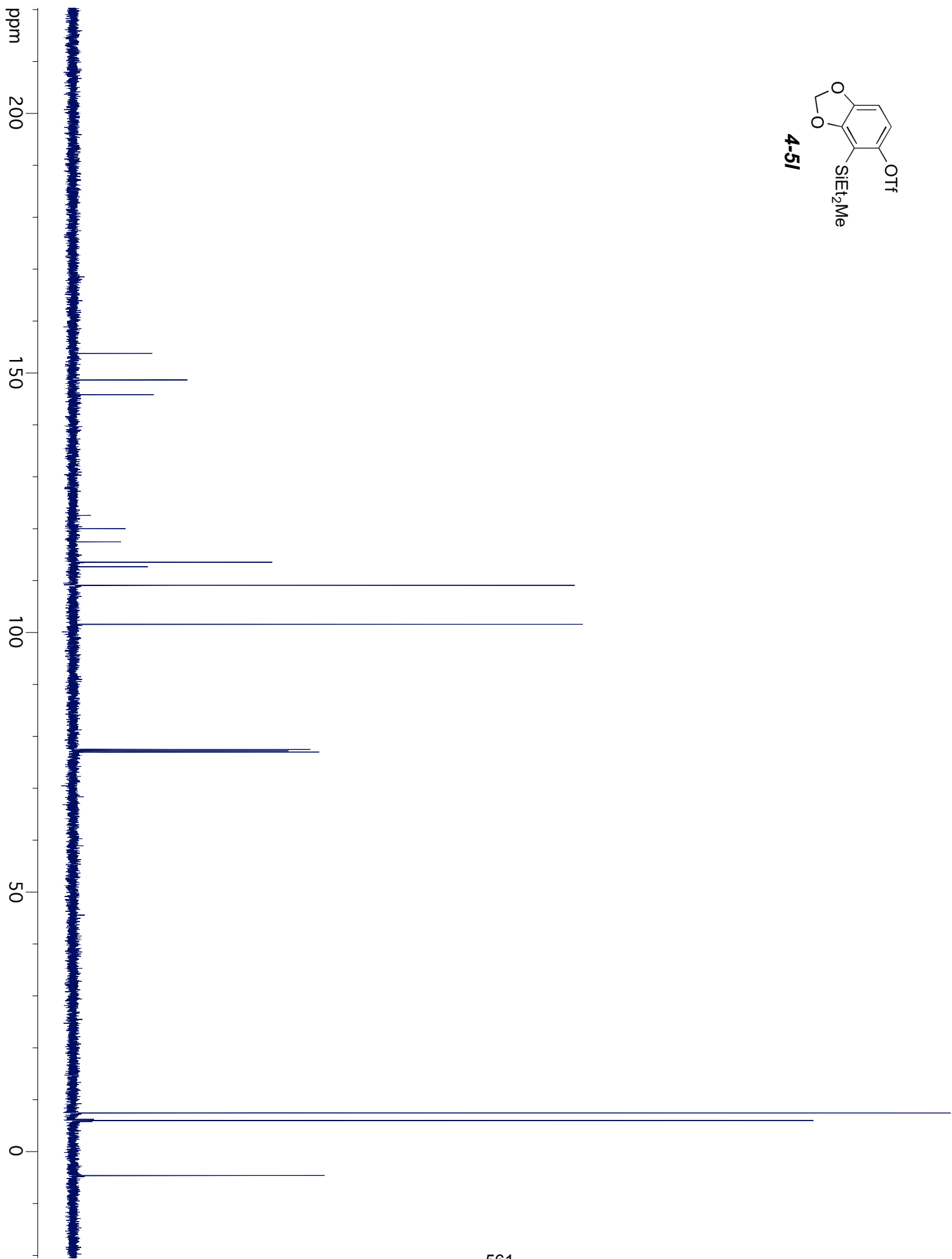
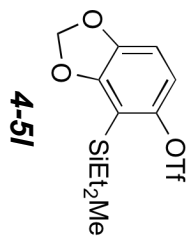
4-5k

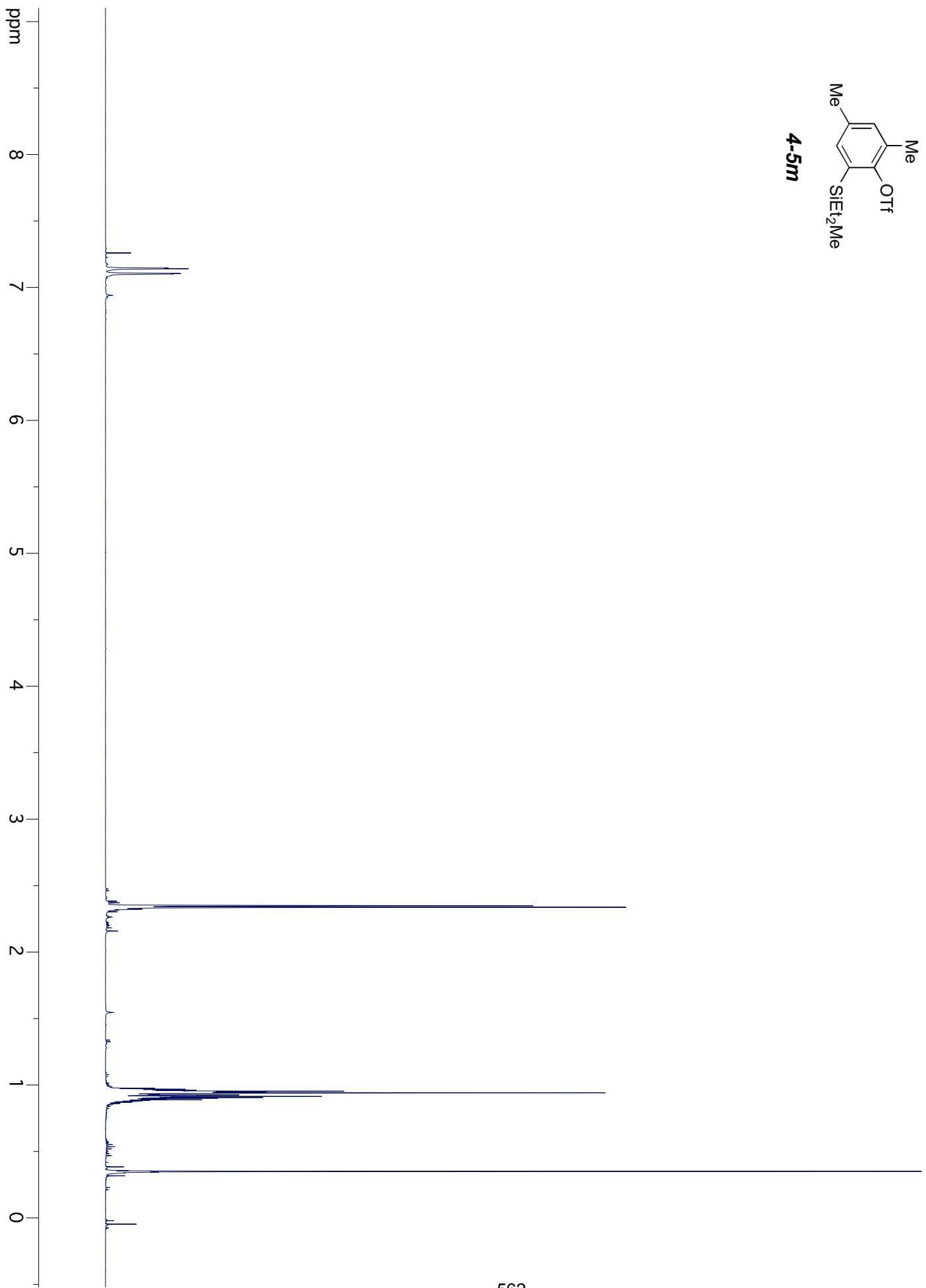
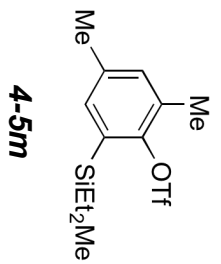


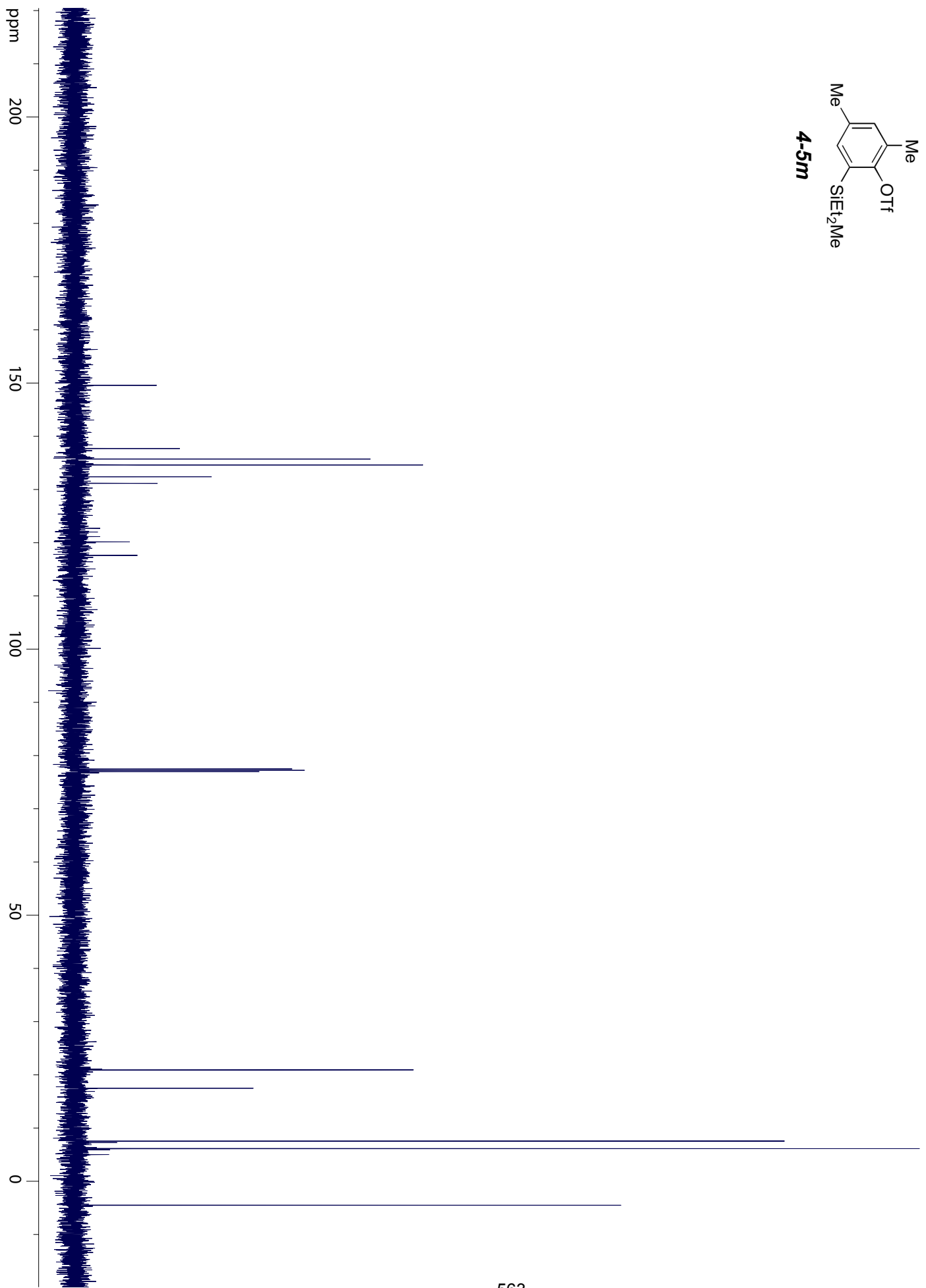
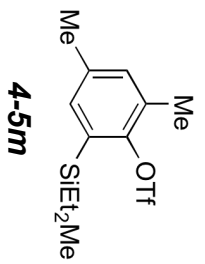


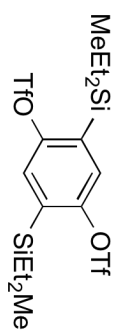
4-51



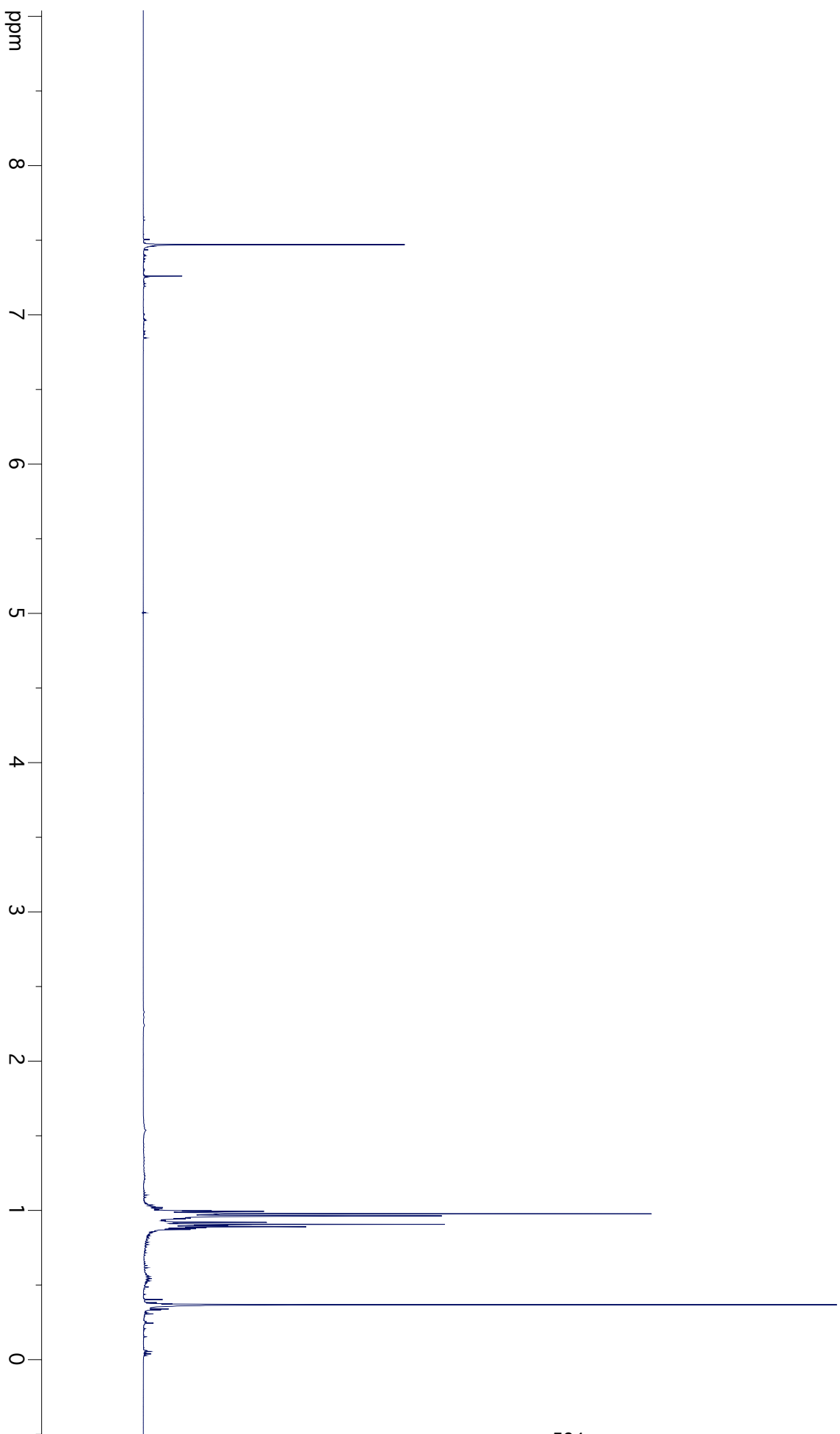


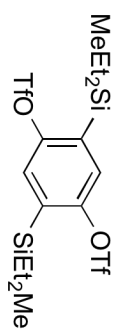




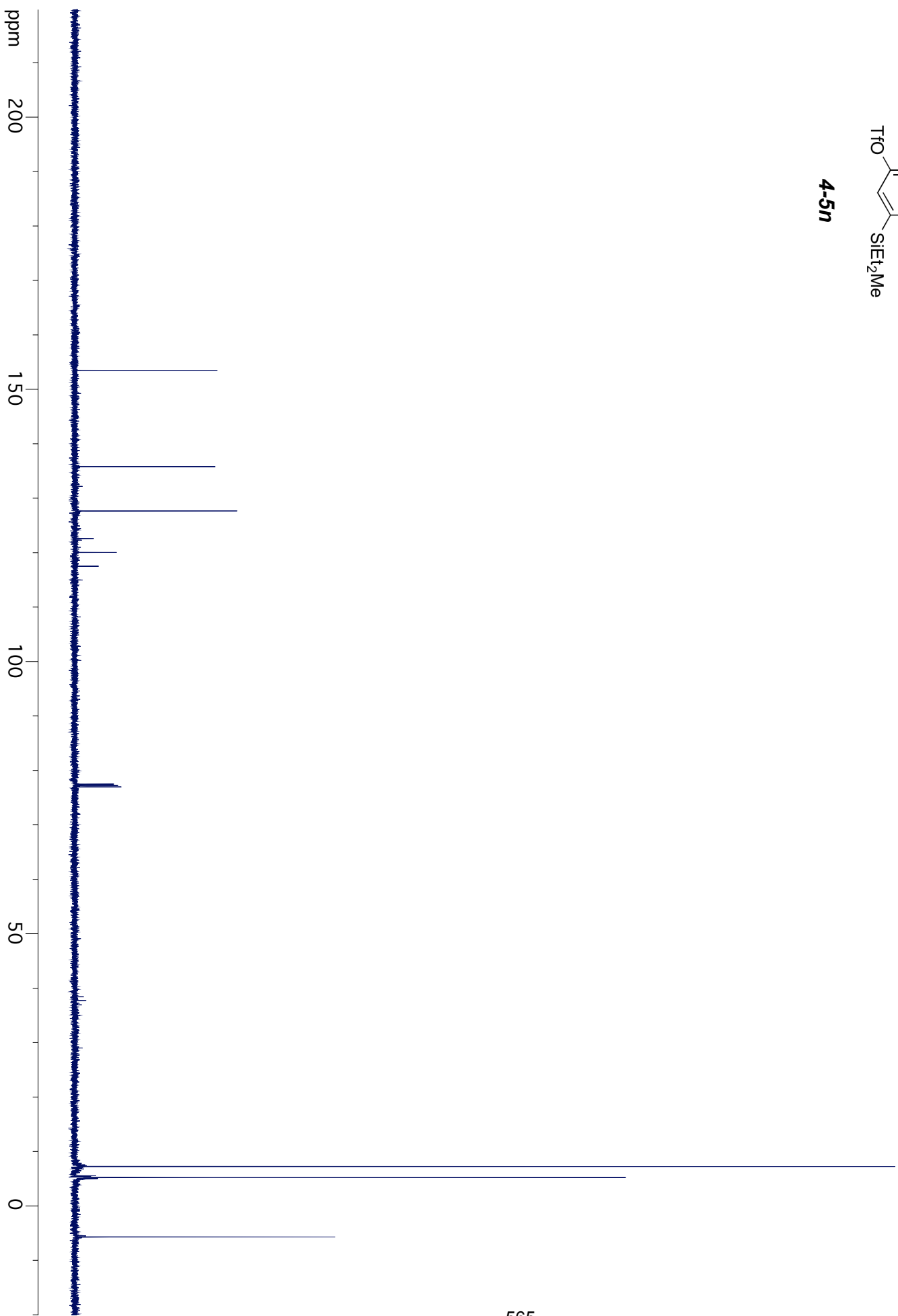


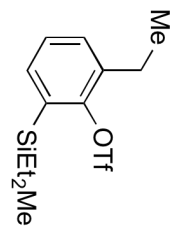
4-5n



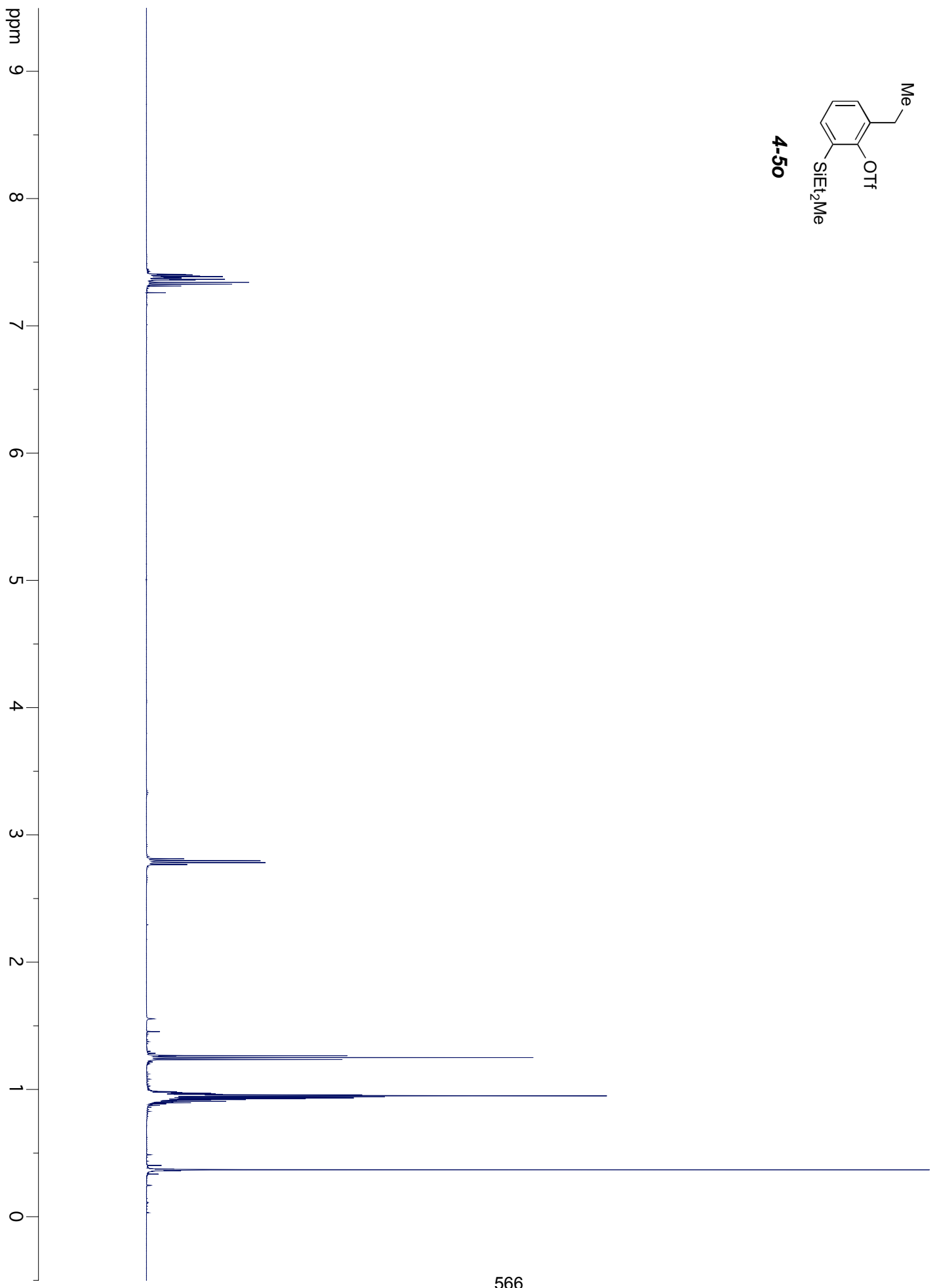


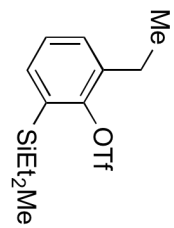
4-5n



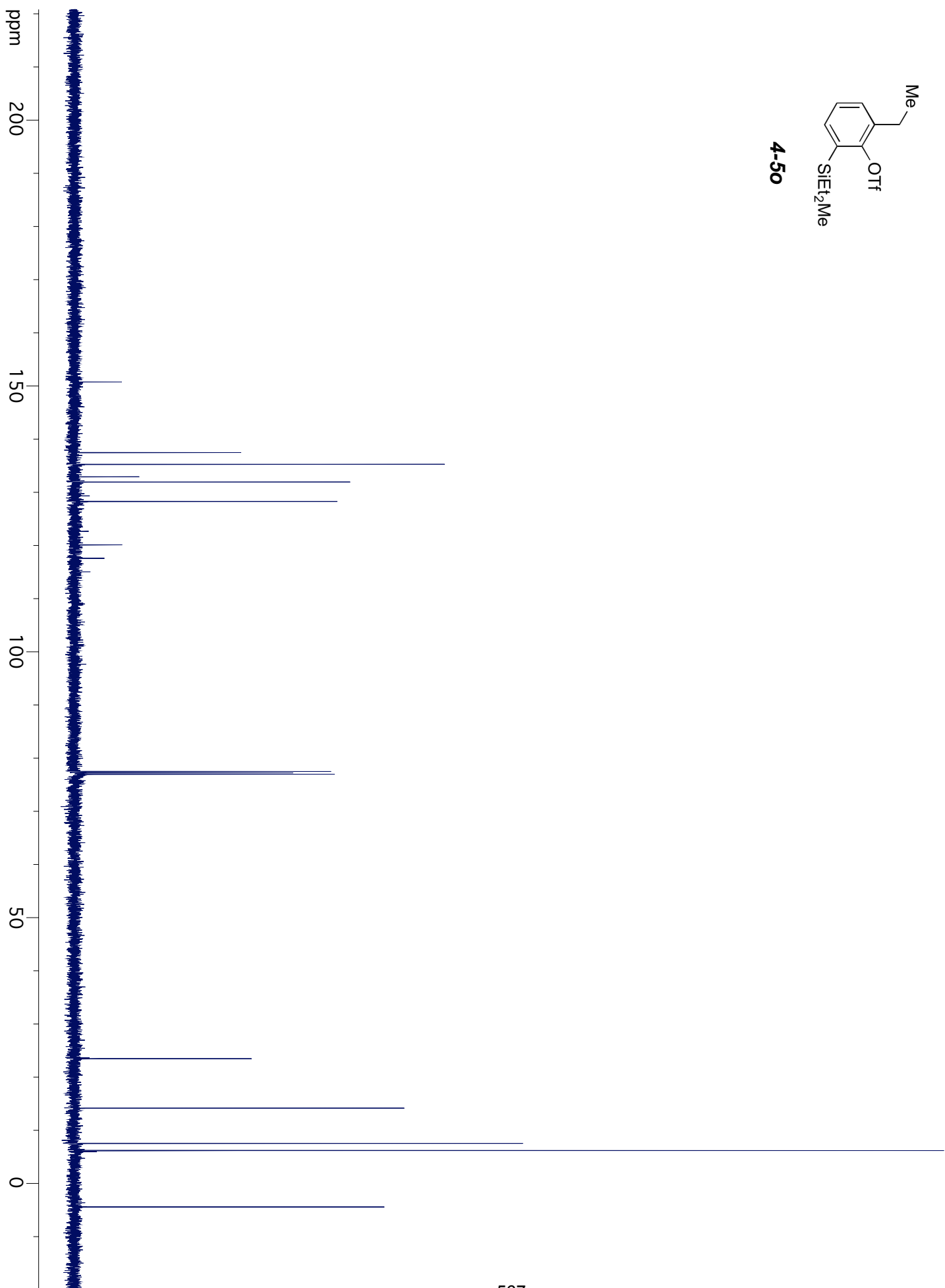


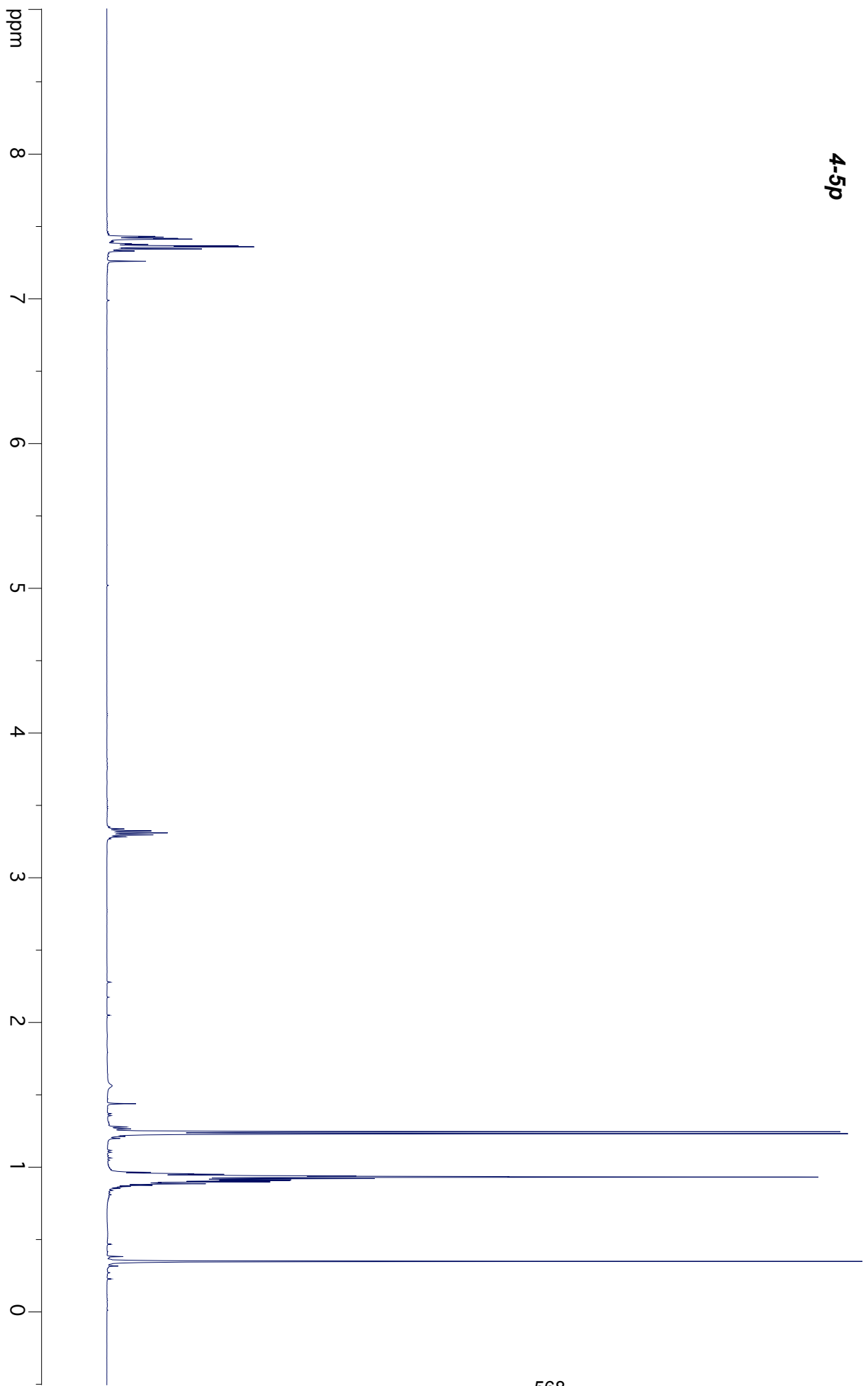
4-50

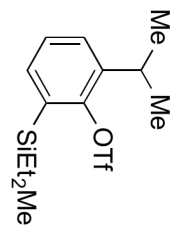




4-50



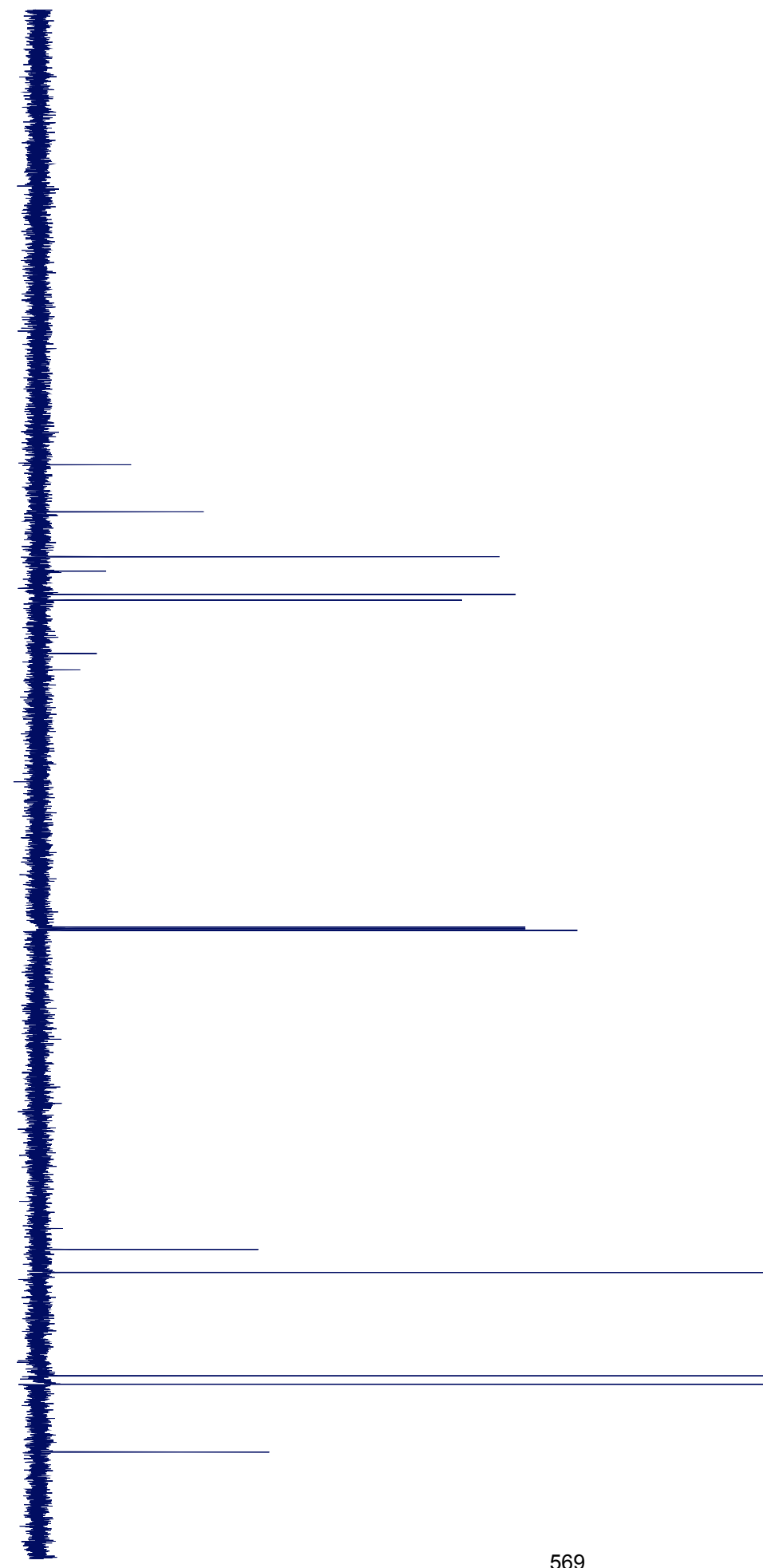


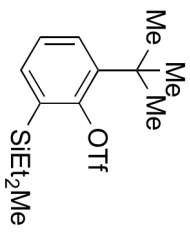


4-5p

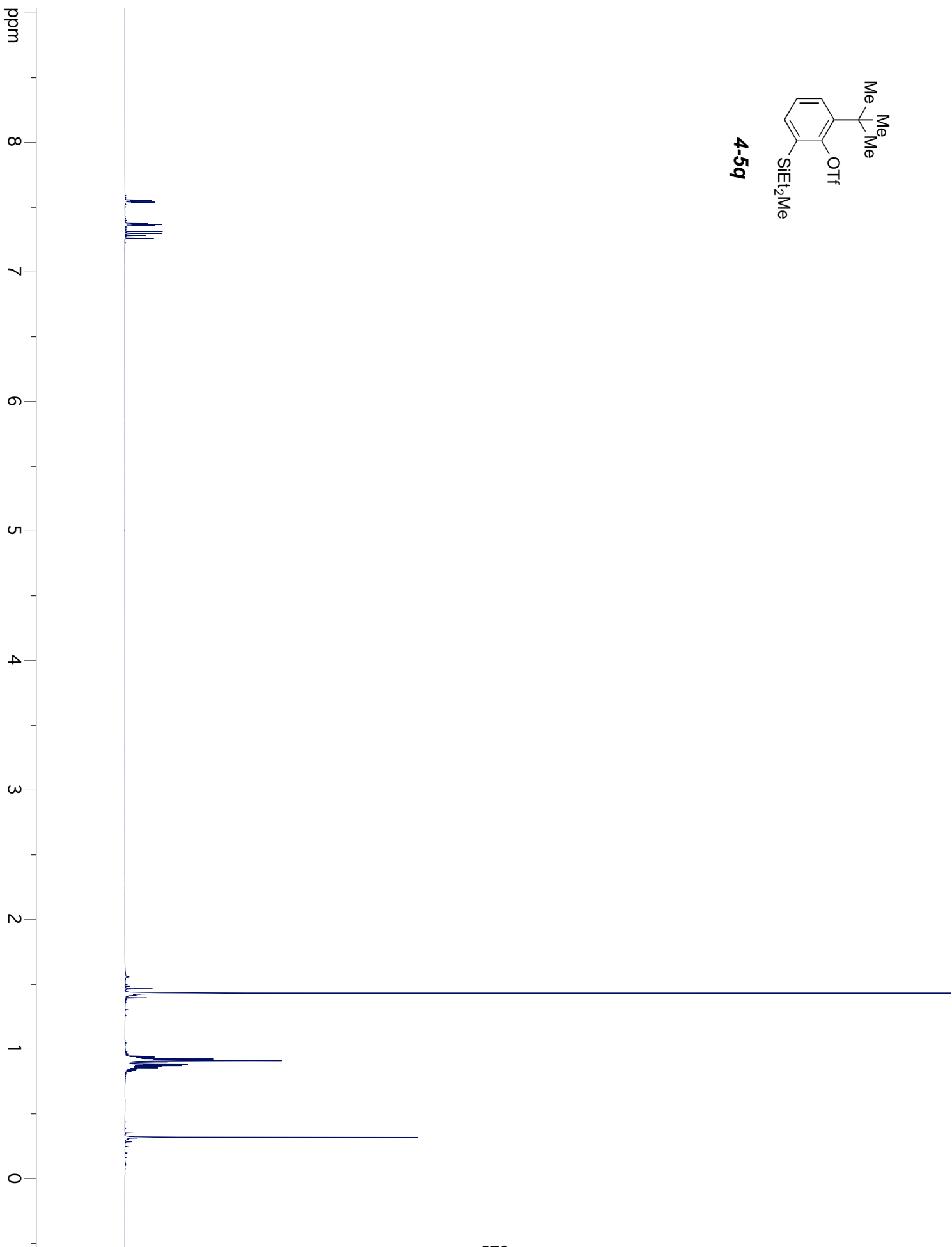
ppm

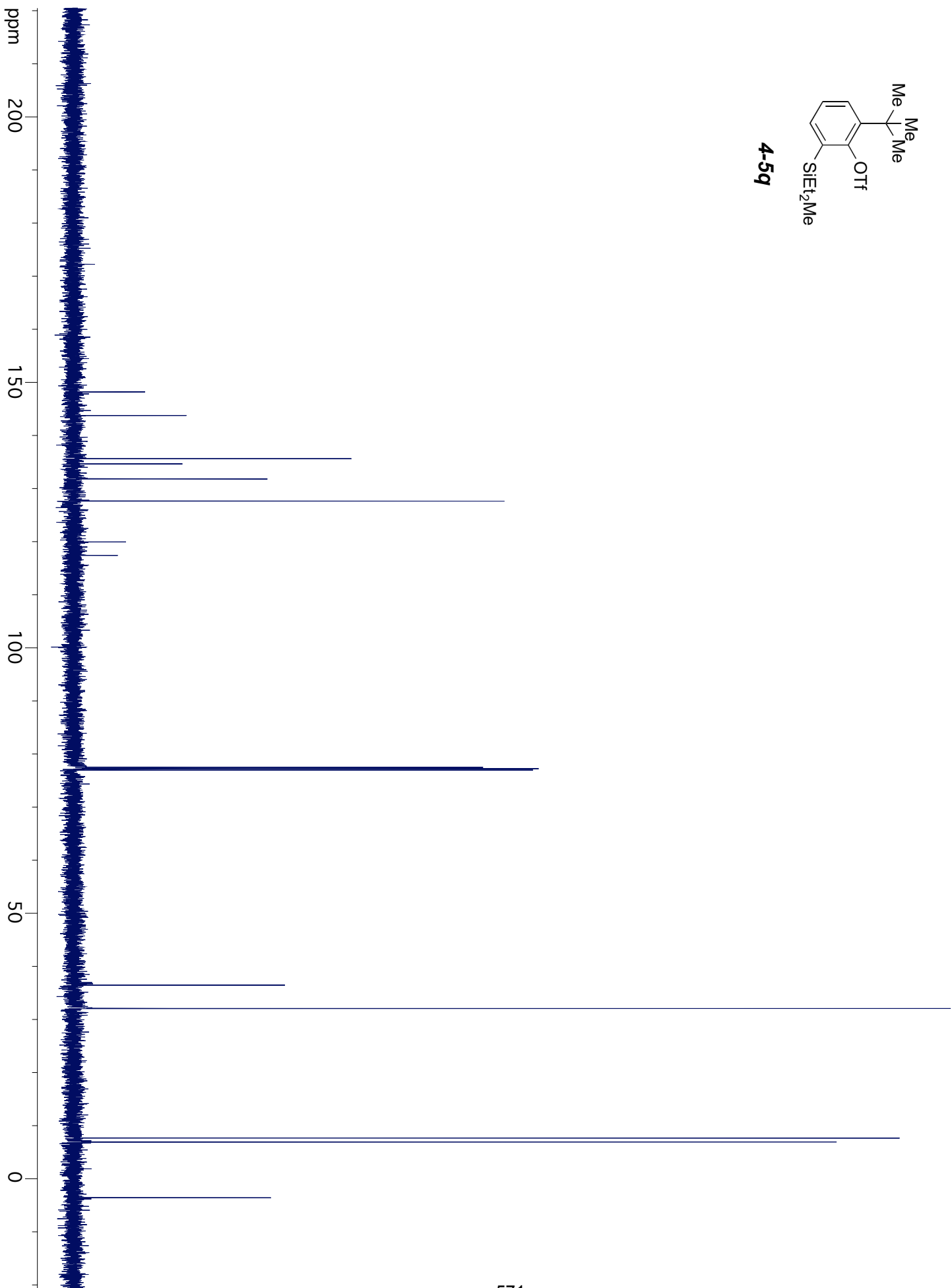
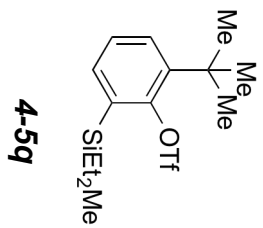
200
150
100
50
0

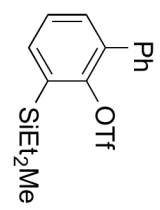




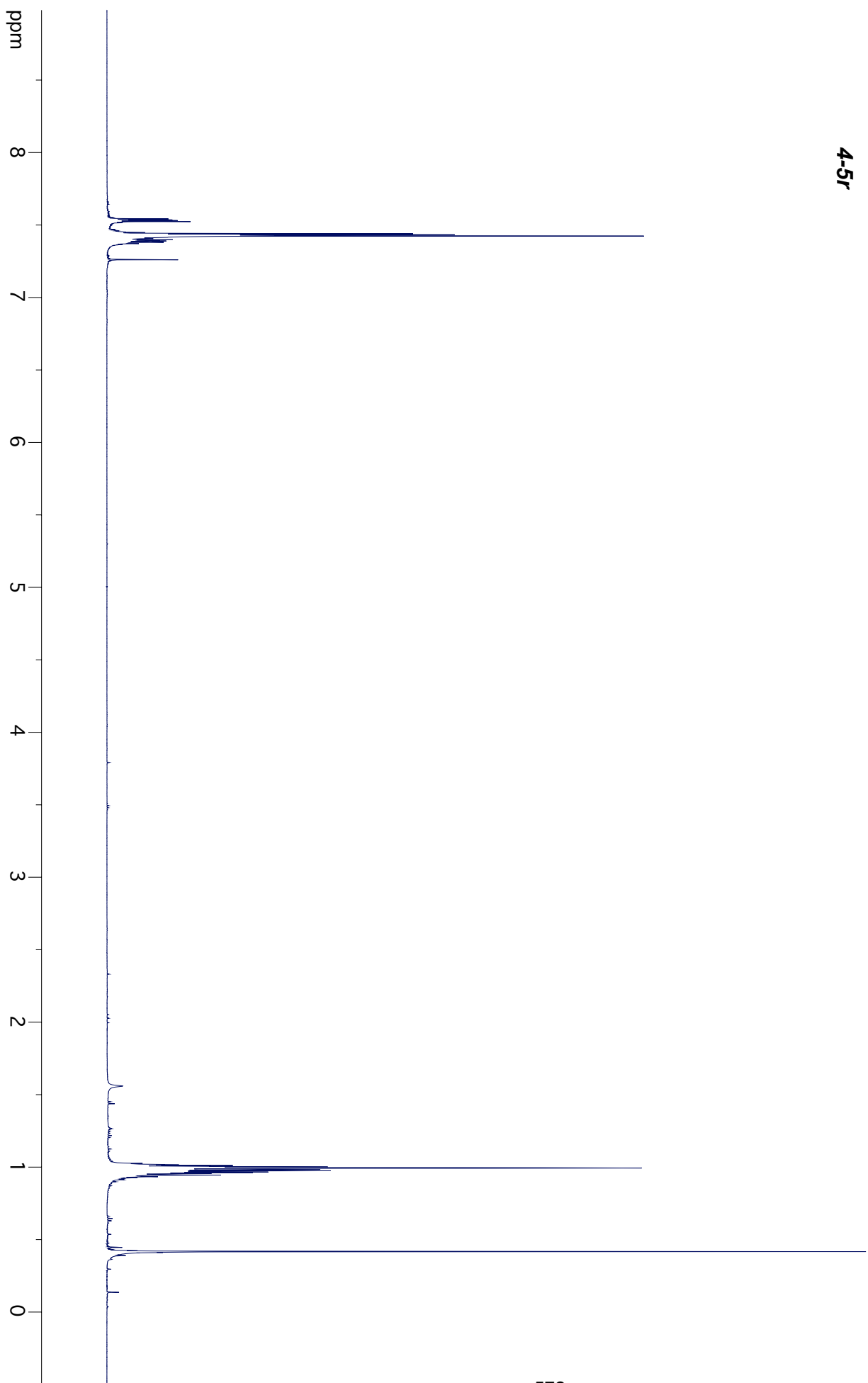
4-5q

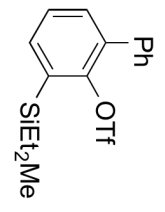




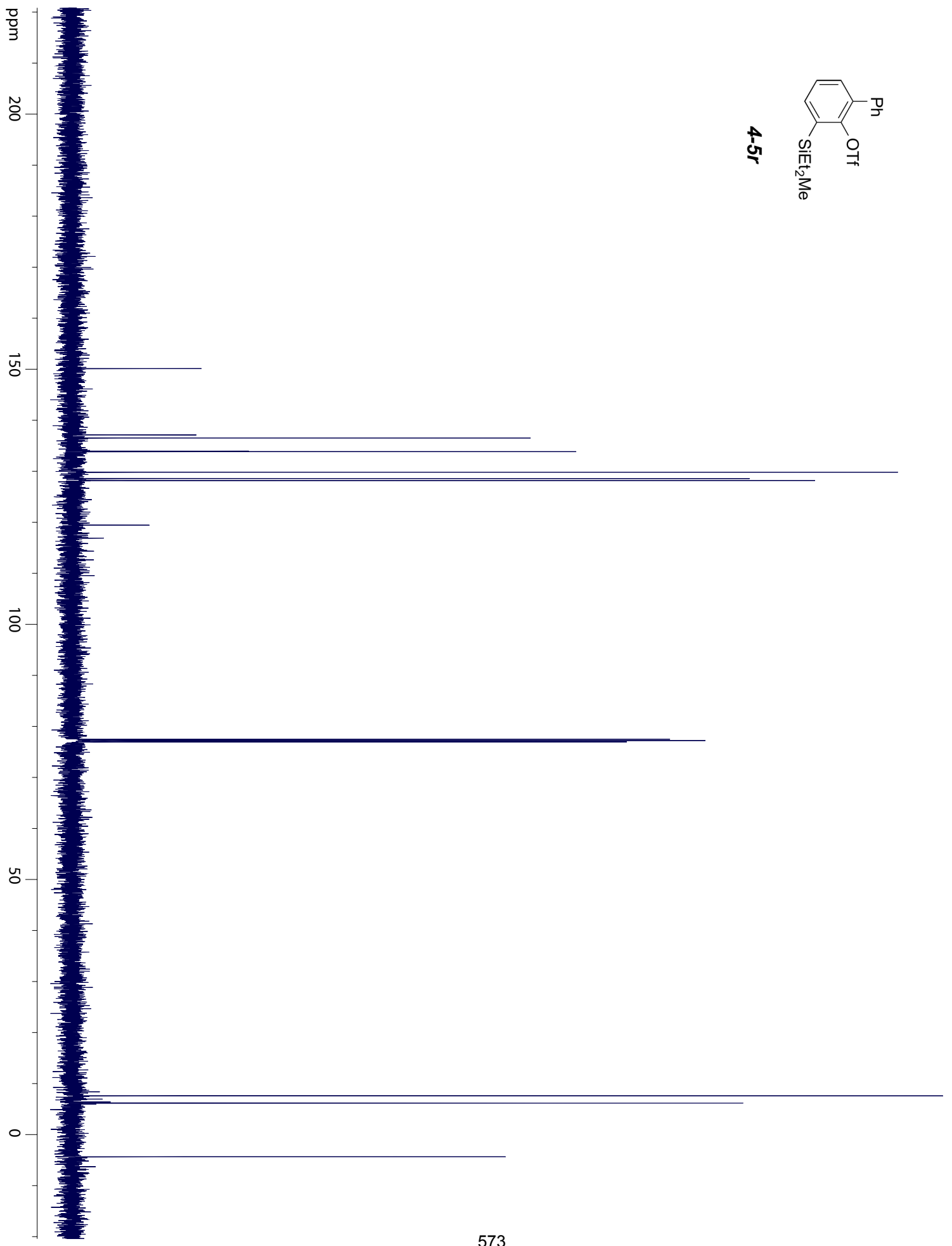


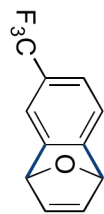
4-5r





4-5r

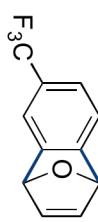




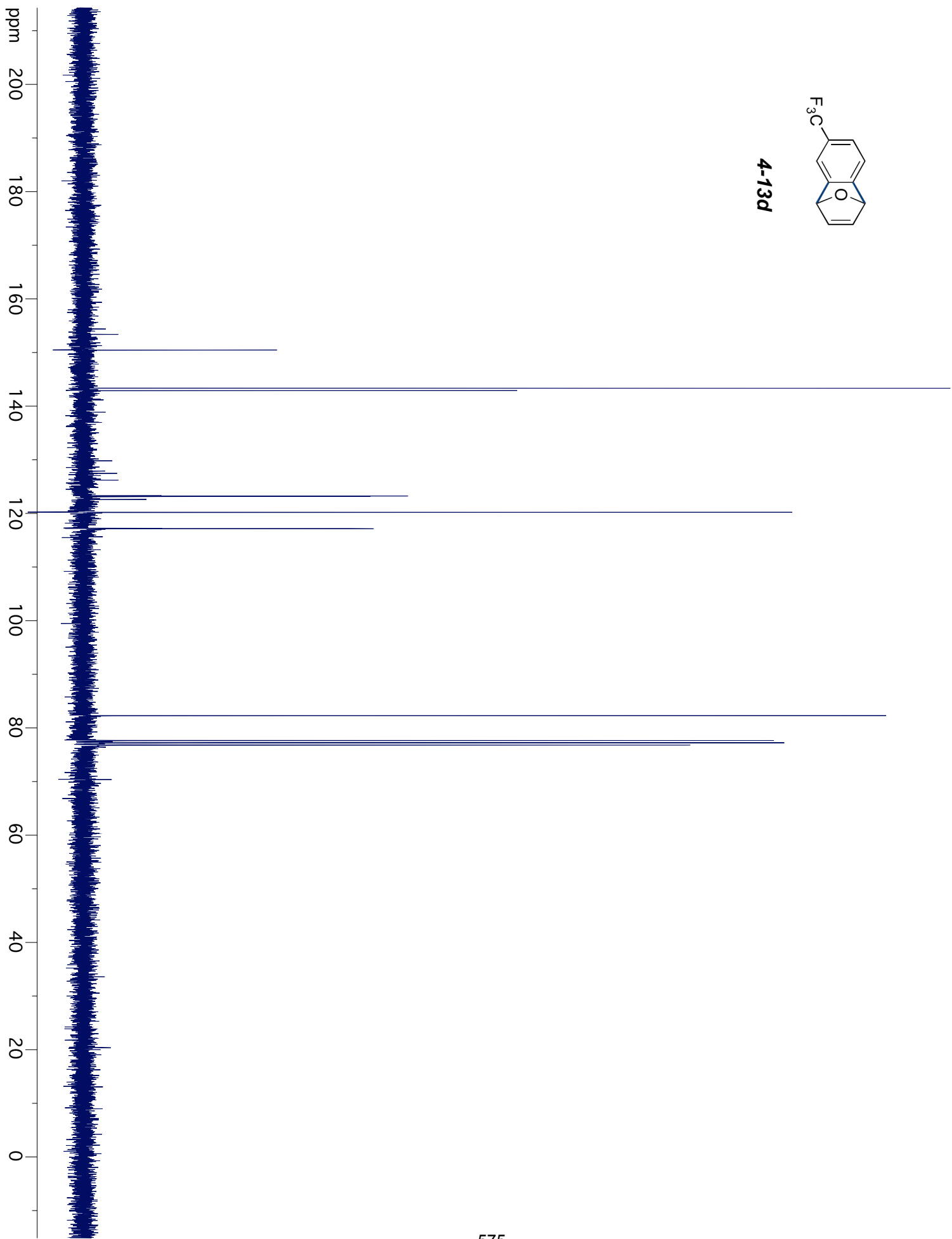
4-13d

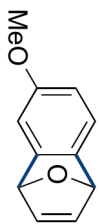
ppm



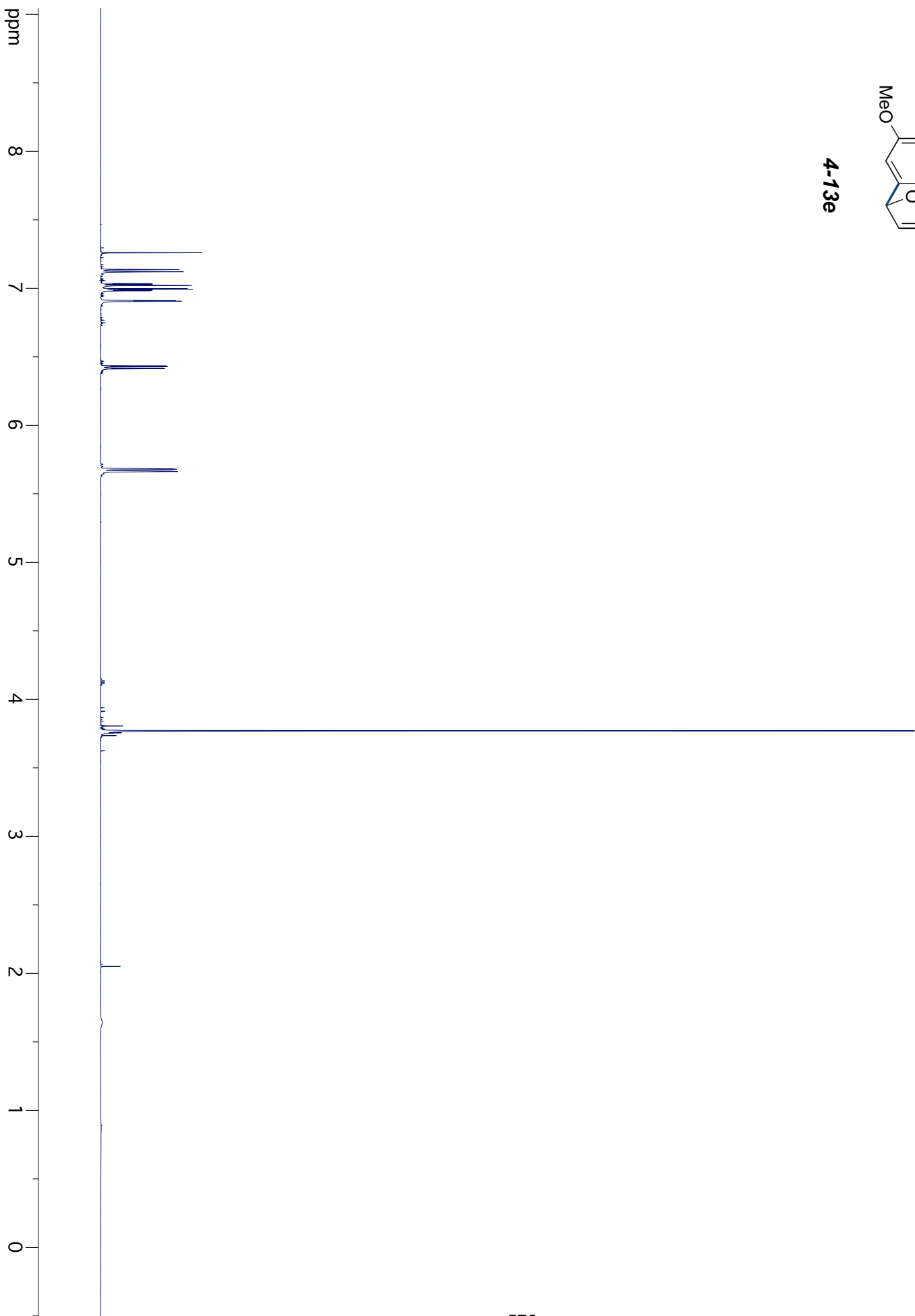


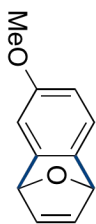
4-13d



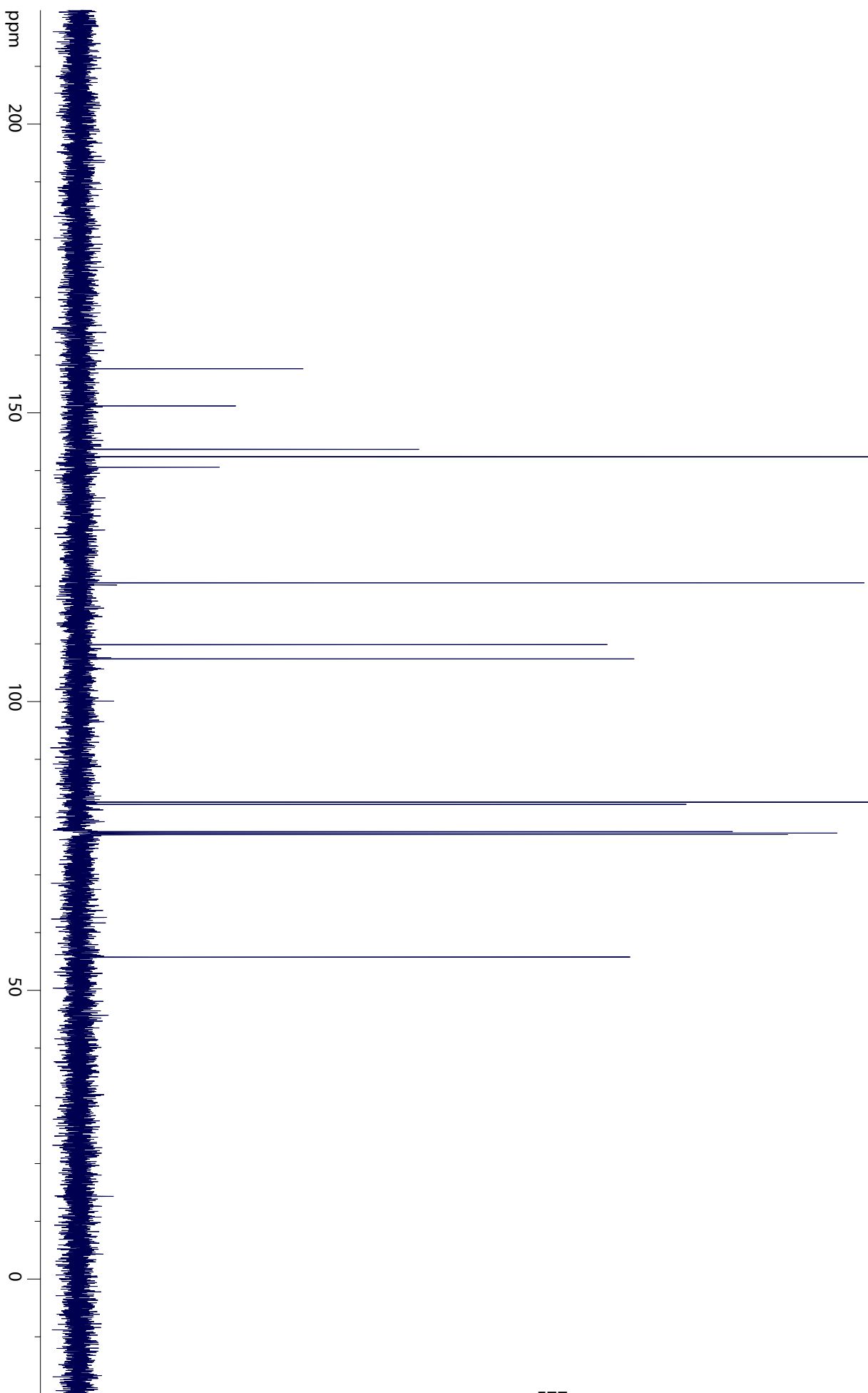


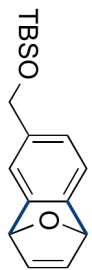
4-13e



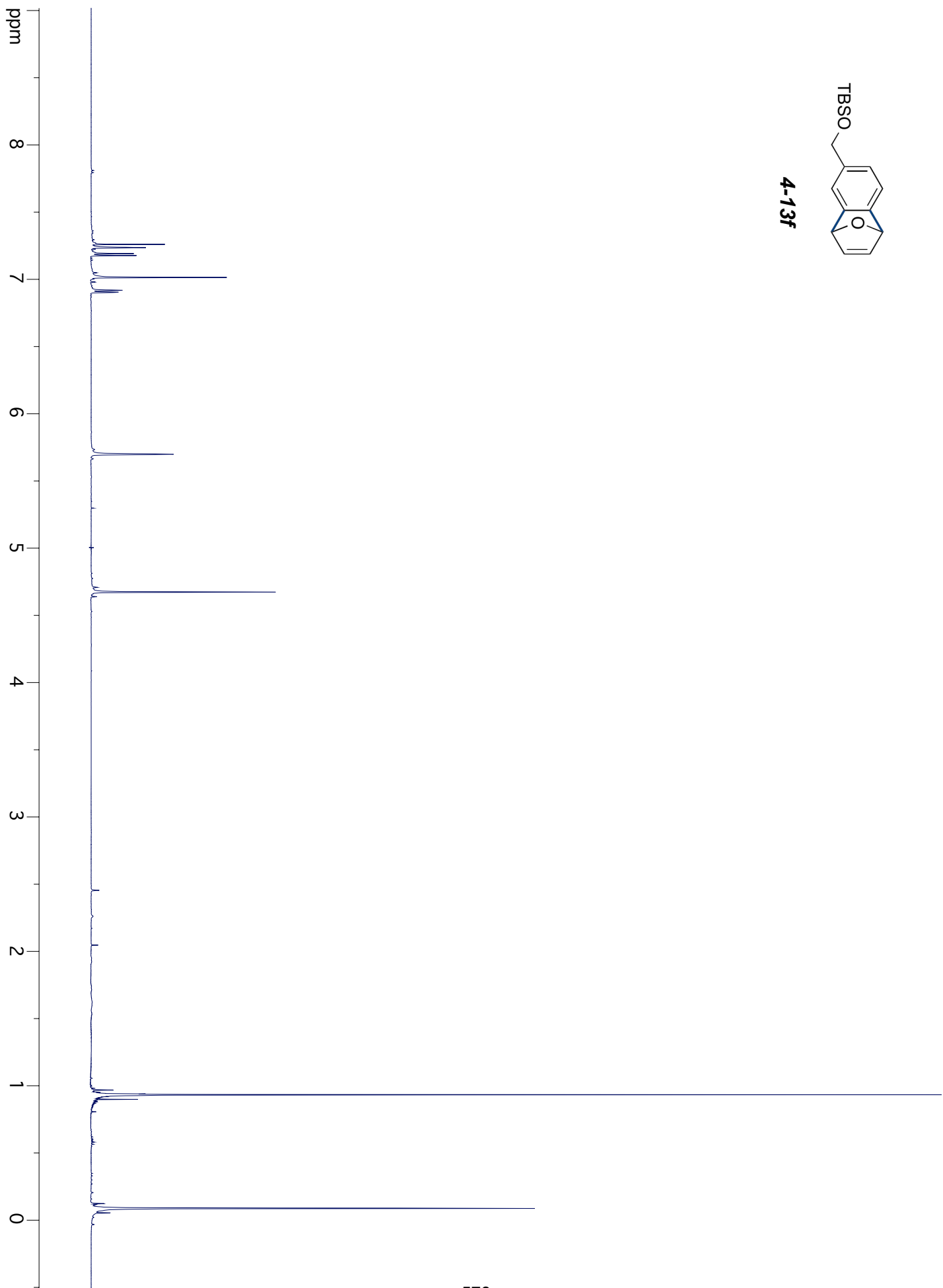


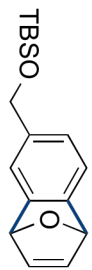
4-13e



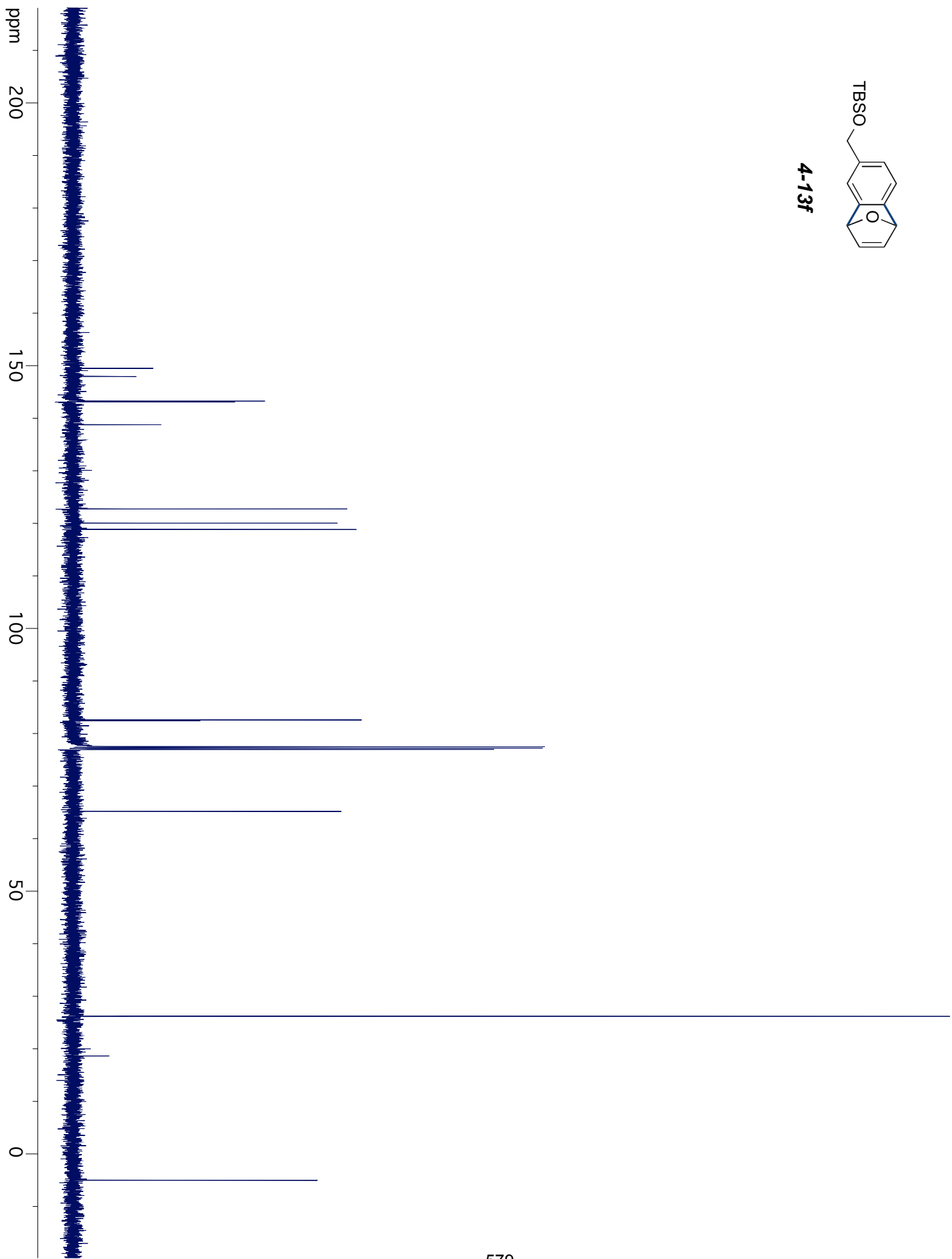


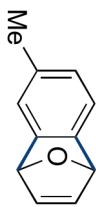
4-13f



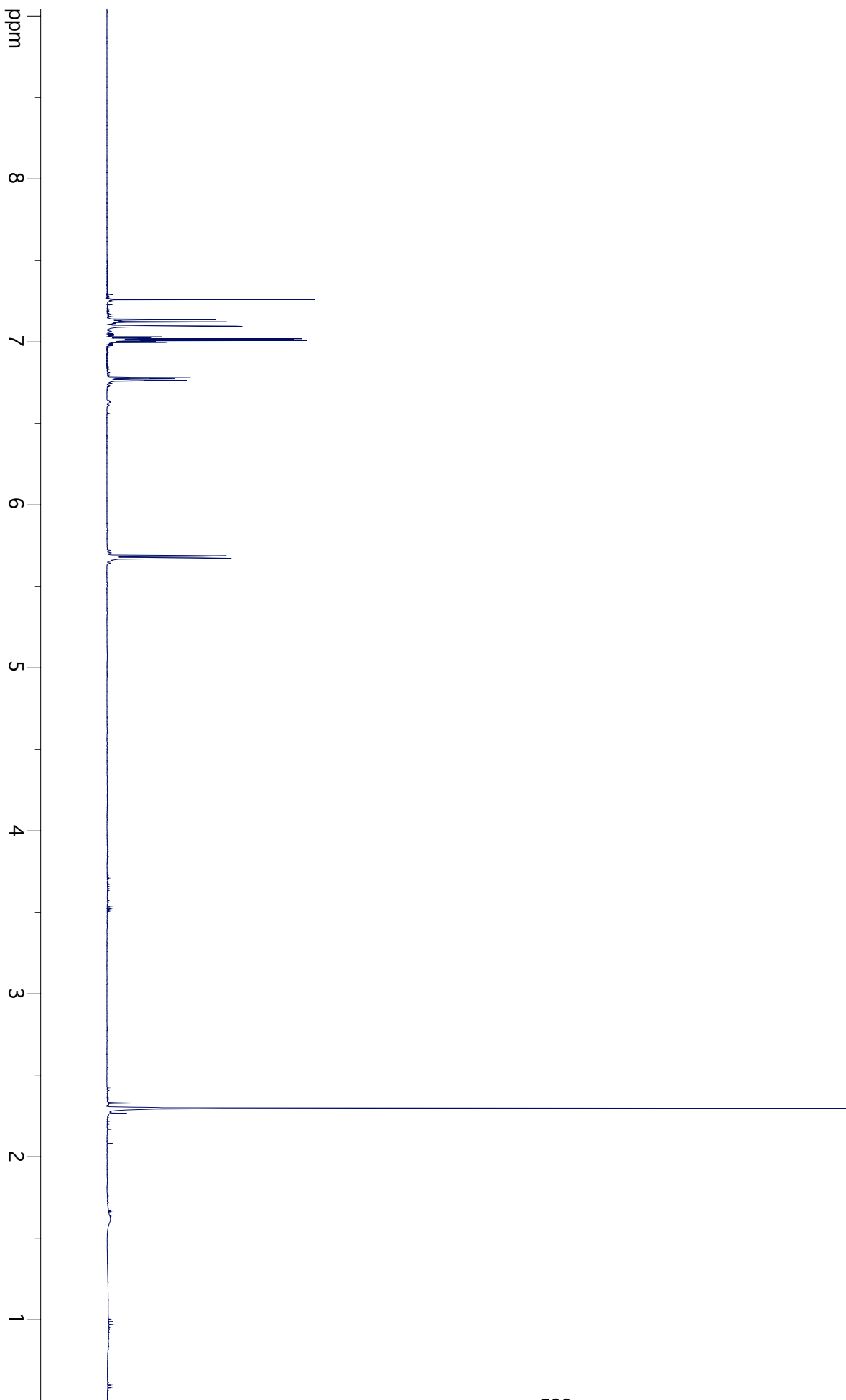


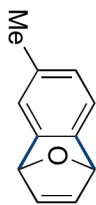
4-13f



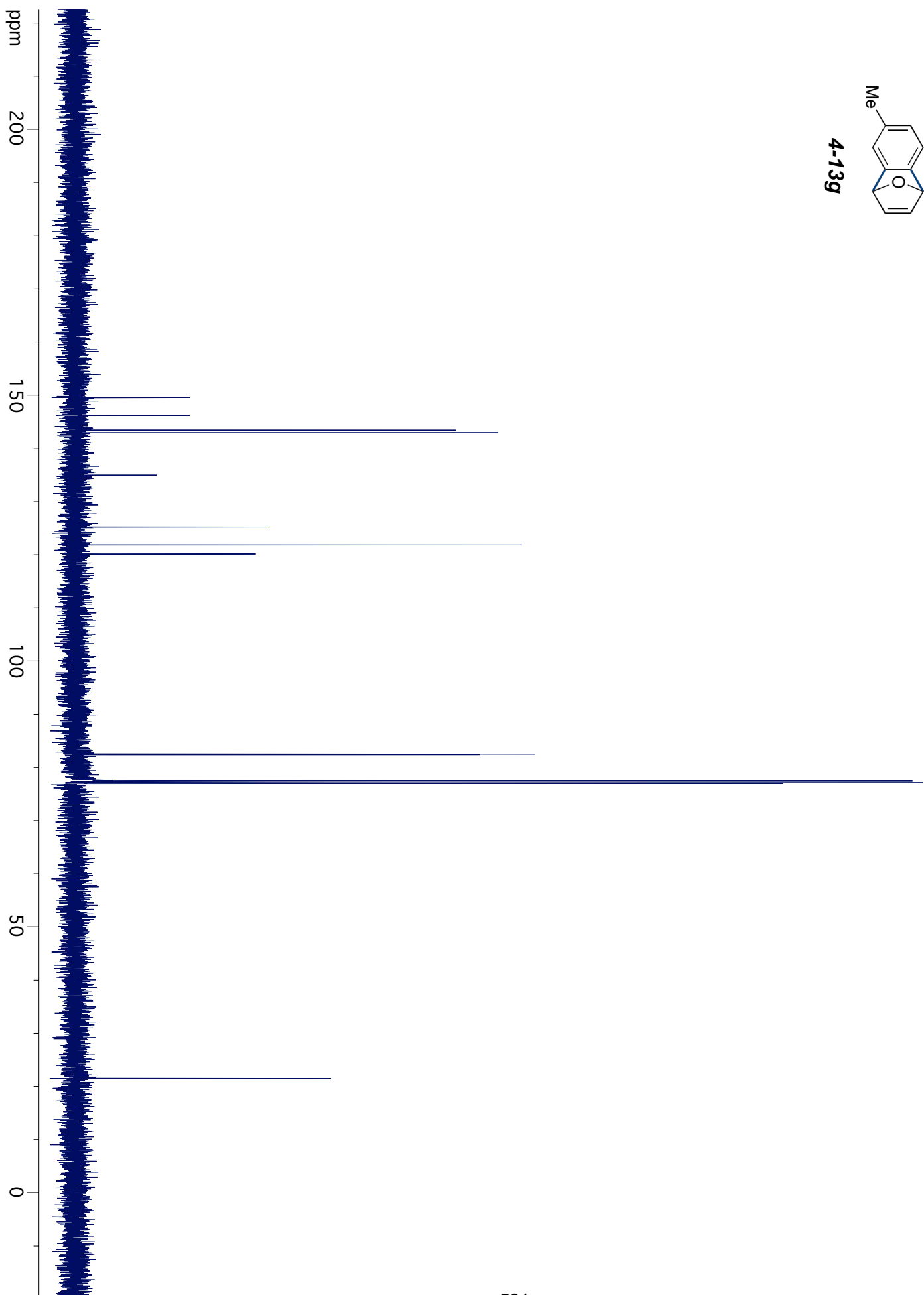


4-13g





4-13g





4-13h

ppm

8

7

6

5

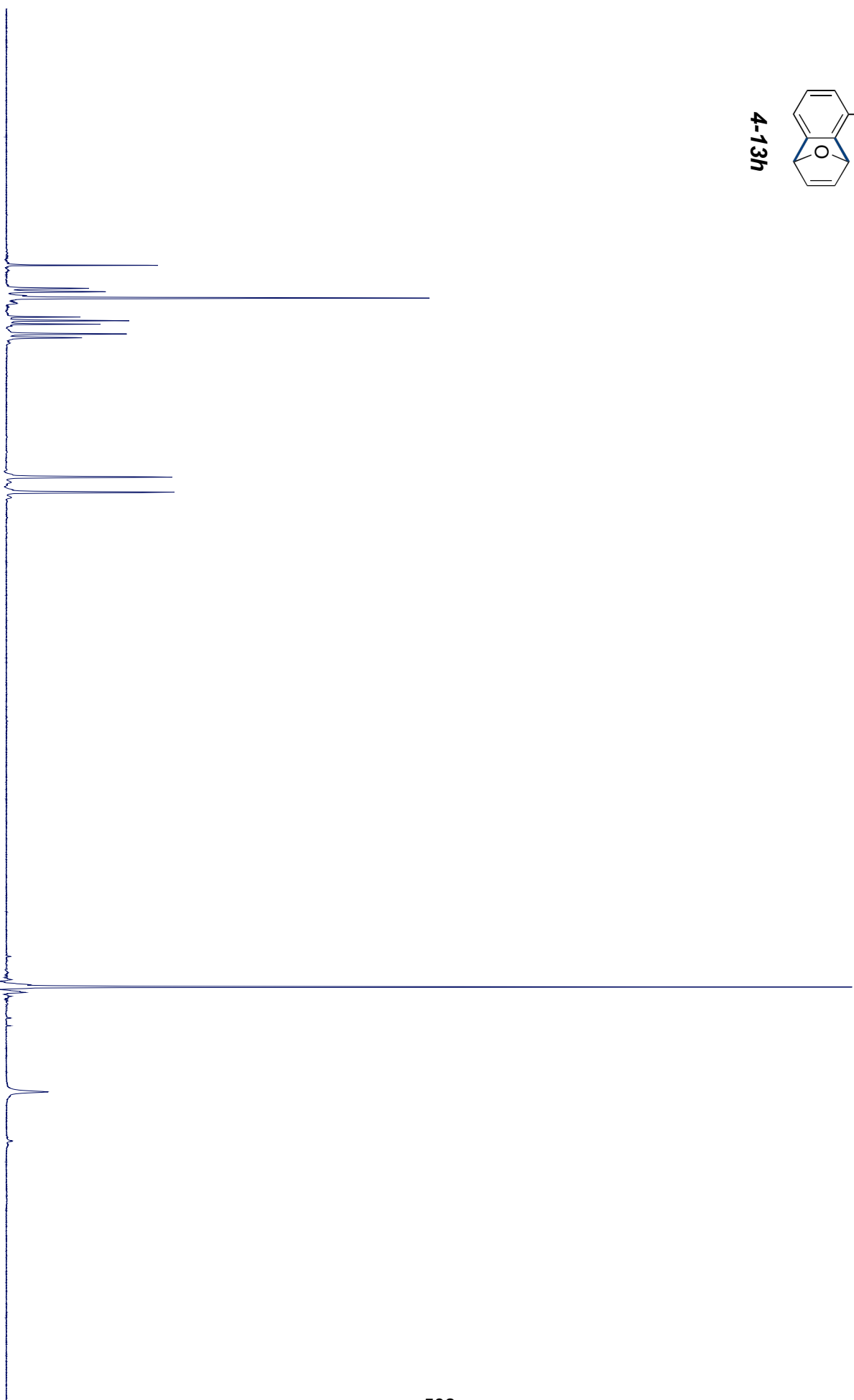
4

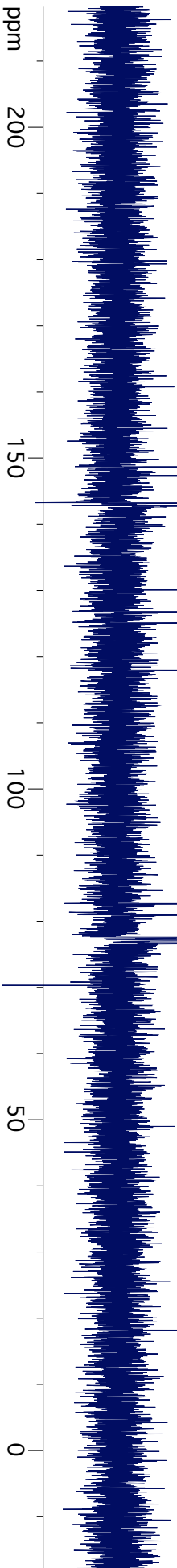
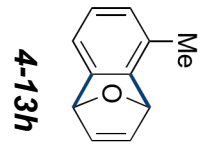
3

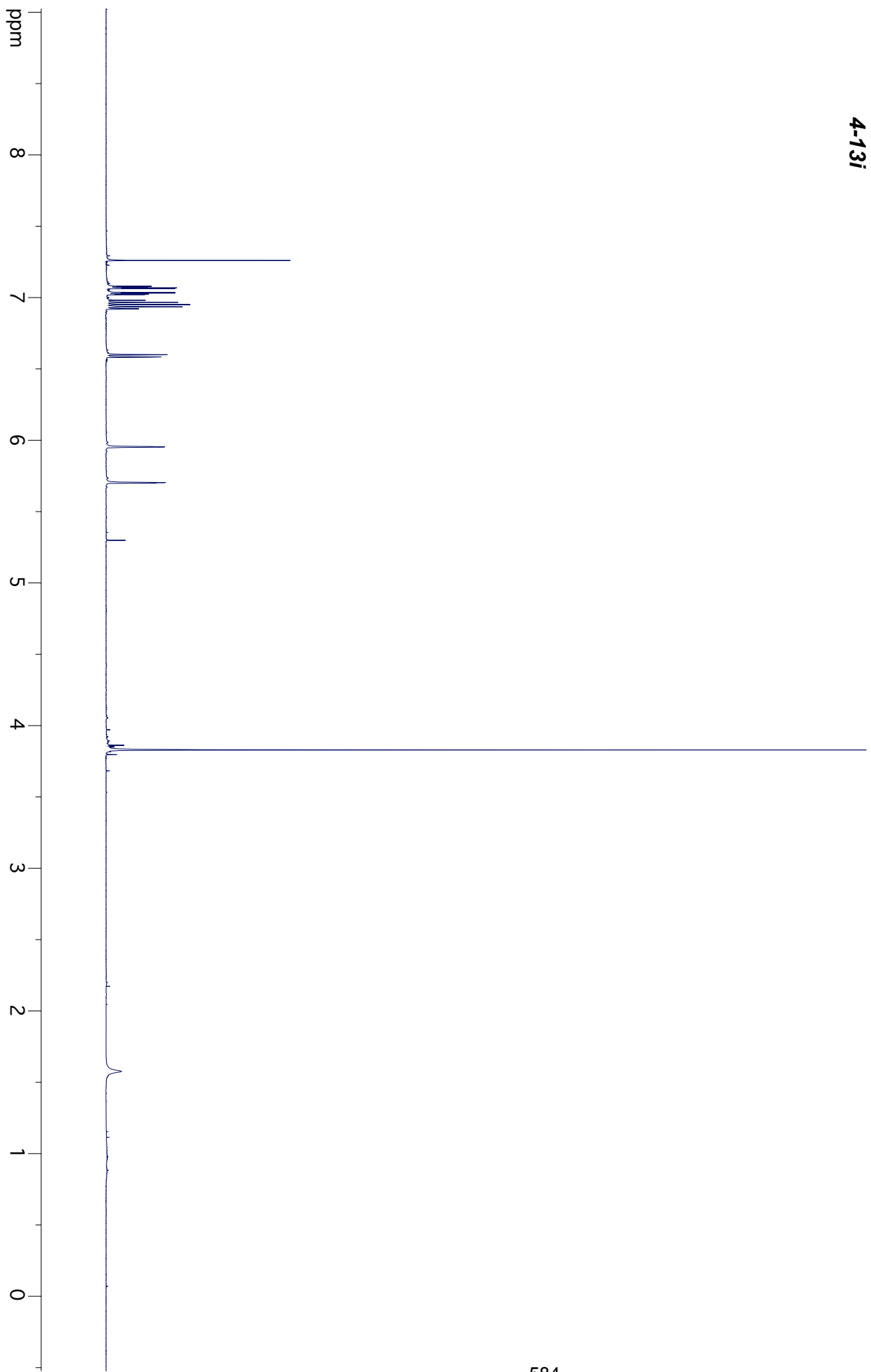
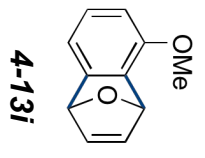
2

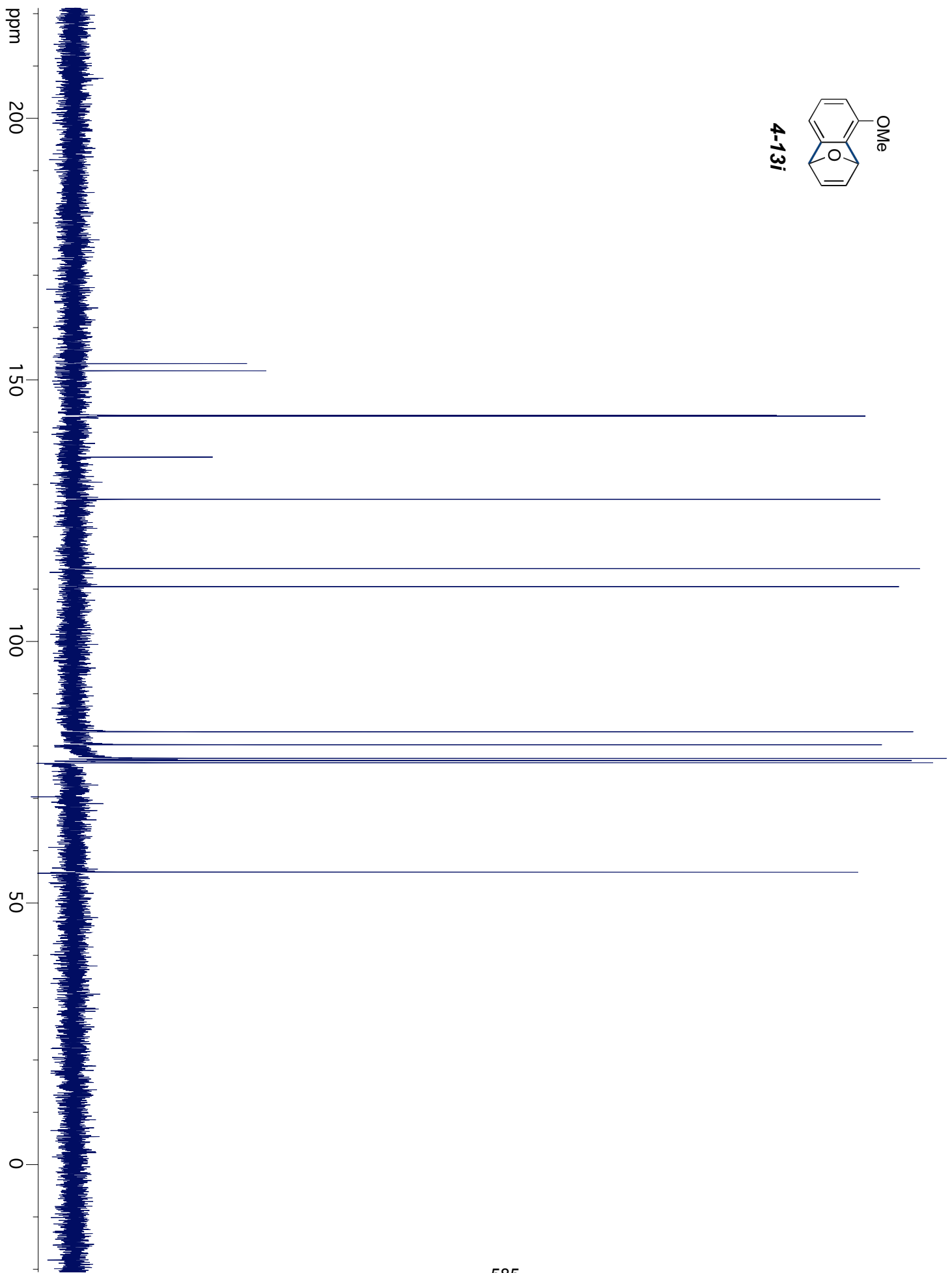
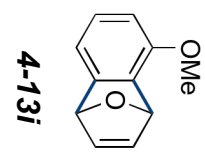
1

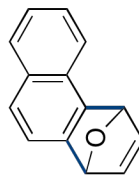
0



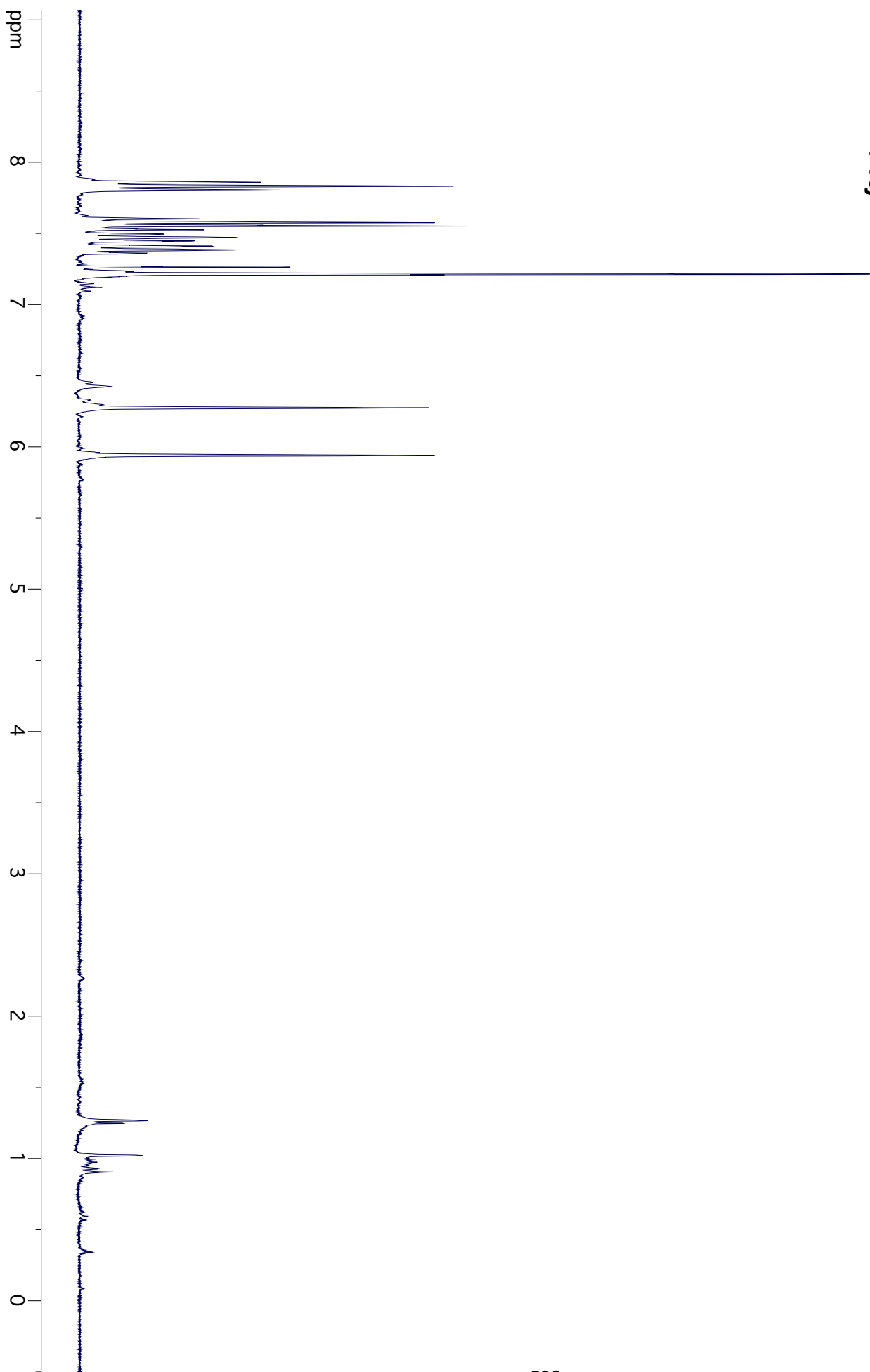


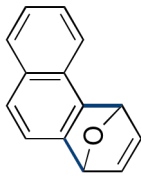




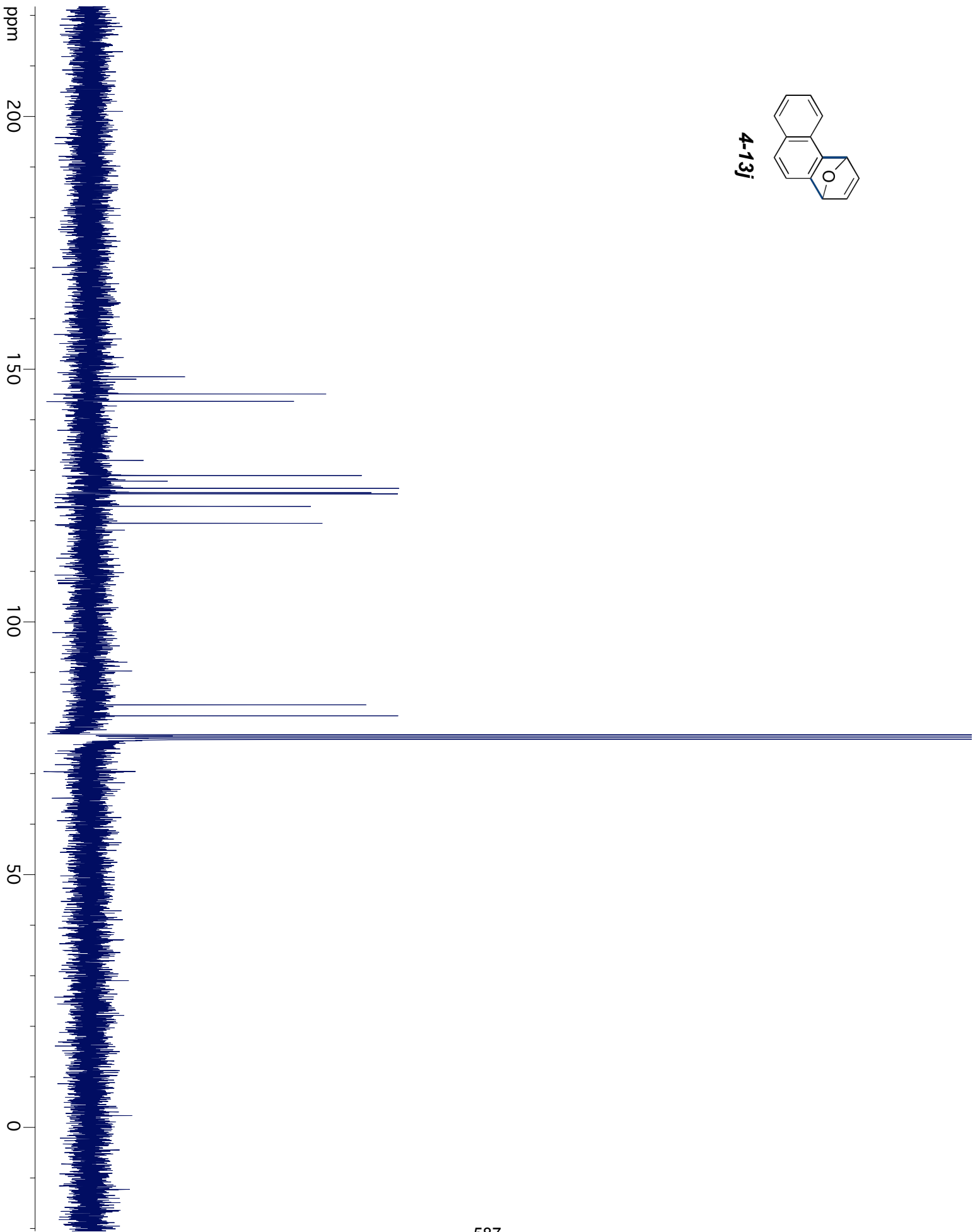


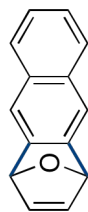
4-13j





4-13j





4-13K

ppm

8

7

6

5

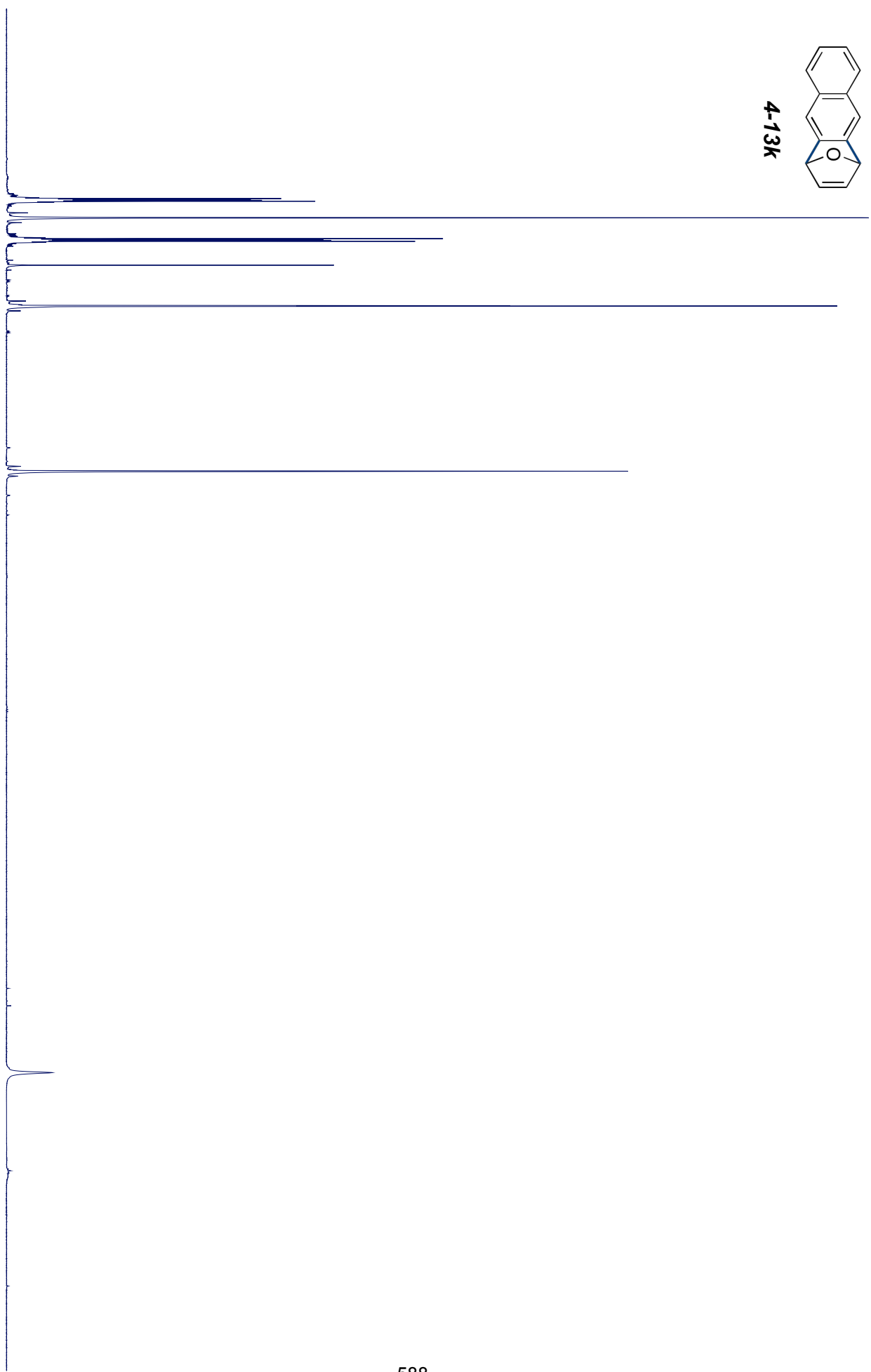
4

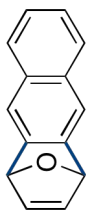
3

2

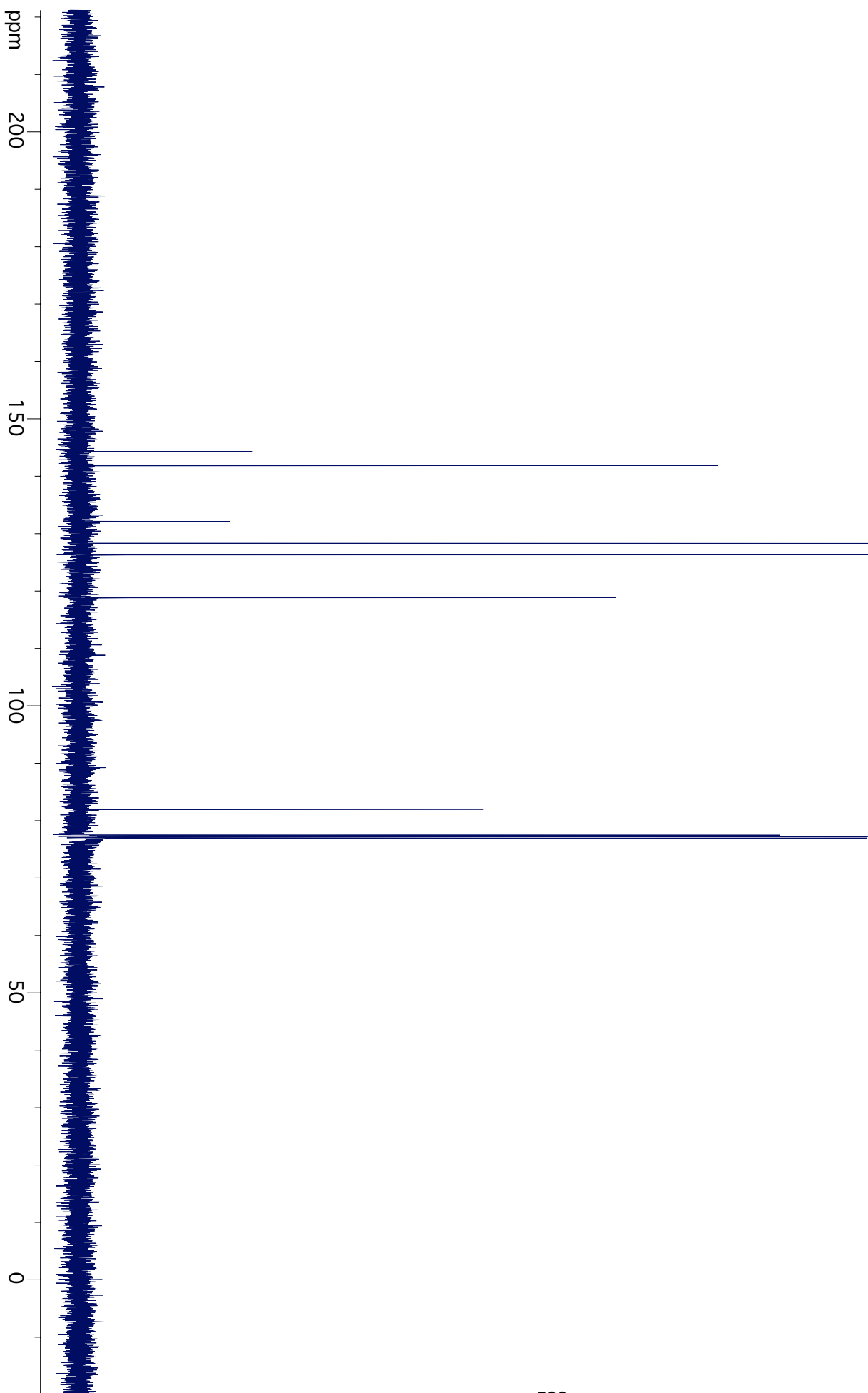
1

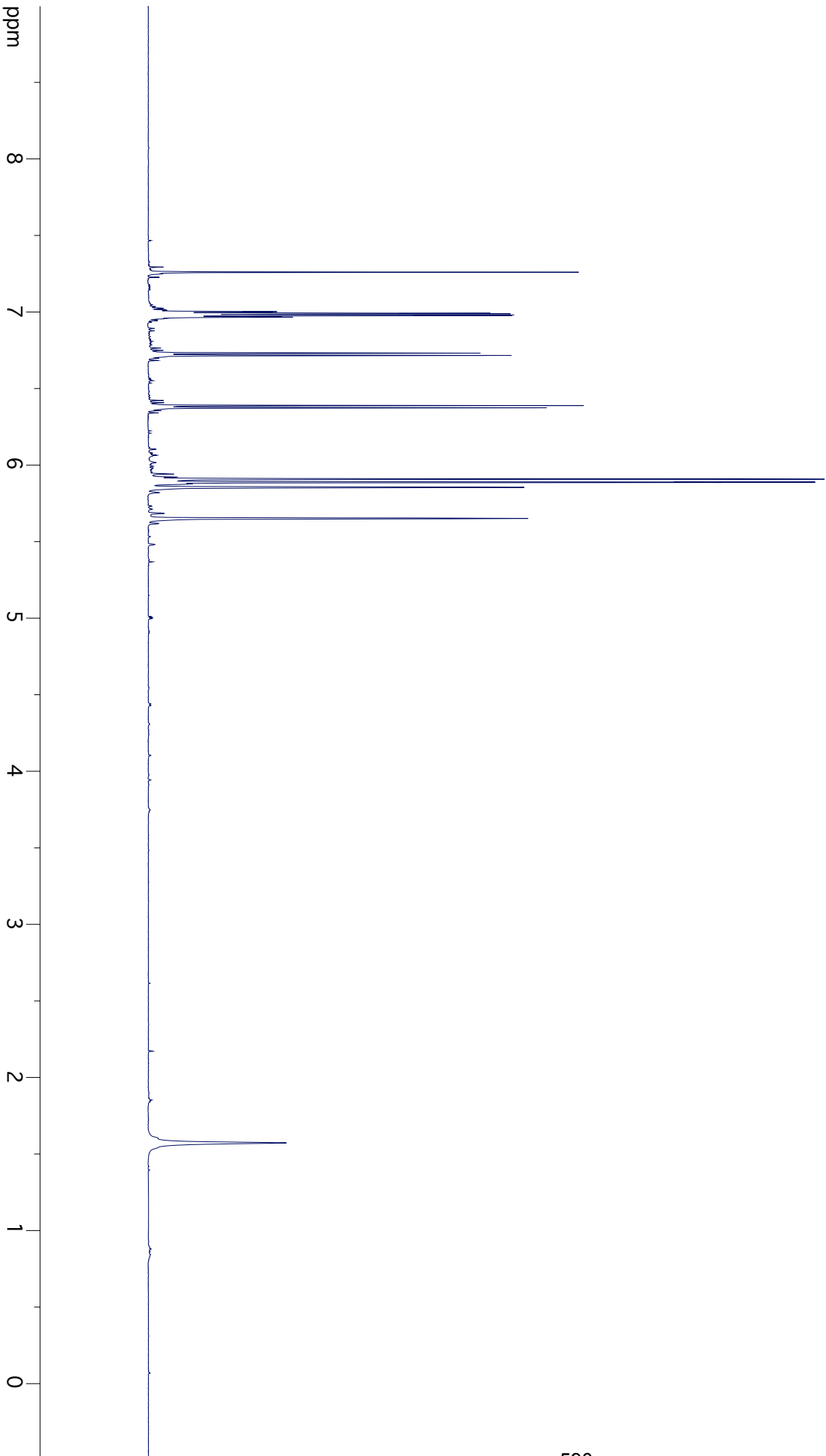
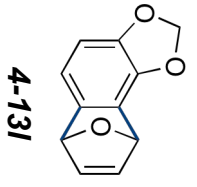
0

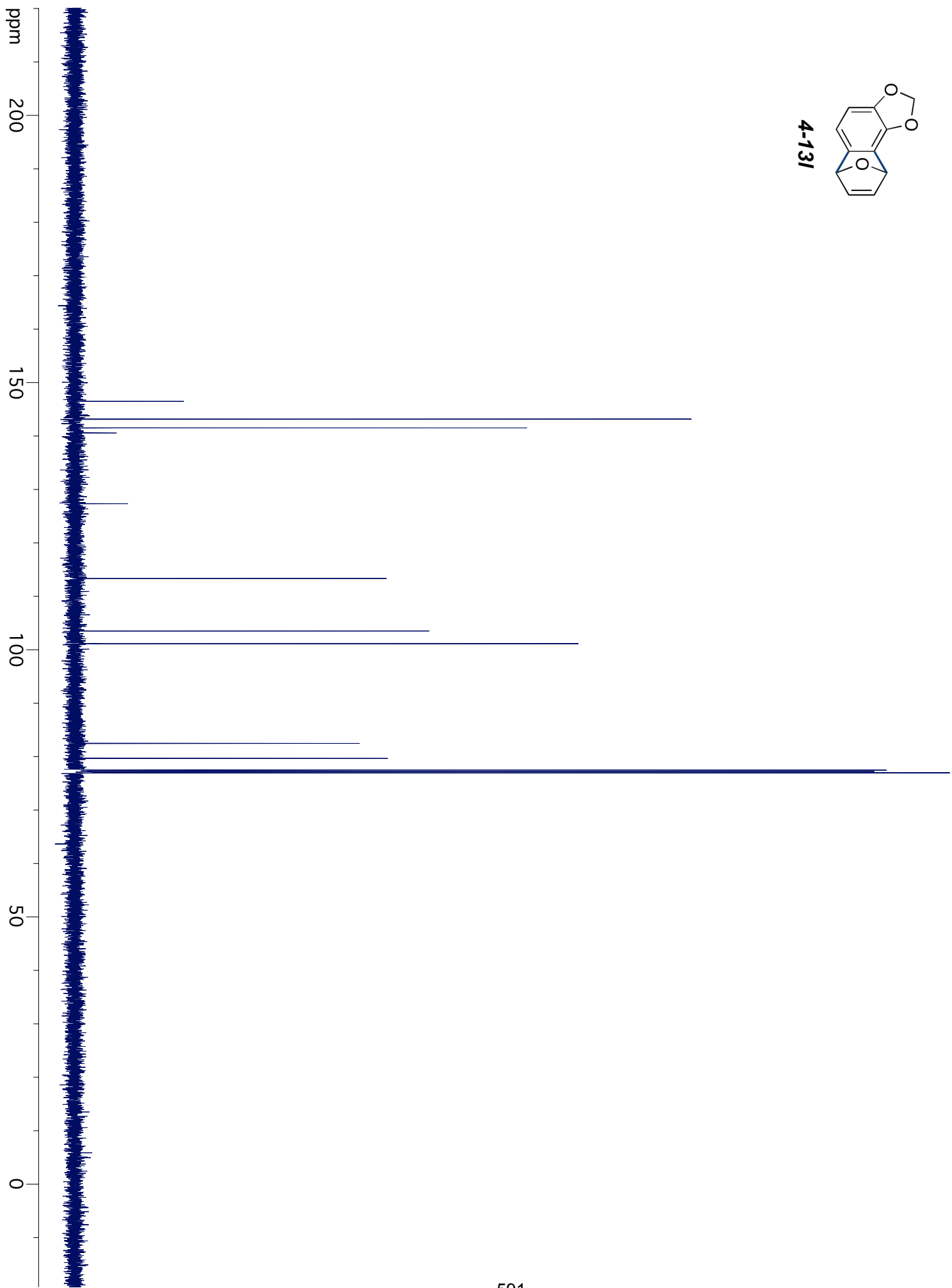
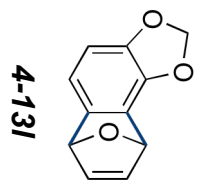


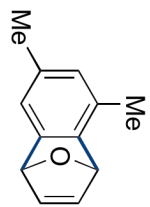


4-13K

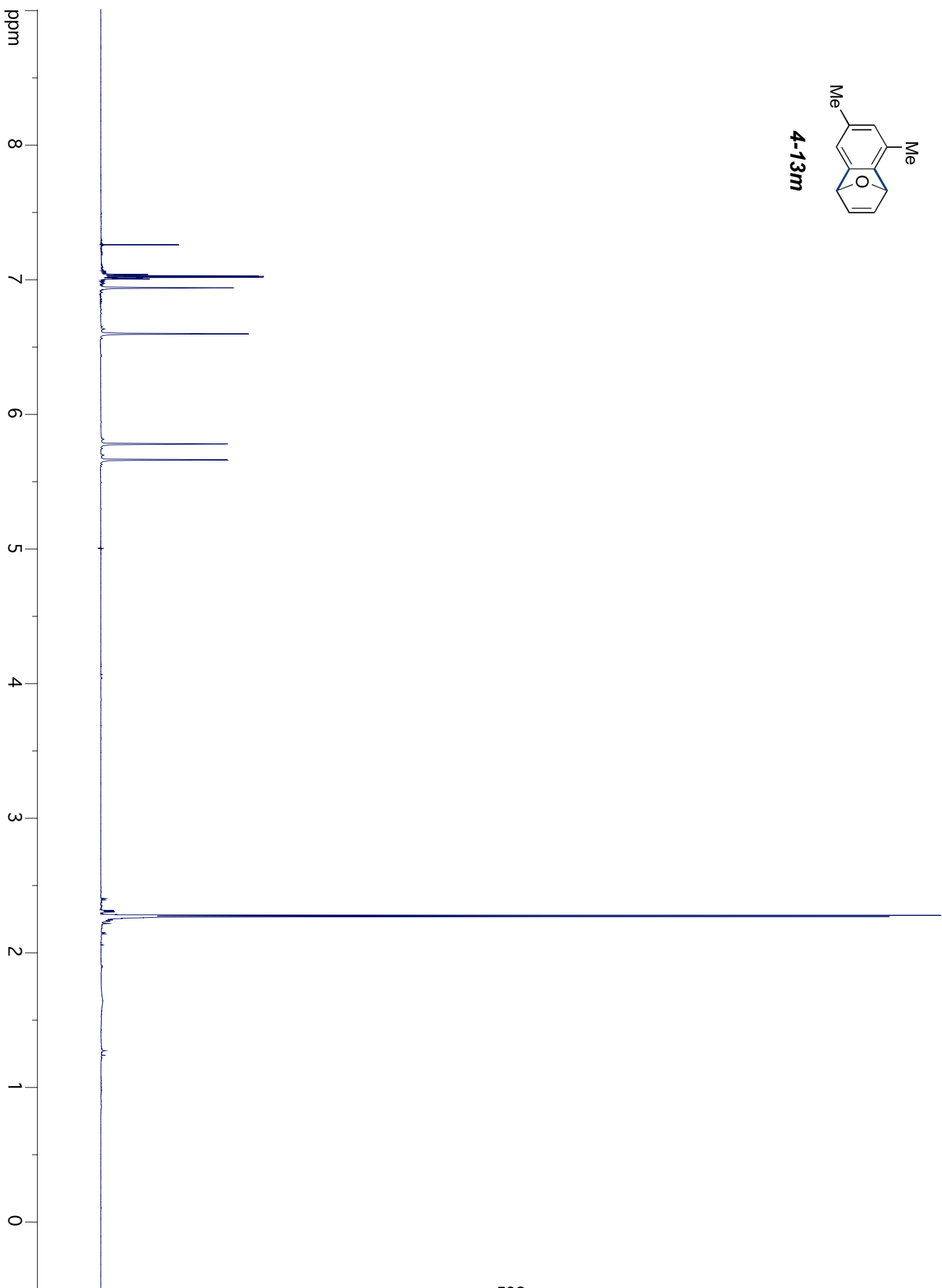


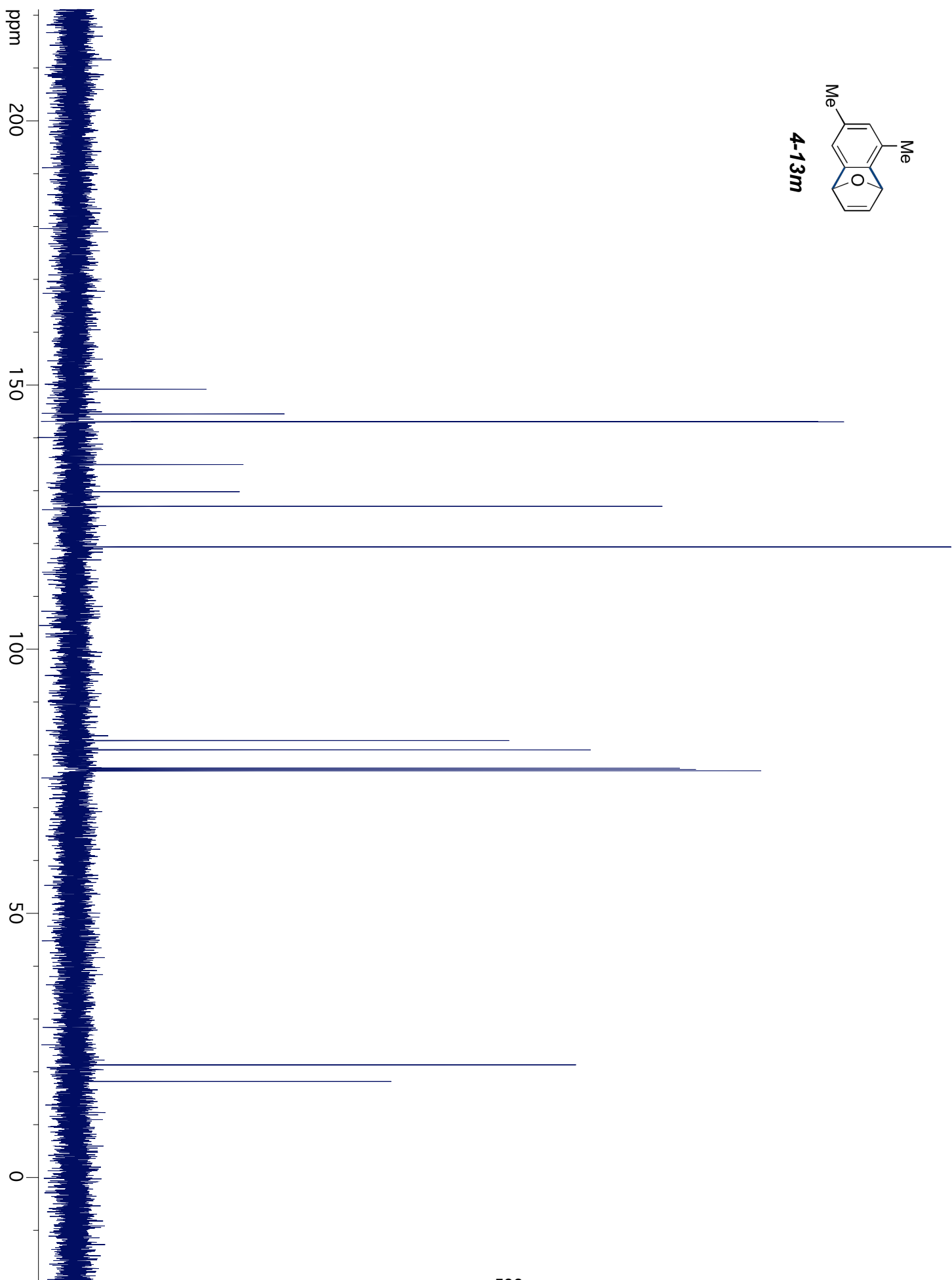
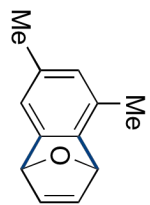


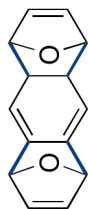




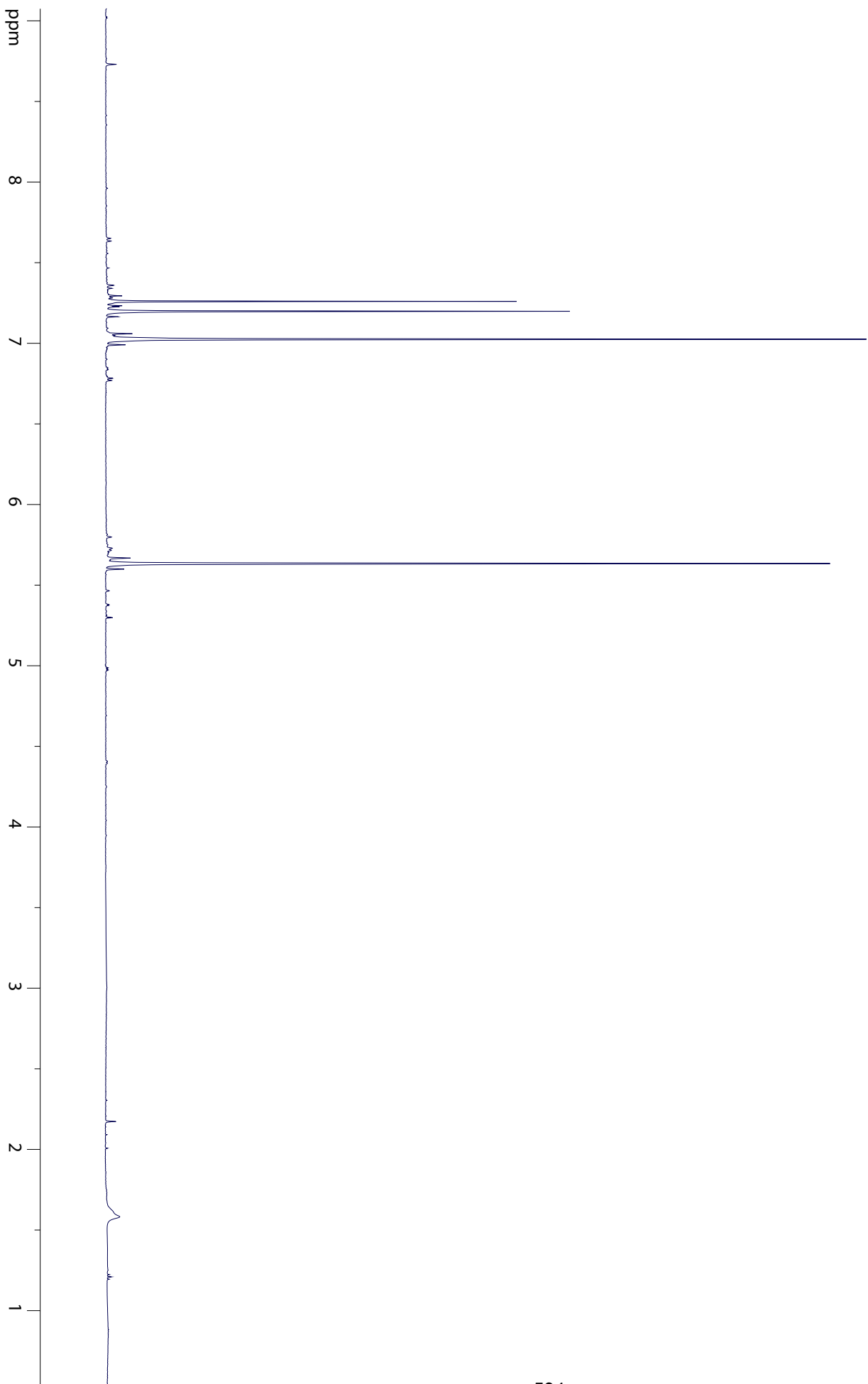
4-13m

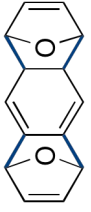






4-13n





4-13n

ppm

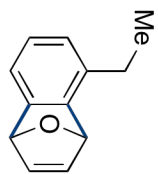
200

150

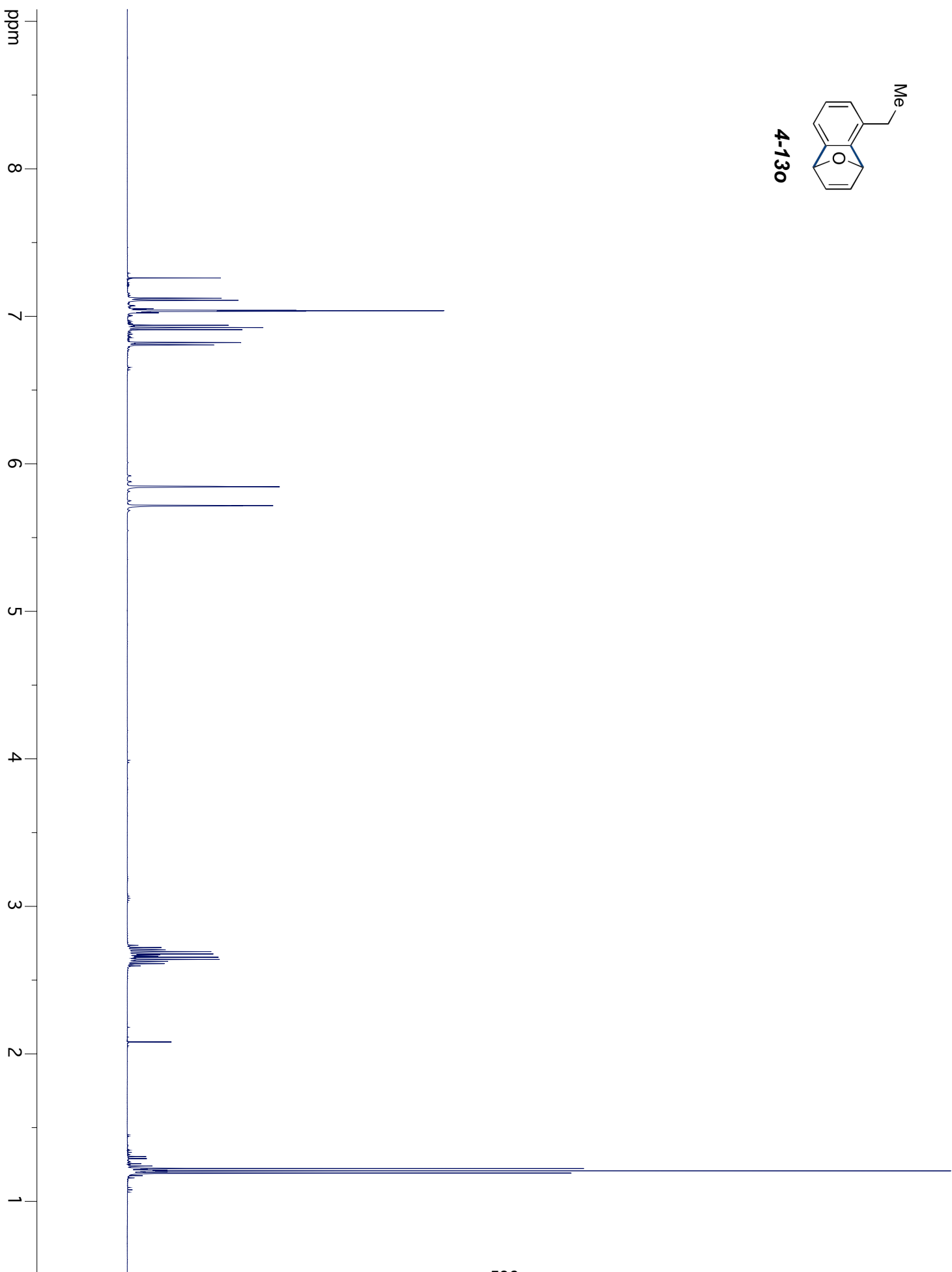
100

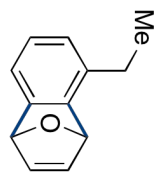
50

0



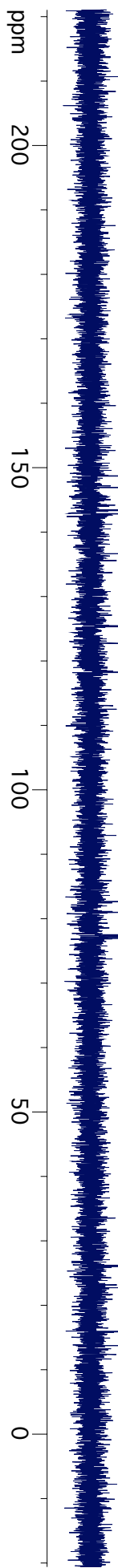
4-130

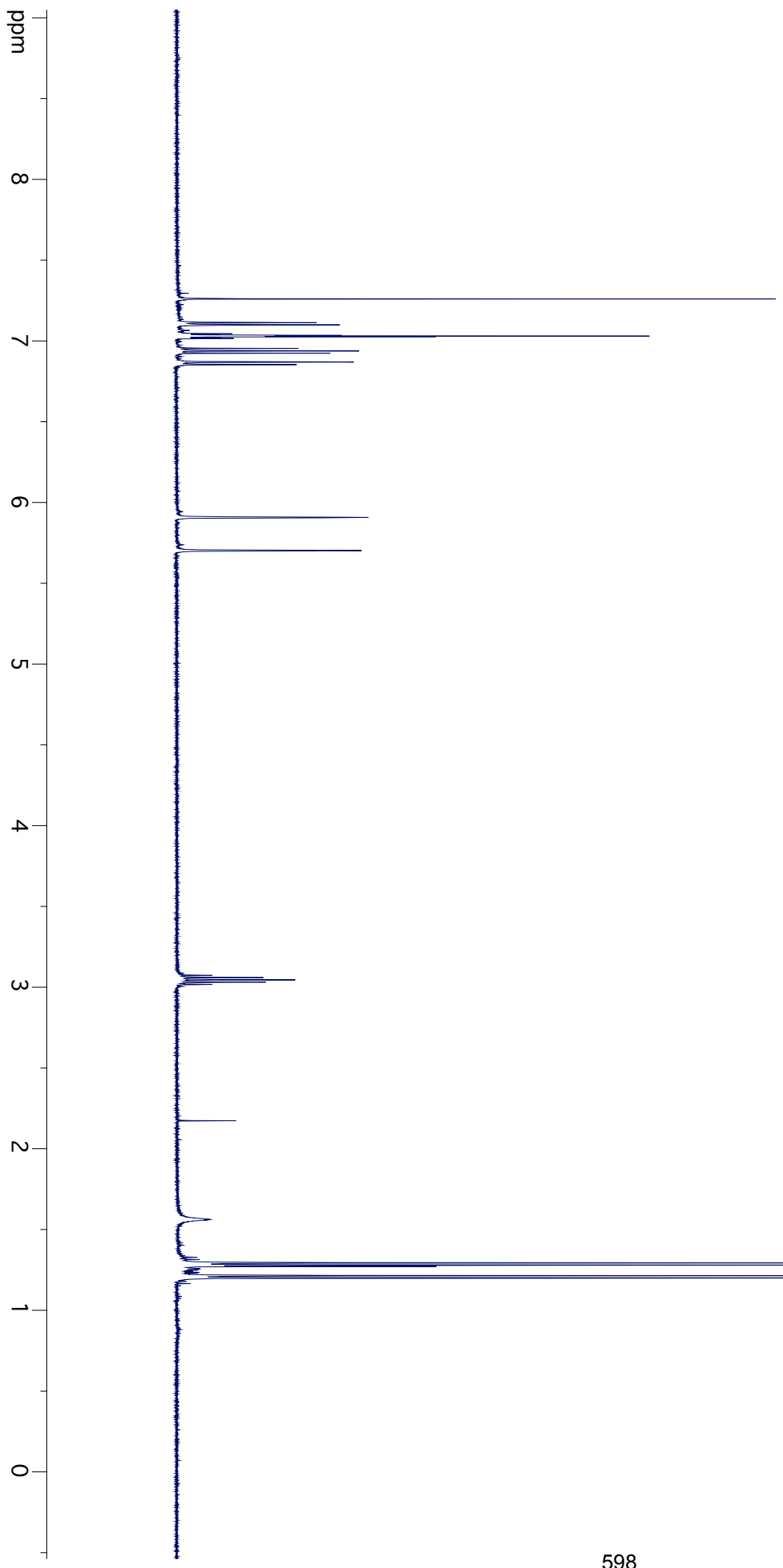
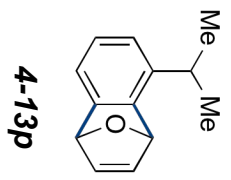




4-130

ppm

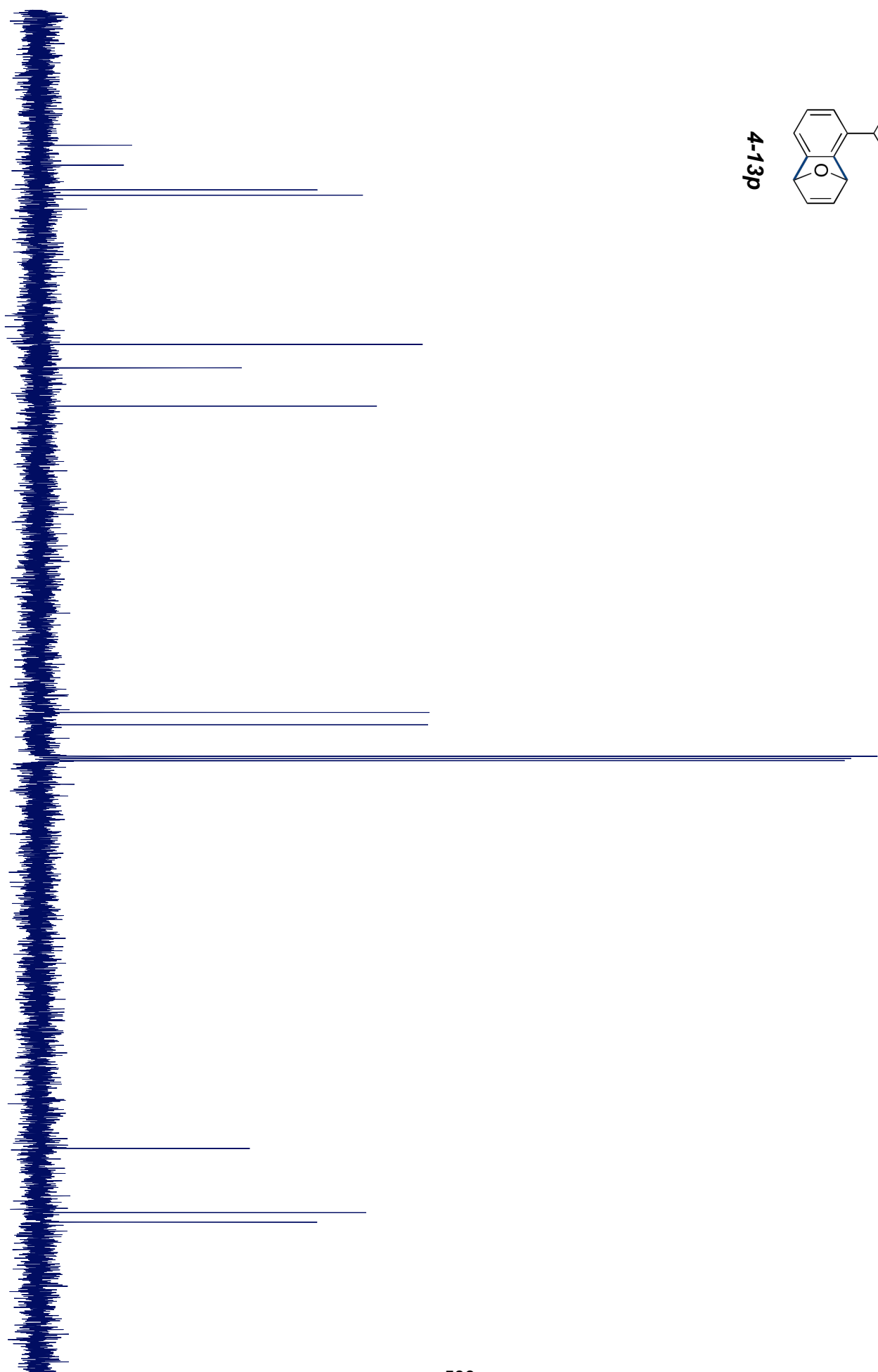


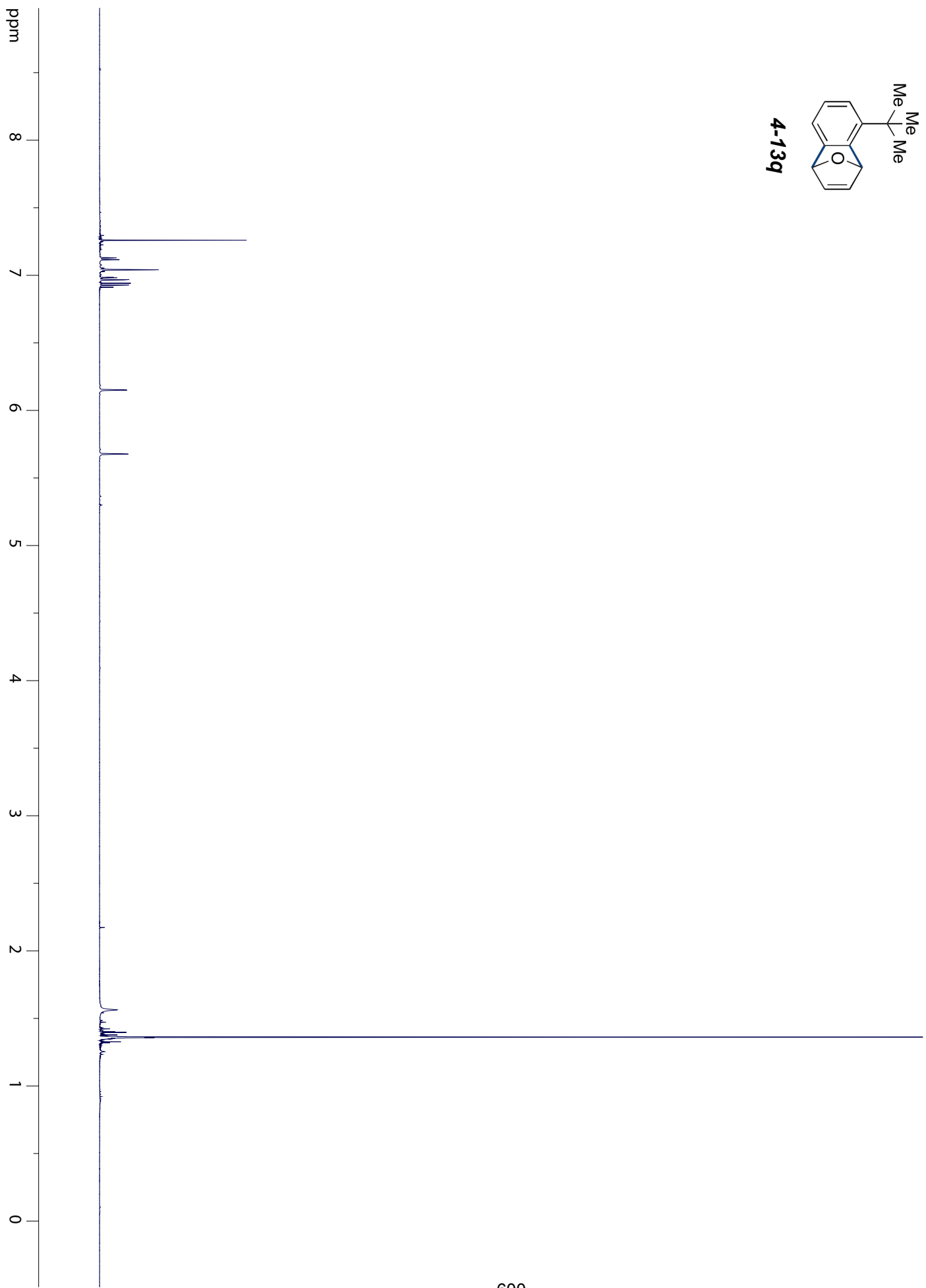
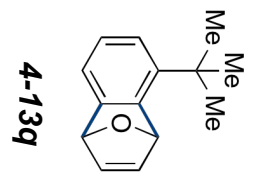


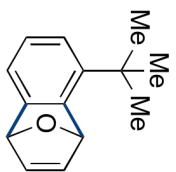


4-13p

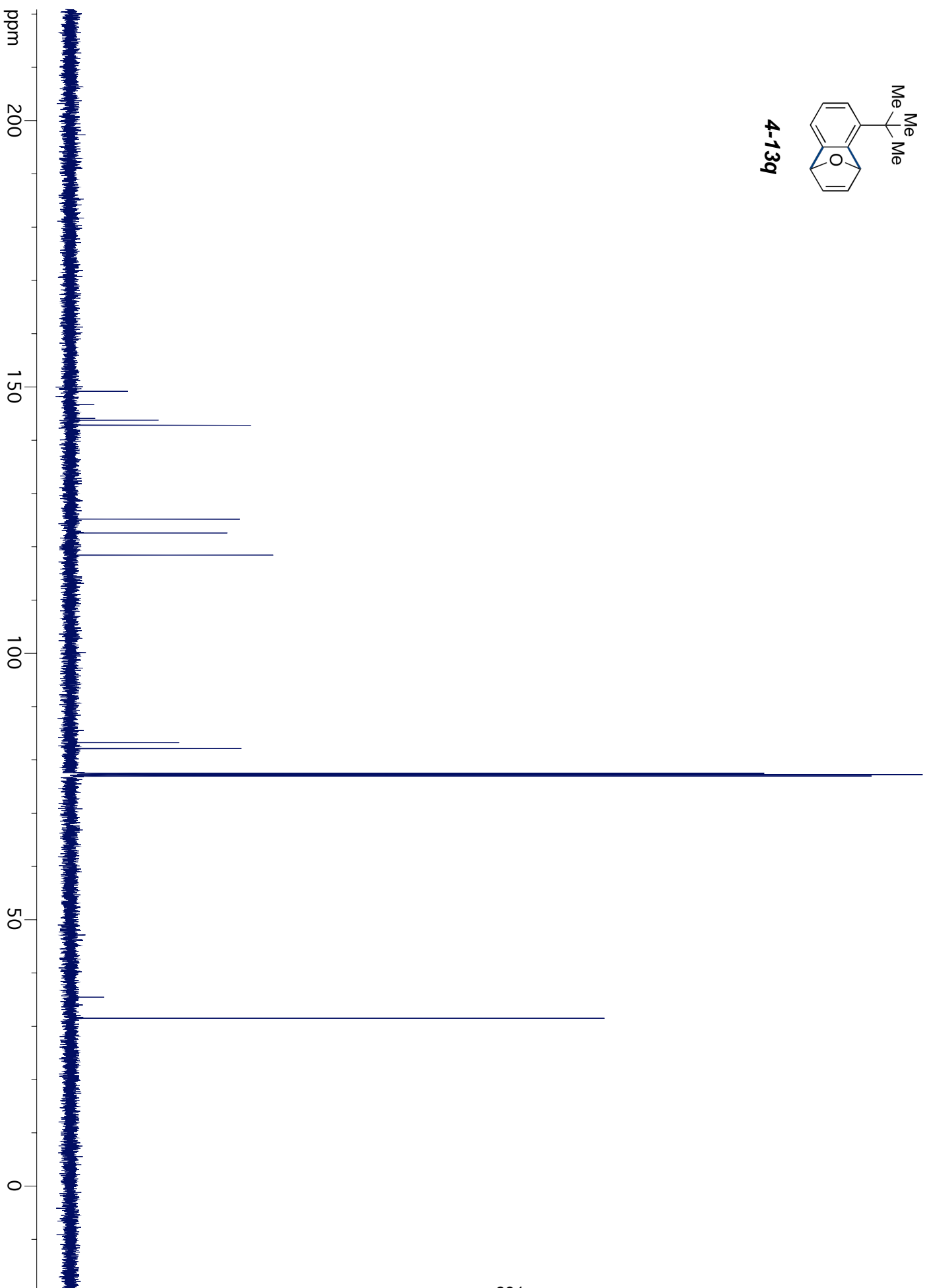
ppm

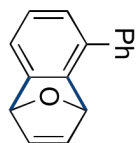




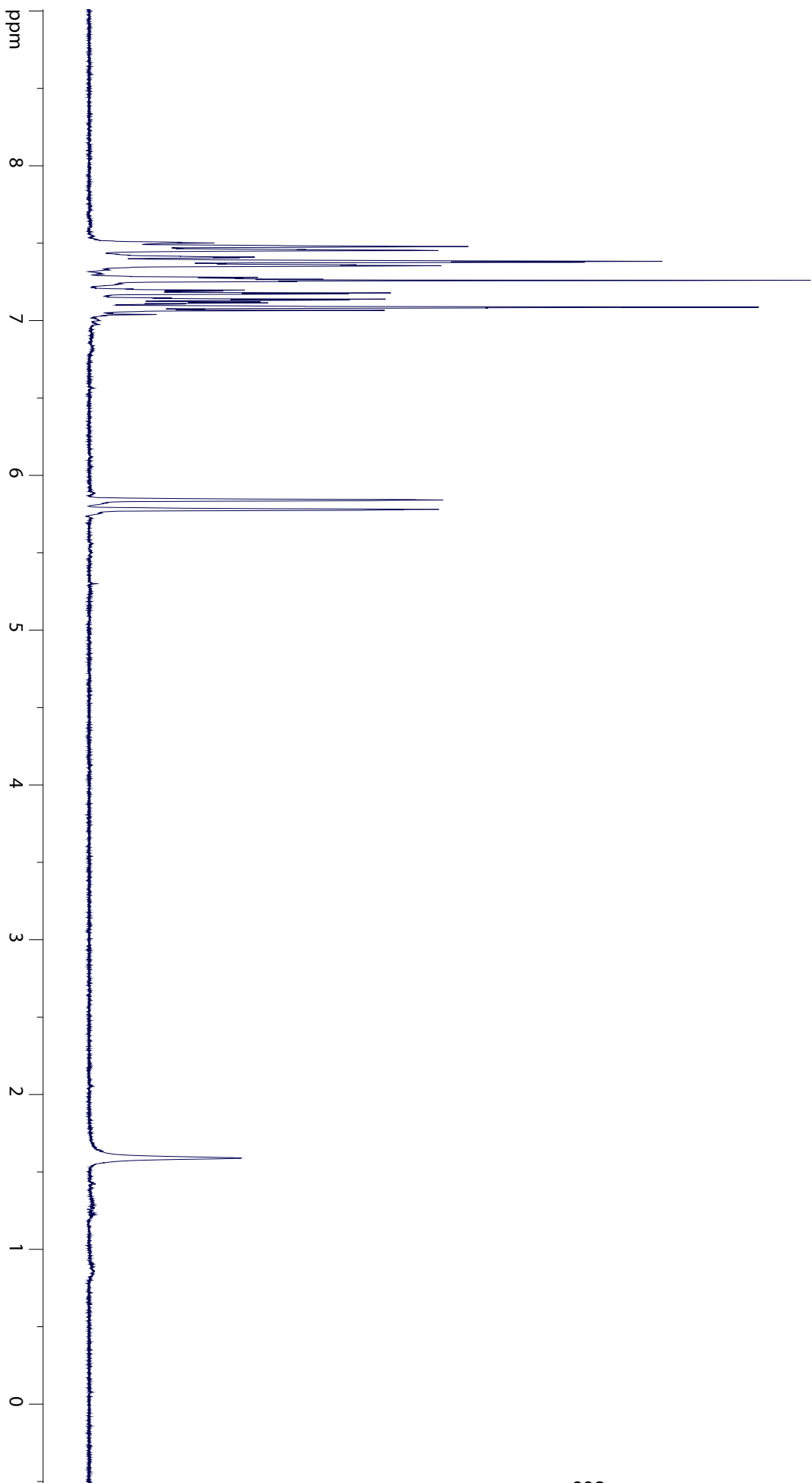


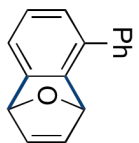
4-13q



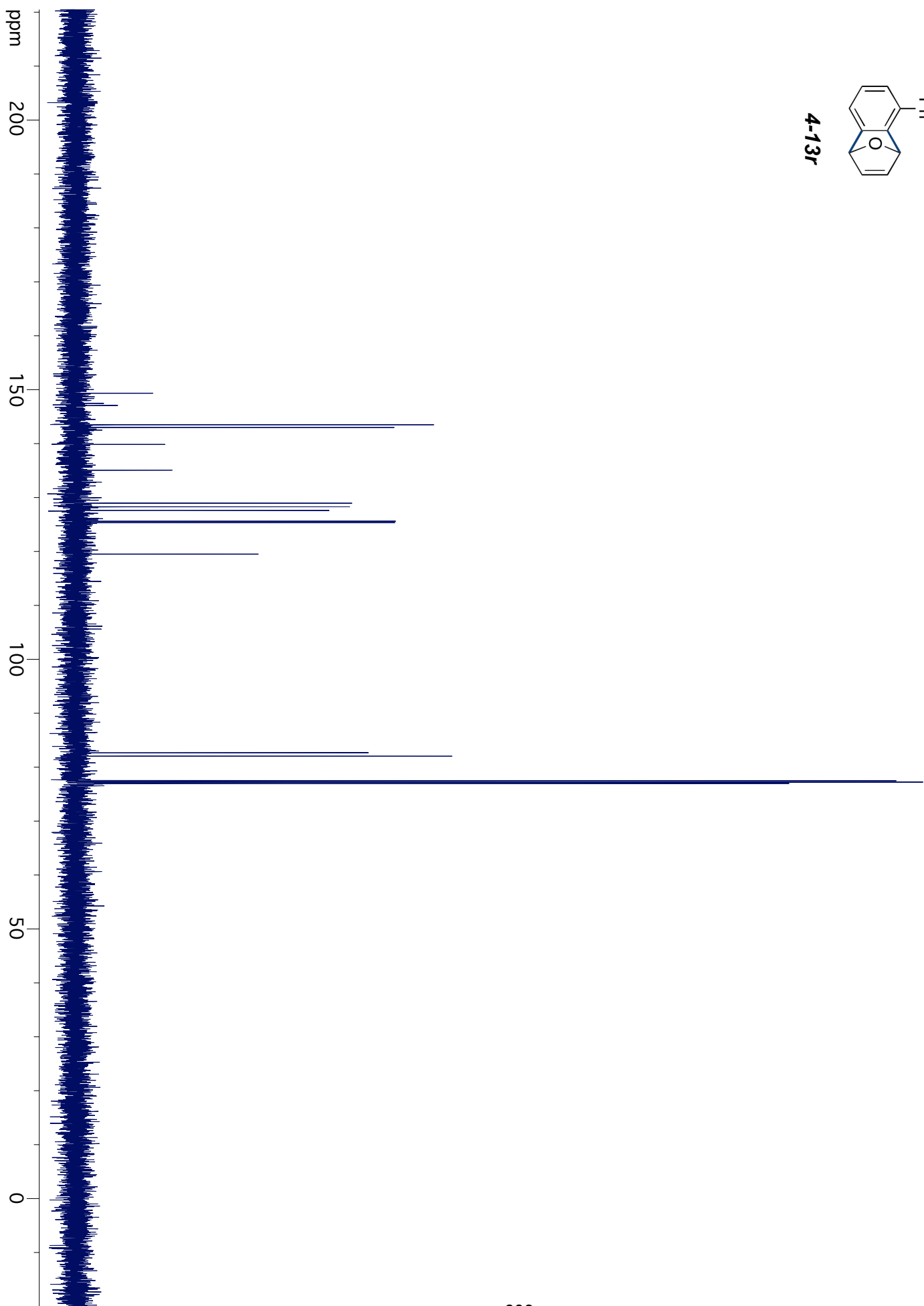


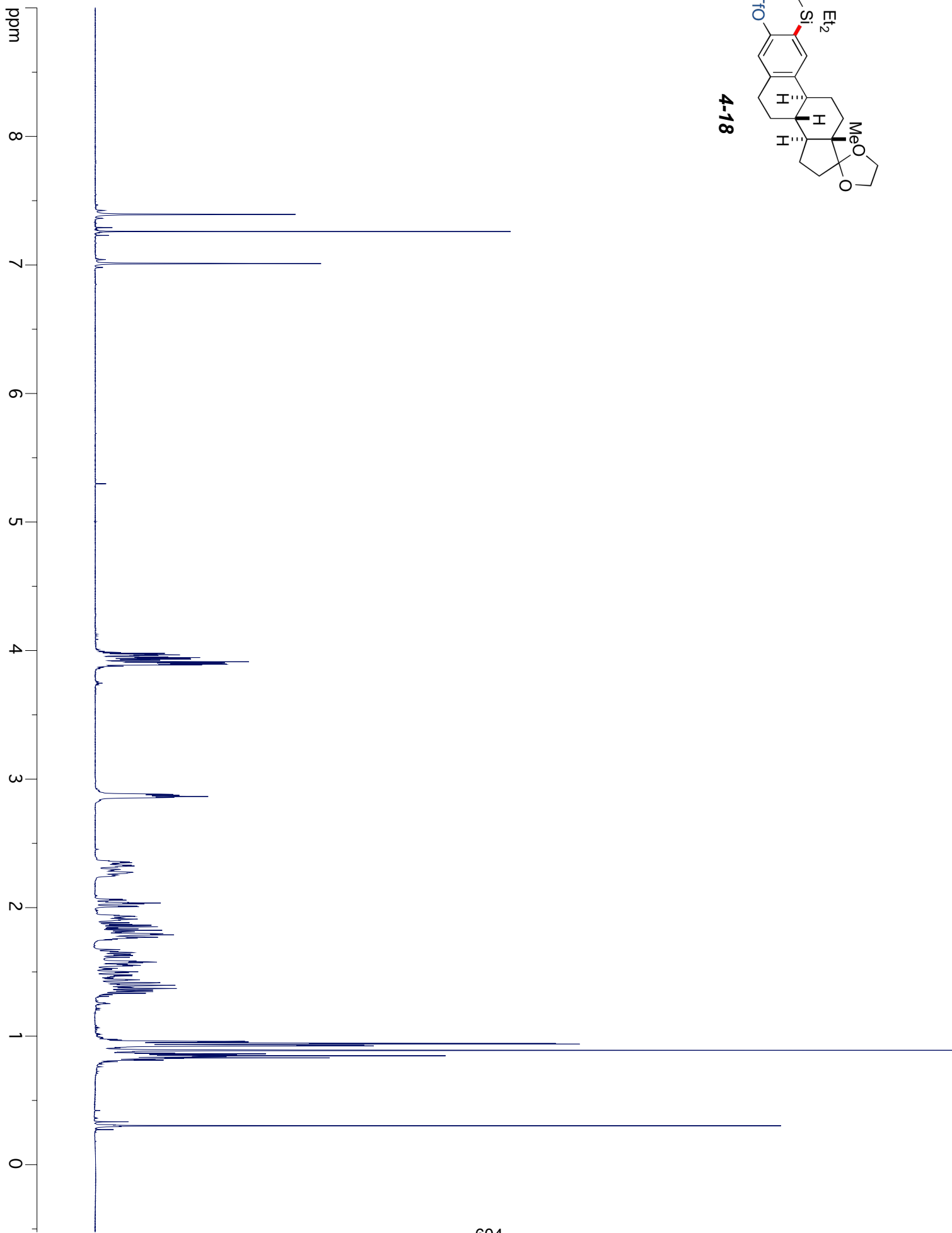
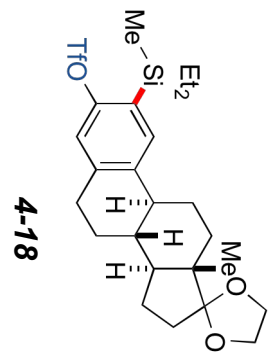
4-13r

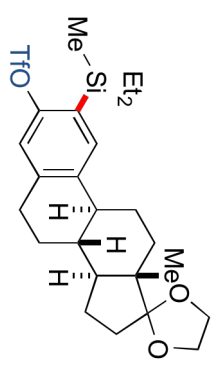




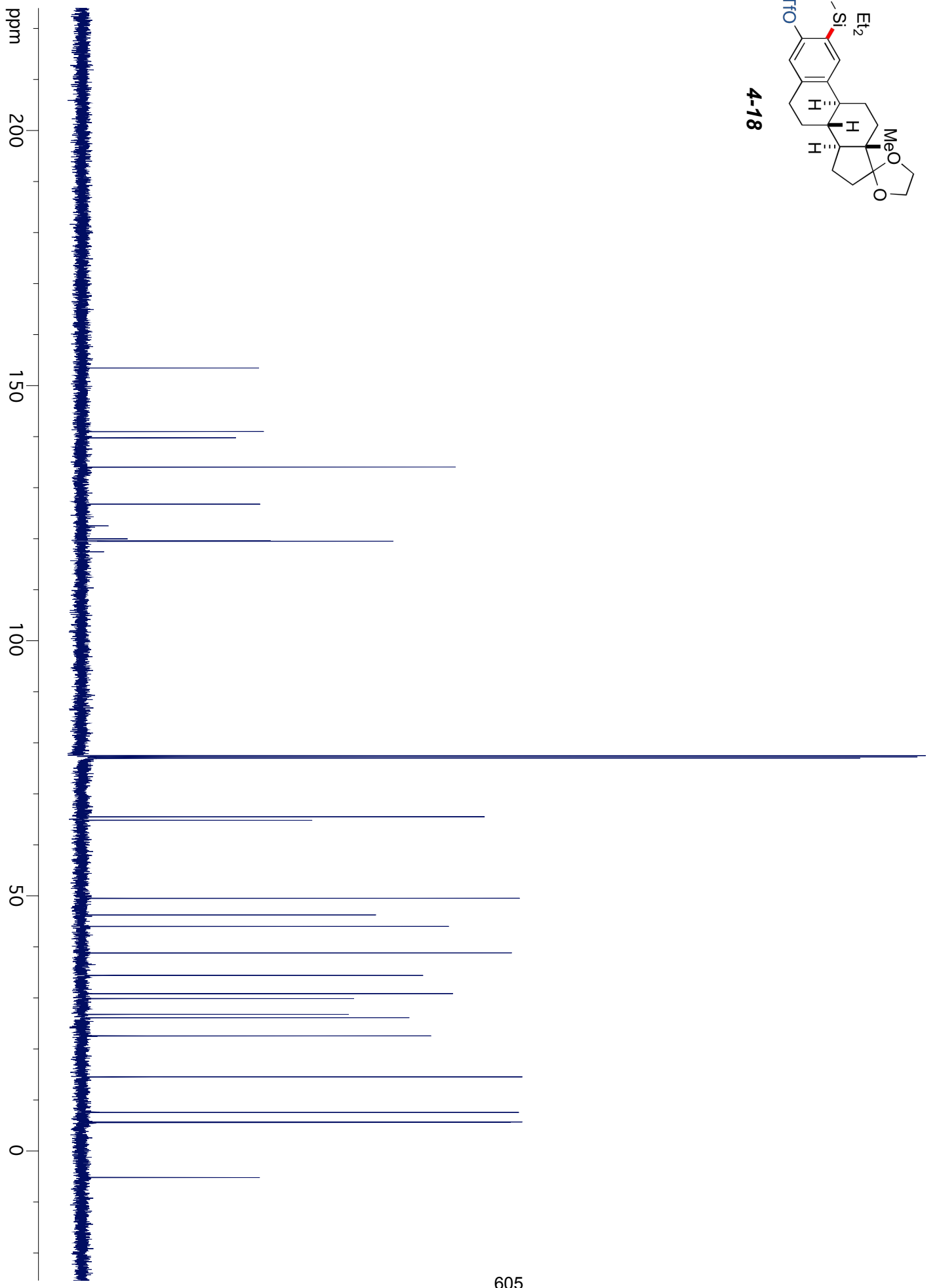
4-13r

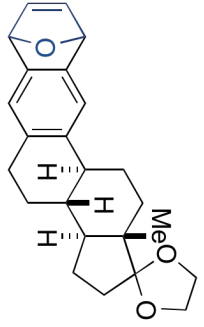




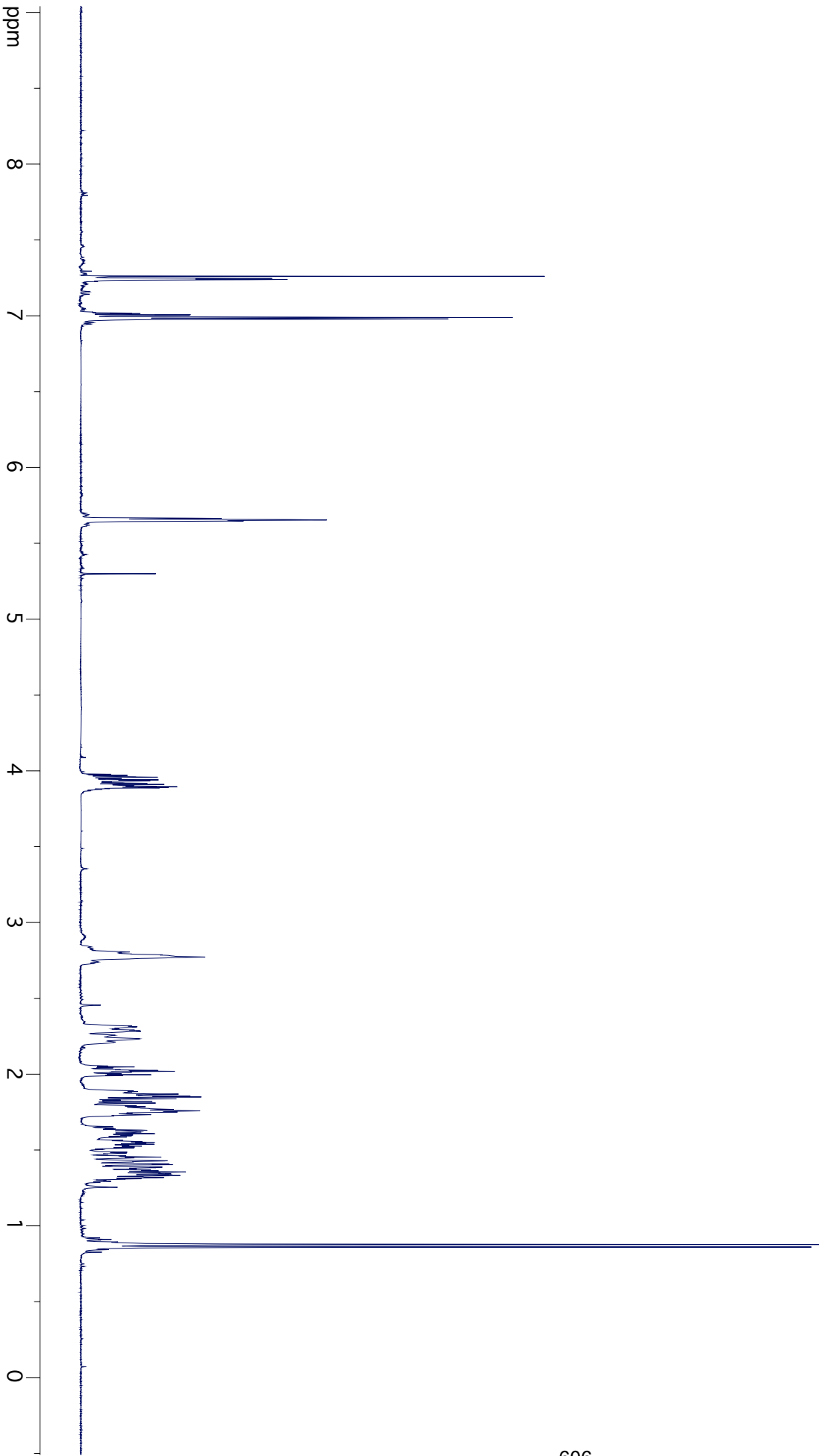


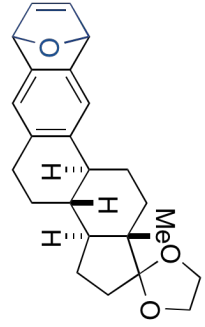
4-18



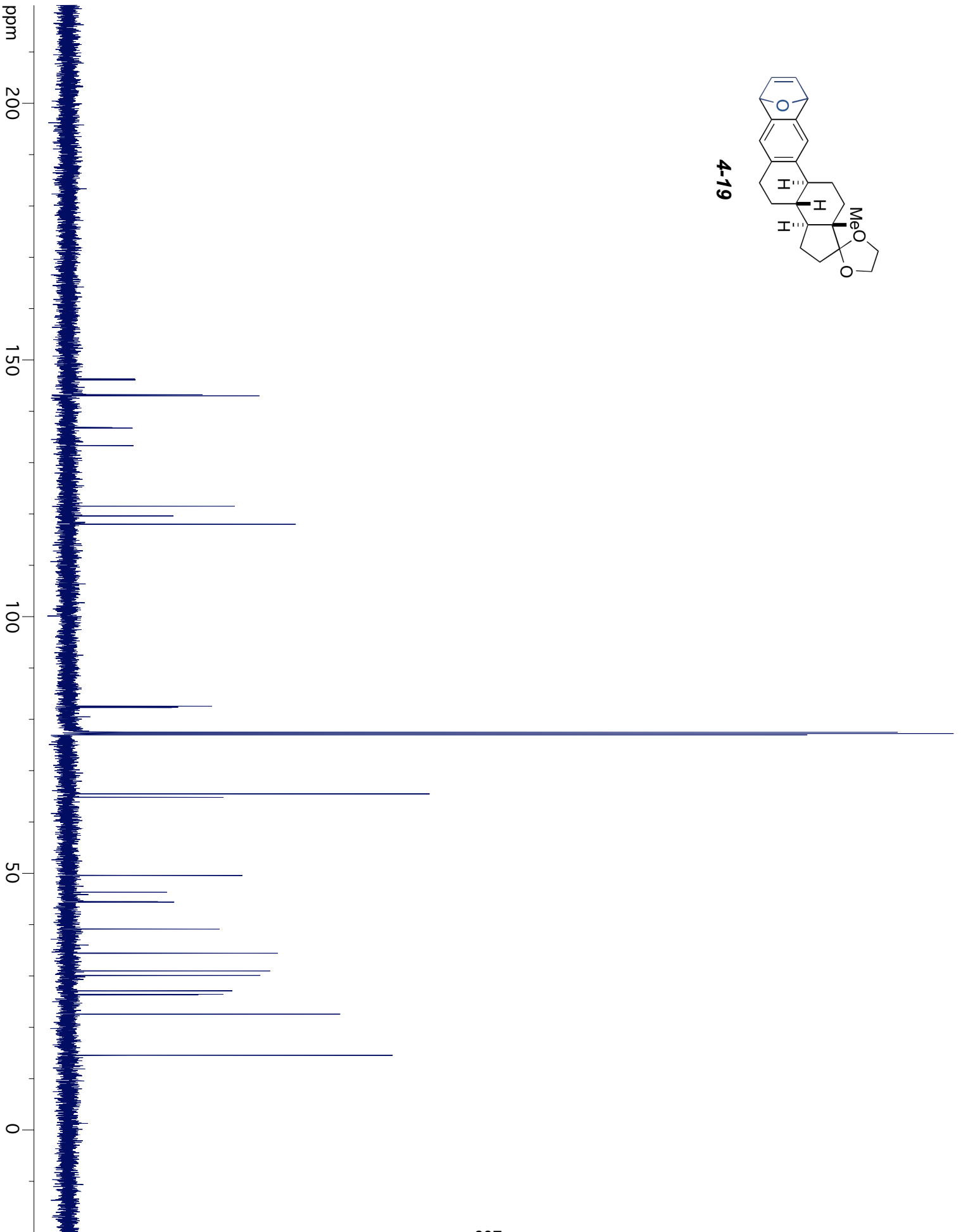


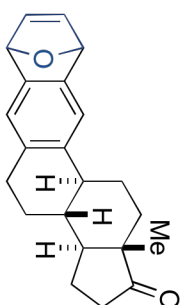
4-19



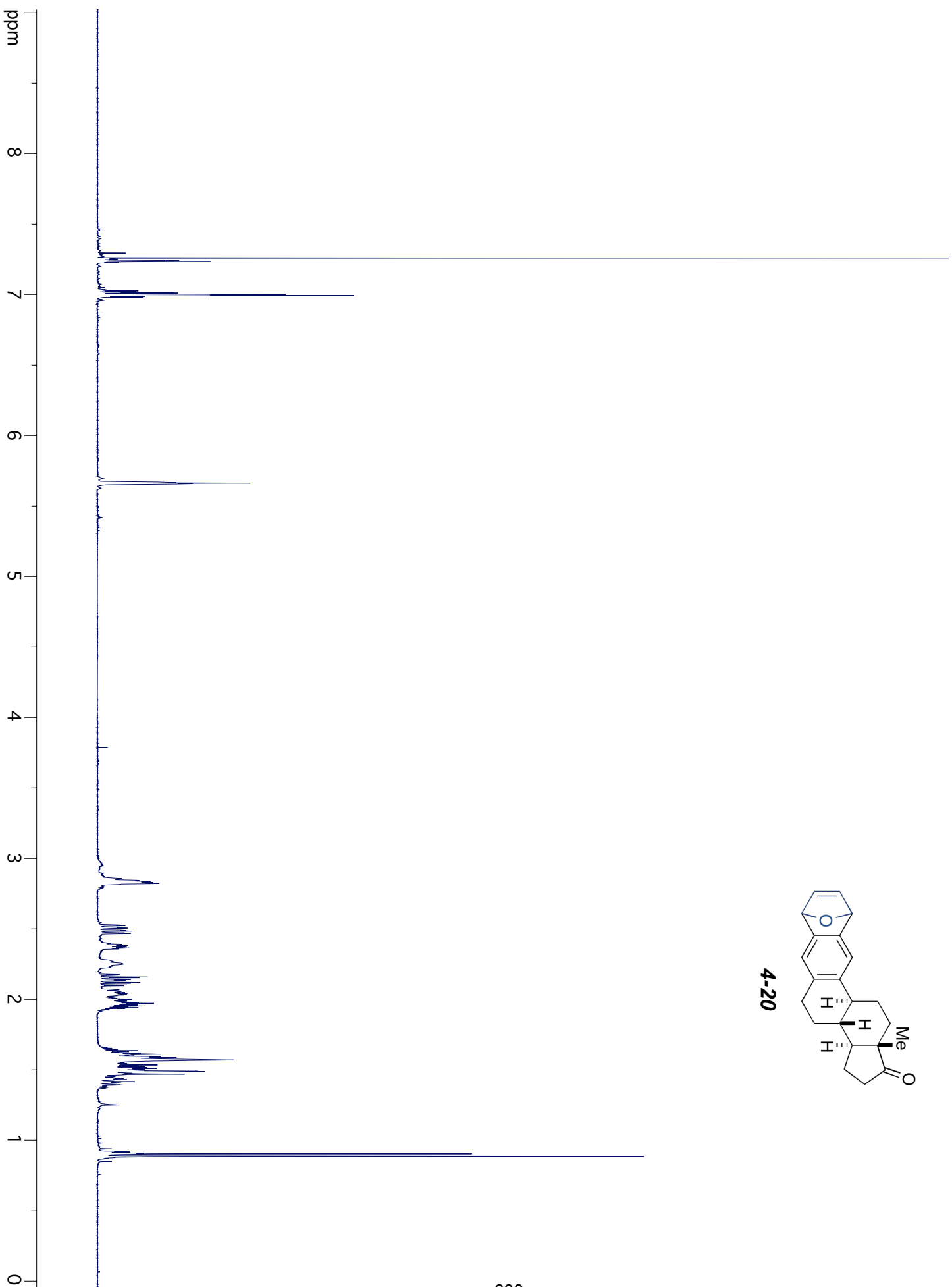


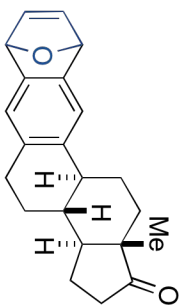
4-19



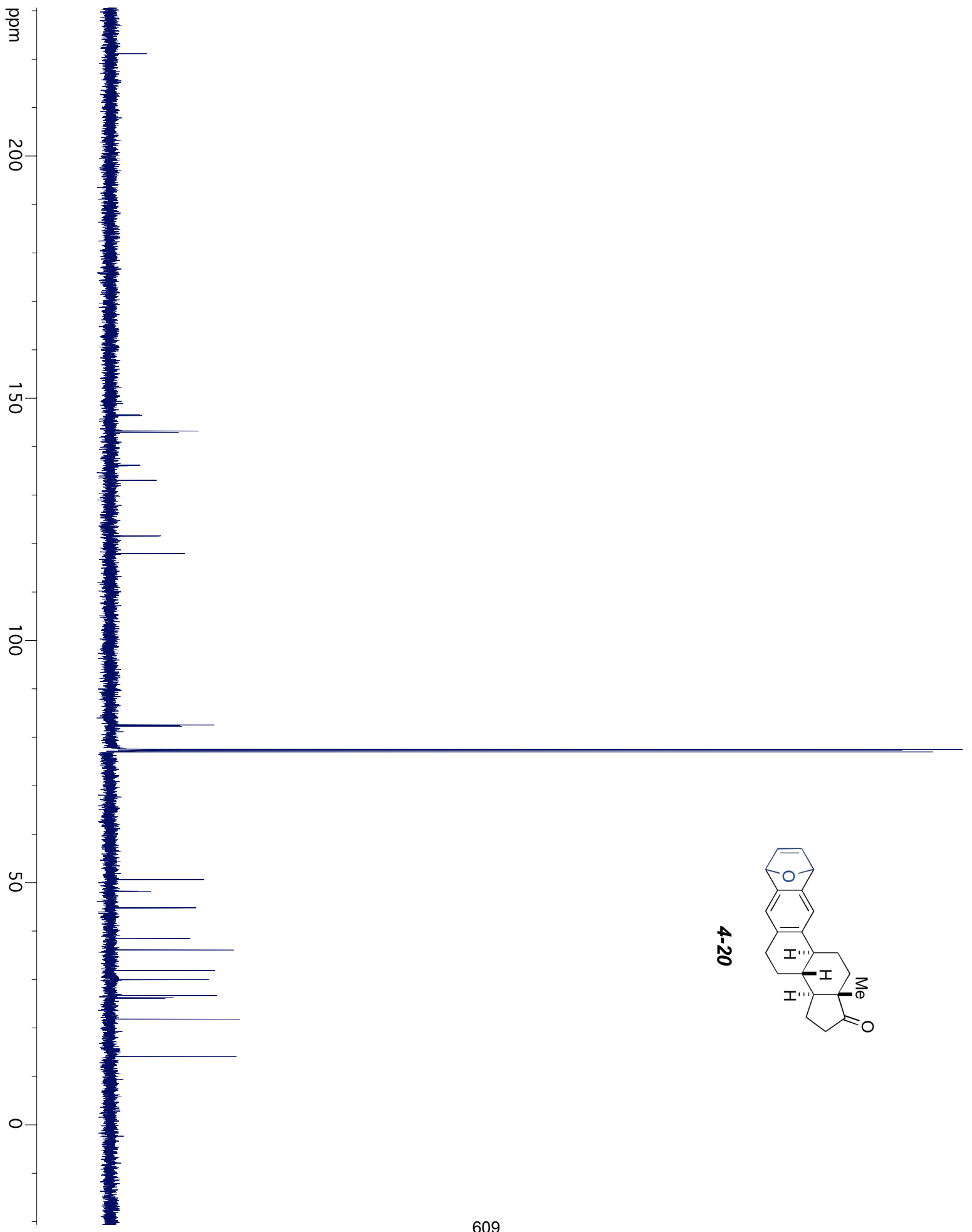


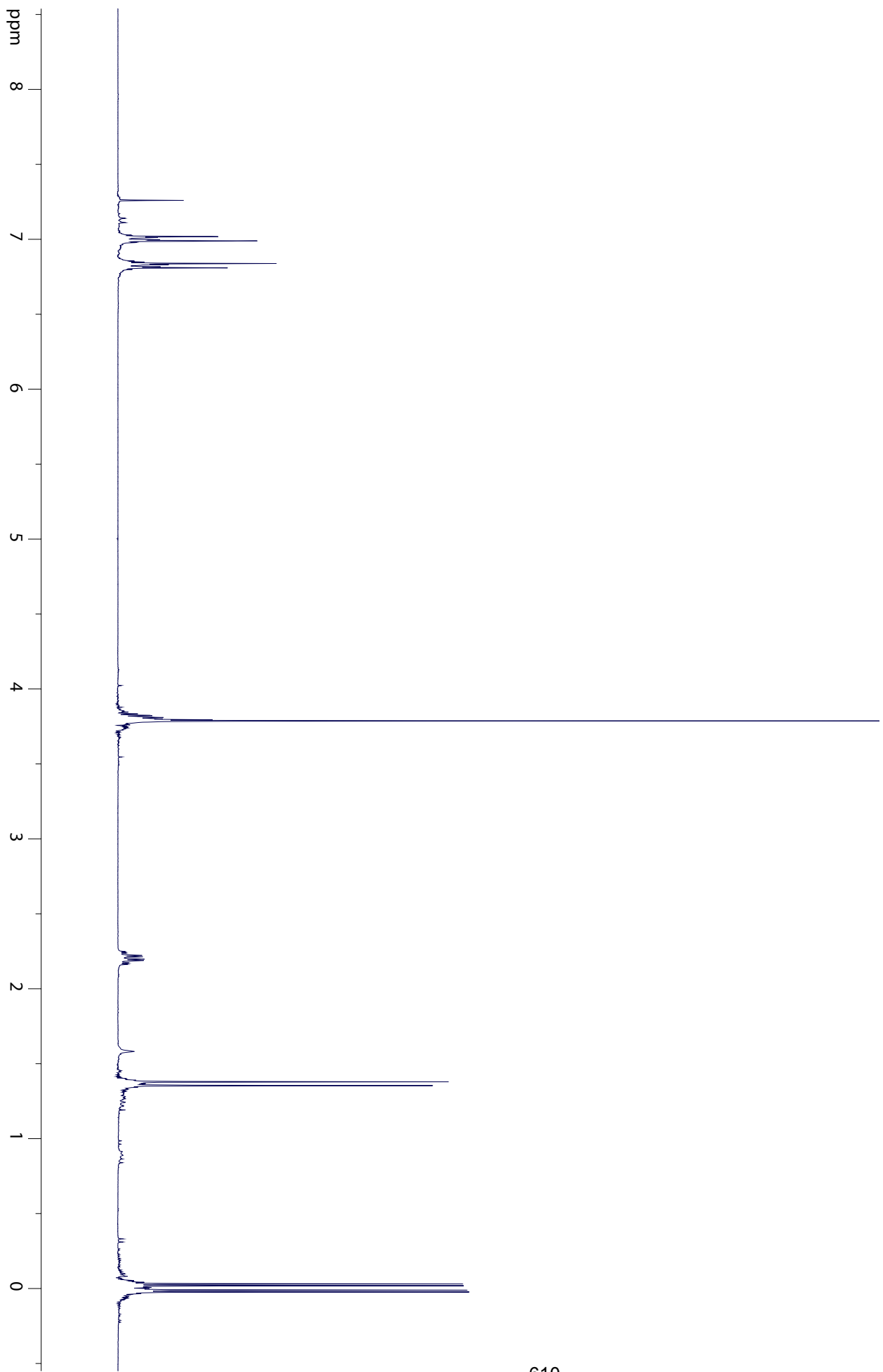
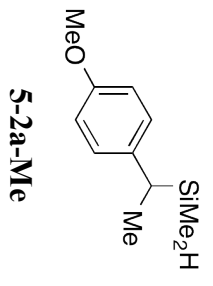
4-20

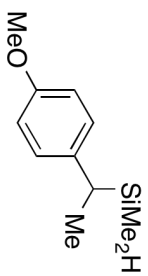




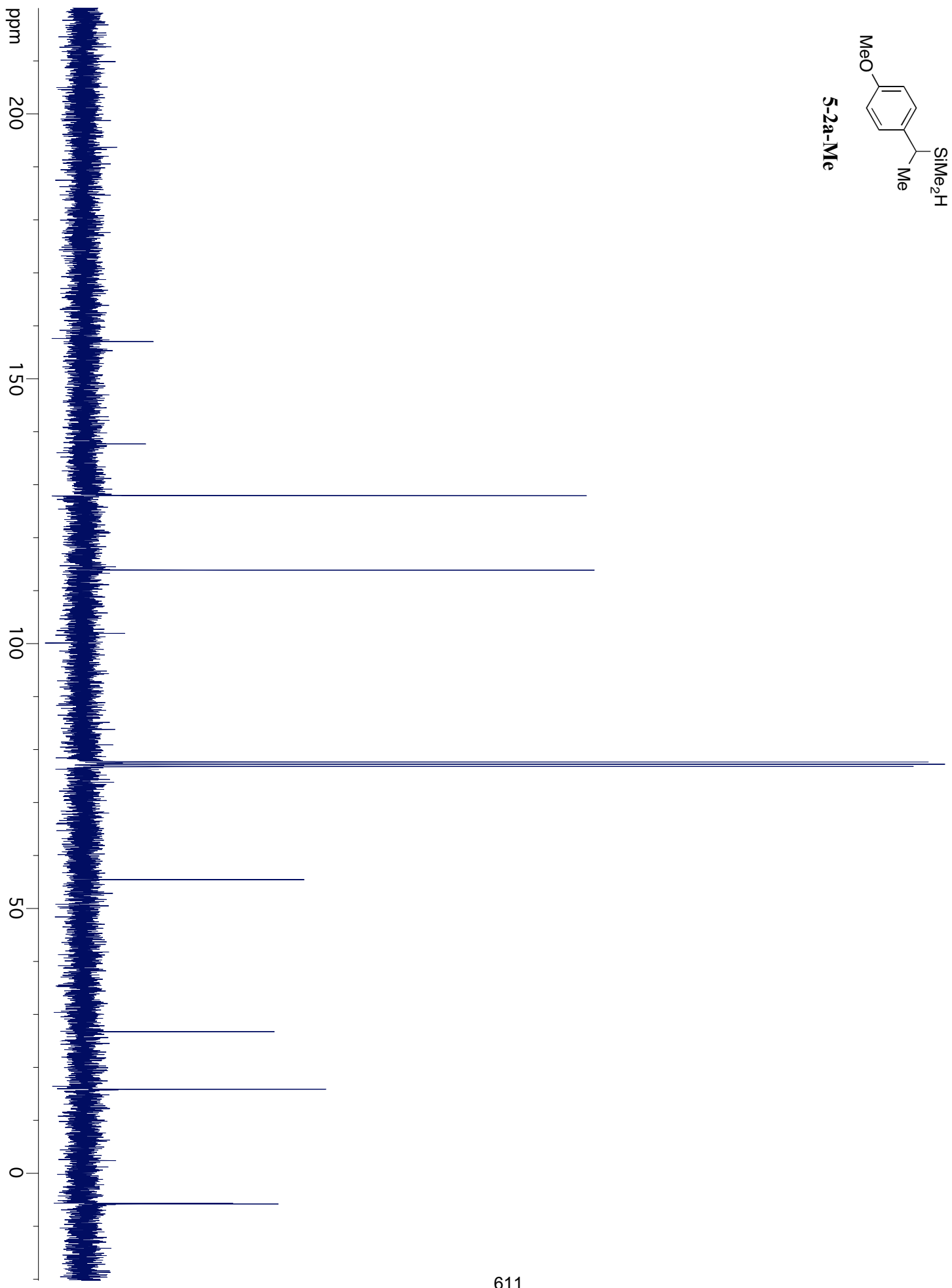
4-20

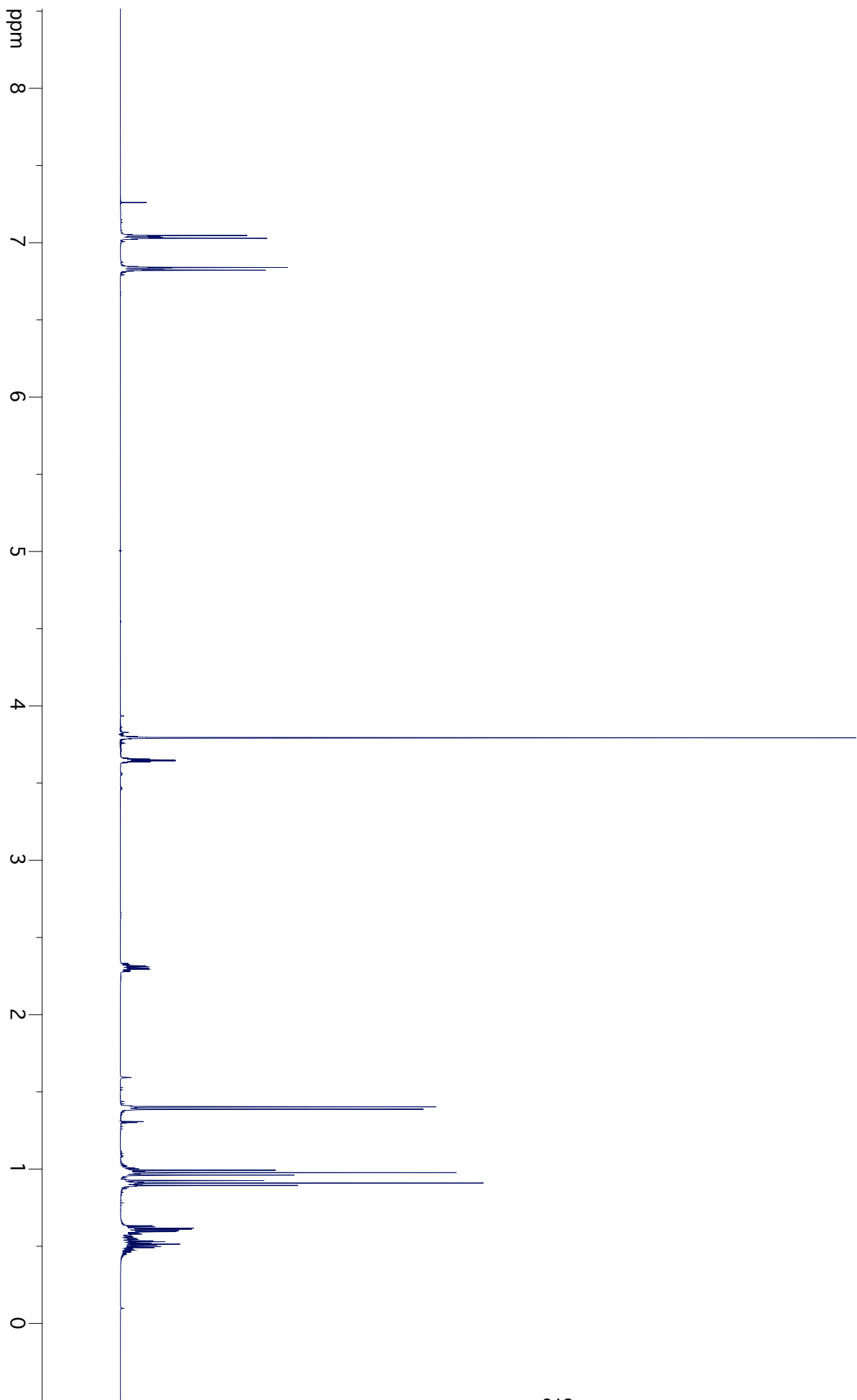
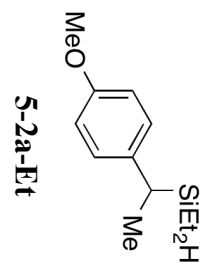


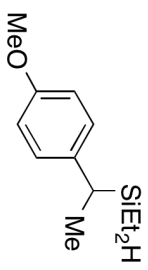




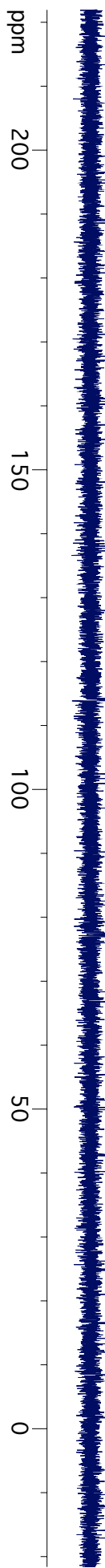
5-2a-Me

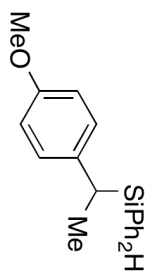




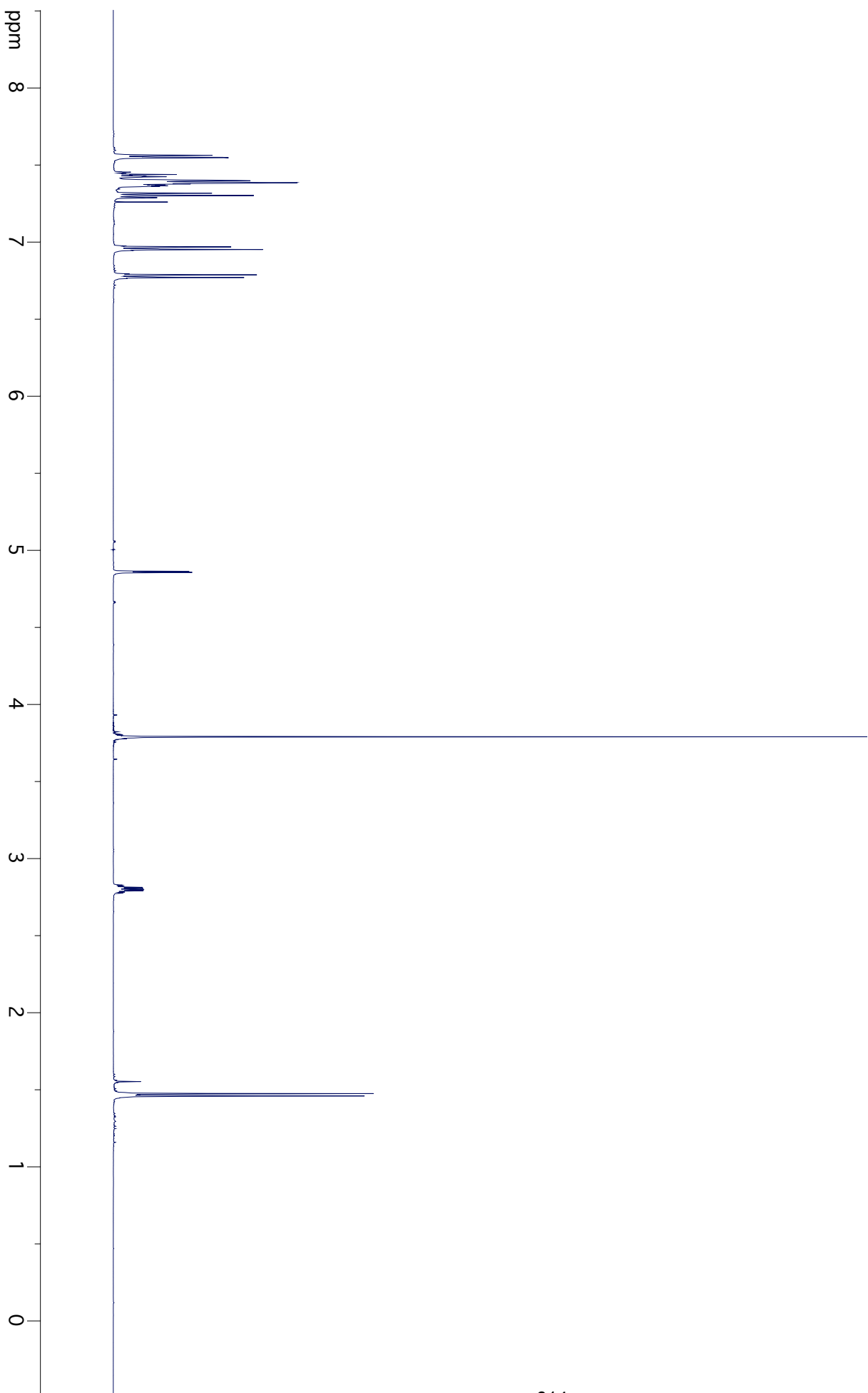


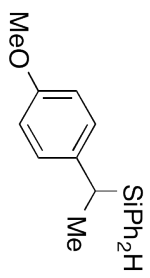
5-2a-Et



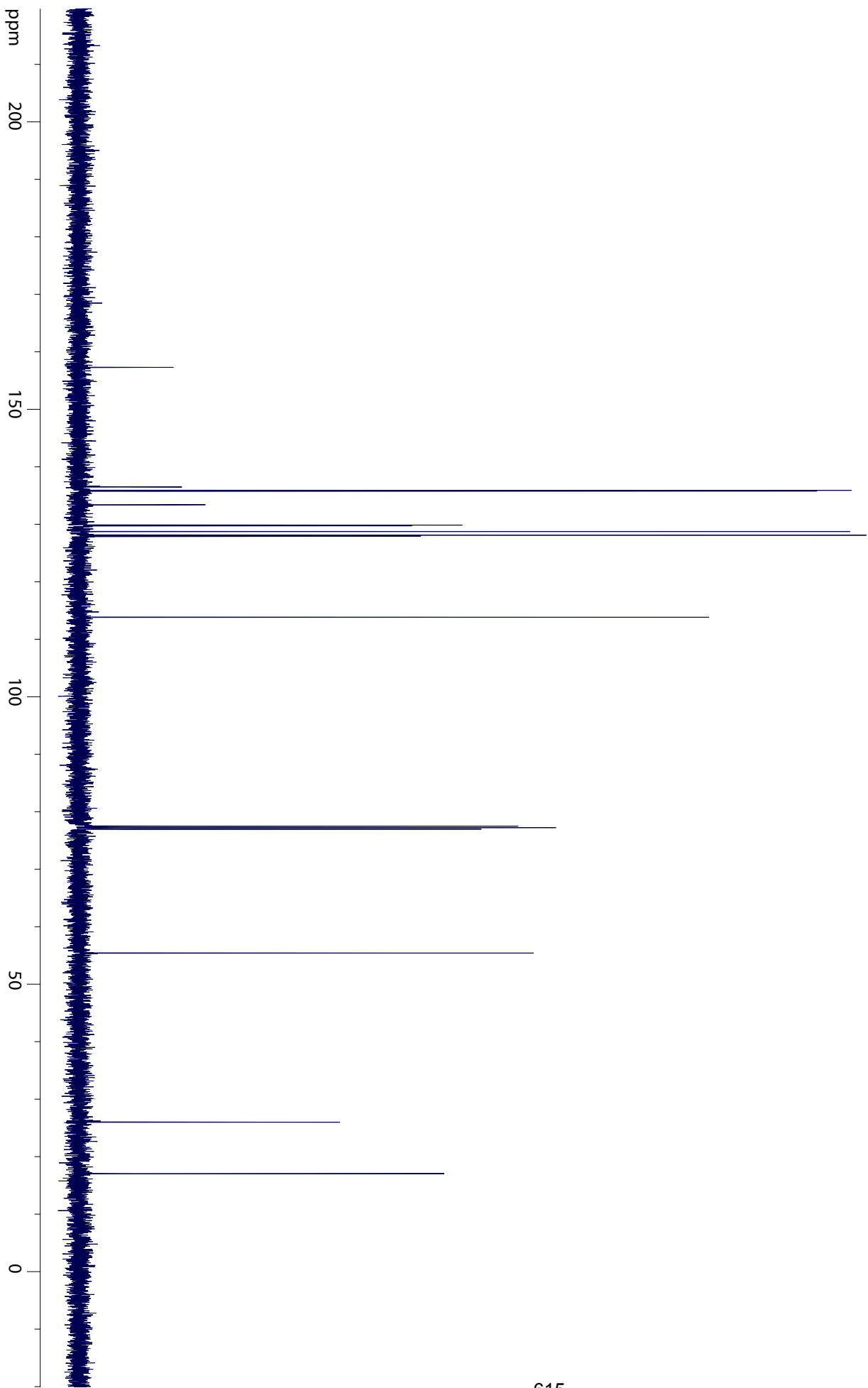


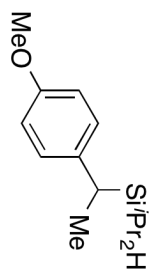
5-2a-Ph



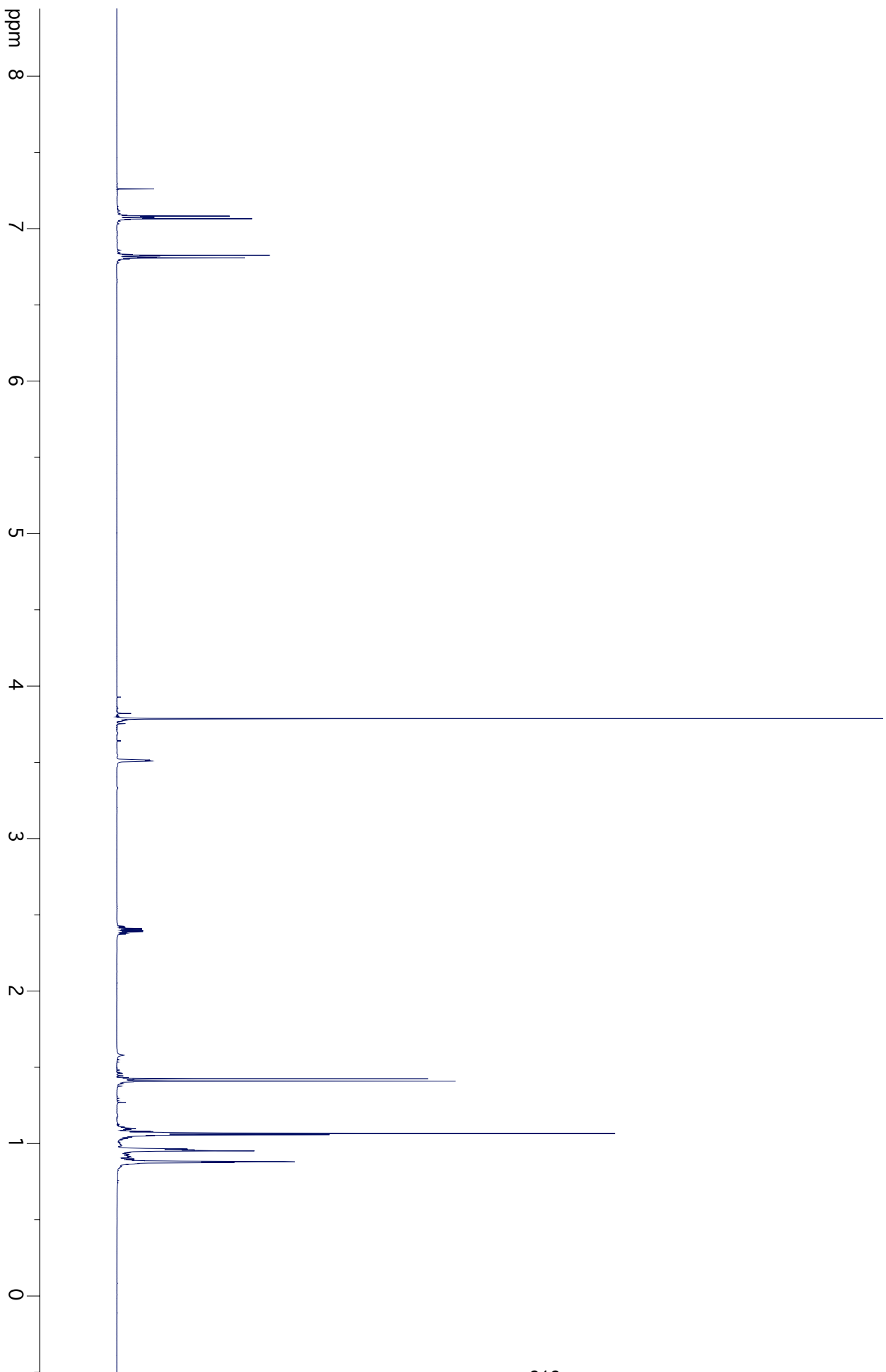


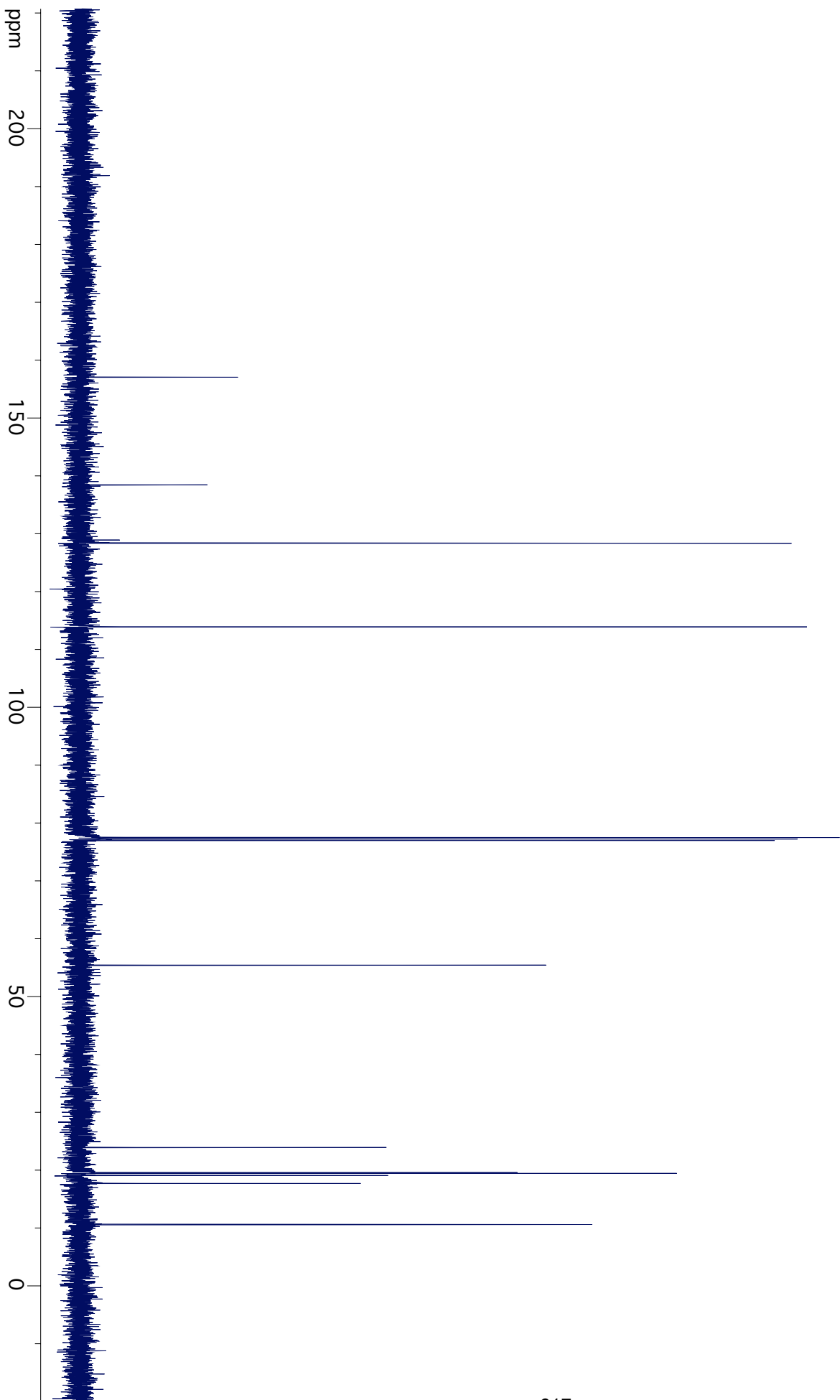
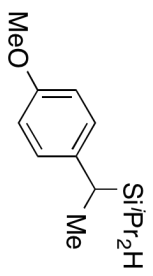
5-2a-Ph

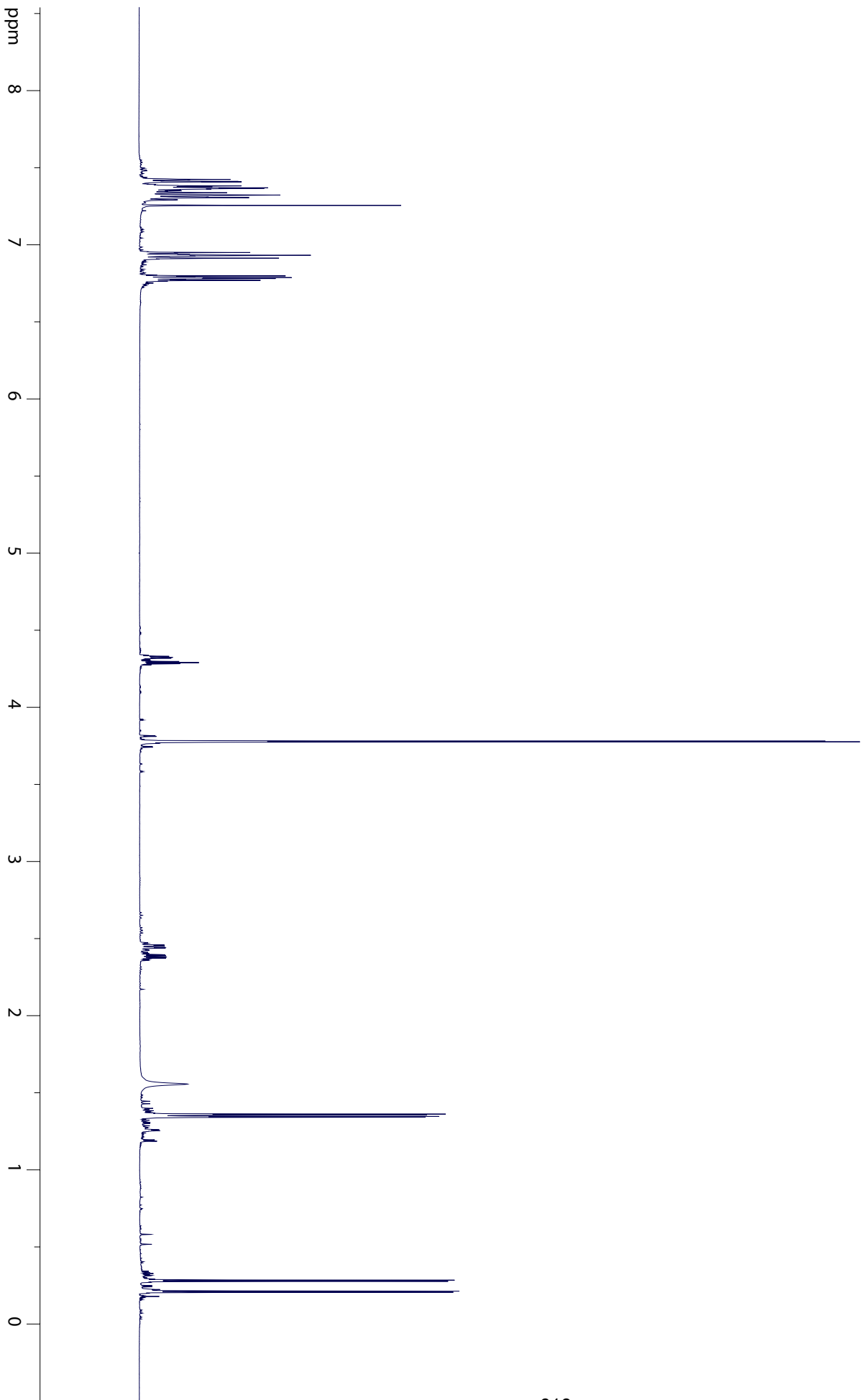
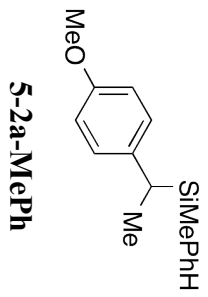


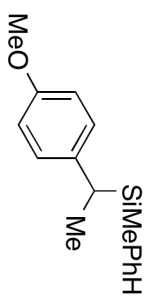


5-2a-*i*Pr





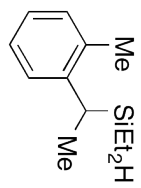




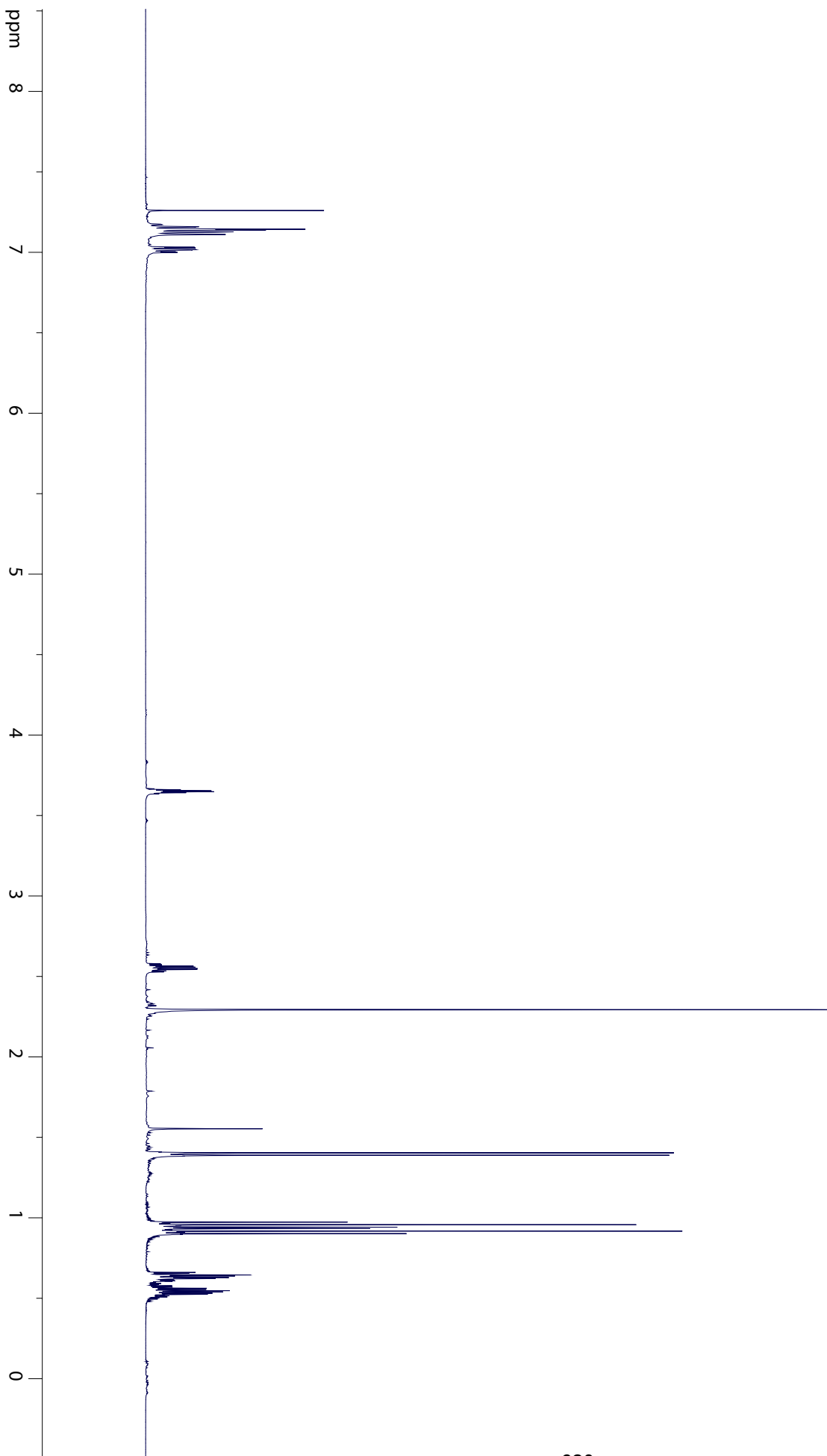
5-2a-MePh

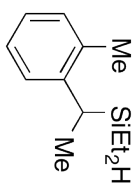
ppm



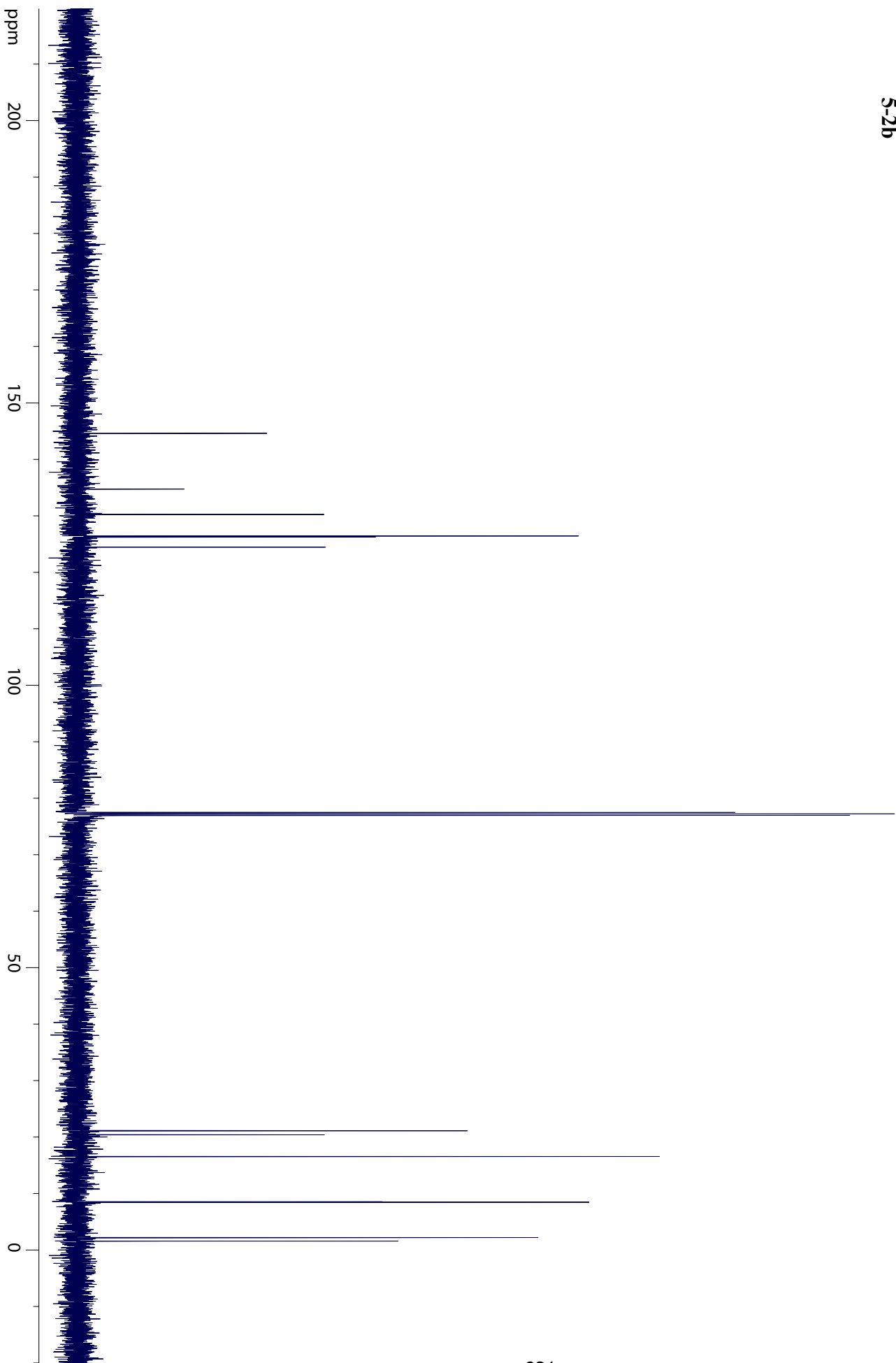


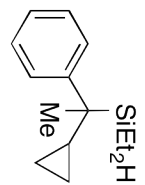
5-2b



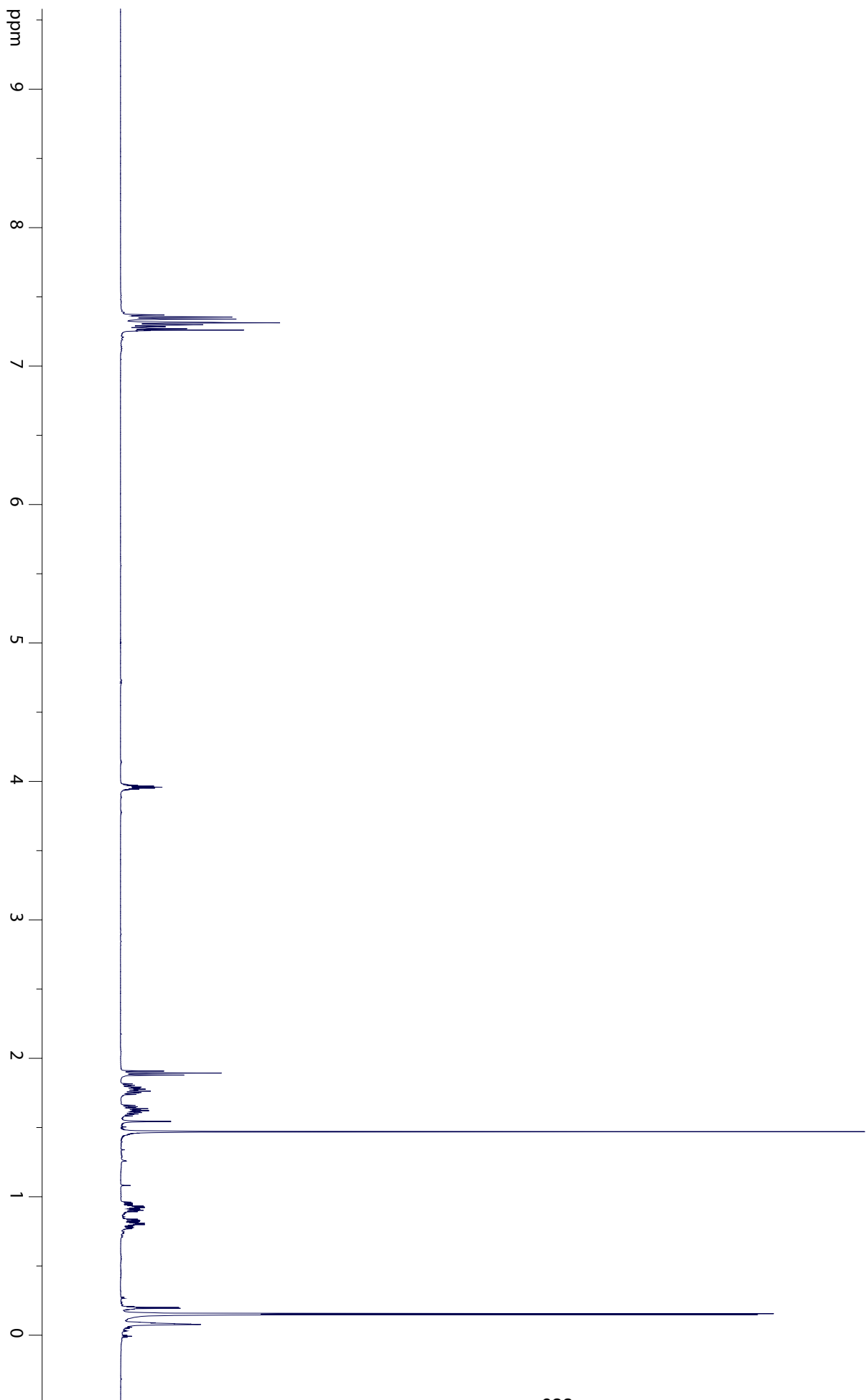


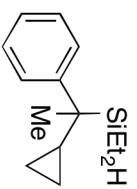
5-2b



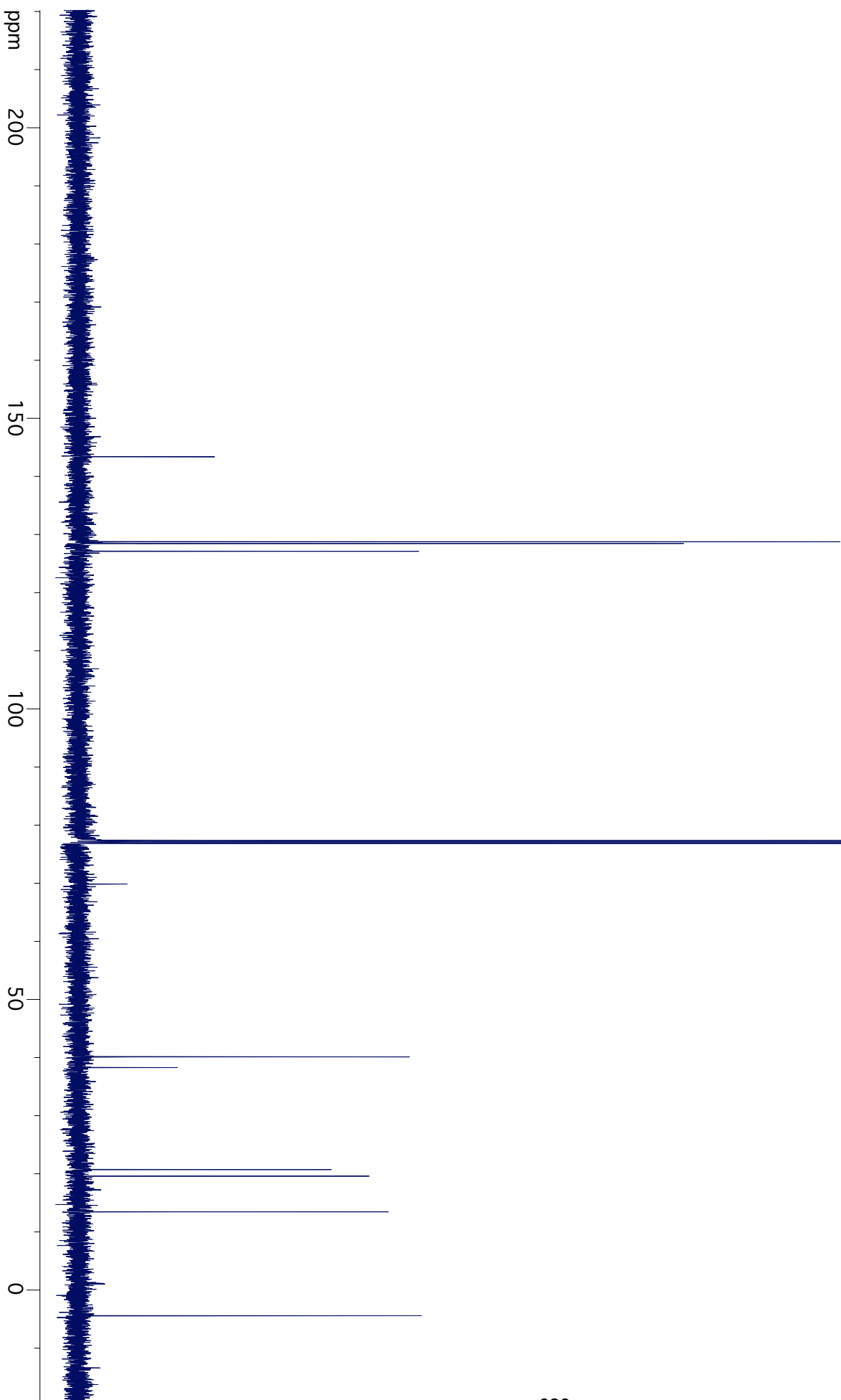


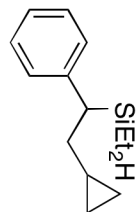
5-2-c- α -Me



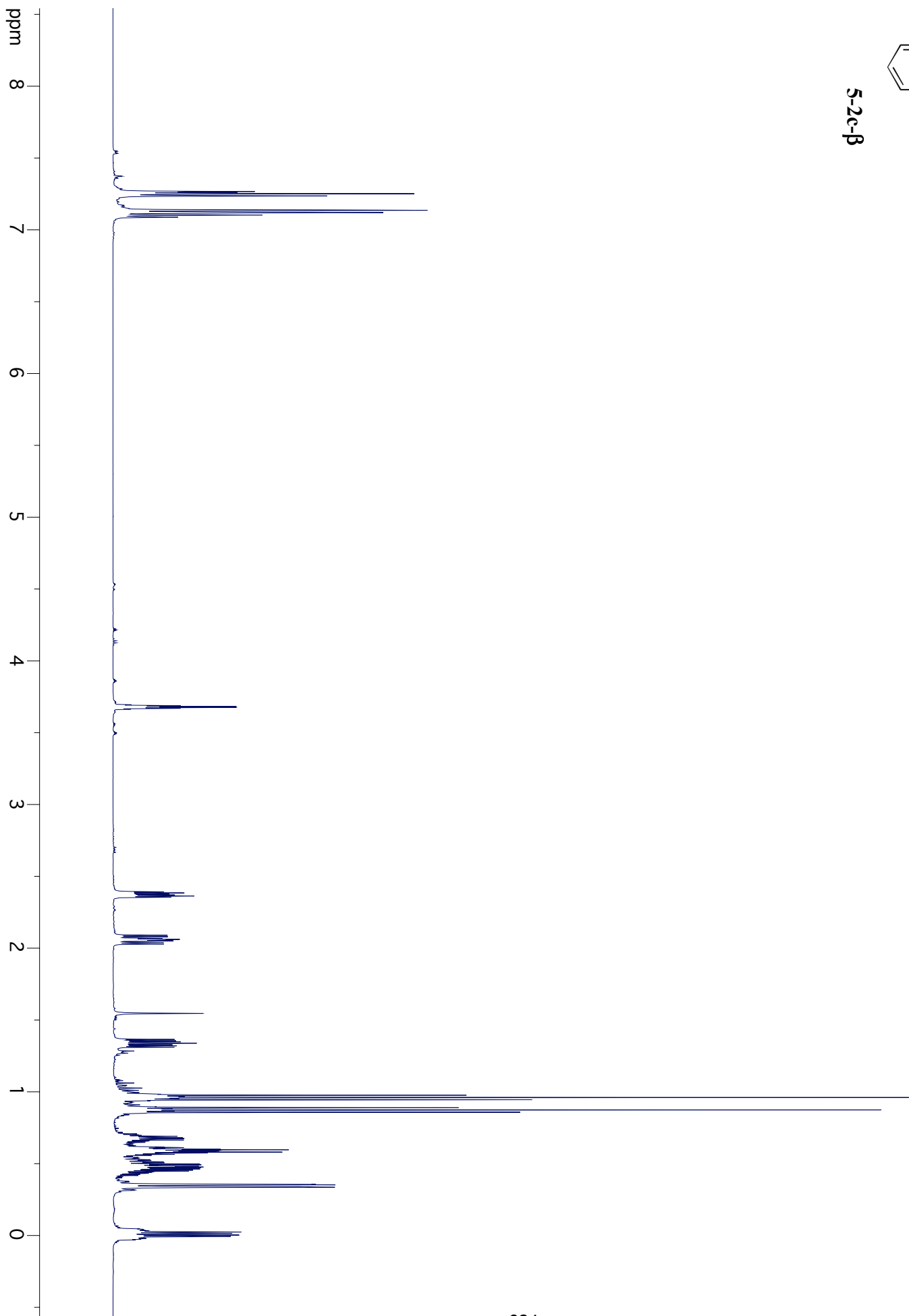


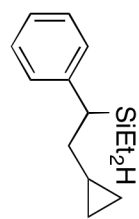
5-2c- α -Me



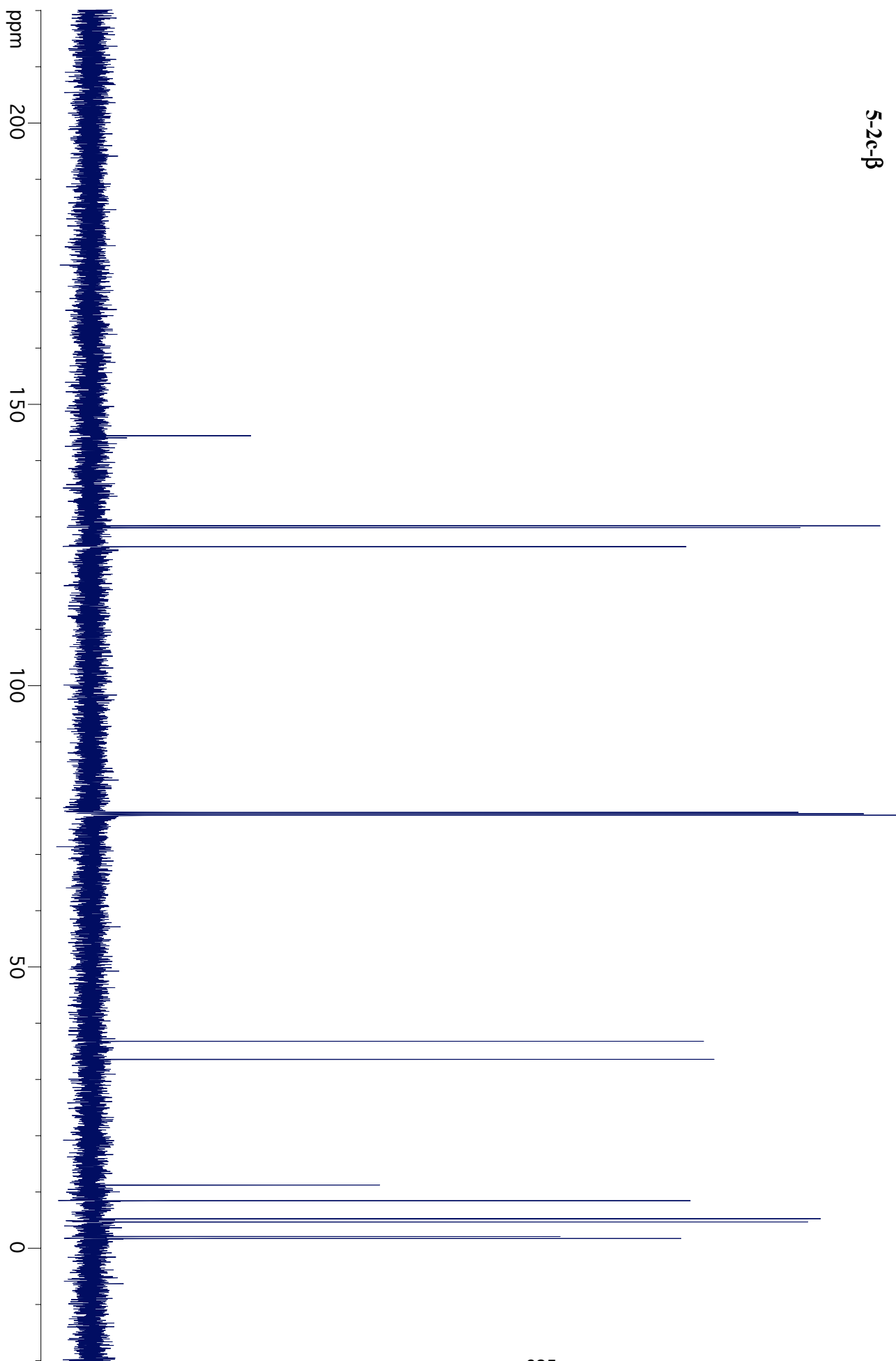


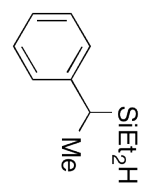
5-2c-β



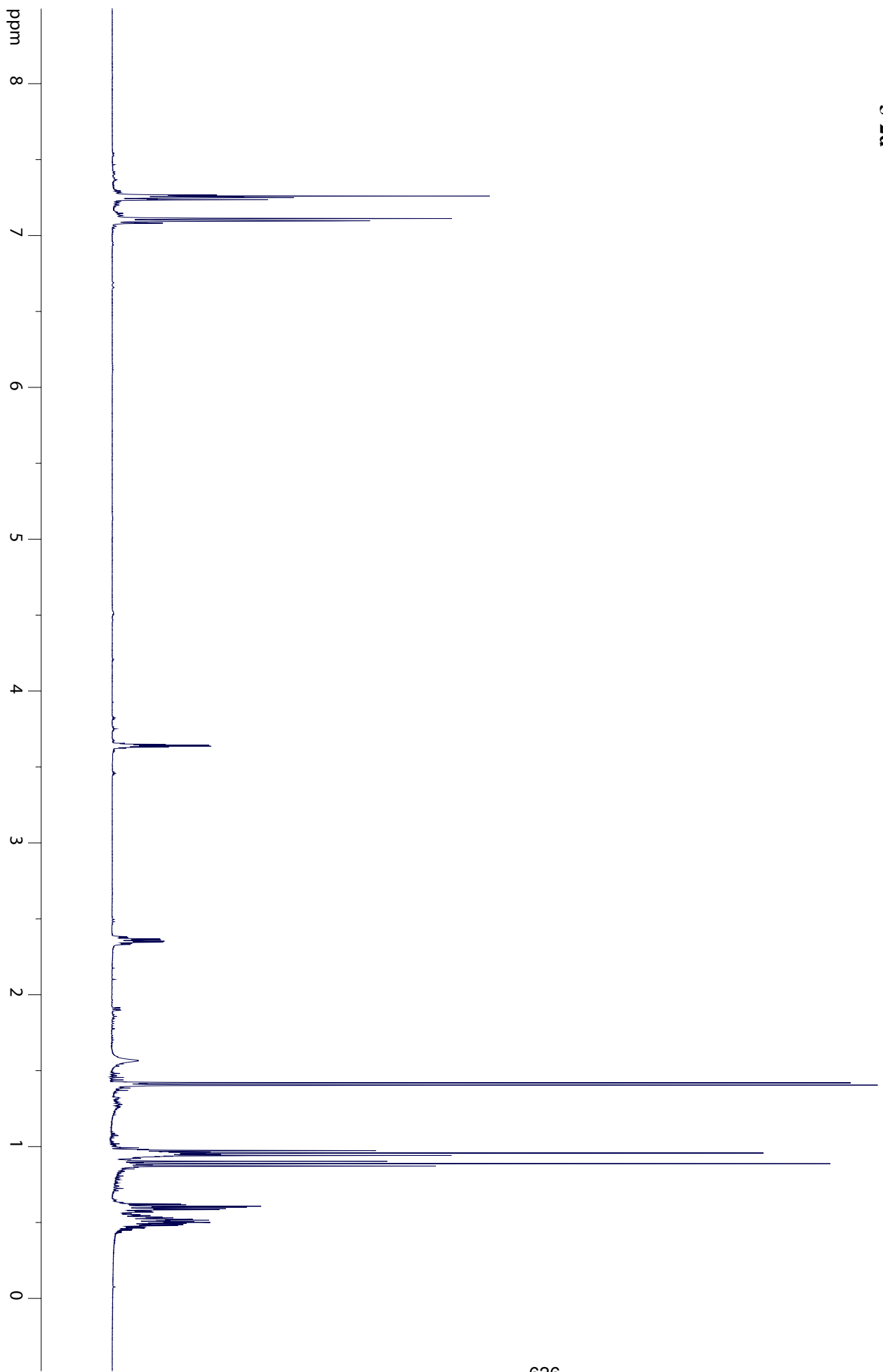


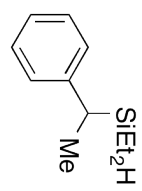
5-2c-β



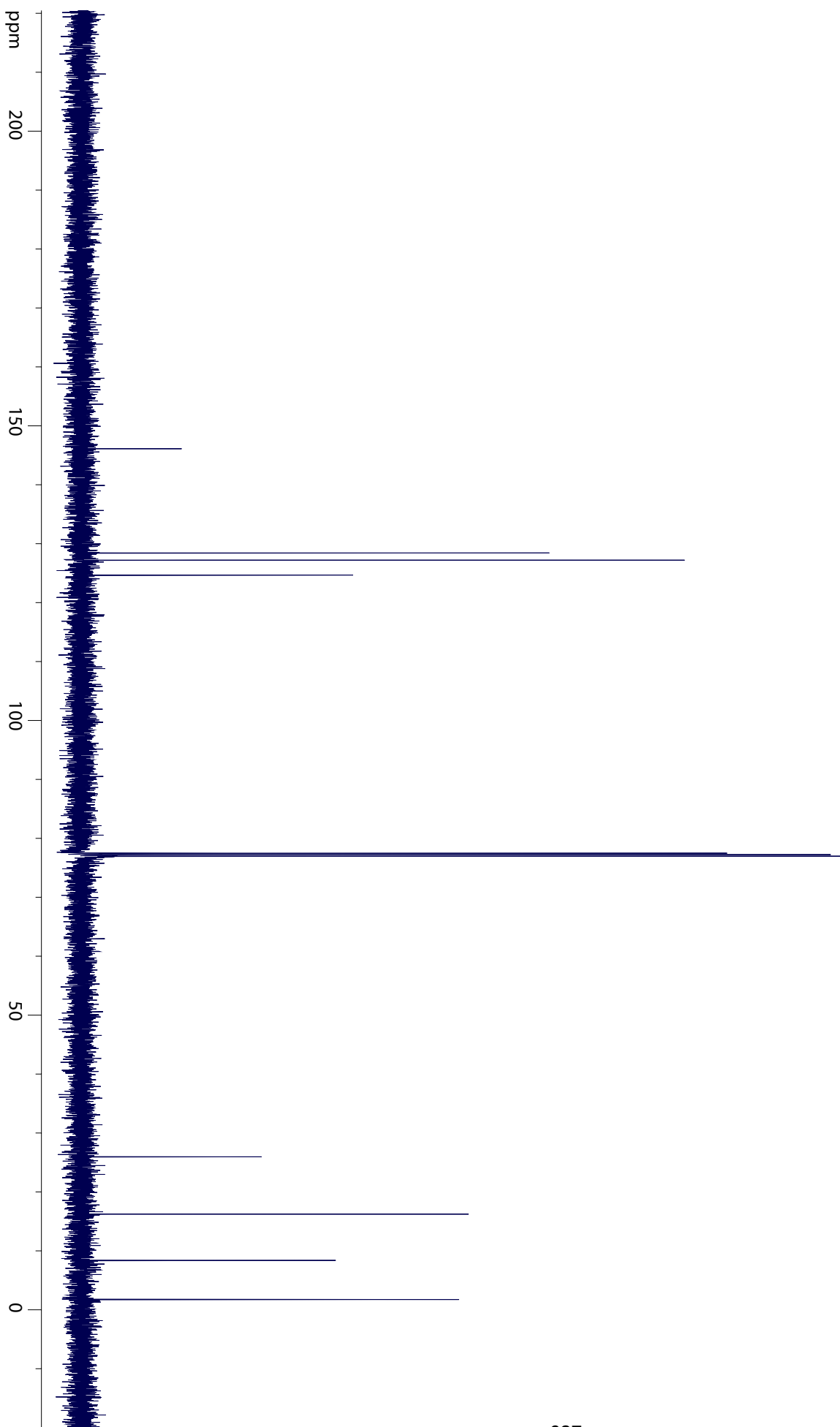


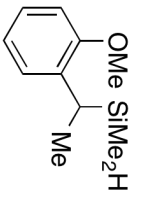
5-2d



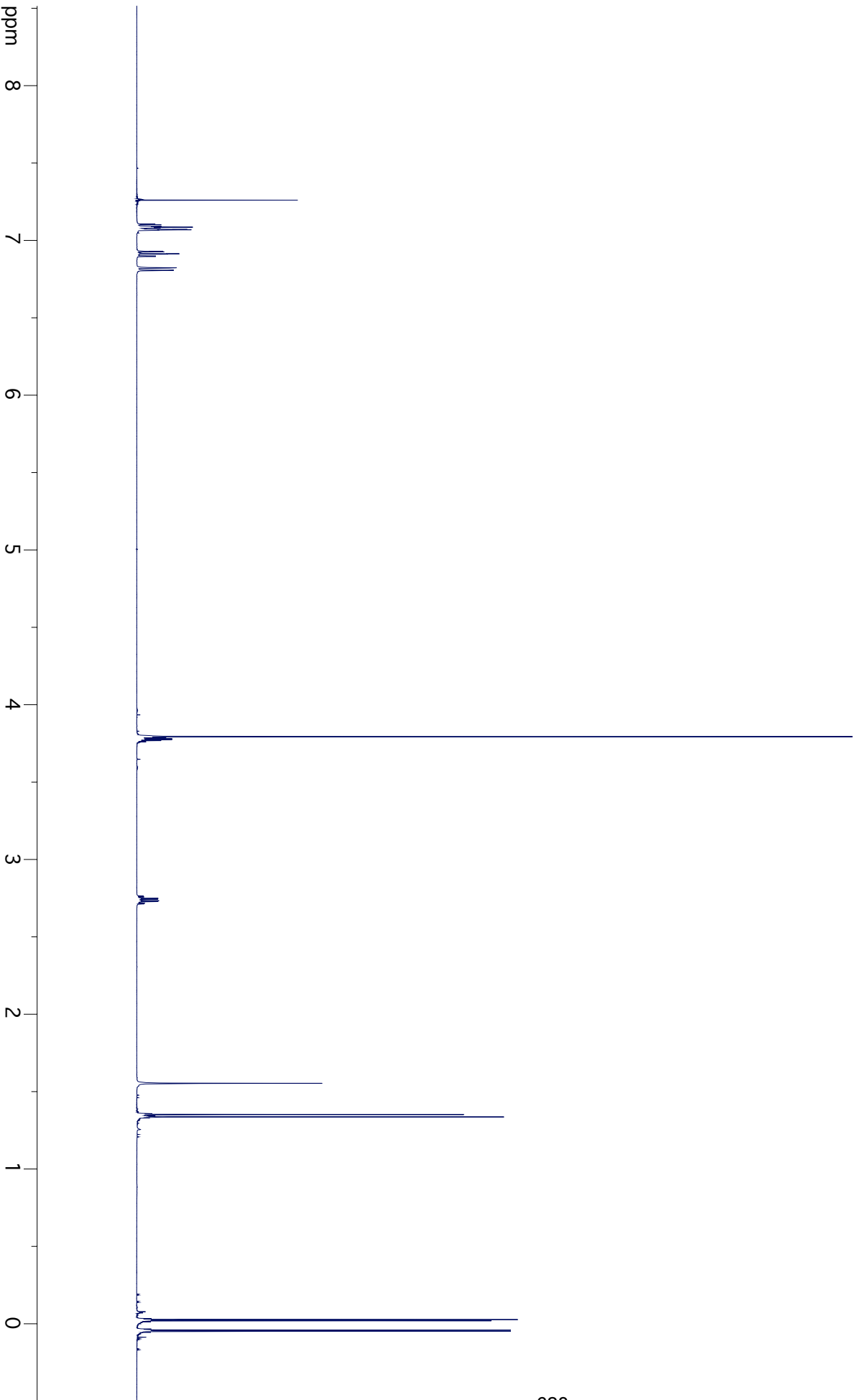


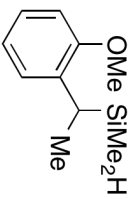
5-2d



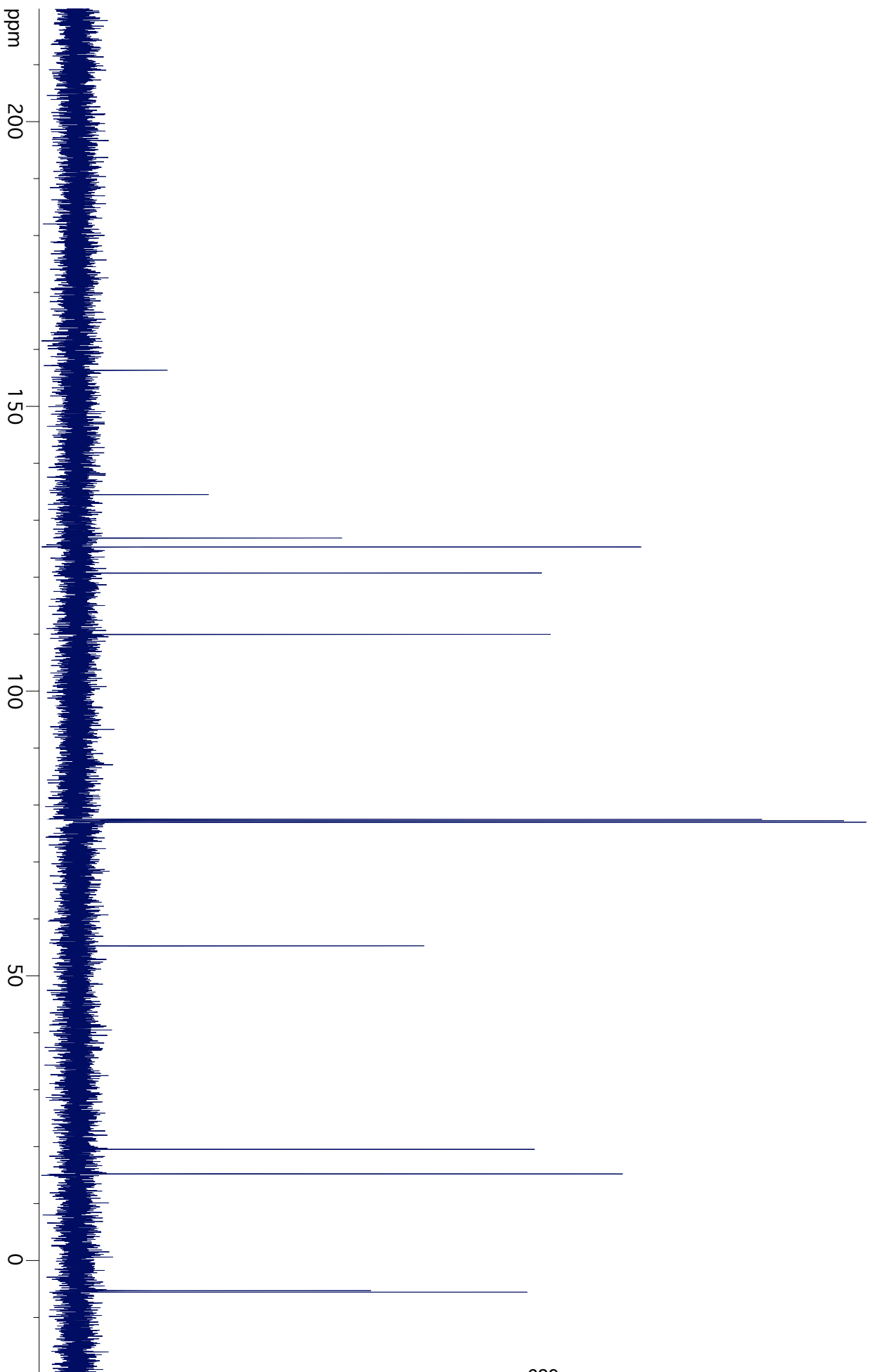


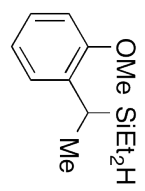
5-2e



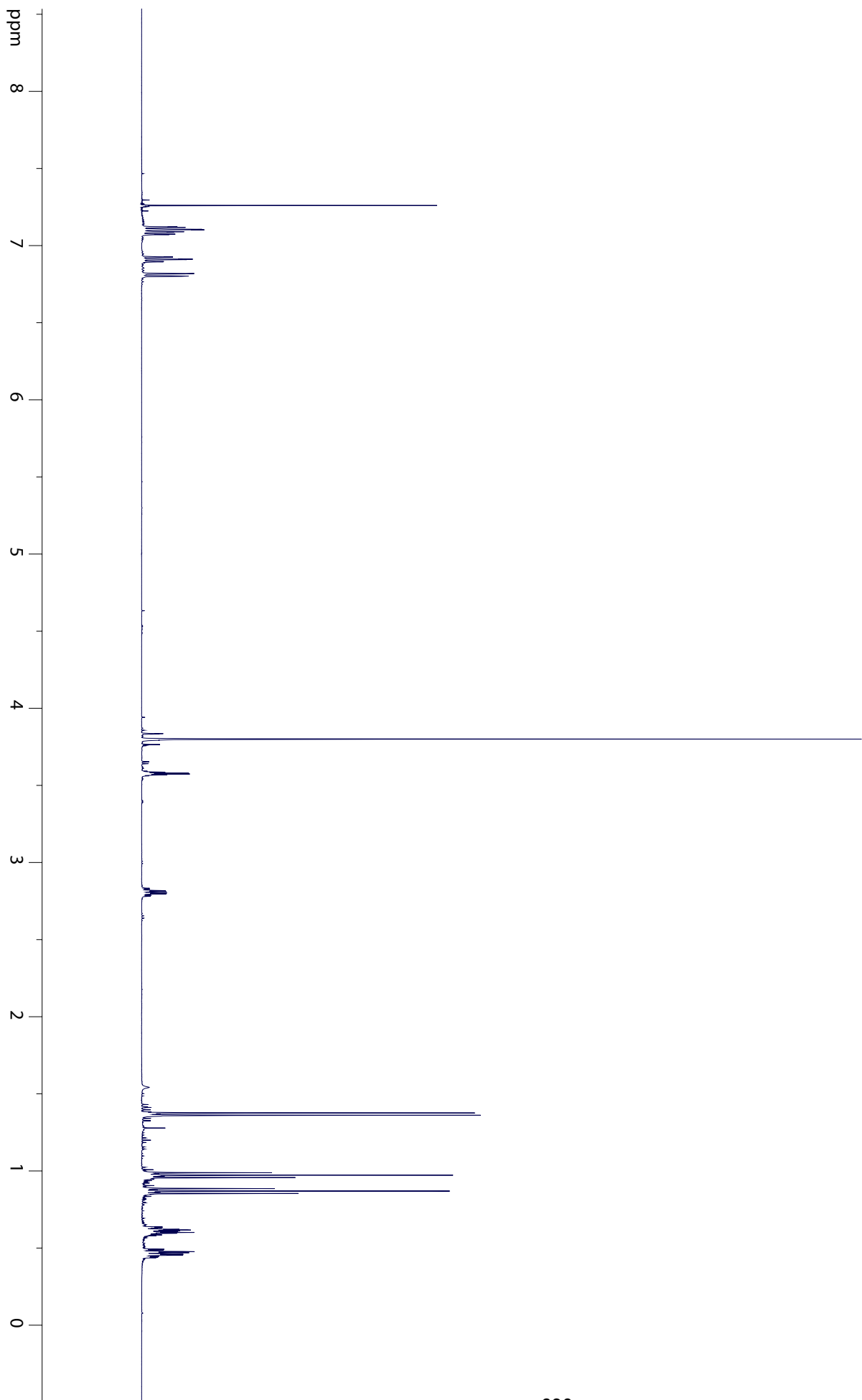


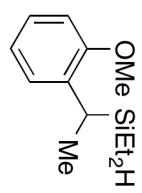
5-2e



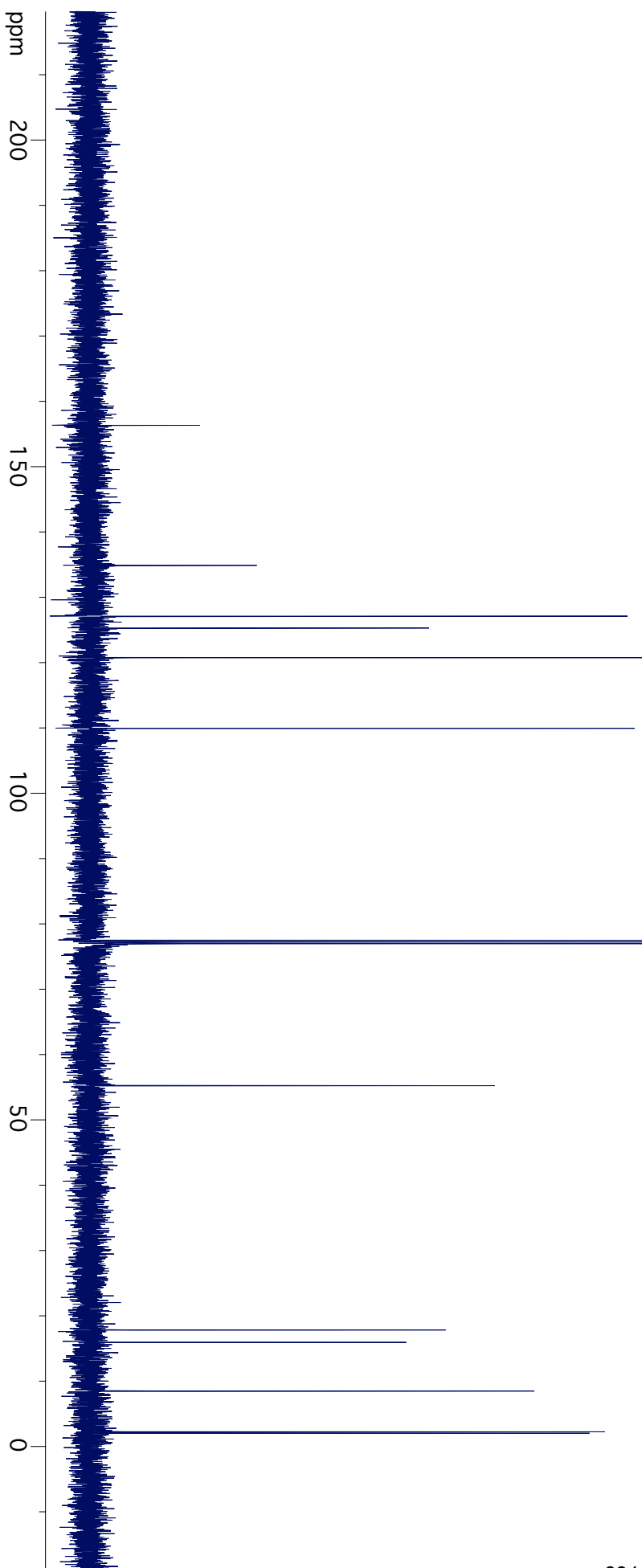


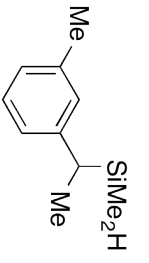
5-2f



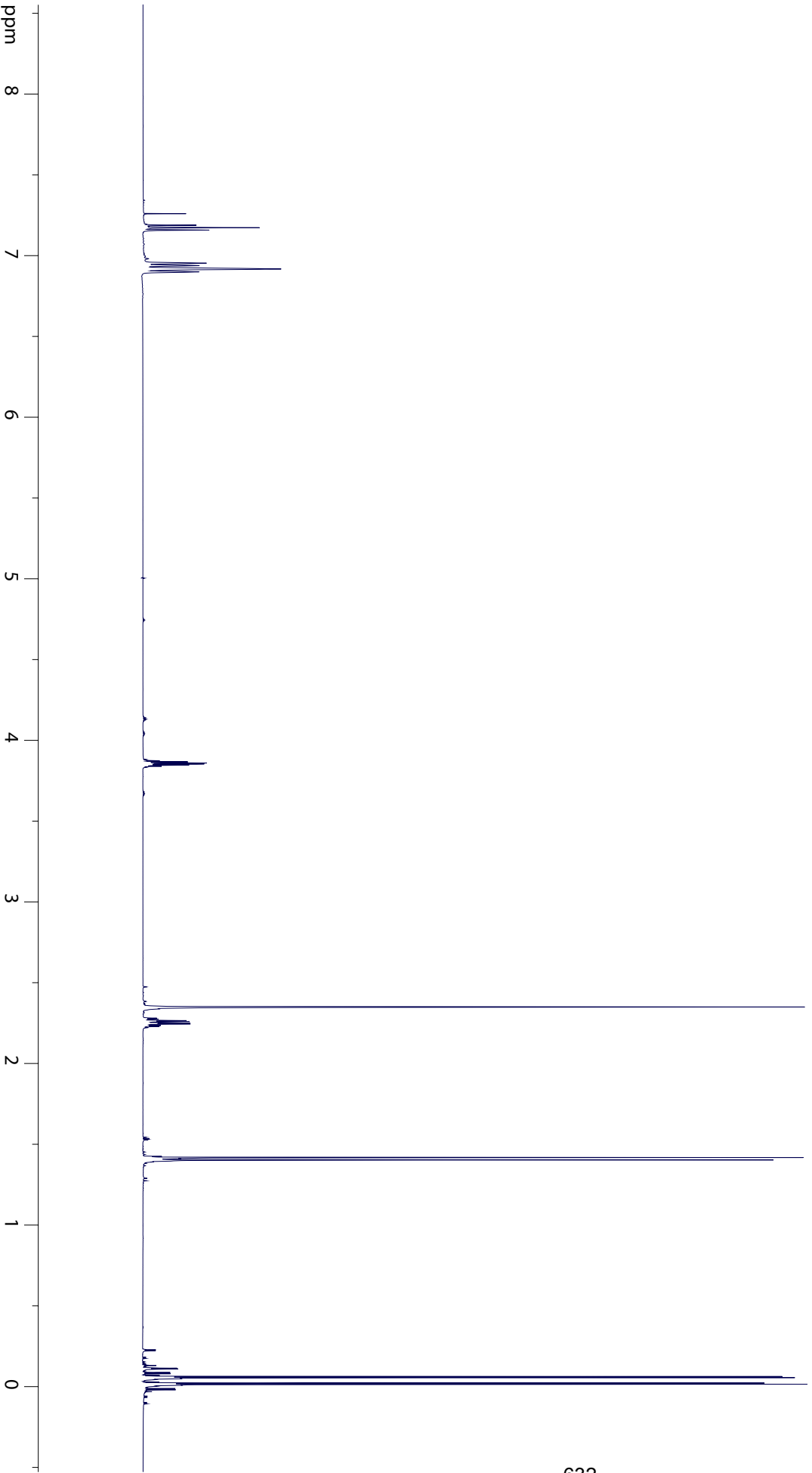


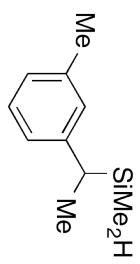
5-2f



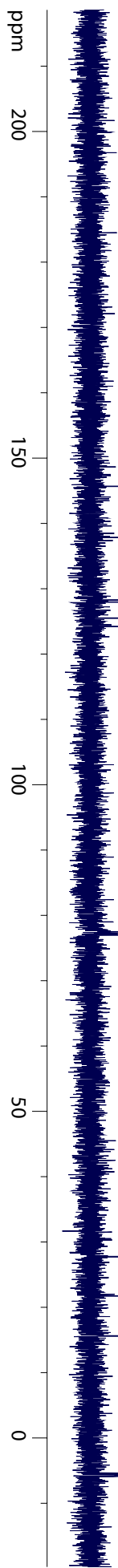


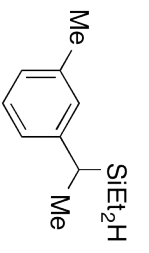
5-2g





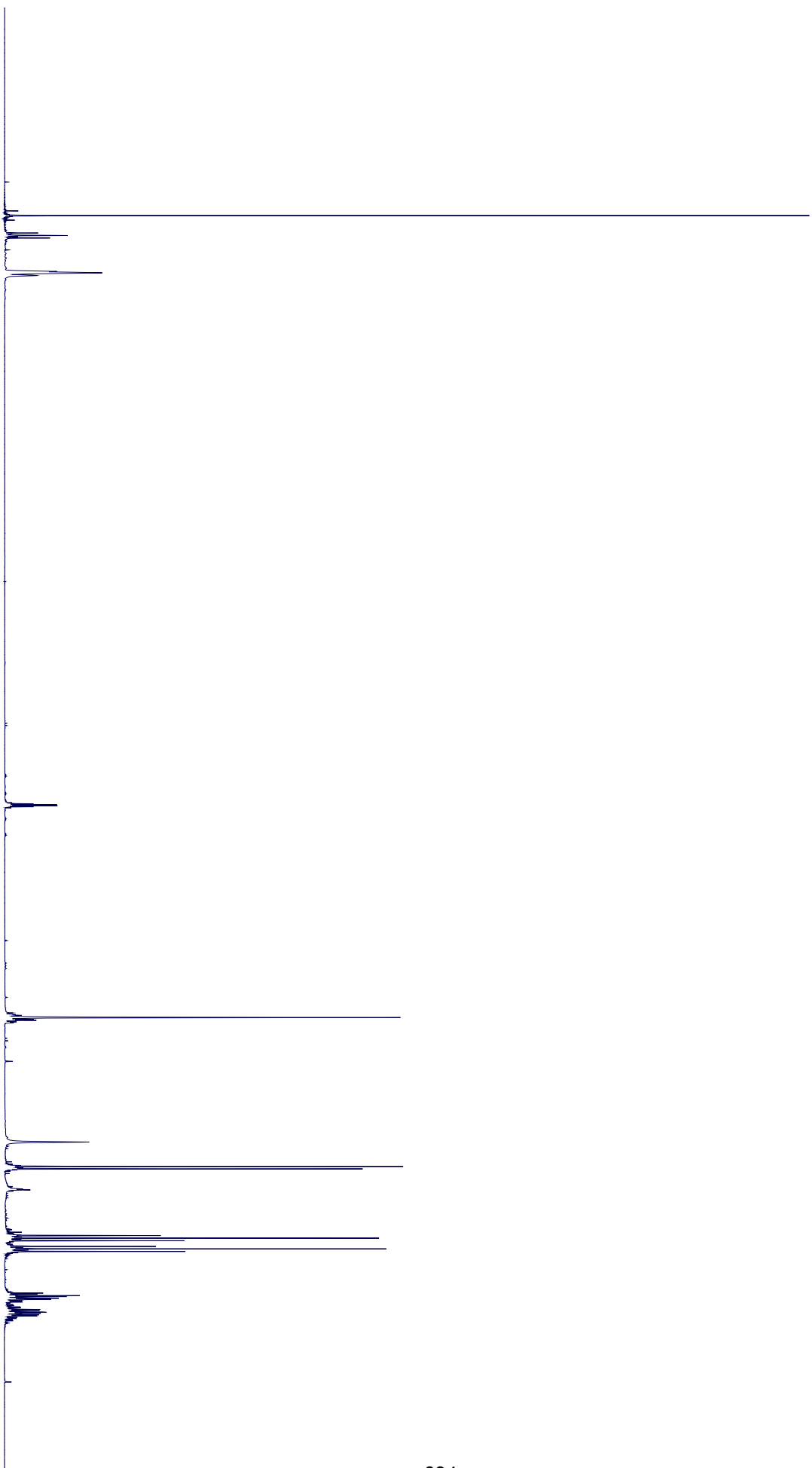
5-2g

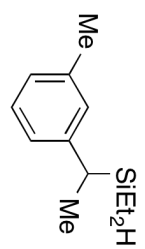




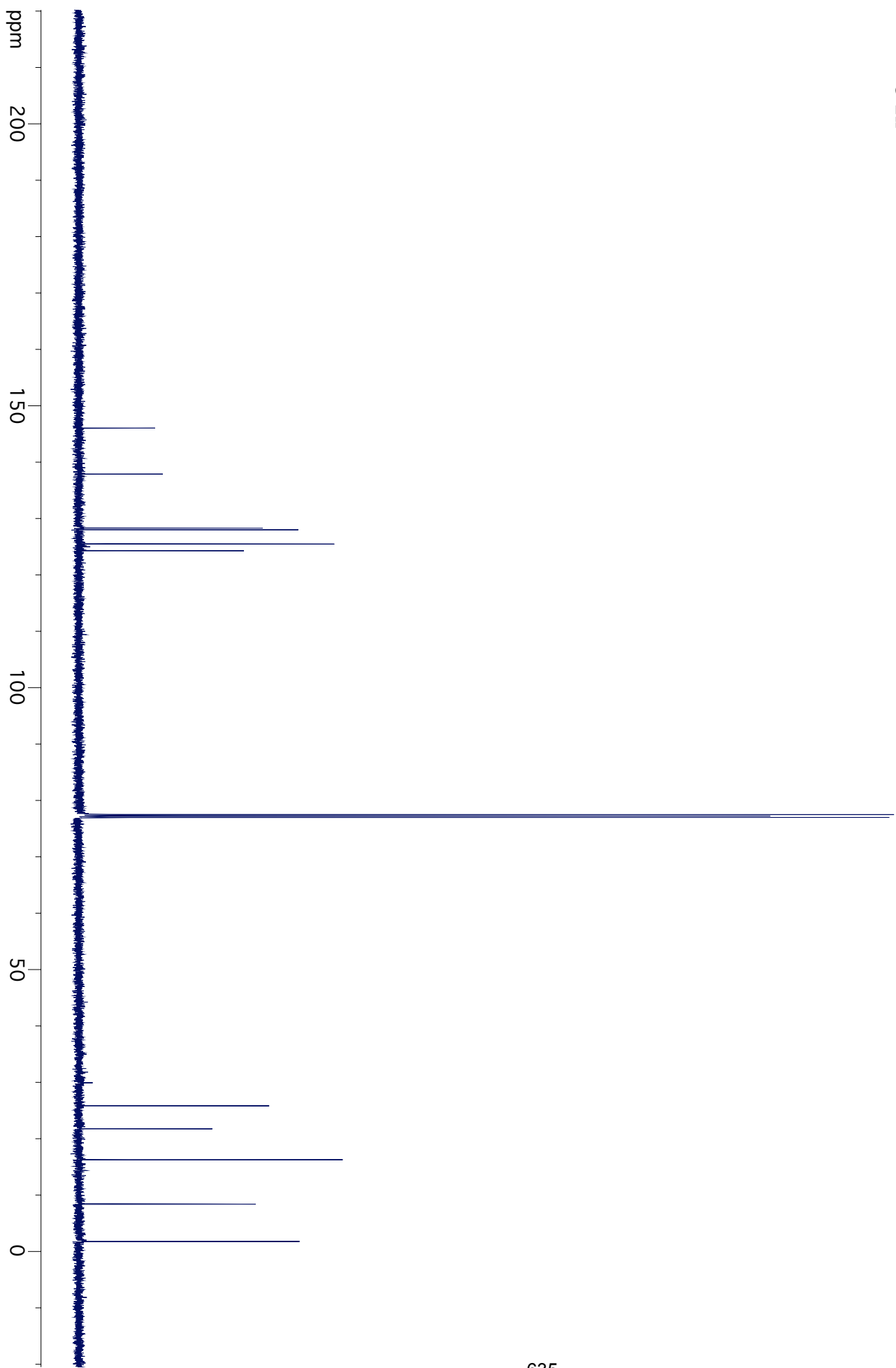
5-2h

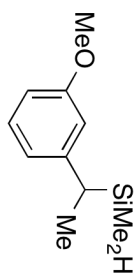
ppm 8 7 6 5 4 3 2 1 0



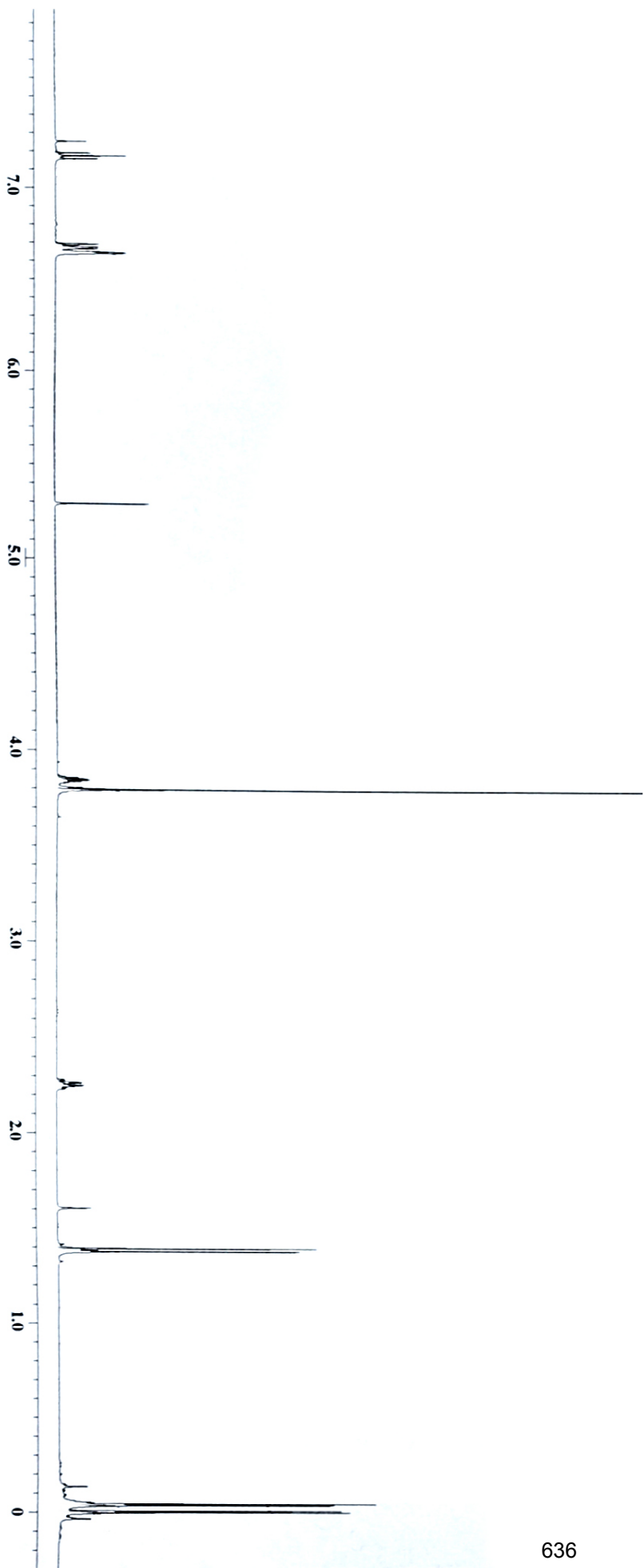


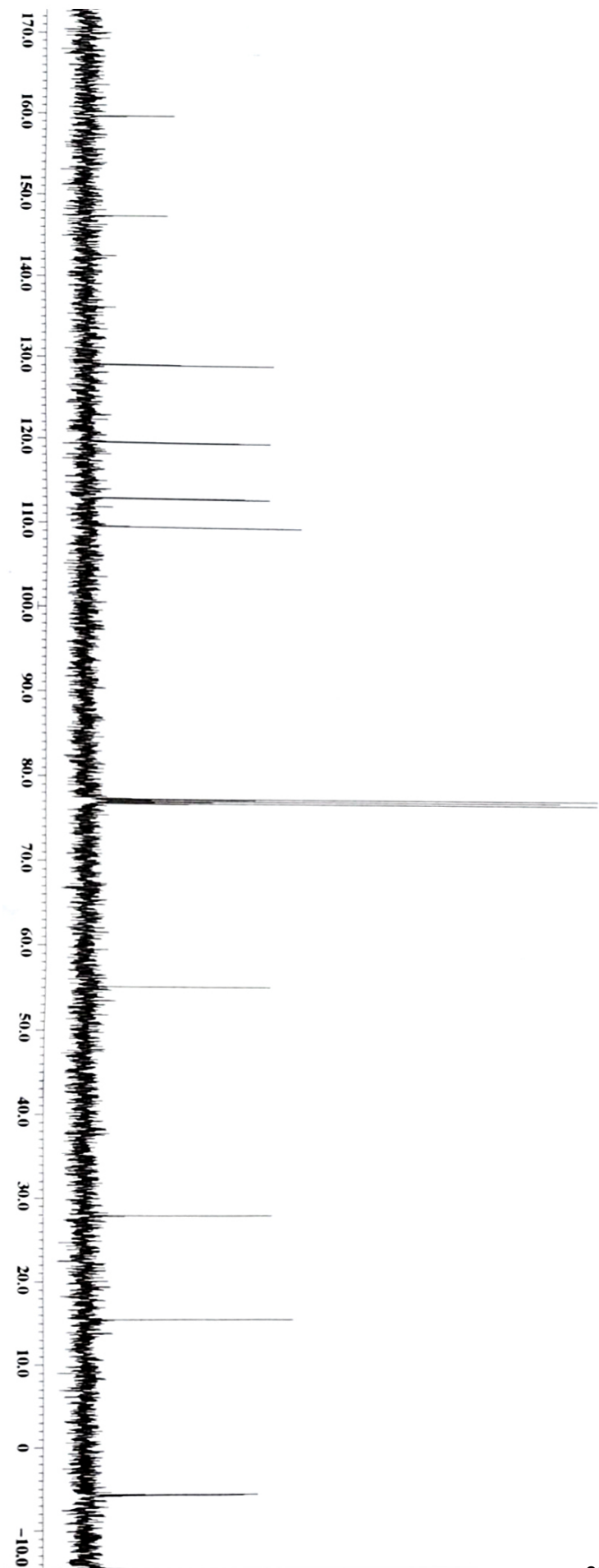
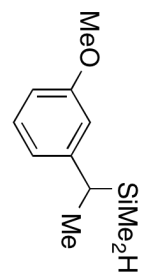
S-2h

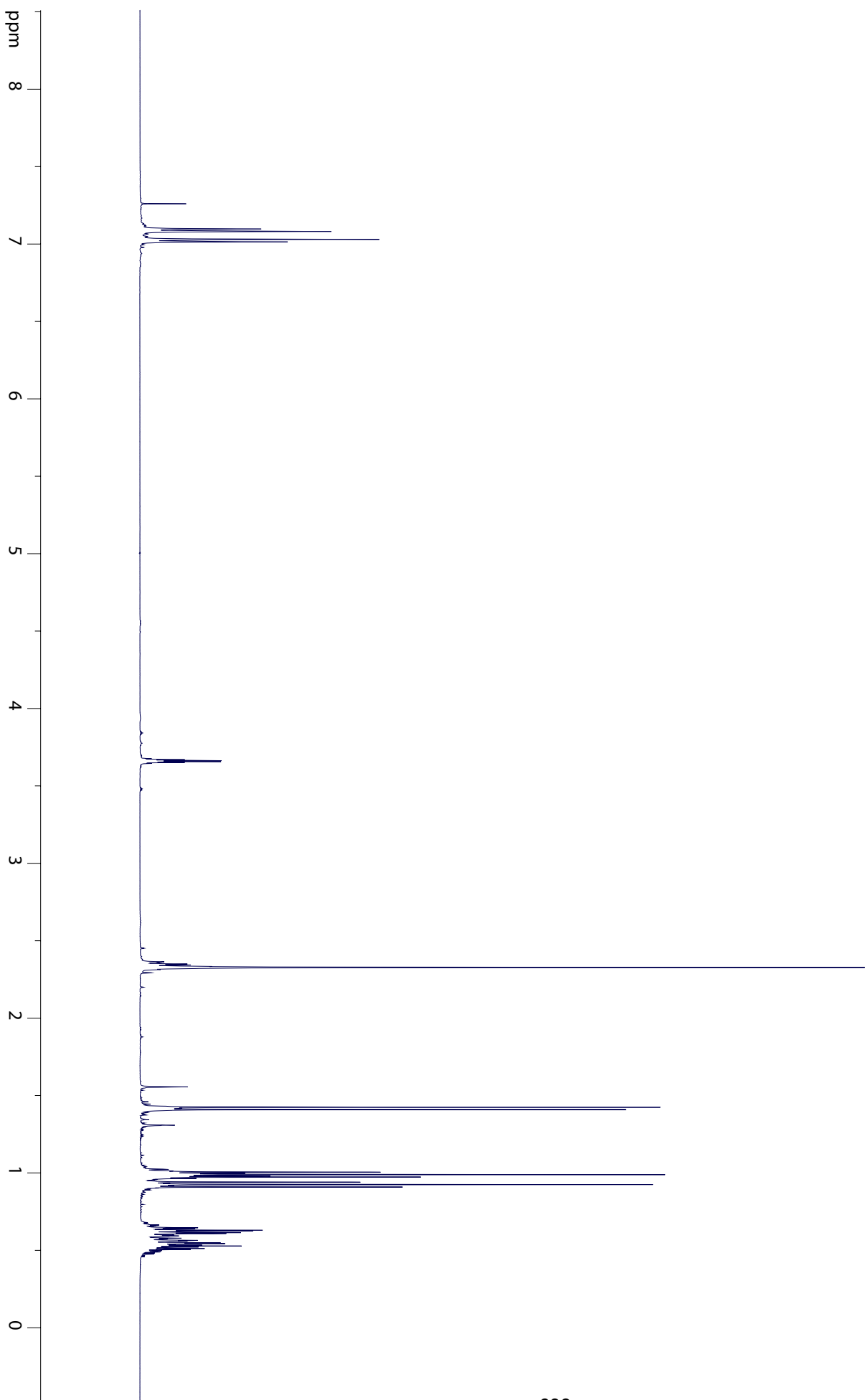
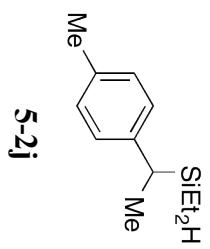


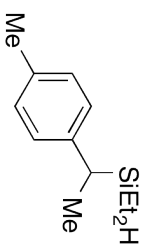


5-2i

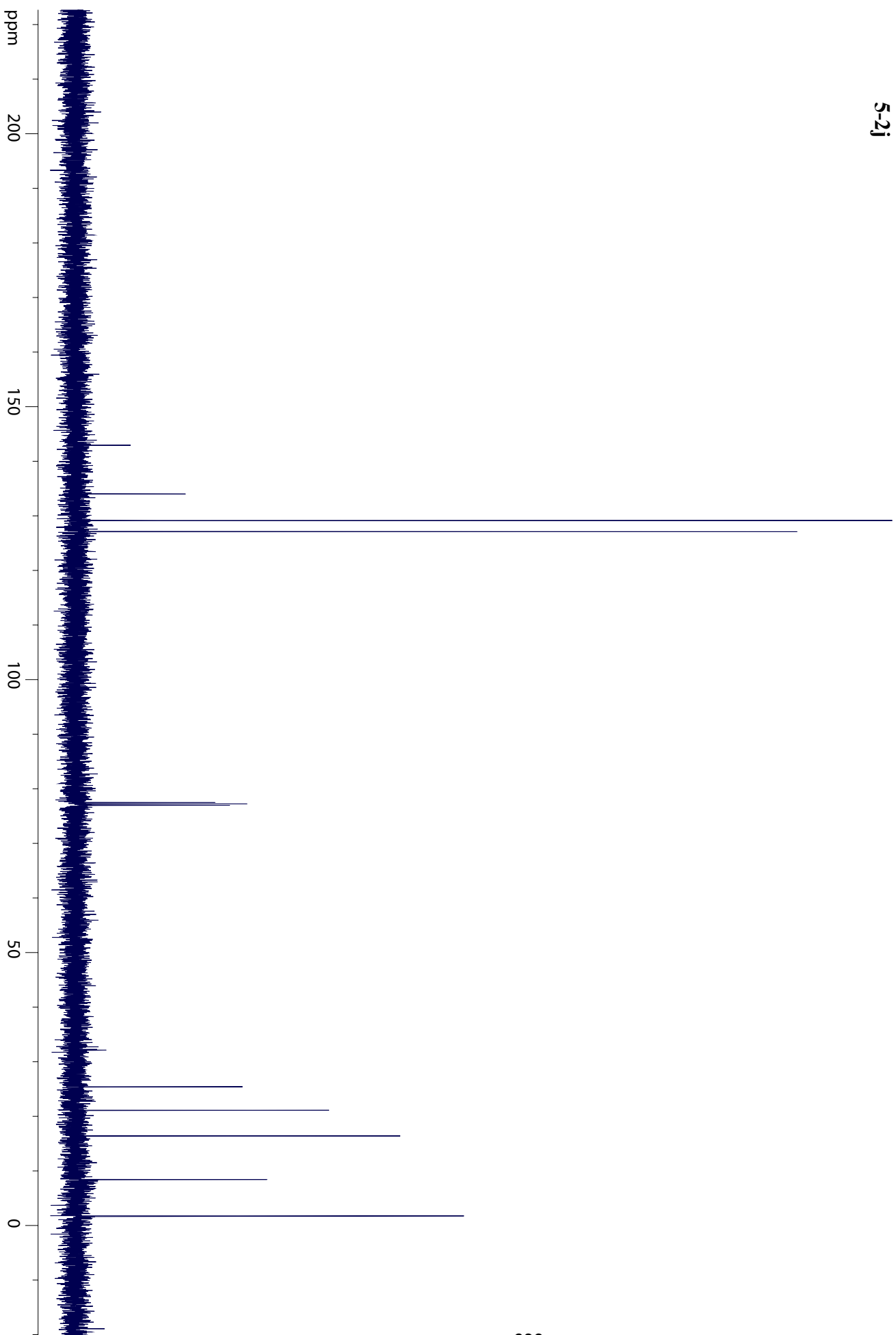


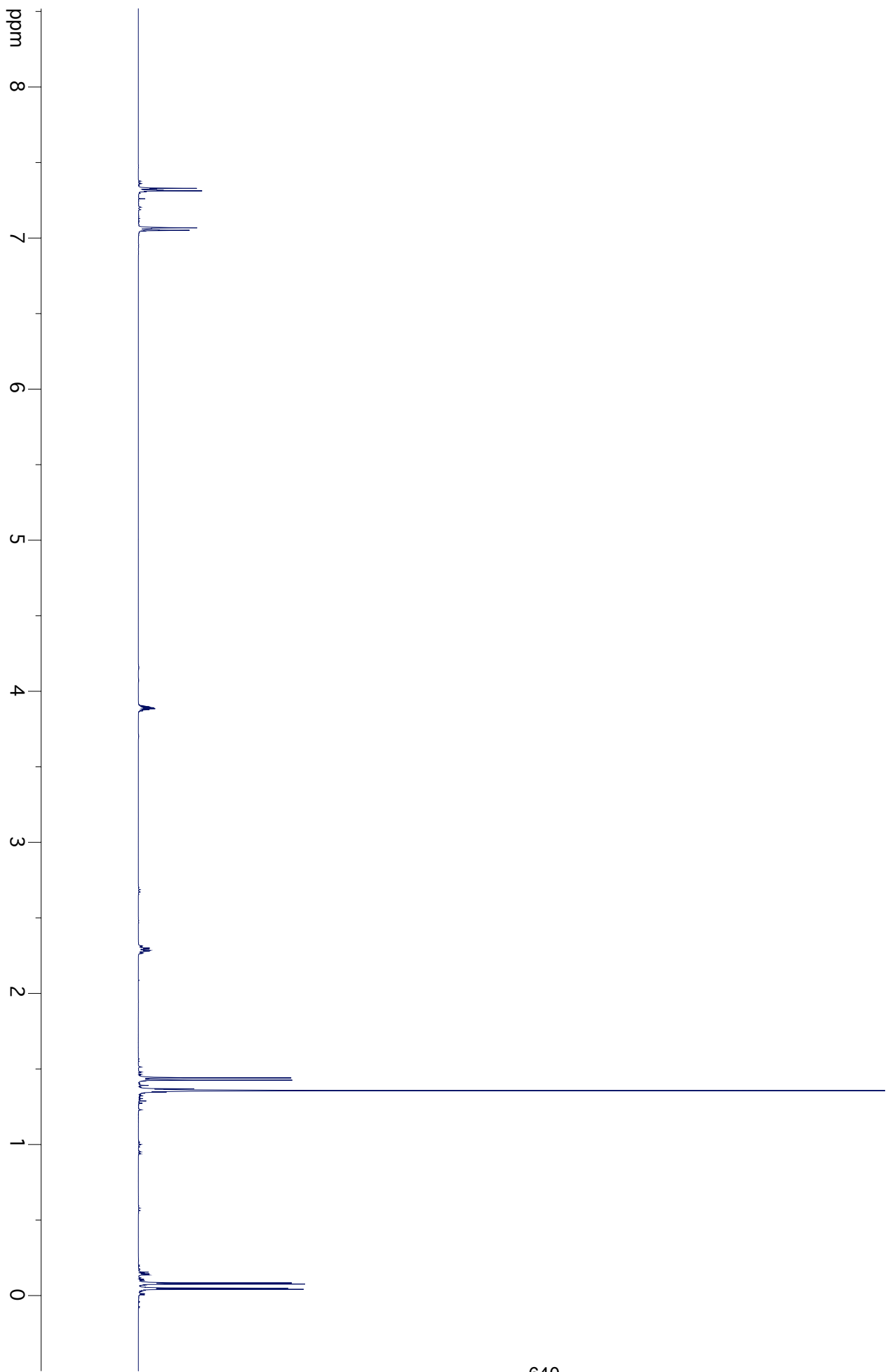
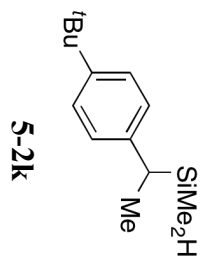


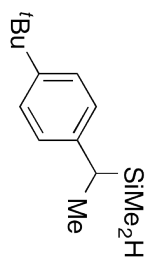




5-2j







5-21k

ppm

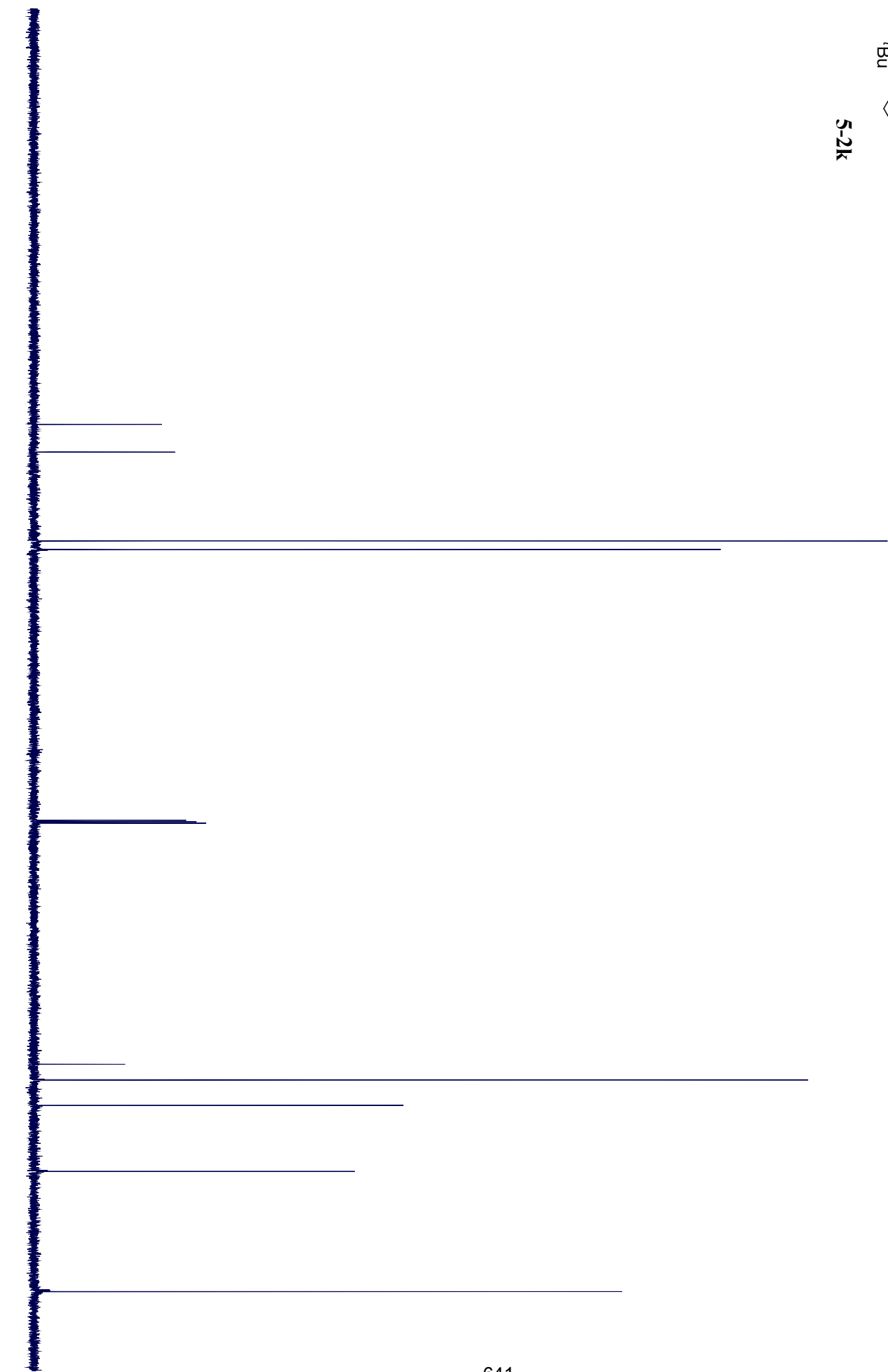
200

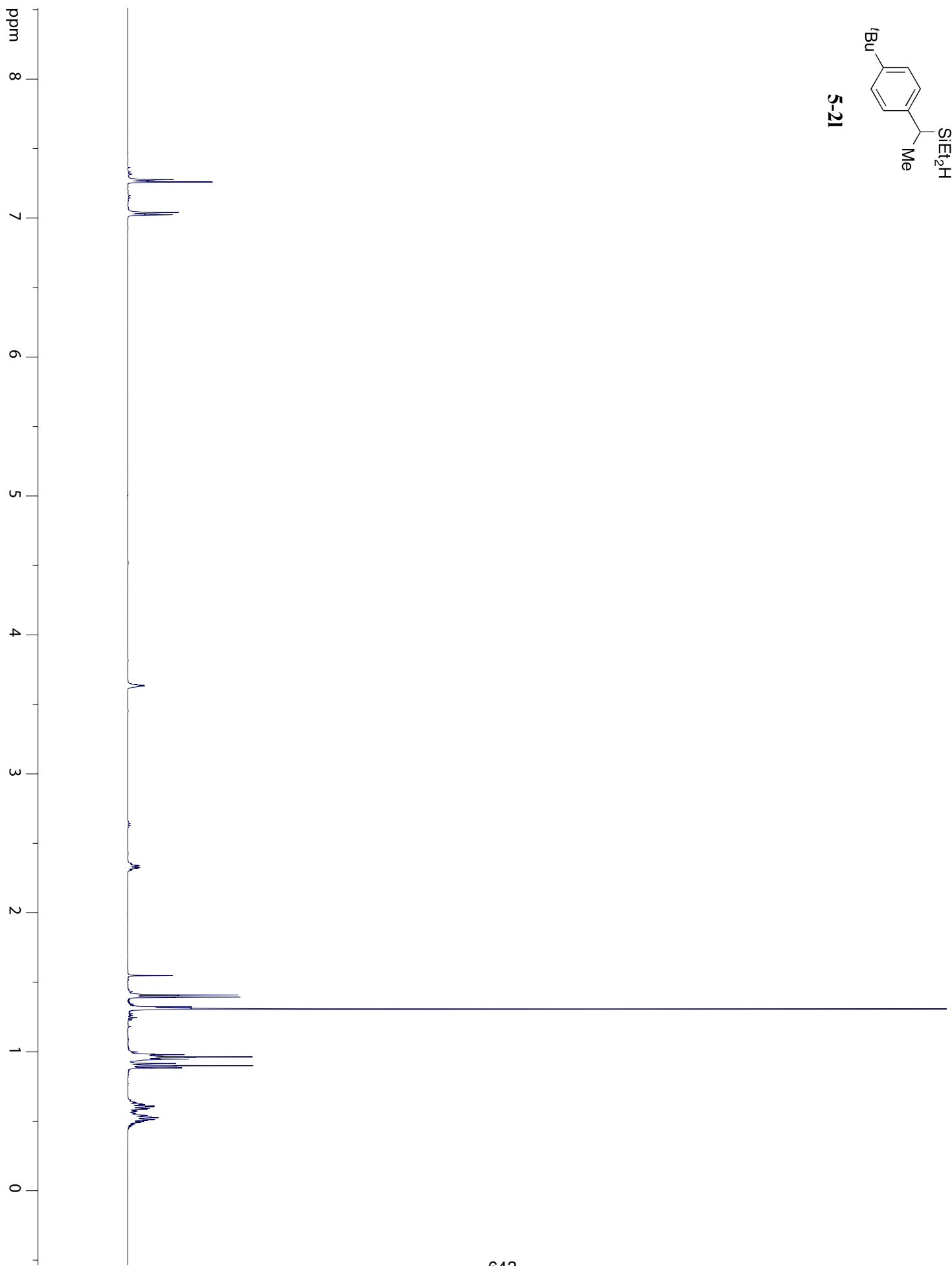
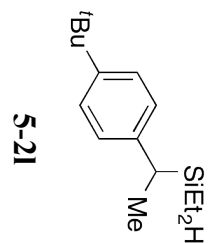
150

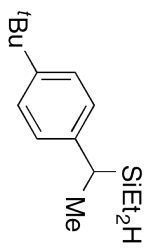
100

50

0

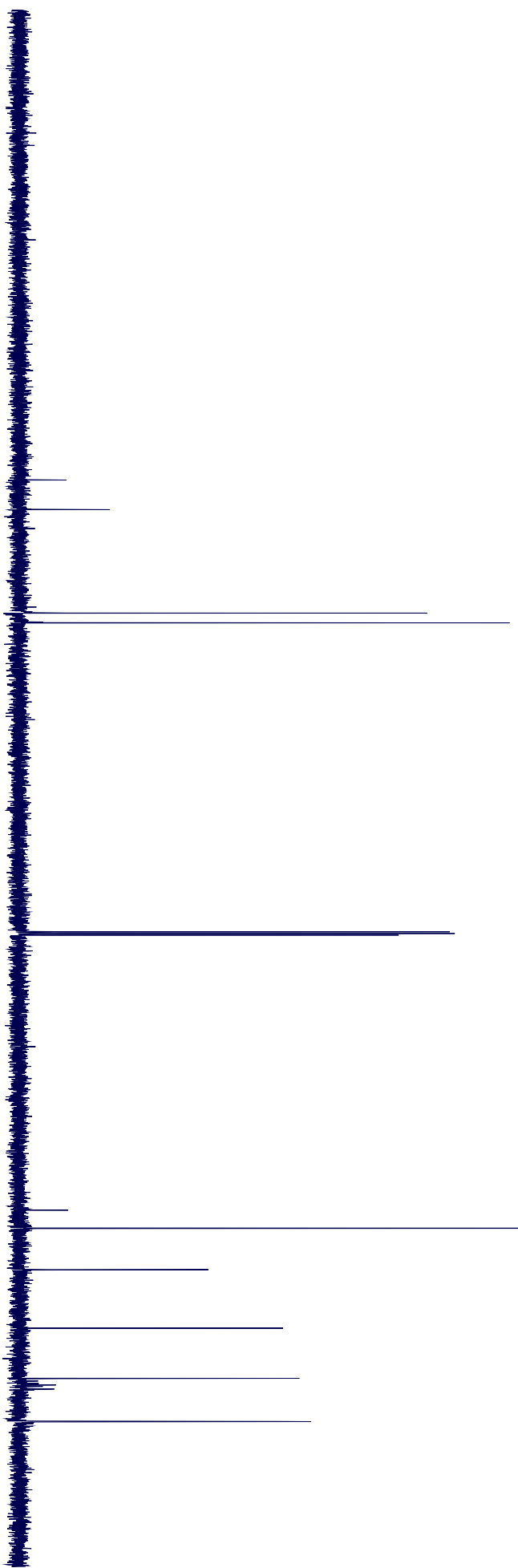


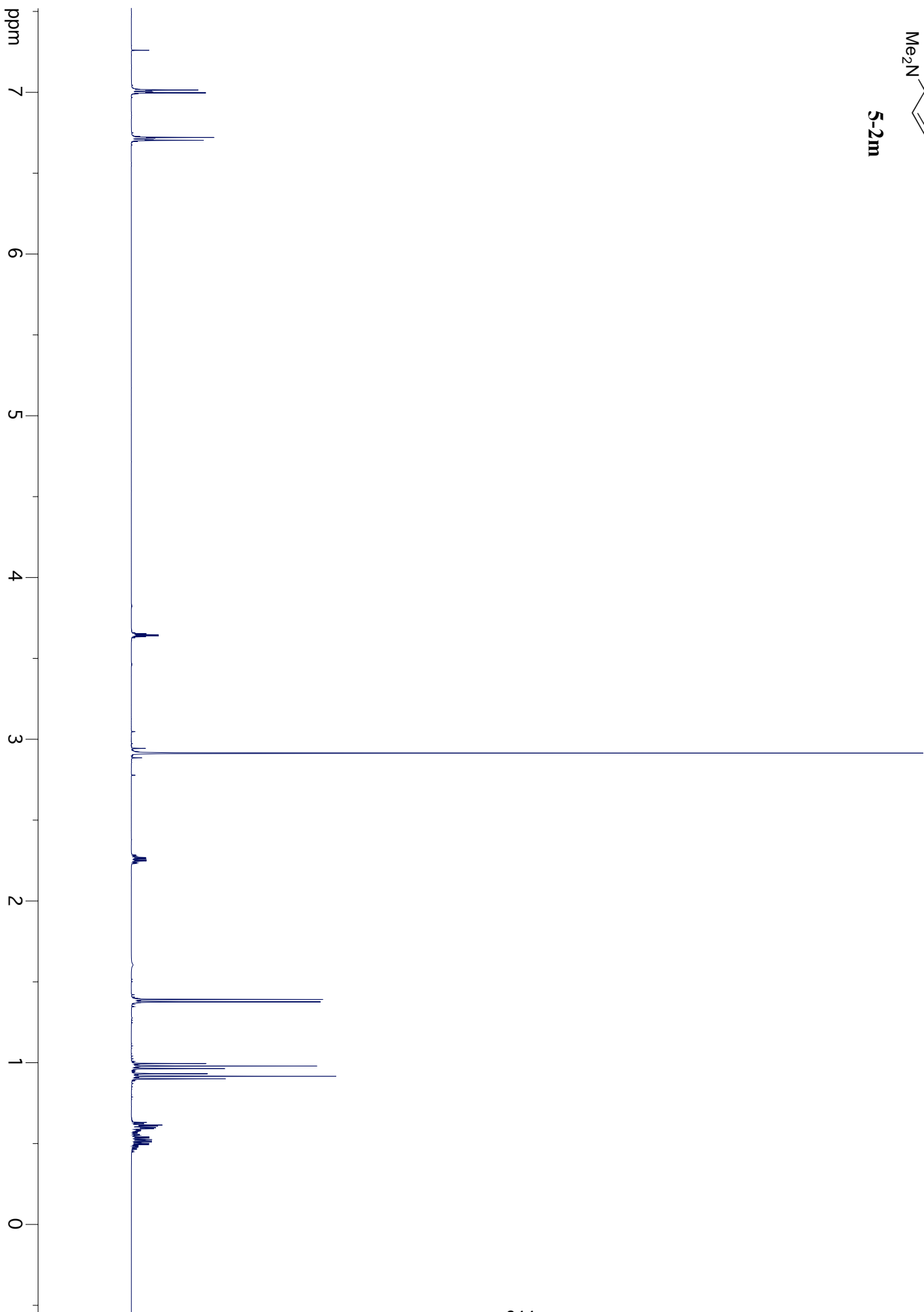
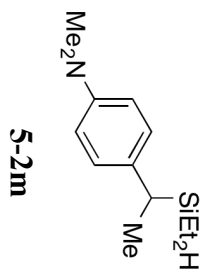


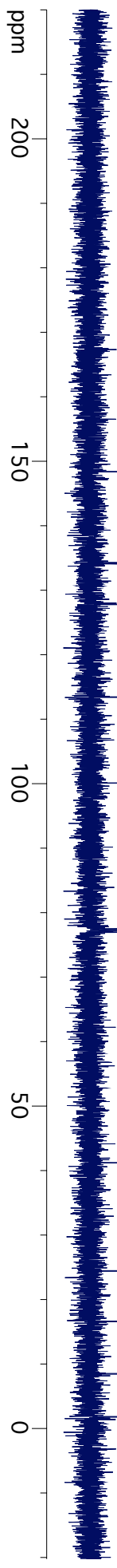
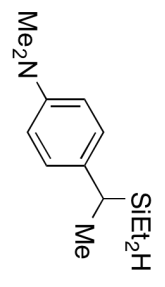


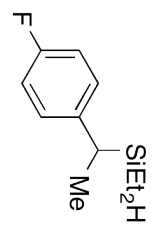
5-21

ppm 200 150 100 50 0

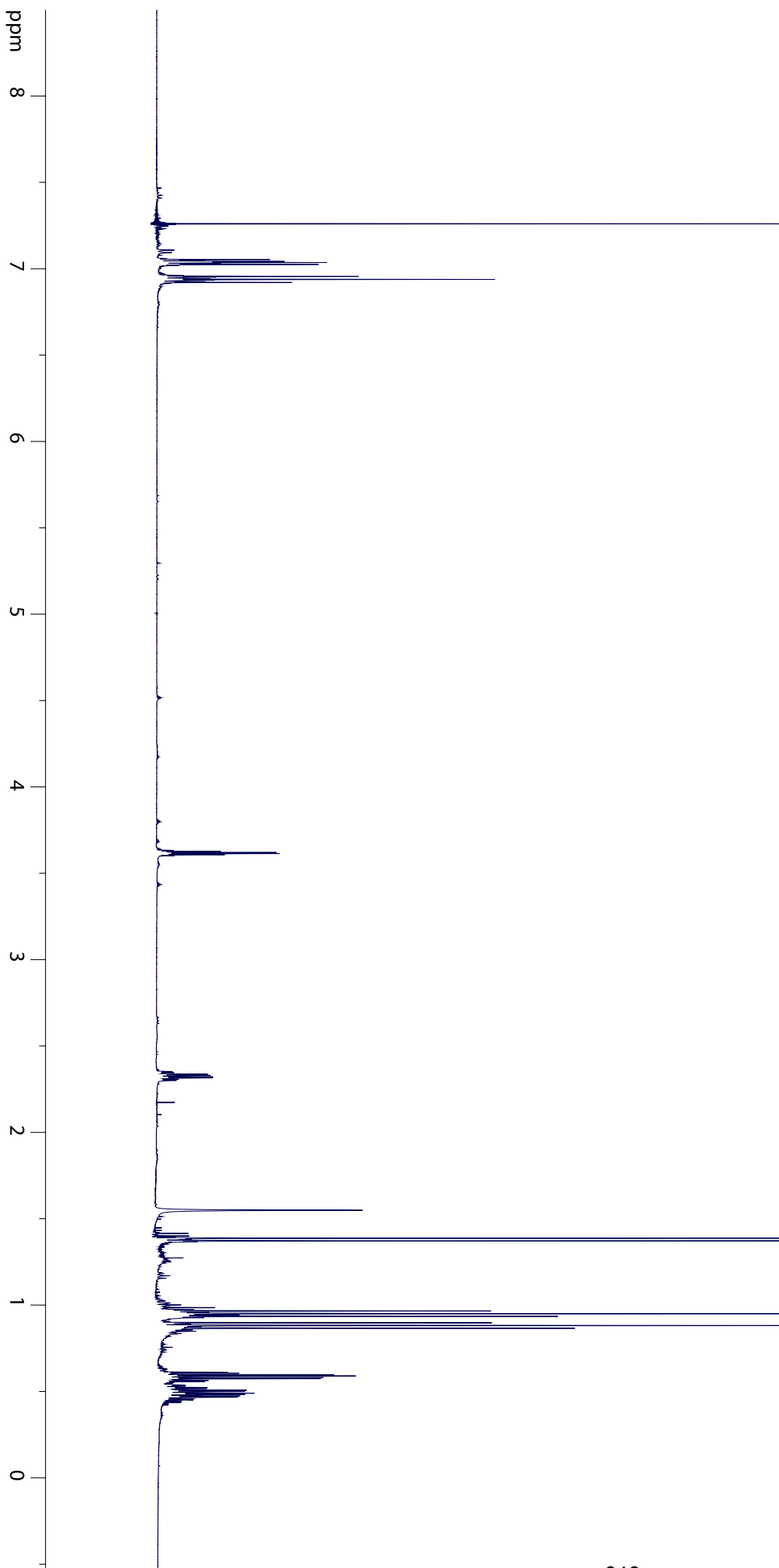


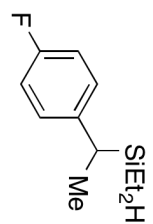




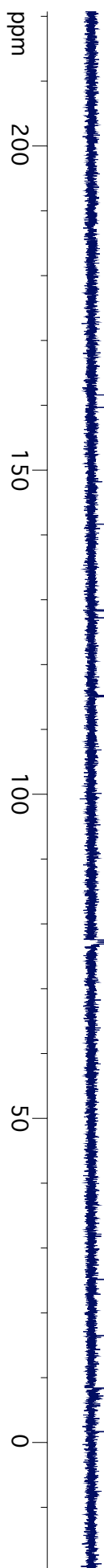


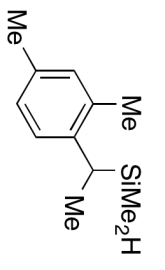
5-2n



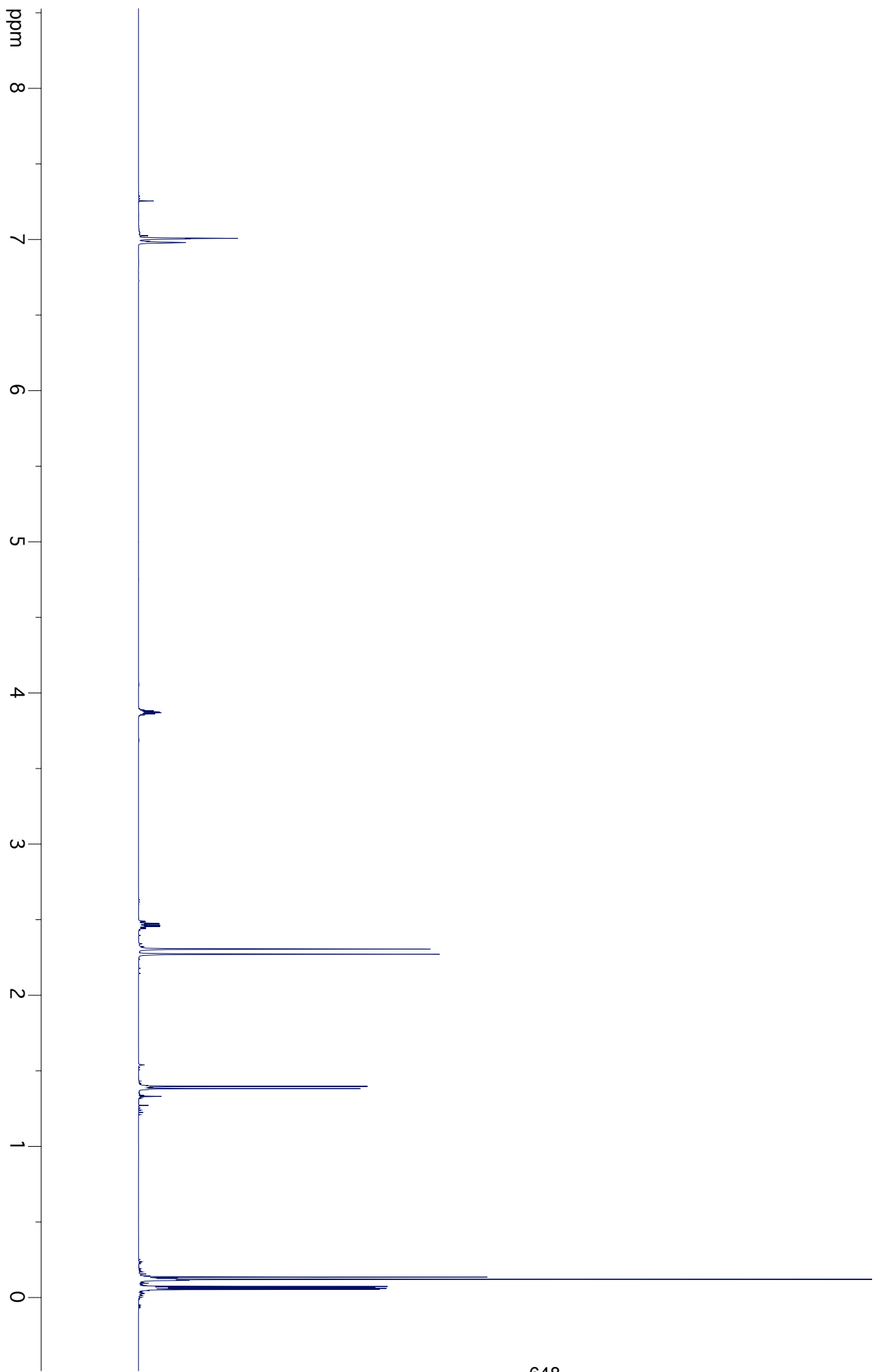


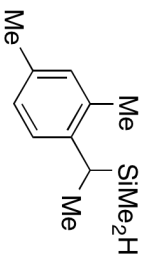
5-2n





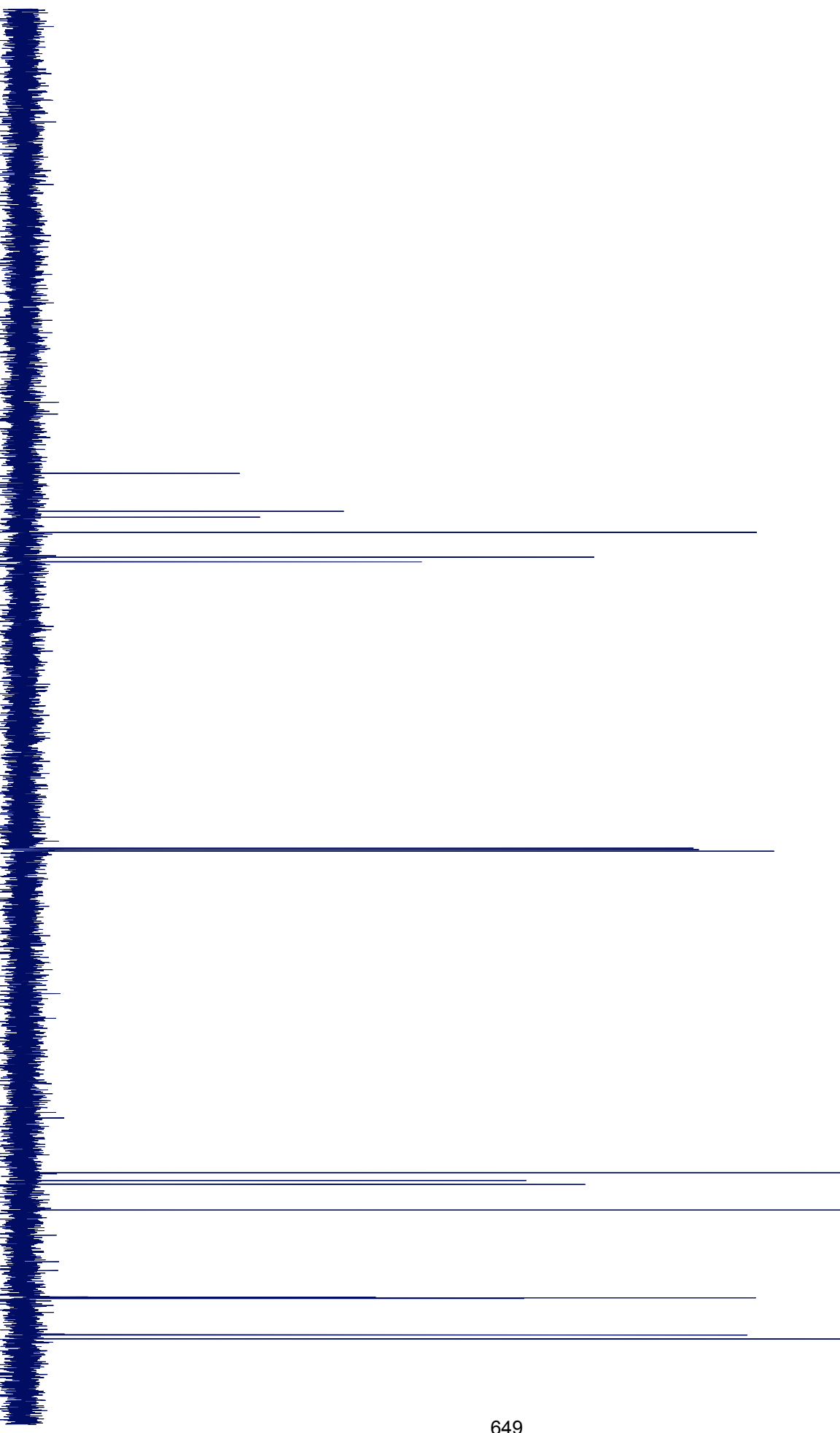
5-20

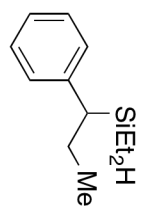




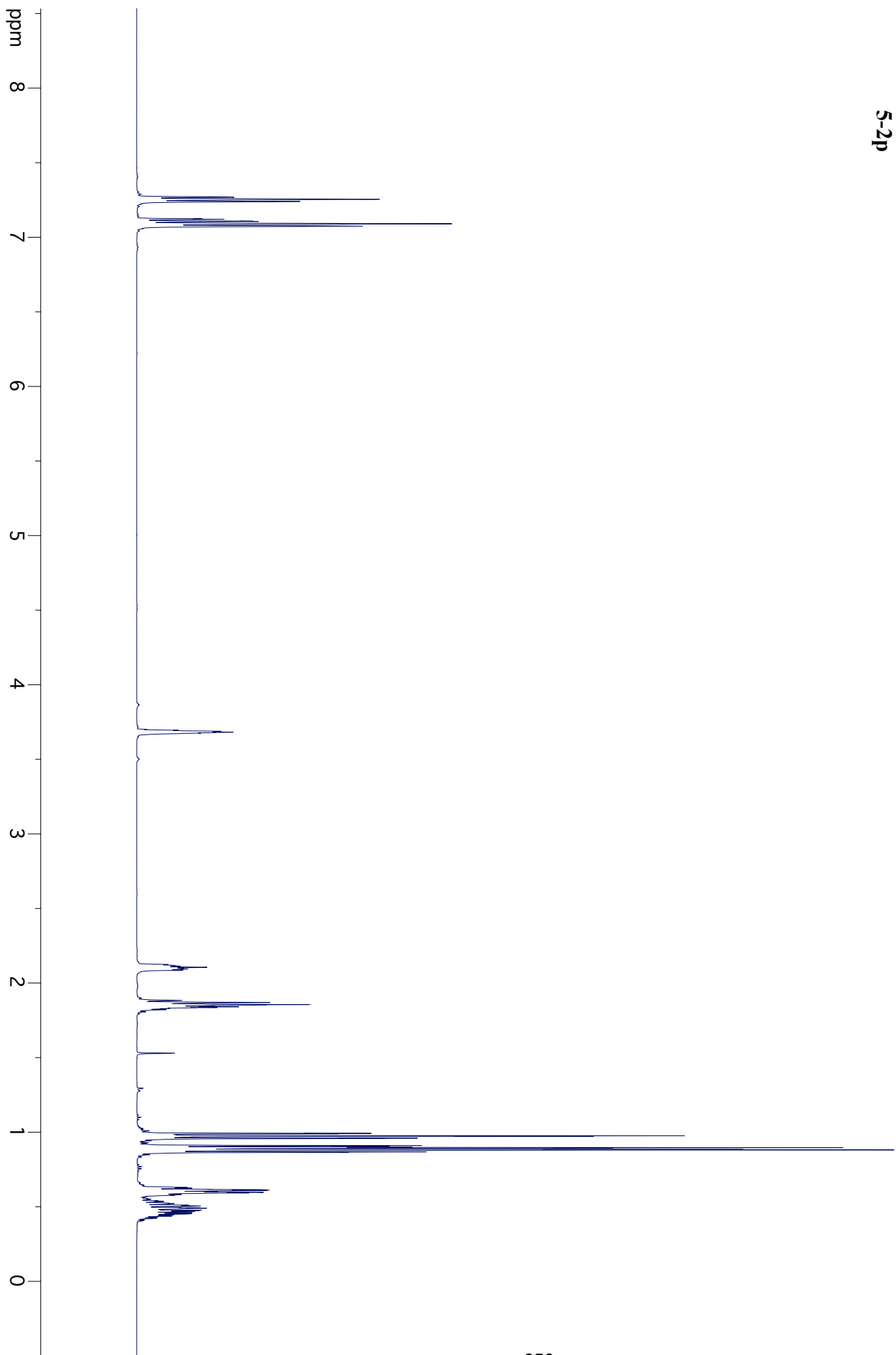
5-20

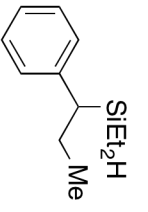
ppm 200 150 100 50 0



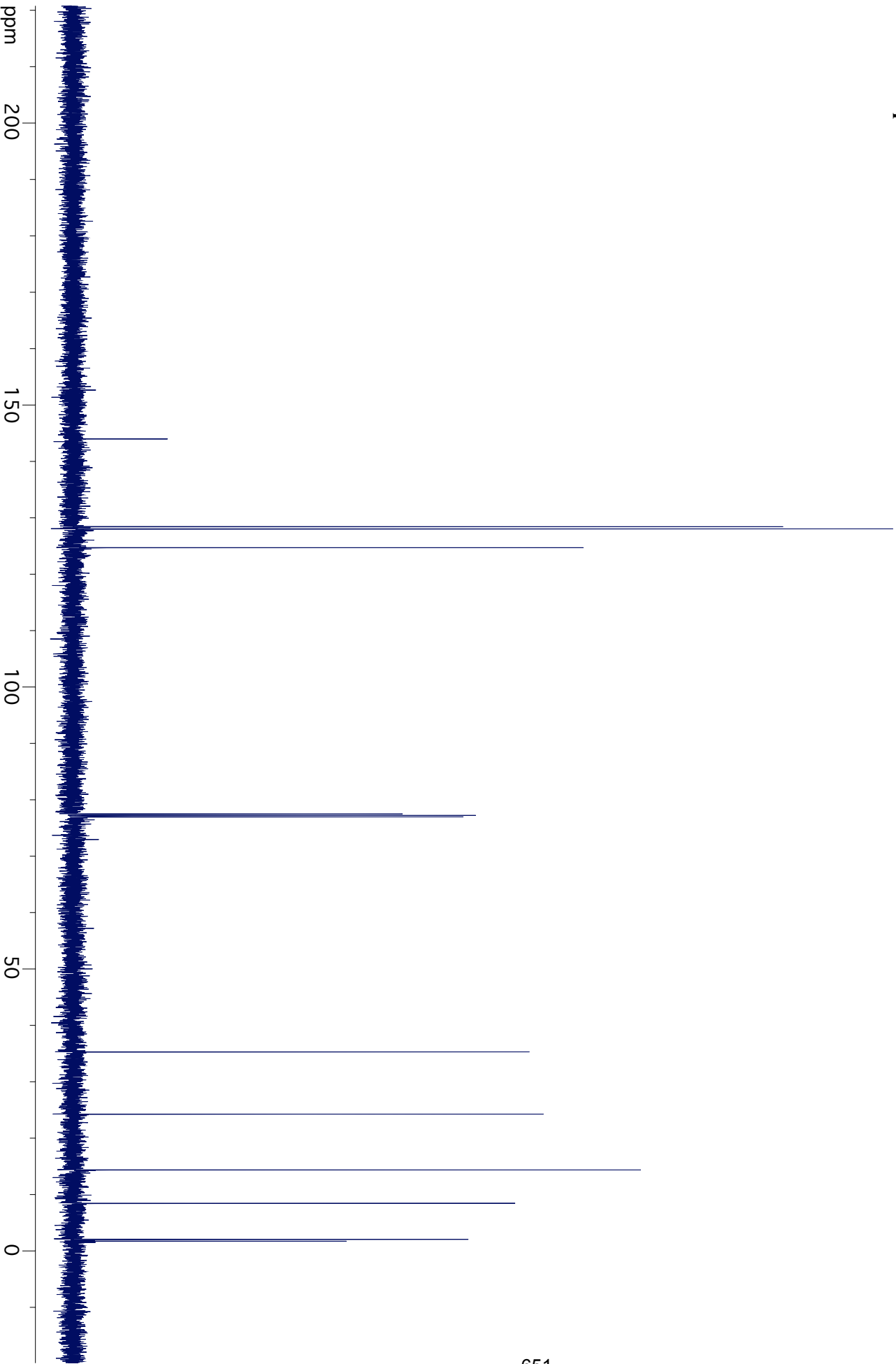


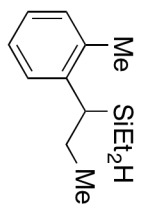
5-2p



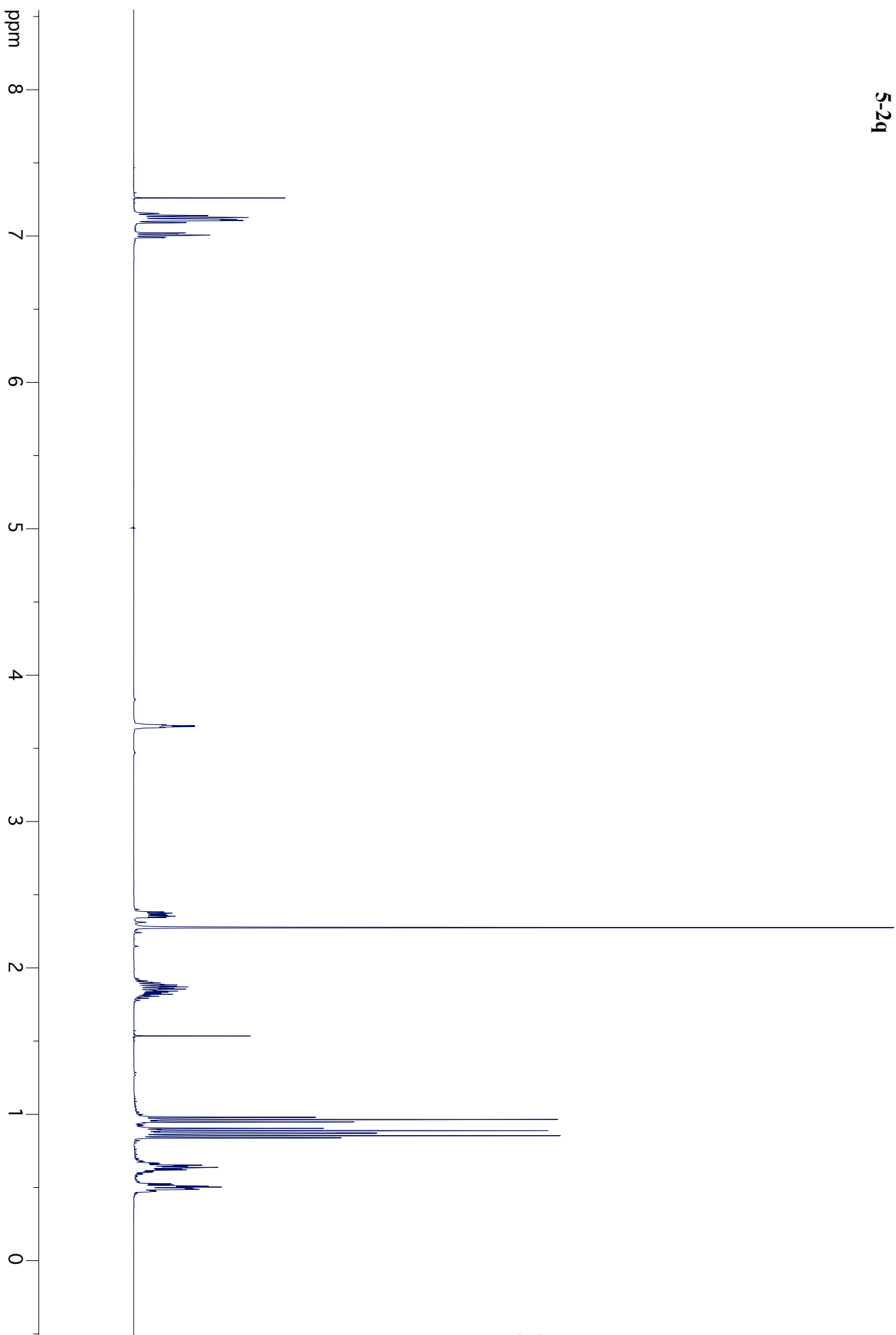


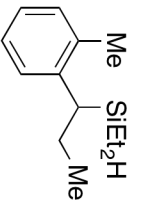
5-2p





5-2q

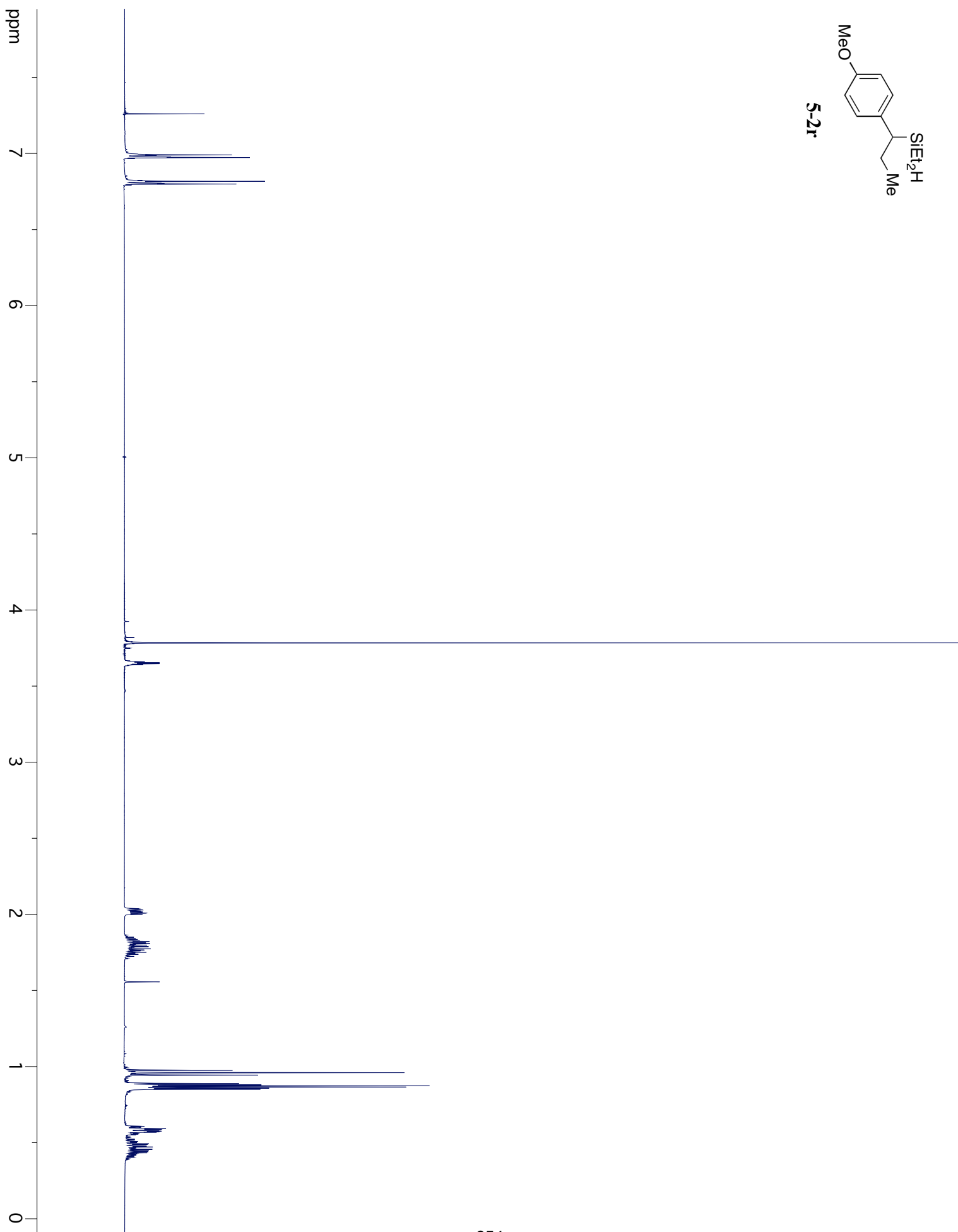
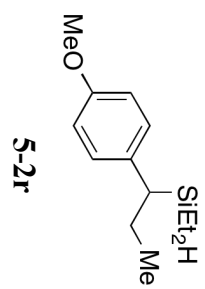


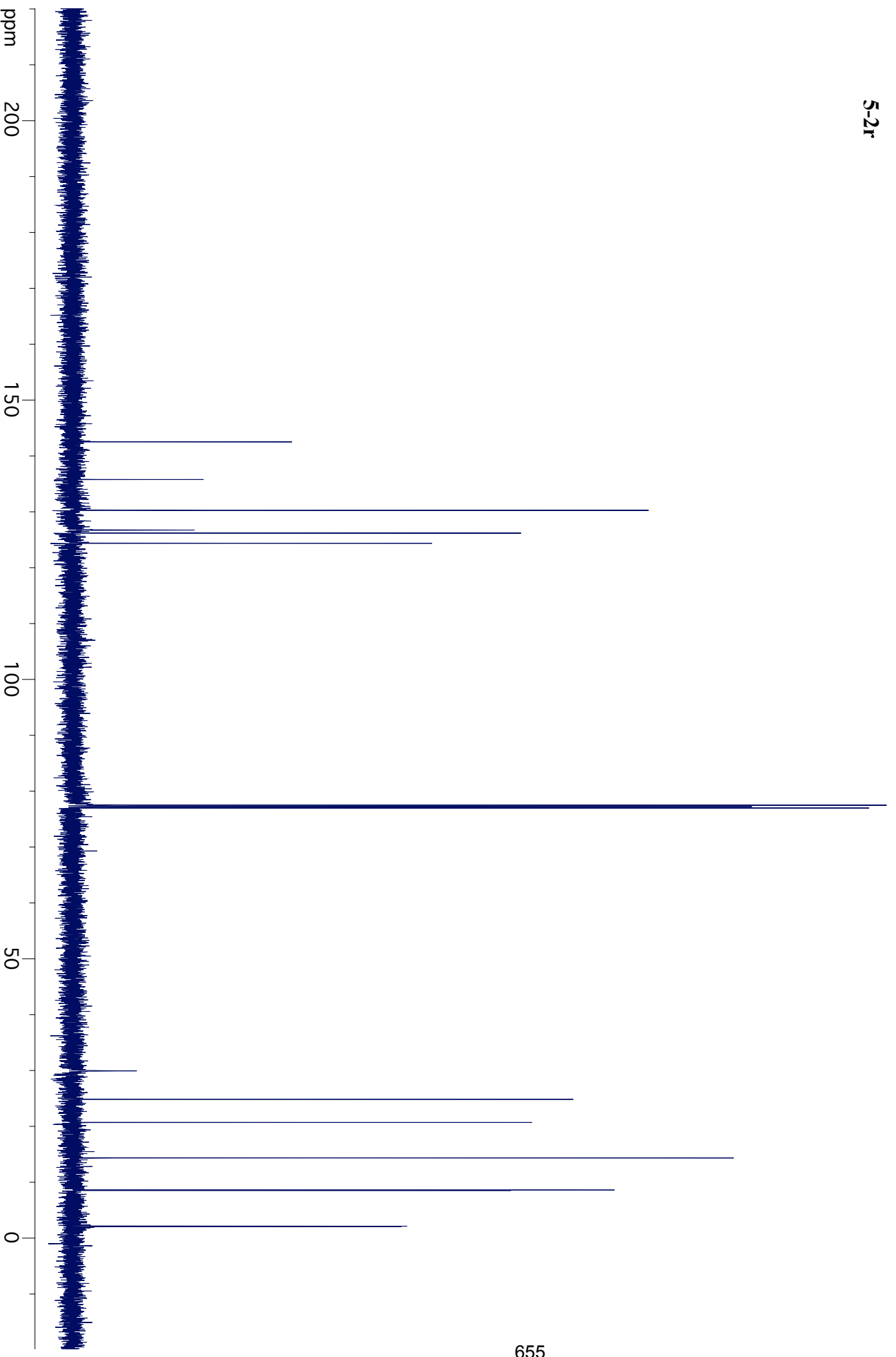
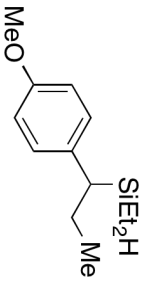


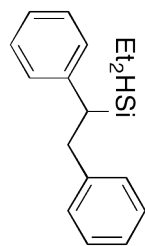
5-2q

ppm

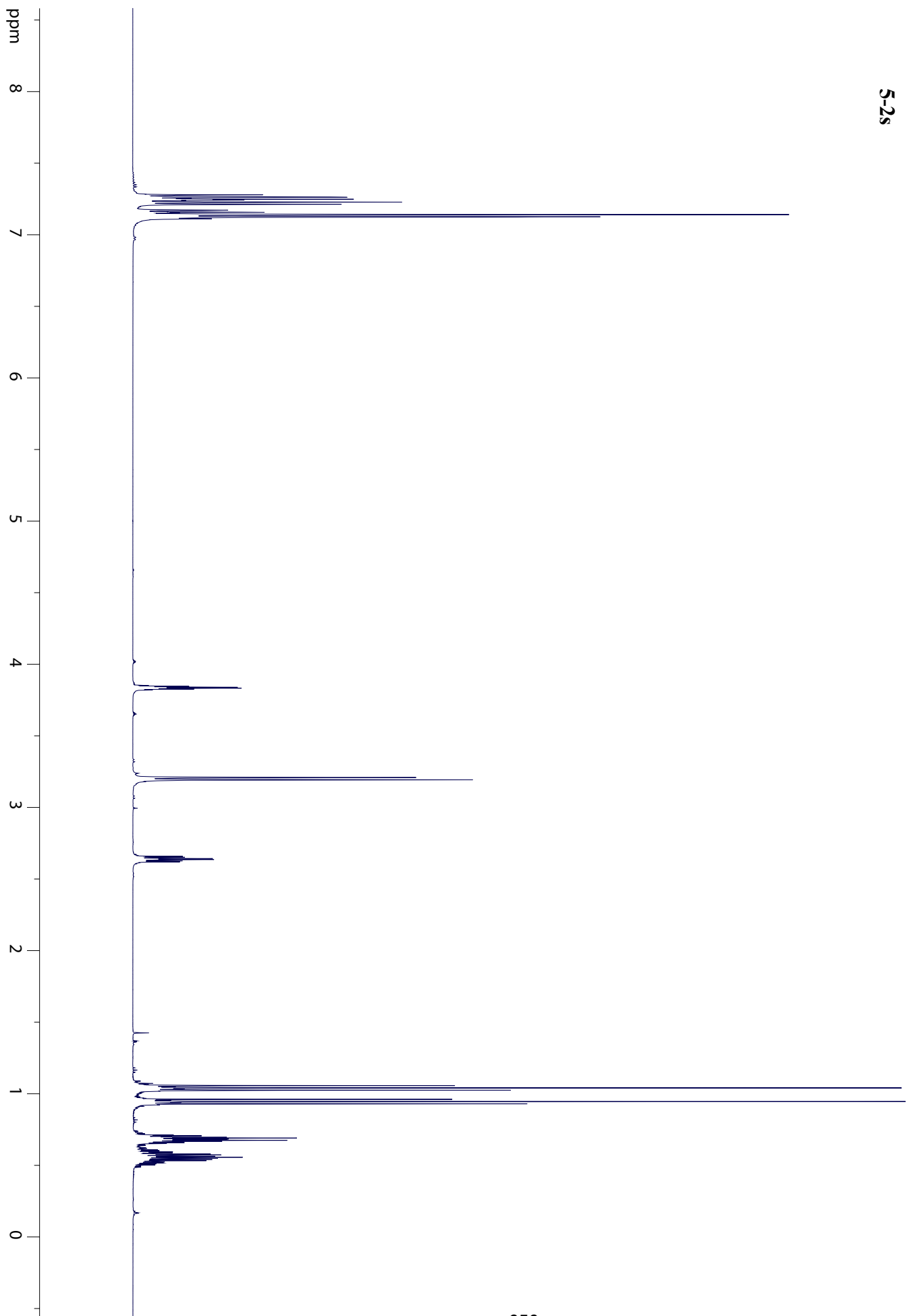


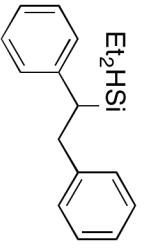






5-2s

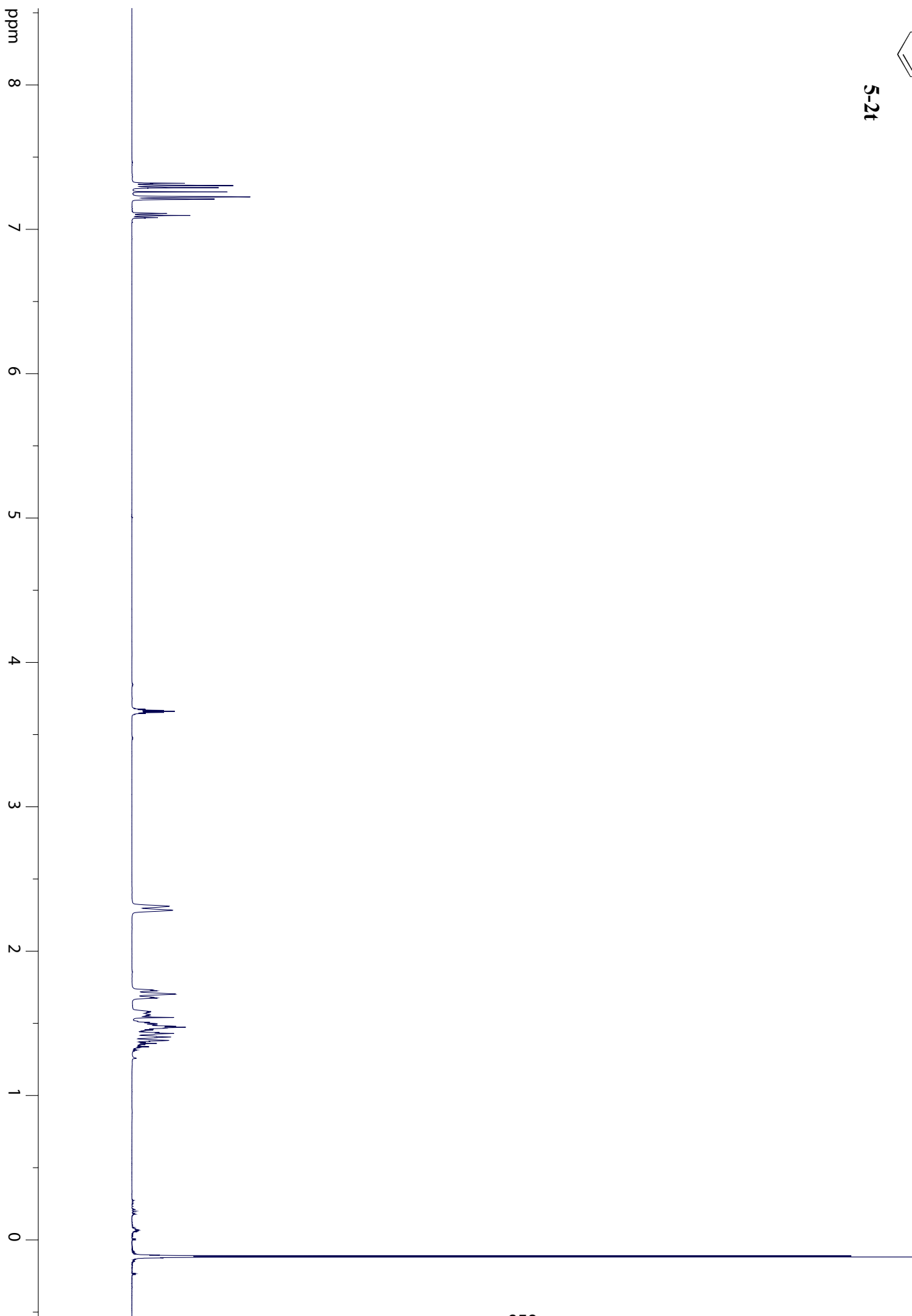
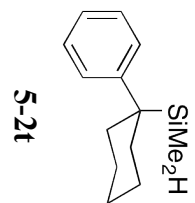


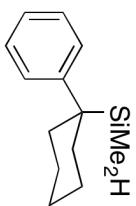


5-2s

ppm



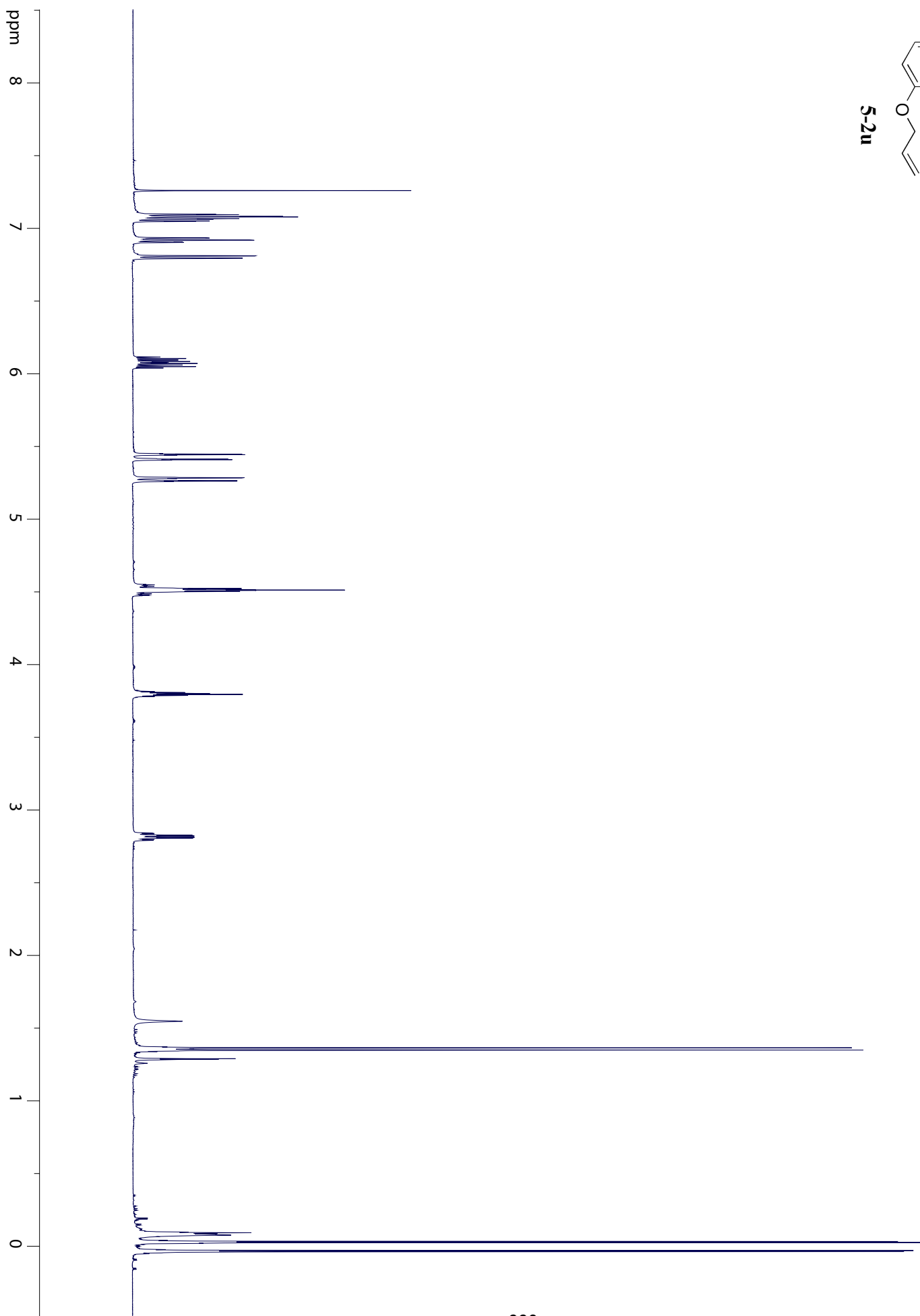
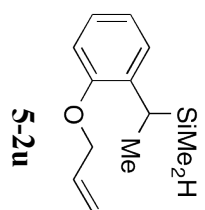


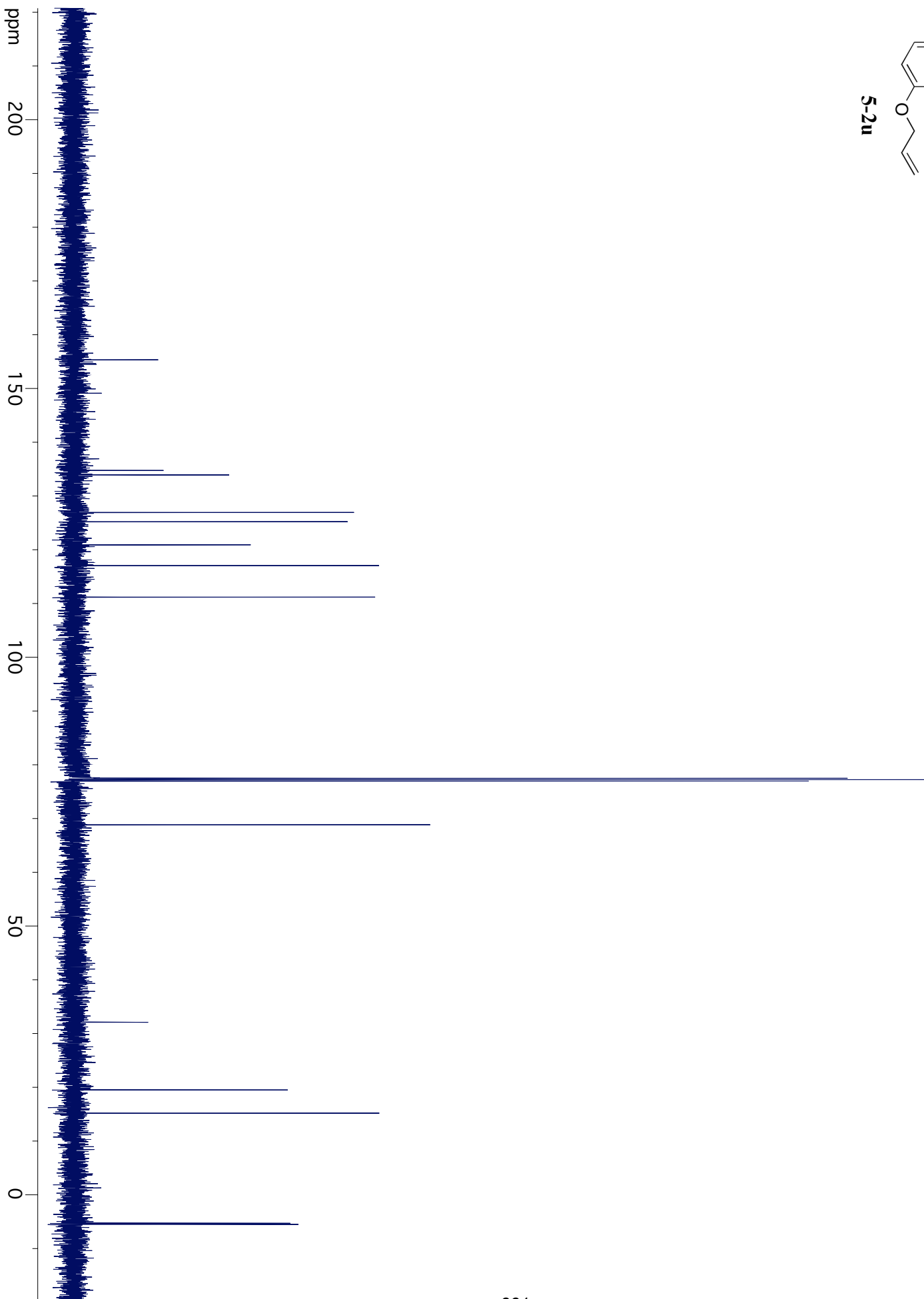
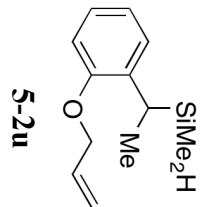


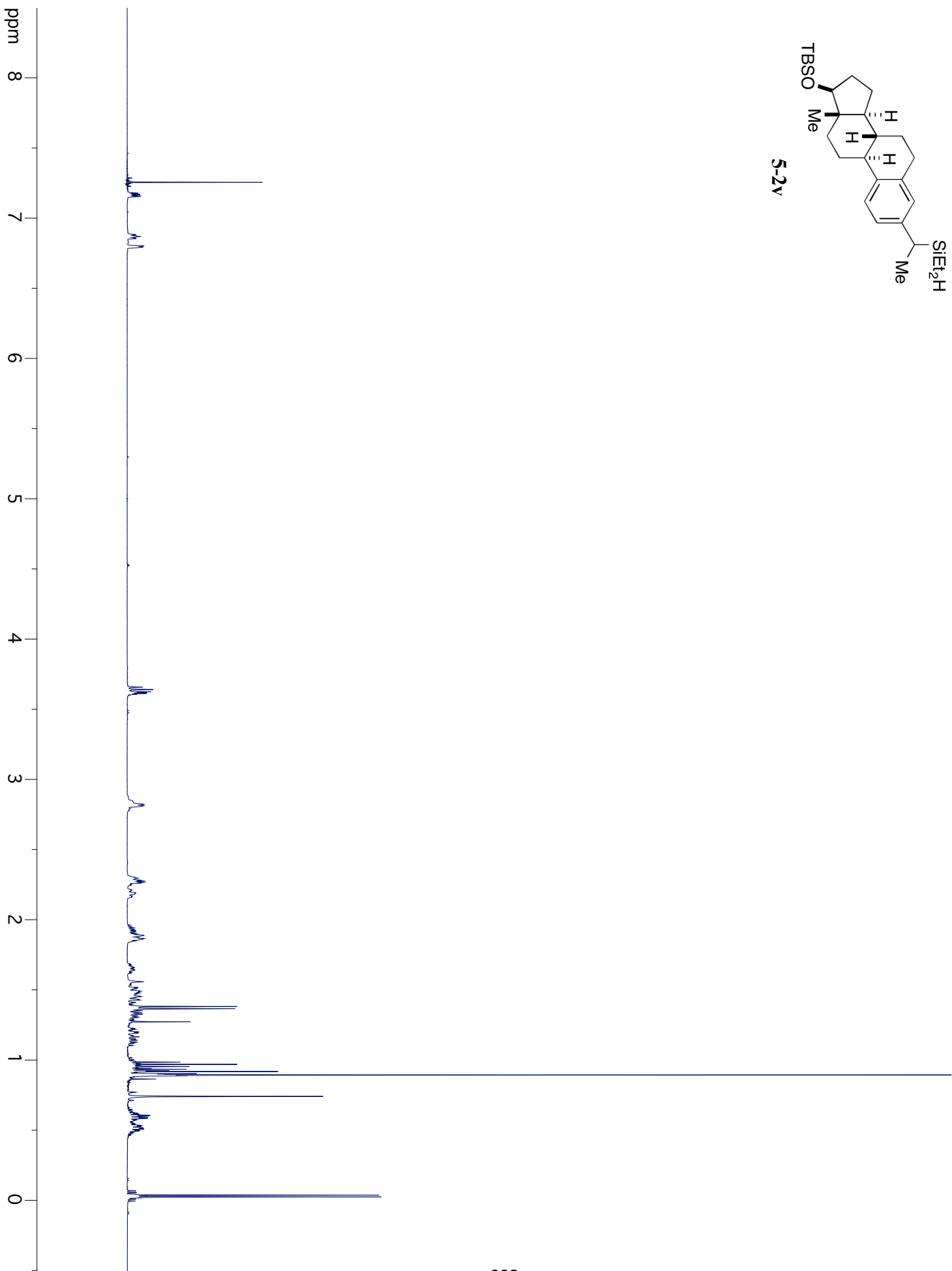
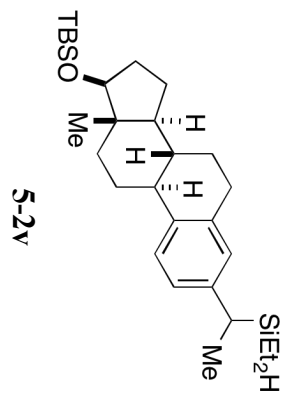
5-2t

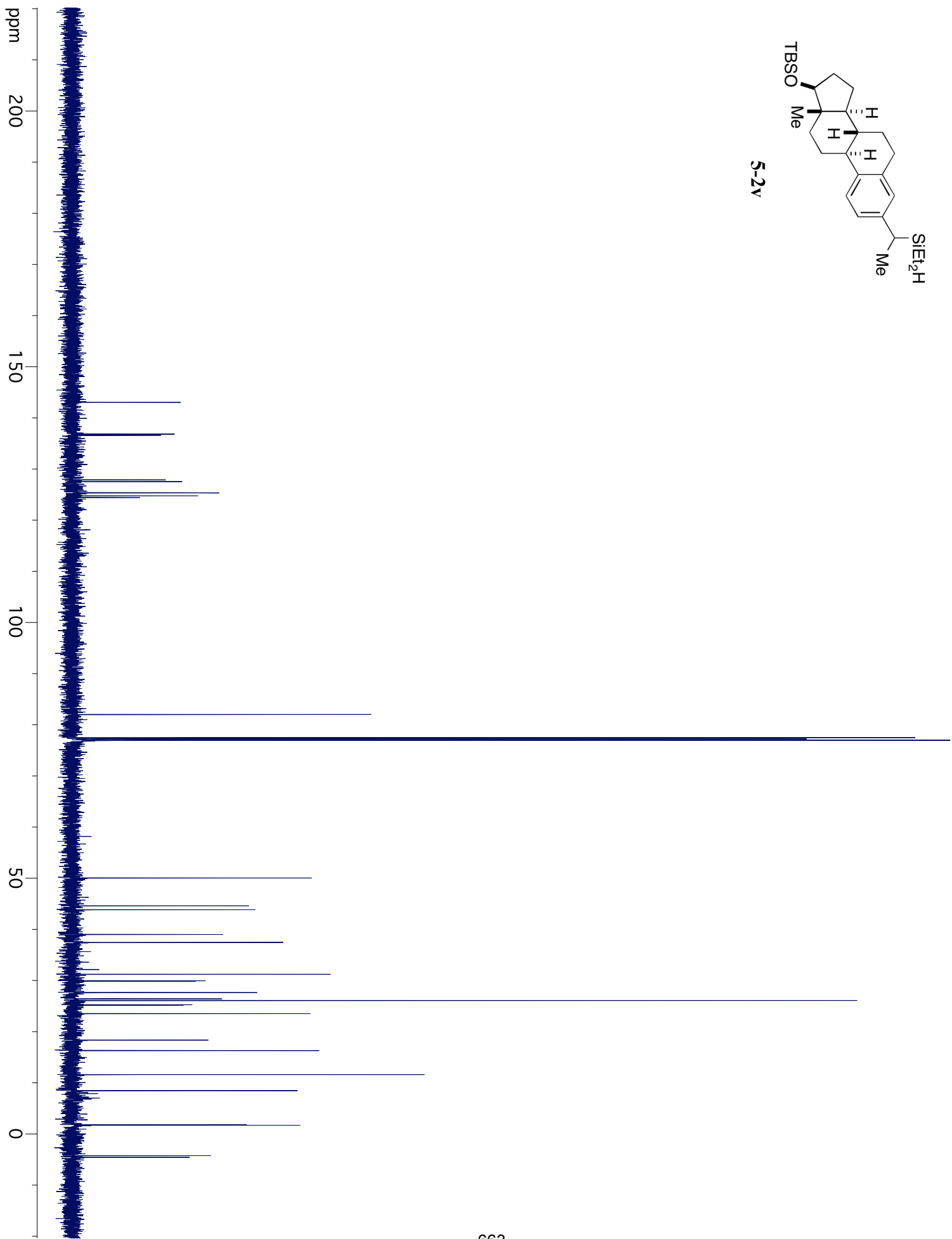
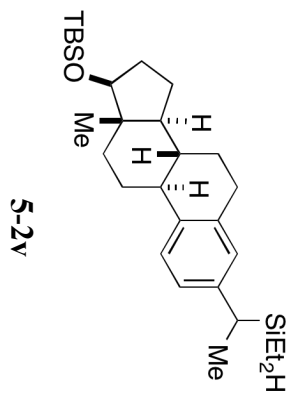
ppm

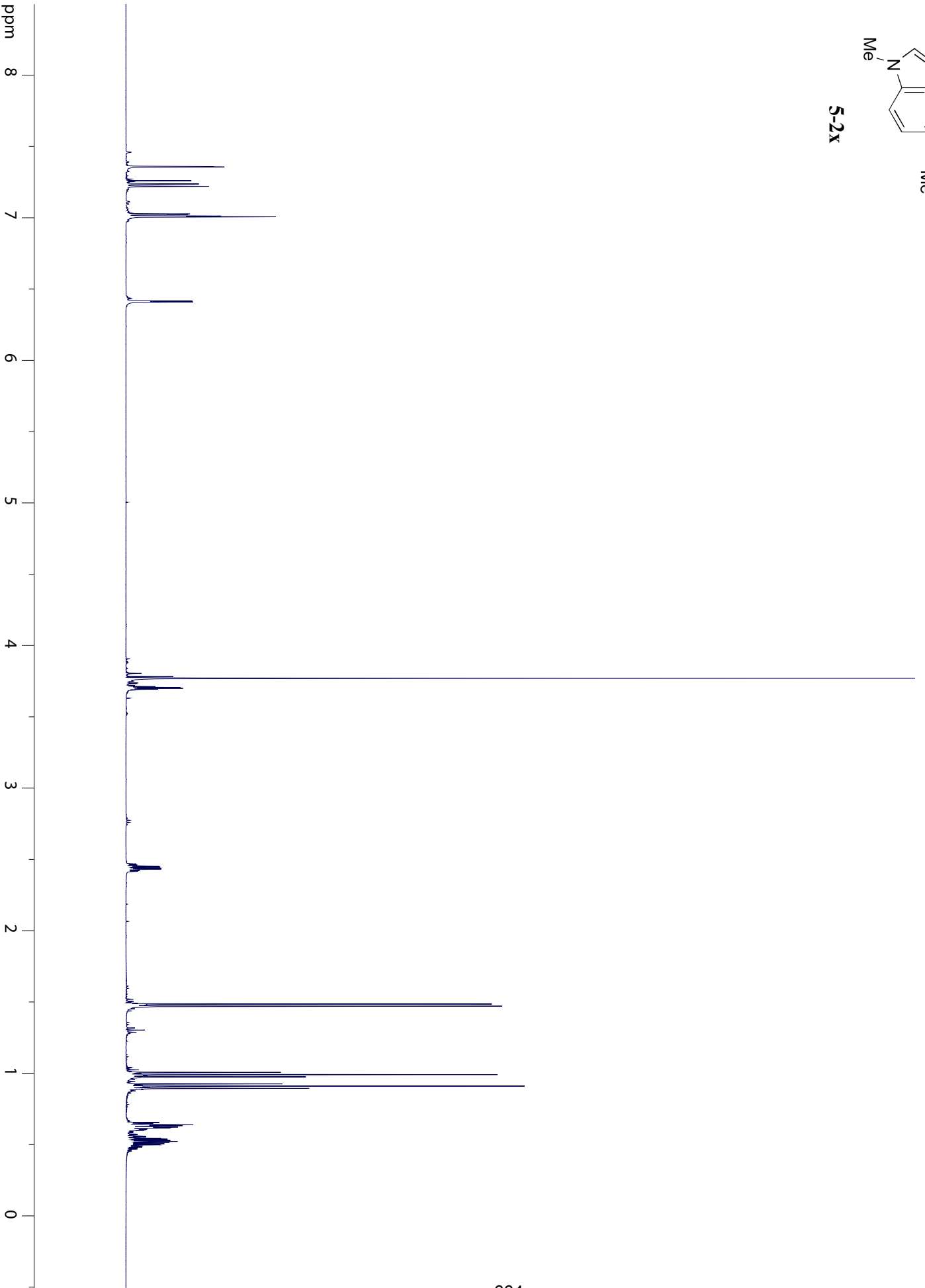
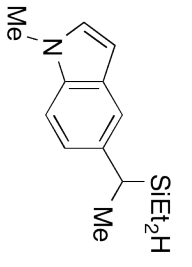


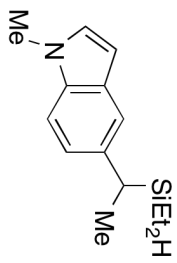








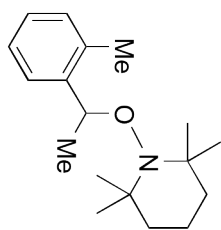




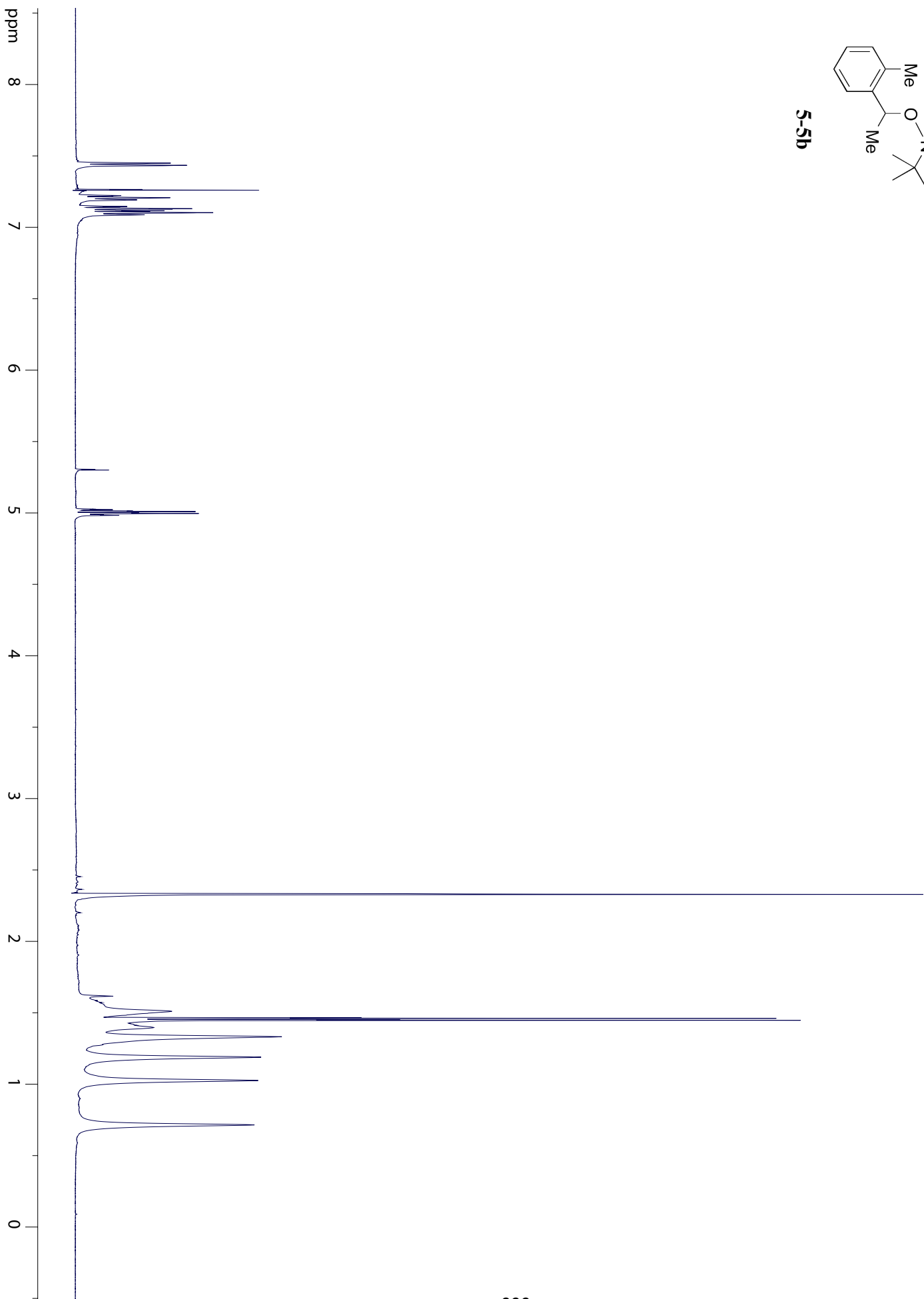
5-2x

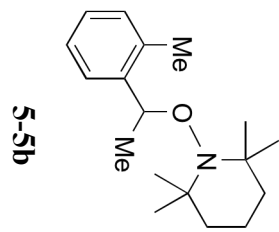
ppm





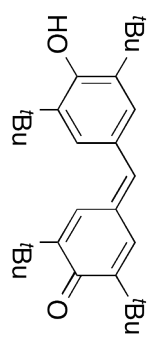
5-5b



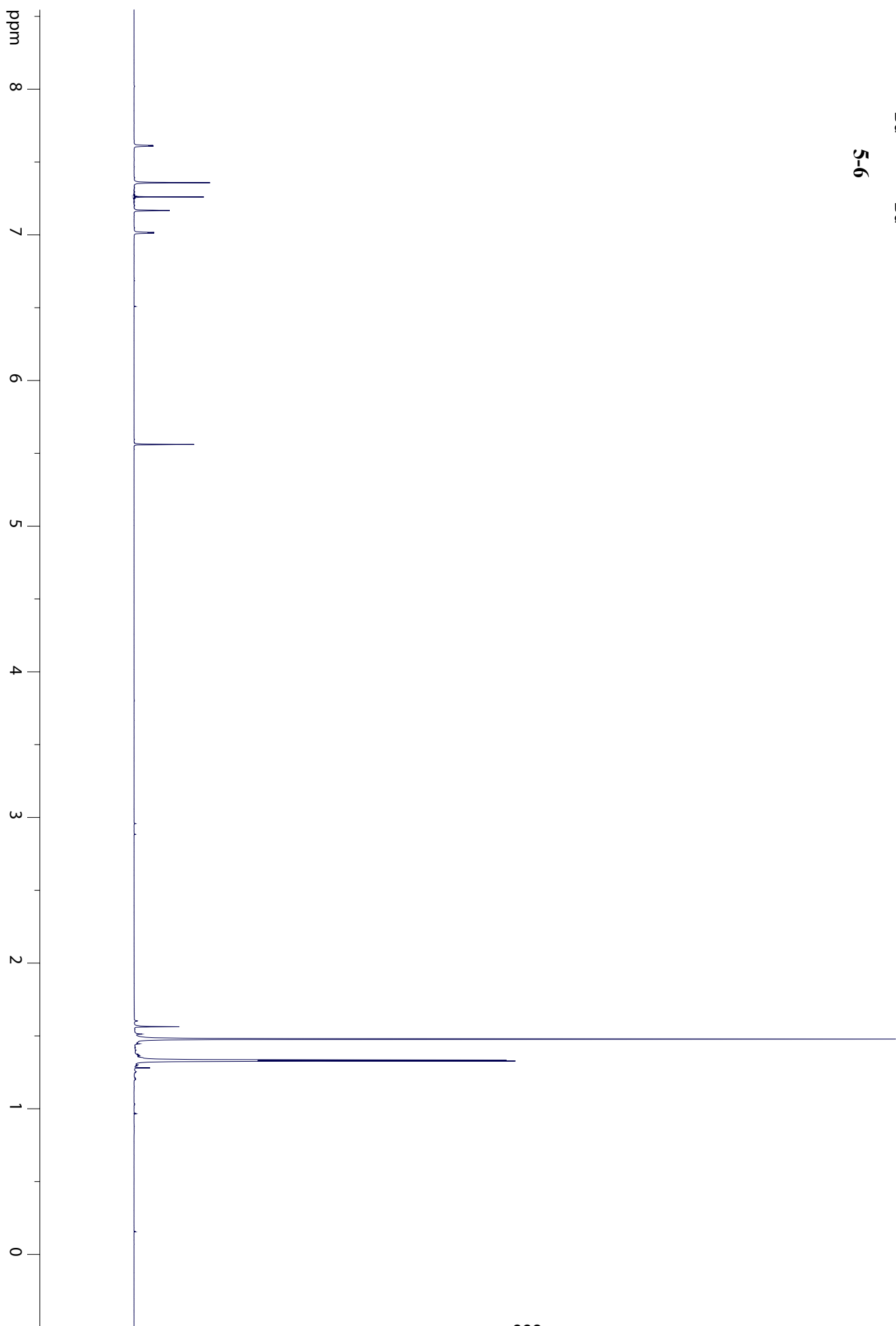


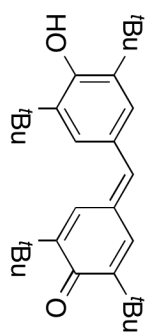
ppm 200
150
100
50
0





5-6

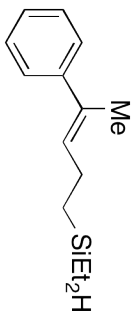




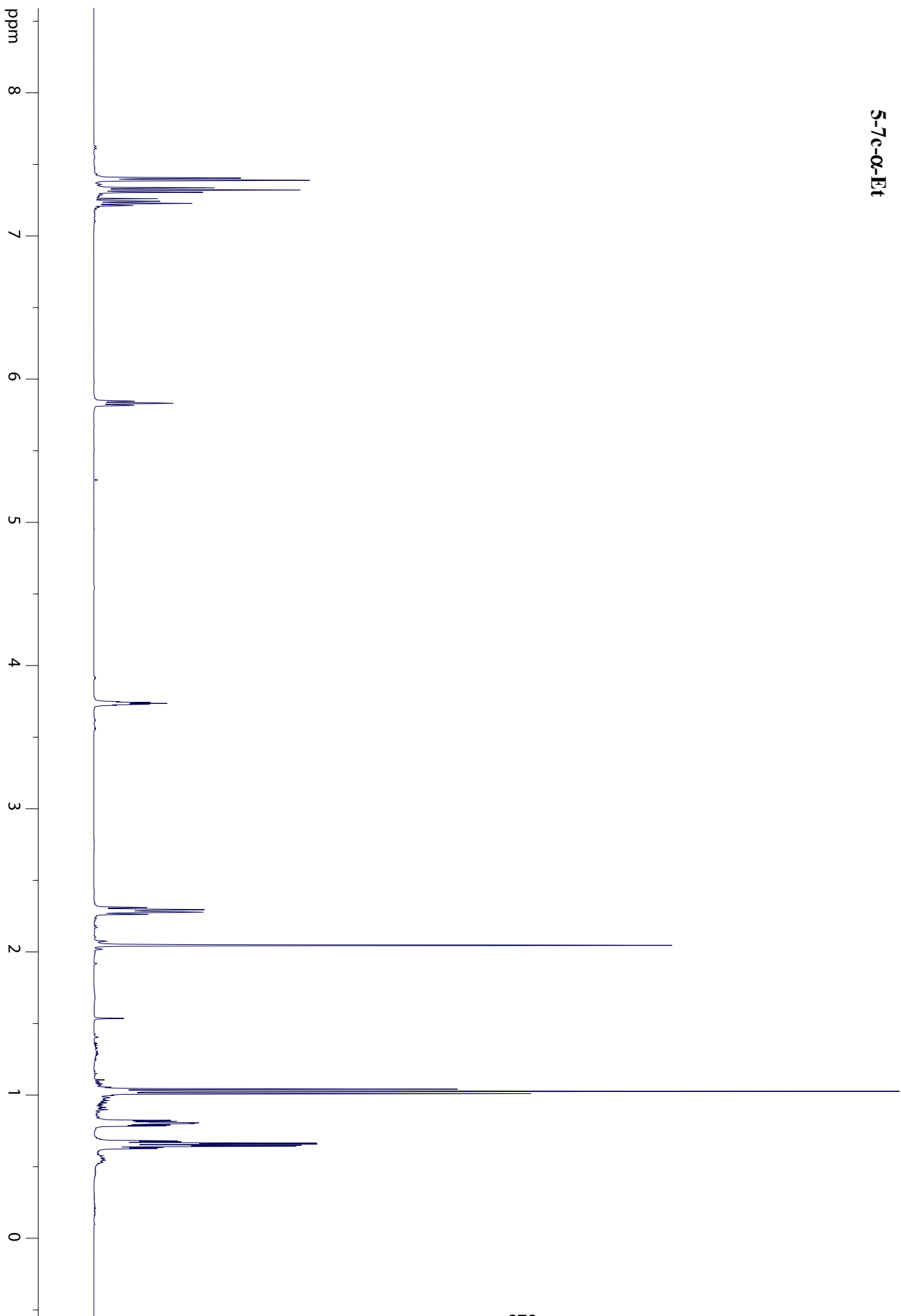
5-6

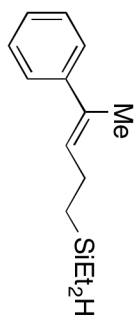
ppm





5-7-c- α -Et

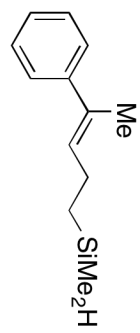




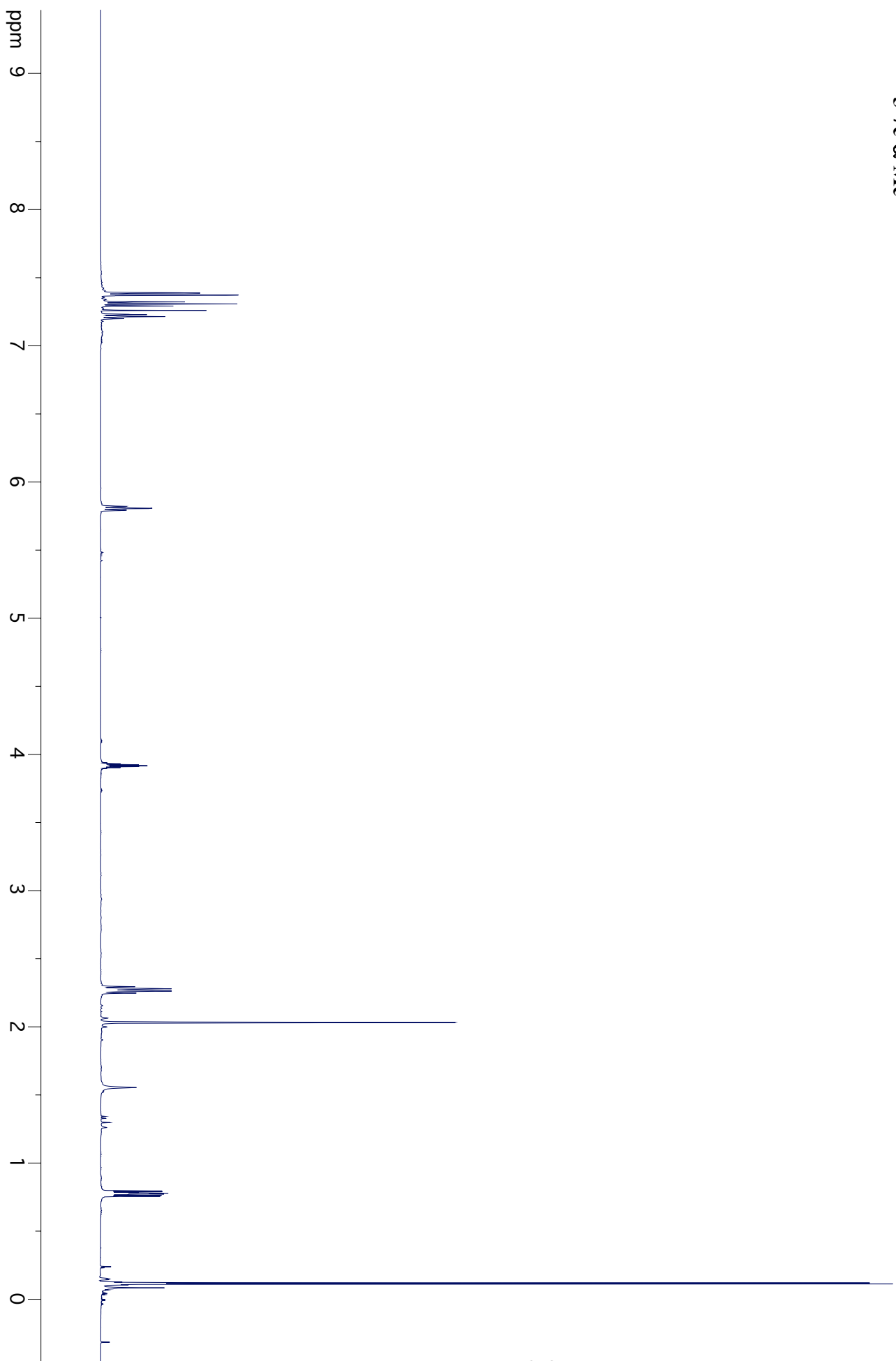
5-7-c- α -Et

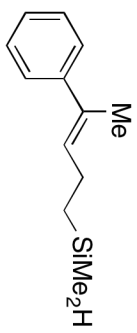
ppm





5-7-c- α -Me

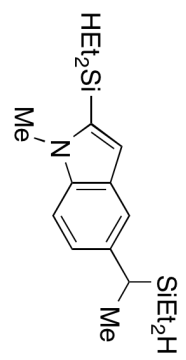




5-7c- α -Me

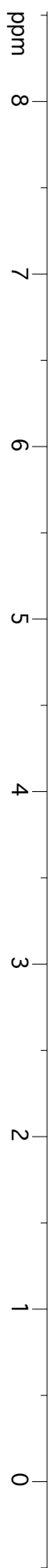
ppm

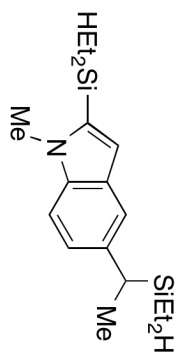




5-11

ppm





S-111

ppm

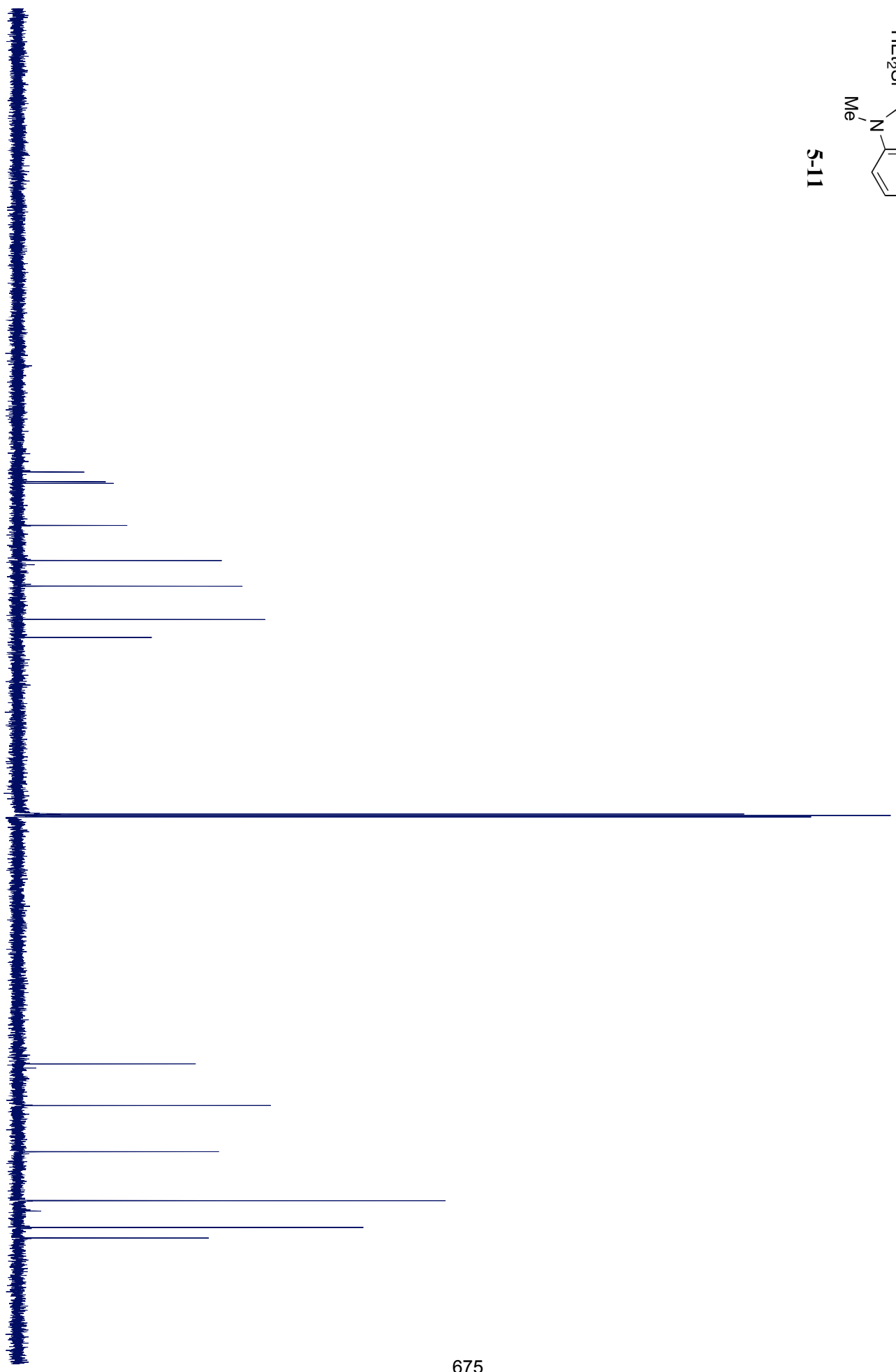
200

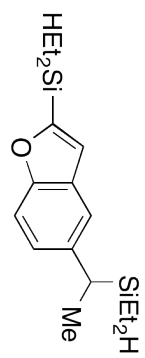
150

100

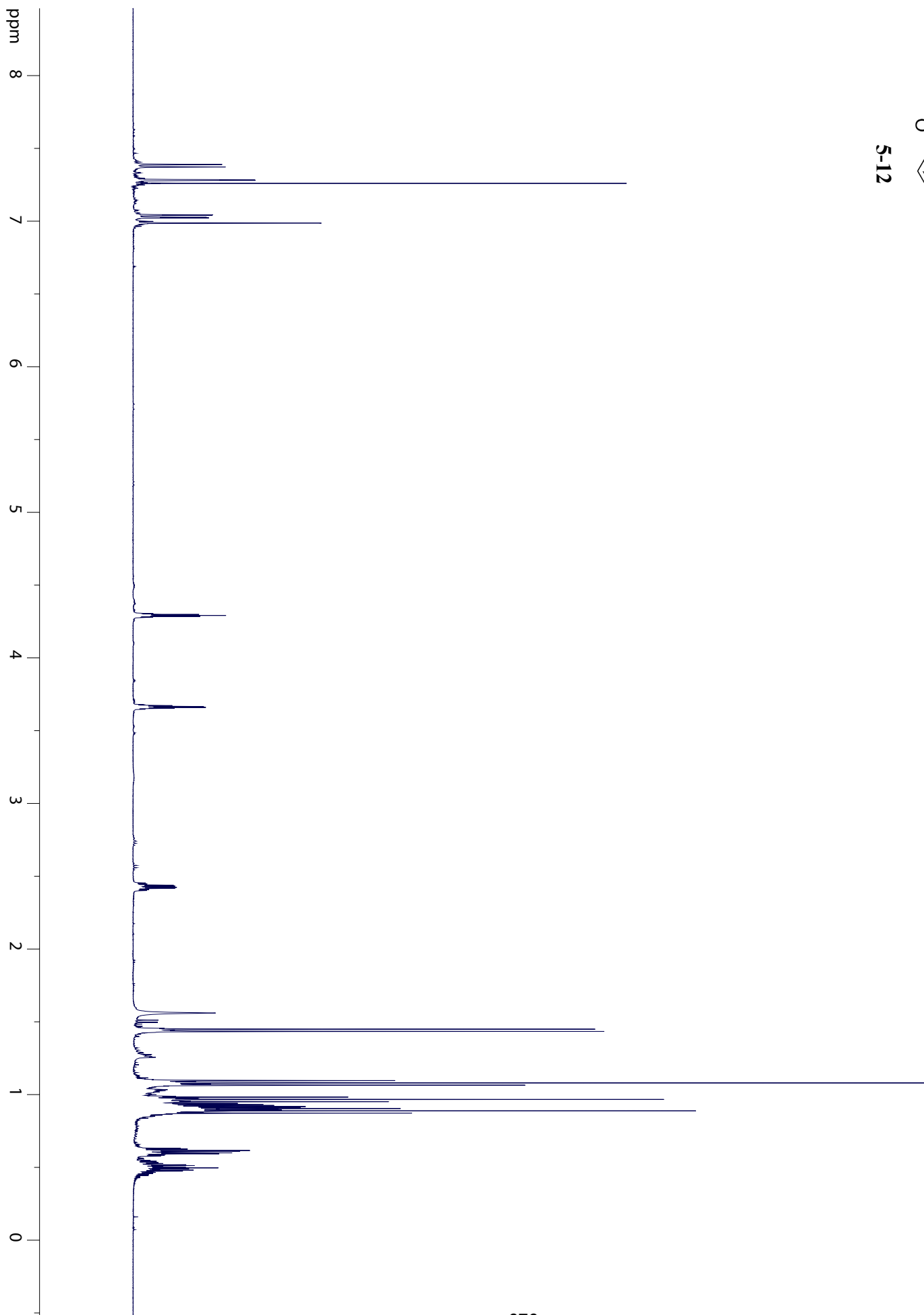
50

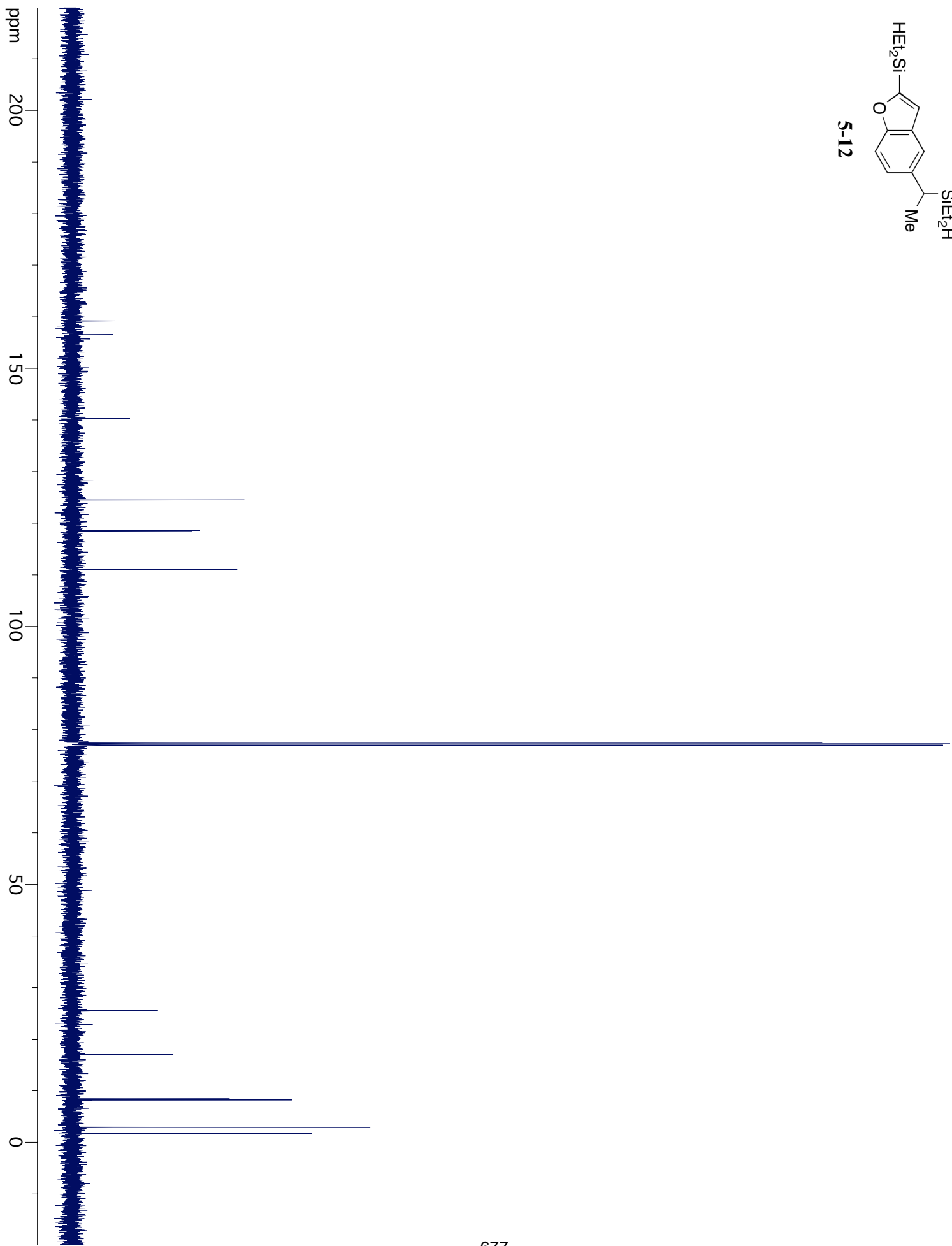
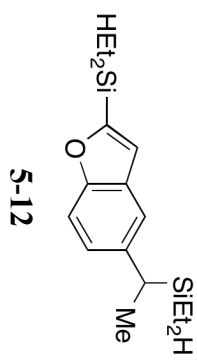
0

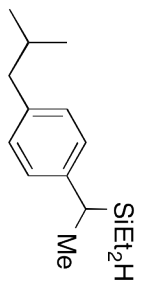




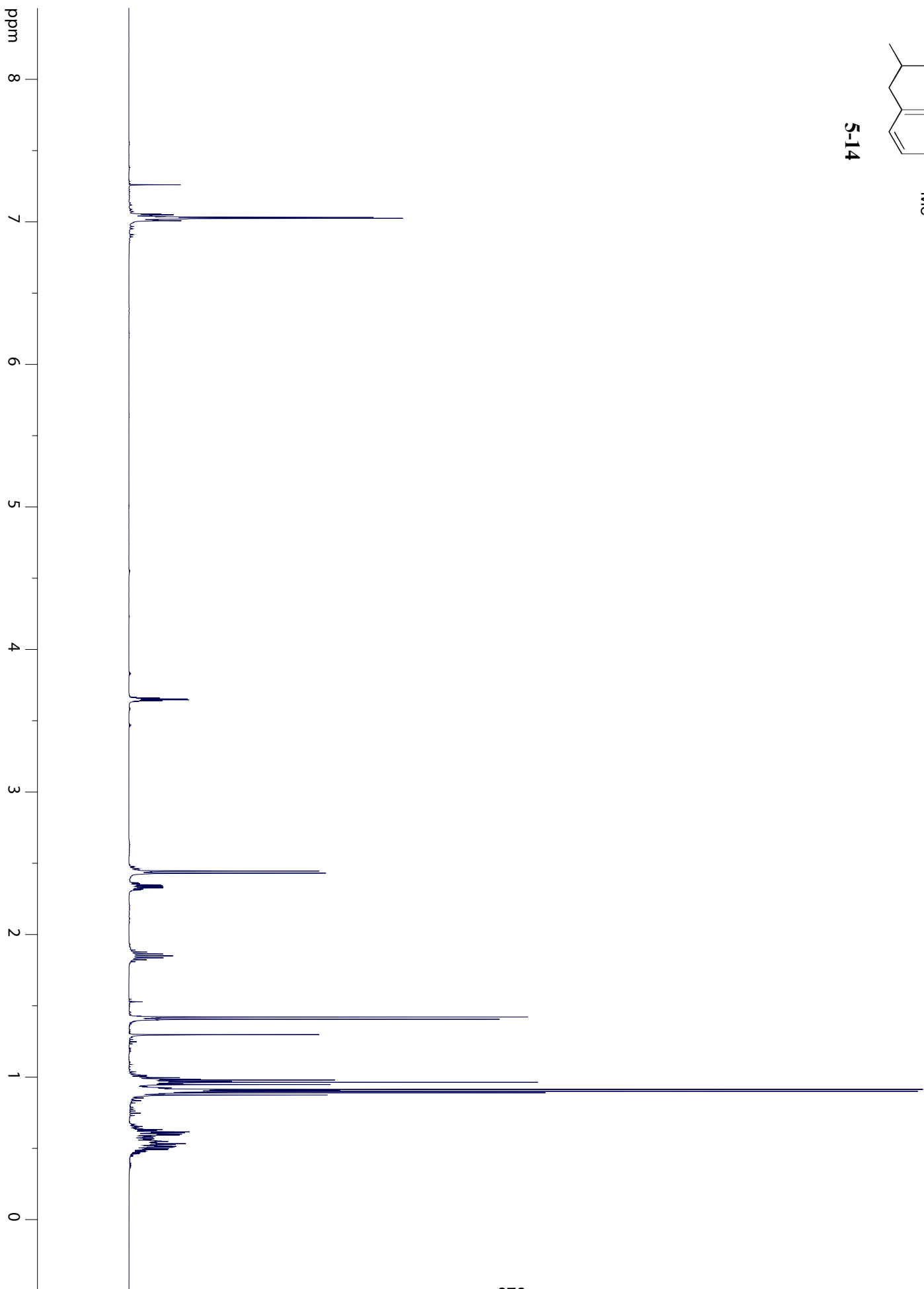
S-12

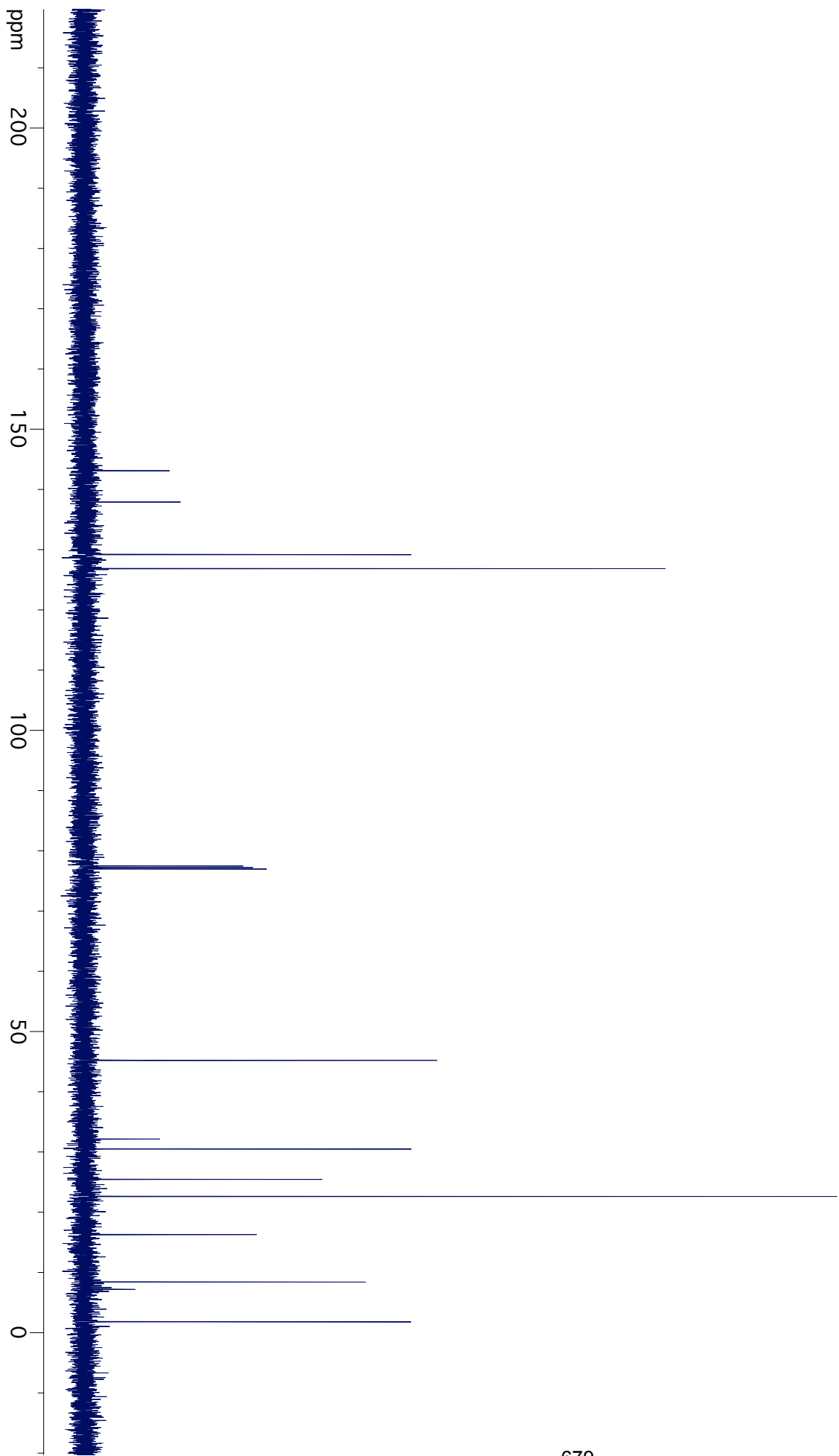
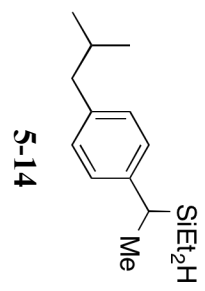


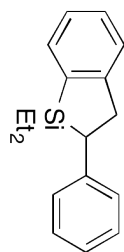




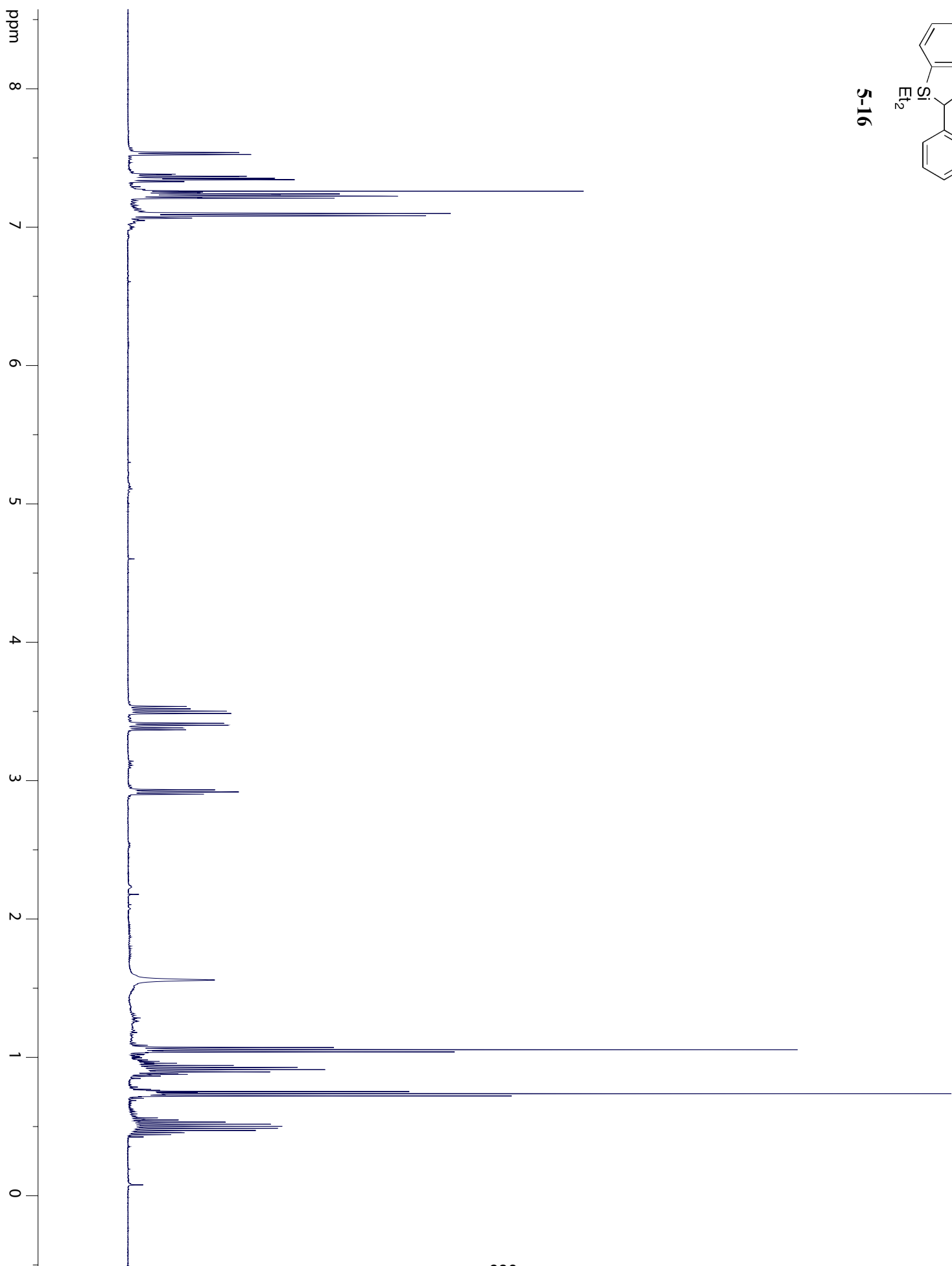
S-14

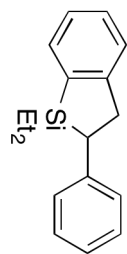




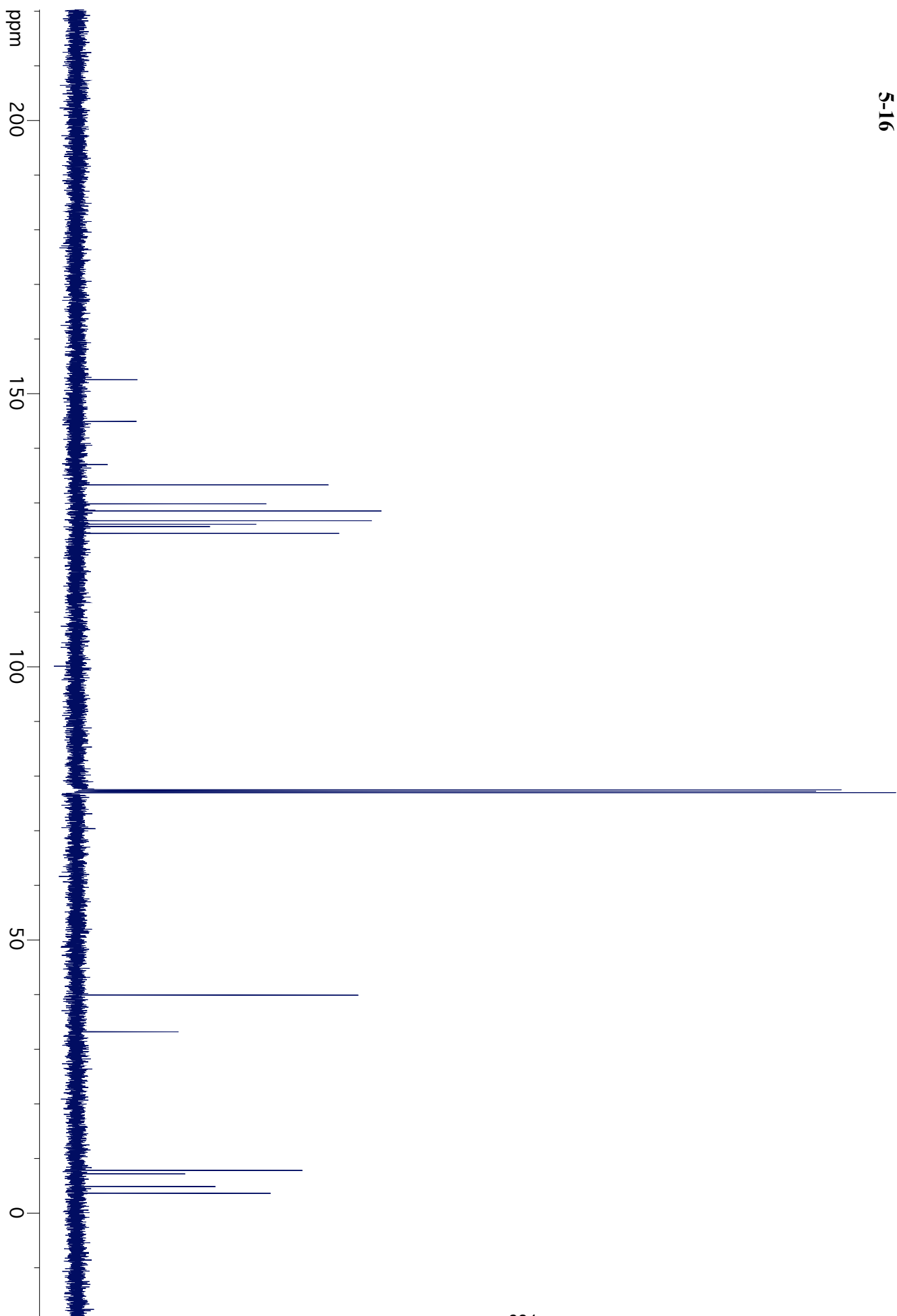


5-16





5-16



References:

- (1) Tacke, R.; Wannagat, U., Syntheses and properties of bioactive organo-silicon compounds. In *Bioactive Organo-Silicon Compounds*, Springer: 1979; pp 1-75.
- (2) Zbik, M.; Jasieniak, M.; Smart, R. S. C. *Meteorit. Planet. Sci.* **2000**, 943.
- (3) Miller, R. D.; Michl, J. *Chem. Rev.* **1989**, 89, 1359-1410.
- (4) Sieburth, S. M.; Nittoli, T.; Mutahi, A. M.; Guo, L. *Angew. Chem., Int. Ed.* **1998**, 37, 812-814.
- (5) Franz, A. K.; Wilson, S. O. *J. Med. Chem.* **2012**, 56, 388-405.
- (6) Denmark, S. E.; Regens, C. S. *Acc. Chem. Res.* **2008**, 41, 1486-1499.
- (7) Nakao, Y.; Hiyama, T. *Chem. Soc. Rev.* **2011**, 40, 4893-4901.
- (8) Jones, G. R.; Landais, Y. *Tetrahedron* **1996**, 52, 7599-7662.
- (9) Denmark, S. E.; Neuville, L. *Org. Lett.* **2000**, 2, 3221-3224.
- (10) Lickiss, P. D. *Adv. Inorg. Chem.* **1995**, 147.
- (11) Denmark, S. E.; Wehrli, D. *Org. Lett.* **2000**, 2, 565-568.
- (12) Hirabayashi, K.; Ando, J.-i.; Kawashima, J.; Nishihara, Y.; Mori, A.; Hiyama, T. *Bull. Chem. Soc. Jpn.* **2000**, 73, 1409-1417.
- (13) Manoso, A. S.; DeShong, P. *J. Org. Chem.* **2001**, 66, 7449-7455.
- (14) Murata, M.; Ishikura, M.; Nagata, M.; Watanabe, S.; Masuda, Y. *Org. Lett.* **2002**, 4, 1843-1845.
- (15) Cheng, C.; Hartwig, J. F. *Chem. Rev.* **2015**, 8946-8975.
- (16) Tsukada, N.; Hartwig, J. F. *J. Am. Chem. Soc.* **2005**, 127, 5022-5023.
- (17) Simmons, E. M.; Hartwig, J. F. *J. Am. Chem. Soc.* **2010**, 132, 17092-17095.
- (18) Li, Q.; Driess, M.; Hartwig, J. F. *Angew. Chem., Int. Ed. Engl.* **2014**, 53, 8471-8474.
- (19) Cheng, C.; Brookhart, M. *Angew. Chem., Int. Ed.* **2012**, 51, 9422-9424.
- (20) Cheng, C.; Brookhart, M. *J. Am. Chem. Soc.* **2012**, 134, 11304-11307.
- (21) Kuninobu, Y.; Yamauchi, K.; Tamura, N.; Seiki, T.; Takai, K. *Angew. Chem.* **2013**, 125, 1560-1562.
- (22) Ureshino, T.; Yoshida, T.; Kuninobu, Y.; Takai, K. *J. Am. Chem. Soc.* **2010**, 132, 14324-14326.
- (23) Chandrasekhar, V.; Boomishankar, R.; Nagendran, S. *Chem. Rev.* **2004**, 104, 5847-5910.
- (24) Zeigler, J. M.; Fearon, F. W. G., *Silicon-Based Polymer Science*. American Chemical Society: 1989; Vol. 224, p 832.
- (25) Zakir, M.; Ashraf, U.; Tian, T.; Han, A.; Qiao, W.; Jin, X.; Zhang, M.; Tsoi, J. K.-H.; Matinlinna, J. P. *Current Oral Health Reports* **2016**, 3, 244-253.
- (26) Kim, Y.-m.; Farrah, S.; Baney, R. H. *Int. J. Antimicrob. Agents* **2007**, 29, 217-222.
- (27) Kim, Y.-m.; Farrah, S.; Baney, R. H. *Electron. J. Biotechnol.* **2006**, 9, 0-0.
- (28) Graiver, D.; Farminer, K.; Narayan, R. *J. Polym. Environ.* **2003**, 11, 129-136.
- (29) Mutahi, M. w.; Nittoli, T.; Guo, L.; Sieburth, S. M. *J. Am. Chem. Soc.* **2002**, 124, 7363-7375.
- (30) Sieburth, S. M.; Nittoli, T.; Mutahi, A. M.; Guo, L. *Angew. Chem., Int. Ed.* **1998**, 37, 812-814.
- (31) Denmark, S. E.; Sweis, R. F., In *Metal-Catalyzed Cross-Coupling Reactions*, de Meijere, A.; Diederich, F., Eds. Wiley-VCH: New York, 2004; p Chapter 4.
- (32) Özçubukçu, S.; Schmidt, F.; Bolm, C. *Org. Lett.* **2005**, 7, 1407-1409.
- (33) Schafer, A. G.; Wieting, J. M.; Mattson, A. E. *Org. Lett.* **2011**, 13, 5228-5231.
- (34) Tran, N. T.; Min, T.; Franz, A. K. *Chem. - Eur. J.* **2011**, 17, 9897-9900.

- (35) Huang, C.; Chattopadhyay, B.;Gevorgyan, V. *J. Am. Chem. Soc.* **2011**, *133*, 12406-12409.
- (36) Frye, C. L.; Salinger, R. M.; Fearon, F.; Klosowski, J.;DeYoung, T. *J. Org. Chem.* **1970**, *35*, 1308-1314.
- (37) Lee, M.; Ko, S.;Chang, S. *J. Am. Chem. Soc.* **2000**, *122*, 12011-12012.
- (38) Denmark, S. E.;Kallemeyn, J. M. *Org. Lett.* **2003**, *5*, 3483-3486.
- (39) Wilson, S. O.; Tran, N. T.;Franz, A. K. *Organometallics* **2012**, *31*, 6715-6718.
- (40) Simmons, E. M.;Hartwig, J. F. *Angew. Chem., Int. Ed.* **2012**, *51*, 3066-3072.
- (41) Chen, S.;Foss, F. W. *Org. Lett.* **2012**, *14*, 5150-5153.
- (42) Padwa, A.; Chiacchio, U.; Fairfax, D. J.; Kassir, J. M.; Litrico, A.; Semones, M. A.;Xu, S. L. *J. Org. Chem.* **1993**, *58*, 6429-6437.
- (43) Pereira, D. M.; Valentão, P.; Pereira, J. A.;Andrade, P. B. *Molecules* **2009**, *14*, 2202-2211.
- (44) Carlsson, A.; Lindqvist, M.;Magnusson, T. *Nature* **1957**, *180*, 1200.
- (45) Kaldor, S. W.; Kalish, V. J.; Davies, J. F.; Shetty, B. V.; Fritz, J. E.; Appelt, K.; Burgess, J. A.; Campanale, K. M.; Chirgadze, N. Y.; Clawson, D. K.; Dressman, B. A.; Hatch, S. D.; Khalil, D. A.; Kosa, M. B.; Lubbehusen, P. P.; Muesing, M. A.; Patick, A. K.; Reich, S. H.; Su, K. S.;Tatlock, J. H. *J. Med. Chem.* **1997**, *40*, 3979-3985.
- (46) O'Brien, I.; Cox, G.;Gibson, F. *Biochim. Biophys. Acta, Gen. Subj.* **1970**, *201*, 453-460.
- (47) Shimizu, M.; Mochida, K.;Hiyama, T. *Angew. Chem., Int. Ed.* **2008**, *47*, 9760-9764.
- (48) Denmark, S. E.; Smith, R. C.; Chang, W.-T. T.;Muhuhi, J. M. *J. Am. Chem. Soc.* **2009**, *131*, 3104-3118.
- (49) Whisler, M. C.; MacNeil, S.; Snieckus, V.;Beak, P. *Angew. Chem., Int. Ed.* **2004**, *43*, 2206-2225.
- (50) Toutov, A. A.; Liu, W.-B.; Betz, K. N.; Fedorov, A.; Stoltz, B. M.;Grubbs, R. H. *Nature* **2015**, *518*, 80-84.
- (51) Dick, A. R.;Sanford, M. S. *Tetrahedron* **2006**, *62*, 2439-2463.
- (52) Godula, K.;Sames, D. *Science* **2006**, *312*, 67-72.
- (53) Alberico, D.; Scott, M. E.;Lautens, M. *Chem. Rev.* **2007**, *107*, 174-238.
- (54) Seregin, I. V.;Gevorgyan, V. *Chem. Soc. Rev.* **2007**, *36*, 1173-1193.
- (55) Davies, H. M.;Manning, J. R. *Nature* **2008**, *451*, 417-424.
- (56) Ackermann, L.; Vicente, R. n.;Kapdi, A. R. *Angew. Chem., Int. Ed.* **2009**, *48*, 9792-9826.
- (57) Chen, X.; Engle, K. M.; Wang, D. H.;Yu, J. Q. *Angew. Chem., Int. Ed.* **2009**, *48*, 5094-5115.
- (58) Daugulis, O.; Do, H.-Q.;Shabashov, D. *Acc. Chem. Res.* **2009**, *42*, 1074-1086.
- (59) Ishihara, Y.;Baran, P. S. *Synlett* **2010**, 1733-1745.
- (60) Lyons, T. W.;Sanford, M. S. *Chem. Rev.* **2010**, *110*, 1147-1169.
- (61) Sun, C.-L.; Li, B.-J.;Shi, Z.-J. *Chem. Commun.* **2010**, *46*, 677-685.
- (62) Gutekunst, W. R.;Baran, P. S. *Chem. Soc. Rev.* **2011**, *40*, 1976-1991.
- (63) McMurray, L.; O'Hara, F.;Gaunt, M. J. *Chem. Soc. Rev.* **2011**, *40*, 1885-1898.
- (64) Neufeldt, S. R.;Sanford, M. S. *Acc. Chem. Res.* **2012**, *45*, 936-946.
- (65) Yamaguchi, J.; Yamaguchi, A. D.;Itami, K. *Angew. Chem., Int. Ed.* **2012**, *51*, 8960-9009.
- (66) Ackermann, L. *Acc. Chem. Res.* **2013**, *47*, 281-295.
- (67) Colby, D. A.; Bergman, R. G.;Ellman, J. A. *Chem. Rev.* **2009**, *110*, 624-655.
- (68) García-Rubia, A.; Urones, B.; Gómez Arrayás, R.;Carretero, J. C. *Chem. - Eur. J.* **2010**, *16*, 9676-9685.
- (69) Cornella, J.; Righi, M.;Larrosa, I. *Angew. Chem., Int. Ed.* **2011**, *50*, 9429-9432.

- (70) Dai, H.; Stepan, A.; Plummer, M.; Zhang, Y.; Yu, J. *J. Am. Chem. Soc.* **2011**, *133*, 7222-7228.
- (71) Huang, C.; Ghavtadze, N.; Chattopadhyay, B.; Gevorgyan, V. *J. Am. Chem. Soc.* **2011**, *133*, 17630-17633.
- (72) Richter, H.; Beckendorf, S.; Mancheño, O. G. *Adv. Synth. Catal.* **2011**, *353*, 295-302.
- (73) Rousseau, G.; Breit, B. *Angew. Chem., Int. Ed.* **2011**, *50*, 2450-2494.
- (74) Wang, C.; Ge, H. *Chem. - Eur. J.* **2011**, *17*, 14371-14374.
- (75) Yu, M.; Liang, Z.; Wang, Y.; Zhang, Y. *J. Org. Chem.* **2011**, *76*, 4987-4994.
- (76) Huang, C.; Ghavtadze, N.; Godoi, B.; Gevorgyan, V. *Chem. - Eur. J.* **2012**, *18*, 9789-9792.
- (77) Wang, C.; Chen, H.; Wang, Z.; Chen, J.; Huang, Y. *Angew. Chem., Int. Ed.* **2012**, *51*, 7242-7245.
- (78) Wang, Y.; Gevorgyan, V. *Angew. Chem., Int. Ed.* **2015**, *54*, 2255-2259.
- (79) Djurovich, P. I.; Dolich, A. R.; Berry, D. H. *J. Chem. Soc., Chem. Commun.* **1994**, 1897-1898.
- (80) Ezbiansky, K.; Djurovich, P. I.; LaForest, M.; Sinning, D. J.; Zayes, R.; Berry, D. H. *Organometallics* **1998**, *17*, 1455-1457.
- (81) Sakakura, T.; Tokunaga, Y.; Sodeyama, T.; Tanaka, M. *Chem. Lett.* **1987**, 2375-2378.
- (82) Tobisu, M.; Ano, Y.; Chatani, N. *Chem. - Asian J.* **2008**, *3*, 1585-1591.
- (83) Furukawa, S.; Kobayashi, J.; Kawashima, T. *Dalton Trans.* **2010**, *39*, 9329-9336.
- (84) Oyamada, J.; Nishiura, M.; Hou, Z. *Angew. Chem. Int. Ed.* **2011**, *50*, 10720-10723.
- (85) Klare, H. F.; Oestreich, M.; Ito, J.-i.; Nishiyama, H.; Ohki, Y.; Tatsumi, K. *J. Am. Chem. Soc.* **2011**, *133*, 3312-3315.
- (86) Tobisu, M.; Hasegawa, J.; Kita, Y.; Kinuta, H.; Chatani, N. *Chem. Commun.* **2012**, *48*, 11437-11439.
- (87) Mita, T.; Michigami, K.; Sato, Y. *Org. Lett.* **2012**, *14*, 3462-3465.
- (88) Kuznetsov, A.; Gevorgyan, V. *Org. Lett.* **2012**, *14*, 914-917.
- (89) Sakurai, T.; Matsuoka, Y.; Hanataka, T.; Fukuyama, N.; Namikoshi, T.; Watanabe, S.; Murata, M. *Chem. Lett.* **2012**, *41*, 374-376.
- (90) Kuninobu, Y.; Yamauchi, K.; Tamura, N.; Seiki, T.; Takai, K. *Angew. Chem., Int. Ed.* **2013**, *125*, 1560-1562.
- (91) Kuninobu, Y.; Nakahara, T.; Takeshima, H.; Takai, K. *Org. Lett.* **2013**, *15*, 426-428.
- (92) Li, Q.; Driess, M.; Hartwig, J. F. *Angew. Chem. Int. Ed.* **2014**, *53*, 8471-8474.
- (93) Cheng, C.; Hartwig, J. F. *Science* **2014**, *343*, 853-857.
- (94) Cheng, C.; Hartwig, J. F. *J. Am. Chem. Soc.* **2014**, *136*, 12064-12072.
- (95) Ishiyama, T.; Sato, K.; Nishio, Y.; Miyaura, N. *Angew. Chem. Int. Ed.* **2003**, *42*, 5346-5348.
- (96) Cheng, C.; Hartwig, J. F. *J. Am. Chem. Soc.* **2015**, *137*, 592-595.
- (97) Hua, Y.; Jung, S.; Roh, J.; Jeon, J. *J. Org. Chem.* **2015**, *80*, 4661-4671.
- (98) Hua, Y.; Asgari, P.; Dakarapu, U. S.; Jeon, J. *Chem. Commun.* **2015**, *51*, 3778-3781.
- (99) Ojima, I. L., Z.; Zhu, J., Recent Advances in the Hydrosilylation and Related Reactions. In *The Chemistry of Organic Silicon Compounds*, Rappoport, Z.; Apeloig, Y., Eds. Wiley: Chichester, U.K., 1998; Vol. 2, pp 1687-1792.
- (100) Parks, D. J.; Piers, W. E. *J. Am. Chem. Soc.* **1996**, *118*, 9440-9441.
- (101) Parks, D. J.; Blackwell, J. M.; Piers, W. E. *J. Org. Chem.* **2000**, *65*, 3090-3098.
- (102) Igarashi, M.; Mizuno, R.; Fuchikami, T. *Tetrahedron Lett.* **2001**, *42*, 2149-2151.
- (103) Nakanishi, J.; Tatamidani, H.; Fukumoto, Y.; Chatani, N. *Synlett* **2006**, 869-872.
- (104) Maciejewski, H.; Pietraszuk, C.; Pawluc, P.; Marciniak, B., In *Hydrosilylation: A Comprehensive Review On Recent Advances. Advances in Silicon Science*, Springer: Berlin: 2009; Vol. 1.

- (105) Roberts, J. D.; Simmons, H. E.; Carlsmith, L. A.; Vaughan, C. W. *J. Am. Chem. Soc.* **1953**, *75*, 3290-3291.
- (106) Wenk, H. H.; Winkler, M.; Sander, W. *Angew. Chem., Int. Ed.* **2003**, *42*, 502-528.
- (107) Gampe, C.; Carreira, E. *Angew. Chem., Int. Ed.* **2012**, *51*, 3766-3778.
- (108) Hoye, T. R.; Baire, B.; Niu, D.; Willoughby, P. H.; Woods, B. P. *Nature* **2012**, *490*, 208-212.
- (109) Tadross, P. M.; Stoltz, B. M. *Chem. Rev.* **2012**, *112*, 3550-3577.
- (110) Goetz, A. E.; Garg, N. K. *J. Org. Chem.* **2014**, *79*, 846-851.
- (111) Ball, L. T.; Lloyd-Jones, G. C.; Russell, C. A. *Science* **2012**, *337*, 1644-1648.
- (112) Ball, L. T.; Lloyd-Jones, G. C.; Russell, C. A. *J. Am. Chem. Soc.* **2013**, *136*, 254-264.
- (113) Yamaguchi, S.; Tamao, K. *J. Organomet. Chem.* **2002**, *653*, 223-228.
- (114) Hissler, M.; Dyer, P. W.; Réau, R. *Coord. Chem. Rev.* **2003**, *244*, 1-44.
- (115) Brunel, J. M. *Chem. Rev.* **2005**, *105*, 857-898.
- (116) Kampen, D.; Reisinger, C.; List, B. *Top. Curr. Chem.* **2010**, *291*, 395-456.
- (117) Nielsen, L.; Lindsay, K. B.; Faber, J.; Nielsen, N. C.; Skrydstrup, T. *J. Org. Chem.* **2007**, *72*, 10035-10044.
- (118) Ojima, I.; Li, Z.; Zhu, J., The Hydrosilylation Reaction. In *The Chemistry of Organic Silicon Compounds*, Eds. ed.; Patai, S.; Rappoport, Z., Eds. Wiley: Chichester, U.K., 1989; Vol. 1, pp 1479-1526.
- (119) Ghosh, P.; Shabat, D.; Kumar, S.; Sinha, S.; Grynszpan, F.; Li, J.; Noodleman, L.; Keinan, E. *Nature* **1996**, *382*, 339-341.
- (120) Eliel, E. L.; Satici, H. *J. Org. Chem.* **1994**, *59*, 688-689.
- (121) Marzabadi, C.; Anderson, J.; Gonzalez-Outeirino, J.; Gaffney, P.; White, C.; Tocher, D.; Todaro, L. *J. Am. Chem. Soc.* **2003**, *125*, 15163-15173.
- (122) Park, S.; Brookhart, M. *J. Am. Chem. Soc.* **2011**, *134*, 640-653.
- (123) Hanamoto, T.; Fuchikami, T. *J. Org. Chem.* **1990**, *55*, 4969-4971.
- (124) Mohanta, P. K.; Davis, T. A.; Gooch, J. R.; Flowers, R. A. *J. Am. Chem. Soc.* **2005**, *127*, 11896-11897.
- (125) Malamakal, R. M.; Hess, W. R.; Davis, T. A. *Org. Lett.* **2010**, *12*, 2186-2189.
- (126) Stanton, G. R.; Norrby, P.-O.; Carroll, P. J.; Walsh, P. J. *J. Am. Chem. Soc.* **2012**, *134*, 17599-17604.
- (127) Horton, D. A.; Bourne, G. T.; Smythe, M. L. *Chem. Rev.* **2003**, *103*, 893-930.
- (128) Seganish, W. M.; DeShong, P. *J. Org. Chem.* **2004**, *69*, 6790-6795.
- (129) Zhang, L.; Wu, J. *J. Am. Chem. Soc.* **2008**, *130*, 12250-12251.
- (130) Wu, X.; Li, M.-L.; Wang, P.-s. *J. Org. Chem.* **2014**, *79*, 419-425.
- (131) Lafrance, M.; Fagnou, K. *J. Am. Chem. Soc.* **2006**, *128*, 16496-16497.
- (132) Yang, S.; Sun, C.; Fang, Z.; Li, B.; Li, Y.; Shi, Z. *Angew. Chem., Int. Ed. Engl.* **2008**, *47*, 1473-1476.
- (133) Wen, J.; Zhang, J.; Chen, S. Y.; Li, J.; Yu, X. Q. *Angew. Chem., Int. Ed.* **2008**, *47*, 8897-8900.
- (134) McGlacken, G. P.; Bateman, L. M. *Chem. Soc. Rev.* **2009**, *38*, 2447-2464.
- (135) Phipps, R. J.; Gaunt, M. J. *Science* **2009**, *323*, 1593-1597.
- (136) Hachiya, H.; Hirano, K.; Satoh, T.; Miura, M. *Angew. Chem., Int. Ed.* **2010**, *49*, 2202-2205.
- (137) Ciana, C.-L.; Phipps, R. J.; Brandt, J. R.; Meyer, F.-M.; Gaunt, M. J. *Angew. Chem. Int. Ed.* **2011**, *50*, 458-462.
- (138) Funaki, K.; Kawai, H.; Sato, T.; Oi, S. *Chem. Lett.* **2011**, *40*, 1050-1052.
- (139) Schön, U.; Messinger, J.; Solodenko, W.; Kirschning, A. *Synthesis* **2012**, 3822-3828.
- (140) Roberts, J. D.; Simmons, H. E.; Carlsmith, L.; Vaughan, C. W. *J. Am. Chem. Soc.* **1953**, *75*, 3290-3291.

- (141) Goetz, A. E.; Shah, T. K.; Garg, N. K. *Chem. Commun.* **2015**, 51, 34-45.
- (142) Pérez, D.; Peña, D.; Guitián, E. *Eur. J. Org. Chem.* **2013**, 2013, 5981-6013.
- (143) Wu, D.; Ge, H.; Liu, S. H.; Yin, J. *RSC Adv.* **2013**, 3, 22727-22738.
- (144) Truong, T.; Daugulis, O. *Chem. Sci.* **2013**, 4, 531-535.
- (145) Allan, K. M.; Gilmore, C. D.; Stoltz, B. M. *Angew. Chem.* **2011**, 123, 4580-4583.
- (146) Smith, A. B.; Kim, W.-S. *Proc. Natl. Acad. Sci. U. S. A.* **2011**, 108, 6787-6792.
- (147) Goetz, A. E.; Garg, N. K. *Nat. Chem.* **2013**, 5, 54.
- (148) Yoshida, H.; Yoshida, R.; Takaki, K. *Angew. Chem., Int. Ed.* **2013**, 52, 8629-8632.
- (149) Hendrick, C. E.; McDonald, S. L.; Wang, Q. *Org. Lett.* **2013**, 15, 3444-3447.
- (150) Bhojgude, S. S.; Thangaraj, M.; Suresh, E.; Biju, A. T. *Org. Lett.* **2014**, 16, 3576-3579.
- (151) Liu, F.-L.; Chen, J.-R.; Zou, Y.-Q.; Wei, Q.; Xiao, W.-J. *Org. Lett.* **2014**, 16, 3768-3771.
- (152) Pandya, V. G.; Mhaske, S. B. *Org. Lett.* **2014**, 16, 3836-3839.
- (153) Sumida, Y.; Harada, R.; Kato-Sumida, T.; Johmoto, K.; Uekusa, H.; Hosoya, T. *Org. Lett.* **2014**, 16, 6240-6243.
- (154) Hendrick, C. E.; Wang, Q. *J. Org. Chem.* **2014**, 80, 1059-1069.
- (155) Yoshida, S.; Yano, T.; Misawa, Y.; Sugimura, Y.; Igawa, K.; Shimizu, S.; Tomooka, K.; Hosoya, T. *J. Am. Chem. Soc.* **2015**, 137, 14071-14074.
- (156) Peng, X.; Ma, C.; Tung, C.-H.; Xu, Z. *Org. Lett.* **2016**.
- (157) Shu, W.-M.; Zheng, K.-L.; Ma, J.-R.; Wu, A.-X. *Org. Lett.* **2016**.
- (158) Dhokale, R. A.; Mhaske, S. B. *Org. Lett.* **2016**.
- (159) Shah, T. K.; Medina, J. M.; Garg, N. K. *J. Am. Chem. Soc.* **2016**, 138, 4948-4954.
- (160) Stoermer, R.; Kahlert, B. *Ber. Dtsch. Chem. Ges.* **1902**, 35, 1633-1640.
- (161) Gilman, H.; Avakian, S. *J. Am. Chem. Soc.* **1945**, 67, 349-351.
- (162) Huisgen, R.; Sauer, J.; Hauser, A. *Chem. Ber.* **1958**, 91, 2366-2374.
- (163) Wittig, G.; Hoffmann, R. W. *Chem. Ber.* **1962**, 95, 2718-2728.
- (164) Stiles, M.; Miller, R. G.; Burckhardt, U. *J. Am. Chem. Soc.* **1963**, 85, 1792-1797.
- (165) Campbell, C.; Rees, C. *Journal of the Chemical Society C: Organic* **1969**, 742-747.
- (166) Meyers, A.; Pansegrau, P. D. *J. Chem. Soc., Chem. Commun.* **1985**, 690-691.
- (167) Hart, H.; Harada, K.; Du, C. J. F. *J. Org. Chem.* **1985**, 50, 3104-3110.
- (168) Niu, D.; Willoughby, P. H.; Woods, B. P.; Baire, B.; Hoye, T. R. *Nature* **2013**, 501, 531-534.
- (169) Yun, S. Y.; Wang, K.-P.; Lee, N.-K.; Mamidipalli, P.; Lee, D. *J. Am. Chem. Soc.* **2013**, 135, 4668-4671.
- (170) Mesgar, M.; Daugulis, O. *Org. Lett.* **2016**, 18, 3910-3913.
- (171) Himeshima, Y.; Sonoda, T.; Kobayashi, H. *Chem. Lett.* **1983**, 12, 1211-1214.
- (172) Kitamura, T.; Yamane, M. *J. Chem. Soc., Chem. Commun.* **1995**, 983-984.
- (173) Yamanoi, Y.; Nishihara, H. *J. Org. Chem.* **2008**, 73, 6671-6678.
- (174) Peña, D.; Cobas, A.; Pérez, D.; Guitián, E. *Synthesis* **2002**, 2002, 1454-1458.
- (175) Bronner, S. M.; Garg, N. K. *J. Org. Chem.* **2009**, 74, 8842-8843.
- (176) Atkinson, D. J.; Sperry, J.; Brimble, M. A. *Synthesis* **2010**, 2010, 911-913.
- (177) Hua, Y.; Asgari, P.; Avullala, T.; Jeon, J. *J. Am. Chem. Soc.* **2016**, 138, 7982-7991.
- (178) Brook, A. G. *Acc. Chem. Res.* **1974**, 7, 77-84.
- (179) Moser, W. H. *Tetrahedron* **2001**, 57, 2065-2084.
- (180) Austin, W. F.; Zhang, Y.; Danheiser, R. L. *Tetrahedron* **2008**, 64, 915-925.
- (181) Cooper, G. D. *J. Org. Chem.* **1961**, 26, 925-929.
- (182) Eastham, S. A.; Ingham, S. P.; Hallett, M. R.; Herbert, J.; Quayle, P.; Raftery, J. *Tetrahedron Lett.* **2006**, 47, 2299-2304.
- (183) Schön, U.; Messinger, J.; Solodenko, W.; Kirschning, A. *Synthesis* **2012**, 44, 3822-3828.

- (184) Esguerra, K. V. N.; Fall, Y.; Petitjean, L. n.;Lumb, J.-P. *J. Am. Chem. Soc.* **2014**, *136*, 7662-7668.
- (185) Billedau, R.; Sibi, M.;Snieckus, V. *Tetrahedron Lett.* **1983**, *24*, 4515-4518.
- (186) He, H.-M.; Fanwick, P. E.; Wood, K.;Cushman, M. *J. Org. Chem.* **1995**, *60*, 5905-5909.
- (187) Eisenberg, D. C.;Norton, J. R. *Isr. J. Chem.* **1991**, *31*, 55-66.
- (188) Kumar, M.; Sinha, A.;Francisco, J. S. *Acc. Chem. Res.* **2016**, *49*, 877-883.
- (189) Mukaiyama, T.;Yamada, T. *Bull. Chem. Soc. Jpn.* **1995**, *68*, 17-35.
- (190) Crossley, S. W.; Obradors, C.; Martinez, R. M.;Shenvi, R. A. *Chem. Rev.* **2016**, *116*, 8912-9000.
- (191) Mayer, J. M. *Acc. Chem. Res.* **1998**, *31*, 441-450.
- (192) Guallar, V.; Baik, M.-H.; Lippard, S. J.;Friesner, R. A. *Proc. Natl. Acad. Sci. U. S. A.* **2003**, *100*, 6998-7002.
- (193) Mandal, S. K.;Roesky, H. W. *Acc. Chem. Res.* **2011**, *45*, 298-307.
- (194) Brunel, J. M. *Int. J. Hydrogen Energy* **2017**, *42*, 23004-23009.
- (195) Peng, W.; Rupich, S. M.; Shafiq, N.; Gartstein, Y. N.; Malko, A. V.;Chabal, Y. J. *Chem. Rev.* **2015**, *115*, 12764-12796.
- (196) Ting, R.; Adam, M. J.; Ruth, T. J.;Perrin, D. M. *J. Am. Chem. Soc.* **2005**, *127*, 13094-13095.
- (197) Komiyama, T.; Minami, Y.;Hiyama, T. *ACS Catal.* **2016**, *7*, 631-651.
- (198) Nakajima, Y.;Shimada, S. *RSC Adv.* **2015**, *5*, 20603-20616.
- (199) Simonneau, A.;Oestreich, M. *Nat. Chem.* **2015**, *7*, 816–822.
- (200) Marciniak, B., *Comprehensive handbook on hydrosilylation*. Elsevier: 2013.
- (201) Uozumi, Y.;Hayashi, T. *J. Am. Chem. Soc.* **1991**, *113*, 9887-9888.
- (202) Gribble Jr, M. W.; Pirnot, M. T.; Bandar, J. S.; Liu, R. Y.;Buchwald, S. L. *J. Am. Chem. Soc.* **2017**, *139*, 2192-2195.
- (203) Cheng, B.; Lu, P.; Zhang, H.; Cheng, X.;Lu, Z. *J. Am. Chem. Soc.* **2017**, *139*, 9439-9442.
- (204) Docherty, J. H.; Peng, J.; Dominey, A. P.;Thomas, S. P. *Nat. Chem.* **2017**, *9*, 595–600.
- (205) Simoes, J. M.;Beauchamp, J. *Chem. Rev.* **1990**, *90*, 629-688.
- (206) Uddin, J.; Morales, C. M.; Maynard, J. H.;Landis, C. R. *Organometallics* **2006**, *25*, 5566-5581.
- (207) Lo, J. C.; Gui, J.; Yabe, Y.; Pan, C.-M.;Baran, P. S. *Nature* **2014**, *516*, 343-348.
- (208) Kuo, J. L.; Hartung, J.; Han, A.;Norton, J. R. *J. Am. Chem. Soc.* **2015**, *137*, 1036-1039.
- (209) Ma, X.;Herzon, S. B. *J. Am. Chem. Soc.* **2016**, *138*, 8718-8721.
- (210) Green, S. A.; Matos, J. L.; Yagi, A.;Shenvi, R. A. *J. Am. Chem. Soc.* **2016**, *138*, 12779-12782.
- (211) Boyer, J.; Corriu, R.; Perz, R.;Reye, C. *Tetrahedron* **1981**, *37*, 2165-2171.
- (212) Toutov, A. A.; Betz, K. N.; Schuman, D. P.; Liu, W.-B.; Fedorov, A.; Stoltz, B. M.;Grubbs, R. H. *J. Am. Chem. Soc.* **2017**, *139*, 1668-1674.
- (213) Liu, W.-B.; Schuman, D. P.; Yang, Y.-F.; Toutov, A. A.; Liang, Y.; Klare, H. F. T.; Nesnas, N.; Oestreich, M.; Blackmond, D. G.; Virgil, S. C.; Banerjee, S.; Zare, R. N.; Grubbs, R. H.; Houk, K. N.;Stoltz, B. M. *J. Am. Chem. Soc.* **2017**, *139*, 6867-6879.
- (214) Banerjee, S.; Yang, Y.-F.; Jenkins, I. D.; Liang, Y.; Toutov, A. A.; Liu, W.-B.; Schuman, D. P.; Grubbs, R. H.; Stoltz, B. M.; Krenske, E. H.; Houk, K. N.;Zare, R. N. *J. Am. Chem. Soc.* **2017**, *139*, 6880-6887.

- (215) Smith, A. J.; Young, A.; Rohrbach, S.; O'Connor, E. F.; Allison, M.; Wang, H.-S.; Poole, D. L.; Tuttle, T.; Murphy, J. A. *Angew. Chem., Int. Ed.* **2017**, *56*, 13747-13751.
- (216) Corriu, R. J.; Guerin, C.; Henner, B.; Wang, Q. *Organometallics* **1991**, *10*, 2297-2303.
- (217) Maifeld, S. V.; Lee, D. *Org. Lett.* **2005**, *7*, 4995-4998.
- (218) Gatineau, D.; Zhao, Q.; Curran, D. P.; Malacria, M.; Lacote, E.; Fensterbank, L.; Goddard, J. P. *Dalton Trans.* **2013**, *42*, 7458-7462.
- (219) Kanabus-Kaminska, J.; Hawari, J.; Griller, D.; Chatgililoglu, C. *J. Am. Chem. Soc.* **1987**, *109*, 5267-5268.
- (220) Denmark, S. E.; Beutner, G. L. *Angew. Chem., Int. Ed.* **2008**, *47*, 1560-1638.
- (221) Couzijn, E. P.; Ehlers, A. W.; Schakel, M.; Lammertsma, K. *J. Am. Chem. Soc.* **2006**, *128*, 13634-13639.
- (222) Chuit, C.; Corriu, R. J.; Reye, C.; Young, J. C. *Chem. Rev.* **1993**, *93*, 1371-1448.
- (223) Baboul, A. G.; Curtiss, L. A.; Redfern, P. C.; Raghavachari, K. *J. Chem. Phys.* **1999**, *110*, 7650-7657.
- (224) Kumpf, R. A.; Dougherty, D. A. *Science* **1993**, *261*, 1708-1710.
- (225) Ibrahim, M. R.; Jorgensen, W. L. *J. Am. Chem. Soc.* **1989**, *111*, 819-824.
- (226) Fischer, H. *Chem. Rev.* **2001**, *101*, 3581-3610.
- (227) Masnovi, J.; Samsel, E. G.; Bullock, R. M. *J. Chem. Soc., Chem. Commun.* **1989**, 1044-1045.
- (228) Hu, S.-W.; Wang, Y.; Wang, X.-Y.; Chu, T.-W.; Liu, X.-Q. *J. Phys. Chem. A* **2004**, *108*, 1448-1459.
- (229) Chandra Mondal, K.; Roy, S.; Roesky, H. W. *Chem. Soc. Rev.* **2016**, *45*, 1080-1111.
- (230) Weil, J. A.; Bolton, J. R.; Wertz, J. E., *Electron Paramagnetic Resonance. Elementary Theory and Practical Applications*. 1st ed.; Wiley: 1994.
- (231) Eaton, G. R.; Eaton, S. S.; Salikhov, K. M., *Foundations of Modern EPR*. World Scientific: 1998.
- (232) Amorati, R.; Lucarini, M.; Mugnaini, V.; Pedulli, G. F. *J. Org. Chem.* **2003**, *68*, 5198-5204.
- (233) Kirste, B.; Krueger, A.; Kurreck, H. *J. Am. Chem. Soc.* **1982**, *104*, 3850-3858.
- (234) Takashi, K.; Shoichi, M.; Teijiro, Y. *Bull. Chem. Soc. Jpn.* **1967**, *40*, 1111-1115.
- (235) Segal, B. G.; Kaplan, M.; Fraenkel, G. K. *J. Chem. Phys.* **1965**, *43*, 4191-4200.
- (236) Du, J. L.; Eaton, G. R.; Eaton, S. S. *J. Magn. Reson. A* **1995**, *115*, 213-221.
- (237) Novak, I.; Kovač, B. *Chem. Phys. Lett.* **2005**, *413*, 351-355.
- (238) Layfield, R. A., Highlights in low-coordinate group 14 organometallic chemistry. In *Organometallic Chemistry: Volume 37*, The Royal Society of Chemistry: 2011; Vol. 37, pp 133-148.
- (239) Peters, S. J.; Turk, M. R.; Kiesewetter, M. K.; Reiter, R. C.; Stevenson, C. D. *J. Am. Chem. Soc.* **2003**, *125*, 11212-11213.
- (240) Sekiguchi, A.; Kinjo, R.; Ichinohe, M. *Synth. Met.* **2009**, *159*, 773-775.
- (241) Drago, R. S. *Acc. Chem. Res.* **1992**, *25*, 382-383.
- (242) Wertz, J. A. W. J. R. B. a. J. E., *Electron Paramagnetic Resonance: Elementary Theory and Practical Applications*. 1st Ed. ed.; John Wiley & Sons Inc.: New York, 1994.
- (243) Qiu, J.; Matyjaszewski, K. *Macromolecules* **1997**, *30*, 5643-5648.
- (244) Gao, J.; Grofe, A.; Ren, H.; Bao, P. *Journal of physical chemistry letters* **2016**, *7*, 5143-5149.
- (245) Grofe, A.; Chen, X.; Liu, W.; Gao, J. *The journal of physical chemistry letters* **2017**, *8*, 4838-4845.

- (246) Cembran, A.; Provorse, M. R.; Wang, C.; Wu, W.; Gao, J. *J. Chem. Theory Comput.* **2012**, *8*, 4347-4358.
- (247) Luo, S.; Averkiev, B.; Yang, K. R.; Xu, X.; Truhlar, D. G. *J. Chem. Theory Comput.* **2013**, *10*, 102-121.
- (248) Shaik, S. S.; Schlegel, H. B.; Wolfe, S., *Theoretical Aspects of Physical Organic Chemistry: The SN2 Mechanism*. Wiley: New York, 1992.
- (249) Wu, W.; Su, P.; Shaik, S.; Hiberty, P. C. *Chem. Rev.* **2011**, *111*, 7557-7593.
- (250) Lai, W.; Li, C.; Chen, H.; Shaik, S. *Angew. Chem., Int. Ed.* **2012**, *51*, 5556-5578.
- (251) Adamo, C.; Barone, V. *J. Chem. Phys.* **1999**, *110*, 6158-6170.
- (252) Liu, Q.; Wu, L.; Jackstell, R.; Beller, M. *Nat. Commun.* **2015**, *6*, 5933.
- (253) Salzner, U.; Lagowski, J.; Pickup, P.; Poirier, R. *Synth. Met.* **1998**, *96*, 177-189.
- (254) Abragam, A.; Bleaney, B., *Electron Paramagnetic Resonance of Transition Ions (International Series of Monographs on Physics)*. 1970; p 912 pp.
- (255) Golombek, A. P.; Hendrich, M. P. *J. Magn. Reson.* **2003**, *165*, 33-48.
- (256) Snyder, L. *J. Chromatogr. Sci.* **1978**, *16*, 223-234.
- (257) Zhao, Y.; Truhlar, D. G. *Theor. Chem. Acc.* **2008**, *120*, 215-241.
- (258) M. J. Frisch, G. W. T., H. B. Schlegel, G. E. Scuseria, M. A. Robb, J. R. Cheeseman, G. Scalmani, V. Barone, B. Mennucci, G. A. Petersson, H. Nakatsuji, M. Caricato, X. Li, H. P. Hratchian, A. F. Izmaylov, J. Bloino, G. Zheng, J. L. Sonnenberg, M. Hada, M. Ehara, K. Toyota, R. Fukuda, J. Hasegawa, M. Ishida, T. Nakajima, Y. Honda, O. Kitao, H. Nakai, T. Vreven, J. A. Montgomery, Jr., J. E. Peralta, F. Ogliaro, M. Bearpark, J. J. Heyd, E. Brothers, K. N. Kudin, V. N. Staroverov, R. Kobayashi, J. Normand, K. Raghavachari, A. Rendell, J. C. Burant, S. S. Iyengar, J. Tomasi, M. Cossi, N. Rega, J. M. Millam, M. Klene, J. E. Knox, J. B. Cross, V. Bakken, C. Adamo, J. Jaramillo, R. Gomperts, R. E. Stratmann, O. Yazyev, A. J. Austin, R. Cammi, C. Pomelli, J. W. Ochterski, R. L. Martin, K. Morokuma, V. G. Zakrzewski, G. A. Voth, P. Salvador, J. J. Dannenberg, S. Dapprich, A. D. Daniels, Ö. Farkas, J. B. Foresman, J. V. Ortiz, J. Cioslowski, and D. J. Fox, , *Gaussian 09* Gaussian, Inc.: Wallingford CT, 2009.
- (259) *Theory and Applications of Computational Chemistry: the first forty years*. C.E.Dykstra, G. F., K.S.Kim, G.E.Scuseria, Ed. Elsevier: Amsterdam, 2005; pp 1167-1189.
- (260) Schmidt, M. W.; Baldridge, K. K.; Boatz, J. A.; Elbert, S. T.; Gordon, M. S.; Jensen, J. H.; Koseki, S.; Matsunaga, N.; Nguyen, K. A.; Su, S. *J. Comput. Chem.* **1993**, *14*, 1347-1363.
- (261) Asgari, P.; Dakarapu, U. S.; Nguyen, H. H.; Jeon, J. *Tetrahedron* **2017**, *73*, 4052-4061.